Carnegie Institution

OF WASHINGTON

Year Book 68

1968-1969

Director's Office

Carnegie Institution

OF WASHINGTON

Year Book 68

1968-1969

Library of Congress Catalog Card Number 3-16716
Port City Press, Baltimore, Maryland

Contents

President and Trustees

Staff

MOUNT WILSON AND
PALOMAR OBSERVATORIES

813 Santa Barbara Street
Pasadena, California 91106

Horace W. Babcock, *Director*
Halton C. Arp
Ira S. Bowen, *Distinguished Service Member*
Edwin W. Dennison
Armin J. Deutsch
Jesse L. Greenstein [1]
Robert F. Howard
Jerome Kristian [2]
Robert B. Leighton [3]
Guido Münch [4]
J. Beverley Oke [4]
George W. Preston III [5]
Bruce H. Rule
Allan R. Sandage
Wallace L. W. Sargent [6]
Maarten Schmidt [4]
Arthur H. Vaughan, Jr.
Olin C. Wilson
Harold Zirin [7]

GEOPHYSICAL LABORATORY

2801 Upton Street, N.W.
Washington, D.C. 20008

Philip H. Abelson, *Director*
Peter M. Bell
Francis R. Boyd, Jr.
Felix Chayes
Gordon L. Davis
Gabrielle Donnay
Joseph L. England
P. Edgar Hare
Thomas C. Hoering
Thomas E. Krogh
Gunnar Kullerud
Donald H. Lindsley
J. Frank Schairer
Hatten S. Yoder, Jr.

DEPARTMENT OF
TERRESTRIAL MAGNETISM

5241 Broad Branch Road, N.W.
Washington, D. C. 20015

Ellis T. Bolton, *Director*
L. Thomas Aldrich, *Associate Director*
Merle A. Tuve, *Distinguished Service Member*

Roy J. Britten
Louis Brown
Dean B. Cowie
Scott E. Forbush [8]
W. Kent Ford, Jr.
Stanley R. Hart
Bill H. Hoyer [9]
David E. James [10]
David E. Kohne
Richard B. Roberts
Vera C. Rubin
I. Selwyn Sacks
John S. Steinhart [11]
Kenneth C. Turner

[1] Professor of Astrophysics and Executive Officer for Astronomy, California Institute of Technology.
[2] From September 1, 1968.
[3] Professor of Physics, California Institute of Technology.
[4] Professor of Astronomy, California Institute of Technology.
[5] From July 1, 1968.
[6] Associate Professor of Astronomy, California Institute of Technology.
[7] Professor of Astrophysics, California Institute of Technology.
[8] Retired June 30, 1969.
[9] From November 1, 1968.
[10] From September 1, 1968.
[11] On leave of absence from October 7, 1968, resigned June 30, 1969.

Staff (continued)

DEPARTMENT OF PLANT BIOLOGY
Stanford, California 94305

C. Stacy French, *Director*
Olle Björkman
Jeanette S. Brown
Jens C. Clausen, *Emeritus*
David C. Fork
William M. Hiesey [1]
Malcolm A. Nobs
James H. C. Smith, *Emeritus*

DEPARTMENT OF EMBRYOLOGY
115 West University Parkway
Baltimore, Maryland 21210

James D. Ebert, *Director*
Bent G. Böving
Donald D. Brown
Igor B. Dawid
Robert L. DeHaan
Douglas M. Fambrough [2]
Elizabeth M. Ramsey
Ronald H. Reeder [2]

GENETICS RESEARCH UNIT
Cold Spring Harbor
New York 11724

Alfred D. Hershey, *Director*
Barbara McClintock, *Distinguished Service Member*
Elizabeth Burgi

Cytogenetics Laboratory
Ann Arbor, Michigan

Helen Gay

[1] Retired June 30, 1969.

[2] Beginning July 1, 1969.

Staff (continued)

OFFICE OF ADMINISTRATION

1530 P Street, N.W., Washington, D.C. 20005

Caryl P. Haskins	*President*
Edward A. Ackerman	*Executive Officer, Acting Director of Publications*
James W. Boise	*Bursar; Secretary-Treasurer, Retirement Trust; Executive Secretary to the Finance Committee*
Marjorie H. Walburn	*Assistant to the President*
Sheila A. McGough	*Editor*
Kenneth R. Henard	*Assistant Bursar; Assistant Treasurer, Retirement Trust*
Pamela W. Thomas	*Associate Editor*
Joseph M. S. Haraburda	*Assistant to the Bursar*
A. Gerald Thompson	*Assistant to the Director of Publications*
Marshall Hornblower	*Counsel*

STAFF MEMBERS IN SPECIAL SUBJECT AREAS

Tatiana Proskouriakoff

Staff (continued)

RESEARCH ASSOCIATES OF THE CARNEGIE INSTITUTION

Mateo Casaverde
Lima, Peru

Richard A. Chase
Johns Hopkins University

Louis B. Flexner
University of Pennsylvania

Irwin Konigsberg
University of Virginia

J. D. McGee
Imperial College of Science and Technology, University of London

Jan H. Oort
University of Leiden

Harry E. D. Pollock
Carnegie Institution

Reynaldo Salgueiro
La Paz, Bolivia

Shigeji Suyehiro
Japan Meteorological Agency

Former Presidents and Trustees

Under the original charter, from the date of organization until April 28, 1904, the following were ex officio members of the Board of Trustees: the President of the United States, the President of the Senate, the Speaker of the House of Representatives, the Secretary of the Smithsonian Institution, and the President of the National Academy of Sciences.

Report OF THE *President*

My soul can find no staircase to Heaven unless it be through Earth's loveliness.

MICHELANGELO

Peace with the earth is the first peace.

HENRY BESTON—*Herbs and the Earth*

You are a child of the universe no less than the trees and the stars; you have a right to be here. And whether or not it is clear to you, no doubt the universe is unfolding as it should. Therefore be at peace with God, whatever you conceive Him to be. And whatever your labors and aspirations, in the noisy confusion of life, keep peace in your soul.

MAX EHRMANN—"Desiderata," from *The Poems of Max Ehrmann*

THE YEAR THAT WITNESSED THE CLIMAX of the most audacious and technically brilliant triumph of exploration in the history of man's wanderings, the year when the conquest of the moon has lifted the hearts of men and reinforced their pride in their humanity, has likewise been the year when the deepest social problems of our age—the intractable welter of urban blight, of academic crises, of worldwide social unrest, and perhaps most fundamental, of individual alienation—also reached a climax. This striking conjunction of opposites has been noted and commented upon many times. It is often primarily seen against the immediate background of that stringent ratio of limited human and material resources to almost unlimited requirements that characterizes the combination of military and civilian demands of our day. The questions of policy inherent in these contradictory challenges are, as we are all vividly aware, probably the most critical of the age.

How are we to maintain and nurture those qualities of hope and humility and reverence that have provided the foundation for all we have done? How are we to combat the sense of alienation, of total frustration, even of the fruitlessness of existence, that threaten all too menacingly today? How are we to preserve—and, where restoration is needed, restore—the sense of an individual oneness with the world, of a personal anchor in the universe, which is so essential

to our spiritual welfare and which, in some quarters, seems to be irrevocably slipping away?

It is often said that much of this alienation is consonant with the unexampled enlightenment of our age; that science, as it is often popularly conceived, has added its share to the spiritual burdens of our time. And so, in this day especially, it is worth recalling for a moment what science actually is, and its real relation to the spiritual crises that beset us. For science may have a most important part to play in these critical times, and its role may be quite the opposite of the one it is sometimes superficially imagined to play.

The year 1969 was not only the year of the first successful voyage to the moon. It was not only witness to the most serious social problems that have beset us. It also marked the centenary of a great scientific achievement by the Swiss biochemist Friedrich Miescher—an historic achievement that will soon be commemorated by the establishment of the first research training group of the Max Planck Institutes in Germany, the Friedrich Miescher Institute at Tübingen. Miescher succeeded in chemically isolating a new and peculiar substance, lying deep within the nuclei of the sperm cells of the salmon which in his day still ascended the Rhine as far as his home in Basel. Miescher, even then recognizing its fundamental distinctness from proteins, and noticing that its occurrence seemed strictly confined to the nuclei of cells, named the amorphous powder *nuclein.* Eighty-four years later two papers were published in England by James Watson and Francis Crick. They dealt with the molecular structure of that same amorphous white powder, and visualized the nature of its function in a way that revolutionized our ideas of the fundamental mechanisms of heredity. Over the decade and a half following the appearance of those papers in 1953, the tide of newly oriented investigation that they released has emphasized more specifically and at a deeper level than we have ever known the basic physical identity of man with all the rest of living nature: in inheritance, in evolution, perhaps in destiny. After that discovery and all its consequences, never again could modern man rationally view himself as other than an integral part of his animate world.

The terms in which that vision was conceived and expressed were peculiarly suited to our contemporary generation. But in fact, of course, they simply reaffirmed in a more powerful and explicit way an insight achieved before Miescher's time, and emphasized by his discovery. For the isolation and characterization of DNA followed by only ten years the first publication of the *Origin of Species.* Darwin was still being persuaded by certain critics to make some emendations in its text which we regard in retrospect as less penetrating than the first conclusions of his genius. In many quarters the theory of evolution was still being hotly argued, was still in its plastic, formative stage, still far from universally affirmed. Only four years previously Mendel had demonstrated the unitary character of the elements of inheritance. In retrospect we can discern in that era what we are experiencing today—the special and highly significant complex of effects that ensue when man's world view and view of himself in it are suddenly transformed by a major conceptual advance. In the context of the conjunctions that this year has brought, it is worth pursuing one of those effects a bit further.

It is believed to have been about the year 270 B.C. when Aristarchus of Samos propounded the doctrine—probably then wholly novel—that the earth, far from being the center of the universe, was instead a satellite of the sun. Little record of the reception accorded this germinal idea survives today save for a comment

of Cleanthes the Stoic. He is reported to have declared that for propounding so heretical a notion Aristarchus ought to be indicted for impiety.

Beyond that flicker of shock and outrage, the idea itself seems to have sunk into virtual oblivion for the next eighteen centuries. It was not to reappear in any commanding way until the publication in 1543 of *De Revolutionibus Orbium Coelestium* by Rhäticus, the devoted disciple and expositor of Copernicus. We know that Copernicus was aware of the thinking of Aristarchus, for he mentioned it in a passage of his own work. But except for such faint indications of its survival in at most a very few minds of originality and genius, the idea of an earth revolving about a central sun seems never, over eighteen centuries, to have risen again strikingly in man's consciousness. And even after Copernicus's life work was done and his theory had become widely current publicly as well as professionally, a full fifty years were to pass before the notions of a Ptolemaic universe were finally abandoned.

In the same context some aspects of the initial reception of the *Origin of Species* take on special interest. The long and hostile reviews of Richard Owen and of Bishop Wilberforce may well have been impelled, at least in part, by other than purely intellectual motives. But the famous debate between Wilberforce and Thomas Henry Huxley before the British Association for the Advancement of Science in June of 1860 clearly represented a watershed in the history of man's view of himself and of his place in nature, and it is against this background that the acerbity of the struggle takes on a special significance. Its intensity and scope, quite beyond the context of the personal ambitions or special prejudices of a few of Darwin's countrymen, were emphasized by the castigation of the *Origin* in the United States by no less eminent an authority than Louis Agassiz, who called it "a scientific mistake, untrue in its facts, unscientific in its methods, and mischievous in its tendencies." In France, there was strong initial opposition to the theory led by Élie de Beaumont and Pierre Flourens. The French Academy refused to admit Darwin as a Corresponding Member in 1870. And in England the Royal Society of London, in presenting its Copley Medal to Darwin, curiously suggested in the accompanying citation that the writing of the *Origin* was not reckoned high among the achievements for which the award was bestowed. Clearly, the reception of the theory of evolution, however enthusiastic in some quarters, was far from universally favorable. Nor was the opposition to be short-lived. For not until the great revival of Darwinism in its modern garb during the middle decades of this century could it be considered to have achieved a firm base in the thinking of all men.

In this context, again, one recalls the forty-five years of disregard that attended the work of Mendel following the reading and the publication of his two-parted paper dealing with the inheritance of genetic characteristics in peas. It is particularly interesting to note that, although Mendel repeatedly stressed that his own demonstration of the discrete apportionment of hereditary characteristics from generation to generation clearly showed that, contrary to the notions of blending inheritance current when Darwin was writing the *Origin,* interbreeding of forms does not extinguish variation but actually increases it, and although he made specific reference to the implications of that demonstration for the theory of evolution—with which he had thoroughly familiarized himself after the publication of the *Origin*—that portion of his work received no more general attention than the rest. Finally, within the same context, one

recalls that more than eight decades separated the findings of Miescher and the solving of the riddle of DNA.

Some of these long delays had obvious causes. Neither the world's technology nor the conceptual framework of biological science could, in all probability, have taken Miescher's findings much further or faster than they did. It has been suggested that the long winter of Mendelism resulted primarily from the fact that the paper was initially published in a little-known journal. But in fact the *Journal of the Society of Naturalists of Brünn* was not particularly obscure. Indeed it enjoyed a fairly wide circulation among the libraries of the day—probably at least as wide as that of the *Journal of the Royal Horticultural Society* of Great Britain, where its republication in English in 1901 soon caught worldwide attention. A more likely contributing cause, often suggested, was the widespread lack of understanding and appreciation of mathematics and its use as a major tool of biological investigation among nineteenth-century naturalists. Finally, of course, the underlying ideas of organic evolution, though they had been foreshadowed by a number of English naturalists of a previous generation—not least Erasmus Darwin himself—were, like the ideas of Aristarchus and Copernicus in their day, of a cast profoundly unfamiliar to the general audience of their times.

There may be another quality common to the public impact of these great dividing ranges in human thought that lies deeper than the initial unfamiliarity of great conceptual advances. That quality may have a more comprehensive significance for the human condition, especially in our own day. Each of these conceptual watersheds profoundly altered man's view of himself in his universe. And often, at the outset, they were interpreted as markedly *diminishing* the stature of man in that relationship. The substitution of the notion of man's planet as a satellite of a remote sun for the picture of his home as the center of the universe can hardly have been welcome at first. The long delay in its reception suggests subliminal rejection by many men. Our firmer, broader, and more detailed knowledge of the early hostility to Darwinism and the delay in its definitive acceptance in a world already at a stage of scientific enlightenment seemingly well equipped to appreciate and absorb it speaks for an underlying trauma inherent in the sudden shift in the image of man's position from that of a specially created being to that of an integral element of the natural world. Even after the shift was generally accepted, hostility and resentment were long in dying.

But as the years rolled on, a curious paradox appeared. It became increasingly apparent that a corollary to the acceptance of what had once seemed an almost insupportable diminution in stature for man in his universe was, surprisingly, a wholly new order of human sensitivity—a wholly new order and intensity of appreciation of the scope and the wonder and the glory of that universe itself. Moreover—and especially in connection with the final acceptance of Darwinism—there came a new feeling for the essential integrity of man with the rest of a natural system which once he had regarded with uncertainty and fear, which once had seemed thoroughly alien and hostile: a sense of essential unity with nature that was soon to be intellectually reinforced. A whole spectrum of biological discoveries, ranging from the revival of Mendelism by de Vries, Correns and Tschermak in 1900 to the most recent demonstrations that at the very level of his genetic code man is truly one with the rest of the living world, could leave our own society in little reasonable doubt of man's place in nature.

From that ultimate demonstration of his essential and rightful niche in a system of almost unimaginable beauty, variety, and dynamism there inevitably followed a reinforced sense of personal identity, a new feeling of security of place in the workings of the natural universe that may well have been a quite new and heady experience. And that sense of personal identity, that feeling of place and significance, has surely been deepened and reinforced over the years by the highly individual and personal nature of the critical advances of understanding that mark the evolution of all science. Accumulating over the years and the centuries, this contribution of the scientific way to man's view of himself may well represent a contribution to humanity as great as all the specific and substantive accomplishments of science itself. And never has this contribution been so intensely relevant as in the present decade.

A prescient observer has recently remarked that the deepest crises of our day, alike for individuals and for society, which are so often seen as political crises, are in fact much more profound. One of the damaging misconceptions that currently afflicts us is that the most severe of the social traumas that we experience, the confusion and agony which we presently suffer at the level of the individual, are within reach of direct political remedy. In fact, their essence lies far deeper. It may lie in a search for meaning, and with it a sense of individual identification, by a society that has in large measure abandoned the easier and simpler framework of religious thinking that characterized another era and now desperately seeks the same values through secular channels. The passion that motivates this search, and which generates an intensity of overt political involvement quite new in many ways to the American experience, is in fact the product of that very same eighteenth-century Enlightenment which, two centuries ago, shaped the American experience and the American civilization. It is the validations and the forms of this philosophy that are outworn and at hostile issue in our day and in our world, a world whose secular aspects and demands have changed beyond all recognition. In this time of crisis, of transition, and of miasma, it is perhaps worth remembering that the very structure and deepest values of modern science were also shaped by that same Enlightenment, and that, of all its manifestations, perhaps the structure and values of modern science have persisted most faithfully to the present day. It has been suggested that the essential question of how to maintain the spiritual health of a great civilization too advanced in size and power and complexity and sophistication to be content with the older shapes of religious belief, yet still deeply committed to the essence of that belief, may be on the agenda of this century and the next as their most central concern. In a day when the real nature of science is perhaps more vulnerable to public misunderstanding than at any time within recent experience, it is worth pondering what resources directly pertinent to that problem can be provided from the experience and the example of the scientific way.

Perhaps there has never been a year when this aspect of the scientific enterprise has been more clearly exemplified; never a year when the challenges to new knowledge have been more compelling, or our mechanical inability to meet so many of them more frustrating.

In all the long history of man's scanning of the heavens, there has surely never been a time when the scope and the range of its mysteries have seemed greater than at this moment, nor the opportunities for new discovery richer or more

varied. The radio and infrared galaxies, sources of vast quantities of energy in ranges of the spectrum quite unexplored by astronomers even a decade ago, continue to challenge understanding. It is only a very few years since the first quasi-stellar sources were discovered. Yet now they are thought to number at least a hundred thousand over the whole sky. Typically they show redshifts in their spectra of an order wholly new in the experience of astronomy. So great are some of the redshifts that, if interpreted in conventional fashion, it must be concluded that these energy sources lie at distances so immense as to set, in effect, new boundaries to the observed universe, redshifts lying far beyond what astronomers could have imagined a mere ten years ago.

Yet the output of quasars can fluctuate greatly and this surely suggests that their volumes cannot be very large. How, then, can these bodies, lying at such vast distances in the heavens, emit sufficient quantities of light to be visible on earth even through the most powerful telescopes?

The severity of this paradox has led to suggestions that the usual interpretation of the relationship between the distance of an object in the universe and the redshift of its spectrum, based on the fundamental concept of an expanding universe advanced by Edwin Hubble at the Mount Wilson Observatory a quarter of a century ago and tested by Hubble and Humason over nearly twenty-five years, may not be valid in this cosmological environment and that other physical factors special to the situation of the quasi-stellar sources could invalidate the conclusion that they lie at such immense distances. In particular it has been suggested that the redshift may be caused, at least in part, by an actual lengthening of light waves due to the Einstein redshift of radiation in intense gravitational fields. But, as Greenstein and Schmidt showed some time ago, such an extreme gravitational field is incompatible with any tenable model of a quasar. In addition, recent studies of the distribution of quasi-stellar sources throughout the sky, taken together with the other considerations, strongly suggest at present that such alternative explanations are unlikely to be correct. So we are returned to the original interpretation of the spectral shift, and with it to the belief that the enormity of the distances of the quasars is indeed real. Yet it may still be possible that there are profound reasons for these great redshifts that are yet to be discovered. The grand mystery, and the grand paradox, in some sense remain.

It was a bare two years ago that Anthony Hewish and his colleagues at Cambridge University discovered an entirely new kind of object in the heavens—a source of radio energy whose emission came in sharply defined pulses of about 10 to 30 milliseconds at extraordinarily regular intervals. Since that time, more than 35 sources of this kind have been detected. The great majority emit their pulses at intervals of 0.5 to 1.5 seconds. So consistent are they that a single object has been found to hold its pulse intervals predictable to one part in 10^9 over periods of weeks, although a gradual slowing over longer times seems characteristic.

With a single exception, all pulsars have been found to emit energy only in the radio range, and consequently are quite invisible to optical telescopes. That exception, however, is peculiarly dramatic. The possibility that pulsars might be associated with the remains of ancient explosions of supernovae was considered shortly after their discovery. Speculation along these lines was heightened when a new pulsar, PSR-0833-45, was discovered in the southern hemisphere within an extensive, roughly circular zone of unusual radio intensity in the constellation Vela, a zone believed to mark the remnants of an ancient nova. An especially striking feature of this pulsar was the period of its pulses—at 89 milliseconds

the shortest then detected. In 1968 another "fast" radio pulsar, NP 0532, was more certainly detected in the vicinity of another supernova, this time the famous Crab nebula, the explosion of which is known from records in the annals of Chinese astronomy to have been observed in A.D. 1054. Interestingly, and in terms of the evolutionary history of pulsars perhaps significantly, this object was yet "faster" than that in Vela, with a period of only 33 milliseconds, and with two distinct pulses. Early in 1969 three astronomers of the Steward Observatory at the University of Arizona succeeded in demonstrating strong optical pulses from this object, with a period corresponding to that of its pulsations in the radio region, and with the corresponding two components. Astronomers at the Lick Observatory, and Kristian, Westphal, and Snellen of the Mount Wilson and Palomar Observatories, made detailed observations of the phenomenon. So the first—and thus far the only—optical pulsar had been identified and characterized. It is especially interesting that the star emitting these pulses is the very one that Walter Baade and Rudolf Minkowski, twenty-seven years before, had predicted would be found to constitute the remnant of the supernova itself. In May of this year (1969) X-ray pulses were detected in the region of the Crab nebula, pulsating with frequencies clearly matching those of light and radio energy, and almost certainly proceeding from the same source.

Early in the spring of this year, a startling new observation of pulsars was made that further complicates their interpretation. Between late February and early March 1969 the pulsar in the constellation Vela, PSR-0833-45, which, next to the pulsar in the Crab nebula, has the shortest period known, but which had shown a consistent gradual slowing of its pulse rate—as is characteristic of pulsars in general—suddenly speeded up. However, the burst was short-lived. By mid-March the rate was back to that of late February, before the aberration had occurred. What had happened to bring about this unexpected, dramatic, short-lived acceleration? Currently, the cause of the phenomenon remains uncertain.

What, in fact, are pulsars? Unlike quasars, which appear to occupy regions of the universe so vastly remote from us, pulsars seem comparatively near neighbors. Recent distance measurements reported for pulsar CP 0328 suggest that it may lie less than 3000 light-years away, and the distance of the Crab nebula itself is reckoned at some 5500 light-years. If these distances are at all typical of the class, it is conceivable that vast numbers of pulsars may exist within the confines of our own galaxy. But the question of their basic nature is still open. Opinion of astrophysicists and cosmologists has increasingly converged to the view that they may be rotating, oscillating, highly magnetic neutron stars. Yet the surprising "hiccup" in the pulse rate of pulsar PSR-0833-45 is not easily explained in the framework of that model, at least in its original version. As with quasars, the frontier of our understanding of the nature of pulsars stands open, presenting us with one of the greatest mysteries in our cosmos, and one of great challenge to future investigation.

When, in 1943, Edwin Hubble and Milton Humason presented their completed velocity-distance curves, based on the period-luminosity law for distance of extragalactic nebulae and upon the redshifts, as shown by photographs for the velocities of recession, a new landmark of cosmology had been set. For the implication that they carried—that of an ever-expanding universe in which all the galaxies were moving steadily away from one another—represented a radical change in man's notions of his environment. Sir Arthur Eddington remarked

that it was "so preposterous that I feel almost an indignation that anyone should believe in it except myself." It posed an alternative, and a sharp challenge, to the "static" models of the universe that had been current since long before its day. Even now, a generation later, static theories still have some able proponents. Yet many telling arguments can be, and have increasingly been, advanced in favor of the "big-bang" model of the evolution of our universe, as Hubble's theory has currently come to be called. The sum total of work on counts of radio sources and of quasars in the heavens offers strong evidence for it.

Yet difficulties remain. Essential to this concept is the "Hubble constant"—the factor connecting the distance of a galaxy and the redshift in its spectrum. And problems in determining the distances of galaxies in space persist—problems connected with those guideposts of the heavens, the cepheid variables, which in the northern hemisphere provided the essential yardsticks for Hubble's work. Indeed, galactic distances today are generally estimated at some ten times the original figures proposed by Hubble. It has even been suggested that the value of the constant itself may change with cosmic circumstances. It is upon the concept of the Hubble constant, of course, that estimates of the enormous distances of the quasars are based today. And fundamentally, it is upon the accepted value of the constant that estimates of the elapsed time since the "big-bang" may have occurred must rest. Clearly few things can be more central to cosmology than an accurate determination of its value.

That determination, however, faces great experimental difficulties so long as observations are confined to the skies of the northern hemisphere. The local anisotropy of the Hubble kinematic field must be mapped for the nearby galaxies before the Hubble expansion rate, with its associated time scale, can be accurately determined. This can be done only by combining data from both the northern and southern hemispheres. It is necessary to establish distances for southern groups of galaxies by studying their stellar content, using photoelectric and photographic photometry. A large amount of data must be collected. And in the heavens of the southern hemisphere lie the Magellanic Clouds, as well as a series of more distant galaxies, which can provide observational "yardsticks" for a redetermination of the Hubble constant: a redetermination which could be of the highest significance to all our concepts of the universe. For such reasons, and for others only less obviously compelling, the southern hemisphere offers immense opportunities for astronomy in the future. But even the physical facilities for exploring them on a truly adequate scale are yet meager. There is surely no greater need in optical astronomy today than that of a really powerful telescope in the southern hemisphere.

It is not only in the realms of quasars and pulsars, or of galaxian astronomy—critical to questions of cosmology—that the great frontiers of astronomy are expanding in our day. That fact was brought vividly home during the year just past in the startling detection by Charles H. Townes and his colleagues at the University of California of the signature of ammonia in the radio spectrum of a small but dense cloud lying in the direction of Sagittarius, near the center of the Milky Way and perhaps 30,000 light-years from earth. It was the first time that a molecule of this order of complexity had been identified in space, and analysis of its microwave radio spectral lines suggested that it may have been present in

a density of the order of one molecule per liter. Against this discovery, it is difficult to remember that only forty years ago, or even less, the space between the stars in our galaxy was thought to be a complete vacuum.

Astronomy is not the only field of research where exciting vistas of new knowledge and understanding have opened during the year just past. Indeed, a convincing case can be made that challenges to our vision as fundamental and moving, and lying much closer to our own immediate concerns, have been posed over the past few months by the life sciences.

Some time ago the British biologist N. W. Pirie, discussing the chemical constitution of viruses, remarked: "Twenty years ago it was prudent to stress, in articles or reviews dealing with the properties of viruses and the processes of virus infection, that the viruses about which we had any significant amount of information were not necessarily representative of the group as a whole. Chemical criteria controlled the selection of viruses for study; chemical uniformity among them was therefore not surprising. However, so many viruses have now been purified and investigated that there will be justifiable amazement should one turn up that does not contain nucleoprotein." That statement may still be correct. But in the last several years it has received one extraordinary challenge for which there is, as yet, no satisfactory answer.

For at least two centuries shepherds in several countries have stood in dread of a mysterious disease. It struck their flocks unexpectedly, and once established was likely to proceed slowly but inexorably through the whole population, killing sheep after sheep in a characteristic and curious way. In France, the disease was given the name *la tremblante,* reflecting the shivering, the progressive loss of muscular power and coordination, and the hypersensitivity that were typical of the disease, and suggesting a primary involvement of the nervous system. In England it came to be called *scrapie* from another behavioral peculiarity that characteristically accompanied the early stages of the disease: the compulsive rubbing of the afflicted sheep against trees or fence posts, until whole patches of the body were bared of wool.

Fifty years of research were of no avail in solving the riddle of the nature of the disease or of its causative agent. Not until 1938 were two investigators, J. Cuillé and P. Chelle, able to produce the disease at will in experimental animals, particularly goats, using tissues taken from infected sheep. It was even longer before the infection of small laboratory animals was achieved. A decade of study of the tissues of infected animals failed to demonstrate the existence of any viral agent. Electron microscope photographs were negative. Serological studies failed to detect the production of antibodies in animals with the disease, or to detect a scrapie antigen. And, whatever the agent might be, it proved astonishingly resistant to treatments that would be expected to destroy nucleic acids in short order. Brain tissues from an infected animal, preserved in 10 percent formalin for from 6 to 28 months, proved capable of transmitting the disease. Heating to 100°C for half an hour did not destroy the agent or the infectiveness of material so treated. Exposure to chloroform or phenol did not inactivate it. And very recently it has been shown that the agent, whatever it may be, is unaffected by

doses of ionizing radiation that will virtually destroy a "standard" virus by wholesale inactivation of its nucleic acid.

Could it be that the agent of scrapie does represent an exception to Pirie's comment—a first exception to that crucial assumption of virology? Is it possible that an agent can exist, so minute as to escape the electron microscope, "living" in the sense that the numbers of its particles can increase within its host, infect new hosts and yet not contain a core of DNA or RNA?

That would indeed be an extraordinary exception to all that we know of earthly life at every level, and one that could be accepted only after exhaustive proof. Yet the extraordinary properties of this infective particle, if such it is, for some years encouraged such speculation in more than one quarter, and the possibility still remains. But some evidence obtained in the last two or three years may weigh against so radical a conclusion. It has recently been demonstrated that when homogenates of scrapie-infected tissues are passed through viral filters with a pore diameter in the range of 20 to 40 millimicrons their infectivity is indeed suppressed. If this in fact represents a truly limiting pore dimension, it suggests a molecular weight for the particle of about 50 million—comparable to that of some known viruses.

Other recent experiments have demonstrated that, though the agent is indeed astonishingly resistant to irradiation with ultraviolet, it is not completely immune. So it has been possible to construct a curve relating extent of inactivation to radiation dose. The portion of the "particle" vulnerable to the radiation can then be determined by the statistical "target" methods first developed in the laboratory of Mme. Curie. When this was done, yet another anomaly appeared. For this target diameter did not turn out to be the 20 to 40 millimicrons indicated by the filter experiments, but rather proved to be of the order of 7 millimicrons. A possible interpretation of this discrepancy, retaining the assumption that RNA or DNA is involved, might be that a small strand of naked nucleic acid, susceptible to ultraviolet, may bind to the membrane of the infected cell, forming a larger aggregate which then is somewhat more resistant to the radiation. But a strand of nucleic acid of these dimensions would hardly seem able to accommodate base-pairs sufficient to code for a single determinant of structure! The enigma of scrapie still stands as a highly challenging puzzle at the very frontier of life.

And the challenge, fascinating and fundamental at the theoretical level, goes further. For scrapie is in some ways remarkably reminiscent of other dread diseases of the nervous system, such as encephalomyelitis and disseminated sclerosis. And in many ways it is suggestive of *kuru*. This strange human nervous disease, discovered early in the 1950's, is wholly confined to the single, minute Foré tribe of the eastern New Guinea highlands and to persons who have intermarried with them. Like scrapie, the disease typically traces a deliberate but inexorable course to death. The brains of its victims show remarkable etiological similarities to scrapie-infected neural tissues. Moreover these pathological changes may simulate to a remarkable degree brain changes sometimes accompanying extreme normal senility, as though kuru might precociously model such normal changes.

Is kuru related to scrapie? Is it infective? If so, how does it infect? D. Carlton Gadjusek and his colleagues, who have supplied much of our information about kuru, have succeeded in infecting the chimpanzee with the disease and, very recently, have infected a species of New World spider monkey. Serial transmission has been achieved with the chimpanzee. But the nature and the size of the

transmitting agent, and its relationship to the agent of scrapie—or to those of such superficially similar nervous diseases as the recently prominent encephalopathy of mink—remain unknown. Ahead lie opportunities for discovery of far-reaching significance in both biological theory and medical practice.

Exciting and important as these particular frontiers of biology are, they represent only particular facets of the wide range of challenges that the life sciences pose today, but one restricted group among hundreds of equally luminous fascination. If problems involving the structure and functioning of DNA occupied the center of the stage during the decade that is closing, it is easy to see that during the next that place will be preempted by far more diverse questions of structure and function involving the various species of RNA through the action of which the coded genetic message is brought to reality. Surely the manifold problems of cell growth, differentiation, and organization; of the maintenance of continuity and stability in the living organism; of the miracles of embryology and birth and senescence, will over the coming years provide as stimulating and important challenges, as multifarious and extensive frontiers, as have ever engaged the mind of man.

In fact, it is inaccurate to cast such challenges as a part of the future, for already they are very much a part of the present. Clearly emphasis will shift more and more in the future to the question of *reaction systems* in biological research. There will be issues of the utmost difficulty here—especially since the scientific method is still ill equipped to formulate them in terms susceptible to experimental test. Yet the significance of even slight alterations of a few components in biological systems can be profound, and can affect all their evolution. One recalls, for example, the virtual identity of the amino acid sequences in the alpha chain of hemoglobin in man and the great apes. Man and the gorilla, for example, appear to differ in only one out of more than one hundred and forty such amino acids, and in the chimpanzee the sequences seem to be identical. There has been little evolutionary divergence here. Yet think what the simple evolution of vocal cavities in man, and of the ability to use them, has meant for his divergence in evolution from the great apes!

Indeed, no questions can be more challenging than those involving the mechanisms by which the panoply of cell differentiation and specialization—so characteristic of higher animals is brought about during growth, and how such specializations are then maintained. Thanks in good part to the powerful and versatile laboratory techniques for the hybridization—the base-pair matching—of DNA and RNA developed in recent years and now employed in a wide variety of investigations, it has become amply clear that in most multicellular organisms every cell of the body, however specialized its structure and however narrowly circumscribed its normal functions, carries the full complement of genetic information inherited from its parental egg cell, specifying in its own chromosomes every trait of body and nervous system of the complete organism.

It has been recognized for a long time that mechanisms of the utmost delicacy and precision must exist to "mask" the great bulk of that potential information store, permitting translation and expression of only that critical fraction required in the growth and function of a particular cell of hair or bone, of skin

or brain. But the elucidation of the precise means by which this delicate discrimination of information is brought about will surely continue to be an absorbing task through the coming decade.

It is clear, for instance, that selective "masking" of information can be imposed at different levels in the translation and transcription of the genetic code. The determination of the significant stage or stages in any particular situation alone offers a formidable challenge. For various reasons, however, the step involving selective decoding of the DNA itself has received particular attention. At one time it was speculated that certain histones, a class of proteins containing large amounts of arginine and lysine and complexing readily with DNA, might act as gene regulators. The difficulty with such a concept, however, is that a vast library of distinct and specific histones would surely be required to selectively inhibit the wealth of gene-sites on the cell chromosomes. Actually, only about five types of appropriate histones are known, and they occur in widely varying amounts in different plants and animals. Their structural range is clearly insufficient for so delicate and versatile a function.

As is often the case with major conceptual advances, a fertile approach to this puzzle has been generated from a reversal of viewpoint. It is possible that histones do indeed "mask" gene action, but in a general and nonselective kind of way. The essential process of selecting a particular portion of the total store of genetic information may not be the *masking of the unwanted* but rather the *unmasking of the wanted,* the removal of the "covering" at correct sites in the DNA at crucial times in the development of the cell and of the organism containing it. So the critical questions become: What is the nature of the unmasking agent? And how does such an agent achieve its extraordinary specificity? Probably many answers will ultimately be revealed. Recently, for example, it has been proposed that glucagon, a pancreatic hormone inducing the synthesis of enzymes in liver cells, causes a large increase in the phosphorylation of a particular fraction of liver histone, and that changes produced by this phosphorylation could inactivate the repressive effect normal to a histone, thus "uncovering" some DNA sites in the liver cell.

It is interesting to examine some of these specific questions with reference to the wider panorama of the general principles around which living things in general are organized and through which they operate. For the principle of selectively de-repressing elements normally held in bondage is indeed, as we are now discovering, a widespread and fundamental element of biological organization at many levels. It clearly lies at the base of the dramatic reorganization of tissues that transforms the caterpillar into the butterfly. It is clearly responsible for the development and the remarkable maintenance of organization in colonies of the social insects at levels of both structure and behavior. It is emphasized in the recent proposal to designate a functionally new class of biological substances as chalones: substances which, alone or in combination with other body products such as hormones, can exert a continuing suppressive action on the normal growth potentials of cells. Such suppression may be released, with overall adaptive consequences, when the concentration of the inhibitor is lowered. The effect is well illustrated, for instance, in the accelerated proliferation of tissues after wounds that reduce the normal concentration of their chalones.

All these observations, of course, address but the tips of the iceberg, as it were, in the grand panoply of biological organization at the level of molecules and genes. A theoretical approach to this whole question was made this year by Roy J.

Britten of the Carnegie Institution of Washington and Eric H. Davidson of the Rockefeller University. It proposes that regulations of this sort could be the province of special genes which may be present in thousands or even millions of replicates or near-replicates in the nuclei of the cells of higher organisms. This concept, which may well prove a "takeoff" point for the achievement of new levels of understanding of biological systems—and of evolution itself—is described elsewhere in this Report.

The whole field of the mechanisms of operation of living systems, for which quantitative studies of the interaction of cell systems at the biochemical level form such vivid paradigms, constitutes one of the major biological research frontiers of our time. The vast and informationally rich situations that include not only the interactions of cells and the viruses that inhabit them but also those among the organelles of single cells—spherosomes, lysosomes, provacuoles, tenoplasts, and the rest—involve analogous dynamic systems. And at the other end of the spectrum of size and kind, similar principles of biological organization almost certainly operate in those associations of organisms independently derived in development which are nonetheless closely associated, physically and functionally. Such associations, of course, may range from the specialized, fused "individuals" that make up the constitution of that great "jellyfish," the Portuguese man-of-war, through the colonies of the social insects that have for so long captured the human imagination, on to the infinitely complex and contemporary and urgent problems of human societies. Internal structuring of feedbacks, especially of a negative sort, or the formation of functional hierarchies in biological organizations—nowhere more dramatically suggested than in the fragmentary evidence that we have of the mode of functioning of the human brain in its vast and infinitely delicately operating organization of 10^9 cells or more—a congeries vastly greater and far more highly evolved in its organization than the greatest conurbations that the human race has ever known—takes on special interest in this context. In this context, too, one recalls the contrasting metamorphoses of the migratory locusts that form the great swarms which long before Biblical times must have posed a legendary menace to man and continue to do so today. If such locusts have matured in populations of low density, they are likely to be solitary, sedentary green insects which may eke out their lives almost unnoticed. If, on the other hand, they have attained adulthood in massed crowds, they become restless, long-winged, black-and-yellow creatures which gather into those immense, ravenous, tireless armies that since the dawn of argiculture have been the scourge of man. One recalls in this context, too, the effects of unaccustomed experimental crowding upon mammals ranging from rats and nutrias to cats and baboons. The onset of organic diseases of unprecedented severity and with unprecedented frequency, the hypertrophied adrenal glands, the widespread antisocial behavior, the steady deterioration of the ordered social structures which mark these experimental populations lead the observer to wonder about the human condition.

Alfred North Whitehead once remarked that science as we know it could have arisen only in the matrix of centuries of Christian civilization, since only a profound faith in the values of the natural order could have provided the initial impetus for its dedicated and total commitment to the elucidation of that order. It is indeed in this aspect of science, so vividly memorialized in those multifarious

conquests of understanding—in those bursts of vision that over and over have brought home anew the beauty and intricacy and sometimes the might of our universe; in those bursts of vision that often enough have seemed at first to diminish our own stature in the universe, and so on occasion have been greeted with a popular resentment ultimately converted to a fresh humility—that some of the finest epics of the human spirit have been written. Clearly, this face of science provides a resource for the spirit that is enormously significant in our troubled day, and must remain so for all the future.

A complementary aspect of science, and one of major human significance, has been conspicuous ever since the days of Francis Bacon. In our workaday world, indeed, it sometimes preempts attention so effectively as to be regarded as the essential characteristic of the scientific way. It is "scientific-research-with-a-goal." The goal is the important one of bettering man's condition through the *control* of nature. That control and that betterment, as three centuries of experience have deeply impressed upon us, are best achieved, in the first instance, through a better understanding of nature. A predominant part of our material civilization, of our comfort and affluence, of our physical health, as we are acutely aware, is the cumulative consequence of investigative work directed to those ends over a span of at least two hundred years. In our day we should not need to be reminded—although there is now real and growing evidence that we do need to be reminded—that, materially as well as spiritually, scientific research is one of the most significant of all our activities.

At their proximate margins, there is little visible difference between scientific investigation undertaken with the primary object of understanding nature and that initiated with the primary object of controlling nature. Indeed, the two motivations may be inextricably entwined within a common program, as they so often are, for example, in medical research. Understanding and power can indeed proceed together.

But despite the fact that both motivations are extremely important to the progress of science; despite the fact that they are highly complementary and that, often enough, the kinds of scientific investigation that they inspire may be quite indistinguishable, it is undeniable that the motivations themselves do differ in important ways, and in certain circumstances it is important to distinguish them.

Two reasons for this are worth emphasis. First, the second orientation is basically derivative, and in that sense is inherently dependent on the first. Typically, research with predominantly practical motivation extends frontiers of knowledge already touched by investigations of the first kind, often expanding and refining them with discrimination and power. But less frequently does it open wholly novel salients, and rather rarely is it prosecuted consistently in an area where tangible benefits do not appear within a reasonable length of time. This, of course, is as it should be. But it also means that if the second motive were ever to *replace* the first on a general scale we would be in great difficulty, for a good share of our initial impetus would necessarily be lost. There is an ever-present risk here, which, if remote, is also dangerously real. The nature of the practical world is clearly such that, unless both the distinction between the two motivations, and their complementarity, are borne constantly in mind, the second view, instead of interweaving with the first, might indeed come to supplant it. That would be catastrophic indeed.

The second danger inherent in the failure to make this distinction is more subtle, and surely even more important. For just as the first motivation of the scientific way can provide a constantly renewing source spring for the human spirit, the second, if fully dominant, could, on occasion, stanch the flow of those springs, thus actually increasing the weight of so many other dangerous forces of our time. For it is a curious but unmistakable circumstance that the most striking successes in controlling the natural world, in contrast to the greatest advances in understanding it, have on the whole tended in the short run to *enhance* man's vision of his stature in the universe. We have been exposed to the heady euphoria of that experience so often, and with such ever-increasing intensity, over the past half century, that it is worth reflecting most soberly upon some of the effects that can follow. Just as the painful experience of a diminution of man's view of his place and stature that has so often accompanied the great discoveries has typically been succeeded by a tautening of inner fiber, by a refreshing of inner wellsprings, by a sense of oneness with a universe enhanced in his respect; so the euphoric experience of success in control of the natural environment can have —and often enough is having—precisely the reverse impact. It can lead to manipulation of the natural world unguided by reverence or comprehension, to the philosophy of "it works, therefore it is right." Unless we are both wise and vigilant, such experiences, accumulating through almost every day of our lives, can ultimately reinforce those spiritual scourges of our time: insecurity; alienation; total identification of nature with the man-made environments, and as a corollary to this view, a crushing sense of individual and personal responsibility for all that takes place—and particularly for all that goes wrong—in that world. Finally, and most seriously, there can be a contrary reaction: the total personal frustration inherent in the view that the human world is already so completely molded and fashioned that the only way the individual can make a significant impact upon that world is by destroying it. These are the dangers that we face: dangers that are to be mitigated only by a steadfast and widespread cultivation of a deep and sensitive understanding of the very nature of the scientific way.

As the year 1969 marks the hundredth anniversary of the discovery of DNA by Friedrich Miescher, it also marks the one hundred and forty-first of another major scientific accomplishment of a somewhat different kind. In 1828 the German chemist Friedrich Wöhler, student and friend of Gmelin and Berzelius and collaborator of Liebig, succeeded in producing the compound urea by heating an aqueous solution of ammonium cyanate, formed in turn from a mixture of potassium cyanate and ammonium sulfate. In the light of modern chemistry this was a simple and straightforward reaction, and no one today would pay particular attention to its first accomplishment. Yet it represented a historic watershed in man's conquest of nature. For in that day no chemical compound elaborated by a living organism had been synthesized in the laboratory. Urea was universally conceived as the product of life—almost as a part of life. The chemist had taken a step so radical as to seem well-nigh incredible to some.

One speculates what Wöhler, the pioneer of that frontier, would have thought of some of the analogous syntheses of life-materials achieved today—syntheses so extraordinary that they could only have filled him with wonder, yet which we, as contemporary and sometimes oversophisticated observers, are all too prone to

take for granted. What, for example, would Wöhler, were he living at this hour, have to say about the total laboratory synthesis of the enzyme ribonuclease achieved for the first time this year independently by two teams, one at the Rockefeller University and the other at the Merck Sharp and Dohm Laboratories of Merck & Company? The approaches of the two teams were wholly different; yet in each case the final product showed the same biological activity as the natural one, splitting ribonucleic acid but having no measurable effect on DNA. If one enzyme which takes so central a part in the direction of life processes can thus be synthesized in the laboratory, others, equally vital, can and will. Their potentialities in the combating of disease and in achieving further levels of understanding of life processes need no emphasis.

One wonders, too, what Wöhler would have thought of the artificial synthesis of polypeptide compounds with properties very similar to those of natural collagen, completed at the Weizmann Institute during the year just past. Or again, what would he have thought of the first crystallization of a multienzyme complex, the fatty acid synthetase, at the Max Planck Institute for Cell Chemistry in Munich; or of the transfer-RNA used by the colon bacterium in adapting formyl methionine to recognize starting points of the messages in messenger RNA, through which the initiation of protein synthesis is effected, at the Laboratory of Molecular Biology of the British Medical Research Council at Cambridge? This remarkable accomplishment may well open the door to the use of X-ray crystallography to determine the tertiary structures of the specific kinds of RNA molecules involved in translation of the genetic code.

These and similar investigations during recent years have dramatically illustrated the rate and scope of growth in our power to create in the laboratory many of the most central components of life itself, and through that power to manipulate life processes with new sophistication and effectiveness. It is a power with immense and still only dimly understood implications for man's health and welfare and even his physical destiny.

There are many other approaches to this power. One need only cite such recently developed techniques as the artificial hybridization of cells from tissues of animals as different as a man and a mouse. With suitable techniques, hybrid somatic cells can be produced that include chromosomes of both the contributing partners within their single nuclei. Such cells can be made to grow and propagate. Over successive cell divisions, however, excess chromosomes in the composite nucleus are gradually lost. The way they disappear, and the kinds of changes the cells undergo as they are eliminated, is providing extraordinarily interesting evidence for the study of chromosome dysfunction. Furthermore this evidence may permit the mapping of human chromosomes with an order of precision and comprehensiveness never before approached. For example, this method has made it possible to accurately locate in human somatic chromosomes certain genes involving deficiency diseases of metabolism. It has been possible to demonstrate X-linkage for the determinant, or determinants, of 8-azaguanine resistance in man. Perhaps most exciting, cancerous mouse cells have recently been fused with noncancerous mouse fibroblasts by Professor Henry Harris and Dr. O. J. Miller at Oxford and by Dr. G. Klein, Dr. P. Worst, and Dr. T. Tachibana of the Karolinska Institutet at Stockholm. Similar experiments have been attempted before, in the hope of exploring a means to suppress cancer, but the results were discouraging since the hybrid cells turned out to be cancerous. In this instance, however, malignancy was initially suppressed. But as the descend-

ants of the polyploid hybrids shed chromosomes in the course of further divisions, the daughter cells reverted to malignancy. Thus it seems clear that the non-malignant partner contained some chromosome-linked determinant capable of suppressing malignancy. It may now be possible, through long and patient cytological work, to "map" the hybrid cell genome for this factor, precisely as with some human metabolic deficiencies. Extensive work obviously lies ahead, and certainly no "cancer cure" is even remotely in the offing. Yet even the tentative location of a cancer-inhibiting genetic locus would be highly significant.

Perhaps even more theoretically important, evidence seems to have been obtained that histocompatibility antigens can be suppressed under certain conditions. This finding may have even greater significance for the future, particularly in view of the growing suspicion that a whole range of "autoimmune" reactions suggesting the attack of certain body cells upon other cells in the same body—"target" cells perhaps rendered unrecognizable to the attackers by some means—may be responsible for some of the most intractable of the long-range degenerative diseases of the general character of kuru and scrapie, and, as such disorders could be hinting, might possibly be relevant to the very process of aging.

Again, the feat of growing complete organisms from single cells of the body offers spectacular practical corroboration of the fact, already so well demonstrated in experiments in DNA hybridization, that the complete range of genetic information contained in the developing egg of an organism is typically preserved in every somatic cell of the mature body. This impressive achievement is not, to be sure, particularly new in principle, for entire plants were developed in cultures derived from single somatic cells some years ago. But the accomplishment has recently been extended by J. B. Gurdon and his colleagues at Oxford University to technically far more difficult animal material. Gurdon and his associates succeeded in removing the nucleus from a body cell of the primitive clawed frog, *Xenopus laevis,* and implanting it in an unfertilized egg cell, the original nucleus of which had been inactivated by radiation. A complete individual developed from this egg, recalling the results of earlier experiments of Briggs and King made with the more advanced frog *Rana.* This achievement is of course technically far more difficult than the corresponding one with plants. But its striking and vivid character has caught the imagination of those who would extrapolate our biological future to embrace a capacity of this kind in human terms.

The remarkable technical feat of growing and fertilizing mammalian egg cells outside the body, accomplished in hamsters some four years ago, has been extended to human ova by three investigators from Cambridge University and the Oldham General Hospital in England. This surely represents a new dimension in the manipulation of life, and may open the way to a detailed future understanding of the metabolism of human oocytes. In turn, it suggests new means for interfering with the processes of maturation in human ova—knowledge that might become of real significance in the general field of birth control.

In yet another arena, techniques developed in recent years to permit the physical examination of the chromosomes in cells from many tissues of the human body have enormously extended our powers of diagnosis. These powers have also increased our awareness of some of the effects that gross chromosome abnormalities may have on the lives and the happiness of the unfortunate individuals that bear them. For instance, it has been recognized for a number of years that the inclusion of an extra chromosome 21 in the human genome is commonly

accompanied by characteristic physical and mental abnormalities. But recently it has become feasible to detect such gross chromosome aberrations in the affected infant before birth. The sinister effects of LSD and other drugs in inducing abnormalities of the somatic chromosomes have only recently been fully recognized, thanks largely to techniques of this kind. And such techniques are currently permitting much more comprehensive research on the still-moot question of whether the possession of an extra sex chromosome—an X or a Y in the human male, the XXY and XYY syndromes—is accompanied by a statistically greater tendency to criminality or violence.

Last but by no means least in this array of latter-day medical conquests come the remarkable surgical achievements of recent years in the transplantation of organs—achievements which, although they must be judged differently in different circumstances, are in any case highly noteworthy. But, like so many other accomplishments in the realms of biomedicine, they too are vulnerable to being popularly cast in a dangerously spectacular role.

Given all these advances in our power over biological nature, reaching so far beyond what was imaginable only a few years ago, it is little wonder that our dreams for the future can on occasion run wild—sometimes cruelly, and even dangerously, wild. It is here, perhaps, that public consequences of the euphoria that so typically accompanies great strides in the control of nature are to be viewed with the greatest reserve, and circumscribed with the greatest vigilance. Uninterrupted progression to the reliable control of cancer, to reliable genetic engineering eliminating inborn and metabolic diseases on a grand scale, to the production of identical copies of notable men and women by the methods of cell cloning that have succeeded in rare and special instances with carrots and with frogs, to the artificial fertilization and transplantation of human ova as a standard procedure, to the transplantation of human organs on a wholesale scale with the establishment of widespread and numerous storage banks for them, all too often seem to the uninitiated simply further and more imaginative conceptual extensions of the present.

As a result of the confluence of several conceptual streams, we stand today at a curious crossroad in this aspect of the public concept of science, and particularly of science in medicine. We live in the grand tradition exemplified by the work of Wöhler and epitomized even more vividly in our day by that epoch-making paper of 1927, wherein Hermann Muller demonstrated for the first time that X rays, generated in a wholly man-engineered device, could bring about considerable genetic mutations, modifying the very materials of Darwinian evolution hitherto thought invulnerable to any outer influence. That is the tradition of our still-growing power to modify life processes in ways and on a scale inconceivable before our time. Simultaneously we are working in another tradition which a century of brilliant successes has made so much a part of us that we rarely question it—the tradition symbolized by the life and work of Louis Pasteur, the tradition of the germ theory of disease. But as Dr. Philip Burch has presciently commented, the discovery of the role of bacteria in disease, that brilliant jewel in the medical and biological crown of another century, and the contemporary spectacularly successful applications of the vision, have indeed resulted in the virtual eradication of what in Pasteur's world were among the most severe of human scourges. But they may also have bequeathed to us a legacy of custom and orientation that in future could be less helpful. That is the doctrine, understandably entrenched in most public health programs, of "cause-then-cure"—the

doctrine that every disease must be identified with some external causal agent. The conquest of such diseases, then, is a matter first of identifying the agents with the conditions which they bring about, and then by suitable large-scale attacks wiping them out, as we have wiped out typhus and yellow fever in many areas. But conditions like the genetically mediated metabolic deficiencies, or the countless subnormal syndromes in which genetic constitution and some outside agent seem to cooperate, may be trying to tell us something else. They may be suggesting that the conquests of disease and the challenges of public health in the last century, magnificent as they were, lay only at the easier peripheries. Increasingly in our day, and surely in the next century, medicine will be preoccupied with chronic illnesses—with cardiovascular and malignant disorders, with arthritis and diabetes, with psychoses and multiple sclerosis. We will surely become more generally familiar with Sir Macfarlane Burnet's brilliant "forbidden-clone" theory of autoimmunity: with the idea that single mutant cells in an individual may, in the course of that individual's life, generate clones of somatic descendants which, either directly or through their products, can then attack cells of neighboring tissues. As the massiveness and severity of that attack exceed some limit of tolerance, symptoms of long-term degenerative conditions may appear. When we have truly comprehended possibilities of this sort and accorded them equal emphasis with the more conventional philosophy that ascribes diseases wholly to agents entering from outside the body, we may come to regard certain medical projections that seem particularly apposite and dramatic in our day in a somewhat different light.

At present, for example, we are greatly—and properly—concerned with the development of antilymphocyte sera, and we are preoccupied with their use in suppressing the tendency of the human body to reject the graft of a foreign organ, such as a heart. At least one hundred and forty-two heart transplants have been made since the first operation was performed on Louis Washansky on December 3, 1967. Of these, some thirty-seven patients now survive. At least two survived for more than a year, and this has been considered a triumph in the control of rejection reactions. But it is certainly worth consideration that if selective suppression of host elements that are incompatible with a foreign graft can thus be achieved, then surely it should also be possible to develop sera to suppress the cells within the patient that destroyed the organ in the first place. The development of fully successful means to ensure the acceptance of the foreign grafts might thus significantly contribute to by-passing the whole transplantation process itself. Perhaps we shall look on this as a primary objective of future research on sera. There may be a moral here applying equally to other of the more immediate and extravagant projections of current laboratory developments in biological manipulation and control to fields of medicine and sociology that are so often heard. Surely it is upon further growth in the processes of *understanding* that the main thrusts of biology and medicine should be concentrated over the next decades.

But there is of course a broader and yet more serious aspect to the tendency of our day to overweigh the image of science in the direction of practical—indeed sometimes of wildly practical—application and control. A century ago the great French physiologist Claude Bernard remarked to his colleagues, "True science teaches us to doubt, and in ignorance to refrain," or, in Lord Ritchie Calder's

contemporary expression: "Science feels its way, with a mine detector, from one safe foothold to another." This is deeply true. And yet it is a truth often difficult to keep in mind in an age when the marvels of biological vision surpass all earlier imagining, when the spread and dominance of computers bid fair to change not only the styles of our thought but major substantive aspects of our thinking too, and when the topographies and climates of planets have become of immediate and practical concern.

Indeed, it is often difficult to keep in mind in this day what science *is*. Sir Herbert Dingle has recently pointed out an important and threatening aspect of this confusion. The circumstance that the final arbiter in science is the crucial experiment, as it has always been, provides critical assurance of the ultimate verity of the scientific way. But there is an obverse to this picture which becomes particularly important in times of fantastically rapid scientific change like the present. Since this awareness that the ultimate safeguard of confirmation by experiment is always present lies just below public consciousness, and since, moreover, controlled speculation indeed forms the essence of the scientific way, it is but a short step to the popular conclusion that speculation in itself spells reality—and to the accompanying judgment that, since the court of ultimate experiment is ever present to exclude the groundless and untenable, unless current scientific advances are extrapolated as boldly as they can possibly be, speculation about them is timid and dull, and has somehow not fulfilled its proper function.

Several things of practical importance, of course, are neglected in such judgments. One is that, whatever the intent of a public speculation or the frame in which it is made, it is likely to be widely regarded as, in some measure, a prediction, and following experiments may be looked to not primarily as tests but rather as confirmations. Again, in a world heavily populated with such predictions the competition for the dollars, the time, and above all for the talent that indiscriminate experimental testing might require could stretch our limited resources in all these fields far beyond the breaking point. So we would often be forced to make the dangerous choice of abandoning either the experiment or the speculation. Further, as Dingle points out, given the very magnitude of the scientific concerns of our time, even individual validating experimental programs are unlikely ever again to be transient or minor undertakings. A high proportion become major enterprises, expensive and not infrequently damaging.

Among those who often are asked to take speculation at its face value are laymen with the most important public responsibilities for ordering the magnitude, the shape, and the character of science in the nation. Such, notably, are the members of the Congress. What are they to do in an atmosphere where uncritical extrapolation, all too often representing merely the large-scale projection of but one among many possible sets of ideas, has never been so prevalent or so tempting? There have been many suggestions of means to provide appropriate and needed aid. Among them is a recent one that there be set up within the Congress something like a Joint Committee on Science and Technology with functions similar to that of the Joint Committee on the Economic Report—to educate, to investigate, to recommend.

In this connection, J. G. Crowther has recently made an interesting proposal for Britain. He suggests the formation of an Institute for the Strategy of Science, analogous, as he points out, to the British Institute for Strategic Studies. The task of such an Institute would be to supply information of the broadest scientific

nature, including engineering science as well, and embracing relevant aspects of many other areas—economic, administrative, commercial, historical, political, and sociological, to name a few. In Crowther's view it is extremely important that this extensive spectrum of disciplines, centered about science, should be housed in the same organization, and that every possible provision should be made to ensure constant and fruitful communication across it. The Institute should be located within government, to secure maximum accessibility to the wide range of institutions concerned with problems of science and to provide maximum coherence and relevance in the information and analyses generated. The very proposal of this major and difficult idea emphasizes the widespread and growing recognition that there has never been a time when a public understanding of the real nature of the scientific way has been more urgently demanded, in terms not only of our cultural and spiritual welfare, but of our material future too.

Thoughtful students of scientific progress have commented again and again that the central step in the achievement of any new order of scientific understanding is basically nonlogical: truly a step of imagination. As T. S. Kuhn has cogently observed, in each age all the workers in the mainstream of any branch of science have typically accepted without serious question a given frame of reference of work and thought inherited from the founders of the discipline. The very structure of science, the maintenance of its quantitative excellence, the assurance of its genuine progress within an arena determined to be sound, demand such a framework. But the converse is that the adoption of a truly new viewpoint typically demands a radical fracturing of that structure. Such qualitative change is not to be achieved through work of ever-greater intensity along the old lines, nor through the accumulation of more data or the improvement of old, nor by further refinement in the tools of analysis, nor, above all, by simplistic but grandiose speculation that merely extends old modes of thinking to more arresting planes. The process by which major new scientific ideas are generated is, as Bronowski long ago emphasized, closely akin to the great insights of philosophy or literature or painting. The notions of Copernicus and of Darwin were clearly of this kind. Numbers of analogous modern examples come to mind: the theory of an expanding universe, for example, or of continental drift, or of the ultimate structure of DNA and the mode of its action. In this, its central process, science is clearly at one with the central processes of literature and art—belying the old assertions of their separateness. In the genesis of their great ideas scientists, artists, and writers alike must deal essentially with resemblances, with analogies, and often enough with ambiguities unresolved. It is only in dealing with those ambiguities that the single significant distinction, that of the role of experiment, appears. For in literature and in art the ambiguity remains and must be resolved, if at all, by the receiver of the message. In science, neither the author of the ambiguity nor the audience can be allowed to act as the court of last resort. The court of nature, with experiment as its plea, alone can serve.

Once again, it is strikingly evident that the need for a general public understanding of the real nature of the scientific way has never been so great. How is it to be achieved? There is no one way, of course, no single campaign, no single plan that can suffice. It can only be attained, gradually and persistently, at many levels of concept and of execution. The channels are especially important, and must be especially subtle, at the deeper levels of feeling and philosophy

which ultimately must be the most socially significant of all. For it is at precisely those levels where a truly widespread comprehension of the real nature of the scientific way could perhaps go farther than any other single factor in helping to span that disastrously serious gap left by the decline of formal religion in a society still fundamentally moved by its deep needs for reverence and an abiding sense of identification with the natural world.

As the nation catches its breath in the wake of the voyage to the moon, as reflection and planning for the future follow, we are faced with some unpleasant considerations. One is that the breadth and the depth of the scientific resources that should stand ready to exploit its results to the full, now and in the future, have become unfortunately thin and show scant prospect of improvement in the immediate future. The remarkable academic program of NASA, which gave effective support to a great number of graduate students at universities in the early and middle part of the decade, has been drastically sacrificed to the moon landing. So has the program of more purely investigational space shots—shots that were not very directly related to the moon program.

Observers of the American scene have long noted a national quality deeply ingrained among us. Frederick Jackson Turner might have argued—and with convincing impact—that it is indeed a basic heritage from the American frontier. We have always shown ourselves conspicuously strong—perhaps the strongest people in history—in accepting great challenges *if they are well-defined*; of organizing ourselves superbly to meet and to conquer them, of concentrating the whole will of a great people on crossing a lofty and inhospitable mountain range, as it were, in the faith that beyond that range lie fertile valleys that will nourish and sustain us and our children; that will bring to us and to those who follow the blessings that our supreme effort has earned. Countless events in our earlier history have reaffirmed that faith. Indeed the growth and development of the nation, in its most formative phases, were deeply rooted in such patterns of episodic and heroic conquest.

But there is an obverse to this picture which, with the years, may become increasingly significant. The expected corollary of the windswept range crossed is indeed for us the smiling, fertile valley beyond. Even late in the twentieth century we still instinctively claim that valley as an expected right. At the end of the First World War we withdrew long before the patterns that should have been stabilized had even begun to be consolidated, certain that, as we had fought that war well, respite was properly due: secure in the belief that inevitably the rest would take care of itself. Even at the end of the Second World War we displayed a strong inclination to leave the real ordering of the world that was emerging to others, convinced at heart that our part was completed. Only now is it becoming evident how much we could have accomplished if we had been willing to stay the course a little longer. And though the exigencies of the last decades have taught us something valuable about all this, national traditions that are so ingrained die hard. Though we were early trained to cross mountain ranges, and to recognize and honor the strengths and gifts that let us do so, we did not, early on, value so highly the sustaining talents that would enable us to plod tenaciously through endless hills of shifting sands, placing our faith not so much in the magnitude of any one achievement as in the consistency and endurance of continuing effort.

It would spell tragedy if we were to exchange one pattern for the other. Such an

exchange could dim a unique drama of glory. But in a world increasingly crowded, increasingly inchoate, where clear victories are rare, it is evident beyond all doubt that we cannot maintain one pattern unless we are also well practiced in the other. We must learn, at very peril of our existence, that there are deserts to be crossed as well as ranges, and that to expect those deserts to have boundaries is illusory. As a wise contemporary American has remarked: "The essential feature of success in any venture is *that it permits you to go on.*" We must come to look on that next chance as our highest and most pertinent reward. It will not be an easy lesson to learn.

That is precisely the lesson that is facing the scientific enterprise in the wake of the first moon shot. Moon exploration can avail us little, over the coming years, unless we have the will, and apply the resources, constantly to build the necessary base of fundamental knowledge. Already Europe is aware that, if the Americans should neglect the academic aspects of space, it must be Europe that picks up the pieces, supplying in brains and judgment and diligence what dollars cannot buy except through the subsidy of consistent, long-range effort in research. Already some Europeans are wondering whether the coming decade could mark a return to the pattern of the 1930's—to that "division of labor" where Europe was predominant in pure research, America in the applied field.

In the year 1964, the government of the Federal Republic of Germany devoted approximately 1.3 percent of its gross national product to the field of research and development. By last year that figure had risen to about 2.4 percent, and 2.5 percent or better is projected for 1972. During the period from 1968 to 1971, although the total budget of the German federal government is expected to expand by only some 6 percent per year, increase in that part devoted to research and development is projected at the rate of approximately 16 percent per year. Adding to this the amount contributed by industry, it is anticipated that the entire expenditure on research and development in the Federal Republic may, by this next year, total between 13,000 and 14,000 million deutsche marks.

It was only in 1955 that the Germans were permitted to enter the field of large-scale nuclear development. Since then, propelled by a rapidly growing need for added sources of energy keenly felt throughout the Federal Republic; reinforced by indigenous talented personnel as well as by nationals who had been trained in nuclear research and technology in the United States and elsewhere abroad; empowered by funds made available with minimum complication by the government for the support of well-conceived projects, progress in this field has been so rapid that in many aspects the German nuclear power program has now caught up with that of the United States and in some areas has surpassed it. It is expected that by 1972 the installed capacity of nuclear power stations will have a capacity of 2300 megawatts. Moreover, it is considered a serious possibility that by then additional nuclear production will be on order capable, when completed, of producing 12,000 megawatts of electricity. The merchant ship, *Otto Hahn,* was designed especially for nuclear propulsion, and as such is the most highly developed nuclear-powered vessel in the world today, being considerably in advance of the U.S.S. *Savannah.*

Space programs have been very much at the forefront in this spectacular resurgence. Clearly the Germans are determined to master the technology of space exploration and research, in the confidence that this field must ultimately

become of major industrial significance. It is interesting to note—especially in the light of our own program—that no less than three of the six experimental packages designed for a NASA space shot to investigate the magnetosphere were developed and produced in the German Max Planck Institutes. Equally interesting, an ambitious rocket launch under German management designed to measure the zodiacal light, planned to take off physically from the United States, will include six German experiments combined with six complementary American ones. The plan is to have the flight actually directed from West Germany, under the control of a 100-meter radio telescope near Bonn planned for completion during the coming year. The anticipated cost of this enterprise to the West German government is reported to be in the neighborhood of 200 million deutsche marks.

The German Federal Ministry for Scientific Research has outlined four clearly defined "priority programs," all touching current frontiers of industrial development as well as basic investigation. They include data processing, space research, atomic energy, and oceanography. The venture into oceanography is the most recent. It was prompted, at least in part, by the large expenditures planned in the United Kingdom and France, as well as by us, and is clearly being approached with some caution. In the field of data processing, no less than eight regional computing centers are planned, with an initial contribution from the science budget of 34 million deutsche marks, in a total program that is expected to reach a level of at least 500 million deutsche marks expended by 1971.

In France, the proportion of the G.N.P. spent on research has doubled in the last decade. The budget of the Centre National de la Recherche Scientifique has been increasing over the past several years on an average of 17 percent per year. Oceanography is being given a good deal of encouragement, in parallel with similar movements in the United States.

In Japan, government funding for research and development in 1966 amounted to 1.4 percent of the G.N.P., and the proportion projected for 1971 is 2.5 percent. This is particularly impressive when it is recalled that unlike most European countries and the United States, the proportion spent on research and development for military purposes is almost negligible. For the Japanese fiscal year 1966 the total spent on research was reckoned at 1.35 billion yen, exceeding that of 1965 by nearly 15 percent. Later expansion, though not quite so dramatic, has been continuous. As in Germany, very high priorities have been set by the government in the fields of space research, including the development of satellites and rockets. Atomic energy research, with special emphasis on the nuclear powering of ships and the development of efficient nuclear fuels, is also being pushed very actively. For centuries the Japanese have been avid investigators and exploiters of the marine environment, both physical and biological, as we fully recognized for the first time only in World War II. It is natural, therefore, that programs in marine science and marine technology should be given a high priority.

All over the world, among developed and developing nations, research is being accorded an increasingly high priority by governments, and is being supported at an accelerating rate. In many of the most important of these countries —notably in Germany and Japan—morale has probably never been higher nor productivity greater in the sector devoted to research and to development.

Against this background, it is particularly melancholy that our own federal parsimony in this area, for the third successive year, has had to be so great. To be sure, the percentage of G.N.P. spent on research in the United States has long

led the world, a fact that has been a particular source of pride, and also of practical satisfaction. For nothing is more certain in the modern world than the high correlation between the research activities of a nation and the level of its prosperity—and indeed, on occasion, its very survival. So well is this recognized in Europe that some of the proportionate figures for total expenditure in research in the United States—such as the 4.3 percent of G.N.P. reckoned for 1966—have come to constitute specific goals, to be equaled or if possible surpassed.

Over the decade from 1958 to 1968, federal outlays for research and development in the United States grew at a compound rate of about 9 percent per annum. During the last four years of this period, however, the rate slowed to 6 percent or less, and for the last two years it has remained almost constant in dollar terms. However, maintenance at a constant level does not, of course, imply constancy of support. Not only does ordinary cost inflation drastically affect the level of research accomplishment at a constant dollar level, but there is a kind of "research inflation" at work also. As investigation proceeds on a scientific frontier, the field characteristically grows in sophistication. The tools essential for continued original investigation typically increase in sensitivity, complexity, and cost. Expenditure for each investigator will inevitably rise even should there be no increase in the cost of living, and even if dollar values were to remain constant. For example, the National Science Foundation, in its budget for fiscal year 1969, was allotted the total sum of $435 million, including some carryover funding from the previous year. This represented a very tight restriction indeed, and one quite drastically disturbing to the equilibrium of federally funded academic research which over a number of years had become established in the nation. This year the corresponding total is slightly larger, at $440 million. This appears to be an advance, however slight—and indeed an advance against heavy odds, considering the weight of other commitments facing the nation—and it symbolizes a continuing federal commitment to growth in this area. Unfortunately, however, the actual impact can only be a token one. The overall effect, indeed, has been to constrict expected programs by 20 to 25 percent in some 550 institutions in the country. The National Institutes of Health reduced their existing grants by about 20 percent and may be expected to make about 600 fewer awards than originally planned. Far from merely holding a ceiling on expansion, it would appear that the current budgetary commitment actually restricts the scope of the Foundation to less than that of 1966. The National Aeronautics and Space Administration will have reduced their commitments to colleges and universities about 30 percent—precisely in this year of the moon triumph. Fewer federal fellowship awards were made for the fall of 1968 than were made either in 1967–1968 or in 1966–1967.

It is quite clear that federal funding for research in the nation cannot—and undoubtedly should not—continue to expand in the coming decade at the rate which characterized the first half of the last. Persistent maintenance of such a rate could only result in a serious imbalance in the nation's commitments—and that in no distant future. It is equally obvious that current competing claims on the national purse are overwhelming in both magnitude and importance. And even presuming an early and optimal settlement in Vietnam, other major demands upon the nation's resources—above all the crucial issues of the cities—must press very heavily upon federal funding of research and development. These are "givens" that must be reckoned with.

But they are "givens" that characterize a situation none the less difficult and dangerous on that account. For there can be no such thing as an "equilibrium" in the quality and the scope of American research and development. Failure to progress is itself to decline. Decades have passed since Alfred North Whitehead commented: "In the conditions of modern life the rule is absolute, the race which does not value trained intelligence is doomed. . . . Today we maintain ourselves. Tomorrow science will have moved forward yet one more step; and there will be no appeal from the judgment which will then be pronounced on the uneducated." How much more true his words are now!

The internal effects of scientific regression are as damaging as the external. One of the most conspicuous and significant is the extent to which such currents tend to be mirrored in the public estimate of the value of scientific research and education as a national asset, and in the public view of their place in the scale of national priorities. Equally grave is their reflection in the morale of the scientific profession itself—in the feeling of the profession for its own place in the national scheme, and correspondingly in its enthusiasm and verve.

In any generation of scientific investigators, a stationary phase of research support inevitably tends to affect adversely the very sector that ought to be most encouraged—the youngest, liveliest, and often the most inherently original group just entering the arena. This is another grave consequence of the arrest of growth for any considerable length of time. Even more serious for the nation, such a pause can markedly affect the numbers and the quality of those from the oncoming generation who will wish to enter the ranks of science. Already one can see some effects of the three past years. Already there is visible in some quarters a disenchantment with science and a derogation of its importance that is at times truly alarming. This contrasts disturbingly with the optimism and vigor so characteristic of earlier years, and at present so conspicuous in some other parts of the world.

In this area we sometimes act almost as though we were running head-on into an insidious danger which through all history has threatened established leadership in every field—a danger characterized by a growing weariness in sustaining the role of leadership; a growing unwillingness to continue to carry undiminished the burdens that its maintenance and protection demand. And this dangerous dip coincides in time with the bold and inspiring bid of others for leadership—with that kindling vigor and hope and energy that the vision of freshening growth can bring. This recrudescence is of the highest importance for the world, and is something in which we should surely rejoice. But there can be the most serious failure —and the most serious material danger, too—for this nation if we do not continue to uphold the standard that others are quite properly striving to match or surpass.

Accepting, as we must, the limitations to which we shall be bound over the next years—conditions some of which grow inevitably from the very order of energy and success of preceding years—what are we to do? A controlled assured expansion of federal support, proportioned against the expansion of the G.N.P. itself, would assist the situation a great deal. A figure of approximately 10 percent annual growth in the budget for research and development has often been mentioned. More important than the precise figure would be the long-term assurance of growth itself.

But what of the immediate future? Several intrinsic features about support for science are significant in this context. One is the extraordinary importance, not

so much of *amount* of support as of its *consistency*. Nothing is so disastrous for the conduct of any scientific enterprise (short of serious shortcomings in talent and in the organization to implement it) as erratic, unanticipated changes in the level of its material support. This is obvious when support is suddenly withdrawn. It is not so generally recognized that a situation of equal difficulty arises when support is suddenly and unexpectedly *expanded*—as in many instances over the past years the programs of the National Institutes of Health have illustrated.

The development of a scientific enterprise of real consequence is as precarious as that of a delicate plant. And to the same degree, it is an organic process. Training to real research competence involves a long, slow, and expensive growth. The participants in a new and original program in a difficult field cannot be prepared overnight, and the more original and difficult the enterprise, the more this will be true. Thus the sudden and unexpected expansion of a program, especially if it is forced by the pressing of funds upon it in the hope of attaining a specific objective, can quickly lead to lowered quality, to dilution of purpose, to waste, and ultimately, often enough to failure. And equally, of course, sudden and unexpected withdrawal of support from a healthy program can lead to disorganization, disruption, and, if the contraction be sufficiently severe, to actual inviability. Even considerable swings in *expectation* of research support can be damaging, though they may be difficult to avoid. Thus rumors of an impending cut of $100 million—20 percent—in the total funding of the National Science Foundation were widely disquieting at both federal and academic levels. There followed a rumor that the cut would be reduced to $50 million, and finally it was established at $80 million. These fluctuations had adverse effects upon morale through a wide sector of the scientific community.

All this argues strongly for gradualism in our approaches to the federal funding of research. But most strongly it argues for the establishment of some stable, relatively fixed formula for determining a consistent and reliable *floor* to research expenditures from year to year. There are many criteria to aid in determining such a floor. Evidently the definition should be in terms proportionate to the growth of the economy at some level. But most important of all, it should indeed be treated as a *stable minimum* base, even in years when other demands on the national economy may be unusually great. Perhaps nothing could contribute more to stability and productiveness in this arena than a widespread knowledge and understanding of an assurance of public confidence of this kind, however modest the actual amounts involved might have to be.

There is a particular practical measure which might be of real aid in dealing with these problems of the federal support for science, and especially in assuring the continuing healthy deployment of that support in the future. It would simply involve a return to an older method of federal budgetary accounting. It is extremely difficult, at any practical level, to make a valid distinction between "pure" and "applied" research. Volumes have been written on this subject, and, while there is clearly a discernible and perhaps definable difference at the extremes of the spectrum, the two activities are often almost identical in their substantive aspects, identical in their general climates, and identical in the quality and the training required of those who prosecute them. Moreover they frequently intergrade and are interwoven functionally in well-nigh inextricable fashion. Accordingly, any attempt to categorize or to separate activities of research along this line would clearly be futile, deceptive, and self-defeating.

On the other hand, there are real differences between science and technology.

Between an activity having as its primary objective the winning and communication of new knowledge *per se,* and one devoted primarily to developing, perfecting, and distributing specific technical items, clear contrasts in orientation and methodology are evident. That the two activities can be distinguished was demonstrated in the structuring of the federal budgets for their support over several years in the second half of the present decade. Although this procedure was very successful, it was abandoned in the budget for 1969, for reasons not clear, and has not been restored. Why should it not be desirable to do so?

The curves of federal support in these two categories have typically varied independently from year to year. Thus, in the category of "basic" research, it has been estimated that federal support grew by 29 percent a year between 1956 and 1964, then dropped to 9 percent between that year and 1969. In the "technology" category the earlier growth rate was 21 percent, the later, 5 percent. Thus the rate curves for the two classes were preferential to the "basic" category in both time divisions. But the actual dollar budgeting in the "technology" category was much the larger of the two. The separation of the two items, therefore, made possible a continuing real, if modest, increase in the support of research. In the year 1966–1967, for example, it proved possible, even in the face of quite radically stringent circumstances, to increase the separated research budget by more than 10 percent—a figure above what many today would regard as an acceptable increment for the future. Such a move, moreover, noticeably sharpened the concepts that govern the budgeting process. Finally, restoration of this distinction might well facilitate the establishment of the stable "floor" in budgeting for basic research that is clearly so very desirable. There indeed seem to be telling reasons why the policy of separate budgeting in the categories of "research" (including both "basic" and "applied") and "development" should be restored in future years.

If one speaks of growth in the federal support of research in the nation for the coming years on the order of 8 to 10 percent, however, the mechanical problems of organization and administration become formidable, and multifarious questions of planning and procedure are insistently posed. They are as comprehensive as the whole organization of scientific support within government.

One of the more specific of these questions, widely debated at present, relates to the optimum form that federal support for both research and training in the universities should take. In this context, it is pertinent to recall that, important though it be, government support of science and of scientific training forms but one leg of a tripod in the overall support and conduct of science in the nation. The others are of course the universities and industry. Government support is critically important for both the other members. But the support of the universities, in turn, is altogether vital both to industry and to government, and indeed to the overall national scientific effort. For by their very nature the universities must continue to be primary resources, not only for the successful maintenance of research itself but for the constant renewing of the human resources for both research and teaching. Those resources are the successive waves of young men and women who, year after year, are trained at great expense in effort and money —at great expense both to themselves and their society—and who go out to take their places in the everlasting renewal of prepared commitment through which alone we as a nation can survive and prosper.

So there can be few subjects in this whole field more important than the relationships of support between universities and research institutes and the federal government. Discussion in this area over the last several years has tended to become polarized around two extreme patterns, commonly referred to as "institutional" on the one hand, and "project" on the other. In this context the rubric of "project support" is commonly used to describe the pattern in which specific research enterprises are individually judged on the basis both of their substantive importance and of the excellence of the personnel engaged on them, usually by expert panels comprising professional peers of the potential grantees. This pattern, of course, is derived from one of long standing in many private foundations. If a favorable judgment is reached, the grantee may, in extreme cases, retain more or less personal control over his award. Although it is customarily administered through some mechanism within his university, often it may be really his, and can travel with him if he changes his institutional affiliation. This pattern, often in this extreme form, was widely adopted during the years of most rapid growth of federal support of science. Much can be said in favor of such a system. The careful and knowledgeable scrutiny to which the applications for such grants can be exposed, though it does not guarantee uniformly high quality, surely promotes it. Unfortunately, the procedure may also, in certain circumstances, tend to reinforce conventionality in research, sometimes leading to the loss or rejection of striking new ideas or approaches which, at the outset, may have been difficult to distinguish from the merely speculative. For such a system inevitably tends to reinforce the middle ground—the sound proposals of meritorious quality—while reducing the extremes—the unsound proposals at one end of the spectrum, and the rare flashes of genius at the other. And in a time of limited budgets, the risk is considerable that the little-known junior investigator of high potential talent will fare poorly in competition with the older, better-established applicant of sound reputation and predictable performance. It should be added, however, that this serious hazard is well recognized by most scientific investigators. A large proportion of the panel judges have kept it clearly in mind and have tried to allow for it.

The project system has considerable disadvantages, however, which have become obvious only in recent years. By its very nature it tends to emphasize proficiency in research above proficiency in teaching, since the rewards go predominantly to the research side. Moreover, while the excellence of a research proposal, and hence of the research capacity of the applicant, can be objectively judged, such objectivity becomes quite impossible in a field where the requirements for and the manifestations of excellence are as complex and varied as in teaching. With the growing realization of the cardinal necessity of reinforcing the teaching function in the universities, the shortcomings of the project grant system in this respect have been brought into sharp focus.

Again, the project grant by its nature shifts the administrative—and possibly to some degree the moral—responsibility for the conduct of the grant, as well as its award, from the institution where the awardee operates to the federal government. An unwise federal centralization of responsibility and obligation for an impossible welter of detail of both administration and judgment was thus early encouraged —to which, it must be added, some private institutions have latterly been guilty, wittingly or unwittingly, of contributing.

Finally, over the years a much graver and longer-term liability has appeared in the system of project grants, especially when they are fully attached to the individual rather than to his institution. It was inevitable that a certain number of

new or impoverished academic institutions, seeking to better their status both economically and in prestige, should have encouraged their more eminent faculty members in the sciences to seek grants as energetically as possible. And so an inevitable, pernicious cycle was initiated. Investigators whose special abilities might trend more toward mastering the techniques of grant-seeking than toward highly original work could be—and sometimes were—selectively rewarded in such institutional environments, with a perceptible lowering of research quality. This situation likewise provided an obvious opportunity for institutional maneuvering of a kind irrelevant to the best scientific progress, if not actually invidious to it. A final and most serious effect was that the social "center of gravity" shifted from institution to individual. There was little reason why an individual in such an environment should maintain any very special loyalty to, or even personal identification with, either his institution or his primary teaching responsibility. As serious difficulties of this kind recurred with increasing frequency over the years, resistance to the project system rose.

These disadvantages of the project system are indeed serious. But it would be a great mistake to neglect its many virtues, or to fail to appreciate the magnitude of the growth of scientific knowledge in almost every conceivable field that the federally supported project system, monitored by its host of dedicated, selfless, highly qualified consultants, has made possible over the last dozen years. Recognizing all the dangers and the shortcomings of the system, now more widely evident than ever before, it still would be the gravest error simply and irresponsibly to throw the baby out with the bath.

The institutional system, as its name implies, is designed to operate in opposite fashion. Support under it is normally given in the form of bloc grants, to be administered by institutions as they judge best to support both research and teaching. Such grants have commonly been used to defray expenses of research and of formal graduate training, and have also helped to meet overhead costs at the institutions concerned—a subject of particular controversy over a number of years. The defects of the project grant system are the virtues of the institutional one. It allows far greater latitude in the expenditure of monies than does the project system, permitting a more effective distribution between the support of teaching and research and even making possible a better balance within the research category itself. Given an able and sensitive university administration, the institutional system probably permits a more effective expenditure of federal dollars in the interest of general scientific *education*. Furthermore, by shifting the main responsibility both of judgment and administration from the government to the recipient body, an otherwise impossibly concentrated federal responsibility is diffused. The system also restores to the university the authority that it needs so badly in dealing with grantees who are members of its faculty and helps to sustain the institutional integrity so essential to hard-pressed educational organizations in our time. In the context of generally raising the standard of *both* teaching and research in American science, it seems, on the whole, better adapted to the present day than is the project system. Still it has its own shortcomings. It will be hard to match the high standards of the best research grants made through the project system: grants that have made possible some outstanding conquests of difficult and important frontiers.

In fact, of course, the terms "project grant" and "institutional grant" are unreal abstractions. They merely signify opposite ends of a long spectrum of devices through which federal monies can be channeled to the support of science

in nonfederal institutions. Don Price has recently put this general situation very clearly. He remarks that we have made a "political judgment that our national purposes will be advanced by supporting and enlarging the amount of scientific research that is carried on in independent universities." But, "The qualities of independence and critical scholarship and leadership in basic theory, upon which the whole research and development enterprise depends, will be threatened unless the central structure of the universities is made strong enough to sustain the structure of specialized research grants."

It is both unrealistic and unhelpful to regard the project and institutional systems as rival or mutually exclusive patterns. The great task over the years to come in this area will surely not be to decide irrevocably *between* them, but rather to *combine* them in ways that complement their purposes and their strengths, and that compensate for their respective weaknesses. There can be no successful project grant system without a strong university structure on which to base it, and that structure, in the field of science as elsewhere, will be more and more strongly dependent, as the years go by, on federal institutional grants.

Our vision here is still somewhat occluded by our devotion, ever since World War II, to the project grant pattern, and by the delusion, perpetuated to the present in many quarters, that the most important aspect of government support for science is that of "buying" specific bits of research rather than of building excellent and comprehensive scientific resources, material and most especially human. That is a misconception peculiarly damaging to both donor and receiver, and to the nation at large. Here a close scrutiny of the British experience, as Christian Arnold has suggested, could serve us well. For in many respects the British system has developed in an opposite direction from our own. It began with heavy emphasis on institutional aspects, through the work of the University Grants Committee, and proceeded to the project grant pattern in a context of more massive undertakings—an evolution, it must be said, that for all the difficulties attending it may have been more logical than our own. Nowhere, indeed, has the intimate dependence of the project system upon the institutional foundations which institutional grants alone can sustain been more poignantly illustrated than in the British pattern, where external grants for special purposes have increased from approximately 8 percent of the total research expenditures in the universities for 1950–1951 to approximately 36 percent in 1966–1967. In this context it is encouraging to notice the current support for the institutional grant system provided in a recent report of our own National Science Board.

An inevitable accompaniment of the immense growth in the volume of federal funding and conduct of science in recent years has been the revival of an old, difficult, and perhaps deceptive query. Should there be a single central department or other center of planning and management within government, devoted to the coordination of all of federal science? The question is not necessarily contingent upon the present massiveness of federal involvement, although it is clearly underlined by that situation. In fact, it was raised by the National Academy of Sciences as long ago as the latter part of the nineteenth century. The issue of centralized or diffuse government management of scientific affairs has been debated from time to time ever since. It has recently been given a new focus by a proposal from the National Academy for a government organization tentatively called the National Institutes of Research and Advanced Studies, which perhaps might act as a central manager of federal science. This model has not been put forward literally,

but only to provide an "anchor" for speculation on the relative merits of diffuse and centralized systems.

Current concern with this question in the United States is no doubt intensified by the picture of federal research in some of the nations of Europe where the resurgence of science has been so spectacular. In West Germany, for instance, the Federal Ministry for Scientific Research has powers of coordination throughout the government as a whole, and assumes direct charge of programs of high national priority, including space research, oceanography, and atomic energy. Further, the Ministry has the responsibility of channeling the federal funds appropriated for science to a group of autonomous research societies, which also receive contributions for the same purposes from the various länder governments. In addition, the Ministry undertakes the critical task of overall scientific planning, including what appears to be an essentially decisive determination of major priorities in fields of research and development which shall engage the nation for some time ahead. This emphasis on planning which is centrally conducted but nevertheless has the flexibility conferred by close cooperation with the scientific societies, with the länder governments, and with the universities and industry, has so far proved remarkably efficient and successful.

Such highly centralized European patterns for the governmental management of science are echoed in Japan, where the central bureaucracy has customarily maintained tight controls on the planning and execution of governmentally supported research, with the universities and industry traditionally functioning as the other corners of a triangle. A National Council for Science and Technology is chaired by the Prime Minister and includes several powerful Cabinet members. The day to day work of assembling and organizing the facts and projections upon which the Council will base its determination of overall science policy for the nation is carried out by a Planning Bureau, which also serves as secretariat for the Council. There are many specialized planning and executive bodies at lower levels which assume derivative responsibilities for particular aspects: the Atomic Energy Commission, the Science and Technology Agency, the Space Activities Council, the Council for Marine Sciences and Technology, the Radiation Council, and, in a somewhat broader advisory frame, the Science Council of Japan, established in 1949 with the encouragement of the American Occupation. But despite the multiplicity and the varied nature of these specialized bodies, final authority for a national policy in science and technology is unmistakably concentrated at the highest governmental level. Small wonder that the question of a nationally centralized policy-making body for science in the United States has recently been raised with renewed urgency.

And what of that question? A first caveat to be observed in all comparisons of this kind is to recall that science, while an immense practical resource of any society, is above all a particularly vivid and sensitive expression of that society's own philosophy, its own history and its own peculiar organizational genius. If the organization of science policy runs faithfully concurrent with the political history and aspirations and philosophy of a people, it will successfully serve that people in the scientific sector of their endeavors and will accurately reflect their aims. If it fails in this, the overall effort is sure to fail as well. Such concordance of character and aim has clearly been established in Germany, in Japan, and in several of the most progressive of the Socialist countries. The essential question for us is how concordant this kind of structuring would be with our own national philosophy. And, indeed, it is a very real question.

There can be no doubt that effectiveness of forward planning has been enhanced in the countries of Europe which have adopted a centralized pattern, or that its adoption has accompanied the verve and vigor of a notable scientific revival. On the purely practical side, however, there is also no question that the situations of those nations with respect to indigenous resources for research and technology are still far more elementary than our own. And it is worth remembering that, so long as this is the case, technologically advanced nations like the United States still provide the overall models toward which such countries can direct their planning. It remains to be seen how effective centralized structuring may prove to be when these countries have drawn abreast of the most technically advanced nations, and must assume an equal share of the burden of innovation and real scientific leadership on a wide scale.

It is also worth recalling that, though governments can often make centralized and overriding scientific decisions which in particular cases can prove extraordinarily efficient—because of the overriding power of implementation which they can carry—*so long as they are correct,* governments can also on occasion make the grossest of mistakes in these difficult areas. They are no more immune than any other human assembly to following the fashions of the moment, to succumbing to the flashy attractions—and sometimes the real brilliance—of fields of scientific research and development which may offer quite illusory promise. And when they do this, with power and assurance sufficient to override quieter but more knowledgeable dissenting voices, major disasters can ensue. As yet this has not happened to any serious degree in countries with tight central control. It is to be hoped that wisdom is such that it will not happen. But the record is not yet long.

There is, however, a danger that is already becoming manifest in some of these countries, and that could take a serious turn. In a number of the nations that have evolved most markedly toward centralization in their governmental planning and conduct of science, all is clearly not well with the universities. Increasingly some universities, at least, have felt pressured to diminish both their uncommitted science teaching and their programs of uncommitted scientific investigation, and to shoulder larger and larger loads of applied work coming to them from government. Many members of university faculties are complaining that, though material resources for research have never appeared so abundant, the precious assets of time and energy free for devotion to basic science are more limited than they have ever been. These hazards are threatening the universities just when other difficulties are at a maximum for them—and indeed may be compounding those difficulties. So far, there are only hints of these possible accompaniments of extreme centralization in the federal planning and funding of science and technology. But they seem real, and they could grow, ultimately causing incalculable damage both to education and to pluralism of research. It is well to remember that these could be "type" dangers of overcentralization that might easily threaten us too.

There seems to be no doubt that a really tightly centralized structure of planning and administration for science and science support in our federal government could be seriously inconsonant with the diversity of concept and action that has always been a hallmark of American philosophy. It is a philosophy that, though often inefficient and clumsy, permits a flexibility that throughout our history has consistently proved salutary. However practically attractive a

thoroughly centralized pattern of federal control and planning for federal science may appear, these are considerations to be kept most seriously in mind.

Whatever may prove to be the ultimate reality of such conjectures, we enjoy a number of inherent safeguards for continued scientific pluralism. For our own federal scientific structure, like that of all scientifically vigorous countries, necessarily works in the closest partnership with the other members of that inevitable triangle—the universities and industry. And we must make quite certain that these safeguards are not overstrained. The heart of the matter lies in the kinds of relationships that are formulated and maintained among them. Here we will do well to bear constantly in mind the essential qualities of the other members of the partnership and their central roles in the affairs and the fortunes of our society.

The importance of the role of the universities needs little emphasis. Discussions and events over the years immediately past have brought their immense contributions, and their immense problems and vulnerabilities, into sharp public focus. But perhaps not enough public attention has been focused on the extraordinary importance of the industrial sector in the research affairs of a nation. In Germany's resurgent science, industry has supplied an indispensable resource and has regularly been brought into research projects at the earliest possible time. The nuclear power industry, for instance, has been primarily responsible for the spectacular German successes in that field. In France, in Japan, and in most other countries experiencing a fresh surge of scientific effort today, the contribution of industry is extremely important. These countries are learning apace that industrial laboratories offer fertile resources for the prosecution of government-financed research—more fertile, often, than the government laboratories themselves.

Of all the nations in the world, we are the leaders of this trend—though we do not always realize it—in time, in magnitude, in variety and ingenuity of arrangement. In a recent survey made by the Economics Department of the McGraw-Hill publishing company it has been estimated that by the end of the next decade, in 1978, industry in the United States will be investing some $33.6 billion in research and development, in comparison with the $17.6 billion expended last year. In 1978, colleges and universities are expected to conduct $5.6 billion worth of research, compared with $3.5 billion last year, while the corresponding figure for nonprofit laboratories is anticipated to reach about $1.6 billion, compared with $840 million last year. So the contribution of industrial research projected over the coming decade is, in dollar terms, by far the most spectacular.

Not only is the cumulative expansion of industrial research and development likely to considerably exceed that of other sectors of the research economy over the coming decade, but the current cutbacks in research funding that have so affected the government are not reflected in the industrial scene. The McGraw-Hill survey predicts that industry will undertake about $19.2 billion of research this year—a gain of 9 percent over last year. Industrial employment of scientists and engineers grew at an average rate of 3.2 percent during the past decade. Between 1969 and 1972 the rate of increase is expected to average 4 percent. In addition, it is anticipated that over those years there will be a gradual shift in the proportion of basic and applied research undertaken in industry to favor the former.

In considerable measure, indeed, it is this faith of industry in the worth of scientific and technological research that is importantly bridging a time of danger

in the federal sphere. It accounts in large part for the prediction that in 1970 the United States will actually be devoting 4.6 percent of her G.N.P. to research and development, against an average of 2.5 percent for Europe. Seen against this background, the picture looks by no means dark. It suggests, moreover, that the current leveling of federal support may not represent any fundamental shift in American attitudes toward research and technology, but only a shift in the major channels of its expression.

Perhaps the deepest and most significantly helpful aspect of this whole matter has recently been set out with extraordinary clarity by Jean-Jacques Servan-Schreiber. A predominant factor in American industrial growth, he emphasizes, is the talent for accepting—and even maneuvering—change. That indeed has historically been a salient character of American society at least since de Tocqueville noted it in his travels in North America in 1831, and no doubt even earlier. It is one of the hallmarks of the frontier and of the germinal experience of opening and occupying new lands that we have never lost or abandoned. A second factor, which Servan-Schreiber is able, perhaps, to evaluate with better perspective than could any American, is the extent to which the American society, by its very nature, is dedicated, as a principal commitment, to the development of men and women. Here idealism and practicality can be welded in an effective partnership, for the investment in men and women that is so characteristic of America is indeed as much practical as idealistic. It is an investment in brainpower, and in personal and organizational effectiveness, on a scale probably unprecedented in world history. The old saw that America gambles far more on human intelligence than it wastes on gadgets is indeed true. And as Servan-Schreiber emphasizes, "The wager on man is the origin of America's new dynamism."

It is this wager on man which we must encourage through all the years as the deepest commitment of American society. Whether in policies of research and development or through those aspects of substantive science so vital in the larger context of the human spirit, we have a solemn and a compelling and a continuing duty to guard and to foster that philosophy in every possible way over the decades to come. This is a consideration of high importance in planning the organization of science in the federal government. It must be a unifying consideration in all that we think and plan and do in the conduct of substantive science itself, now and as far into the future as we can foresee.

And science, we should insist, better than any other discipline, can hold up to its students and followers an ideal of patient devotion to the search for objective truth, with vision unclouded by personal or political motive, not tolerating any lapse from precision or neglect of any anomaly, fearing only prejudice and preconception, accepting nature's answers humbly and with courage, and giving them to the world with an unflinching fidelity. The world cannot afford to lose such a contribution to the moral framework of its civilization, and science can continue to offer it only if science can remain free.

Sir Henry Hallett Dale—*An Autumn Gleaning*

Other desires perish in their gratification, but the desire of knowledge never; the eye is not satisfied with seeing, nor the ear with hearing . . . the sum of things to be known is inexhaustible, and however long we read we shall never come to the end of our story book.

A. E. Housman—*Introductory Lecture at University College, London, 1892*

The Year in Review

"I have . . . learned from others of whom I made the most careful and particular inquiry."

—THUCYDIDES, *Peloponnesian War,* Book I, 22, (Jowett translation)

The Carnegie Institution engages in fundamental scientific research and training. It is an operating organization using the methods of physics, chemistry, mathematics, biology, geology, and observational astronomy to investigate the research frontier of the natural sciences. Integral with its research is a postdoctoral training program that has been and is a significant source of professors and scientists for universities and research organizations in the United States and abroad.

The Carnegie Institution spent $4.9 million in the fiscal year 1968–1969 for research and fellowship support, its only activities. This report will describe the specific purposes of the expenditures and the results of operations.

The relevance of science is not that of today's press. Nor is it short-term. It is one of concentration on the unknown; it is served by dedication, by utmost economy, by patience, and by an ever-present willingness to admit error. Science is highly relevant not only to the advancement of thought and understanding, but also to material progress.

This is the kind of relevance within which the Institution can undertake an accounting, and for which its operations are designed.

The Institution conducted research in fifteen distinct fields in 1968–1969. All but two were among the biological and physical sciences. The choice of these fields has been determined largely in decisions by individual Staff Members or Fellows, or by collaborating groups of Directors, Staff Members, and Fellows. In the "system" of scientific research the Institution has always emphasized the importance of the individual scientist. Although it also recognizes the importance of other parts of the system, such as the position of the frontier of research in a field, the "critical mass" of collaborators and colleagues, the availability of proper equipment, and long-range security, it has built all its programs around individual research workers. The pattern of activities and results here described represents a summation of the choices of more than 120 Staff Members and Fellows who were the Institution during 1968–1969. What they did during the year has a high degree of relevance to scientific progress and to the cultural and social progress of the future.

Of the $4.9 million spent by the Institution in 1968–1969, 85 percent was spent

Plate 1. Types of galaxies studied by Sandage, Freeman, and Stokes for intrinsic flattening. *Top left:* A typical elliptical galaxy of the E1 type (NGC 4278). *Top right:* A spheroidal (S0) galaxy (NGC 1201). *Bottom:* A spiral galaxy (Sa type) (NGC 3898). All photographs from A. Sandage, *The Hubble Atlas of Galaxies,* Carnegie Institution of Washington, 1961.

by the research departments. The Office of Administration and general expenses accounted for about 15 percent of the Institution's 1968–1969 expenses. Ninety percent of its operations are carried out through five operating departments: The Mount Wilson and Palomar Observatories at Pasadena, California; the Department of Terrestrial Magnetism and the Geophysical Laboratory, both at Washington, D. C.; the Department of Embryology at Baltimore, Maryland; and the Department of Plant Biology at Stanford, California. A sixth group, the Genetics Research Unit, at Cold Spring Harbor, Long Island, New York, continues a long tradition of distinguished genetics research within the Institution. The research and training activities of each of these groups during the year are described in the pages that follow.

Mount Wilson and Palomar Observatories

1968–1969 Expenditures:
Operating $1,005,663.04*
Equipment $255,710.59†

Ten years ago Allan Sandage wrote in *The Hubble Atlas of Galaxies,* "A renaissance is occurring today in astronomy. . . . we do stand a chance of understanding the universe." The renaissance continues. The 1960's have indeed been an exciting period for astronomy and astrophysics, one to which Sandage and his colleagues at the Observatories have contributed so much. The discovery and optical identification of many quasi-stellar sources, the discovery of pulsars, the finding of a series of objects with almost incredibly large redshifts, and the increasing understanding of what may be an appropriate model of the observed universe are intellectual landmarks of the first magnitude.

The work of the Observatories continued during the year in very much the same direction as during the preceding years of the decade. Indeed, the scope, penetration, and profundity of studies undertaken by the Observatories' staff maintain the position of leadership that has been traditional with them for sixty-five years, despite mounting support for astronomy elsewhere in the United States and among other advanced nations. The Observatories are a center not only for research but also for the training of young astronomers.

Study of Galaxies from the Southern Hemisphere. Pursuing his interest in achieving a definitive cosmological model, and in a refinement of the Hubble constant,[1] Sandage turned this year to the southern hemisphere, spending most of the year at the Mount Stromlo and Siding Spring Observatories in Australia. Observations of southern galaxies are considered crucial both for more accurate redeterminations of the Hubble constant, and in investigations of the symmetry of the universe as viewed from the earth. Sandage therefore gave first priority to studies of galaxies in groups and clusters in the interest of mapping the local dissymmetry (anisotropy) of the expansion of the universe. Another objective of the work was to test the possible dependence of the absolute luminosity of the brightest cluster or group galaxy on the star population of the group. In the course of the year he obtained 267 spectra of 221 galaxies of elliptical (E) and spheroidal (S0) galaxies (Plate 1). He also began a survey for the brightest red

* The Observatories (renamed the Hale Observatories in December, 1969) were jointly supported by California Institute of Technology and the Institution. The sum noted here represents the Carnegie Institution's expenditures in the operation of the Observatories for the fiscal year July 1, 1968–June 30, 1969.

† Includes $182,675.47 construction costs of new 60-inch telescope at Palomar.

[1] The Hubble constant gives the increase in velocity of an astronomical object with distance as it recedes from the earth.

supergiant stars in the Large and Small Magellanic Clouds, the closest external galaxies to our own. These form important reference points in the recalibration of the Hubble constant. The reduction of Sandage's data is not yet complete. But preliminary calculations suggest that southern galaxies showing recessional velocities of less than 4000 kilometres per second have smaller redshifts for a given apparent magnitude than their counterparts in the northern hemisphere. This could indicate a "local" dissymmetry in the universe as viewed from the two hemispheres.

Sandage, K. C. Freeman, and R. N. Stokes of the Mount Stromlo Observatory also studied the intrinsic flattening of elliptical, spheroidal, and spiral galaxies in the southern hemisphere (Plate 1). It was found that spiral and spheroidal galaxies are equally flat, with axial ratios of 0.25, but that elliptical galaxies have a large range of shapes, with axial ratios from 1 to 0.3. Furthermore, the intensity profiles of the spheroidal component of all three types of galaxies are remarkably similar. From these studies Sandage and his Australian colleagues concluded that elliptical and spheroidal galaxies cannot have been directly connected in evolution. These investigations confirmed that the central spheroidal component of all these galactic types is formed very rapidly (on the order of a few hundred million years) from matter having a low angular momentum, whereas the surrounding disk is formed of material with higher-than-average angular momentum. The galaxy type was determined essentially by the amount of free gas left over after collapse into the spheroid.

The importance of southern hemisphere observations in Sandage's cosmological study at this time underlines the dilemma that at present there are no major telescopes in the southern hemisphere. In this connection it is gratifying to report that the Institution took a step toward establishing its own southern hemisphere optical observatory. Although it established a radio astronomy observatory at La Plata, Argentina, several years ago, and has studied the seeing conditions for optical astronomy in the southern hemisphere for several years, an observatory site was not finally decided upon until this year. The institution has acquired from the Chilean government a 20,000-hectare property on the boundary between Coquimbo and Atacama Provinces, known as Las Campanas, about 80 miles northeast of the coastal town of La Serena. Development of the property will commence in 1969–1970.

Pulsar Observations. One of the more remarkable astronomical discoveries of the decade has been that of the pulsar. First detected by Hewish and his collaborators at Cambridge University, England, early in 1968, pulsars have commanded the attention of many astronomers and astrophysicists in the months since. An immediate search for optical pulsars followed the initial discovery. The first optical identification came almost a year after the radio discovery, when optical pulsation was detected in the Crab nebula by Cocke, Disney, and Taylor at the Steward Observatory of the University of Arizona in January 1969. The Crab nebula pulsar proved to be a star first singled out by W. Baade and R. Minkowski of the Mount Wilson Observatory in 1942. Baade and Minkowski's study of this object showed it to have a highly unusual featureless blue continuous spectrum. They considered it to be the central star of the nebula, and the primary remnant of the spectacular supernova explosion observed in 1054 A.D.

Employing a new specially designed digital data system for analyzing the rapidly pulsing light signals, J. Kristian, J. A. Westphal, and G. Snellen of the Mount Wilson and Palomar Observatories studied the Crab pulsar with the prime-focus photometer of the Palomar 200-inch telescope. They recorded digital

photon counts in time increments of one millisecond. Two distinct pulses were found in each 33-millisecond period, the main pulse extending only five milliseconds. Both the primary and secondary pulses are extremely sharp. The Crab pulsar has the shortest period of the dozen or so pulsars which have been detected by radio observation. This very precise photometry revealed a remarkable stability of pulse shapes and amplitudes, with an accuracy of better than one percent for one-minute averages compared at intervals of two hours. The optical stability of pulses differs from the large variations observed at the pulsar's radio wavelength. The light of the pulses was also shown to be plane-polarized to the extent of about ten percent.

The physical causes of the pulses and the energy background for the emissions of the pulsars are of course fascinating subjects for astrophysical theory. T. Gold of Cornell University has suggested that pulsars are rotating magnetic neutron stars formed in supernova explosions like that of the Crab nebula. P. Goldreich of the Astronomy and Geological Sciences Divisions of California Institute of Technology, and W. Julian, a Research Fellow at the Observatories, have investigated a simple model of such a star. They have concluded that the star must possess a dense magnetosphere, that particles within the star's light cylinder [2] rotate with the star, and that magnetic field lines which extend beyond the light cylinder close in a boundary zone near the supernova shell. Rotational energy lost by the star is transported out by the magnetic field and transmitted to particles in the boundary zone.

Another Unusual Quasi-Stellar Source. The investigation of quasi-stellar sources, another of the remarkable discoveries of the decade, was continued by several of the Staff Members and Fellows of the Observatories.

D. DuPuy, J. Schmitt, R. McClure, S. van den Bergh, and R. Racine, a Fellow at the Observatories, studied the remarkable radio source BL Lacertae, a quasi-stellar object that varied in visual magnitude between 12.0 and 15.5 during a period of seven months in 1968. Light variations of as much as 0.3 magnitude per day were observed. This anomalous object has a continuous spectrum, so its distance remains unknown. According to the assumptions made, it could be either the nearest quasi-stellar source, or the most luminous object known in the universe. Other infrared photometric and spectrometric observations by B. Oke, G. Neugebauer, and E. Becklin suggest the radiation of BL Lacertae is largely nonthermal.

Studies of Stellar Evolution. Studies of the processes of evolution of stars are fundamental to the progress of astronomy. Theories of stellar evolution, as Sandage has expressed it, "consolidate many of the isolated facts in astronomy."

One of the anomalies between observation and theory, hitherto unresolved, concerns stars in the final stages of degenerate evolution. According to the Schwarzschild theory the cooling of degenerate stars from the white dwarf through the red degenerate stages should proceed very slowly. Thus, if there are large numbers of white dwarfs there also should be large numbers of degenerate red stars. However, hundreds of white dwarfs have been observed but only about 20 of the degenerates, none of them very faint. J. Greenstein has now shown that new knowledge of convection outside the core but inside the surface of white dwarfs resolves the discrepancy. The fainter degenerate stars cool at a rapid rate,

[2] A light cylinder, a mathematical concept, has a radius such that, co-rotating with the star, its surface speed is equal to that of light.

and thus pass through the red stage quickly. Therefore they may be expected to be less numerous, conforming to the observations.

Instrumentation. As in most other physical sciences, progress in instrumentation plays a vital part in the progress of astronomy itself. In the last few years, especially, new techniques and auxiliary instrumentation at the Observatories have added substantially to the number of observations which can be made with the telescopes, and have increased the sensitivity of these basic instruments. In addition, a new 60-inch photometric telescope of the most modern design and with modern auxiliary instrumentation was nearing completion on Palomar Mountain at the end of the year. Its construction was made possible by National Science Foundation and National Aeronautics and Space Administration grants, and by a gift made to the California Institute of Technology by the Oscar G. Mayer family.

The program for conversion of observational outputs into digitally recorded form, under the supervision of E. W. Dennison of the California Institute of Technology Astroelectronics Laboratory, continued its progress during the year. A program for the adaptation of small computers to direct use at the telescopes also was started. These computers will be used as Central Processing Units at the Mount Wilson 100-inch and 60-inch telescopes, and at the Palomar 200-inch and photometric 60-inch telescopes, as well as at the 150-foot Mount Wilson solar tower. These new Central Processing Units will permit rapid change in the interrelation of important auxiliary devices, such as counters, timers, and encoders, with the telescope drives. The new computer control systems will be able to set the telescopes on any object in the sky rapidly and accurately. During the year integrating TV cameras were used experimentally in an attempt to reduce the time now required to find, set, and guide the larger telescopes on very faint stars or galaxies.

For several years these reports have described the image-intensifier tube, developed under the supervision of the Committee on Image Tubes for Telescopes. Now in use in many observatories, it has proven a most effective time-saver at the 200-inch telescope. Indeed, the speed of the image-tube spectrograph used at the 200-inch is so great that a substantial fraction of the total observing time is occupied, not in the making of the observations, but actually in loading and changing plate holders. I. Bowen, former Director of the Observatories and a Distinguished Service Member of the Institution, and B. Rule have designed a new reimaging camera with a rapid-change mechanism that will further increase the effectiveness of this highly useful instrument. The camera functions with optics of a new design by Bowen that will yield better image quality than that hitherto available.

Fellows and Students at the Observatories. The place of the Mount Wilson and Palomar Observatories in postdoctoral training and in graduate study of astronomy deserves special mention. The Institution supported five postdoctoral Fellows at the Observatories in 1968–1969. Another 12 Research Fellows were supported by funds made available by the California Institute of Technology, and 14 graduate student observers from the Institute studied at the Observatories. The assistance and advice of Observatories' Staff Members from both the Institution and the Institute thus were made available to 17 Fellows and 14 graduate students during 1968–1969. This is one of the major instructional programs in astronomy and astrophysics in the world. Both graduate students and Fellows have access to telescopes appropriate to their research programs, and to plate files, data reduction equipment and computers. Students participate in observing runs at the

major instruments by senior Astronomers. Students from the Institute's Division of Geological Sciences also regularly conduct research on the moon and planets with the use of Observatory telescopes and other instruments. A special project manned largely by graduate students and Research Fellows has been the infrared sky survey from Mount Wilson, made with a special 62-inch infrared telescope.

Students participate in every phase of Observatory life, including the reconstruction of instruments. An example is the modernization of the Mount Wilson 60-inch telescope in progress during the year. Student observers voluntarily aided technical employees in the extensive mechanical, electrical, and optical improvements that will soon give a new usefulness to this famous instrument. The Mount Wilson 60-inch is the instrument most used by student observers; a large part of the available observing time on it is allocated to students.

Geophysical Laboratory

1968–1969 Expenditures:
Operating $736,753.95
Equipment $66,300.42

Dr. Philip H. Abelson, Director of the Geophysical Laboratory, says in the Introduction of his report: "This past year has been a great one for earth scientists." At the end of the report year, geologists and geophysicists were awaiting samples from the moon, as well as samples from the deepest sea bottoms. Although the interest generated by these unprecedented events is great, other advances have been quite as stimulating for both the professional and the layman. Outstanding among these has been the accumulation of increasingly convincing evidence of the widening geographical separation of some of the great land masses of the earth in the course of geological history.

First proposed in France about 110 years ago [3] and elaborated by A. Wegener in the early years of this century, the theory of "continental drift" has been largely ignored by North American geologists and geophysicists until very recently. Since the discovery of the midocean basalt ridges, to be found in all of the oceans, and study of the magnetic properties of rocks on the ocean bottom, the theory of continental drift is receiving increasingly serious consideration as a working hypothesis in geophysics. Various models have been proposed within the last year for the primeval grouping of continents (Fig. 1), the dynamics of the "spreading" of the ocean floors, and the components of the earth's mantle and crust in movement (Fig. 2).

One long-standing program of investigation at the Geophysical Laboratory is designed to produce definitive evidence on the composition of the earth's crust and mantle. The data and methods of analysis developed at the Laboratory are most useful in testing models and theories such as these, as they will be in analyzing new and unusual materials like those from the moon. They are equally useful in revealing the finer structure of the earth's composition and history, as in studies on ore minerals, on the origins of petroleum, or indeed in the discovery of new minerals.

Magnetization of Oceanic Sediments and Lavas. An important part of the currently available evidence for the continental drift theory and for the "spreading" of the ocean floor is based on measurements of the remnant magnetism of ocean lavas and sediments. Yet there has been very little systematic study of the magnetic minerals of the sediments. The reliability of measurements of magnetic

[3] A. Snider, *La Création et ses Mystères Dévoilés* (Franck), Paris, 1858.

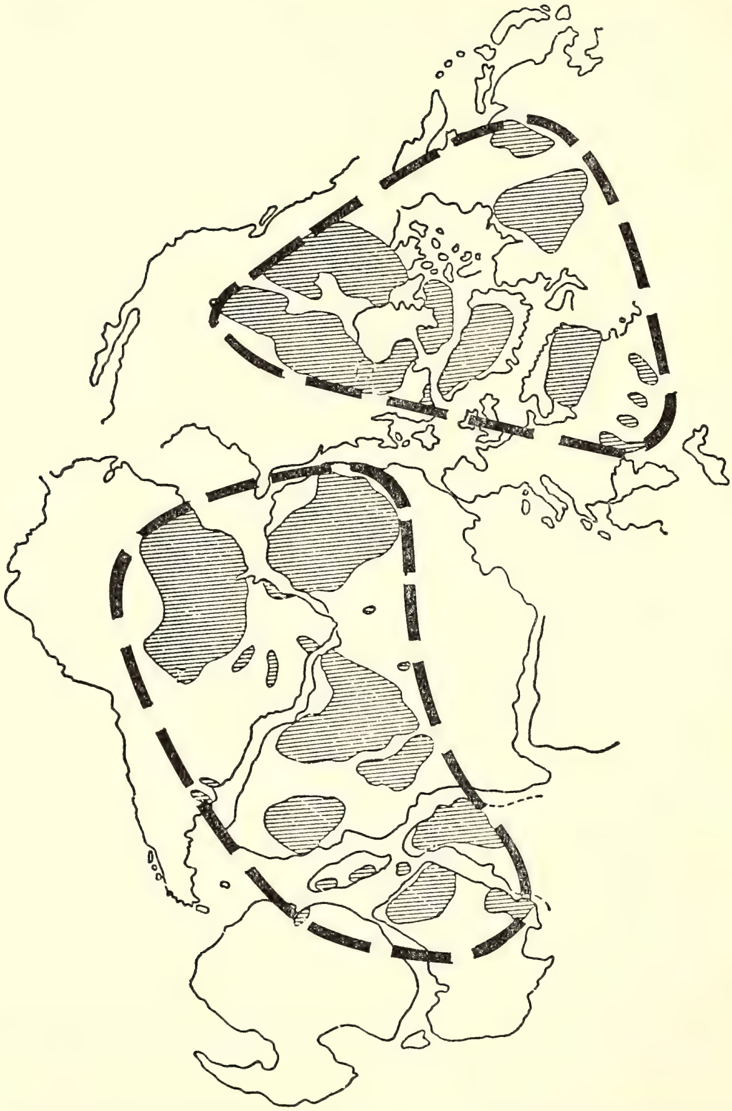

Fig. 1. A reconstruction of the world land mass before drift of the continents. The continental "blocks" having apparent ages of 1700 million years or more (hatched areas) appear in a coherent grouping within two regions. These blocks are transected and circumscribed by belts of younger rocks. Nonmoving ancient nuclei and continental accretion are thought to have existed up to the time of the great drift. (P. M. Hurley and J. R. Rand, *Science,* 13 June 1969: 1238.)

orientation in strata on the ocean floor depends on concordance with direction of the earth's magnetic field at the time of deposition of the sediment. To be a good indicator of magnetic and stratigraphic history the sediment must be sufficiently mobile for natural realignment of particles to occur under the influence of the earth's magnetic field at the time of deposition. The source of such mag-

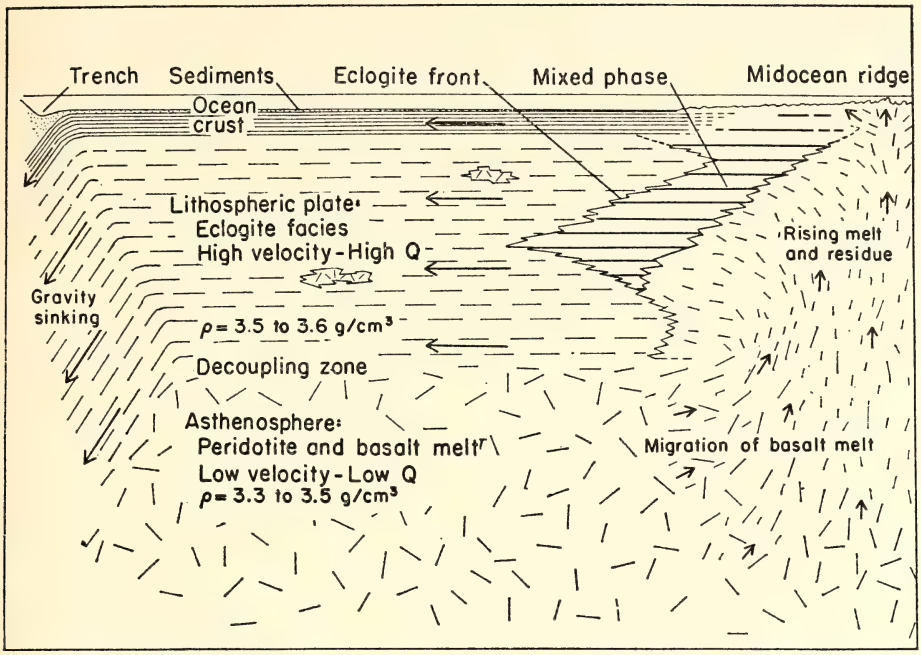

Fig. 2. One current model of the earth's crust and mantle composition in the oceanic basins. Volcanic rocks are extruded at the midocean ridge, and a suboceanic "plate" moves gradually toward a "trench," where the crust is reassimilated into the mantle. (F. Press, *Science,* 11 July 1969: 175.)

netic mineral material for the oceans as a whole, however, has not been determined.

S. E. Haggerty, a Fellow of the Geophysical Laboratory, has undertaken a study of the magnetization of pelagic sediments from the Atlantic, Pacific, and Indian Oceans, and from beneath the Antarctic ice sheet. He notes that the simple mechanical breakdown of primary volcanic material, like that observed on the mid-Atlantic ridges, does not apply to the deep oceans. Haggerty's study has shown that a major part of the magnetic material in deep-sea sediments is composed of detrital iron-titanium oxides of very small particle size (10 μm or less). He believes that atmospheric transportation of these materials from the continents to the deep oceans is likely. The wide distribution of wind-blown ash through the atmosphere following violent volcanic eruptions is well known, and sedimentation rates in the deep oceans (0.5–1 cm per thousand years in the Pacific Ocean) suggest that this is a reasonable hypothesis.

Conditions determining the magnetization and polarity of certain lavas, also critical in studies of the ocean floor, have been investigated by Haggerty and D. H. Lindsley. Systematic correlations have been shown recently between lavas that exhibit reversed directions of magnetization (i.e., antiparallel to the direction of the earth's magnetic field) and highly oxidized lavas. The relation between this reversed polarity and lava oxidation is not understood. In a study of the stability of the pseudobrookite (Fe_2TiO_5)-ferropseudobrookite ($FeTi_2O_5$) series, Haggerty and Lindsley believe they have found an indicator for the question whether the direction of magnetization in highly oxidized lavas is primary, that

is, whether it is developed during the initial cooling. They conclude that the oxidation of titanomagnetite and ilmenite ($FeTiO_3$) in nature to form members of the pseudobrookite solid solution series takes place between 600° and 800°C. Oxidation of lavas in this temperature range is most likely to occur during initial cooling. Field studies of cooling lavas corroborate these laboratory results. Accordingly, they also conclude that the presence of pseudobrookite suggests that the remnant magnetization of the rocks in which pseudobrookite appears is primary—that is, it is parallel to the direction of the earth's field at the time of cooling.

Mineralogy of the Mantle and Crust. Over the long run the most definitive evidence about the structure and dynamics of the earth's crust and mantle will probably depend on mineralogical and petrological study. Such investigations have been pursued by the staff of the Geophysical Laboratory for many years. More than 40 mineralogy and petrology studies were undertaken at the Geophysical Laboratory during this year. Their range and content, methods, and results may be illustrated by a selection of studies attempting to reveal the content of the earth's mantle, the relationships of minerals and rocks in the crust, and crust-mantle relations. Experiments depend heavily upon high temperature–high pressure apparatus, but the new electron microprobe has been very useful, and statistical methods have had their place also.

Statistical Petrology. Volcanic rocks have an exceedingly wide distribution in the earth's crust, particularly in the ocean basins, and on continental margins.

F. Chayes has continued the compilation of a "library" of chemical analyses of Cenozoic volcanic rocks, which have been placed on computer tapes. The tapes now contain more than eight thousand analyses that can be processed singly or in groups, by geographical occurrence, rock name, or any linear combination of chemical or normative characteristics. During the year Chayes used this data file to complete a summary study of the chemical composition of andesite, one of the broad groupings of volcanic rocks. He also made a survey of the relative frequency of rhyolite and andesite in ocean basins. Using the groupings rhyolite and andesite and five other classes of volcanic rocks: trachyte, trachyandesite, basalt, and trachybasalt, Chayes studied the incidence of corundum in more than 3500 analyses.[4] He found that the groups arrange themselves according to corundum content, from the rhyolites, with the highest average corundum percentage, to basalts, which have the lowest average content. At the end of the year Chayes also had under way a study of the "alumina balance" of these rocks, that is, the ratio of alumina (Al_2O_3) to the summation of sodium, potassium, and calcium (Na_2O+K_2O+CaO) in the rock.

Crustal Volcanic Materials from the Pacific Ocean Area. Two laboratory studies have produced interesting new information on tectonically active areas within the oceans and seas. The electron microprobe has been used to analyze the Coral Sea drift pumice, which is produced along the Tonga-Kermadec ridge in the southwest Pacific. Microprobe analyses by W. B. Bryan, a Fellow at the Laboratory, showed that the feldspar of the pumice is a more sodic type (bytownite) than had been determined from prior optical analyses, which showed it to be anorthite, the most calcic of the plagioclase feldspars.

[4] The seven groups of volcanic rocks are composed of varying combinations of feldspar, quartz, pyroxene minerals, mica, and a number of other minerals in lesser amounts. All of them contain a sodium potassic or a sodium-calcium feldspar. Rhyolite, for example, contains a potassic feldspar and quartz, whereas basalt contains a sodium-calcic feldspar and pyroxene minerals.

The drift pumice is of more than passing interest because it may be an important source of fragmented materials in deep-sea sediments. It is known to have been transported over thousands of miles by ocean currents, and not infrequently in large volume. A pumice "raft" from the 1962 submarine eruption in the South Sandwich Islands had an estimated area of about 2000 square miles, and had an estimated volume of about 750 million cubic yards. Bryan considers that knowledge of the source, composition, and ultimate distribution of the pumice is essential to a more complete understanding of sedimentations in the deep oceans and of the geochemical balance between continents and ocean basins.

Bryan also undertook a microprobe study of rocks from the Revillagigedo Islands (Mexico), located on the East Pacific Rise. Rocks from this area are considered to have special interest as genetic indicators. The Rise is an area of thin crust and high heat flow, a setting, according to Bryan, "that seems to preclude the role of granitic or other typical continental crustal rocks in the genesis of the lavas." The chemical and mineralogical relations between pantellerite [5] and a closely associated titanium-rich basalt from Socorro Island were studied. Bryan concluded that the pantellerite could have been derived by fractional crystallization of the basalt at fairly shallow depths, probably above 12 kilometers.

Mineral Composition of the Mantle. The composition of the earth's mantle, which lies below the crust, and the manner of mineral formation within it are other subjects of great interest for the Laboratory. In recent years even more effort has been concentrated on these studies, particularly on the phase equilibria of important mineral systems. The phase equilibria studies, of which more than a score were undertaken at the Laboratory during the year, will be illustrated by a set of experiments by F. R. Boyd on one "pyroxene-garnet system," and experiments by I. Kushiro, a Fellow of the Laboratory, on melting of the upper mantle under hydrous conditions.

Boyd's experiments are of special interest because they mark the first time that electron microprobe techniques have been used at the Geophysical Laboratory as a primary means of phase identification in high pressure studies of a mineral system.

Boyd says in his report that most petrologic models for the upper mantle favor garnet lherzolite as a major rock type.[6] This choice is made because garnet lherzolite is considered a possible parent material for the basaltic lavas commonly found near the surface. Garnet lherzolite also is abundant among the ultramafic nodules found in kimberlites,[7] which are considered to have been formed within the mantle. The nodules within which the garnet lherzolite is found are believed to be relatively unaltered mantle materials.

Garnet lherzolites are composed of only four essential minerals: the olivine forsterite $Mg_2(SiO_4)$, pyrope garnet, and the pyroxenes enstatite and diopside. The simplicity of this composition gives promise that the variations of the minerals in solid solution can be interpreted in considerable detail through experiment. Boyd experimented with the system $CaSiO_3$-$MgSiO_3$-Al_2O_3, which he considered to model the natural solid solutions closely. The phase relations of this

[5] Found also on the Mediterranean Island of Pantelleria, from which the rock received its name.

[6] Lherzolite is a coarse granitoid rock containing olivine and the pyroxenes diopside and enstatite. A garnet lherzolite contains garnet as well as the olivine and pyroxenes.

[7] Kimberlite is a granular rock chiefly composed of olivine ($Mg \cdot Fe_2SiO_4$), biotite mica, and calcite. It is found in the diamond "pipes" of South Africa and elsewhere.

system not only model the mineral assemblage in garnet lherzolites but also have similarities to the assemblages known in eclogites [8] and grospydites.[9] In general the results of these experiments agree with those of earlier studies on binary systems undertaken with conventional X-ray and optical methods. However, they are more detailed and precise. They show that the prior experimentally determined solvus for diopside in equilibrium with enstatite can be applied to natural assemblages of minerals in the mantle containing moderate amounts of alumina.

An understanding of the effect of water on systems of upper mantle components is necessary to understand the origin of magmas in that region. I. Kushiro, a Fellow, this year experimented on additional mineral systems containing most of the major components in hypothesized upper-mantle materials. His studies of the forsterite-nepheline-anorthite-silica-water system (Fig. 3) showed that the hypothesized garnet-lherzolite of the upper mantle could form andesitic magmas in the presence of water at depths of 60–80 km. Other peridotite upper-mantle rocks could form tholeiitic basalt magmas at the same depths but lower water contents. The study suggests that the formation of some common volcanic rocks of the crust is consistent with hypothesized mineralogical composition in parts of the upper mantle. Further application of the system seems promising when phase relations within it have been yet more precisely determined.

A Thermal Radiation Barrier in the Mantle. P. M. Bell and H. K. Mao, a Fellow at the Laboratory, undertook an intriguing study of the crystal field spectra at high pressure of two minerals considered to be important components of rocks in the mantle, fayalite (Fe_2SiO_4) and almandite garnet ($Fe_3Al_2Si_3O_{12}$). Their observations suggest that there are mineralogical reasons for a radiation barrier at great depths in the earth's mantle.

Atoms isolated in space tend to be spherical. In a crystal they are no longer spherical but are distorted in response to the influence of neighboring atoms, that is, the crystal field. The effects of the crystal field are especially large in transition elements such as iron, manganese, chromium, and titanium and can be measured by means of optical absorption spectra. Exposure of crystals to high pressure enhances the optical effects because the atoms are forced closer together and the crystal field is intensified as pressure is increased.

Thermal properties of the earth's mantle are sensitive to crystal field effects because radiation depends on the amount of absorption in the near-infrared and infrared regions of the spectrum. There is a broad "transmission window" in silicates at surface temperatures and pressures. This window is "closed" at high temperatures but tends to reopen on application of pressure. Bell and Mao also observed strong absorption at approximately 50 kb pressure. The results of the experiments suggest a mechanism for the shielding of thermal radiation within the mantle, which could be an important feature affecting its energy states and transfers.

Phase-Equilibrium Studies of Ore Systems. For the past 15 years G. Kullerud and his collaborators at the Laboratory have studied the mineral phase relations in a large number of sulfide and arsenide two-member systems that include many ore minerals. These studies have produced knowledge of the characteristics and behavior of these systems in previously unparalleled detail and precision. The binary systems most studied are those of sulfur, selenium, tellurium, arsenic,

[8] An eclogite is a coarse-grained mafic rock, mainly pink garnet and green pyroxene, thought at one time to be a component of the upper mantle, but not favored in recent hypotheses.

[9] A grospydite is an inclusion (xenolith) composed of garnet pyroxene and kyanite found in some kimberlite pipes.

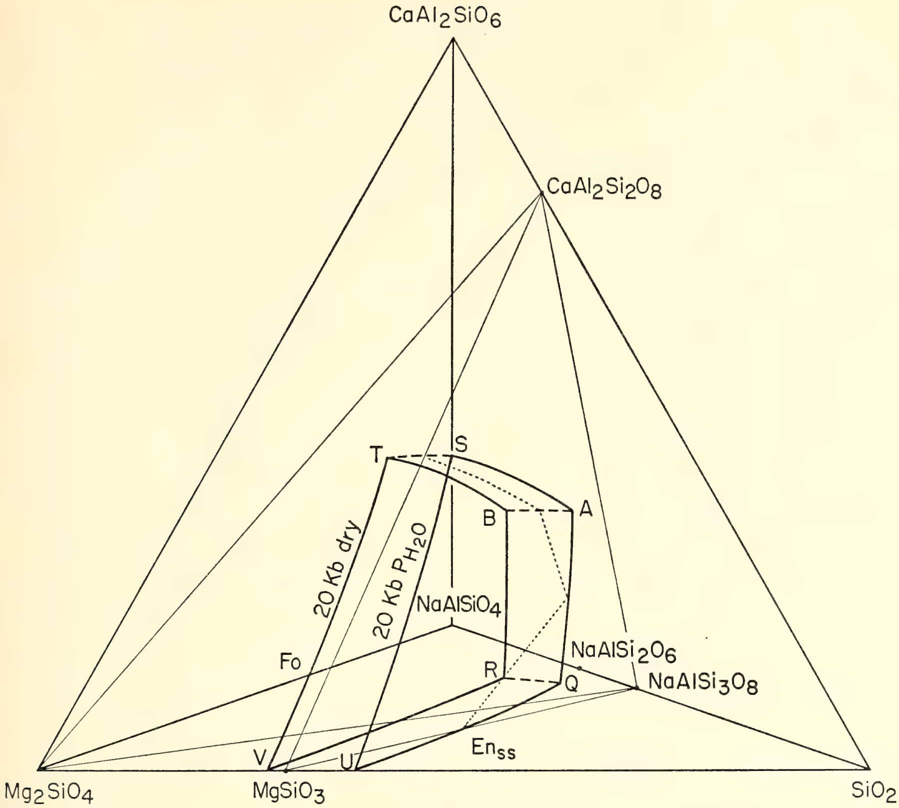

Fig. 3. Phase relations in a quaternary mineral system showing effects of the pressure of water. The diagram models the forsterite-orthopyroxene liquidus boundaries in the system forsterite-nepheline-$CaAl_2SiO_6$-silica-H_2O at 20 kb under water-saturated and dry conditions.

antimony, and bismuth. Kullerud states in his report that a "sulfide-type system" in the past has been understood to include any one of these elements in combination with one or more typical metals. This generalization has implied that a typical metal in combination with selenium, tellurium, arsenic, antimony, or bismuth, would have characteristics at least similar to the same metal in a system with sulfur. Kullerud and his collaborators have studied more than a hundred mineral systems that are composed of these five elements in combination with each other and with 24 metals of six different mineral groups, including nickel, copper, gold, silver, zinc, aluminum, iron, cobalt, chromium, and others. The results, classified by Kullerud for the first time this year, now show that the more than 100 pertinent systems divide into two groups. One is a sulfide type that includes the sulfides, selenites, and some tellurides. The second system, which is quite distinct, includes most tellurides, the arsenides, the antimony compounds, and most bismuth compounds. The bismuthide systems also appear to be transitional into alloy-type systems. Kullerud's classification would appear to have real value in predicting the behavior of about 40 mineral systems among these types that have not yet been adequately investigated. It may be considered an excellent key for future study of a number of minerals in these ore systems.

Discovery of New Minerals. Discoveries of new minerals in the experimental and field studies undertaken by the Laboratory have been reported several times in earlier accounts. This year has seen the detection of two new minerals. S. E. Haggerty describes a new iron phosphate mineral which he discovered in a study of specimens from the extrusive Laco magnetite lava flow in Chile (Plate 2). The new mineral, as yet unnamed, has the formula $Fe_4(Po_4)_3$. It was found as minute crystals in cavities interstitial to magnetite and hematite, which are more common iron-bearing minerals. It is opaque and crystalline, and has a yellow to bluish gray coloration. It is considered to be a late-stage precipitate in the lava flow.

The second new mineral, discovered by H. O. A. Meyer, a Fellow at the Laboratory, and B. M. French of the NASA Goddard Space Flight Center, has a somewhat more complex formula. It is thought to be the first example of the natural occurrence of a β-quartz solid solution, and is a combination related to spodumene ($LiAlSi_2O_6$), one of the pyroxene group of minerals. The formula of this mineral is given as $(LiAlSi_2O_6)_{63}$ $(SiO_2)_{37}$. It was found in a specimen of "Macusani glass" which occurs as pebbles and cobbles in glacial and alluvial deposits near Macusani, Southern Peru. It is not comparable to any naturally occurring volcanic glass hitherto observed. The β-quartz–spodumene mineral occurs as numerous small rosettes in the glass.

Amino Acids in Organic Earth Materials. As Dr. Philip H. Abelson writes in the Introduction to his report this year, one of the major puzzles of organic geochemistry occurs in the process wherein the relatively simple components of living matter are incorporated into the sediments of the earth. Microorganisms have long been accorded an important role. However, kerogen, a complex organic material, comprises the greater part of the organic matter in sediments. And the nature of kerogen strongly suggests that nonbiological processes must be involved.

Abelson and P. E. Hare have discovered that kerogen itself participates in an important nonbiological mechanism in sediments leading to the disappearance of small molecules like amino acids. Starting from a chance observation that both fatty acid tracers and amino acid tracers were not completely recovered when exposed to kerogen, they found that kerogen reacts rapidly and irreversibly with amino acids and peptides. The most reactive amino acids included cystine, arginine, histidine, lysine, phenylalanine, and tyrosine. Most of these are the basic and longer aliphatic chained amino acids. Only glutamic acid and aspartic acid remained after exposure of amino acids to kerogen for relatively long periods at 110°C. It is thought that a considerable portion of the nitrogen of the amino acids is bound into the kerogen, although some of it is evolved as ammonia. Humic acid, usually found mixed with kerogen, has about the same effect on amino acids as kerogen. An important nonbiological "sink" thus has been identified for destroying components of living matter in crustal sediments over long periods, at ambient temperatures.

Seeking additional insight into the amino acid–kerogen reaction Abelson and Hare conducted a series of experiments whose results suggest some equally significant inferences about life origins. They are another instructive example of the importance of chance in science, but the chance that comes to the prepared. Their experiments started with the reactions of kerogen and the peptides glycylleucine and leucylglycine. In the course of the experiments they observed that after long-term exposure of one or the other of the two peptides to kerogen, new peptides appeared. When glycylleucine and kerogen were heated, some leucylglycine was formed, and similarly, glycylleucine was formed from leucylglycine.

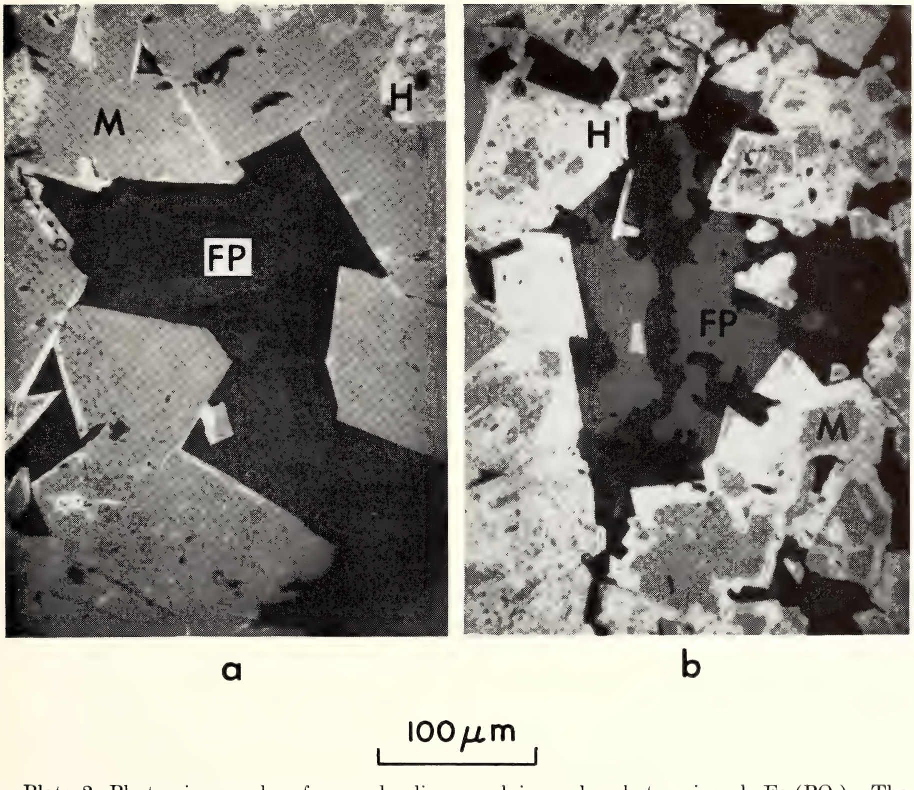

Plate 2. Photomicrographs of a newly discovered iron phosphate mineral, $Fe_4(PO_4)_3$. The mineral (FP) is dark gray, and in photograph (a) it is unaltered and crystallographically twinned. In photograph (b) thin alteration veinlets have developed along the grain boundaries and in cracks. The iron phosphate is surrounded by magnetite (M) and hematite (H).

One peptide, leucylglycine, was more stable than the other. Further experiment without kerogen, in which the cyclic amide diketopiperazine appeared as an intermediate, resulted in production of consistently higher proportions of leucylglycine than glycylleucine from the parent material.

Abelson and Hare conclude their report with the observation that these experiments "have profound implications for the abiotic synthesis of peptides and proteins since they indicate a preferred production of certain amino-acid sequences by a nonbiological, non-genetic code mechanism."

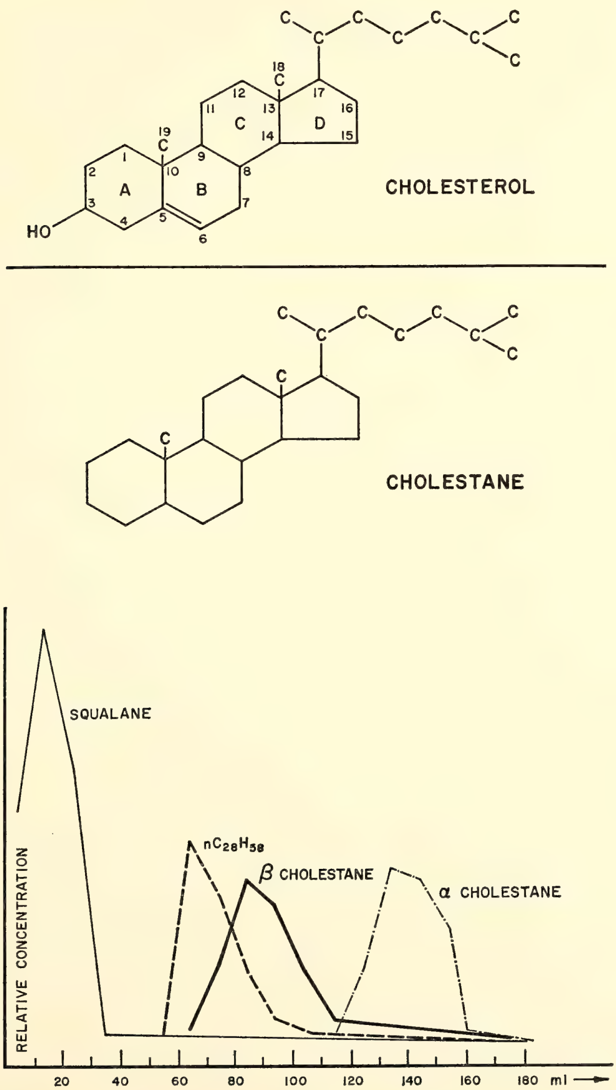

Fig. 4. Two steranes (steroid deviatives), and cholestane, as they are identified by alumina chromatography. The relation of the chemical structure of cholestane to cholesterol is shown by the two models. Cholestane lacks only the 3-hydroxyl group.

Steranes in Petroleum. T. C. Hoering, of the Laboratory, succeeded in isolating some of the optically active components of petroleum. Optically active molecules are widely synthesized by living organisms but are rarely found in nonliving systems. A strong argument for the biological origin of petroleums resides in the optical activity associated with high-boiling, saturated, cyclic hydrocarbon components. They include the four-ringed molecules of the sterane class, probably formed through the hydrogenation of optically active steroids commonly found in living organisms (Fig. 4).

With new methods of chromatographic separation and new instrumental methods of structure determination Hoering has isolated and identified ten sterane hydrocarbons from a crude oil taken from the Los Angeles Basin. They were highly active optically and had the molecular structures to be expected from the hydrogenation of common plant and animal steroids. Hoering's method will permit the examination of the high-boiling fractions of sedimentary organic matter in a degree of detail not before possible. Many classes of compounds of great biogeochemical interest, such as very old petroleums and rocks, are now open to detailed analysis and characterization.

Department of Terrestrial Magnetism

1968–1969 Expenditures:
Operating $726,419.19
Equipment $172,320.65

Commencing more than 60 years ago with studies of the magnetic properties of the earth, the Department of Terrestrial Magnetism has gradually broadened its scope until it now has the widest range of research interests of all the Institution departments. The Department applies the methods of physics to a great variety of problems from the evolution of life forms to astrophysics. This year's report notes astrophysical studies that include optical astronomy, radio astronomy, nuclear physics, and atomic physics. Geophysical studies, which are described below, display an increasing convergence of interest on problems generally similar to those which engage the Geophysical Laboratory. The DTM, however, applies some different research techniques. Staff Members from the Department and the Laboratory together form a joint study group that has specialized for some years on geochronologic study by means of isotopic dating. Besides these techniques, the DTM also has a very active seismology program, and the year's reports also show a fruitful and far ranging use of the techniques of geochemistry. As illustrations of the work of the Department, selected studies from the Geophysical Section and Biophysical Section will be described.

Geophysical and Geochemical Studies Related to the Evolution of the Continents and Other Parts of the Earth's Crust. Like the Geophysical Laboratory, the DTM has designed its program in geophysics and geochemistry to attack the global problems of the evolution of the earth's crust, including both continental and ocean basin areas.

The objectives of the Geophysics Section,[10] which undertakes these studies, are very fittingly stated in a reference to its seismological observations on the Andean plateau: ". . . we have sought to describe with increasing depth and

[10] L. T. Aldrich, Chairman, S. E. Forbush, S. R. Hart, I. S. Sacks, J. S. Steinhart, M. A. Tuve, C. Brooks, D. E. James; Fellows: A. J. Erlank, A. T. Linde, G. Saa; Research Associates: S. Suyehiro, M. Casaverde, R. Salgueiro; Collaborators: P. Aparicio, A. Rodriguez, D. Simoni, L. Tamayo, A. A. Giesecke, Jr., E. Deza, J. Frez, E. Kausel, E. Gajardo, F. Volponi, J. Mendiguren, R. Cabre, L. Fernandez, S. del Pozo, J. Santa Cruz.

precision the physical properties of this unusual part of the earth's crust. These properties must be satisfied by any model describing the process of continent formation." The process of continent formation itself was in mind in geochronological studies of ancient volcanic rocks on the Canadian shield. A contribution to understanding of sea-floor spreading likewise was the objective of a study of sea-floor basalts.

Trace Elements in Sea-Floor Basalts. S. R. Hart of the Geophysics Section notes in his report that the hypothesis of sea-floor spreading includes formation of an igneous crust on the oceanic ridges and rises, followed by lateral spreading and re-assimilation of the crust into the mantle along the oceanic trenches (Fig. 2). The material of the ocean floor appears to be a tholeiitic (high-alumina) basalt with a low potassium content, and relatively high ratios of potassium to rubidium, potassium to cesium, and strontium to barium. These characteristics are unlike continental or oceanic island basalts. Increasing alteration of the sea-floor basalts with distance from the zone of origin had previously been observed. Hart therefore undertook investigation of the possible role of sea water in producing the anomalous nature and proportions of the trace elements found.

Analyzing specimens from the East Pacific Rise, Hart found severalfold differences between recent unaltered interior and sea-water-altered rock margins in the proportions of the elements potassium, rubidium, and cesium that they contained. Little difference in strontium was found. It would appear that as the basalts move away from the ridges and age they are increasingly altered and become more difficult to date by isotopic methods. Hart considers the prospects for accurate potassium-argon dating, a familiar and convenient method, to be poor for sea-floor basalts.

In collaboration with A. Nalwalk, of the University of Connecticut, Hart also studied trace elements in much older basalts dredged from the Puerto Rico Trench. Evidence of alterations in the proportions of calcium, rubidium, cesium, and strontium, as compared to silica, was found in these specimens. Hart concludes that trace element values for the alkali metals and alkaline earths in the sea-floor basalts must be regarded with "considerable caution." This, of course, has obvious meaning for achieving precise geochronology of rocks on the ocean floor.

Evidence from Strontium Isotopes on the Early Heterogeneity and Continuous Differentiation of the Earth's Mantle. The evolution of the earth's crust from earliest time is of no less geological interest than that during recent epochs. Much of the evidence for an interpretation of this earliest history resides in the great continental blocks of ancient rocks (greater than 1.7 million years) like the Canadian shield (Fig. 1). One means of interpreting this history is through a study of a strontium^{87}-strontium^{86} ratio. The ratio is a useful tracer because strontium^{87} is always formed through natural decay of rubidium^{87}, whereas strontium^{86} is nonradiogenic. Information on the evolution of rubidium and strontium in the mantle can be obtained by calculation of the rate of change in this ratio of strontium^{87} to strontium^{86}.

Application of this tool to a study of the evolution of the earth's mantle depends on the discovery of rocks directly derived from the mantle. Most such rocks are modern volcanics. But almost no analysis has been undertaken on ancient volcanics in the old continental blocks. C. Brooks, a Fellow at DTM; S. R. Hart of DTM, and T. E. Krogh and G. L. Davis of the Geophysical Laboratory, undertook to close this data gap on mantle evolution by studying volcanics

from the 2.7-million-year-old Superior Province of the Canadian shield. The rocks analyzed are of zeolite, greenschist, and amphibolite facies, that had been metamorphosed from original rhyolites and basalts. The basalts are similar in chemical composition to modern basalts dredged from the ocean basins.

The results of these studies strongly suggest that a higher strontium^{87}-strontium^{86} value existed in the earth's mantle 2.7 million years ago than that predicted from the model in use, which projects linear growth from observed values in meteorites. The strontium^{87}-strontium^{86} data also suggest that the variation in this ratio inferred for the present-day mantle appears also to have existed in the mantle of 2.7 million years ago. In arriving at these conclusions, Brooks, Hart, Krogh, and Davis evaluated possible effects of metamorphic processes, crustal contamination, magma aging, and magma regeneration. They note that present-day heterogeneities in the submarine mantle of the earth appear to be somewhat larger than the inferred ancient mantle values.

On the basis of the data derived from study of these ancient volcanics, Brooks and Hart have derived a new model for the evolution of rubidium and strontium in the crust of the earth (Fig. 5). They propose a nonlinear continuous transport model in which rubidium and strontium are transported from mantle to crust continuously. They consider their model to be consistent with data on modern submarine basalts. They note that further testing of the validity of the model will require analyses of volcanic rocks intermediate between Archaean and modern.

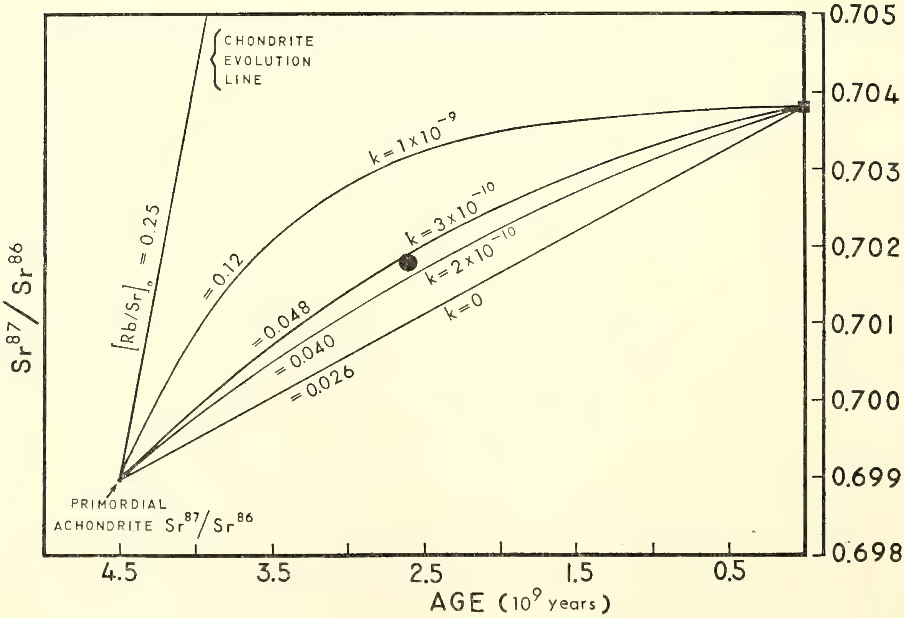

Fig. 5. Diagram for a model of rubidium-strontium evolution. Curves connecting primordial strontium ($Sr^{87}/Sr^{86} = 0.6990$) and modern oceanic strontium (0.7038) are calculated for a continuous transport model. K values are the transport parameters; other values are the initial Rb-Sr ratios required by the model. Also shown is the evolution line of a typical chronditic meteorite with initial Rb-Sr ratio of 0.25. Black dot at 2.6 billion year age is the best average value for Archaean metavolcanics determined at the Department of Terrestrial Magnetism.

If the model proves valid, it would imply a relatively constant rate of continental growth from Archaean times.

Other studies by Hart, Davis, Brooks, and Krogh showed that the continuous transport model was consistent with the evolution of cesium, rubidium, and potassium in the mantle, as well as strontium.

Potassium as a Tracer for Mantle Origins of Crustal Rocks. One important requirement for accurate determination of mantle parent materials for crustal rocks is a source of potassium sufficiently abundant to account for the high potassium contents of alkali basalts, a relatively common rock among modern volcanics. A. J. Erlank, a DTM Fellow; and I. Kushiro and L. W. Finger, Fellows at the Geophysical Laboratory, undertook analyses of the distribution of potassium in mafic and ultramafic nodules found especially in the kimberlites of South Africa. They are thought to represent fragments of the upper mantle. Erlank, Kushiro, and Finger found that most of the minerals present in these nodules did not have enough primary potassium to account for the potassic content of alkali basalts. Only two possible potassium sources were discovered: (1) part of a pyroxene mineral series known as omphacites, found especially in eclogite nodules; and (2) a somewhat rare amphibole mineral known as richterite, found in a mica nodule from a South African kimberlite. According to Erlank and Finger the richterite may represent the type of amphibole likely to occur in the upper mantle. If it amounts to even one percent of the upper mantle material it could account for the potassium in basalt lavas. These analyses were all undertaken by electron microprobe methods, permitting the measurement of relatively minute quantities of potassium (as little as 20 parts per million).

Seismological Techniques for Probing the Crust and Mantle. In a currently accepted model of the dynamics of the crust and mantle (Fig. 2) one of the clearly stressed regions is where the ocean floor moving out from the "rises" plunges under continental blocks. The western coast of South America appears to be such a region. It has been an attractive area for seismological study by the DTM for a number of years.

This year the DTM staff, in collaboration with the University of Wisconsin, the Southwest Center for Advanced Studies, the Instituto Geofísico Boliviano, the Instituto Geofísico del Peru, and the Instituto Geofísico of San Agustín University, Arequipa, Peru, engaged in the most active program of seismological observation in southern Peru and eastern Bolivia undertaken since 1957. This newest series of measurements confirmed the earlier anomalously high absorption of seismic energy in southern Peru, and gave indication that the seismic attributes of the crust could be fully measured through later observations in Bolivia.

I. S. Sacks, of the DTM staff, G. Saa, a DTM Fellow, and P. Aparicio, of La Paz, Bolivia, report on a study made at the Carnegie Analysis Center in Lima, Peru, of the correlation between crustal features like the Andes and anomalous velocities of earthquake waves in the upper mantle. They find that the Andes Mountains chain has a "root" of lower velocity material that dips away from the Pacific Coast. The width of this root is about 100 km, and the length may be as much as 400 km. The earthquake activity, which also dips away from the Pacific Coast, lies along the seaward side of the low velocity tongue and may reach a depth of 600 km. Aside from the low velocity tongue below the Andes, the behavior of seismic waves between the Pacific Coast and the pampas of western Brazil appears to be relatively normal. One is tempted to correlate the low velocity tongue with the dipping "plate" postulated in current hypotheses on ocean floor movement.

An Extraordinarily Sensitive New Seismic Instrument. Probably the most exciting seismological achievement of the year was the invention by I. S. Sacks of DTM and D. W. Evertson of the University of Texas, of a borehole strainrate meter. Dr. Ellis Bolton, the Director of DTM, refers in his report to the remarks made 60 years ago by H. F. Reid of Johns Hopkins University, describing the great value that discovery of a method of determining strains would have for the prediction of earthquakes. Strains in the crust always precede major earthquakes. Bolton adds, "Reid's dream may be on the verge of becoming a reality."

Sacks and Evertson's meter is both inexpensive and extraordinarily sensitive. The principal element of the meter is a water-filled resilient stainless steel tube in intimate contact with the walls of a borehole (150 ft. deep for the DTM prototype). The tube is cemented to the bottom of the borehole, and as the strain changes in the surrounding rock the tube is deformed, forcing liquid through a flow sensor into an air space. The sensor used is a linear solion developed at the Applied Research Laboratory of the University of Texas (Fig. 6). The meter is omnidirectional and its frequency response covers many types of geophysical measurement. Not only are microseisms detected, but also microbarometric pressure influences on solid rock, and the gravitational deformation of the earth by the moon. Distortions as minute as 10^{-7} microns (one-thousandth the distance between atoms in an ordinary chemical bond) are readily detected (Fig. 7). It has been calculated that strain changes of "somewhat over 1 part in 10^{13}" can be measured. The system is many times more sensitive than the most precise strainmeters heretofore available. The prototype meter has operated without fail for more than a year. One may be confident that this revolutionary new instrument will accelerate considerably our acquisition of precise knowledge on the geophysics of the earth. Furthermore, it offers unusual promise of assisting

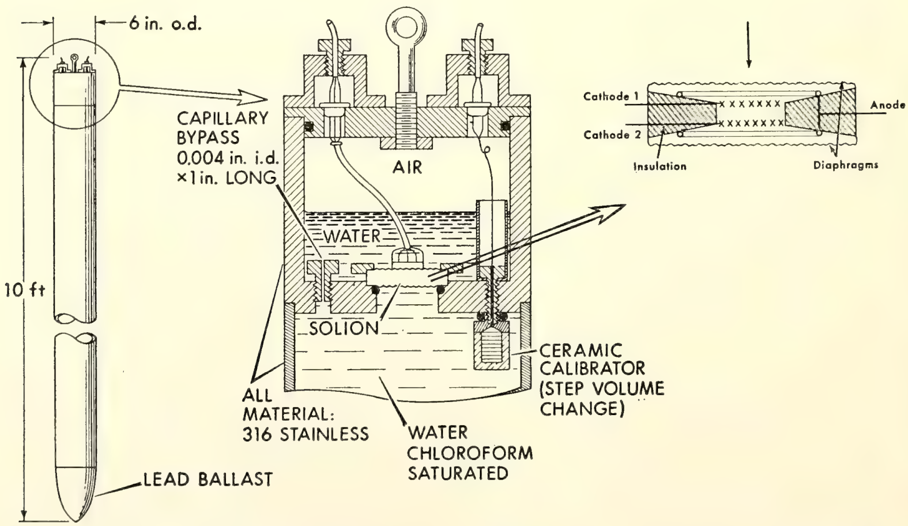

Fig. 6. Prototype borehole strainrate meter, including a schematic drawing of the solion flow velocity sensor. The cathodes are made from very fine platinum basketweave. The electrolyte is potassium iodide and free iodine, and the solion body is made of Kel-F, a plastic. The two half cells have a bias voltage of about 0.5 volts applied; the current in each cathode is a measure of the flow velocity of the electrolyte through the cathodes.

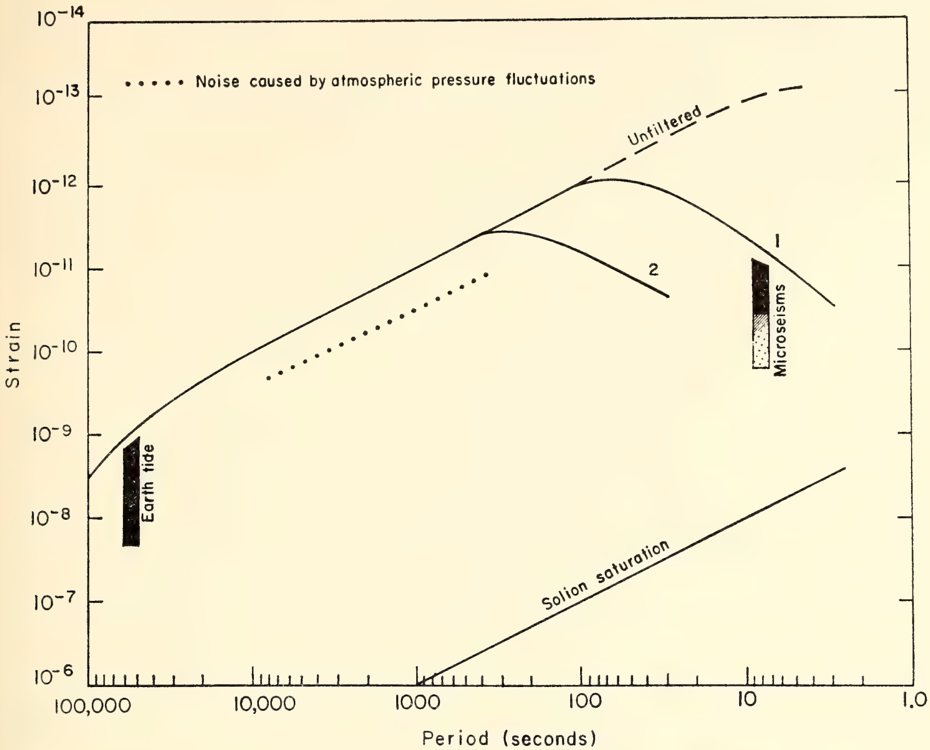

Fig. 7. Frequency response of the prototype strainmeter. The response at short periods is modified by electronic double integration to reduce the sensitivity in the microseism range, 6–20 second period.

in the achievement of a long-held dream in earthquake susceptible regions—the timely prediction of major shocks.

The Biophysics Section. The direct descendant of the interest in biology and biophysics developed more than 20 years ago by a group of nuclear physicists at the Department of Terrestrial Magnetism. Its Biophysics Section (E. T. Bolton, R. J. Britten, J. A. Chiscon, D. B. Cowie, L. J. Grady, B. H. Hoyer, D. E. Kohne, N. J. Reed, and R. B. Roberts) continued during the year its distinguished program of research on molecular processes within individual cells. In recent years the Section's interest has centered on the distinction between the relation of the large amounts of repeated DNA sequences in the genomes of higher organisms, and on the nonrepetitious DNA contained in all living cells. Noteworthy among the achievements this year, which included detailed studies of the DNA of many organisms including bacteria, algae, and higher organisms, was the discovery of a new virus infecting blue-green algae, the development of a new and much more rapid and efficient method of DNA extraction, and, most exciting, the formulation of a new theory for gene regulation in the cells of higher organisms.

Since the first recognition of repeated sequences in DNA within cell genomes about four years ago, many different properties of these sequences have been described. A large number of these descriptions have come from the Biophysics Section itself, and still others from other departments of the Institution. In this

year's report R. J. Britten suggests that the repeated sequences now have a major role in transcription of messages from the DNA and probably have had such a role throughout evolution. However, the way in which they originate and the manner in which they function still remain unknown. Britten summarizes the knowledge thus far obtained about this apparently important part of the genome:

1. Repeated sequences have been observed in all the species tested thus far above the level of fungi.

2. Although the definition of a repeated sequence is currently considered somewhat arbitrary, the amount in individual species varies from twenty percent (sea urchin) to eighty percent (salmon and wheat). Britten believes that future observations will increase the total quantity of repetitive DNA recognized.

3. The number of repetitions within a single genome among the species observed varies from fifty times that expected for single copy DNA (the fruit fly, *Drosophila*) to two million times (guinea pig).

4. There is a wide range of thermal stability for repeated sequences which have been "reassociated." The "families" of sequences with the highest thermal stability also have the largest number of members in the family. It is thought that they originated most recently in the evolutionary process. Since a range of thermal stabilities may be found within a single genome, it is possible that different stages of evolution among higher organisms are represented physically in the repeated sequences.

5. The repeated sequences appear to be scattered throughout the genome, the interspersion being at a surprisingly fine scale. Fragments of about 1.5 million daltons[11] appear to contain both repeated and nonrepeated sequences.

6. Some families of repeated sequences apparently are of great age on the evolutionary scale. This is suggested by the wide degree of difference in nucleotide sequences among the members of some families. Additional strong inferences are given by the sequences held in common among organisms such as fish and mammals, whose common ancestors date back hundreds of millions of years.

7. Each species appears to have a distinct pattern of frequency and precision among the repeated sequences. During the year, for example, Britten and Jean Smith analyzed the bovine genome and found that calf DNA is dominated by a 66,000-copy component that makes up 37 percent of the original DNA in the calf genome. In the human being there is a component with about the same frequency, but it contains much less of the total DNA. The usual pattern appears to be a small number of "families" of repeated sequence within an individual species.

8. RNA complementary to the repetitive DNA sequences has been observed in every cell type examined thus far by the Biophysics Section. It is also known that individual sets of repetitive sequences are transcribed in different tissues and at different stages of development. The large redundancy of RNA during the embryonic development of the toad, *Xenopus laevis,* which has been studied extensively by the Department of Embryology, is an example referred to later in this report.

Blue-Green Algae and Their Viruses. It thus appears that the repetitive sequences of DNA may offer an extraordinarily good indicator for pathways of evolution. One of the groups of organisms on which the Biophysics Section centered its attention during the year was the class of blue-green algae or Cyano-

[11] A dalton is a unit of physical measure equal to about one-sixteenth the mass of the oxygen atom.

phyta. The blue-green algae and the bacteria both lack well-defined nuclei. In this they are basically different from all higher cell types, which have true nuclei bounded by nuclear envelopes. The Section's laboratory studies have brought out another significant distinction between bacteria and blue-green algae on the one hand and organisms with nucleated cells on the other: The DNA of the former is generally nonrepetitive, whereas the DNA of nucleated cells contains large quantities of repeated DNA sequences in addition to the nonrepetitive DNA. At the same time the blue-green algae (but not most bacteria) share with the higher plants the capacity for oxygen-evolving photosynthesis. These characteristics have led the Section to study the blue-green algae as a system bridging "the apparent evolutionary discontinuity" between bacteria and higher organisms.

D. B. Cowie and L. K. Prager report this year on their progress in the first experiments undertaken by the Section on the blue-green algae. Prior studies by other research workers had resulted in the isolation of a virus (LLP-1) that can lyse some species of three genera of blue-green algae (*Lyngbya, Plectonema,* and *Phormidium*). The common viral host-range specificity of these species suggested to Cowie and Prager that they might be evolutionarily related. Cowie and Prager's studies indeed did reveal homologies among them in nucleotide sequences (Fig. 8). Furthermore, a high degree of precision in base-pairing was found when the DNAs of species from the three genera were reacted with each other. However there were no DNA-DNA reactions between the lysing virus (LLP-1) and the algae, indicating that the algae virus-host system is similar to those of nonlysogenic phages and their bacterial hosts.

In the course of experiments with another blue-green species of the genus *Oscillatoria* (1270) Cowie and Prager discovered a new lysogenic virus carried within the algae but capable of infecting the three blue-green species of *Lyngbya* (488), *Plectonema* (597), and *Phormidium* (485). Hitherto lysogeny [12] has been known only among bacteria. It would appear that the *Oscillatoria* virus discovered during the year is the first lysogenic one known outside the bacterial class.

Further studies designed to test relationships among the lysed and lysogenic blue-green species disclosed information suggesting some rearrangements in the prevailing taxonomy of the class of blue-green algae as a whole. For example, DNA-DNA agar tests showed one species of *Lyngbya* (621) to be less closely related to another *Lyngbya* (488) than to *Phormidium* (485) and *Plectonema* (597). A still more precise reaction with another species (*Anacystis nidulans*) strongly suggested a taxonomic reclassification of this species.

The year's studies with blue-green algae thus have yielded a more detailed—and new—picture of relationships within the class, and have revealed an important new characteristic shared with bacteria: the possibility of the presence of a lysogenic virus on the genome of one blue-green species, which is able to infect at least three others.

New Method of DNA Purification. A new method of DNA purification was developed during the year by R. J. Britten, M. Pavich, and J. Smith. Mr. Pavich, a summer student with the Biophysics Section, was making a series of exploratory measurements on the effect of urea and various concentrations of a phosphate buffer on the binding of DNA and RNA to hydroxyapatite in a column, a material customarily employed for this purpose. Unexpectedly, experiments showed that no RNA was bound when urea and the phosphate buffer were present in certain

[12] The presence of a virus on the genome of one species benign to it but infective to other species.

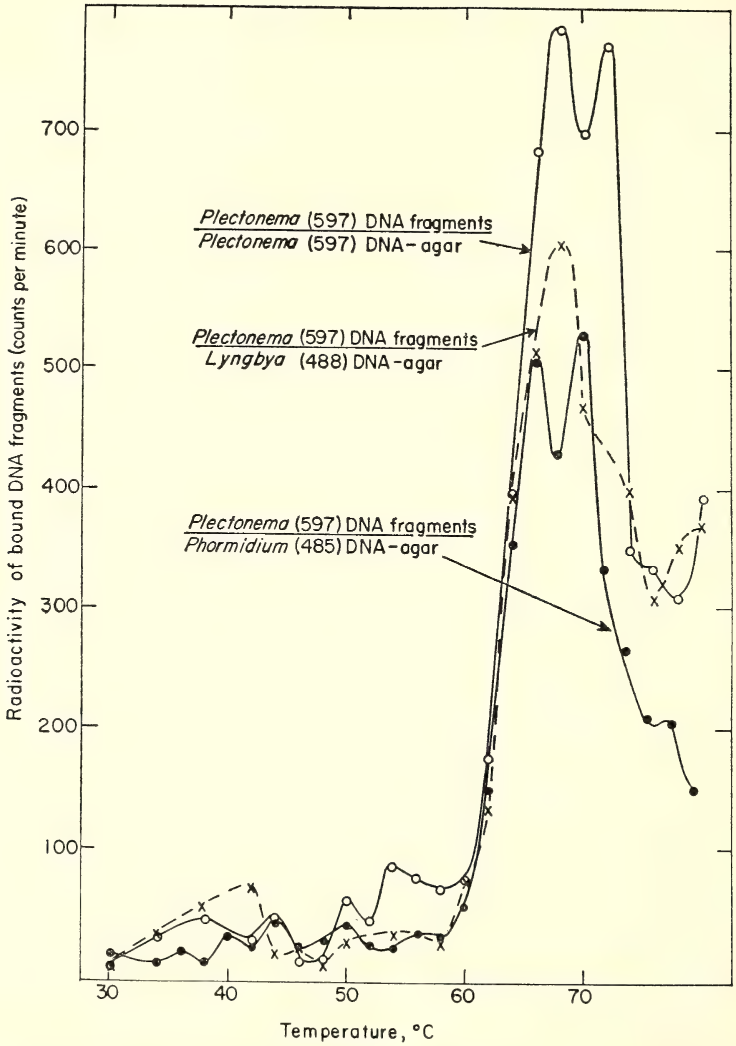

Fig. 8. Thermal elution profiles characteristic of the reaction of radioactive *Plectonema* (597) fragments with *Plectonema* (597) DNA-agar (open circles); with *Lyngbya* (488) DNA-agar (crosses); and with *Phormidium* (485) DNA-agar (solid circles). The homologies of *Plectonema* with the other two algae are clearly visible in the higher temperature fractions.

concentrations. It was then found that DNA of an unusually high degree of purity could be prepared directly from tissues by the urea, or MUP, method, as it has come to be known. DNA of comparable purity, if prepared by standard methods, requires a lengthy procedure that includes successive stages of enzyme treatment, deproteinization, and precipitation.

Not only is the MUP method more rapid, less expensive, and more efficient, but it also appears capable of recovering DNA fractions not hitherto separated by the standard methods. Britten, Pavich, and Smith found that a low melting temperature fraction of *Neurospora* DNA was separated in quantity for the first

time by the MUP method. This DNA fraction amounts to about 25 percent of the total DNA recovered. A new view of the DNA of a widely used experimental organism has already been obtained.

The new method has been successfully used for extraction of DNA from tissues of many widely differing organisms, including blue-green algae, amoebae, *Neurospora, Lactobacillus, Escherichia coli, Amphioxus,* Brachiopods, King crab, iguana, chicken, calf, mouse, and man.

Repeated Sequences in Bacterial DNA. The identification last year of nucleotide sequences that code for ribosomal RNA has led J. A. Chiscon and D. E. Kohne to look for repetitive DNA sequences in bacteria. By employing repeated cycling in the usual DNA separation procedures they isolated multiple copies of DNA from *Escherichia coli* cells. They estimate that these copies may represent as much as 4–5 percent of the total DNA of the stationary stage of *Escherichia coli* cells. The fraction appears to be heterogeneous, with at least two components, and differing degrees of multiplicity at different stages of culture growth. Chiscon and Kohne suggest that this multiple copy DNA is not part of the actual bacterial genome. If this proves to be true, it will be a radical discovery, for, as earlier stated, it has been generally believed that such replication is characteristically absent in bacteria and the blue-green algae. The matter will be pursued further, using a relatively quick and simple method now available for isolation and characterization of episomal and plasmid DNA.

A New Theory of Gene Regulation for Higher Cells. The observations and experiments that have gradually enlarged our knowledge of repeated sequences in the DNA of higher organisms have led R. J. Britten of the Section, and E. H. Davidson of Rockefeller University to propose a new model of gene regulation for all higher organisms.

One of the great contemporary issues of biology concerns an understanding of the mechanisms of cell differentiation. This is a principal objective of the entire Department of Embryology of the Institution, described later in this report. Britten and Davidson introduce their model by observing that "Cell differentiation is based almost certainly on the regulation of gene activity, so that for each state of differentiation a certain set of genes is active in transcription and other genes are inactive." Evidence for this observation is provided by current knowledge of the genome of the cell. The cells of any given organism generally contain identical genomes. In higher cell types much of the genome is known to be inactive. Different cell types are known to synthesize different ribonucleic acids. Britten and Davidson state that their model suggests a contemporary function for the repeated DNA sequences, and also suggests their possible evolutionary role as the raw material for creation of new gene sequences.[13]

Britten and Davidson identify as parts of their model (Fig. 9) producer genes, receptor genes, integrator genes, sensor genes, and activator RNA. A sensor gene is a nucleotide sequence serving as a binding site for agents that induce specific responses in the genome. An integrator gene synthesizes the activator RNA in response to a signal from the sensor gene. The activator RNA forms a sequence-specific complex with receptor genes that are linked to producer genes. Britten and Davidson postulate a single-stranded RNA molecule, but double-stranded (native) DNA as part of the receptor-producer complex. The receptor gene is linked to the producer gene, and causes a transcription of the producer gene to occur when the sequence-specific complex is formed between the receptor and the

[13] Roy J. Britten and Eric H. Davidson, "Gene Regulation for Higher Cells: A Theory," *Science,* 25 July 1969: 349–357.

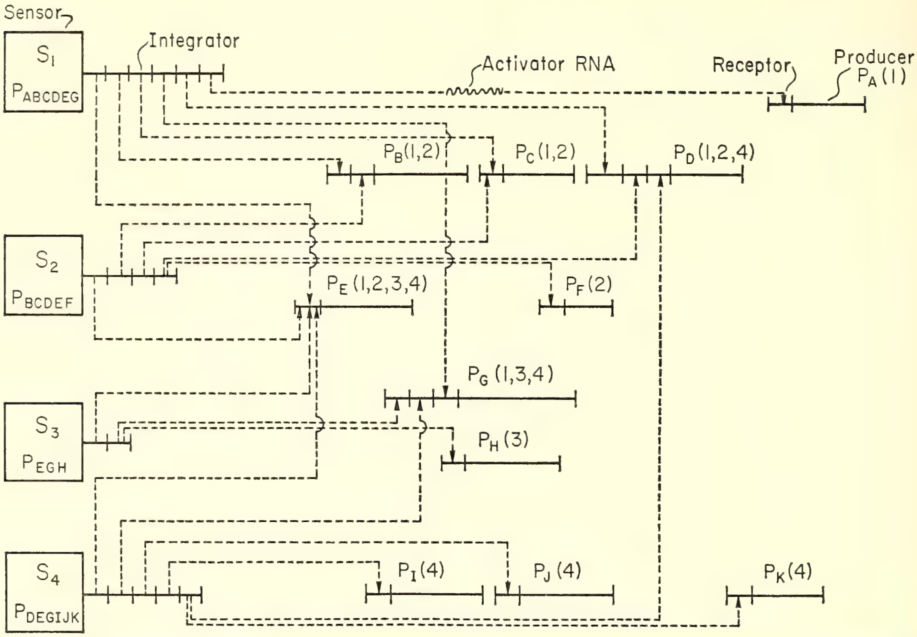

Fig. 9. A diagram of the Britten-Davidson model, suggesting the existence of overlapping batteries of genes, and the manner in which control of their transcription might occur. The dotted lines symbolize the diffusion of activator RNA from its sites of synthesis, the integrator genes, to the receptor genes. The numbers in parentheses show which sensor genes control the transcription of the producer genes. At each sensor the battery of producer genes activated by that sensor is listed. In reality many batteries will be much larger than those shown and some genes will be part of hundreds of batteries.
(R. J. Britten and E. H. Davidson, *Science,* 25 July 1969: 351.)

activator RNA. The producer gene usually is part of a set of producer genes activated in the process started by the sensor gene. The producer genes yield template RNA molecules or other species of RNA, excepting those directly concerned with gene regulation. Britten and Davidson mention as examples of the producer genes those on which the messenger RNA template for a hemoglobin subunit is synthesized.

They cite in support of their theory previous experimental observations on regulatory genes, the known sensor elements in physiological systems, the number of functionally linked enzyme systems, and the known existence of RNAs for which there is no known function.

Barbara McClintock, of the Genetics Research Unit of the Institution, in particular has produced evidence of regulator genes through her pioneering studies of the maize genome. Britten and Davidson consider that McClintock's results fit their model very well. They further note the functional linkage in at least 16 enzyme systems, more than half of which contain more than ten different enzymes. The citric acid cycle, for example, has 17 different enzymes associated with it. Furthermore, the same enzyme is to be found in widely differing types of tissue. The authors of the theory say that direct contiguity of active producer genes could not account for such a pattern of overlapping activity if only a single copy of each gene were present in the genome. A mechanism is required

for coordinating the activity of noncontiguous systems of producer genes for each state of differentiation.

The existence of many chemically defined agents that can induce large-scale changes in specific target tissues is cited as fitting the role of sensor elements in the Britten-Davidson model, including the integrator gene function. Such agents include steroid hormones, polypeptide hormones, plant hormones, vitamins, and embryonic inductive agents.

Among the RNAs that have been described thus far are some that appear to be specific to the nucleus, where the Britten-Davidson activator RNA would be located. Furthermore, these nuclear-specific RNAs perform experimentally in the manner assigned to the activator RNAs in the Britten-Davidson model.

Britten and Davidson state that the model supplies a new means of visualizing the process of the evolution of life. The inactivity of DNA sequences, unless specifically activated, allows for the accommodation of new and "even useless or dangerous segments of DNA such as might result from a saltatory replication." The model appears to have a needed combination of conservatism and flexibility. Preexisting useful batteries of genes will tend to continue functioning. At the same time new integrative combinations of preexisting producer genes can occur. Lastly, a mechanism for divergence is afforded, through base changes in the individual sequences within a DNA family. Thus new nonrepetitive DNA sequences could arise from repetitive ones. Such changes could also be reversible. Britten and Davidson conclude, "The potentiality for smoothly changing patterns of integration among many sets of producer genes supplies a mechanism for direct adjustment by natural selection of the organization of systems of cellular activity." Selective factors may influence the integrative gene configurations of any organism. The rate of evolution, and its direction (i.e., toward greater or less complexity) are thus themselves subject to control by natural selection.

The model stimulates further consideration of a fascinating field—the evolution of regulatory systems in all life.

Genetics Research Unit

1968–1969 Expenditures:
Operating $186,744.17
Equipment $5,464.43

In an extraordinarily rewarding essay that forms a major part of this report, Dr. Alfred D. Hershey, Director of the Genetics Research Unit, examines the relation of microbiological and biochemical genetics to classical genetic theory.

Hershey commences his essay by noting the distinction between genotype, the genetic constitution of an organism, and its phenotype, or the visible expression of its genes in an individual, probably first observed by Mendel.[14] Mendel's great contribution against a background of this complex concept was the demonstration that inheritance depends on unit factors. Mendel indeed set the direction that has characterized the study of inheritance to this day. Noting the work of T. H. Morgan and others who followed directly, but much more elaborately, the lines set by Mendel, Hershey concentrates on the important steps taken in biochemical genetics after 1940. First came the one gene–one enzyme hypothesis evolved from the work of Beadle and Tatum and their colleagues on the bread mold, *Neurospora.* This important hypothesis, which Hershey restates in terms of current understanding as "one gene determines the amino acid sequence of one enzyme," was not accepted until about 1951 when Horowitz and Leupold demon-

[14] Gregor Mendel: 1822–1884.

strated that only one gene functions in the synthesis of a single enzyme. In the context of the one gene–one enzyme hypothesis, principal subsequent developments were the discovery of two subclasses of genes—the regulator genes and genes that encode the structures of ribosomal and transfer RNA—and of course the famous elucidation of the structure and function of DNA, the material of the gene itself.

The initial aim of chemical genetics, Hershey says, was an understanding of the structural and functional basis of genotypic determination of phenotype. This has been achieved, thanks to the revelation of the structure of DNA, which commenced with the Watson-Crick hypothesis in 1953. He summarizes this knowledge: (1) the genotype resides in DNA; (2) nucleotide sequences in single DNA strands afford a code for one-to-one transcription in DNA replication, and synthesis of RNAs; (3) sequences in one of the two DNA strands represent a second code translatable into amino acid sequences; and (4) gross structure can be directly determined by subunit structure. As proof of the latter Hershey cites the reconstruction of certain virus particles from their molecular constituents, and the joining of separated bacteriophage tails and heads to make viable virus particles. The most surprising thing about the denouement in elucidating gene action, according to Hershey, was its simplicity. The universality of these gene relations and the exploitation of a common genetic code in all living forms points to a unique origin of life, "the only economical explanation."

Hershey then goes on to discuss some limitations of the gene theory as it has been refined by molecular genetics. Perhaps the foremost question is the old one as to whether or not all heritable characteristics are determined by genes—a question that has never been finally answered. In spite of the dramatic evidence yielded by experiments with viruses, Hershey suggests "The inference that all three-dimensional structure is encoded in nucleotide sequences does not necessarily follow." Observations on protozoans like *Paramecium* and *Stentor* raise serious questions about such an inference. In *Stentor* a "primordium" in the cell cortex (outer membrane) has been shown to be indispensable to development and persistent through both sexual and asexual reproduction. Growth, division, and continuity thus are exhibited by a cellular element that persists in the cell in only one copy.

A second question not answered by gene theory is the phenomenon of cell polarity, shown in experiments with *Stentor coeruleus* by Tartar and others.[15] Cell polarity is the capacity of the cell to reorient itself into normal pattern when parts are displaced by surgical intervention and then rejoined in abnormal configurations. Polarity has been demonstrated to reside in every part of the cell cortex.

Hershey adds that supramolecular patterns also are observable in bacteriophages, apparently residing in the structures of individual molecules. He considers cortical polarity a phenomenon whose structure and processes should be analyzable. This poses an intriguing task for future molecular biologists.

DNA Phenotypes. Relatively few years ago it would have been inconceivable that DNA itself might be considered to manifest a phenotype. Hershey shows, however, that this concept is now supported by a great variety of experimental evidence. The discovery in 1953 that the bacteriophages T2, T4, and T6 contain glucosylated hydroxymethylcytosine led to a series of experiments in which Kornberg and others showed that a dozen or more bases, including artificial ones, are equivalent to the guanine, cytosine, adenine, and thymine of which DNA typically

[15] V. Tartar, *The Biology of Stentor,* Pergamon, London, 1961.

is composed. The genetic message thus is "a specified sequence of four nonequivalent units." The similar chemical differences (methylation of adenine and cytosine) have been observed in strains of *Escherichia coli.* There are thus optional phenotypes exhibited in DNA composition among bacteria and phages. Diverse phenotypes are also seen in DNA structure (rings, terminal repetitions, terminal cohesive sites, etc.). The amount of DNA per cell also varies. This poses a highly significant question about the amounts of nongenic DNA: "What functions of DNA remain to be discovered?" Hershey summarizes the evidence on DNA variability by saying, "The general implication seems to be that nucleotide sequences are subject to evolutionary constraints that have nothing to do with the genetic message proper."

Hershey concludes with a discussion of recent work in his own laboratory. He remarks that the most puzzling aspect of DNA phenotypes is the distribution of nucleotides in the molecules. Nucleotide composition is generally expressed in terms of the molar fraction of guanine plus cytosine (GC). More than ten years ago analyses of a number of bacterial DNAs showed a range from 26 to 74 percent in GC content. Later study (Sueoka, 1961) found no correlation in the frequencies of the amino acids leucine, valine, and threonine from whole cellular protein with the GC content of DNA in a number of microbial species. Other amino acids showed only weak positive or negative correlations. These observations, together with the fact that proteins also vary phenotypically and that, as Hershey says, "functional requirements do not impose severe restrictions on the composition of proteins," led to the conclusion in 1962 that the composition of DNA was determined mainly by "mutational habit," that is, mutational interconversion between guanine-cytosine pairs and adenine-thymine pairs. If this conclusion were correct, guanine-cytosine pairs should be distributed at random among DNA fragments of gene size or larger. However, recent analyses by A. M. Skalka and H. Yamagishi, Fellows at the Genetics Research Unit, show that the distributions are never random.

Yamagishi during the year analyzed the DNA of *E. coli,* and showed that fragments of the size of individual genes range in GC content from 39 to 56 percent, with an average at 51 percent (Fig. 10). A similar distribution of DNA was observed in the genome of *Bacillus subtilis.* In collaboration with I. Takahashi of McMaster University, Yamagishi showed by genetic tests that regions of exceptional GC content in *B. subtilis* include typical genes of the species. This means that local variations in composition do not reflect a temporary condition of the chromosome.

Skalka examined a number of phage DNA species by density analysis of molecular halves and smaller fragments. She found that the DNA of some phages (lambda 434, 82, 21, P2, P22) consist of dissimilar halves containing 37 percent, 43 percent, 48.5 percent and 57 percent GC. Hershey calls these asymmetric DNAs. Phage lambda, he thinks, may be considered a representative of a class. If so, "asymmetry of DNA structure, clustering of genes of related function . . . and propensity toward interspecific genetic recombination form a seemingly harmonious set of class characteristics."

The conclusions from Skalka's and Yamagishi's experiments may be viewed in the light of a remark made by Hershey in introducing their experiments. Noting that GC content is not random in the genome he said, "One must conclude either that DNA composition does reflect specialized functional adaptations or that interspecific genetic recombination is frequent with respect to the evolutionary time scale. Perhaps both possibilities should be considered likely. In any

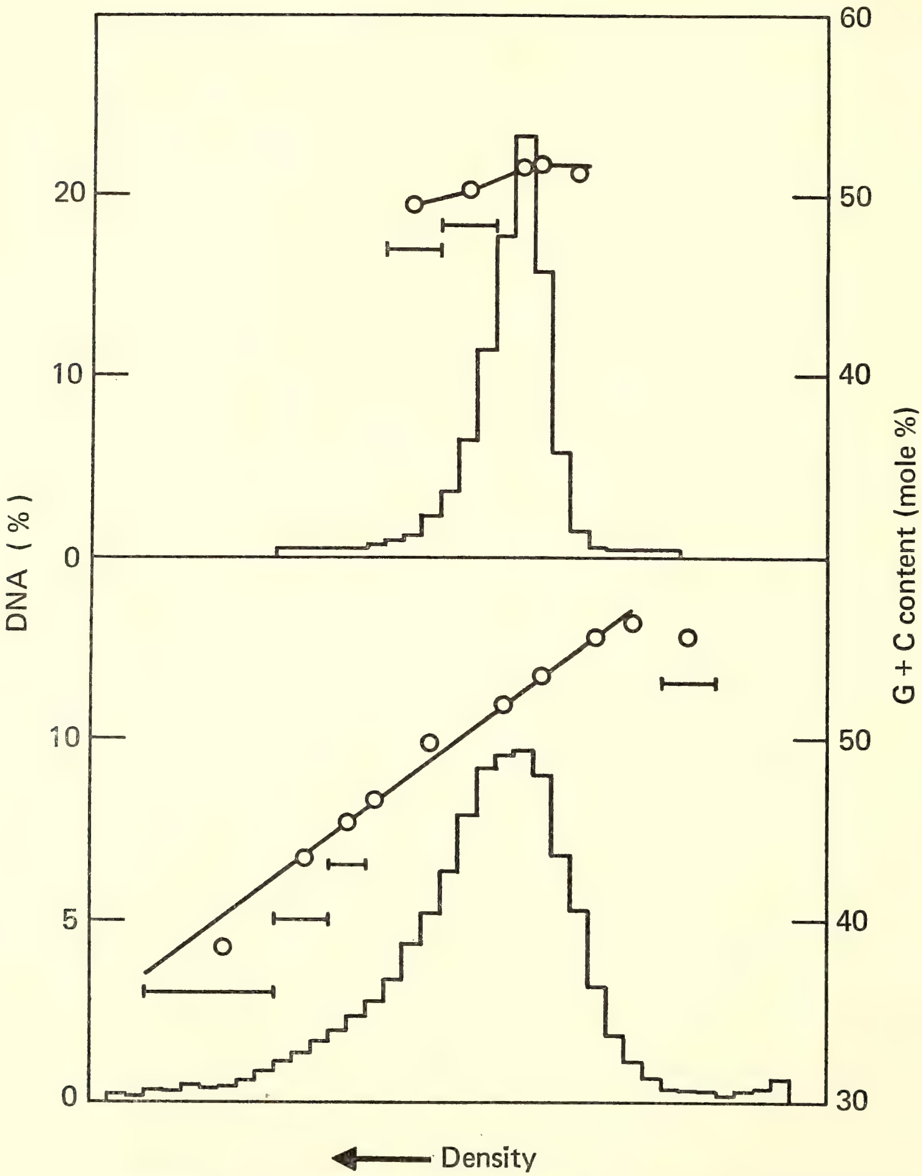

Fig. 10. Distribution of guanine + cytosine (GC) content in fragments of *Escherichia coli* DNA. Upper: fragments of molecular weight 70 million (about 10^5 nucleotide pairs). Lower: fragments of molecular weight 1.3 million (1800 nucleotide pairs). In both parts, histograms show distributions of DNA with respect to buoyant density in Hg-Cs_2SO_4, and curves show the GC content of fractions. Single fractions or pooled fractions (indicated by horizontal bars) were analyzed directly to get the points on the curves.

case, the hypothesis of domination by mutational equilibria loses its force." It is clear that there are still very important questions before molecular biology, and that its methods may continue to provide a significant tool of scientific discovery for some time to come.

Department of Embryology

1968–1969 Expenditures:
Operating $554,348.13
Equipment $96,258.05

The Department of Embryology is devoted to the study of the processes of development in living organisms. Dr. James D. Ebert, Director of the Department, has observed that the spectrum of development grades into the rapid processes of biochemistry at one end, and into the slow processes of evolution at the other. Just as the continuous presence of a chemically defined hereditary material, DNA, in successive generations of a species permits quantitative study of cause and effect in evolution, the presence of like DNA in all the cells of a single developing organism is the starting point for the study of developmental mechanisms. Dr. Ebert further believes that the most fruitful new generalizations in embryology are likely to emerge from "the frame of perception provided by molecular genetics: the concept of levels of control and their interactions, [and] of regulation." The work of the Department during the year reflects this judgment. Molecular biology and genetics are receiving increasing emphasis in a department that for forty years has been a leader in two other subfields, those of human embryology and reproductive physiology.

The most important techniques in the current progress of embryology are interdisciplinary. The Department's research during the year illustrated this trend, not only in the application of molecular genetics but also in the use of virology to probe into developmental processes at the cellular level. Three experimental research projects, in which seven members of the Departmental staff participated during the year, illustrate very clearly the Department's judgment as to where the research frontier in embryology and developmental biology lies. They concern mechanisms inhibiting genetic transcription, the nature of mitochondrial replication within a cell, and the relation of tumor-causing viruses to cells.

Experimental Embryology—the Mechanisms of RNA Transcription. A glimpse of the possibilities that lie ahead in applying the concepts and techniques of molecular genetics to problems of development is provided by the progress reported by D. D. Brown, I. B. Dawid, R. H. Reeder, and P. C. Wensink, a Johns Hopkins graduate student, in their continuing study of the genes coding for ribosomal RNA. These genes are the first to be isolated from an animal genome. The ribosomal DNAs of the toad *Xenopus laevis* and of other amphibians, and their products, have been analyzed in detail by Brown and others. The object of the Brown-Dawid-Reeder-Wensink study is a charting of one of the very first steps in development, the action of rDNA and the formation of ribosomal RNA.

Some parts of the process already are known from studies of *Xenopus* cells. In *Xenopus,* ribosomal RNA sequences are initially transcribed from rDNA as a large "precursor" molecule (40S), which then cleaves into one 18S and one 28S rRNA molecule. The precursor contains few (if any) sequences other than those for 18S and 28S rRNA. DNA sequences for the precursor rRNA correspond to half the total length of the isolated homogenous DNA component, which has been designated as ribosomal DNA (rRNA). The precursor sequences have an average deoxyguanylic-deoxycytidylic acid (GC) content of 62 percent. The other half of the rDNA, called "spacer," is interspersed with the precursor

sequences and has a GC content of about 77 percent. The "spacer" sequences are probably not transcribed *in vivo*. The precursor and "spacer" sequences alternate along the length of the DNA. The active and inactive lengths of rDNA have actually been seen and photographed through the electron microscope for the first time this year, by O. L. Miller, Jr., and Barbara R. Beatty of the Oak Ridge National Laboratory. They are illustrated in the reproduction of their photograph in Plate 3.

There are two forms of the *Xenopus* rDNA: that found in oocytes, and a second distinct rDNA found in somatic cells (present in the nucleolar organism). In primary oocytes the rDNA is replicated multiply so that an individual oocyte contains about 4000 nuclear equivalents of rDNA, a thousandfold more rDNA than would be predicted from its complement of chromosomes. Somatic cell rDNA does not have this great redundancy.

It has been reported previously that the somatic rDNA and the extra replicas of oocyte rDNA differ from each other in buoyant density (*Year Book 67*). The buoyant density of somatic rDNA is lower by 6 mg/cm^3 than that of the extra copies. Having obtained both the somatic rDNA and extra copies of oocytes in pure form, Brown and his colleagues were then able to show that the two DNAs differ in the degree to which they are methylated, the somatic rDNA containing about 4–5 percent 5-methyl deoxycytidylic acid (MeC) while the extra copies contain less than 0.2 percent MeC. The presence of methyl groups is known to lower the density of DNA in cesium chloride and the content of MeC in somatic rDNA is probably sufficient to account for its lower buoyant density.

At this point the trail on this research frontier becomes less definite. The location and description of these genes is only a beginning. Knowledge must be obtained about the way in which gene activities are regulated. What is the basis for differential gene expression? Little is known about the way in which cytoplasmic factors may affect the genome. It is known that in *Xenopus,* rDNA functions during oogenesis and again after gastrulation, but not during cleavage. K. Shiokawa and K. Yamana of Kyushu University have described a cytoplasmic factor obtained from cleaving embryos which inhibits the formation of rDNA when it is added to embryonic cells at stages when the rDNA is otherwise known to be active. However, the evidence presented does not show whether the cytoplasmic factor inhibits transcription (i.e., inhibits synthesis of 40S rRNA) or "processes" 40S rRNA to the 28S and 18S components. The potential importance of the observation is clear: there are few leads to the isolation of possible repressors in embryonic cells. It will be necessary to establish the *level* of the inhibition in order to understand the basis for differential gene expression.

Establishing the level of inhibition and the manner of functioning of the genes requires: (1) isolation and characterization of both the rDNA and rRNA, and (2) the development of a system for synthesis of the products of rDNA *in vitro*. The first has been accomplished. During the year Brown, Reeder, and their colleagues also report substantial progress on the second. Using a system in which *Xenopus* rDNA is transcribed by *E. coli* RNA polymerase they appear to have obtained high fidelity transcription of rDNA *in vitro*. They have developed a sensitive assay which measures how much of each strand of the double-stranded rDNA is transcribed, as well as the amount and kind of RNA transcribed from the spacer region of the rDNA. The rDNA contains two strands, the heavy (H), which is the one transcribed *in vivo,* and the light (L) strand. The technique actually separates the two. Studies of the complementary RNA synthesized from rDNA as template show both rRNA and some RNA corresponding to the

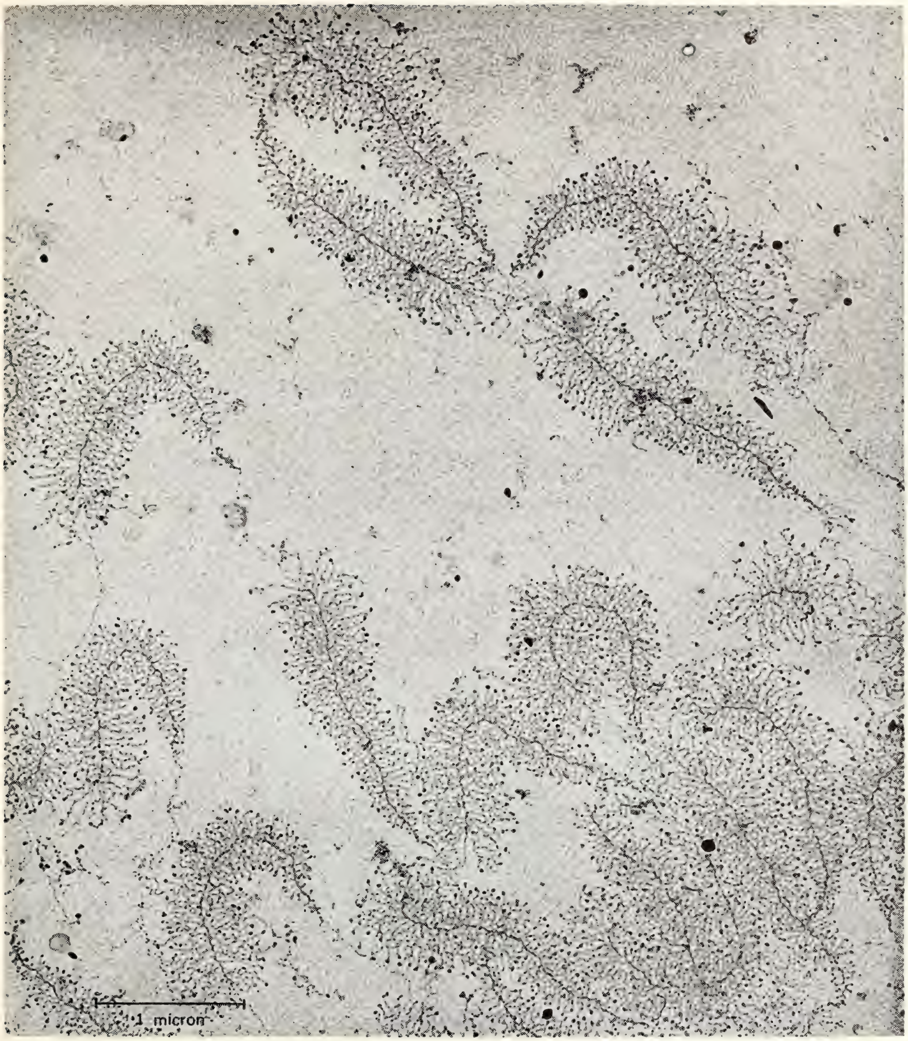

Plate 3. Electron micrograph of the transcription of precursor RNA from rDNA of a *Xenopus laevis* oocyte. The branching patterns show the transcribing segments, which are separated by "spacer" DNA (thin lines along the main axes). Photograph by O. L. Miller and B. R. Beatty, Oak Ridge National Laboratory.

spacer DNA. Chain initiation appears to be very accurate in the *in vitro* system developed, but chain termination less so. Some polymerase molecules apparently continue to transcribe beyond the precursor (40S) sequences, moving into the spacer region of the rDNA.

Mitochondrial DNA. A similar approach is being taken by I. B. Dawid and his colleague, R. F. Swanson, a Fellow of the U. S. Public Health Service, in their study of the role of mitochondrial DNA.

Dawid has continued to focus his attention on mitochondrial DNA in *Xenopus* and its immediate RNA products. He has now obtained evidence that the 21S and 13S RNAs of mitochondria differ clearly from the 28S and 18S ribosomal RNAs previously described. In addition, preliminary hybridization experiments suggest that the 21S and 13S do not share sequence homologies. It seems likely, therefore, that different sequences of the mitochondrial DNA act as templates in their formation.

At the same time Swanson has progressed significantly in studying protein synthesis in mitochondria isolated from ovaries of *Xenopus laevis*. It is known that mitochondria have the ability to synthesize proteins *in vitro*. However, little is known of the source of informational RNA, the products themselves, or the details of the process. Swanson has developed a system in which the three polynucleotides polyuridylic acid, polyadenylic acid, and polycytidylic acid are taken up by isolated mitochondria. The transport of poly-U across the mitochondrial membrane results in an increase in the incorporation of phenylalanine. The system appears to offer promise of identifying the sites of protein synthesis within mitochondria.

Virus-Cell Relations. Another striking example of the effectiveness of interdisciplinary studies is seen in the relationship between virology and developmental biology. More than 50 years ago Peyton Rous discovered the tumorigenic virus that bears his name. In his studies Rous used two pioneering techniques later to be carried further and exploited by students of development. The first was the technique of the transplantation of tissue fragments to the membranes of the chick embryo. This technique was used by several generations of embryologists to study the differentiation of isolated embryonic tissues and to study the graft-versus-host reaction. The second pioneering technique was the use of the enzyme trypsin to liberate cells from clotted plasma on which they were growing. Use of this enzyme was the forerunner of today's techniques of dissociating tissues into component cells, now widely employed in studies of the interaction of embryonic cells to form their characteristic patterns of tissue architecture.

Virology contributed these most useful techniques to the study of development. But it was an embryologist, Ross Harrison, who contributed the technique of tissue culture, a method now widely recognized as one of the methodological cornerstones of virology. Viruses may be now propagated in clonal lines of cells from a variety of sources, normal and abnormal; and clonally derived cells provide the most convenient and reproducible material for studying viral destruction or transformation of cells.

In keeping with this tradition several new research techniques offer promise for the future. One depends on the knowledge that in order to transform a cell a tumor virus must first stimulate the synthesis of the cell's DNA. During the year M. Yoshikawa-Fukada, a Carnegie Fellow, and J. D. Ebert have continued to probe the mechanism whereby oncogenic viral infection activates part of a cellular genome. Their earlier studies (*Year Book 67*) showed that Rous sarcoma virus RNA (RSV-RNA) contains base sequences complementary to those of DNA

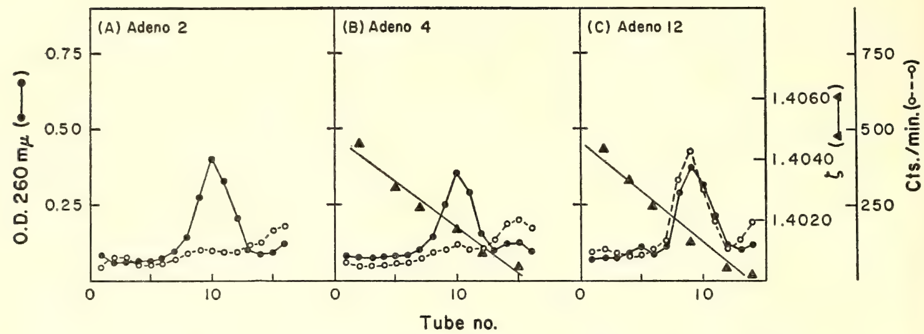

Fig. 11. Hybridization of P^{32}-labeled Rous sarcoma virus DNA with three adenovirus DNAs. The homology of "Adeno 12" and Rous sarcoma virus DNA is shown in the right-hand curves.

from a number of sources. They now report further progress in characterizing these sequences and are attempting to determine their significance in oncogenesis.[16] They noted last year that the part of RSV-RNA which hybridizes with DNA from chicken cells has a high content of adenylic acid. Further studies now reveal this to be a general pattern. The segment of RSV-RNA that is enriched in adenylate is also observed in hybrids with fish and mammalian DNAs. This specific segment of RSV-RNA may be directly involved in the transformation process. It is noteworthy that DNAs of other oncogenic viruses, like the adenoviruses and SV 40 virus, also have a high content of deoxyadenylate. There also is evidence that DNA from oncogenic viruses is integrated into the genome of the host cell.

These and other findings suggest that there may be a "viral oncogenic sequence" and possibly a corresponding sequence in the cellular genome. If such a "viral oncogenic sequence" exists, it should be revealed in viral homologies. As a first test of this hypothesis, Yoshikawa-Fukada and Ebert have studied the relations between RSV-RNA and the DNAs of three adenoviruses—types 2, 4, and 12. This family of adenoviruses is especially interesting in that types 2 and 4 are not oncogenic, while type 12 is highly oncogenic. The results are striking (Fig. 11). RSV-RNA hybridizes far more extensively with DNA from type 12 (oncogenic) than with DNAs from types 2 and 4. Moreover, preliminary analyses indicate that the RSV-RNA combining with adenovirus 12-DNA again has a high adenylate content. Experiments are in progress further to characterize the part of the cellular DNA involved and to determine its role.

Human Embryology and Reproductive Physiology. During the current year the Department of Embryology came to a decision that marked the end of an era that had extended from its founding in 1914. Almost from its beginning the Department has supported two further lines of research in addition to experimental embryology—the fields of human embryology and of reproductive physiology. As Dr. Ebert states in his report: "what were once three relatively small fields of research, in which the subject matter and techniques could be mastered by one or two devoted, energetic investigators, have become three vast areas for exploration, requiring a new depth and range of knowledge and technical sophistication. The 'critical mass' of investigators in each of these areas is no longer one or two." The Department has decided therefore to concentrate its future efforts on experimental embryology. The programs in human embryology and in reproductive physiology will gradually be terminated.

[16] Oncogenesis—the origin of neoplasmic (tumor) growth.

This decision has resulted from a gradual shift in the interests of a department that for more than forty years was outstanding in these fields. Indeed, in human embryology it was preeminent. But it also follows a pattern within the Institution of terminating a line of work that has become so well established elsewhere in the nation that its progress is assured. Research on reproductive physiology, for example, now is expanding rapidly in the United States under the leadership of the National Institute of Child Health and Human Development. The building of a new center for research in human embryology will be assisted by the Department in the transfer of its unique human embryo collection to Wayne State University, Detroit, Michigan. Dr. B. G. Böving, a Staff Member of the Department, will transfer to the University in 1970. Professor Ronan O'Rahilly, a Fellow at the Department, also will move to the University upon the expiration of his fellowship at the Department in 1971 to become Director of Embryology at the University's Kresge Eye Institute.

Department of Plant Biology

1968–1969 Expenditures:
Operating $254,999.85
Equipment $6,340.36

Another most important realm in the world of life is that of plants which capture and store the sun's energy. The Department of Plant Biology, whose work has formed a part of the Institution program since its beginning, centers its attention on this realm.

The student of plants and vegetative processes who seeks precision must be patient, for the complexities of the photosynthetic process seem to be just as recalcitrant to investigation as those of development in higher animals. For many years now the Department's principal line of research has focused on these processes of photosynthesis. Such research was undertaken at the Institution as early as 1911. Much progress has been made, but there is a great deal about photosynthesis that remains to be discovered, as in other significant fields.

Dr. C. Stacy French, Director of the Department of Plant Biology, in a review of the status of research in his field says, "The main tide of scientific effort in photosynthesis flows increasingly toward the more precise refinement of a theoretical picture describing the interrelations between the pigments, enzymes, and intermediate compounds that make up the photosynthetic system." In this system carbon dioxide from the air is turned into the organic components of living matter by a linked series of complex chemical reactions. The reactions are oxidation-reduction processes coupled with phosphorylation systems that store chemical energy. The energy for the system is supplied by light, which causes a flow of electrons from water to reduce carbon compounds and begin the building of life materials.

French notes that the recent tide of scientific effort in his field "left an ebb" in the area from which it originated. The ebb was in descriptive and comparative plant physiology, currently being revived in the United States under the pressures to understand ecology. But the Department of Plant Biology has never allowed its interests in plant physiology to lapse. This continued interest, as will shortly be illustrated, is one of its current strengths. Largely as a result of it, the Department is in a position to apply effectively the intricate concepts of photosynthesis to broader biological questions, such as those of plant evolution.

Evaluation of a New Photosynthetic Pathway. Until recently it was assumed that one general system of photosynthesis was universal among plants. This

system uses the enzyme carboxydismutase to capture carbon dioxide. In 1965 a different "pathway" was discovered in Hawaiian sugar cane by G. O. Burr and his colleagues. M. D. Hatch and others, working in Australia, subsequently demonstrated that the same pathway occurs in a number of other tropical plant species. The new pathway is known as β-carboxylation photosynthesis. The common maize used in agriculture proves to be one of the β-carboxylation species. The β-carboxylation of phospho(enol)pyruvate (PEP) is the reaction that makes this pathway distinctive. It is probably catalyzed by the enzyme PEP carboxylase. At high light intensities and temperatures many of the species using β-carboxylation are capable of considerably higher rates of CO_2 fixation than plants employing the conventional pathway. A peculiarity of the new pathway is that closely related species may or may not have it. Within each of four different plant genera some species have the β-carboxylation pathway, but others use the carboxydismutase system.

O. Björkman, M. A. Nobs, of the Experimental Taxonomy Group, and E. Gauhl, a Fellow at the Department, describe in their report some interesting experiments undertaken with two species of the salt bush, *Atriplex,* a genus widely distributed in North America and Eurasia. One species, *Atriplex patula,* which has the "normal" carboxydismutase pathway, is found mostly in the salt marshes of cool areas. Another, *Atriplex rosea,* which employs the β-carboxylation pathway, typically grows on warm, semiarid sites.

Björkman and Gauhl found that the photosynthetic characteristics of these two species differ greatly. *Atriplex patula* (from the salt marshes), which has a high level of enzyme carboxydismutase, showed a marked inhibition of photosynthesis in the oxygen concentration of normal air (21 percent) as compared to low oxygen concentrations (1.5 percent). By contrast *Atriplex rosea* (warm, semiarid), which has a high level of the enzyme PEP carboxylase, showed no inhibition of photosynthesis by the oxygen concentration present in normal air. *A. rosea* was also capable of higher photosynthetic activity at high light intensities and high temperatures than *Atriplex patula* (Fig. 12). *Atriplex rosea,* like all other known species with the β-carboxylation photosynthesis, has a highly specialized leaf anatomy. Large chloroplast-rich cells surround the vascular bundles of the leaves in a characteristic pattern.

Toward the close of the year Nobs was able to cross the two *Atriplex* species and obtain first-generation hybrids. This achievement opens for the first time the possibility of studying the inheritance of the two pathways of CO_2 fixation in photosynthesis. Preliminary studies suggest that the photosynthetic and biochemical characteristics associated with β-carboxylation photosynthesis are not transmitted by the plastids of the female parent to the offspring. Instead they appear to be under control of the nucleus.

In external morphology, internal leaf anatomy, and some biochemical characteristics, the hybrid is intermediate between the parents. The activity of the enzyme carboxydismutase in the hybrid is about one-half that in *Atriplex patula* and the PEP carboxylase activity is about one-tenth that in *Atriplex rosea.* Photosynthesis in the hybrid is at least as strongly inhibited by the oxygen content of normal air as in the *Atriplex patula* parent. Thus the hybrid is definitely not intermediate between the parental species in photosynthetic activity. Instead, the rate of photosynthesis in the hybrid is lower than in either parent under normal oxygen concentration. It is also interesting that the chlorophyll content of the leaves in the hybrid is lower than in either of the parental species.

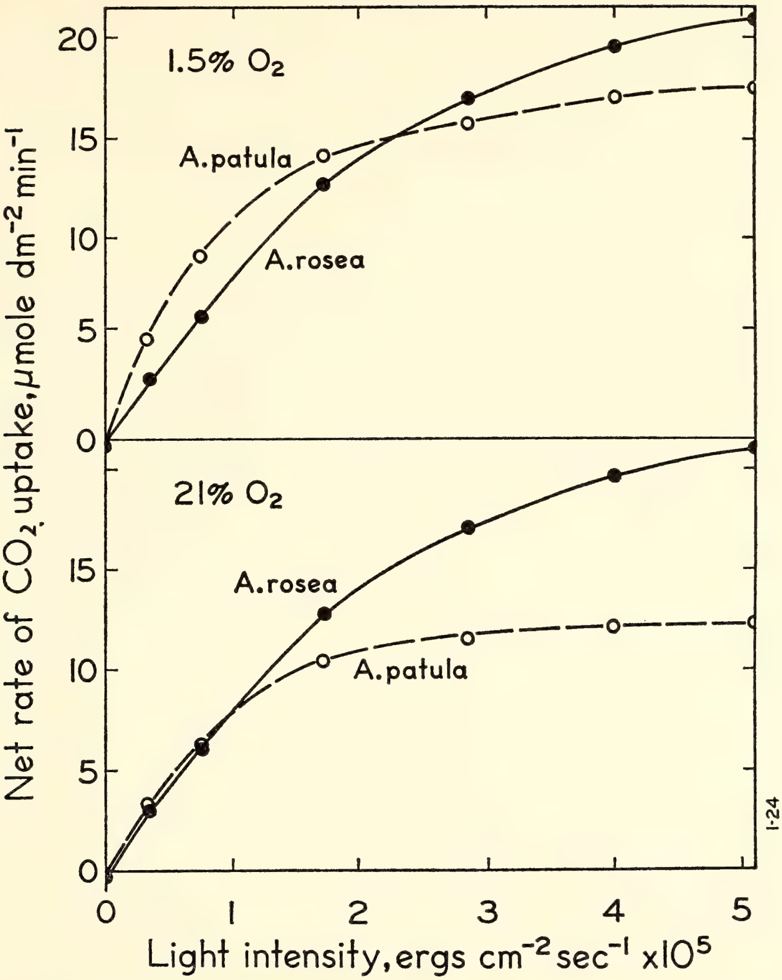

Fig. 12. Effect of light intensity on the rate of photosynthesis CO_2 uptake in 1.5 percent and 21 percent oxygen concentrations by *Atriplex patula* and *Atriplex rosea* leaves. Leaf temperature was 25°C and CO_2 concentration 0.030–0.034 percent. The greater efficiency of the *Atriplex rosea* system at higher light intensities is shown under both O_2 concentrations.

Attempts are now being made to obtain second-generation hybrids, as well as backcross progeny with both parent species. If these attempts are successful they may open the way to an understanding of the physiological, biochemical, and anatomical characteristics essential in β-carboxylation photosynthesis. If this is achieved, our understanding of the molecular mechanism of adapted differentiation and natural selection in plants can be much enhanced.

Biochemical Investigations. The Biochemical Investigations Group of the Department continued its interest in the functional relations between photosynthetic pigments and associated enzymes. There are two subsystems, which have been labeled system I and system II, each of which is comprised of a mixture of pigments and enzymes contained within solid particles. The separation of these two

systems of chloroplasts is a problem that has compelled the attention of many laboratories, including the Biochemical Investigations Group itself (C. S. French, D. C. Fork, J. S. Brown, K. E. Mantai, E. E. Loos, L. O. Björn). These systems of chloroplasts have different reactions, are composed of different pigments, and show striking contrasts in their absorption spectra.

The biochemical group during the year continued the analysis of the spectral characteristics of the two systems, with particular attention to comparing the absorption spectra with the action spectra. Action spectra reveal the light wavelengths that cause specific chemical effects, and hence identify the effective pigments only. Absorption spectra characterize all the pigments present, whether functional or nonfunctional. Dr. French says in the Introduction to his report that action spectra for system I and system II effects in whole cells and in isolated chloroplasts have been measured with adequate accuracy. However, for the partial reactions representing the separate steps of photosynthesis in chloroplast fractions "the precision so far . . . is lamentable."

Efforts were made in several directions during the year to improve the precision of measurement and to uncover functional relationships within and among chloroplast fractions. Thus photochemical reduction of the dye methyl viologen was tried by E. Loos, a Fellow. His first results showed close agreement between the action spectra and absorption spectra of system I particles. Loos' technique gives easily measurable rate determinations at low light intensities.

Another approach to understanding a biological system is to identify the minimum structural unit that can perform a given function. It has long been known that chlorophyll molecules do not act separately in photosynthesis, but cooperate in groups. A few hundred molecules make up the unit for primary conversion of light into chemical energy, but several such units may form larger ones capable of more complex functions. One such larger grouping may depend on a single enzyme for its association and activity. Thus the size of such a unit can be determined if the enzyme molecule can be made ineffective by a single molecule of an enzyme poison.

L. O. Björn, also a Fellow at the Department, undertook such an experiment during the year. He studied the delayed light emission (afterglow) given off by plants transferred from light to darkness. Björn found that the application of *N*-methylphenazonium methosulfate (PMS) accelerates the emission of a long wavelength component of the afterglow known as component V. The afterglow followed the activation of photosystem I by far-red light. Björn estimates the size of the functional unit so measured to be about 100,000 chlorophyll molecules, the size of a morphological unit called a "thylacoid" that is visible in electron micrographs of chloroplasts (Plate 4).

Björn's experiments, like almost every other experiment or observation in such research, emphasizes the complexities of photosynthesis. Component V is only one of several components of the afterglow emission spectrum. The grouping of molecules here postulated only applies to component V. As Björn observes, "the other afterglow components may emanate from units of different sizes." The afterglow is only a secondary phenomenon being used as a small mirror for the activity of system I.

Fellows and Students

The preceding reports of the Departments' scientific activities have included many references to work by Fellows and students who are in residence at the Departments. Two years ago I discussed the place of Fellows in the work of the

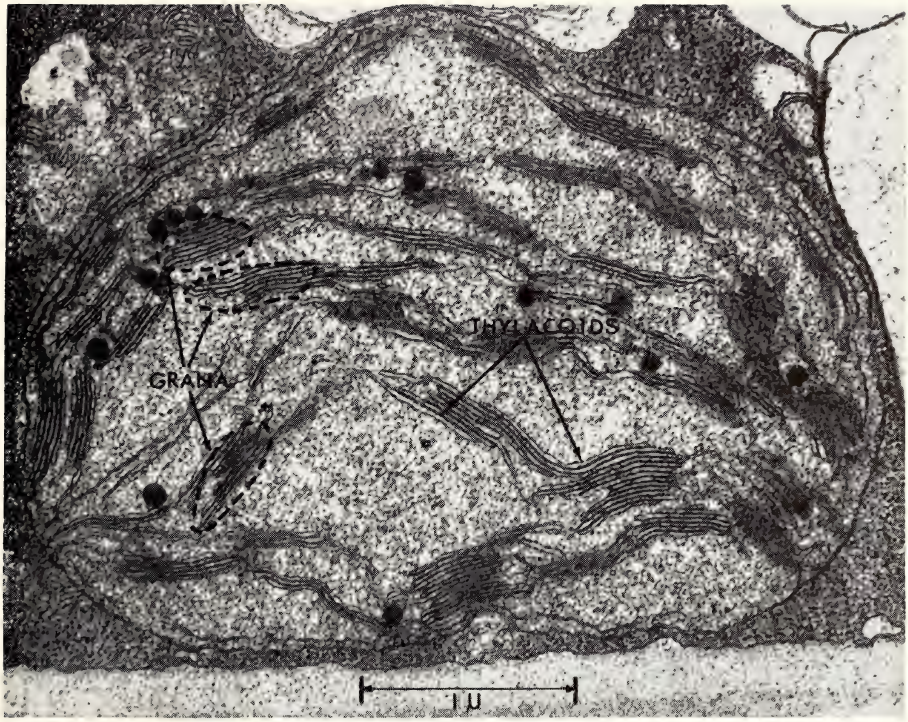

Plate 4, Electron micrograph of a well-developed chloroplast in a vascular bundle cell, showing thylacoids and their grouping as grana. The cell is a mature leaf of the F_1 hybrid *Atriplex rosea* × *Atriplex patula hastata.* (Taken by Dr. John Boynton, Carnegie Institution Fellow, at the Advanced Instrumentation Center, University of California, Davis, California.)

TABLE 1. Fellows at the Carnegie Institution, 1967–1969

Department	Total number 1967–68	Total number 1968–69	Status as of August 1, 1969: Academic positions	Fundamental research	Industrial research	Fellows or students
Mount Wilson and Palomar Observatories	8	5[a]	5	2	...	2
Geophysical Laboratory	21	15[b]	16	1	1	7
Department of Terrestrial Magnetism	10	16[c]	8	2	1	7
Genetics Research Unit	4	4[d]	2	1	...	2
Department of Embryology	12	9[e]	9	3	...	2
Department of Plant Biology	7	7[f]	6	3	...	4
Totals	62	56	46	12	2	24

Number of individuals		84[g]
Individuals' subjects of study:		
Biology	36	
Geophysics and geochemistry	35	
Astronomy	11	
Atomic physics	2	

[a] 4 for second year.
[b] 11 for second year.
[c] 8 for second year.
[d] 3 for second year.
[e] 7 for second year.
[f] 1 for second year.
[g] After subtraction of two-year Fellows.

Institution.[17] Postdoctoral training and the original research of the Fellows have become such important parts of the Institution's life that it is appropriate to bring that general account of their work up to date.

During 1967–1968 the number of Fellows reached a peak of 62 in residence at the five Departments and the Genetics Research Unit. Most were supported from Institution funds, but some fellowship grants were made from private foundation funds, notably those of the Carnegie Corporation of New York, and Federal Government research agencies. In 1968–1969 the number declined by six because of budget constraints, but a very lively program was continued in all of the Departments.

As has been usual in the Institution program, more than half of the 1967–1968 Fellows (34 of 62) remained for a second year. Thus, for two years, 84 individuals participated in the fellowship program. Two-fifths of them were interested in the several branches of geophysics and geochemistry (35), and another two-fifths (36) undertook research in the biological fields, which were about evenly divided between embryology and the two other principal subjects, genetics and plant biology. Eleven Fellows carried out programs in astronomy: all but two in optical astronomy.

I have already mentioned the Mount Wilson and Palomar program of graduate student instruction. In the past every Department has provided some service, facilities, and guidance to Ph.D. candidates. During 1968–1969 there were 47 graduate students associated with four other Departments, for a total of 61 in all Institution facilities. Some were supported by Institution predoctoral fellowship grants or by technical assistantships; all received instruction by members of the senior staff, and all used the Institution's laboratory or observing equipment.

We value our graduate student programs, but the opportunities the Institution offers for postdoctoral training are perhaps even more rewarding. In the post-

[17] *Year Book 66,* Report of the President: 68–70.

doctoral program, which has been enthusiastically developed by all the Departments, promising young scientists can investigate problems of their own choosing, take time to fill in any gaps in their training through seminars and other means, and benefit from the guidance of senior staff members. Most, if not all, of the senior staff members are interested in guiding and actively collaborating with these younger men. The modest numbers and intellectual diversity of the staff at each of our Departments make it possible for a Fellow to have a broad range of highly stimulating intellectual experiences. For the postdoctoral Fellows experience at the Institution generally has led to the attainment of true professionalism in their fields in the shortest possible time.

The range of subjects studied by the Fellows covers almost the entire list of the Table of Contents in the *Year Book*. The Bibliography of each of the Departments for this last year, shown at the end of this report, gives most abundant evidence of the Fellows' productivity and capacity.

When I last reported on our postdoctoral fellowship program in *Year Book 66*, I noted that many of our "alumni" either returned to or took up professorships and other teaching positions. Many of them were considered leaders in their fields at relatively young ages. I also noted the very high rate of return of foreign Fellows to responsible academic posts in their own countries. These same statements continued to be true of the Fellows for 1967–1968 and 1968–1969. More than half (46) of the Fellows have either accepted new positions in academic institutions or returned to those from which they had leave. An additional 12 turned to positions in fundamental research organizations, and 2 went into industrial research. As of August 1969, 24 of the 84 still remained with the Institution in fellowship or equivalent status. Of the approximately 400 Fellows who have become Institution "alumni" since 1952, more than half (215) now hold positions in universities or other academic institutions. Another 81 are occupied in fundamental research, and 28 more are in applied research.

About 40 percent of our Fellows in recent years have been foreign. In 1967–1969, as before, nearly all the Fellows from foreign lands returned, or will return, to posts in their own countries. Almost without exception these people seem to have achieved a sympathetic understanding of the United States in addition to their professional training.

Concluding Note. As in other years, we count among our highest accomplishments in the year 1968–1969 the provision of a useful, even vital, experience to young scientific leaders through our resident fellowships. The meaning of this experience can best be understood by relating it to the earlier descriptions of research results. The Fellows have been able to witness discovery and invention, to share in precise experiment and observation, to see, or even share in, the construction of theory and hypotheses, and to share in searching and methodical evaluations of research frontiers.

Among discovery and invention at the Institution in 1968–1969 was that of the strainrate meter, an instrument of most extraordinary sensitivity for measuring the strains preceding earthquakes, and other earth movements; the invention of an inexpensive new method of purifying DNA, that recovers fractions hitherto lost; the discovery of a new lysogenic virus; and the first isolation of genes from an animal cell.

Experiment and observation in the Institution's program gave new knowledge about the asymmetry of the universe; added substantially to precise knowledge of rock formation, of the energy balance in the earth, and of continental movement; showed an important nonbiological route by which the materials of life disappear into the earth's crust; produced significant information on tumor

virus relations to virally infected cells; charted more precisely the differences between the two principal photosynthetic "pathways," and produced for the first time a hybrid incorporating both the pathways.

Theoretical work resulted in the Britten-Davidson model of gene operation, which distinguishes and articulates the known functional units of DNA and RNA, and in a new model of the evolution of radiogenic elements within the earth's crust and mantle from primordial time.

Among the important critical evaluations of research frontiers mentioned in our reports is one on genetics, another on cosmology, one on the dynamics of the earth's crust and mantle, and one on the relation of biochemical and biophysical research to plant physiology.

It has been a rewarding and exciting year at the Institution.

List of Fellows in Residence Carnegie Institution, 1967–1969

1967–1968	Research Field at the Institution	Employment or Fellowship Status as of August 1, 1969
Mount Wilson and Palomar Observatories		
Arvind Bhatnagar	magnetic fields in and around sunspots	Fellow, Carnegie Institution
Robert J. Dickens	dynamic theory of equilibrium, forms of globular star clusters	Royal Greenwich Observatory, England
Jerome Kristian	determination of the Hubble constant	Staff Member, Mount Wilson and Palomar Observatories
Wojciech Krzeminski	the eruptions of eclipsing binary stars	Polish Academy of Sciences, Institute of Astronomy, Warsaw
John Vincent Peach	the short-period light variations of quasars	Faculty, Department of Astrophysics, University Observatory, Oxford University, England
René Racine	photometry and spectroscopy of clustering of reflection nebulae	Faculty, Astronomy Department, University of Toronto, Canada
David Maurice Rust	solar magnetic field structure outside active regions	Astronomer, Sacramento Peak Observatory, Sunspot, New Mexico
Natarajan Visvanathan	interstellar polarization	Fellow, Carnegie Institution
Geophysical Laboratory		
G. Malcolm Brown	pyroxenes and the genesis of mafic and ultramafic rocks	Professor and Chairman of the Department of Geology, University of Durham, England
Wilfred B. Bryan	numerical and statistical analysis of marine volcanic petrography	Fellow, Carnegie Institution
James R. Craig	silicate-sulfur relationships in ore deposits	Assistant Professor of Geosciences, Texas Technological College

1967–1968	Research Field	Employment or Fellowship Status as of August 1, 1969
Larry W. Finger	crystal chemistry and physics of silicate rock-forming minerals	Staff Member, Geophysical Laboratory, Carnegie Institution
M. Charles Gilbert	high pressure studies of mineral phase relations	Assistant Professor of Petrology, Virginia Polytechnic Institute
Ahmed El Goresy	investigation of sulfides in meteorites	Research Associate, Max Planck Institute für Kernphysik, Heidelberg, Germany
Necip Güven	interaction of micas with X-ray and other radiation	Assistant Professor of Geology, University of Illinois
Stephen E. Haggerty	composition of basaltic iron-titanium oxides	Fellow, Carnegie Institution
Edward C. Hansen	rock deformation under extreme conditions	Shell Development Company, Houston, Texas
Hans G. Huckenholz	mineral phase relations	Professor, Institute for Mineralogy and Petrology, University of Munich, Germany
Jon E. Kalb	experimental techniques in mineralogy	Graduate Student, American University
Ikuo Kushiro	mineral phase relations in the upper mantle	Faculty, Geological Institute, University of Tokyo, Japan
Henry O. A. Meyer	crystal X-ray and electron microprobe analysis of diamonds and their inclusions	Fellow, Carnegie Institution
Richard M. Mitterer	amino acids in fossils	Assistant Professor of Geosciences, Southwest Center for Advanced Studies
S. A. Morse	mineral phase relations	Professor of Geology, Franklin and Marshall College
James L. Munoz	stability relations of staurolite	Assistant Professor, Department of Geological Sciences, University of Colorado
Anthony J. Naldrett	geologic history of sulfide minerals in the Sudbury Basin	Assistant Professor, Department of Geology, University of Toronto, Canada
Harold R. Puchelt	fractionation of sulfur isotopes in geologic processes	Faculty, Institute for Mineralogy and Petrology, University of Tübingen, Germany
Stephen W. Richardson	high temperature and high pressure studies of mineral phase relations	Research Assistant, National Environment Research Council, Grant Institute of Geology, University of Edinburgh, Scotland
William H. Scott	geophysical processes occurring during tectonic activity	Yale University
Josef Zemann	sulfide minerals crystallography	Professor, Mineralogical Institute, University of Vienna, Austria

1967–1968	Research Field	Employment or Fellowship Status as of August 1, 1969
Department of Terrestrial Magnetism		
George E. Assousa	foil excitation spectroscopy	Fellow, Carnegie Institution
Christopher Brooks	isotopic geochronology	Faculty, University of Montreal, Canada
Alfred Chiscon	isolating episomal factor in a strain of *E. coli*	Professor, Department of Biological Sciences, Purdue University
Kyoichi Ishizaka	isotopic geochronology	Faculty, Geological and Mineralogical Institute, Kyoto University, Japan
David E. James	explosion seismology	Staff Member, Department of Terrestrial Magnetism, Carnegie Institution
Peter N. S. O'Brien	measurements of ground motions due to large explosions	British Petroleum Company, Ltd., Middlesex, England
Claude Petitjean	data on polarization in the elastic scattering of protons by lithium-8 nuclei	Swiss Institute of Nuclear Research, Cyclotron Planning, Zurich
Adrian V. Rake	changes in macromolecular components of cultured neural tissue as a result of electrical stimulation	Faculty, Pennsylvania State University
German Saa	seismology in western South America	Faculty, Universidad del Norte, and Universidad de Chile
Alan Stueber	isotope geology of the upper mantle	Faculty, Miami University, Oxford, Ohio
Genetics Research Unit		
Phyllis Bear	growth and inheritance in bacteriophage	Associate Professor, Division of Microbiology and Veterinary Medicine, University of Wyoming
Shraga Makover	replication of DNA in lambda phage at molecular sites	Fellow, Carnegie Institution
Anna Marie Skalka	DNA structure and function	Assistant Member, Department of Microbiology, Roche Institute of Molecular Biology, Nutley, New Jersey
Hideo Yamagishi	nucleic acid structure and function	Molecular Biology Laboratory, Department of Biophysics, Kyoto University, Japan
Department of Embryology		
Hayden G. Coon	somatic cell hybridization	Associate Professor of Zoology, Indiana University

1967–1968	Research Field	Employment or Fellowship Status as of August 1, 1969
Douglas Fambrough	clonal culture of muscles and nerves	Staff Member, Department of Embryology, Carnegie Institution
Masako Fukada	nucleic acid chemistry of cultured animal cells	Fellow, Carnegie Institution
Harold R. Kasinsky (USPHS)	histone synthesis in cleaving embryos of *Xenopus laevis*	Assistant Professor of Zoology, University of British Columbia
Harold R. Misenhimer	placental physiology	Assistant Chief, Obstetrics and Gynecology, Baltimore City Hospital
Ronan O'Rahilly	study of embryo collection	Director of Embryology (designate), Kresge Institute, Wayne State University
Ronald H. Reeder*	methods of covalently joining double-stranded DNA molecules	Staff Member, Department of Embryology, Carnegie Institution
John Sinclair (USPHS)	comparative studies of genes for ribosomal RNA	Assistant Professor, Department of Zoology, University of Indiana
Helge Stalsberg	controlled growth of specific parts of chick embryo heart	Department of Pathology, Ulleval Hospital, Oslo, Norway
Peter Tuft	uptake of water by embryos and its role in morphogenesis	Faculty, Department of Zoology, University of Edinburgh, Scotland
Mary C. Weiss (USPHS)	somatic cell hybridization	Centre de Génétique Moleculaire, Gif-sur-Yvette, France
Shuhei Yuyama	quantifying evidence for stimulation of DNA synthesis by Rous sarcoma virus	Faculty, Department of Zoology, University of Toronto, Canada
Department of Plant Biology		
Eckhard Gauhl	photosynthetic reactions	Botanisches Institut der J. W., Goethe Universität, Frankfurt, Germany
Ulrich Heber	electron transport chain in mutants of higher plants deficient in photosynthesis	Professor, Botanisches Institut der Universität Düsseldorf, Germany
Eckhard E. Loos	production of oxygen in plants during photosynthesis	Fellow, Carnegie Institution
Jean-Marie Michel Marie-Rose Michel	fractionation of chloroplasts	Centre de Recherches de Gorsem, St. Trond, Belgium
James M. Pickett	improved electrode for measuring photosynthesis rates	Assistant Professor, Department of Botany and Microbiology, Montana State University

* Helen Hay Whitney Foundation Fellowship.

1967–1968	Research Field	Employment or Fellowship Status as of August 1, 1969
James H. Silsbury	influence of light intensity on ratio of leaf area to leaf weight	Senior Lecturer in Agronomy, University of Adelaide, Waite Agricultural Research Institute, Glen Osmond, South Australia
1968–1969		
Mount Wilson and Palomar Observatories		
Arvind Bhatnagar*	magnetic fields in and around sunspots	Fellow, Carnegie Institution
Jerome Kristian*	determination of the Hubble constant	Staff Member, Mount Wilson and Palomar Observatories
Deane M. Peterson	astrophysics; short-period light variations in stars	Fellow, Carnegie Institution
René Racine*	photometry and spectroscopy of clustering of reflection nebulae	Faculty, Astronomy Department, University of Toronto, Canada
Natarajan Visvanathan*	interstellar polarization	Research Astronomer, Harvard Observatory, Harvard University
Geophysical Laboratory		
Wilfred B. Bryan*	numerical and statistical analysis of marine volcanic petrography	Fellow, Carnegie Institution
Larry W. Finger*	crystal chemistry and physics of silicate rock-forming minerals	Staff Member, Geophysical Laboratory, Carnegie Institution
M. Charles Gilbert*	high pressure studies of mineral phase relations	Assistant Professor of Petrology, Virginia Polytechnic Institute
Ahmed El Goresy*	investigation of sulphides in meteorites	Research Associate, Max Planck Institut für Kernphysik, Heidelberg, Germany
Stephen E. Haggerty*	composition of basaltic iron-titanium oxides	Fellow, Carnegie Institution
Edward C. Hansen*	rock deformation under extreme conditions	Shell Development Company, Houston, Texas
Jon E. Kalb*	experimental techniques in mineralogy	Graduate Student, American University
Ikuo Kushiro*	mineral phase relations in the upper mantle	Faculty, Geological Institute, University of Tokyo
Ho Kwang Mao	X-ray diffraction studies of effects of pressure on crystal structures and lattice parameters of materials	Fellow, Carnegie Institution

* Also a Fellow in 1967–1968.

1968–1969	Research Field	Employment or Fellowship Status as of August 1, 1969
Henry O. A. Meyer*	crystal X-ray and electron microprobe analysis of diamonds and their inclusions	Fellow, Carnegie Institution
S. A. Morse*	mineral phase relations	Professor of Geology, Franklin and Marshall College
H. R. Puchelt	fractionation of sulfur isotopes in geological processes	Faculty, University of Tübingen, Germany
William H. Scott*	geophysical processes occurring during tectonic activity	Yale University
Douglas Smith	mineral phase relations at high pressure	Fellow, Carnegie Institution
Lawrence A. Taylor	geochemistry and experimental petrology	Fellow, Carnegie Institution
Department of Terrestrial Magnetism		
George E. Assousa*	atomic physics	Fellow, Carnegie Institution
Willy Z. Barreda	seismology	Fellow, Carnegie Institution
Christopher Brooks*	isotopic geochronology	Faculty, University of Montreal, Canada
Alfred Chiscon*	isolating episomal factor in a strain of *E. coli*	Professor, Department of Biological Sciences, Purdue University
Sandro D'Odorico	radio astronomy	Fellow, Carnegie Institution
Joseph W. Erkes	radio interferometry and other aspects of radio astronomy	Fellow, Carnegie Institution
A. J. Erlank	trace elements in ultrabasic rocks	Faculty, Department of Geochemistry, University of Capetown, South Africa
Leo J. Grady	DNA analyses	Fellow, Carnegie Institution
Jaime Guzman	determination of earthquake hypocenters	International Institute of Seismology and Earthquake Engineering, La Paz, Bolivia
Kyoichi Ishizaka*	isotopic geochronology	Faculty, Geological and Mineralogical Institute, Kyoto University, Japan
David E. James*	explosion seismology	Staff Member, Department of Terrestrial Magnetism
Alan T. Linde	seismic studies of the upper mantle	Fellow, Carnegie Institution

* Also a Fellow in 1967–1968.

1968–1969	Research Field	Employment or Fellowship Status as of August 1, 1969
Claude Petitjean*	data on polarization in the elastic scattering of protons by lithium-8 nuclei	Swiss Institute of Nuclear Research, Cyclotron Planning, Zurich
Adrian V. Rake*	changes in macromolecular components of cultured neural tissue as a result of electrical stimulation	Faculty, Pennsylvania State University
German Saa*	seismology in western South America	Faculty, Universidad del Norte, and Universidad de Chile
Erich Steiner	nucleic acid interactions	Fellow, Carnegie Institution
Genetics Research Unit		
Shraga Makover*	replication of DNA in lambda phage at molecular sites	Fellow, Carnegie Institution
David H. Parma	structure of stable heterozygotes in T4 phage	Postdoctoral Fellow, National Science Foundation
Anna Marie Skalka*	DNA structure and function	Assistant Member, Department of Microbiology, Roche Institute of Molecular Biology, Nutley, New Jersey
Hideo Yamagishi*	nucleic acid structure and function	Molecular Biology Laboratory, Department of Biophysics, Kyoto University, Japan
Department of Embryology		
Hayden G. Coon*	somatic cell hybridization	Associate Professor of Zoology, Indiana University
Douglas Fambrough*	clonal culture of muscles and nerves	Staff Member, Department of Embryology, Carnegie Institution
Masako Fukada*	oncogenic viral studies	Fellow, Carnegie Institution
Harold R. Kasinsky* (USPHS)	histone synthesis in cleaving embryos of *Xenopus laevis*	Assistant Professor of Zoology, University of British Columbia
Harold R. Misenhimer*	placental physiology	Assistant Chief, Obstetrics and Gynecology, Baltimore City Hospital
Ronan O'Rahilly*	study of embryo collection	Director of Embryology (designate), Kresge Institute, Wayne State University

* Also a Fellow in 1967–1968.

1968–1969	Research Field	Employment or Fellowship Status as of August 1, 1969
Kenjiro Ozato	developmental biology	Instructor in Biology, Yoshida College, Kyoto University
Ronald H. Reeder*	methods of covalently joining double-stranded DNA molecules	Staff Member, Department of Embryology, Carnegie Institution
Yoshiaki Suzuki	gene coding in the silkworm (*Bombyx mori*)	Fellow, Carnegie Institution

Department of Plant Biology

John E. Boynton	barley chloroplast mutants	Fellow, Carnegie Institution
Lars Olof Björn	determination of accurate action spectra in *Chlorella*	Associate Professor, Lunds Universitet, Sweden
Eckhard Gauhl*	photosynthetic reactions	Botanisches Institut der J. W. Goethe Universität, Frankfurt, Germany
Eckhard E. Loos*	production of oxygen in plants during photosynthesis	Fellow, Carnegie Institution
Kenneth E. Mantai	effects of ultraviolet light on pigment systems using fluorescence and absorption spectroscopy	Brookhaven National Laboratories, Upton, New York
Norio Murata	fluorescence spectra of photosynthetic pigments and transfer of energy between them	Fellow, Carnegie Institution
Colin Wraight	influence of conformational changes on chloroplast fluorescence	Fellow, Carnegie Institution

* Also a Fellow in 1967–1968.

1968–1969 BIBLIOGRAPHIES

Two hundred and four papers were published by Staff Members, Research Associates, Fellows, and members of technical staffs of the Observatories and Laboratories in professional journals and books during the year 1968–1969. The journals were published in 11 different countries and had worldwide circulation. Reference to each of these papers follows. They have been included in this report as an indication of the work of Staff Members and Fellows during the year, the range and importance of their subjects, and their written communication with the scientific and technological world. This list does not include oral presentations at scientific meetings, or published abstracts of such presentations.

Mount Wilson and Palomar Observatories

Abt, Helmut, Peter S. Conti, Armin J. Deutsch, and George Wallerstein, The mass and other characteristics of the magnetic star HD 98088. *Astrophys. J., 153,* 177–186, 1968.

Adelman, Saul J., Peculiar stars in the Lac OB1 association. *Publ. Astron. Soc. Pacific, 80,* 329–331, 1968.

Arp, Halton, Optical observations of two Seyfert galaxies. *Astron. J., 73,* 847–848, 1968.

Arp, Halton, Relation between quasi-stellar radio sources and radio compact and radio N galaxies. *Astrophys. J. (Letters), 153,* L33–L38, 1968.

Arp, Halton, Further comments on the ring around M81. *Soviet Astron.–AJ, 12,* 715–716, 1968.

Bahcall, John N., Jesse L. Greenstein, and Wallace L. W. Sargent, The absorption-line spectrum of the quasi-stellar radio source Pks 0237-23. *Astrophys. J., 153,* 689–698, 1968.

Bahcall, John N., Patrick S. Osmer, and Maarten Schmidt, On the absorption spectrum of Ton 1530. *Astrophys. J. (Letters), 156,* L1–L6, 1969.

Barbon, Roberto, The frequency of supernovae in clusters of galaxies. *Astron. J., 73,* 1016–1020, 1968.

Baschek, Bodo, and Leonard Searle, The chemical composition of the λ Bootis stars. *Astrophys. J., 155,* 537–554, 1969.

Bergh, Sidney van den, Observation of the nucleus of the radio galaxy M82. *Astrophys. J. (Letters), 156,* L19–L20, 1969.

Bergh, Sidney van den, Globular clusters in the Andromeda nebula. *Nature, 221,* 48–49, 1969.

Boesgaard, Ann Merchant, Isotopes of magnesium in stellar atmospheres. *Astrophys. J., 154,* 1185–1190, 1968.

Bradt, H., S. Naranan, S. Rappaport, F. Zwicky, H. Ogelman, and E. Boldt, Upper limit on X rays from a new supernova. *Nature, 218,* 856–857, 1968.

Bradt, H., S. Rappaport, W. Mayer, R. E. Nather, B. Warner, M. MacFarlane, and J. Kristian, X-ray and optical observations of the Pulsar NP 0532 in the Crab Nebula. *Nature, 222,* 728–730, 1969.

Bumba, V., and Robert Howard, On the solar source of recurrent geophysical effects. *Bull. Astron. Inst. Czech., 20,* 61–62, 1969.

Bumba, V., and Robert Howard, On long-term forecasts of solar activity. *Solar Flares and Space Research,* pp. 387–396, Z. Sveska and C. de Jager, eds. North-Holland Publishing Co., Amsterdam.

Bumba, V., and Robert Howard, Solar activity and recurrences in magnetic-field distribution, *Solar Physics, 7,* 28–38, 1969.

Bumba, V., R. Howard, M. Kopecký, and G. V. Kuklin, Some irregularities in the distribution of large-scale magnetic fields on the Sun. *Bull. Astron. Inst. Czech., 20,* 18–21, 1969.

Cohen, Judith G., The carbon abundance of Population II stars. *Astrophys. Letters* (England), *2,* 163–164, 1968.

Cohen, Judith G., A. J. Deutsch, and Jesse L. Greenstein, The spectrum of α^2 CVn, 5000–6700 Å. *Astrophys. J., 156,* 629–652, 1969.

Davis, D. N., and P. C. Keenan, Is there NbO in S-type stars? *Publ. Astron. Soc. Pacific, 81,* 230–237, 1969.

Demarque, Pierre, F. D. A. Hartwick, and M. D. T. Naylor, Some uncertainties in Population II models near the main sequence. *Astrophys. J., 154,* 1143–1146, 1968.

Deutsch, Armin J., O. C. Wilson, and P. C. Keenan, High-dispersion classification of K2–M6 giants of high and low velocity. *Astrophys. J., 156,* 107–115, 1969.

Difley, John A., Two photographic developers for astronomical use. *Astron. J., 73,* 762–769, 1968.

DuPuy, David, John Schmitt, Robert McClure, Sidney van den Bergh, and René Racine, Optical observations of BL Lac = VRO 42.22.01. *Astrophys. J.* (*Letters*), *156,* L135–L139, 1969.

Eggen, Olin J., Narrow- and broad-band photometry of red stars, II, Dwarfs. *Astrophys. J., Suppl. Ser., 16,* No. 142, 49–96, 1968.

Eggen, Olin J., Luminosities, colors, motions, and distribution of faint blue stars. *Astrophys. J., Suppl. Ser., 16,* No. 143, 97–142, 1968.

Garrison, Robert F., Erratum re "The spectrum of star No. 1 in NGC 2024." *Publ. Astron. Soc. Pacific, 80,* 755, 1968.

Greenstein, Jesse L., Red and black degenerate stars. *Comments in Astrophys., 1,* 62–72, 1969.

Greenstein, Jesse L., Faint, metal-poor, subluminous and red degenerate stars, in *Low-Luminosity Stars,* pp. 281–295, S. S. Kumar, ed., Gordon and Breach, Publishers, London, 1969.

Greenstein, Jesse L., and Halton Arp, A spectroscopic flare of Wolf 359. *Astrophys. Letters* (England), *3,* 149–152, 1969.

Greenstein, Jesse L., and Valdar Oinas, Two K dwarfs with enhanced carbon molecular bands. *Astrophys. J. (Letters), 153,* L91–L94, 1968.

Hardorp, J., and M. Scholz, On the surface gravity and temperature of Vega. *Z. Astrophys., 68,* 350–362, 1968.

Hartwick, F. D. A., A two-dimensional classification for galactic globular clusters. *Astrophys. J., 154,* 475–481, 1968.

Hartwick, F. D. A., and Allan Sandage, The color-magnitude diagram for the abnormally strong-line globular cluster M69. *Astrophys. J., 153,* 715–722, 1968.

Heintze, J. R. W., Temperature, gravity, and mass of Vega, Sirius, and τ Herculis. *Bull. Astron. Inst. Netherlands, 20,* 1–25, 1968.

Heintze, J. R. W., A tentative model of the solar atmosphere and the low chromosphere. *Bull. Astron. Inst. Netherlands, 20,* 137–153, 1969.

Heintze,, J. R. W., On the temperature scale of B-type stars. *Bull. Astron. Inst. Netherlands, 20,* 154–162, 1969.

Howard, Robert, Solar research at the Mount Wilson and Palomar Observatories. *Solar Physics, 7,* 153–158, 1969.

Julian, William H., Overstability of thin stellar systems. *Astrophys. J., 155,* 117–122, 1969.

Kodaira, K., Jesse L. Greenstein, and J. B. Oke, Abundances in two horizontal-branch stars. *Astrophys. J., 155,* 525–536, 1969.

Kowal, Charles T., The absolute magnitudes of supernovae. *Astron. J., 73,* 1021–1024, 1968.

Kozlovsky, Ben-Zion, and Harold Zirin, The O VI emission from the Sun. *Solar Physics, 5,* 50–54, 1968.

Kraft, Robert P., and Jesse L. Greenstein, A new method for finding faint members of the Pleiades, in *Low-Luminosity Stars,* pp. 65–82, S. S. Kumar, ed., Gordon and Breach, Publishers, London, 1969.

Kristian, Jerome, An upper limit for the optical luminosity of the pulsating radio sources CP 0950 and CP 1133. *Astrophys. J. (Letters), 154,* L99–L100, 1968.

Lambert, D. L., Radiation pressure and the composition of the solar corona. *Astrophys. Letters* (England), *2,* 37–39, 1968.

Lambert, D. L., and B. E. J. Pagel, The dissociation equilibrium of H^- in stellar atmospheres. *Monthly Notices Roy. Astron. Soc., 141,* 299–315, 1968.

Lambert, D. L., E. A. Mallia, and B. Warner, The abundances of the elements in the solar photosphere, VII: Zn, Ga, Ge, Cd, In, Sn, Hg, Tl, and Pb. *Monthly Notices Roy. Astron. Soc., 142,* 71–95, 1969.

Lambert, D. L., E. A. Mallia, and B. Warner, Forbidden lines of Ca II in the photospheric spectrum. *Solar Physics, 7,* 11–16, 1969.

McClure, Robert D., and Sidney van den Bergh, UBV observations of field galaxies. *Astron. J., 73,* 1008–1010, 1968.

Manwell, Tom, and Michal Simon, Application of a random-event quasar model to the optical variability of 3C 273. *Astron. J., 73,* 407–411, 1968.

Münch, Guido, Small-scale thermal homogeneity of the Orion Nebula, in *Interstellar Ionized Hydrogen,* pp. 507–516, Yervant Terzian, ed., W. A. Benjamin, Inc., New York, 1968.

Neugebauer, G., and R. B. Leighton, *Two-Micron Sky Survey, A Preliminary Catalog,* National Aeronautics and Space Administration, Washington, D. C., 1969.

Neugebauer, G., J. B. Oke, E. E. Becklin, and G. Garmire, A study of visual and infrared observations of Sco XR-1. *Astrophys. J., 155,* 1–10, 1969.

Neugebauer, G., E. E. Becklin, J. Kristian, R. B. Leighton, G. Snellen, and J. A. Westphal, Infrared and optical measurements of the Crab pulsar NP 0532. *Astrophys. J. (Letters), 156,* L115–L120, 1969.

Newell, E. B., A. W. Rodgers, and Leonard Searle, The blue horizontal-branch stars of ω Centauri. *Astrophys. J., 156,* 597–608, 1969.

Oke, J. B., Continuum energy distributions of Seyfert galaxies and related objects. *Astron. J., 73,* 849–850, 1968.

Oke, J. B., Photoelectric spectrophotometry of the Crab pulsating radio source NP 0532. *Astrophys. J. (Letters), 156,* L49–L53, 1969.

Oke, J. B., A multichannel photoelectric spectrometer. *Publ. Astron. Soc. Pacific, 81,* 11–22, 1969.

Oke, J. B., and Allan Sandage, Energy distributions, K corrections, and the Stebbins-Whitford effect for giant elliptical galaxies. *Astrophys. J., 154,* 21–32, 1968.
Oke, J. B., G. Neugebauer, and E. E. Becklin, Spectrophotometry and infrared photometry of BL Lacertae. *Astrophys. J. (Letters), 156,* L41–L43, 1969.
Peach, John V., Optical variations in quasi-stellar objects. *Nature, 222,* 439–442, 1969.
Preston, George W., The magnetic field of HD 215441. *Astrophys. J., 156,* 967–982, 1969.
Preston, George W., The nature of the variability of HD 19216, *Astrophys. J., 156,* 1175–1176, 1969.
Preston, George W., and Kazimierz Stepién, The light, magnetic, and radial veolcity variations of HD 10783. *Astrophys. J., 154,* 971–974, 1968.
Preston, George W., Kazimierz Stepién, and Sidney Carne Wolff, The magnetic field and light variations of 17 Comae and κ Cancri. *Astrophys. J., 156,* 653–660, 1969.
Racine, René, The distance of the Cepheid SU Cassiopeiae. *Astron. J., 73,* 588–589, 1968; erratum and addendum, *ibid., 74,* 572, 1969.
Racine, René, 2000 globular clusters in M87. *J. Roy. Astron. Soc. Canada, 62,* 367–376, 1968.
Racine, René, Preliminary colors of faint objects around M87. *Publ. Astron. Soc. Pacific, 80,* 326–329, 1968.
Rees, M. J., Polarization and spectrum of the primeval radiation in an anisotropic universe. *Astrophys. J. (Letters), 153,* L1–L2, 1968.
Rees, M. J., Proton synchrotron emission from compact radio sources. *Astrophys. Letters* (England), *2,* 1–4, 1968.
Rudnicki, Konrad, The dependence of the velocity body of stars on space location, in *Vistas in Astronomy,* Vol. 11, pp. 173–180, A. Beer, ed., Pergamon Press, Oxford and New York, 1968.
Rudnicki, Konrad, and Irena Tarrare, Redshifts of six galaxies in the vicinity of the Coma cluster. *Acta Astron., 19,* 171–172, 1969.
Sandage, Allan, The time scale for creation (Part I). *Astron. Soc. Pacific Leaflet No. 477,* 8 pp., March 1969; (Part II) *ibid., No. 478,* 8 pp., April 1969.
Sandage, Allan, and Basil Katem, The color-magnitude diagram for the globular cluster NGC 5897. *Astrophys. J., 153,* 569–576, 1968.
Sandage, Allan, and Willem J. Luyten, On the nature of faint blue objects in high galactic latitudes, II, Summary of photometric results for 301 objects in seven survey fields. *Astrophys. J., 155,* 913–918, 1969.
Sandage, Allan, and G. A. Tammann, Photometrie des Haufen-Doppel-Cepheiden CE Cas. *Mitt. Astron. Gesellschaft, No. 25,* 147, 1968.
Sandage, Allan, Basil Katem, and Jerome Kristian, An indication of gaps in the giant branch of the globular cluster M15. *Astrophys. J. (Letters), 153,* L129–L134, 1968.
Sandage, Allan, J. A. Westphal, and Jerome Kristian, Results of five nights of continuous monitoring of the optical flux from Sco X-1. *Astrophys. J., 156,* 927–942, 1969.
Sargent, W. L. W., New observations of compact galaxies. *Astron. J., 73,* 893–895, 1968.
Sargent, W. L. W., The redshifts of galaxies in the remarkable chain VV 172. *Astrophys. J. (Letters), 153,* L135–L138, 1968.
Scargle, Jeffrey D., Activity in the Crab Nebula. *Astrophys. J., 153,* 569–576, 1968.
Schild, Rudolph E., W. A. Hiltner, and N. Sanduleak, A spectroscopic study of the association Scorpius OB 1. *Astrophys. J., 156,* 609–616, 1969.
Schmidt, Maarten, Quasistellar objects, in *Annual Review of Astronomy and Astrophysics, 7,* Annual Reviews, Inc., Palo Alto, Calif., 1969.
Searle, Leonard, and J. G. Bolton, Redshifts of fifteen radio sources. *Astrophys. J. (Letters), 154,* L101–L104, 1968.
Searle, Leonard, and Wallace L. W. Sargent, The strength of Hβ in extragalactic objects with broad emission lines. *Astrophys. J., 153,* 1003–1006, 1968.
Simon, Michal, Asymptotic form for synchrotron spectra below Razin cutoff. *Astrophys. J., 156,* 341–344, 1969.
Simon, Michal, Time dependence on Razin spectra in Type IV solar radio bursts. *Astrophys. Letters* (England), *3,* 23–24, 1969.
Spinrad, Hyron, Benjamin J. Taylor, and Sidney van den Bergh, The M7 giants in the nuclear bulge of the Galaxy. *Astron. J., 74,* 525–528, 1969.
Stephenson, C. B., N. Sanduleak, and Rudolph E. Schild, A new hot, rapid variable star. *Astrophys. Letters* (England), *1,* 247–248, 1968.
Stoeckly, Robert, and Jesse L. Greenstein, Spectrophotometry of a B-type star in the globular cluster M13. *Astrophys. J., 154,* 909–922, 1968.

Swings, J. P., D. L. Lambert, and N. Grevesse, Forbidden sulphur lines in the solar spectrum. *Solar Physics, 6,* 3–11, 1969.

Terzan, Agop, Six nouveaux amas stellaires (Terzan 3–8) dans la région du centre de la Voie lactée et les constellations du Scorpion et du Sagittaire. *Compt. Rend. Acad. Sci. Paris, 267,* 1245–1248, 1968.

Trimble, Virginia, Motions and structure of the filamentary envelope of the Crab Nebula. *Astron. J., 73,* 535–547, 1968.

Tsuji, Takashi, Model atmospheres of M dwarf stars, in *Low-Luminosity Stars,* pp. 457–482, S. S. Kumar, ed., Gordon and Breach, Publishers, London, 1969.

Visvanathan, N., Optical polarization in quasi-stellar sources. *Astrophys. J. (Letters), 153,* L19–L22, 1968.

Weart, Spencer R., and Harold Zirin, The birth of active regions. *Publ. Astron. Soc. Pacific, 81,* 270–273, 1969.

Westphal, J. A., and G. Neugebauer, Infrared observation of Eta Carinae to 20 microns. *Astrophys. J. (Letters), 156,* L45–L48, 1969.

Westphal, J. A., Allan Sandage, and Jerome Kristian, Rapid changes in the optical intensity and radial velocities of the X-ray source Sco X-1. *Astrophys. J., 154,* 139–156, 1968.

Westphal, J. A., Jerome Kristian, Grant Snellen, Allan Sandage, Maarten Schmidt, J. B. Oke, Gerry Neugebauer, and E. E. Becklin, On the nature of Ryle and Bailey's candidate star for the pulsating radio source CP 1919. *Astrophys. J., 155,* L109–L114, 1969.

Wilcox, John M., and Robert Howard, A large-scale pattern in the solar magnetic field. *Solar Physics, 5,* 564–574, 1968.

Wilson, Olin C., Flux measurements at the centers of stellar H and K lines. *Astrophys. J., 153,* 221–234, 1968.

Wilson, Olin C., Calibration apparatus at Mt. Wilson and Mt. Palomar. *Bull. Am. Astron. Soc., 1,* 154, 1969.

Wilson, Olin C., Chromospheric variations in main-sequence stars, in *Low-Luminosity Stars,* pp. 103–106, S. S. Kumar, ed., Gordon and Breach, Publishers, London, 1969.

Zirin, Harold, Abundance analyses from extreme-ultraviolet emission lines. *Astrophys. J., 154,* 799–801, 1968.

Zirin, Harold, Mass motions in loops, sprays, surges, etc., in *Nobel Symposium 9, Mass Motions in Solar Flares and Related Phenomena,* pp. 131–136, Yngve Öhman, ed., John Wiley & Sons, New York, 1969.

Zirin, Harold, Observations of stellar chromospheres using the He 10830 line, in *Nobel Symposium 9, Mass Motions in Solar Flares and Related Phenomena,* pp. 239–242, Yngve Öhman, ed., John Wiley & Sons, New York, 1969.

Zirin, Harold, George Ellery Hale, 1868–1938. *Solar Physics, 5,* 435–441, 1968.

Zirin, Harold, Two prominence eruptions and the problem of emission. *Solar Physics, 7,* 243–252, 1969.

Zirin, Harold, and Dora R. Lackner, The solar flares of August 28 and 30, 1966. *Solar Physics, 6,* 86–103, 1969.

Zwicky, Fritz, *Catalogue of Galaxies and of Clusters of Galaxies,* Vols. IV and VI, California Institute of Technology, Pasadena, Calif., 1968.

Zwicky, Fritz, Physics and chemistry on the Moon, in *Research in Physics and Chemistry, Proc. Third Intern. Laboratory (LIL) Symp., 1967,* pp. 1–27, C. H. Roadman, H. Strughold, and R. B. Mitchell, eds., Pergamon Press, Oxford and New York, 1969.

Zwicky, Fritz, Physics of the universe, in *Proc. 4th Intern. Symp. on Bioastronautics and the Exploration of Space,* pp. 63–81, 527, 533, 595–608, Brooks Air Force Base, Texas, 1969.

Zwicky, Fritz, 1967 Palomar supernova search. *Publ. Astron. Soc. Pacific, 80,* 462–465, 1968.

Zwicky, Fritz, W. L. W. Sargent, and C. Kowal, The 1968 Palomar supernova search. *Publ. Astron. Soc. Pacific, 81,* 224–229, 1969.

Geophysical Laboratory

Bell, P. M., and F. R. Boyd, Phase equilibrium data bearing on the pressure and temperature of shock metamorphism, in *Shock Metamorphism of Natural Materials,* pp. 43–50, B. M. French and N. M. Short, eds., Mono Book Corp., Baltimore, Md., 1968 (Geophysical Laboratory Paper 1533).

Bell, P. M., and B. T. C. Davis, Melting relations in the system jadeite-diopside at 30 and 40 kb. *Am. J. Sci., Schairer Vol., 267A,* 17–32, 1969 (Geophys. Lab. Paper 1521).

Boyd, F. R., Electron-probe study of diopside inclusions from kimberlite. *Am. J. Sci., Schairer Vol., 267A,* 50–69, 1969 (Geophys. Lab. Paper 1522).

Bryan, W. B., L. W. Finger, and F. Chayes, Estimating proportions in petrographic mixing equations by least-squares approximation. *Science, 163,* 926–927, 1969 (Geophys. Lab. Paper 1532).

Chayes, F., A least squares approximation for estimating the amounts of petrographic partition products. *Mineral. Petrogr. Acta, 14,* 111–114, 1968 (Geophys. Lab. Paper 1519).

Davis, G. L., S. R. Hart, and G. R. Tilton, Some effects of contact metamorphism on zircon ages. *Earth Planet. Sci. Letters, 5,* 27–34, 1968 (Geophys. Lab. Paper 1515).

Donnay, G., and R. Allmann, Si_3O_{10} groups in the crystal structure of ardennite. *Acta Cryst., B24,* 845–855, 1968 (Geophys. Lab. Paper 1506).

El Goresy, A., and G. Donnay, A new allotropic form of carbon from the Ries crater. *Science, 161,* 363–364, 1968 (Geophys. Lab. Paper 1513).

El Goresy, A., and G. Kullerud, Phase relations in the system Cr-Fe-S, in *Meteorite Research,* pp. 638–656, P. M. Millman, ed., D. Reidel Publishing Co., Dordrecht, Holland, 1969 (Geophys. Lab. Paper 1536).

Finger, L. W., and C. W. Burnham, Peak-width calculations for equi-inclination diffraction geometry. *Z. Krist., 127,* 101–109, 1968 (Geophys. Lab. Paper 1507).

Gaines, R. V., G. Donnay, and M. H. Hey, Sonoraite. *Am. Mineralogist, 53,* 1828–1832, 1968 (Geophys. Lab. Paper 1517).

Gilbert, M. C., High-pressure stability of acmite. *Am. J. Sci., Schairer Vol., 267A,* 145–159, 1969 (Geophys. Lab. Paper 1523).

Hadidiacos, C. G., Solid-state temperature controller. *J. Geol., 77,* 365–367, 1969 (Geophys. Lab. Paper 1537).

Huckenholz, H. G., Synthesis and stability of Ti-andradite. *Am. J. Sci., Schairer Vol., 267A,* 209–323, 1969 (Geophys. Lab. Paper 1524).

Kullerud, G., The lead-sulfur system. *Am. J. Sci., Schairer Vol., 267A,* 233–256, 1969 (Geophys. Lab. Paper 1525).

Kullerud, G., G. Donnay, and J. D. H. Donnay, Omission solid solution in magnetite: kenotetrahedral magnetite. *Z. Krist., 128,* 1–17, 1969 (Geophys. Lab. Paper 1514).

Kushiro, I., The system forsterite-diopside-silica with and without water at high pressures. *Am. J. Sci., Schairer Vol., 267A,* 269–294, 1969 (Geophys. Lab. Paper 1526).

Kushiro, I., H. S. Yoder, Jr., and M. Nishikawa, Effect of water on the melting of enstatite. *Geol. Soc. Am. Bull., 70,* 1685–1692, 1968 (Geophys. Lab. Paper 1516).

Lindsley, D. H., I. S. E. Carmichael, and J. Nicholls, Iron-titanium oxides and oxygen fugacities in volcanic rocks: a correction. *J. Geophys. Res., 73,* 3351–3352, 1968 (Geophys. Lab. Paper 1504).

Lindsley, D. H., and J. L. Munoz, Subsolidus relations along the join hedenbergite-ferrosilite. *Am. J. Sci., Schairer Vol., 267A,* 295–324, 1969 (Geophys. Lab. Paper 1527).

Naldrett, A. J., and G. Kullerud, Emplacement of ore at the Strathcona Mine, Sudbury, Canada, as a sulfide-oxide magma in suspension in young noritic intrusions. *Intern. Geol. Congr., 23rd, 7,* 197–213, 1968 (Geophys. Lab. Paper 1503).

Richardson, S. W., Staurolite stability in a part of the system Fe-Al-Si-O-H. *J. Petrol., 9,* 467–488, 1968 (Geophys. Lab. Paper 1509).

Richardson, S. W., P. M. Bell, and M. C. Gilbert, Kyanite-sillimanite equilibrium between 700° and 1500°C. *Am. J. Sci., 266,* 513–541, 1968 (Geophys. Lab. Paper 1508).

Richardson, S. W., M. C. Gilbert, and P. M. Bell, Experimental determination of kyanite-andalusite and andalusite-sillimanite equilibria; the aluminum silicate triple point. *Am. J. Sci., 267,* 259–272, 1969 (Geophys. Lab. Paper 1518).

Schreyer, W., and F. Seifert, High-pressure phases in the system MgO-Al_2O_3-SiO_2-H_2O, *Am. J. Sci., Schairer Vol., 267A,* 407–443, 1969 (Geophys. Lab. Paper 1534).

Tilton, G. R., and R. H. Steiger, Mineral ages and isotopic composition of primary lead at Manitouwadge, Ontario. *J. Geophys. Res., 74,* 2118–2132, 1969 (Geophys. Lab. Paper 1535).

Wones, D. R., and M. C. Gilbert, The fayalite-magnetite-quartz assemblage between 600° and 800°C. *Am. J. Sci., Schairer Vol., 267A,* 480–488, 1969. (Geophys. Lab. Paper 1528).

Yoder, H. S., Jr., and I. Kushiro, Melting of a hydrous phase: phlogopite, *Am. J. Sci., Schairer Vol., 267A,* 558–582, 1969 (Geophys. Lab. Paper 1529).

Department of Terrestrial Magnetism

Bolton, E. T., The evolution of polynucleotide sequences in DNA, in *Mendel Centenary: Genetics, Development and Evolution,* pp. 76–85, R. M. Nardone, ed., Catholic University of America Press, Washington, D.C., 1968.

Britten, R. J., and D. E. Kohne, Repeated sequences in DNA. *Science, 161,* 529–540, 1968.

Brooks, C., S. R. Hart, T. E. Krogh, and G. L. Davis, Carbonate contents and $^{87}Sr/^{86}Sr$ ratios of calcites from Archaean metavolcanics. *Earth and Planetary Sci. Letters, 6,* 35–38, 1969.

Brown, L., W. K. Ford, Jr., Vera Rubin, W. Trächslin, and W. Brandt, Foil- and gas-excitation of sodium spectra, in *Beam-Foil Spectroscopy, I,* pp. 45–77, S. Bashkin, ed., Gordon and Breach, New York, 1968.

Brown, L., and C. Petitjean, $^6Li(p, {}^3He){}^4He$ reaction with polarized protons from 0.4 to 3.2 MeV. *Nucl. Phys., A117,* 343–352, 1968.

Davis, G. L., S. R. Hart, and G. R. Tilton, Some effects of contact metamorphism on zircon ages. *Earth and Planetary Sci. Letters, 5,* 27–34, 1968.

Erlank, A. J., Microprobe investigation of potassium distribution in mafic and ultramafic nodules (abstract). *Trans. Am. Geophys. Union, 50,* 343, 1969.

Falkow, S., and D. B. Cowie, Intramolecular heterogeneity of the deoxyribonucleic acid of temperate bacteriophages. *J. Bacteriol., 96,* 777–784, 1968.

Fischer, G. von, W. Schreyer, G. Troll, G. Voll, and S. R. Hart, Hornblendealter aus dem ostbayerischen Grundgebirge. *N. Jb. Miner. Mh., 11,* 385–404, 1968.

Flexner, L. B., J. B. Flexner, G. De La Haba, and R. B. Roberts, Loss of memory as related to inhibition of cerebral protein synthesis. *J. Neuro-chem., 12,* 535–541, 1965.

Forbush, S. E., Variation with a period of two solar cycles in the cosmic-ray diurnal anisotropy and the superposed variations correlated with magnetic activity. *J. Geophys. Res., 74,* 3451–3468, 1969.

Forbush, S. E., S. P. Duggal, and M. A. Pomerantz, Monte Carlo experiment to determine the statistical uncertainty for the average 24-hour wave derived from filtered and unfiltered data. *Can. J. Phys., 46,* S985–S989, 1968.

Ford, W. K., Jr., Electronic image intensification, in *Annual Review of Astronomy and Astrophysics, 6.* pp. 1–12, L. Goldberg, ed., Annual Reviews, Inc., Palo Alto, Calif., 1968.

Ford, W. K., Jr., A. T. Purgathofer, and Vera C. Rubin, Optical spectra near 1 micron: the Seyfert galaxy NGC 4151 and the planetary nebula NGC 6543. *Astrophys. J., 153,* L39–L40, 1968.

Ford, W. K., Jr., and Vera C. Rubin, The spectrum of the 1968 supernova in NGC 2713. *Publ. Astron. Soc. Pacific, 80,* 466–469, 1968.

Hart, S. R., Discussion of 'K/Rb in amphiboles and amphibolites from northeastern Minnesota.' *Earth and Planetary Sci. Letters, 4,* 30–31, 1968.

Hart, S. R., and G. L. Davis, Zircon U-Pb and whole-rock Rb-Sr ages and early crustal development near Rainy Lake, Ontario. *Geol. Soc. Am. Bull., 80,* 595–616, 1969.

Hart, S. R., G. L. Davis, R. H. Steiger, and G. R. Tilton, A comparison of the isotopic mineral age variations and petrologic changes induced by contact metamorphism, in *Radiometric Dating for Geologists,* pp. 73–110, E. I. Hamilton and R. M. Farquhar, eds., Interscience Publications, 1968.

Kohne, D. E., Isolation and characterization of bacterial ribosomal RNA cistrons. *Biophys. J., 8,* 1104–1118, 1968.

Kohne, D. E., Taxonomic applications of DNA hybridization techniques, in *Chemotaxonomy and Serotaxonomy, 2,* pp. 117–130, J. G. Hawkes, ed., Academic Press, Inc, New York, 1968.

Petitjean, C., L. Brown, and R. Seyler, Polarization and phase shifts in $^6Li(p,p){}^6Li$ from 0.5 to 5.6 MeV. *Nucl. Phys., A129,* 209–219, 1969.

Roberts, R. B., *et al., A Report on National Uses and Needs for Separated Stable Isotopes.* National Academy of Sciences–National Research Council, Washington, D.C., 37 pp., July 29, 1968.

Rubin, Vera C., and W. K. Ford, Jr., Spectrographic study of the Seyfert galaxy NGC 3227. *Astrophys. J., 154,* 431–445, 1968.

Steinhart, J. S., and S. R. Hart, Calibration curves for thermistors. *Deep-Sea Res., 15,* 497–503, 1968.

Stueber, A. M., Abundances of K, Rb, Sr and Sr isotopes in ultramafic rocks and minerals from western North Carolina. *Geochim. Cosmochim. Acta, 33,* 543–553, 1969.

Tuve, M. A., Letters: An Open Forum, Re: Solid-earth geophysics after the termination of the Upper Mantle Project. *Trans. Am. Geophys. Union, 49,* 448–449, 1968.

Tuve, M. A., Odd Dahl at the Carnegie Institution, 1926–1936, in *Festskrift til Odd Dahl,* pp. 40–46, Fra Venner Og Kolleger, Bergen, A. S. John Griegs Boktrykkeri, 1968.

Varsavsky, C. M., Dust and atomic hydrogen in interstellar space. *Astrophys. J., 153,* 627–632, 1968.

Genetics Research Unit

Bear, P. D., and A. Skalka, The molecular origin of lambda prophage mRNA. *Proc. Natl. Acad. Sci. U.S., 62,* 385–388, 1969.

Makover, S., A preferred origin for the replication of lambda DNA. *Cold Spring Harbor Symp. Quant. Biol., 33,* 621–622, 1968.

Skalka, A., Nucleotide distribution and functional orientation in the deoxyribonucleic acid of phage ϕ80. *J. Virology, 3,* 150–156, 1969.

Yamagishi, H., Single strand interruptions in PBS 1 bacteriophage DNA molecule. *J. Mol. Biol., 35,* 623–633, 1968.

Department of Embryology

Böving, B. G., and Billingsley, L. M., Rat conceptus spacing. *Anat. Rec., 163,* 158, 1969.

Coon, H. G., and M. C. Weiss, A quantitative comparison of spontaneous and virus-produced viable hybrids. *Proc. Natl. Acad. Sci. U.S., 62,* 852–859, 1969.

Cooper, M. H., and R. O'Rahilly, The development of the human heart at seven postovulatory weeks. *Anat. Rec., 163,* 172, 1969.

Dawid, I. B., Cytoplasmic DNA in differentiation and development. *J. Animal Sci., 27,* Suppl. I, 61–69, 1968.

Dawid, I. B., and D. R. Wolstenholme, The structure of frog oocyte mitochondrial DNA, in *Biochemical Aspects of the Biogenesis of Mitochondria,* pp. 83–90, E. C. Slater, J. M. Tager, S. Papa, and E. Quagliariello, eds., Adriatica Editrice, Bari, 1968.

Dawid, I. B., and D. R. Wolstenholme, Renaturation and hybridization studies with mitochondrial DNA. *Ibid.,* pp. 283–297.

DeHaan, R. L., Emergence of form and function in the embryonic heart. *Develop. Biol., Suppl., 2.,* 208–250, 1968.

DeHaan, R. L., *Review of* Epithelial-Mesenchymal Interactions. *Science, 162,* 784, 1969.

DeHaan, R. L., and S. H. Gottlieb, The electrical activity of embryonic chick heart cells isolated in tissue culture singly or in interconnected cell sheets. *J. Gen. Physiol., 52,* 643–665, 1968.

Ebert, J. D., Preface I, in *Dynamics of Development: Experiments and Inferences,* pp. v-vi, by Paul A. Weiss; Academic Press, New York, 1968.

Ebert, J. D., Discussion, in *Symposium on Molecular Aspects of Differentiation, J. Cell. Physiol., 72* (Suppl. 1), 222–223, 227, 1968.

Ebert, J. D., Levels of control: A useful frame of perception? in *Current Topics in Developmental Biology,* volume 3, pp. xv-xxv, A. A. Moscona and A. Monroy, eds., Academic Press, New York, 1968.

Green, H., B. Goldberg, M. Schwartz, and D. D. Brown, The synthesis of collagen during the development of *Xenopus laevis. Develop. Biol., 18,* 391–400, 1968.

Harbert, G. M., C. B. Martin, Jr., and E. M. Ramsey, Placenta extrachorialis in rhesus monkeys. *Anat. Rec., 163,* 195, 1969.

Manasek, F. J., Myocardial cell death in the embryonic chick ventricle. *J. Embryol. Exp. Morph., 21,* 271–284, 1969.

Misenhimer, H. R., and D. F. Kaltreider, Preterm delivery of patients with decreased glucose tolerance. *Obstet. Gynecol., 33,* 642–646, 1969.

Ramsey, E. M., Radioangiography of the placenta, in *Fetal Homeostasis,* Vol. III., pp. 151–170, Ralph M. Wynn, ed., Appleton-Century-Crofts, New York, N. Y., 1968.

Reeder, R. H., and D. D. Brown, An assay for the control of ribosomal RNA gene transcription *in vitro. Fed. Proc., 28,* 349, 1969.

Stalsberg, H., The origin of heart asymmetry: right and left contributions to the early chick embryo heart. *Develop. Biol., 19,* 109–127, 1969.

Stalsberg, H., and R. L. DeHaan, Endodermal movements during foregut formation in the chick embryo. *Develop. Biol., 18,* 198–215, 1968.

Stalsberg, H., and R. L. DeHaan, The precardiac areas and formation of the tubular heart in the chick embryo. *Develop. Biol., 19,* 128–159, 1969.

Wolstenholme, D. R., and I. B. Dawid, A size difference between the mitochondrial DNA molecules of urodele and anuran Amphibia. *J. Cell Biol., 39,* 222–228, 1968.

Wolstenholme, D. R., I. B. Dawid, and H. Ristow, An electron microscope study of DNA molecules from *Chironomus tentans* and *Chironomus thummi. Genetics, 60,* 759–770, 1968.

Department of Plant Biology

Björkman, Olle, Characteristics of the photosynthetic apparatus as revealed by laboratory measurements. *IBP/PP Technical Meeting, Trebon, Czechoslovakia, Productivity of Photosynthetic Systems, Models and Methods.* Czechoslovakia Academy of Science, ed., Preliminary texts of invited papers, 136–148, April 10, 1969 (DPB No. 462).

Fork, David C., and Jan Amesz, Action spectra and energy transfer in photosynthesis. *Ann. Rev. Plant Physiol., 20,* Leonard Machlis, ed., Annual Reviews, Palo Alto, Calif., 305–328, 1969 (DPB No. 449).

French, C. S., M. R. Michel-Wolwertz, J. Michel, J. S. Brown, and L. Prager, Naturally occurring chlorophyll types and their functions in photosynthesis. *Biochim. Soc. Symposia, 28,* Porphyrins and Related Compounds, T. W. Goodwin, ed., London, 147–162, 1969 (DPB No. 442).

French, C. S., Biophysics of plastid pigments, Closing Session Summary. Internatl. Congr. of Photosynthesis Research, Freudenstadt, June 4–8, 1969, *Photosynthetica, 3*(1), 94–96, 1969 (DPB No. 445).

Gauhl, Eckard, and Olle Björkman, Simultaneous measurements on the effect of oxygen concentration on water vapor and carbon dioxide exchange of leaves. *Planta, 88,* 187–191, 1969 (DPB No. 454).

Heber, Ulrich, Conformational changes of chloroplasts induced by illumination of leaves in vitro. *Biochim. Biophys. Acta, 180,* 302–319, 1969 (DPB No. 446).

Losses . . .

It is with deep regret that I must report the retirement of General Omar N. Bradley, who was a Trustee of the Institution from 1949 to 1968. General Bradley's magnificent military career and his public service in civil life following World War II sum to a record that seems hardly possible within the lifetime of one man. He brought to the Board of the Carnegie Institution the same deep concern and tremendous moral force that he has given the whole nation in war and in peace. We shall greatly miss his counsel.

Dr. Leason H. Adams, Director of the Geophysical Laboratory from 1938 until his retirement in 1952, died on August 20, 1969. First as a Staff Member, and then as Director, he served the Laboratory and the Institution for forty-two years. He was a founder of the American Geophysical Union, and served as its President from 1944 to 1947. He was also a prominent member of many other learned and scientific societies, and received many scientific honors, particularly in the field of his research specialty, the study of high-pressure chemical reactions of silicate rock, a subject which, after his retirement from the Institution, he continued to explore and teach at the University of California until only a few years before his death. We mourn deeply the loss of this distinguished scientist who spent so many productive years with the Institution and contributed so much to the development of the Geophysical Laboratory.

In August we also lost Dr. Elias A. Lowe, a Research Associate of the Institution for three different periods totaling twenty-three years. Dr. Lowe was devoted to paleography, the science of deciphering and describing ancient writings. He was checking proofs for the twelfth volume of his monumental *Codices Latini Antiquiores* at the time of his death at the age of 89 in Bad Nauheim, Germany.

Two of the Staff Members retiring in 1969 are capping their careers at the Institution with a final publication in a distinguished series. Dr. William M. Hiesey, who has headed the Experimental Taxonomy Group at the Department of Plant Biology from 1956 until this year, has concluded the fifth volume of

the famous series *Experimental Studies on the Nature of Species,* which will be published by the Institution during the coming year. Dr. Hiesey's work has spanned so many and such critical years in the development of his field that he can truly be considered a creator of his science. One of the men who first formulated the basic questions of the evolution of plant species, he opened avenues of research that are being entered by more and more investigators. Dr. Hiesey made original and important contributions to his field of study and a no less fine contribution to the spirit and operation of our Department of Plant Biology. We are sorry indeed to lose him as a Staff Member but anticipate a continuing association with the Department for many years to come.

This year, also, we lose another Carnegie Staff Member, retiring after forty-two years of service, Mr. Scott E. Forbush of the Department of Terrestrial Magnetism. His *Cosmic-Ray Results,* Volume XXII of the Researches of the Department of Terrestrial Magnetism, completed this year dramatically illustrates the progress made in Mr. Forbush's field in recent years. The great body of cosmic-ray data assembled by Mr. Forbush over many years comprises an invaluable store of data for future investigators of cosmic-ray patterns. Mr. Forbush joined the Department in 1927 at age 23, and continued that association throughout his working life. Shortly after coming to DTM, Mr. Forbush sailed with the nonmagnetic ship *Carnegie.* He also worked at the seismic station at Huancayo, Peru, in its early days. His career has been filled with adventure of the most scientifically exciting kind.

. . . and Gains

The Board of Trustees at its spring meeting elected to its membership a distinguished new Trustee, Mr. William T. Golden. Mr. Golden, whose government service has associated him over the years with the Atomic Energy Commission, the Bureau of the Budget, the Hoover Commission, and the Department of State Advisory Committee on Private Enterprise in Foreign Aid, is now Chairman of the Board of Federated Mortgage Investors, of United Ventures, Inc., and of the Kirkeby-Natus Corporation. In addition, he is a Director of Crowell-Collier and Macmillan, Inc.; of the Paribas Corporation; of Woodward Iron Co.; of Verde Exploration, Ltd.; and of General American Investors Co., Inc. His wide experience in public affairs and in finance will be of great service to the Institution, particularly in this time of change. We are honored and privileged to have Mr. Golden with us.

With great pleasure I record the following honors accorded to Staff Members during the past year.

Dr. Alfred D. Hershey, Director of the Genetics Research Unit, together with Dr. Max Delbrück of the California Institute of Technology and Dr. Salvator Luria of the Massachusetts Institute of Technology, was awarded the Nobel Prize for 1969 in Physiology and Medicine for his discoveries in the genetics of viruses.

Dr. Philip H. Abelson, Director of the Geophysical Laboratory, received an honorary Doctor of Science degree from Southern Methodist University on May 25, 1969. He was also elected to membership on the Council of the National Academy of Sciences for a two-year term beginning July 1, 1969.

Dr. James D. Ebert, Director of the Department of Embryology, received the honorary degree of Doctor of Science from Washington and Jefferson College on June 7, 1969. Dr. Ebert was also elected to the Presidency of the American Society of Zoologists for 1970.

Dr. H. W. Babcock, Director of the Observatories, was elected an Associate of the Royal Astronomical Society in February 1969. Dr. Babcock also received the Bruce Medal from the Astronomical Society of the Pacific in June 1969.

Dr. Elizabeth M. Ramsey of the Department of Embryology was elected an Associate Fellow (Honorary) of the American College of Obstetricians and Gynecologists.

Dr. Maarten Schmidt of Mount Wilson and Palomar Observatories received the Rumford Medal from the American Academy of Arts and Sciences in December 1968 and was elected a member of that Academy.

Dr. Jesse L. Greenstein of the Observatories was made Chairman of the United States Committee of the International Astronomical Union.

Mr. Jan Kowalik of the Department of Plant Biology was awarded the Jurzykowski Award by the Alfred Jurzykowski Foundation on January 24, 1969, in recognition of his outstanding achievements in the field of bibliography.

Reports of Departments and Special Studies

Mount Wilson and Palomar Observatories

Geophysical Laboratory

Department of Terrestrial Magnetism

Committee on Image Tubes for Telescopes

Department of Embryology

Department of Plant Biology

Genetics Research Unit

Mount Wilson and Palomar Observatories

Operated by Carnegie Institution of Washington
and California Institute of Technology

Pasadena, California

Horace W. Babcock
Director

OBSERVATORY COMMITTEE

Horace W. Babcock
Chairman

Armin J. Deutsch

Jesse L. Greenstein

Robert B. Leighton

J. Beverley Oke

Olin C. Wilson

Contents

INTRODUCTION

The Crab nebula, remnant of the supernova of 1054 A.D. in our Galaxy, is one of the most fascinating objects in the sky, particularly now that its central star has been found to be emitting its light in the form of pairs of sharp pulses recurring at a rate of 30 per second. The nebula, at a distance of some 5500 light years, has a fragmented, roughly spheroidal filamentary structure, with an apparent major axis of 6 minutes or 10 light years. It consists of material ejected from the supernova explosion. The nebula is expanding at a rate that is measurable both photographically and spectroscopically. The Crab emits not only optical radiation, but also radio pulses and X rays. Near the center of the nebula appear two stars of about the 16th magnitude. One is presumably a foreground object. The other star was found by Baade and Minkowski at Mount Wilson in 1942 to show a highly unusual featureless blue continuous spectrum. They suggested that it is almost undoubtedly the central star of the nebula and the primary remnant of the supernova.

Radio astronomers at Puerto Rico in 1968 found that radio emission from the source NP 0532 in the approximate position of the Crab is in the form of sharp pulses that recur with great regularity. Optical astronomers attempted to detect and identify the pulsing source. Success came in January 1969 when Cocke, Disney, and Taylor at the Steward Observatory detected optical pulsation. The source was identified a few days later by Lynds, Maran, and Trumbo at the Kitt Peak National Observatory as the star that had been suggested by Baade and Minkowski. The light arises almost entirely from the short rapid pulses emitted at the rate of 30 pairs per second.

The Crab pulsar was observed early in 1969 by Kristian, Westphal, and Snellen with the prime-focus photometer of the 200-inch telescope at Palomar. For this work they quickly assembled a digital data system capable of recording and analyzing the rapidly pulsating light signals. Digital photon counts were recorded in time increments of one millisecond for extended intervals to permit later analysis. In each 33-millisecond period, two distinct pulses occur. The main pulse is 3 milliseconds wide and asymmetric, the decline being steeper than the rise. The secondary pulse occurs 13.5 milliseconds later; its amplitude is 30% that of the main pulse. It also is asymmetric, but in the opposite sense. Both the primary pulse and the secondary pulse are extremely sharp, the width of the main peak at 90% of maximum being less than 300 microseconds. The light-intensity level between pulses is very low, but detectable. An upper limit of a few tenths of an arc second for the size of the optically pulsating source was determined by knife-edge occultation of the pulsar in the focal plane. The precise photometry accomplished by Kristian and his colleagues shows a remarkable stability of pulse shapes and amplitudes, with accuracy of better than one percent for one-minute averages compared over time intervals of two hours. This result shows that the large variations observed at radio wavelengths are probably not inherent in the source, but are most likely caused by atmospheric scintillation.

Kristian, Visvanathan, Westphal, and Snellen have shown that the light of the pulses is plane-polarized to the extent of about 10%.

Among the dozen or more radio pulsars that are known, the Crab pulsar has the shortest period. A search by Kristian has failed to show any other radio pulsars that are optically detectable. It is tempting to speculate that as the rapidly spinning neutron star slows down (assuming that Gold's model is correct), the

pulse intensity in the optical spectrum diminishes rapidly.

Turning to the subject of degenerate stars in the final stages of their evolution, Greenstein has attempted to resolve the apparent discrepancy in the number of white as compared with red degenerate stars. According to the Schwarzschild theory, the cooling of degenerate stars from the white dwarf through the red stages should proceed very slowly, and we should expect to find a substantial proportion of these that are passing through the red stage on their way to ultimate extinction. But, observationally the number of white dwarfs is in the hundreds, while the search by Eggen and Greenstein for yellow and red degenerate stars resulted in the listing of only about twenty, none of which is fainter than the 16th visual magnitude. Greenstein's study of the problem shows that new knowledge of convection interior to the surface but outside the degenerate core of the star alters the situation. In a white dwarf having a surface temperature near that of the sun, it develops from the work of K.-H. Böhm that convection provides rapid heat transport. Thus, the core temperature is far lower than that inferred from the earlier theory. This has the effect of greatly reducing the specific heat. Greenstein finds that a simplified stellar model can be derived in this way, showing that the fainter degenerate stars cool at a comparatively rapid rate rather than on a slow and decelerating time scale. He concludes that such stars therefore pass quickly through the red stage as they grow fainter, and that they are therefore much less numerous than had been predicted. Further tests will come from surveys of stars to the 20th magnitude with an image-tube spectrograph. The proper-motion catalog being compiled by Luyten from plates obtained with the 48-inch schmidt telescope should aid by providing candidate stars with large proper motions.

Preston has made noteworthy progress on the study of stars with strong magnetic fields. It has been known that fields in excess of about 20 kilogauss are required to produce resolved Zeeman triplets in stellar spectrograms, but such fields are very rare; indeed, the 8th magnitude star HD 215441 with its field of 34 kilogauss is the only known example. Preston now finds that magnetic fields stronger than 5 kilogauss can be studied by concentrating on those occasional lines showing the anomalous Zeeman effect in which the most intense π components have displacements that are comparable to those of the σ components. Such a pattern results in a doublet that is more readily resolved than is a triplet of the same width because the central component is absent. No analyzer is required in deriving the absolute value of the mean field strength. From the measured separations, a mean value of the surface field on the disk is found. This shortcut method significantly supplements the standard procedure whereby an "effective" field is measured from blended patterns. From such doublet measurements, Preston has derived a mean surface field of 15 kilogauss for 53 Camelopardalis and one of 6 kilogauss for β Coronae Borealis, both at specified phases.

During a year's stay at the Mount Stromlo and Siding Spring Observatories of the Australian National University, Sandage began an observational program to obtain redshifts and photometry of elliptical (E) and spheroidal (S0) galaxies brighter than the 13th photographic magnitude and within 60° of the South Pole. He obtained 267 spectra of 221 galaxies, thus observing nearly 95% of the available systems. Observations of southern galaxies are considered to be crucial for the problem of finding the Hubble constant by determining the anisotropic shear field of the local Hubble flow. First priority was therefore given to galaxies in groups and clusters in mapping the local anisotrophy of the general expansion and in testing the possible dependence of the absolute luminosity of the brightest cluster or group galaxy on group population. While the reductions are not yet complete, prelimi-

nary indications are that southern galaxies with velocities less than 4000 km/sec have smaller redshifts for a given apparent magnitude than the galaxies in the northern hemisphere.

Sandage with K. C. Freeman and R. N. Stokes of the Mount Stromlo Observatory completed a study of the intrinsic flattening of elliptical, spheroidal, and spiral galaxies. The distribution of apparent flattening for each class was determined for all classified galaxies brighter than photographic magnitude 12.5 in the *Reference Catalogue.* The distribution of true flattening was then obtained from the integral equation of the problem. In agreement with previous results, it was concluded that spirals and S0 galaxies are equally flat with an axial ratio of 0.25. Elliptical galaxies, however, exist throughout the entire range of intrinsic flattenings, with axial ratios from 1 to 0.3. Because flattening is a dynamical property that can change only with extreme slowness, the difference in the intrinsic distribution of axial ratios between E and S0 galaxies shows that one form cannot evolve into the other. The initial conditions at the time of formation must have been different for the two types. Freeman, analyzing the photometric properties of disks, showed that the central surface brightness of the exponential disks in S and S0 galaxies is remarkably constant from one to another and does not vary along the Hubble classification sequence. The mass density of free neutral hydrogen appears to be the sole systematic variable. These facts, combined with D. Lynden-Bell's theory of violent relaxation, led Sandage, Freeman, and Stokes to a number of significant conclusions regarding the formation of galaxies. They confirmed that the spheroidal galaxian component is formed very rapidly, largely from matter having low angular momentum per unit mass, whereas the disk is formed from material having higher-than-average angular momentum per unit mass. The galaxy type, the authors conclude, was determined essentially by the amount of free gas that was left over in the disk after collapse. No appreciable evolution along the Hubble sequence has occurred since the galaxies were formed.

OBSERVING CONDITIONS

Mount Wilson received 81.23 inches of precipitation during the year, far above the average of 36 inches. The total snowfall was 80.5 inches.

Palomar Mountain received a total rainfall in excess of 60 inches. Storms in January and February resulted in an unusually poor observing record for these two months, with only 8 clear nights and 14 partial nights.

The work of modernizing the 60-inch required placing this telescope out of service for several weeks beginning on June 6, 1969. As limited by this and by weather conditions, the hours worked with the major telescopes were as shown in the tabulation below.

TABLE 1. Observations

Telescope	Complete Nights	Partial Nights	Total Hours Worked
60-inch	203	59	2291
100-inch	242	56	2591
200-inch	211	86	2550

PHYSICS OF THE SUN

Routine Solar Observations

Routine solar observations were made by Adkins, Cragg, Howard, and Utter on 313 days. The records of various kinds made between June 1, 1968, and May 31, 1969, were as follows:

Direct photographs	304
Hα spectroheliograms, 30-foot focus	579
K2 spectroheliograms, 30-foot focus	573
Full-disk magnetograms	237
Sunspot drawings	271

Magnetograms

The attempt to obtain daily full-disk magnetograms at the 150-foot solar tower telescope continued during the year despite difficulties with some of the electronic instruments. Observational data are normally recorded digitally on a tape recorder, and later the tape is taken to the Caltech Computing Center where magnetograms and other results are extracted. During the year a change in the basic computer from an IBM 7094 to an IBM 360/75 necessitated an extensive conversion of the magnetogram programs. Planning has started for a new data system that will permit carrying out most of the data reduction at the telescope.

A preliminary examination by Howard of recent data on the polar magnetic fields of the sun shows that both polar fields decreased during the summer of 1968 to a value of one or two tenths of a gauss and remained at about that level at least through the first two months of 1969. During that period there was no indication of a polarity reversal at either pole.

The magnetograph observations and much of the data reduction continue to be supported partially by the Office of Naval Research through contract number NR 013-230, N00014-66-C-0239.

Active Regions

Mrs. Sara F. Smith of the Lockheed Solar Observatory, Burbank, California, and Howard continued their work on the magnetic classification of solar active regions using the daily magnetogram data. The classification scheme includes the orientation of the magnetic axis of the region as well as the size and magnetic configuration.

Solar Rotation and Velocity Fields

Howard has studied 2½ years of differential-rotation data on Doppler velocity obtained from the magnetogram scans. The results indicate clearly that the rotation of the visible layers of the photosphere is nearly 5% slower than the rotation of sunspots. It seems very unlikely that a bias in the proper motion of preceding sunspots could account for the entire discrepancy in angular velocity. It is reasonable to assume that the faster rotation of sunspots results from the fact that they are rather rigidly attached by large amounts of magnetic flux to magnetic-flux tubes in deeper, more rapidly rotating layers. Thus the spots are dragged through the slower-moving photospheric material.

Dopplergrams that are usually obtained along with magnetograms suggest that large-scale motions occur occasionally. The larger active regions are generally seen as loci of downward motions. Only the largest and most magnetically-complex active regions show both downward and upward motions.

Howard, together with Andrew S. Tannenbaum, John M. Wilcox, and Edward N. Frazier of the Space Sciences Laboratory, University of California, Berkeley, has analyzed one-dimensional magnetograph scans to study the 5-minute photospheric velocity oscillations and the supergranulation. The oscillations in wing brightness lead the oscillations in velocity by less than 90° in the photosphere, and by about 90° in the chromosphere. This suggests that the 5-minute oscillations are traveling waves at lower levels and standing waves at higher levels. Downward flows are observed at the bright parts of the chromospheric network, and upward flows are observed at the centers of network cells. This confirms the association of supergranular cells and network cells. Some of the observations for this study were obtained at the Kitt Peak National Observatory.

Solar Archives Copying Project

During the year, Mrs. Clare Neal and Mrs. Paula Swanson, under the supervision of Howard, microfilmed Mount

Wilson solar spectroheliograms from the plate vault. This material, covering the period from about 1905 to the present, is a rich source of fundamental solar data. Microfilming will ensure the preservation of the images and make it possible for solar physicists to obtain these records in a useful form. As a part of the project, the original plates are being washed and placed in new envelopes.

Studies of Velocity Fields

The Mount Wilson fine-scan (apertures $5'' \times 5''$ and $10'' \times 25''$) magnetograms and Dopplergrams of active solar regions are being studied by Howard. Dopplergrams, obtained with the $\lambda 5250$ line, show that the velocity pattern persists for several hours and that the regions of receding velocity are invariably the most active regions.

Doppler Heliograms

Dr. J. O. Stenflo of Lund and Bhatnager developed a new technique to obtain Doppler spectroheliograms directly on a single plate. The principle is to oscillate the exit slit between the two wings of a line profile while a spectroheliogram is being made. This is achieved by oscillating two tilted plane-parallel glass plates in front of the second slit of a spectroheliograph. The resulting spectroheliogram made in the wing of a line appears crossed by a fringe pattern. Successive fringes correspond to the images obtained in the two wings of the line profile. The density differences between the fringes are directly related to the velocity fields on the sun. The rate of oscillation and the scanning speed of the spectroheliograph define the width of the fringes and thus the angular resolution on the sun. The advantage of this method is that one obtains directly a Doppler heliogram, without doing elaborate photographic laboratory work. Preliminary results show that the sensitivity of the velocity determination is about 0.1 km/sec.

Solar Spectrum

Howard and Bhatnagar have analyzed a very fine solar spectrogram for the estimation of an upper limit of the magnetic field in the granular and intergranular regions. The plate was obtained with the 150-foot solar tower and spectrograph combination. From the digital output of the microphotometer of the Sacramento Peak Observatory, the scans made in the dark, intergranular regions were separated from those made in the bright, granular regions. A program written for the IBM 7094 computes half width, equivalent width, central density, and the line positions of the granular and intergranular regions; a systematic increase of the half width of lines is observed in the darker regions compared with the spectrum of bright regions. The relation between the increase of half width and Zeeman broadening of lines gave an upper limit to the magnetic field of 20 ± 14 gauss. This investigation shows that the difference of the magnetic field between the granular and intergranular regions is probably below 20 gauss.

Isophotes obtained of the same spectrum plate show conspicuous line variation. Profiles acquire cusp and scallop shapes in the dark streaks, due to continuum brightness variations.

Structure of the Chromosphere

Preparatory to attempting eclipse observations of the chromosphere in the 0.3- to 2-cm band, Simon and Zirin observed the sun at 9 mm with the National Radio Astronomical Observatory's 36-foot antenna at Kitt Peak. The ratio of the flux of the quiet sun to that of the center of the moon at its last quarter was found to be 31.2 ± 0.8. North–south scans showed that the brightness distribution was flat to at least $r/R_{\odot} \sim 0.7$.

Coronal Physics

Lambert, in collaboration with R. A. Chevalier (Caltech student) has per-

formed new calculations of the excitation of coronal ions responsible for the prominent forbidden lines. The calculations incorporate several recent improvements in the necessary collision rates. A novel feature of these calculations is the introduction of the proton excitation of the fine-structure collisions with the appropriate rates taken from a recent study (J. N. Bahcall and R. A. Wolf, *Astrophys. J., 152,* 701, 1968).

An initial study was made of the ions Fe XIII and Ca XV for which the ^3P ground state provides two observable forbidden lines, $^3P_2 \rightarrow {}^3P_1$ and $^3P_1 \rightarrow {}^3P_0$. The intensity ratio of these lines can be interpreted without detailed information on the ionization equilibrium. The measurements available in the literature are in good agreement with the predicted intensity ratios. This agreement is not maintained when the proton collisions are excluded.

The calculations for ions of Ca, Fe, and Ni are being used in analyses of coronal condensations. There is evidence that the abundances in some condensations are in excess of the photospheric values. This result may be attributed to diffusion processes, as suggested by S. Chapman and E. Tandberg-Hanssen (*Extremely High Temperatures,* p. 139, H. Fischer and L. C. Mansur, eds., Wiley and Sons, New York, 1958). The possibility that diffusion processes operate throughout the corona has been examined.

The observations available in the literature are insufficiently detailed to provide information. It is apparent that an eclipse experiment to measure simultaneously the intensities of the coronal lines of Fe X, XI, XIII, and XIV would provide much vital information. Of special importance are observations at distances of more than 1 $R_\odot$ above the solar limb because at these heights the excitation is primarily radiative and the uncertainties in the collisional rate constants are negligible.

An analysis of the 1952 eclipse spectra of a coronal condensation (M. K. Aly, J. W. Evans, and F. Q. Orrall, *Astrophys. J. 136,* 956, 1956) is in progress. This condensation was apparently symmetrical. Aly *et al.* derived radial distribution of the number density of excited ions. An attempt was made to determine the temperature profile. No satisfactory solution was found to accommodate the wide range of ions from Ca XV to Fe X. This result implies that the condensation is composed of filaments. Average properties of the filaments are being determined.

The Quiet Sun

A program of analysis of eclipse measurements of solar continua, begun by Weart at the Joint Institute for Laboratory Astrophysics, is being continued in collaboration with Drs. R. N. Thomas and K. Gebbie of JILA. Their extreme photosphere limb-darkening curves, the most accurate available to date, are in agreement with simple equilibrium theory.

The horizontal motions of spicules, observed at the sun's limb in Hα movies by Zirin and Lambert, were analyzed by Weart. These motions are violent and complex. The time spectrum of line-of-sight motions, as indicated by Doppler shifts, shows no significant peaks, but resembles a (1/frequency) noise spectrum with half height at a period of roughly 200 sec.

Composition of the Solar Photosphere

Lambert has continued to collaborate with Dr. E. A. Mallia of the Department of Astrophysics, Oxford, England, in a program of analyses of Fraunhofer lines.

Improved observations of the [Ca II] λ7323 line were secured with a spectrometer at a high-altitude station in the Swiss Alps. The spectrometer is operated by the Department of Astrophysics in Oxford, England. The new spectra show λ7323 to be partially resolved from the blending atmospheric H_2O line. The

equivalent width of the forbidden Ca II line is in good agreement with a prediction based upon the calcium abundance log $N(\mathrm{Ca}) = 6.33$ that was reported last year.

Photoelectric scans near λ4140 were searched for lines from (0, 0) band of the SiH system $A^2\Delta - X^2\Pi$. Eleven lines were positively identified and are the first convincing identification of SiH in the spectrum of the solar disk. Isotope shifts were computed for Si^{30} and Si^{29} isotopes. The solar spectrum is too confused to permit the identification of the very weak isotopic lines; the result $N(Si^{30})/N(Si^{28}) \lesssim 0.15$ is consistent with the terrestrial ratio $N(Si^{30})/N(Si^{28}) = 0.033$.

Other problems under active investigation include a search of the C_2 Swan band for isotopic lines, an analysis of the neutral calcium autoionization lines (λλ6318, 6342, 6371) and improved abundance analyses for chlorine, copper, rubidium, mercury, and thallium.

Studies of Solar Activity

Early in the operation of the Caltech photoheliograph, it was recognized that growing active regions observed in Hα were characterized by very high surface brightness and by dark parallel streaks, presumably loop prominences in absorption. This phenomenon had been noted earlier by Waldmeier and by Bruzek. Weart and Zirin now find that such bright regions with loops (BRL) are generally characteristic of emerging sunspot groups. Weart reports that the orientation of the loops is at first tilted at an angle to the equator, but this angle invariably decreases during the first day or two; sometimes the reorientation occurs in less than an hour. Apparently an active region begins where a kink in the latitudinal subsurface field rises to the surface and straightens out. It is surmised that the greatest activity occurs in bright regions with loops whose polarities are not oriented in the normal east–west bipolar configuration.

Zirin has studied the further development of sunspot groups in some detail. The bright regions will often exist for a few days and disappear. Others will arise rapidly in ten or fifteen hours to levels of moderate activity, climaxed by large flares, and either die out or stabilize into bipolar spot groups. The major sunspot groups associated with the largest solar-flare activity appear to arise out of a secondary growth in such regions. For example, a new sunspot group (Mount Wilson No. 16951) was born September 1, 1968, in the center of the disk at the end of a long filament. It grew rapidly to bipolar structure with a moderate amount of activity and was carried off the disk September 7. The same region reappeared on September 27 as a simple round spot, again with moderate activity. The spot grew rapidly, however, in its disk transit, and was fairly active when it transited the west limb October 7. When it reappeared October 20, it was still a large spot of preceding polarity completely surrounded by magnetic regions of opposite polarity. This peculiar magnetic configuration resulted in an extremely high level of flare activity that persisted to the next rotation. This two-stage development has been found in a number of other active regions.

Another important facet is the high level of activity associated with some rather simple round spots, which until now have been considered the end product of the sunspot evolution. Mount Wilson No. 16999, which appeared on the east limb September 23, 1968, and was classed αp, was a simple round spot with no associated plage; it subsequently produced a large number of flares, including one solar proton event. This phenomenon is not understood.

Subsequent work has shown that great activity occurs when small sunspots of following polarity are formed anomalously ahead of a large mature spot of preceding polarity. Although N and S polarities coexist stably when the "correct" one precedes, the situation de-

scribed is apparently unstable and gives rise to many flares. This occurred, for example, after December 21, 1968, when Mount Wilson group 17097 appeared on the east limb as a stable βp configuration. On the next day small spots of following polarity grew just ahead of the preceding spots. Flares followed, along with more spots of the "wrong" polarity, and a number of large flares occurred. The reason for the instability of magnetic fields when the Hale-Nicholson polarity law is violated is obviously of fundamental importance in the theory of solar activity.

Round-the-clock Hα movies of an active region which produced hundreds of surges during November 1968 show that surges can occur with great regularity. Weart, collaborating with Dr. U. Feldman and R. Zach of the University of Tel Aviv, found a number of examples of surge-producing centers less than 10 arc-sec across, with lifetimes of about two days, each producing up to a half dozen nearly identical surges. These centers are often located along the boundary between areas of opposite magnetic polarities. No existing theory of surge production adequately explains them.

Solar Magnetic Fields

By comparing Mount Wilson magnetograms with high-resolution photographs made with the Caltech photoheliograph, Glen Veeder (graduate student) and Zirin have reached two interesting conclusions:

1. The association between plages with regional magnetic fields greater than 30 gauss and Hα brightness, first pointed out by Howard and Harvey, is apparently valid only for "following" polarities. For preceding polarities, equivalent magnetic-field intensities do not result in visible Hα brightness, probably because the bright layer tends to be masked by an overlying pattern of fibril structure. Therefore, magnetic polarity may be inferred (with caution) from the presence or absence of Hα brightness in regions determined from off-band pictures to have large magnetic fields. In calcium K both the leading and following plages are bright.

2. In off-band pictures there is a one-to-one correspondence between dark structures in the disturbed chromospheric network and the presence of strong magnetic fields of 50 gauss or more. Because the fields cover only part of the surface, and the magnetograph is customarily used with a 17-sec aperture, the boundary of the enhanced chromospheric region is the 5-gauss contour on the daily Mount Wilson magnetograms. Where the field is not too complex, it is easy to draw the 5-gauss contours on the magnetograms directly from these Hα pictures. The "enhanced network" region is immediately evident on off-band pictures as an area showing a strong dark network and a reduced level of chromospheric oscillation. Outside of the 5-gauss contour there is normally a disturbed region in which the field appears to be horizontal, bounded by prominences that mark the change to the chromospheric network.

Solar X Rays

In a study of the relationship between optical and X-ray activity, a close collaboration was begun between solar physicists of the Observatories and experimenters of the University of California at San Diego and Berkeley. Almost every X-ray event observed with satellite apparatus was found to correspond to some sort of Hα phenomenon, typically a simple flare. Almost every small flare appears to produce substantial numbers of X rays in the 7- to 12-kilovolt range and higher. Because the satellite X-ray measurements are not directional, great interest attached to an event behind the west limb on December 2, 1967. As a bright arch arose from behind the limb of the sun, the X-ray

flux increased rapidly to nearly 100 times the quiet sun value. The total X-ray flux between 7 and 12 kilovolts was directly proportional to the projected area of the flare, up to the time of maximum, when the arch broke up and the energetic electrons appear to have disappeared. From these data, as well as the energy distribution on the X rays, Zirin and William Ingham, collaborating with Hugh Hudson and David McKenzie of UCSD, determined a density of 10^{10} cm^{-3} for electrons at a temperature of 50 million degrees in the flare. The decay time of the X-ray burst also gave maximum values for the electron density of ambient particles because of the absence of coulomb braking. These derived densities were of roughly the same order. A continuing investigation and comparison of Hα data with X-ray observations is in progress.

PLANETS AND THE MOON

Mars

During the current opposition of Mars, Münch and Neugebauer have been observing the planet radiometrically in the 8–14 μ and 4.6–5.2 μ channels at the Cassegrain focus of the 200-inch telescope. Scans of the planetary disk in various directions have been made with apertures as small as 1 arc sec, when the seeing conditions warrant it. The irradiance of dark areas appears, in general, higher than that of light ones, although the correlation between visual darkness and excess temperature is not yet clear. Further observations of the brightness of Mars in the 8–14 μ range will be carried out prior to the encounter of the Mariner VI and VII fly-by spacecraft, from which Neugebauer, Münch, and S. Chase, of the Santa Barbara Research Center, will carry out an absolute radiometric measurement in two spectral channels, one of them very nearly coinciding with the 8–14 μ channel used from ground. In this fashion a fundamental calibration of the 8–14 μ magnitude system will be established. Measures in the other channel, 18–24 μ, of the Mariner radiometer will also be compared with ground-based observations which will be carried out in Hawaii, to establish a calibration of the 20-μ magnitude system.

Photoelectric observations of the weak absorption lines in the $5\nu_3$ CO_2 band at λ8690 in the spectrum of Mars are being carried out at Mount Wilson by Münch with the Fabry-Perot interferometer used in the 1967 opposition (*Year Book 66*, p. 16). The purpose of the measures is to detect and measure differences in the CO_2 columns above dark and light areas. Preliminary inspection of data so far obtained indicates that over dark areas (Syrtis Major) detectably less CO_2 absorption takes place than over deserts (Arabia).

Jupiter

The brightness distribution of the disk of Jupiter in the wavelength ranges 4.6–5.2 μ and 8–14 μ is being studied by Neugebauer and Münch at the Cassegrain focus of the 200-inch telescope. The observations in the 5-μ channel are made through a dichroic filter, which permits photographing the field being measured through a boresighted reticle. In this fashion the nature of the relation between the 5-μ brightness and the visual features in the equatorial belt may be clarified. The observations in the 10-μ channel are done by driving the telescope in slow motion along chosen paths crossing the disk. Scans made along directions normal to the banded structure of the planet have clearly shown that, contradicting the earlier findings of Murray, Wildey, and Westphal (*Year Book 62*, p. 42), there is a distinct temperature difference between belts and zones—the zones being appreciably cooler.

The darkening toward the limb of Jupiter has been measured by Münch on photographic images taken at the coudé focus of the 200-inch telescope in a variety of broad-band wavelength regions. Theoretical limb-darkening curves for semi-infinite homogeneous atmospheres with various scattering phase functions have been fitted to the observations to derive characteristic values for the single scattering albedo and asymmetry factors in belts and zones. On this basis the variations in the strength of the CH_4 absorption bands over the Jovian disk, measured earlier by Münch and Younkin, can be quantitatively accounted for as arising by diffuse reflection. Very strong bands, however, increase in strength at the equatorial limb, indicating the existence of a thin high-level gas layer over the scattering medium. The phase-angle effect shown by the brightness at the extreme equatorial limb cannot be explained in terms of existing model calculations and presumably implies a strong forward lobe in the scattering function.

Spectrograms of Jupiter in the region of the $3\nu_3$ band of CH_4 at λ10900 have been obtained by Münch with a Carnegie image tube at the 72-inch camera of the 200-inch coudé. On this basis, differences in the rotational temperatures at various points in the planetary disk will be searched for.

Saturn

The darkening toward the limb of Saturn has been measured in photographic images taken by Münch with various emulsion-filter combinations. As for Jupiter, the purpose of the measures is to derive parameters for the scattering processes in the continuum, which in turn are needed to interpret the intensity of absorption bands or lines. For Saturn, an attempt has been made to rectify the observed limb-darkening profiles for seeing effects. Toward this end a "seeing smearing function" has been derived from tracings of the ring system and an assumed photometric profile. The brightness distribution at the extreme limb, where the seeing effects are important, contains information mostly about the asymmetry factors of the scattering phase functions. Existing calculations of diffusely reflecting planetary atmospheres are not sufficiently general to permit interpretation of these effects.

Infrared Limb Darkening

Using the 200-inch telescope, Westphal obtained infrared limb-darkening measurements of several planets with the highest spatial resolution possible. Measurements of Venus were made at wavelengths of 5, 9, 11, 13, 17, and 21 μ. Measurements of Jupiter and Saturn could be made at 8–14 and 16.5–22.5 μ. Attempts to measure the 5-μ limb-darkening of Jupiter led to the discovery of intense thermal radiation from localized areas where the brightness temperatures are at least 310°K. This thermal radiation is apparently coming from regions where the cloud layer is absent and the flux can escape from deep in the atmosphere. During April and May 1969 the flux was being emitted from localized regions between 5°N and 20°N latitude, which appeared extremely dark during times of excellent seeing.

Limb-darkening measurements of Saturn at 1.2, 1.65, 2.2, and 3.4 μ indicate an anomalously high albedo for the equatorial region at 2.2 μ. This effect, first seen by Younkin and Münch in 1963 in the region around 8870 Å, is apparently due to the reduced methane absorption over cloud layers that are higher in the atmosphere than the clouds in the surrounding areas.

A similar situation was observed when scans across the Red Spot on Jupiter at 8870 Å on 25 April 1967 indicated a higher albedo than that of the surrounding area. Thus the cloud tops in the Red Spot are apparently considerably higher than the general level over the planet.

STELLAR SPECTROSCOPY AND PHOTOMETRY

White Dwarfs

Greenstein continued the survey of the spectroscopic properties of the white dwarfs at two extremes of their cooling tracks. The small-proper-motion Lowell blue stars (the GD series) yielded 54 white dwarfs that were found to have very low space motions and, preferentially, an abnormally high percentage of spectroscopically interesting stars. The DB helium-rich type, in fact, has its highest frequency in the Lowell GD list—about 17% of those observed. Reexamination of the earlier lists of Eggen-Greenstein objects shows that the DB stars are progressively more common as one proceeds toward lower space motion, with a frequency as low as 4% among the Population II group. It is interesting to note that the surface anomaly connected with the next nucleosynthetic stage, production of C^{12}, which is represented by the λ4670 stars, seems confined to high-velocity stars, or white dwarfs in binary systems. Both these results are somewhat unexpected, since Population I white dwarfs may, in part, be the cores of or descendants of massive stars which burn He^4 to C^{12} (or further). One would therefore expect the low-velocity white dwarfs to be λ4670, not DB type. The subsequent shell-burning, or details of mixing, may be involved.

While at the Institute for Advanced Study, Greenstein studied the cooling times of old white dwarfs. He found that the rarity of red degenerate stars is connected with the solid-state theory of cooling at low core temperatures. In a star like van Maanen 2, which has a surface temperature near the sun, K.-H. Böhm had found that convection provides rapid heat transport, and begins near the degeneracy boundary. The core temperature is then far lower than on the Schwarzschild theory—in fact, near 10^6 °K. If so, not only has ion solidification occurred, which changes the specific heat, but the specific heat is low. A simplified model can be derived from the Debye theory of specific heats, which shows that stars fainter than van Maanen 2 cool at a rate such that they fade by one magnitude in 1.3×10^9 years, rather than on a time scale that increases with decreasing luminosity. Thus the faint red degenerates have shortened lives and are much rarer than previously expected. Greenstein has attempted to find cool red degenerate stars by various methods but with poor success. The total number of candidates studied spectroscopically now approaches 50. A new compilation of degenerate or possibly degenerate stars shows that a total of 17 yellow and red degenerates are now known, as compared to 6 known when the work of Eggen and Greenstein began. Nevertheless, few are very cool, and none is fainter than $M_v = +16$. Thus the suspected acceleration of cooling by solid-state effects seems to be supported by observational evidence, at least for stars brighter than $m_v = 16.5$. Only image-tube spectral surveys of stars to 20th magnitude will make this result definite.

Oke has continued to obtain spectral-energy distributions of selected white dwarfs. Some of the objects studied are normal A- and B-type objects. Many, however, are objects found by Greenstein to have peculiar spectra. Observations, particularly in the near infrared, reveal many other peculiar spectral features, of which few have been identified.

Dwarf M Stars

Infrared photometry can provide nearly complete coverage of the energy maximum of faint M dwarfs. After the flare of Wolf 359 was noted by Arp and Greenstein, Neugebauer and Becklin observed this star and the faint companion of +4°4048, known as Van Biesbroeck 11, which are the two stars of faintest

known visual magnitude for which spectra and far infrared observations can be made. Both are dMe stars, have flared, and are representative of the intrinsically faintest and least massive stars known. Greenstein has analyzed the data and restudied the photometry by H. L. Johnson for other faint M dwarfs (later than M3) by fitting black-body curves at the energy maximum, where molecular bands are weak, and allowing for reasonable blocking in the *UBVRI* photometric band passes (where TiO may be very strong). The empirical result is a recalibration of the effective temperature-bolometric-magnitude scale for stars of low mass. Fitting the energy maximum suggests very serious depression by TiO (and atomic lines) must occur even in the *I* band, and certainly at all shorter wavelengths. This disagrees with Tsuji's theoretical predictions. The effective temperatures are raised and the bolometric correction increased. The temperature for Wolf 359 is raised to the range 2625–2750°K, above that given (2200°K) in *Year Book 1967*, p. 18. For VB 11 the temperature is 2250–2375°K. The M_{bol}, log T_e diagram is then nearly a straight line down to $M_{bol} = +13$. VB 11 is brighter than expected, and suggests that the smallest masses so far known are well above the theoretical lower limit of 0.07 $\mathfrak{M}_\odot$ for main-sequence stars.

Model Atmospheres for M Dwarfs

Tsuji has studied convective energy transport in cool stars, with a result that raises the surface temperatures over those obtained with a radiative model including molecular opacities. The flux is not substantially changed, with a flux excess at 1.0 and 1.6 μ but a general infrared deficiency caused by high molecular opacity. He suggests an effective-temperature scale for types M0.5V, M3V, and M5V as $T_e = 3600$, 3000, and 2600°K, respectively.

Tsuji also computed a model ($T_e =$ 3000°K) with 1% of the solar metal abundances to represent a halo M dwarf. Collisionally induced H_2 absorption is high in the infrared because of high gas pressure. The TiO opacity is low, while SiH, MgH, and CaH remain important in the blue to red spectral regions. He suggests that a halo M dwarf will also show flux excess at 1 μ and deficiency at $\lambda > 2\ \mu$, with smaller deficiencies at $\lambda < 1\ \mu$ as compared to dwarfs.

Subdwarf Radial Velocities

Radial velocities of 112 subdwarf candidates, chosen from the unpublished photometric catalogue of 1700 proper-motion stars reported in earlier *Year Books,* have been obtained by Sandage. The work has been carried as a stand-by 200-inch coudé program from 1962 to 1968 during observing runs scheduled for other problems on which work was interrupted because of partially cloudy weather.

Many of the stars have quite large velocities. The two highest are G64-12 = LTT 13980 with $\rho = +438.6$ km/sec and G20-8 ≡ LTT 15239 with $\rho = -395.5$ km/sec. There may be nine possible radial-velocity variables, four of which are certain.

Photometric parallaxes were estimated for each star and preliminary *UVW* space motions were computed. There is a good correlation between asymmetrical drift velocity and the observed ultraviolet excess $\delta(0.6)$, normalized to $B-V=0.60$ (to correct for the guillotine). The velocity dispersions in U and W also correlate well with $\delta(0.6)$, as expected from prior work by Stromberg, Oort, Greenstein, and others. The results can be interpreted by, and generally are consistent with, the galactic collapse model of Eggen, Lynden-Bell, and Sandage. In particular, the good correlation between $\delta(0.6)$ and the velocity dispersion in W again emphasizes the presence of a chemical composition gradient perpendicular to the galactic plane.

A few high-angular-momentum sub-

dwarfs which lead the sun in V are present in the sample, but there are not yet enough examples to establish whether a correlation exists between $\delta(0.6)$ and increasingly positive V velocity. A program to find more such stars has been started by Sandage.

CE Cassiopeiae a and b and the Calibration of the Cepheid P-L-C Relation

Sandage and G. A. Tammann completed a two-color photometric investigation of the double Cepheid CE Cas in the galactic cluster NGC 7790. The binary consists of two Cepheids separated by 2.″3. Separate light curves for each component in B and V were obtained by relating (1) photoelectric data of the combined light of both components measured with a large aperture, and (2) relative photometry of short-exposure plates made between 1956 and 1962 with the 200-inch telescope diaphragmed to 100 inches, where the components are clearly separated. Final values of $\langle V \rangle$ $\langle B-V \rangle$ for each star are estimated separately to be accurate to ± 0.02 mag or better.

The stars differ in color, luminosity, and period. The data permit a test of the $P\langle\rho\rangle^{1/2} \doteq Q$ relation. The components of CE Cas, as well as CF Cas in the same cluster, obey the relation to within the probable error set by the photometric accuracies. This provides evidence that the formulation of the Cepheid period-luminosity-color relation via the $P\langle\rho\rangle^{1/2}$ function is valid. The calibration of the *P-L-C* relation was rediscussed using the new data for CE Cas, together with new data on RS Puppis (Westerlund) at $P=41.4$ days, SU Cas (Racine) $P=1.95$ days, 1 Carinae ($P=35.^d6$), and α Ursae Minoris ($P=4^d$) from Fernie. Thirteen fundamental Cepheids covering the large period range from 1.95 days to 41 days are now available. In agreement with theory, the scatter in the trace of the full *P-L-C* relation in the period-luminosity plane is tightly correlated with color. Cepheids brighter than average at a given period are bluer than average, and conversely. The coefficients expressing the observed correlation are $\Delta M_V/\Delta(B-V)=2.52$, $\Delta M_B/\Delta(B-V)=3.52$, in good agreement with predictions based on $P\langle\rho\rangle^{1/2}=Q$.

Sandage and Tammann found that the equations

$$M_V = -3.425 \log P(\text{days}) + 2.52\ [\langle B\rangle^\circ - \langle V\rangle^\circ] - 2.459$$
$$M_V = -3.425 \log P(\text{days}) + 3.52\ [\langle B\rangle^\circ - \langle V\rangle^\circ] - 2.459$$

reproduce absolute magnitudes of the 13 calibrating Cepheids to within 0.064 mag (AD) over the available period range. The new calibration differs from their 1967 discussion, based on a smaller sample, by 0.05 mag. The new calibration gives brighter values.

Discussion of the evolutionary history of the components of CE Cas shows that in the absence of perturbing effects, such as rotation, mass loss, or different main-sequence formation times, the mass-ratio of the components must now be less than 1.007 for both stars to be in the Cepheid instability strip. This stringent requirement results from the short time scale for stars in the Cepheid phase compared to their main-sequence lifetime, and explains why so few binary stars are Cepheids at any given time.

Variation of Chromospheric Radiation

Wilson has continued his work with the 100-inch telescope coudé scanner and its associated pulse-counting equipment in a search for stellar analogs of the solar cycle. A number of main-sequence stars are being followed, covering the spectral-type range F5 to M2. The fluxes at the center of the H and K lines of Ca II are measured as frequently as possible in order to detect changes in the chromospheric components of the radiation.

As this work was begun in 1966, there are now observations of some stars in

four seasons, extending over a 3-year period. For most of the later-type stars, however, observation did not begin until 1967.

With the assistance of Riley, Wilson has made a preliminary analysis of the observations. It is found that nearly all stars whose spectra reveal H and K reversals on 10 Å/mm spectrograms have undergone some change in chromospheric emission. In a number of instances these changes are well in excess of the standard deviations for the observing seasons, which are computed in the usual manner. No periods can be determined yet, but the fact that apparently real variations can be seen over two- or three-year intervals provides impetus to continue the work.

The most striking results are those for 61 Cygni A and B. These stars can be observed during nine months of the year and have been followed as closely as possible. Measures in 1967, 1968, and early 1969 show that the chromospheric fluxes in both objects are varying in a roughly cyclical manner. The period for 61 Cyg A appears to be about six and one-half months, while that for the fainter star is probably somewhat more than twice as long. It is not known whether these are intrinsic cycles of some kind or whether they are the rotation periods of the stars. In any case, further observation is clearly required.

Absolute Magnitude Criterion

A linear correlation between the logarithm of the width of the chromospheric H and K reversals in stars and the absolute visual magnitude was established by Wilson and Bappu in 1957. Various studies of this relationship indicate that it may be capable of yielding rather accurate luminosities. There is, however, a troublesome question of whether the correlation depends significantly on the metal abundances of the stellar atmosphere. In an effort to shed some light on this matter, Wilson has obtained 10 Å/mm spectrograms of several stars for which published analysis show greatly reduced metal abundance as compared to the Sun. This work was done with the 200-inch telescope and proceeds slowly, since most of the stars concerned are rather faint and require long exposures even when the seeing is good.

Of the stars observed, measurable H and K reversals can be seen in the spectra of HD 26, 165195, and 221170, for which the published [Fe/H] values are -0.67, -2.70, and -2.70, respectively. These spectrograms have not yet been measured. However, when they are examined on a comparator against spectra of ordinary giants, it is seen that the line widths are very similar. Additional spectrograms will be obtained to strengthen this result.

Stellar Chromospheres in Cluster Members

The color-magnitude diagrams of the Pleiades and the Hyades have shown considerable scatter at the faint end, with important implications for the theory of stellar contraction and evolution and for the Hayashi time scale. For clarification of this situation, field M dwarfs must be excluded and good photometry provided despite the relatively bright reflection background. Kraft and Greenstein chose to study the K-line emission of Ca II, which is expected to be strong in young stars. (O. C. Wilson and other investigators found that the strong chromospheres of young stars fade in about 4×10^8 years.)

Low-dispersion spectrograms (90–400 Å/mm) were obtained for 49 stars in the magnitude range 13–15, presumed to be cluster members on the basis of proper motion. It was found that emission became strong at about K3.5V and was extremely strong in the M stars. The equivalent widths approached 5 Å. Comparison with field stars studied by Wilson showed that the faint stars in the

Pleiades have extremely strong emission features.

The use of the emission-line criterion for young clusters does, in fact, clear up the H-R diagrams. The resultant scatter is very small. In the Hyades, photoelectric colors and spectral type are highly correlated; omission of three stars without emission lines produces an apparent-magnitude–spectral-type diagram of negligible scatter, from K5 to M2.

The Pleiades are more difficult because of the sparse V and $B-V$ data, the effect of the nebulous background on the photographic colors, and differential absorption and reddening. Below $V=12.0$, the spread in the color-magnitude diagram is mainly the result of fairly large observational errors. The selection of members, however, is easy. In a $B-V$ (Iriarte) photoelectric-spectral-type diagram, the scatter is small. In a V (Johnson and Mitchell) spectral-type diagram for members selected on the basis of emission, the total spread is 1.2 mag and is nearly symmetrical about the standard zero-age main sequence. Field stars, i.e., stars without emission, deviated up to 4 magnitudes. If any turnaway above the faint end of the main sequence exists, it is fainter than M1. Thus, stars of $M_V=+10$ lie essentially on the main sequence. At present, theoretical contraction times computed for such stars are longer than the nuclear age of 3×10^7 years. Probably the Hayashi time scales should be reconsidered in the light of pre-main-sequence evolutionary stages, such as the T Tauri stars, with very strong chromospheres and mass loss. In order to posit that all the Pleiades stars have the same age as the B stars, we require a mechanism that accelerates the Hayashi contraction.

Stellar Composition

A detailed analysis of the extremely metal-poor star +39°4926 was completed by Kodaira, Greenstein, and Oke; its temperature is 7500°K and log $g=1$, with microturbulence 5 km/sec. While the metal abundance is 1% that in the sun, abundances of carbon, oxygen, and nitrogen are essentially normal and insensitive to errors of temperature. There is an unusually large odd-even alternation in abundances, absolutely and differentially. Rapid synthesis of carbon and oxygen occurred either when the star was more massive or in a nearby explosive event with α-particle capture predominant. The radial velocity seems variable in a 775-day period, the luminosity near $M=-3$, the mass less than $\mathfrak{M}_\odot$. The unusual location in the H-R diagram may be connected with rapid evolution with mass exchange. Kodaira has obtained 27-Å/mm infrared spectra of the horizontal-branch A stars HD 86986, 109995, and 161817 at the 200-inch. These very metal-poor stars (see *Year Book 67*, p. 24) show the oxygen triplet at λ7771 as strong as in standard A stars, indicating normal oxygen abundance (as for +39°4926, which is much more luminous). He is studying the non-LTE effects in the triplet, compared to weaker oxygen lines in the red.

Mrs. Locanthi is preparing a wavelength table for lines in S-type stars, and has partially completed one for V Cancri (intermediate between the barium and S stars). With Keenan she studied the evidence for bands of niobium-oxide in S stars. They conclude that only $\lambda\lambda$6484, 6591 are suitable, and find them weakly present in R Cygni at a cool phase.

Much work is being done on Population I stars of earlier types. Scholz, collaborating with J. Hardorp of Hamburg and Cambridge, has reinvestigated the spectrum of α Lyrae, A0 V. They cannot find an atmospheric model that predicts the continuum, the metallic-line spectrum, and the Balmer lines simultaneously. An effective temperature of 9700°K and log $g=3.9$ is recommended. In τ Scorpii, $T_e=32{,}000$°K, log $g=4.1$; and for λ Leporis, 30,900°K, log $g=4.05$, with microturbulence of 4.5 km/sec.

Kodaira observed 27 bright B3 V stars

with the 60-inch Cassegrain scanner. The 1964 Oke system of standards is used with $T_e=9600°K$, log $g=4.0$ as the paramaters for α Lyr, based on a 1966 blanketed model by Mihalas. Effective temperatures for program stars were determined from color and Balmer jump, and were 16,000–18,000°K. Some rapidly rotating stars showed an excess Balmer jump equivalent to a gravity change of Δ log $g=1$. Mihalas also obtained spectra for velocity variation of these stars over a period of 11 months.

A detailed model-atmosphere analysis was carried out by Kodaira and Scholz for ι Herculis (v sin $i\approx0$), a moderate rotator η Hydrae (v sin $i\approx$ 100 km/sec), and HD 58343, a pole-on rapid rotator (B3e, v sin $i\approx$ 30 km/sec). Spectra were taken also by Lambert. The parameters were $T_e=18{,}000°K$, log $g=3.75$ for ι Her and HD 58343; $T_e=20{,}000°K$, log $g=4.0$ for η Hya, microturbulence 5.0 km/sec. The chemical composition of these stars is not distinguishable from that of the sun. The He/H abundance, which is of cosmological importance, is 0.063 by number, i.e., $Y=0.20$. A dependence of rotational velocity on lines used was found in η Hya, as predicted by Hardorp and Strittmatter. A pole-on model of HD 58343 was used to study the effect of gravity-darkening on a fine analysis. The chemical composition scarcely changes, while the discrepancy between the temperature derived from the hydrogen spectrum and that from ionization equilibria decreases.

Magnetic and Peculiar A Stars

Preston, K. Stepien (Warsaw University), and S. C. Wolff (University of Hawaii) have derived a period of 5.08 days for the light and magnetic variations of 17 Comae A. The star also exhibits periodic spectrum variations of small amplitude in the lines of Ti II, Sr II, and Eu II. A provisional period of 5.00 days was obtained also for κ Cancri, but the light and magnetic ranges are very small. This star is in need of further study.

A period of 3.7220 days has been established for 78 Virginis by Preston. This period, derived from a study of the occurrence of the crossover effect in the line profiles, successfully represents the magnetic observations, the radial velocity data, and the occurrence of the crossover effect during the past 20 years.

R. C. Henry (thesis, Princeton University, 1966; *Astrophys. J. Suppl., 18,* No. 156, 1969) recently has given values of his k-index for a number of Ap stars. The k-index measures the equivalent width of the K-line of Ca II in A-type stars. Henry's data clearly indicate periodic variations of the K-line in 17 Com A and 78 Vir and suggest that k-index measurements may be one of the easiest ways by which to detect periodic spectrum variables, at least among the Ap stars of later types.

Preston has found that the radial velocities and line intensities in the spectrum of 21 Persei vary periodically in the 2.88-day photometric period derived by Stepien. The velocity curve for the singly-ionized rare earths consists of two branches that overlap near primary light maximum and overlap again one-half cycle later when a weak secondary light maximum may occur. The range of the velocity variation is about 30 km/sec. The velocity variation for Ti II and Mn II resembles those for the rare earths, while lines of Si II, Sr II, and Fe II yield velocity curves of small amplitude with double waves. The velocity curve for Cr II lines varies in antiphase with the other elements. The line components of the rare earths appear as sharp, weak, shortward-displaced features that first increase and then decrease in strength as they move longward.

From measurements of the displacements of resolved Zeeman patterns in the spectrum of HD 215441, Preston has found evidence for a periodic variation of the magnetic field. The field appears to oscillate with a range of about 3000

gauss in phase with the 9.5-day light variation. Comparison of the measured intensities and displacements of the Zeeman components with those calculated for dipoles inclined to the line of sight indicate that the magnetic field of HD 215441 is not dipolar.

Magnetic fields in excess of about 20 kilogauss are required to produce resolved Zeeman triplets in stellar spectrograms. However, magnetic fields in the range 5–20 kilogauss can profitably be studied by means of those cases of the anomalous Zeeman effect in which the most intense π components have displacements that are comparable to those of the σ components. The result is a doublet which, by virtue of the absence of a central component, is more readily resolved than is a triplet of similar pattern width. A typical example is the ${}^4P_{1/2}-{}^4D^{\circ}{}_{1/2}$ transition Fe I λ4385.38. Preston has found such doublets in the spectrum of 53 Camelopardalis near the phase of positive crossover. The doublet separations correspond to a mean surface field over the disk of 15 kilogauss. More recently, Preston has found a number of such doublets on very high-dispersion spectrograms of β Coronae Borealis at the phases of positive and negative crossover. The mean surface field derived from these doublets is 6 kilogauss at these phases. Within the framework of the oblique-rotator theory, it can be shown that this mean surface field is compatible with the period, $v \sin i$, and the maximum value of the effective longitudinal field (+1000 gauss) if the star is viewed at small inclination and if the magnetic axis lies near the rotational equator.

Preston is using Zeeman doublets to study the large ($\sim$15 kilogauss) magnetic field of HD 126515. Both the mean surface field and the effective field of this star appear to vary smoothly in a period of 130 days.

Stepien (*Astrophys. J., 154,* 1968) recently reported that HD 19216 (HD spectral type B9) is a variable star with a period of 7.7 days and with V, $B-V$, and $U-B$ variations similar to those of a number of Ap stars. Palomar coudé spectrograms (dispersion 9 Å/mm) obtained by Preston show that HD 19216 closely resembles the B9 V standard star v Capricorni. However, the lines are exceedingly sharp ($v \sin i \leq 10$ km/sec). Thus, HD 19216 appears to be an example of a normal late B-type star with two of the secondary characteristics of the Ap star; viz., slow rotation and a periodic photometric variation.

Preston is obtaining rotational velocities from coudé spectrograms of all known Ap stars brighter than the 9th magnitude and north of $\delta = -40°$. The purpose of the program is to delineate better the rotational velocity-distribution functions for the various subclasses of Ap stars.

Preston is also surveying the spectra of a large number of B0–B5 stars (dispersions$\sim$20 Å/mm) to determine the frequency of occurrence of stars like 3 Centauri A in this interval of spectral type. Rotational velocities are being determined as a by-product of the program.

Miss Judith Cohen has discussed recent observations by Deutsch, Oke, and Greenstein of the continuum and the line spectrum of the magnetic-variable star α^2 Canum Venaticorum. She finds $T_e = 12{,}000$°K and $\log g = 4.0$, with abundances ranging from <0.05 the normal value for helium to $>10^6$ times the normal value for europium. Her analysis takes into account the strong spectrum variation and is consistent in all respects with a rigid-rotator model. The chief problems that remain are the variations of color with phase, which differential line-blanketing cannot explain, and the unknown process that concentrates the elements in different areas over the surface of the star.

Kodaira and Unno (of Tokyo) reexamined the oblique-rotator model for α^2 Canum Venaticorum by analyzing Si II $\lambda\lambda$4128, 4130 on high-dispersion spectra with four polarimetric strips,

taken at Okayama. They determined the position angle and effective longitudinal magnetic-field strength for the lines of force. The solution is well represented by the oblique-rotator model developed by Böhm-Vitense, which also predicts the strong variations of the profiles of Eu II (λ4129) and Cr II $\lambda\lambda$4555, 4559.

The star 38 Draconis, which Eggen has described as "the brightest horizontal-branch star in the old disk population," was found by W. L. W. Sargent and Adelman to be a new Mn-type peculiar star. A quantitative analysis revealed several composition anomalies, including excesses of Mn, Y, and Zr.

The study of neon lines in Ap stars by A. I. Sargent, Greenstein, and W. L. W. Sargent shows that neon is detectable only in the hotter objects. In those with temperatures above 13,000°K, indicated by Q from colors, they find that neon shares the deficiency of helium, carbon, and oxygen. In the λ4200 Si II stars, the deficiency of neon exceeds a factor of 3; the Mn stars may also be neon-deficient. Earlier work on deficiencies of He, C, and O is confirmed.

Kodaira observed the continuous energy distribution of HD 221568, period 159 days. When the star was red, it showed a flux excess in the visible to near-infrared, and a deficiency in the blue. Broad depressions exist at $\lambda\lambda$4200, 5300 and in the red phase at λ6300. An unknown opacity source perturbs the B9 IV–V continuum when the star is in the red phase. Work continues with Peterson.

In addition to examining the effects of C I and N I opacity in the Balmer continuum, D. M. Peterson has also investigated the effects of silicon bound-free absorption on the emergent flux of the Ap stars. It now appears that at higher temperatures ($T_e \geq 13{,}000$°K), Si II is a more important opacity source in the ultraviolet than Si I. Thus the effects of enhanced silicon abundance on the atmospheres of these stars are significant to much higher temperatures than originally suggested by Strom.

Furthermore, in those stars with varying silicon abundance over the surface, the changing ultraviolet opacities provide a natural explanation for light variability through the rotation of the objects. Thus, it is not necessary to assume a variable effective temperature over the surface of the star nor a deformation of the star due to the pressure of magnetic fields. To first order, i.e., moderate overabundances, the increased ultraviolet opacity acts simply to backwarm, and the light and color variations appear as if due to effective-temperature variations. With increasing overabundance, however, the ultraviolet metal continua begin to contribute significantly to the flux derivative and hence tend to lower the surface temperature. This affects only the strong features in the star. In particular, the cores of the hydrogen—and in cooler stars, calcium—line profiles become wider and deeper. The primary effect on the colors of the objects is to increase U and V more rapidly than the B magnitude, which is most sensitive to the hydrogen-line absorption. In exceptional cases, the flux shortward of the Balmer discontinuity may be affected also.

Finally, in the cooler Ap objects, large overabundance will allow silicon to contribute significantly to the opacity in the visual regions of the spectrum. HD 221568, as recently observed by Kodaira, seems to represent an example of such an object.

Pulsation of μ Cephei

From coudé spectrograms of μ Cephei, Deutsch has found this M2 Ia star to be in radial pulsation with a period of 1100 days. The amplitude of light variation is known to be small, and other periods also occur in the light curve in addition to the 1100-day cycle. The phase relation between the changes of radial velocity and brightness is the same as in classical

Cepheids, with maximum expansion velocity near maximum brightness. If the mass of μ Cephei is about 12 $\mathfrak{M}_\odot$, its pulsation constant $Q \simeq 0^d.06$, in accord with theoretical estimates.

The pulsation of μ Cephei is unique because of the large amplitude (in R) and the pronounced stratification effects. The radius of the star is $\sim 1 \times 10^3$ $R_\odot$ and, if the reversing layer moved with the gas, the pulsation amplitude would be $\sim R_*/5$. The strong lines that originate higher in the atmosphere systematically lag behind the velocity curve of the weaker lines by $\sim 90°$ in phase, and their velocity amplitude is only about half as large. At the greatest heights, the circumstellar envelope produces at least two distinctive sets of absorption lines from zero-volt energy levels; these lines appear to have constant velocities of expansion.

M Giants: Balmer-Line Intensities

Deutsch, Keenan, and Wilson last year noted that the absorption lines at $H\gamma$ and $H\delta$ are subject to large intensity variations in the spectrum of HR 6128, and M2.5 III star with a relatively high velocity. Now Deutsch has found that the M2 and M3 giants are a generally heterogeneous group with respect to their Balmer-line intensities. The differences among stars are least at $H\alpha$ and increase toward the higher Balmer lines, with $H\epsilon$ going over into emission in some weak Balmer-line stars. The M2 III stars show other differences in the metallic lines on the damping part of the curve of growth. These lines are systematically weaker in some stars than in others—a result like that recently found in the K giants by Spinrad and Taylor. Differences also occur in the doubly reversed profiles of Ca II H and K. On a time scale of months, some M giants show large changes in the Balmer lines, and Deutsch has some evidence as well for variations in the damped metallic lines and in the H and K reversals. The correlations among these features are not yet clear, but it seems that the Balmer lines and the Ca II emissions do not vary together, although both originate in the stellar chromosphere.

Mass Loss

Red giant stars of the Mira variable class include both R Andromedae and R Cygni of the Se type. Tsuji finds circumstellar lines of K I and Rb I to be quite strong. In R And the expansion velocity is 23 km/sec; the doublet ratio gives a Doppler parameter of 2 km/sec for the Rb I atoms, and a surface density of 4×10^{11} cm^{-2}. From his earlier work on shock fronts in this atmosphere, Tsuji concludes that the circumstellar envelope is matter ejected in the previous pulsational cycle. From the normal Rb/H ratio he finds a total mass loss of 10^{-5} $\mathfrak{M}_\odot$ per year. So rapid a mass loss suggests that an S star can last only 10^5 years, consistent with the presence of technetium in its atmosphere.

Tsuji also obtained spectral scans of 20 carbon stars between 0.4 and 1.1 μ to study the opacity in these stars and to interpret the ultraviolet depression.

O-Type Stars

D. M. Peterson has prepared a series of opacity subroutines for computer calculation of the first four ionization states of C, N, O, and Ne utilizing the most recent "quantum defect" and "close coupling" calculations of the bound-free cross-sections. These elements represent important sources of opacity in stars sufficiently hot to emit a substantial amount of their flux shortward of the Lyman discontinuity. In addition, C I and N I have been found to be important opacity sources between λ1440 and the Lyman discontinuity for stars as cool as the sun. Further computer programs are being prepared to calculate the effects of departures from LTE in hydrogen and helium in stellar atmospheres. In collaboration with M. Scholtz, these

programs will be used for the construction of realistic model atmospheres to be used in the analysis of O stars.

Rapid Variable, HDE 310376

Observations of a rapid variable similar to Scorpius XR-1 have been made at the Cerro Tololo Interamerican Observatory by Schild. The star, HDE 310376, exhibits brightness fluctuations of the order of 0.1 mag in 90 sec and also shows some night-to-night variation. No appreciable color change accompanies the rapid brightness fluctuations. The spectrum of the star varies from night to night. It is ordinarily nearly continuous with emission at λ4650 and λ4686, similar to that of Sco XR-1. A hydrogen absorption spectrum is sometimes weakly present; when it is at maximum strength, a faint helium spectrum characteristic of a B5 star is observed. If Sco XR-1 is to be understood as a hot star below the main sequence, surrounded by a hot plasma, HDE 310376 may be similar in most respects, except that the plasma is less well developed.

Line Identifications

Spectra of the southern slow nova RR Telescopii (A. D. Thackeray, *Monthly Notices Roy. Astron. Soc., 113,* 211, 1953, and *115,* 236, 1955) have proved a fascinating source of unidentified emission lines. Recently, Thackeray of the Radcliffe Observatory in South Africa identified several strong lines as forbidden transitions in the ground configuration of Fe IV. Lambert, in collaboration with Thackeray, has identified four other lines as forbidden transitions in the ground configuration of Ni IV. The newly identified lines include λ5041.6, which has long been a prominent and unidentified line in the spectra of peculiar emission-line objects. The relative intensity of the [Ni IV] and [Fe IV] emission lines is qualitatively consistent with a normal solar abundance ratio N(Fe)/N(Ni) = 0.05.

Spectrophotometry of Symbiotic Stars

The Cassegrain scanning spectrometer has been used by Lambert at the 60-inch and 100-inch telescopes to measure the flux distribution for several symbiotic stars. The observations extend from $\lambda\lambda$3300 to 11000 and include measures of prominent emission lines. In 1967, five stars were observed: CH Cygni, AG Pegasi, Z Andromedae, AX Persei, and BX Monocerotis. The program is continuing and T Coronae Borealis and MH 2328-116 were observed in 1968.

Reddening Determination

Racine, in collaboration with R. D. McClure of Kitt Peak National Observatory, has developed an accurate reddening-determination method based on broad- and intermediate-band photometry of late-type giants. Application of the method to four high-galactic-latitude fields gave $E(B-V) = 0^{m}.00 \pm 0^{m}.02$ m.e. for the globular clusters M3 and M13, and $E(B-V) = 0^{m}.11 \pm 0^{m}.02$ and $0^{m}.03 \pm 0^{m}.02$ for the spirals M31 and M33, respectively.

Peculiar Objects

Oke, Neugebauer, and Becklin have used an infrared photometer and the multichannel spectrometer to study the peculiar object BL Lacertae, which is also a radio source. No spectral features were detected, so that no redshift was determined. The spectral-energy distribution suggests that the radiation is largely nonthermal.

INFRARED STELLAR SPECTROSCOPY

Infrared Sources

Many of the reddest objects identified on the infrared sky survey have been measured photometrically by Becklin and Neugebauer from 1.2 to 3.5 μ on the 24-inch, 60-inch, and 100-inch Mount Wilson telescopes. These measurements are now being extended to 5 and 10 μ

and have resulted in the discovery of several very bright 10-μ sources.

The most interesting source so far discovered is IRC+10216, which is the brightest object known at 5 μ outside the solar system, while its visual magnitude is probably fainter than 19 mag. Photometric measurements from 1.2 to 20 μ and spectra in the regions 1.6–1.8 μ, 2.1–2.5 μ, 3.3–4.0 μ, 4.5–5.5 μ, and 8.5–13.5 μ have been made by Becklin, Frogel, Hyland, and Neugebauer. The energy distribution is close to that of a 600°K blackbody, and no molecular absorption features have been found in the spectra. The object lies in an unreddened field in Leo, and appears elliptical on a 48-inch schmidt plate and also on a 200-inch E plate taken by Arp. The exact nature of this peculiar object is unknown.

Orion Nebula

For some time it has been known that the Orion nebula has a rather different distribution of light in the infrared than would be indicated by visual photographs. Accordingly, a study of this anomaly has been undertaken. Hilgeman has obtained infrared spectrometer observations of the nebula during 11 nights on the 60-inch telescope at Mount Wilson, and photometric observations from 1.2 to 5 μ on the 24-inch telescope. The analysis of these data is being undertaken to obtain information on various physical properties of the nebula, such as electron temperature, electron density, dust temperature, gas–dust ratio, and particle-size distribution. An average electron temperature of 5700°K has been derived for the central 4′ region, and there is a suggestion that the electron temperature increases with distance from the center. The small optical depth at 2 μ has enabled Hilgeman to derive a nebular reddening from the infrared to visual hydrogen-line ratios, and he obtains a value similar to that found for the trapezium stars. From the He I 1.70-μ triplet line, he has derived an abundance of helium lower by approximately a factor of 2 than that found from the visual observations.

Galactic Center

New observations of the nucleus of the Galaxy in the wavelength region between 1.65 and 19.5 μ have been made by Becklin and Neugebauer. The 10- and 20-μ radiation originates in a source approximately 1 pc in diameter. The energy distribution of the galactic-center source is similar to that measured in the nuclei of Seyfert galaxies (F. Low and D. Kleinman, *Astron. J., 73,* 868, 1968). Unfortunately, the observations cannot be used to distinguish between two possible mechanisms for producing the infrared radiation: (1) thermal reemission of starlight by dust and gas, and (2) nonthermal radiation.

OH Sources

Infrared photometry to 20 μ and spectra in the 2–2.5-μ region have been obtained for several infrared stars associated with OH radio emission. One of the OH sources associated with an infrared star, VY Canis Majoris, has been found to be one of the brightest sources in the sky at 20 μ. This source has been studied in detail by Hyland, Becklin, and Neugebauer in collaboration with George Wallerstein of the University of Washington. Spectra at optical and infrared wavelengths indicate that it is a supergiant with an effective temperature of 2500–3000°K. Its OH emission, near infrared spectra, and far infrared energy distribution are similar to those of the NML Cygnus source, but visually it is 10 mag brighter. A simple dust-shell model is proposed to explain the observations of VY CMa. Reradiation of energy by the shell is found to be the predominant source of radiation for wavelengths longer than 3 μ. The currently available evidence favors the interpretation that VY CMa and NML Cyg are evolved stars.

Red Stars

The f/5 Ebert-Fastie spectrometer has been used by Hyland and Frogel on 30 nights at the Mount Wilson 60-inch and 100-inch telescopes and on 3 nights at the Cassegrain focus of the 200-inch. Most of the spectra obtained have been of the 2.1–2.5-μ and 1.5–1.8-μ regions with resolutions of 32.5 Å and 65 Å. Some have been taken in the 2.6–4.0-μ region.

The major areas of study have been:

1. Spectra of the very red stars identified from the 62-inch 2-μ survey have been obtained for classification purposes. The infrared sources that have been identified also as 1612 mHz OH sources have been studied in some detail. Several of these, unlike the NML Cygnus source and VY CMa, appear to have many of the characteristics of normal late-type Mira stars.

2. Two-micron spectra of Mira variable stars are being studied around their cycles to monitor changes. Several striking changes have been found among as yet unidentified molecular bands. These spectra have proved to be very useful in classifying the spectra of the OH sources.

3. Spectra of M0–M5 supergiants have been studied to aid in luminosity classification for late-type stars. The strength and shape of the 2.3-μ CO bands prove to be excellent luminosity criteria, especially for the earlier M stars.

Image-Converter Spectra

Zirin has continued his studies with the single-stage image converter at the coudé focus of the 200-inch telescope of late-type stars evincing chromospheric activity by absorption or emission in the λ10830 helium line. A number of these stars have been found to change with time: ϵ Geminorum, which showed λ10830 in emission is now in absorption; a strong emission line is now exhibited by 12 Pegasi, which once showed very slight emission. These stars are being followed. An interesting sidelight on these investigations has been the comparison with observations of the CN bands at $\lambda\lambda$10867 and 10914. The infrared spectrograms that have been extended to this region show strong CN absorption in ϵ Gem and θ Herculis, two of the stars with strongest chromospheric activity. According to the Redman and Griffin catalog, these two stars had abnormally strong CN absorption in the visual region. In fact, Redman and Griffin pointed out that absolute-magnitude differences do not suffice to explain the great intensity of the CN band in these and other stars. This observation suggests that the CN-band intensity may be a measure of chromospheric activity in stars.

ABSOLUTE SPECTROPHOTOMETRY

The program of absolute calibration of the flux of α Lyrae is being continued by Oke and Schild. The 4-inch telescope and scanner, together with the portable data system, are being routinely used in observations of standard stars and fundamental sources.

A new fundamental source in the form of a blackbody cavity operated at the temperature of the melting point of copper has been constructed. The new source utilizes a pure copper sample supplied by the National Bureau of Standards. The sample is contained in graphite crucibles, and the blackbody cavity is immersed in the copper. The copper sample is heated to its melting point by a resistive wire surrounding the crucible. Observations made when the copper sample is being melted and being frozen are in excellent agreement.

An additional new standard recently acquired will permit the calibration to be related to the fundamental sources maintained by the Bureau of Standards. The new source is in the form of a tungsten-filament lamp which has been accurately calibrated at a number of wave-

lengths by comparison with the gold furnace maintained by the Bureau. Observations of the new source will be made in the coming months.

Three sources are now available for the calibration of α Lyrae. The platinum furnace is effective from λ3500 to the near infrared and has been used extensively. The copper furnace is too cool to be used shortward of λ6000, but it provides an important check on the red and infrared calibration. The calibrated lamp has sufficient flux to be used at all wavelengths.

A new calibration based on observations of the two blackbody sources and α Lyrae has recently been completed. The platinum furnace was observed from λλ3500 to 11400, and the copper furnace was observed from λλ6000 to 11400. Agreement of the two furnaces is excellent in the region of the overlap. The new calibration substantiates the revision recently suggested by Hayes (thesis, University of California, 1967) from λλ4000 to 7000, but suggests that the revision is too great in the infrared. The new calibration is still uncertain in the ultraviolet.

The 4-inch telescope is being used extensively for observations of bright stars and extended composite sources. Observations of a number of bright elliptical galaxies in the Coma and Virgo clusters have been obtained. The energy distributions of these ellipticals are strikingly similar to one another but suggest important differences from that of M67. A number of bright globular and galactic clusters have been measured also. These energy distributions will be compared with one another, and also with synthetic energy distributions derived from energy distributions of individual stars added together with a weighting function based on density in the H-R diagrams.

STAR CLUSTERS

Main-Sequence Gap and Age of NGC 188

Eggen and Sandage completed discussion of photoelectric data for the old galactic cluster NGC 188. New *UBV* measurements by Eggen with the 200-inch were combined with the original data of Sandage to provide high weight for stars in the magnitude range $16 > V > 11$. A gap on the evolving main sequence was located between $4.33 \geq M_V \geq 4.53$. The feature represents hydrogen exhaustion at the center of evolving stars, followed by gravitational contraction and the subsequent firing of a hydrogen shell immediately outside the helium-rich core. The presence of the gap is important for stars of such faint absolute magnitude and such small mass because it fixes some combination of the stellar opacity, the core temperature, or the ratio of the p-p to CNO reaction rates. Early theoretical calculations of evolutionary models by Iben, Demarque, and others failed to predict a gap using either Keller-Meryott opacities or a special set of values without line opacity. Later models by Demarque, Miller, and Aizenman using Cox's opacities with lines have now produced a gap, consistent with the present observations.

Sandage and Eggen calculated a set of theoretical isochrones in the H-R diagram using models by Iben and by Aizenman, Demarque, and Miller. Comparison with the new observational data gives ages of $T = (9.5 \pm 0.5) \times 10^9$ years using the Iben models, or $T = 7.7 \times 10^9$ years with the ADM models.

A slight ultraviolet excess is present for main-sequence stars, amounting to $\delta \simeq 0.03$ mag relative to the Hyades. A normal interpretation in terms of a mental deficiency is uncertain in view of Spinrad and Taylor's results of strong metal lines for giant stars in NGC 188. The problem presents an important and unsolved anomaly.

The new color-magnitude diagram for NGC 188 was combined with that for

M67 (with the recent extension of its giant branch incorporating bright stars found to be members by C. A. Murray's proper motion studies) and with other old to intermediate age clusters to form a new composite color-magnitude diagram. The funnel effect is well shown—all giant branches converge to a common region and presumably terminate on the Hayashi limiting sequence. A new effect appears to be present in the observations, as predicted by the calculated isochrones. Near $M_V = +3$, the main sequences cross over one another due to the special conditions at the phase of hydrogen exhaustion in the core. In this luminosity region the slopes of the evolving main sequences near the termination point are not monotonic functions of age. New data are needed to establish positively the reality of the effect.

Reddening, Helium Abundance, and Age Difference of M3, M13, M15, and M92

Sandage completed the analysis of photoelectric data for blue horizontal-branch stars in the four globular clusters M3, M13, M15, and M92. The data had previously been obtained with the 200-inch between 1959 and 1967. Reddening values were obtained from the $U-B$, $B-V$ diagrams, interpreted by using Mihalas' calculations of $I(\lambda)$ for line-blanketed B, A, and F stars over the relevant range of log g. The low values of $E(B-V)$ derived in 1964 were confirmed at 0.00 mag for M3, 0.03 mag for M13, 0.12 mag for M15, and 0.02 mag for M92.

New photometric data of the main-sequence termination colors of these clusters, corrected for differential line blanketing and reddening, agree to within 0.01 mag in $(B-V)^\circ, c$, indicating equal ages for M15 and M92, and M3 and M13 separately to better than $\Delta t/t \lesssim 0.03$, or $\Delta t \lesssim 3\times 10^8$ years, in agreement with the galactic collapse model.

The blue-boundary colors of the RR Lyrae instability gap in the C-M diagrams of M3, M15, and M92 are all within 0.025 mag of $(B-V)^\circ$, $c=0.175$ mag when reddening and differential blanketing corrections (to the $\Delta S=6$ line-blanketing system) are applied. The difference in mean period between the Oosterhoff-Sawyer groups cannot then be due to a temperature difference, but may arise from a luminosity difference of $\Delta M_V \simeq 0.3$ mag, as previously supposed.

From R. F. Christy's calculations, the color of the blue boundary of the RR Lyrae gap was found to depend on M_V, $\mathfrak{M}/\mathfrak{M}_\odot$, T_e, and the helium abundance as

$$Y = -3.138\,\theta_e - 0.34\,\mathfrak{M}/\mathfrak{M}_\odot - 0.16\,M_V + 2.830.$$

Use of this equation with the new observational data for horizontal-branch stars gives a mean helium abundance of $Y = 0.32 \pm 0.09$ (total range). The helium abundances for M3, M15, and M92 are the same to within the observational error despite the large differences in metal abundance among the clusters.

If this is a valid way to determine Y, enough information is available, in principle, to make a proper photometric fit of the four globular clusters to the appropriate age-zero main sequence (whose position is a function of Y and Z) to obtain thereby a theoretically correct age determination. An analysis of the new photometric data has been started using these precepts.

Photometry of Southern Globular Clusters

Direct plates of ω Centauri, 47 Tucanae, M4, and NGC 6398 in B and V were obtained by Sandage at the f/8 Cassegrain focus of the Siding Spring 40-inch reflector to study fine-structure of the C-M diagrams. Preliminary measurements of 1000 stars in 47 Tuc on one pair of plates indicates the presence of gaps along the giant branch at $V=13.3$ and $V=12.8$. They are similar to gaps reported last year in M15. The horizontal branch in 47 Tuc occurs at $V=14.0$, giving $\Delta V=0.7$ and 1.2 mag for the gap

positions relative to the horizontal branch. The gaps in the much more metal-poor cluster M15 had previously been found at $\Delta V = 0.3$, 0.9, and 2.0.

A four-color (*UBVR*) photoelectric sequence was obtained in M4. Measurement of this cluster, together with ω Cen and 47 Tuc, should provide more complete data on the gaps because these clusters are among the most populous in the Galaxy, thus providing adequate statistics.

NGC 6397 and ω Centauri

Searle, in collaboration with Dr. A. W. Rodgers and E. B. Newell of Mount Stromlo Observatory, completed a study of the blue horizontal-branch stars in the globular clusters NGC 6397 and ω Cen. The surface gravities and effective temperatures of these stars were obtained from an analysis of spectroscopic and photoelectric observations. This work located the horizontal-branch stars in the theoretical Hertzsprung-Russell diagram and facilitates a comparison of observation with the predictions of the theory of stellar interiors. The mass-to-luminosity ratio of these stars is also determined. It is $\log \mathfrak{M}/\mathfrak{L} = -2.0$ (in solar units) and appears to be the same in both clusters and constant along the horizontal branch. This value, combined with measurements of the cluster reddenings and distance moduli, leads to a mass determination $\mathfrak{M} = 0.55\ \mathfrak{M}_\odot$ for the globular cluster horizontal-branch stars.

INTERSTELLAR GAS AND GASEOUS NEBULAE

Interstellar Absorption Lines

Profiles of the interstellar K line in a number of stars of high galactic latitude are being obtained by Rickard with the scanning Fabry-Perot spectrometer at the 100-inch telescope with a resolution of 50,000. Several stars brighter than $V = 7.0$ mag previously observed photographically have been studied with the purpose of detecting high-velocity clouds off the galactic plane, which may be detected also in 21-cm line radiation.

Interstellar Matter

An analysis of interferometer observations by Vaughan and Dr. I. J. Danziger of Harvard College Observatory in a search for interstellar lithium in the direction of the star ζ Ophiuchi has been carried out. The observations were designed on the assumption that lithium, if present, and interstellar Na I may be distributed alike in radial velocity in the direction of the star. If the hypothesis is correct, the present observations imply an upper limit for [Li^7/Si] that is within a factor 2 of the value for chondritic meteorites. Further observations to test this result are planned.

Galactic Emission Nebulae

The spectrum of emission nebulae in the region of the Paschen 12 line of hydrogen, at $\lambda 8750$, is being studied by Rickard and Münch with the purpose of verifying the detection of an H_2 quadruple emission line recently reported. An interference photometer specially constructed for the purpose is being used at the Cassegrain focus of various telescopes. To date, only the H II region of M8 has been studied in some detail, and no indications for the presence of the H_2 line have been found.

INFRARED SKY SURVEY

During the current report period the catalog of the survey for objects that radiate at 2.2 μ was completed (G. Neugebauer and R. B. Leighton, *Two-Micron Sky Survey, A Preliminary Catalog,* National Aeronautics and Space Administration, Washington, D. C., 1969). The infrared catalog includes a total of

5600 objects north of declination −33°, of which approximately three quarters have been previously identified in the catalog of the Smithsonian Astrophysical Observatory; this catalog includes stars with visual magnitude brighter than about $V=10$.

Preliminary analyses of the catalog data have been undertaken and were incorporated in the thesis of E. E. Hughes. These showed that the reddest stars observed in the survey could be seen to distances of roughly 2 kpc. About 200 extremely red stars form an excess concentration within one or two degrees of the galactic equator. These excess stars are interpreted as being supergiants which are seen to about 5 kpc. The long baseline available also enabled Hughes to get an estimate of the gradient of late-type stars in the Galaxy.

With the effective completion of the survey catalog, the 62-inch infrared telescope was utilized primarily in two programs:

1. The normal 2.2-μ survey has shown that certain of the extremely red stars vary by as much as 2 magnitudes at 2.2 μ. Although the time-scale of these variations is generally about a year, very rapid changes have been noted. Some 200 selected red stars were observed nearly every second night during the summer. The merging of this data with that extending over a four-year period has yielded valuable information on the variability of these stars.

2. Certain regions of the sky are clearly of greater potential interest than others with respect to investigation of galactic structure. A program was undertaken to examine five selected areas with a slower scanning speed and consequently higher sensitivity than was used in the normal survey. The data from these areas are now being reduced.

GALAXIES

Nucleus of M31

Photoelectric photometry of the central $\pm 120''$ of M31 was completed by Sandage, Becklin, and Neugebauer using the 200-inch, 100-inch, and 60-inch telescopes. Intensity profiles with 5″ resolution were obtained from $\lambda=0.36\ \mu$ to $\lambda=2.2\ \mu$ along the major and minor axes and along an east-west line passing through the center. A steep radial color gradient was found in $U-B$ in the range $40'' > |r| > 0$, but there was no evidence for a gradient at longer wavelengths. The color varies from $U-B=0.79$ at the center to $U-B=0.60$ at $|r|=60''$. The effect is interpreted either as (1) a gradient of metal abundance, such that stars at the center are more metal-rich than stars farther out, or (2) a change in the ratio of giants to dwarfs in the stellar-luminosity function, such that the CN break at λ3889 is progressively diluted by increasing dwarf light as one approaches the center. The existence of the gradient shows that no radial-orbit mixing occurs in the center of M31; otherwise, the effect, once established, would be destroyed in several mixing times. This is taken as proof that stars within $|r| \simeq 40''$ of the nucleus of M31 move in predominantly circular orbits.

Combining the $I|r|$ distributions in the blue and visual regions with those at 1.6 μ and 2.2 μ shows that M31 has no excess nuclear infrared radiation as is present in some Seyfert galaxies and related objects. The conclusion rests on the similarity of the $I|r|$ distributions over all wavelengths.

The measured surface brightness at the center of M31 at 2.2 μ, averaged over the central 13 pc (17″.62 along the diameter), is 2.2×10^{-28} Wm^{-2} Hz^{-1} $(\square'')^{-1}$. This is a factor of 2.4 fainter than that of the galactic center (measured several years ago by Neugebauer and Becklin), averaged over the same equivalent linear diameter.

Globular Clusters in M31 and Fornax

Van den Bergh has used the 200-inch telescope to obtain classification spectra, radial velocities, and *UBV* photometry for the brightest clusters in M31. The principal results of this study are:

1. The average metallicity of globular clusters in the Andromeda nebula, as determined from spectroscopic line strengths and the photometric metallicity parameter Q, is significantly higher than it is in the Galaxy.

2. There is no clear-cut evidence for a dependence of cluster metallicity on position. Some quite strong-lined clusters occur far out in the halo of M31.

3. Most of the *stars* in the inner halo of M31 are not extremely metal poor.

Available evidence indicates that the globular clusters in M31 are systematically brighter than are those in the Galaxy and in M87. This suggests that considerable caution should be exercised in using globular clusters to determine the extragalactic distance scale.

Van den Bergh finds that Baade's best 200-inch plates provide evidence in favor of the view that the red giants in M31 globulars obey the same relation between metal abundance and luminosity as do their counterparts in galactic globular clusters.

Observations of the highly reddened cluster B327 in M31 suggest that $A_V/E_{B\text{-}V}<3.0$ in the Andromeda nebula.

Comparison of the colors of galactic and M31 globulars with similar spectra yields a galactic foreground reddening $E_{B\text{-}V}(\mathrm{B0}) = 0.09 \pm 0.02$ m.e. in the direction of the Andromeda nebula.

Spectroscopic observations by van den Bergh of the globular clusters associated with the Fornax system show that the Fornax globulars exhibit a significant range of metallicity and that the average metal abundance of the globular cluster in Fornax is very low.

Red Supergiants in the Magellanic Clouds

Sandage began a survey for the brightest red supergiants in the Large and Small Magellanic Clouds, using a 5-inch Zeiss chart-camera and the Uppsala 20/26-inch schmidt telescope at Mount Stromlo. Previous work on NGC 2403 by Tammann and Sandage (reported in *Year Book 66*, p. 280) suggested that such stars redder than $B-V \simeq 2.0$ mag reach a stable upper luminosity of $M_V = -8.0$, which, if true, will provide a new distance indicator useful in the calibration of the Hubble constant.

Blue and yellow plates covering the complete area of the Clouds were taken. Plates taken with the Zeiss 5-inch give for the Clouds a relative scale and resolution similar to 100-inch plates of M33. The plates were blinked by Peter Hooper and Anthony Wier (summer vacation scholars at Mount Stromlo), and several hundred red supergiants were located. Preliminary photometry relative to known photoelectric sequences in both Clouds show that $M_V \simeq -8.0$ applies to the LMC, whereas the brightest red stars in the SMC are about 1 magnitude fainter. This suggests that M_V for the brightest red stars is a function of total magnitude of the galaxy. The relation $M_V = f(M_{\mathrm{total}})$ can be calibrated by combining these data with those from dwarf Sm and Im galaxies in the M81 group (NGC 2366, IC 2574, HO I, HO II), together with members of the Local Group. Sandage and Tammann have begun this more extended phase of the work. When the calibration is complete, it is expected that good distances can be obtained for field galaxies to the modulus limit of $m-M \simeq 29$, as a continuing step toward the Hubble constant.

The Virgo Cluster

Using the 48-inch schmidt and Kodak IIIa-J emulsions, Racine has completed a survey of the Virgo cluster to a limiting magnitude of $B \simeq 23.0$. This homogene-

ous material allows the detection of the globular clusters of many cluster galaxies and will be used to study the dependence of the luminosity of these globulars on their total population, on the parent-galaxy type, and to assess their value for the determination of the extragalactic distance scale. Preliminary results seem to indicate that NGC 4486 (M87) has by far the largest population of globular clusters and that its brightest clusters are appreciably more luminous than those of any other galaxy in Virgo.

Galaxies in Chains and Small Groups

Sargent has completed work on the determination of redshifts of galaxies in chains and small groups. Most of the systems studied are illustrated in Arp's *Atlas of Peculiar Galaxies.* In *Year Book 67* (p. 35), Sargent summarized results for the systems VV 144, 150, 165, and 172. During the present year, he determined redshifts for 4 galaxies in the NGC 833 group, 4 in the VV 169 group, 7 in the VV 282 group, 3 in the VV 159 group, 5 in the NGC 6027 sextet, 6 in the chain Arp 330, 3 in the VV 197 group, 5 in the VV 101 group, and 3 in the VV 208 group. In addition, *UBV* photometry was obtained for galaxies in the NGC 833 group, VV 161, VV 169, VV 282, VV 165, VV 159, NGC 6027 sextet, and VV 208.

Only one group was found to have a galaxy with a strikingly discrepant velocity similar to VV 172 described last year. This is the NGC 6027 group, otherwise known as Seyfert's Sextet. It has been described by Seyfert (*Publ. Astron. Soc. Pacific, 63,* 72, 1951) who published a photograph obtained by Baade with the Hale telescope. Seyfert also quoted Baade's opinion that two of the galaxies in this group (c and d in Seyfert's illustration) were field galaxies because, unlike the remaining members, they did not show signs of tidal distortion. Sargent finds that four of the galaxies, including c, have redshifts near 4000 km/sec, but that d has a redshift of 19,885 km/sec. On grounds of angular size, Sargent concludes that this object, a spiral, is probably a background galaxy. Sargent finds that one chain, VV 159, which consists of three galaxies elongated roughly in the direction of the line joining them, is probably not physical. The redshift of the central galaxy differs by 2700 km/sec from the other two. This would imply a mass-to-light ratio of 4800 solar units for a bound system. Application of the virial theorem shows that rather high mass-to-light ratios are required to bind most of the systems; e.g., 59 for VV 165, 74 for VV 282, 80 for VV 169, 50 for Seyfert's Sextet (including galaxy d), and 55 for VV 150. On the other hand, the NGC 833 group requires a more reasonable mass-to-light ratio of about 10. This work adds considerably to the available statistics on galaxies in small groups.

Redshifts and Photometry of Southern Galaxies

During the year's stay in Australia, Sandage began a program to obtain redshifts and photometry of E and S0 galaxies brighter than $m_{pg} \simeq 13$ south of $\delta = -30°$. Spectra have been obtained with the Mount Stromlo 74-inch reflector using the Cassegrain image-tube spectrograph on loan from the Department of Terrestrial Magnetism. Photometry on a six-color system [*UBVR,* 0.35-μ (UG11 filter), and 0.47-μ (narrow-band interference filter)] was started with the 40-inch reflector at Siding Spring Observatory.

First priority has been given to E and S0 galaxies in groups and clusters (1) to map the local anisotropy of the general expansion and (2) to test the dependence, if any, of the absolute luminosity of the brightest cluster or group galaxy on group population. Solutions for the anisotropic shear field of the local Hubble flow are necessary as the next step in finding the Hubble constant. Observations of southern galaxies are considered to be crucial for the problem.

During the report year, Sandage obtained 267 spectra of 221 galaxies. Nearly 95% of the available southern E and S0 systems have been observed. The reductions are not yet complete, but preliminary indications suggest that southern galaxies with $cz \lesssim 4000$ km/sec have smaller redshifts for a given apparent magnitude than galaxies in the northern hemisphere. The sense of the anisotropy is consistent with earlier work by de Vaucouleurs. The Hubble constant cannot be determined adequately until the shear field is mapped completely. It must then be related to the expansion parameters for redshifts greater than 4000 km/sec via the Hubble diagram at large distances.

New Seyfert and Related Galaxy Types

A by-product of Sandage's southern redshift program has been the isolation of several new Seyfert-like galaxies.

NGC 1705, a particularly interesting case, is of type E4 or S0, with a bright starlike object displaced from the centroid by about one third the apparent diameter of the galaxy. The object was believed at first to be a superposed foreground star, but photometry showed quasarlike colors, and spectra show redshifted narrow emission lines of Hβ, N1, N2, Hα, [N II], and [S II].

Other galaxies found to show bright emission lines are IC 4329 [S0] with very wide Hβ and Hα (rotal width $\simeq 125$ Å), but with narrow N1, N2, [N II], and [S II]; and NGC 5643, NGC 5728, and IC 5063 with intense moderately narrow ($\simeq 10$ Å) Hα, [N II], [S II], N1, N2, but moderately intense [O I, λ6300], which is uncommon in non-Seyfert galaxies.

Flattening of S0 Systems

Sandage, K. C. Freeman, and R. N. Stokes (of the Mount Stromlo Observatory) completed a study of the intrinsic flattening of E, S0, and spiral galaxies using Hubble's statistical method. All classified galaxies brighter than $m_{pg} = 12.5$ that had angular diameter measurements tabulated in the Reference Catalogue were used to obtain the distribution of apparent flattenings for each class. The distribution of true flattenings follows from the integral equation of the problem.

In agreement with previous results, spirals and S0's are equally flat with $\langle b/a \rangle \simeq 0.25$, distributed with a dispersion close to $\sigma = 0.06$. Elliptical galaxies exist throughout the entire range of intrinsic flattenings from $b/a = 1$ to $b/a \simeq 0.3$, with indications of a peak near $b/a \simeq 0.6$.

Because flattening is a dynamical property that cannot change in times less than $\sim 10^{14}$ years, the difference in the intrinsic distribution of b/a between E and S0 galaxies shows that one form cannot evolve into the other. The initial conditions at the time of formation must then have been different for the two galaxy types.

Freeman's analysis of the photometric properties of disks in S and S0 galaxies shows that the central surface brightness of the exponential disks in such systems is remarkably constant from galaxy to galaxy, and does not vary along the Hubble classification sequence. The only systematic variable appears to be the mass density of free, neutral hydrogen.

In addition to these properties, the intensity profiles, $I(r)$, of the spheroidal component of S and S0 galaxies and of E systems are remarkably similar. Furthermore, they have the form of a pseudo-isothermal-sphere distribution, which is a relaxed configuration. These facts, combined with the theory of violent relaxation by D. Lynden-Bell, led Sandage, Freeman, and Stokes to the following conclusions:

1. Stars in the spheroidal component of all galaxies were formed very rapidly on a time scale comparable to the collapse time of the protogalaxy (a few times 10^8 years). The argument is inde-

pendent of that used in 1961 by Eggen, Lynden-Bell, and Sandage based on orbital characteristics.

2. The halo stars were formed from matter in the low-angular-momentum tail of the distribution of angular momentum per unit mass, i.e., the spheroidal component, during the collapse time. Other, higher-angular-momentum matter, collapsed to a disk.

3. The galaxy type was determined essentially by the amount of free gas left over in the disk after collapse. No appreciable evolution along the Hubble sequence has occurred since the galaxies were formed.

4. The dominance of the disk in spiral and S0 systems betrays their mean angular momentum per unit mass, higher than that which exists in less flattened E galaxies.

5. All stars in the spheroidal component of galaxies should be of the same age to within less than 10^9 years, in agreement with observational data on the ages of halo globular clusters in our own Galaxy.

Markarian Galaxies

Sargent completed work begun last year with the Cassegrain image-tube spectrograph on the spectra of 30 Markarian galaxies with ultraviolet continua. Twenty-six of the 30 galaxies were found to have emission lines. Two of these, Markarian 50 and 69, are new galaxies of the Seyfert type, with broad Balmer emission lines and sharper forbidden lines. Their redshifts are $z=0.023$ for Markarian 50 and $z=0.076$ for 69. Markarian 50 has $m_p=15.5$ and $M_p=-19.6$, while No. 69 has $m_p=16.5$ and $M_p=-21.2$. Of the 24 sharp emission-line galaxies, only 3 have absorption lines, in each case of early type, detectable at the dispersion of 190 Å/mm used in the survey. The remaining 21 galaxies have a range in absolute magnitude of $-14.7 > M_p > -21.5$ with $\langle M_p \rangle = -19.6$. The mean size is about 5 kpc and the mean redshift about 6900 km/sec. The range in excitation of the emission lines in these objects is the same as in galactic H II regions. Some of these objects are probably Type I irregular galaxies observed at large distances.

H II Regions in Galaxies

As a necessary preliminary to determining the Hubble constant from the sizes of the H II regions in late-type galaxies, Kristian has completed *UBVR* photometry, using the 60-inch and 100-inch reflectors, of stars in the fields of 35 galaxies for which 200-inch Hα plates have been obtained by Sandage. The measurements are needed in order to correct the size measurements for the characteristic curve and instrumental spread function of each plate.

Searle began a survey of the spectra of gaseous nebulae in external galaxies, looking for evidence that the composition of the interstellar medium in one galaxy differs from that in another. To establish a standard sequence of spectra, the H II regions in nearby Sc galaxies were surveyed. With the Cassegrain image-tube spectrograph of the Hale telescope, spectra of 15 regions in NGC 2403 and 35 in M33 were obtained.

These spectra can be classified in a one-parameter sequence, all line ratios being strictly correlated with, for example, the $(N_1+N_2)/H\beta$ ratio. There are no detectable differences from one galaxy to another. There is, however, in each of the Sc galaxies surveyed a remarkably strict relation between the distance of the H II region from the center of the galaxy and the appearance of its spectrum. The $(N_1+N_2)/H\beta$ ratio increases from 0.1 to H II regions located in the innermost spiral arms to 5 in the outermost regions. At a particular distance from the center, this ratio shows only a small scatter and is uncorrelated with surface brightness, size, or appearance of the H II region.

A program of photoelectric measure-

ment of emission-line intensities in these regions is under way using the multichannel spectrometer.

Compact Galaxies

Sargent is completing work begun last year on a spectroscopic survey of selected compact galaxies in Zwicky's first five lists. Additional work during the present year included spectroscopic observations of a further 20 galaxies and direct photographs with the f/3.67 Ross corrector on the Hale telescope of 30 objects having a wide variety of spectral characteristics. An account of the properties of 130 galaxies is in preparation. Some of the more interesting results are briefly summarized as follows.

1. Two new Seyfert-type galaxies, II Zw 1 and III Zw 55 were discovered. Galaxy II Zw 1 has $m_p=15.1$, $M_p=-21.8$, and $z=0.054$. III Zw 55 has $m_p=14.7$, $M_p=-20.6$, and $z=0.025$. It is NGC 1409 and forms an interacting double system with NGC 1410.

2. Thirty-five of the galaxies show sharp emission lines on a blue continuum, with no absorption lines visible on the available spectra. Examples were mentioned in *Year Book 67,* p. 38. These galaxies cover a wide range in absolute magnitude, from $M_p=-14.9$ to $M_p=-22$. Their emission lines have a range in excitation similar to galactic H II regions, so it is tentatively concluded that the gas in these galaxies is excited by hot stars. Some of these galaxies may be similar to the Haro galaxies. Many of the sharp emission-line galaxies, however, are too bright to be distant irregulars of known types. Several of them show signs of disruption, and some were found to be weak radio sources in the survey by Moffet and Sargent (*Year Book 67,* p. 37).

3. Most of the galaxies, about 50 in number, show late-type absorption spectra with prominent H and K lines. The mean absolute luminosity of these objects is about $M_p=-20$. Most of them resemble N-type galaxies, with a hard, sharply bounded core and a faint halo. Not all of the galaxies have this structure; two in particular, I Zw 155 and II Zw 188, have smooth external rings, about 30 kpc in diameter, around a much smaller, bright core.

An important problem remaining is the determination of the compact objects revealed by the preliminary, more or less random spectroscopic surveys of Zwicky's galaxies. Zwicky has undertaken to survey completely a small region of the sky in the southern extension of the Virgo cluster down to a given apparent magnitude, using schmidt plates provided by Sargent. Spectra of the resulting compact galaxies are to be obtained by Sargent in collaboration with astronomers at the Mount Stromlo Observatory. A preliminary investigation of the spectra of ten galaxies discovered in this new survey has revealed several interesting emission-line objects.

Energy Distribution of Peculiar Galaxies

Oke is using the multichannel spectrometer to measure absolute spectral-energy distributions of various kinds of peculiar galaxies. Included are (1) all the known N-type galaxies, (2) a selection of Markarian galaxies, (3) several radio galaxies, and (4) some of Zwicky's compact galaxies. The continuum is being studied to determine what fractions of the radiation are produced by stars, hot hydrogen gas, and nonthermal sources. The stronger emission lines are being measured also.

The multichannel spectrometer is being used by Oke to obtain spectral-energy distributions of the more luminous members of distant clusters of galaxies. Up to the present time, only clusters with redshifts $z<0.20$ are being observed, since the spectrometer is temporarily limited to 16 channels. More distant galaxies will be observed as soon as all 32 channels can be operated simultaneously.

In a continuing program to study certain subclasses contained in the *Atlas of Peculiar Galaxies,* Arp has now completed an analysis showing that companions on the ends of arms of spiral galaxies tend to be of higher surface brightness and earlier spectral type than the central galaxy. The systems involved are all spirals characterized by young, hot stars and loose, open spiral arms.

One of these systems, *Atlas* 82 (NGC 2535 and NGC 2536), has a redshift of about 4000 km/sec. To obtain a picture of this system in Hα light, use was made of an interference filter of 100-Å transmission half-width centered at the position of the redshifted Hα line. Arp and Vaughan then used the Carnegie image tube (S-20 cathode) at the prime focus of the 200-inch to obtain a direct photograph of NGC 2536 in the light of its own redshifted Hα line. Although the recorded field is limited in size, the net resolution is comparable to that of photographic plates. The speed of the image tube permitted this photograph to be obtained in one hour, whereas with the normal, unintensified image a prohibitively long exposure time would have been required.

Some multichannel scanner observations of the companions on the ends of spiral arms have been made in cooperation with John Danziger of Harvard College Observatory in order to gain more information on the physical processes taking place in these companions.

Redshifts of Galaxies

In a continuing investigation of smaller galaxies that appear, by reason of their concentration in the vicinity of larger galaxies, to be statistically associated with the larger galaxies, Arp has continued to measure redshifts with the Cassegrain image-tube spectrograph at the 200-inch. Recently reduced are data for six small galaxies nearest to NGC 2403. Their redshifts are 0.022, 0.022, 0.018, 0.021, 0.014, and 0.023. It should be emphasized that only when a sufficient number of redshifts are available can statistically significant inferences be drawn about the redshift properties of these smaller galaxies that are in excess density about the larger galaxies. In some parts of this investigation Arp is informally cooperating with Prof. E. B. Holmberg of Uppsala University Observatory, who has recently studied faint companions around nearby galaxies.

Braccesi Galaxies

In the course of his work on the blue quasi-stellar objects, Dr. A. Braccesi of Bologna obtained photographs of a field at the north galactic pole with a coarse diffraction grating over the 48-inch schmidt telescope. This accidentally revealed five galaxies with point secondary images. Braccesi inferred that these galaxies must have unusually concentrated nuclei and suggested that they should be observed spectroscopically. Image-tube spectra of all five objects were obtained by Sargent. No unusual spectral features were observed, although several of the galaxies appeared visually to have abnormally bright nuclei.

Colors of Elliptical Galaxies

McClure and van den Bergh have obtained *UBV* colors of 32 noncluster elliptical galaxies. These observations show that the colors of elliptical galaxies do not depend on cluster membership. This result suggests that the stellar-luminosity function and the mean metal abundance of stars in elliptical galaxies are not affected by the cluster environment.

Radio Galaxies

Searle, in collaboration with John Bolton of C.S.I.R.O., Australia, completed the study of the spectra of 38 identified radio sources from the *Parkes Catalogue.* Redshifts were obtained of the 15 emission-line objects found in this survey.

Sargent obtained an image-tube spectrogram of the radio galaxy PKS 1345+12, which C. Hazard pointed out to have unusual radio properties, implying very small angular dimensions for the radio source. The spectrogram revealed very prominent emission lines of [O II], 3727 and [O III], N_1 and N_2, leading to a redshift of $z=0.121$. No Balmer emission lines were found; possibly they are present but exceedingly broad. The galaxy has $m_p \simeq 17$.

The compact radio galaxy 3C 371, shown by Oke to be variable, has been studied spectroscopically by Arp, and the results are being analyzed by Arp and Visvanathan (*Year Book 67,* p. 37). Deep 200-inch photographs have shown a very low-surface-brightness halo around the semistellar nucleus. The halo extends to the nearest galaxies in the field.

Van den Bergh has obtained red and infrared plates of the nearby radio galaxy M82 with the 200-inch telescope. These plates show that the nuclear region of this galaxy, which exhibits very complex structure, is much brighter in the infrared than it is at shorter wavelengths. A spectrum of the nucleus of M82 does not exhibit the broad Hα profile that is characteristic of Seyfert galaxies.

Catalog of Compact Galaxies

Zwicky, as a post-retirement project, is compiling a catalog of about 5000 compact galaxies, compact parts of galaxies, and probable post-eruptive galaxies. This will include objects from a number of shorter preliminary lists. Details as to structural features, apparent photographic magnitude, and color will be given, together with mention of spectroscopic results obtained by Zwicky or collaborators for about 500 of the objects.

THE GALAXY

Local Galactic Structure

Racine's investigation of the spatial distribution of R associations (young, hot stars associated with reflection nebulae) shows that these objects outline the same pattern as the H II regions and O–B2 clusters, and indicate that gas and dust are well mixed over distances of a few hundred parsecs. The interstellar material in the Orion arm appears distributed in roughly parallel, overlapping "sheets" 1.2 kpc long, 0.1 kpc thick, and tilted by 10° to 15° to the formal galactic plane, their high side leading in the galactic rotation. The present survey is sufficiently complete over a distance of 3 kpc along the Orion arm to reveal the existence of three such tilted sheets.

Galactic Center

See "Infrared Stellar Spectroscopy," p. 122.

SUPERNOVAE

Supernova Search

The supernova search has been reorganized under the supervision of Oke and Sargent, with Kowal conducting the observations. Nineteen supernovae were discovered at Palomar during the report period: 10 by Kowal, 8 by F. Zwicky, and 1 by M. Zwicky. Six of these were found on plates of the *Palomar Sky Survey,* and the rest were discovered during the course of the monthly supernova search with the 48-inch schmidt telescope.

Photoelectric magnitudes are being determined by Kowal and Christensen at the Mount Wilson 100-inch telescope for selected stars in each of the regular supernova search fields. It is hoped that the availability of these "standard stars" will permit the prompt and accurate determination of supernova light curves.

Absolute Magnitudes of Supernovae

In 1968, Kowal derived the absolute magnitudes of 33 supernovae in terms of an assumed Hubble constant of 100 km/sec/Mpc. Type I supernovae were found to have an average magnitude of $M_{pg} = -18.6$, and Type II supernovae had an average of -16.5. In both cases the observed dispersion in absolute magnitude is $0^m.6$.

Some new data for Type I supernovae indicate that their absolute magnitudes may be closer to -18.7 and that the *intrinsic* dispersion in their maximum magnitudes is about $0^m.3$. With the accumulation of new light curves and radial velocities, it is hoped that a definitive redshift-magnitude relation can shortly be derived for Type I supernovae.

Supernovae and the Structure of the Virgo Cluster

If the intrinsic dispersion in absolute magnitude among supernovae is as small as present data suggest, the supernovae can be used as excellent indicators of distance. Kowal has used the apparent magnitudes of 10 supernovae in the Virgo cluster to determine the relative distances of their parent galaxies. The data support the traditional view that the Virgo cluster is a single dynamical unit. The magnitudes of the supernovae, and therefore the distances of the galaxies, do not differ by more than the back-to-front ratio to be expected for such a large, nearby cluster, thus ruling out any multiple-group interpretation of the structure of the cluster.

Cassiopeia A

Van den Bergh and W. W. Dodd of the University of Toronto are continuing their investigation of the expansion of the optical remnant of the radio source Cassiopeia A on 200-inch plates covering the time interval 1951–1968. No star brighter than $m = 23$ is visible within two standard deviations of the adopted position of central expansion. The central star in Cas A is therefore at least 7 mag fainter than the central star in the Crab.

A widened spectrogram, at a dispersion of 50 Å/mm, was obtained of the central star in the Crab. The spectrum of this star (which was subsequently found to be a pulsar) was seen to be continuous. This observation confirmed earlier low-dispersion observations by Minkowski and by Zwicky.

Slow Supernova in NGC 1058

The spectrum of Wild's slow supernova in NGC 1058 (SN 1961e) has relatively sharp lines in emission and absorption. It is related to η Carinae, but is much more luminous. It was found on Harvard plates, as early as 1937, near $m = 18$ until 1955, and then was found to brighten from 1960 to the end of 1962, reaching nearly $m = 12$. It was still visible in 1967 near $m = 20$. Spectra were taken by Greenstein until about two years after the outburst began—one at 18 Å/mm. Descriptions of spectra by Zwicky and Bertola have been published. The total emission, at a modulus of 29.7, is 10^{50} erg, in visible light, neglecting any bolometric correction. A conservative total thermal energy is between 5 and 23×10^{50} erg, quite comparable to a typical supernova of Type I, although not as bright at maximum.

Greenstein finds that the spectrum evolved with time. The emission lines became sharper, shifted to the red by 1.5 Å, and developed P Cygni-type absorption wings. The mean wavelengths of the emission give different velocity shifts; the nebula is at +440 km/sec, but the supernova hydrogen lines are at +765 km/sec, He I at +650 km/sec, and Fe II at 960 km/sec. One sharp absorption line of He I from the 2^3S metastable level, λ3888, is displaced to −320 km/sec, i.e., −760 km/sec with respect to the nebula. There was a short-lived outburst when the supernova reached 12th magnitude, which did not substan-

tially affect the emission-line spectrum but which eliminated the λ3888 line.

The most startling fact about this object is the strength of Fe II absorption and emission lines. Spectra of Type II supernovae show H, He, and C; the quasar 3C 273 shows weak Fe II emission blends. In SN 1961e there are about 40 Fe II lines partially resolved. The spectrum is so crowded that weaker metallic ions might not be seen; a search for Co II and Ni II (interesting for the theory of nucleosynthesis) is inconclusive. They are certainly not very strong. Forbidden lines also are not seen. The energy-level diagram of Fe II is such that the lines studied can be produced by photoexcitation via the ultraviolet Fe II lines, followed by cascades or by collisional excitation. Dependent on details of the excitation process, the abundance Fe/H can vary over a wide range, but seems to be abnormally high. In ordinary novae and 3C 273, Fe II emission is extremely weak compared with hydrogen emission, but in the supernova Hδ is weaker than λ4233 of Fe II. In Merrill's iron star, XX Ophiuchi, many lines of Fe II and [Fe II] are present far weaker than Hγ.

The mass ejected can be determined from the Hβ emission, the electron density, which is high, and an assumed age. It is at least 0.1 $\mathfrak{M}_\odot$, and may be much larger. The anomalous composition will need further detailed study; the parent star may have been a massive Type II supernova detonating in a dense gas cloud. A slow supernova is a contradiction in terms, but in total energy and iron anomaly this object seems to qualify as a supernova.

PULSARS

NP 0532

The only pulsating radio source so far identified with a visible object is NP 0532 in the Crab nebula, first optically observed to be pulsing on January 16, 1969, by Cocke, Disney, and Taylor at Steward Observatory, and identified a few days later by Lynds, Maran, and Trumbo at Kitt Peak National Observatory as the "south preceding star" of the pair near the center of the nebula. This star was suggested as the central star of the Crab by Baade and Minkowski in 1942, on the basis of its position near the center of expansion and its spectroscopic peculiarity (a featureless blue continuum). It is seen on photographic plates as a star of about 16.5 mag; in fact, the light arises almost entirely from the 60 short pulses emitted each second. The object has been observed by Kristian, Westphal, and Snellen with the prime-focus photometer of the 200-inch. Photon counts were averaged at multiples of the known period of the pulsar and simultaneously recorded directly on digital magnetic tape with 1-msec integration times for later analysis.

Two distinct pulses occur during each 33-msec period (Fig. 1). The main pulse is 5-msec wide and asymmetric, the trailing edge being steeper than the leading edge. It is followed 13.5 msec later by a secondary pulse having an amplitude 30% that of the main pulse and 55% as much energy as the main pulse. The secondary pulse is also asymmetric, but in the opposite sense. Both pulses are extremely sharp near the peak. With a time resolution of 60 microsec, the peaks are still cusps, and the full width of the main peak at 90% of maximum is less than 300 microsec.

The light level following the main pulse is slightly higher than that following the secondary pulse. The latter has a very long, shallow tail, with a nonzero slope up to within at least 2 msec of the beginning of the succeeding main pulse. The intensity level between pulses, however, is very low. At its lowest point, it is within a few percent of the nearby nebular background of the Crab, as

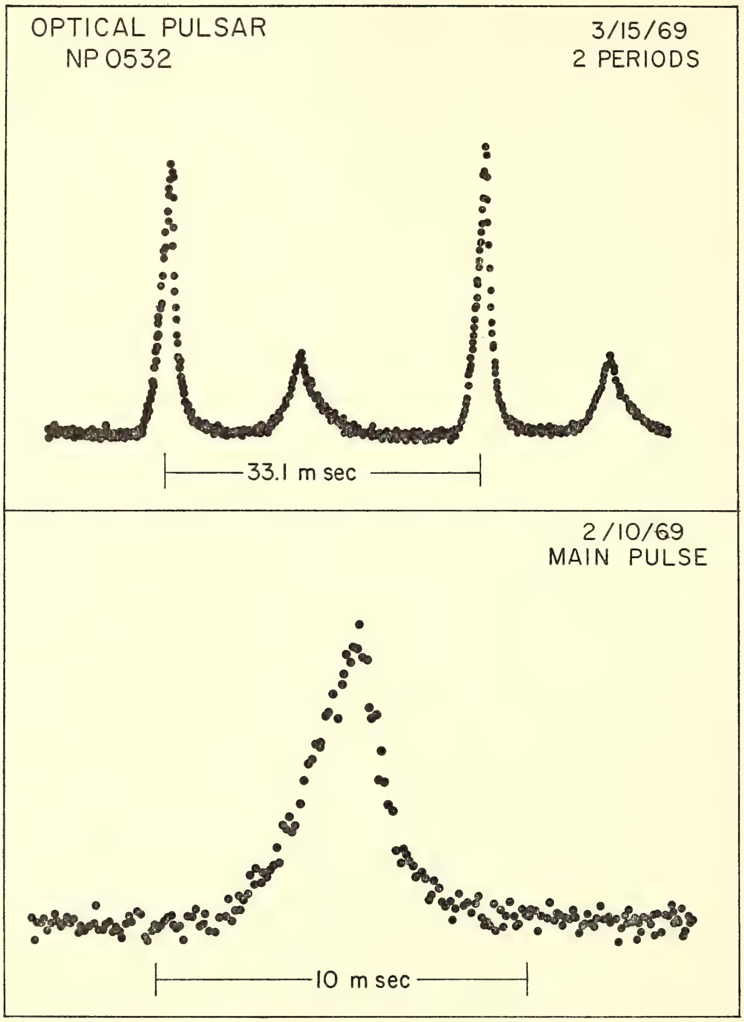

Fig. 1. Light curves of the optical pulsar in the Crab nebula. The data were obtained by averaging photon counts from the 200-inch prime-focus photometer in a 1024-channel multiscaler, cycled at twice the pulsar period. The time resolution is 66 μsec per point. *Upper:* A 2-minute average recorded on 15 March 1969. Note the very sharp peaks on both the main and the secondary pulses; the asymmetry of both pulses; the higher background level following the main pulse; and the long nonzero slope following the secondary pulse. *Lower:* A 1-minute average recorded on 10 February 1969. The detail of the main pulse only is shown, with an expanded time scale. A comparison with the upper light curve indicates the stability in pulse shape on a time scale of a month.

shown by a drift scan in which the edge of the focal-plane diaphragm was allowed to occult the pulsar. This experiment also sets an upper limit of a few tenths of an arc second for the size of the pulsating source. At the 2-kpc distance of the Crab, this corresponds to about 500 astronomical units, which is 10^7 times larger than the diameter of the speed-of-light cylinder for an object

rotating at 30 Hz. It therefore is not a stringent limit for rotating neutron star models.

The data that have so far been analyzed in detail show a remarkable stability of pulse shapes and amplitudes, with accuracies ranging from a factor of a few for successive pulses to less than 1% for 1-min averages compared over times of the order of 2 hours. This indicates that the large variations that are observed at radio wavelengths are probably caused by scintillation, either interstellar or at the source, as has been suggested by several authors.

On time scales of months and years, Kristian has examined plates in the files and finds no changes in the integrated intensity of the pulsar from 1920 to the present, with an uncertainty of 30% from 1939 to the present and 45% from 1920 to 1939. The mechanism that produces the pulses is clearly a stable, long-lived feature of the source.

Polarization measurements of the Crab pulsar were made by Kristian, Visvanathan, Westphal, and Snellen. These show plane polarization of the order of 10% in both pulses, and an upper limit of 5% for circular polarization. The nebular background (when the pulses are off) has a plane polarization of 10.3% in position angle 156°. This is the same position angle and about 40% of the amount of the general polarization of the Crab nebula at the position of the pulsar. Absolute timing was lost between measurements at successive analyzer angles, so the data do not give direct information on the crucial question of possible changes of polarization during the pulses.

On April 26, 1969, Kristian measured the absolute arrival times of the pulses, as did R. E. Nather and his colleagues at McDonald Observatory, in order to compare these with the pulse arrival times in the X-ray region of the spectrum, as measured by Bradt, Rappaport, and Mayer of M.I.T., using a rocket-borne X-ray detector. After correction for the difference in light-travel times from the pulsar to Palomar, White Sands, and McDonald, the optical and X-ray pulses were found to arrive simultaneously to within the measuring uncertainty of 1 msec. Assuming that there is no dispersion along the light path at optical and X-ray frequency, this means that the X-ray and optical pulses are generated within 300 km of one another. Alternatively, if it is assumed that the X-ray and optical pulses are generated at the same place, it implies that the velocity of light at the two wavelengths is the same to less than 1 part in 10^{14}. The X-ray pulses are qualitatively similar to the optical pulses, although there is more relative energy in the secondary X-ray pulses. Most of the energy of the pulsar is in the short wavelength (X-ray) region of the spectrum.

The spectral-energy distribution of NP 0532 has been studied by Oke. The star-sky chopper of the multichannel spectrometer was synchronized with the pulsar period and operated in such a way that the aboslute-energy distributions of the pulses themselves were obtained. After correcting for interstellar reddening, the energy distribution in the pulses in the optical region can be fitted accurately to a Planck function with $T=$ 10,000°K. This fit should not be interpreted as meaning that there is a thermodynamic blackbody present, since the energy density must be enormously higher than that of a 10,000°K blackbody.

Coordinated observations of the pulsed component of NP 0532 were made at 2.2 μ, 1.65 μ, and in the visual region by Neugebauer, Becklin, and Kristian. The pulse shapes, relative amplitudes, and spacing were consistent between the visual and infrared. The infrared amplitude fits smoothly onto the visual data of Oke, but the data suggest that the energy spectrum is not smooth throughout the visual, infrared, and radio regions.

CP 1919

Additional attempts were made by Westphal, Kristian, Snellen, Sandage, and Schmidt to detect variations in Ryle and Bailey's candidate for the pulsar CP 1919, following earlier reports of such variations by other observers. The light from the star was found to be constant, with an accuracy as high as 0.1%. On the basis of a spectral scan by Oke, an infrared measurement at 2.2 μ by Neugebauer and Becklin, and *UBV* photometry of stars in the field by Sandage and Kristian, it was concluded that the star is a normal main-sequence star of spectral type near F0, unrelated to the pulsar.

Optical Pulsar Search

The search for optical objects associated with other pulsating radio sources has been continued by Kristian, using averaging techniques to look for pulsations at the known radio frequencies. No pulsing optical objects have been found in the fields of CP 0328, CP 0808, AP 0823, PSR 0833–45 (the Vela pulsar), CP 0834, CP 0950, CP 1133, HP 1506, PSR 1749–28, AP 2015, or PSR 2045–16, with limits ranging from 20th to almost 25th magnitude.

X-RAY SOURCES

Identification of Centaurus X-2

Working from an improved position (due to Lewin, Clark, and Smith of M.I.T.) for the highly variable X-ray source Cen X-2, Eggen, Freeman, and Sandage made a probable optical identification with the irregular blue variable WX Centauri. The optical position at $\alpha(1950)=13^h09^m38^s$, $\delta=-63°08'$ is within the 1°5 error radius of the X-ray position at $\alpha(1950)=13^h09^m$, $\delta=-62°$. Photometry by Eggen at Siding Spring Observatory showed that WX Cen varies by 0.4 mag from night to night and has the unusual colors $B-V=0.4$, $U-B=-0.7$, similar to those of the positively identified Scorpius X-1.

Image-tube spectrograms taken by Sandage and Freeman with the Mount Stromlo 74-inch reflector show strong emission lines of Hα, Hβ, Hδ, He II λ4686, He II λ5412, C IV λ5802, together with many fainter lines. The unusual spectrum closely resembles that of Sco X-1 in the overlap region $4300<\lambda<5000$ Å, where the broad diffuse high-excitation band near 4640 Å, due to N III, C III, and possibly O II, is present.

Sandage attempted to identify the Vela X-ray source from the new position at $\alpha(1950)=8^h57^m$, $\delta=41°15'$ by the American Science and Engineering X-ray group. Two-color plates were taken with the Uppsala schmidt at Mount Stromlo, but no candidate object was found. The limit of the search was $B=15$ mag.

Sco X-1

In May 1969 a number of observations of Sco X-1 were made by Kristian, simultaneously with other observers, in an attempt to correlate changes in the source photoelectrically and spectroscopically. The Palomar observations were made with Oke's multichannel spectrophotometer at the Cassegrain focus of the 200-inch. Complete spectral scans were obtained continuously, every one minute or less, for periods up to 90 minutes. One such measurement was made simultaneously with a measurement in the far ultraviolet by the Wisconsin Experimental Package of the Orbiting Astronomical Observatory, launched in December. The Wisconsin group detected the source near the limit of their equipment, and preliminary data indicate that the spectrum is approximately flat between 2700 and 5500 Å. Other measurements were made in con-

junction with spectroscopic observations by C. R. Lynds at Kitt Peak National Observatory and satellite X-ray observations by H. Hudson of the University of California at San Diego. These observations are being reduced and correlated.

QUASI-STELLAR SOURCES

Position Measurements

Kristian and Sandage have carried out a program of position measurements of the optical objects associated with 45 unresolved radio sources, mostly previously identified quasi-stellar sources. The measurements were made on plates taken with the 48-inch schmidt telescope, using the newly refurbished and digitized x-y machine at the Santa Barbara Street offices. Position accuracies of the order of 0.2 arc seconds have been achieved by the use of a large number of AGK reference stars, typically 20 on each plate. This program was carried out in cooperation with Dr. C. M. Wade of the National Radio Astronomy Observatory, who has measured the radio positions of the same sources with the 3-element interferometer at Green Bank. The estimated accuracy of the radio positions is also a few tenths of an arc second, and the agreement between the radio and optical positions is entirely satisfactory. This program will supply a fundamental reference grid of well-determined radio-source positions.

Spectroscopy

Spectroscopic observations of quasi-stellar radio sources are being continued by Schmidt. Most of the sources are 4C radio sources in the declination range +20° to +40°, for which identifications are being published by Edward T. Olsen, now at the University of Michigan. Further identifications in this declination zone have been supplied by radio astronomers at Parkes and at the National Radio Astronomical Observatory. It is expected that a sample of quasi-stellar sources complete to well-defined optical and radio limits will be obtained, allowing the determination of optical- and radio-luminosity functions and their variation with redshift.

Schmidt is continuing systematic spectroscopic work on the blue stellar objects identified by Sandage and Luyten in a number of fields at intermediate and high galactic latitude. This should eventually yield an optical-luminosity function of radio-weak or radio-quiet quasars, as well as its variation with redshift.

Bahcall, B. A. Peterson, and Schmidt have studied the absorption spectrum of the radio-quiet quasar Ton 1530, which has an emission redshift $z_{\mathrm{em}}=2.05$. Following a method first used by Bahcall on PKS 0237-23, three acceptable absorption redshifts ($z_{\mathrm{abs}}=1.9365$, 1.9215, and 1.8866) were found, as well as one plausible redshift ($z_{\mathrm{abs}}=1.9800$). The same method applied to similar but random absorption spectra yielded on the average only 0.1 acceptable redshift.

Oke and Wampler (at the Lick Observatory) are continuing to monitor 3C 446 to determine whether the emission lines are variable. No positive results have yet been obtained, indicating that the time scale for changes is at least one year.

Energy Distribution

Oke, Neugebauer, and Becklin have completed a study of the energy distribution of quasi-stellar sources. Twenty-five objects have been observed from 0.33 μ to 2.2 μ with the prime-focus scanner, the multichannel spectrometer, and infrared photometers. Eighteen additional quasi-stellar sources have been observed at 2.2 μ. It is found that the continuum energy distributions can be represented reasonably well by power-law spectra, $f_v \propto v^{\alpha}$, with $0.0<\alpha<-1.7$. There is in no sense a "universal" continuum energy

distribution that represents all QSS. A comparison of the optical and radio fluxes leaves completely open the question of whether most of the radiation from a QSS is in the infrared. Only for 3C 273 has such been demonstrated to be the case. The equivalent widths of the emission lines $H\alpha$, Lyman α, and $\lambda\lambda 1550$ of C IV are remarkably constant. The number of photons in Ly α is significantly smaller than the number beyond the Lyman limit predicted by extrapolating the observed continuous energy distribution. This suggests that a substantial part of the Lyman continuum radiation may escape from the object. The almost constant ratio of intensity of $\lambda 1550$ to Ly α may put very severe limitations on the electron temperature and carbon-to-hydrogen abundance.

BL Lacertae

The remarkable radio source VRO 42.22.01 = BL Lacertae has been studied by DuPuy, Schmitt, McClure, van den Bergh, and Racine. During the period April–November 1968, the visual magnitude of this object varied between 12.0 and 15.5. Light variations as fast as 0.3 mag per day were observed. The spectrum of this object is continuous, so that its distance remains unknown. The very bright apparent magnitude of BL Lac at maximum light makes it improbable that this object is a normal quasi-stellar source. BL Lac would have to be the nearest quasi-stellar if it has a typical QSO luminosity. On the other hand, a distance greater than that of 3C 273 would make it the most luminous object known in the universe.

Distribution

Over the past few years, Arp has studied the distribution of QSS on the sky. Recently he has concentrated on an analysis of 93 QSS with known redshifts. Using the California Institute of Technology 7094 computer with a program designed by F. Bartlett, he reports the result that the distribution of these QSS on the sky is significantly nonrandom. He believes that the distribution changes markedly as a function of apparent magnitude (V) of the QSS, such that the fainter QSS are concentrated in the vicinity of the brighter galaxies in the sky.

The densest grouping of faint QSS, according to Arp, is centered near the position of the exploding galaxy NGC 520 (*Atlas of Peculiar Galaxies,* No. 157). In an analysis recently completed, he discusses the statistical relationships of the properties of the QSS, such as their radio spectral indices and flux strengths as well as their optical apparent magnitudes and redshift with respect to the galaxies in the same region of the sky.

THEORETICAL STUDIES

Theory of Pulsars

T. Gold of Cornell University has suggested that pulsars are rotating magnetic neutron stars which formed in supernova explosions. P. Goldreich of the Astronomy and Geological Sciences Divisions and W. Julian (1969) have investigated the simplest such model, one in which the magnetic dipole moment is aligned with the rotation axis, and have reached the following conclusions. Notwithstanding its intense surface gravity, the star must possess a dense magnetosphere. The particles in the region threaded by those field lines which close within the *light cylinder* (of radius 5×10^9 P cm, where P is the stellar rotation period in seconds) rotate with the star. In the corotating zone the space charge density is 7×10^{-2} B_z/P electronic charges per cm^3, where B_z is the component of magnetic field parallel to the rotation axis in gauss. The field lines which extend beyond the light cylinder

close in a boundary zone near the supernova shell. Charged particles escape along these lines and are electrostatically accelerated up to energies of 3×10^{12} ZR_6^3 $B_{12}P^{-2}$ eV in the boundary zone. (The stellar radius is $R_6 \times 10^6$ cm, and the polar surface magnetic field is $B_{12} \times 10^{12}$ gauss.) Beyond the light cylinder, the magnetic field becomes predominantly toroidal. Its strength is 6×10^{-9} R_6^3 $B_{12}P^{-2}$ r_{pc}^{-1} gauss at a distance of r_{pc} parsecs from the central star. The magnetic torque on the star causes its rotational period to lengthen at the rate P^{-1} $dP/dt = 10^{-8}$ B_{12}^2 R_6^4 P^{-2} M^{-1} yr^{-1} for an M solar mass star. The rotational energy lost by the star is transported out by the electromagnetic field and is then transmitted to the particles in the boundary zone.

Extragalactic Radio Sources

In a continuing study of the variable extragalactic radio sources, Simon investigated the possibility that the positive curvature in the high-frequency radio spectra of such sources might be due to the suppression of synchrotron radiation in an ionized medium (Razin effect). Analytic formulae valid for frequencies below the Razin cutoff were calculated for the spectrum radiated by relativistic electrons. It could be shown, on the basis of the best available data, that the Razin effect is not likely to be responsible for the cutoff observed in 3C 120 and 3C 273, and that synchrotron self-absorption continues to be the most reasonable explanation. In the simplest models that have been suggested to explain these sources, the variable flux arises in an expanding component emitting synchrotron radiation. From an analysis of the millimeter wavelength data for the 1966–1967 variable component of 3C 273 it was shown that there is evidence that the model is breaking down at an early stage of the evolution of the source because the synchrotron and Compton losses of the relativistic electrons are very severe then. Since later observations of the same source at longer wavelengths fit the model well, this provides evidence for a continued acceleration of electrons during the first few months of the bursts' existence. The intrinsic size of the source, over which particle acceleration must have taken place, was ~0.4 pc. Work on possible stochastic acceleration mechanisms is continuing.

Type IV Solar Bursts

The analytic formulae developed for the asymptotic form of synchrotron spectra below the Razin cutoff were used to test the hypothesis that the low-frequency cutoff in Type IV solar bursts is due to the Razin effect. If the observed frequency cutoff is caused by the Razin effect, then the coronal electron density may be derived from the intensity variation in the burst as it propagates outwards from the Sun. Bohlin and Simon analyzed the moving Type IV burst observed by Boischot and Clavelier, and showed that the electron density profiles obtained from K-coronameter data (appropriate to $1.125 \leq r/R_\odot \leq 2$) and from the radio data ($2.2 \leq r/R_\odot \leq 2.5$) form a continuous distribution. It is possible to conclude then that the cutoff was due to the Razin effect, that the radiation in the burst is due to relativistic electrons having a steep inverse power-law energy distribution, and that the coronal magnetic field at $r/R_\odot = 2.2$ was 0.26 gauss at the time of the burst.

Interstellar Gas

K.-H. Schmidt of the University Observatory, Jena, Germany, and van den Bergh have studied the ejection of dust from the Galaxy by radiation pressure. They find that significant dust loss can occur when a dust cloud arches over a bright spiral arm. It is found that the heavy-element abundance and the interstellar gas might be a *decreasing* fun-

tion of time if a significant fraction of the heavy elements are locked up in grains. Dust ejection is expected to be particularly important during the early high-luminosity phase of galactic evolution.

GUEST INVESTIGATORS

Dr. George O. Abell of the University of California at Los Angeles has recently determined the luminosity function of the elliptical galaxies in the central $6.6° \times 6.6°$ region of the Virgo cluster. The luminosity function of the Virgo ellipticals resembles that found by Abell for the elliptical galaxies in other clusters (Coma, Corona Borealis, Abell 151, and Abell 2199). However, if the luminosity functions of the Virgo cluster and the Coma cluster are compared, the ratio of the distance of the Coma to that of the Virgo cluster is found to be about 50% greater than the ratio derived from the difference in apparent magnitudes of the first brightest cluster galaxies.

On the other hand, the Virgo cluster is much less rich than the other clusters investigated, and the critical part of the Virgo luminosity function represents only about the 20 brightest galaxies in the observed field. To obtain a sample of Virgo galaxies roughly twice that previously available, Abell, in March, obtained sets of 48-inch schmidt plates covering four additional fields in the cluster surrounding the central field already studied. It is expected that the reduction of magnitudes of the additional galaxies in these fields will be complete by September 1969, and comparison with the earlier results should be possible then.

Dr. Lawrence Aller and Dr. Stanley J. Czyzak of the University of California at Los Angeles used the 60-inch telescope with Oke's Cassegrain scanner to obtain photoelectric observations of five planetary nebulae in the visible and blue regions. Companion stars were observed in each case. Coudé spectrograms of two of the objects were obtained with the 100-inch telescope, but the program was hampered by unfavorable weather. The study of physical processes in gaseous nebulae is proceeding on the basis of the photoelectric and photographic photometry with the latest theoretical results on collision strengths.

Dr. J. M. Beckers of the Sacramento Peak Observatory, Sunspot, New Mexico, and Dr. J. O. Stenflo of the Astronomical Observatory, Lund, Sweden, in a joint investigation with Howard used the solar magnetograph with 10-second resolution, together with high-resolution spectrograms of $\lambda 5250$, to study very small regions of high magnetic-field strength ("magnetic knots") that occur near sunspots. While the resolution achieved was not really adequate for the purpose, many interesting details were recorded and these are now being examined by Dr. Stenflo.

A program intended to detect the faint outer regions of galaxies has been carried out by Dr. F. Bertola of the Astrophysical Observatory of Asiago, Italy, in collaboration with Arp. Plates obtained with the 48-inch schmidt telescope on the new IIIa-J emulsion were analyzed with the isodensitometer. Several elliptical galaxies were found to possess faint extended halos. Faint extensions of M87, the large elliptical radio-source galaxy in the Virgo cluster, have been detected out to a diameter corresponding to 300 kpc.

Spectra of the galaxies NGC 128, NGC 1808, NGC 3077, and NGC 7753 were secured with the image-tube spectrograph (dispersion 80 Å/mm) at the Cassegrain focus of the 200-inch reflector for dynamical study. NGC 128 is a peculiar S0 galaxy well suited for the determination of the rotation curve from both the absorption and emission lines. In the spectra of the nuclear region of NGC 1808, a galaxy with hot spots,

taken with the slit set at three different position angles, the emission lines are strongly inclined or broken, suggesting the occurrence of some kind of explosion. Spectra of NGC 3077, morphologically similar to M82 and belonging to the same group, were taken for a precise determination of the velocity field. The study of the rotation curve of NGC 7753, the main component of an M51-type system, may permit conclusions as to dynamic stability.

Professor Alessandro Braccesi of the Istituto di Fisica di Bologna, Italy, has continued his program of investigation of the radio-quiet quasi-stellar objects, using the method of the infrared excess. Five high-galactic-latitude fields were observed with the Palomar 48-inch schmidt. Reductions have been completed for one field, and the number-magnitude relation for the QSO has been shown to be rather steep, in agreement with the cosmological evolution suggested by Schmidt.

Dr. John G. Bolton, of the Radiophysics Laboratory, C.S.I.R.O., Australia, obtained a series of two-color plates centered on *Sky Survey* centers taken for the region Dec 0° between R.A. 17^h and 13^h. Exposures were 8 min in the blue and 1 hour in the ultraviolet. The purpose of these plates was to aid in the identification of radio sources as quasi-stellar objects from the Parkes survey of Dec $\pm 4°$ at 2700 MHz. An average of 3 QSO per plate have been identified for most of the region where the radio-survey limit is 0.35 flux units, and as many as 10 per plate in selected areas where the radio-survey limit is 0.08 flux units.

Examination of the plates in the positions of previously unidentified sources from the Parkes general catalog had disclosed 2 QSO that have become visible since the original *Sky Survey* was made. The sources are PKS 0950+00 and 1218−02. (The same happened in the case of 3C2, which was not visible on the *Sky Survey* plates.) Twenty-four position plates of new identifications were taken to provide additional position calibrators.

In an investigation of rotation and internal motion in galaxies, Dr. G. Courtes of the Marseilles Observatory made intensive observations of M33, NGC 6496, NGC 253, and NGC 6888 with the 200-inch telescope. He used a Fabry-Perot interferometer of his own design, working on the Hα line with a dispersion of 25 Å/mm. In M33, five interferograms were taken on the major axis and radial velocities of 2500 points have been measured. Courtes confirmed the existence of the disk of diffuse ionized hydrogen, as well as the fact that its circular velocity is 15 km/sec slower than that of the spiral arms.

Strong noncircular motions were found in NGC 6946 and NGC 253. A preliminary examination of plates of M31 gave more than 60 radial velocities in a field 6′ in diameter; it confirmed the absence of expansion in the arms.

Dr. I. J. Danziger, in collaboration with graduate students at Harvard, has analyzed high-dispersion spectra of the bright K giant, ζ Cygni. It is a moderately pronounced example of a Ba II star, the brightest now known, with enhancements among the *s*-process elements. Danziger and Jura have analyzed high-dispersion spectra of HD 137569, a halo B star. The helium abundance appears to be normal, but silicon and magnesium are very underabundant. This star has a low surface gravity ($\log g = 2.3$) and appears to have a variable radial velocity. It may be a member of a sequence of early evolved stars of Population II which so far are unaccounted for theoretically.

Danziger is continuing a program of observations of centers of normal galaxies of various types containing radio sources. Low-resolution scans of approximately 30 objects have been obtained with the Mount Wilson scanner and the Palomar multichannel scanner. There is significant variety in the continuous

spectra, which are receiving further study.

Mr. Joseph R. Bruman of the Jet Propulsion Laboratory used the 48-inch schmidt during the lunar eclipse of October 1968 in a search for the reported clouds of dust circling the earth near the libration points of the moon's orbit. It was possible to make the observations near the zenith, but neither diffuse clouds nor discrete objects were found.

Dr. Robert F. Garrison of the David Dunlap Observatory used the 100-inch telescope and Newtonian spectrograph for five nights for four different programs. These included a search for physical members of the association II Scorpii among the faint apparent companions to the bright stars, a search for variations in the spectra of the peculiar B stars in II Sco, and obtaining spectrograms of selected Mira-type variables near minimum light.

Dr. Hugh M. Johnson of the Lockheed Palo Alto Research Laboratory used the 48-inch schmidt telescope with 5×7-inch plates centered on positions of the X-ray sources GX9+9, GX5−1, GX9+1, GX13+1, GX17+2, Serpens XR−1, Cygnus X−1, Cygnus X−3, Cygnus X−4, and Cassiopeia A. Five exposures per plate, shifted 4″, were the standard procedure in a search for rapid variable stars that might be candidates for optical identification, but so far the examination of the fields has not produced a positive result. Exposures on Cas A in various passbands were made to improve the composite-plate imaging of the yellow continuum reported in 1967, and to compare the yellow imaging directly with Hα (filamentary) imaging.

The one coudé run at Palomar and the two with the 100-inch at Mount Wilson were used by Dr. Philip C. Keenan of Ohio State University primarily to obtain spectrograms of Mira variables for the pending revision of the catalog of their spectral types. A slight modification of the classification of the coolest M-S was found necessary on the basis of the spectrograms of χ Cygni in the blue region. In most M stars the number of blue TiO bands observable continues to increase at least as far as type M8, but in the M-S stars the bands from vibrational levels with $v = 3$ or higher can remain very weak or invisible, while bands originating in the lowest vibrational levels increase. This is the same effect that is conspicuous in the yellow region, and apparently reflects the lesser absolute concentration of TiO in M-S stars. Consistent temperature classification of these stars can be carried out by using such band ratios as 4395 (8, 3)/4422 (4, 0).

Following the discovery at Flagstaff of peculiarities in the spectrum of the B star HD 191980, coudé spectrograms were taken to confirm the abnormally strong C II/He I line ratio. Since a 1963 spectrogram of the red region in this spectrum was available, the coudé plates provided the following radial velocities: Pc 7484, -15.0 ± 0.7 km/sec, August 12, 1963; Ce 191287, 8, -15.4 ± 1.0, August 9, 1968.

Because these velocities are much more accurate than the earlier published values from Lick and Victoria, the large disagreements between the new and old sets do not necessarily indicate variation. The mean of the interstellar D-line velocities in 1963 and 1968 was +11.7 km/sec.

In cooperation with O. C. Wilson and A. J. Deutsch, Keenan completed the paper on classification of K and M giants by line ratios (*Astrophys. J., 156,* 107, 1969).

Dr. Willem J. Luyten of the University of Minnesota, working with the 48-inch schmidt, has continued taking second-epoch plates for comparison with the *National Geographic Society–Palomar Observatory Sky Survey.* To date, 833 fields of a total of 936 have been repeated in this *Proper Motion Survey.*

Luyten has completed examination and analysis of the North Polar Cap and has published a *General Catalogue* giving proper motions for more than 10,500 stars north of Dec $+75°$.

Dr. T. B. McCord of M.I.T. used the 60-inch, 100-inch, and 200-inch telescopes for a variety of projects concerning solar-system objects. A special two-beam photometer was used to observe the spectral reflectivity, 0.30 to 1.10 μ ($\Delta\lambda \simeq$ 200 Å), of the rings and some bands of Saturn and of the satellites of Saturn at several positions in their orbits. Also, several asteroids were observed at various points in their spin period.

The spectral reflectivity of the brightest satellites of Jupiter was observed also. This is part of a complementary program carried out on the Mount Wilson 24-inch telescope by Mr. T. Johnson, a graduate student, to observe the changes in reflectivity of the satellites as a function of orbital position.

During the early spring of 1969, Mr. Carl Pilcher, another graduate student, and McCord used the 60-inch telescope to measure the spectral reflectivity of various bands on Jupiter. These observations are being analyzed along with similar observations made with the prime-focus scanner of the 200-inch telescope.

The 24-inch telescope was used by McCord and several graduate students to observe the larger satellites of Jupiter and some asteroids. The spectral reflectivity (0.30–2.5 μ) of various regions on the lunar surface also was studied.

Dr. D. H. McNamara of Brigham Young University obtained intermediate-band photometric observations of several RR Lyrae variables in the globular star clusters M92, M3, and M15. These observations have proved to be extremely useful in showing that the color excesses of M92 and M3 are essentially zero, while M15 is definitely reddened. They also have proved useful for estimating the metal abundance of the RR Lyrae variables in these clusters.

In November 1968, McNamara attempted to secure some spectrograms of metal-strong RR Lyrae variables at minimum light for the purpose of estimating the line blanketing in the ultraviolet. The program was unsuccessful because of poor weather conditions. The program was revised, however, and good high-dispersion spectrograms of several bright Cepheids were secured. These spectrograms are proving useful for estimating the effects of line blanketing on narrow-band photometric indices. The spectrograms were exposed very strongly in the ultraviolet for the purpose of gaining information on absorption-line strengths in the wavelength region of $\lambda\lambda$3200–3800.

Dr. Walter E. Mitchell, Jr., of Ohio State University used the Snow Telescope on Mount Wilson in August and September 1968 to obtain solar-spectrum observations with the McMath-Hulbert spectrometer. The instrument was used in the double-pass mode to obtain a high-resolution atlas of integrated sunlight, a mosaic of flat mirrors being used to feed the spectrograph. The atlas, requiring 17 observing days, covers the spectral range $\lambda\lambda$3900–5900. This atlas, being recorded near time of solar maximum, will serve for the intercomparison of Fraunhofer-line central intensities with a similar atlas made near the time of the minimum of solar activity in 1964.

A number of digitally recorded spectral scans were made at the center of the sun's disk in the ultraviolet range shortward of λ3010.

Also, the program of photoelectric limb scans for the measurement of mean chromospheric heights was extended to include one polar limb as well as an equatorial limb. Scans in the Hβ and Ca II H lines were obtained simultaneously in the core and continuum.

Dr. Jeffrey D. Scargle of the Lick Observatory, working with the 48-inch schmidt, obtained plates of a number of quasi-stellar objects (with $z \sim 2.0$) using narrow filters to isolate their Lyman-α emission. The goal was to detect possible

reemission of Lyman-α from intergalactic hydrogen near the QSO, most likely in the form of clouds. Such emission would be produced by direct scattering, and also could be the result of recombination if enough ionizing radiation escaped from the QSO. So far no circum-QSO emission has definitely been detected, a result that places an upper limit on the density of intergalactic hydrogen.

Plates were taken also of the Crab nebula and the Cygnus Loop using G-emulsion and a Wratten 15 filter, a combination that avoids all but a few weak emission lines. In the case of the Crab, the aim was to go as deep in the continuum as possible to see if there is a halo of synchrotron emission from electrons escaping from the nebula.

Dr. Jan O. Stenflo of the Astronomical Observatory of Lund, who was in residence for several months, worked on a number of solar problems, mostly with the magnetograph of the 150-foot tower telescope. He recorded the magnetic field near the north and south heliographic poles on most days during the period July 3 to August 23, 1968. The aperture was $5'' \times 5''$, but on some days with very good seeing in the morning the $2''.3$ aperture was used also. The main reduction and the isogauss drawings were made on the IBM 7094 computer at Caltech, with funds provided by the Office of Naval Research. A computer program was written to draw the isogauss contours in a polar coordinate system to show the sun as viewed along its axis.

These polar synoptic charts show that the magnetic field was directed predominantly outward at both poles of the sun; i.e., the situation during this observational period was similar to that during the preceding maximum of solar activity. If these synoptic charts are given a straightforward interpretation, they mean that the field at the north pole had already reversed sign, but that the field at the south pole had not.

To investigate the problems of interpretation of solar-magnetograph observations, Stenflo made a number of magnetograph records with the $17''.5$ aperture in the lines Fe I λ5250, Fe II λ6149, Ca I λ6103, Si I λ5690, Cr I λ5248, and in the Zeeman-insensitive lines Fe I λ5576 and Fe I λ5124. Smaller apertures were also used. The analysis of these observations is under way.

A method to obtain a map of solar magnetic fields directly in one spectroheliogram was developed and successfully tested with the spectroheliograph in the 60-foot tower. The principle of the method is to modulate the light with a reversible quarter-wave plate while the spectroheliograph is scanning. The method was extended in cooperation with Dr. A. Bhatnagar to make it possible to obtain maps of solar-velocity fields as well.

Stenflo investigated theoretically the transformation of the kinetic energy of rotational motion of a sunspot to electromagnetic energy in filamentary electric currents. With this mechanism, the time needed for preconditioning the solar atmosphere for a flare may be of the order of minutes for small flares and of the order of hours or days for large flares.

A spectrogram of the O-type star Von Zeipel 1128 in the globular cluster M3 was obtained with the Carnegie image-tube spectrograph at the Hale telescope by Dr. S. E. Strom of the Smithsonian Astrophysical Observatory. From analysis of the spectrum it was concluded that this unusual object had $\mathfrak{M} \gtrsim 0.6\ \mathfrak{M}_\odot$ and a He/H ratio close to that of Population I O and B stars. Despite the fact that other stars in M3 have metal deficiencies of at least a factor of 10, the measured strength of N III and O II lines suggests much higher metal abundances in Von Zeipel 1128. Various arguments concerning its evolutionary history lead to the tentative conclusion that this star is in a post-double-shell source phase and most likely has a carbon-burning core. Spectra were

obtained of several A stars in the young galactic cluster NGC 2264, which falls below the zero-age main sequence. Analysis of these spectra is currently under way.

As a guest investigator, Dr. G. A. Tammann of the University of Basel completed in eight nights at the 48-inch schmidt telescope the three-color observations for four fields, including a field around *h* and χ Persei. The plates, taken in the *R, G, U* system, will be used for W. Becker's extensive program of investigation of the density and luminosity functions in different directions of the Galaxy and for the photometry of the galactic clusters contained on the plates. Since photoelectric sequences are known in all four fields, the reduction of the fields can be begun immediately.

Tammann rediscovered on a 48-inch schmidt plate, taken on November 19/20, 1968, the periodic comet Perrine-Mrkos (1968h). He has completed, in cooperation with Sandage, a photometric investigation of the cluster double-Cepheid CE Cassiopeia. The results, which include a calibration of the period-color-luminosity relation for galactic Cepheids and the indication that the components of CE Cas suffer mass loss, are in press.

Dr. A. Terzan of the Lyons Observatory was a guest investigator for two months in the summer of 1968. He worked with the 48-inch schmidt telescope, obtaining three-color (*B,V,R*) plates of the central region of the Galaxy. The aims were to investigate red and extremely red objects for interstellar absorption; to detect new variable stars, in particular those of RR Lyr type; to establish sequences of *B,V,R* magnitudes for certain globular clusters situated in the direction of the Galactic center; and to attempt resolution of the stars in the large observing cloud "C." Six new star clusters were discovered, to be further investigated with the 1.93-meter telescope of the Haute-Provence Observatory. Sequences were established in the vicinity of NGC 6304, and the amplitudes of 83 variables in the field of the cluster were determined. Numerous other variables will be studied with the blink comparator of the Lyons Observatory.

Dr. R. van Helden of York University, Toronto, used the coudé spectrograph of the 100-inch telescope to obtain *UV* spectrograms of a number of B-type stars. This is the first phase of a program to investigate the hydrogen content of early-type supergiants.

Dr. N. Visvanathan of the Harvard College Observatory has used the multichannel scanner of the 200-inch telescope to acquire linear polarization and continuum measurements of BL Lacertae from λλ5820 to 7980. *UBV* data and polarization observations at 4700 Å have been obtained at the Cassegrain focus of the 100-inch telescope. The continuum is highly polarized (10.8%), and the polarization is constant in the wavelength range observed. The red and infrared continuum is smooth and straight, having a steep slope $P(\eta)\alpha\eta^{-2.78}$ that fits nicely to all the observed scanner points. There is no indication of any strong emission lines or bands in the region between λλ5820 and 10,860. These results can be explained if the major portion of the continuum of BL Lac is of synchrotron origin. Further identification of the radio source VRO 42.22.01 with BL Lac can be taken to confirm the nonthermal nature of the continuum of BL Lac.

Polarization observations of the Crab pulsar at about 4700 Å were made by Visvanathan in collaboration with Kristian at the prime focus of the 200-inch telescope. The observations were made at position angles 0, 90, 180, 270, 0, 30, 120, 210, 300, 30, 60, 150, 240, 330, and 60 degrees. Each angle was observed continuously for about 2 minutes with a time resolution of 1 msec. The areas under the main pulse and the secondary pulse have been computed for each angle, and the radiation is found to be polarized. Polarization is the same for the two pulses and is equal to $10\% \pm 0.2\%$; the position

angle of the electric vector is 98° (measured from north toward east). Background radiation, which is composed mainly of nebular background, has been analyzed for polarization. It is constant in all parts of the light curve and is equal to $11\% \pm 0.2\%$; the position angle of the electric vector is $159° \pm 1°$. The position angle of the electric vector of the nebular background within 50 sec of arc around the pulsar is nearly constant. These observations show that the polarization of pulses is different from that of the background radiation. Further, the energy emitted between the pulses has the same polarization angle as the surrounding nebula.

Visvanathan has observed the following optically variable QSS, N-type or Seyfert galaxies for both polarization and color: 3C 279, 3C 345, 3C 454.3, 3C 446, 3C 147, PKS 1510−08, 3C 371, 3C 390.3, ZW 1727+50, 3C 109. Some of these objects were observed many times during the year. All were found to be polarized in the range from 3 to 10%. Except for 3C 454.3 and ZW 1727+50, all were faint and therefore were observed at the 200-inch prime focus or Cassegrain focus. Those that have been observed frequently showed variation of position angle from 9° to 80°. The source 3C 454.3 showed variation of position angle from 48° to 82° and change of polarization from 5 to 3%. Wavelength dependence of polarization, both with multichannel scanner and filter, showed the following important results: (1) Lines of Mg II in 3C 446, 3C 345 are found to be unpolarized; and (2) 3C 371 (N-type galaxy) showed a strong wavelength dependence of polarization similar to NGC 1068:— $P_U=10\%$, $\theta=57°$; $P_B=7\%$, $\theta=56°$; $P_V=5\%$, $\theta=56°$. Thus there is clearly a mixture of thermal (galactic) and nonthermal in the continuum of 3C 371.

Dr. G. Wallerstein of the University of Washington obtained spectrograms of the C^{13}-rich CH star HD 209621 in September 1968. An analysis has been completed and submitted for publication. The composition is similar to that of the C^{13}-poor CH stars in that the metals are deficient by a factor of 20 as compared to normal stars. The rare earths are enhanced, relative to the metals, by a factor of 8. There is some evidence that the nitrogen content is high, which may be expected from the CNO cycle reactions when C^{13} is enhanced.

Spectrograms of the 45-day Cepheid SV Vulpeculae have been taken during rising light to study the behavior of Hα and other lines formed at various optical depths. Metallic lines show the expected effect that high-excitation lines of Si II begin their shift to the violet first, while zero-volt lines of Sr II are last affected by the progressing wave. Hα absorption is double at minimum light, then single and displaced to the red of the metallic lines by 50 km/sec. At maximum a new absorption component of Hα appears displaced 40 km/sec to the violet of the metallic lines. From maximum to at least phase 0.10 both components are present. This behavior is entirely different from that reported by Kraft for the 16-day Cepheid X Cygni.

ASTROELECTRONICS LABORATORY

Future Data Systems

With a staff of twelve, under the supervision of Dennison, the Laboratory has started a program to adapt small computers for use directly at the telescopes. The current plans call for these computers to be used as Central Processing Units (CPU) with the 100-inch, 60-inch, and the 150-foot tower at Mount Wilson, and the 200-inch and the new photometric 60-inch at Palomar Mountain. The concept for the new CPU systems was created by Sachs and Hall to improve efficiency and to satisfy the spe-

cial requirements of modern photoelectric observing instruments. The goal of this effort was to find the best data and programming system that would provide for the maximum possible flexibility at reasonable cost. The possibility of changing the inter-relationship of peripheral telescopic devices; i.e., counters, timers, encoders, telescope drives, etc., is essential to a system of this type. With the new concept, these changes can be accomplished by altering only the program that is stored in the CPU memory. Furthermore, new peripheral devices can be added without changing any of the existing circuitry. In addition to handling data, these new systems will be capable of controlling the telescopes, setting on any object in the sky rapidly and accurately. Projects for the 150-foot tower at Mount Wilson and the 200-inch and 60-inch telescopes at Palomar Mountain are in progress. Work on the Mount Wilson 100-inch and 60-inch telescopes will begin as soon as funds become available.

Multichannel Spectrophotometer

The largest single project completed in the last year was the multichannel spectrophotometer electronic system, which was installed on the 200-inch during July. This project was carried on by the Laboratory staff in consultation with Oke. The spectrophotometer itself has 32 photomultipliers used for simultaneous pulse-counting photometry. The high-speed pulse-amplifier discriminators are mounted on the spectrophotometer, and 32 coaxial cables conduct the signals from the Cassegrain observing location to the data room for the 200-inch.

A special observer-oriented control panel was designed and constructed for the spectrophotometer. This display panel indicates the angle of the grating, as well as which of several gratings is in place. It further indicates the slit mask for the red and blue cold boxes, and which of the pairs of entrance apertures is in place. All of this information is transmitted by multiconductor cables from the spectrophotometer to the data room for display and subsequent recording.

The data system for the spectrophotometer is the basic 200-inch data system that was installed last year. At present, this system records raw data from the spectrophotometer counters, the grating wavelength, slit-mask position, grating number, and aperture size, as well as the sidereal time, civil time, data-acquisition time, telescope coordinates, the star name, and other miscellaneous information. All of this information is recorded on summary punch cards and printed paper tape.

The spectrophotometer has two circular entrance apertures: one admits the light from the observed object plus the night-sky background, and the other admits light from an equivalent area of the sky. A motor-driven mechanical chopper wheel alternately covers the apertures. A phase-reference signal is generated by a magnetic pick-up near the outer edge of the chopper wheel. Electronic counters accumulate the pulses that are generated by the light that is detected by the 32 photomultipliers. After all the data have been recorded on punched cards, the computer at a later time can calculate the difference between the two apertures, and thereby give the net star intensity.

This design was reevaluated last year. The system will now be revised by using 16 counter pairs (32 counters total) instead of the 32 counter pairs (64 counters total) that were originally planned. In the new system, after each half cycle of the chopper (approximately 16 msec) the contents of the counters will be transferred to a small computer and the differences calculated for display on a television-type monitor. A small monitor will be placed in the observing cage near the observer to permit him to examine the data being collected. The basic raw data and pertinent observing informa-

tion will be recorded on magnetic tape for later computer analysis.

Mount Wilson TV Tests

With the advent of instruments such as the multichannel spectrophotometer and the new image-tube spectrograph, which are capable of measuring radiation from objects that cannot be seen in a telescope eyepiece, it is imperative that additional visual aids be developed for field viewing. To explore the possibility of using closed-circuit television, arrangements were made with Dr. John Lowrance of the Princeton University Observatory to use the 60-inch telescope for evaluation tests. The purpose of these tests was to allow the Princeton group to test their cameras and equipment under good conditions with a large telescope, dark sky, and typical star images; and to provide an opportunity for evaluation of a well-designed system operating under typical conditions.

The two camera tubes were tested, a Westinghouse Secon and an RCA Image Isocon. Observations were made of a number of different astronomical objects. One was a cluster in which stars ranging from magnitude 13 to 22 had been measured photoelectrically. Extended objects such as the Ring nebula in Lyrae and the nucleus of a galaxy were also examined. Observations were made with a bright sky caused by the moon and Los Angeles lights, and with a dark sky after moonset and while the valley was covered by a dense fog. The camera system uses integration times that are multiples of 12 seconds. Both systems in times of the order of one minute or less could detect stars as faint as magnitude 20. At the same time, experienced observers were able consistently to see stars of magnitude 17. Thus, apart from integration time considerations, both TV camera tubes are capable of detecting stars approximately 3 mag fainter than those which are visible to the unaided eye.

It can be anticipated that these TV systems will work effectively with large telescopes such as the 200-inch. A finite integration time of 10 sec will require new guiding techniques, but developments in this area appear to be relatively straightforward. The use of integrating TV cameras will substantially reduce the time required to find, set, and guide on very faint stars or galaxies.

Other Activities

Numerous small projects were carried out in the Astroelectronics Laboratory, in addition to maintenance of all the electronic instrumentation for the Observatories. Approximately 220 trips were made to the mountain tops to set up and check out electronic equipment prior to observing runs. This procedure reduced lost observing time resulting from electronic failures to an almost negligible level.

INSTRUMENTATION

Mount Wilson 60-Inch Modernization

With general coordination by Vaughan, the 60-inch telescope drive, gears, and auxiliary mechanical subassemblies have been completed, and final installation along with a temporary control console will be completed shortly. The installation includes a new declination gear and both polar axis and declination drive systems, as well as new cables and wiring compatible with other Mount Wilson and Palomar telescope drive and data systems. The coudé flat-mirror mechanism has been modified for use with the new coudé spectrograph. This work is being funded under NASA Contract NSR 09-140-001.

Palomar 60-Inch Photometric Telescope

The 60-inch photometric telescope mount fabrication and shop assembly tests under the supervision of Rule were

completed on schedule in March. All components have now been shipped to Palomar, and are awaiting erection after the Oscar G. Mayer Memorial Dome has been completed, about midsummer. Mechanical and electrical components of the telescope have been constructed under National Science Foundation Grant GP-5566.

The Oscar G. Mayer Memorial Dome is nearing completion, although construction was delayed somewhat by severe winter rains and by road and manpower problems of the contractors. Concrete construction, steel dome room partitions, and all of the building's mechanical systems are finished, with final hardware, dome drives, and auxiliary systems to be installed by late July 1969.

Multichannel Spectrometer

The multichannel spectrometer has now been in operation for one year. All 32 photomultipliers have been installed and any 20 of these can be selected for operation. A small computer has been purchased and is being interfaced with the instrument and the data system. Within the next few months, when installation is complete, it will be possible to operate all 32 channels simultaneously. A magnetic-tape output is also being incorporated into the system. This will eliminate the one hour of observing time per night now devoted to punching the large number of output cards. The reliability of the over-all system has proved to be excellent. Occasional component failures still occur, but these are usually detected and corrected before observing runs begin. The rate of acquisition of data is at least as high as that predicted when the instrument was being designed.

Spectrograph Camera

The speed of the Cassegrain image-intensifier-tube spectrograph installed at Palomar in 1967 is so high that exposures in the blue are limited by the sky background to 15 or 20 minutes. Because of this, a substantial fraction of the observing time is used in loading and changing plate holders. To reduce this operating time, Bowen and Rule have designed a new reimaging camera that will use IIa-O emulsion on 16-mm Estar-base motion picture film and will have a rapid-change mechanism. The camera reimages the phosphor on the film at 1:1 and is of a solid block, all-reflecting design with an effective focal ratio on each side of f/1.6. A field of 4×38 mm is covered with all the light from a point source falling in an 8-micron circle.

To reduce the instabilities of the film, the change mechanism provides for each section of the film to be open to ambient conditions for two exposure periods prior to its own exposure. During the exposure, the film is sealed against the fused silica block of the camera.

Interferometric Photometer

A photoelectric photometer with a Fabry-Perot scanning filter has been constructed under the supervision of Münch and Rickard, to be used for the observation of extended emission-line sources. The instrument utilizes a pressure-scanned etalon with 1-inch clear aperture and interference filters for order isolation. It is designed for operation at the Cassegrain focus in pulse-counting modes.

Photometric Calibration of Direct Plates

A new technique for photographic photometry has been successfully tested by Racine with the 60-inch and 200-inch reflectors. In the converging beam ahead of the photographic plate, he inserts a small optical wedge that produces secondary images of field stars, bearing a calculable intensity ratio to the primary images. He has succeeded in reproducing photoelectrically calibrated sequences with a systematic accuracy better than $0\overset{m}{.}1$ at the plate limit. The method can

be used to set up reliable photometric sequences to the limit of any direct photograph, a few bright photoelectric standards being sufficient to determine the zero point of the magnitude scale. The main advantage of this technique is that both the primary and secondary images are obtained simultaneously on the same plate and under identical conditions of guiding, seeing, and transparency, thus ensuring identical photometric characteristics for the two sets of images.

Fast Data System

To permit an early and effective attack on the problem of measuring very rapid light variations in pulsars and other objects, Kristian assembled a special portable data system. Its main components are a 1024-channel signal-averaging computer for averaging photoelectric data at the telescope, a digital magnetic-tape recorder for recording the data from the averager and for collecting raw photon pulse counts with integration times down to 100 microsec, and a frequency synthesizer with a very good quartz-crystal time base and 8-digit frequency resolution. Interfacing was done by G. H. Snellen of the Caltech Computing Center.

PHOTOGRAPHIC LABORATORY

The Photographic Laboratory, under the general supervision of Miller with Difley assisting, continued the program of routine tests of all photographic materials obtained for use at the Mount Wilson and Palomar telescopes. These tests assure quality control of the photographic materials reaching the astronomers and provide the observers with emulsion-sensitivity data useful in estimating exposure times. Development of improved testing apparatus is proceeding.

Consultation with staff and visiting astronomers on photographic aspects of research programs is a routine service by the Photographic Laboratory. Effort is made to have the latest and best information immediately available on all aspects of astronomical photography.

Requests for work prints and publication prints have been heavy. Difley has performed most of the routine plate tests and measurements as well as many experiments required to solve problems in commercial packaging of the Observatories' new MWP-2 photographic developer. This new developer, reported last year, is in great demand. It has become standard for most photographic work done on Mount Wilson and Palomar Mountain, and has been adopted by a number of other observatories. Full details concerning the developer have been published and a patent application is in preparation.

Equipment was tested and installed at Palomar for baking 10×10-inch and 14×14-inch plates for the 48-inch schmidt telescope. Such baking makes possible application of the relatively new Kodak Type IIIa-J plates with an increase of nearly 2 magnitudes in the limiting magnitude of the 48-inch telescope.

Miller was appointed chairman of the American Astronomical Society's Working Group on Photographic Materials and in this capacity has initiated investigations of a number of problems related to astronomical photography. Information of general interest gathered by the Group will be published in a new series of papers called the *AAS Photo Bulletin*.

In connection with the centennial of the birth of George Ellery Hale, several displays of material related to the history of the Observatories and Hale's contributions to astronomy were prepared. These exhibits have traveled widely.

BIG BEAR SOLAR OBSERVATORY

Construction was begun on the tower and laboratory of the Big Bear Solar Observatory at Big Bear Lake in the San Bernardino Mountains in October 1968 and completed in April 1969 by the J. Putnam Hank Construction Company. Great difficulties were occasioned by the unusually severe winter, which necessitated suspension of the work for some time. Installation of the dome by technicians of the solar group is under way, and it is expected that the solar equatorial telescope and the coudé spectrograph will be installed during the summer. Scientific activity at the new site is scheduled to begin in July 1969.

The California Institute of Technology has purchased the land formerly leased from the Bear Valley Development Company with the exception of the strip of land under the lake, which is still under long-term lease from the Bear Valley Mutual Water Company.

SOUTHERN HEMISPHERE OBSERVATORY

After a careful appraisal of the available observatory sites in Chile, and with consideration of the technical, legal, and political factors, a decision was made to acquire an area including Las Campanas, an 8100-foot mountain at a latitude of about 29°02′S. Steps were taken to purchase 20,800 hectares (208 square kilometers) from the Government of Chile and, after authorization by the Congress, as well as approval by the Ministry of Lands and by the President of the Republic, the transaction was scheduled for final completion in July 1969.

Under the supervision of Adkison, who was appointed Associate for Administration on October 1, 1968, the work of the project was organized to provide for development of water, construction of an access road, protection from interfering mining claims, and detailed topographic mapping of the summit ridge, among other requirements. Plans developed earlier by Rule for mountain-top installation of observatory facilities and services are now being reviewed by Rule and Adkison to adapt them to requirements of the new location. Meteorological observations are being continued on Las Campanas.

Property known as Colina El Pino in La Serena was purchased as a site for a future project office, warehouse, and vehicle yard.

BIBLIOGRAPHY

Abt, Helmut, Peter S. Conti, Armin J. Deutsch, and George Wallerstein, The mass and other characteristics of the magnetic star HD 98088. *Astrophys. J., 153,* 177–186, 1968.

Adelman, Saul J., Peculiar stars in the Lac OB1 association. *Publ. Astron. Soc. Pacific, 80,* 329–331, 1968.

Arp, Halton, Optical observations of two Seyfert galaxies. *Astron. J., 73,* 847–848, 1968.

Arp, Halton, Relation between quasi-stellar radio sources and radio compact and radio N galaxies. *Astrophys. J. (Letters), 153,* L33–L38, 1968.

Arp, Halton, Further comments on the ring around M81. *Soviet Astron.–AJ, 12,* 715–716, 1968.

Arp, Halton, *see also* Greenstein, Jesse L.

Bahcall, John N., Jesse L. Greenstein, and Wallace L. W. Sargent, The absorption-line spectrum of the quasi-stellar radio source Pks 0237-23. *Astrophys. J., 315,* 689–698, 1968.

Bahcall, John N., Patrick S. Osmer, and Maarten Schmidt, On the absorption spectrum of Ton 1530. *Astrophys. J. (Letters), 156,* L1–L6, 1969.

Barbon, Roberto, The frequency of supernovae in clusters of galaxies. *Astron. J., 73,* 1016–1020, 1968.

Baschek, Bodo, and Leonard Searle, The chemical composition of the λ Bootis stars. *Astrophys. J., 155,* 537–554, 1969.

Becklin, E. E., *see* Neugebauer, G.; Oke, J. B.; Westphal, J. A.

Bergh, Sidney van den, Observation of the nucleus of the radio galaxy M82. *Astrophys. J.* (*Letters*), *156,* L19–L20, 1969.

Bergh, Sidney van den, Globular clusters in the Andromeda nebula. *Nature, 221,* 48–49, 1969.

Bergh, Sidney van den, *see also* DuPuy, David; McClure, Robert D.; Schmidt, Karl-Heinz; Spinrad, Hyron.

Boesgaard, Ann Merchant, Isotopes of magnesium in stellar atmospheres. *Astrophys. J., 154,* 1185–1190, 1968.

Boldt, E., *see* Bradt, H.

Bolton, J. G., *see* Searle, Leonard.

Bradt, H., S. Naranan, S. Rappaport, F. Zwicky, H. Ogelman, and E. Boldt, Upper limit on X rays from a new supernova. *Nature, 218,* 856–857, 1968.

Bradt, H., S. Rappaport, W. Mayer, R. E. Nather, B. Warner, M. MacFarlane, and J. Kristian, X-ray and optical observations of the Pulsar NP 0532 in the Crab Nebula. *Nature, 222,* 728–730, 1969.

Bumba, V., and Robert Howard, On the solar source of recurrent geophysical effects. *Bull. Astron. Inst. Czech., 20,* 61–62, 1969.

Bumba, V., and Robert Howard, On long-term forecasts of solar activity. *Solar Flares and Space Research,* pp. 387–396, Z. Svestka and C. de Jager, eds., North-Holland Publishing Co., Amsterdam, 1969.

Bumba, V., and Robert Howard, Solar activity and recurrences in magnetic-field distribution. *Solar Physics, 7,* 28–38, 1969.

Bumba, V., R. Howard, M. Kopecký, and G. V. Kuklin, Some irregularities in the distribution of large-scale magnetic fields on the Sun. *Bull. Astron. Inst. Czech., 20,* 18–21, 1969.

Bumba, V., *see also* Howard, Robert.

Cohen, Judith G., The carbon abundance of Population II stars. *Astrophys. Letters* (England), *2,* 163–164, 1968.

Cohen, Judith G., A. J. Deutsch, and Jesse L. Greenstein, The spectrum of α^2 CVn, 5000–6700 Å. *Astrophys. J., 156,* 629–652, 1969.

Conti, P. S., and Armin J. Deutsch, Color anomalies and metal deficiencies in solar-type disk-population stars. *Bull. Astron. Inst. Czech.,* 19, 263–264, 1968.

Conti, Peter S., *see* Abt, Helmut.

Davis, D. N., and P. C. Keenan, Is there NbO in S-type stars? *Publ. Astron. Soc. Pacific, 81,* 230–237, 1969.

Demarque, Pierre, F. D. A. Hartwick, and M. D. T. Naylor, Some uncertainties in Population II models near the main sequence. *Astrophys. J., 154,* 1143–1146, 1968.

Deutsch, Armin J., O. C. Wilson, and P. C. Keenan, High-dispersion classification of K2–M6 giants of high and low velocity. *Astrophys. J., 156,* 107–115, 1969.

Deutsch, Armin J., *see also* Abt, Helmut; Cohen, Judith G.; Conti, P. S.

Difley, John A., Two photographic developers for astronomical use. *Astron. J., 73,* 762–769, 1968.

DuPuy, David, John Schmitt, Robert McClure, Sidney van den Bergh, and René Racine, Optical observations of BL Lac = VRO 42.22.01. *Astrophys. J.* (*Letters*), *156,* L135–L139, 1969.

Eggen, Olin J., Narrow- and broad-band photometry of red stars, II, Dwarfs. *Astrophys. J., Suppl. Ser., 16,* No. 142, 49–96, 1968.

Eggen, Olin J., Luminosities, colors, motions, and distribution of faint blue stars. *Astrophys. J., Suppl. Ser., 16,* No. 143, 97–142, 1968.

Garmire, G., *see* Neugebauer, G.

Garrison, Robert F., Erratum re "The spectrum of star No. 1 in NGC 2024." *Publ. Astron. Soc. Pacific, 80,* 755, 1968.

Greenstein, Jesse L., Astronomy, in *Americana Annual,* pp. 103, 105–106, The Americana Corporation, New York, 1969.

Greenstein, Jesse L., The pulsars: cosmic riddle, in *Americana Annual,* p. 104, The Americana Corporation, New York, 1969.

Greenstein, Jesse L., Red and black degenerate stars. *Comments in Astrophys., 1,* 62–72, 1969.

Greenstein, Jesse L., A night on Palomar Mountain. *Engineering and Science, 32,* 12–14, 1969.

Greenstein, Jesse L., Introductory address, in *Low-Luminosity Stars,* pp. xv–xviii, S. S. Kumar, ed., Gordon and Breach, Publishers, London, 1969.

Greenstein, Jesse L., Faint, metal-poor, subluminous and red degenerate stars, in *Low-Luminosity Stars,* pp. 281–295, S. S. Kumar, ed., Gordon and Breach, Publishers, London, 1969.

Greenstein, Jesse L., and Halton Arp, A spectroscopic flare of Wolf 359. *Astrophys. Letters* (England), *3,* 149–152, 1969.

Greenstein, Jesse L., and Valdar Oinas, Two K dwarfs with enhanced carbon molecular bands. *Astrophys. J.* (*Letters*), *153,* L91–L94, 1968.

Greenstein, Jesse L., *see also* Bahcall, John N.; Cohen, Judith G.; Kodaira, K.; Kraft, Robert P.; Stoeckly, Robert.

Grevesse, N., *see* Swings, J. P.

Hardorp, J., and M. Scholz, On the surface gravity and temperature of Vega. *Z. Astrophys., 68,* 350–362, 1968.

Hartwick, F. D. A., A two-dimensional classification for galactic globular clusters. *Astrophys. J., 154,* 475–481, 1968.

Hartwick, F. D. A., and Allan Sandage, The color-magnitude diagram for the abnormally strong-line globular cluster M69. *Astrophys. J., 153,* 715–722, 1968.

Hartwick, F. D. A., *see also* Demarque, Pierre.

Heintze, J. R. W., Temperature, gravity, and mass of Vega, Sirius, and τ Herculis. *Bull. Astron. Inst. Netherlands, 20,* 1–25, 1968.

Heintze, J. R. W., A tentative model of the solar atmosphere and the low chromosphere. *Bull. Astron. Inst. Netherlands, 20,* 137–153, 1969.

Heintze, J. R. W., On the temperature scale of B-type stars. *Bull. Astron. Inst. Netherlands, 20,* 154–162, 1969.

Hiltner, W. A., *see* Schild, Rudolph E.

Howard, Robert, An astronomer in Czechoslovakia. *Engineering and Science, 32,* 22–24, 1969.

Howard, Robert, Reply to K. R. Sivaraman. *Solar Physics, 6,* 154, 1969.

Howard, Robert, Solar research at the Mount Wilson and Palomar Observatories. *Solar Physics, 7,* 153–158, 1969.

Howard, Robert, and V. Bumba, On forecasts of interplanetary and geophysical conditions. *Solar Flares and Space Research,* pp. 397–404, Z. Svestka and C. de Jager, eds., North-Holland Publishing Co., Amsterdam, 1969.

Howard, Robert, *see also* Bumba, V.; Wilcox, John M.

Julian, William H., Overstability of thin stellar systems. *Astrophys. J., 155,* 117–122, 1969.

Katem, Basil, *see* Sandage, Allan.

Keenan, P. C., *see* Davis, D. N.; Deutsch, Armin J.

Kodaira, K., Jesse L. Greenstein, and J. B. Oke, Abundances in two horizontal-branch stars. *Astrophys. J., 155,* 525–536, 1969.

Kopecký, M., *see* Bumba, V.

Kowal, Charles T., The absolute magnitudes of supernovae. *Astron. J., 73,* 1021–1024, 1968.

Kowal, Charles T., *see also* Zwicky, Fritz.

Kozlovsky, Ben-Zion, and Harold Zirin, The O VI emission from the Sun. *Solar Physics, 5,* 50–54, 1968.

Kraft, Robert P., and Jesse L. Greenstein, A new method for finding faint members of the Pleiades, in *Low-Luminosity Stars,* pp. 65–82, S. S. Kumar, ed., Gordon and Breach, Publishers, London, 1969.

Kristian, Jerome, An upper limit for the optical luminosity of the pulsating radio sources CP 0950 and CP 1133. *Astrophys. J. (Letters), 154,* L99–L100, 1968.

Kristian, Jerome, *see also* Bradt, H.; Neugebauer, G.; Sandage, Allan; Westphal, J. A.

Kuklin, G. V., *see* Bumba, V.

Lackner, Dora R., *see* Zirin, Harold.

Lambert, D. L., Radiation pressure and the composition of the solar corona. *Astrophys. Letters* (England), *2,* 37–39, 1968.

Lambert, D. L., and B. E. J. Pagel, The dissociation equilibrium of H^- in stellar atmospheres. *Monthly Notices Roy. Astron. Soc., 141,* 299–315, 1968.

Lambert, D. L., E. A. Mallia, and B. Warner, The abundances of the elements in the solar photosphere, VII: Zn, Ga, Ge, Cd, In, Sn, Hg, Tl, and Pb. *Monthly Notices Roy. Astron. Soc., 142,* 71–95, 1969.

Lambert, D. L., E. A. Mallia, and B. Warner, Forbidden lines of Ca II in the photospheric spectrum. *Solar Physics, 7,* 11–16, 1969.

Lambert, *see also* Swings, J. P.

Leighton, R. B., *see* Neugebauer, G.

Luyten, Willem J., *see* Sandage, Allan.

McClure, Robert D., and Sidney van den Bergh, *UBV* observations of field galaxies. *Astron. J., 73,* 1008–1010, 1968.

McClure, Robert D., *see also* DuPuy, David.

MacFarlane, M., *see* Bradt, H.

Mallia, E. A., *see* Lambert, D. L.

Manwell, Tom, and Michal Simon, Application of a random-event quasar model to the optical variability of 3C 273. *Astron. J., 73,* 407–411, 1968.

Mayer, W., *see* Bradt, H.

Münch, Guido, Small-scale thermal homogeneity of the Orion Nebula, in *Interstellar Ionized Hydrogen,* pp. 507–516, Yervant Terzian, ed., W. A. Benjamin, Inc., New York, 1968.

Naranan, S., *see* Bradt, H.

Nather, R. E., *see* Bradt, H.

Naylor, M. D. T., *see* Demarque, Pierre.

Neugebauer, G., and R. B. Leighton, *Two-Micron Sky Survey, A Preliminary Catalog,* National Aeronautics and Space Administration, Washington, D. C., 1969.

Neugebauer, G., J. B. Oke, E. E. Becklin, and G. Garmire, A study of visual and infrared observations of Sco XR-1. *Astrophys. J., 155,* 1–10, 1969.

Neugebauer, G., E. E. Becklin, J. Kristian, R. B. Leighton, G. Snellen, and J. A. Westphal, Infrared and optical measurements of the Crab pulsar NP 0532. *Astrophys. J. (Letters), 156,* L115–L120, 1969.

Neugebauer, G., *see also* Oke, J. B.; Westphal, J. A.

Newell, E. B., A. W. Rodgers, and Leonard Searle, The blue horizontal-branch stars of ω Centauri. *Astrophys. J., 156,* 597–608, 1969.

Ogelman, H., *see* Bradt, H.

Oinas, Valdar, *see* Greenstein, Jesse L.

Oke, J. B., Continuum energy distributions of Seyfert galaxies and related objects. *Astron. J., 73,* 849–850, 1968.

Oke, J. B., Photoelectric spectrophotometry of the Crab pulsating radio source NP 0532. *Astrophys. J. (Letters), 156,* L49–L53, 1969.

Oke, J. B., A multichannel photoelectric spectrometer. *Publ. Astron. Soc. Pacific, 81,* 11–22, 1969.

Oke, J. B., and Allan Sandage, Energy distributions, *K* corrections, and the Stebbins-Whitford effect for giant elliptical galaxies. *Astrophys. J., 154,* 21–32, 1968.

Oke, J. B., G. Neugebauer, and E. E. Becklin, Spectrophotometry and infrared photometry of BL Lacertae. *Astrophys. J. (Letters), 156,* L41–L43, 1969.

Oke, J. B., *see also* Kodaira, K.; Neugebauer, G.; Westphal, J. A.

Osmer, Patrick S., *see* Bahcall, John N.

Pagel, B. E. J., *see* Lambert, D. L.

Peach, John V., Optical variations in quasi-stellar objects. *Nature, 222,* 439–442, 1969.

Preston, George W., The magnetic field of HD 215441. *Astrophys. J., 156,* 967–982, 1969.

Preston, George W., The nature of the variability of HD 19216. *Astrophys. J., 156,* 1175–1176, 1969.

Preston, George W., and Kazimierz Stepien, The light, magnetic, and radial velocity variations of HD 10783. *Astrophys. J., 154,* 971–974, 1968.

Preston, George W., Kazimierz Stepien, and Sidney Carne Wolff, The magnetic field and light variations of 17 Comae and κ Cancri. *Astrophys. J., 156,* 653–660, 1969.

Racine, René, The distance of the Cepheid SU Cassiopeiae. *Astron. J., 73,* 588–589, 1968; erratum and addendum, *ibid., 74,* 572, 1969.

Racine, René, 2000 globular clusters in M87. *J. Roy. Astron. Soc. Canada, 62,* 367–376, 1968.

Racine, René, Preliminary colors of faint objects around M87. *Publ. Astron. Soc. Pacific, 80,* 326–329, 1968.

Racine, René, *see also* DuPuy, David.

Rappaport, S., *see* Bradt, H.

Rees, M. J., Polarization and spectrum of the primeval radiation in an anisotropic universe. *Astrophys. J. (Letters), 153,* L1–L2, 1968.

Rees, M. J., Proton synchrotron emission from compact radio sources. *Astrophys. Letters* (England), *2,* 1–4, 1968.

Rodgers, A. W., *see* Newell, E. B.

Rudnicki, Konrad, The dependence of the velocity body of stars on space location, in *Vistas in Astronomy,* Vol. 11, pp. 173–180, A. Beer, ed., Pergamon Press, Oxford and New York, 1968.

Rudnicki, Konrad, and Irena Tarrare, Redshifts of six galaxies in the vicinity of the Coma cluster. *Acta Astron., 19,* 171–172, 1969.

Sandage, Allan, The time scale for creation (Part I), *Astron. Soc. Pacific Leaflet No. 477,* 8 pp., March 1969; (Part II) *ibid., No. 478,* 8 pp., April 1969.

Sandage, Allan, Age of creation, in *Science Year 1968, World Book Science Annual,* pp. 56–69, World Book Field Enterprises Educational Services, Chicago, Ill., 1969.

Sandage, Allan, and Basil Katem, The color-magnitude diagram for the globular cluster NGC 5897. *Astrophys. J., 153,* 569–576, 1968.

Sandage, Allan, and Willem J. Luyten, On the nature of faint blue objects in high galactic latitudes, II, Summary of photometric results for 301 objects in seven survey fields. *Astrophys. J., 155,* 913–918, 1969.

Sandage, Allan, and G. A. Tammann, Photometrie des Haufen-Doppel-Cepheiden CE Cas. *Mitt. Astron. Gesellschaft,* No. 25, 147, 1968.

Sandage, Allan, Basil Katem, and Jerome Kristian, An indication of gaps in the giant branch of the globular cluster M15. *Astrophys. J. (Letters), 153,* L129–L134, 1968.

Sandage, Allan, J. A. Westphal, and Jerome Kristian, Results of five nights of continuous monitoring of the optical flux from Sco X-1. *Astrophys. J., 156,* 927–942, 1969.

Sandage, Allan, *see also* Hartwick, F. D. A.; Oke, J. B.; Westphal, J. A.

Sanduleak, N., *see* Schild, Rudolph, E.; Stephenson, C. B.

Sargent, W. L. W., New observations of compact galaxies. *Astron. J., 73,* 893–895, 1968.

Sargent, W. L. W., The redshifts of galaxies in the remarkable chain VV 172. *Astrophys. J. (Letters), 153,* L135–L138, 1968.

Sargent, W. L. W., *see also* Bahcall, John; Searle, Leonard; Zwicky, Fritz.

Scargle, Jeffrey D., Activity in the Crab Nebula. *Astrophys. J., 153,* 569–576, 1968.

Schild, Rudolph E., W. A. Hiltner, and N. Sanduleak, A spectroscopic study of the association Scorpius OB 1. *Astrophys. J., 156,* 609–616, 1969.

Schild, Rudolph E., *see also* Stephenson, C. B.

Schmidt, Karl-Heinz, and Sidney van den Bergh, Zur zeitlichen Variation des Metallgehaltes in der Galaxis. *Astron. Nachr., 291,* 115–124, 1969.

Schmidt, Maarten, Quasistellar objects, in *Ann. Rev. Astron. Astrophys., 7,* pp. 527–552, Annual Reviews, Inc., Palo Alto, Calif., 1969.

Schmidt, Maarten, *see also* Bahcall, John N.; Westphal, J. A.

Schmidt, Maarten, Quasi-stellar radio sources and objects, in *Intern. Astron. Union Symp. No. 29, Instability Phenomena in Galaxies,* pp. 239–244, M. Arakeljan, ed., Mezdunarodnaja Kniga, Moscow, 1967.

Schmitt, John, *see* DuPuy, David.

Scholz, M., *see* Hardorp, J.

Searle, Leonard, and J. G. Bolton, Redshifts of fifteen radio sources. *Astrophys. J. (Letters), 154,* L101–L104, 1968.

Searle, Leonard, and Wallace L. W. Sargent, The strength of Hβ in extragalactic objects with broad emission lines. *Astrophys. J., 153,* 1003–1006, 1968.

Searle, Leonard, *see also* Baschek, Bodo; Newell, E. B.

Simon, Michal, Asymptotic form for synchrotron spectra below Razin cutoff. *Astrophys. J., 156,* 341–344, 1969.

Simon, Michal, Time dependence of Razin spectra in Type IV solar radio bursts. *Astrophys. Letters* (England), *3,* 23–24, 1969.

Simon, Michal, *see also* Manwell, Tom.

Snellen, G., *see* Neugebauer, G.; Westphal, J. A.

Spinrad, Hyron, Benjamin J. Taylor, and Sidney van den Bergh, The M7 giants in the nuclear bulge of the Galaxy. *Astron. J., 74,* 525–528, 1969.

Stenflo, J. O., *see* Bhatnagar, A.

Stephenson, C. B., N. Sanduleak ,and Rudolph E. Schild, A new hot, rapid variable star. *Astrophys. Letters* (England), *1,* 247–248, 1968.

Stepien, Kazimierz, *see* Preston, George W.

Stoeckly, Robert, and Jesse L. Greenstein, Spectrophotometry of a B-type star in the globular cluster M13. *Astrophys. J., 154,* 909–922, 1968.

Swings, J. P., D. L. Lambert, and N. Grevesse, Forbidden sulphur lines in the solar spectrum. *Solar Physics, 6,* 3–11, 1969.

Tammann, G. A., *see* Sandage, Allan.

Tarrare, Irena, *see* Rudnicki, Konrad.

Taylor, Benjamin J., *see* Spinrad, Hyron.

Terzan, Agop, Six nouveaux amas stellaires (Terzan 3–8) dans la région du centre de la Voie lactée et les constellations du Scorpion et du Sagittaire. *Compt. Rend. Acad. Sci. Paris, 267,* 1245–1248, 1968.

Trimble, Virginia, Motions and structure of the filamentary envelope of the Crab Nebula. *Astron. J., 73,* 535–547, 1968.

Tsuji, Takashi, Model atmospheres of M dwarf stars, in *Low-Luminosity Stars,* pp. 457–482, S. S. Kumar, ed., Gordon and Breach, Publishers, London, 1969.

Visvanathan, N., Optical polarization in quasistellar sources. *Astrophys. J. (Letters), 153,* L19–L22, 1968.

Wallerstein, George, *see,* Abt, Helmut.

Warner, B., *see,* Bradt, H.; Lambert, D. L.

Weart, Spencer R., and Harold Zirin, The birth of active regions. *Publ. Astron. Soc. Pacific, 81,* 270–273, 1969.

Westphal, J. A., and G. Neugebauer, Infrared observation of Eta Carinae to 20 microns. *Astrophys. J. (Letters), 156,* L45–L48, 1969.

Westphal, J. A., Allan Sandage, and Jerome Kristian, Rapid changes in the optical intensity and radial velocities of the X-ray source Sco X-1. *Astrophys. J., 154,* 139–156, 1968.

Westphal, J. A., Jerome Kristian, Grant Snellen, Allan Sandage, Maarten Schmidt, J. B. Oke, Gerry Neugebauer, and E. E. Becklin, On the nature of Ryle and Bailey's candidate star for the pulsating radio source CP 1919. *Astrophys. J., 155,* L109–L114, 1969.

Westphal, J. A., *see also* Neugebauer, G.; Sandage, Allan.

Wilcox, John M., and Robert Howard, A large-scale pattern in the solar magnetic field. *Solar Physics, 5,* 564–574, 1968.

Wilson, Olin C., Flux measurements at the centers of stellar H and K lines. *Astrophys. J., 153,* 221–234, 1968.

Wilson, Olin C., Calibration apparatus at Mt. Wilson and Mt. Palomar. *Bull. Am. Astron. Soc., 1,* 154, 1969.

Wilson, Olin C., Chromospheric variations in main-sequence stars, in *Low-Luminosity Stars,* pp. 103–106, S. S. Kumar, ed., Gordon and Breach, Publishers, London, 1969.

Wilson, Olin C., *see also* Deutsch, Armin J.

Wolff, Sidney Carne, *see* Preston, George W.

Zirin, Harold, Abundance analyses from extreme-ultraviolet emission lines. *Astrophys. J., 154,* 799–801, 1968.

Zirin, Harold, Mass motions in loops, sprays, surges, etc., in *Nobel Symposium 9, Mass Motions in Solar Flares and Related Phenomena,* pp. 131–136, Yngve Öhman, ed., John Wiley & Sons, New York, 1969.

Zirin, Harold, Observations of stellar chromospheres using the He 10830 line, in *Nobel Symposium 9, Mass Motions in Solar Flares and Related Phenomena,* pp. 239–242, Yngve Öhman, ed., John Wiley & Sons, New York, 1969.

Zirin, Harold, George Ellery Hale, 1868–1938. *Solar Physics, 5,* 435–441, 1968.

Zirin, Harold, Two prominence eruptions and the problem of emission. *Solar Physics, 7,* 243–252, 1969.

Zirin, Harold, and Dora R. Lackner, The solar flares of August 28 and 30, 1966. *Solar Physics, 6,* 86–103, 1969.

Zirin, Harold, *see also* Kozlovsky, Ben-Zion; Weart, Spencer R.

Zwicky, Fritz, *Catalogue of Galaxies and of Clusters of Galaxies,* Vols. IV and VI, California Institute of Technology, Pasadena, California, 1968.

Zwicky, Fritz, *Discovery, Invention, Research,* The Macmillan Co., New York, 1969.

Zwicky, Fritz, Physics and chemistry on the Moon, in *Research in Physics and Chemistry, Proc. Third Intern. Laboratory (LIL) Symp., 1967,* pp. 1–27, C. H. Roadman, H. Strughold, and R. B. Mitchell, eds., Pergamon Press, Oxford and New York, 1969.

Zwicky, Fritz, Physics of the universe, in *Proc. 4th Intern. Symp. on Bioastronautics and the Exploration of Space,* pp. 63–81, 527, 533, 595–608, Brooks Air Force Base, Texas, 1969.

Zwicky, Fritz, 1967 Palomar supernova search. *Publ. Astron. Soc. Pacific, 80,* 462–465, 1968.

Zwicky, Fritz, Zukunftsbild eines Astrophysikers, in *Was Wird Morgen Anders Sein?,* pp. 1–12, O. Herreche, ed., Walter Verlag, Olten, Switzerland, 1969.

Zwicky, Fritz, W. L. W. Sargent, and C. Kowal, The 1968 Palomar supernova search. *Publ. Astron. Soc. Pacific, 81,* 224–229, 1969.

Zwicky, F., *see also* Bradt, H.

STAFF AND ORGANIZATION

Dr. Sidney van den Bergh of the University of Toronto came to the Observatories as Research Associate for one year. While here, he engaged in a number of investigations, including especially the study of globular clusters in M31.

Sandage spent the year on leave, working on a variety of Southern Hemisphere problems at the Mount Stromlo and Siding Spring Observatories in Australia.

Research Division

Distinguished Service Member, Carnegie Institution of Washington

Ira S. Bowen

Staff Members

Halton C. Arp
Horace W. Babcock, Director
Edwin W. Dennison
Armin J. Deutsch
Jesse L. Greenstein [1]
Robert F. Howard
Jerome Kristian
Robert B. Leighton [2]
Guido Münch [3]
J. Beverley Oke [3]
George W. Preston III
Bruce H. Rule, Chief Engineer
Allan R. Sandage
Wallace L. W. Sargent [4]
Leonard T. Searle

Maarten Schmidt [3]
Arthur H. Vaughan, Jr.
Olin C. Wilson
Harold Zirin [5]

Staff Members Engaged in Post-Retirement Studies

Alfred H. Joy
Henrietta H. Swope
Fritz Zwicky

Research Associate

Sidney van den Bergh

Staff Associates

Bruce C. Murray [6]
Gerry Neugebauer [7]
James A. Westphal [8]

Carnegie Fellows

Arvind Bhatnagar
Deane M. Peterson
René Racine [9]
Natarajan Visvanathan [10]

Research Fellows

J. David Bohlin
Ardon R. Hyland
William H. Julian
Keiichi Kodaira
Ben-Zion Kozlovsky [11]
David L. Lambert
James J. Rickard
Rudolph E. Schild [9]
Michael Scholz
Michal Simon
Takashi Tsuji [10]
Spencer R. Weart

Senior Research Assistants

Sylvia Burd
Dorothy D. Locanthi
A. Louise Lowen
Anneila Sargent

Research Assistants

John M. Adkins
Frank J. Brueckel
Thomas A. Cragg
Basil N. Katem
Charles Kowal
James D. Pederson
Malcolm S. Riley
Merwyn G. Utter [12]
Grace D. Vess

Graduate Student Observers

Saul J. Adelman
Dennis D. Baker
Clark G. Christensen
Jay A. Frogel
Theodore Hilgeman
Torrence V. Johnson
Hugh H. Kieffer
Dennis L. Matson
Robert W. O'Connell
Valdar Oinas
Patrick S. Osmer
Sven E. Persson
Edward W. Ritz
Donna E. Weistrop

Photographic Laboratory

William C. Miller, Research Photographer
John A. Difley, Photographer
Clare Neal, Solar Photographic Assistant [13]
Paula Swanson, Solar Photographic Assistant

Librarians

Charlotte Fournier [14]
Marjorie A. Henderson

Instrument Design and Construction

Lawrence E. Blackeé, Supervisor, Electronic Services
Maynard K. Clark, Senior Engineering Assistant
John P. Cowley, Laboratory Specialist
Floyd E. Day, Head Optician
Stephen Doro, Machinist
Raymond Dreiling, Machinist
Eugene B. Fair, Optician
Robert D. Georgen, Machinist
Donn M. Hall, Electronics Engineer
Joseph P. Hsu, Associate Electronics Engineer
Fred Idzinga, Senior Electronics Specialist
Melvin W. Johnson, Optician
Margaret Katz, Technical Assistant
Wilfred H. Leckie, Draftsman
Ernest O. Lorenz, Engineering Field Assistant
Richard Lucianio, Engineering Assistant [15]
Martin J. Olsiewski, Electronics Specialist
Frederick G. O'Neil, Machinist
Gerald Preston, Technical Aide [16]
John D. Raphael, Electronics Specialist [17]
Edward H. Rehnborg, Senior Engineer
Rudolf E. Ribbens, Designer and Shop Superintendent
Howard G. Sachs, Senior Engineer

Benny W. Smith, Electronics Specialist [18]
Robert G. Stiles, Optician
David Thompson, Senior Technical Assistant
William Thompson, Electronics Technician
Eli A. Tilajef, Junior Engineer
Virgal Z. Vaughan, Electronics Specialist
Madeline B. Williams, Draftswoman
Ralph W. Wilson, Machinist [19]
Felice Woodworth, Draftswoman-Illustrator

Maintenance and Operation

Mount Wilson Observatory and Offices

Fern V. Borgen, Telephone Operator–Typist
Clyde B. Bornhurst, Mechanic
Herman E. Carpentier, Carpenter
Hugh T. Couch, Superintendent of Buildings and Grounds
Helen S. Czaplicki, Typist-Editor
Sue H. DeWitt, Secretary
Hazel M. Fulton, Stewardess
Eugene L. Hancock, Night Assistant
Elsie Hanlon, Stewardess
Judith A. Harstine, Secretary
Anne Hopper, Accountant [20]
Mario Jacques, Night Assistant
Rienaldo M. Jacques, Head Steward
Ethel Marzalek, Stewardess [20]
Frances Maynor, Stewardess [20]
Alfred H. Olmstead, Custodian
William D. St. John, Construction Aide
Glen Sanger, Driver
Henry P. Schaefer, Night Assistant
Clair E. Sharp, Accountant
Elizabeth M. Shuey, Secretary [11]
Benjamin B. Traxler, Mountain Superintendent
Frank Trylko, Custodian
Frederick P. Woodson, Assistant to the Director

Palomar Observatory and Robinson Laboratory

Ray L. Ballard, Senior Administrative Assistant
Doris J. Brenner, Secretary
Betty Browne, Secretary
Jan Adriian Bruinsma, Painter and General Maintenance
Maria J. Bruinsma, Lodge Stewardess
Eleanor Ellison, Librarian
Beulah Greenlee, Lodge Stewardess
Frank V. Greenlee, Sr., Custodian
Daniel J. Hargraves, Mechanic and Relief Night Assistant
Liselotte M. Hauck, Secretary
Victor A. Hett, Night Assistant
Helen Holloway, Secretary
Charles E. Kearns, Assistant Mountain Superintendent
J. Luz Lara, Mechanic
Carl D. Palm, Night Assistant
Catherine T. Paul, Secretary
Marilynne J. Rice, Secretary
Kenneth R. Robinson, Night Assistant and Maintenance
Robert T. Snow,[21] Temporary Assistant
Gary M. Tuton, Senior Night Assistant
William C. Van Hook, Mountain Superintendent
Ardith Walthers, Secretary

[1] Professor of Astrophysics and Executive Officer for Astronomy, California Institute of Technology.

[2] Professor of Physics, California Institute of Technology.

[3] Professor of Astronomy, California Institute of Technology.

[4] Associate Professor of Astronomy, California Institute of Technology.

[5] Professor of Astrophysics, California Institute of Technology.

[6] Professor of Planetary Science, California Institute of Technology.

[7] Associate Professor of Physics, California Institute of Technology.

[8] Senior Research Fellow in Planetary Science, California Institute of Technology.

[9] Resigned June 30, 1969.

[10] Resigned September 30, 1968.

[11] Resigned March 31, 1969.

[12] Terminated March 27, 1969.

[13] Resigned February 28, 1969.

[14] Resigned October 18, 1968.

[15] Resigned September 27, 1968.

[16] Resigned August 11, 1968.

[17] Resigned January 24, 1969.

[18] Resigned January 31, 1969.

[19] Resigned March 15, 1969.

[20] Resigned November 30, 1968.

[21] Resigned August 15, 1968.

Warren L. Weaver, Mechanic and Electrician

Carnegie Southern Observatory Project
Pasadena, California

Bruce Adkison, Associate for Administration
Wilma J. Berkebile, Secretary

[22] Resigned May 7, 1969.

La Serena, Chile

Manuel Blanco, Laborer
Donald L. Buck, Project Supervisor
Manuel Casanova, Foreman [22]
Pedro La Paz, Laborer
Fernando Peralta, Foreman
Roberto Ramos, Laborer
Manfred Wagner, Camp Chief

Geophysical Laboratory

Washington, District of Columbia

Philip H. Abelson
Director

Carnegie Institution Year Book 68, 1968–1969

Contents

INTRODUCTION

If man is to have an enduring future, he must learn to husband his environment and to live with its realities. Some of the important realities of the environment are the physical and chemical nature of the planet itself and the processes that have shaped it and are even now changing it. Thus man must continue to exploit resources of the earth, but he will devote increasing attention to management of the earth—controlling erosion, pollution, and the like. At the same time a restless planet will command fearful concern with floods, earthquakes, and volcanism.

Of great interest during the next decades will be exploration of that great frontier the sea bottom, which represents 72% of the earth's surface. All these factors together guarantee continued interest in the earth sciences. There is yet another factor. Man will continue to study the earth because he is a curious animal. He wonders, what and why.

This past year has been a great one for earth scientists. The sediments beneath the oceans have been made accessible to intensive study. The moon awaits further exploration. During the report year specimens from the deep sea and the moon were not yet distributed. In coming years, however, these materials will surely be the source of much new information. As these materials become available for study the Geophysical Laboratory will participate in studies in which our knowledge, techniques, and equipment are especially relevant. At the same time we will continue investigations of basic problems of long-term significance. During the past year some of these areas of geochemical and petrological research have been fruitful as new ideas, techniques, and instrumentation have facilitated the work or created new opportunities. In the following paragraphs highlights of some of the year's work at the Geophysical Laboratory are reviewed.

With the activation of our medium-speed computer terminal, Chayes resumed work on his library of chemical analyses of Cenozoic volcanic rocks. The library tape now contains over 8000 analyses that can be referenced, singly or in groups, by area of occurrence, rock name(s), or any linear combination of chemical or normative parameters. He has completed a summary study of the chemical composition of andesite, an examination of the compositional relations between andesite, dacite, and rhyodacite, and a survey of the relative frequencies of analyses of rhyolite and andesite in ocean basins. A detailed study of the "alumina balance"—i.e., the molar ratio of Al_2O_3 to the sum (Na_2O+K_2O+CaO)—and a restudy of the oceanic basalt-trachyte association are in progress.

Meyer and Boyd show that silicate inclusions in natural diamonds from a variety of sources in Africa and South America resemble, in kind, the minerals of ultramafic xenoliths from kimberlite. In detail, however, the chemical compositions of the inclusions show a number of consistent and characteristic differences that are independent of provenance and age. It is notable, for instance, that the garnet, olivine, chromite, and enstatite inclusions in diamond are particularly rich in Cr. These differences cannot yet be rationalized satisfactorily, but it seems possible that the diamonds crystallized from silicate magmas, and that the inclusions, armored by diamond, reflect crystal-liquid equilibria, whereas the minerals of the xenoliths have equilibrated below the solidus.

Boyd has used the electron probe to determine the compositions of coexisting phases in high-pressure runs in the system $CaSiO_3$-$MgSiO_3$-Al_2O_3 at 1200°C and 30 kb. This study is the first to be

published in our report in which electron-probe techniques, rather than more conventional X-ray and optical methods, were the primary means of phase identification. Probe analysis can sometimes provide a much more detailed view of phase relations in a complex system than has hitherto been possible. Phase relations in the system $CaSiO_3$-$MgSiO_3$-Al_2O_3 closely model the mineral assemblage found in garnet lherzolites and also show similarities to the assemblages of eclogites, corundum eclogites, and grospydites. Synthetic pyroxenes containing 3 to 4 wt % Al_2O_3 in equilibrium with garnet in this system have Ca/(Ca+Mg) ratios that are little changed from Al-free pyroxenes on the join $CaMgSi_2O_6$-$MgSiO_3$ at the same temperature and pressure. Hence, the experimentally determined solvus for diopside in equilibrium with enstatite can safely be applied to natural assemblages containing moderate amounts of Al_2O_3.

Bryan has continued optical and electron-microprobe studies of minerals in volcanic rocks. Microprobe analysis of plagioclase in Coral Sea drift pumice shows that it is bytownite rather than anorthite, as previously deduced from optical data; substitution of iron for aluminum apparently causes the anomalously high refractive index. Unusual in both mineralogy and bulk composition, this pumice seems to be produced in relatively large volume along the Tonga-Kermadec ridge and is widely distributed by ocean currents.

Electron-microprobe analyses of minerals in basalt associated with pantellerite both in the type area at Pantelleria, and at Socorro Island, Mexico, provide new evidence for a genetic relation between basalt and pantellerite. In both areas, aluminous titanaugite and titaniferous magnetite are important constituents of the basalts. Using the least-squares calculation described last year (Bryan, Finger, and Chayes, *Year Book 67*), Bryan has shown that relatively large amounts of pantellerite could be derived from the basalt at Socorro Island. The removal of aluminous titanaugite and titaniferous magnetite from the basalt could yield a residue having the alumina deficiency and high iron/titanium ratio characteristic of pantellerite.

Petrologic and meteoritic evidence suggests that iron oxides are important components of the earth's mantle. Mao has studied the behavior of magnetite (Fe_3O_4) under pressures as high as 300 kb. This work is a continuation of studies begun with Bassett and Takahashi at the University of Rochester. By X-ray identification of products formed in a diamond-anvil cell, Mao has found that magnetite undergoes a first-order phase transformation at approximately 250 kb. This phase reverts to the original spinel structure on release of pressure to 1 bar. Mao, Takahashi, and Bassett have also found that ordinary lead with face-centered cubic structure starts to transform to the hexagonal close-packing structure at 130 ± 10 kb and room temperature. They also observed that the two phases of lead can coexist in a range of 60 kb. This transformation is presumably the same one first observed by Balchan and Drickamer at 160 kb, which is currently widely used as a pressure calibration point. The uncertainty arising from the broad pressure range of the phase transition leads to the suggestion that precautions must be taken when this transformation is used for calibration.

One of the major puzzles of organic geochemistry is the process by which the relatively simple components of living matter disappear in sediments. Microorganisms have been accorded an important role in the process, but kerogen, which makes up the bulk of the organic matter in sediments, is different in nature from ordinary biological substances. Other factors must be involved. Abelson and Hare have uncovered an important nonbiological mechanism in sediments for the disappearance of small molecules such as amino acids. They have found

that kerogen reacts rapidly and irreversibly with amino acids and peptides. The most reactive amino acids include cystine and the basic amino acids followed by the aromatic and longer aliphatic chained amino acids. The reactions yield substantial amounts of ammonia and involve, at least in some instances, attachment of portions of the amino acid moiety to the kerogen. For example, reaction of arginine with kerogen changed the C/N ratio of the kerogen from 14.4 to 8.2.

Optically active molecules are synthesized routinely by living organisms but are rarely produced by nonbiological systems. The presence of optical activity in petroleums (due mainly to steranes) is a strong argument for the biological origin of crude oils. Hoering has developed new methods for the chromatographic separation of steranes from petroleum and applied new instrumental methods of structure determination. He has isolated and identified ten sterane hydrocarbons from a crude oil from the Ventura Basin. The steranes were highly optically active and had molecular structures expected from a hydrogenation of common plant and animal steroids. The methods are generally applicable and permit study of steranes in very old petroleums and rocks.

One of the major developments of the 1960's was the accumulation of evidence of continental drift. Much of this evidence is based on measurements of the remanent magnetism of oceanic sediments. Oddly enough, there has been little systematic study of the magnetic minerals of the sediments. Such a study of the magnetic mineralogy of pelagic sediments from the Atlantic, Pacific, and Indian Oceans and from beneath the Antarctic ice sheet has been undertaken by Haggerty. His results show that a major portion of the magnetic material in deep-sea sediments consists of detrital iron-titanium oxides. These phases are considered to have been wind-transported from the continents.

Kushiro studied the system forsterite-nepheline-anorthite-silica-water and showed that the liquids formed by partial melting of peridotitic compositions in the presence of water are tholeiitic or andesitic up to at least 20 kb. The results are important for understanding the origin of tholeiitic and andesitic magmas. Kushiro has also determined the pressure-temperature conditions of crystallization of amphibole from a peridotite composition and the stability of phlogopite in the presence of diopside and enstatite. The results indicate that amphibole and phlogopite could be present at considerable depths in the upper mantle where water pressure is high. Kushiro and Erlank showed, however, that potassic richterite, an alkali amphibole found in a nodule in kimberlite, is not stable in eclogites and garnet-bearing peridotites and appears to be stable only in rocks in which potassium is present in excess over aluminum.

The effects of a multicomponent gas on the behavior of some of the minerals important in the mantle are being studied by Yoder. The melting of the hydrous phase phlogopite was found to be suppressed by the presence of CO_2. The CO_2, relatively insoluble in the silicate liquid, reduces the effective pressure of H_2O. The presence of CO_2 will greatly affect, therefore, the melting temperature of the hydrous rocks now believed to be present in the mantle. Furthermore, the assumption of vapor-absent conditions in magmas in the mantle may not be valid if a relatively insoluble gaseous component is present. Rocks such as kimberlite will vary greatly in their thermal behavior, depending on the ratio of CO_2 to H_2O in the gas phase, if a gas phase exists.

Important advances have been made during the past few years in our knowledge of the crystallization relations in basalts and related alkaline rocks. From the many studies reported from this Laboratory it became obvious that before attempting to interpret detailed re-

lations in the quinary system Na_2O-CaO-MgO-Al_2O_3-SiO_2, it was necessary to know more about relations in the tetrahedron akermanite-diopside-anorthite-spinel in the quaternary system CaO-MgO-Al_2O_3-SiO_2, without the complication of Na_2O. During the past year Schairer and Yoder determined the precise relations in this tetrahedron.

Important clues in the crystallization behavior of the melilite-bearing rocks were uncovered in this tetrahedron, and a possible solution of the plagioclase-melilite dilemma was evolved. The coexistence of clinopyroxenes and spinel, commonly observed in nature, was observed experimentally. A new flow sheet for the system CaO-MgO-Al_2O_3-SiO_2 was developed, which shows in detail the thermal relations between four of the most important oxides present in rocks.

Boyd and Nixon have found that the distribution of the ratio Ca/(Ca+Mg) in diopsidic pyroxenes from African kimberlite concentrates and nodules appears to be markedly bimodal. Interpretation of this distribution in terms of the continuous solvus curve in the system $CaMgSi_2O_6$-$MgSiO_3$ suggests that these kimberlites have originated under two distinct temperature regimes, perhaps at two separate levels in the mantle. Such an origin seems improbable, however, and Boyd and Nixon suggest that the bimodal distribution may be due to undiscovered features in the phase diagram for $CaMgSi_2O_6$-$MgSiO_3$ at pressures well above 30 kb.

Kushiro and Yoder continued their study of the stability field of iron-free pigeonite and showed that this material is stable, at least in the pressure range 5 to 20 kb and at near-solidus temperatures. Kushiro and Schairer confirmed that the system diopside-anorthite-albite is not ternary and showed that the diopside solid solutions crystallized from this system at 1 atm probably contain several percent of enstatite and Tschermak's components. Erlank and Kushiro measured potassium contents of clinopyroxenes and garnets made at high pressures in the presence of phlogopite and potassium-bearing liquids and found that only a very small amount (<200 ppm) of potassium can enter the clinopyroxenes and garnets. The results indicated that these minerals in the upper mantle are not the major source of potassium in basalts.

The stability of iron-rich orthopyroxene relative to the compositionally equivalent assemblage of olivine + quartz has been investigated by Smith. The stability relationships determined for these phases at low pressure provide a necessary basis for subsolidus investigations in the iron-rich portion of the pyroxene quadrilateral. With increasing pressure, orthopyroxenes of progressively greater iron content become stable. Because the reaction of orthopyroxene to olivine + quartz is pressure sensitive, the presence of the phases in a rock may serve as a guide to the depth at which it crystallized.

Meyer and French have discovered the first natural occurrence of a member of the β-quartz–spodumene solid solution series. This new mineral has the composition $(LiAlSi_2O_6)_{62}(3SiO_2)_{38}$ mole % and has a hexagonal β-quartz type structure. It occurs as crystals in a unique glass obtained from near the town of Macusani in southern Peru. In this same glass they have found the first occurrence of andalusite that has apparently grown in equilibrium with a melt.

Lindsley pursued his interests in the iron-titanium oxides on a variety of fronts. An uncompleted study of the magnetite-ulvöspinel join confirms that the critical temperature of the miscibility gap lies at or below 600°C. A joint study with Haggerty on the stability of intermediate pseudobrookite solid solutions places important constraints on the oxidation temperatures of certain oxidized basalts of paleomagnetic significance. In addition, Lindsley spent the last 6 months of the report year preparing a review of the experimental petrology,

synthesis, and crystal chemistry of the iron-titanium oxide minerals.

Bell and Chao have determined the effects of annealing on dense feldspar glasses produced by shock-wave experiments and by natural meteorite impacts. By relating annealing temperatures and times with the effects of the shock-release adiabats they provide a qualitative interpretation of the pressure-temperature history of feldspar glasses that are found in debris produced by meteorite impact. Such interpretations will be useful for samples returned to the earth from the surfaces of other celestial bodies.

Bell and Mao have measured the crystal-field spectra of the olivine and spinel forms of fayalite (Fe_2SiO_4), and of almandite garnet ($Fe_3Al_2Si_3O_{12}$), at 1 atm and at 100 kb. They observed spectral shifts that slightly open the "window" for radiative transfer of heat at high pressure. In addition, strong absorption was observed in fayalite, presumably because of the onset of nucleation of the spinel phase. This strong absorption may provide a heat barrier at great depths in the earth's mantle.

Finger has refined the crystal structure of an anthophyllite from Montana and determined the occupancies of the octahedral sites with the bulk composition constrained to agree with the chemical analysis. The sample has a very ordered distribution, suggesting a low temperature of formation or annealing.

Finger and Rapp have refined the crystal structure of the mineral triphylite, $Li(Fe,Mn)PO_4$, from South Dakota, as a first step in the study of a solid-state reaction in which the lithium is removed from the structure and the iron or manganese converted from the divalent to the trivalent state.

Erlank and Finger have described the occurrence of an amphibole with high potassium and low aluminum content. This amphibole is in the form of subhedral grains contained within diopside in a mica pyroxenite nodule from the Wesselton kimberlite pipe, South Africa.

The chemical analysis of a new mineral species often leads to more than one possible structural formula. Sonoraite, $Fe_2Te_2O_{10}H_6$, is a case in point; the structural formulae $Fe_2Te_2O_4(OH)_6$, $Fe_2Te_2O_5(OH)_4 \cdot H_2O$, $Fe_2Te_2O_6(OH)_2 \cdot 2H_2O$, and $Fe_2Te_2O_7 \cdot 3H_2O$ are equally likely. X-ray diffraction data lead to the oxygen coordinates but do not reveal hydrogen positions. Using the principle of local neutralization of charge first formulated by L. Pauling in 1929, G. Donnay has suggested a general procedure that distinguishes oxygen ions from hydroxyl groups and from water molecules and gives information on hydrogen bonding that may be present.

Kullerud has classified and grouped binary systems containing As, Bi, S, Sb, Se, and Te, based on the behavior of such systems in both the liquid and solid states, into the sulfide and arsenide types. This classification points up certain discrepancies between the reported and predicted behavior of many systems and thus identifies the systems that should be restudied with modern methods.

Pyrite and the various species of pyrrhotite, the commonest sulfide minerals, are compounds in the binary system Fe-S. Because of retrograde equilibration, the high-temperature chemistry of many Fe-S phases is masked by the low-temperature phase relations. Taylor has investigated the Fe-S system and has significantly extended our knowledge of the important low-temperature regions of this system.

By combining the results of age determinations made on a rock and on the minerals separated from that rock, Krogh and Davis have been able to determine within close limits the time of occurrence of significant events during the history of the rock. They show that in the Grenville province in Ontario, gneissic rocks were formed from preexisting sediments

during a period of major metamorphism 1800 m.y. ago and that these rocks were then subjected to a period of less intense metamorphism 900 m.y. ago. They also show that some of the structural features of the Front zone of the province are at least 1600 m.y. old and probably as old as 1800 m.y.

PETROGRAPHY

Experimentation in the Electronic Storage and Manipulation of Large Numbers of Rock Analyses *

F. Chayes

In January of the report year, after nearly a year of delay and improvisation, regular communication was established between a medium-speed data terminal at the Geophysical Laboratory and the University of Maryland's Univac 1108 computer. The work is done under a multiprogramming monitor, so that turnaround is ordinarily very rapid. Once received at the central facility, our work is processed exactly as if it had been submitted through an on-site card reader; in our programming we may accordingly take full advantage of the speed, large core memory, and immense mass storage capacity of a third generation computer operating under optimum conditions. This section of the petrography report is a review of work made physically practical by the presence of the terminal in the laboratory. The programming has benefited greatly from the generous assistance of L. W. Finger.

The Rock File

A collection of rock analyses on punched cards, begun in connection with a study of published Harker diagrams (Chayes, 1964), has been expanded gradually into a library of analyses of Cenozoic volcanic rocks. For some time the library has been too large for efficient exploitation by physical manipulation of the cards, and the first major petrographic application of the data terminal was the transfer of this information to magnetic tape. The library tape in use at the present writing, from which most of the information summarized below was drawn, is a preliminary version, completed in mid-February. It contains 8300 analyses that can be referenced, individually or in groups, geographically, by modified Tröger numbers denoting rock names used in the source publications, and by a variety of chemical and/or normative criteria. The geographic reference is essentially an accession number; the world is divided into large, numbered areas, and within each of these the analyses are grouped in numbered suites, the analyses in each suite being obtained either from a single publication or from a number of publications describing the same occurrence. Each suite of the card library is a logical record of the library tape. The tape generator contains updating options which permit deletion or replacement of existing records as well as insertion of new ones.

* Supported in part by National Science Foundation grant GA 1612.

The Normative Color Index and Plagioclase Content of Andesite

Andesite, the most abundant volcanic rock in the circumoceanic environment, is common throughout orogenic belts on the present continental land masses and rare or lacking in the ocean basins. A résumé of the chemical composition of andesite, prepared for a recent field symposium at Eugene, Oregon, and published in its proceedings (Chayes, 1969), was carried through as a pilot operation of the rock analysis storage project. Copies were made (mostly by D. Velde) of all andesite analyses in the punched card library, and from this set a precursor of

the library tape was prepared; the tape-building program now in use was tested and corrected with the andesite data, and a few months later, when our terminal was finally activated, the current version of the library tape was generated from the andesite tape by an extended series of editings.

The distributions of two normative parameters of considerable interest, color index and *an* content of plagioclase, were not available at the time of the Eugene summary; they are given here in Table 1. The normative color index of the calculation is essentially the complement of the CIPW statistic "Sumsal," i.e., it is the sum of all normative parameters other than *Q, or, ab, an, ne,* and *lc.* Although the current version of the library tape contains 1946 analyses of rocks called andesite in the source references, only the analyses used in the summaries compiled for the Eugene symposium have been included in the preparation of Table 1; for a bibliography of source references the reader is referred to the published proceedings of the symposium.

TABLE 1. Distribution of (I) Normative Color Index and (II) Normative Ratio (100*an/pl*) in 1775 Analyses of Andesite (Upper-Class Mark of Class k = Origin + k Times Class Width)

	I	II
Average	21.32	50.0
Standard deviation	6.13	11.0
Origin	9.00	0.0
Class width	1.00	3.3
Class Number	**Frequencies**	
1	24	0
2	21	2
3	23	1
4	37	6
5	44	11
6	69	14
7	92	20
8	90	32
9	113	35
10	122	53
11	111	97
12	114	128
13	120	184
14	100	217
15	92	238
16	90	231
17	83	188
18	72	135
19	70	99
20	45	48
21	52	20
22	48	10
23	29	2
24	23	1
25	27	0
26	11	
27	6	
28	4	
29	3	
30	2	

The So-Called Andesites of the Oceanic Islands

All petrologists agree that andesites are very rare in the ocean basins, and probably most believe that andesites do not occur at all in this environment. As of the present writing, nevertheless, 57 of the analyses of oceanic island volcanics on the library tape are of rocks called andesite in the source references. Over half of these are from the Pacific basin, viz., one from West Maui; five each from East Maui and Kohala; six from Mauna Kea; three each from Pitcairn, the Tubuai archipelago, and the Marquesas; two each from Easter and the Galapagos; and one from the Society Islands.

Of the seventeen Hawaiian analyses, only seven contain more than 50% and only two more than 52% of SiO_2; fifteen are *ol* and thirteen *ne* normative; only one—the one richest in SiO_2—contains less than 2% of TiO_2; in the remainder TiO_2 ranges from 2.09 to 5.10%. These are preeminently the rocks for which Iddings proposed and Macdonald revived the name hawaiite. The analyses are decidedly richer in alkalies and poorer in MgO than most Hawaiian basalts, which in other respects they closely resemble. As Macdonald points out, they are certainly not andesites, and in Iddings' definition hawaiite denotes andesine *basalt.*

The other fourteen Pacific basin "andesites" are much like the Hawaiian examples; thirteen are *ol* and seven *ne* normative; ten contain less than 52%

of SiO_2 and only the other four contain less than 2% of TiO_2; all contain considerably more alkalies than would be expected in feldspathoid-free basalt; the alkali content of the four relatively siliceous examples ranges from 8.5 to 10%, far more than is found in andesite.

With the possible exception of one specimen from Easter Island, none of these rocks appears to be an andesite in the now fairly standard usage of that term. Six might qualify as one or other variety of trachyandesite. For most of the remaining twenty-four, hawaiite would be a suitable varietal name but mugearite might be more appropriate for the more siliceous ones. In a few—one each from the Galapagos, Pitcairn, the Marquesas, and the Tubuai archipelago —SiO_2 is less than 50%, normative *ne* is scarce or lacking, and *an* equals or exceeds *ab*; these seem to be ordinary oceanic-island basalts. Andesites, which abound along much of the margin of the Pacific, do indeed seem to be lacking in the Pacific basin despite the fact that the name andesite has been attached to more than 5% of the published analyses of rocks from that region.

The tape library now contains sixteen analyses of Atlantic island rocks called andesite in the source references, one from Possession, three from the Canaries, and twelve from the Azores. Of these, thirteen are *ol* and 11 *ne* normative. Three of the Azores specimens and all from Possession and the Canaries are far too poor in silica to be called andesite and far too rich in alkalies to be called basalt.* Like much of the Pacific material, they are trachybasalts for which either hawaiite or mugearite would be appropriate varietal names. The silica content of the remaining nine Azores analyses is, with one exception, between 50.5 and 53.8%, within but certainly at the low end of the normal andesite range, but the alkali content of the six that lack normative *Q* is far too high for andesite; they are trachyandesites of one variety or other. We are left with three quartz normative analyses; one contains only 47.6% SiO_2, the highest normative *Q* (4.3%) occurs in one containing only 50.5% SiO_2, and in all three TiO_2 is well over 2%. In the continental or circum-oceanic environments, where andesites abound, not one of these specimens would be given that name. The name is nevertheless assigned, in the source references, to nearly 3% of the analyses of specimens from the Atlantic basin, and in a recent summary essay (Gaskell, 1962) the volcanism of the Azores is confidently described as "andesitic." †

To my knowledge, no analyzed samples of rocks called andesite have been described from oceanic islands of the Arctic or Antarctic, but if Reunion is accepted as an oceanic island the current library tape contains ten examples from the Indian Ocean. Six of the ten are highly aluminous, with normative *c* in amounts far too large to be explained away as analytical error: five of these also contain normative *Q*; in one *Q* is 28% though SiO_2 is only 61.2%, and in another *Q* is 20.7% though SiO_2 is only 52.4%. Probably all six corundiferous norms are of laterized or hydrothermally altered specimens. There are in addition four analyses, all of specimens from Piton des Neiges, whose norms lack both *Q* and *c*; three of these are *ne* normative, though the amount of *ne* is small. Two of the four contain less than 47% SiO_2 but are rather rich (3.18%, 3.57%) in Na_2O for basalt; either basalt or trachybasalt would do as a group name for them, but andesite is clearly inappro-

* In the journal and reference literature the name basalt is rarely applied to a rock containing more than 3% Na_2O.

† This author states (*op. cit.*, p. 305), "there is no doubt that both Bermuda and the Azores would be placed to landward of the andesite line if they were in the Pacific." But surely there is very considerable doubt! As we have just seen, the published analyses of Azores specimens called andesite offer no support whatever for this dictum, and *all* of some 62 other published Azores analyses are of drastically nonandesitic materials.

priate. The other two contain sufficient SiO_2 for andesite, but the total alkali content of one is 6.68% and of the other 9.62%. The first is perhaps marginally admissible as a highly aberrant andesite, the second is clearly trachyandesite.

In sum, although more than 4% of the 1325 analyses of oceanic volcanics now on the library tape are named andesite in the source references, only two of the specimens in question, one from Reunion and one from Easter Island, have chemical and normative compositions appropriate for andesite, and these two barely qualify.

Rhyolites of the Oceanic Islands

The library tape now contains twenty analyses of oceanic island volcanics called rhyolite in the source references, nine from the Canaries, four from Easter Island, three from Reunion, and one each from American Samoa, Bouvet, Ascension, and Waianae. Although fewer in number than oceanic "andesites," the oceanic rhyolites seem a much more cohesive group.

Although less than 23% of the 485 named rhyolites on the library tape are peralkaline, 60% of the analyses of oceanic rhyolites fall in this category; twelve of the twenty norms are acmitic but only two contain *ns*. Nine of eleven specimens from the Atlantic islands, two of six from the Pacific, and one of three from the Indian Ocean are *ac* normative. Five of the eight remaining analyses are *c* normative and in two (both from Reunion) normative corundum is so abundant as to suggest that the specimens are extensively altered, whether by hydrothermal action or weathering. The characteristic rhyolite of the oceanic islands is evidently a peralkaline rock with a marked (molar) excess of alkalies over available Al_2O_3. Peralkalinity is less pronounced than in the famous rhyolites of Pantelleria, in which there is usually an excess, and often a very considerable excess, of alkalies over the sum (Al_2O_3 + Fe_2O_3). Oceanic rhyolite is perhaps more similar to comendite; it is on the whole an exceedingly rare rock but there can be no question that it does indeed occur in the oceanic island basalt-trachyte association.

On the Amounts of Silica and Normative Quartz in Analyses of Andesite, Dacite, and Rhyodacite

Innumerable text and reference books encourage the petrographer to suppose that, in silica and normative quartz contents, dacites are intermediate between andesite and rhyolite. In terms of group averages this generalization is both important and correct. The words andesite, dacite, and rhyodacite are primarily names applied to individual rocks, however, and the now generally accepted notions of their relative silica and normative quartz contents, usually offered both as broad genetic insights and as practical aids in classification, prove of little taxonomic value.

The distributions of SiO_2 and normative quartz in analyses of Cenozoic rocks called andesite, dacite, and rhyodacite stored on the current library tape are summarized in Table 2 and Fig. 1. An analyzed lava of this general type containing less than 66% SiO_2 is far more likely to be called andesite than dacite or rhyodacite, and 56% of the 338 dacites stored on the library tape contain less than 66% SiO_2; further, the probability that a rock containing more than 66% SiO_2 will be called andesite, though small, is not negligible. Similarly, an analyzed lava of this type whose norm shows less than 27% normative quartz is far more likely to be called andesite than dacite, and in the norms of more than two-thirds of the dacite analyses stored on the tape, *Q* is in fact less than 27%. The overlap between rhyodacite and dacite is even more extreme than that between dacite and andesite. The same hopelessly broad overlap characterizes the distributions of other im-

TABLE 2. Distribution of SiO_2 and Normative Q in Analyses of (A) 1864 Andesites, (B) 338 Dacites, (C) 36 Rhyodacites

	SiO_2			Q		
	A	B	C	A	B	C
Average	57.91	65.34	69.09	13.49	24.00	30.30
Standard deviation	4.24	4.44	3.40	6.79	8.10	8.13
Origin	44.00	44.00	44.00	0.00	0.00	0.00
Class width	1.00	1.00	1.00	1.50	1.50	1.50
Class Number	Frequencies					
1				41	0	
2	0			55	1	
3	7			67	0	
4	6			89	1	
5	16			132	2	
6	14			108	0	0
7	29			129	4	1
8	50			159	8	
9	92	0		161	10	
10	111	2		147	13	1
11	118			167	18	
12	171	3		116	22	
13	164	7		108	23	
14	189	4	0	92	30	3
15	187	10	1	75	25	1
16	168	14		55	22	1
17	136	15		45	32	2
18	121	18	1	24	19	5
19	66	25		16	20	1
20	65	24		14	16	1
21	62	33	1	4	17	3
22	30	33	2	6	11	4
23	27	29	1	5	8	2
24	9	32	3	0	7	
25	5	31	9	0	5	6
26	4	17	4	0	6	1
27	4	12	5	2	4	
28	5	6	4	1	6	2
29	1	10	3	0	3	
30	3	2	0	1	1	1
>30	0	11	2	1	4	1

portant chemical and normative variables in rocks called andesite and dacite.

Nowadays usually mocked or condescendingly ignored, classification and nomenclature are as important in petrology as in every other branch of natural science, and our inability to agree upon a satisfactory classification of igneous rocks must bear a heavy share of responsibility for the relative stagnation of our subject. It is the first requirement of a sound classification that the different names used in it denote appreciably different sets of properties. Barring redefinition so extreme as to be utterly unrealistic, a petrographic system retaining the names andesite and dacite probably cannot satisfy this requirement. These, like certain other common rock names, are old bottles into which it is unwise, if not actually impossible, to pour the new wine of sound taxonomy. Unappealing and foolish as they may sometimes seem, systems that impose a completely synthetic nomenclature—the Linnaean academicism of CIPW, the nonsense syllables of Holmes, the symbolism of Shand—probably offer more hope of success than those that attempt, whether by fiat or plebiscite, to impose consistency and mutual exclusiveness on the common names of common rocks. No matter how democratically—or arbitrarily—we decide how these names ought to be used in the future, we can do nothing about how they have been used in the past.

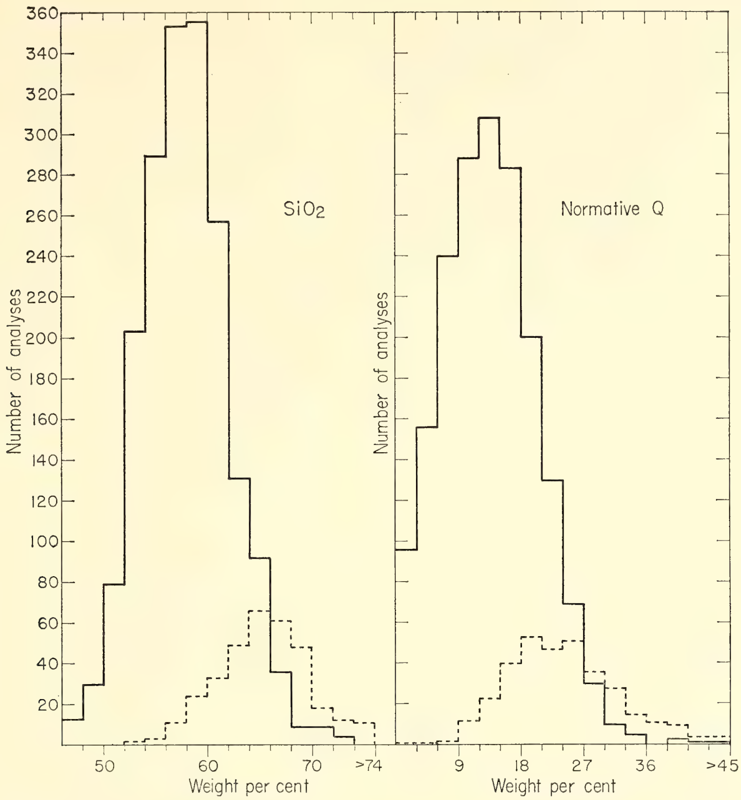

Fig. 1. Distribution of SiO_2 and normative quartz in andesite (solid lines) and dacite (dashed lines). Data from Table 2.

On the Occurrence of Corundum in the Norms of the Common Volcanic Rocks

In a norm computed according to the standard CIPW conventions, *c* will occur if and only if the molar inequality $Al_2O_3 > (Na_2O+K_2O+CaO)$ is satisfied. Of the essential minerals of the eruptive rocks, only certain aluminous micas satisfy the limiting inequality. These are rarely abundant, and the peraluminous character they would otherwise give to the rock analysis is usually counterbalanced by associated amphiboles, chlorites, or other micas. There is thus no reason why the norms of most eucrystalline eruptive rocks should be corundiferous, and, in the absence of modal corundum—on the whole a very rare mineral—the presence of *c* in the norm of an intrusive rock is usually taken as evidence either of alteration or of a questionable analysis.

Modal corundum is virtually unknown in extrusive rocks, and except in the andesites, the occurrence of *c* in the norms of such rocks seems to have attracted little attention. It has long been known that a little *c* is not at all uncommon in the norms of andesites, and this is usually considered additional evidence that the assimilation of aluminous sediments or metamorphic rocks plays an important role in their formation. (The principal evidence for this view is the restriction of andesites to the orogenic environment and the not-infrequent occurrence in them both of metamorphic minerals, such as garnet and cordierite, and of inclusions of sedimentary and metamorphic rocks.)

Little has previously been known about the distribution of *c* in the norms of Cenozoic volcanics, but the existence of the library tape makes it possible to survey this matter in any desired detail. Some of the results of a preliminary survey are shown in Table 3. The rock names shown there require some explanation, since all are used as broad group designations. Specifically, their denotations are:

A. *Rhyolite.* Rocks identified in the source references as rhyolite, quartz-porphyry, nevadite, liparite, tordrillite, comendite, cantalite, pantellerite, dellenite, or pitchstone, modified by any one or combination of the following: aegerine, riebeckite, arfvedsonite, amphibole, soda, plagi-, and comendite.

B. *Dacite.* Rocks identified in the source references as dacite, santorinite, weiselbergite, shastaite, peleeite, or bandaite, with mineral modifiers.

C. *Trachyte.* Rocks identified in the source references as trachyte, arsoite, vulsinite, sanidinite, orendite, modified by one or more of the following: fayalite, mica, nepheline, sodalite, hauyne, tephritic, soda.

D. *Andesite.* Rocks identified in the source references as andesite, palatinite, tholeiite in the sense of Tröger, alboranite, aleutite, modified by any one or combination of the following: mica, biotite, hornblende, augite, hypersthene, oligoclase, andesine, labradorite (all *ne*-normative analyses rejected).

E. *Trachyandesite.* Rocks identified in the source references as latite, latite-phonolite, vulsinite-vicoite, dancalite, ordanchite, or trachyandesite, modified by the names of feldspathoids.

F. *Trachybasalt.* Rocks identified in the source references as ciminite, kohalaite, mugearite, hawaiite, andesine basalt, dorgalite, trachybasalt, trachydolerite, with mineral name modifiers.

G. *Basalt, basanite, tephrite.* Rocks identified in the source references as basalt, ankaramite, oceanite, basanite, tephrite, limburgite, scanoite, atlantite, vesuvite, braccianite, modified by one or more of the following: plagioclase, labradorite, leucite, analcime, hauyne, sodalite, mica, hornblende, olivine, hypersthene, picrite, basaltic, alkali.

The most important and unexpected information in the table is that the relative frequency of *c* in the various groups varies inversely with average CaO and

TABLE 3. Incidence of Normative Corundum in Some Common Volcanic Rocks, and Related Sample Statistics

Group	No. of Analyses	% in which $c >$ 0	1%	2%	Averages, % c	SiO_2	Al_2O_3	CaO
A	491	58.5	37.9	19.3	1.05	71.83	13.04	1.25
B	338	44.4	22.2	10.1	0.63	65.34	15.63	4.44
C	216	36.6	19.4	10.6	0.63	61.91	17.45	1.99
D	1864	18.7	9.3	4.8	0.30	57.91	17.26	6.96
E	104	9.6	4.8	3.8	0.17	56.73	17.45	5.17
F	133	5.3	3.0	1.5	0.10	48.78	16.79	8.08
G	425	1.9	1.2	0.9	0.05	46.21	14.65	9.99
All	3571	24.9	13.7	7.0				

A. Rhyolites, complete tape search.
B. Dacites, complete tape search.
C. Trachytes, complete tape search.
D. Andesites, complete tape search.
E. Trachyandesites associated with trachyte on oceanic islands.
F. Trachybasalts associated with trachyte on oceanic islands.
G. Basalts, basanites, and tephrites associated with trachyte and trachyandesite or trachybasalt on oceanic islands.

directly (and also monotonically) with average SiO_2. It does not appear to vary meaningfully with average Al_2O_3. Andesite is not the only common volcanic rock the norms of which often contain *c*; the relative frequency of normative *c* is far greater in trachytes, dacites, and rhyolites.

It is to be noted, however, that the amounts of *c* under consideration are nearly always very small. It is present, to be sure, in almost a quarter of the 3571 norms under review but in almost half of the corundiferous norms the amount of *c* is less than 1%, and in well over 70% of them it is less than 2%.

Even for the trachytes and dacites the average value of *c* is probably not an impossible result for a passable analysis of a material lacking normative *c*, and except for rhyolite the other averages are well within analytical tolerances. It is to be remembered that, like the conventional analytical value for Al_2O_3, normative *c* is not a direct estimate. Its variance cumulates many perfectly legitimate uncertainties attaching to analytical values for oxides other than Al_2O_3. Considering a rather unlikely source of interaction, for instance, an overestimate of K_2O in the partitioning of alkalies would tend to generate *c* in a norm calculated from an otherwise errorless analysis of a material containing no molar excess of Al_2O_3 over (Na_2O+K_2O+CaO). If the rock in question were sufficiently high in CaO, the norm could easily be free of *c*, the alumina misbalance finding expression only in a ratio of *an* to *di* somewhat greater than the true value. Since the true value of this ratio is unknown, the effect would probably escape detection altogether. If the CaO content were low enough, however, the molar excess of CaO over $(Al_2O_3-Na_2O-K_2O)$ might well be too small to compensate for the error in alkali partition, and the norm would then contain *c*. Errors in the partition of CaO and MgO would have similar effects. Effects of this kind are generated largely by the CIPW calculating conventions, but more direct analytical interactions are of course possible; the monotonic variation of average SiO_2 with relative frequency of occurrence of normative corundum certainly suggests that the amount of SiO_2 that may be identified as Al_2O_3 varies directly with the amount of SiO_2 in the rock. (The interactions discussed here are those that might occur in a classical wet analysis, for so far the library tape contains very few analyses done by X-ray spectrography, nuclear activation, etc.)

The gist of this discussion is that the amounts and relative frequencies of normative *c* in Table 3 should not be taken as an indication that either the rocks in question or the immediate parent magmas are commonly peraluminous. Should one then use the occurrence of normative *c* in the absence of satisfactory modal rationalization as a means of identifying faulty or inadequate analyses? Under the circumstances, one cannot help thinking that a norm containing more than a few percent of *c* indicates either a very unusual analysis or a very unusual rock, and if modal information does not support the latter possibility the former clearly cannot be ignored. The mere occurrence of *c* in *any* amount, however, is not a desirable criterion for rejection; in the greatly oversimplified analytical situation described above, for instance, such a criterion would eliminate analyses in which the ratio K_2O/Na_2O had been overestimated, but not those in which it had been underestimated. The long-range effect would be to introduce a bias leading to overestimates of Na_2O.

In dealing with so many interdependent variables it is probably wise to refrain from imposing fixed rejection criteria. For specific purposes analyses will certainly have to be rejected, and sometimes in considerable number, but rejection criteria suitable for one situation may be wasteful, ineffective or misleading in another.

Whatever the detailed interpretation of *c*, in norms of volcanic rocks, there

seems little doubt that its occurrence in amounts of the order of 2% or less is either a consequence of surficial or hydrothermal alteration or a combined analytical-computational artifact. In illustration of the former possibility, *c* is present in the norms of only 13% of the andesite analyses containing less than 2% H_2O but in almost 32% of the norms of those containing over 2% H_2O. Both factors no doubt contribute to a striking result obtained as a by-product of work described below, in which norms were generated for the 200 andesite analyses selected, by a systematic ranking procedure, as closest to the grand mean for the group. Although, as already noted, 18.7% of all andesite analyses on the current library tape are *c* normative, *only two of this central subset of 200 yielded norms containing* c. At the time of writing, similar calculations have not been carried through on the dacites, trachytes, and rhyolites.

On Selecting the Centrally Located Members of a Large Group of Analyses

Nothing is better calculated to reveal the inadequacy of the sampling concepts of descriptive petrography than careful study of a really well-exposed complex. The availability of a large reservoir of readily retrieved rock analyses places broader petrological and geochemical notions—such matters as the definitions of petrographic provinces or major rock types, for instance—in similar jeopardy. Questions that seem reasonably clear and specific so long as there is no possibility of answering them definitely may prove vague, tenuous, and decidedly unclear as emerging technology provides means by which, in principle at least, answers could be provided. Accustomed to suppose that the central difficulty in each specific instance is the lack of a demonstrably sound answer, we are then often chagrined to discover that what is actually lacking is an answerable question.

A case in point, and perhaps the simplest of all possible examples, is the selection of analyses thought to be similar to each other. This is of course a nearly trivial operation if only a single variable is involved. "Complete" rock analyses contain estimates of at least ten variables, however, and the assertion that the members of a subset of such analyses resemble each other more closely than they do the remaining members of the set is essentially meaningless without some specification of what is meant by resemblance. In most practical work the master set is reasonably small, each of the analyses is examined by the petrologist making the selection, and the subset finally selected is small enough so that it can be published in full in a table occupying at most a few pages and usually no more than a single page. Under these circumstances it usually does not matter much that the purveyor does not provide and the consumers do not demand an explicit specification of resemblance. Each uses his own implicit specification, and although no two of these may agree exactly, most have so much in common that serious differences of opinion about the closeness of the suggested resemblances are quite rare.

To some extent this is perhaps because the function of tables of this sort is often largely ornamental, but I believe there is more to it than that. The standard techniques of descriptive petrography are both very old and very stable. Early in our careers we are all taught what little there is to know about the astatistical comparison of analyses. We suppose we are all doing about the same thing when we examine sets of allegedly similar analyses, and our intuition is probably substantially correct even though we cannot—or, at any rate, do not—say just what it is we are doing. If really large numbers of analyses are to be sorted, however, time alone dictates that the sorting be by machine, and the background of common petrographic experience that makes it unnecessary to define operating procedures explicitly is of

no use whatever when we attempt to transfer the selection function to the computer. Unless the selection process can be completely and explicitly specified, it cannot be computerized.

A reviewer of the andesite work described in an earlier section requested the identities and source references for a subset of chemically typical andesites, i.e., andesites whose analyses were in some sense central. Given an appropriate definition of "centrality," this is a straightforward problem in data retrieval. The definition finally adopted, and some of its numerical properties, are described here.

Oxide ranks and the rank sum. Distance from the group mean is of course the criterion one would apply to any oxide individually, but because of extreme variance differences the distances for all oxides are not readily compounded into a single statistic meaningfully characterizing the centrality of a whole analysis. If the unweighted distances are used, the net distance will be essentially that of a few components only. The simplest escape, and the one taken here, is to abandon deviations in favor of ranks, using the sum of ranks rather than of deviations as a centrality statistic. In the absence of ties, this has the effect of giving equal weight to all oxides; in fact, however, the range of the minor oxides is so small that in any large collection of analyses the incidence of tie ranks for them will be very large and, in general, the more ties in the rankings for a particular oxide, the less that oxide contributes to differences between rank sums. (A weighting of deviations would probably involve less loss of information than their abandonment, but the selection of weights involves difficult and rather arbitrary decisions.)

In most work of this type it is probably desirable to assign ranks from the signed deviations, but in this particular application retention of the signs of the deviations would introduce considerable ambiguity. Because of the closure restraint the sum of deviations in any analysis is in principle zero and in fact very nearly zero; thus the sum of ranks assigned from the signed deviations for a particular analysis might fall close to the mean rank sum either because the individual oxide ranks all lie close to the mean oxide rank or because oxide ranks far above and below the mean oxide rank contribute to it. The appropriate remedy is to assign oxide ranks from the absolute or *un*signed deviations, so that *the more central a particular analysis, the smaller its rank sum.*

Mean and variance of the oxide rank and rank sum. If X_{ij} is the rank of oxide j in analysis i, $j=1, k$ and $i=1, n$, the mean oxide rank is

$$\bar{x}=\frac{1}{n}\sum_{i=1}^{n}(X_{ij})=(n+1)/2 \qquad (1)$$

for all j, and the average rank sum is

$$\bar{y}=k\bar{x}=k(n+1)/2, \qquad (2)$$

a rather large number even for fairly small values of k and n.

The variance of an oxide rank if there are no ties is

$$\text{Var }(X)=\frac{1}{n-1}\left[\sum_{i=1}^{n}(X_{ij}^{2})-\frac{1}{n}\left(\sum_{i=1}^{n}(X)\right)^{2}\right]=\frac{n(n+1)}{12}, \qquad (3)$$

again the same for all j. If the X's were independent the expected variance of the rank sum would be

$$\text{Var }(Y)=k\text{ var }(X)=\frac{kn(n+1)}{12}, \qquad (4)$$

and Y, being the sum of k uniformly distributed numbers, would be asymptotically normal about $k(n+1)/2$ with standard deviation $(kn(n+1)/12)^{\frac{1}{2}}$.

The variance of the rank sum, however, is always considerably larger than indicated by equation 4. In the oxide ranking procedure used here each element of a tie extending from ranks j through k inclusive is assigned the rank $(j+k)/2$. Ties have no effect on oxide rank means, for

the sum of the untied ranks would be

$$j+(j+1)+(j+2)+\ .\ .\ .\ +k=(k-j+1)\ (j+k)/2,$$

but it was at first feared they might be responsible for the excess of observed over expected variance. In fact, however, their effect on variance, whatever its magnitude, must be in the opposite direction. Although a tie treated in this fashion contributes to the sum exactly what would be contributed by the same sequence of untied ranks, its contribution to the sum of squares is always less than that of the untied ranks it replaces. Thus ties must always reduce the first but cannot affect the second term inside the square bracket of equation 3, with the result that if ties do in fact occur the oxide rank variance must be *smaller* than its expectation calculated from equation 3. On the hypothesis of independence the expected variance of the rank sum is merely the sum of the expected oxide rank variances; treatment of ties can therefore not be responsible for the excess of observed over expected rank sum variance.

There is only one other assumption involved in calculation of the expected variance of the rank sum which is not realized in the practical situation, namely, that the oxide ranks are independent. If there is interdependence, the term in covariance cannot be ignored and equation 4 becomes

$$\text{Var }(Y)=k\text{ var }(X)+\sum_{j\neq m}\text{cov }(X_j,X_m). \quad (5)$$

Now the oxide ranks are uniformly distributed about the same mean for all oxides and are assigned from the absolute values of deviations whose algebraic sum in any analysis is actually or nearly zero; under the circumstances there *must* be positive correlation between oxide ranks, high rank in any constituent being associated with high rank in one or more of the others. Clearly, rank sum variances greater than expectations calculated from equation 4 should have been anticipated; indeed, observed rank sum variances may be used to obtain an estimate of the average covariance between oxide ranks.

Recalling that the oxide rank variance is the same for all oxides, we may restate equation 5 as

$$\rho=\frac{1}{k-1}\left[\frac{\text{var }(Y)}{k\text{ var }(X)}-1\right] \quad (6)$$

where ρ is the correlation calculated from the average covariance between pairs of oxides. Estimates of ρ obtained by using the observed variance of the rank sum for var (Y) in equation 6 are so far rather small; for the world andesite group of Table 4, for instance, r is only

TABLE 4. Some Sample Statistics for Rank Sums in Groups of Analyses of Rhyolites, Andesites, and Basalts

	A	B1	B2	B3	B4	C
Number of analyses	528	778	189	134	1946	1880
Average rank sum, $\bar{x}$	2645	3895	950	675	9735	9405
Expected standard deviation (from eq. 4)	482.45	710.67	172.99	122.78	1776.90	1716.65
Observed standard deviation, s	638.02	1115.05	221.89	178.80	2587.82	2150.96
Number of rank sums $\leqslant (\bar{x}-3s)$	0	0	0	0	0	0
Number of rank sums $\leqslant (\bar{x}-2s)$	14	5	3	0	18	29
Number of rank sums $> (\bar{x}+2s)$	15	23	9	22	42	39
Number of rank sums $> (\bar{x}+3s)$	1	0	0	0	3	0
Percentage of rank sums outside $\bar{x}\pm 2s$	5.5	3.6	6.3	6.1	3.1	3.6
Percentage of rank sums outside $\bar{x}\pm 3s$	0.19	0	0	0	0.15	0

A. Rhyolites (Tröger numbers 40–44, 47–49, 72, 96, 102, 118).

B. Andesites (Tröger numbers 127, 154, 324, 340, 342, 343, 890): 1, Japan; 2, Kuriles, Kamchatka, Aleutians; 3, Mexico, Central America; 4, world.

C. Basalts (Tröger numbers 151, 159–162, 344, 378–382, 384–387, 407–410, 801, 855, 864, 888).

0.114. It is a striking illustration of the difference between significance testing and estimation that a correlation too small to warrant rejection of the hypothesis of zero covariance between any pair of variables except in very large samples may more than double the variance of the sum of ten variables.

The coefficient of concordance suggested by Kendall (1948) provides another means for summarizing the interdependence of oxide ranks. If the oxide ranks were perfectly concordant, i.e., if the ranks for all oxides in each analysis were the same (and there were no ties), the rank sums would be k, $2k$, $3k$, . . ., nk. The variance of these perfectly concordant rank sums is $k^2n(n+1)/12$ * and no other arrangement of k sets of n ranks can have a larger variance. Kendall's coefficient of concordance is the ratio of the observed rank sum variance to that for perfect concordance, or

$$W = 12s_y^2/k^2n(n+1),$$

which clearly lies in the interval 0, 1. In terms of this statistic, incidentally, equation 6 may be written $\rho = (kW-1)/(k-1)$.

As we have seen, if the oxide ranks were independent, the expected variance of the rank sum would be $kn(n+1)/12$. For this null point, accordingly,

$$W_i = k \text{ var } (X)/[k^2n(n+1)/12] = 1/k.$$

Sample values greater than $1/k$ indicate some degree of concordance, and those less than $1/k$ some degree of discordance, between ranks; concordance, in turn, results from a net positive, and discordance from a net negative, correlation between the variables being ranked. Every sample value of W so far computed is greater than 0.1, the null value for $k=10$. The excess, however, is never large; for the world andesite group of Table 4, for example, $W=0.203$.

*If $j = 1, 2, 3, \ldots, n$, then, from (3), var $(j) = n(n+1)/12$, and for any constant, k, var $(kj) = k^2$ var (j).

Some examples. As already mentioned, the work on rank sums was stimulated by a request for a set of analyses "typical" of the andesites on the library tape. A program was constructed that would search all or any part(s) of the library tape for analyses of rocks denoted by any of a set of names, save all such analyses and their tape locations in a temporary file, generate rank sums for all analyses in this file, and print out each of the i smallest rank sums, together with the number of the logical record containing the analysis that gave rise to it and the sequence number of the analysis within that record. (From this latter information the analysis itself, associated analyses, and source reference or references are easily reclaimed.) The parts of the tape to be searched, the names of the rocks whose analyses are to be processed, and the number of rank sums to be printed out are at the option of the user. The desired information was thus readily obtained—although the whole procedure would have been impractical or impossible on anything but a very fast and very large computer—but the rank sums were much larger than had been anticipated, the smallest in each of a considerable set of rankings being of the order of two to three times the number of analyses being ranked.

The work described above, prompted by these excessively large minimum rank sums, soon showed, however, that the *average* rank sum (equation 2) would be a very large number indeed and suggested that the observed minimum values, far from being too large, were too small; in samples of the sizes used, values as small as those found would not occur in anything like the observed frequency if the parent population was indeed normal with mean and variance as indicated by equations 2 and 4. Accordingly, the program was modified so that it would find the sample mean and standard deviation of the rank sum and generate a sample frequency distribution with class width equal to one-third of the

(observed) standard deviation. Results of some of the runs made with the modified program are summarized in Table 4. The average rank sum is precisely that given by equation 2, but the observed variance is always considerably larger than indicated by equation 4; in the examples shown in the table the ratio of observed to expected standard deviation ranges from 1.24 to 1.66, so the observed variance may be 1.5 to 2.75 times as large as that calculated from equation 4. In the three largest samples, the relative frequency of rank sums distant from the mean rank sum by more than 2*s* is somewhat less than the normal expectations of 5%, and that of values distant from the mean by more than 3*s* is far less than the expected 1%. Thus a dispersion markedly greater than normal against a standard deviation calculated on the hypothesis that the oxide ranks are independent is in fact subnormal against the sample standard deviation.

Chemical and Mineralogical Petrography

Knowledge of the chemical composition of individual minerals in volcanic rocks is essential both for proper classification of the rock and for an understanding of fractionation trends arising from crystal-melt equilibria. Traditional gravimetric analysis undoubtedly remains the most accurate method for properly purified, homogeneous mineral concentrates, but the minerals of rapidly cooled volcanic rocks are rarely homogeneous, and the purification of fine mineral intergrowths is sufficiently tedious and wasteful of material that such analyses can hardly be produced routinely. In such a situation the electron microprobe is of obvious value; with its aid all but the most minute mineral grains can be identified and analyzed. Though the individual analyses are of considerable value, qualitative comparisons of phenocryst and groundmass crystals of a given mineral or scans across marginal zones of phenocrysts with the probe beam provide important information on possible variation trends in both minerals and residual liquids. Examined in this detail, most volcanic rocks prove to be much more complex than traditional thin-section study would suggest.

All electron-microprobe * analyses were made with standards and correction procedures described by Boyd (*Year Book 66*) and Boyd, Finger, and Chayes (*Year Book 67*), except that a natural cossyrite analyzed and described by Zies (1966) was used as a standard for Na and Ti in the aenigmatite (cossyrite) from Socorro Island. The ratio $\sigma/\sqrt{\overline{N}}$, where $\overline{N}$ is the mean count and σ is the standard deviation, provides a useful measure of homogeneity and is given for the major elements; a value greater than 3 indicates a distinctly inhomogeneous mineral.

Volcanic rocks examined during the report year include material from Australia, Pantelleria, the Revillagigedo Islands on the East Pacific Rise, and drift pumice, collected from beaches in Australia but probably originating in the Tonga-Kermadec volcanic zone north of New Zealand. Over fifty minerals have been analyzed so far, many of them replicated against different standards or with different operating conditions as a check on the procedures used. The minerals discussed here, along with the rocks in which they occur or with which they are associated, represent some of the more important observations and the petrologic problems toward which the work has been directed.

Among the common silicate minerals in the rocks examined this year, zoning is usually most pronounced in feldspar, and the next most variable mineral is olivine. Pyroxenes are usually relatively homogeneous in terms of the major elements but typically show considerable

* The electron probe was purchased with the assistance of the National Science Foundation under grant GP 4384.

sympathetic variation in titanium and aluminum. Alkali feldspars range from potassic oligoclase to sodic sanidine or anorthoclase with a composition close to the "dry" eutectic of $Ab_{65}Or_{35}$. In the basalts examined, feldspar consists of a relatively uniform core of intermediate plagioclase, surrounded by a narrow zone of potash oligoclase in which there is a rapid transition to a rim of anorthoclase. This partitioning of sodium between plagioclase and alkali feldspar probably largely accounts for the common observation that modal plagioclase is distinctly more calcic than normative plagioclase. The discrepancy may disappear if normative albite is partitioned between normative anorthite and orthoclase, on the assumption that the alkali feldspar has the eutectic composition. As a practical matter, grains sufficiently free from zoning for reliable microprobe analysis can usually be found, but it must be realized that such an analysis may not correspond to the average composition for the whole assemblage of crystals of that mineral phase in the rock. Indeed, the problem of determining the bulk composition of a feldspar in a rock, discussed by Suzuki and Chayes (*Year Book 60,* pp. 169–172), appears to apply in a less extreme way to all other mineral phases.

In volcanic areas one can usually be sure that magmas having the compositions of each of the major rock types did in fact exist, and the sequence of magmatic development can sometimes be inferred with reasonable assurance. With regard to plutonic rock complexes the situation is very different. Although chilled margins may provide direct evidence of magma composition, the other facies of a complex are not merely frozen magma; rather, they are fractionation products that in general must be presumed to differ in composition both from the magma that precipitated them and from the magma remaining after their precipitation. Reconstruction of the path of magmatic development is nevertheless of prime interest. It is nearly always accomplished by graphical devices, and there is probably little to choose between solving a "partition" problem by graphical or analytical means if the numerical work is to be done by hand. If a programmed computer or a good desk calculator is available, however, an analytical solution will ordinarily be more reliable and much more quickly reached than a graphical one. An analytical solution for the composition of successive liquids in the important "Skaergaard model"—in which a single mass of magma of some known or assumed composition is partitioned into a number of zones or fractions, one of which is unexposed—is briefly described here. An application of the procedure to summary data for the well known Skaergaard complex has been published elsewhere (Chayes, 1970); the burden of the argument is that the exposed portion of the complex may be a very much smaller part of the whole than Wager (1960) suggests, and that there is no evidence for the progressive alkali enrichment indicated by his graphical analysis.

Mineralogy of Coral Sea Drift Pumice

W. B. Bryan

Pumice that accumulates on mainland beaches and barrier reef islands of Queensland, Australia, probably originates from submarine eruptions along the Tonga-Kermadec volcanic zone north of New Zealand. Menard (1964, p. 58) has considered the effect of sea water pressure on the vesiculation of magma and concludes that the possibility of explosive volcanism increases very rapidly above a depth of 1500 meters. Many submarine volcanoes along the Tonga-Kermadec zone extend above this depth and could have been the source of the pumice. The samples described here were collected in November 1966, by Dr. J. C. Yaldwyn, of the Australian National Museum, from the beach on One Tree Island near the southern end of the Great

Barrier Reef. In megascopic appearance and in terms of refractive index of the glass and plagioclase (Table 5) this pumice appears identical to that collected on the Herald Cays, Queensland, in December 1964, and to that which appeared on beaches of the Fiji Islands in March 1965. Optical data and chemical analyses of light and dark varieties of the Herald Cays pumice have been published previously (Bryan, 1968).

The One Tree Island pumice may be readily subdivided into light, dark, and intermediate varieties on the basis of the color of the glass. As was true of the Herald Cays and Fiji samples, the light pumice forms the largest pieces, some lumps measuring 3–4 inches in diameter, and the intermediate and dark pumice lumps average about 1 inch in diameter. The light pumice is almost pure white or chalky in hand specimen, with yellowish or brownish iron oxide stain along fractures. The glass appears colorless under the microscope. The intermediate pumice is pale tan in hand specimen, but small fragments also appear almost clear in transmitted light. The dark pumice is a dark chocolate brown color, appearing reddish brown in small fragments under the microscope. Small nodules, 1–2 mm in diameter, are especially common in the light and dark varieties; they are aggregates of interlocking green clinopyroxene, hypersthene, and calcic plagioclase with minor amounts of magnetite.

TABLE 5. Refractive Index of Pumice Glass and Plagioclase from Herald Cays, One Tree Island, and Fiji

Pumice Variety	Light	Intermediate	Dark
	Pumice Glass		
One Tree Island	1.508	1.523	1.532
Herald Cays *	1.5075	1.5220	1.5300
Fiji *	1.5075	1.5212	1.5306
	Plagioclase α' on Cleavage		
One Tree Island	1.576	...	...
Herald Cays *	1.5760	...	1.5773
Waya Island, Fiji *	1.5755	...	1.5740

* Bryan, 1968.

Note: Values are midpoints of ranges given in Table 1 (*op. cit.*).

Microprobe analyses of the light pumice glass (Table 6) and minerals (Table 7) reveal the same compositional peculiarities noted in the Herald Cays pumice. Chemically and mineralogically this material may be classified as a dacite, but the high ratio of lime to alkalies, and especially the low potash, are unusual in a rock containing over 70% SiO_2, even among the relatively calcic circumpacific lavas.

Analyses of the plagioclase indicate a distinctly less calcic composition than would be inferred from the α' refractive index on cleavage fragments, although the extinction $\alpha' \wedge 010$ on 001 cleavage fragments averages about 23°, giving a composition of An_{83} on the determinative chart of Deer, Howie, and Zussman (1963, p. 137), in good agreement with the compositions obtained by microprobe analysis. The refractive index is apparently raised appreciably by the relatively high iron content of the feldspar. As care

TABLE 6. Chemical Analyses of Pumice and Pumice Glass

	1	2	3	4	5
SiO_2	72.3	73.38	73.50	65.84	73.04
Al_2O_3	11.4	12.66	11.90	12.02	13.61
TiO_2	0.45	0.45	0.58	0.76	0.30
Fe_2O_3	...	1.11	0.76	1.05	0.69
FeO	4.34	2.84	4.84	8.25	2.13
MnO	0.13	0.06	0.00	0.13	0.08
MgO	0.62	0.84	0.63	1.29	0.50
CaO	3.59	3.79	3.80	6.22	3.25
Na_2O	3.50	3.09	2.81	2.66	4.66
K_2O	0.80	1.52	0.75	0.77	0.67
P_2O_5	...	0.00	0.09	Tr	0.12
H_2O^+	...	<0.10	0.46	0.84	1.04
H_2O^-	...	0.03	...	0.16	0.04
Totals	97.13	99.77	100.12	99.99	100.13

1. Interstitial glass, pumice *C*, One Tree Island, Queensland. Partial analysis by electron microprobe.
2. Pumice glass, Metis Shoals, Tonga. E. Jarosewich, analyst (Melson, 1969).
3. Light pumice, Herald Cays, Queensland, L. J. Sutherland, analyst (Bryan, 1968).
4. Drift pumice, 1928 Falcon Island eruption, Tonga. A. LaCroix, analyst (LaCroix, 1939).
5. Pumice, 1962 eruption, South Sandwich Islands. P. G. Harris and M. Kerr, analysts (Gass, Harris, and Holdgate, 1963).

TABLE 7. Composition of Plagioclase, Pyroxene, and Magnetite from Gabbroic Nodules in Drift Pumice, One Tree Island, Queensland

	1		2		3		4		5	
SiO_2	48.7	*3*	46.2	*3*	51.4	*1*	51.7	*1*	0.12	
Al_2O_3	32.1	*4*	33.3	*4*	0.73		1.19		2.21	*1*
TiO_2	...		...		0.19		0.31		12.4	*2*
Fe_2O_3	0.90	*3*	0.89	*2*	...		...		50.3	*2*
FeO	...		...		26.4	*2*	14.0	*1*	32.4	
MnO	...		0.01		1.02		0.57		0.48	
MgO	0.08		0.11	*2*	18.1	*2*	12.8	*1*	1.46	*1*
CaO	16.6	*4*	17.8	*5*	1.68	*2*	19.5	*1*	0.03	
Na_2O	2.07	*4*	1.24	*5*	0.00		0.13		...	
K_2O	0.01		0.00		0.00		0.00		...	
Cr_2O_3	...		...		Tr		0.00		0.00	
Totals	100.5		99.6		99.5		100.2		99.4	
O	32.00		32.00		6.00		6.00		32.00	
Si	8.902		8.570		1.975	2.000	1.960	2.000	0.035	
Al					0.025		0.040			
Al	6.921	15.946	7.264	15.959	0.008		0.013		0.764	
Ti	...		...		0.005		0.009		2.725	
Fe^{3+}	0.123		0.125		...		...		11.096	23.31
Fe^{2+}					0.849		0.443		7.924	
Mn					0.033	2.002	0.018	2.009	0.120	
Mg	0.022		0.030		1.038		0.725		0.637	
Ca	3.241	3.999	3.525	4.001	0.069		0.792		0.009	
Na	0.734		0.445		...		0.009		...	
K	0.002		...		...		...		...	
Ca	82.0	Ca	89.0	Ca	3.5	Ca	40.4		...	
Na	18.0	Na	11.0	Fe	43.4	Fe	22.6		...	
K	0.0	K	0.0	Mg	53.1	Mg	37.0		...	

1. Bytownite, pumice *A nodule,* all Fe as Fe_2O_3.
2. Calcic bytownite, pumice *C* nodule, all Fe as Fe_2O_3.
3. Orthopyroxene, pumice *A* nodule, all Fe as FeO.
4. Clinopyroxene, pumice *A* nodule, all Fe as FeO.
5. Titanomagnetite, pumice *C* nodule, recalculated to give FeO and Fe_2O_3 on ilmenite-magnetite basis.

Note: Numbers in italics are $\sigma/\sqrt{N}$.

was taken to select especially clear crystals for analysis, and inclusions are easily avoided with the probe beam, the iron must be contained in the feldspar structure. In both analyses alumina is insufficient to balance the alkalies, and iron may be presumed to make up the deficiency. Apparently this iron content does not seriously affect the optic orientation.

The pyroxenes in such a siliceous rock might be expected to be relatively enriched in iron, but the analyzed compositions are in fact more typical of a gabbroic rock. These pyroxenes, along with the very calcic plagioclase, would not be expected to be in equilibrium with a magma of this composition. It seems more likely that the rock nodules are small xenoliths incorporated into the frothy pumice magma during its ascent in the volcanic vent. The mixture of at least three pumice varieties, presumably erupted almost simultaneously at the same vent, is also suggestive of hybridization of acid and basic material in the magma chamber. It is strange, however, that in none of the three separate collections from Fiji, from the Herald Cays, and from One Tree Island do any of the pumice fragments show banding or transitional compositional features; each fragment seems to fall distinctly into one of the three categories.

Drift pumice may be an important source of fragmental material in deep-sea sediments, and the transport of pumice for thousands of miles by ocean currents provides effective distribution over a

large area. The transfer of material from oceanic sites of eruption to distant sites of deposition on the sea floor or on the continental shelves may have important geochemical implications that have yet to be evaluated. Fiske (1969) has discussed criteria by which pumice fragments, often overlooked in marine sedimentary rock, may be recognized. He described examples dating back to the Precambrian. The size and ultimate distribution of pumice rafts may be judged from a few recent examples. Richards (1958) cited linear dimensions of 64 to 324 miles for the pumice raft from the eruption of San Benedicto Island, Mexico; although he gave no estimate of the volume of the raft, the estimated volume of tephra in the new cone produced by the 1952 San Benedicto eruption is 350 million cubic yards (Richards, 1959). If the eruption had been submarine, all of this material would have been ejected into the sea. Pumice from this eruption drifted at least as far as the Marshall Islands, a distance of 4700 miles. Pumice from the 1962 submarine eruption in the South Sandwich Islands circled the Antarctic continent in the "roaring forties." The area of the original pumice raft was estimated to be about 2000 square miles, with an estimated volume of pumice of about 750 million cubic yards or about 0.15 cubic mile (Gass, Harris, and Holdgate, 1963).

The frequency of submarine pumice eruptions is very poorly established; of those observed or detected, probably most are never reported in geologic literature. If such eruptions average only four per year, a reasonable figure, they could easily produce about one-half cubic mile of pumice per year. Even allowing for void space in the pumice, this amount would represent almost two-tenths of a cubic mile of rock, a significant figure compared with other estimates of material moved by erosion or produced by terrestrial eruptions. For example, Gilluly (1955) suggested 13.6 km^3, about three and one-quarter cubic miles, as the amount of material removed annually from the continents by erosion. Wilson (1952) noted that the building of the continents to their present size by accretion through available geologic time requires an addition of about one-third of a cubic mile of material per year, and he suggested that the rate of terrestrial volcanic eruption alone is sufficient to add this amount. It is difficult to estimate the proportion of eroded material that bypasses the continental shelf and is lost to the ocean basins; similarly, it is not yet possible to estimate the proportion of material transported as drift pumice that becomes incorporated in sediments on the continental shelves. It is clear, however, that knowledge of the source, composition, and ultimate distribution of drift pumice is essential to a more complete understanding of sedimentation in the deep oceans and of the geochemical balance between continents, ocean basins, and active volcanic areas in and around the oceans.

Mineralogy of a Mugearite from Clarion Island, Mexico

W. B. Bryan

Chayes (1963*a*) showed that bulk chemical analyses of alkaline rocks of composition intermediate between basalt and trachyte are relatively rare in the literature. Even less detailed information is available on the mineralogy of these rocks. Muir and Tilley (1961) gave data for olivines, pyroxenes, feldspars, and iron-titanium oxides for eighteen rocks that they then classified as mugearite; of these, only three lie in or close to the "Daly gap" as defined by Chayes's histograms. In a later paper, Tilley and Muir (1964) discussed the nomenclature of rocks lying in the "Daly gap" and noted that, though most would be called trachyandesite, this term has been too loosely used to be meaningful. They suggested instead the names "tristanite" for the potassic varieties and "benmoreite" for the sodic variants. Under this termi-

nology, the "mugearite trachyte" from Totardor, Skye, and the "mugearite" of Ben More, Mull, described in their earlier paper, are now defined as benmoreite. For these two rocks the earlier paper gave analyses only for the pyroxenes, and no new mineral data were given in the later paper. Baker *et al.* (1964) provided data on trachyandesites (tristanites) from Tristan da Cunha, but further accounts of tristanites and benmoreites from other areas remain minimal. Accordingly, it has seemed desirable to examine in more detail the mineralogy of some rocks lying in or near the Daly gap. The trachyandesite described here is of particular interest, as it is one of the very few intermediate alkaline rocks known from volcanic islands along the East Pacific Rise and is also sufficiently well crystallized to permit satisfactory microprobe analyses of most groundmass minerals as well as of phenocrysts. The rock has been briefly described elsewhere (Bryan, 1967, p. 1468); its chemical analysis is given in Table 8.

The bulk chemical composition of this rock resembles more nearly some of the rocks described as mugearite by Muir and Tilley (1961), being distinctly lower in SiO_2 and total alkalies than the type examples of benmoreite and tristanite described by Tilley and Muir (1964). It most closely resembles the mugearite from the Hawi volcanic series, Hawaii, with which it is compared in Table 8. The greatest differences in the norm are due to the different ratio of ferric to ferrous iron, the much higher ferrous iron in the Hawaiian rock being largely responsible for the normative olivine and nepheline. The Clarion trachyandesite also appears to lie well outside the limits of hawaiite as defined by Macdonald (1960); in particular it is distinctly lower in dark minerals, the normative color index being 19.2, compared to 38.3 for the average hawaiite cited by Macdonald. The ratio of Na_2O to K_2O is also well outside the limit of 2:1 set by Macdonald.

TABLE 8. Chemical Analysis and CIPW Norm of Trachyandesite CL-16, Clarion Island, Mexico, and a Mugearite from Hawaii

	1	2		1	2
SiO_2	53.17	51.84	Q	4.56	...
TiO_2	2.40	2.18	Or	18.35	11.95
Al_2O_3	17.70	18.11	Ab	38.77	39.43
Fe_2O_3	6.26	2.41	Ne	...	5.81
FeO	3.54	7.27	An	16.21	16.54
MnO	0.14	0.24	Di	...	7.74
MgO	2.07	3.25	Hy	5.20	...
CaO	4.20	5.93	Ol	...	9.08
Na_2O	4.56	5.95	Mt	4.87	3.48
K_2O	3.09	2.04	Il	4.56	4.26
P_2O_5	0.73	0.55	Ap	1.68	1.34
H_2O^+	1.47	0.28	C	0.92	...
H_2O^-	0.24	0.09	Hm	2.88	...
CO_2	0.00	...	Rest	1.71	0.37
Totals	99.58	100.14	Totals	99.52	100.00

1. Trachyandesite, Clarion Island, Mexico. H. B. Wiik, analyst (Bryan, 1967, p. 1468).
2. Mugearite, Hawi volcanic series, Hawaii. J. H. Scoon, analyst (Muir and Tilley, 1961, p. 192).

Microprobe analyses of the principal minerals of the trachyandesite are set out in Table 9. The plagioclase phenocrysts range in size from 1 to 2 mm in length and are subhedral and often marginally corroded, with an outer zone clouded with opaque oxides, largely magnetite. On many phenocrysts, including the one analyzed, the outer zone of alkali feldspar is separated from the core by a narrow zone of more calcic plagioclase, ranging up to An_{55-60}, as indicated by the relative intensity of the $CaK\alpha$ peak. Groundmass plagioclase laths may be as calcic as An_{60}; they are marginally zoned to calcic anorthoclase and are surrounded by blocky unzoned crystals of alkali feldspar. Comparison of $K\alpha$ intensities for Na, K, and Ca with those of the alkali feldspar rims on plagioclase shows that these crystals are also calcic anorthoclase.

The olivine, a small microphenocryst, was selected for analysis both because it is free from impurities and because it appears typical in composition among the grains tested with the probe beam. Only a few of the grains show the elongation noted by Muir and Tilley (1961, p.

TABLE 9. Microprobe Analyses of Minerals from Trachyandesite CL-16, Clarion Island, Mexico

	1		2		3		4			5	
SiO_2	59.3		34.8		0.02		49.6			49.7	
Al_2O_3	24.5		...		...		3.69			3.89	
TiO_2	...		...		50.7		1.38			1.73	
Fe_2O_3	0.26		...		6.36		...			...	
FeO	...		35.7		37.7		10.1			12.0	
MnO	0.00		0.97		0.80		0.33			0.28	
MgO	0.02		28.4		3.99		14.5			16.6	
CaO	7.05		0.25		0.01		19.6			8.95	
Na_2O	6.99		...		...		0.51			4.04	
K_2O	0.90		...		...		0.00			1.21	
Totals	99.0		100.1		99.6		99.7			98.4	
O	32.000		4.000		6.000		6.000		O	23.000	
Si	10.722		0.975		0.001		1.864	2.000	Si	7.230	
Al	5.214		...		...		0.136		Al	0.668	8.000
Al	...	15.972	...		...		0.027		Ti	0.102	
Ti	...		...		1.881	4.001	0.039		Ti	0.088	
Fe	0.036		0.835		1.790		0.318		Mg	3.593	5.000
Mn	...		0.023	2.050	0.034		0.010	2.034	Fe	1.319	
Mg	0.004		1.184		0.294		0.814		Fe	0.137	
Ca	1.366	4.030	0.008		0.001		0.789		Mn	0.035	2.000
Na	2.452		...		...		0.037		Ca	1.395	
K	0.208		...		...		0.000		Na	0.433	
									Na	0.705	0.930
									K	0.225	

Atomic Ratios

Ca	33.9	Ca	0.4	Ilm	94.0	Ca	40.9	Ca + Alk	35.2
Na	60.9	Mg	57.8	R_2O_3	6.0	Mg	42.2	Fe + Mn	19.0
K	5.2	Mn + Fe	41.9			Mn + Fe	17.0	Mg	45.8

1. Plagioclase phenocryst, all Fe as Fe_2O_3.
2. Olivine microphenocryst, all Fe as FeO.
3. Ilmenite phenocryst, FeO and Fe_2O_3 computed on assumption of ideal ilmenite-hematite mixture.
4. Augite microphenocryst, all Fe as FeO.
5. Groundmass amphibole, all Fe as FeO.

194), but the composition lies within the range of average values they obtained from X-ray data.

Iddingsite forms pseudomorphs of much of the phenocryst olivine; qualitative examination with the probe beam shows that it also has an Fe/Mg ratio similar to the olivine, and the amounts of other elements, except Si, are negligible.

Pyroxene is present as stubby prismatic microphenocrysts up to 0.5 mm in diameter and as interstitial groundmass granules. The larger crystals, like the one analyzed, have optic angles of 35°–45°, but in some groundmass grains the angle approaches 10°–15°; nevertheless, all grains tested with the probe beam contained appreciable calcium. Possibly the low $2V$ is due to entry of Ti and Al into the structure, but this question has not been satisfactorily resolved. Although the rock is not sufficiently well crystallized for an accurate point count, olivine seems more abundant than pyroxene and certainly is if iddingsite is included with the olivine. This observation again is in agreement with the observations of Muir and Tilley (1961, p. 194).

Ilmenite apparently was not common in mugearites examined by Muir and Tilley, who stated (1961, p. 197) that "no ilmenite has crystallized directly as a separate phase." In the Clarion rock, ilmenite appears as a conspicuous phenocryst over 2 mm in length and is also abundant in the groundmass, where it is joined by magnetite. The latter mineral

is usually partly oxidized to maghemite, which appears both as veins and as more indistinct patches. Ilmenite is rarely present as exsolved blebs or lamellae in magnetite but is mostly present as distinct crystals. These ilmenites may be xenocrysts derived from basic inclusions described below. Pyrite appears in traces, associated with magnetite.

An alkaline amphibole is closely associated with iddingsite and magnetite in the groundmass, where it usually forms irregular patches less than 0.1 mm in diameter, interstitial to feldspar. The analysis in Table 9 is an average of two such grains. The amphibole is weakly pleochroic with α, very pale yellow; β, pink; and γ, pale greenish yellow. The grains analyzed show normal extinction and are almost identical in composition. Other grains, however, which show more intense pink absorption for β and patchy, anomalous extinction colors, may not be of the same composition. The optic angle is also variable, being always negative but ranging in size from about 10° up to more than 40°. The optical properties and composition indicate that the mineral is intermediate in composition between arfvedsonite and richterite. Apatite is a conspicuous accessory mineral, forming stout rounded prisms up to 0.3 mm long, pale pink in color, with abundant acicular inclusions parallel to the *c* axis.

An inclusion, 1.5 cm in diameter, consists of optically continuous, dark brown kaersutite, which ophitically encloses rectangular crystals of plagioclase and rounded crystals of ilmenite and titaniferous magnetite. The plagioclase yields CaKα intensities identical with those given by the cores of groundmass plagioclase laths. The contact between kaersutite and enclosed plagioclase is sharp and without evidence of reaction, but where it is in contact with the groundmass of the rock or with enclosed iron-titanium oxides the kaersutite is bordered by a reaction rim, 5–20 mm thick, which consists of a very fine-grained mixture of magnetite, plagioclose, hematite, and reddish-brown granules, resembling iddingsite. The groundmass of the rock immediately adjacent to these rims also is enriched in finely divided magnetite, hematite, and iddingsite. It is possible that the bulk composition of this rock was derived by reaction of trachytic liquid with a more mafic rock, the latter now represented by the kaersutite-bearing inclusion. The kaersutite may have formed by reaction of olivine or augite with hydrous alkaline magma, as described by Aoki (1959, p. 304). Gabbroic nodules have been observed in older basalt flows on Clarion (Bryan, 1967, p. 1465). Reaction with a relatively calcic contaminant is also suggested by the reverse zoning in the phenocrysts of sodic plagioclase and by the mixture of anorthoclase and labradorite appearing in the groundmass. In view of the possibility of contamination or hybridization, the composition of this rock should not be accepted as that of a liquid on a genetic "line of descent" from basalt to trachyte.

If Chayes's (1963*b*) specifications for the "Daly gap" are taken literally, the Clarion rock qualifies on two criteria and fails on two others. The weight percentage of SiO_2 falls just above the lower limit of the specified interval; the weight percentage of CaO is well within it; the Thornton-Tuttle index is about 2 points below, and the total iron is more than 1.0% above the specified intervals. There is of course no reason to suppose that a perfect correlation exists between these four criteria, such that they will all be simultaneously satisfied by any given rock, and this will be especially true of marginal cases. A purely numerical and chemical definition will probably prove to be as unsatisfactory for intermediate alkaline rocks as it has proved to be for other aspects of rock classification; a number of the rocks listed by Tilley and Muir (1964) as typical intermediate rocks also fall slightly outside one or more of the defined chemical and norma-

tive limits. As more mineralogical data become available it may be increasingly possible to set modal qualifications for membership in the clan of intermediacy, but criteria for entry must be based on far more information than is now available.

Alkaline and Peralkaline Rocks of Socorro Island, Mexico

W. B. Bryan

A peralkaline rock as formally defined by Shand (1943, p. 190) contains a molecular proportion of alumina which is less than that of soda and potash combined. Perhaps the best known occurrence of such rocks is on the island of Pantelleria in the Mediterranean, the type area for the oversaturated peralkaline rock pantellerite. Pantellerites from the type area and from many other localities around the world have been the subject of numerous papers in recent years. Descriptions of the natural rock occurrences have stimulated experimental studies (Carmichael and MacKenzie, 1963; Bailey and Schairer, 1966; Thompson and MacKenzie, 1967) and have prompted discussions of alternative and presumably more informative methods of graphical representation of the rock data (Bailey and Schairer, 1964; Bailey and MacDonald, 1969). Most of the discussion has centered on rocks and synthetic mixtures lying in or close to the oversaturated "Residua System" $NaAlSi_3O_8$-$KAlSi_3O_8$-SiO_2. Although basalt has been recognized on Pantelleria at least since the work of Foerstner (1883) and has been reanalyzed by Washington (1913), Zies (1962), and Romano (1968), the possibility of deriving pantellerite from this basalt has not been seriously considered. Genesis of pantellerite from associated alumina-saturated trachyte poses problems for which no entirely satisfactory solution has been offered. The development of alumina deficiency is generally attributed to the "plagioclase effect" (see, for example, discussions by Yoder and Tilley, 1962, p. 416; Carmichael and MacKenzie, 1963, pp. 394–395; Bailey and Schairer, 1964, p. 1205; Thompson and MacKenzie, 1967, pp. 730–731), but demonstrations of this mechanism in natural rocks are extremely rare. The best example (Carmichael, 1964) has been observed in phonolite rather than in pantellerite or in trachyte associated with pantellerite. Bailey and Schairer (1966, pp. 147–148) considered briefly the possibility that peralkaline rocks may be derived from basalt and suggested that aluminous minerals other than feldspar may be effective in producing the alumina deficiency that is the critical characteristic of peralkaline rocks. However, such effects have not been demonstrated within suites of natural rocks.

The volcanic rocks of Socorro Island provide an excellent opportunity to examine some of the genetic problems noted above. The island is located on the East Pacific Rise, an area of thin crust and high heat flow, a setting that seems to preclude the role of granitic or other typical continental crustal rocks in the genesis of the lavas. The general geology and eruptive history have been discussed elsewhere (Bryan, 1966), and it has been shown that an earlier period of extrusive activity was terminated with formation of a caldera. Renewed activity, predominantly explosive, accompanied faulting along a north-south rift and nearly filled the caldera, building a central volcanic peak composed of numerous overlapping pyroclastic cones. Each of the explosive central eruptions typically ended with quiet extrusion of trachyte or pantellerite domes into the crater of the pyroclastic cone. The most recent eruptions are confined to low-level flank extrusions along well-defined rifts, with little or no preliminary explosive activity, and basalt appears only as flows of relatively small volume erupted from low-level flank vents. It was suggested that these relationships could be explained by a stratified magma column

beneath the caldera, in which basalt is overlain by an accumulation of volatile-poor trachytic or pantelleritic liquid, topped by a highly vesicular, vapor-rich salic liquid (Bryan, 1966, pp. 474–480). In many respects the topography and geologic history of Socorro Island appear very similar to those outlined for Pantelleria by Washington (1913, pp. 665–670).

Petrography. The basalts of Socorro Island contain modal and normative olivine and small to large amounts of normative hypersthene, the latter mainly reflecting different degrees of oxidation. Total alkali ranges from slightly over 4.00% to over 5.00% in the analyzed rocks, the latter being similar to the typical hawaiite as defined by Macdonald (1960). The least siliceous and least alkalic basalt, S141, is also probably the youngest. As this basalt is well crystallized and is closely associated with recent domes of pantellerite obsidian on the north rift zone of Socorro, its mineralogy has been studied in the greatest detail.

The chemical analysis and norm of basalt S141 are given in Table 10, where it is compared with the basalt PRC 2006 from Pantelleria, analyzed by Zies (1962). The two rocks differ most notably in the ratio of ferric to ferrous iron. As the basalt PRC 2006 was collected from a small intrusive dike, it probably more nearly reflects the true oxidation state of the magma. The ferric-ferrous ratio of S141, collected near the surface of a lava flow, is similar to those given by Romano (1968, p. 777) for new analyses of basalt lavas and scoria from Pantelleria.

TABLE 10. Chemical Analyses and Norms of Olivine Basalts from Pantelleria and Socorro Island

Chemical Analyses			CIPW Norms		
	1	2		1	2
SiO_2	46.31	46.96	Or	6.40	6.97
TiO_2	3.94	3.07	Ab	27.17	26.15
Al_2O_3	14.18	13.53	An	21.09	19.56
Fe_2O_3	1.91	6.44	Di	16.85	15.72
FeO	11.76	7.28	Hy	2.17	12.21
MnO	0.23	0.18	Ol	12.48	1.03
MgO	5.43	7.14	Mt	2.78	9.34
CaO	10.07	9.06	Il	7.48	5.83
Na_2O	3.21	3.09	Ap	3.16	1.97
K_2O	1.08	1.18	Rest	0.63	0.54
P_2O_5	1.33	0.85			
H_2O^+	0.36	0.43			
H_2O^-	...	0.11			
Totals	100.14	99.32			

1. PRC 2006, Pantelleria; E. G. Zies, analyst (Zies, 1962). Includes Cr_2O_3 0.01, V_2O_5 0.11, BaO + SrO 0.04, S 0.06, Cl 0.06, F 0.09.

2. S141, Socorro Island; H. B. Wiik, analyst.

The basalt PRC 2006 has been described elsewhere (Zies, 1962, p. 177) and little need be added here, except with regard to the "brown and black globulites," which have been examined in more detail in reflected light. They consist of two generations of titaniferous magnetite and a skeletal groundmass ilmenite. The first magnetite forms subhedral crystals 10–50 μm in diameter, often with a sutured or dendritic outer boundary zone, intergrown with groundmass silicate crystallites. The core is slightly anisotropic, and a traverse of several grains with the microprobe shows that it is unusually rich in magnesium. The outer rim, extending into the dendritic overgrowths, is distinctly less magnesian and relatively enriched in titanium, chromium, and aluminum. Some grains show small exsolved lenses of spinel, probably hercynite. The second generation of magnetite consists of barblike skeletal groundmass crystallites, which may be partly replaced by blebs of maghemite. These crystallites are too tiny for satisfactory probe analysis but appear to be similar in composition to the outer zones of the first-generation magnetite. The skeletal ilmenite can be distinguished from the skeletal magnetite both by its stronger anisotropism and by its blocky habit, each plate being made up in detail of tiny interlocking rectangular segments.

The Socorro Island basalt S141 is much better crystallized than PRC 2006, the texture being virtually that of a microgabbro or diabase. The average grain size is about 0.5 mm, and olivine

forms conspicuous phenocrysts up to 1.5 mm in diameter. A point count indicated about 12.5 volume % olivine, considerably in excess of the normative amount. This is almost certainly due to surface oxidation of the flow, resulting in too high a value for Fe_2O_3 with consequent reduction in the amount of iron expressed as silicate in the norm. Pale pink augite is in subophitic intergrowth with plagioclase and opaque oxides. The latter share many of the features of the titanomagnetite and ilmenite in PRC 2006, although slower cooling and complete crystallization have precluded the formation of second generation "quench" magnetite. For the same reason, the paragenesis is not as evident, but the texture and zoning in the titanomagnetite again suggest that ilmenite is the later of the two minerals. The magnetite forms relatively stout subhedral crystals, zoned similarly to those in PRC 2006, although the effect is much less extreme. Chromium is higher and magnesium is lower, and again chromium, aluminum, and titanium are concentrated toward the edge of the crystals. Irregular veins of hematite traverse some grains. The ilmenite has the typical platy habit, appears much more uniform in composition than the magnetite, and shows no unusual compositional features. Plagioclase consists of randomly oriented laths in which the cores are almost homogeneous labradorite, An_{60}. Many grade marginally through a narrow transition zone to rims of alkali feldspar. Most of the latter mineral, however, tends to be concentrated in the interstitial triangular areas between plagioclase laths.

Microprobe analyses of magnetite and augite of PRC 2006, and of all the minerals of S141 except the interstitial alkali feldspar, are given in Table 11. Among the more interesting features are the relatively high iron in the plagioclase, which appears essential to fill out the tetrahedral site, and the very aluminous titanaugite in both rocks.

Trachybasalt appears on the south flank of Socorro Island as flows of very restricted extent. Microphenocrysts of augite are sparingly distributed in a very fine-grained groundmass in which plagioclase laths up to 0.1 mm in length are arranged in subparallel clusters, giving a distinct platy structure and flow-banded texture to the rock. There are rare rounded phenocrysts of plagioclase with distinct albite twinning. Olivine appears in the groundmass, where it may

TABLE 11. Microprobe Analyses of Minerals in Olivine Basalts S141, Socorro Island, and PRC 2006, Pantelleria

	Basalt S141										Basalt PRC 2006			
	Plagioclase		Olivine		Ilmenite		Magnetite		Augite		Augite		Magnetite	
SiO_2	52.9	*1*	38.3	*1*	0.21		0.21		46.4	*2*	46.0		0.10	
TiO_2	...		...		50.3	*3*	24.8	*5*	4.18	*6*	3.27	*27*	18.3	*2*
Al_2O_3	28.9	*2*	...		0.08		1.26	*4*	5.86	*7*	5.95	*9*	2.71	*4*
Fe_2O_3	0.57	*2*	...		4.90		34.2		...		...		33.0	
FeO	...		21.6	*12*	40.9	*1*	35.6	*2*	9.13	*2*	10.1	*3*	40.4	*1*
MnO	...		0.29		0.73		0.58		0.18		0.20		0.41	
MgO	0.11		39.7	*7*	2.14	*2*	1.89	*1*	12.3	*2*	12.6	*8*	5.17	*1*
CaO	12.6	*2*	0.31		0.05		0.05		21.3	*1*	21.1	*3*	...	
Na_2O	4.40	*2*	...		...		...		0.55		0.52		...	
K_2O	0.29		...		...		...		...		...		...	
Cr_2O_3	...		...		...		1.69	*20*	...		0.03		0.03	
Totals	99.8		100.2		99.3		100.3		99.9		99.8		100.2	
							Mole %							
	Ca 60.3		Ca 0.5		Ilm 95.1		Usp 70.2		Ca 46.8		Ca 45.4		Usp 49.7	
	Na 38.1		Mg 76.0		R_2O_3 4.9		Mgt 29.8		Mg 37.5		Mg 37.7		Mgt 50.3	
	K 1.6		Mn + Fe 23.5						Fe 15.6		Fe 16.9			

Note: Numbers in italics are $\sigma/\sqrt{N}$

be associated with aggregates of tiny magnetite grains. Microprobe analyses show the composition of the plagioclase phenocryst to be about An_{47}, whereas an analyzed groundmass microlite is about An_{42}. Analyzed groundmass olivine is about Fo_{40}. The presence of augite microphenocrysts suggests that augite is on the liquidus, in contrast to its invariable late crystallization in the basalts. Analyses of two augite microphenocrysts (Table 12) give some indication of the changes in augite composition as crystallization proceeds. One of the largest microphenocrysts is a normal augite; one of the smallest, virtually a groundmass augite, is distinctly enriched in titanium and aluminum. This enrichment is consistent with the experimental data and natural examples discussed by Yagi and Onuma (1969, p. 546).

A distinct compositional hiatus exists between the trachybasalt and trachyte on Socorro (Bryan, 1964). In mineralogy and composition the trachytes range through increasingly peralkaline types to pantellerite. Trachyte S84, the most calcic of the analyzed trachytes, is the only one that contains plagioclase. The latter is a potassic oligoclase that forms abundant phenocrysts marginally zoned to lime-poor alkali feldspar. The oligoclase is zoned outward to lime-poor alkali feldspar. Groundmass feldspar is extremely variable in composition, but the average composition is that of a sodic anorthoclase. There are a very few large, rounded phenocrysts of fayalitic olivine. Ferroaugite forms scattered small euhedral phenocrysts. An alkali amphibole pleochroic in pink and violet is abundant in the groundmass. Magnetite, apparently originally titaniferous, shows abundant exsolved ilmenite lamellae and blebs of hematite, apparently due to secondary oxidation. Microprobe analyses of all major minerals except the magnetite are given in Table 12.

Pantelleritic trachytes contain phenocrysts of lime-poor anorthoclase, close to Ab_{65} in composition. No appreciable zoning or exsolution has been detected in these feldspars. Olivine is common and is almost pure fayalite; ferrohedenbergite forms scattered phenocrysts and also appears in the groundmass with an alkaline amphibole. Quartz may appear as irregular watery patches in the groundmass but never appears as phenocrysts. The more peralkaline varieties may contain a few phenocrysts of aenigmatite, and in these rocks the ferrohedenbergite is relatively more sodic. Opaque oxides are not abundant. Ilmenite typically predominates over magnetite, the ferric iron apparently being taken up by amphibole and ferrohedenbergite.

Chemical analyses of three pantellerite obsidians, widely separated in the field, are nearly identical; one of these, S138, is given in Table 13. The pantellerites are found almost invariably as obsidian domes that may have been breached on one side to yield very rough, blocky flows. Where exposed by marine erosion, the interiors of the domes are badly altered to a gray, chalky rock completely unsuitable for mineralogical study. The obsidian contains phenocrysts of anorthoclase, sodic ferrohedenbergite, and aenigmatite, with traces of ilmenite. The glass contains abundant microlites of anorthoclase, aenigmatite, and ferrohedenbergite. Quartz does not appear among the modal minerals in any of these rocks. They most resemble the hyalopantellerites of Pantelleria, although the samples from Socorro contain a much higher proportion of microlites in the glass. Analyses of the phenocryst minerals of S138 are given in Table 12.

Petrogenesis. A complete account of the relations between the various lavas of Socorro Island is being prepared for publication, and only a brief summary will be given here. The possibility of deriving trachyte, pantellerite, and trachybasalt from appropriate parent magmas as deduced from field association has been tested with the least-squares approximation described by Bryan, Finger, and Chayes (1969). The

TABLE 12. Microprobe Analyses of Various Minerals from Trachybasalt S77, Trachyte S84, and Pantellerite S138

	S77 Augite				S84 Minerals										S138 Minerals					
	Phenocryst		Groundmass		Plagioclase		Anorthoclase *		Augite		Olivine		Amphibole		Anorthoclase		Augite		Aenigmatite	
SiO_2	51.3	*2*	48.4	*2*	64.7	*2*	66.3		50.7	*1*	31.0	*2*	49.5	*2*	65.7	*2*	48.2	*6*	40.3	*3*
TiO_2	1.02	*2*	2.13	*5*	...		...		0.48		...		2.79	*6*	...		0.44		9.61	*4*
Al_2O_3	1.98	*12*	4.04	*5*	20.8	*3*	19.6		0.79		...		0.60		19.1	*4*	0.24		0.45	
Fe_2O_3 †	...		...		0.20		...		...		...		...		1.00		...		...	
FeO †	12.3	*10*	12.9	*4*	...		...		17.2	*5*	56.6		32.3	*4*	...		30.6	*1*	41.3	*1*
MnO	0.55		0.43		...		...		0.89		2.85	*2*	0.96		...		1.16		1.03	
MgO	12.3	*5*	11.4	*3*	0.00		...		8.85	*3*	8.66	*2*	2.16	*5*	0.00		0.04		0.01	
CaO	20.6	*2*	19.5	*5*	2.60	*8*	0.68		20.0	*2*	0.43		3.68	*8*	0.01		18.3	*1*	0.93	*9*
Na_2O	0.39		0.40		8.39	*1*	7.67	*9*	0.47		...		4.99	*4*	7.73	*2*	1.95	*2*	6.69	*1*
K_2O	...		...		2.91	*6*	5.31	*9*	...		...		1.31	*2*	6.07	*4*	...		0.04	
Totals	100.4		99.2		99.6		99.6		99.4		99.5		98.3		99.6		100.9		100.4	
									Atomic %											
Ca	43.7	Ca	43.0	Ca	12.2	Ca	3.3	Ca	43.7	Ca	0.8		...	Ca	0.1	Ca	43.4		...	
Mg	36.0	Mg	34.8	Na	71.5	Na	66.4	Mg	26.9	Mg	21.2		...	Na	65.9	Mg	0.1		...	
Fe	20.3	Fe	22.2	K	16.3	K	30.3	Fe	29.4	Fe	78.0		...	K	34.0	Fe	56.5		...	

* Calculated from partial analysis for Na, K, and Ca; average of five groundmass grains.
† All Fe as Fe_2O_3 in feldspar and as FeO in all other minerals.

Note: Numbers in italics are $\sigma/\sqrt{N}$.

TABLE 13. Chemical Analyses and CIPW Norms of Pantellerite S138, Socorro Island, Mexico, and Pantellerite PRC 2007, Pantelleria

Chemical Analyses			CIPW Norms		
	1	2		1	2
SiO_2	68.91	69.56	Q	19.84	21.34
Al_2O_3	10.83	11.27	Z	...	0.11
Fe_2O_3	2.91	1.87	Or	26.36	27.17
FeO	4.56	4.18	Ab	30.88	32.57
MgO	0.22	0.23	Ac	8.42	5.41
CaO	0.24	0.44	Ns	4.30	2.70
Na_2O	6.96	6.28	Di	0.94	1.19
K_2O	4.46	4.60	Hy	8.23	7.41
MnO	0.25	0.28	Wo	...	...
TiO_2	0.40	0.47	Il	0.76	0.90
P_2O_5	0.02	0.10	Ap	0.05	0.24
H_2O^+	0.26	0.13	Hl	...	0.63
H_2O^-	0.10	0.02	Rest	0.36	0.21
Totals	100.12	99.90		100.14	998.8

1. Pantellerite S138, Socorro Island, Mexico; H. B. Wiik, analyst.
2. Pantellerite PRC 2007, Pantelleria; E. G. Zies, analyst (Zies, 1960). Includes ZrO_2 0.12, SO_3 0.06, Cl 0.38.

calculations show that it is quite feasible to derive the salic rocks from the basalts with which they are most closely associated. In spite of the apparent chemical gradation from trachyte to pantellerite, however, calculations do not support a parental relation of trachyte to pantellerite. As might have been anticipated from the relevant experimental work, it appears impossible to derive pantellerite from alumina-saturated trachyte by crystallizing any combination of the minerals appearing as phenocrysts in the trachyte. Calculations using peralkaline trachyte as parent yield lower sums of squares, but the discrepancies remain too large for the mechanism to appear very convincing.

A test of the possible genesis of pantellerite S138 from basalt S141, with which it is closely associated on the north rift zone of Socorro, is far more successful. Table 14 shows the results of a least-squares solution, using a linear combination of the pantellerite and minerals observed in the basalt (Table 11) to calculate an approximation to the basalt composition. The sum of squares is satisfactory, and the amount of pantellerite

TABLE 14. Least-Squares Estimate of the Composition of Basalt S141, Calculated as a Linear Combination of Pantellerite S138 and Minerals Observed in the Basalt

	1	2	3	4
SiO_2	47.84	47.85	Pantellerite S138	24.90
Al_2O_3	13.79	13.78	Plagioclase S141	33.66
FeO	13.21	13.32	Olivine S141	12.52
MgO	7.35	7.28	Augite S141	17.08
CaO	9.20	9.23	Magnetite S141	10.18
Na_2O	3.32	3.15	Apatite *	2.11
K_2O	1.21	1.20		
MnO	0.19	0.18		
TiO_2	3.41	3.13		
P_2O_5	0.91	0.87		

Sum of squares of residuals = 0.1286

1. Composition of basalt S141 estimated by least-squares approximation.
2. Observed composition of basalt S141.
3. Rock and mineral variables used in calculation (see Tables 11 and 13 for compositions).
4. Proportions of pantellerite and minerals in basalt S141, wt %.
* Not analyzed; ideal calcium phosphate formula assumed.

that could be extracted from the basalt is about twice that necessary to account for the total amount of salic eruptive rocks observed on the island (Bryan, 1966, p. 473). The crystallization of aluminous titanaugite and titaniferous magnetite in particular appears essential to derive the proportions of alumina and iron oxide characteristic of pantellerite. Basalts associated with pantellerite at Pantelleria and at Socorro are relatively rich in titanium, and perhaps this is the critical factor in the genesis of pantellerite. The conditions favoring crystallization of aluminous titanaugite have been discussed by Kushiro (1960), who suggested that relatively low silica content in the magma causes substitution of alumina for silica, with simultaneous substitution of titanium in the octahedral site to balance charges. Verhoogen (1962) suggested that the partial pressure of oxygen may be the controlling factor, a high p_{O_2} favoring precipitation of iron as an oxide, and titanium in the silicate phase. In this case, substitution of alumina for silica to balance charges

would be a consequence, rather than a cause, of the entry of titanium into the structure. It seems clear that low silica, a relatively high p_{O_2}, and a relatively high titanium/iron ratio in the magma will all favor the crystallization of aluminous titanaugite, and a delicate balance of all three factors may operate in natural magmas. Kushiro (1960, p. 553) cited several well-known intrusive complexes in which variation in titanium content of pyroxenes does not seem to correlate with variation in titanium in the bulk rock composition, but noted that as he has not considered the role of iron-titanium oxides, the influence of TiO_2 concentration on the composition of pyroxene cannot be ruled out.

Crystal fractionation of basalt leading to a peralkaline residual liquid would have to take place within the volcanic cone, and if the magma chamber model outlined by Bryan (1966, p. 473) is valid, this crystallization would have taken place at a depth of about 12 km below sea level, implying pressures of not more than 4 kb. It is evident that the appropriate distribution of elements can be achieved at low pressures, as the basaltic mineral assemblage used in the calculation crystallized in a surface flow. MacGregor (1969) has suggested that titanium-rich basalts may be expected to form by partial fusion at relatively high pressures and hence at relatively great depths in the mantle. On the crest of the East Pacific Rise, however, the thin crust and high heat flow (Menard, 1964, p. 129) would probably permit melting at relatively shallow depths, so that it is not essential to postulate a deep-mantle origin.

At present, then, the evidence is largely circumstantial. At Socorro, as at Pantelleria, association of pantellerite with titaniferous basalt suggests a parental role for the latter in the genesis of pantellerites. Calculations show that the observed mineral assemblage in the Socorro basalt, separated in appropriate proportions, could yield a residual liquid having the composition of pantellerite found in close association with that basalt. Separation of aluminous titanaugite and titaniferous magnetite seems essential to account for the observed balance of alumina, iron, and titanium between basalt and pantellerite, and these minerals are also found in the basalt at Pantelleria.

The Simplified or Idealized "Skaergaard" Model

F. Chayes

Whether performed graphically or numerically, derivation of the successive residual liquids of the Skaergaard (or other similar complex) presumes a very simple but restrictive descriptive hypothesis, namely, that a single mass of magma of some known or assumed composition is partitioned into a number of zones or fractions, one of which is unexposed. Using compositions, relative ages, and relative magnitudes of the exposed zones estimated from field observation and chemical analyses of rock specimens, we wish also to estimate—perhaps, more properly, to calculate *ex hypothesis*—the compositions of the unexposed portion of the complex and of residual liquids at successive stages of solidification. The magnitude of the unexposed portion of the complex may be estimated either by extrapolating from data concerning the shape and dimensions of the intrusion or by materials-balance calculations based on the compositions of the assumed parent magma and the exposed portion of the complex. Obviously preferable in principle, the former procedure is nearly always impracticable. The materials-balance solution is outlined here.

Notation. $\mathbf{X}_j$ is a vector whose ith element, X_{ij}, is the estimated percentage of constituent i in

(a) the unexposed portion of the complex if $j=1$

(b) the $(j-1)$th exposed zone or facies if $j>1$.

M is a vector whose jth element, $j>1$, is the value, for the $(j-1)$th exposed zone, of the sample statistic used as an estimator of the magnitudes of the exposed zones.

P is a vector whose jth element, $j \geq 1$, is the proportion of the whole complex formed by the jth zone, hidden or exposed.

$\mathbf{L}_j$ is a vector whose ith element, L_{ij}, is the percentage of constituent i in the liquid existing just before the jth zone, $j \geq 1$, begins to solidify.

Compositions of the exposed and unexposed portions of the complex. If there are n zones and the first is unexposed, the estimated composition of the exposed portion of the complex is

$$\mathbf{E} = \mathbf{YM} \Big/ \sum_{j=2}^{n} (M_j), \qquad (1)$$

in which **Y** is the matrix formed of (column) vectors $\mathbf{X}_j$, $j=2$, n, in order.

Since by definition no element of $\mathbf{X}_1$, the composition vector of the unexposed portion of the complex, may be negative, it will be necessary to use a multiple, K, of parent magma equal to or greater than the largest ratio of analogous elements of **E** and $\mathbf{L}_1$, i.e., $K \geq (E_i/L_{i1})_{\max}$. Specifically, if the maximum ratio of E_i to L_{i1} occurs for, say, $i=b$, and $X_{b1}=B$, then

$$K = (E_b - B)/(L_{b1} - B). \qquad (2)$$

For $B=0$, the supply of magma is just sufficient if *all* of the critical constituent reports in the visible facies.

The total supply of magma is proportional to K, the amount contained in the unexposed portion of the complex is proportional to $(K-1)$, and the composition vector of the unexposed portion is

$$\mathbf{X}_1 = (K\,\mathbf{L}_1 - \mathbf{E})/(K-1). \qquad (3)$$

Relative magnitudes of the zones. The unexposed portion of the complex is $(K-1)/K$ of the whole, the ratio of the exposed portion to the whole is $1/K$, and the vector **P** may be written

$$\mathbf{P} = \left[\left(\frac{K-1}{K}\right), \left(\frac{M_2}{K\Sigma(M)}\right), \left(\frac{M_3}{K\Sigma(M)}\right), \ldots, \left(\frac{M_n}{K\Sigma(M)}\right)\right], \qquad (4)$$

in which the summation of M is over the range 2, n, and the jth element of **P** is, as previously specified, the proportion of the entire complex formed by zone j. $P_1 = (K-1)/K$ is the proportion of unexposed material compatible with the assumptions that (a) the exposed zones of the complex are partition products drawn from the proposed parent magma and (b) the unexposed portion of the complex contains $B\%$ the constituent undergoing maximum enrichment during the partition process.

The amounts and compositions of residual liquids. The proportion of the initial magma solidified after the consolidation of, say, zone k is evidently $\sum_1^k P_j$. The proportion of the original liquid surviving at this time is $\left(1 - \sum_1^k P_j\right)$, and its composition vector is

$$\mathbf{L}_{k+1} = \left(\mathbf{L}_1 - \sum_1^k (P_j \mathbf{X}_j)\right) \Big/ \left(1 - \sum_1^k P_j\right) \qquad (5)$$

for k in the range $0 \leq k < n$.

It is to be noted that the calculated composition of liquid 2, the magma remaining after separation of the hidden zone, is in fact the estimated composition of the exposed portion of the complex. A direct consequence of the definitions involved, this identity is perhaps not immediately obvious; symbolically, solving (3) for **E** and (5) at $k=1$, we have at once that $\mathbf{L}_2 = \mathbf{E} = K\mathbf{L}_1 - (K-1)\mathbf{X}_1$. From this point onward, accordingly, the assumed initial liquid, *whatever its composition,* exerts no influence on the further development of the magma.

PHASE-EQUILIBRIUM STUDIES, CHIEFLY OF SILICATES AND OXIDES

PYROXENES AND RELATED SYSTEMS

Critical Planes and Flow Sheet for a Portion of the System CaO-MgO-Al_2O_3-SiO_2 Having Petrological Applications

J. F. Schairer and H. S. Yoder, Jr.

Important advances have been made during the past few years in our knowledge of the crystallization relations in basalts and related alkaline rocks. Schairer and Yoder (*Year Book 63,* pp. 65–74) showed the relations in the expanded basalt tetrahedron nepheline-forsterite-silica-larnite between quartz-normative (tholeiitic) and nepheline-normative (alkaline) rocks where the feldspar is nearly pure albite, i.e., a highly sodic plagioclase with only a small anorthite content. Since most basaltic rocks carry a feldspar with a moderate to large anorthite content, it was clearly necessary to ascertain phase-equilibrium relations on synthetic analogues in which anorthite plays the dominant role. Schairer, Tilley, and Brown (*Year Book 66,* pp. 467–471) studied the join nepheline-diopside-anorthite and showed the complex relationships between the solid phases nepheline, spinel, anorthite, olivine, and diopsidic pyroxenes at liquidus temperatures and with melilites below liquidus temperatures. Schairer and Yoder (*Year Book 65,* p. 206, Fig. 2; *Year Book 67,* pp. 104–105, respectively) studied the joins albite-anorthite-forsterite and albite-anorthite-akermanite where the whole range of plagioclases are present with olivines or with melilites, diopsidic pyroxenes, and wollastonite solid solutions. Kushiro and Schairer have just studied (this report) a line between diopside and the feldspar albite$_{50}$ anorthite$_{50}$ in the system albite-anorthite-diopside. Schairer and Yoder in their study of albite-anorthite-akermanite clearly indicated that this join is a triangular section through a system that is not quaternary but quinary. It became obvious that before attempting to interpret detailed relations in the quinary system Na_2O-CaO-MgO-Al_2O_3-SiO_2 it was necessary to ascertain the precise relations between forsterite, diopside solid solutions, the melilites gehlenite and akermanite, anorthite, and spinel in the system CaO-MgO-Al_2O_3-SiO_2 without the complication of Na_2O.

Considerable previous data on the petrologically important portion of CaO-MgO-Al_2O_3-SiO_2 were available. The system diopside-anorthite-akermanite was studied by deWys and Foster (1958). Segnit (1956) reported on the section $CaSiO_3$-$MgSiO_3$-Al_2O_3. Hytönen and Schairer (*Year Book 60,* p. 135, Fig. 28) also provided information on the join $MgSiO_3$-$CaSiO_3$-Al_2O_3 and at the same time (pp. 125–139) presented some data on the join CaTs (Ca-Tschermak's molecule, $CaO \cdot Al_2O_3 \cdot SiO_2$)-diopside. O'Hara and Schairer (*Year Book 62,* p. 108, Fig. 32) provided additional data on $MgSiO_3$-$CaSiO_3$-Al_2O_3. Chinner and Schairer (1962, p. 619, Fig. 4), on the basis of previous studies and with additional data on the single join grossularite-pyrope at 1 atm, drew a flow sheet for the silica-rich portion of CaO-MgO-Al_2O_3-SiO_2. Subsequently O'Hara and Schairer (*Year Book 62,* p. 114, Fig. 37) suggested that three different quaternary invariant points may replace the points C and D of the Chinner and Schairer flow sheet. Recently O'Hara and Biggar (1969) and Biggar and O'Hara (1969) presented additional data to confirm this contention. Clark, Schairer, and de Neufville (*Year Book 61,* pp. 59–68) presented additional data on the join CaTs-diopside. Kushiro and Schairer (*Year Book 64,* p. 101, Fig. 21) gave some information on the join diopside-spinel. W. R. Foster (personal communication) and his students are now studying the join akermanite-anorthite-forsterite and have located the

field of diopside solid solutions as predicted by Chinner and Schairer (1962, p. 624, Fig. 6). Some years ago DeVries and Osborn (1957, especially Fig. 9) studied the Al_2O_3-rich portion of CaO-MgO-Al_2O_3-SiO_2 and obtained data on four quaternary invariant points which we have integrated with the data in our new flow sheet, shown below as Fig. 11. We now present the data on CaO-MgO-Al_2O_3-SiO_2 that we have obtained during the past year.

The Join Akermanite-Spinel-Anorthite and the Akermanite-Spinel Portion of the Coplanar Join Akermanite-Spinel-Gehlenite-Forsterite

As shown in Fig. 2, there are three piercing points of univariant lines: K, mel+mont$_{ss}$+sp+liquid at 1368° ±3°C; *L*, mel+an+sp+liquid at 1248° ±2°C; and *F*, corundum+an+sp+liquid at 1485° ±5°C. All points in the side akermanite-spinel, except $Ak_{96}Sp_4$ (which consists of a melilite and a forsterite solid solution when completely crystalline), pass during crystallization through the quaternary invariant point mel+mont$_{ss}$+fo$_{ss}$+sp+liquid at 1348° ±2°C. The three compositions $Ak_{80}Sp_{17}An_3$, $Ak_{82}Sp_{14}An_4$, $Ak_{77}Sp_{15}An_8$ also pass through this same quaternary invariant point (labeled *S* in Fig. 11) during crystallization.

Four compositions in the join akermanite-spinel-anorthite ($Ak_{80}Sp_{17}An_3$, $Ak_{82}Sp_{14}An_4$, $Ak_{77}Sp_{15}An_8$, and $Ak_{76}Sp_{13}An_{11}$) produce liquids during crystallization that go down the univariant line mel+fo$_{ss}$+sp+liquid to the quaternary

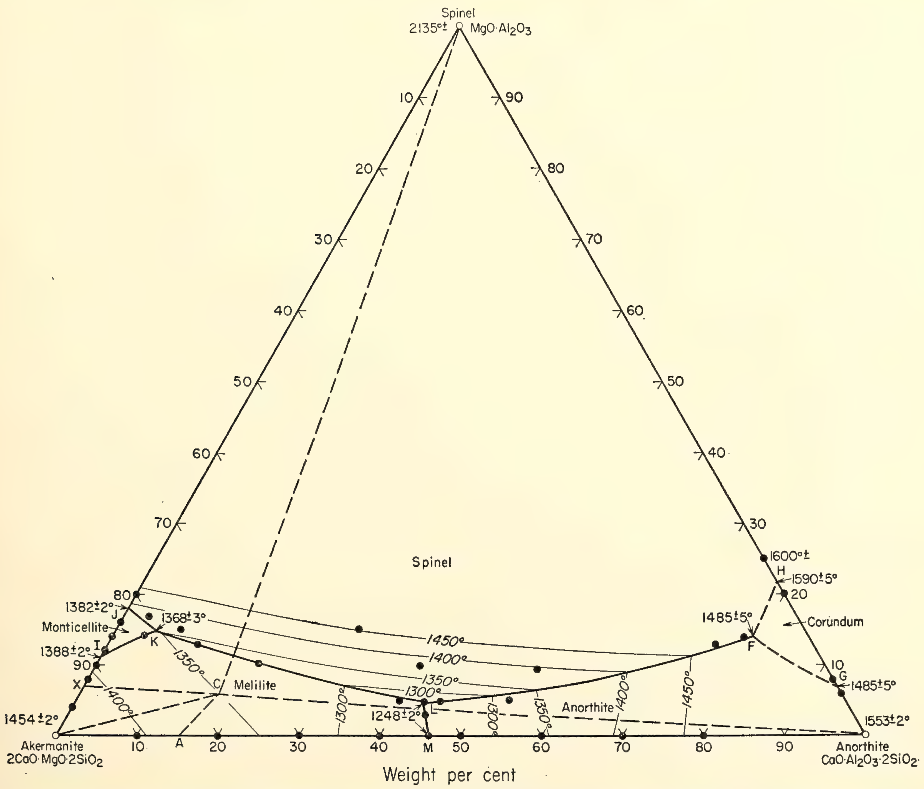

Fig. 2. Phase-equilibrium diagram for the join akermanite-spinel-anorthite. Black dots indicate compositions studied by the method of quenching. *C* is the piercing point of the tie line between melilite and diopside solid solutions. Dashed lines outline assemblages at the solidus described in the text.

invariant point $di_{ss}+fo_{ss}+sp+mel+liq$-uid at 1238° ± 2°C (labeled Q in Fig. 11).

Seven compositions in the join akermanite-spinel-anorthite yield liquids during crystallization that go down the univariant line mel+an+sp+liquid to the quaternary invariant point mel+an+sp+di_{ss}+liquid at 1238° ± 2°C (labeled R in Fig. 11). The seven compositions are $Ak_{55}Sp_5An_{40}$, $Ak_{50}Sp_{10}An_{40}$, $Ak_{52}Sp_5An_{43}$, $Ak_{50}Sp_5An_{45}$, $Ak_{41.57}Sp_{5.42}An_{53.01}$, $Ak_{35.82}Sp_{9.35}An_{54.83}$, $Ak_{12}Sp_{13}An_{75}$. There are two compositions in the join akermanite-spinel-anorthite ($Ak_{55}Sp_{15}An_{30}$ and $Ak_{70}Sp_{10}An_{20}$) where sp+mel+liquid are joined by both an and di_{ss} at the quaternary invariant point mel+an+sp+di_{ss}+liquid at 1238° ± 2°C (R of Fig. 11).

The join CaTs-diopside pierces the join akermanite-spinel-anorthite at $Ak_{35.82}Sp_{9.35}An_{54.83}$ at $CaTs_{57.32}Di_{42.68}$, and the join grossularite-pyrope * pierces it at $Ak_{41.57}Sp_{5.42}An_{53.01}$ at grossular-ite$_{74.39}$pyrope$_{25.61}$.

The dashed lines radiating from C divide the join akermanite-spinel-anorthite into several areas of complete crystallization. The point C is the piercing point of the tie line connecting the maximum solid solutions of melilite and diopside solid solution at the solidus and is only known approximately because of the complexities of the solid solutions.

1. Compositions that lie in C An Sp consist of mel+sp+an+$di_{ss(maximum)}$ at and below the temperature of R (Fig. 11) at 1238° ± 2°C.

2. Compositions that lie in C X Sp consist of mel+sp+fo_{ss}+$di_{ss(maximum)}$ at and below the temperature of Q (Fig. 11) at 1238° ± 2°C.

3. Compositions that lie in C A An consist of mel+$di_{ss(maximum)}$+an+wo at and below the temperature of B (Fig. 11), which is not known precisely.

4. Compositions that lie in C A Ak consist of mel+$di_{ss(maximum)}$+wo at and below some temperature between 1350°C and that of B (Fig. 11).

5. Compositions that lie in C X Ak consist of mel+$di_{ss(maximum)}$+fo_{ss} at and below some temperature between 1357°C and that of Q (Fig. 11) at 1238° ± 2°C.

The phase diagram for akermanite-spinel is shown here in Fig. 3. In the system akermanite-spinel the following reaction occurs: akermanite ($Ca_2MgSi_2O_7$) + spinel ($MgAl_2O_4$) → forsterite (Mg_2SiO_4) + gehlenite ($Ca_2Al_2SiO_7$). There is probably some monticellite in solid solution in the forsterite phase as well, and there may be more complex solid solutions in the akermanite to yield the melilite phase. Attention is called to the behavior of pure akermanite composition as described by Schairer, Yoder, and Tilley (*Year Book 65*, pp. 217–218). Only pure akermanite crystals are present between the congruent melting temperature 1454° ± 2°C and 1385°C. At this latter temperature crystals of pseudowollastonite appeared, and then at 1345° ± 10°C crystals of wollastonite solid solution also appeared. Both of them were present over a range of about 40°C, below which only twinned crystals of wollastonite solid solution were present with the melilite crystals. Finally, at 1240° ± 10°C diopside crystals appeared along with the wollastonite solid solution crystals, both of them well distributed in the melilite. The products of all the quenching experiments were examined for the presence of monticellite, but none was observed. In the join akermanite-spinel the composition $Ak_{96}Sp_4$ was the richest in akermanite studied. A melilite is present on the liquidus at 1428°C; $mont_{ss}$ appears as an additional solid phase at 1402°C; fo_{ss} appears at 1363°C;

* Chinner and Schairer (1962, p. 617, Fig. 2) show the complication "pyroxene + other phases." We have just shown that grossular-ite$_{74.39}$pyrope$_{25.61}$ cuts the join akermanite-spinel-anorthite. During crystallization, liquid produced in that composition goes down the univariant line mel + an + sp + liquid and is joined by di_{ss} at 1238° ± 2°C, the temperature of R in the flow sheet shown later in Fig. 11. There is never any fo_{ss} present in grossular-ite$_{74.39}$pyrope$_{25.61}$.

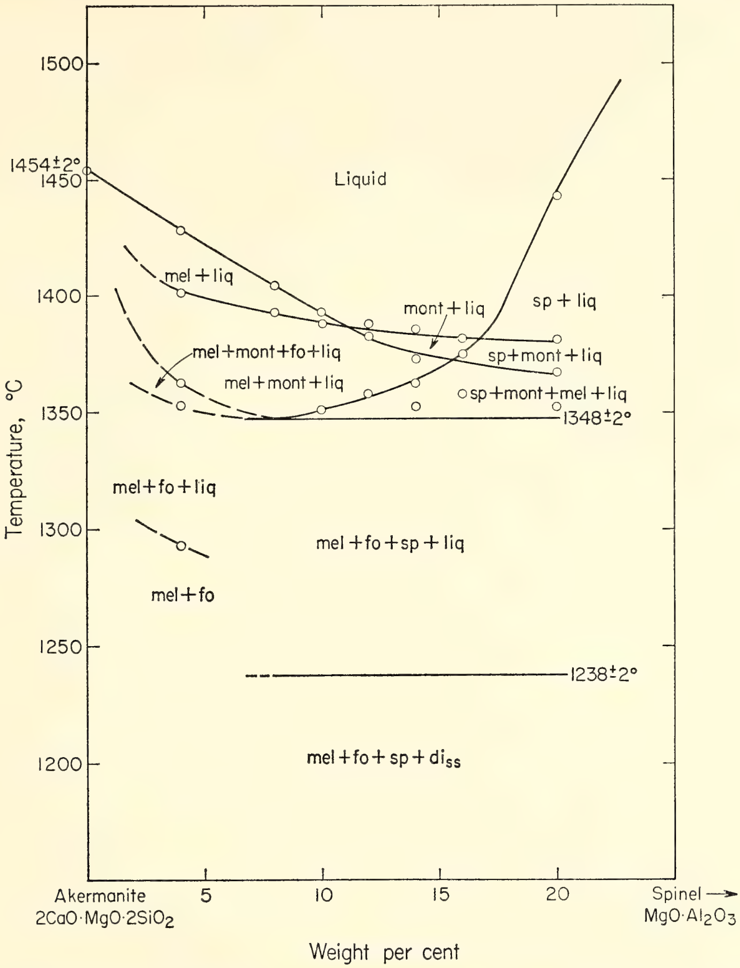

Fig. 3. Phase-equilibrium diagram for the join akermanite-spinel. This join is coplanar with akermanite-spinel-gehlenite-forsterite. Abbreviations: mel, melilite; fo, forsterite solid solutions with monticellite; mont, monticellite solid solutions; sp, spinel; di$_{ss}$, diopside solid solutions with CaTs and possibly $MgSiO_3$; liq, liquid.

mont$_{ss}$ disappears at 1353°C; there is mel + fo$_{ss}$ + liquid below this temperature to 1295° ± 5°C, where it becomes completely solid with the two phases mel + fo$_{ss}$. No crystals of pseudowollastonite, wollastonite solid solution, or di$_{ss}$ were observed in this composition at any temperature at or above the solidus.

In the join akermanite-spinel a horizontal line is drawn at 1348° ± 2°C. In all compositions studied between 8 and 20% spinel, mont$_{ss}$ is present at 1350°C but absent at 1345°C, and the horizontal line is drawn on the basis of the presence or absence of mont$_{ss}$. In the compositions $Ak_{80}Sp_{20}$, $Ak_{84}Sp_{16}$, and $Ak_{86}Sp_{14}$, fo$_{ss}$ appears at a temperature slightly above this horizontal line, represented by the three circles shown, presumably because our run times were too short for equilibrium. In $Ak_{88}Sp_{12}$, $Ak_{90}Sp_{10}$, and $Ak_{92}Sp_8$, fo$_{ss}$ appears as monticellite disappears at 1348°C. We have already shown that three compositions in the join aker-

manite-spinel-anorthite yield this same temperature of disappearance of $mont_{ss}$ at 1348°C. It is concluded that the change of solid solution in monticellite is apparently small. The results of Biggar and O'Hara (1969) suggest that considerable solid solution of forsterite in monticellite exists at this temperature.

The (211) spacings for the melilite present in runs at 1200°C in the join akermanite-spinel are plotted in Fig. 4. The spacing changes measurably from pure akermanite to about 7 wt % spinel and then approaches constant composition. In the absence of liquid, metastable solid solutions persist and equilibrium between the four solid phases does not obtain, thereby accounting for the variability of the spacings in the mel + fo_{ss} +

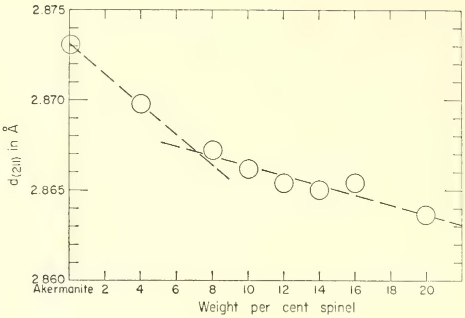

Fig. 4. (211) X-ray spacings for the melilites present in runs at 1200°C in the join akermanite-spinel.

sp + di_{ss} region. Because akermanite-spinel is coplanar with gehlenite-forsterite, the X-ray data suggest that the maximum solid solution of gehlenite in

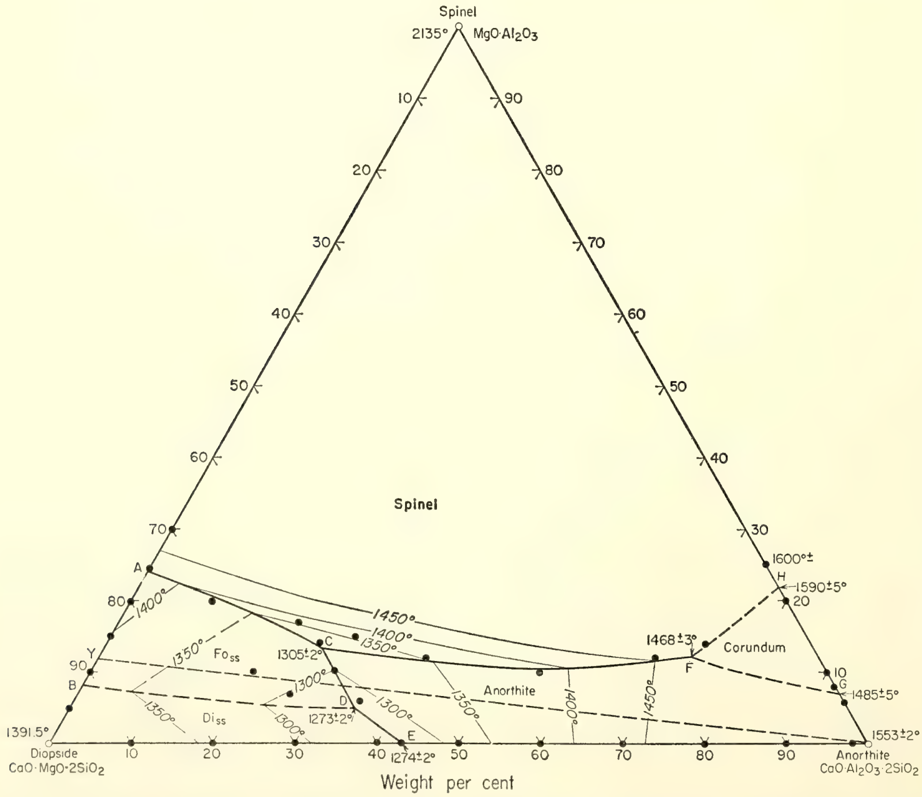

Fig. 5. Phase-equilibrium diagram for the join diopside-spinel-anorthite. Abbreviations: an, anorthite; others as in Fig. 3.

akermanite for the assemblage mel+ fo_{ss}+sp is about 16 wt %, assuming no other types of solid solution are present.

The Join Diopside-Spinel-Anorthite and Its Relations to Coplanar Di-Fo-CaTs-Sp

As shown in Fig. 5 there are three piercing points of univariant lines: *C*, fo_{ss}+an+sp+liquid at 1305°±2°C; *D*, fo_{ss}+di_{ss}+an+liquid at 1273°±2°C; and *F*, corundum+an+sp+liquid at 1468°±3°C. The behavior of points in the side line diopside-spinel will be discussed later. Four compositions—$Di_{70}Sp_{20}An_{10}$, $Di_{48}Sp_{12}An_{40}$, $Di_{35}Sp_{10}An_{55}$, and $Di_{20}Sp_{12}An_{68}$—yield liquids that during crystallization go down the univariant line fo_{ss}+an+sp+liquid to the quaternary invariant point an+di_{ss}+fo_{ss}+sp +liquid at 1238°±2°C (*P* in Fig. 11). Five other compositions—$Di_{70}Sp_{10}An_{20}$, $Di_{61}Sp_{17}An_{22}$, $Di_{60}Sp_{14}An_{26}$, $Di_{60}Sp_{10}An_{30}$, and $Di_{55}Sp_{15}An_{30}$—yield liquids that during crystallization go down the univariant line fo_{ss}+an+di_{ss}+liquid to the same quaternary univariant point, an+ di_{ss}+fo_{ss}+sp+liquid, at 1238°±2°C (*P* of Fig. 11).

In Fig. 5 the dashed line *Y* An divides the join into two portions. Those in the area *Y* Sp An when completely crystalline consist of an+fo_{ss}+sp+$di_{ss(maximum)}$ at 1238°±2°C, the temperature of point *P*, shown below in the flow sheet (Fig. 11). Those in the area *Y* Di An when completely crystalline consist only of the three solid phases an+fo_{ss}+di_{ss} because Di-Fo-CaTs-Sp are coplanar. However, if the di_{ss} involves enstatite as well as CaTs there may be two small triangular areas near the diopside corner of the join with the three solid phases wo_{ss}+di_{ss}+mel and fo_{ss}+di_{ss}+mel, as well as the narrow fields of an+di_{ss}+ mel and sp+di_{ss}+mel. None of the necessary data were collected to test this possibility.

The Join Akermanite-Spinel-Diopside and Its Relations to Coplanar Fo-Geh-Ak-Sp

Only three compositions were prepared in the join akermanite-spinel-diopside, and the data on these points indicate the relations as shown in the diagram for this join given here as Fig. 6. There are three piercing points of univariant lines: *K*, mel+$mont_{ss}$+sp+liquid; *N*, mel+ sp+fo_{ss}+liquid; and *O*, mel+di_{ss}+fo_{ss} +liquid. The exact temperatures and compositions of these three piercing points were not determined, and boundary curves are shown as dashed lines.

The light dashed line *XY* divides the join into two areas. Compositions that are in the area *X* Sp *Y* when completely crystalline consist of the four solid phases $mel_{ss(maximum)}$ + $di_{ss(maximum)}$ + sp +fo_{ss} and begin to melt at the temperature 1238°±2°C of the quaternary invariant point *Q* of the flow sheet shown below as Fig. 11. As a first approximation, those compositions in the area Ak *X Y* Di would be expected to consist of the three solid phases mel+di_{ss}+fo_{ss}. These relations result from the coplanar character of Fo-Geh-Ak-Sp; however, more complex relations may arise in the vicinity of Di if some enstatite is also in solid solution with the aluminous diopside. The three compositions prepared in the join akermanite-spinel-diopside should contain sp when completely crystalline in addition to the three phases fo_{ss}, di_{ss}, and mel. However, if present, there was too little sp to show in the X-ray diagrams or to be observed under the microscope.

The Join Ca-Tschermak's Molecule (CaTs)-Diopside and Its Relationship to Coplanar Ak-Geh-Di-CaTs

During the past year we have obtained considerable new data on this join. We prepared a batch of $CaTs_{85}Di_{15}$ and a new batch of $CaTs_{90}Di_{10}$. We crystallized the latter at 1470°C first to get crystals

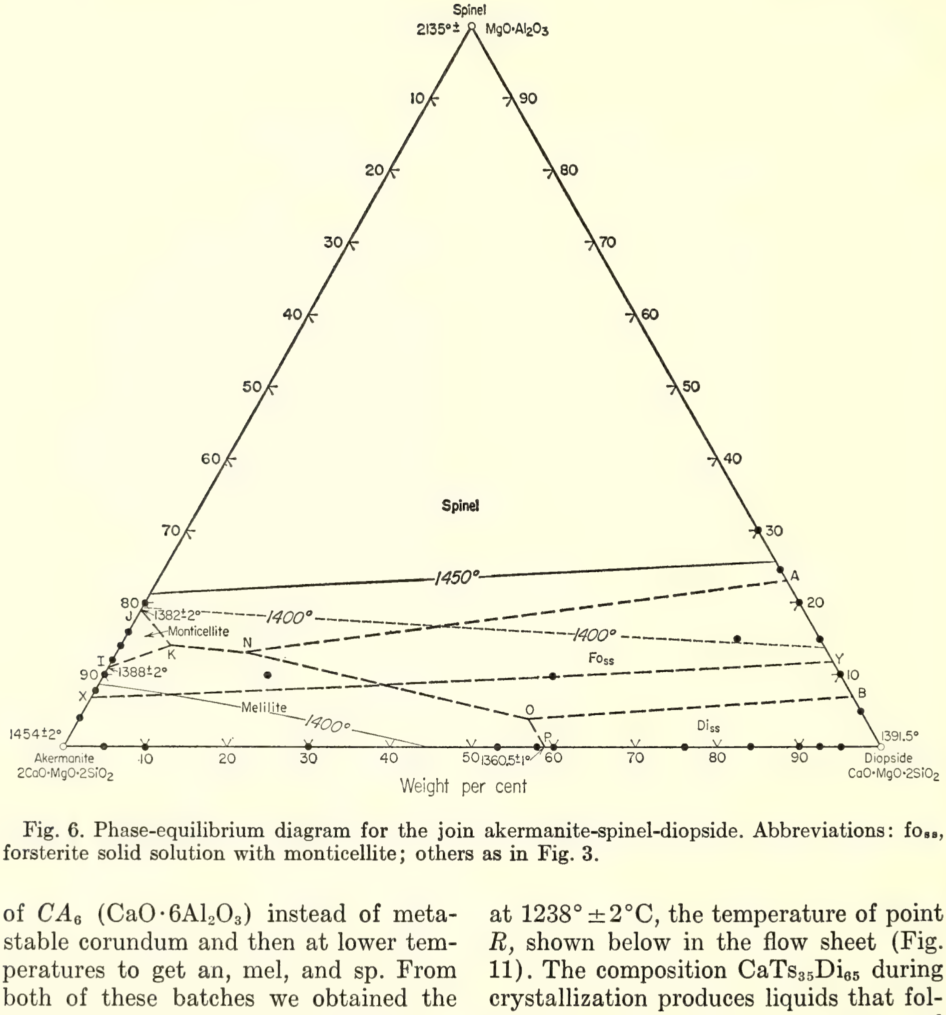

Fig. 6. Phase-equilibrium diagram for the join akermanite-spinel-diopside. Abbreviations: fo_{ss}, forsterite solid solution with monticellite; others as in Fig. 3.

of CA_6 ($CaO \cdot 6Al_2O_3$) instead of metastable corundum and then at lower temperatures to get an, mel, and sp. From both of these batches we obtained the value 1360° ± 5°C for the quaternary invariant point CA_6+an+mel+sp+liquid. The composition $Ak_{35.82}Sp_{9.35}An_{54.83}$ in the join akermanite-spinel-anorthite also has the composition $CaTs_{57.32}Di_{42.68}$ and, as shown before, reaches the point R at 1238° ± 2°C of the flow sheet shown below as Fig. 11.

The data for the join CaTs-Di are plotted in Fig. 7. It should be noted that geh-an-sp and ak-an-sp cut this join. The composition $CaTs_{50}Di_{50}$ during crystallization produces liquids that follow the surface an+sp+liquid, and these phases are joined by both di_{ss} and mel at 1238° ± 2°C, the temperature of point R, shown below in the flow sheet (Fig. 11). The composition $CaTs_{35}Di_{65}$ during crystallization produces liquids that follow the surface di_{ss}+an+liquid and these phases are joined by both mel and sp at 1238° ± 2°C, the temperature of point R (Fig. 11). The two compositions $CaTs_{55}Di_{45}$ and $CaTs_{40}Di_{60}$ during crystallization follow the univariant line an+di_{ss}+sp+liquid where they are joined by mel at the quaternary invariant point mel+sp+an+di_{ss}+liquid at 1238° ± 2°C, the temperature of point R (Fig. 11). The dotted line at about $CaTs_{33}Di_{67}$ is an observational line to the right of which sp was not observed. The constancy of the melting relations suggests that the phase is there and not

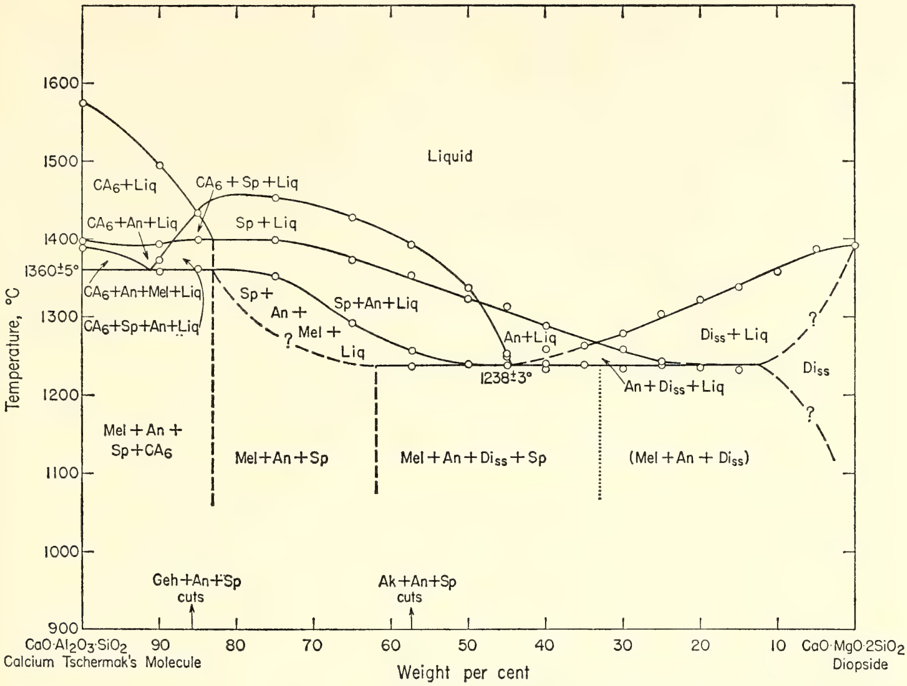

Fig. 7. Phase-equilibrium diagram for the join CaTs-diopside. This join is coplanar with akermanite-gehlenite-diopside-CaTs. Abbreviations: CA_6, $CaO \cdot 6Al_2O_3$; An, anorthite; Geh, gehlenite; Ak, akermanite; others as in Fig. 3.

readily observable. Alternatively, the di_{ss} may contain enstatite as well as CaTs and the polyhedron an-di_{ss}-mel would be cut by CaTs-Di. CaTs-Di is coplanar with Ak-Geh.

The Join Diopside-Spinel

Data for this join are plotted in Fig. 8. Two compositions, $Di_{70}Sp_{30}$ and $Di_{75.27}Sp_{24.73}$, produce liquids during crystallization that go down the univariant line sp + fo_{ss} + an + liquid to the quaternary invariant point di_{ss} + fo_{ss} + sp + an + liquid at 1238° ± 2°C (*P* of Fig. 11). Two compositions, $Di_{80}Sp_{20}$ and $Di_{85}Sp_{15}$, produce liquids during crystallization that go down the univariant line di_{ss} + fo_{ss} + an + liquid to this same quaternary invariant point (*P* of Fig. 11). Two compositions, $Di_{95}Sp_5$ and $Di_{90}Sp_{10}$, become completely crystalline with the three solid phases di_{ss} + fo_{ss} + mel in the experiments, but there is reason to believe the melilite persists or grows metastably.

Experimental difficulties were encountered in our study of this join. Melilite crystallizes readily and in excessively large amounts even in those compositions where it is a metastable phase. In order to circumvent this we found it necessary to hold appropriate compositions at temperatures above the appropriate quaternary invariant point, X-ray them to be sure no metastable melilite was present, and then lower the temperature to that of the quaternary invariant point. Only by this means were we able to ascertain the correct equilibrium relations with no metastable solid phases. However, in the compositions $Di_{95}Sp_5$ and $Di_{90}Sp_{10}$ metastable melilite appeared during crystallization at 1200°C, and because so little liquid is present it persists metastably at temperatures just

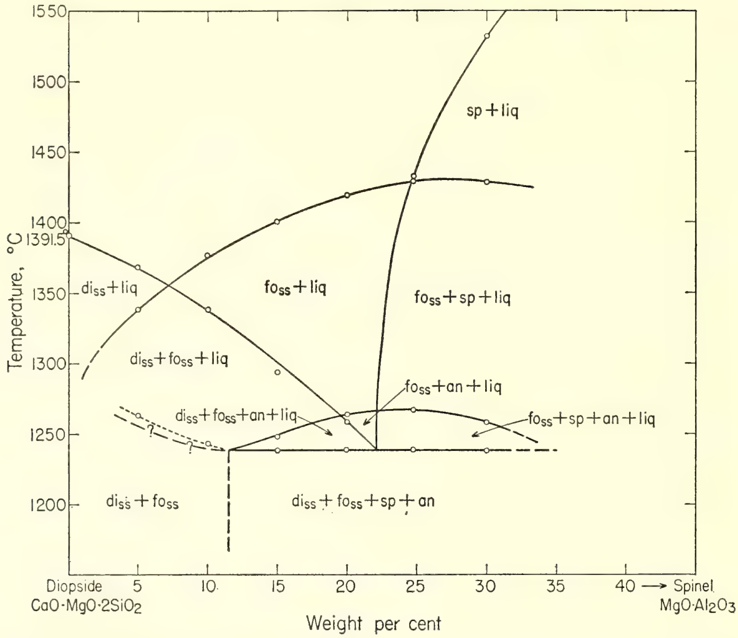

Fig. 8. Phase-equilibrium diagram for the join diopside-spinel. This join is coplanar with forsterite-CaTs. Abbreviations as in Fig. 5.

above the beginning of melting, as indicated by the dotted line in Fig. 8.

The diagram for diopside-spinel given by Schairer and Kushiro (*Year Book 64,* p. 101, Fig. 21) suggests that some of the liquids freeze up at *Q* (Fig. 11). In their study, as well as in the early stages of this study, however, the excessively large amounts of melilite indicate its metastability.

Positions of the Joins Studied in the Tetrahedron CaO-MgO-Al_2O_3-SiO_2

The relationship of the various joins studied in the context of the CaO-MgO-Al_2O_3-SiO_2 tetrahedron are displayed in Fig. 9. The three principal planes studied and the data on Di-An-Ak by deWys and Foster (1958) form the subtetrahedron An-Di-Ak-Sp. As will be demonstrated below, at least two of the three most critical invariant points of the entire system lie within this subtetrahedron. Because of the extensive solid solution in Ak and Di, primarily in the direction of Geh and CaTs, respectively, the compositions of phases crystallizing at the solidus are more closely represented by the dashed lines outlining An-Sp-Ak_{ss}-Di_{ss} and consequent Fo-Sp-Ak_{ss}-Di_{ss}. In short, the subtetrahedra just described are not only compositional tetrahedra but also represent the final products obtained in the experiments.

As determined by experiment the array of primary phase volumes for the principal portion of CaO-MgO-Al_2O_3-SiO_2 can be outlined. These subsolidus tetrahedra are displayed in Fig. 10 as an exploded view. The lettered tetrahedra correspond to the quaternary invariant points shown in the flow sheet presented below as Fig. 11. In brief, liquids generated in tetrahedron *P* fractionate along an + fo_{ss} + sp + liquid and an + di_{ss} + fo_{ss} + liquid through the face An-Di_{ss}-Sp into tetrahedron *R*. Liquids generated in the tetrahedron *Q* fractionate through

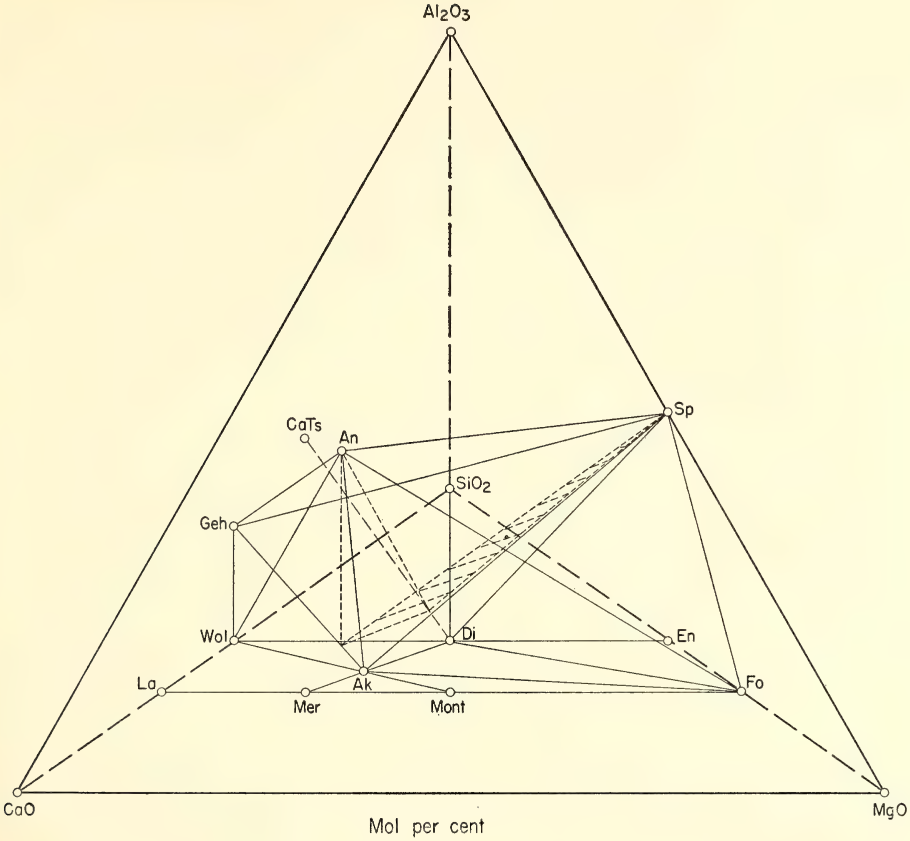

Fig. 9. Relationship of the joins studied in the tetrahedron $CaO\text{-}MgO\text{-}Al_2O_3\text{-}SiO_2$ (in mole %). The dashed lines represent an estimate of the subtetrahedron anorthite-spinel-melilite-diopside solid solution at the solidus as determined by experiment.

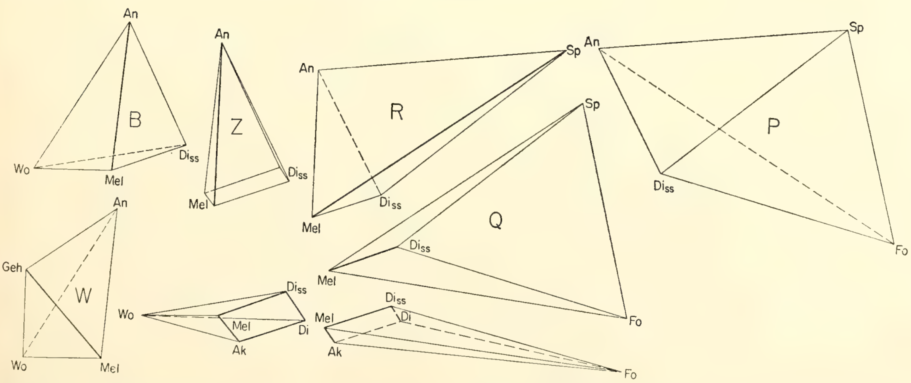

Fig. 10. Subsolidus tetrahedra in $CaO\text{-}MgO\text{-}Al_2O_3\text{-}SiO_2$ as determined by experiment. Upper-case letters in the tetrahedra and prisms represent assemblages at the solidus corresponding to the quaternary invariant points similarly lettered in Fig. 11. The liquids at the quaternary invariant points do not necessarily lie in these volumes.

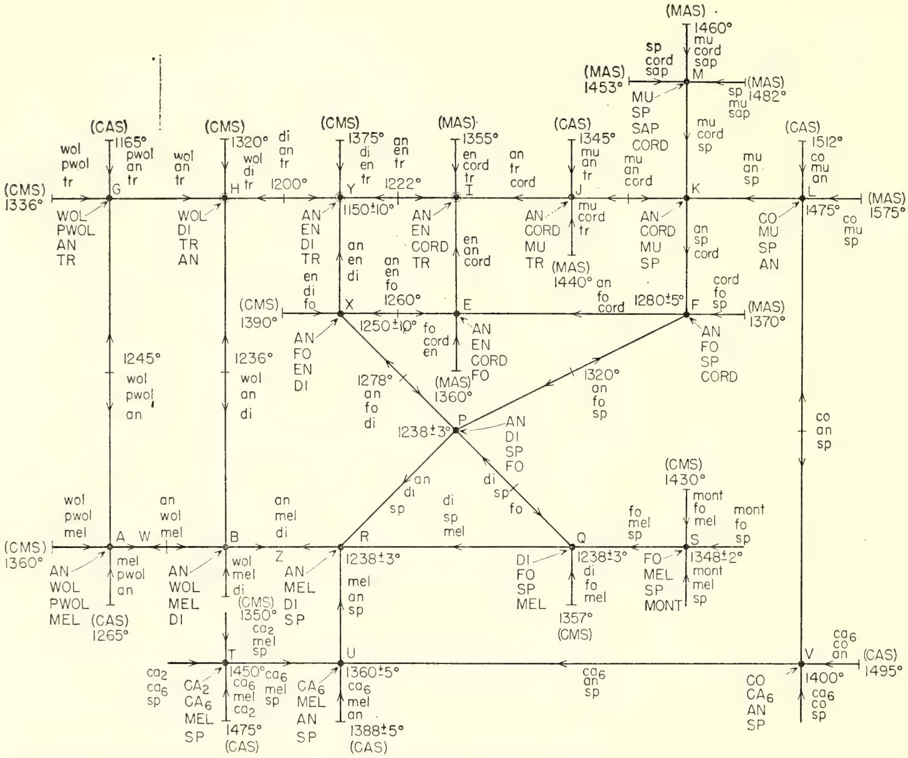

Fig. 11. Flow sheet for the geologically relevant portion of the quaternary system CaO-MgO-Al_2O_3-SiO_2. Diagram showing univariant lines and their relation to ternary invariant points (indicated by a small bar) in limiting systems and to quaternary invariant points (large black dots and upper-case letters). These lines and points do not lie in a plane. Only their relations to one another are shown in this diagram, which is not intended to depict their angular spatial relations. The lengths of lines and the position of temperature maxima or minima on a line are arbitrary and without significance. Arrows indicate the direction of falling temperature. Abbreviations: wol, wollastonite solid solutions; pwol, pseudowollastonite; tr, tridymite; an, anorthite; mel, melilite; di, diopside solid solutions; sp, spinel; fo, forsterite solid solutions; mont, monticellite solid solutions; CA_2, CaO·$2Al_2O_3$; CA_6, CaO·$6Al_2O_3$; co, corundum; mu, mullite; sap, sapphirine; cord, cordierite; en, enstatite. Attention is called to the three eutectics *H*, *Y*, and *I* and to the two minima *W* and *Z*. There are four univariant lines that originate in portions of CaO-MgO-Al_2O_3-SiO_2 not considered here.

the face Mel-Di_{ss}-Sp along mel + fo_{ss} + sp + liquid and mel + di_{ss} + fo_{ss} + liquid. The piercing points on the bounding faces of An-Di-Sp and Ak-Di-Sp indicate that the invariant points *P* and *Q* must lie in An-Mel-Di_{ss}-Sp. The invariant point *R* may lie in its own tetrahedron An-Sp-Mel-Di_{ss} as a eutectic or may lie in a subsidiary polyhedron An-Mel-Di_{ss}, in which case it becomes a reaction point leading to a minimum positioned in the same subsidiary polyhedron. The data on the plane Di-An-Ak studied by deWys and Foster (1958) are not sufficient to arrive at an unambiguous choice. The temperature of their "eutectic," which is presumably a piercing point, at 1226°C (see Schairer and Yoder, *Year Book 67*, p. 104) is lower than *R*, and, therefore, suggests but is not conclusive evidence that *R* may be a reaction point. However, if *R* is a reaction point, then a small field of spinel should appear on the liquidus of the join Di-An-Ak. Reli-

ance is placed on their temperature data (given in their Table 1, eutectic horizontal data) and the flow sheet, drawn accordingly.

From the experimental data on the joins presented we have seen that (1) all compositions studied in the join diopside-spinel-anorthite and four of the compositions studied in diopside-spinel ($Di_{70}Sp_{30}$, $Di_{75.27}Sp_{24.73}$, $Di_{80}Sp_{20}$, and $Di_{85}Sp_{15}$) have their final crystallization at P (Fig. 11); (2) four compositions in the join akermanite-spinel-anorthite crystallize completely at Q (Fig. 11); (3) nine compositions in the join akermanite-spinel-anorthite and four compositions in the join CaTs-Di became completely crystalline at R (Fig. 11). In the discussion of Fig. 2, the join akermanite-spinel-anorthite, we have shown that compositions that lie in the area C A An become all crystalline at B (Fig. 11).

Because of the analogy between the flow sheet of Schairer and Yoder (*Year Book 63*, p. 72, Fig. 8) for compositions where the feldspar is nearly pure albite, Schairer, Tilley, and Brown (*Year Book 66*, p. 470, Fig. 70), in their flow sheet for the corresponding compositions where the feldspar is anorthite, show the points F', C', and L with a temperature maximum in $F'C'$. They had no experimental evidence for this maximum, which was based on the analogy. Attention is called to the close proximity in temperature between F', C', and L at 1155°, 1152°, and 1148°C (all ±3°), respectively. Note the similarity between the quaternary invariant points P, Q, and R of the flow sheet for CaO-MgO-Al_2O_3-SiO_2 in Fig. 11. These three points lie at 1238° ± 3°C, that is, at the same temperature within experimental error. These same three points, investigated by O'Hara and Biggar (1969), are 1233.5°, 1232°, and 1230°C, respectively, that is, in an interval of only 3.5°C. From an examination of data in their Table 4 (pp. 374–375), it may be seen that there is no evidence indicating temperatures along their curve di+sp+fo+liquid, although they show an arrow for falling temperature, from P to Q of our flow sheet, Fig. 11.

In view of the lack of experimental temperature evidence and the absence of petrographic observations on an anorthite reaction relation with liquid, it seems more likely that there is a temperature maximum in the small temperature range along PQ of our flow sheet, Fig. 11. The absence of piercing points in the plane fo-di-sp tends to support this interpretation.

Attention is called to the nature of some of the solid solutions. The melilites are not pure akermanite or pure gehlenite but an akermanite-rich melilite (usually with approximately 16 wt % gehlenite). The clinopyroxene is not pure diopside but must have CaTs in solid solution and might also have an appreciable enstatite content. The forsterite should have appreciable monticellite in solid solution, and even the spinel may not be pure $MgO \cdot Al_2O_3$.

Petrologic Applications to Rocks and a Possible Solution to the Plagioclase-Melilite Dilemma

The flow sheet presented in Fig. 11 is in fact that for the expanded basalt tetrahedron, based not on nepheline and albite but on calcium Tschermak's molecule and anorthite. The presence of spinel in the geologically relevant assemblages, however, limits its application to magma fractionation problems. The occurrence of clinopyroxene and spinel, herein confirmed, has already been pointed out by O'Hara and Schairer (*Year Book 62*, p. 115) and O'Hara and Biggar (1969). However, spinel appears to react out early in the fractionation scheme when Na_2O is added to the system, as outlined by Schairer, Tilley, and Brown (*Year Book 66*, p. 470), and is not represented among the final products of the common alkali igneous rocks. With the present construction of the flow sheet, liquids fractionating from olivine gabbro would

then pass into regions (R of Figs. 10 and 11) of composition more calcic than those represented by natural magmas. Such rocks appear to be generated mainly by assimilation of limestone as illustrated at Scawt Hill, northern Ireland (Tilley and Harwood, 1931). The reaction behavior assigned by Chinner and Schairer (1962), p. 630) to the aluminous pyroxene does not appear to be operative; in fact, the pyroxene may become slightly more aluminous with the onset of melilite.

Liquids generated in Q would be represented by the olivine melilite nephelinites. Accepting the maximum on P-Q (for which there are no experimental data), the liquid at Q would fractionate on the loss of olivine toward R with calcium enrichment of the liquid. The high liquidus temperatures of the natural olivine-melilite nephelinites support the view that they have a liquid line independent of the olivine gabbros at 1 atm. Ignoring this limitation for purposes of discussion, it is seen that the assemblage at P is essentially representative of an olivine gabbro.

The new subtetrahedra point to a possible solution of the plagioclase-melilite dilemma described in detail last year by Yoder and Schairer (*Year Book 67,* p. 101). Although plagioclase and melilite do not occur together in igneous rocks, those phases were stable together in liquid over a wide range of bulk compositions and conditions in the laboratory. Examination of the volume enclosed by An-Ak-Di-Fo-Sp (see Fig. 10) reveals that Ak is stable with An only in the absence of Fo. That is, the more calcium-rich assemblage An-Ak-Di-Sp is found only in the metamorphic rocks, whereas the assemblage Fo-Ak-Di-Sp has representatives among the igneous rocks. In brief, plagioclase and melilite are indeed stable together in certain assemblages, but not in those characteristic of the igneous rocks. If Sp in the above-named assemblages is replaced by Ne, then the assemblages are those displayed in Fig. 12. These assemblages are just those deduced

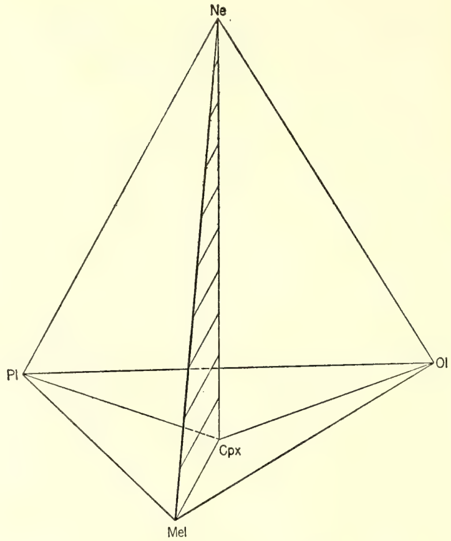

Fig. 12. The generalized volume plagioclase (Pl)-nepheline(Ne)-olivine(Ol)-melilite(Mel)-clinopyroxene(Cpx), illustrating the coexistence of plagioclase and melilite in the absence of olivine and their incompatibility in the presence of olivine. The tetrahedron Pl-Ne-Ol-Cpx represents the basanites; Mel-Ne-Ol-Cpx represents the olivine melilite nephelinites; and Pl-Ne-Cpx-Mel, metamorphic rocks or those resulting from assimilation.

by Schairer, Tilley, and Brown (*Year Book 66,* p. 470) in their flow sheet at the points F', C', and L. It appears that the incompatibility of plagioclase and melilite can be explained in the presence of olivine; however, the melilite nephelinites do not have this constraint. The commitment to that particular fractionation trend may have been made at an earlier stage, as suggested in the flow sheet by Schairer and Yoder (*Year Book 63,* p. 72).

The System $CaSiO_3$-$MgSiO_3$-Al_2O_3

F. R. Boyd

Most petrologic models for the upper mantle favor garnet lherzolite as a major rock type. Among the reasons for this choice is the belief that it is a possible parent material for basaltic lavas. Garnet lherzolite is also abundant among

the ultramafic nodules that have been recovered from kimberlites, and these nodules are believed to be relatively unaltered mantle rocks.

Garnet lherzolites contain only four essential minerals: forsterite, pyrope-rich garnet, enstatite, and diopside. The simplicity of this assemblage offers hope that compositional variations of the constituent minerals can be interpreted in considerable detail from studies on synthetic systems. Solid solutions in garnet, in pyroxenes, and between garnets and pyroxenes are sensitive to temperature and pressure and are the most important aspects of these phase relations. The system $CaSiO_3$-$MgSiO_3$-Al_2O_3 models the natural solid solutions rather well. This system contains the joins pyrope-grossularite and enstatite-diopside and shows the solid solutions of these pyroxenes toward Al_2O_3. This ternary also contains the composition $CaAl_2SiO_6$, or "calcium Tschermak's molecule," a pyroxene that is stable under limited conditions of high temperature and pressure.

Subsolidus synthesis relations in the system $CaSiO_3$-$MgSiO_3$-Al_2O_3 have been determined at 1200°C and 30 kb with analysis by electron probe as the means of establishing the compositions of coexisting phases. This is the first phase study to be published in an Annual Report in which the probe has been used as the principal analytical instrument, rather than the petrographic microscope and the X-ray diffractometer. Electron-probe techniques have many advantages over optical and X-ray methods. They are more accurate and more direct, and for complex equilibria they are faster. A disadvantage is that the grain size of a synthetic run must be at least 6–8 μm to permit accurate probe analysis. Nevertheless, this minimum grain size can be obtained in silicate systems under favorable circumstances.

Phase Relations

Phase relations in $CaSiO_3$-$MgSiO_3$-Al_2O_3 appear to be completely ternary at 1200°C and 30 kb. Figure 13 shows the whole ternary, and portions of it together with plots of the analytical data are shown in expanded form in Figs. 14 and 15. Explanations of abbreviations used in these figures and in the text are given in Table 15. The ternary contains four three-phase fields, one of which $Di_{ss}+En_{ss}+Mg\text{-}Gt_{ss}$ is of primary geologic interest because it models the garnet-lherzolite assemblage. There is a very extensive solid solution of diopside toward $CaAl_2SiO_6$ (CaTs) extending to a composition of 56 wt % CaTs. This solid solution "finger" pierces the garnet join and interrupts the extensive solid solution between pyrope and grossularite. CaTs is not a stable phase at 1200°C and 30 kb. At higher temperatures and lower pressures it becomes a stable phase (Hays, *Year Book 65;* Hijikata and Yagi, 1967) and the solid solution along the join diopside-CaTs becomes complete (Clark, Schairer, and de Neufville, *Year Book 61*).

The compositions of diopsidic pyroxenes in equilibrium with garnet in this system are of particular interest because they reveal the effect of aluminum on the solid solution of enstatite in diopside. The basic phase relations for this part of the ternary were outlined and discussed on a theoretical basis by O'Hara and Mercy (1963) and Banno (1965). These authors correctly deduced that solid solution toward garnet would reduce the solid solution of enstatite in diopside. O'Hara and Yoder (1967) have provided experimental data in support of the theoretical treatments. The diopside solution field (Fig. 14) lies along the join $CaMgSi_2O_6$-$CaAl_2SiO_6$, extending to compositions considerably richer in Mg at the low-Al_2O_3 end. As the Al_2O_3 contents of these pyroxenes increase, the extension of this field toward $MgSiO_3$ decreases.

Nevertheless, there is an inflection in the boundary of the diopside solid solution field (Fig. 14) such that diopside in equilibrium with *both enstatite and gar-*

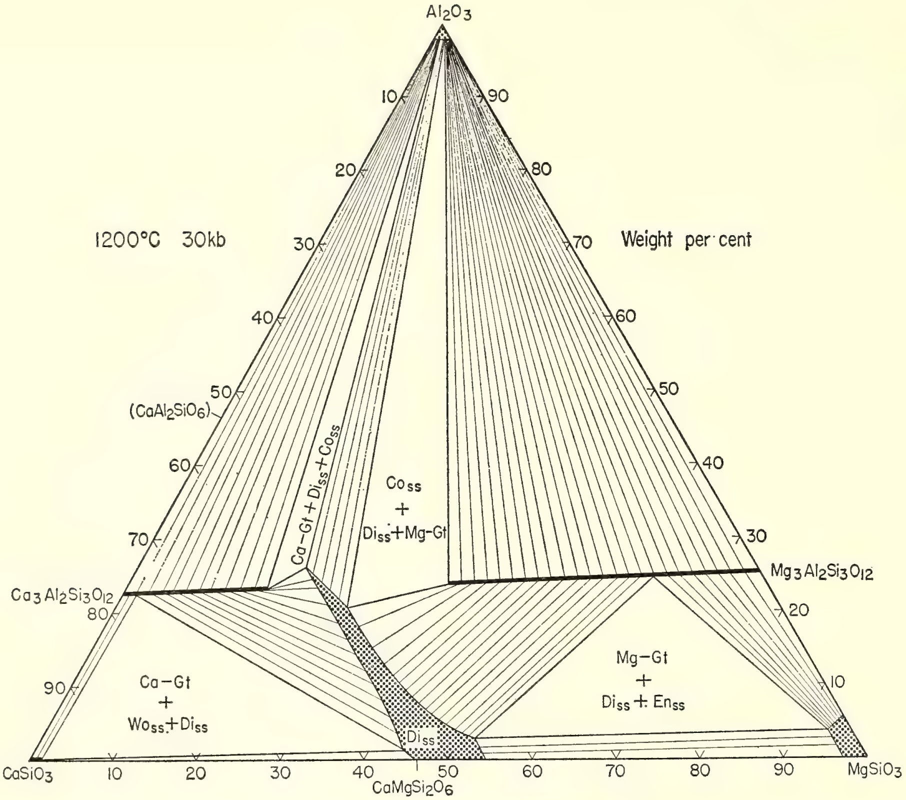

Fig. 13. Synthesis diagram for phase relations in the system $CaSiO_3$-$MgSiO_3$-Al_2O_3 at 1200°C and 30 kb. Data points are shown in Figs. 14 and 15.

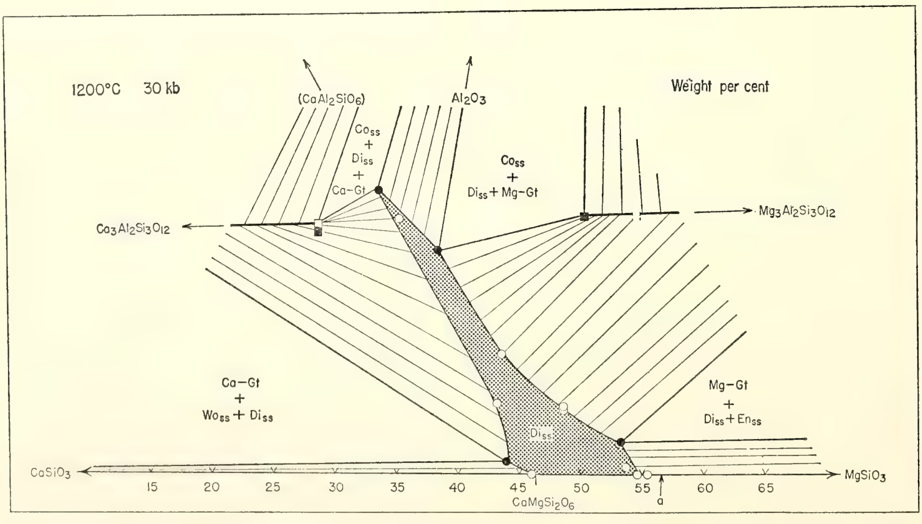

Fig. 14. A portion of the system $CaSiO_3$-$MgSiO_3$-Al_2O_3 at 1200°C and 30 kb showing the solid solution field for diopside. Open points represent analyses of phases in two-phase assemblages, and solid points are for phases in three-phase assemblages. Circles are pyroxenes, and squares are garnets. Point *a* is the Di(*en*) solvus in the system $CaMgSi_2O_6$-$MgSiO_3$ determined by Davis and Boyd (1966).

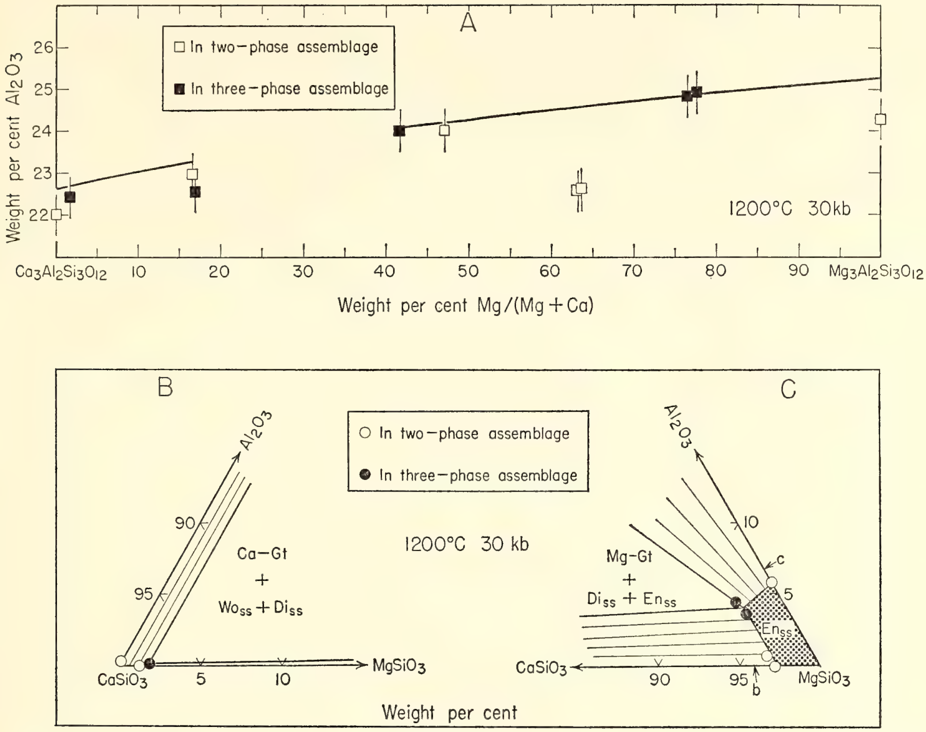

Fig. 15. Portions of the system $CaSiO_3$-$MgSiO_3$-Al_2O_3 showing the analytical data. (A) The garnet join with wt % Al_2O_3 plotted against the weight ratio Mg/(Mg + Ca) in order to expand the Al_2O_3 axis. Vertical bars on the points are error limits of ±2 relative % Al_2O_3. (B) The wollastonite solid solution field. (C) The enstatite solid solution field. Point *b* is the En(*wo*) solvus in the system $CaMgSi_2O_6$-$MgSiO_3$ determined by Davis and Boyd (1966), and point *c* is the En(*co*) solvus in the system $MgSiO_3$-$Mg_3Al_2Si_3O_{12}$ determined by Boyd and England (*Year Book 63*).

net has a Ca/(Ca+Mg) ratio that is only slightly larger than that of a diopside in equilibrium with enstatite on the join $CaMgSi_2O_6$-$MgSiO_3$. Specifically,

TABLE 15. Abbreviations Used in this Report

Di	Diopside, $CaMgSi_2O_6$
En	Orthorhombic enstatite, $MgSiO_3$
Wo	Wollastonite, $CaSiO_3$
Mg-Gt	Mg-rich garnet on the join $Mg_3Al_2Si_3O_{12}$-$Ca_3Al_2Si_3O_{12}$
Ca-Gt	Ca-rich garnet on the join $Mg_3Al_2Si_3O_{12}$-$Ca_3Al_2Si_3O_{12}$
CaTs	Ca-Tschermak's molecule, $CaAl_2SiO_6$
Co	Corundum, Al_2O_3
$wo_x en_y co_z$	Composition ($x + y + z = 100$ wt %)
ss	Subscript denoting solid solution
En(*co*)	Notation indicating the solvus for the component Al_2O_3 in enstatite

diopside in the three-phase field Di_{ss}+En_{ss}+$Mg\text{-}Gt_{ss}$ at 1200°C and 30 kb contains 3.0±0.1 wt % Al_2O_3 and has a Ca/(Ca+Mg) ratio of 0.43±0.01 (mole fraction), compared with 0.42±0.01 for Al-free diopside in equilibrium with enstatite at the same pressure and temperature. Thus application of the pure Di(*en*) solvus (Davis and Boyd, 1966) to garnet peridotites in which the pyroxenes contain only a few percent of Al_2O_3 would be in error because of the effect of Al by an amount which is clearly small in relation to other uncertainties. These other uncertainties include an uncertainty in the experimental location of the Di(*en*) solvus of about ±0.01 in

mole fraction $CaSiO_3$ where the data are best, as well as uncertainties about the effects on this solvus of small amounts of Na, Cr, Fe^{2+} and Fe^{3+}, in the natural pyroxenes.

Boyd (1967) has suggested that the Al_2O_3 content of enstatite in equilibrium with garnet might be used in combination with the Ca/(Ca+Mg) ratio of coexisting diopside to fix the *P-T* conditions of equilibration of garnet peridotites. O'Hara (1967) has more fully developed an analogous approach using the R_2O_3 content and Ca/(Ca+Mg) ratio of diopside in equilibrium with enstatite +forsterite+"an Al_2O_3-rich phase." O'Hara's treatment takes into account the interrelationships of these solid solutions, and it is interesting to note that the experimental determination of the three-phase field $Di_{ss}+En_{ss}+Mg\text{-}Gt_{ss}$ described in this report fits his provisional diagram (*op. cit.*, p. 396, Fig. 12.4) relatively well. As shown above the Ca/(Ca+Mg) ratio of diopside in equilibrium with enstatite is slightly affected by several percent of Al_2O_3. The Al_2O_3 content of enstatite in equilibrium with garnet is affected in a similar way by solid solution of diopside in the enstatite. Data in Fig. 15 show that the Al_2O_3 content of enstatite that coexists with pyrope on the join $MgSiO_3$-$Mg_3Al_2Si_3O_{12}$ at 1200°C and 30 kb is 5.8 wt %, whereas enstatite in equilibrium with garnet and diopside under these conditions contains about 4 wt % Al_2O_3. There is a discrepancy in the Al_2O_3 analyses of duplicate runs on this point (Fig. 15), but the apparent effect of Ca on the solid solution of enstatite toward garnet is most likely real. When more data on these ternary equilibria become available, it is probable that the Al_2O_3 content of enstatite will be of more use in constructing a *P-T* grid for peridotites than will the analogous solid solution in diopside, because natural enstatites contain less Cr_2O_3 and show less solid solution toward jadeite and acmite than do the coexisting diopsides.

The experimental determination of the $Di_{ss}+En_{ss}+Mg\text{-}Gt_{ss}$ field is compared in Fig. 16 with analytical results for two garnet-lherzolite nodules from kimberlite. The agreement for the point of intersection of the three-phase field with the garnet join is remarkable. Experimental results obtained by Kushiro, Syono, and Akimoto (1967*a*) are also shown (Fig. 16). They determined the cell dimensions of garnets coexisting with enstatite and diopside solid solutions in runs crystallized in the pressure range 18–96 kb and found a systematic variation corresponding to a compositional range of 81–88 mole % pyrope. Results on the garnets are thus concordant. Nevertheless, there is a large variation in the points of intersection of the three-phase field with the solid solution fields for diopside and enstatite. The A-3 nodule (Fig. 16) has a calcic diopside, typical of most diopsidic pyroxenes from kimberlites, whereas the diopside in the E-3 nodule is of the rarer, subcalcic variety. Elsewhere in this report Boyd and Nixon suggest that these results may not be understandable in terms of present experimental data and that studies at higher pressures are needed.

The pair of three-phase fields for corundum, garnet, and pyroxenes (Fig. 13) seem to model the mineral assemblages found in grospydite and kyanite-eclogite xenoliths in kimberlite. These rocks sometimes contain corundum, but more frequently kyanite is the highly aluminous phase. The garnets in the grospydites and kyanite eclogites contain 10–35% almandine, and the pyroxenes are omphacites containing 30–50% jadeite. Hence, application of the phase relations from the ternary studied in this investigation to these rocks involves a long reach. O'Hara and Mercy (1966) have projected compositions of garnets and pyroxenes from a corundum eclogite and grospydite from Yakutia and garnet from a kyanite eclogite from the Roberts Victor mine onto the plane $CaSiO_3$-$MgSiO_3$-Al_2O_3 and obtained an arrange-

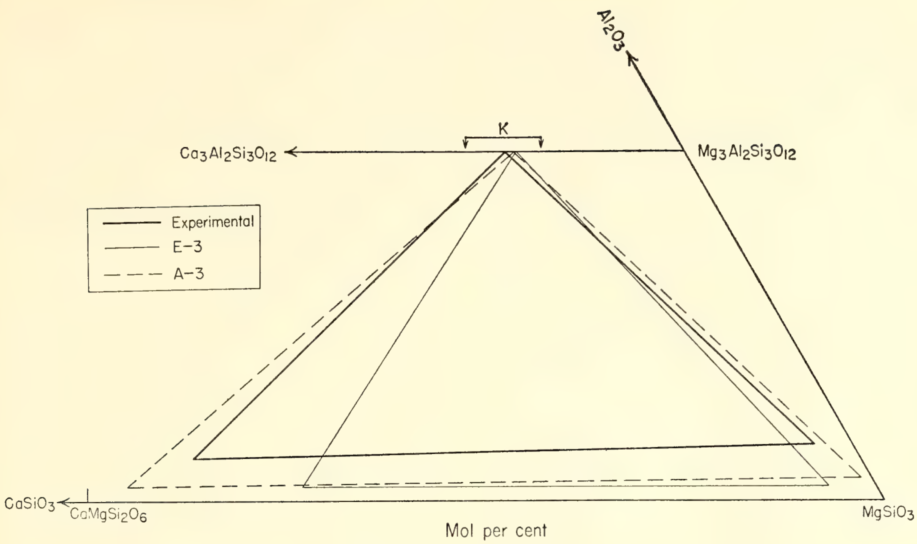

Fig. 16. A portion of the system $CaSiO_3$-$MgSiO_3$-Al_2O_3 showing the experimental determination of the phase field $Mg\text{-}Gt + Di_{ss} + En_{ss}$ at 1200°C and 30 kb together with analytical data for the pyroxenes and garnets of two lherzolite nodules. A-3, O'Hara and Mercy (1963); E-3, Nixon, von Knorring, and Rooke (1963), Boyd (1969). The range of garnet compositions obtained in experiments by Kushiro, Syono, and Akimoto (1967) is shown as bracket *k*. The two natural garnets are assumed to lie on the join $Ca_3Al_2Si_3O_{12}$-$Mg_3Al_2Si_3O_{12}$. For the natural pyroxenes "Al_2O_3" $= 0.5[Al - Na(Al/Al + Cr + Fe^{3+})]$, where Al, etc., are in atomic proportions.

ment of three-phase fields similar to that determined by experiment (Fig. 13). However, Sobolev, Kuznetsova, and Zyuzin (1968) have presented a large number of analyses of pyroxenes and garnets from grospydites and kyanite eclogites and concluded that there is a complete solid solution between grossularite and pyrope under the *P-T* conditions of grospydite equilibration. The relatively high almandine contents of the garnets they analyzed leave some uncertainty about this conclusion. One would certainly expect that the pyrope-grossularite join would be continuous at pressures high enough to stabilize diamond. Diamonds have been found in eclogites (Sobolev, 1968), although apparently not in kyanite eclogites or grospydites. In this connection it is interesting to note that one of the garnet inclusions from diamond described by Meyer and Boyd (this report) is very similar to those from kyanite eclogites.

Both the wollastonite and corundum in this system show detectable solid solutions, but they are rather small. Analyses for wollastonites in three assemblages are plotted in Fig. 15, and it can be seen that the wollastonite dissolves 1–2% $MgSiO_3$ but only about 0.1–0.2% Al_2O_3. The corundum in these assemblages is too fine grained to permit accurate analysis. However, significant signals for Mg, Ca, and Si were obtained. They are extremely variable but correspond to a solid solution of about 1% $MgSiO_3$ and 2% $CaSiO_3$ in corundum in the assemblage $Co_{ss}+Di_{ss}+Ca\text{-}Gt$. Silicon is definitely present in the corundum, but the analyses made were not of sufficient accuracy to make it certain that the composition of the corundum is in the plane $CaSiO_3$-$MgSiO_3$-Al_2O_3.

All the probe analyses of garnets obtained in these runs are shown in Fig. 15 in a plot of wt % Ca/(Ca+Mg) against wt % Al_2O_3. This plot permits expansion

of the Al_2O_3 axis, and it can be seen that although most of the garnet analyses fall on the garnet join within expectable error limits, there are a number that fall significantly below. Ringwood (1967) has shown that a large solid solution of garnet toward pyroxene develops at pressures on the order of 100 kb. The onset of this solid solution with increasing pressure is rather abrupt in the experiments he describes, but it is possible that with the greater sensitivity of electron-probe techniques in comparison to cell size measurements a beginning of this solid solution might be detected at lower pressures. If best-fit curves were drawn through the garnet analyses in Fig. 15, they would lie below the garnet join and might be taken as evidence of such a solid solution. Nevertheless, the scatter in these results does not support such an interpretation and suggests instead that the garnets in some runs have incorporated minute inclusions of pyroxenes that could not be detected and avoided during analysis.

There are several discrepancies between the phase relations shown in Figs. 13–15 and earlier work on binary joins. Chinner, Boyd, and England (*Year Book 59*) reported a complete solid solution on the join pyrope-grossularite at 30 kb and 1250°C on the basis of cell edge and refractive-index measurements. Present results (Fig. 13) show that this solid solution is interrupted in the composition interval 23–51 wt % (25–54 mole %) pyrope. The pressure listed by Chinner *et al.* contained a −8% friction correction, whereas it is our present practice to list load pressures. Using the load-pressure convention, the pressure of the runs made by Chinner *et al.* was 32.3 kb. It is possible that garnet-pyroxene phase relations change sufficiently rapidly with pressure that the increment of 2.3 kb in pressure over the pressure of the present study is sufficient to stabilize this garnet solid solution.

The probe determinations reported here show that solid solutions between enstatite and diopside and in enstatite toward pyrope are consistently more restricted than indicated by earlier work (Davis and Boyd, 1966; Boyd and England, *Year Book 63*). These discrepancies are small (Figs. 14 and 15), and it is questionable whether they are significant. The earlier determinations were made by optical identification of one or two phases in runs closely spaced in composition. Possibly trace amounts of garnet mixed with enstatite or trace amounts of one pyroxene mixed with another were consistently missed. There may also be a small bias in the probe analyses in that one tends to avoid grains that give somewhat extreme counts because they usually indicate intergrowths. This tendency could lead to a small but consistent underestimate of solid solutions.

Experimental Technique

Starting materials for the high-pressure runs made to determine these phase relations were prepared as powdered glass and were moistened with small amounts of H_2O. They were loaded in platinum capsules. Inasmuch as the capsules were not sealed by welding, the H_2O diffused away in the course of a run. Samples were held at temperature and pressure for 2–5 hours. This technique sometimes yields run products with a grain size up to 50 μm, but grain growth is very erratic. At times too much H_2O was added and the samples melted; at other times grain growth was inadequate for electron-probe analysis. Approximately a third of the total number of runs that were made could be probed. They were mounted in epoxy on glass slides, and each was polished to as thin a section as practical.

It proved very difficult to distinguish individual grains under the probe in many samples. Use of transmitted light is helpful, but small differences in relief, cathodoluminescence, cleavage, etc., were also employed. At least a dozen grains of

each phase in each assemblage were analyzed for Ca, Mg, and Al, and the output was processed by computer programs described by Boyd, Finger, and Chayes (*Year Book 67*). An addition to program ABFAN converted the Ca and Mg analyses to $CaSiO_3$ and $MgSiO_3$ and formed a total with Al_2O_3. Thirty-three out of thirty-six analyses of individual phases totaled between 98.0 and 102.0, and the remaining three are only slightly outside these limits.

The analytical techniques used in this study have been shown to yield an accuracy within $\pm 2\%$ of the amount of a major element present in a relatively coarse-grained sample (Boyd, 1969). The fine-grained run products produced in these experiments are inherently more difficult to analyze, but the reproducibility and internal consistency of a majority of the results shown in Figs. 14 and 15 are within error limits of ± 2 relative %. Inasmuch as the absolute error of a probe analysis depends upon the amount of an element present, this error will generally not be the same for each element in a given analysis. Ideally, the points plotted in Figs. 14 and 15 should show this variable absolute error, but to do so obscures the visual presentation of the data. A simpler but less rigorous procedure has been adopted wherein the size of the data points in Figs. 14 and 15 corresponds to a relative error of $\pm 1\%$ for a composition in the center of the ternary.

Phase relations for two of the bounding joins, $CaMgSi_2O_6$-$MgSiO_3$ (Davis and Boyd, 1966) and $MgSiO_3$-$Mg_3Al_2Si_3O_{12}$ (Boyd and England, *Year Book 63*), have been reversed by the same high-pressure techniques at the same pressure and temperature as were used to study ternary compositions. Reversing ternary solid solution fields is obviously a more complex problem than reversing solvus curves in binary systems. Reversal experiments within the ternary have not yet been attempted, and it will be necessary to study the ternary under *P-T* conditions where these solid solution fields are both more extensive and more limited to provide starting materials for such experiments.

Quenching Experiments in the Systems Jadeite ($NaAlSi_2O_6$)-Forsterite (Mg_2SiO_4) and Jadeite ($NaAlSi_2O_6$)-Anorthite ($CaAl_2Si_2O_8$)

H. K. Mao and J. F. Schairer

Behavior of the components jadeite, forsterite, and anorthite is important in the interpretation of deep-seated igneous processes. During the past year we have prepared mixtures of pure jadeite, jadeite with 5, 15, 25, and 35 wt % of forsterite, and jadeite with 5, 15, 25, and 35 wt % of anorthite to carry out a study of these systems at low and high pressure. This report describes results obtained by the quenching method at 1 atm.

Schairer and Yoder (*Year Book 64*, p. 106) studied the system forsterite-nepheline-silica. Jadeite-forsterite is a join through this system. Results of the present quenching experiments agree with the value of 1068° ± 5°C (Greig and Barth, 1938) for the binary eutectic between nepheline and albite. The value 1138° ± 5°C (Yoder, 1950, p. 316) was confirmed for the nepheline liquidus for jadeite composition. Additional confirmation was obtained for the value 1058° ± 5°C (Schairer and Yoder, *Year Book 60*, p. 142) for the ternary eutectic among nepheline, albite, and forsterite from the compositions $Jd_{95}Fo_5$, $Jd_{85}Fo_{15}$, $Jd_{75}Fo_{25}$, and $Jd_{65}Fo_{35}$. New data for the join jadeite-forsterite include the appearance of nepheline as a second solid phase at 1098° ± 5°C in all cases and the forsterite liquidus temperatures of 1197°, 1358°, 1428°, and 1478°C, respectively.

The join jadeite-anorthite lies in the system nepheline-albite-anorthite, and the results of quenching experiments on the compositions $Jd_{95}An_5$, $Jd_{85}An_{15}$, $Jd_{75}An_{25}$, and $Jd_{65}An_{35}$ are in good agreement with the data previously obtained by Schairer (unpublished data on the system

nepheline-anorthite-silica; see Schairer, 1957, p. 232, Fig. 35). In $Jd_{95}An_5$ the crystalline assemblage nepheline + plagioclase began to melt at 1048° ± 5°C and the nepheline liquidus was at 1153° ± 5°C. In $Jd_{85}An_{15}$, $Jd_{75}An_5$, and $Jd_{65}An_{35}$, respectively, nepheline + plagioclase began to melt at 1058°, 1073°, and 1085°C, the temperature shift being in response to the changing compositions of plagioclase. The plagioclase liquidus temperatures for these compositions were 1268°, 1333°, and 1378°C; nepheline appeared as a second solid phase at 1168°, 1197°, and 1213°C.

Experiments on the liquidus and in the subsolidus region in the range 10–50 kb have been started for all of the compositions prepared at 1 atm. It is hoped that an understanding of the influence of anorthite and forsterite on the behavior of jadeite at high pressure will be gained from these experiments. Combinations of anorthite, forsterite, and jadeite will clarify the roles of anorthite, calcium Tschermak's molecule, and diopside in the pressure-temperature stabilization of omphacite.

Diopside Solid Solutions in the System Diopside-Anorthite-Albite at 1 Atm and at High Pressures

I. Kushiro and J. F. Schairer

The liquidus relations in the system diopside-anorthite-albite were studied by Bowen (1915) at 1 atm for an understanding of the crystallization behavior of basaltic and dioritic magmas. Bowen (1928) described this system as the simplest example of a ternary system with a binary series of solid solutions. Osborn (1942) found, however, that the join diopside-anorthite is not binary and showed that diopside crystallizing from this join is not pure diopside but a solid solution containing some alumina. This result was confirmed by Hytönen and Schairer (*Year Book 60,* pp. 125–141) and Clark, Schairer, and de Neufville (*Year Book 61,* pp. 59–68). Schairer and Yoder (1960) also found that the join diopside-albite is not binary and showed that the feldspar crystallizing from this join is not pure albite but is a solid solution containing a small amount of the anorthite component and that the diopside is also a solid solution. These results suggest that the system diopside-anorthite-albite is not ternary and that the diopside crystallizing within this system is not pure diopside but a solid solution. The join diopside-plagioclase ($An_{50}Ab_{50}$ wt %) has been studied carefully to ascertain and define the nature of the diopside solid solution. Four compositions were selected along this join: (1) $Di_{70}An_{15}Ab_{15}$, (2) $Di_{50}An_{25}Ab_{25}$, (3) $Di_{42}An_{29}Ab_{29}$ and (4) $Di_{40}An_{30}Ab_{30}$ (wt %). Starting materials were glasses crystallized at temperatures between 1050° and 1175°C for 10 to 22 days.

The liquidus temperatures are 1318°, 1268°, 1237°, and 1233°C for compositions 1, 2, 3, and 4, respectively. Diopside solid solution is the liquidus phase for compositions 1, 2, and 3, and both diopside solid solution and plagioclase are the liquidus phases for composition 4. Composition 4 is, therefore, at the liquidus boundary between diospide solid solution and plagioclase. These liquidus results are nearly the same as those obtained by Bowen (1915); the temperatures at which diopside solid solution and plagioclase began to crystallize simultaneously, however, are 1251°, 1246°, 1237°, and 1233°C for compositions 1, 2, 3, and 4, respectively. Since the uncertainties of these temperatures are ±3°, these differences are significant. If diopside is of pure $CaMgSi_2O_6$ composition, diopside should be joined by plagioclase at the same temperature for all of these mixtures. The present results indicate, therefore, that diopside crystallizing in this system is not pure $CaMgSi_2O_6$ but a solid solution.

Determination of the temperature of beginning of melting was not easy because of the difficulty of detecting a small amount of glass in the fine-grained

products. In the present experiments, the temperature of beginning of melting has been estimated by whether the products are loose powder or fritted. If the products are barely fritted or fritted, the temperature of the run is considered to be above the beginning of melting. It is noted that temperatures estimated by this method could be slightly different from the temperature of beginning of melting. The glasses for these experiments were crystallized at 1080°C, a little below the beginning of melting, for 7 to 15 days. The temperatures of "beginning of melting" thus estimated are 1103°, 1115°, 1140°, and 1145°C for mixtures 1, 2, 3, and 4, respectively. They are considerably lower than 1200°C, the temperature of beginning of melting given by Bowen (1915) for the composition $Di_{50}(An_1Ab_1)_{50}$ (mole %), which lies very close to the present join. The temperature of "beginning of melting" increases systematically from composition 1 to composition 4. This evidence also indicates that diopside crystallizing in this system is a solid solution whose composition is off the plane diopside-anorthite-albite. The composition of liquids formed at temperatures at or near the "beginning of melting" (1100°–1150°C) should be very rich in albite, on the basis of the liquidus diagram of Bowen (1915). As suggested below, however, the liquid may be enriched in silica and off the plane diopside-anorthite-albite.

The unit-cell dimensions of diopside solid solutions crystallized from the mixtures $Di_{70}An_{15}Ab_{15}$ and $Di_{50}An_{25}Ab_{25}$ (wt %) have been determined to ascertain the nature of the solid solution. Least-squares refinement of the data from the powder X-ray diffraction patterns was carried out on the basis of $C2/c$ symmetry, with a program for the IBM 7094 digital computer by Burnham (*Year Book 61,* pp. 132–135). The reflections measured against the internal silicon standard were $\bar{2}23$, 150, 510, $\bar{4}02$, 041, $\bar{4}21$, $\bar{3}31$, 330, 311, 221, 002, $\bar{1}31$, $\bar{3}11$, 310, $\bar{2}21$, 220, and 021. The results are shown in Table 16, with the unit-cell dimensions of pure diopside determined by Clark, Schairer, and de Neufville (*Year Book 61,* pp. 59–68) and diopsides crystallized at high pressures from the mixtures $Di_{70}An_{15}Ab_{15}$ and $Di_{50}An_{25}Ab_{25}$. As

TABLE 16. Unit-Cell Dimensions of Diopside Solid Solutions Crystallized in the System Diopside-Anorthite-Albite at 1 Atm and at High Pressures

		a, Å	b, Å	c, Å	β, deg.	V, Å^3
	Pure diopside (Clark, Schairer, and de Neufville, *Year Book 61*)	9.745 ±0.001	8.925 ±0.001	5.248 ±0.001	105.87 ±0.01	439.08 ±0.07
a	$Di_{70}An_{15}Ab_{15}$ 1 atm, 1250°C, 3 days	9.741 ±0.002	8.918 ±0.001	5.253 ±0.001	105.98 ±0.02	438.72 ±0.19
b	$Di_{70}An_{15}Ab_{15}$ 1 atm, 1080°C, 8 days	9.722 ±0.003	8.905 ±0.002	5.254 ±0.003	106.12 ±0.03	436.96 ±0.38
c	$Di_{50}An_{25}Ab_{25}$ 1 atm, 1235°C, 7 days	9.738 ±0.002	8.914 ±0.001	5.253 ±0.001	106.06 ±0.02	438.19 ±0.20
d	$Di_{50}An_{25}Ab_{25}$ 1 atm, 1080°C, 8 days	9.715 ±0.004	8.884 ±0.003	5.265 ±0.003	106.23 ±0.03	436.31 ±0.38
e	$Di_{70}An_{15}Ab_{15}$ 25 kb, 1350°C, 2 hours	9.672 ±0.005	8.855 ±0.004	5.263 ±0.004	106.28 ±0.06	432.67 ±0.53
f	$Di_{50}An_{25}Ab_{25}$ 30 kb, 1350°C, 2 hours	9.622 ±0.007	8.787 ±0.004	5.267 ±0.004	106.52 ±0.06	426.93 ±0.55

shown in the table, the unit-cell dimensions of the diopsides crystallized at 1 atm are significantly different from that of pure diopside; *a, b,* and unit-cell volume *V* of these four diopsides are smaller and *c* and β are slightly larger than those of pure diopside. Particularly, the diopsides crystallized at 1080°C for 8 days show greater differences of unit-cell parameters from those of pure diopside. The diopsides crystallized at 1240°C from the mixture $Di_{70}An_{15}Ab_{15}$ and at 1235°C from the mixture $Di_{50}An_{25}Ab_{25}$ coexisted only with liquid, whereas those crystallized at a subsolidus temperature of 1080°C coexisted with plagioclase. The variation in the unit-cell parameters is similar to those observed for the clinopyroxenes formed in the joins diopside-$CaAl_2SiO_6$ and diopside-anorthite at high pressures (Clark, Schairer, and de Neufville, *Year Book 61,* pp. 59–68; Kushiro, 1969), suggesting that the differences between the unit-cell dimensions of these diopside solid solutions and those of pure diopside are mainly due to the presence of Ca-Tschermak's component. However, the $MgSiO_3$ component would also be present in these clinopyroxenes, since the diopside solid solutions in the join diopside-anorthite contain measurable amounts of excess $MgSiO_3$ at about 1150°C, as shown by Hytönen and Schairer (*Year Book 60,* pp. 125–141). Jadeite solid solution is also possible but would not be significant at 1 atm. On the assumption that the differences in the unit-cell dimensions of these diopsides are essentially due to the presence of the Ca-Tschermak's component, the contents of the Ca-Tschermak's component can be estimated roughly from the relations between the unit-cell parameters and compositions of the clinopyroxenes crystallized from the join diopside-$CaAl_2SiO_6$ (Clark, Schairer, and de Neufville, *Year Book 61,* pp. 59–68). The contents thus estimated are about 3, 10, 5, and 13 wt % $CaAl_2SiO_6$ for diopsides *a, b, c,* and *d* in Table 16, respectively. The content of $CaAl_2SiO_6$ is larger for the clinopyroxene crystallized from the more plagioclase-rich mixture and also at lower temperatures. If the relation between composition and *d* values of the (510) and (150) planes of diopside solid solutions given by Hytönen and Schairer is used, the present diopside solid solutions contain about 3 to 7% Al_2O_3 and up to about 8% excess $MgSiO_3$.

The presence of the $CaAl_2SiO_6$ and excess $MgSiO_3$ components (and possibly a very small amount of $NaAlSi_2O_6$) in diopside solid solutions crystallizing from the present system indicates that the liquids coexisting with the diopside solid solutions must be off the plane diopside-anorthite-albite and contain excess silica and $CaSiO_3$ components, and that free silica must exist at temperatures below the solidus at 1 atm. No reflections of silica minerals were detected, however, in the powder X-ray diffraction patterns of the mixtures crystallized at subsolidus temperatures. This could be explained by a diopside solid solution containing a small amount of excess silica, suggested by Schairer and Kushiro (*Year Book 63,* pp. 130–132), but the amount of excess silica would be very small at temperatures below 1300°C, as they suggested. Even if the silica mineral is present in the products, it may be in too small amount to be detected by X ray. Under the microscope, crystals formed at subsolidus temperatures are very fine grained and the presence of the silica mineral was not confirmed.

The subsolidus phase relations in the join diopside-plagioclase ($An_{50}Ab_{50}$ wt %) have been studied in the pressure range 15 to 31 kb at 1150° and 1350°C with the solid-media, piston-cylinder apparatus. The starting materials were glass and glass crystallized at 1 atm. At 1150°C, only glass was used because the crystalline mixtures did not react at this temperature even in long runs. At 1350°C, it was shown that the results obtained from glass are identical with those obtained from the crystalline mixtures. The subsolidus phase relations at

1150°C are shown in Fig. 17. As shown in the figure, the range of the clinopyroxene (diopside solid solution) + quartz assemblage expands to about 30 wt % $CaAl_2Si_2O_8 + NaAlSi_3O_8$ at 20 kb and 1150°C, indicating that the clinopyroxene contains about 25 wt % $CaAl_2SiO_6$ and $NaAlSi_2O_6$ components at 20 kb and 1150°C. The range of the solid solution may attain its maximum at about 25 kb and 1150°C. More detailed subsolidus phase relations are described elsewhere (Kushiro, 1969).

The unit-cell dimensions of diopside solid solutions crystallized from the mixtures $Di_{70}An_{15}Ab_{15}$ and $Di_{50}An_{25}Ab_{25}$ at 25 and 30 kb at a subsolidus temperature of 1350°C are shown in Table 16. The parameters *a, b,* and *V* of these clinopyroxenes are much smaller than those of pure diopside and the diopside solid solutions crystallized at 1 atm. These high-pressure diopside solid solutions, which coexist only with quartz, must contain jadeite as well as Ca-Tschermak's component.

The results of the present experiments indicate that diopside or augite crystallizing from silica-saturated basaltic magmas at 1 atm would contain small amounts (up to several weight percent) of $CaAl_2SiO_6$ and excess $MgSiO_3$ components. Those crystallizing from silica-undersaturated basaltic magmas would contain more $CaAl_2SiO_6$ and less $MgSiO_3$ components, on the basis of the results of Hytönen and Schairer (*Year Book 60*, pp. 125–141) and de Neufville and Schairer (*Year Book 61*, pp. 56–59). Present results also indicate that the plane

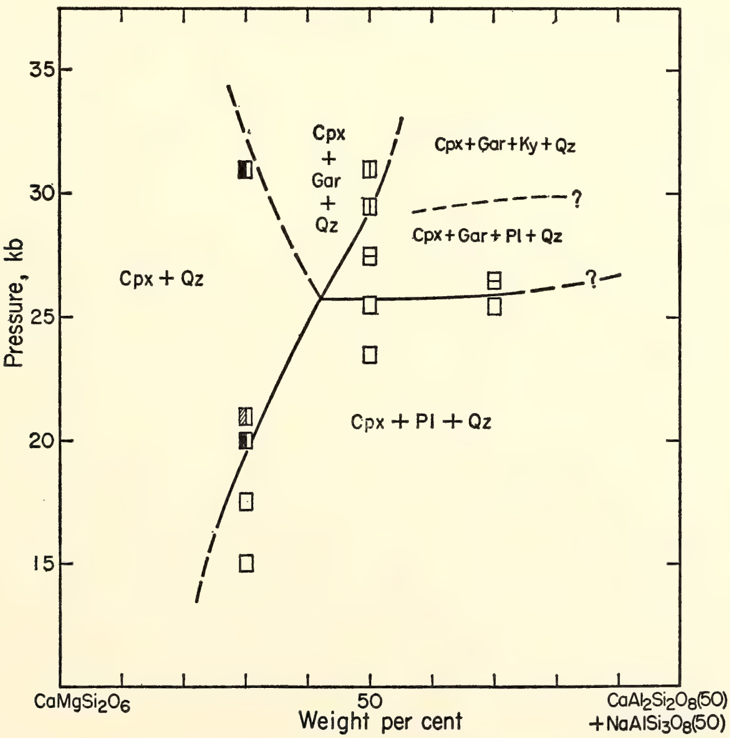

Fig. 17. Subsolidus phase-equilibrium relations on the join diopside-plagioclase ($An_{50}Ab_{50}$ wt %) at 1150°C. Abbreviations: Cpx, clinopyroxene (diopside solid solution); Gar, garnet; Ky, kyanite; Pl, plagioclase; Qz, quartz.

diopside-anorthite-albite is not ternary and is not a thermal barrier between silica-saturated and silica-undersaturated compositions at 1 atm nor at high pressures.

Stability Field of Iron-Free Pigeonite in the System $MgSiO_3$-$CaMgSi_2O_6$

I. Kushiro and H. S. Yoder, Jr.

Iron-free "pigeonite" has been synthesized on the join diopside-enstatite at 20 kb, and its stability field at 20 kb has been outlined (Kushiro, *Year Book 67,* pp. 80–83; 1969). Since pigeonite occurs in igneous rocks crystallized on or near the surface of the earth's crust, it is important to understand the stability field of pigeonite at lower pressures. Therefore, additional experiments have been undertaken to determine the stability field of iron-free "pigeonite" at lower pressures. The starting materials used in the present experiments were several different crystalline mixtures and glass of the composition $Di_{20}En_{80}$ (wt %) whose Ca/(Ca+Mg) atomic ratio is very close to the Ca/(Ca+Mg+Fe^{2+}) ratios of natural pigeonites. In the previous experiments a mixture of this composition was crystallized to a single-phase pigeonitic clinopyroxene at 1630°C and 20 kb. In the present experiments a solid-media, piston-cylinder apparatus was used for the runs at pressures higher than 10.5 kb and a gas-media, internally heated apparatus for those at and below 10 kb. The gas-media apparatus is considered to generate hydrostatic pressure, whereas the piston-cylinder apparatus has some shearing effects.

The experimental results are shown in the pressure-temperature diagram (Fig. 18). The boundary between the field of a single-phase pigeonitic clinopyroxene and that of orthoenstatite solid solution +pigeonitic clinopyroxene for the composition $Di_{20}En_{80}$ is about 1540°C at 20 kb, about 1480°C at 15 kb, and about 1430°C at 12.5 kb. The lower stability limit of the pigeonitic clinopyroxene, which is more important, may be a little below 1480°C at 20 kb, about 1450°C at 17.5 kb, and a little above 1400°C at 12.5 kb. At 17.5 and 20 kb, the amount or orthoenstatite solid solution relative to that of pigeonitic clinopyroxene in the Pig+En_{ss} field decreases with increasing temperature. These relations are interpreted in a schematic diagram of the enstatite-rich part of the join diopside-enstatite at 17.5 kb (Fig. 19).

At and below 10 kb, three or four different starting materials were used in a single run. Many of the results are different for different starting material, and they are described below in more detail. At 10 kb, clinoenstatite and diopside solid solutions were not reacted but converted to a mixture of orthoenstatite and diopside solid solutions, held for 4 hours at 1350° and 1375°C and for 2 hours at 1400° and 1425°C. Orthoenstatite solid solution grew from a single-phase pigeonitic clinopyroxene, and glass was crystallized to orthoenstatite and diopside solid solutions at 1350° and 1375°C. The results indicate that pigeonitic clinopyroxene is not stable but orthoenstatite and diopside solid solutions are stable at 1350° and 1375°C at 10 kb. At 1450°C, neither the mixtures of clinoenstatite and diopside solid solutions nor orthoenstatite and diopside solid solutions were reacted, and mixtures of orthoenstatite and diopside solid solutions were obtained in the 4-hour run; however, glass was crystallized into a single-phase pigeonitic clinopyroxene under the same conditions. The temperatures at least above 1400°C would be in the stability field of pigeonitic clinopyroxene at 10 kb if the stability field determined at pressures higher than 12.5 kb can be extrapolated to 10 kb. Therefore, three runs made on the crystalline mixtures at 1400°, 1425°, and 1450°C do not agree with the phase relations determined at higher pressures, although the runs made on glass at 1350°, 1375°, and 1450°C are consistent with those at higher pressure. In the

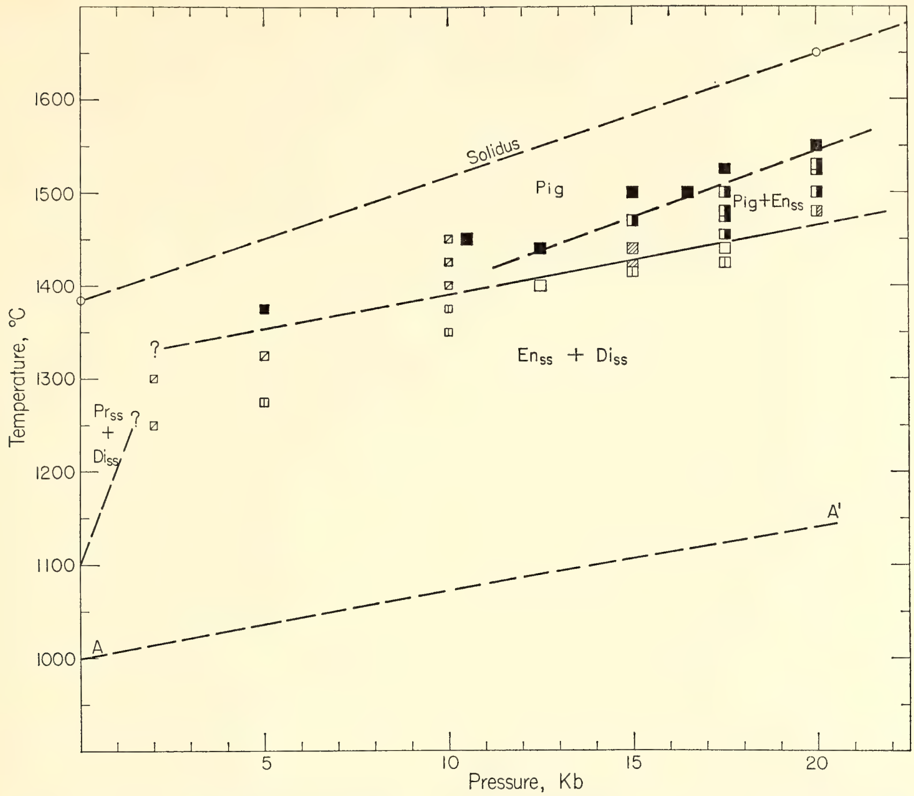

Fig. 18. Pressure-temperature plane for composition $Di_{20}En_{80}$ (wt %). Abbreviations: Pig, pigeonitic clinopyroxene; Di_{ss}, diopside solid solution; En_{ss}, orthoenstatite solid solution; *L*, liquid; Pr_{ss}, protoenstatite solid solution. Symbols: solid square, Pig formed from En_{ss} + Di_{ss} or clinoenstatite$_{ss}$ + Di_{ss}; half-solid square, Pig + En_{ss} formed from En_{ss} + Di_{ss} or clinoenstatite$_{ss}$ + Di_{ss}; shaded square, Pig unchanged; half-shaded square, Pig + En_{ss} formed from Pig; square with vertical line, En_{ss} + Di_{ss} formed from clinoenstatite$_{ss}$ + Di_{ss}; open square, En_{ss} + Di_{ss} formed from Pig; square with diagonal line, run that is not satisfactorily interpreted (see text). Dashed line *A–A'* is the lower stability limit of pigeonite ($Wo_{7.6}En_{40.7}$-$Fs_{51.7}$ mole %) determined by Brown (*Year Book 66,* pp. 347–353).

solid-media apparatus, orthoenstatite and diopside solid solutions were reacted to form a single-phase pigeonitic clinopyroxene at 10.5 kb and 1450°C in the 3-hour run, whereas they were not reacted at 10 kb and 1450°C in the 4-hour run made with the gas-media apparatus. The discrepancy between the results obtained by the gas-media and the solid-media apparatus suggests that the nonhydrostatic pressure in the solid-media apparatus stabilizes the pigeonitic clinopyroxene in wider *P-T* ranges or the reaction rate is greater in the solid-media apparatus than in the gas-media apparatus.

At 5 kb and 1375°C, a mixture of orthoenstatite and diopside solid solutions was reacted to form orthoenstatite solid solution and pigeonitic clinopyroxene, and glass crystallized to pigeonitic clinopyroxene in the 6-hour run. These results indicate that the composition $Di_{20}En_{80}$ is in the field of pigeonitic clinopyroxene or of pigeonitic clinopyroxene + orthoenstatite solid solution at 1375°C. At 1325°C, glass was crystallized to pigeonitic clinopyroxene, and

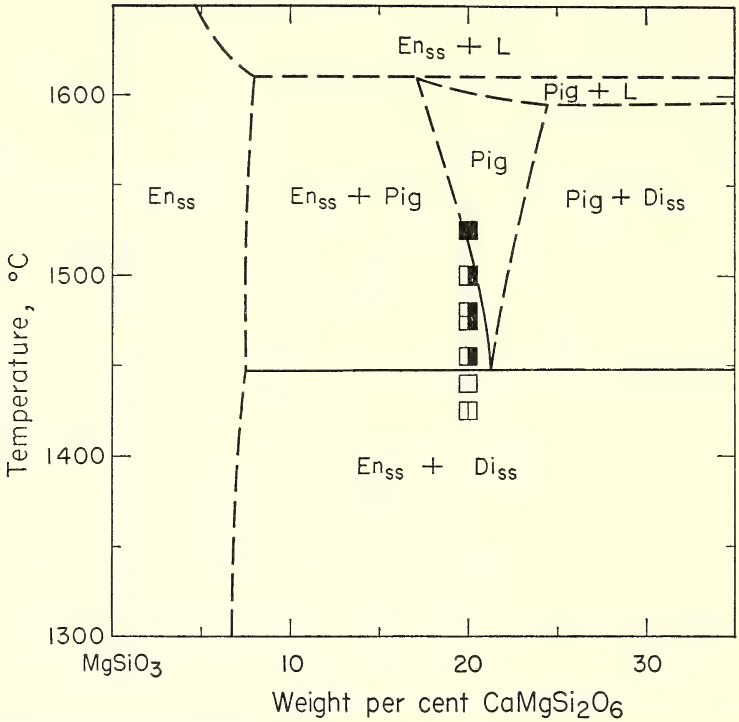

Fig. 19. Schematic diagram showing the phase relations for composition $Di_{20}En_{80}$ (wt %) at 17.5 kb. Abbreviations as in Fig. 18.

pigeonitic clinopyroxene was unchanged; however, a mixture of clinoenstatite and diopside solid solutions was converted to a mixture of orthoenstatite and diopside solid solutions in the 24-hour run. These results are ambiguous, presumably because of the different starting materials. The results obtained from glass and pigeonitic clinopyroxene suggest the stability of pigeonitic clinopyroxene at 1325°C, but the result obtained from the mixture of clinoenstatite and diopside solid solutions fails to confirm this possibility. This same problem is encountered at 10 kb and 1450°C. At 2 kb, the results obtained at 1300° and 1250°C are nearly the same as those obtained at 5 kb and 1325°C. These results strongly suggest that the reaction rates, particularly those of the homogenization of two pyroxenes and the breakdown of a single pyroxene, are very slow at relatively low pressures and temperatures.

Although there are problems with reaction rates and a discrepancy in the results between the solid-media and gas-media apparatus, the present experiments indicate that the stability field of pigeonitic clinopyroxene exists near the composition $Di_{20}En_{80}$ in the pressure range at least between 20 and 5 kb and near the solidus temperatures. It is likely that the stability field of pigeonitic clinopyroxene extends to lower pressures and possibly to 1 atm. At pressures lower than 2 kb, however, the field of protoenstatite solid solution may appear even near the composition $Di_{20}En_{80}$ and the phase relations may be more complicated. In the iron-bearing system the stability field of pigeonite will be more easily determined because of a more favorable reaction rate. For the compositions $Wo_{7.6}En_{40.7}Fs_{51.7}$ (mole %), Brown (*Year Book 66*, pp. 347–353) determined the lower stability limit of pigeonite in the

pressure range 1 atm to 20 kb, shown for comparison in Fig. 18. Comparison of the present results and those of Brown suggests that the lower stability limit of pigeonite drops about 300°C from the iron-free composition to the composition having the ratio $Fe/(Mg+Fe)=0.56$ in the pressure range from near 1 atm to 20 kb. It should be mentioned that temperatures of basaltic and andesitic magmas (1250°–1100°C) are between the lower stability limit of pigeonite estimated in the iron-free system and that in the ratio $Fe/(Mg+Fe)=0.56$ at pressures lower than 5 kb. The evidence that the natural pigeonites have $Fe^{2+}/(Mg+Fe^{2+})$ ratios larger than 0.3 can be explained by the magma temperatures crossing the lower stability limit of pigeonite at the $Fe^{2+}/(Mg+Fe^{2+})$ ratio near 0.3, as first suggested by Hess (1941).

Stability of Iron-Rich Orthopyroxene

Douglas Smith

Orthopyroxene occurs in most rocks instead of the compositionally equivalent assemblage of olivine+quartz. In rocks with high Fe/Mg ratios, however, the assemblage olivine+quartz is more common than orthopyroxene. The iron end member of the orthopyroxene series, ferrosilite, was shown to be stable at high pressures relative to fayalite and quartz by Lindsley, MacGregor, and Davis (*Year Book 63*, pp. 174–176) and by Akimoto, Fujisawa, and Katsura (1964). The purposes of this investigation were (1) to establish limits of orthopyroxene stability as a function of pressure and composition for possible use as a barometer for rocks of crustal origin and (2) to provide a basis for subsolidus investigations in the iron-rich portion of the pyroxene quadrilateral. The only previous comprehensive investigation of the relative stabilities of orthopyroxene and olivine in the system $FeO\text{-}MgO\text{-}SiO_2$ was made by Bowen and Schairer (1935); experimental limitations at that time precluded studies with iron-rich synthetic phases at temperatures much below 1000°C.

The relative stabilities of these minerals were investigated over a range of pressures and temperatures. Either orthopyroxene or olivine+silica was used as a starting material for each experiment. Equimolar mixtures of silica and olivine of the desired compositions were made from oxide mixes in evacuated silica glass tubes and in controlled gas mixtures. Silica was present as glass, quartz, and tridymite in various starting materials. Orthopyroxenes were synthesized at 20 kb from mixtures of olivine+silica in a large volume, piston-cylinder apparatus. All hydrothermal runs were conducted in the presence of excess silica, added to saturate the fluid phase.

The experimental results shown in Fig. 20 clearly establish that the most iron-rich orthopyroxene stable at temperatures of 800° to 950°C and pressures of 0.3 to 1 kb is more magnesian than $En_{25}Fs_{75}$. The results suggest that the actual composition of the most iron-rich orthopyroxene stable under these conditions is close to $En_{30}Fs_{70}$. In runs at 1000°C in evacuated silica glass tubes, orthopyroxenes of compositions $En_{30}Fs_{70}$ and $En_{25}Fs_{75}$ broke down to yield orthopyroxene, olivine, silica, and minor multiply twinned clinopyroxene in the quench product. The clinopyroxene presumably inverted from a proto form (Boyd and Schairer, 1964, p. 297).

In hydrothermal experiments at 1 kb and 800°C, olivine ($Fo_{20}Fa_{80}$) reacted with silica to form some orthopyroxene, whereas orthopyroxene ($En_{20}Fs_{80}$) partially broke down to olivine and silica. These results establish a point in the three-phase field orthopyroxene-olivine-silica in the system $FeO\text{-}MgO\text{-}SiO_2$. The hydrothermal experiments at 800°C in which olivine reacted with silica lasted about 80 days. In contrast, the hydrothermal experiments at 900° and 950°C lasted only a few days, and olivine as magnesian as $Fo_{35}Fa_{65}$ failed to react

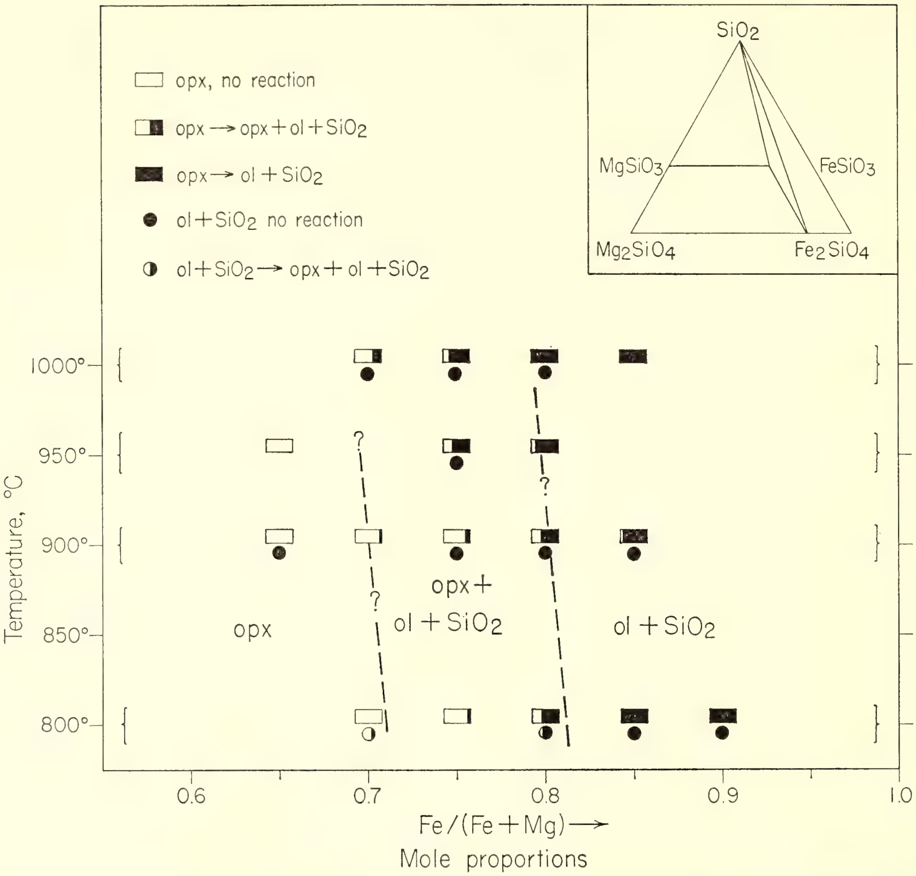

Fig. 20. Experimental results on orthopyroxene and on olivine plus quartz at low pressures. The brackets by the temperature axis of the figure indicate that the plotted experiments were conducted at 800°, 900°, 950°, and 1000°C, *not* at temperatures slightly above and below these values. Hydrothermal experiments at 800°C were conducted at 1 kb, and those at 900° and 950°C were conducted at 0.3 kb. Experiments at 1000°C were performed in evacuated silica-glass tubes. The amount of shading is approximately proportional to the amount of olivine + silica in the reaction products. The quartz-tridymite inversion and the inversion of orthopyroxene to a proto form have been ignored in drawing this diagram.

with silica during these time periods. Likewise, olivine and silica failed to react in evacuated tube experiments at 1000°C. Medaris (1969) has studied the partition of Fe and Mg between coexisting orthopyroxene and olivine at temperatures from 700° to 900°C. The Fe/(Fe+Mg) ratios of the two phases coexisting with silica should lie on the boundaries of the three-phase field as drawn in Fig. 20. The studies of Medaris show that the field (Fig. 20) should extend over an interval of Fe/(Fe+Mg) of about 0.1. Further experiments are being carried out to define more precisely the position of the three-phase field.

Experiments at high pressure at 900°C (Fig. 21) bracket at least part of the three-phase field orthopyroxene-olivine-silica within the pressure interval 10 to 11 kb for a bulk composition with Fe/(Fe+Mg) = 0.9 and within the interval 12 to 13 kb for Fe/(Fe+Mg) = 0.95. At

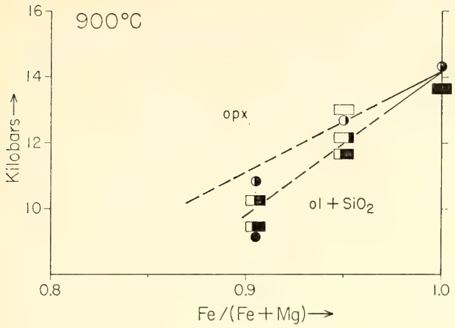

Fig. 21. Experimental results on orthopyroxene and on olivine + quartz at 900°C and high pressures. Symbols are the same as in Fig. 20.

900°C, pure orthorhombic ferrosilite was found to be stable above 14.5 kb. These experiments were conducted in a solid-media piston-cylinder apparatus by the modified piston-out procedure of Richardson, Bell, and Gilbert (1968, p. 517), and nominal, uncorrected pressures are reported here.

The experimental results establish that the most iron-rich orthopyroxene stable from 800° to 950°C at pressures lower than 1 kb is somewhat more magnesian than $En_{25}Fs_{75}$. This value contrasts with the limit of about $En_{15}Fs_{85}$ suggested by Bowen and Schairer (1935, Fig. 8). The present results also show that with increasing pressure, orthopyroxenes of progressively greater iron enrichment become stable, pure ferrosilite being stable at 900°C above 14.5 kb. Natural orthopyroxenes more iron-rich than $En_{25}Fs_{75}$ have been described (e.g., Henry, 1935; Kuno, 1954). Some such orthopyroxenes may have been stabilized by the presence of minor elements like calcium and manganese. Some may have formed at low pressure but at temperatures considerably below 800°C in a possible low-temperature expansion of the orthopyroxene field. Others may have been stabilized by high pressure. For instance, Wheeler (1965) described an olivine adamellite with complex intergrowths of calcic pyroxene, orthopyroxene, fayalitic olivine, and quartz in which the olivine and quartz apparently formed by the breakdown of orthopyroxene. Lindsley and Munoz (1969, p. 319) suggested that the orthopyroxene was initially stabilized by pressure. In this and other instances, the presence of high-iron orthopyroxene may serve as a useful geobarometer. At a given temperature and neglecting minor elements, the composition of orthopyroxene in the three-phase assemblage orthopyroxene-olivine-quartz uniquely characterizes the pressure of equilibration. The occurrence of iron-rich orthopyroxene alone may be useful in establishing a minimum pressure of formation if the temperature can be estimated by other means.

Stability of Potassic Richterite

*I. Kushiro and A. J. Erlank**

The occurrence of potassic richterite, a member of the alkali amphiboles, in a diopside-phlogopite nodule in the Wesselton kimberlite pipe, South Africa, is described in the preceding section. This discovery suggests that potassic richterite is a possible amphibole in the upper mantle. To examine this possibility, preliminary experiments have been conducted on the stability of potassic richterite at high pressures.

The starting material was a potassic richterite from a leucite lamprophyre from Wolgidee, Australia, collected by B. Mason. Partial analysis (Table 17) shows that it is similar in composition to that described originally by Wade and Prider (1940). The chemical composition of this richterite indicates that its chemical formula is close to $KNaCa(Mg,Fe,Ti)_5Si_8O_{22}(OH)_2$. Mixtures of this richterite and synthetic minerals were also used. The experiments were conducted in solid-media, piston-cylinder apparatus in sealed Pt capsules with water contents varying from 4.7 to 10.5 wt %.

* Department of Terrestrial Magnetism.

TABLE 17. Partial Analyses of Potassic Richterites by Electron Microprobe

	1	2		3		4
		Core	Rim	Core	Rim	
TiO_2	3.0	3.2	0.5	3.0	0.6	0.6
MgO	21.3	22.0	23.7	21.5	23.6	21.2
CaO	6.9	7.3	8.8	7.1	7.8	7.1
Na_2O	3.6	3.6	3.0	3.5	3.3	3.2
K_2O	5.6	5.6	4.6	5.7	5.0	4.7

1. Potassic richterite, starting material. Locality: Wolgidee, Australia.
2. Potassic richterite run at 30 kb, 1000°C, 3 hours.
3. Potassic richterite run at 30 kb, 1100°C, 2½ hours.
4. Potassic richterite, average of three grains, mica nodule, Wesselton kimberlite pipe, South Africa.

Potassic richterite in the runs at 30 kb, 1100°, and 1000°C, showed euhedral-subhedral crystals and appeared to have been well recrystallized. Very small amounts of rutile and very fine-grained unidentified granular crystals were observed with the richterite. Some relatively large richterite crystals had cores, which were slightly different in color and refractive indices from the marginal parts of the crystals. The cores would represent the original richterite, surrounded by the newly recrystallized richterite. These features suggested that electron-probe analysis of the products of these two runs would be worthwhile. Partial analyses of a few of the larger grains of this material, of the starting material, and of the Wesselton richterite described previously are given in Table 17. Analyses 1, 2, and 3 have not been corrected for matrix interference effects, as in the case of analysis 4. Because of the overall similarity of these materials, however, the trends shown in Table 17 are relatively accurate. It is clear from the analyses that the cores of the richterites in the runs at 1000° and 1100°C are similar to the starting material and the rims of these materials differ in composition, supporting the recrystallization process. The marked decrease in TiO_2 in the rim is readily accounted for by the presence of rutile in the reaction products. The slight depletion in Na_2O and K_2O is presumably related to solution in the vapor phase, whereas the increase in the CaO and MgO contents is simply a reflection of the above-mentioned decreases in concentration. Our second observation concerns the similarity in composition between the analyzed rims (recrystallized potassic richterites) and the potassic richterite found in the Wesselton kimberlite nodule. In particular the similarity in the low TiO_2 contents is striking. Because the original TiO_2-rich richterite is believed to have formed at very low pressures, it appears that the TiO_2 content of potassic richterite depends on pressure as well as bulk chemical composition.

In the run on the 1:1 mixture (by weight) of the richterite and pure diopside at 24 kb and 1000°C, richterite and diopside were well recrystallized and no other phases were observed after the run. These results indicate that, under water-saturated conditions, potassic richterite would be stable at least at 30 kb at 1100° and 1000°C and at least at 24 kb and 1000°C in the presence of diopside. In the run on the 2:1 mixture by weight of the richterite and the mixture of garnet composition (pyrope 2 grossular 1, by mole) at 20 kb and 1000°C, a considerable amount of phlogopite was crystallized and the assemblage was phlogopite + clinopyroxene + richterite. It is evident that potassic richterite and a mixture of garnet composition reacted to form phlogopite. In the event of complete reaction, the simplified process may be as follows.

$$\underset{\text{potassic richterite}}{KNaCaMg_5Si_8O_{22}(OH)_2} + \underset{\text{pyrope 2 grossular 1}}{CaMg_2Al_2Si_3O_{12}} =$$

$$\underset{\text{phlogopite}}{KMg_3AlSi_3O_{10}(OH)_2} + \underset{\text{omphacite}}{2CaMgSi_2O_6 \cdot NaAlSi_2O_6} + \underset{\text{enstatite}}{3MgSiO_3}$$

Part or all of enstatite may be dissolved in omphacite to make a complex clinopyroxene solid solution. In the present experiment the mole ratio of potassic richterite and garnet is nearly 1:1; potassic richterite is still present after the run, however, probably because of incomplete reaction or the effect of solid solution. Because of the fine-grained nature of the products, electron-probe analysis was not successful in determining in detail the compositions of pyroxene phases. The present experiment suggests that in the presence of garnet, potassic richterite reacts to form phlogopite and clinopyroxene or clinopyroxene+orthopyroxene. In the presence of spinel, potassic richterite may also react to form phlogopite, clinopyroxene, and forsterite. Potassic richterite and Ca-Tschermak's pyroxene component are also isochemical with phlogopite+omphacite. The phlogopite+diopside assemblage is stable in a wide pressure range, as shown elsewhere in this report, and the phlogopite+clinopyroxene (omphacite) assemblage would also be stable in a wide pressure range. It is suggested, therefore, that potassic richterite is not stable in the presence of garnet, spinel, or aluminous pyroxenes. The alumina content of diopside from the Wesselton nodule is only 0.71 wt %. To conclude, potassic richterite would not be expected to occur in eclogites and garnet- or spinel-bearing peridotites under equilibrium conditions. To the best of our knowledge it has not been found in rocks of this type occurring in kimberlite. Potassic richterite may, however, occur in alumina-poor pyroxenites and peridotites or in the rocks in which K is in excess over Al and is still present after forming phlogopite and/or other potassium minerals (e.g., K-feldspar and leucite). The occurrence of potassic richterite in the Wesselton nodule is explained by the presence of excess K over Al.

Potassium Contents of Synthetic Pyroxenes at High Temperatures and Pressures

A. J. Erlank and I. Kushiro*

Electron-probe analyses of presumed upper-mantle materials, in particular kimberlite nodules, have revealed that olivines, garnets, and orthopyroxenes in general contain <30 ppm potassium and hence do not play an important role in the distribution of potassium in the upper mantle. The K content of clinopyroxenes is considerably larger and is crucial when considering the production of basaltic liquids with K contents varying from 0.05 to 1.5%.

Garnet peridotites, such as those found in kimberlites, are often assumed to be the dominant rock type present in the upper mantle. Chrome diopsides from these nodules generally contain on the order of 100 ppm K or less. The highest concentrations measured to date by electron-probe analysis have been observed in two subcalcic diopsides (Boyd, *Year Book 66,* pp. 331–334); concentrations of 280 and 340 ppm K in these two pyroxenes have been measured in this study. Even allowing for 15% modal abundance for diopsides in garnet peridotite, the K content of the resultant assemblage does not satisfactorily account for the high K contents of alkali basalts, provided at least 1% direct partial melting is involved in the production of the basalt.

Potassium contents of eclogitic omphacites from African kimberlites are more difficult to interpret. Electron-probe analyses given elsewhere in this report demonstrate that the K distribution of omphacites is apparently bimodal, with some containing 20–150 ppm K and others 800–1400 ppm K. The comments expressed above with respect to the diopsides obviously apply to the low K omphacites. The K content of the second group is larger than expected, however,

* Department of Terrestrial Magnetism.

and is difficult to explain on crystal-chemical grounds. It is clear that the presence of clinopyroxene with K contents of this order as an upper-mantle phase would be important for controlling the distribution of K in basaltic liquids. Hence, it appeared desirable to seek confirmation for this feature.

We have attempted to determine experimentally the amount of K that could enter the clinopyroxene structure under upper-mantle conditions by reacting together, at high temperatures and pressures, various clinopyroxenes and potassium-rich phases and measuring the potassium content of the resultant pyroxenes by electron-probe analysis. The experiments were made in the pressure range 15 to 32 kb with a piston-cylinder type apparatus similar to that designed by Boyd and England (1960). Sealed Pt tubes were used for the hydrous runs. The starting materials are mechanical mixtures of the following materials: synthetic pure diopside made by Hytönen and Schairer; a mixture of phlogopite composition consisting of forsterite, quench forsterite, and glass; a mixture crystallized at 1 atm from a glass of composition anorthite 50 forsterite 50 (mole %); a natural omphacite from Kaminaljuyu, Guatemala, originally described by Foshag (1957), with a composition close to diopside 45 jadeite 55 (mole %) (Clark and Papike, 1968); and a natural potassic richterite from Wolgidee, Australia, which is similar in composition to that analyzed by Wade and Prider (1940) and is described elsewhere in this report (see Table 17, No. 1).

In all the hydrous runs, diopside and omphacite were recrystallized to euhedral or subhedral crystals even at subsolidus temperatures. During the electron-probe analysis for K the other two spectrometers were set for Ca and Mg, and comparison of the starting materials and reactants indicated the recrystallization of the clinopyroxenes. Additional measurements for Na also revealed the nature of the pyroxenes formed. Phlogopite occurs as hexagonal plates forming thick books; when glass is present, however, it often appears as feathery crystals, believed to be quench crystals. Richterite that had been ground finely was also recrystallized to relatively large, euhedral or subhedral crystals. Because of recrystallization in the presence of excess vapor, equilibrium is believed to have been attained in the hydrous runs. In the anhydrous run made for the 1:1 mixture of diopside and phlogopite composition, the temperature was raised above the solidus to secure equilibrium.

A great deal of difficulty has been experienced in making the electron-probe measurements. The small size of the reaction products necessitated the use of a 1–2 μm electron beam and low sample current (0.025 μa), with resultant low intensity. The main problem has, however, been caused by the presence of minute inclusions and intergrowths of these crystals with K-rich phases (phlogopite and glass), frequently resulting in anomalously high K contents for apparently clear clinopyroxene grains. Consequently several runs have been discarded, and only those measurements in which a fair amount of consistency has been established are reported here. Particular care has been taken in making background measurements, often by using the pure starting materials, which were always mounted together with the reaction products. It is to be noted that the results have been corrected only for background and drift, but it is believed that they are accurate to within 10–20% of their true values; this level of accuracy is adequate for present purposes. A detailed account of the technique used will be given elsewhere.

The assembled data are listed in Table 18. It is immediately apparent that regardless of variation in mineral assemblage, temperature, pressure, and water content, the amount of K that has entered the clinopyroxene reaction products is small, <150 ppm. Even where clinopyroxene has crystallized directly

TABLE 18. Potassium Contents of Synthetic Clinopyroxenes and Garnets

Reactants	P, kb	T, °C	Duration, hours	H_2O %	Products	K in Clinopyroxene, ppm
Di + Anhy Phl (1:1)	15	1100	4	11.4	Di, Fo, Phl, Gl, gl	140
	30.5	1150	3⅔	13.1	Di, Fo, Phl, Gl, gl	90
	32	1000	4	4.6	Di, Phl, gl	70
	21	1450	2¼	...	Di, Fo, Gl	140
Omph + Anhy Phl (1:1)	25	1000	5⅙	5.0	Omph, Phl	110
(2:1)	25	1000	6	40.0	Cpx, Phl, Fo, gl	50
(1:1)	26.5	1050	4	7.4	Cpx, Phl, Gl	<50
	30	1100	3	22.2	Cpx, Fo, Phl, gl	50
Rich + An_1Fo_1 (2:1)	20	1000	3	4.7	Rich, Phl, Cpx	120
Rich + Di (1:1)	24	1000	2	10.4	Rich, Cpx	<50
						K in garnet, ppm
Anhy Phl + An_1Fo_1 (1:4)	30	1100	3	12.6	Gt, Cpx, Phl	<50
Phl *	70	1500	⅔	...	Gt, Phl, q-Phl, X	<100

* Run prepared by Kushiro, Syono, and Akimoto (1967).

Abbreviations: Di, diopside; Anhy Phl, anhydrous phlogopite composition; Phl, phlogopite; Fo, forsterite; Gl, glass; gl, glass balls considered to be quenched vapor; Omph, omphacite; Cpx, clinopyroxene solid solution; Rich, potassic richterite; Gt, garnet; An_1Fo_1, crystalline mixture of anorthite and forsterite (1:1 by mole) = pyrope-grossular (2:1 by mole); q-Phl, quench phlogopite; X, unknown phase.

from liquid under anhydrous conditions and in the absence of phlogopite, nearly all the K has remained in the liquid, as measured by the K content of ~13% in the glass. At this stage it is not clear to what extent variations in temperature, pressure, and sodium content affect the substitution of potassium. These results seem in accord with the natural diopsides and low K omphacites previously discussed, and no experimental evidence has been found to explain the presence of 1000–1500 ppm K in omphacite. The most likely explanation appears to be that these high K contents are due to the presence of submicroscopic intergrowths of amphibole in the omphacite structure, as suggested by J. J. Papike (personal communication, 1968) on the basis of X-ray studies. This possibility has important implications regarding the genesis of eclogites and basaltic lavas, and requires further confirmation. In the runs with amphibole and pyroxene no reaction has occurred between these minerals.

Also given in Table 18 are measurements made on garnets produced in two runs. Potassium was not detected in either one. One of the runs had previously been analyzed with an electron probe, and up to 5.8% K was reported in the garnets (Kushiro, Syono, and Akimoto, 1967*b*). The original electron-probe section was available, and further study showed that the earlier analysis was in error. The discrepancy is most likely due to the beam overlapping high K mica in the original analysis. During the analysis of this section, one of the breakdown products of phlogopite was found to have a very high potassium content (phase X in Table 18). Semiquantitative analysis indicates that this phase has on the order of 29% K_2O and 32% MgO but an anomalously low SiO_2 content of 1% or less. Unfortunately, the fine-grained nature of this phase and poor surface of the section prevented proper analysis, and it is not possible at this stage to identify this phase. It seems clear that clinopyroxenes and garnets will not accept sufficient potassium in their structures, even at high temperatures and pressures, to provide that required to form basalt by simple partial

melting. In this case, the rocks that are parental to basalt must contain potassium-rich phases such as phlogopite and/or K-rich amphibole.

HYDROUS SYSTEMS

Phlogopite-H_2O-CO_2: An Example of the Multicomponent Gas Problem

H. S. Yoder, Jr.

The study of phlogopite-H_2O by Yoder and Kushiro (1969) revealed extensions of the stability field of phlogopite in the absence of a gas phase and documented the existence of new melting relationships of hydrous phases where gas is absent. It was suggested that melting in the mantle was best approximated by gas-absent conditions rather than gas-present conditions because of the belief that the H_2O content of the mantle was very small and was mainly in hydrous minerals.

Many rocks contain other potentially gaseous components in addition to water, and it is pertinent to investigate the effects of these components on the melting behavior of hydrous minerals. For example, excluding those minerals in rock fragments adventitiously incorporated, the rock kimberlite consists primarily of olivine, phlogopite, and calcite. The presence of the latter two minerals implies H_2O and CO_2 in the magma if such existed. Inclusions in olivine from some nodules in kimberlite contain both liquid and gaseous CO_2, as well as H_2O (Roedder, 1965, p. 1760, 1764). The effect of CO_2 on the melting of phlogopite is, therefore, relevant to the general problem of melting under conditions where the H_2O pressure is less than the total pressure.

Phlogopite-H_2O

The join $K_2O \cdot 6MgO \cdot Al_2O_3 \cdot 6SiO_2$-$H_2O$ was first restudied in the more H_2O-rich compositions (Fig. 22), following the experimental procedures of Yoder and Kushiro (1969). The boundary between the forsterite (Fo) + liquid (L) + gas (G) region and the Fo + G region was delineated for $P = 10$ kb and $T = 1225°C$. The criterion was the presence or absence of interstitial glass, which was presumed to represent in part the more siliceous liquid phase distinct from glass spheres believed to represent a portion of the less siliceous gas phase. The relations deduced from these data are shown in projection on the plane leucite:kalsilite (1:1 mole)-forsterite-H_2O. Only the gas compositions in the G region are believed to lie on the plane. The ratio of dissolved silicate to H_2O in the less siliceous gas in the Fo + L + G region appears to be about 1:1 by weight, whereas the ratio of silicate to water in the more siliceous liquid phase was previously determined to be about 4:1. Partial confirmation of the H_2O content of the more siliceous liquid is obtained from an examination of the inclusions in the larger forsterite crystals. Several types of inclusions were observed, which contained the following phases after quenching to room temperature and an undetermined pressure.

Most of the inclusions consisted of a glass with a very low index of refraction, containing a globule of liquid in which was suspended a small gas bubble in constant thermal motion. The relations in an exceptionally symmetrical inclusion from the Fo + L + G region are shown in the photograph of Plate 1A. Assuming that the inclusion is circular in cross-section, was entrapped at the conditions of the experimental run, and is solely representative of the total fluid phase, the volume proportions of silicate to H_2O can be calculated, neglecting mutual solubility at containment conditions and diffusion through the forsterite crystal. The silicate:H_2O is approximately 56:44 by volume and is approximately 74:26 by weight. In the light of the large possible errors, the agreement with the composition of the more siliceous liquid phase estimated by construction is surprising.

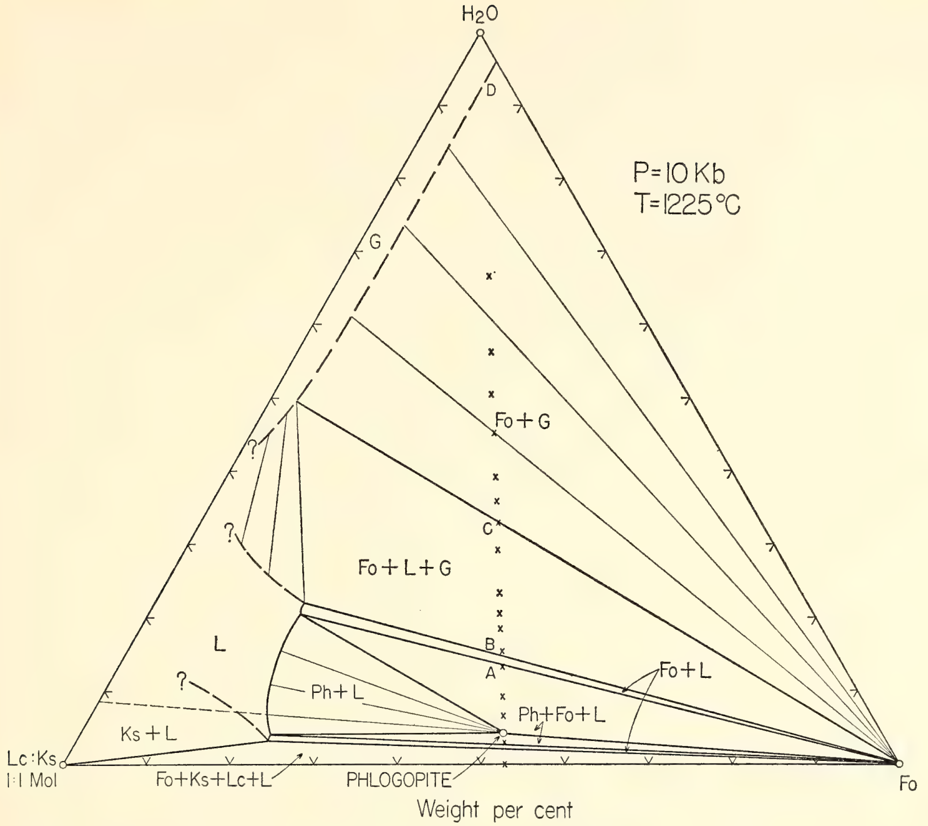

Fig. 22. The join phlogopite-H_2O in the pseudoternary section Fo-H_2O-Lc:Ks (1:1 mole) at 1225°C and 10 kb. Fo, forsterite; Ks, kalsilite; Lc, leucite; Ph, phlogopite; *G*, gas; *L*, liquid.

A second type of inclusion consisted of minute (<1 μm) spheres of water-rich fluid having a gas bubble in constant thermal motion. Glass may coat the inside of the sphere, but it was not resolved optically with certainty. This type of inclusion is presumed to be related to the gas phase; the proportions of its present constituents, however, seem to be at variance with the inferred gas composition. A third rare type consisted of glass, having a very low index of refraction relative to the forsterite, with a minute immobile bubble. It is believed to be representative of the less siliceous gas phase under the conditions of the run.

The inclusions in the forsterite in the Fo+*G* region were usually less than 1 μm in diameter. A few were about 2 μm in diameter and where resolvable appeared to be a water solution with a minute gas bubble in rapid thermal motion. The presence or absence of glass could not be ascertained with certainty.

Phlogopite-H_2O-CO_2

Known amounts of carbon dioxide were added to the $K_2O \cdot 6MgO \cdot Al_2O_3 \cdot 6SiO_2$-$H_2O$ join by using (1) requisite amounts of $KHCO_3$ with the remainder of the constituents as glass or (2) synthetic sanidine and a natural magnesite from Brazil. Two compositional lines were studied by adding various amounts of water to these powders in platinum capsules sealed by

welding. The resulting compositions run at 1225°C and 10 kb total pressure are plotted in Fig. 23 along with those from Fig. 22. The products in the two major fields Fo + L + G and Ph + Fo + G will be described. In the region Fo + L + G (Fig. 23) the products were euhedral to subhedral forsterite, balls of glass having a low, variable index of refraction, and some quench mica, concentrated mainly on the surface of the forsterite crystals. The glass balls were considered to represent part of the gas phase. No glass was observed that could be attributed to the liquid phase with certainty; the evidence provided by the inclusions in forsterite described immediately below, however, indicates the presence of a liquid phase during the run. The variation of index of refraction of the glass balls (due to diffusion of water out of the balls during and after quench) does not preclude the possibility that some of the glass balls may in fact represent liquid. On the other hand, supercritical phenomena may be involved where liquid and gas are no longer distinguishable. The forsterite contained a variety of inclusions, usually less than 2 μm and rarely reaching 10 μm on the longest dimension. Most consisted of a liquid with a minute gas bubble in rapid motion. Glass may coat the inside of the inclusion, and it is presumed that the CO_2 is in solution in the liquid or forms a thin invisible film of liquid CO_2 on the surface of the gas bubble. Rarely

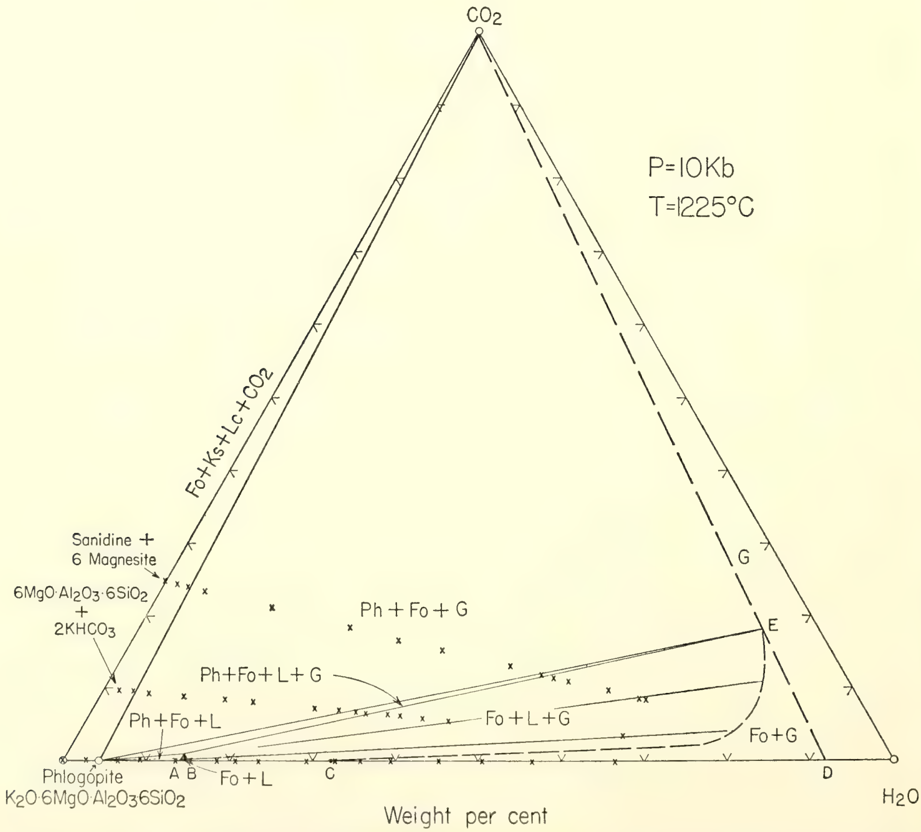

Fig. 23. The section $K_2O \cdot 6MgO \cdot Al_2O_3 \cdot 6SiO_2$-$H_2O$-$CO_2$ showing the compositions studied along three compositional joins. Points *A–D* are also illustrated in Fig. 22.

a liquid (mainly H_2O) inclusion was observed, containing a slowly moving large bubble of another liquid (mainly CO_2) which in turn contained a minute gas bubble (mainly CO_2) in rapid motion. Again, glass is assumed to coat the inside of the inclusion. Some inclusions consisted of glass with a liquid bubble (mainly H_2O) of moderate size (Plate 1B). The existence of these latter types of inclusion is taken as evidence that a liquid phase existed during the run, and the two former types of inclusion are taken as variant representatives of the gas phase.

In the region Ph + Fo + G (Fig. 23) the phases observed were faceted phlogopite (Ph), anhedral forsterite (Fo), and skins of glass of low index of refraction, giving way to glass balls as the H_2O content of the run increased to the boundary phlogopite-E. The glass skins and balls are interpreted as part of the gas (G) phase. The forsterite crystals contained minute inclusions, usually irresolvable in character, diminishing in number with decreasing H_2O content of the run. Where resolvable they consisted of glass with a minute immobile gas bubble or glass with a large liquid bubble containing a minute gas bubble in rapid motion. In one run a spectacular display of relatively large inclusions occurred in which glass, often containing a faceted crystal, held a liquid (mainly H_2O) having a large bubble of another liquid (mainly CO_2) and moving slowly under the heat from the microscope illumination (Plate 1C). Phlogopite contained no discernible inclusions, and many crystals of forsterite contained no inclusions (Plate 1D). Crystals of both minerals may be found in glass inclusions (Plate 1E) and appear to be faceted. Complex combinations of these inclusions were also observed (Plate 1F).

It was hoped that the study of the inclusions would aid in defining the nature of the fluid in both major assemblages. However, the wide variety of inclusions, the uncertainty of conditions under which the inclusions were incorporated in the growing crystal, i.e. during run-up or under the run conditions, the heterogeneous distribution of inclusions within and between crystals, and the changing of the immediate chemical environment about the growing crystal cast doubts on interpretation. Both forsterite and phlogopite grow exceptionally fast relative to other silicates in the laboratory, and yet one commonly entraps the surrounding fluid and the other does not. These phenomena of crystal growth preclude a definitive conclusion on the character of the fluid phase at the present state of knowledge. Similar difficulties arise from the interpretation of the variety of some of the fluid inclusions found in rocks from Ascension Island (Roedder and Coombs, 1967).

The region between Fo + L + G and Ph + Fo + G in Fig. 23 is presumed to consist of Ph + Fo + L + G, one fluid being relatively enriched in silicate components and the other relatively enriched in volatile components. Only two runs yielded products that suggested two fluid phases. There are too few data in the H_2O-poor region to the left of the join phlogopite-CO_2 to outline the various fields. The assemblage Ph + Fo + Lc + G was obtained where some H_2O was initially present, and Fo + Ks + Lc was obtained in the absence of H_2O. No data were obtained in the Ph + Fo + L or Fo + L region except in the absence of CO_2.

The principal observation is the expansion of the stability region of phlogopite in the presence of CO_2. Melting of phlogopite appears to be suppressed because of the relative insolubility of CO_2 in the liquid in equilibrium with phlogopite. Evaluation of these surprising results must await further study at other temperatures and pressures. It is likely that the proportions of CO_2:H_2O in the gas phase, determined herein to be about 1:4 at 1225°C and 10 kb, will change rapidly with T and P. The assumption of vapor-absent conditions in the mantle

will have to be reexamined if CO_2 and other gases relatively insoluble in silicate magmas are present in appreciable amounts. These factors also have important bearing on the genesis of diamond in kimberlite pipes, on kimberlite itself, and on the association of carbonatites with alkalic rocks.

Systems Bearing on Melting of the Upper Mantle under Hydrous Conditions

I. Kushiro

To understand the origin of magmas formed in the upper mantle, it is important to evaluate the effect of water on the liquidus relations of the systems containing components present in upper-mantle materials. Last year the liquidus relations of the system forsterite-diopside-silica-H_2O were studied at 20 kb (Kushiro, *Year Book 67,* pp. 158–161). The experiments have been extended to the systems forsterite-nepheline-silica-H_2O and forsterite-$CaAl_2SiO_6$-silica-H_2O, which contain most of the major components present in the suggested upper-mantle materials.

The System Forsterite-Nepheline-Silica-H_2O

Four compositions have been studied in the system forsterite-nepheline-silica-H_2O to determine the liquidus boundary between forsterite and enstatite solid solution, since this boundary is most relevant to the melting of the peridotitic composition. The compositions of four mixtures are shown by circles in Fig. 24.

The experiments were carried out in the pressure range 17.5 to 30 kb with a solid-media, piston-cylinder apparatus similar to that designed by Boyd and England (1960) and with sealed Pt capsules surrounded by powdered alumina. On the basis of the experimental results on the four compositions and those on the join forsterite-silica-H_2O at 20 kb (Kushiro, *Year Book 67,* pp. 158–159), the forsterite-orthopyroxene liquidus boundary at 20 kb is drawn (Fig. 24). It is noted that the boundary is projected from the H_2O apex onto the plane forsterite-nepheline-silica. The projected liquidus boundary at 17.5 kb is also shown in this figure. The water contents in these experiments were relatively high (22.8 to 42.5 wt %), and glass balls with low refractive index were observed in most of the runs. The glass balls are considered to be "quenched vapor" (Kushiro, Yoder, and Nishikawa, 1968; Yoder and Kushiro, 1969), and the experiments were under water-saturated or vapor-present conditions. Experiments have also been conducted with water content less than 9 wt %. In these experiments the orthopyroxene liquidus field is considerably expanded relative to that of forsterite.

The boundary and phase relations close to the join nepheline-silica are not certain because of the possible appearance of glaucophane on the liquidus in this low-temperature area. However, it is certain that the forsterite-orthopyroxene liquidus boundary under water-saturated conditions extends into the Ne-normative region at 20 kb above the temperature range where glaucophane could appear.

In Fig. 24, the forsterite-orthopyroxene liquidus boundary at 20 kb under anhydrous conditions determined by Kushiro (1968) is shown for comparison. It is nearly parallel with the boundary under water-saturated conditions at the same pressure but is located considerably on the silica-poor side of the latter.

On the basis of the results of the present experiments, it is indicated that the first liquid formed by melting of peridotitic mixtures consisting of forsterite and enstatite solid solution with small amounts of jadeite (or albite) component and water is silica saturated at 17.5 kb or less; however, the first liquid is critically silica undersaturated or Ne-normative at 20 kb. If partial melting proceeds at 20 kb, the composition of the liquid changes

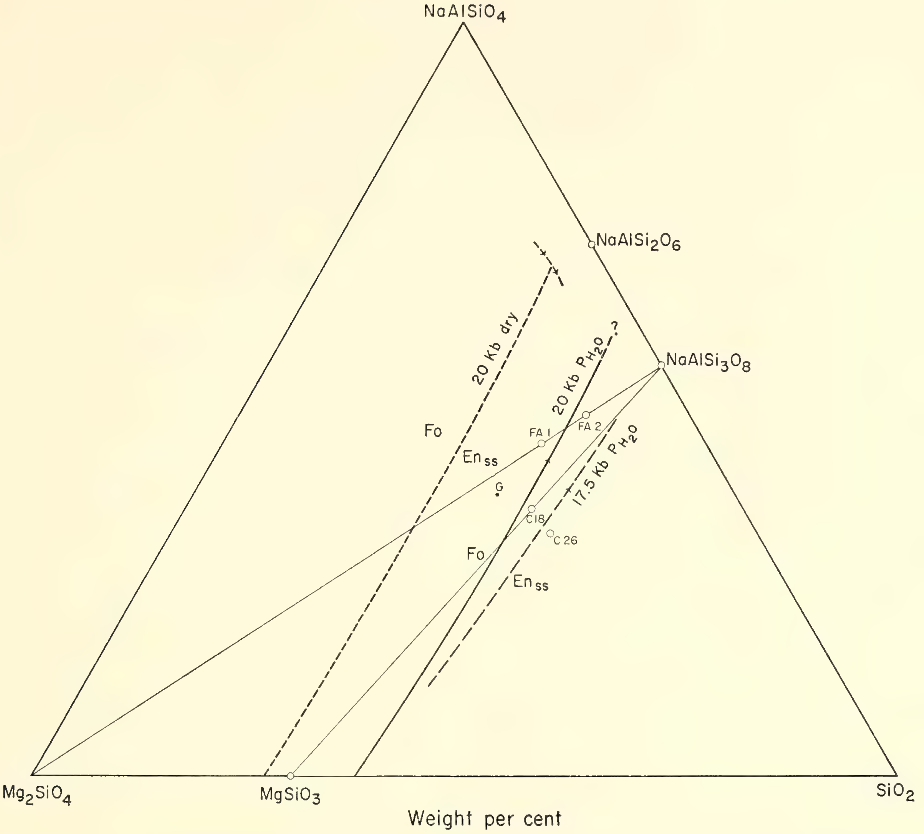

Fig. 24. The forsterite-orthopyroxene liquidus boundaries in the system forsterite-nepheline-silica-H_2O at 20 and 17.5 kb under water-saturated conditions, and at 20 kb under dry conditions. The boundaries under water-saturated conditions are projected from the H_2O apex onto the plane forsterite-nepheline-silica. Point *G* indicates the composition of anhydrous glaucophane.

from Ne-normative to (Ol+Hy) normative and further to Qz-normative. That the first liquid formed by partial melting of a peridotitic mixture is Ne-normative and the liquid formed after further melting is (Ol+Hy) normative and even Qz-normative appears to agree with the hypothesis on the genesis of alkali basalt and tholeiite proposed by Gast (1968) on the basis of the trace-element abundances in these basalts.

The present experimental results indicate that orthopyroxene may crystallize from the liquids of Ne-normative composition at pressures higher than 20 kb under water-saturated conditions as well as under anhydrous conditions. This may agree with some of the experiments by Baltitude and Green (1967), although their observation that the field of orthopyroxene expands relative to that of olivine under hydrous conditions is not in accord with the present results.

The System Forsterite-$CaAl_2SiO_6$-Silica-H_2O

The system forsterite-$CaAl_2SiO_6$-silica-H_2O is also important for understanding the liquids formed in the upper mantle under hydrous conditions. Five mixtures have been studied in the pressure range

15 to 33 kb and in the temperature range 1100° to 1150°C. The forsterite-orthopyroxene liquidus boundary at 20 kb is shown in Fig. 25, which is projected from the H_2O apex onto the plane forsterite-$CaAl_2SiO_6$-silica. The water content of the experiments ranges from 17.2 to 31.7 wt % (most of them are more than 20 wt %), and glass balls with low refractive index ("quenched vapor") were found in most of the runs. The conditions of the experiments are, therefore, considered to be water saturated or nearly water saturated. As shown in Fig. 25, the projected forsterite-orthopyroxene liquidus boundary under water-saturated conditions lies on the silica side of the join enstatite-anorthite, i.e., in the Qz-normative region at least at 20 kb. At 30 kb, forsterite is still on the liquidus for the mixture EAN-40, indicating that at least a part of the forsterite-orthopyroxene boundary is still on the silica side of the join enstatite-anorthite at 30 kb. Therefore, the first liquid formed by melting of a mixture consisting of forsterite, enstatite solid solution, and small amounts of anorthite or garnet of the pyrope-grossular series is silica saturated up to about 30 kb under water-saturated conditions. Under anhydrous conditions, however, the forsterite-orthopyroxene liquidus boundary lies in the (Ol+Hy) normative area in the pressure range about 10 to at least 30 kb (Kushiro, 1968). The boundary at 20 kb under anhydrous conditions is shown in Fig. 25 for comparison. It is parallel to but much to the silica-poor side of the boundary under water-saturated conditions. These results also indicate that the liquids formed by melting of peridotitic mixtures under hydrous conditions are consider-

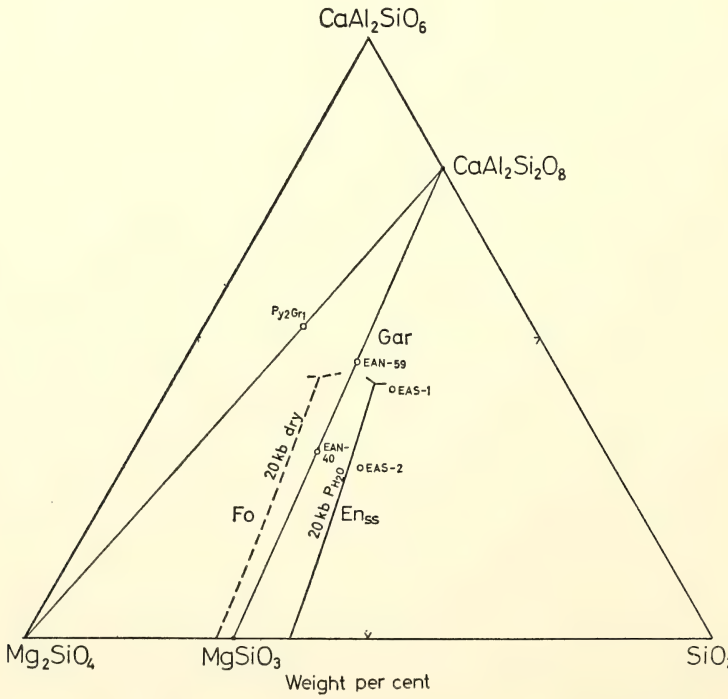

Fig. 25. The forsterite-orthopyroxene liquidus boundaries in the system forsterite-$CaAl_2SiO_6$-silica-H_2O at 20 kb under water-saturated and dry conditions. The boundary under water-saturated conditions is projected from the H_2O apex onto the plane forsterite-$CaAl_2SiO_6$-silica.

ably more silica rich than those under anhydrous conditions.

The System Forsterite-Nepheline-$CaAl_2SiO_6$-Silica-H_2O

For a better understanding of the compositions of liquids formed under upper-mantle conditions, the liquidus relations in the system forsterite-nepheline-$CaAl_2SiO_6$-silica-H_2O should be known. This system consists of the two systems described in the previous sections and includes most of the major components in the upper-mantle materials, except iron. Two mixtures on the plane enstatite-anorthite-albite ($En_{24.6}An_{35.4}Ab_{40.0}$ and $En_{32.8}$-$An_{47.2}Ab_{20.0}$ wt %) and two mixtures on the plane forsterite-anorthite-albite ($Fo_{20.16}An_{39.84}Ab_{40.0}$ and $Fo_{36.8}An_{33.2}Ab_{30.0}$) have been studied in the pressure range 20 to 30 kb and in the temperature range 1000° to 1150°C. The water content of the experiments ranged from 21.7 to 30.9 wt %.

Among the four mixtures studied, the mixture $En_{32.8}An_{47.2}Ab_{20.0}$, which is on the plane enstatite-anorthite-albite, was found to be most critical for the understanding of the melting relations of peridotitic mixtures in this system. At 20 kb and 1050°C the assemblage for this mixture is forsterite + orthopyroxene with glass and quench crystals, whereas at 1025°C the assemblage is forsterite + orthopyroxene + clinopyroxene + garnet with glass and quench crystals. All the crystals show euhedral or subhedral form. Glass balls ("quenched vapor") were observed in very small amount. Therefore, six phases coexist together at this temperature and pressure. If compositions of garnet and pyroxenes remain in the system forsterite-$CaAl_2SiO_6$-nepheline-silica, this six-phase assemblage represents a univariant relation or isobaric invariant relation; that is, the liquid is just at the isobaric invariant point. If the composition of pyroxene or garnet is outside the system mentioned above, this assemblage represents the isobaric univariant relation. The composition of garnet is slightly out of the system, as shown below, and the compositions of clinopyroxene and orthopyroxene may also be out of the system. Their deviations would be relatively small, however, and in the following discussion the relations at 1025°C and 20 kb are taken to be isobaric invariant as an approximation. The composition of the liquid at this "point" is most relevant to the melting of garnet-lherzolite; that is, the first liquid formed by melting of the mixture, forsterite + orthopyroxene + clinopyroxene + garnet with a small amount of water, has this composition, which is clearly in the silica-saturated (Qz-normative) region at 20 kb and probably up to 25 kb under water-saturated conditions. At this "point," forsterite reacts with liquid to form probably two pyroxenes and garnet. Amphibole is not involved at this "point," but it crystallizes at 1000°C with orthopyroxene, clinopyroxene, and garnet. The unit-cell dimension of garnet formed at 1000°C is 11.569 Å, which corresponds to that of pyrope 72 grossular 28 (by mole) on the basis of the unit-cell–composition curve for pyrope-grossular garnet (Chinner, Boyd, and England, *Year Book 59,* pp. 76–78).

On the basis of these experimental results and those in the systems forsterite-nepheline-silica-H_2O and forsterite-$CaAl_2SiO_6$-silica-H_2O, the projection of the forsterite-orthopyroxene liquidus boundary at 20 kb under water-saturated conditions is shown in the system forsterite-nepheline-$CaAl_2SiO_6$-silica (plane *A-Q-U-S* in Fig. 26). Point *A* is the projection of the composition of the liquid under the "isobaric invariant" conditions described above. It may be a piercing point, if the conditions are isobaric univariant. Even so, the true isobaric invariant point would be close to point *A*. Along the line *A-S,* forsterite, orthopyroxene, and garnet coexist with liquid and vapor, and along the line *A-Q,* forsterite, orthopyroxene, and clinopyroxene coexist with liquid and vapor. In the

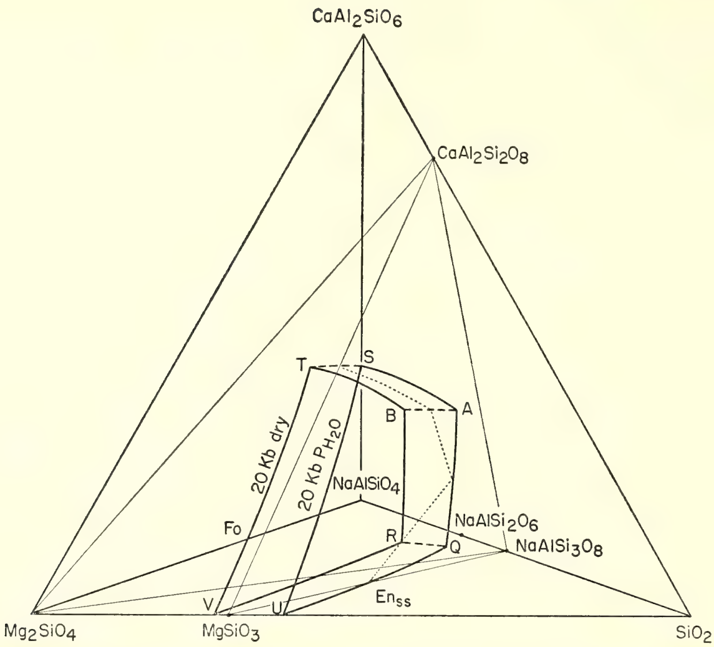

Fig. 26. The forsterite-orthopyroxene liquidus boundaries in the system forsterite-nepheline-$CaAl_2SiO_6$-silica-H_2O at 20 kb under water-saturated and dry conditions. The dotted line indicates a trace of the intersection of the plane $MgSiO_3$-$CaAl_2Si_2O_8$-$NaAlSi_3O_8$ with the volume *A-Q-U-S-T-V-R-B*.

present experiments, the exact positions of point *A* and the lines *A-S* and *A-Q* at 20 kb could not be determined. At lower pressures, point *A* would also lie in the Qz-normative region; spinel or plagioclase would appear instead of garnet at lower pressures, however, and the phase relations are not the same as those at 20 kb. The forsterite-orthopyroxene liquidus boundary at 20 kb under anhydrous conditions is shown for comparison in Fig. 26 (plane *B-R-V-T*). Point *B* is probably in the Ne-normative region at 20 kb.

The first liquid formed by partial melting of garnet-lherzolite in the presence of water is silica saturated at pressures up to 25 kb. The composition of the liquid is not certain, but the solidified liquid appears to be andesitic. Accordingly, it is possible that andesite magmas could be generated by direct partial melting of the upper mantle in the presence of water at depths of 60–80 km. The possibility of generation of andesite magma by direct partial melting of the upper mantle has been suggested by O'Hara (1965) and discussed in more detail by Yoder (1969).

In Fig. 26, if partial melting of peridotitic mixtures with small amounts of water proceeds as a closed system, water vapor disappears and the liquid leaves point *A* and changes its composition toward *B* along the dashed line *A-B*. The liquid becomes undersaturated with water. The composition of liquid is Qz-normative and may be andesitic at *A;* when the liquid crosses the plane enstatite-anorthite-albite, however, its composition becomes (Ol+Hy) normative. The compositions of liquids may change from andesite to tholeiite and olivine tholeiite. If the liquid crosses the plane forsterite-anorthite-albite, it becomes Ne-normative, although this possibility was not tested in the present experiments. How

far the liquid can move from A toward B depends on the water content of the initial material melted. If the water content is lower, the liquid may reach a point closer to B. Of course, the first liquid is always A regardless of the water content, its amount being smaller for the lower water content of the initial material. Thus, the peridotitic materials with the lower water content can generate less silicic liquids as far as the process of partial melting can proceed, to a considerable extent at constant pressure. It may be possible, therefore, that tholeiitic and olivine tholeiitic magmas can be generated by direct partial melting of the peridotite upper mantle with lower water contents, at depths at least near 60–80 kb. If the water content is high, a considerable amount of silica-rich andesitic magma may be produced by direct partial melting of the upper mantle. The results of the present study suggest interesting possibilities on the relationship between tholeiites and alkali basalts and on the origin of andesites, and determination of the compositions near points A and B is important in the further application of the system.

Stability of Amphibole and Phlogopite in the Upper Mantle

I. Kushiro

Amphibole is a possible hydrous mineral in the upper mantle. It has been found in the peridotites of the St. Paul's Rocks (Tilley, 1947; Melson *et al.*, 1967) and in some peridotite inclusions in basaltic rocks (e.g., Lausen, 1927; White, 1966; Kuno, 1967). In addition, high-pressure experiments on amphibole suggest that same amphibole can be stable under the P-T conditions of the upper mantle (Yoder and Tilley, 1962; Ernst, 1968; Lambert and Wyllie, 1968; Gilbert, *Year Book 67,* pp. 167–170; M. Nishikawa, unpublished data). Phlogopite is also a possible hydrous mineral in the upper mantle. The possibility of the presence of phlogopite in the upper mantle has been suggested recently by several investigators (e.g., Nicholls, 1967; Kushiro, Syono, and Akimoto, 1967*b*; Green, 1968; Yoder and Kushiro, 1969). In the present studies, stability of amphibole and phlogopite has been examined at high pressures in the presence of minerals of the upper mantle.

Formation of Amphibole in Peridotite Composition

Amphibole has been shown to form from various basalt compositions up to at least 10 kb under hydrous conditions (Yoder and Tilley, 1962). Yoder (*Year Book 65,* pp. 269–279) has also shown that amphibole forms from synthetic forsterite + anorthite (1:1 by mole) composition. Kushiro, Syono, and Akimoto (1968) carried out experiments on a natural lherzolite under hydrous conditions in the pressure range 26 to 50 kb at temperatures above 980°C and determined the solidus temperatures, but they did not find amphibole or other hydrous minerals within the P-T range of their experiments. The present experiments have been conducted on the same lherzolite under hydrous conditions in the pressure range 15 to 28 kb to determine the P-T range of crystallization of amphibole if it forms in the lherzolite + H_2O composition.

The experiments have been performed with the solid-media, piston-cylinder apparatus and with sealed Pt capsules. The water content of the capsules ranged from 5.8 to 9.3 wt %. The starting material used was a spinel-bearing lherzolite, which occurs as a nodule in the tuff of Salt Lake crater, Hawaii, and has been described by Kuno (1969).

The results are shown in Fig. 27. As shown in the figure, the upper limit of the amphibole-bearing assemblage has a negative slope. At 1030°C and 15 kb, no amphibole was found and feathery quench crystals were observed with glass, indicating that the solidus temperature at 15 kb is 1015° ± 15°C, consistent with

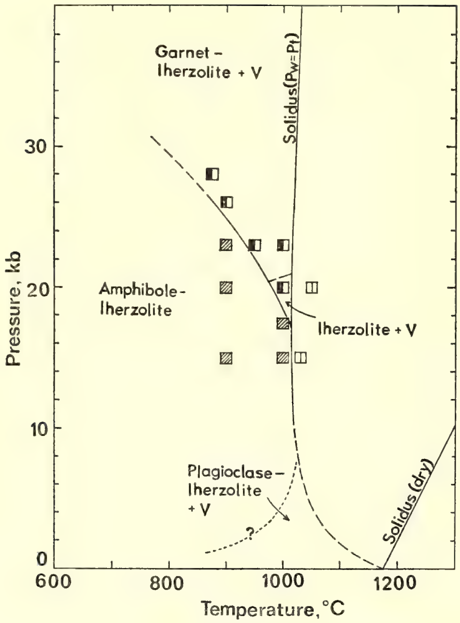

Fig. 27. Pressure-temperature diagram for a lherzolite nodule from the tuff of Salt Lake, Hawaii, in the presence of excess water. The solidus under dry conditions and a part of the solidus in the presence of excess water are from Kushiro, Syono, and Akimoto (1968). Symbols: shaded square, olivine + orthopyroxene + clinopyroxene + amphibole ± garnet; half-solid square, olivine + orthopyroxene + clinopyroxene ± garnet; square with vertical line, olivine + orthopyroxene + clinopyroxene + quench crystals and glass.

the results obtained by Kushiro, Syono, and Akimoto (1968). In the present experiments, the water content is considerably higher than that required for the formation of amphibole. As suggested by Yoder and Kushiro (1969), hydrous minerals have the maximum thermal stability at solidus temperatures when the water contents are the same as those of the corresponding hydrous minerals. If the water content of the experiments is lower, therefore, amphibole may persist to temperatures above the solidus of the lherzolite.

The amphibole obtained in the present experiments is almost colorless or very pale green. It is thin and prismatic, its average length being 0.05 mm. The composition of the amphibole was not determined but is probably pargasitic. The amounts of amphibole in the five runs are estimated to be about 10% or less from the intensity of reflection in the powder X-ray diffraction patterns and from the microscopic observation. Clinopyroxene, orthopyroxene, and garnet are euhedral to subhedral and appear to be well recrystallized. Olivine also shows euhedral to subhedral form but the centers of many of the crystals are cloudy. Garnet crystallizes at 900°C at 20 kb or higher, and at 950° and 1000°C at 23 kb, although its amount is very small; it does not crystallize, however, at 1000°C and 20 kb. The unit-cell dimension of garnet formed at 28 kb and 875°C is 11.571 Å, indicating that the garnet is pyrope and almandine rich. In the previous experiments by Kushiro, Syono, and Akimoto (1968), garnet was not found in the run conducted at 26 kb and 980°C for one-half hour. The duration of the run was probably too short for the formation of garnet at subsolidus temperatures and at pressures relatively close to the transition. No other hydrous minerals were found to form in the present experiments.

The stability of synthetic pure pargasite has been studied by Boyd (1959) at pressures below 2 kb and by Gilbert (*Year Book 67,* pp. 167–170) at 30 and 40 kb. Gilbert has shown that pure pargasite is stable up to at least 900°C at 20 kb in the presence of clinopyroxene and is not stable at 950°C and higher near 30 kb or at 900°C and higher near 40 kb. Although the data are too few for comparison, the stability field of pure pargasite in the presence of clinopyroxene is not much different from the field of crystallization of amphibole in natural lherzolite.

The present results would be useful in estimating the maximum depth of formation of amphibole in the upper mantle if the upper-mantle materials are similar in chemical composition to the present

lherzolite. Assuming that the geotherms in the oceanic and continental areas are represented by those given by Clark and Ringwood (1964) and the water pressure is nearly equal to the total pressure in the upper mantle, it would be predicted that amphibole could form at pressures up to about 20 and 27 kb or at depths of about 60 and 85 km in the oceanic and continental areas, respectively. If the water pressure is less that the total pressure, amphibole breaks down at lower temperatures and would not be stable to such depths.

Stability of Phlogopite in the Presence of Pyroxene

Pure phlogopite is stable up to at least 37.5 kb at about 1200°C in the presence of forsterite (Yoder and Kushiro, 1969), and a natural phlogopite is stable up to at least 72 kb at about 1000°C (Kushiro, Syono, and Akimoto, 1967*b*). The stability field of phlogopite, however, may change in the presence of other phases. Lambert and Wyllie (1968) noted that in the presence of "mantle pyroxenes" phlogopite would become unstable at lower pressures than pure phlogopite and assumed that phlogopite is not stable at pressures higher than about 20 kb at about 900°C. In the present preliminary experiments, therefore, phlogopite + enstatite and phlogopite + diopside assemblages have been examined at high pressures.

The starting materials are a 1:1 mixture (by weight) of synthetic pure diopside and a mixture of anhydrous pure phlogopite composition, and a 1:1 mixture (by weight) of synthetic pure orthoenstatite and a mixture of anhydrous pure phlogopite composition. Three runs were conducted on the diopside + phlogopite composition—at 15 kb and 1100°C, at 30.5 kb and 1150°C, and at 32 kb and 1000°C—with sealed Pt capsules having water contents of 11.4, 13.1, and 4.6 wt %, respectively. In all the runs a large amount of phlogopite crystallized, and the assemblage is phlogopite + diopside + forsterite with or without a small amount of glass, including glass balls condensed from vapor. Phlogopite crystals are mostly euhedral. Diopside is also well recrystallized. Crystallization of forsterite indicates that vapor or liquid would dissolve excess potassium and alumina over phlogopite composition, as already shown by Yoder and Kushiro (1969). These experimental results indicate that the diopside + phlogopite assemblage is stable up to at least 32 kb at about 1000°C.

Two runs were conducted on the enstatite + phlogopite assemblage, at 26 and 33 kb and 1100°C, with water contents of 22.4 and 15.4 wt %, respectively. In these runs a large amount of phlogopite crystallized, and the assemblage was phlogopite + orthoenstatite + forsterite with a small amount of glass balls and glass coatings. Phlogopite crystals are mostly euhedral; orthoenstatite is also well recrystallized and mostly euhedral. These experimental results indicate that the phlogopite + orthoenstatite assemblage is stable up to at least 33 kb at 1100°C. As shown above, the presence of diopside and enstatite does not seem to change significantly the stability field of phlogopite. Although the effect of iron and other elements on the stability of the phlogopite + pyroxene assemblage is not known, it is suggested from the above experimental results that phlogopite may be stable at depths of at least 100 kb if the water pressure is equal or nearly equal to total pressure and the temperature is not much higher than 1100°C.

OXIDES AND OTHERS

Stability of the Pseudobrookite (Fe_2TiO_5)-Ferropseudobrookite ($FeTi_2O_5$) Series

S. E. Haggerty and D. H. Lindsley

Members of the pseudobrookite series are ubiquitous as high-temperature oxidation products of titanomagnetite and

ilmenite, and a knowledge of the lower thermal stability limit of the series has now become significant in terms of magnetic mineral studies because the series can serve as a temperature indicator. Recent investigations relating magnetic properties with petrography have revealed that systematic correlations exist between lavas that show reversed directions of magnetization (i.e., antiparallel to the direction of the earth's magnetic field) and lavas that are highly oxidized (Wilson and Haggerty, 1966). Although self-reversing physiochemical models have been proposed, they are rarely demonstrable in the laboratory. The relationship between reversed polarity and lava oxidation is not understood. An insight into the mechanism controlling these correlations obviously depends, first of all, on whether it can be proved that magnetization and mineral oxidation are coeval or are separated in time. Our results suggest that in highly oxidized lavas a possible mineralogical method of deciding whether a direction of magnetization is primary, having developed during the initial cooling, or whether the polarity is secondary and developed at some later time, can be made on the presence or absence of pseudobrookite as an oxidation product.

The alteration of titanomagnetite and ilmenite, in nature, to members of the pseudobrookite series is a nonequilibrium oxidation process. Although the thermal-stability determinations described here are equilibrium values, they nevertheless provide an important and initial framework for delineating the problem.

Akimoto, Nagata, and Katsura (1957) have shown that the pseudobrookite series is complete above 1150°C; this observation has been confirmed in the present study. Results from quenched, evacuated silica-glass-tube experiments are presented in Fig. 28, for the temperature range 750°–1150°C; other points included on the diagram are hydrothermal experiments at 2 kb and the f_{O_2} of the

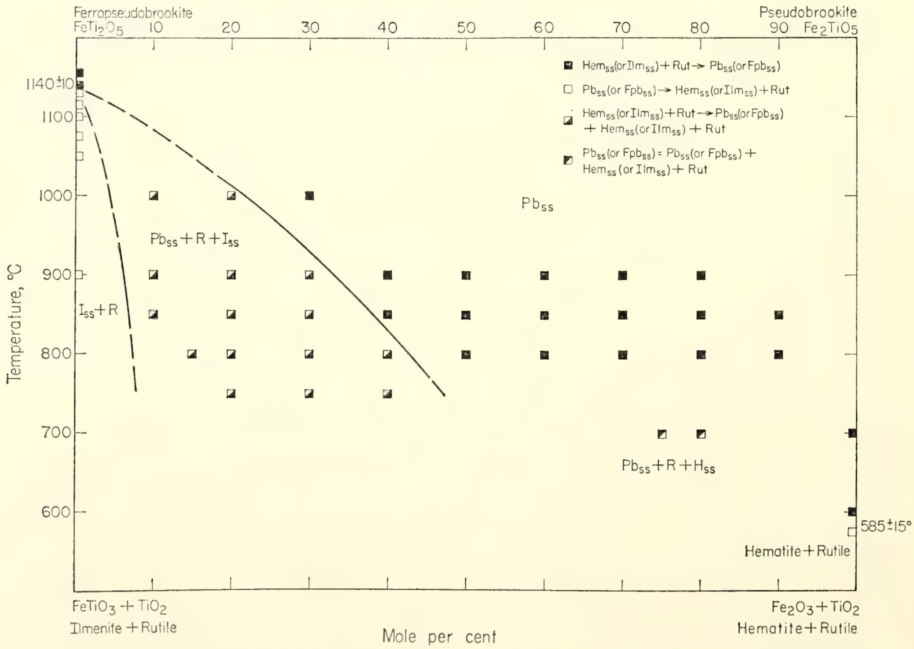

Fig. 28. Stability relations in the pseudobrookite-ferropseudobrookite series.

buffer controlled by hematite+hydrogen peroxide. Starting material for the primary breakdown experiments consisted of crystalline pseudobrookite; and reversible experiments, to establish true equilibrium, were carried out by reacting rutile and members of the ilmenite-hematite solid solution series in 1:1 ratios.

Ferropseudobrookite ($FeTi_2O_5$) decomposes to $FeTiO_3+TiO_2$ at $1140° \pm 10°C$, and the pseudobrookite (Fe_2TiO_5) end member (based on hydrothermal experiments) breaks down to $Fe_2O_3+TiO_2$ at $585° \pm 10°C$. Intermediate members break down between 700° and 800°C, but the decomposition curve between the two end members is not linear. The effect of Mn and Mg (elements that are known to be present in small quantities in titanomagnetite and ilmenite) on the stability limit of the series has not been determined.

The silica-glass-tube technique has a limited application below 800°C in this system because of very slow reaction rates; Fe_2TiO_5-rich members and members of the series having intermediate compositions, for example, remained only partially reacted, at 750°C, even after 3 years. The Pb_0-Pb_{50} region above 750°C is relatively simple, and three distinct fields—(a) ilmenite+rutile, (b) ilmenite+rutile+pseudobrookite, (c) pseudobrookite—have been defined. The Pb_{50}-Pb_{100} region, which has a direct application to magnetic mineral studies, however, is far more complex and has not yet been fully resolved.

Identification of the synthetic phases was made by X-ray powder diffraction and in polished section. An interesting feature demonstrated by compositions in the pseudobrookite field is that crystals frequently show a tendency to be zoned by a rim that is darker and shows a lower reflectivity than the central core. Electron-probe scans for Fe and Ti across the core and the rim showed no observable variation in concentration, and it is inferred that the rim represents a quenched polymorphic inversion product of pseudobrookite. Attempts to grow large crystals for a detailed X-ray study have been made but have not yet been successful. In experiments containing the assemblages ilmenite+rutile and ilmenite+rutile+pseudobrookite these minerals occur as discrete grains or in mutual intergrowths. Textures resembling the exsolution or oxidation products that are observed in nature do not occur in the synthetic phases.

It is concluded that the oxidation of titanomagnetite and ilmenite in nature to form members of the pseudobrookite solid solution series in association with rutile and titanohematite must take place between 600° and 800°C. For lavas, oxidation in this temperature range is most likely to occur during initial cooling. The presence of migrating oxidation zones in the cooling Makaopuhi lava lake between 550° and 750°C (Sato and Wright, 1966), the systematic oxidation zones that are observed in single lava units (Watkins and Haggerty, 1967), and the presence of pseudobrookite toward the center of these units (Haggerty, 1968) support this conclusion and the high-temperature deuteric origin of pseudobrookite. On the basis of these high temperatures the presence of pseudobrookite would suggest that a measured direction of thermoremanent magnetization would be primary and would have occurred concurrently with mineral oxidation.

High-Pressure Phase Transformation in Magnetite

H. K. Mao, W. A. Bassett, and T. Takahashi**

Knowledge of the phase relations in the system Fe_3O_4 under high *P-T* conditions is useful for an understanding of the mineralogy of the earth's mantle. Iron oxides are important mantle components, as indicated in petrologic and meteoritic occurrences. Magnetite (Fe_3

*University of Rochester, Rochester, New York.

O_4) with spinel structure is stable at 1 atm. In most proposed mantle models, a major phase transformation of (Mg, $Fe)_2SiO_4$ from the spinel structure to a high-pressure phase or phase assemblage is predicted to occur in the lower part of the transition zone. This high-pressure phase or phase assemblage should predominate in the lower mantle. So far, this transformation in $(Mg,Fe)_2SiO_4$ spinel has not been discovered in nature, nor has it been observed in the laboratory. By analogy, the high-pressure phase of magnetite may offer information on which a good prediction of the high-pressure phase of $(Mg,Fe)_2SiO_4$ spinel might be based.

Thermodynamic calculations of free energy and entropy data on the basis of conditions at room temperature and pressure and high-pressure compression data indicate that magnetite has a higher free energy than either the assemblage hematite + wüstite or the assemblage hematite + ϵ iron at pressures above 150 kb (Mao, 1967). Theoretically, experiments above 150 kb should transform magnetite into one of these two assemblages or possibly to an unknown state, kinetics permitting. In the present study, a pressure-induced, first-order phase transformation in magnetite was observed in a diamond anvil, high-pressure X-ray diffraction cell. Natural magnetite from Mineville, New York ($a_0 = 8.394 \pm 0.002$ Å), was used as starting material.

The present technique has been described by Bassett, Takahashi, and Stook (1967). Experiments were conducted at temperatures up to 310°C and pressures up to 300 kb, equivalent to the pressures predicted for a depth of 800 km in the earth. The pressure cell was heated to 310°C momentarily after the pressure was applied, in order to accelerate the phase transformation. All X-ray diffraction photographs were taken after the samples had been cooled to room temperature but were still under high pressure. The pressures were determined by using the lattice constant of NaCl, or in some runs, the lattice constant of the low-pressure magnetite phase as internal standard. The exact pressure during heating was unknown, but it was believed to be somewhat lower than the pressure after cooling.

In both heated and unheated runs, magnetite underwent a phase transformation at approximately 250 kb but reverted to the original spinel structure with the original a_0 value upon release of pressure to 1 bar. The reaction was very sluggish at room temperature, and the true equilibrium pressure might be far below 250 kb. No reversion of the high-pressure form to magnetite was observed above 50 kb. At 1 bar, remnants of the high-pressure form can persist for a few weeks to a month before completely reverting to magnetite.

The crystal structure of the high-pressure form has not been determined. Its X-ray powder diffraction pattern, in comparison with the magnetite pattern, is given in Table 19. Many of its diffraction lines overlap those of magnetite, but the intensities are very different. This pattern could not be indexed as a single cubic phase nor as a single tetragonal or hexagonal phase with a reasonably small unit cell.

It is interesting to note that the *d*

TABLE 19. *d* Values of the High-Pressure Form of Magnetite and of Magnetite, Both at 250 Kb, 25°C

High-Pressure Form			Magnetite		
No.	*d*, Å	I/I_{10}*	(*hkl*)	*d*, Å	I/I_{10}*
			(111)	4.671	1
			(220)	2.860	3
1	2.60	10			
2	2.44	1	(311)	2.439	10
3	2.34	3	(222)	2.335	1
4	2.14	1			
5	2.03	4	(400)	2.023	3
6	1.90	4			
7	1.79	2			
			(422)	1.651	2
8	1.55	4	(333)(511)	1.557	4
9	1.40	5	(440)	1.430	5
10	1.23	1	(533)	1.234	1

* Intensities were estimated by eye.
Note: $MoK\alpha_1$ radiation was used.

values and intensities of diffraction lines 1, 2, 4, and 7 (Table 19) are remarkably close to those of the (104), (110), (113), (204), and (115) reflections, respectively, of hematite at the same pressure. It is not likely that the high-pressure assemblage contains hematite, which is stable at atmospheric oxygen pressure. If hematite formed from magnetite at high pressure, it could not revert to magnetite when the pressure was released and the sample exposed to the air. The X-ray pattern does not correspond to that of an assemblage containing wüstite or ϵ iron, according to the data measured at 250 kb by Mao *et al.* (1969) and Mao, Bassett, and Takahashi (1967). No transformation was observed in wüstite at 300 kb and 325°C.

The complete reversion of the high-pressure form to magnetite at atmospheric oxygen pressure suggests a single phase instead of a phase assemblage. Overlapping of a large part of the X-ray pattern of the high-pressure form with magnetite lines may be due to a reordering in magnetite, probably involving a move of iron from tetrahedral oxygen coordination into octahedral coordination. Such a coordination change in the magnetite structure requires decrease in the intensity of the (311) reflection, with corresponding increases in the intensities of the (222), (400), and (440) reflections. All of these requirements are consistent with our observations.

Study of Lead up to 180 kb

H. K. Mao, T. Takahashi, and W. A. Bassett**

The lead transformation was first recognized by Balchan and Drickamer (1961), reportedly at 161 kb and room temperature, on the basis of a 23% increase in electrical resistance. The crystal structure of the high-pressure phase was not determined, but under room conditions lead is in a face-centered cubic (fcc) structure. Currently, this transformation is used as a pressure calibration point.

* University of Rochester, Rochester, New York.

In the present study at room temperature, the high-pressure phase of lead has been identified. In addition, its transformation pressure has been correlated with the fixed-point pressure of $\alpha \rightarrow \epsilon$ iron at 130 kb and with the pressure-volume equation of state of iron. The *P-V* equation of state of lead was also determined. This was accomplished by the X-ray diffraction method, with a polycrystalline sample compressed in a diamond-anvil, high-pressure cell (Bassett, Takahashi, and Stook, 1967).

The sample of lead used for this study is a high purity ingot (99.999% Pb) supplied by the American Smelting and Refining Company.

Determination of the High-Pressure Phase

Zr-filtered MoKα radiation was used to study lead under pressure in the diamond-anvil cell. X-ray diffraction lines were recorded on a cylindrical film having a radius of 50 mm, allowing dispersion of a maximum angle of 48° 2θ. Seventeen diffraction lines of the high-pressure phase of lead were observed. They can all be indexed as hexagonal with c/a ratios of 1.650. Systematic extinctions in the pattern are consistent with a hexagonal close-packed (hcp) structure.

The d values and intensities of a set of diffractions observed at 139 ± 10 kb are compared in Table 20 with the calculated d values and intensities for a hcp structure of lead. The calculated lattice parameters are $a = 3.265 \pm 0.004$ Å and $c = 5.387 \pm 0.007$ Å. Observed and calculated d values agree within the experimental uncertainty. The observed and calculated intensities were generally in good agreement, with the exception of (100) and (110) reflections, for which the observed intensities are considerably higher than the calculated ones. A possible explana-

TABLE 20. Observed and Calculated d Values and Intensities for hcp Lead at 139 ± 10 Kb and 25°C

(hkl)	d_{obs}, Å	d_{calc}, Å	$(I/I_{100})_{obs}$	$(I/I_{100})_{calc}$
100	2.820	2.827	75	23
002	2.685	2.694	32	27
101	2.507	2.504	100	100
102	1.947	1.951	12	17
110	1.633	1.632	71	21
103	1.514	1.516	22	25
200	...	1.414	...	3
112	1.397	1.396	33	26
201	1.367	1.367	36	18
004	...	1.347	...	4
202	1.254	1.252	5	5
104	*	1.216	*	4
203	1.110	1.111	17	9
210	...	1.069	...	1
211	1.047	1.048	18	16
114	*	1.039	*	10
105	*	1.007	*	8
212	0.9927	0.9933	9	6
204	...	0.9752	...	3
300	...	0.9426	...	5
213	0.9195	0.9183	15	14
006	...	0.8984	...	1
302	*	0.8897	*	8

* Observed in other photograph but not in this one, which is the best for intensity measurement; (...) indicates not observed.

Note: MoKα radiation was used.

tion is that the X-ray diffraction pattern of the high-pressure form was always spotty, probably due to preferred orientation, even though we started with a fcc lead having a perfectly smooth pattern. If the change from fcc to hcp only involves a glide along the (111) plane of fcc, equivalent to the (002) plane of hcp, then shear stress along this plane should favor the transformation. In the diamond-anvil cell the maximum shearing stress is parallel to the anvil face, and consequently the (002) plane would tend to be so oriented. If this parallelism of (002) occurs, the planes perpendicular to (002) should be in better orientation for diffraction. Thus (100) and (110) would have higher intensities in a diamond-anvil cell than those calculated on the basis of random orientation.

Precise Measurement of the Transformation

Two samples of lead, one intimately mixed with an iron standard and the other alone, were used to study the transformation pressure. In experiments with the lead-iron mixture, pressures were determined from the known P-V relations of iron (Takahashi, Bassett, and Mao, 1968). In the pure lead sample, pressures were determined from the P-V data for the fcc form of lead determined in the Fe+Pb experiments. The effect of pressure on the volume of the fcc lead was first studied by Bridgman (1945) up to 100 kb at room temperature. It was redetermined in the present study of the iron-lead mixture, based on the seven diffraction lines (111), (200), (220), (311), (222), (331), and (420) of the fcc phase. The results can be fitted to a first-order Birch equation of state: $P = \frac{3}{2} B_0[V_0/V)^{7/3} - (V_0/V)^{5/3}]$, where B_0 represents the zero pressure isothermal bulk nodules, $B_0 = 458 \pm 30$ kb; V_0 and V are volumes at zero pressure and pressure P, respectively. Our results agree within 0.5% with those of Bridgman (1945), and B_0 is close to the value ($B_0 = 439$ kb) calculated from the elastic constant at zero pressure (Swift and Tyndall, 1942).

To avoid overshooting the transformation, pressure was increased at an extremely slow rate (less than 1 kb per hour). The onset of the lead transformation was determined by the first appearance of the (101) diffraction line of hcp lead. In the lead-iron mixture the onset of the lead transformation occurred close to but always at lower pressure than the fixed point of 130 kb for the onset of the $\alpha \rightarrow \epsilon$ iron transformation. In both the lead-iron mixture and the pure lead sample, the onset pressure of the fcc-hcp transformation was determined to be 130 ± 10 kb by internal-standard calibration (lattice constants of iron or fcc lead), but the transformation was not completed until 160 ± 10 kb in the lead-iron mixture and 145 ± 10 kb in the pure lead sample. In both samples, when pressure was reduced remnants of the hcp lead persisted to pressures as low as 100 ± 10 kb before completely reverting to fcc. The total observed range of coexisting fcc-hcp lead was $P = 100$ kb to $P = 160$ kb, or $V_{fcc} = 15.58$ cm^3/mole, $V_{hcp} = 15.41$ cm^3/mole, to $V_{fcc} = 14.65$ cm^3/mole, $V_{hcp} = 14.54$ cm^3/mole, respectively.

The volume change for the fcc-hcp phase transformation was determined when these two phases coexisted in the high-pressure cell. On the basis of twelve measurements, the change was determined to be -0.18 ± 0.06 cm^3/mole, or 1% in $\Delta V/V_0$, where $V_0 = 18.269$ cm^3/mole is the molar volume of fcc lead under room conditions. Since the volume change is small, it increases confidence that the coexisting fcc and hcp phases were at the same pressure. The pressure inhomogeneity in an intimate mechanical mixture of NaCl and Nb reported by Jamieson and Olinger (1968) did not exist in the coexisting fcc and hcp lead. If the hcp phase were at a higher pressure the volume change would have been overestimated, and therefore the true volume decrease would have been less than 1% but still larger than zero. A 1% change in $\Delta V/V_0$ at 130 kb is only equivalent to 9 kb in the P-V relation of fcc lead, setting an upper limit for the possible pressure difference between the two coexisting phases.

Using a belt apparatus Bundy (1967) found, in agreement with Balchan and Drickamer (1961), that the electrical-resistance change of the lead transformation was 30 kb higher than that of the iron transformation and was always sharp. The discrepancy between their results and the present ones may be due to the following factors: the length of time of the runs (resistance measurement is on the order of minutes, and the present technique is on the order of months); the stress distribution in different types of apparatus; and the type of observation (resistance versus X-ray). As described above, in the present study a range of 60 kb for coexistence of fcc and hcp lead was observed. Precaution must therefore be taken when the lead transformation is used as a calibration point in other than X-ray diffraction methods.

Crystal-Field Spectra at High Pressure

P. M. Bell and H. K. Mao

Theory

An ion loses its spherically symmetrical environment when bonded in a crystal. Cations commonly occur in octahedral and tetrahedral coordination with oxygen atoms in mineral structures and as a result are influenced by the crystal field. Primarily, the effect of pressure as a parameter is to increase the field intensity, because of the closer proximity of neighboring electronic fields, and to alter the d and f electronic levels in a transition metal cation.

For the transition elements the Hund rule of maximum spin multiplicity describes the ground state in a weak or zero field. Owing to filling of the lowest crystal-field levels, a different ground state occurs in strong fields. Competition between spin-pairing energy and crystal-

field energy determines whether the strong or weak field case results.

Another effect is the prediction of molecular orbital theory for the occurrence of more states at higher energies. Here transitions may occur from orbitals having predominantly *d* characteristics to those having ligand character, i.e., transitions of *d* electrons to *s* and *p* levels.

In actually relating the crystal-field strength to pressure, Zahner and Drickamer (1961) have calculated the difference in energy between a free ion and one in an octahedral field. This energy, sometimes called the crystal-field parameter Δ or 10 Dq, should vary as R^{-5} for a point charge and R^{-6} for point dipoles in a cubic field (R = interatomic distance). Clearly, compression causing a decrease in R is the important factor. One should be able to make the following observations: a shift of spectral absorption bands with pressure; an increase of Δ with pressure, which will be independent of the transition (in the zeroth order); and a shift with pressure of certain electronic transitions (such as charge transfer).

Minerals that contain transition elements are subject to crystal-field effects, which become increasingly important at high pressure. Excellent reviews of this subject have been recently completed by Burns and Fyfe (1967) and Burns (1969). Three of the recognized effects of interest in geophysics are pressure-sensitive transitions, control of geochemical fractionation of the transition elements, and thermal properties of minerals at great depths in the earth. Geologically, the most important elements showing crystal-field effects are iron, manganese, chromium, and titanium.

Two distinct types of pressure transition involving iron have been predicted, and some observations have been made. The first, spin-pairing, was suggested by Fyfe (1960) and is described in detail by Burns (1969); the second, a change in the oxidation state of iron, was observed by Drickamer (1965). Spin-pairing results in a shift or transition of iron in the high-spin state to the low-spin state, with a sharp transition. The depths in the earth where this type of transition might occur have been calculated for several minerals by Burns (1969). The oxidation-state effect is one of the reduction of Fe^{3+} to Fe^{2+} and has been observed as occurring gradually with pressure in organic compounds. Drickamer, Lewis, and Fung (1969) made this observation at pressures of the order of 100 kb using the Mössbauer technique.

Crystal fields tend to lower the free energy of a compound containing a transition element, i.e., the crystal-field energy of a transition ion in an octahedral or tetrahedral site tends to stabilize this ion relative to a nontransition ion. Chromium has the highest crystal-field stabilization energy (CFSE), and starting at this highest point, Curtis (1964) has demonstrated a striking correlation of the fractionation of transition elements in ultramafic deposits with their relative CFSE's. Burns (1969) observed the concentration of transition elements in carbonaceous chondrites and drew analogies with the upper and deep mantle of the earth. El Goresy, Bell, and England (*Year Book 67*, pp. 197–198) reported an iron-chrome sulfide from a meteorite which is stable at high pressure. In a high-pressure environment the transition elements should be concentrated in the first solids to crystallize from a melt. Results of a study by Meyer and Boyd (this report) of inclusions in natural diamonds are in agreement with this prediction.

Thermal properties of the earth's mantle are sensitive to crystal-field effects because the radiative component of heat transfer will depend on the amount of absorption in the near infrared (NIR) and infrared (IR) regions. Clark (1957) observed a broad transmission window in silicates at 1 atm and room temperature, but Fukao, Mizutani, and Uyeda (1968) have shown that crystal-field absorption

bands tend to limit transmission severely at high temperature. Shankland (1969) observed the opposite effect in olivine with increasing pressure, but below 50 kb the pressure effect is not strong enough to cancel the temperature effect.

Preliminary Experiments

We have employed a diamond cell of the type described by Weir, Van Valkenburg, and Lippincott (1962) to make measurements of crystal-field spectra at high pressure. This cell is mounted on the stage of a Leitz polarizing microscope, through which the beam of a Perkin-Elmer spectrophotometer is transmitted. A lead-sulfide detector and a photomultiplier sample the beam for absorption bands in the NIR and visible regions. This apparatus, described by Lippincott, Whatley, and Duecker (1966), is located in the U. S. National Bureau of Standards. The instrument had previously been used in the visible region only, and difficulties were encountered in the NIR, owing to strong absorption by the optical elements of the microscope. These difficulties could have been overcome by placing a microscope in the reference beam as well as the sample beam (Burns, 1966), but it was not possible to modify the borrowed instrument. Therefore, it was necessary to determine the absorption of the microscope without sample or diamond cell so the overlapping absorption bands could be subtracted.

Powdered samples were used because the diamonds caused multiple scattering, making the measurement of polarized spectra of a single crystal sample difficult. No attempt was made to assign bands.

Crystal-field spectra were measured in the NIR for fayalite and spinel (both Fe_2SiO_4) and almandine-garnet ($Fe_3Al_2Si_3O_{12}$). Additional measurements of olivine were made in the visible region. In all measurements strong absorption bands due to the crystal field were observed.

At low pressure a strong crystal-field band was observed at 1.22 μm. This shifts toward higher energy by 100 nm (nanometers) at approximately 100 kb, and the phenomenon is entirely consistent with the widening of the transmission window observed by Shankland (1969) at 50 kb. (The band defining the lower limit of the window is at approximately 5 μm in the IR and was not measured in the present study.)

Spinel measured in this study was synthesized at approximately 80 kb by F. R. Boyd. The crystal-field absorption band was observed at 1.35 μm at 1 atm and shifted by 50 nm toward higher energy at approximately 100 kb. Maximum transmission at 1 atm was observed at 1.6 μm; at 100 kb, transmission was a maximum at 1.68 μm. These results suggest that spinel transmits well in the low-energy region at least to 2 nm.

Almandine-garnet used in the study was synthetic, supplied by H. S. Yoder. Two absorption bands were observed: at 1 atm they occurred at 1.23 and 1.70 μm; at high pressure they shifted to higher energy by 100 and 150–200 nm, in agreement with the observations of Balchan and Drickamer (1961).

Observations of fayalite in the ultraviolet (UV)–visible (V) were intriguing. At 1 atm the visible cut-off of the charge-transfer band occurred at 380 nm. At about 50 kb this absorption edge had shifted to 400 nm. Above 50 kb strong absorption centers appeared with increasing pressure, and very rapidly absorption was complete throughout the visible region. The effect was reversible without hysteresis, probably because of incipient formation of the high-pressure phase (spinel). Similar phenomena are well known to occur at polymorphic transitions, presumably owing to the scattering of light in minute nucleation particles (Burns, 1969). In this case it could also be due to the rather strong absorption in the visible region of spinel, which we have observed to be continuous

to about 800 nm, where a sharp edge occurs. Burns (1969) has pointed out that strong absorption at a phase transition will shield thermal radiation. This process could be important in the earth's mantle.

PHASE-EQUILIBRIUM STUDIES OF SULFIDE SYSTEMS

Sulfide- and Arsenide-Type Binary Systems

G. Kullerud

During the past 15 years we have studied the phase relations in a considerable number of binary sulfide- and arsenide-type systems. We have approached this study from the mineralogical point of view and have concentrated on those systems that contain compounds with mineral equivalents. Compilation of our data and those produced in metallurgical studies (reviewed by Hansen and Anderko, 1958, and Elliott, 1965) brings out some interesting features that may serve to classify or group these systems. Such grouping of empirical systems, if properly executed, is useful for numerous purposes. For instance, comparison of the behavior of one such group with that of another can (1) lead to conclusions of general value not attainable by comparison of large numbers of individual systems, (2) lead to prediction of the behavior of systems not yet investigated, and (3) point up discrepancies between reported (mostly in the old literature) and predicted behavior of many systems and thus single out those systems which should be restudied with modern methods.

The distinguishing features that permit classification pertain to the behaviors of the individual systems both in the liquid and solid states. In this first effort at grouping we shall emphasize melting relations and the liquid state.

Sulfide-Type Systems

In experimental work sulfide-type systems generally are considered to involve selenides and tellurides as well as sulfides. We shall first examine binary systems containing two of these group VIA elements and then the binary relations of each of these elements to the elements arsenic, antimony, and bismuth from group VA; germanium, tin, and lead from group IVA; aluminum, gallium, indium, and thallium from group IIIA; zinc, cadmium, and mercury from group IIB; copper, silver, and gold from group IB; nickel, palladium, platinum, cobalt, rhodium, iridium, and iron from group VIII; Mn from group VIIB; and chromium, molybdenum, and tungsten from group VIB.

Data on melting relations in these systems are compiled in columns 1–3 of Table 21. It is noted that in each of the S-Se, S-Te, and Se-Te systems homogeneous liquid exists above the liquidus over its entire length. Congruently melting compounds do not exist in these systems. Column 1 of Table 21 shows that liquid immiscibility fields exist in all other sulfide systems.

About one-half of the listed sulfide systems on which information exists contain one liquid immiscibility field, whereas the others contain two. A cursory look down the sulfur column does not give the impression of orderly grouping of one versus two liquid immiscibility field systems. We shall make no attempt as yet to group or classify these systems on the basis of the occurrence of one or two liquid immiscibility fields. Such a classification is premature for several reasons, the main one being lack of knowledge of melting relations in the sulfur-rich portions of the systems. Only recently have methods been devised to yield this kind of information, and so far the sulfur-rich portions of only the

TABLE 21. Melting Relations in Binary Sulfide- and Arsenide-Type Systems

		S	Se	Te	As	Sb	Bi
VIA	Se	hom *l*, no cc, eut					
	Te	hom *l*, no cc, eut	hom *l*, ss				
VA	As	1 im *l*, 1–2 cc	no inf	hom *l*, eut, 1 cc			
	Sb	2 im *l*, 1 cc	1 im *l*, 1 cc	hom *l*, eut, 1 cc	hom *l*, ss		
	Bi	1 im *l*, 1 cc	1 im *l*, eut, 1 cc	hom *l*, eut, 1 cc	hom *l*, no cc	hom *l*, ss	
IVA	Ge	2 im *l*, 2 cc	no inf	hom *l*, eut, no cc	hom *l*, eut(?), 2 cc(?)	hom *l*, eut, no cc	hom *l*, no cc
	Sn	2 im *l*, 2 cc	1 im *l*, 2 cc, eut	hom *l*, eut, 1 cc	hom *l*, eut, 2 cc	hom *l*, no cc	hom *l*, eut, no cc
	Pb	2 im *l*, 1 cc	2 im *l*, 1 cc	hom *l*, eut, 1 cc	hom *l*, eut, no cc	hom *l*, eut, no cc	hom *l*, eut, no cc
IIIA	Al	1 im *l*, 1 cc	hom *l*, eut, 1 cc	hom *l*, eut, 1 cc	no inf	hom *l*, 1 cc	1 im *l*, no cc
	Ga	no inf	no inf	1 im *l*, 2 cc	hom *l*, 1 cc	hom *l*, eut, 1 cc	1 im *l*, eut, no cc
	In	1 im *l*, 1 cc	no inf	1 im *l*, 2 cc	hom *l*, eut, 1 cc	hom *l*, eut, 1 cc	hom *l*, eut, 2 cc
	Tl	2 im *l*, 1 cc	2 im *l*, 2 cc	1 im *l*, 1 cc, eut	1 im *l*, no cc, eut	hom *l*, eut, no cc	hom *l*, eut, 1 cc
IIB	Zn	2 im *l*, 1 cc	no inf	hom *l*, 1 cc	hom *l*, eut, 2 cc	hom *l*, eut, 1 cc	hom *l*, eut, no cc
	Cd	2 im *l*, 1 cc	2 im *l*, 1 cc	hom *l*, 1 cc	hom *l*, eut, 1 cc	hom *l*, eut, 1 cc	hom *l*, eut, no cc
	Hg	2 im *l*, 1 cc	no inf	no inf	no inf	no inf	hom *l*, no cc
IB	Cu	2 im *l*, 1 cc	2 im *l*, 1 cc	1 im *l*, eut, 1 cc	hom *l*, eut, 1 cc	hom *l*, eut, 1 cc	hom *l*, eut, no cc
	Ag	2 im *l*, 1 cc	2 im *l*, 1 cc	1 im *l*, eut, 1 cc	hom *l*, eut, no cc	hom *l*, eut, no cc	hom *l*, eut, no cc
	Au	1 im *l*, 1 cc(?)	1 im *l*, 1 cc(?)	hom *l*, eut, 1 cc	hom *l*, eut, no cc	hom *l*, eut, no cc	hom *l*, eut, no cc
VIII	Ni	1 im *l*, eut, 2 cc	1 im *l*, eut, 2 cc	no inf	hom *l*, eut, 2 or 3 cc	hom *l*, eut, 2 cc	hom *l*, eut, no cc
	Pd	1 im *l*, 1 cc(?)	no inf	hom *l*, eut, 1 cc	no inf	hom *l*, eut, 2 cc	hom *l*, eut, 1 cc
	Pt	no inf	no inf	no inf	hom *l*, eut, no cc	hom *l*, eut, 1 cc	hom *l*, eut, 1 cc
	Co	1 im *l*, eut, 2 cc	1 im *l*, eut, 1 cc(?)	hom *l*, eut, 1 cc	hom *l*, eut, 1 cc	hom *l*, eut, 1 cc	eut, no cc, 1 im *l*
	Rh	no inf	no inf	no inf	no inf	hom *l*, eut, no cc	hom *l*, eut, no cc
	Ir	no inf	no inf	no inf	no inf	hom *l*, eut, no cc	eut, 1 cc, 1 im *l*
	Fe	1 im *l*, eut, 1 cc	2 im *l*, 1 cc	no inf	hom *l*, eut, 2 or 3 cc	hom *l*, eut, 1 cc	eut, no cc, 1 im *l*
VIIB	Mn	2 im *l*, 1 cc	no inf	no inf	hom *l*, eut, 2 cc	hom *l*, eut, 1 cc	eut, no cc, 1 im *l*
VIB	Cr	2 im *l*, 1 cc	no inf	no inf	no inf	hom *l*, eut, 1 cc	eut, no cc, 1 im *l*
	Mo	1 im *l*, 1 or 2 cc	no inf	no inf	no inf	no inf	no inf
	W	1 im *l*, eut, 1 cc	no inf	no inf	no inf	no inf	no inf

Abbreviations: hom *l*, homogeneous liquid; im *l*, immiscible liquids; eut, eutectic; cc, congruently melting compound; ss, complete solid solution between end members; no inf, no information on melting relations.

mineralogically important systems have been investigated. Additional study is likely to increase the number of systems having two liquid immiscibility fields. It is interesting to note that those systems that contain a true compound (i.e., a compound that melts at an invariant temperature to a liquid of the same composition as the solid in the presence of a vapor that has the same composition as the solid and liquid) also contain two liquid immiscibility fields. In these systems one liquid immiscibility field occurs on the metal side of the true compound and one on the sulfur side.

The generalization emerging from the data in column 1 of Table 21, that all binary metal-sulfur systems contain one or two fields of liquid immiscibility, may perhaps be expanded. The extended rule

would include the statement that when a true compound occurs in a binary metal-sulfur system a field of liquid immiscibility exists on the metal side as well as the sulfur side of the compound. It does *not* follow that a compound is "true" if liquid immiscibility fields occur on both its metal and sulfur sides.

The metal-sulfur systems without exception each contain one or two congruently melting compounds (Table 21, column 1). Classification of these systems based on the number of compounds does not appear feasible at this stage, although as many as seventeen of the listed systems contain one congruently melting compound and only six systems contain two such compounds.

The selenide systems behave very much like the sulfide systems, as noted from column 2 of Table 21. The only exception to the general rule of liquid immiscibility is displayed by the aluminum-selenium system, in which a homogeneous liquid field reportedly transects the entire system. The experimental data (obtained by Chikashige and Aoki, 1917) are incomplete, especially in the Al-Al_2Se_3 portion of the system. A restudy with modern equipment might reveal the existence of a liquid immiscibility field in this region.

The tellurides are more metallic than the sulfides and the selenides and display very different band structures and optical properties. The melting relations of sulfide and selenide systems, on the one hand, and telluride systems, on the other, are markedly different. Binary tellurium systems involving the elements from groups V and IVA all contain homogeneous liquids over their entire width. The IIIA elements-tellurium systems contain immiscible liquid fields. The only recorded exception again appears to be provided by aluminum. Reinterpretation of the experimental data obtained by Chikashige and Nosé (1917), however, indicates that liquid immiscibility probably exists above 800°C in the Al-Al_2Te_3 portion of the Al-Te system.

The group IIB and group VIII metals-tellurium binary systems apparently contain homogeneous liquids, as does the Au-Te system, whereas the other group IB metals, copper and silver, produce immiscible liquid fields when associated with tellurium.

Perusal of Table 21 demonstrates that tellurium in the majority of the listed systems behaves much more like arsenic than like sulfur or selenium. Therefore the term sulfide-type system should, in general, be applied to sulfide and selenide systems only, and tellurides should be classified with the arsenide-type systems. The systems As-S, Sb-S, Bi-S, and As-Se, Sb-Se, and Bi-Se belong to the sulfide-type systems, not to the arsenide-type.

Arsenide-Type Systems

The melting relations in arsenide-type systems are characterized by the existence of a homogeneous liquid field along the entire length of the liquidus. The arsenide-metal systems listed in Table 21 indicate only one exception to this rule, namely, Tl-As. The phase relations in this system were studied by Mansuri (1922), who employed open crucibles.

The antimony-metal systems all behave like the arsenic-type systems, with formation of homogeneous liquids. Most of the bismuth systems behave like the arsenide systems, but because of the metallic character of bismuth a number of them are essentially alloy systems. Bismuth does not take on the role of anion and therefore contrasts to sulfur and selenium, which are the anions in all their metal compounds, and to tellurium, arsenic, and antimony, which are generally anions.

Conclusions

The term sulfide-type system in the past has been commonly used to indicate a system that, in addition to one or more typical metals, also contains one or more of the elements sulfur, selenium, tellurium, arsenic, antimony, or even bis-

muth. This term would imply that the behavior of systems containing a typical metal together with any one of the last five elements should be at least similar to that of the system involving the same metal and sulfur. In other words, the sulfide-type systems would be expected to behave somewhat like the sulfide system. Compilation of experimental data on melting relations in more than 100 pertinent binary systems shows that such similarity in behavior does not exist. If the term sulfide type is to have any relevance to classification or grouping of binary systems, it must be confined to sulfides and selenides. Only a few telluride systems (those involving the IIIA and IB groups of metals) are of the sulfide type.

If we accept this limitation, a general rule emerges for which no exception is known: Binary sulfide-type systems contain one or two fields of liquid immiscibility as well as one or two congruently melting compounds.

The arsenide-type systems, according to the present classification, include all binary arsenic and antimony systems as well as most tellurium and bismuth systems. These systems, without exception, each contain a homogeneous liquid field; liquid immiscibility does not occur. Most of the arsenide-type systems contain one congruently melting compound, although very many contain none, a fair number contain two, and a few three.

All sulfide and selenide binary systems are of the sulfide type, and all arsenide and antimonide systems are of the arsenide type. Telluride systems are transitional but most belong to the arsenide type. Bismuthide systems are transitional between the arsenide-type and alloy-type systems but most are of the arsenide type.

Low-Temperature Phase Relations in the Fe-S System

L. A. Taylor

It has repeatedly been shown (e.g., Desborough and Carpenter, 1965) that all pyrrhotites in nature represent low-temperature assemblages that are definitely stable below 320°C and probably near 25°C, regardless of the initial temperature of deposition. Thus, the high-temperature chemistry of many pyrrhotites is masked by the low-temperature phase relations.

As a result of the present investigation, knowledge of the phase relations involving the various species of pyrrhotite below 320°C has been extended by means of X-ray diffraction studies at controlled temperatures and by shear pressure experiments. In addition, a new find of the mineral smythite ($Fe_{3+x}S_4$) has permitted a systematic study of its chemical and physical properties and its relationship to the other iron sulfide phases. This smythite from Cobalt, Ontario, is distinctly different from the type specimens from Indiana.

Monoclinic Pyrrhotite

Monoclinic pyrrhotite (abbreviated hereafter as m-po), generally referred to as Fe_7S_8, is the most common of the pyrrhotite minerals and possesses a measurable solid solution field. This is shown in Fig. 29, which summarizes the low-temperature phase relations in the central portion of the Fe-S system.

Compositional limits. The sulfur-rich limit of m-po, the subject of much recent concern (e.g. Arnold, 1969; Yund and Hall, 1969; Clark, 1966), was reexamined in the present study by the following method. $Fe_{1-x}S$ with 46.0 atomic % Fe, synthesized as a homogeneous phase at 700°C, was annealed at various temperatures between 290° and 75°C for periods of up to 12 weeks. The $Fe_{1-x}S$ exsolved pyrite (py), became monoclinic, as determined by X-ray examination of supercell reflections, and adjusted to a compo-

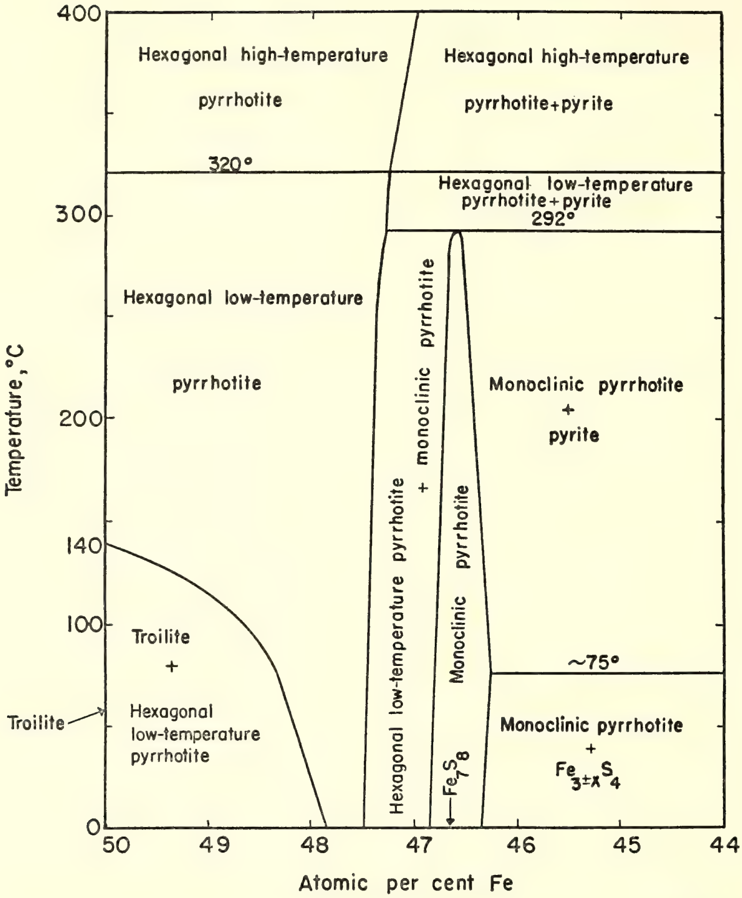

Fig. 29. Phase relations at low temperatures in the region from 44 to 50 atomic % Fe in the condensed Fe-S system.

sition on the m-po solvus.* This m-po was annealed at 330°C for 5–10 minutes and thereby was converted completely to hexagonal pyrrhotite (h-po), the compostion of which was determined from the curve for $d_{(10.2)}$ versus composition of Arnold (1962). The present study indicates that m-po coexisting with py contains more sulfur (i.e., ~0.25 atomic % at 200°C, ~0.35 atomic % at 100°C) than indicated by the Fe_7S_8 formula (see Fig. 29). The solvus below 250°C is, within the experimental error, in good agreement with the experimental findings of Clark (1966) and Yund and Hall (1969) and with the reported compositions of m-po in ores (Arnold, 1967).

The iron-rich limit of the m-po solid solution field was investigated in the present study by exsolution experiments conducted by annealing homogeneous high-temperature pyrrhotites with various compositions between 47.5 and 46.5

* Arnold (1969) has reported that equilibrium is not atttained in such experiments. When using etching techniques for phase identification, he always observed h-po + m-po + py as products, and on the basis of the relative proportions of these phases, he interpreted his results as indicating that m-po is a metastable phase with respect to h-po + py.

atomic % Fe at temperatures from 280° to 200°C. Difficulties were encountered in obtaining consistent results in these "appearance of phase" experiments because (1) an uncertainty exists in the optical identification of small amounts of h-po occurring with m-po even when etching techniques are used and (2) the intensities of the split "10·2" peaks of m-po are not necessarily indicative of the presence or absence of h-po, as explained below. Therefore, supercell reflections were used to identify the presence of h-po and/or m-po. Figure 29 shows the iron-rich solvus of the m-po phase as a nearly vertical line below 290°C with a composition of 46.75 ± 0.10 atomic % Fe.

Thermal stability. The maximum thermal stability of m-po, in equilibrium with vapor, has been variously reported as 320°C (Grønvold and Haraldsen, 1952), 310°C (Kullerud, 1967), 308°C (Clark, 1966), and 304°C (Arnold, 1969). However, none of these investigators was able to successfully reverse the reaction m-po $\rightleftarrows$ h-po + py. During the present study it was determined that m-po broke down to h-po + py only above 310°C. This breakdown can be represented by the reaction m-po $\rightleftarrows$ h-po$_1$ $\rightarrow$ h-po$_2$ + py, where the subscripts refer to different compositions of the h-po. The m-po transforms rapidly (in minutes at 330°C) to an h-po of the same composition; this h-po only slowly (in months at 312°C) exsolves py and adjusts to a composition on the pyrrhotite solvus. Therefore, the inversion of m-po to an h-po of the same composition was investigated during the present study.

Monoclinic pyrrhotite of Fe_7S_8 composition was found to invert to h-po of Fe_7S_8 composition rapidly and reversibly at $292° \pm 4°C$, and unit-cell dimensions of m-po were determined at various temperatures below the inversion. A 19-cm Debye-Scherrer camera on a modified Unicam unit, calibrated with Si ($a_{25°} = 5.4306$ Å), was used to X-ray the samples in sealed, evacuated silica capillaries at elevated temperatures. Figure 30 shows detailed cell data obtained from this study after a least-squares refinement (LCLSQ) of the X-ray data according to the program of Burnham (*Year Book 61*). The h-po reflection data obtained at 300°C were given monoclinic indices and resulted in the calculated cell parameters, based on the m-po unit cell, shown in Fig. 30. Theoretically, the breakdown of m-po to h-po + py must occur at a slightly lower temperature than the inversion to the metastable h-po; however, the maximum thermal stability of m-po is stated here as $292° \pm 4°C$. The high-temperature, single-crystal study of Corlett (1968) indicated a somewhat lower inversion temperature for m-po $\rightleftarrows$ h-po, $225° \pm 10°C$, whereas Yund and Hall (1969) concluded that m-po is metastable above 290°C and possibly lower.

Although h-po of Fe_7S_8 composition is metastable above 292°C, it is not possible to retain this hexagonal species as a product of "normal" quench experiments with annealing temperatures below 310°C. Consideration of the kinetics involved in the isochemical reaction of h-po to m-po explains the discrepancy between the high-temperature X-ray (292°C) and quenching experiments (310°C). An m-po (Fe_7S_8) that is annealed at 330°C for 10 minutes to convert it to h-po and then is rapidly cooled by immersion of the silica tube in water yields an h-po having the same composition as the original m-po. In an experiment conducted at 330°C, the silica tube was allowed to cool in air for 15 seconds before being chilled to 25°C. The h-po completely reverted to the monoclinic structure in these few seconds, a finding previously reported by Taylor (1968). An m-po annealed at $304° \pm 1°C$ and rapidly chilled in water produced m-po, whereas an original m-po annealed at the same temperature but quenched by immersion in liquid N_2 gave X-ray evidence of having retained the hexagonal structure. Therefore, the determination of the

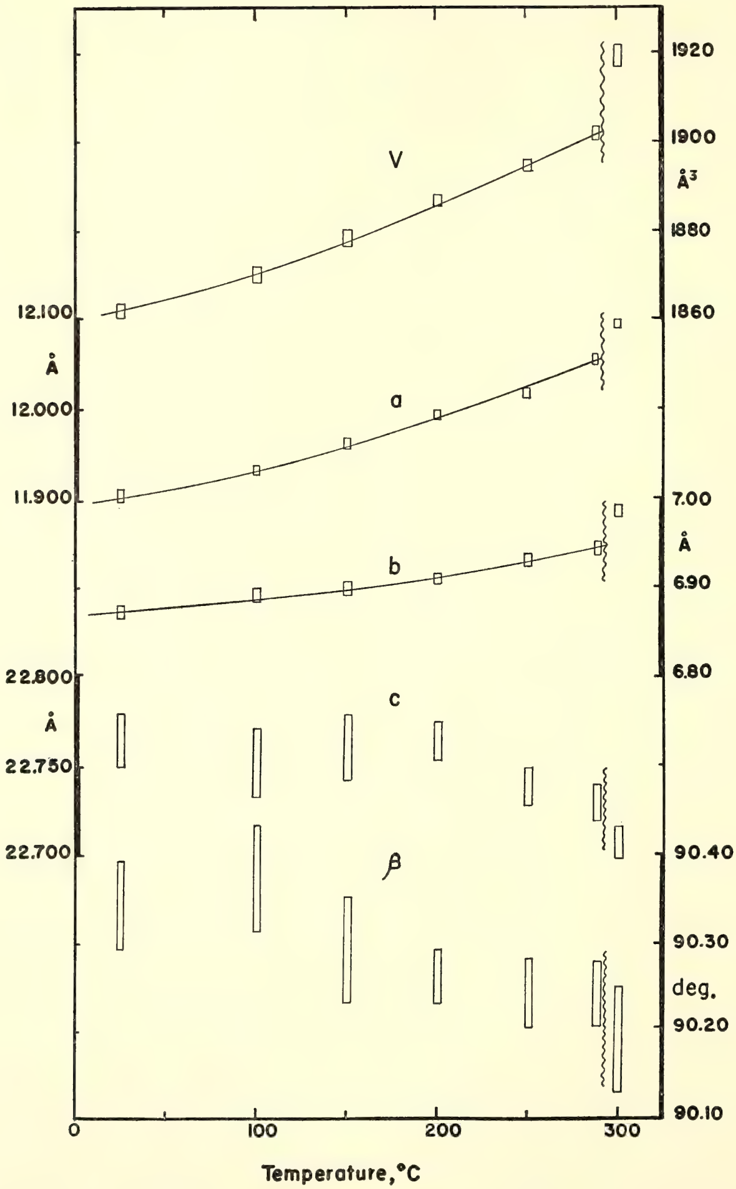

Fig. 30. Data on unit-cell parameters versus temperature for monoclinic pyrrhotite of Fe_7S_8 composition. For the cell used $a = 2A\sqrt{3}$, $b = 2A$, $c = 4C$. Maximum thermal stability of the monoclinic phase is shown by the wavy line at 292°C. The 300°C data are explained in the text.

upper stability temperature in this manner is largely a matter of quenching rate.

Attempts to synthesize m-po from its presumed equilibrium breakdown products, h-po + py, produced m-po at 280°C but not at 296°C and thus agree with the 292°C upper stability temperature obtained from the X-ray study. Experiments with reactants of h-po (48.0 atomic % Fe) + py and h-po (47.0 atomic

% Fe) + py at 296°C equilibrated to an assemblage of h-po + py; the h-po compositions plot on an approximate extension of the high-temperature pyrrhotite solvus (i.e., ~47.35 atomic % Fe). At 280°C a charge of h-po (47.5 atomic % Fe) + py, after 86 days and several regrindings, had partially reacted to produce m-po.

"10·2" reflections. X-ray diffraction charts of m-po usually show a characteristic splitting of the "10·2" reflection into two peaks, the (408)-(228) and the ($\bar{4}08$)-($\bar{2}28$) reflections. With a mixture of m-po + h-po, the (10·2) of the h-po is superimposed on the (408)-(228) peak of the m-po, usually resulting in a greater intensity for this peak versus the ($\bar{4}08$)-($\bar{2}28$). Thus, when the lower 2θ—i.e., the (408)-(228)—peak is the larger of the two resolved peaks, it is usually attributed to the presence of h-po in addition to the m-po (Arnold, 1966). Frequently, however, the reverse situation is encountered (i.e., $I_{\bar{4}08} > I_{408}$). Kullerud (1967) suggested that this "reversed" intensity situation may be a function of the temperature of formation of the m-po. During the present study it was determined that the resolution and relative intensities of the (408)-(228) and ($\bar{4}08$)-($\bar{2}28$) reflections are not correlative with annealing temperature but are largely a function of grain size and smear-mount preparation for X-ray study. Different portions of the same smear mount may show grossly different relative intensities.

From X-ray diffraction studies at 25°C of m-po formed by annealing previously synthesized high-temperature h-po of Fe_7S_8 composition at 300°, 200°, and 100°C, it was found by least-squares refinement based on 15 reflections that the β angle does not vary as a function of the temperature of formation, as suggested by von Gehlen (*Year Book 62*) based on the resolution and measurement of the "10·2" peaks. The β angle does change slightly as a result of thermal expansion (see Fig. 30), but the higher temperature β angle is not preserved upon cooling to 25°C.

Effects of grinding and pelletizing. In order to hasten the attainment of equilibrium, certain techniques are routinely incorporated as part of the experimental procedure; charges are commonly (1) finely ground to produce more fresh surface areas for reaction and/or (2) pressed into pellets to provide more intimate contact for the reacting phases. The effects of shear pressures introduced by these techniques, however, can lead to contradictory results (Taylor, 1968).

The effect of grinding on the X-ray powder diffraction pattern of m-po is pronounced. An m-po of Fe_7S_8 composition was subjected to various durations of regular hand grinding under toluene (to prevent oxidation). At the end of each grinding interval, a portion of the ground material was X-rayed. Examination of the diffractometer tracings revealed that the (408)-(228) and ($\bar{4}08$)-($\bar{2}28$) reflections of m-po became diffuse and were gradually replaced, with increased grinding time, by a single reflection. Supercell reflections became diffuse and could not be positively identified because of the weak intensities encountered. The thermal effects of grinding were not large; a thermocouple placed in the toluene during grinding showed a temperature increase of <1°C. Grinding may have transformed the monoclinic phase into a hexagonal one, or broadening of the (408)-(228) and ($\bar{4}08$)-($\bar{2}28$) reflections may have caused them to merge.

Monoclinic pyrrhotite of Fe_7S_8 composition was also subjected to directed pressure in a small cylinder press to see if simple deformation of the crystals would cause the "10·2" and supercell reflections to become diffuse. Instead, after only 5 minutes, the (408)-(228) and ($\bar{4}08$)-($\bar{2}28$) peaks of the m-po were replaced by a single sharp peak. Supercell reflections remain relatively sharp; although the results obtained from several experiments are not entirely reproducible,

the general effect of this pressure was to produce new supercell reflections, listed below for a typical experiment (Table 22).

The significance of these shear-pressure induced effects is not known at present. Monoclinic pyrrhotite might be a stable phase in the condensed system, the pressures produced during grinding or pelletizing transforming it into a high-pressure modification of h-po, or perhaps m-po is a metastable phase in the condensed system, as originally suggested by Hall and Yund (1966) and recently stressed by Arnold (1969). The effects of shear pressure on m-po should be considered when we interpret results obtained using reactants that have been subjected to grinding or pelletizing.

Hexagonal Pyrrhotite

Compositional limits. The low-temperature iron-rich limit of h-po (coexisting with troilite [tr] as shown in Fig. 29) was investigated by exsolution experiments in which previously synthesized homogeneous po exsolved to a mixture of tr and h-po. A diffractogram of the charge showed a split "10·2" peak similar in appearance to that of m-po; however, one peak was from tr and the other was from the h-po. The *d* values of these peaks were used to obtain the composition of the phases. The tr was always stoichiometric, and the compositions of the h-po are in good agreement with the results of Yund and Hall (1968) but differ slightly from those of Arnold (1969). It is this splitting of the "10·2" that led Moh and Kullerud (*Year Book 63*) to believe that they had synthesized m-po from FeS+S in aqueous solutions held at 100°C for 11 days; they produced a tr+h-po assemblage whose compositions were similar to those found during the present study.

TABLE 22. Effects of Pelletizing on Supercell Reflections of Monoclinic Pyrrhotite (Fe_7S_8)

Total Time of Applied Pressure, minutes	Supercell Reflections, Å				
0	4.70	...	5.27	5.72	...
10	...	4.92	5.29	5.72	...
40	...	4.92	...	5.74	5.88
2520	...	4.90	...	5.72	5.87

The sulfur-rich limit of the low-temperature h-po field from ~290°C down is depicted as approximately vertical in Fig. 29, in agreement with the observation that h-po in association with m-po in natural assemblages is restricted in composition (Arnold, 1967). A point of 47.35±0.10 atomic % Fe at 296°C was determined during the present investigation. This value is in agreement with previous values of 47.45 (Yund and Hall, 1969) and 47.2 atomic % Fe (Arnold, 1969).

X-ray diffraction at elevated temperatures. High-temperature X-ray data were obtained on hexagonal pyrrhotites with the Unicam unit. The pyrrhotites were prepared at 700°C, quenched to 25°C, and then annealed at 250°C for 1 month prior to X-ray examination. At least 15 reflections between 40° and 180° 2θ (FeKα) were measured. Most of the unit-cell data presented refer to the simple NiAs cell. This convention was adopted because it would provide some common factors for comparison at various temperatures and compositions and because of the uncertainties associated with the presence of various $Fe_{1-x}S$ supercells, many of which are undoubtedly quench products.

The maximum thermal stability of the troilite superstructure (i.e., α transition), in equilibrium with vapor, has been variously reported by Roberts (1935), Haraldsen (1941), Moh and Kullerud (*Year Book 63*), Sugaki and Shima (1965), and Arnold (1969) as 139°–144°, 138°, 139°, 155°, and 150°C, respectively. High-temperature X-ray examination of FeS during the present study places this transition temperature at 140°±5°C, confirming the earlier experimental work.

Figure 31 shows the breaks in slope in a plot of cell volume versus temperature

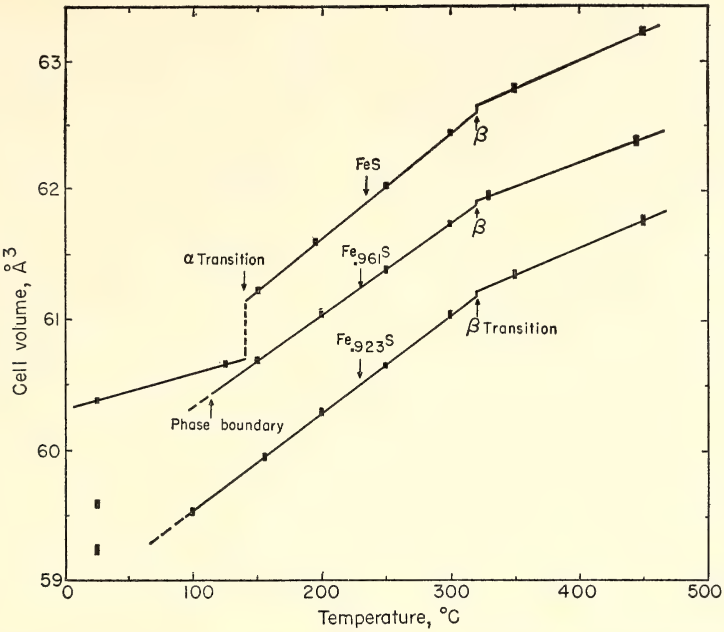

Fig. 31. Data on unit-cell volume versus temperature for selected $Fe_{1-x}S$ compositions. The simple NiAs (*B*8) cell was used.

of FeS due to the α and β transitions at 140° and 320°C, respectively. The ΔV associated with the α transition is $\approx +0.22$ Å^3/mole-FeS and the effect of pressure on the transition, using the ΔH from Robie and Waldbaum (1968), would be to raise the temperature about 2.3°C/kb. However, Kullerud, Bell, and England (*Year Book 64*) determined the curve by differential thermal analysis from about 2 to 19.7 kb and found that pressure lowers this transition temperature by 2.2°C/kb, indicating a negative ΔV. This apparent discrepancy suggests that a high-pressure polymorph of FeS becomes stable below 2 kb, resulting in an arrangement of univariant curves similar to those reported for Ni_3S_4 by Kullerud (*Year Book 67*).

At temperatures below the α transition, FeS has the troilite superstructure. Above 140°C but below 320°C several weak reflections were observed for FeS, as well as for the other compositions examined, which could not be indexed on the basis of the simple NiAs cell, suggesting the presence of some supercell. Systematic changes in these reflections were not observed, however, possibly owing to the insensitive nature of the examination of the specimens—as powder samples. Above 320°C no such reflections were observed, and it is concluded that $Fe_{1-x}S$ above the β transition possesses the simple hexagonal *B*8 structure of NiAs.

In a refinement based on 41 reflections, troilite (with supercell $a=\sqrt{3A}$, $c=2C$) at 25°C was determined to have $a=5.966\pm0.001$ Å, $c=11.755\pm0.003$ Å, and $V=362.2\pm0.1$ Å^3, in close agreement with values previously reported.

Hexagonal pyrrhotites of various compostions were also examined at elevated temperatures. Figure 31 depicts plots of cell volume versus temperature for pyrrhotites with 50.0 (FeS), 49.0 ($Fe_{0.961}S$), and 48.0 ($Fe_{0.923}S$) atomic % Fe. It should be noted that the 25°C volumes for the last two compositions do not plot on an extension of the higher temperature

data and may be related to the discontinuity in the plot of cell parameters versus composition described by Fleet (1968). The pyrrhotites with 48 and 49 atomic % Fe at 25°C are within the tr+h-po+V univariant field (Fig. 29) and are thus metastable at this temperature.

Thermal Expansion Data

Thermal expansion is commonly expressed by means of the thermal-expansion coefficient: $\alpha = 1/V(\partial V/\partial T)_P$. The pressure over Fe-S phases within the temperature range of examination are low ($f_{S_2} \approx 10^{-50}$ to 10^{-5} atm), and for all practical purposes, $\alpha \simeq 1/V_0(dV/dT)$, where V_0 represents the volume at some reference temperature.

The procedures for obtaining the thermal-expansion data were described in the previous sections. Figure 32 shows isotherms at 50°C intervals for the homogeneous $Fe_{1-x}S$ field. Thermal-expan-

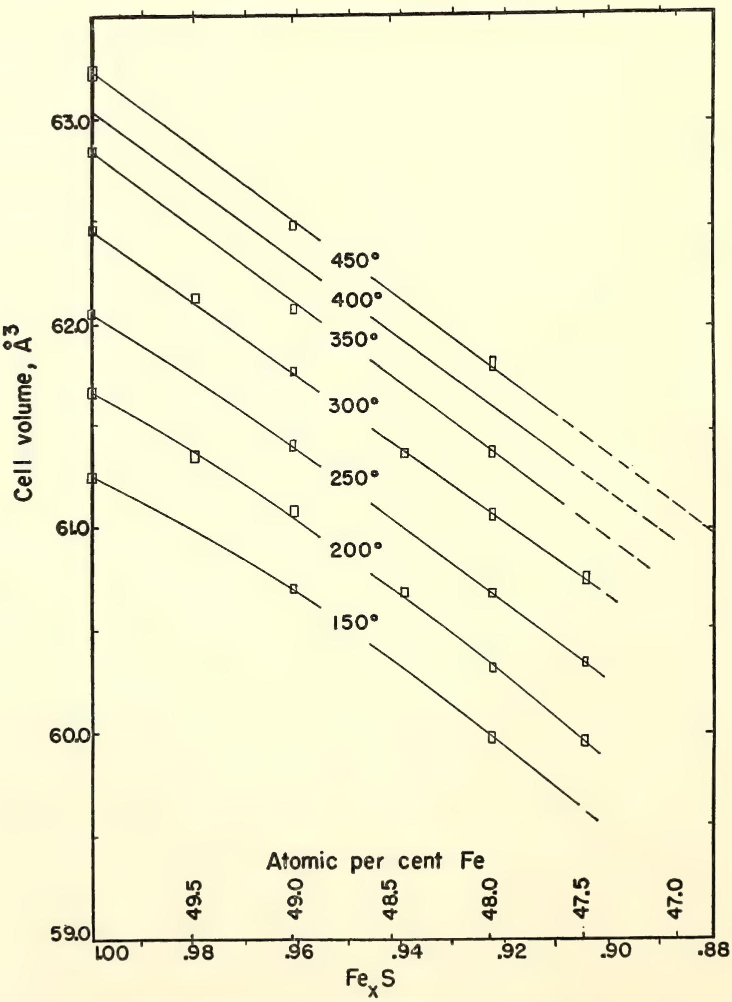

Fig. 32. Data on unit-cell volume versus composition at elevated temperatures for $Fe_{1-x}S$ compositions. The simple NiAs ($B8$) cell was used.

TABLE 23. Thermal Expansion Data for the Fe-S Compounds

Composition *	Temperature Range, °C	$\alpha, T \times 10^{-6}$ †	$\Delta a/100°C$, % ‡	$\Delta c/100°C$, % ‡
$Fe_{1.000}S$	25–140	4.5	0.25	−0.34
	140–320	12.5	0.84	−0.37
	320–450	7.2	0.28	−0.04
$Fe_{0.961}S$	115–320	11.6	0.67	−0.24
	320–450	6.1	0.30	−0.05
$Fe_{0.923}S$	75–320	12.6	0.70	−0.17
	320–450	6.9	0.34	−0.02
$Fe_{0.875}S$	25–292 §	9.0	0.54	~0
	292–320 ‖	~8	0.43	−0.22
$Fe_{3.25}S_4$ (smythite)	25–75	15.7	0.74	~0
	75–155	11.1	0.38	+0.37
FeS_2 ¶ (pyrite)	25–300	1.1	0.11	...

* All compounds listed are synthetic except for the smythite, which was found at Cobalt, Ontario.

† $\alpha \cong 1/V_0(dV/dT)$, where V_0 represents the volume at the lowest temperature of the temperature range under consideration.

‡ a and c are not strictly linear functions of temperature; however, the cell parameters versus temperature were plotted and a "best-fit" straight line was drawn through the data points. % $\Delta a/100°C = \Delta a \times 100/a_0 \times 100°C$, where a_0 represents the a dimension at the lowest temperature of the temperature range under consideration.

§ Refers to the monoclinic cell, $a = 2A\sqrt{3}$, $b = 2A$, $c = 4C$.

‖ Metastable hexagonal pyrrhotite.

¶ $a_{25°} = 5.4175 \pm 0.0001$ Å.

sion coefficients (α) determined during this study for several h-po compositions and for other iron sulfides are compiled in Table 23.

Anisotropy in pyrrhotite is well displayed by the thermal data obtained during this study. At a given temperature, the c dimension varies greatly with composition, whereas the a dimension varies much less. For a given composition, however, a increases greatly and c actually decreases slightly with increasing temperatures; the net effect is an increase in volume with increase in temperature. This volume increase with temperature is much larger than that reported for any other sulfide mineral except pentlandite (Morimoto and Kullerud, *Year Book 63*).

Smythite, $Fe_{3+x}S_4$

Smythite was discovered with calcite and sulfide minerals in a nearly horizontal cross vein closely associated with silver-bearing veins at the Silverfields Mine, Cobalt, Ontario. Chemical and physical data show that this smythite is distinctly different from that of the type locality at Bloomington, Indiana (Erd, Evans, and Richter, 1957).

Smythite from Cobalt occurs in two distinct mineral assemblages. In one it is associated with pyrite, marcasite, and sphalerite containing 9 ± 1 mole % FeS; in the other with galena, chalcopyrite, monoclinic pyrrhotite, and sphalerite containing 13 ± 1 mole % FeS (sphalerite compositions were determined by microprobe analyses). Bladed pyrite inclusions within smythite contain 5.4 wt % Ni. This Ni content is one of the highest reported for a natural pyrite and is not consistent with the "dry" phase relations as determined at low temperatures in the Fe-Ni-S system; it may be related to the metastable pyrite compositions described by Clark and Kullerud (1963).

Electron-microprobe analyses of the smythites from these two assemblages are shown in Table 24. No other elements in amounts greater than 0.1 wt % were detected. The analyses show a difference in the compositions of the smythites; the one coexisting with monoclinic pyrrhotite

TABLE 24. Electron-Microprobe Analyses of Smythites from Cobalt, Ontario, wt %

	Smythite			Theoretical Formulae	
	po Assemblage	py Assemblage	Precision	Fe_3S_4	$Fe_{3.25}S_4$
Fe	58.5	58.1	0.2	56.64	58.60
Ni	0.4	0.5	0.1	...	...
S	40.9	41.5	0.3	43.36	41.40

contains 0.4 wt % more Fe than the one with pyrite, but the difference is near the limits of precision. These compositions indicate a metal/sulfur ratio of approximately 13/16, halfway between Fe_7S_8 (monoclinic pyrrhotite) and Fe_3S_4 (stoichiometric smythite), and lead to the formula $Fe_{3+x}S_4$, where $x \simeq 0.25$ (see theoretical formula in Table 24), a cell content of $Fe^{3+}_{4.5}Fe^{2+}_{5.25}S_{12}$.

Density determinations with Clerici solution were made at 25°C on the smythite from Cobalt and gave 4.33 ± 0.01 g/cc. The calculated density, for a composition of $Fe_{3.25}S_4$ and the cell parameters mentioned below, is 4.319 g/cc. In comparison, the Indiana specimen has a measured density of 4.06 g/cc and a calculated density of 4.09 g/cc (Erd, Evans, and Richter, 1957).

Smythite does not break down readily upon heating in sealed, evacuated silica tubes. After 194 days at 210° ± 5°C, only partial breakdown to monoclinic pyrrhotite and pyrite was observed, a result compatible with the phase relations as shown in Fig. 29. Attempts to synthesize smythite in the "dry" Fe-S system with pelletized mixtures of monoclinic pyrrhotite (Fe_7S_8) + pyrite and monoclinic pyrrhotite + S were unsuccessful. A hexagonal pyrrhotite of 46.0 atomic % Fe presynthesized at 700°C was observed to exsolve pyrite and change to the monoclinic form at temperatures down to 75°C, suggesting that smythite is stable only below this temperature.

The unit-cell parameters of the smythite from Cobalt were determined at various temperatures (Fig. 33) by the high-temperature X-ray technique previously described. At 25°C, $a = 3.4651 \pm 0.0005$ Å, $c = 34.34 \pm 0.02$ Å, $V = 357.1 \pm 0.2$ Å^3, referred to the cell used by Erd, Evans, and Richter (1957), apparently not the true cell (see below). These dimensions are approximately the same as those of the original samples from Indiana (i.e., $a = 3.47$ Å, $c = 34.5$ Å). Figure 33 shows a discontinuity in the cell volume of smythite as a function of temperature at approximately 75°C. These curves were determined by X-ray analysis of smythite, first at 25°C, and then at successively higher temperatures, followed by a reexamination of each temperature, proceeding from 152°C down to 25°C. The exact nature of this break is not known at present; the apparent "transition" is reversible, however, and may be indicative of the presence of a high-temperature polymorph of this smythite.

Monoclinic pyrrhotite and smythite are indistinguishable in polished section and were identified with certainty only by X-ray diffraction studies. Precession photographs of smythite single crystals showed that twinning by reticular merohedry (twin law: 180° rotation about [00·1]) is universal; an intensity study indicated equal volumes for the two individuals of the twin. The basal cleavage that is very prominent in the Indiana specimens is completely lacking in the Cobalt samples. Additional Fe between S layers of the basic Fe_3S_4 sheet structure, with accompanying omission of Fe from other sites, could account for this physical property. Precession photographs of powdered smythite from Cobalt show complete randomness of orien-

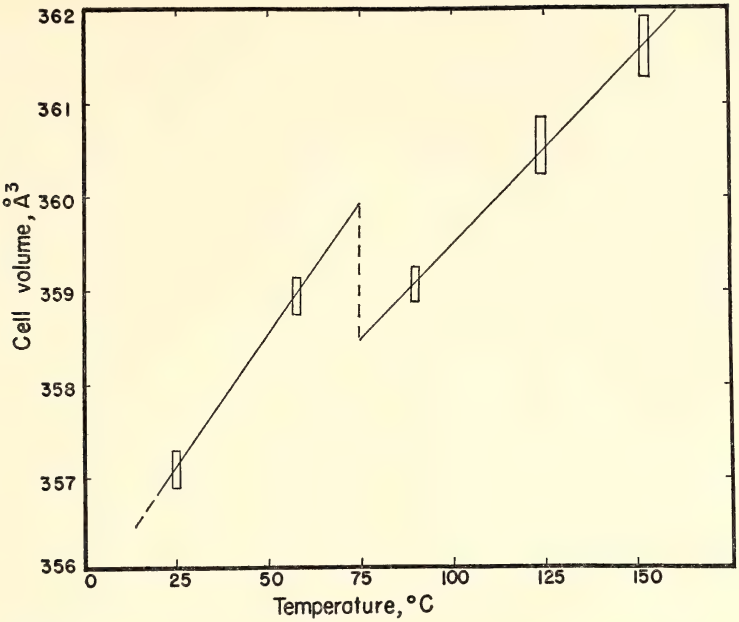

Fig. 33. Data on unit-cell volume versus temperature for smythite from Cobalt, Ontario.

tation. The very weak basal reflections in diffractometer tracings obtained on powder-smear mounts of the Cobalt samples are probably caused by this general absence of basal cleavage, which if present would produce some preferred orientation.

The space group of the Indiana smythite was given as $R\bar{3}m$ (Erd, Evans, and Richter, 1957). Precession photographs of the smythite from Cobalt contain diffuse spots which would require a cell with a doubling of the *a* axis. This larger cell, the true cell, does not possess the R^{xx} aspect of the subcell. Preliminary investigations show the diffraction aspect of the true cell to be of lower symmetry, possibly monoclinic.

Much of the smythite at Cobalt is present as single pure masses. The occurrence of monoclinic pyrrhotite and pyrite in the correct proportions to react upon cooling to form smythite with no excess pyrrhotite or pyrite seems exceedingly unlikely. The chemical inertness of pyrite is also not favorable to such a reaction. It therefore appears probable that this smythite was deposited directly from solution at a low temperature.

A second compound of Fe_3S_4 composition has been reported as the mineral greigite (Skinner, Erd, and Grimaldi, 1964). Actual polymorphic relationship between greigite and smythite, as suggested in the literature, has never been demonstrated. The 2 wt % Fe in the Cobalt smythite in excess of that present in an Fe_3S_4 formula would seem to indicate that these minerals are not polymorphs. By analogy with other M_3S_4-type sulfides, Kullerud (*Year Book 67*) concluded that if smythite and greigite are polymorphs, smythite should be the higher temperature phase. Therefore, the breakdown of smythite, with increasing temperature, should be to monoclinic pyrrhotite (composition near $Fe_{0.875}S$) and pyrite (see Fig. 29). Equations 1 and 2 show this reaction for stoichiometric

smythite and iron-rich smythite, respectively.

$$Fe_3S_4 \rightleftarrows 2.667\ Fe_{0.875}S + 0.667\ FeS_2 \quad (1)$$

$$Fe_{3.25}S_4 \rightleftarrows 3.333\ Fe_{0.875}S + 0.333\ FeS_2 \quad (2)$$

At ~75°C, using the cell volumes as calculated from the thermal-expansion data given in the previous section and assuming that the thermal-expansion coefficient for Fe_3S_4 is approximately the same as for $Fe_{3.25}S_4$, we obtain for equations 1 and 2:

$$72.78\ cm^3 = 46.86\ cm^3 + 16.02\ cm^3 \qquad \Delta V = -9.90\ cm^3 \quad (1)$$

$$72.25\ cm^3 = 58.54\ cm^3 + 8.01\ cm^3 \qquad \Delta V = -5.70\ cm^3 \quad (2)$$

These ΔV values, the largest calculated to date for any sulfides, indicate that the upper stability curve for smythite should have a decided negative slope, a factor perhaps responsible for the scarcity of smythite in nature.

The calculations above also suggest that pressure tends to favor the formation of the iron-rich variety, a suggestion compatible with the occurrence of stoichiometric smythite in geodes at Bloomington, Indiana, and the formation of iron-rich smythite in the silver-bearing veins at Cobalt, Ontario. The composition of smythite may be indicative of the pressures existing during its formation.

The Ni-Sb-S System

*K. L. Williams * and G. Kullerud*

Antimonides and sulfantimonides are constituents of many sulfide ore deposits, but despite the existence of at least four binary compounds in the Ni-Sb system, nickel antimonides appear to be rare in nature. The only one described to date is the mineral breithauptite (NiSb). Ullmannite (NiSbS) is the only mineral belonging to the Ni-Sb-S system that has been reported. The present study was undertaken to clarify confusing aspects concerning the existence and stabilities of phases in the Ni-Sb binary system and to determine the phase relations in the ternary Ni-Sb-S system. Isotherms at 500° and 350°C in the Ni-Sb-S system were studied by quenching experiments, followed by optical, X-ray diffraction, and electron-microprobe examination of the quenched products. Experiments were performed at temperatures between 350° and 500°C to resolve previous conflicts in that portion of the Ni-Sb phase diagram of geological interest and to establish solid solution limits.

Nickel takes considerable amounts of antimony into solid solution. All runs of bulk compositions between 20 and 40 wt % Sb contained this $(Ni,Sb)_{ss}$ phase saturated on Sb. It is readily identified in polished sections by its creamy white color and high reflectivity. No substantial change in composition with temperature was observed; analyses of $(Ni, Sb)_{ss}$ from four runs between 335° and 500°C all showed 15.5 ± 1.0 wt % Sb.

Ni_3Sb was identified in all runs of bulk composition between 20 and 42 wt % Sb. It is characterized in reflected light by a distinctive mauvish brown color; it is weakly anisotropic, with no detectable "reflection pleochroism." Its X-ray diffraction pattern is identical with that given by Fürst and Halla (1938). Results of microprobe analyses were in agreement with the stoichiometric composition (40.9 wt % Sb).

The Ni_5Sb_2 phase was produced in all runs of bulk composition between 46 and 62 wt % Sb. In reflected light it is pale brownish in color, with weak bireflection; it is moderately anisotropic, with brown polarization colors. Microprobe analyses showed a composition of 45.0 ± 0.5 wt % Sb for this phase in all runs of bulk composition between 46 and 62 wt % Sb; this result agrees well with the Ni_5Sb_2 formula proposed by Eremenko and Kruchinina (1951) rather than the Ni_7Sb_3 formula (47.1 wt % Sb) suggested by Sibata (1941). No variation of composition with annealing temperature was observed.

NiSb was identified in all binary runs of bulk composition between 46 and 80 wt % Sb. In reflected light it is superficially similar to Ni_5Sb_2, but NiSb is more pinkish in color, with higher reflec-

* The Australian National University.

tivity and bireflectance, and is more strongly anisotropic.

Microprobe analyses showed the composition of homogeneous NiSb to vary from 64.0 wt % Sb (when in equilibrium with Ni_5Sb_2) to 67.5 wt % Sb (in equilibrium with $NiSb_2$); the latter is the composition of stoichiometric NiSb. Neither limit showed any significant variation with annealing temperature.

The $NiSb_2$ phase was observed in all binary runs containing more than 70 wt % Sb. It is creamy white in reflected light, with moderately high reflectivity, and is fairly strongly anisotropic. Microprobe analyses showed a compositional range from 80.7 wt % Sb (corresponding almost exactly to stoichiometric $NiSb_2$) to 84.0 wt % Sb (close to 83.8 wt % Sb, the composition of Ni_2Sb_5). These data support the formula $NiSb_{2+x}$ given by Rosenqvist (1953) and indicate that x may range from 0 to 0.5; the latter agrees with the formula Ni_2Sb_5 proposed by Osawa and Sibata (1940). No change in the limiting compositions of $NiSb_{2+x}$ was observed over the temperature range investigated. Microprobe analyses of Sb in equilibrium with $NiSb_{2+x}$ confirmed the negligible solubility of Ni—of the order of 0.2 wt % or less.

The only ternary compound known in the Ni-Sb-S system is NiSbS, corresponding to the mineral ullmannite. Ullmannite is cubic, space group $P2_13$, $a_0=5.88$ Å, $Z=4$, S.G. $=6.90$ (Takéuchi, 1957). Its structure resembles that of pyrite, with the S_2 group in pyrite replaced by SbS. In natural occurrences, cobalt and small amounts of iron may substitute for nickel, and arsenic and bismuth for antimony. It occurs most frequently in association with other nickel minerals, such as gersdorffite, niccolite, and breithauptite. Ternary isotherms for 500° and 350°C are shown in Figs. 34 and 35 (all

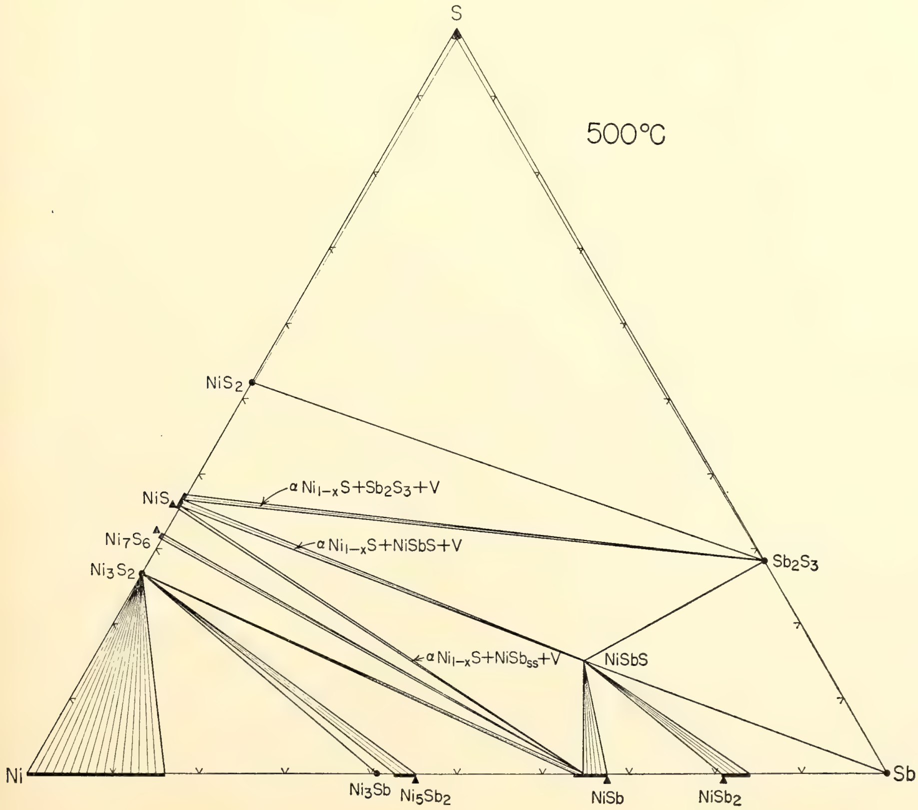

Fig. 34. Phase relations in the Ni-Sb-S system at 500°C. All phases and phase assemblages coexist with vapor.

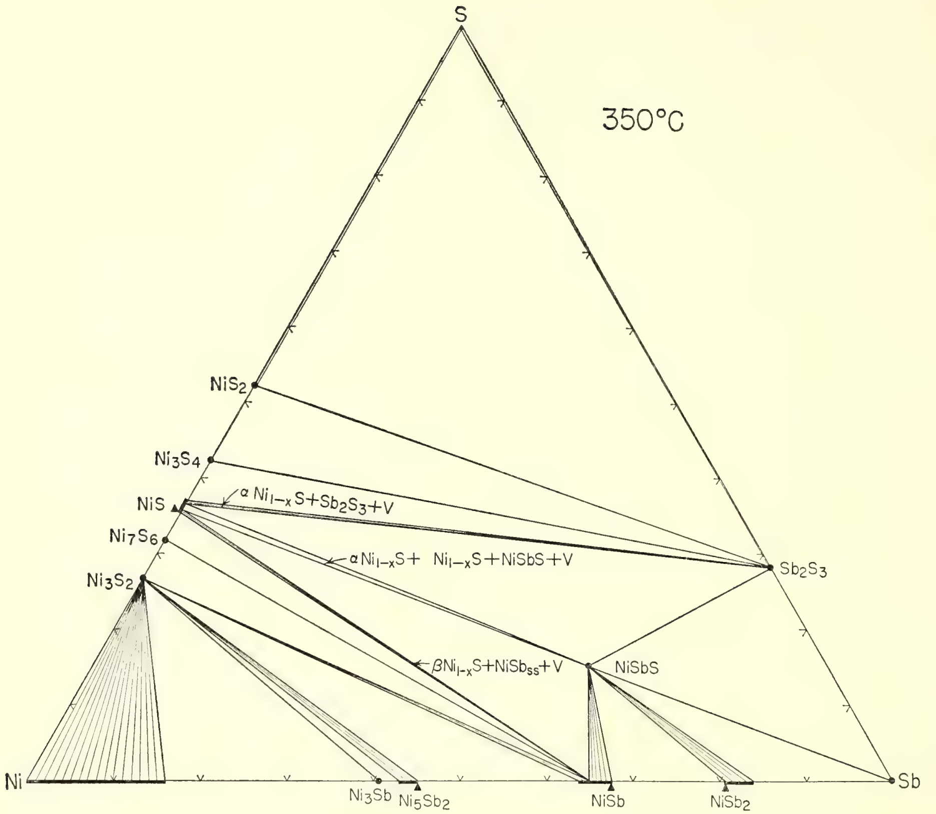

Fig. 35. Phase relations in the Ni-Sb-S system at 350°C. All phases and phase assemblages coexist with vapor.

phases and phase assemblages coexist with vapor).

The solubility of the third element in each of the binary compounds was investigated by microprobe analysis of phases from appropriate runs. The solubilities were found to be uniformly low, in no run exceeding 0.2% and in most runs being lower than the detection limits.

Within the limits of experimental and analytical error, NiSbS showed no departure from stoichiometry in any of the equilibrium assemblages. Its thermal stability was investigated by differential thermal analysis on homogeneous synthetic material, and melting was observed at 752° ± 6°C.

The compositions of Ni_{1-x} and NiSb in various three-phase (+vapor) assemblages were investigated by X-ray diffraction and microprobe analyses. At 500°C $\alpha Ni_{1-x}S$ coexisting with Sb_2S_3 and NiSbS was, from interplanar spacings, found to contain 36.5 wt % S, whereas in equilibrium with NiSb and NiSbS it contains 35.5 wt % S. Microprobe analyses were consistent with these average compositions but again showed some internal variation (+0.3 wt % S). At 350°C $\alpha Ni_{1-x}S$ coexisting with Sb_2S_3 was, from microprobe analyses, found to contain 36.8 ± 0.3 wt % S, and $\beta Ni_{1-x}S$ contained 35.8 ± 0.2 wt % S. These compositions are all consistent with the data of Kullerud and Yund (1962).

The compositions of $NiSb_{ss}$ when coexisting with Ni_3S_2, Ni_7S_6, or NiS, de-

termined by microprobe analysis, all fall within the range 64.8±0.2 wt % Sb at 500°C and 64.7±0.4 wt % Sb at 350°C.

This study shows that the compounds Ni_3Sb and Ni_5Sb_2 can exist only under very low sulfur fugacities, consistent in magnitude with those stabilizing heazlewoodite (Ni_3S_2). Under such conditions, attained for instance during serpentinization of peridotites, the activity of antimony is generally too low to stabilize Ni_3Sb and Ni_5Sb_2 as mineral species.

Breithauptite (NiSb) is not uncommon in ores. The phase relations diagramed in Figs. 34 and 35 show that it coexists stably with minerals such as millerite (NiS) and ullmannite. The $NiSb_2$ compound has not been reported as a mineral species. Since it can coexist with breithauptite and ullmannite or with ullmannite and antimony, which has been reported from many localities, we expect $NiSb_2$ to occur as a mineral in many ores.

The System Cu-S-O

L. A. Taylor and G. Kullerud

Minerals of the Cu-Fe-S-O and Cu-S-O-H systems occur in thousands of localities, and knowledge of the Cu-S-O system is prerequisite to exploration of these geologically important quaternary systems. The metallurgical literature contains abundant data on the Cu-S-O system, obtained from high-temperature experiments performed in containers open to the air or in apparatus designed to measure vapor pressures. With the exception of a few publications (e.g., Reinders and Goudriaan, 1923), the presence of a ternary liquid phase is not mentioned. Kullerud and Yund (*Year Book 61*) conducted a preliminary examination in this system and found that a liquid field transects the system, prohibiting tie lines between the ternary and binary sulfide phases even at temperatures as low as 250°C.

The ternary solid phases encountered during our current investigation are $CuSO_4$, corresponding to the mineral chalcocyanite, and $CuO \cdot CuSO_4$, corresponding to the mineral dolerophanite. No evidence was found for the stable existence of Cu_2SO_4 or any other ternary compounds above 200°C. Both $CuSO_4$ and $CuO \cdot CuSO_4$ are stable from 200°C to temperatures in excess of 700°C.

Figure 36 shows a schematic plot of the phase relations at 500°C. The assemblage $Cu + Cu_2O + Cu_2S$ is stable from high temperatures (>850°C). Tie lines between Cu_2O and $CuSO_4$ are stable below 510°±5°C. Above this temperature the ternary liquid field expands to intersect this join. With decreasing temperature the homogeneous liquid field is divided into two fields by the establishment of tie lines between Cu_9S_5 and $CuSO_4$ at 434°±5°C, as determined by quenching experiments. The presence of H_2O in the $CuSO_4$ drastically lowers this temperature (i.e., to below 360°C). The Cu_2S-$CuSO_4$ join is stable below 390°C. The vapor pressures on the sulfur side of this join are appreciable. A DTA tube containing a mixture of very pure $CuSO_4$ and Cu_9S_5 broke at 520°C in spite of an external confining pressure of 65 bars, and the internal pressure must have been well in excess of 150 bars. The gaseous species are mainly sulfur oxides, principally SO_2. Even higher vapor pressures are encountered on the CuS-$CuSO_4$ join. A silica tube containing a mixture of CuS and $CuSO_4$ exploded at ~270°C. One containing a mixture of $CuSO_4$ and S exploded below 200°C, and the vapor pressure over this assemblage must approximate that of pure SO_2 (i.e., ~100 bars at 180°C).

Charges consisting of CuO and $CuSO_4$ react to form $CuO \cdot CuSO_4$ at temperatures from 700° to 200°C. The positions and intensities of X-ray reflections of the synthetic phase are not wholly consistent with the data for the mineral dolerophanite (Mrose, 1961). Tie lines between Cu_2O and $CuO \cdot CuSO_4$ are stable at high temperatures (i.e., >500°C) but are not observed at 350°C. The details of the changes in phase relations as a conse-

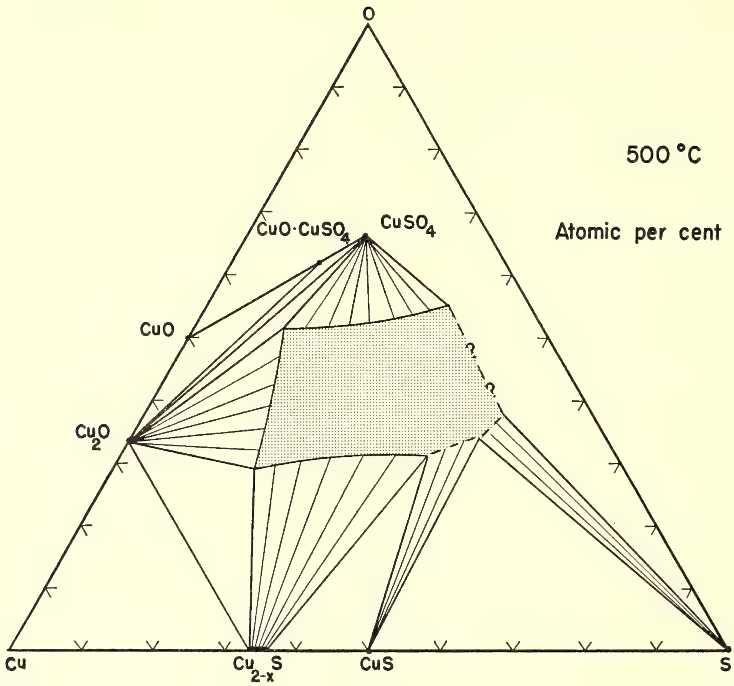

Fig. 36. Phase relations in the Cu-S-O system at 500°C. All phases and phase assemblages are in equilibrium with vapor. Portions of the system are schematic.

quence of the disruption of the Cu_2O-$CuO \cdot CuSO_4$ join are not known at present.

The establishment of the Cu_2S-$CuSO_4$ join restricts the positions of liquid fields as shown schematically in Fig. 37. The liquid present in the Cu_2O-Cu_2S-$CuSO_4$ field persists with decreasing temperature, to a ternary eutectic at $340° \pm 4°C$, as determined by quench-type and DTA experiments. The ternary liquid is ruby red to resinous brown and is readily quenched to a glass; this behavior is unique for liquids containing metal, sulfur, and oxygen. Depending on the cooling rate, the liquid partially crystallizes to a mixture of Cu_2O, $CuSO_4$, and Cu_2S.

Below 340°C the remaining ternary liquid field is restricted to the S side of the $Cu_{2-x}S + CuSO_4$ join, and with decreasing temperature the boundaries of this liquid field withdraw toward the S-O join, which apparently is reached at about 100°C. Tie lines exist between $Cu_{2-x}S$ (Cu_9S_5) and this liquid to below 260°C, prohibiting stable coexistence of CuS and $CuSO_4$.

Mixtures of CuS and $CuSO_4$ heated at $250° \pm 5°C$ for 90 days show partial reaction to produce a small amount of Cu_9S_5 and possible liquid, suggesting that the CuS-$CuSO_4$ join becomes stable below 250°C. This ternary liquid cannot be quenched but crystallizes, on even the fastest possible chilling, to sulfur and a waterlike phase, which in turn commonly partially crystallizes below 50°C to icelike needles, interpreted here as being a form of $CuSO_4$. A silica tube containing this ternary liquid at 25°C possesses a vapor pressure in excess of 1 atm, for the tube will "pop" when broken and the liquid evaporates rapidly (in seconds), giving off a very strong SO_2 odor. The behavior of this liquid field at low

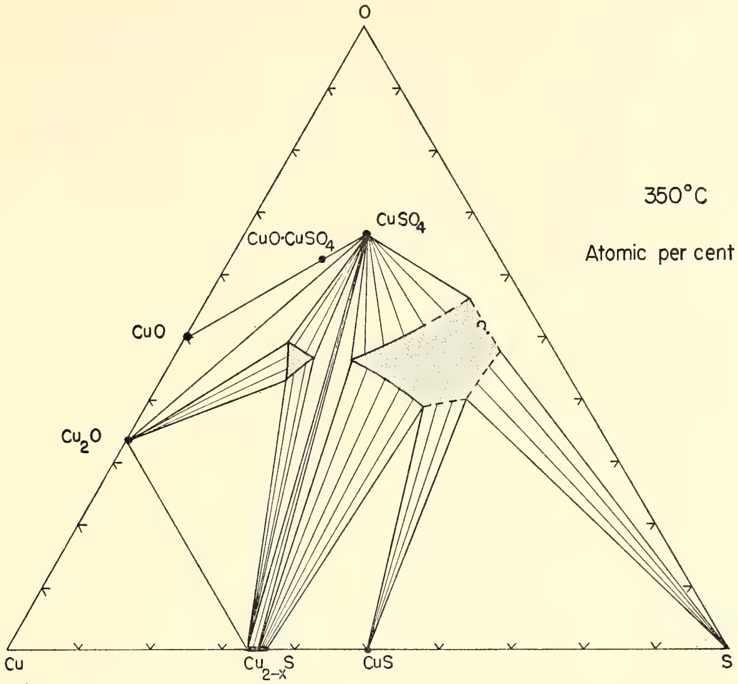

Fig. 37. Phase relations in the Cu-S-O system at 350°C. All phases and phase assemblages are in equilibrium with vapor. Portions of the system are schematic.

temperatures near the sulfur-oxygen join was not determined.

Below the ternary eutectic temperature of 340°C, the assemblage $Cu_2O+Cu_2S+CuSO_4$ remains stable with decreasing temperature to $215° \pm 15°C$, the temperature of the reaction point represented by the equation $Cu_2O+CuSO_4+V \rightleftarrows Cu_2S+CuO$. At 215°C tie lines are established between Cu_2S and CuO; this assemblage is stable to below 130°C and may well exist at room temperature.

Tie lines between Cu_9S_5 and $CuSO_4$ exist to temperatures below 130°C. At some lower temperature, as yet undetermined, the assemblage CuS+CuO becomes stable, as represented by the equation $Cu_9S_5+CuSO_4+V \rightleftarrows CuO+CuS$. Additional complications exist at low temperatures in this portion of the system as a result of developments on the Cu-S join (e.g., stabilization of blue-remaining covellite, djurleite, and anilite [Cu_7S_4]).

The mineral assemblages of geologic interest within the Cu-S-O system at low temperatures but above 157°C are native copper + cuprite + chalcocite, cuprite + tenorite + chalcocite, and digenite + tenorite + covellite. The copper oxide minerals are widespread in occurrence and are common in oxidation zones of many copper deposits, where they generally occur as alteration products of chalcocite, chalcopyrite, and other copper sulfides. The present study shows that even though the assemblage copper + cuprite + chalcocite is stable to high temperature (>850°C), the assemblage cuprite + tenorite + chalcocite is stable only below 215°C and the assemblage digenite + tenorite + covellite (aside from complications discussed above) is stable only to a temperature, as yet undetermined, below 130°C. Occurrences of the minerals chalcocyanite and dolerophanite are very restricted in nature and are reported from fumaroles associated with recent

eruptions of Mt. Vesuvius. That they are very unstable in the presence of water accounts for their rarity. Although many sulfates of copper are found in nature, most are hydrous and belong to the complex Cu-S-O-H system.

High-Pressure Differential Thermal Analysis

Acanthite-Type Compounds

P. M. Bell and G. Kullerud

The acanthite group of compounds contains about twenty known species, of which more than a dozen have been reported to occur as minerals. These compounds are sulfides, selenides, and tellurides of group IB metals and have a cation-to-anion ratio of, or about, 2:1. The common minerals acanthite (Ag_2S) and chalcocite (Cu_2S) belong to this group. In the condensed system these compounds all have been reported to occur in at least two distinctly different crystallographic forms, of which the room-temperature polymorph apparently is monoclinic in all instances and the high-temperature form, which is nonquenchable, is cubic.

We have performed high-pressure differential thermal analysis (DTA) experiments on synthetic Ag_2S to increase our knowledge of the behavior of this mineral and particularly to gain a better general understanding of the acanthite type of compounds.

Kracek (1946) found that in the condensed system the monoclinic form of Ag_2S is stable at room temperature and inverts at 177°C to a body-centered cubic polymorph, which in turn inverts to a face-centered cubic form at 586°C when excess Ag is present and at 622°C when excess S occurs. Stoichiometric synthetic Ag_2S, which was used in our experiments, inverts in the presence of vapor to the face-centered cubic form at about 600°C.

Roy, Majumdar, and Hulbe (1959) studied the effect of pressure on the temperature of the monoclinic $\rightleftarrows$ body-centered cubic inversion and found that pressures up to 1225 atm increase the inversion temperature by about 4°C/kb. Bridgman (1937) found Ag_2S to have a high-pressure nonquenchable polymorphic form. The data by Bridgman (1937) and by Roy, Majumdar, and Hulbe (1959) are incorporated in the pressure-temperature diagram of Fig. 38. As recorded by our method, the heat effect associated with the transition reported by Bridgman (1937) is very weak and diffuse. The crystal structure of the high-pressure form is not known, and the form is not preserved on cooling and release of pressure. In analogy with the behavior of Cu_2S under pressure, as reported by Skinner, Boyd, and England (1964), the high-pressure form of Ag_2S (which we shall refer to as the δ form) may have tetragonal crystal structure. Extrapolation of the monoclinic $\rightleftarrows \delta Ag_2S$ reaction curve toward decreasing temperature indicated that the δ form may be stable in the condensed system at temperatures below about -100°C.

The monoclinic $\rightleftarrows$ body-centered cubic inversion manifests itself very strongly on the high-pressure DTA charts. It is readily recorded both on heating and on cooling, as seen in Fig. 38. The slope of the P-T curve is about 2.2°C/kb, according to our results.

Extrapolation of the monoclinic $\rightleftarrows$ body-centered cubic and the monoclinic $\rightleftarrows \delta$ reaction curves indicates intersection of these curves in a point situated at about 25 kb and 230°C. At this point the three forms of Ag_2S—monoclinic, body-centered cubic, and δ—apparently coexist stably. If this is correct, a third curve delineating the reaction $\delta \rightleftarrows$ body-centered cubic must exist. Strong DTA peaks believed to be caused by this reaction were recorded as noted in Fig. 38.

The high-temperature body-centered cubic $\rightleftarrows$ face-centered cubic inversion could not be detected with our equipment. The enthalpy of this reaction is small, about one-tenth that of the monoclinic $\rightleftarrows$ body-centered cubic reaction,

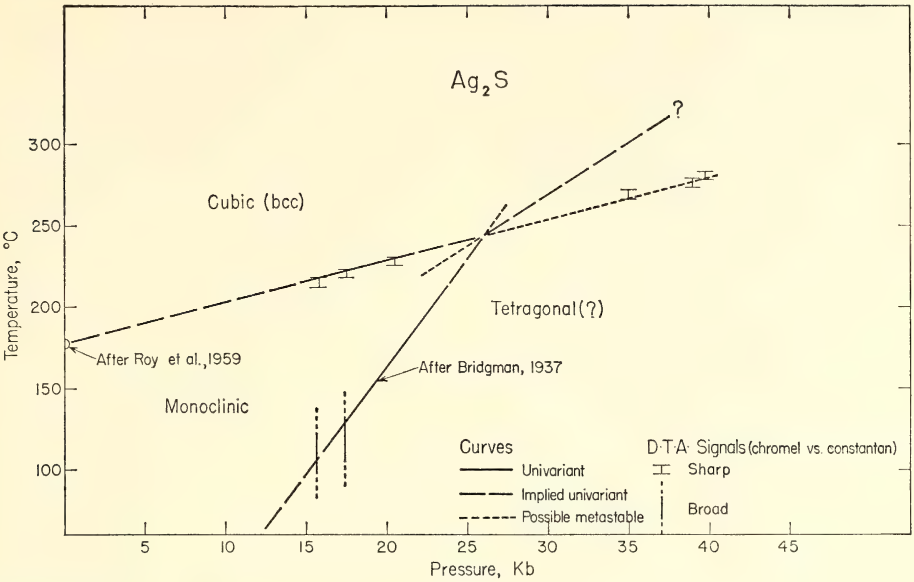

Fig. 38. Proposed phase diagram for Ag_2S.

according to Rosenqvist (1949) and Richardson and Jeffes (1952).

Pressure-Temperature Diagram for Cr_2FeS_4

P. M. Bell, A. El Goresy, J. L. England, and G. Kullerud

Daubréelite (Cr_2FeS_4) is a common mineral in chondritic, achondritic, and iron meteorites; a better knowledge of its chemical behavior might provide information useful in geophysical correlation.

The present study is an attempt to determine the *P-T* phase diagram of daubréelite (*Year Book 67*, pp. 197–198). The results of Rooymans and Albers (1967) for a system of nearly the same composition included a phase boundary with a negative slope. The possibility that a similar phenomenon might exist in daubréelite was examined with high-pressure differential thermal analysis (DTA). The results indicate a boundary that is nearly horizontal with the pressure axis but with a slight dip in the central portion of the curve, shown in Fig. 39. No other significant DTA signals were observed (except for melting of the gold capsule at temperatures approaching and above 1100°C at low pressures). The dip in the curve suggested the possibility that another phase boundary was involved, but this could not be verified with DTA. Quenching experiments with 1:1 mixtures of the low- and high-pressure forms of daubréelite showed that a phase boundary existed. Procedures identical with those of Richardson, Bell, and Gilbert (*Year Book 66*, pp. 392–397) for examination of solid reactions with 1:1 mixtures produced the results that are also shown in Fig. 39. The sharp negative slope of the boundary obtained from quenching experiments intersects the DTA boundary at about 800°C, 14 kb.

At 1 atm a strong DTA signal was observed at 1060°C, with the low-pressure phase always forming during the quench. Several exploratory experiments at temperatures above 1100°C and at pressures high enough to avoid melting of the gold capsule were performed. No DTA signals were observed, and in every experiment the quench product was the high-pressure form of daubréelite. This

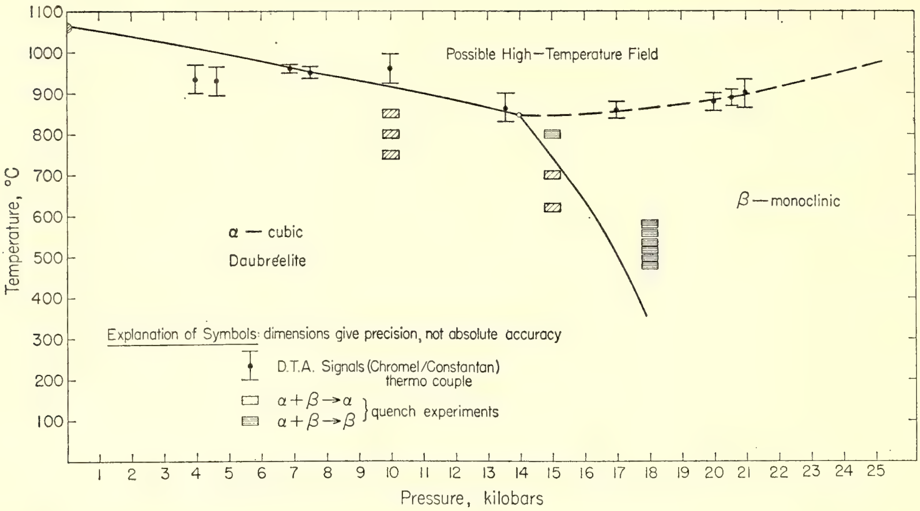

Fig. 39. Pressure-temperature diagram for Cr_2FeS_4.

phenomenon is difficult to explain because the quench occurred in the low-pressure field. Possibly the high-pressure form crystallized upon crossing the metastable extension of the high-pressure stability curve. X-ray diffraction and microprobe analyses showed no differences between these products, all the other experimental products, and the starting materials.

That the high-temperature field is very likely a breakdown curve is based on a strong analogy with the polydymite system (Ni_3S_4) (see Kullerud, *Year Book 67*, p. 181, Fig. 68). Except for its location in *P-T* space, the diagram of Fig. 39 is nearly identical with the one for polydymite.

On the basis of the present information it is clearly difficult to determine the *P-T* history of daubréelite in meteorites without supporting textural evidence.

CRYSTALLOGRAPHY

Fifty Years of X-ray Crystallography at the Geophysical Laboratory, 1919–1969

Gabrielle Donnay, with the help of R. W. G. Wyckoff, T. F. W. Barth, and George Tunell

It is difficult for us today to realize the rudimentary state of the art of structural crystallography in 1919, only seven years after Laue's discovery of X-ray diffraction. A letter of December 22, 1920, from Dr. Arthur L. Day, the first Director of the Geophysical Laboratory, to Dr. Ralph W. G. Wyckoff, its first structural crystallographer (1919–1927), telling Wyckoff of his first raise, conveys the vision of this Director, whose birth dates back one hundred years, to 1869:

"The field of activity in which your work falls is entirely new to this Laboratory, and for the most part new in this country. It is, I think, rare that a man at the outset of his career has such an unusual opportunity to enter and exploit a field of such vital importance to our knowledge of the structure of matter, a field, by the way, which will probably take you far beyond the immediate application which this Laboratory will wish to make of it. I heartily commend both

your choice and your opportunity, and wish you every success in your work."

Dr. Day's good wishes were fulfilled: of the many honors and recognitions later bestowed on Dr. Wyckoff, we need only mention that he became President of the International Union of Crystallography, which was founded in 1948.

The only laboratories in the United States where crystal-structure work was being attempted prior to 1919 were found at Massachusetts Institute of Technology, the General Electric Company in Schenectady, and the Chemistry Department of Cornell University, where graduate student Wyckoff, under the guidance of Professor Shoji Nishikawa, became acquainted with space-group theory and its usefulness to X-ray diffraction. In 1919 the M.I.T. group moved to the California Institute of Technology, and Dr. Wyckoff joined the staff of the Geophysical Laboratory of the Carnegie Institution in Washington, D. C.; only in these two places has X-ray crystallography been carried on continuously ever since.

The first determinations of atomic positions in crystals were inspired guesses supported by the few X-ray diffraction intensities that could be obtained with the primitive spectrometers then available. Additional data were needed if many more structures were to be analyzed, and some orderly procedure was required for finding possible atomic arrangements from which the correct choice could be made. Wyckoff grasped the fact that space-group theory offered the means of enumerating possible structures, and following Nishikawa, he saw in the original patterns of Laue a promising source of additional data. These ideas were developed in his early publications from the Geophysical Laboratory. R. G. Dickinson, moving from M.I.T. to Pasadena, spent a short time at the Laboratory, familiarizing himself with these methods of approach, and Wyckoff supplemented this visit by working during the following year at the newly established California Institute of Technology. The work in Pasadena expanded rapidly, first under Dickinson and then under Linus Pauling; under Pauling it has played a dominant role in the development of structural chemistry throughout the world. In contrast, crystallography at the Geophysical Laboratory has remained in the hands of a very few people. Nevertheless, their contributions have dealt with many aspects of their science, such as theoretical crystallography, crystal-structure determinations and their interpretations and refinements, solid solutions, computing techniques, and biocrystallography. Compilations of crystallographic data, beginning with Wyckoff's "Survey of existing crystal structure data," filling 68 pages in 1923, his first edition of *The Structure of Crystals* in 1927, through Donnay and co-workers' *Determinative Tables of Crystal Data,* comprising 1300 pages in 1963, show how aware of the retrieval problem were the "isolated" crystallographers at the Laboratory.

Let us look back at some of the highlights of the contributions, as we judge them now, for in our present-day group approach to scientific research, such a miniature crystallographic laboratory as the one at the Geophysical Laboratory might be called upon to justify its existence.

The value of space-group theory was not quickly recognized by the crystallographic fraternity, and Wyckoff's *Analytical Expression of the Results of the Theory of Space Groups* could not find a publisher. It finally appeared in 1922, as a publication of the Carnegie Institution of Washington, through the personal interest and intervention of Dr. Robert S. Woodward, originally a mathematician, who was President of the Institution. This book was the forerunner of the *International Tables of X-ray Crystallography,* the third edition of which is now in preparation and in which, as in the preceding editions, the atomic positions in the 230 space groups will be

designated by their Wyckoff letters. Of the sixty-four crystallographic publications that came out of the Geophysical Laboratory during the nine-year period when Wyckoff was here, we need mention only the first crystal-structure determination to illustrate how much new information could then be packed into one structure paper. This one dealt with the "Crystal structures of some carbonates of the calcite group" and covered 44 pages in the *American Journal of Science*. In addition to determining the correct unit cell of calcite and the structures of magnesite, rhodochrosite, smithsonite, and siderite, and recognizing that dolomite would have a different structure, the author proved the existence of planar $CO_3^=$ groups, which Bragg's determination of the calcite structure with the X-ray spectrometer had failed to do, since the oxygen atoms could not be located. By making $CO_3^=$ the anions, the close relation of the calcite structure to the NaCl structure became evident. It was stressed that $NaNO_3$ and $CaCO_3$ are even more closely isostructural than $CaCO_3$ and $MnCO_3$. The faces of calcite were explained by recognizing that the nodes of a nonstructural lattice, based on the cleavage rhombohedron, are occupied by morphologically equivalent Ca^{2+} and $CO_3^=$ ions. The extinction criterion for a rhombohedral lattice ($-h+k+\ell=3n$) was derived; the relation of the gnomonic projection to the Laue photograph was elucidated and a ruler to construct the projection directly from the photograph was described. All this, in 1920!

Experimental work with gas X-ray tubes was very difficult and time-consuming in the early days, and the Laboratory was fortunate in having a Swiss-trained instrument maker, C. J. Ksanda, employed at the Laboratory from 1914 to 1940, who carried out much of the laboratory work and in 1932 designed the Ksanda twin gas tubes, which were built by a local firm.

A Laboratory colleague who was introduced to X-ray crystallography by Wyckoff was Dr. Eugene Posnjak (Staff Member, 1913–1947). Russian by birth, he was trained in physical chemistry at Leipzig, Germany, and had joined the Laboratory after a year with A. A. Noyes at M.I.T. Posnjak published "The crystal structure of ammonium chloroplatinate" jointly with Wyckoff in 1922. The authors proved once and for all the validity of Werner's Coordination Theory, which until then had been only a hypothesis: platinum is octahedrally surrounded by six chlorine ions. The structure is of the fluorite type with $PtCl_6^=$ replacing Ca^{2+} and NH_4^+ replacing F^-. Also jointly, they described the alkali halides and cuprous halide. Posnjak determined the crystal structure of the alkali metal potassium and together with Dr. Sosman discovered the naturally occurring ferromagnetic iron-deficient magnetite of composition Fe_2O_3, to which the name maghemite was later given. In 1928 he published the cell dimensions of spinel ($MgAl_2O_4$) and other compounds of the spinel group. He had exceptional skill in preparative and experimental work, and in order to study the magnetic properties of crystals, he produced various compounds and solid solutions containing both ferrous and ferric iron. He had begun a study of the powder diagrams of such samples exhibiting spinel structure when Dr. Tom F. W. Barth joined the Laboratory in 1929.

Barth (Staff Member, 1929–1936) had received his introduction to the field from the greatest geochemist of the time, V. M. Goldschmidt, then a professor at the University of Oslo, Norway. Barth let his active interest in petrology guide his choice of crystallographic problems and concentrated his efforts on important rock-forming minerals. He soon joined forces with Posnjak on the spinel problem, and this happy collaboration resulted in 1931 in their classical paper "The spinel structure: an example of variate atom equipoints," in which it was proved that crystallographically equiva-

lent sites can be occupied by chemically different atoms. Five months later they showed that the structure of lithium ferrite, $Li_2Fe_2O_4$, belongs to the NaCl type, with univalent lithium and trivalent iron substituting randomly for each other on the sites of one and the same crystallographic position. The new concept of "variate atom equipoints" proved to be essential for understanding and solving most mineral crystal structures. Aluminum, for example, to some extent replaces silicon in all aluminosilicates, and studies of gehlenite, sodalite, related minerals, and the feldspars clarified the principle involved. Barth also studied the cristobalite structure, showed that nonsilicates can exist with the same structure type, and recognized considerable solid solution in the system SiO_2-$Na_2Al_2O_4$, also with the cristobalite structure.

Dr. Sterling B. Hendricks, who had been a Fellow at the time of Wyckoff, was back in Washington, at the Fixed Nitrogen Laboratory, and cooperated throughout the thirties with the crystallographic group at the Laboratory. In 1931 and 1932 Hendricks, Kracek, and Posnjak verified Pauling's hypothesis that in sodium nitrate and ammonium nitrate molecular rotation takes place in the solid state. This was another new phenomenon first described at the Geophysical Laboratory. Brandenberger had pointed out that in the case of sodium nitrate there exists a particular stationary position for the NO_3 group which would be difficult to distinguish from the rotating group. It was important, therefore, that Barth could prove the existence of two polymorphic forms of KNO_3: one in which the nitrate group was rotating and another in which it had the location predicted by Brandenberger.

Dr. George Tunell (Staff Member, 1925–1947), a Harvard-trained economic geologist, mineralogist, and crystallographer, specialized in ore minerals. He promptly became the friend of Tom Barth and learned from him the techniques of crystal-structure determination. With his wife Ruth helping with the computations, he determined the structures of tenorite, calaverite, sylvanite, and krennerite, and later published a paper with Linus Pauling on "The atomic arrangement and bonds of the gold-silver ditellurides." Tunell also derived the Lorentz correction factor for equi-inclination Weissenberg films, without which the photographic intensities of diffracted X rays could not be used. He had taken great interest in the computing of Fourier syntheses, as is evidenced by the "Patterson-Tunell stencils and strips," which rapidly became popular and helped crystallographers in their laborious calculations of the precomputer era. (They are, to this day, used as a teaching aid to make the student appreciate what really goes on in a Fourier summation.)

By 1933 the X-ray laboratory was so well equipped—it had a Weissenberg camera, the first to be converted to equi-inclination outside of M.I.T., an oscillation camera, several powder cameras, including one in which the sample could be studied at high temperature—that Dr. Barth could report to Dr. Day: "for a considerable length of time we have had the best X-ray goniometer [Weissenberg camera] in the U.S. and probably in the world" and "we have concrete problems already well under way which we believe are of more than ordinary interest, as is evidenced, for example, by the fact that Dr. [J. D. H.] Donnay, Professor of Mineralogy at the Johns Hopkins University, desires to study with us in the fall and that Professor Palache has sent us his assistant, Mr. Berman, for advice and instruction." The association with the morphological crystallographers of Harvard and of Johns Hopkins was both a fruitful and a happy one, as witness the formation of the delightful "Calaverite Club," composed of Palache, Peacock, Donnay, Tunell, and Barth. Calaverite is a mineral whose morphology apparently violates the Law of Rationality and which, even now, is not fully under-

stood. In those days all the papers on calaverite were written by members of the club! The enthusiastic cooperation also led to a joint publication in 1934 on "Various modes of attack in crystallographic investigations."

The association with Professor Donnay continues to the present time. His wife, Dr. Gabrielle Donnay, joined the Laboratory in 1950 as a Fellow and in 1955 as a Staff Member. Her undergraduate training in chemistry at U.C.L.A. was followed by a Ph.D. in crystallography under M. J. Buerger at M.I.T. Her first research problem at the Laboratory, carried out with the help of the Director, Dr. L. H. Adams, was a test of the precision of the then-new powder diffractometer and led to the cell dimensions and cell volumes of a complete solid-solution series of well-documented alkali feldspars. It showed the existence of a high-order transition. A study of chalcopyrite, performed jointly with Drs. L. M. Corliss, J. D. H. Donnay, N. Elliott, and J. M. Hastings at Brookhaven National Laboratory, led to the first application of "generalized symmetry" to magnetic-structure determinations. Complex crystalline edifices resulting from twinning (in digenite), epitaxy, and syntaxy (in the bastnaesite-vaterite series) have been studied. Solid solutions, omission as well as substitution and organic as well as inorganic, have been investigated, and the theory of limited solid solutions between end members of different structure types has been considered. In addition to describing five new minerals (among them ewaldite, a simple new carbonate structure), a novel building block composed of three corner-linked SiO_4 groups we found in the structure of the rare silicate mineral ardennite. Together the Donnays have investigated the relation of morphology to structure, which led to further generalizations of the Law of Bravais. Most recently an X-ray survey of the orientation relations between crystallographic axes and morphological features of calcite "biocrystals" in Echinodermata was carried out with Dr. David L. Pawson of the Smithsonian Institution.

The tremendous help which modern computers can give crystallographers has not been overlooked at the Laboratory. Computing and its use for structure refinement to obtain meaningful temperature factors was of special interest to another student of Professor Buerger, Dr. Charles W. Burnham, who became a Fellow in 1961 and was a Staff Member from 1963 to 1966. He refined the structures of sillimanite and kyanite and wrote several computer programs that are now widely used.

This account would not be complete without mentioning the following postdoctoral Fellows who contributed to the crystallographic output: J. V. Smith (1951–1954), N. Morimoto (1957–1960, seven months in 1962, three months in 1963, and four months in 1966–1967), E. W. Radoslovich (1962–1963), N. Güven (1965–1967), and L. W. Finger (1967–1969). Dr. Finger became a Staff Member on July 1, 1969. He is working on order-disorder problems in amphiboles and is now setting up a second X-ray laboratory.

A bibliography of 183 crystallographic publications that have come out of the Laboratory in the period 1919–1969 is available on request.

Looking back at the historical facts, it seems to us that the Geophysical Laboratory was different from most other places in its approach to X-ray crystallography. Most early workers in this field were classical physicists rather than crystallographers. After the initial discovery, the methods employed in working out actual crystal structures were slow and cumbersome, and lacked the elegance and ease that only crystallographic theory could provide. It was fortunate for the Geophysical Laboratory that Wyckoff, who demonstrated the use of the theory of space-groups and always insisted on applying it in his work, became the first X-ray crystallographer of the

Laboratory. The same approach was used by Tunell and Barth, both educated in classical crystallography; this trend was strengthened by the inspiring cooperation of morphological and optical crystallographers, in and out of the Laboratory, who brought in the best traditions of the European schools. Together with this mode of approach, the freedom of research that has been the rule at the Geophysical Laboratory has served its crystallographers well. It is a pleasure, in conclusion, to quote Professor Barth's enthusiastic reply to our call for help when we started writing this short history: "I shall be happy to do so; I spent the most pleasant time of my life at the Geophysical Laboratory."

Refinement of the Crystal Structure of an Anthophyllite

L. W. Finger

The anthophyllite structure models proposed by Warren and Modell (1930) and Ito and Morimoto (1950) have been refined as part of the continuing investigation of Fe-Mg ordering in the ferromagnesian amphiboles. The specimen (no. 30 of Rabbitt, 1948) is from the Dillon Complex, Beaverhead and Madison Counties, Montana (U. S. National Museum, catalogue no. 117227). The chemical formula from an analysis is $Mg_{5.53}Fe_{1.47}Si_8O_{22}(OH)_2$. Single crystals of this material display diffraction symmetry *mmmPn-a*, which corresponds to space group *Pnma* if centric or $Pn2_1a$ if noncentric. A satisfactory refinement was accomplished with the centrosymmetric space group. The unit-cell parameters were determined from back-reflection Weissenberg photographs taken about the *b* and *c* axes with Cu ($\lambda_{K\alpha_1}=$ 1.54051 Å, $\lambda_{K\alpha_2}=1.54433$ Å) and Fe ($\lambda_{K\alpha_1}=1.93597$ Å, $\lambda_{K\alpha_2}=1.93991$ Å) radiations. The data were refined with the use of program LCLSQ of Burnham (*Year Book 61*, pp. 132–135), with correction terms for absorption, film shrinkage, and eccentricity errors. The resulting cell parameters at 23°C are $a=18.560\pm 0.003$ Å, $b=18.013\pm0.002$ Å, $c=5.2818 \pm0.0009$ Å, $V=1765.8\pm0.7$ Å^3. There are four formula units per cell. A cleavage fragment, $0.15\times0.26\times0.40$ mm in size, was selected for intensity collection at the U. S. Geological Survey, Washington, D. C., on a Picker four-circle automated diffractometer, equipped with a scintillation detector. All nonequivalent reflections with sin $\theta\leq0.5$ for MoKα ($\lambda=0.7107$ Å) radiation were measured using a Nb filter and the 2θ-scan technique, with the scan range calculated according to Alexander and Smith (1964). The resulting data were corrected for background, Lorentz and polarization effects, and absorption ($\mu_l=20.07$ cm^{-1}). The reflections with a negative integrated intensity were assigned the most probable value of the structure factor for a centric crystal (Hamilton, 1955). Any reflection with an intensity less than three times its standard deviation based on counting statistics was marked for special treatment in the refinement. These data will henceforth be called "less-thans." A total of 2656 symmetry-independent reflections were measured, of which 532 were less-thans.

Because the site nomenclature used by Warren and Modell (1930) did not agree with that of Ito and Morimoto (1950) and neither scheme agreed with previous work on the clinoamphiboles, the nomenclature has been changed to reflect the relationship of the structure to the C-centered monoclinic amphiboles. In addition, we have tried to conform as closely as possible to the conventions proposed by Burnham *et al.* (1967) for clinopyroxenes and to agree with the work of Whittaker (1969) on holmquistite which is isostructural with anthophyllite.

The anthophyllite structure may be imagined as a unit of the cummingtonite structure, composed of a strip of octahedra sandwiched between two double chains of tetrahedra. In cummingtonite the chains are symmetrically related by

two-fold axes and the two halves of a chain are related by a mirror plane. In anthophyllite the mirror exists but the two-fold axes are not present, and the two chains are not related by symmetry. In accord with the structure of clinoferrosilite (Burnham, *Year Book 65,* pp. 285–290), the more extended or regular chain has been labeled the *A* chain and the distorted chain, the *B* chain. The number of crystallographically distinct octahedral cations is not affected, and they are called M1, M2, M3, and M4 as in cummingtonite. Within a chain, the conventional nomenclature shown in Fig. 40 is used. The chain-linking oxygens O5 and O6 create a slight problem. The distortion from the ideal chain causes the hole in the double chain to be deformed from a pseudohexagonal to a pseudoditrigonal shape. The selection of O6 is made such that the bond angle O6-O7-O6 is less than the bond angle O5-O7-O5, as shown (cf. cummingtonite, Ghose, 1961; Fischer, 1966). This choice could not be made *a priori* for both chains since the tetrahedra of the *A* chain are rotated in the opposite sense from the rotation of chains in cummingtonite, a point which will be discussed later. To complete the site nomenclature, O3 is the hydroxyl atom that is not bonded to a tetrahedron, and the *A* site, which is empty in anthophyllite, lies between the backs of two tetrahedral chains. Table 25 shows the correspondence between the site nomenclature used here and those of Warren and Modell, and Ito and Morimoto.

Full matrix least-squares refinement was accomplished with the use of pro-

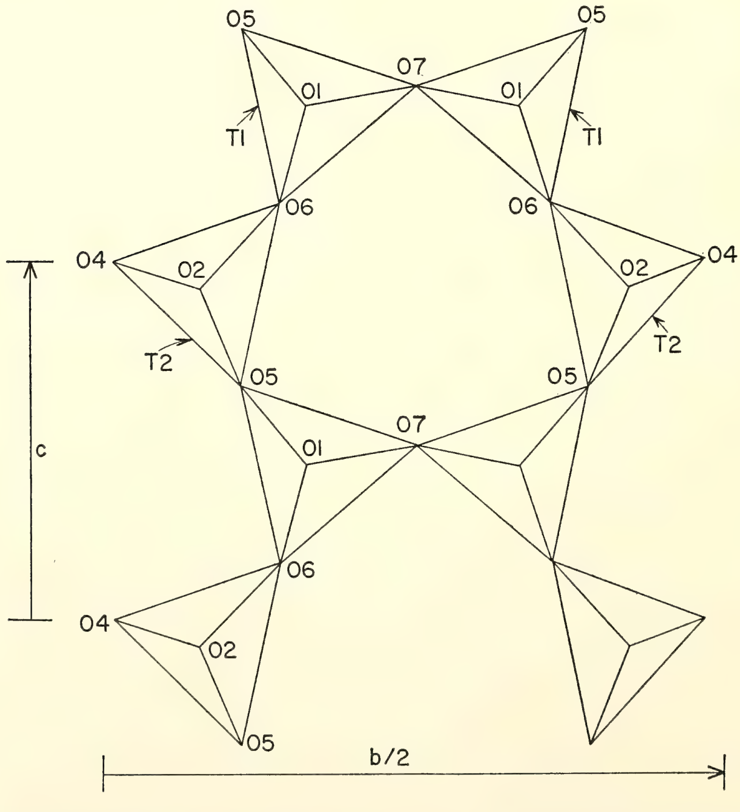

Fig. 40. Site nomenclature for idealized amphibole double chain projected parallel to a^*.

TABLE 25. Anthophyllite Site Nomenclature Derived from Clinoamphiboles Compared with Schemes Proposed Previously

This Study	Warren and Modell	Ito and Morimoto
M1	Mg_1	Mg_1
M2	Mg_2	Mg_2
M3	Mg_4	Mg_4
M4	Mg_3	Mg_3
T1*A*	Si_4	$Si_I(2)$
T1*B*	Si_1	$Si_I(1)$
T2*A*	Si_3	$Si_{II}(2)$
T2*B*	Si_2	$Si_{II}(1)$
O1*A*	O_8	$O_{II}(2)$
O1*B*	O_2	$O_{II}(1)$
O2*A*	O_9	$O_I(2)$
O2*B*	O_1	$O_I(1)$
O3*A*	$(OH)_2$	$(OH)_2$
O3*B*	$(OH)_1$	$(OH)_1$
O4*A*	O_{10}	$O_V(2)$
O4*B*	O_5	$O_V(1)$
O5*A*	O_{13}	$O_{VII}(2)$
O5*B*	O_6	$O_{VI}(1)$
O6*A*	O_{14}	$O_{VI}(2)$
O6*B*	O_7	$O_{VII}(1)$
O7*A*	O_{11}	$O_{III}(2)$
O7*B*	O_3	$O_{III}(1)$

gram RFINE, with scattering curves for neutral atoms from Cromer and Mann (1968) and the anomalous dispersion coefficients of Cromer (1965) for Si, Mg, and Fe, the anomalous scattering of oxygen being ignored. The positional parameters of Warren and Modell (1930), isotropic temperature factors of 0.5, and fully disordered occupancies were selected as the initial values. The program minimized the function $\Sigma w(|F_o| - |F_c|)^2$, and the weights, w, were the inverse of the variance of the structure factors as computed from counting statistics. In the refinement the less-thans were not included in the least-squares solution, but the structure factors were computed for comparison of the observed and calculated values. The positional parameters and the scale factor were refined for three cycles, and the isotropic temperature factors were then refined for one cycle. At this stage of the refinement the occupancies were varied, with the use of the chemical constraints described in *Year Book 67* (pp. 216–217). The sum of Fe+Mg for each octahedral site was required to be unity, and the total amount of iron was restricted to 1.47 atoms per formula unit. The structure converged in four cycles. At this point the structure factor data were investigated to determine if any of the highly discrepant values were due to previously undetected diffractometer errors. Approximately 45 reflections were found to be affected by interference. Because the unit cell of anthophyllite has two axial lengths of approximately 18 Å and is primitive, the diffraction from neighboring planes is closely spaced for Mo radiation. For those data in question, the background measurement was made after the scan had intercepted the diffracted ray from the next *hkl* plane, and therefore the integrated intensity was too small. A better value for the intensity was obtained by estimating the true background from the strip-chart record and recalculating. Because this procedure is not very accurate, the reflections recalculated in this fashion were marked as less-thans so they could not influence the least-squares solutions obtained later.

With the data revised as outlined above, the structure converged in three cycles. Next, the M sites were converted to anisotropic temperature factors, and the parameters were refined. Finally, all the atoms were refined with anisotropic temperature factors. The weighted residuals were tested according to Hamilton (1965), the results showing that the hypothesis that the oxygens vibrate isotropically may be rejected at the 0.005 level. The final value of the weighted residual, $r = [\Sigma w(|F_o| - |F_c|)^2/\Sigma w F_o^2]^{\frac{1}{2}}$, was 0.040 for all data and 0.027 for the unrejected reflections. The corresponding values for the conventional residual, $R = \Sigma||F_o| - |F_c||/\Sigma|F_o|$, were 0.063 and 0.044. The final values for the occupancies, positional parameters, and equivalent isotropic temperature factors (Hamilton, 1959) are presented in Table 26. The error for the occupancy of M4 is derived from propagation of error considerations, neglecting any error in the analysis, and

TABLE 26. Atomic Coordinates, Equivalent Isotropic Temperature Factors, and Site Chemistry for Anthophyllite

Atom	x	y	z	B	Occupancy
M1	0.12489(9)	0.16329(7)	0.3911(3)	0.54(3)	0.960(3) Mg
M2	0.12488(9)	0.07317(7)	−0.1099(3)	0.55(3)	0.973(3) Mg
M3	0.12579(14)	¼	−0.1089(5)	0.49(4)	0.966(4) Mg
M4	0.12371(4)	−0.00982(4)	0.3877(2)	0.78(2)	0.349(4) Mg
T1*A*	0.23039(7)	−0.16540(7)	−0.4344(2)	0.37(2)	Si
T1*B*	0.01863(8)	−0.16626(7)	0.2760(2)	0.38(2)	Si
T2*A*	0.22731(8)	−0.07956(7)	0.0622(2)	0.38(2)	Si
T2*B*	0.02469(8)	−0.08177(7)	−0.2227(2)	0.43(2)	Si
O1*A*	0.1825(2)	0.1635(2)	0.0573(6)	0.43(6)	
O1*B*	0.0685(2)	0.1635(2)	−0.2746(6)	0.52(6)	
O2*A*	0.1855(2)	0.0777(2)	−0.4377(6)	0.43(5)	
O2*B*	0.0630(2)	0.0773(2)	0.2187(6)	0.54(5)	
O3*A*	0.1822(3)	¼	−0.4437(8)	0.51(8)	OH
O3*B*	0.0694(3)	¼	0.2267(9)	0.49(8)	OH
O4*A*	0.1869(2)	−0.0011(2)	0.0721(6)	0.59(6)	
O4*B*	0.0668(2)	−0.0065(2)	−0.2920(6)	0.70(6)	
O5*A*	0.1978(2)	−0.1168(2)	0.3293(6)	0.59(5)	
O5*B*	0.0508(2)	−0.1112(2)	0.0570(6)	0.54(5)	
O6*A*	0.2009(2)	−0.1303(2)	−0.1739(6)	0.67(5)	
O6*B*	0.0484(2)	−0.1402(2)	−0.4493(6)	0.68(5)	
O7*A*	0.2027(3)	−¼	0.5397(8)	0.72(8)	
O7*B*	0.0450(3)	−¼	0.2221(9)	0.71(8)	

Note: Standard deviations, σ, are in parentheses.

is therefore a measure of the internal consistency of the structure-factor data.

Discussion

The refined structure of anthophyllite shows a high degree of cation ordering in the M sites with very little iron in the small octahedral sites, probably indicating a relatively low temperature of formation or annealing. This material would therefore be a good sample for the determination of equilibrium distributions at

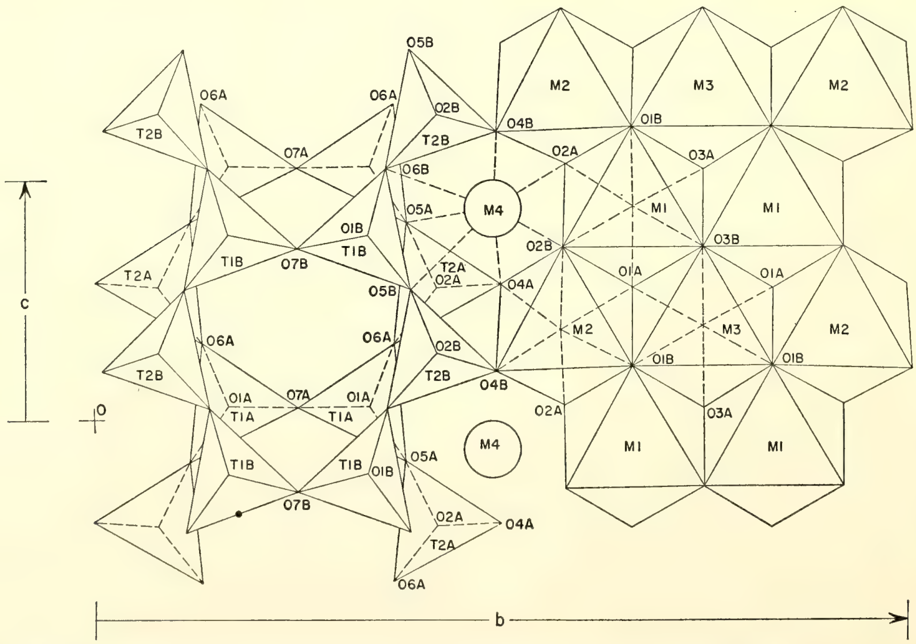

Fig. 41. A partial projection of the anthophyllite structure projected parallel to *a*.

various temperatures. The fine details of the ordering are similar to those in the refined structures of cummingtonite (Fischer, 1966) and grunerite (Finger, 1969) and are essentially as predicted by Ghose (1965). M1 and M3 have similar Fe:Mg ratios, whereas M2 is more enriched in Mg and M4 is greatly enriched in iron.

A partial projection of the structure on (100) is presented in Fig. 41, with selected bond distances in Table 27 and the bond angles of the silicate double chains in Table 28. The major difference between the cummingtonite-grunerite structure (Ghose and Hellner, 1959; Ghose, 1961; Fischer, 1966; and Finger, 1969) and the anthophyllite structure concerns the coordination of M4. In each structure there are four M-O bonds in the range 2.0–2.1 Å. Grunerite has two bonds at about 2.8 Å, and the next closest oxygens are at a distance of about 3.3 Å. In order to accommodate the smaller Mg ion in M4, the packing must be denser in this region of the structure. To accomplish this the *B* chain is distorted from the O6-O5-O6 angle of 172°C in grunerite to an angle of 157° in anthophyllite, allowing both of the chain-linking oxygens to be 2.87 Å from M4. In addition, the *A* chain is distorted in the opposite sense

TABLE 27. Selected Interatomic Distances (in Ångstroms) from Anthophyllite

Atoms	Distance: *A* Chain	Distance: *B* Chain
T1 tetrahedron		
T1-O1	1.618(3)	1.618(3)
T1-O5	1.640(3)	1.636(3)
T1-O6	1.611(3)	1.622(3)
T1-O7	1.615(2)	1.617(2)
T1-O	1.621	1.623
O1-O5	2.664(4)	2.667(4)
O1-O6	2.657(4)	2.648(5)
O1-O7	2.643(5)	2.649(5)
O5-O6	2.636(5)	2.659(5)
O5-O7	2.646(3)	2.649(3)
O6-O7	2.635(4)	2.632(4)
O-O	2.647	2.651
T2 tetrahedron		
T2-O2	1.619(3)	1.630(3)
T2-O4	1.601(3)	1.608(3)
T2-O5	1.655(3)	1.643(3)
T2-O6	1.621(3)	1.653(3)
T2-O	1.624	1.634
O2-O4	2.742(4)	2.753(4)
O2-O5	2.679(4)	2.638(4)
O2-O6	2.627(4)	2.654(4)
O4-O5	2.496(4)	2.655(4)
O4-O6	2.677(4)	2.570(4)
O5-O6	2.669(5)	2.725(5)
O-O	2.648	2.666
Tetrahedral chains		
T1-T1	3.049(2)	3.017(2)
T1-T2(+*z*)	3.045(2)	3.055(2)
T1-T2(—*z*)	3.076(2)	3.044(2)

Atoms	Distance: *A* Chain	Distance: *B* Chain
Octahedral strip		
M1-O1	2.062(3)	2.053(4)
M1-O2	2.112(3)	2.133(3)
M1-O3	2.082(3)	2.063(3)
M1-O	2.084	
M2-O1	2.138(3)	2.121(3)
M2-O2	2.067(3)	2.082(3)
M2-O4	2.010(3)	2.037(3)
M2-O	2.076	
M3-O1(2*x*)	2.075(3)	2.079(3)
M3-O3	2.055(5)	2.059(5)
M3-O	2.070	
M4-O2	2.156(3)	2.128(3)
M4-O4	2.044(3)	1.996(3)
M4-O5	2.387(3)	2.867(3)
M4-O6	3.481(3)	2.865(3)
M1-M1	3.124(2)	
M1-M2(—*z*)	3.104(2)	
M1-M2(+*z*)	3.095(2)	
M1-M3(2*x*)	3.068(3)	
M1-M4	3.118(1)	
M2-M3	3.185(1)	
M2-M4(—*z*)	3.046(2)	
M2-M4(+*z*)	3.024(2)	

Note: Standard deviations, σ, are in parentheses.

TABLE 28. Selected Interatomic Angles (in Degrees) from Anthophyllite

Atoms	Angle	
	A Chain	*B* Chain
T1 tetrahedron		
O1-T1-O5	109.7(2)	110.1(2)
O1-T1-O6	110.8(2)	109.6(2)
O1-T1-O7	109.7(2)	109.9(2)
O5-T1-O6	108.4(2)	109.4(2)
O5-T1-O7	108.8(2)	109.0(2)
O6-T1-O7	109.5(2)	108.7(2)
T2 tetrahedron		
O2-T2-O4	116.7(2)	116.5(2)
O2-T2-O5	109.8(2)	107.4(2)
O2-T2-O6	108.3(2)	107.9(2)
O4-T2-O5	100.1(2)	109.5(2)
O4-T2-O6	112.4(2)	104.0(2)
O5-T2-O6	109.1(2)	111.5(2)
Chains		
T1-O7-T1	141.4(3)	137.8(3)
T1-O5-T2	138.0(2)	136.3(2)
T1-O6-T2	140.8(2)	137.8(2)
O6-O5-O6	169.2(2)	157.5(2)

Note: Standard deviations, σ, are in parentheses.

from the equivalent chain in grunerite, allowing O5*A* to be 2.4 Å from M4. If anthophyllite were to be transformed into cummingtonite, one of the M4-O bonds would have to be broken. In addition, alternate strips of octahedra would have to be rotated approximately 180° about the a^* axis to form the cummingtonite stacking sequence. Therefore, a polymorphic transition, if it exists, must be reconstructive, not displacive.

The effect of these changes on the molar volume is shown in Fig. 42. The curve is for the cummingtonite-grunerite series as determined by Klein and Waldbaum (1967). The dashed portion is the extrapolation of their curve outside the compositional limits of their samples and is not intended to portray the stability range of anthophyllite. The points plotted are for aluminum-poor anthophyllites from this study, Johansson (1930), Greenwood (1963), and Lindemann (1965). Clearly, the anthophyllite structure allows denser packing, as noted by Whittaker (1960).

The assistance of the crystallographers at the U. S. Geological Survey in the data collection and reduction is gratefully acknowledged. In addition, Drs. J. J. Papike and M. Ross contributed greatly to the nomenclature scheme and to the description of the structure.

Progress Report on Ewaldite

*G. Donnay and H. Preston**

The first description of ewaldite (*Year Book 67*, pp. 218–219) appeared under

* Chemistry Dept., U. of Maryland.

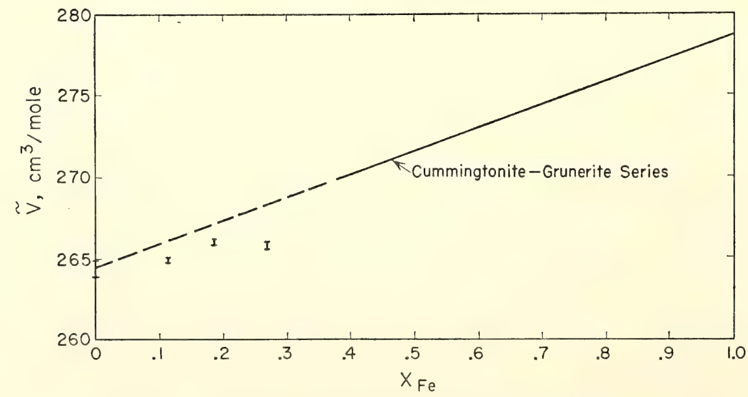

Fig. 42. Molar volumes for ferromagnesian amphiboles. The curve for the monoclinic varieties is drawn as a solid line in the compositional range of samples used to determine the curve. The points are plotted for aluminum-poor anthophyllites.

the heading " 'Mckelveyite,' a syntactic intergrowth of two phases." The mineral as well as its name has now been approved by the I.M.A. Commission on New Minerals and Mineral Names. Its chemical analysis was performed by Dr. Max H. Hey on previously X-rayed single crystals that showed only the faintest reflections due to mckelveyite. Dr. Hey's results (in wt %) follow:

BaO, 45.0; CaO, 7.6; Ln_2O_3, equivalent to 6.5% Y_2O_3, a spectroscopic analysis of the rare earths is underway; Na_2O, 5.6; K_2O, 1.4; SrO, 0.8; Fe_2O_3, 2.0; insolubles, 5.4; CO_2 29.3 (calculated), 30.8 (observed); sum, 103.6.

We collected 321 symmetry-independent reflections on the Supper-Pace automated diffractometer with MoKα radiation. The Miller indices range from 0 to 4 for *h*, from 0 to 5 for *k* and from -16 to $+16$ for *l*. The space group is $P6_3mc$. The cell dimensions of the actual crystal used were obtained from a back-reflection Weissenberg photograph taken with CuKα_1 (1.54051 Å) and CuKα_2 (1.54434 Å) radiations. They are $a=5.284\pm7$, $c=12.78\pm1$ Å. The intensities were corrected with Lorentz and polarization factors and for absorption with the GNABS program. A linear absorption coefficient of 103.9 cm^{-1} was assumed, based on the chemical analysis of mckelveyite (Milton *et al.*, 1965), because the ewaldite analysis was not available at the time. The value we would use now is 98.3 cm^{-1}, not significantly different.

A three-dimensional Patterson synthesis revealed four cations in position 2(*b*) at ⅓, ⅔, *z*; ⅔, ⅓, ½+*z*. The heavier cation was placed at $z=0$; the lighter one was found at $z=0.304$. Electron-density syntheses, with the phases based on cation contributions, show one carbonate group in position 2(*a*) with $z=0.424$ and one in position 2(*b*) with $z=0.675$. There is evidence for omission of carbonate ions in the 2(*b*) position. We therefore converted the chemical analysis to a structural formula with a total of four cations after subtracting the insolubles and the Fe_2O_3, which electron-probe study has shown to be present in the form of hematite inclusions only (*Year Book 67*, p. 219).

The cell content can then be written as: $(Ba_{1.68}K_{0.16}Na_{0.12}Sr_{0.04})(Na_{0.92}Ca_{0.76}Y_{0.32})(CO_3)_{3.56}$ where the cations are grouped by "effective ionic radius" (Shannon and Prewitt, 1969). The ions in the first parentheses, which have coordination number 9, have a weighted average radius of 1.38 Å. Those in the second parentheses have coordination number 6 and a weighted average radius of 0.99 Å.

In order to compare the ewaldite structure type with the most important two structure types of alkaline earth carbonates, those of calcite and of aragonite (Table 29), let us look at their idealized forms. Calcite is a deformed NaCl-type structure; its cations and its carbonate groups are in pseudo-cubic close packing along *c*. Each oxygen has two nearest cation neighbors; each cation is octahedrally surrounded by six oxygens. Aragonite is a deformed NiAs type with Ni (at 0, 0, 0; 0, 0, ½) replaced by $CO_3^=$ and As at (⅓, ⅔, *z*; ⅔, ⅓, *z*+½) replaced by Ca^{2+}; only its cations repeat in pseudohexagonal close packing along *c*. Each oxygen has three nearest cation neighbors; each cation is surrounded by a trigonal prism of six anions.

Ewaldite has a cell edge *a* large enough to accommodate the carbonate groups in the (0001) plane, and thus has true hexagonal symmetry. Its density is correspondingly lower than that of calcite and

TABLE 29. Comparison of Crystal Structures of Composition $(Ba_{0.6}Ca_{0.4})CO_3$ with Ewaldite

	Ewaldite	Calcite Type	Aragonite Type (Alstonite)
Space group	$P6_3mc$	$R\bar{3}c$	*Pmcn*
a, Å	5.284	5.12	5.00
b, Å	...	...	8.79
c, Å	12.78	18.2	6.12
Z	4	6	4
$D_{calc.}$ (g/cm³)	2.884	3.818	3.912

aragonite (Table 29), suggesting a low-pressure stability field on a phase diagram. The structure differs further from the aragonite type in that it is noncentric, its cations have two kinds of coordination polyhedra, and the anions form double hexagonal close-packed layers (Table 30). If, for the purpose of classification, we consider the carbonate groups to be represented by large spheres, the complete ewaldite structure can be described as a layer structure. With the conventional notation of *A, B, C* for the layers that have atoms at 0, 0, z_A; ⅓, ⅔, z_B; ⅔, ⅓, z_C we obtain:

$$\begin{array}{ll} \mathrm{I}\left\{\begin{array}{l} A \\ \quad B \end{array}\right. & \begin{array}{l} (\mathrm{CO_3},\ z=0.924) \\ (\mathrm{Ba..},\ z=0.000) \end{array} \\ \mathrm{II}\left\{\begin{array}{l} \quad\ C \\ \quad B \end{array}\right. & \begin{array}{l} (\mathrm{CO_3},\ z=0.175) \\ (\mathrm{Na..},\ z=0.304) \end{array} \\ \mathrm{III}\left\{\begin{array}{l} A \\ C \end{array}\right. & \begin{array}{l} (\mathrm{CO_3},\ z=0.424) \\ (\mathrm{Ba..},\ z=0.500) \end{array} \\ \mathrm{IV}\left\{\begin{array}{l} B \\ C \end{array}\right. & \begin{array}{l} (\mathrm{CO_3},\ z=0.675) \\ (\mathrm{Na..},\ z=0.804) \end{array} \\ \hline \quad A & (\mathrm{CO_3},\ z=0.924) \end{array}$$

Thus we may describe ewaldite as a quadruple hexagonal close-packed crystal structure (q.h.c.p.).

(Ba. . .) has nine oxygen neighbors at nearly equal distances (~2.87 Å), six below it and three above it. The cation is less than one-third of the way above the bottom layer, thus giving a polar character to the atomic distribution along *z*. The six oxygens below Ba fall at the corners of a truncated equilateral triangle, outlining a six-sided polygon with alternating short (2.25 Å) and long (2.97 Å) edges. The short edges are shared with CO_3 groups; the long edges connect oxygens of translation-equivalent CO_3 groups. In the oxygen layer above Ba, the nearest oxygen neighbors outline a regular triangle, edge length 2.97 Å, with the corners above the midpoints of the long oxygen edges in the six-sided polygon below. This face is shared with the (Na. . .) polyhedron, which consists of a trigonal antiprism, with the central cation at half-height.

Temperature factors of most ions are still too high to be acceptable, and positional disorder involving the *z* coordinates is being studied now.

TABLE 30. Atomic Coordinates of Ewaldite

Atom	Wyckoff Position	Coordinates		
		x	*y*	*z*
(Ba...)	2(*b*)	⅓	⅔	0.000
($C_{1.56}\square_{0.44}$)	2(*b*)	⅔	⅓	0.175
($O_{4.68}\square_{1.32}$)	6(*c*)	0.543	0.457	0.175
(Na...)	2(*b*)	⅓	⅔	0.304
C	2(*a*)	0	0	0.424
O	6(*c*)	0.143	0.857	0.424

Refinement of the Crystal Structure of Triphylite*

L. W. Finger and G. R. Rapp, Jr.†

The crystal structure of a specimen of triphylite from the Dan Patch Mine, Keystone, South Dakota, has been refined as the first step of an investigation of a solid-state oxidation reaction. In this reaction the composition $LiFe^{2+}{}_{1-x}Mn^{2+}{}_x PO_4$ (triphylite-lithiophylite series) may be oxidized to the composition $Li_xFe^{3+}{}_{1-x}Mn^{2+}{}_xPO_4$ by the action of an oxidizer less electropositive than Mn. This is the composition of sicklerite, a naturally occurring member of the series. Finally, the remaining lithium may be removed, the manganese oxidized, and the composition converted to $Fe^{3+}{}_{1-x}Mn^{3+}{}_xPO_4$. In this study we propose to investigate the details of the crystal structures at each step, and we hope to use the same crystal for each determination. In addition, for any reactions that proceed relatively slowly, an attempt will be made to observe the reaction kinetics with X-ray diffraction techniques.

The triphylite studied has been analyzed by C. O. Ingamells (personal com-

* This work was supported in part by National Science Foundation grant GA 707 awarded to the University of Minnesota.

† Department of Geology and Geophysics, University of Minnesota, Minneapolis, Minnesota.

munication), and its composition is very nearly that of $LiFe_{0.76}Mn_{0.24}PO_4$, the composition used in the refinement. Single crystals of the material display diffraction symmetry *mmmP-nb*, consistent with the space group *Pmnb* found by Geller and Durand (1960). Note that this is a reorientation $(00\bar{1}/0\bar{1}0/\bar{1}00)$ from the cells of Gossner and Strunz (1932) and Destenay (1950). The unit-cell parameters were determined from back-reflection Weissenberg photographs taken at 23°C about the *b* and *c* axes with Cu radiation ($\lambda_{K\alpha_1}=1.54051$ Å, $\lambda_{K\alpha_2}=1.54433$ Å, $\lambda_{K\beta}=1.39217$ Å), and the data were refined with the lattice-constant refinement program of Burnham (*Year Book 61,* pp. 132–135). The resulting values are $a=6.0285\pm0.0006$ Å, $b=10.3586\pm0.0009$ Å, $c=4.7031\pm0.0003$ Å, and $V=293.70\pm0.07$ Å^3. There are four formula units per unit cell, giving a calculated density of 3.562 g/cm^3 compared with an observed density range of 3.42–3.56 g/cm^3 (Destenay, 1950).

The X-ray diffraction data were collected at the U. S. Geological Survey, Washington, D. C., on the Picker four-circle automated diffractometer, which is equipped with a scintillation counter. The crystal used was a cleavage fragment, $0.13\times0.16\times0.30$ mm in size. All nonequivalent reflections having sin $\theta \leq 0.7$ for MoKα ($\lambda=0.7107$ Å) radiation were measured with the use of a Nb filter and the 2θ-scan technique, with the scan range calculated according to the method of Alexander and Smith (1964).

The resulting data were corrected for background, Lorentz and polarization effects, and absorption ($\mu_l=54.31$ cm^{-1}). The reflections with a negative integrated intensity were assigned the most probable intensity (Hamilton, 1955). A total of 1240 reflections were measured. The 173 reflections that had an integrated intensity less than three times its standard deviation were treated as unobserved reflections in later refinement.

Starting with the coordinates of Geller and Durand (1960), the structure was refined with the program RFINE. Statistical weights, the scattering factors of Cromer and Mann (1968) for neutral atoms, and the anomalous dispersion coefficients of Cromer (1965) were used throughout this study. After convergence with isotropic temperature factors, the conventional residual, $R=\Sigma||F_o|-|F_c||/\Sigma|F_o|$, was 0.053 for all data and 0.042 for the 1067 reflection data with intensities greater than the minimum observable. The corresponding values for the weighted residual, $r=[\Sigma\omega(|F_o|-|F_c|)^2/\Sigma\omega F_o^2]^{\frac{1}{2}}$, were 0.047 and 0.039. The atoms were then allowed to have anisotropic temperature factors, and the refinement was continued. After convergence, the residuals were $R=0.047$ and $r=0.045$ for all data, and $R=0.037$ and $r=0 036$ for the data with intensities greater than the minimum observable. Applying the significance test of Hamilton (1965), the hypothesis that the atoms of this structure vibrate isotropically may be rejected at the 0.005 level. Some of the important bond distances and angles in the structure are presented in Tables 31 and 32. These quantities and their errors were computed with the unpublished program BADTEA of Finger, and the errors include the full-matrix propagation-of-error formula, including the errors in the lattice constants.

The Keystone triphylite is isostructural with monticellite and consists of serrated bands of edge-sharing octahedra (Birle *et al.,* 1968) cross-linked by phosphate tetrahedra. Each distorted lithium octahedron shares edges with two other LiO_6 groups, two FeO_6 octahedra, and two PO_4 tetrahedra; each iron octahedron shares edges with two lithium octahedra and one tetrahedron; and each phosphate group shares edges with two lithium and one iron octahedra. With this amount of edge-sharing present, there is a great deal of distortion in the polyhedra (Table 31) from shortening of the shared O-O edges; the metal-oxygen bonds, however, are reasonably regular.

TABLE 31. Selected Bond Distances (in Ångstroms) for Triphylite

Atoms	Distance	Atoms	Distance
PO_4 tetrahedron		FeO_6 octahedron	
P-O1	1.535(3)	Fe-O1	2.205(3)
P-O2	1.536(3)	Fe-O2	2.110(3)
P-O3(2x)	1.553(2)	Fe-O3(2x)	2.081(2)
		Fe-O3(2x)	2.251(2)
P-O	1.544	Fe-O	2.163
O1-O2	2.556(4)	O1-O3(2x)	2.907(3)
O1-O3(2x)	2.579(3)	O1-O3(2x)	3.055(3)
O2-O3(2x)	2.479(3)	O2-O3(2x)	3.281(3)
O3-O3	2.442(4)	O2-O3(2x)	2.958(3)
		O3-O3(2x)	2.995(2)
O-O	2.519	O3-O3	2.442(4)
		O3-O3	3.587(4)
LiO_6 octahedron		O-O	3.035
Li-O1(2x)	2.181(2)		
Li-O2(2x)	2.097(2)		
Li-O3(2x)	2.183(2)		
Li-O	2.154		
O1-O2(2x)	2.980(4)		
O1-O2(2x)	3.070(1)		
O1-O3(2x)	2.907(3)		
O1-O3(2x)	3.255(3)		
O2-O3(2x)	2.479(3)		
O2-O3(2x)	3.490(3)		
O-O	3.030		

Note: Standard deviations, σ, are in parentheses.

TABLE 32. Selected Interatomic Angles (in Degrees) in Triphylite

Atoms	Angles
PO_4 tetrahedron	
O1-P-O2	112.7(2)
O1-P-O3(2x)	113.2(1)
O2-P-O3(2x)	106.7(1)
O3-P-O3	103.6(2)
LiO_6 octahedron	
O1-Li-O2(2x)	88.3(1)
O1-Li-O2(2x)	91.7(1)
O1-Li-O3(2x)	83.5(1)
O2-Li-O3(2x)	70.8(1)
O2-Li-O3(2x)	109.2(1)
FeO_6 octahedron	
O1-Fe-O2	178.7(1)
O1-Fe-O3(2x)	81.4(1)
O1-Fe-O3(2x)	90.8(1)
O2-Fe-O3(2x)	89.8(1)
O2-Fe-O3(2x)	97.5(1)
O3-Fe-O3	65.7(1)
O3-Fe-O3(2x)	87.4(1)
O3-Fe-O3(2x)	152.7(1)
O3-Fe-O3	119.0(1)

Note: Standard deviations, σ, are in parentheses.

The deviations of the internal angles (Table 32) from the values for regular polyhedra also show the distortions, as does Fig. 43, in which the details of the octahedral strip and the cross-linking tetrahedra are presented.

The authors gratefully acknowledge the assistance of Drs. D. E. Appleman, J. R. Clark, and J. J. Papike, of the U. S. Geological Survey, who aided in the collection of intensities and preliminary reduction of the data.

Further Use for the Pauling-Bond Concept

Gabrielle Donnay

It frequently happens that the chemical analysis of a new mineral cannot distinguish hydroxyl groups from water molecules incorporated in the crystal structure. A crystal-structure determination will locate all oxygen ions, but unless extreme care can be taken in data

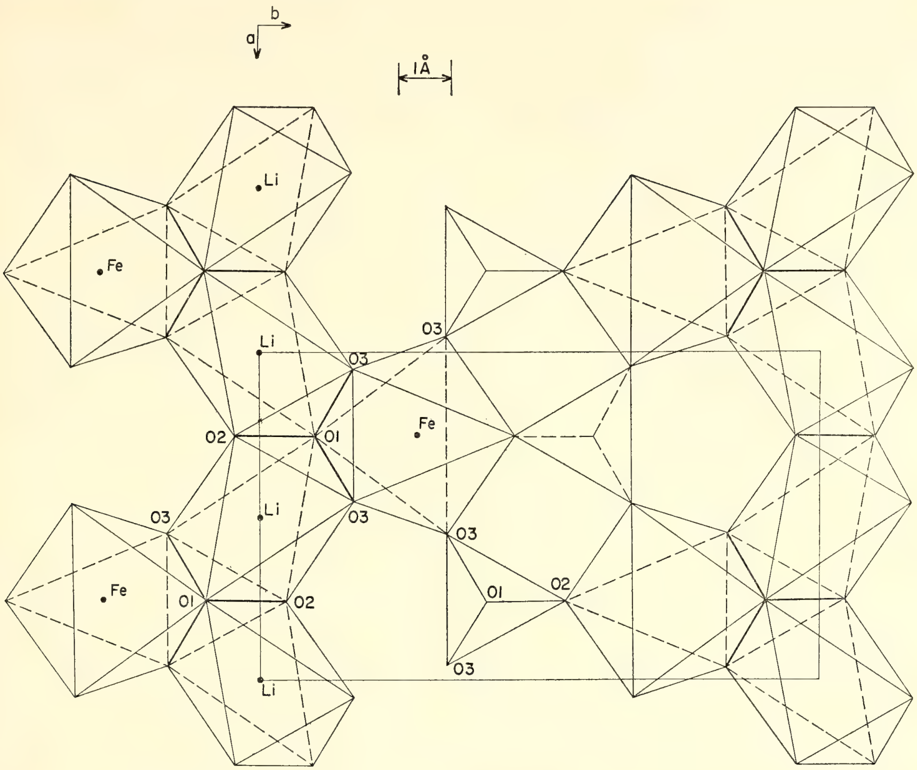

Fig. 43. A partial projection of the triphylite structure parallel to c showing the bands of octahedra cross-linked by phosphate tetrahedra.

collecting, it will not detect protons. Neutron-diffraction data would do this but are not readily available. We wish to draw attention to the fact that Pauling's principle of local neutralization of charge (Pauling, 1929) can be readily applied to solve the problem at hand. As far as the writer knows, only one paper by Zachariasen (1963) has described a related but not identical application for borate structures. We shall illustrate the proposed procedure with the example of sonoraite (Gaines, Donnay, and Hey, 1968), whose structure determination was recently completed (Donnay, Stewart, and Preston, 1969).

The chemical analysis of sonoraite showed that Fe^{3+} and Te^{4+} were present as the only cations in the atomic ratio 1:1. The only other product of the analysis was water. The electron-density map showed eight Fe and eight Te ions in general fourfold position of space group $P2_1/c$ and in addition forty oxygen ions, also in general position. The overall formula thus has to be written $Fe_2Te_2O_{10}H_6$, the six protons being needed to balance the charges. We still had to decide among the formulae $Fe_2Te_2O_4(OH)_6$, $Fe_2Te_2O_5(OH)_4 \cdot H_2O$, $Fe_2Te_2O_6(OH)_2 \cdot 2H_2O$, and $Fe_2Te_2O_7 \cdot 3H_2O$. When the structure determination was completed (with residual R for 1884 reflections equal to 6.2%) bond lengths were known to better than 1% (Table 33), and assuming that the observed bond length uniquely determines the bond valence, we proceeded to estimate these Pauling-

TABLE 33. Bond Lengths (Å) and Estimated Bond Valences (v.u.) for $FeTeO_3(OH) \cdot H_2O$

Oxygen Atoms (numbered)	Te(1)	Te(2)	Fe(1)	Fe(2)	Σ2	Oxygen Associations with Protons
O(1)				2.163(15)		H_2O
				0.25	0.25	
O(2)				2.015(11)		OH^-
				0.49	0.99	
				2.009(12)		
				0.50		
O(3)	1.888(13)			1.943(14)		$O^=$
	1.34			0.62	1.96	
O(4)			2.000(12)	1.983(10)		OH^-
			0.52	0.54	1.06	
O(5)		1.857(12)	1.938(11)			$O^=$
		1.34	0.62		1.96	
O(6)	1.893(10)			1.990(12)		$O^=$
	1.33			0.54	1.87	
O(7)					0	H_2O
O(8)		1.905(11)	2.061(11)			$O^=$
		1.33	0.41		2.16	
			2.055(12)			
			0.42			
O(9)	1.895(13)		2.040(12)			$O^=$
	1.33		0.45		1.78	
O(10)		1.890(11)	1.983(11)			$O^=$
		1.33	0.54		1.87	
Σ1	4.00	4.00	2.96	2.95		
Average bond length	1.892	1.884	2.013	2.017		

Note: Σ1 = valence sum of bonds emanating from cation. Σ2 = valence sum of bonds reaching anion.

bond valences.* The Te-O bonds presented no problem; they range only from 1.857(12) to 1.905(11) Å, where the parentheses contain the standard deviations expressed in units of the last decimal quoted. They overlap within three standard deviations, and we therefore assign valence 1.33 v.u. to each of the longest two bonds and 1.34 v.u. to the shortest bond emanating from each Te ion. The Fe-O bonds, on the other hand, range from 1.943(14) to 2.163(15) Å, and we need an experimental curve for Fe^{3+}-O bond valence versus bond length. Zachariasen (1963, Tables 8 and 9) employed five experimentally determined points to plot the B-O curve and four points for the H-O curve. These points were based on his numerous refined borate-structure determinations. The intermediate range of these plots can be approximated by a straight line, a relation we were obliged to use in any case since only two reference points were available in the literature (*International Tables,* 1962, Vol. 3, p. 269). These points correspond to the average ${}^{vi}Fe^{3+}$-O, and ${}^{iv}Fe^{3+}$-O distances, 2.01 and 1.86 Å, respectively. (The Roman superscript is used to designate the coordination number.) The corresponding bond valences are, of course, $3/6 = 0.50$ v.u. and $3/4 = 0.75$ v.u. Starting with the experimentally determined sonoraite bond lengths, we read from the plot valences that range from 0.62 to 0.25 v.u.; the valence sum of the six bonds coming from an Fe^{3+} ion is 2.96 v.u. in one case, 2.95 v.u. in the other, values that are close enough to the integral value of 3 to show that the linear relation is an acceptable approximation. The valence sum of the bonds that reach any oxygen ion leaves no doubt as to the cor-

* The term "Pauling-bond strength" has been used in the past; it is here replaced by Pauling-bond valence, which is free from physical implication and can naturally be expressed in valence units (v.u.), introduced by Zachariasen (1963).

responding proton association. Values of 0.25 and 0.00 v.u. for O(1) and O(7) identify them as part of water molecules; O(2) and O(4) must belong to hydroxyl groups on the basis of their bond-valence sums, 0.99 and 1.06, respectively. The remaining six oxygens are not associated with protons. The formula is thus found to be $FeTeO_3(OH) \cdot H_2O$, with 8 formula units per cell.

The example of sonoraite involves only cations that have more than one oxygen-coordination number, since tellurium is also known to have four nearest oxygen neighbors. If the observed Te-O bond lengths had indicated the need, a straight-line plot through two points from the literature (Zemann, 1968) would have been used: $^{iii}Te^{4+}$-O with bond valence $\frac{4}{3}$ has average bond length 1.95 Å, and $^{iv}Te^{4+}$-O with bond valence 1.00 has average bond length 2.0 Å. What can be done, however, when a cation occurs with only *one* coordination number? We have learned that the oxygen-coordination number affects the bond length, but we have no direct way of obtaining a reference point with a different bond-valence value. We must proceed in the reverse direction. Let us consider the case of Si as an example. Before $^{vi}Si^{4+}$ had been discovered in stishovite, we used a straight line for Si-O which was obtained from accurately determined silicate structures, in which no substitution of Si^{4+} by Al^{3+}, Fe^{3+}, etc., occurs and all but the Si-O bonds can have their valences estimated. The Si-O bond valences were chosen so as to make the valence sum of bonds reaching the oxygen atoms about Si equal to 2.00. This straight line was found to agree closely with the one now used, which passes through 1.61 Å for bond valence 1.00 and 1.80 Å for bond valence $\frac{2}{3}$.

In mineral crystal-structure determinations, cation substitution further complicates the interpretation of bond lengths. To use the example of Si again, the average tetrahedral bond length (Si, Al)-O in an aluminosilicate has been used to determine the Si/Al atomic ratio on the position in question. Such a determination can be refined to take the average oxygen-coordination number into account, but it cannot otherwise allow for variations in bond lengths that are due to the range in bond valence observed for a single chemical cation. By considering only the average bond length in a coordination polyhedron, errors thus introduced are kept to a minimum.

Taking into account the coordination number of the oxygen ions as well as that of the cations for refinement purposes is now feasible thanks to the compilation of "Effective ionic radii in oxides and fluorides" (Shannon and Prewitt, 1969) in which different oxygen radii for different coordination numbers are given. These data are based on a survey of all pertinent accurate structure determinations and therefore represent the best values now available. In sonoraite, although the effect of coordination number on bond length is strikingly evident—average Fe-^{iii}O bond length is 1.98 Å, average Fe-^{ii}O bond length is 2.04 Å; Te-^{iii}O bond length is 1.905(11) Å, average Te-^{ii}O bond length is 1.88 Å—the refinement was not needed. In general, for locating protons in an oxide structure, the rough approximations used here will be adequate.

A table of bond lengths and bond valences in a description of an ionic structure has additional advantages: it enables one to see at a glance the coordination numbers of all the anions as well as those of the cations, gives average bond lengths for the cations, and shows the departures of the sums of bond valences from their ideal integral values. If such a departure amounts to more than ~25%, experience has shown that the structure determination is open to suspicion.

X-Ray Study of Echinoderm Skeletons

G. Donnay and D. L. Pawson *

Echinoderms have skeletons and spines made of magnesium-rich calcite. Aragonite, which is a common constituent of skeletons of other sea animals, has never been observed in echinoderm plates. The nature of the individual plates had remained uncertain; they were described as subparallel aggregates and as single crystals in the literature (Raup, 1966; Towe, 1967). The shapes and surfaces of the plates are strikingly noncrystallographic. Even on a micrometer scale, scanning electron microscopy shows only curved, spongelike structures, and no planar crystal faces and no constant interfacial angles. It has not been possible to grow any crystal shapes like these in the laboratory, and the biological control leading to their production in the living organism is a fascinating mystery.

We surveyed the orientation relation between crystallographic directions (*a* and *c*) and the plate and body shape of the animal. The orientation relations we are reporting are such as to permit finding the desired reciprocal lattice row on an initial precession orientation photograph. Judging from X-ray precession ($MoK\alpha$) and Weissenberg ($CuK\alpha$) patterns, the skeletal elements studied are indistinguishable from those of cleavage rhombohedra of perfect Iceland spar of comparable size: *they are single crystals.* Some plates were examined optically between crossed nicols; they all showed strain effects when viewed down their *c* axes. No twinning was observed except mechanical twinning induced in echinoid plates when their tubercles are cut off. The tubercles themselves were examined in detail because optical studies on thin sections have led to the impression that they are powders or, at most, crystalline aggregates (Raup, 1965). The tubercles were selected to be representative of those with different functions: spine-bearing and nonspine-bearing, of different ages, and of locations on different parts of the skeletons. They were taken from the species *Evechinus chloroticus* (Valenciennes), *Strongylocentrotus droebachiensis* (Müller), and *Cidaris rugosa* (Clark) and were studied *in situ* on plates. They all bore out the fact that tubercles form as part of the single crystal of the plate on which they grow. Nothing happens to change them when they are nonspine-bearing, as observed, for example, in rudimentary (adapical) tubercles of *Cidaris rugosa.* If, however, they carry spines, their surface becomes pulverized with time, and eventually all of the tubercle may consist only of powder grains, although preserving the rounded shape of the original single-crystal protuberance. The breaking up of the crystal into a powder is very likely brought about mechanically by rubbing of the spine upon the tubercle. Dr. H. U. Nissen, of Zürich, has confirmed this interpretation of our X-ray diffraction data with scanning electron-microscope photographs of a tubercle we had X-rayed.

The spines of the four species of sea urchins (Echinoidea) that we studied are elongated parallel to *c*. No correlation of *a* with shape was found. Each echinoid tooth is an extremely hard subparallel aggregate of single-crystal plates and whiskers; its *c* and *a* directions lie normal to the length of the tooth. The whiskers are aligned along its length so that they are elongated normal to *c*. The plates are curved, difficult to separate, and randomly oriented. In five species of sea cucumbers (Holothuroidea), the *c* axis is perpendicular to the plates. When the plate carries a spine, the latter is part of the same crystal, and the *c* axis points along the length of the spine. These plates show pseudohexagonal rows of perforations, which point along the *a* directions. In three species of sea stars (Asteroidea), the furrow spines are elongated along *c*; those that show a plane

* Smithsonian Institution, Washington, D. C.

of flattening have *a* either in the plane or perpendicular to it. Oral interradial plates in *Patiriella regularis* (Verrill) show *c* perpendicular to the plate and *a* along its direction of elongation. The brittle star *Ophionereis fasciata* (Hutton) (Ophiuroidea) has arm spines elongated along *c*, with *a* parallel or perpendicular to the plane of flattening of the spine. Each ventral arm plate studied has *a* normal to the plate and *c* along its length. In two species of sea lilies (Crinoidea), the *c* axis parallels the axial canal in the cirrus, the stem, the arm, and the pinnule. An *a* axis is directed normal to the plane that contains the cirrus. An axis of morphological pseudosymmetry, often 5-fold, parallels *c* in the stem; an *a* axis lies along the juncture of two repeat patterns. No morphological feature could be correlated to the *a* direction in the arm. The pinnule has a ridge; *a* is perpendicular to it.

Although the present studies are limited to a very small number of species, we are confident that an orientation relation between crystallographic *a* and *c* axes and skeletal shape is to be found throughout the group of *Echinodermata*.

BIOGEOCHEMISTRY

Uptake of Amino Acids by Kerogen

P. H. Abelson and P. E. Hare

The degradation and disappearance of amino acids and other relatively small organic molecules in organic-rich sediments are usually ascribed primarily to microorganisms. Although microorganisms undoubtedly play a significant role in such processes, the experiments reported here demonstrate the existence of another mechanism of degradation, a nonbiological mechanism. This mechanism has a significant role today; it must have been important in the pre-life era of earth's history. We have found that kerogen itself, free of any biological activity, reacts rapidly and to a large degree irreversibly with free amino acids and peptides.

Initial observations leading to these experiments involved the chance observation that fatty-acid tracers were not recovered in experiments with the kerogen from the Tertiary Green River shale and that amino-acid tracers disappeared when exposed to kerogen from the Precambrian gunflint chert. The major amino acids vary substantially in their hydrophilic-hydrophobic character and include a variety of side chains and functional groups; thus the amino acids seem well suited to a comparative study of uptake and reactivity. In our experiments we have noted a wide variation among the individual amino acids in the rate of their irreversible reaction with kerogen and humic acid. We have surveyed the role of a number of experimental variables, including time, temperature, concentration, and *p*H. We have shown that an important factor in the disappearance of the amino acids is reactions involving amine groups.

The kerogens used in this study were isolated from recent mud from the San Pedro basin. On the basis of wet weight, the thick mud had an organic chemical content of 2%. Direct experiments with the mud itself were marginally feasible, but they were difficult to carry out because of contamination of the amino-acid analyzer with cations such as iron. In addition, many of the results would have been suspect because of the flora in the mud. Accordingly, kerogen was prepared by a series of treatments, including extraction with 6 *N* HCl, and a hydrofluoric acid digest, followed by repeated hydrochloric acid extractions. Near the end of the procedure, the light, suspended kerogen was decanted, leaving behind heavy or refractory minerals, such as pyrite. The product was thoroughly

washed and dried. On ignition a weight loss of 94% was noted. The crude kerogen was actually partly humic acid. For many experiments the crude mixture was employed. Humic acid was also isolated from the kerogen, however, so that the two components could be tested separately. The humic acid was extracted by stirring the crude kerogen with 0.1 *N* NaOH for a day and was precipitated from the extract by adjusting to *p*H 1. About 20% of the crude kerogen was isolated as humic acid.

Reactions of the amino acids with humic acid were qualitatively similar to those with kerogen. Quantitative differences were observed but did not seem significant enough to justify extended studies involving isolated humic acid versus kerogen. Accordingly, most of our experiments were conducted with the crude kerogen.

To determine the interaction of kerogen with various amino acids a series of experiments was performed on a solution of standard amino acids sealed under nitrogen with a portion of kerogen, usually in the ratio of 1 ml solution to 50 mg kerogen. For most experiments each amino acid initially was at a concentration of 0.2 μM/ml, with the *p*H adjusted to 8.5. At the end of the incubation period the *p*H was noted and then adjusted with HCl to *p*H 2. The suspension was centrifuged, and an aliquot of the supernatant was applied directly to the ion-exchange column of the amino-acid analyzer. Table 34 summarizes data concerning the effect of time and temperature on the recovery of amino acids from a series of runs at temperatures from 25° to 110°C for various lengths of time. To normalize results with respect to aliquot size the data are expressed in terms of percentage recovery of each individual amino acid, with aspartic acid taken as 100%. We have found consistently that with moderate times and temperatures of incubation aspartic acid reacts only slightly with kerogen.

A wide range of reactivity among the various amino acids can be seen in the data in Table 34. Cystine is the most reactive, followed by the basic amino acids, arginine, lysine, histidine; then the aromatic amino acids, phenylalanine and tyrosine; then leucine and isoleucine. After 8 days at 110°C only aspartic and glutamic acids are relatively abundant. Even at room temperature substantial

TABLE 34. Percentage Recovery of Amino Acids as a Function of Time and Temperature from Kerogen–Amino Acid Mixtures *

	25°C		52°C		80°C			110°C			
Amino Acid	1 hr	97 days	8 days	83 days	1 day	2 days	8 days	6 hr	2 days	4 days	8 days
Lysine	95	13	0	0	6	0	0	0	0	0	0
Histidine	90	10	tr	tr	11	0	0	5	0	0	0
Arginine	90	4	0	0	2	0	0	0	0	0	0
Threonine	98	64	77	27	65	65	36	60	24	13	6
Serine	98	71	79	37	68	69	42	66	31	18	9
Glutamic acid	98	97	100	95	87	90	90	91	76	61	60
Glycine	99	43	64	38	77	57	35	59	32	24	18
Alanine	99	80	81	61	61	60	52	65	35	22	15
Half cystine	29	0	0	0	0	0	0	0	0	0	0
Valine	83	80	62	57	61	54	26	50	19	9	3
Methionine	61	43	31	6	35	25	14	10	0	0	0
Isoleucine	82	66	47	38	46	36	11	33	11	0	0
Leucine	88	60	32	23	40	21	2	16	0	0	0
Tyrosine	36	19	9	3	29	6	0	10	0	0	0
Phenylalanine	30	12	2	1	16	2	0	7	0	0	0

* 0.2 μM of each amino acid originally. Data expressed as percentage recovery with aspartic acid normalized to 100%.

amounts of many amino acids react with kerogen. The trend of the reactions at the lower temperatures is similar to the trend of the reactions at 110°C.

In the absence of kerogen little or no disappearance of any amino acids would be observed at the temperatures and times indicated in Table 34. Even the most unstable of these amino acids endure for at least several thousand years at 25°C in solutions free of reactive materials. The data show that kerogen is an effective scavenger for amino acids and might be expected to reduce the level of many of the free amino acids in the natural environment within a relatively short period of time.

The percentage rate of disappearance of amino acids is strongly affected by initial concentration. In an experiment conducted for 83 days at 52°C, three concentrations of amino acids were employed—0.02, 0.20, and 2.0 μM/ml. Results are shown in Table 35. With the exception of aspartic and glutamic acids, a strong concentration effect was observed.

At a level of 2 μM/ml, cystine reacts completely with kerogen. At the same concentration most of the basic amino acids and a significant amount of the aromatic amino acids disappear. At a concentration of 0.02 μM of each amino acid the reactions are virtually complete for the basic and aromatic amino acids and most of the remaining acids have disappeared. In natural environments like soils and sediments the free amino-acid concentrations are in the range 0.01–400 μg/g of dry sediment (Degens, 1965). Depending on the water content, which in sediments is well over 50%, these amounts of amino acids are in the range of the amino-acid concentrations used in this study. A mud containing 2% organic matter and 20 μg total amino acids per gram would have a ratio of kerogen to amino acids similar to that of the 0.02 μM column of Table 35.

TABLE 35. Effect of Concentration on Percentage Recovery of Amino Acids*

Amino Acid	2.0 μM/ml	0.20 μM/ml	0.02 μM/ml
Lysine	13	0	0
Histidine	21	tr	tr
Arginine	8	0	0
Threonine	70	27	14
Serine	81	37	21
Glutamic acid	99	95	86
Glycine	85	38	29
Alanine	99	61	49
Half cystine	0	0	0
Valine	99	57	40
Methionine	60	6	4
Isoleucine	88	38	13
Leucine	95	23	10
Tyrosine	41	3	0
Phenylalanine	35	1	0

* Data expressed as percentage recovery with aspartic acid normalized to 100%. 83 days at 52°C.

The effect of pH on the amino acid-kerogen reactions was tested in a series of experiments conducted at 80°C for 24 hours with solutions ranging in pH from strong acid to 12.3. The best recovery was effected in 6 N HCl, but even in this medium nearly half of the cystine and substantial amounts of the methionine and tyrosine disappeared (Table 36). The basic amino acids react faster at all of the higher pH values, whereas the leucines and aromatics react best in the intermediate pH range, being recovered fairly well at both low and high pH values. The data show that in the normal pH range found in natural environments there is not an important pH effect.

To determine the extent to which the reactions of kerogen and amino acids are irreversible, samples of kerogen were hydrolyzed with 6 N HCl before and after the treatment with amino acids. In every case, only a small fraction of the reacted amino acids could be recovered. In addition, the amount of ammonia found in the supernatant was significantly greater after reaction with the amino-acid mixture, showing that ammonia was being produced from the degradation of the amino acids. Five amino acids—aspartic acid, isoleucine,

TABLE 36. Effect of pH on Amino-Acid Recovery *

Amino Acid	6 N HCl	1 N HCl	pH 2	pH 5	pH 8.8	pH 11.3	pH 12.3
Lysine	100	78	71	10	6	2	7
Histidine	100	18	39	5	11	14	11
Arginine	85	57	52	2	1	2	6
Threonine	98	93	71	68	63	54	63
Serine	97	87	69	72	65	60	82
Glutamic acid	100	65	50	76	81	76	100
Glycine	100	100	83	80	71	58	73
Alanine	100	99	81	80	77	72	98
Half cystine	52	10	7	0	0	0	0
Valine	100	95	86	90	90	85	94
Methionine	63	9	33	26	28	34	64
Isoleucine	90	85	66	61	61	59	85
Leucine	100	69	51	42	44	41	100
Tyrosine	64	47	39	25	27	29	64
Phenylalanine	80	29	24	14	16	21	59

* Data expressed as percentage recovery with aspartic acid normalized to 100%. 80°C for 24 hours.

phenylalanine, lysine, and arginine—were incubated separately at a concentration of 40 μM/ml with 50 mg kerogen at pH 8.5 for 5 days at 110°C. An aliquot of kerogen was similarly incubated with water, with the pH adjusted to 8.5. The concentrations of amino acid employed were unusually great, and the duration of incubation was long so that products of incubation could be readily detected. In each instance, including the control with H_2O, some NH_3 (2.4 μM) appeared, and in each incubation with amino acid some of the latter disappeared. Subtracting the amount of NH_3 contributed by the control from that observed, the adjusted results are as follows: Of an initial 40 μM, 11 μM aspartic acid disappeared and 4 μM NH_3 appeared. Other corresponding values are 19 μM isoleucine, 9.3 μM NH_3; 25 μM phenylalanine, 10.5 μM NH_3; 29 μM lysine, 17 μM NH_3; and 32 μM arginine, 24 μM NH_3. In a control run with 40 μM NH_4SO_4, 12 μM NH_3 disappeared. Thus one would not expect to observe an exact correspondence of disappearance of amino acids with appearance of NH_3. From previous experiments (see Tables 34–36) the order of reactivity of these amino acids from least reactive to most reactive is aspartic acid, isoleucine, phenylalanine, lysine, and arginine. This is exactly the order of ammonia production, with aspartic acid producing the least and arginine the most.

The kerogen that had been incubated with arginine was later hydrolyzed for 22 hours with 6 N HCl. The supernatant contained 1.2 μM. Our experience with long and repeated hydrolysis of kerogen is that prolonged hydrolysis might have brought off a total of 2.4 μM arginine out of the 32 μM bound. Clearly arginine had disappeared irrevocably. On the other hand, only trifling amounts of urea, citrulline, ornithine, or any other amino acid appeared during the original incubation. The 6 N HCl hydrolysis of the kerogen yielded small amounts of the usual amino acids, as expected. Thus, it appeared that the arginine molecule was largely incorporated into the kerogen.

An analysis of the carbon and nitrogen values of the kerogen residue confirms this observation. The C/N molar ratio of kerogen incubated with water was 14.4, whereas the C/N ratio of the kerogen incubated with arginine dropped to 8.2. To account for such a change, three of the nitrogen atoms of arginine must be incorporated in the kerogen. Most of the fourth nitrogen atom of arginine appears in the supernatant as NH_3.

Operation of our amino-acid analyzer was conducted in two modes; one facilitated resolution of acidic and neutral amino acids, and the other was convenient for identifying basic amino acids and amines. Thus, if interaction of the amino acids with the kerogen gave rise to ninhydrin-sensitive entities, such as amines, we could have easily found and identified them. We can state that no appreciable amount of amines was released. The disappearance of alanine, for example, was not accompanied by the appearance of ethyl amine. These observations rule out simple decarboxylation as the primary mechanism for disappearance of the amino acids. Moreover for lysine, simple deamination is not the mechanism of disappearance. Simple deamination would have yielded a detectable residue.

In the hydrolysis of kerogen samples with 6 *N* HCl a small but significant amount of amino-acid material was released. This was surprising in view of the fact that the preparation of the kerogen involved exposure to hot 6 *N* HCl for long periods of time, which should have hydrolyzed any normally peptide-bound amino acids. After an initial hydrolysis, a second hydrolysis also yielded substantial though smaller amounts of amino acids. To determine the extent of the release of amino acids from kerogen by hydrochloric acid treatment a 7-g sample of kerogen was continuously subjected to hot 6 *N* HCl extraction for 5 weeks in a Soxhlet apparatus. The HCl was evaporated and analyzed for amino acids at 1-week intervals, after each of which the Soxhlet was filled with fresh, constantly boiling HCl for the next period. Four such samples were taken; the final sample covers 2 weeks, and each of the other three covers 1 week. The results are summarized in Table 37 in namomoles (10^{-9} moles) per gram of ash-free kerogen. For most of the amino acids half or more was released in the first week of Soxhlet extraction. The unusually large amount of cystine is noteworthy. For certain amino acids, e.g., tyrosine and phenylalanine, the ratios change, indicating perhaps that some are more tightly bound to the kerogen than others.

It seems unlikely that we are dealing with normal peptide bonds in the release of amino acids from kerogen. It may be that the amino acids recovered are highly adsorbed but have not yet reacted with the kerogen. Incubation of kerogen with water alone results in a marked decrease in the recovery of amino acids on later treatment with 6 *N* HCl. For example, after incubation at 110°C for 30 hours with water, adjusted to *p*H 8.5, subsequent acid treatment yielded only about 50% as much of the amino acids as did acid treatment of the original kerogen.

TABLE 37. Extraction of Amino Acids in Kerogen *

Amino Acid	1st Week	2nd Week	3rd Week	4th and 5th Weeks
Aspartic acid	1500	490	110	90
Threonine	530	87	14	15
Serine	290	85	13	7
Glutamic acid	980	320	57	65
Glycine	2900	1850	340	420
Alanine	950	350	86	105
Half cystine	1250	384	95	74
Valine	2150	470	150	100
Methionine	170	28	...	...
Isoleucine	2130	460	120	120
Leucine	1220	330	73	85
Tyrosine	450	310	90	104
Phenylalanine	700	200	44	64

* Data expressed in nanomoles (10^{-9} moles) per gram of ash-free kerogen.

This result suggests that part of the amino acids are initially bound by adsorption and that these loosely adsorbed amino acids are irreversibly incorporated into the kerogen itself on incubation.

To gain further insight into the mechanism of the amino acid–kerogen reaction a series of experiments with peptides and kerogen were carried out. The two peptides glycylleucine and leucylglycine differ only in the position of the amino acids. The individual constituent amino acids differ in their reactivity with kerogen, leucine being much more reactive than glycine. In glycylleucine the amino group of glycine is free to react, whereas in leucylglycine only the amino group of leucine is free. Breaking of the peptide bond while in solution would of course release equal amounts of both free amino acids, which in turn could react with kerogen. These peptides can be resolved, by ion-exchange chromatography, from each other and from glycine and leucine, making it possible to monitor both peptides and any free glycine and leucine produced during the course of the reactions.

In Table 38 are summarized the results of an experiment in which the two peptides were exposed to kerogen. Although only a small fraction of the peptides was recovered as free glycine and leucine, the proportion of glycine and leucine was consistently different in each peptide. In glycylleucine free leucine always exceeded free glycine; in leucylglycine the reverse was true, glycine exceeding leucine to an even greater extent. These results indicate that the peptide-kerogen reactions involve the free amino group of the peptide. Following attachment to the kerogen, some of the peptide bonds have split.

TABLE 38. Reaction of Peptides with Kerogen *

	Start	1½ hr	6½ hr	1 day	4 days
Glycylleucine + kerogen at 110°C, *p*H 8.8					
Glycine	0	1	3	5	7
Leucine	0	1	5	8	8
Glycylleucine	100	84	49	18	6
Leucylglycine	0	...	tr	1	4
Leucylglycine + kerogen at 110°C, *p*H 8.8					
Glycine	0	2	4	7	11
Leucine	0	tr	1	2	3
Leucylglycine	100	86	57	40	15
Glycylleucine	0	1	1	2	4

* Data expressed as percentage of original peptide. 6 *N* HCl hydrolysis of the 4-day kerogen residue yielded less than 10% of the glycine and leucine originally present.

Although leucine is more reactive than glycine, the peptide glycylleucine is somewhat more reactive than leucylglycine. In these experiments the production of NH_3 was again observed. Thus our studies point toward an important role for the amine group in reactions of amino acids with kerogen. All our observations point toward a mechanism in which the amino acids reacting with kerogen lose NH_3 and the residual portion is bonded to the kerogen, presumably by a carbon-carbon bond.

In our studies of the interaction of kerogen and peptides we observed that after long-term exposures new peptides appeared. When glycylleucine was heated, some leucylglycine was formed, and similarly glycylleucine was formed from leucylglycine. That kerogen was *not* involved was shown by heating each peptide alone, forming in each case the opposite configuration. Our experiments showed that one peptide configuration, leucylglycine, was more stable than the other, and an equilibrium proportion was obtained after prolonged heating. The low recovery of the peptides and constituent amino acids after reaction (without kerogen) indicated that much of the original material was in a ninhydrin-negative form—probably a ring structure such as diketopiperazine. Hydrolysis with 6 *N* HCl permitted recovery of the total amount of glycine and leucine originally present. On passage through Dowex-50 in the sodium form of solutions at *p*H 3 the diketopiperazine was not retarded and could be freed from any free amino acids and peptides present.

Heating of solutions of this diketopiperazine produced leucylglycine, glycylleucine, and some free glycine and leucine. Consistently higher proportions of leucylglycine were formed. These experiments have profound implications for the abiotic synthesis of peptides and proteins since they indicate a preferred production of certain amino-acid sequences by a nonbiological, nongenetic code mechanism.

Optically Active Steranes in a Miocene Petroleum

T. C. Hoering

The optical activity of many petroleums is associated primarily with high-boiling, saturated, cyclic hydrocarbons. These include the four-ringed molecules of the sterane class. Optically active steroids are common constituents of living organisms. After deposition in sedimentary rocks, they are fully saturated with hydrogen to form steranes (see Fig. 44).

This report describes the development and application of a procedure for isolating sterane hydrocarbons from sedimentary organic matter. A petroleum of Miocene age from the Los Angeles Basin, California, was chosen in order that large amounts of starting material would be readily available. Phillipi (1965) has made a detailed study of the geology and petroleum genesis in this area. He kindly provided a quantity of a typical crude oil, which corresponds to sample 36 of his

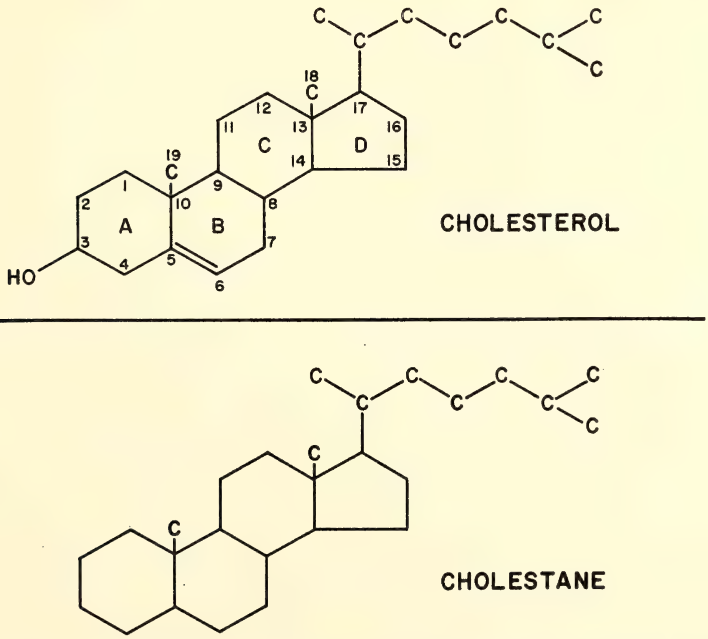

Fig. 44. Structure of a typical steroid, cholesterol. The conventional numbering of the carbon atoms in the molecule and the designation of the rings are shown. A sterane hydrocarbon, cholestane, would result if the double bond at C_5 were saturated with hydrogen and the hydroxyl group at C_3 were replaced by hydrogen. The naturally occurring classes of steroids are grouped on the basis of the structure of the side chain bonded at C-17. Ergostane has a methyl group substituted at C-24, and sitostane has an ethyl group at C-24. Two forms of steranes are considered. They differ only in the configuration at the juncture of rings *A* and *B*. If the added hydrogen at C_5 projects below the plane of the ring, the molecule is designated as 5α and ring *A* lies in the same plane as the other rings. If the added hydrogen projects above the plane of the rings, the molecule is designated 5β and ring *A* projects downward at an angle to the other rings.

publication. He had shown by mass spectrometer analysis that the oil was rich in four-ringed alkanes, but the distribution and types of molecular structures in the sterane fraction were unknown.

The optically active fractions of petroleum are extremely complex mixtures, but new types of chromatographic separation and instrumental methods of analysis make it possible to isolate and characterize individual components. For example, the Bendix-Ericson automatic polarimeter is capable of routinely detecting 0.001° of rotation. It is possible to use samples that are 1 to 2 orders of magnitude smaller than employed by conventional polarimetry. Combined gas-liquid chromatography and mass spectrometry makes possible the separation of complex mixtures and the simultaneous measurement of the mass spectra of microgram quantities of individual components. The mass spectra of sterane hydrocarbons have been studied in great detail by Tokes (1965). Their spectra are unique, and detailed information on molecular weight, number of carbons in the aliphatic side chain, the nature of the juncture between rings *A* and *B*, and the presence of extra methyl substituents is easily obtained. Mass spectrometry, however, does not give useful information on the structure of the side chain at C-17.

Pure steranes are needed for developing the separation procedures and for calibrating the gas chromatograph and the mass spectrometer. Most of them are not available commercially. They were synthesized from readily available steroids by well-established chemical reactions. A set of steranes in both the 5α and 5β configuration was assembled.

In the study of the crude oil, the general experimental procedure was as follows. Saturated hydrocarbons were isolated from the petroleum by alumina and silica-gel column chromatography. They were distilled into thirty-five narrow-boiling-range fractions. Over 90% of the optical activity was concentrated into 7 wt % of the hydrocarbons. A series of separations, selective to molecular size and shape was employed on the fractions containing the optical activity. Straight-chained hydrocarbons were removed by forming their urea adduct. Thiourea forms an adduct with hydrocarbons of bulkier size. Using the synthetic pure compounds, it was found that 5α cholestane and 5α ergostane could be selectively removed from a mixture. Haug (1963) found that five-ringed hydrocarbons are selectively adsorbed by Linde molecular sieve 13X. When the optical activity concentrate from the petroleum was chromatographed on a 6-foot column of the molecular sieve in CCl_4, fractions enriched in steranes and free of hydrocarbons with higher number of rings could be obtained. Gel permeation chromatography substrates, compatible with organic solvents, have become available recently. A 10-foot column of Sephadex LH-20, expanded in acetone-tetrahydrofuran, was effective in concentrating four-ringed hydrocarbons from linear and cyclic hydrocarbons. Adsorption chromatography on a 25-foot column of alumina at low sample loadings was very effective in separating steranes. A chromatogram is shown in Fig. 45.

The individual separation steps were combined as follows. The branched cyclic hydrocarbons in the optical activity concentrate were treated with thiourea and separated into two classes, the adductinated and the nonadductinated. Each of these was then chromatographed successively on the molecular sieve, the gel permeation medium, and the alumina column. Fractions of pure four-ringed hydrocarbons resulted. High-resolution mass spectrometry and field-ionization mass spectrometry showed them to be exclusively steranes of the formulae $C_{26}H_{46}$, $C_{27}H_{48}$, $C_{28}H_{50}$, $C_{29}H_{52}$, $C_{30}H_{54}$, and $C_{31}H_{56}$.

About one-fourth of the sterane fraction formed a thiourea adduct and gave the relatively simple gas-liquid chro-

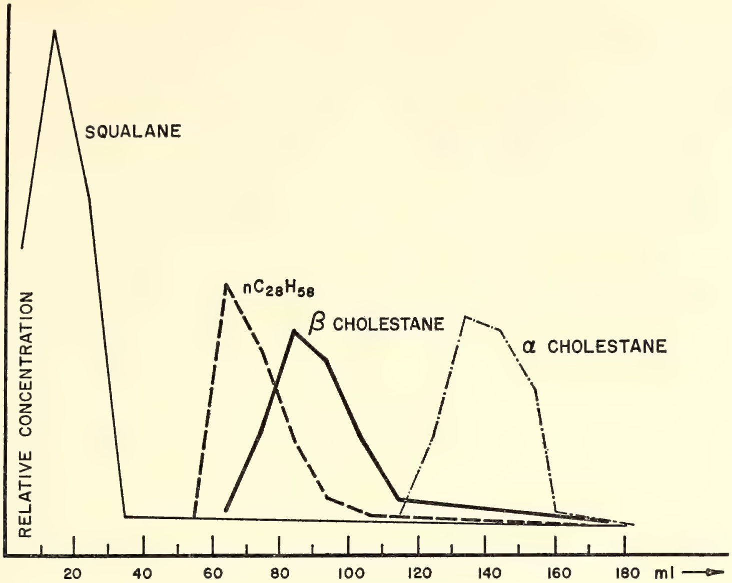

Fig. 45. Separation of hydrocarbon classes by alumina chromatography. A column of neutral alumina, 25 feet × 0.375 inch in diameter, was used. Ten milligrams of a mixture of normal hydrocarbon, *n*-octacosane, $C_{28}H_{58}$; a highly branched hydrocarbon, squalane, $C_{30}H_{62}$; and two sterane hydrocarbons, 5α and 5β cholestane, $C_{27}H_{48}$, was placed on the column and eluted with hexane. Ten milliliter fractions of the eluate were collected and analyzed by gas-liquid chromatography.

matogram shown in Fig. 46. This sample was highly optically active, having a specific rotation of 28.3, as compared to 0.9 for the total hydrocarbons in the petroleum. The individual compounds were separated and identified by combined gas-liquid chromatography and mass spectrometry.

The steranes that did not form a stable thiourea adduct were a complex mixture but could be resolved by gas-liquid chromatography. The mass spectra of over thirty components have been measured. The components are principally isomeric cholestanes, ergostanes, and sitostanes. The mass spectra of every compound examined so far are typical of the 5α configuration. Hence, the steranes in this petroleum differ primarily in the degree of branching of the side chain at C-17.

A number of interesting minor components have been identified. Figure 46 shows the presence of a sterane with a seven-carbon side chain. The corresponding steroid is very rare. This compound may represent a cholesterol with one of the carbons in the side chain removed during petroleum genesis. A series of steranes without the 19-methyl grouping (19-nor steranes) is present. There are a number of steranes with extra methyl substituents on rings *A* and *B*.

There is little doubt that the steranes in this petroleum represent fossil steroids from once-living organisms. They are highly optically active, and the most abundant ones—cholestane, ergostane, and sitostane—are just the ones to be expected from reduction of the major steroid types. An examination of much older sedimentary organic matter may yield information on the biochemical evolution of steroids (Bergman, 1958).

The presence of steranes in predominantly the 5α configuration, but with isomerized side chains, shows that during hydrogenation of steroids in sedi-

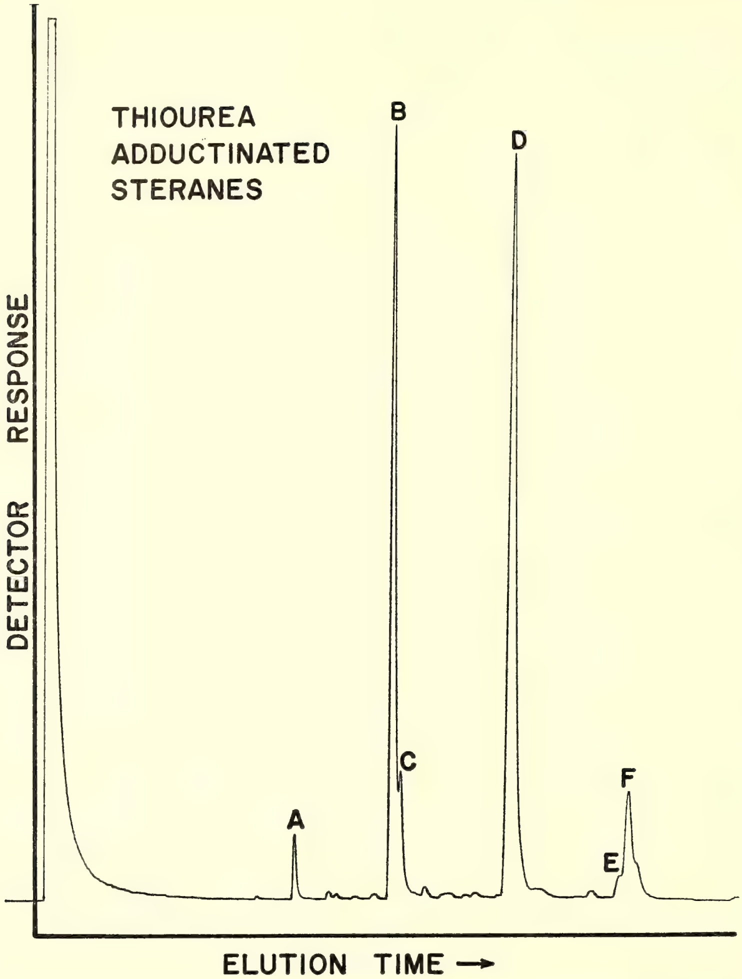

Fig. 46. Gas chromatogram of sterane hydrocarbons isolated from petroleum. The chromatogram was made with a 100-foot × 0.010-inch capillary column coated with Apiezon L and a head pressure of 30 psi at 265°C. The identifications were made by combined gas-liquid chromatography and mass spectrometry. (*A*) 5α sterane, $C_{26}H_{46}$, with a 7-carbon side chain at C-17. (*B*) 5α cholestane, $C_{27}H_{48}$. (*C*) 5α sterane, $C_{27}H_{48}$, isomeric to cholestane. (*D*) 5α ergostane, $C_{28}H_{50}$. (*E*) 5α cholestane with two additional methyl groups on rings *A* or *B*, $C_{30}H_{52}$. (*F*) 5α sitostane, $C_{30}H_{52}$.

mentary rocks the stereochemically more stable ring structure is preferred. A considerable amount of rearrangement of alkyl groups must have already occurred in this geologically young sample.

No detectable optical activity occurred in the lower boiling fraction of the hydrocarbons. Several of them were greatly enriched in the compounds pristane and phytane, the major hydrocarbons present. They are believed to be formed from the phytol side chain of chlorophyll. However, phytol alcohol is optically active, and its hydrogenation products would be expected to be active also. It is difficult to imagine how these compounds could be so thoroughly racemized under the conditions of petroleum formation.

This report shows that it is possible

to examine the high-boiling fractions of sedimentary organic matter in detail that has not been possible before. Many classes of compounds of great biogeochemical interest await exploration. For example, if a range of five-ringed saturated hydrocarbon standards were available, it would be possible to examine triterpanes, which are probably derived from plant triterpenoids.

ISOTOPIC INVESTIGATIONS IN GEOCHEMISTRY AND GEOCHRONOLOGY

G. L. Davis, T. E. Krogh, and S. R. Hart, with C. Brooks* and A. J. Erlank**

The Age of Metamorphism in the Grenville Province, and the Age of the Grenville Front

The Grenville province of the Canadian shield is an area of great extent having structures and rock types that indicate deep burial. Its metamorphic grade is usually higher than that of the Superior, Southern, and Churchill provinces, which bound the Grenville province on the northwest. This boundary, the Grenville Front, is a major northeast-trending zone of both plastic and brittle deformation that extends from Georgian Bay on Lake Huron to the Labrador trough and perhaps as far as the Labrador coast, a distance of about 1800 km. In the Georgian Bay–Sudbury area of Ontario, age relationships between the Grenville gneisses south of the Front and the lower temperature, higher level Huronian metasediments north of the Front were studied by many eminent Canadian geologists of earlier times. The Grenville gneisses in this area have been considered to be older, equivalent to, and younger than the Huronian rocks that were deposited at least 2150 m.y. ago (Van Schmus, Wetherill, and Bickford, 1963), as well as equivalent to the Grenville series in southeastern Ontario that was deposited between 1300 and 1000 m.y. ago (Krogh and Hurley, 1968).

The most detailed geological investigation of this area was published in 1930 by Quirke and Collins, who entitled their memoir "The disappearance of the Huronian." These authors concluded that the Huronian formation, traceable eastward for 225 km from Sault Ste. Marie, does not terminate at the Grenville Front but exists south of the Front in a highly recrystallized and metamorphosed state. Phemister (1961) reached a similar conclusion after a study of the transition southeast of Sudbury.

A great divergence of opinion regarding the age of the metamorphism of the gneisses existed among the early workers. In the past 15 years, however, more than a hundred radiometric age values between 900 and 1300 m.y. have been determined for minerals from various parts of the Grenville province. These ages have been widely accepted as indicating that the major metamorphism occurred about 1000 m.y. ago.

In the past few years we have been able to show that many of the gneisses south of the Front were metamorphosed more than 1500 m.y. ago and that the age of deposition of these rocks is more than 1700 m.y., the age of numerous granites in the region. Because of this, the area provides a unique opportunity to determine the extent of migration of the dating elements during a regional metamorphism, in this case about 1000 m.y. ago. A technique based on isotopic determinations of rubidium and strontium in layered paragneisses has been developed. This is the only direct method available to determine the time of metamorphism if all mineral systems have undergone subsequent isotopic exchange. This report gives the results of a study

* Department of Terrestrial Magnetism.

of the paragneiss that indicates a time of major metamorphism 1800±100 m.y. ago, with isotopic exchange taking place during a younger metamorphism, 900 m.y. ago, restricted in extent to a few millimeters. The older age for the first metamorphism was confirmed by our determination of muscovite ages of 1630 m.y. in a pegmatite 1.5 km south of the Grenville Front.

The proximity of these older gneisses with the plastically deformed northeast-trending migmatitic zone in the Grenville Front implies the same age for the Front itself. We have made considerable progress toward dating the nonrock-forming structural events in the Grenville Front in areas where most of the mineral systems suitable for measurement have been open to exchange during the younger metamorphism. The centers of coarse muscovite crystals yield ages as old as 1630 m.y. in a syndeformational pegmatite and as old as 1470 m.y. in postdeformational pegmatites in the Front zone. Preliminary whole-rock determinations on these pegmatites suggest that their true ages may be as much as 1800±100 m.y.

An age of 1570 m.y. has been determined for a series of elongate granitic bodies that occur along the Front between Sudbury and Georgian Bay for a distance of more than 65 km. These intrusives commonly have a very limited contact metamorphic effect where they intrude the fine-grained Huronian rocks to the northwest, but they are bounded on the southeast by coarsely crystalline gneisses. Field evidence suggests that the late-stage brittle deformation found along the Grenville Front occurred both before and after the emplacement of this granite.

Our results to date imply that the gneisses both in this part of the Grenville province and in the Grenville Front zone underwent metamorphism and deformation between 1500 and 1800 m.y. ago and that the Front zone was again a line of dislocation and probable uplift about 1000 m.y. ago.

Metamorphism 1700±100 m.y. and 900±100 m.y. Ago in the Northwest Part of the Grenville Province in Ontario

T. E. Krogh and G. L. Davis

Paragneiss from the Georgian Bay area 55 miles southeast of the Grenville Front. In *Year Book 67* we presented the variations in Rb and Sr found in a layered felsic paragneiss sample collected south of Pointe au Baril on highway 69 (*Year Book 67,* location 11). To date we have analyzed five 2-cm to 3-cm slices from the 20-cm block, as well as plagioclase and microcline from two of the slices, and a single biotite.

The data for microcline and plagioclase shown in Fig. 47 indicate isotopic exchange of strontium between these two minerals in each of the two samples analyzed (11-2, 11-9) at about 930 m.y. The biotite from sample 11-2 yields a slightly lower age, 890 m.y.

In Fig. 47 the data for the whole-rock samples lie on an isochron for 1800 m.y. Even the three adjacent samples (11-7, 11-8, 11-9), which had distinctly different isotopic compositions during the younger metamorphism, do not indicate any signfiicant between-sample isotopic mixing.

These whole-rock and mineral data demonstrate that the isotopic composition of strontium was homogeneous within this 20-cm section of rock about 1800 m.y. ago and that isotopic mixing since then has been restricted to local exchange between adjacent minerals. In a microcline-plagioclase host, Sr^{87}, once released from its production site, behaves as a relatively nondiffusing trace element.

Paragneiss from the French River area. In *Year Book 66* we discussed the Rb and Sr variations that occur in a layered paragneiss, situated about 30 miles southeast of the Grenville Front in

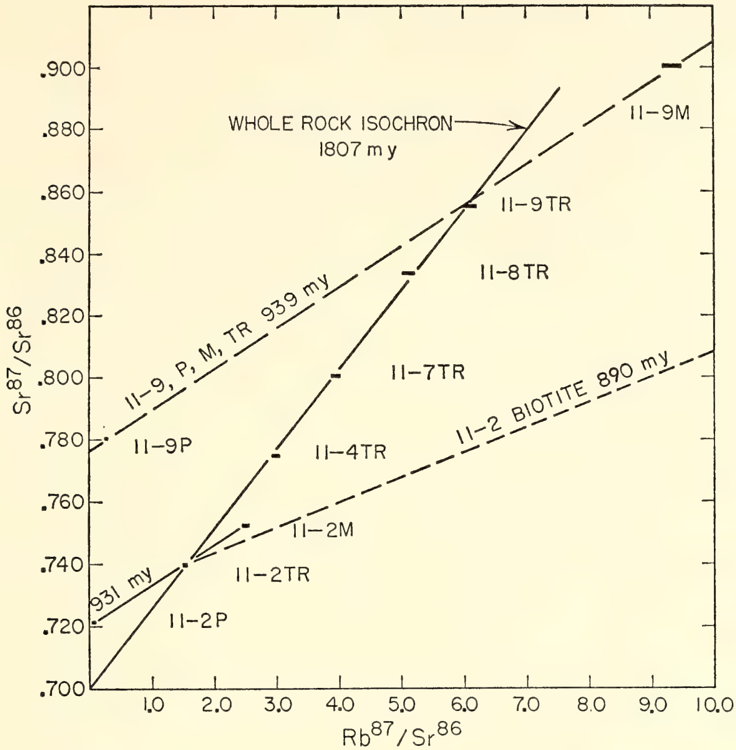

Fig. 47. Isochron plot for the Georgian Bay, Pointe au Baril, paragneiss sample. Solid line is the whole-rock isochron. Broken line is the mineral isochron.

the French River area. Of special interest are the plagioclase-quartz-biotite layers that appear to form as a result of metamorphic reactions between the microcline-bearing layers and the mafic layers (amphibole, plagioclase, biotite). As a test of isotopic mixing during the younger metamorphism, plagioclase from four adjacent layers (2 to 4 cm thick), including a plagioclase-rich reaction zone, was analyzed. The results obtained, as shown in Fig. 48, demonstrate that the isotopic composition of Sr in plagioclase is different in each of the adjacent layers. If these metamorphic layers developed during the younger metamorphism, each part of this 12 cm of rock would have strontium with the same isotopic composition. We propose that the isotopic composition of the strontium was the same across this section at some time between 1500 and 1800 m.y. ago and that the metamorphic changes to form the minerals now present occurred then. Between the first and the second metamorphism each layer developed a different Sr^{87}/Sr^{86} ratio in accordance with its Rb^{87}/Sr^{86} ratio. During the 900-m.y. thermal event each plagioclase exchanged strontium with the minerals in its own layer.

Isotopic Ages Along the Grenville Front in Ontario

T. E. Krogh and G. L. Davis

The Grenville Front southeast of Sudbury, Ontario. Isotopic dating of a pegmatite body situated in the northeast-trending migmatitic Grenville Front zone provides our best estimate of the time of formation of this major structural

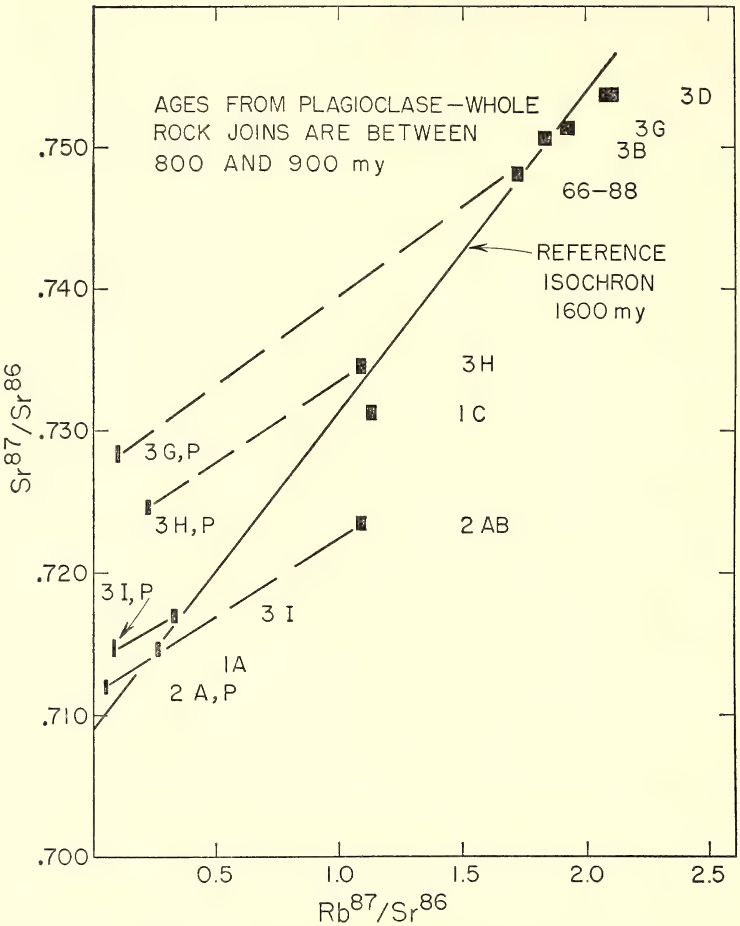

Fig. 48. Isochron plot for the French River paragneiss sample. Solid line is the whole-rock isochron. Broken line is the mineral isochron.

feature. The body, which contains kyanite and garnet, apparently was introduced between the layers of the gneiss during a period of plastic deformation. Phemister (1961) reported that many paragneiss inclusions within the pegmatite strike northeast and dip to the southeast parallel to the host rocks. In places, pegmatite and gneiss are interlayered on a scale of a few centimeters, and together they are folded with the southeast-plunging lineation typical of the Front zone. These relationships imply that the age of emplacement for the pegmatite is the time of plastic deformation in this part of the Front.

Analysis of the magnetic and nonmagnetic zircons from this pegmatite yields a probable diffusion age between 1600 and 1700 m.y. (Fig. 50). The centers of two large muscovite crystals from the pegmatite yield Rb-Sr ages of 1630 m.y. These muscovites, formed during the major regional metamorphism, are the first ever measured within the Grenville province that give ages approaching that of the earlier metamorphism. A single whole-rock aliquot from a 38-kg pegma-

tite sample has a ratio of Rb to Sr of 9.0. It yields an age of 1880 m.y. for the pegmatite if an initial ratio (Sr^{87}/Sr^{86}) of 0.705 is assumed. These results imply that the Front zone may be as old as 1880 m.y. and that the region did not cool until about 1600 m.y. ago.

Killarney Bay, Bell Lake, and Chief Lake areas. In the Sudbury–Georgian Bay area a series of elongated granitic bodies occur along the Grenville Front for a distance of more than 70 km. Along their northwest intrusive contact they have a very limited contact metamorphic effect on the Huronian rocks. Occasionally zones of brecciated quartzite occur. Toward the southeast their contact with the Grenville gneisses is probably intrusive, but the relationships are obscured by development of northeast-trending orthogneisses within the granites as well as a late-stage pervasive mylonite. Quirke and Collins (1930), who did the most detailed early geological work in the area, suggested that the granite seems to have followed a break in the crust and to have been crushed into a zone of weakness.

The authors of recent geological investigations in these areas include M. J. Frarey (paper in preparation) in the Killarney–Bell Lake area, Henderson (1967) in the Chief Lake area, and Brooks (1967) in part of the Bell Lake area. Previous whole-rock Rb-Sr analyses (*Year Books 65* and *67*) indicated an age of about 1700 m.y. for the Chief Lake batholith in the eastern part of the area, but points for some samples were below the isochron.

The results obtained for samples from three localities are presented in Fig. 49:

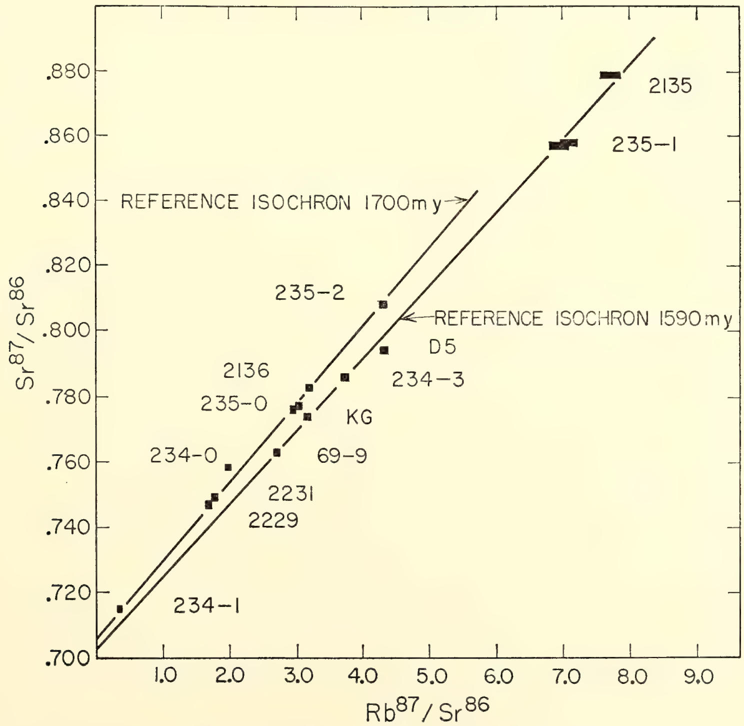

Fig. 49. Isochron plot for granite samples from along the Grenville Front in the Georgian Bay–Sudbury area. Sample designated KG is from the Killarney granite, sample 69-9 is from the Bell Lake granite, and other samples are from the area mapped as the Chief Lake batholith.

the Killarney granite (designated KG) occurs near Georgian Bay, the Bell Lake granite (designated 69-9) occurs about 20 km to the northeast, and the Chief Lake batholith (other points) is situated up to 70 km to the northeast. Two ages of granite emplacement are now apparent from both the whole-rock and zircon data: about 1590 and 1700 m.y. (Figs. 49 and 50). The older granite occurs only in the northern part of the area called the Chief Lake batholith, whereas the younger granites are distributed along the Grenville Front from Georgian Bay to near Conniston, southeast of Sudbury.

A major northeast-trending structure, the Grenville Front must have developed prior to the emplacement of this younger granite almost 1600 m.y. ago. Many of the least deformed granite samples from the Chief Lake batholith area are found to be parts of the younger granite. Much of the mylonitization of the Chief Lake body is probably older than this granite. In other areas, however, the younger granites are also intensely deformed, suggesting that these granites were actually emplaced during the late-stage brittle deformation of the Grenville Front.

Rb-Sr ages of 1440–1470 m.y. were measured on coarse muscovite crystals from pegmatites that cut (1) the lineations immediately north of the Bell Lake granite, (2) the foliation in coarse-grained impure quartzite immediately south of this granite, and (3) the mylonitized granite about 2.5 km south of the Grenville Front. The muscovite ages provide only a minimum age for these features because of the probable loss of radiogenic strontium by diffusion prior to the cooling of the region. Deformation that is later than some of these pegmatites is also apparent. The real age of the pegmatites is uncertain, but they may be as old as 1700 m.y., an age obtained for a single whole-rock pegmatite

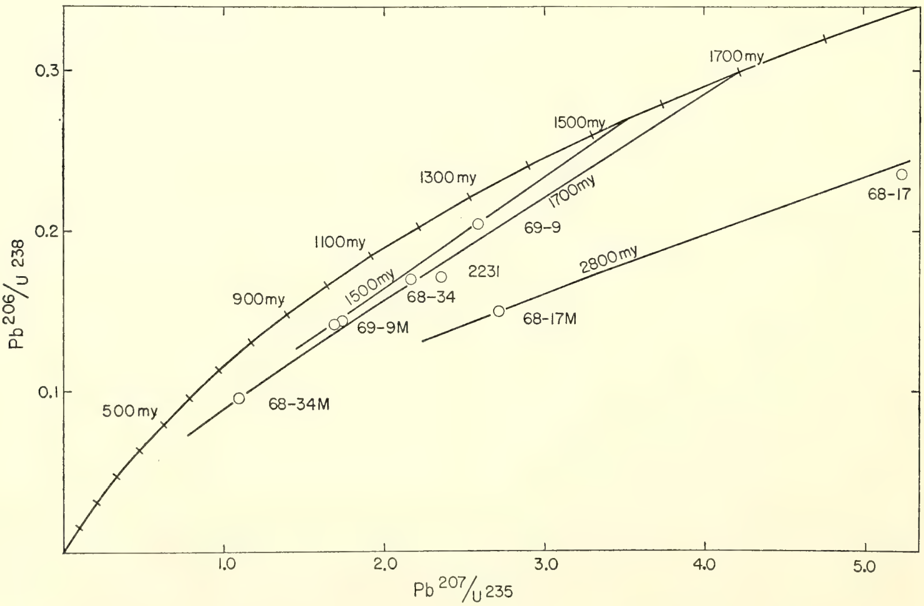

Fig. 50. Concordia diagram for zircons from the pegmatite in the Grenville Front zone near Sudbury (68-34, 68-34M), the Bell Lake granite (69-9, 69-9M), the pegmatite in the Front zone near North Bay (68-17, 68-17M), and the Killarney granite (2231). Parts of continuous diffusion lines are shown for zircons 1500 m.y., 1700 m.y., and 2800 m.y. old.

sample based on an assumed initial ratio of 0.705.

Rb-Sr ages of ten muscovite samples collected north of the Front in the Chief Lake area vary systematically between 1050 and 1950 m.y. as the sample distance from the migmatites of the Grenville province increases from 1 to 5 miles. In one critical location a silty impure quartzite is folded about the southeast-plunging axis of lineation typical of the Front zone. Muscovite from this recrystallized and folded silty layer has a Rb-Sr age of 1390 m.y., but the coarser muscovite from a pegmatite that appears to cut the folding on this outcrop has a Rb-Sr age of 1665 m.y.

The Grenville Front north of North Bay, Ontario. In *Year Books 65* and *67* we reported the presence of an Archean granite body (about 2600 m.y. old) about 12 km south of the Grenville Front, as mapped by Johnston (1954).

A recent study of a pegmatite that cuts across the northeast-trending foliation in a migmatitic granite 0.4 km south of the Front produced some surprising results. The zircons in this dike, although discordant, indicate a U-Pb diffusion age of at least 2700 m.y. (sample 68–17, Fig. 50); the Rb-Sr muscovite age is 2270 m.y., and the plagioclase-microcline line on a Rb-Sr isochron diagram has a slope of 1550 m.y.

These results show that the migmatitic granite probably formed 2700 m.y. ago. It became aligned parallel to the Front at this time or some time before 1550 m.y. ago. The Rb-Sr data for the feldspars indicate that a significant Grenville (1000 m.y.) thermal event did not occur at this location.

The Grenville Front in the Chibougamau–Surprise Lake Area, Quebec

T. E. Krogh, C. Brooks, S. R. Hart,* and G. L. Davis*

A metamorphic transition in the Surprise Lake area near Chibougamau, Quebec, was studied and described as a transitional Grenville Front by Deland (1956). A brief report of preliminary results was included in *Year Book 67*. The Rb-Sr ages of muscovites and biotites from this metamorphic transition are shown in Fig. 51. Figure 52 presents the isotopic data for several whole-rock samples.

It is clear from the muscovite ages that the metamorphic transition had occurred and the region had cooled earlier than 2500 m.y. ago. Biotite Rb-Sr ages, on the other hand, range from a minimum value of about 900 m.y. in the southeastern part of the map area to 2100 m.y. in the northwest. When two biotites were analyzed the coarser fraction always yielded an older age, and biotites from the granites gave older age values than those from the metasediments. The biotites have lost different amounts of radiogenic strontium by diffusion, probably about 900 m.y. ago, whereas under the same conditions the muscovites have retained almost all of their radiogenic strontium.

The occurrence of the Archean metamorphic transition near the Grenville metamorphic zone may be simply a coincidence, but an alternative explanation is possible. A metamorphic gradient, which developed vertically 2500 m.y. ago, may have been exposed in a lateral direction as a result of later uplift and erosion, perhaps at 900 m.y. The time of formation of mineral isograds in the rocks exposed by this mechanism along the Grenville Front would be older than the Front itself.

Isotopic analysis of whole-rock samples of granite from several locations does not show any marked effect of the younger metamorphism. A poorly defined isochron with a slope of 2500 ± 100 m.y. was obtained from several samples from a single outcrop area. Samples from other locations suggest a similar age but had an anomalously high initial ratio. These results are inconclusive.

* Department of Terrestrial Magnetism.

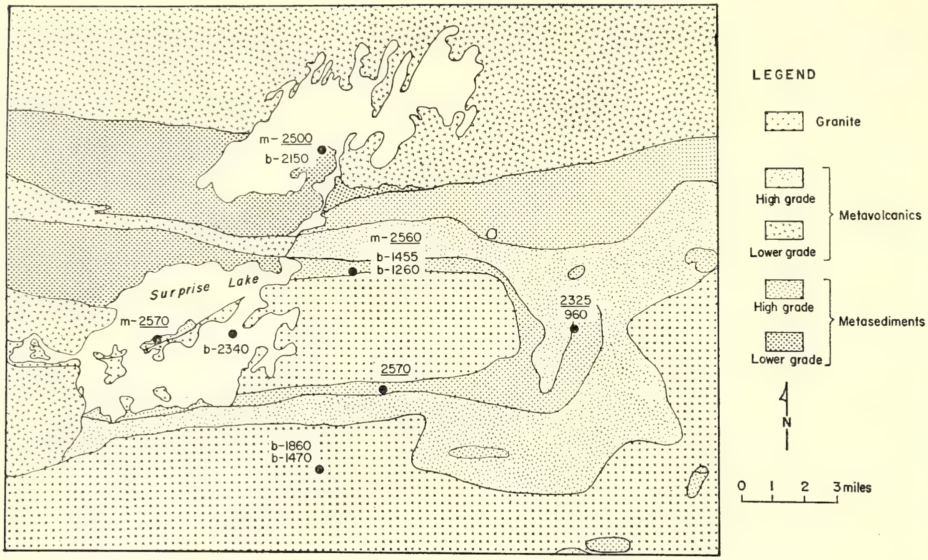

Fig. 51. Mineral age values for muscovite (*m*) and biotite (*b*) in the Surprise Lake area, Quebec.

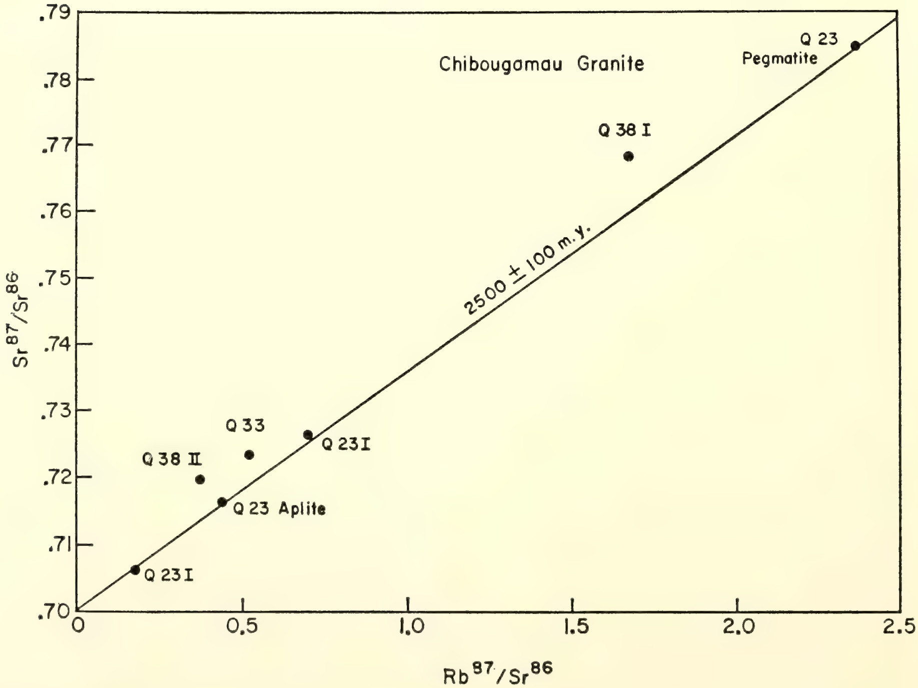

Fig. 52. Isochron diagram for the Surprise Lake granite.

Sr Isotope Variations in Archean Greenstones and the Differentiation of the Earth's Mantle

The isotopic abundance of Sr^{87} increases by natural radioactive decay in proportion to the time elapsed and the abundance of Rb^{87}. The isotopic variations of strontium from modern volcanic rocks indicate that small differences in the Rb/Sr ratio have existed in their mantle source region for some time. The relative abundance of these trace elements varies, as does that of K and Ca, during the extraction of crustal material from the earth's mantle. Thus, strontium isotopes are sensitive tracers that can be used to investigate the differentiation history of the earth.

In our recent studies we have attempted to determine the isotopic composition of strontium in the oldest volcanic rocks available in North America (2700 m.y.). The metamorphism of these rocks to the zeolite, greenschist, or amphibolite facies, as well as the necessity to correct for radiogenic additions of Sr^{87}, complicates the determination of the primary isotopic ratios.

Our results suggest that the Sr^{87}/Sr^{86} ratio in the mantle 2700 m.y. ago was higher than would be predicted from a linear evolution model based on meteorite and modern basalt strontium. Samples from the Michipicoten area, situated just east of Lake Superior in Ontario, indicate a probable difference in the isotopic composition of strontium between the upper and lower series in a single volcanic pile. This difference is supported by similar results for other metavolcanic belts of the Canadian shield and suggests that variations in the Rb/Sr ratio had existed in the mantle more than 2700 m.y. ago.

The discovery that calcite veins in these volcanics contain radiogenically enriched Sr and our observation that the dating elements in some of the rhyolites have undergone migration subsequent to their extrusion require that we interpret initial strontium ratios with caution.

Further details of these topics are discussed in the current Annual Report of the Director of the Department of Terrestrial Magnetism under the following titles:

"Carbonate contents and Sr^{87}/Sr^{86} ratios of calcites from Archean metavolcanics," by C. Brooks, T. E. Krogh, S. R. Hart, and G. L. Davis.

"The initial Sr^{87}/Sr^{86} ratios of the upper and lower series Michipicoten metavolcanics, Ontario, Canada," by C. Brooks, T. E. Krogh, S. R. Hart, and G. L. Davis.

"Initial Sr^{87}/Sr^{86} ratios of regionally distributed metavolcanics from the Canadian shield," by C. Brooks, S. R. Hart, T. E. Krogh, and G. L. Davis.

"Rb-Sr mantle evolution models," by S. R. Hart and C. Brooks.

"The K, Rb, Cs, and Sr geochemistry of Archean metavolcanics," by S. R. Hart, G. L. Davis, C. Brooks, and T. E. Krogh.

MINERALOGY

Inclusions in Diamonds

H. O. A. Meyer and F. R. Boyd

Investigation of inclusions in diamonds over the past several years has revealed a number of singular chemical and physical characteristics. These characteristics are clues to the process by which natural diamonds have formed and clues to the nature of the earth's mantle at the great depths at which diamonds have originated. Nevertheless, the interpretation of these characteristics is enigmatic at present. Understanding the chemical and textural features of igneous and metamorphic minerals requires more than their accurate description. It requires duplication of the essential features by

experiment or by the calculation of models based on limited and reasonable assumptions. Our study of diamond inclusions has provided some of the raw data required to design experiments and provide constraints in the construction of models. The task of synthesis remains.

The most significant feature to emerge this year is the remarkable similarity of inclusions of garnet, olivine, and chromite from one geographic region to another. It should be understood that these inclusions have unique chemical compositions that distinguish them from similar minerals found in kimberlite or in ultramafic xenoliths. Yet inclusions showing these particular chemical characteristics have been found in diamonds * from southern Africa, Sierre Leone, Venezuela, and Ghana. Diamonds we have studied from southern Africa and Sierre Leone were erupted in Mesozoic time, whereas diamonds from Venezuela and Ghana are Precambrian. Evidently the process by which natural diamonds have crystallized and incorporated inclusions with unique compositions has been uniform in space and time.

Inclusions of chrome pyrope are unusually rich in chromium relative to pyropes of other origins, and this feature is also shown by the inclusions of chromite, olivine, and enstatite. Why chromium is concentrated in these inclusions is not understood at present. Indeed there are as yet very few phase studies in silicate systems with Cr_2O_3 and virtually none at high pressures.

Examination of nearly 200 inclusions from over 50 diamonds shows that the order of abundance is Mg-rich olivine, chrome pyrope, chromite, enstatite, and diopside. Pyroxenes appear to be relatively more abundant in mafic and ultramafic xenoliths from kimberlite than as diamond inclusions. So far only two inclusions have been found that contain more than one phase. One consists of olivine + chromite, and the other is a chrome pyrope which itself contains a small (<5 μm) birefringent inclusion—possibly olivine or pyroxene. Positive identification of this birefringent inclusion is difficult because of its small size and the absorption of X rays by the garnet host. The olivine and chromite pair are in firm contact along an apparently plane face. Analyses of other olivine and chromite grains from the same diamond (GL47) that contains the bimineralic inclusion are given in Tables 39 and 42.

Another aspect of this year's study has been the analysis of several groups of inclusions from individual diamonds, i.e., of minerals of different varieties that have been found as separate inclusions in the same diamond host. Olivine-garnet (GL24), olivine-enstatite (G10), olivine-chromite (GL47), and garnet-chromite (G20) "assemblages" have been studied. It will be suggested hereafter that these diamonds and their inclusions have crystallized from magmas. If this is true it is likely that separate, monomineralic inclusions in a given diamond form an equilibrium assemblage because they were at one time in equilibrium with the same liquid. Of course, there could have been a temperature difference in the magma between the times of incorporation of two separate inclusions, but this is unlikely to have been a major effect because there is a relative constancy of composition within varietal groups of inclusions. The data in Figs. 53–56 show that the chrome pyropes are all similar, as are the enstatites and the olivines. There appear to be two groups of chromites.

The data in Figs. 53–56 summarize

* The assistance and generosity of Mr. R. Winston, of Harry Winston, Inc., Mr. W. Cotty, of the Diamond Producers Association, and Dr. George Switzer, of the Smithsonian Institution, in supplying diamonds from various localities is gratefully acknowledged. Dr. J. W. Harris, of University College London, generously allowed us to analyze inclusions that he has obtained from diamonds from Ghana.

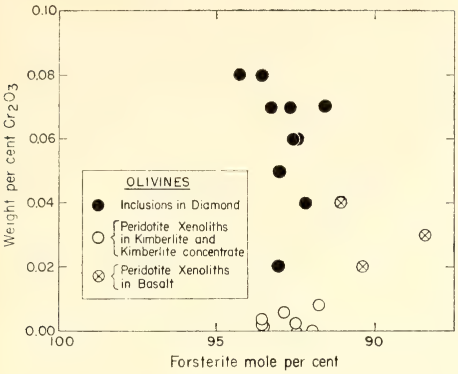

Fig. 53. Comparison of the Cr_2O_3 (wt %) contents of olivine inclusions from natural diamonds with olivines from peridotite xenoliths in kimberlite (O'Hara and Mercy, 1963; Nixon, von Knorring, and Rooke, 1963) and basalt (Ross, Foster, and Myers, 1954) and from kimberlite concentrate (Stockdale pipe, Kansas, *Year Book 67*, p. 132).

the chemical results obtained in the past two years and compare the compositions of diamond inclusions with similar minerals from other environments. The significant features shown by these diagrams are summarized as follows:

1. Cr_2O_3 contents of Mg-rich olivines range up to about 0.1 wt % (Fig. 53). On an average, olivines included in diamond are richer in Cr than those from other environments and they are markedly richer in Cr than olivines from ultramafic xenoliths in kimberlite and kimberlite concentrates.

2. Garnets included in diamond (Fig. 54) are predominantly chrome pyrope, but Cr-poor pyrope-almandine inclusions have been found. The pyrope-almandines resemble eclogite garnets, whereas the chrome pyropes are akin to the garnets of the lherzolite and harzburgite xenoliths. In this regard its is interesting to note that rare inclusions of enstatite and diopside have been found in diamonds, but inclusions of omphacite, the characteristic pyroxene of eclogites, have not yet been discovered.

3. The chrome-pyrope inclusions (Fig. 54) show a range of Cr content, as do

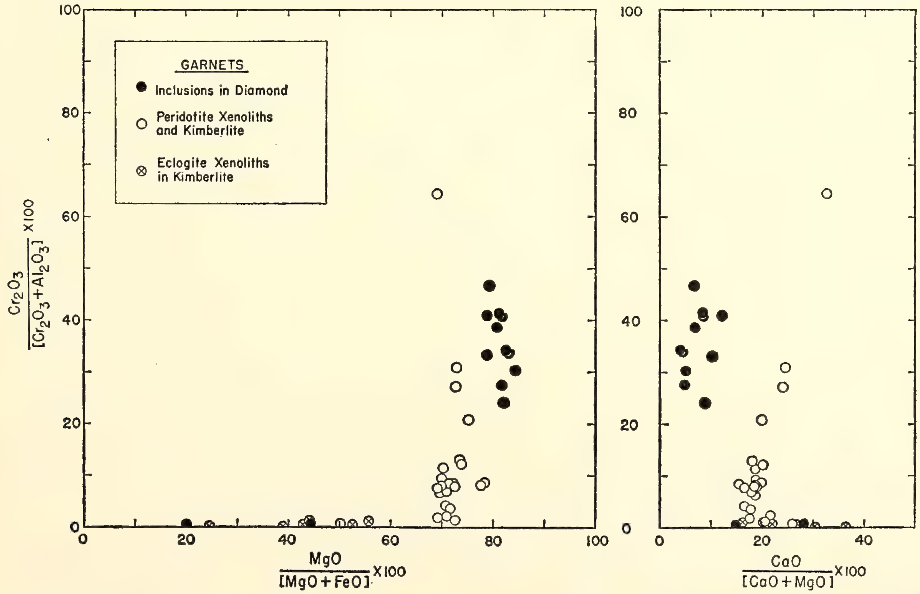

Fig. 54. Analyses of garnet inclusions from natural diamonds compared with garnets from peridotite xenoliths, from kimberlite, and from eclogite xenoliths in kimberlite (O'Hara and Mercy, 1963; Nixon, von Knorring, and Rooke, 1963; Fiala, 1965; Brookins, 1967; Kushiro and Aoki, 1968; Nixon and Hornung, 1968).

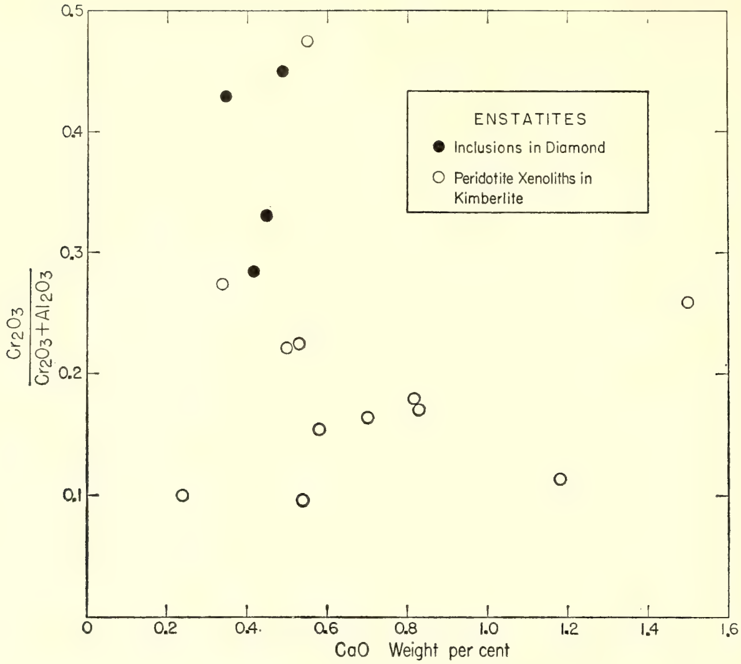

Fig. 55. Analyses of enstatite inclusions from natural diamonds and from peridotite xenoliths in kimberlite (O'Hara and Mercy, 1963; Nixon, von Knorring, and Rooke, 1963; Banno, Kushiro, and Matsuii, 1963; MacGregor and Ringwood, *Year Book 63,* p. 163).

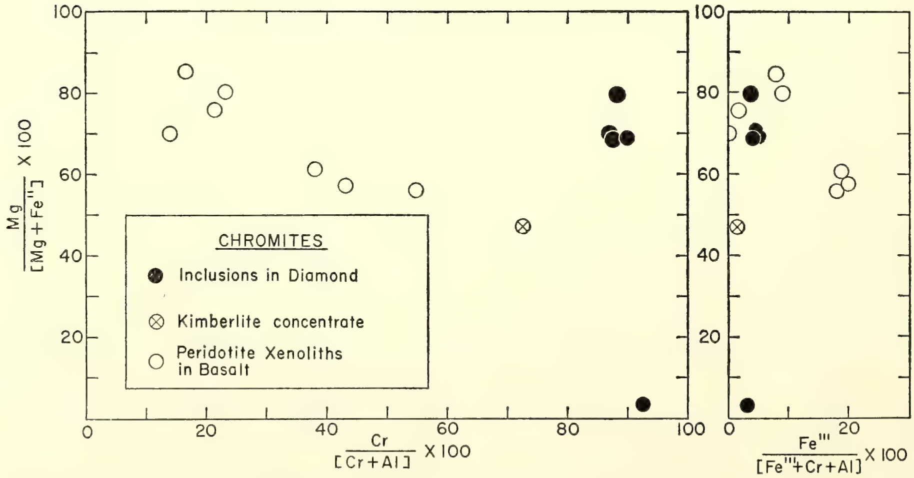

Fig. 56. Plot (after Irvine, 1967) of analyses of chromite inclusions from natural diamonds and from peridotite xenoliths in basalt (Ross, Foster, and Myers, 1954) and from kimberlite concentrate (Nixon, von Knorring, and Rooke, 1963).

their counterparts from xenoliths in kimberlite and kimberlite concentrates. On an average, however, the inclusions contain more Cr, somewhat more Mg, and notably less Ca. The Mg content of the chrome pyropes is in fact the highest yet recorded for any natural garnet.

4. Enstatites (Fig. 55) that occur as inclusions in diamond have higher Cr and lower Al and Ca contents than most enstatites from peridotite xenoliths in kimberlite.

5. Chromite inclusions from diamond (Fig. 56) contain more Cr than those from any other terrestrial environment. Nevertheless, they resemble chromites from pallasites and from silicate inclusions in metallic meteorites (Bunch, Keil, and Olsen, 1969; Bunch and Keil, 1969).

It is now clear that the chemical history of the diamond inclusions has been in some way different than the history of the similar minerals of peridotite and eclogite xenoliths with which diamonds are associated and sometimes even intergrown. Possibly the diamonds and their inclusions are relics of igneous events, whereas the minerals of the peridotites, and perhaps the eclogites, have established their present compositions by reaction and equilibration after cooling below the solidus. It seems possible that the monomineralic inclusions in diamond, being armored, failed to participate in subsolidus equilibration; their compositions may reflect earlier, crystal-liquid equilibria. Little quantitative support of this hypothesis can be mustered at the present time, but Kennedy and Nordlie (1968) have presented other arguments that diamond formation is an igneous process. Meyer and Boyd (*Year Book 67,* p. 130) suggested that the monomineralic nature of diamond inclusions might indicate a subsolidus growth process because in an igneous crystallization, diamond might be expected to include droplets of liquid that would crystallize to polymineralic aggregates. We now doubt this suggestion, but in fact we need to better understand the way in which growing crystals include or exclude foreign matter at their surfaces.

The detailed analyses * of diamond inclusions that have been carried out this year are presented in Tables 39–42. The olivines (Table 39) show little variation from an average composition of $fo_{93}fa_7$ and most of them are relatively rich in Cr. The enrichment in Cr cannot be due solely to crystallization in a Cr-rich environment because olivines associated with chromitites in the Stillwater Complex contain less than 0.01 wt % Cr_2O_3 (E. D. Jackson, personal communication). Analyses for Ni have been made for the olivines described in *Year Book 67* (p. 132, Table 4), and the results are in accord with those presented in Table 39.

New analyses of chrome-pyrope inclusions from Venezuela, Ghana, and Sierre Leone are given in Table 40; in their high Mg and Cr contents and relatively low Ca they resemble those previously analyzed (Meyer, 1968 and *Year Book 67,* p. 133, Table 5). Garnet inclusion GL16 (Table 40) from an unknown locality is a pyrope-almandine, and it is similar to the garnets from eclogite xenoliths in kimberlite. Inclusion D15 (Table 40) is a high-Ca garnet (12.0 wt % CaO) from a South African diamond. It is similar to those in kyanite-eclogites from the Zagadochnaya pipe in Yakutia described by Sobolev, Kutznetsova, and Zyuzin (1968), and to a garnet in a kyanite-eclogite from the Roberts Victor pipe described by O'Hara and Mercy (1963). The discovery in diamond of garnet inclusions with eclogite affinities is interesting in view of the fact that diamond has been found in eclogite xenoliths from kimberlite (Sobolev, 1968).

* These analyses were made with a Materials Analysis Co. model 400 electron probe purchased with the assistance of the National Science Foundation under grant GP 4384.

TABLE 39. Analyses of Olivine Inclusions

	Venezuela			Ghana		
	GL24c	GL29b	GL47a	G10b	G16a	G17a
SiO_2	41.0	40.2	41.1	41.3	40.8	41.2
TiO_2	0.00	0.00	0.00	0.00	0.00	0.00
Al_2O_3	0.02	0.02	0.00	0.05	0.02	0.02
Cr_2O_3	0.07	0.07	0.08	0.05	0.02	0.07
FeO	6.65	7.14	6.21	6.91	7.10	8.34
MgO	52.7	51.9	52.7	51.6	52.5	50.7
CaO	0.01	0.04	0.01	0.04	0.03	0.06
MnO	0.10	0.12	0.10	0.11	0.11	0.11
NiO	0.38	0.40	0.40	0.43	0.43	0.40
Totals	100.9	99.9	100.6	100.5	101.0	100.9
	Number of Cations on the Basis of 4 Oxygens					
Si	0.986 } 0.987	0.981 } 0.982	0.989 } 0.989	0.998 } 0.999	0.983 } 0.984	0.997 } 0.998
Al	0.001	0.001	0.000	0.001	0.001	0.001
Cr	0.001 } 2.034	0.001 } 2.045	0.002 } 2.029	0.001 } 2.010	0.000 } 2.040	0.001 } 2.012
Fe^{2+}	0.134	0.146	0.125	0.140	0.143	0.169
Mg	1.890	1.887	1.892	1.858	1.886	1.831
Ca	0.000	0.001	0.000	0.001	0.001	0.001
Mn	0.002	0.002	0.002	0.002	0.002	0.002
Ni	0.007	0.008	0.008	0.008	0.008	0.008
	Forsterite, mole %					
	93.4	92.8	93.8	93.0	93.0	91.6

Analyst H. O. A. Meyer.

Analyses of enstatite inclusions (Table 41) from diamonds from Sierre Leone and Ghana are the first to be made of this variety of inclusion. They show little solid solution toward diopside, and on an average they contain less Al and more Cr than do enstatites from peridotite nodules in kimberlite (Fig. 56). Boyd and England (*Year Book 63*, p. 157) showed that increase of pressure in the *P-T* region where pyrope is stable reduces the solubility of Al_2O_3 in enstatite. Hence, it is not surprising that these enstatite inclusions in diamond contain very little Al_2O_3.

Three chromite inclusions from Ghana and Venezuela (Table 42) have proved to be Mg-rich in contrast to the Fe-rich chromites discovered last year (*Year Book 67*, p. 134, Table 6). All of these chromites have unusually high chrome contents, however, comparable only to those found in meteorites.

The Occurrence of Potassic Richterite in a Mica Nodule from the Wesselton Kimberlite, South Africa

A. J. Erlank and L. W. Finger*

The presence of amphibole as a constituent of the upper mantle has been suggested by several workers, and cogent geochemical and geophysical arguments have been presented in support of this contention (Oxburgh, 1964; Ringwood, 1966; Hart and Aldrich, 1967). Amphibole, usually in the form of hornblende or pargasite, has been observed in many rocks of possible upper-mantle origin, such as the amphibole peridotites from St. Paul's Rocks on the Mid-Atlantic Ridge, and as xenocrysts and in xenoliths from basic volcanic rocks and tuffs (Mason, 1968) but to our knowledge has not been recorded as a definite primary constituent of the mafic and ultramafic

* Department of Terrestrial Magnetism.

TABLE 40. Analyses of Garnet Inclusions

	Venezuela			Ghana			Sierre Leone	South Africa	Unknown
	GL24a	GL25a	GL26e	G9a	G12a	G20a	GL32b	D15	GL16
SiO_2	41.6	42.5	41.0	42.7	42.1	41.0	42.7	39.9	40.5
TiO_2	0.02	0.05	0.25	0.02	0.00	0.02	...	0.64	0.74
Al_2O_3	16.0	17.3	15.5	18.4	16.3	14.4	18.4	20.7	21.9
Cr_2O_3	10.1	8.77	10.7	5.85	8.14	12.6	6.97	0.05	0.11
FeO	5.92	5.04	6.08	5.38	6.31	6.11	5.65	14.5	17.2
MgO	24.6	25.1	22.8	25.1	24.0	23.6	24.5	9.74	13.7
CaO	1.18	1.77	3.10	2.46	2.79	1.74	1.22	12.0	5.35
MnO	0.27	0.19	0.29	0.18	0.24	0.28	0.29	0.42	0.47
Totals	99.7	100.7	99.7	100.1	99.9	99.8	99.7	98.0	100.0
				Number of Cations on the Basis of 12 Oxygens					
Si	2.989	2.993	2.973	2.999	3.006	2.997	3.028	3.042	2.995 } 3.000
Ti	0.001 } 3.000	0.003 } 3.000	0.014 } 3.000	0.001 } 3.000	0.000 } 3.006	0.001 } 3.000	... } 3.028	0.037	0.005
Al	0.010	0.004	0.013	...	...	0.022	...	...	Ti 0.037
Al	1.341	1.433	1.313	1.528	1.374	1.206	1.537	1.858 } 1.932	1.913
Cr	0.571 } 2.000	0.489 } 2.000	0.611 } 2.000	0.325 } 1.999	0.460 } 1.992	0.721 } 2.000	0.391 } 1.962	0.003	0.006 } 1.991
Fe^{3+} *	0.088	0.078	0.076	0.146	0.158	0.073	0.034	0.034	0.035
Fe^{2+}	0.268	0.219	0.293	0.171	0.219	0.298	0.301	0.891	1.031
Mg	2.631 } 3.006	2.639 } 3.002	2.457 } 3.008	2.633 } 3.000	2.554 } 3.000	2.554 } 3.007	2.589 } 3.000	1.105 } 3.000	1.509 } 2.993
Ca	0.091	0.133	0.240	0.185	0.213	0.138	0.093	0.977	0.424
Mn	0.016	0.011	0.018	0.011	0.014	0.017	0.017	0.027	0.029
				End Members, mole %					
Spessartite	0.5	0.4	0.6	0.4	0.5	0.6	0.6	0.9	1.0
Andradite	3.0	3.9	3.8	6.2	7.1	3.5	1.7	1.8	3.6
Skiagite	1.4	...	...	1.2	0.6	...	...	...	...
Uvarovite	...	0.5	4.2	...	...	1.0	1.4	0.2	0.3
Grossularite	...	...	...	...	...	...	...	31.7	10.3
$Mg_3Cr_2(SiO_4)_3$	28.6	23.9	26.4	16.3	22.9	35.1	18.5	...	...
Pyrope	59.1	64.0	55.5	71.5	62.6	50.0	69.4	36.4	50.4
Almandine	7.4	7.3	9.5	4.4	6.3	9.8	8.3	29.0	34.4

*Fe^{3+} calculated from total Fe as Fe^{2+} to satisfy charge requirements.
Analysts H. O. A. Meyer, F. R. Boyd (GL32b).

TABLE 41. Analyses of Enstatite Inclusions

	Sierre Leone				Ghana			
	GL27a		GL28a		G3a		G10a	
SiO_2	57.7		57.0		56.9		57.3	
TiO_2	0.00		0.00		0.00		0.00	
Al_2O_3	0.78		0.97		0.67		0.44	
Cr_2O_3	0.31		0.48		0.55		0.33	
FeO	4.36		4.48		4.43		4.29	
MgO	36.2		35.8		35.9		37.0	
CaO	0.42		0.45		0.49		0.35	
MnO	0.09		0.12		0.12		0.12	
Totals	99.9		99.3		99.1		99.8	
	Number of Cations on the Basis of 6 Oxygens							
Si	1.976	2.008	1.966	2.006	1.969	1.996	1.966	1.984
Al	0.032		0.040		0.027		0.018	
Cr	0.008		0.013		0.015		0.009	
Fe^{2+}	0.125		0.129		0.128		0.123	
Mg	1.845	1.997	1.839	2.001	1.849	2.013	1.889	2.037
Ca	0.016		0.117		0.018		0.013	
Mn	0.003		0.003		0.003		0.003	
	Enstatite, mole %							
	93.5		93.3		93.5		93.9	

Analyst H. O. A. Meyer.

TABLE 42. Analyses of Chromite Inclusions

	Ghana				Venezuela	
	G4a		G20b		GL47e	
SiO_2	0.26		0.23		0.26	
TiO_2	0.05		0.03		0.00	
Al_2O_3	6.74		5.94		5.81	
Cr_2O_3	63.3		64.0		65.3	
FeO	14.4		15.1		10.3	
MgO	14.4		13.8		16.4	
CaO	0.01		0.00		0.05	
MnO	<0.01		0.00		0.00	
Totals	99.2 *		99.1 *		98.1 *	
	Number of Cations on the Basis of 4 Oxygens					
Si	0.009		0.008		0.009	
Ti	0.001		0.001		0.000	
Al	0.260	1.997	0.231	2.000	0.224	2.000
Cr	1.635		1.667		1.686	
Fe^{3+} †	0.092		0.093		0.081	
Fe^{2+}	0.301	1.000	0.323	1.000	0.199	1.000
Mg	0.699		0.677		0.799	
Ca	0.000		0.000		0.002	
	End Members, mole %					
$MgCr_2O_4$	70.0		67.7		80.0	
$FeCr_2O_4$	11.9		15.7		4.4	
$FeAl_2O_4$	13.5		12.0		11.8	
$FeFe_2O_4$	4.6		4.6		3.8	

* Does not include V_2O_3 and ZnO, both <1.0 wt. %, respectively.
† Fe^{3+} calculated from total Fe as Fe^{2+} to satisfy charge requirements.
Analyst H. O. A. Meyer.

nodules found in South African kimberlite pipes.

During the course of electron-probe analysis of a mica pyroxenite nodule from the Wesselton kimberlite pipe, South Africa, a mineral with an unusual potassium content was encountered and subsequently identified as the rare amphibole potassic richterite (magnophorite). These nodules, also referred to as phlogopite nodules, are distinctive in that they consist almost entirely of phlogopite (>90%), with minor amounts of diopside. Garnet, olivine, and orthopyroxene are absent. A petrographic description and chemical analysis of the nodule in question, WESS 156, are given by Williams (1932, pp. 347, 350).

The potassic richterite found in this nodule is in the form of small subhedral grains, usually about 100 μm in length, contained within the diopside and appears to be of primary origin. Optical characteristics are consistent with those available for other richterites. Three of these grains, together with the associated diopside, have been analyzed by electron probe, and a fourth, identified by probe analysis in a grain mount of separated diopside grains, has been partially isolated and analyzed by single-crystal X-ray diffraction.

Relevant chemical data are presented in Table 43. Multiple measurements show each grain to be homogeneous, with very little, if any, variation between grains. Compared with the type analysis for potassic richterite (Wade and Prider, 1940), the Wesselton richterite has slightly differing FeO and K_2O contents, but the most striking difference is the lower TiO_2 content of the Wesselton

TABLE 43. Electron-Microprobe Analyses of Kimberlitic Potassic Richterites and Diopside

	Richterite			
	1	2	3	Diopside
SiO_2	54.3	54.4	54.1	54.2
TiO_2	0.59	0.60	0.59	0.10
Al_2O_3	1.22	1.25	1.24	0.71
FeO *	4.36	4.34	4.22	5.07
MnO	0.07	0.07	0.07	0.17
MgO	20.9	21.4	21.2	16.0
CaO	7.06	7.14	7.15	20.7
Na_2O	3.19	3.20	3.34	1.50
K_2O	4.70	4.77	4.69	0.01
Cr_2O_3	0.07	0.06	0.04	0.42
Totals	96.5	97.2	96.6	98.8

	Number of Ions on the Basis of 23 Oxygens						Number of Ions on the Basis of 6 Oxygens		
	1		2		3				
Si	7.80		7.75		7.76		Si	2.010	
Al	0.20	8.00	0.21	8.00	0.21	8.00	Ti	0.003	
Ti	...		0.04		0.03		Al	0.031	
Al	0.01		...		...		Ca	0.820	
Ti	0.06		0.02		0.03		Cr	0.012	
Mg	4.46	5.00	4.55	5.00	4.52	5.00	Fe	0.157	2.018
Cr	0.01		0.01		0.01		Mn	0.005	
Fe	0.46		0.42		0.44		Ca	0.820	
Fe	0.05		0.10		0.07		Mg	0.881	
Mn	0.01	2.00	0.01		0.01		Na	0.108	
Ca	1.09		1.09	2.00	1.10	2.00	K	0.001	
Na	0.84		0.80		0.82				
Na	0.05	0.91	0.08	0.95	0.11	0.97			
K	0.86		0.87		0.86				

* Total Fe expressed as FeO.

potassic richterite (0.6% TiO_2) compared with the value of 3.5% TiO_2 given by Wade and Prider. The significance of this feature and its possible dependence on pressure are discussed elsewhere in this report. The average of the three analyses, expressed in the amphibole formula, is $(K_{0.86}Na_{0.08})(Na_{0.82}Ca_{1.09}Mn_{0.01}Fe_{0.07})(Fe_{0.45}Mg_{4.51}Ti_{0.04}Cr_{0.01})(Si_{7.77}Al_{0.21}Ti_{0.02})O_{22}(OH)_2$.

The composition of the enclosing diopside is given for comparison. It has a lower chrome content than diopsides that occur in the peridotite nodules and is similar to a diopside inclusion from a diamond studied by Boyd (*Year Book 67,* pp. 133–135).

The Wesselton potassic richterite grain examined by single-crystal techniques was only partially separated from the enclosing diopside because of difficulties in handling small grains. The interfering diffraction pattern handicapped the orientation of the grain, but the following cell data were obtained from precession photographs: $a = 10.00$ Å, $b = 18.00$ Å, $c = 5.26$ Å, $\beta = 104.8°$, $V = 917$ Å^3. The cell data of the diopside at 23°C were measured from back-reflection Weissenberg photographs and yielded the following results: $a = 9.734 \pm 0.002$ Å, $b = 8.9135 \pm 0.0005$ Å, $c = 5.261 \pm 0.006$ Å, $\beta = 106.06° \pm 0.03°$, $V = 438.6 \pm 0.6$ Å^3.

It is difficult at this stage to assess the importance of the occurrence of potassic richterite in the mica nodule. Certainly it appears to be of primary origin, and work described elsewhere in this report shows that in the absence of phases other than diopside it is stable to higher temperatures and pressures than any other amphibole examined so far. Hence, although it occurs only as a trace constituent in the nodule examined, it may indicate the type of amphibole likely to occur in the upper mantle. Preliminary work described elsewhere in this report, however, indicates that it may not be stable in the presence of nonpotassic aluminous phases such as garnet. Nevertheless, if 1% potassic richterite of the type analyzed occurs in upper-mantle material, the resulting K content of 400 ppm is sufficient, when such material is subjected to partial melting and fractionation along the lines suggested by O'Hara (1968), to account for the K content of most basaltic lavas. This would also apply to other elements related to K, specifically Rb and Ba, and hence it would be of interest to determine the trace element content of potassic richterites.

Kimberlite Diopsides

*F. R. Boyd and P. H. Nixon**

Pyroxenes in mafic and ultramafic rocks have particular petrogenetic value because their compositions are sensitive to variations in the conditions of equilibration or to changes in magmatic composition. They reveal magmatic fractionation by an increase in the ratio Fe/(Fe+Mg). They can also provide information on the conditions of subsolidus equilibrium through the degree of solid solution shown by coexisting Ca-rich and Ca-poor pyroxenes and by the solid solution of these pyroxenes toward garnet or other aluminous phases.

Primary pyroxenes in kimberlite are found as individual crystals and in peridotite and eclogite nodules. Many of the individual crystals undoubtedly come from disaggregated nodules, but there is a possibility that silicate magma is involved in some kimberlite eruptions and that some of the individual crystals may be true phenocrysts rather than fragments of mantle rocks. Opinions differ on this point, and the problem is insufficiently studied for the answer to be clear. Pyroxenes from kimberlites rarely show exsolution, in contrast to pyroxenes from tholeiitic basalts and gabbros. They have evidently crystallized as coarse-grained, relatively homogeneous phases at depth in the mantle and been erupted sufficiently rapidly to become quenched.

Most clinopyroxenes from African

* Department of Mines, Maseru, Lesotho.

kimberlites show restricted solid solution toward enstatite and jadeite and contain an average of 1.3% Cr_2O_3, 2.0% Al_2O_3, and 2.8% Fe as FeO. A much less abundant group from eclogitic assemblages shows a large solid solution toward jadeite. Data presented herein show that there is a third, subcalcic group, examples of which are rare but widely distributed in African kimberlites. Clinopyroxenes in this group exhibit much solid solution toward $MgSiO_3$, having compositions near a mean of $wo_{31}en_{62}fs_7$.

Nixon, von Knorring, and Rooke (1963) first recognized the unusual composition of these subcalcic diopsides and gave analytical data for one they discovered in a garnet lherzolite nodule (E-3) from the Thaba Putsoa pipe in Lesotho (formerly Basutoland). Boyd (1969) described a second, chemically similar specimen from an alluvial deposit in the Shinyanga district, Tanzania. These localities are about 1800 miles apart. Further work described below has led to the discovery of four more subcalcic diopsides, and it now appears that diopsidic pyroxenes from African kimberlites, apart from omphacites, fall into two well-defined groups that differ chiefly in their Ca/(Ca+Mg) ratio. Diopsides in the subcalcic group show a greater solid solution toward enstatite than diopsides from other plutonic rocks.

New analytical results are given in Tables 44 and 45 and are shown along

TABLE 44. Electron-Probe Analyses of Diopsides from Kimberlite

	GL-50			E-5			E-14		
				Weight %					
SiO_2	54.7	*1*		55.2	*3*		54.0	*3*	
TiO_2	0.2	...		0.15	...		0.39	...	
Al_2O_3	2.64	*21*		2.67	*1*		2.55	*1*	
Cr_2O_3	1.36	*17*		0.71	*1*		0.24	...	
FeO *	2.37	*6*		4.40	*1*		5.94	*3*	
MnO	0.1	...		0.14	...		0.14	...	
CaO	18.9	*17*		14.0	*2*		14.5	*3*	
MgO	17.5	*8*		21.9	*1*		20.6	*2*	
Na_2O	2.1	*15*		1.70	*3*		1.63	*1*	
K_2O	0.05	...		0.02	...		0.02	...	
Totals	99.9			100.9			100.0		
				Atomic %					
Si	1.973		2.000	1.955		2.000	1.950		2.000
Ti	0.004			0.007			0.011		
Al	0.023			0.038			0.039		
Al	0.089		2.021	0.074		2.031	0.070		2.041
Cr	0.039			0.020			0.007		
Fe	0.072			0.130			0.179		
Mn	0.003			0.004			0.004		
Mg	0.941			1.155			1.107		
Ca	0.730			0.531			0.559		
Na	0.145			0.116			0.114		
K	0.002			0.001			0.001		
Ca	41.9			29.2			30.3		
Mg	54.0			63.6			60.0		
Fe	4.1			7.2			9.7		
Ca/(Ca + Mg)	0.437			0.315			0.335		

* Total Fe as FeO.

Note: Italicized values are for $\sigma/\sqrt{\overline{N}}$, where σ is the standard deviation and $\overline{N}$ is the mean count. GL-50: Diopside intergrown with diamond and titaniferous phlogopite, South Africa. E-5: Diopside from garnet wehrlite nodule, Thaba Putsoa pipe, Lesotho. See Nixon, von Knorring, and Rooke (1963) for a mode of this nodule. E-14: Diopside from diopside nodule, Thaba Putsoa pipe, Lesotho. Partial wet-chemical analysis by M. H. Kerr shows $Na_2O = 1.84\%$ and $Cr_2O_3 = 0.24\%$.

TABLE 45. Partial Analyses of Kimberlite Diopsides

		Weight %					Atomic %			
	Locality	CaO	MgO	Al_2O_3	FeO	Cr_2O_3	Ca	Ma	Fe	Ca/(Ca + Mg)
E-10 *	Sekameng	18.9	16.5	2.3	2.1	2.7	43	53	4	45
1108 *	KaO	19.5	14.7	4.7	1.3	2.2	48	50	2	49
S58-1	Solane	14.2	20.7	2.6	4.2	0.7	31	62	7	33
S58-2	Solane	21.4	17.2	2.0	1.9	1.5	46	51	3	47
S58-4	Solane	19.9	16.2	2.3	2.5	1.6	45	51	4	47
S58-5	Solane	21.5	17.3	2.0	1.9	1.5	46	51	3	47
2611 †	Kimberley area	19.4	17.6	2.2	2.6	1.2	42	53	4	44
2623 †	Dutoitspan	18.6	16.2	2.6	2.5	2.5	43	52	5	45
1083A-1	Moroto	22.4	16.9	2.3	2.2	1.0	47	49	4	49
1083A-2	Moroto	20.1	16.3	6.1	2.0	0.9	45	51	4	47
1083A-3	Moroto	22.8	17.7	1.7	1.8	0.9	47	50	4	48
PHN-5	Shinyanga	15.0	20.0	2.3	4.4	0.7	32	60	7	35

* With pyrope.
† In garnet lherzolite nodule.
Note: Other specimens are single crystals from heavy mineral concentrates.

with earlier electron-probe analyses (Boyd, 1969) in Fig. 57. The fifteen new analyses bring the total number of probe analyses of these diopsides to sixty-two, of which six are subcalcic. These specimens were collected from about fifteen different pipes in South Africa, Lesotho, Uganda, and Tanzania and are thus believed to be a representative sample.

Some of the diopsides shown in Fig. 57 are from nodules, but the bulk of them have been picked from heavy mineral

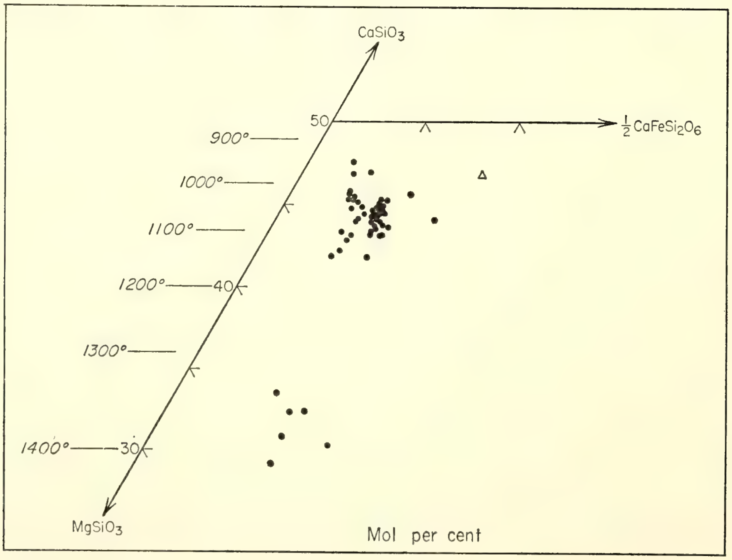

Fig. 57. Electron-probe analyses of diopsidic pyroxenes from African kimberlites plotted in a portion of the pyroxene quadrilateral. Analytical data for 15 new analyses are given in Tables 44 and 45. An additional analysis is from Erlank (this report); the remaining 46 are from Boyd (1969). The analysis shown as an open triangle is for an inclusion from diamond (Boyd, 1969). The temperatures shown are for the diopside solvus in the system $CaMgSi_2O_6$-$MgSiO_3$ (Davis and Boyd, 1966).

concentrates formed in the course of mining or prospecting kimberlite for diamond. Twelve of the sixty-two diopsides are from nodules that also contain enstatite, and two of these are subcalcic. The distribution and range of analyses in this subgroup of diopsides that are known to coexist with enstatite are similar to the distribution and range shown by the whole group. It is probable that most of the diopsides in Fig. 57 are saturated with $MgSiO_3$ because enstatite-bearing garnet lherzolite is a very common rock type among the nodules and because many of the single crystals appear to be from disaggregated nodules.

The analyses in Fig. 57 show that there are significant variations of Fe/(Fe+Mg) and Ca/(Ca+Mg) within the subcalcic and calcic groups. The former variation could be reasonably interpreted as due to minor igneous fractionation, and the latter variation might reflect a range in equilibration temperature. In the event that these diopsides crystallized under static conditions in the mantle, a range in equilibration temperature could reflect simply a range in depth of equilibration. Points on the diopside solvus in the system $CaMgSi_2O_6$-$MgSiO_3$ at 30 kb (Davis and Boyd, 1966) are given in the margin of Fig. 57, and they give an idea of the dependence of the composition of diopside (in equilibrium with enstatite) on temperature.

The large difference in Ca/(Ca+Mg) between the calcic and subcalcic groups is less easy to understand, however. Conceivably this difference could also be due to a difference in equilibration temperature. But if so, it would then be a particular problem to understand why these kimberlites had been erupted from two very distinct regions or levels in the mantle. One would certainly expect that some diopsides of intermediate origin would be found.

Moreover, if the subcalcic diopsides are interpreted as having been erupted in kimberlite that originated at a higher temperature and a greater depth than the calcic group, it is difficult to understand why this kimberlite did not pick up material from a *range* of lower temperatures and shallower levels in the mantle during eruption. The total absence of diopsides with compositions intermediate between the calcic and subcalcic groups is very awkward to explain by any model that attempts to relate composition and temperature by a continuous solvus curve of the sort found in the system $CaMgSi_2O_6$-$MgSiO_3$ at pressures up to 30 kb (Boyd and Schairer, 1964; Davis and Boyd, 1966).

An alternative explanation for the division of these diopsides into calcic and subcalcic groups can be sought in the possibility that there is a miscibility gap between them. The phase relations determined for the Ca-rich portion of the join $CaMgSi_2O_6$-$MgSiO_3$ at pressures up to 30 kb do not show such a gap, but it is probable that these kimberlite diopsides have equilibrated at pressures well above 30 kb because of their association with diamond. The principal two-pyroxene field dividing the Ca-rich and Ca-poor pyroxenes is actually a transition loop because the Ca-rich pyroxenes are monoclinic whereas enstatite and hypersthene are orthorhombic. It is possible, however, that a true miscibility gap in a structurally continuous series of diopsides develops at high pressures in addition to the main two-pyroxene field.

Another possibility is suggested by the narrow field for pigeonite found by Kushiro (*Year Book 67*) on the join $CaMgSi_2O_6$-$MgSiO_3$ at 20 kb. This field is limited to temperatures between 1450° and 1650°C and has a maximum width in composition of 6 wt % *di*. Its axis is at a composition of $en_{82}di_{18}$ (wt %). If the subcalcic diopside analyses are projected onto the join $CaMgSi_2O_6$-$MgSiO_3$, they group around a composition of $en_{31}di_{69}$. This composition is thus far removed from the pigeonite field at 20 kb, but it is conceivable that higher pressures could shift this field to more Ca-rich compositions. If so, it is possible that these sub-

calcic diopsides crystallized as pigeonites in equilibrium with enstatite or calcic diopside or both. It must be emphasized that there is at present no experimental evidence to support either of these alternatives. These suggestions are purely hypothetical.

The cell size and symmetry of one of these subcalcic diopsides (Table 46, E-5) have been determined by Joan R. Clark. The space group is $C2/c$, which together with the cell parameters indicates diopside structure rather than pigeonite. The E-5 pyroxene shows very sparse exsolution lamellae, and these have been identified on the basis of the cell parameters by Clark as being a clinoenstatite-like structure. The relationships between composition and cell parameters in these pyroxenes are not yet sufficiently well understood to permit a precise estimate of the Ca content of these lamellae. Exsolution of Mg-rich pyroxene from diopside or augite as monoclinic rather than orthorhombic lamellae is normal, although the energetics of this relationship are not yet understood (Boyd and Brown, 1969; Bown and Gay, 1960). Hence, if the E-5 diopside had crystallized as primary pigeonite it would be necessary to assume that it had inverted to diopside during eruption.

It is interesting to note that in one case both calcic and subcalcic diopsides have been erupted from the same kimberlite pipe. Analyses of four diopsides picked from a heavy mineral concentrate from the Solane pipe in Lesotho are given in Table 45. One (S58-1) is subcalcic, and the other three are calcic. So far, calcic and subcalcic types have not been found in the same nodule. If their stable association were to be possible, one would expect it to be rare, because it would require a bulk composition rich in Ca pyroxene relative to Mg pyroxene; i.e., a wehrlite rather than the more abundant lherzolites.

TABLE 46. X-Ray Data for Kimberlite Diopsides

	E-5 *		
	Diopside Host	Exsolved Clino-enstatite	GL-50 †
a, Å	9.67	9.67	9.69
b, Å	8.86	8.86	8.87
c, Å	5.26	5.18	5.26
β	106°45′	108°40′	106°43′
Space group	$C2/c$	$P2_1/c$	

* Measured by Joan R. Clark.

† Measured by J. W. Harris.

One of the complete analyses (Gl-50) in Table 44 is of a chrome diopside intergrown with diamond. A small crystal of diopside from this intergrowth was kindly supplied by J. W. Harris, and the cell dimensions determined by him are given in Table 46. This pyroxene is a normal, calcic, chrome diopside. It differs from the single diopside inclusion from diamond thus far analyzed (Fig. 57 and Meyer and Boyd, *Year Book 67*) in being markedly poorer in Fe and Mn and richer in Al and Cr. As suggested by Meyer and Boyd elsewhere in this report, the diamond inclusions have probably experienced a crystallization history very different from that of the nodule minerals with which diamonds are sometimes intergrown.

New, complete analyses of two subcalcic diopsides (E-5 and E-14) from Thaba Putsoa, Lesotho, are also given in Table 44. These are very similar to the analyses of the E-3 and PHN-4 subcalcic diopsides previously published (Boyd, 1969). It was suspected on the basis of the earlier analyses that the subcalcic diopsides might prove to be unusually rich in potassium. However, the K_2O contents of E-5 and E-14 are not especially high and are within the range established for the calcic group. The subcalcic diopsides are slightly richer in Fe than the calcic group (Fig. 57) and on an average they contain less Cr, but the major difference is in the ratio Ca/(Ca+Mg).

Values for $\sigma/\sqrt{N}$ for the analyses in Table 44 show that the two subcalcic diopsides are unusually homogeneous,

which is characteristic of the group as a whole. Kimberlite diopsides are usually not zoned, but some of the calcic ones show variable counts for Al and Cr in particular (e.g., Table 44, GL-50).

Two of the partial analyses in Table 45 (2611 and 2623) are for diopsides that earlier wet-chemical analyses had indicated to be intermediate between the calcic and subcalcic groups (Boyd, 1969, Fig. 1). The new probe analyses (Table 45) show that these diopsides are members of the calcic group, although they are more Mg-rich than the average.

Further experimental and analytical data are obviously needed to provide an understanding of the chemical compositions of these pyroxenes. It is possible that phase studies in the system $CaMgSi_2O_6$-$MgSiO_3$ at pressures higher than 30 kb would clarify the problem. It would also be interesting to know whether subcalcic diopsides occur in kimberlites from continents other than Africa. More detailed study of pyroxenes from kimberlite pipes such as Solane, where both calcic and subcalcic diopsides have been found, would also be illuminating.

The Laco Magnetite Lava Flow, Chile

S. E. Haggerty

An ore microscopic examination of the Laco magnetite lava flows that occur in the highlands of northern Chile has been made as a first step in what is to be a detailed study of the mineralogy of this unique occurrence.* The Laco iron-oxide flows were first discovered in 1958, but only very brief field descriptions have since been reported in the literature (Parks, 1961; Rogers, 1968). The flows occur in an area of volcanic activity and are considered to be Quaternary in age. Field-relationship studies indicate that the iron-oxide bodies were partially intruded into basic tuffs and in places erupted to the surface in large blocky masses of magnetite. The flows are highly vesicular, contain gas tubes, show good contorted banding and ropy surfaces, and in general have all the characteristics of a basalt lava.

The mineralogy of these metallic flows is simple: magnetite and hematite are the primary iron oxides; the accessory minerals include feldspar, calcic pyroxene, apatite, calcite, and a new iron-phosphate mineral. The ore contains up to 98% iron oxide and in many instances this concentration does not fall below 80%. Magnetite and hematite occur in euhedral crystals, which grow up to several centimeters in diameter. These primary oxides are free of exsolution intergrowths, and spectral scans of magnetite and hematite, with the electron-probe microanalyzer, reveal that no detectable concentrations of other elements are present.

Secondary hematite and maghemite develop extensively as oxidation products of the magnetite. Although there are no chemical variations in the magnetite, crystals are nevertheless strongly zoned in a very unusual manner. The zoning is crystallographically controlled with respect to morphology (Plate 2A) but becomes apparent only as selective oxidation of the magnetite takes place; the process of maghematization, on the other hand, does not reveal this zoning. By heating polished specimens of the ore for 1 minute at 920°C, it has been shown that certain concentric zones within the magnetite are more susceptible to oxidation than others, thus demonstrating that the natural observed zonation is an inherent feature and is not due to the crystallization of successive generations of magnetite and hematite from the primary melt. The nature of this zoning is not fully understood but a possible explanation is that the zones reflect metastable intermediate members of the oxidation series Fe_3O_4-Fe_2O_3 and are therefore analogous to the kenotetrahedral magnetites described by Kullerud,

* Material for this study was obtained from D. P. Rogers, Texas Gulf Sulfur Company; their cooperation is gratefully acknowledged.

Donnay, and Donnay (*Year Book 66*).

Colloform goethite is present as a late-stage vesicle and veinlet infilling, and complex overgrowths of goethite and goethite-hematite intergrowths develop on the sharp crystal terminations of primary magnetite and hematite that have grown into open cavities (Plate 2B).

Ilmenite has been identified in one specimen only. This sample contains abundant calcic pyroxene, and the ilmenite is in an advanced stage of alteration to sphene, titanohematite, and rutile.

Large bodies of iron oxide that appear to be intrusive and are considered to be magmatic in origin are characterized by high titanium contents and concentrations of apatite in the ore that are frequently as high as 30% by volume (Philpotts, 1967). Although the discovery of these recent metallic flows in Chile at first appeared to confirm the opinions held for the igneous origin of such ore deposits, these lavas contain neither high concentrations of titanium nor of phosphorous. The absence of titanium is particularly striking in view of the high concentrations that are present in basaltic magnetite and in magnetite associated with large layered intrusions. Analysis of coequilibrated titanomagnetite and ilmenite from naturally occurring oxide-apatite rocks indicate temperatures of formation in the range 850°–1000°C (Philpotts, 1967). If the Laco magnetite deposits were extruded as molten oxides, temperatures in excess of 1500°C would be necessary. The porous nature of these flows, however, indicates that large amounts of gas were present, thus suggesting that a process other than liquid extrusion was involved.

A New Iron-Phosphate Mineral

S. E. Haggerty

An iron-phosphate mineral to which the formula $Fe_3^{2+}Fe^{3+}(PO_4)_3$ is tentatively assigned, on the basis of electron-microprobe results, has been discovered in specimens of extrusive Laco magnetite. The phase occurs as minute crystals (maximum 300 μm) in open cavities interstitial to magnetite and hematite. The mineral is opaque and crystalline and shows good polysynthetic twinning (Plate 2C). It is strongly pleochroic and anisotropic in polished sections. The maximum color variation on rotation of the microscope stage, under oil immersion, is from yellow to bluish gray. The mineral has an estimated reflectivity value in the 10–15% range (cf. magnetite, 22%; hematite, 25%); it is softer than magnetite and takes a good surface polish. Initial breakdown of the mineral takes place along cracks and grain boundaries (Plate 2D). The breakdown product becomes darker in color but continues to retain its strong optical anisotropy. Electron-microprobe scans across these alteration veinlets show no variation in either Fe or P, and it is concluded that the darkening is due simply to the oxidation of ferrous to ferric iron. More advanced alteration produces hematite and an unidentified granular phase, which still contains only iron and phosphorous. This breakdown product is weakly anisotropic, in color tones that are similar to that of the primary phase, and is distinguished from the parent mineral by having deep-red internal reflections.

Electron-microprobe analysis of the new mineral gives Fe, 44.05%; P, 17.93%; in good agreement with the formula $Fe_4(PO_4)_3$. Recalculating the values in terms of oxides we obtain FeO, 42.49%; Fe_2O_3, 15.74%; and P_2O_5, 41.08%; giving a total of 99.31%. The theoretical oxide concentrations for $Fe_4(PO_4)_3$ are FeO, 42.41%; Fe_2O_3, 15.71%; and P_2O_5, 41.88%. Individual grains are compositionally homogeneous, and spectral scans show that no other elements heavier than Na are present in detectable quantities.

Small quantities of the uncontaminated phase were carefully extracted for X-ray purposes from the surface of polished

sections by the microsampling technique described by Kingston (1966). Three Debye-Scherrer patterns (*A, B,* and *C;* Table 47) of the new phase, from different hand specimens, have been measured using a 114.6-mm camera and Mn-filtered FeKα radiation (λ=1.9373). Strong lines corresponding to spacings 3.31 Å, 3.19 Å, 2.09 Å, and 1.60 Å coincide with strong reflections for the synthetic phase lipscombite, $Fe^{2+}Fe_2^{3+}(PO_4)_2(OH)_2$ (Gheith, 1953), but the resemblance ends there; many other strong lines of the two phases do not agree. Polished sections of synthetic lipscombite have been made from material kindly supplied by Professor M. A. Gheith. The color, reflectivity, and degree of optical anisotropy of the synthesized phase are quite distinct from those of the new mineral. Furthermore, lipscombite is hydrated; it contains 42.8% Fe and 15.8% P, compared with 44.1% Fe and 17.9% P for $Fe_4(PO_4)_3$. The X-ray powder data for naturally occurring manganoan lipscombite (Lindberg, 1962) also differ significantly from this new phase. Attempts to index the powder data on the

TABLE 47. X-Ray Powder Data for Three Debye-Scherrer Patterns of a New Iron-Phosphate Mineral Compared with Synthetic Lipscombite (Mn-filtered, FeKα radiation)

Lipscombite *			New Phase			
hkl	*d*, Å	*I*	*A* *d*, Å	*B* *d*, Å	*C* *d*, Å	*I*
101	4.864	1	3.827	3.856	3.861	4
	3.669	2.5				
	3.544	1				
			3.464	3.489	3.479	3
103	3.329	10	3.314	3.311	3.308	10
004	3.200	1	3.191	3.211	3.218	7
			2.928	2.943	...	0.5
	2.880	f				
			2.822	2.825	...	3
			2.704	2.686	2.701	1
200	2.616	2	2.612	2.618	2.607	1
	2.544	f	2.529	2.545	2.546	6
	2.422	1				
			2.378	2.374	2.371	1
	2.267	f				
			2.286	2.313	2.289	1
			2.084	2.082	2.079	6
213	2.056	5.5	2.042	2.064	2.041	0.5
	2.036	1.5				
	1.862	1				
	1.845	2	1.842	1.855	1.839	0.25
	1.773	1				
017	1.747	1				
			1.735	1.737	1.736	1
206	1.664	5				
			1.653	1.656	1.655	0.5
208	1.604	6	1.598	1.601	1.597	9
			...	1.483	1.486	1
	1.449	1.5	1.438	1.445	1.445	0.25
	1.441	1				
			1.402	1.404	1.401	2
	1.374	1	1.371	1.371	1.371	4
			1.312	1.319	1.294	1
			1.236	1.235	1.234	1
			1.147	1.153	1.145	1
			...	1.076	1.077	1
			1.042	1.040	1.042	1
			0.9978	0.9978	0.9974	2
			0.9958	0.9961	0.9959	1

* Gheith (1953, experiment 99B).

basis of the lipscombite structure have been unsuccessful (tetragonal, body-centered, $a = 5.37$ Å, $c = 12.81$ Å; Katz and Lipscomb, 1951).

The iron phosphate is easily broken down at 500°C in air as well as in evacuated silica glass tubes. In both types of experiment the product becomes transparent. In the runs conducted in air, finely textured filaments of hematite are produced that closely resemble the natural breakdown product. Accurate electron-probe analysis of the altered phase was not obtained because of widespread inhomogeneity.

From the textural relations it is clear that the new mineral is a late-stage precipitate in the Laco magnetite lava flow. In a few instances the mineral occurs with apatite but in general apatite and other calcium-bearing minerals are absent. The new mineral has not been found in association with goethite or colloform hematite (also late-stage products), and this is not surprising in view of its high ferrous iron content.

Magnetic Minerals in Pelagic Sediments

S. E. Haggerty

In sediment cores from the deep oceans, extremely good magnetic and fossil stratigraphic correlations have been successfully extended over wide areas of the sea floor (Opdyke *et al.*, 1966; Watkins and Goodell, 1967). These correlations suggest that large areas of active sedimentation are being simultaneously magnetized, the direction of magnetization being either normal or reversed, depending on the direction of the earth's magnetic field.

The present study indicates that high-temperature detrital Fe-Ti oxides are probably responsible for most, if not all, of the magnetic remanence. These minerals have a high magnetic susceptibility and a strong, previously inherited thermoremanent direction. The later diagenetic crystallization of new phases, however, and the concurrent acquisition of new chemically derived magnetic directions are mineralogical factors that will modify and perhaps eventually destroy the primary depositional directions of magnetization. A thorough knowledge of these minerals and the possible post-depositional changes that are likely to occur in oceanic sediments is therefore a necessary prerequisite for a full interpretation of the magnetic record.

One hundred and ten samples from twenty-two sediment cores * from the equatorial and north Pacific, Atlantic, and Indian Oceans and from below the Antarctic ice sheet have been examined. These sediments consist of lutites, calcareous oozes, and red-brown clays. Paleomagnetic stratigraphy is a unique method of dating and correlating deep-sea sedimentary cores, and yet few direct attempts have been made to identify the magnetic mineral component. In the studies by Keen (1960) and Opdyke *et al.* (1966) thermomagnetic analyses were used to show the presence of magnetite. The only other study to appear in the literature is the report by Harrison and Peterson (1965). In their X-ray determination a magnetic mineral "between" magnetite and maghemite in structure was found and was considered (although it was not directly observed) to be an oxidation product of magnetite.

Optical observations are particularly important because of the fine textural distinctions that can be made on the opaque minerals. In contrast, X-ray studies and thermomagnetic analyses give no direct information on whether the phases are discrete or whether they are present in complex exsolution or oxidation intergrowths. Furthermore, clues to the possible origin of magnetic constituents can only be obtained by directly observing the nature and form of these phase intergrowths and noting their

* The sediment cores in this study were obtained from the Lamont-Doherty Geological Observatory, Columbia University; their cooperation is gratefully acknowledged.

disposition toward the sedimentary matrix.

In the present study, examination of polished sections of the core material has yielded unequivocal identification of the magnetic minerals. Vacuum impregnation with an epoxy resin gives the samples sufficient coherence and durability for dry polishing with fine alumina powders (1, 0.3, 0.05 μm) on closely woven metallographic laps.

Mineralogy

The opaque minerals identified consist of oxides, oxyhydroxides, and sulfides. These phases are fine grained (<10 μm) and are present in quantities ranging from 1 to 5% by volume. Exceptions are the oxides and oxyhydroxides of manganese, which occur commonly as small discrete nodules but may also form in high concentrations and large masses.

Oxides. The oxides observed in the core material are members of the magnetite-ulvöspinel solid solution series and members of the hematite-ilmenite solid solution series. Homogeneous titanomagnetite and titanomagnetite with oxidation lamellae of ilmenite are extremely common. Alteration products of these intergrowths are ferri-rutile, rutile, titanohematite, and pseudobrookite; the extent of oxidation, however, is highly variable in any single core sample. Crystals of titanomagnetite are generally euhedral to subhedral in form and are rarely rounded. These oxides occur mostly as single discrete grains but are also present in detrital fragments of crystalline lava, in volcanic ash fragments, and in devitrified glass shards. Exsolution and alteration of these oxides are of the type observed in lavas (Watkins and Haggerty, 1967) and shown by experiment to form at high temperatures (Lindsley, *Year Books 61* and *62;* Haggerty and Lindsley, this report).

Maghemite (γFe_2O_3) is ferrimagnetic and is by far the most common low-temperature oxidation product of titanomagnetite. It occurs typically in curved conchoidal cracks in the titanomagnetite; it is either white or pale blue in color and is optically isotropic. Maghemite is known to invert to the stable α form (hematite) between 250° and 500°C (Gheith, 1952; Lepp, 1957); hence, the material observed in these sediments must have developed below this limit. The effect of titanium on this limiting temperature range is considered to be small but has not been experimentally determined. Akimoto and Kushiro (1960) and Baker and Haggerty (1967) have shown that maghemite can develop as an oxidation product of titanomagnetite during active weathering of basaltic lavas. Unless there has been systematic and controlled sampling of the parent rock, however, alteration products due to superficial weathering cannot be readily distinguished from those products that develop during the waning stages of deuteric cooling. Subsequent diagenetic alteration complicates the problem even further. Therefore, since alteration may be assigned to any one of a number of processes at low to intermediate temperatures, it must be concluded that the time of formation of maghemite as an oxidation product cannot be accurately assessed.

Although members of the rhombohedral series (Fe_2O_3-$FeTiO_3$) are common in these oceanic cores, homogeneous hematite is the most abundant phase present. Members of the hematite-ilmenite series are regarded as high-temperature phases, but Fe_2O_3 may also form authigenically as a primary mineral or as an oxidation product; thus, unless exsolution or alteration intergrowths suggest a high concentration of titanium, formation in situ must be considered. There are no diagnostic textural features in homogeneous hematite, such as colloform banding, that would confirm its formation in situ at low to intermediate temperatures, or indeed whether it is a pseudomorph after magnetite. Grains showing mutual exsolution intergrowths

of titanohematite and ferri-ilmenite are widespread. Titanohematite-rutile intergrowths and titanohematite-rutile-ilmenite intergrowths similar to those described by Ramdohr (1950) have also been observed. These intergrowths are characteristic of deep-seated and slow-cooling conditions in igneous rocks and are texturally different in form and mode of occurrence from the somewhat similar mineral assemblage that develops by simple high-temperature oxidation. One would infer from these observations that minerals containing these intergrowths in deep-sea sediments are detrital.

Oxyhydroxides. Birnessite (7 Å, δMnO_2), todorokite (9.7 Å, δMnO_2), and ranciete (calcium manganese oxide), which are common in manganese nodules (Roy, 1968), are known to be magnetic (Powell and Ballard, 1968), and the formation of these phases at low to intermediate temperatures in highly oxidizing environments on the sea floor is generally accepted (Mero, 1962; Bonatti and Nayudu, 1965). The layered and colloform textures, as well as the radial and concentric syneresis cracks that develop as a result of contraction when a gel hardens, are diagnostic of a metacolloidal origin. Manganese micronodules, which are highly abundant in the core samples, are typical and are similar to those described in the literature (Sorem and Gunn, 1967).

Goethite has been observed to form in minute (1–5 μm) spherical or subspherical accumulations, which bear a striking resemblance to the fossil bacterial forms that have been observed in Precambrian iron ore formations (LaBerge, 1967). Colloform banded goethite, similar to the ferromanganese micronodules, has also been observed. Goethite occurs extensively as an alteration product of pyrite. Such grains contrast with the colloidal forms because of their irregular shape, and many of them are seen to contain relic areas of the primary sulfide phase.

Goethite is magnetic (Strangway *et al.*, 1968) and has an upper thermal stability limit in the region of 140°C (Tunell and Posnjak, 1931); it is hydrated and there is little doubt that its presence in oceanic sediments is authigenic.

Sulfides. Iron sulfides are abundant in the deep-sea sediments examined and occur as discrete grains or in thin parallel bands. Paramagnetic pyrite and ferromagnetic pyrrhotite have been observed only rarely as 10-μm grains; the ferromagnetic Fe_3S_4 minerals are very similar to pyrrhotite in color, and although greigite is optically isotropic and smythite is anisotropic, even these distinguishing features prove difficult to identify on minute single crystals. Sulfides in deep-sea sediments are generally regarded as authigenic in origin. No problem arises in providing a primary source of iron, as is evidenced by the presence and formation of ferromanganese nodules, goethite, and hematite. The bacterial generation of hydrogen sulfide in reducing environments and in association with organic debris is well known. Framboidal structures of the type described by Love and Amstutz (1966), however, have not been observed.

Sediment, Magnetic, and Mineralogical Relationships

In the specimens we have examined, detrital minerals are ubiquitous, regardless of sediment type, depth within a core, or geographical location. The oxyhydroxides are confined almost entirely to the clay-rich sediments. Sulfides are commonly present in dark-brown sediments and are characteristically absent in the manganese-enriched cores. The Antarctic cores are unique in that these sediments contain large proportions of ice-rafted material.

Members of the magnetite-ulvöspinel solid solution series contribute significantly to the magnetic properties of marine sediments. Members of the ilmenite-hematite series are ferromagnetic over a very narrow range of solid solubility, and toward the Fe_2O_3 end are only

weakly magnetic. Pseudobrookite members are paramagnetic, and the polymorphs of TiO_2 (rutile, brookite, and anatase) that form as oxidation products are also paramagnetic, with weak susceptibility values in the region of 0.05×10^{-6} emu/g (Pankey and Senftle, 1959). How far the magnetic behavior of the sediment is influenced by the occurrence of the ferromagnetics in intergrowths such as exsolution or by-products of oxidation depends on the condition under which the intergrowths formed and the way in which the component minerals acquired their magnetization. The authigenic manganese micronodules, goethite, and the magnetic iron sulfides will also contribute and will have an overall influence on the magnetic moment.

Opdyke *et al.* (1966) have observed that the quality and resolution of the magnetic stratigraphy are sometimes lost at depth. An examination of nine polished samples from the Vema 21-177 core (lat. 33° 52′ N; lon. 160° 08′ W) has shown that the disruption of the magnetic vector can be qualitatively * correlated with an increase in manganese micronodule content. The core is 1030 cm in length and varies from a yellowish brown clay at the top to a dusky brown clay at the base. The manganese micronodule content is moderate between 21 and 361 cm and abundant between 461 and 927 cm. At 475 cm the coercivity decreases abruptly and the polarity oscillates with great rapidity down to the base of the core. This loss of a coherent magnetic polarity pattern suggests that the increase in manganese content has taken place during diagenesis and that effective remagnetization of the sediment has followed. Lynn and Bonatti (1965) have shown that manganese will dissolve in a reducing environment and also that it has a tendency to migrate to zones of higher oxidation. Manganese nodules may contain up to 21% Fe (Cronan and Tooms, 1969), and a direct consequence of the preferential migration of Mn (since differential rates of solubility and mobility exist for Fe and Mn) is that an iron-enriched residue will prevail in the reduced zones; these accumulations could give rise to the spontaneously magnetic iron sulfides, greigite and smythite, by bacterial precipitation (Berner, 1964; Doyle, 1968) and are therefore equally likely to be responsible for remagnetization of the sediment.

* Accurate quantitative opaque petrographic study of deep-sea sediments by optical methods is unreliable because of the extremely fine grain sizes involved.

The reliability of magnetic stratigraphic measurements depends on the extent to which the direction of magnetization is the direction of the earth's magnetic field at the time of deposition. Magnetic measurements of the uppermost part of deep-sea sediment cores, which would permit examination of this matter, have been unsuccessful because of the fluidal state of the water-sediment interface. Since major polarity boundaries, as well as minor events within major epochs, can be stratigraphically correlated over wide areas of the ocean, the sediment must still be sufficiently mobile for natural realignment of detrital particles to take place under the influence of the earth's magnetic field.

The present study suggests that the vector properties of the magnetic moment in oceanic sediments are acquired by depositional or detrital remanence. The source of the magnetic mineral detritus is a problem, however. The simple mechanical breakdown of primary volcanic material, such as that described by Fox and Heezen (1965) on the slopes of the Mid-Atlantic Ridge, cannot be evoked for the deep oceans. Since a large proportion of the grains are 10 μm or less, aeolian transportation from the continents to the deep oceans is a likely mechanism. It is well known, for example, that a wide distribution of windblown ash will follow violent volcanic eruptions, and in this context it is of interest to note that in the Pacific the

average sedimentation rate is of the order of 0.5–1 cm per 1000 years.

Annealing Experiments with Naturally and Experimentally Shocked Feldspar Glasses

*P. M. Bell and E. T. C. Chao **

The present study is an attempt to understand meteorite impact phenomena on the earth's surface. Presumably this knowledge can also be used to aid in the interpretation of impact debris from the surfaces of other planets. Previously, Bell and Chao (*Year Book 67,* pp. 126–130) reported the results of annealing experiments with dense feldspar glasses that had been prepared statically at high pressure (10–45 kb). In the present study the same annealing techniques have been applied to dense glasses that were formed during experimental and nautral shock-wave events.

Two of the natural feldspar glasses are plagioclase (An_{41}, An_{22}); the other is an alkali feldspar ($Or_{39}Ab_{61}$). All three are from the Ries Crater in Bavaria. Two synthetically shocked glasses were formed from labradorite crystals (An_{67}) from Lake County, Oregon (the same material studied statically in last year's report). Preparation of the shocked synthetic glasses involved shock pressures of approximately 285 kb for one sample and 325 kb for the other. No vestiges of crystallinity could be observed in either sample. Paul De Carli and Thomas Ahrens, of the Stanford Research Institute, carried out the shock-wave preparations.

Petrographic Setting of the Natural Specimens

All three Ries Crater samples are from brecciated rock fragments known as suevite. The breccias have been interpreted as fallout debris from a meteorite impact (Shoemaker and Chao, 1961).

Two microprobe analyses of the An_{41} glass are given in Table 48. The glass fragments (RC641-14) were extracted from a medium-grained gabbroic rock collected from the Otting quarry. The rock consists essentially of the feldspar glass and oxidized and deformed green monoclinic pyroxene, with accessory apatite and opaque minerals.

The An_{22} glass has been described petrographically and analyzed by microprobe by James (1969). The composition is $An_{22}Ab_{72}Or_6$. It occurs in a biotite-bearing amphibolite (RC647-67) from the Bollstadt quarry. This fine-grained, foliated rock consists of the plagioclase glass with green amphibole (wavy extinction) and oxidized brown biotite, which contains minute opaque particles. James has recognized a few microscopic inclusions of jadeite in some of the shocked glass.

The $Or_{39}Ab_{61}$ glass is calcium free but contains a small amount of barium, as noted in its chemical analysis (Table 48, RC647-41). It occurs in an amphibole-bearing biotite granodiorite (RC647-41) from the Bollstadt quarry. This medium-grained rock contains the alkali-feldspar glass, shocked and mostly isotropic quartz, saussuritized plagioclase, strongly kinked brown biotite, and a deep-green amphibole (lamellar twinning). Acces-

TABLE 48. Probe Analyses of Naturally Shocked Feldspar Glasses

	RC641-14, wt %		RC647-41, wt %
	1	2	
SiO_2	58.9	58.1	64.3
Al_2O_3	26.7	26.5	18.6
CaO	8.41	8.31	...
Na_2O	6.36	6.48	6.67
K_2O	0.24	0.32	6.49
BaO	...	...	0.8
H_2O	...	...	3.1*
Totals	100.6	99.7	(100.0)
	Mole %		
Ab	57.0	57.4	61.0†
An	41.6	40.7	...
Or	1.4	1.9	39.0

Analyst P. M. Bell.
* H_2O by subtraction.
† BaO ignored.

* U. S. Geological Survey.

sory sphene, apatite, and an opaque mineral are present.

Experimental Procedure

In general, the index of refraction of each grain was measured prior to and after annealing at 850°C in a platinum furnace. Each grain was mounted on a spindle stage. In the previously reported study a gradational filter for monochromatic light was used with specially calibrated immersion oils to measure the index of refraction to a precision of ± 0.0004 or better. In the present study indices of refraction were also measured with immersion oils but with an interference microscope that has a precision of ± 0.0002.

After measurement of the index of refraction, each grain was individually wrapped in platinum foil. A grain of dense feldspar glass produced at static pressures (*Year Book 67,* pp. 126–130) was also wrapped in platinum and included as a control sample. In each experiment the two platinum packets were welded to a Pt/Pt-10Rh thermocouple before rapid insertion into the horizontal annealing furnace. As soon as the thermocouple junction reached a preselected temperature (850°C or lower), the packets were quickly removed from the furnace and quenched in an air jet. The time necessary for the sample to come to temperature was recorded. In practice runs the quench time was measured to be 0.5 to 1 second. After the quench, both the sample and control grains were remounted on the spindle stage, and the indices of refraction were again measured.

Annealing Data

Results are shown in Fig. 58. The maximum change of index of refraction of the An_{41} glass was from 1.5250 to 1.5242, a drop of 0.0008. The annealing behavior of this glass is similar to that of statically synthesized and experimentally shocked dense glasses.

The An_{22} and $Or_{39}Ab_{61}$ glasses vesiculated extensively during heating, presumably due to the release of water vapor. Water could have been incorporated in the glass structure during impact or at a later time. Microscopic examination of less severely shocked grains from the same specimens showed crystalline feldspars of the same composition to be relatively unaltered, suggesting that the water was meteoritic in origin. Vesicules were observed in the alkali-feldspar glass at temperatures as low as 450°C. An_{22} glass showed partial vesiculation above 700°C, suggesting a much lower water content. Figure 59 shows the data for An_{22}. Measurements of indices of refraction of the control sample, An_{23} (synthesized statically at 10 kb), are also included for comparison. Vesiculation did not severely affect the results on the An_{22} glass.

Vesiculation in the alkali-feldspar glass was so severe that it appeared cloudy, and the indices of refraction could not be measured. In order to drive off the contained water, several grains of alkali-feldspar glass were heated overnight at various temperatures. Indices of refraction measured after heating are plotted as a function of heating temperature in Fig. 60. In summary, the index of refraction changes rapidly at low temperatures (300°C); apparently the water was bonded into the high-pressure, dense glass structure. The index of refraction was still falling at 800°C. Relaxation of the high-pressure density probably affects refractive index more than water loss.

The indices of refraction of An_{22} and $Or_{39}Ab_{61}$ glasses decreased by 0.0011 and 0.0145 as a result of heating at 300°C overnight; further heat treatment and annealing of these glasses was not accompanied by massive vesiculation. Figure 58 shows the changes in index of refraction after these preheated samples have been annealed.

The two An_{61} glasses, produced by

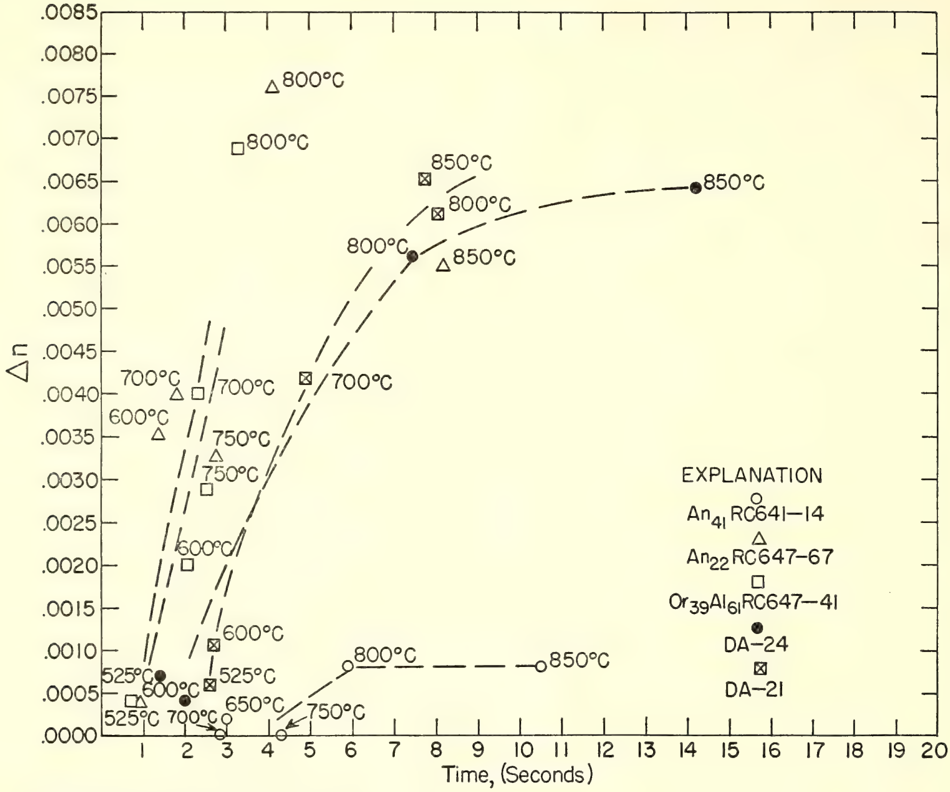

Fig. 58. Change of index of refraction (Δn) during annealing of An_{41}, An_{22}, $Or_{39}Ab_{61}$, DA-21, and DA-24. The change in index occurred as the temperature was raised to the noted value in the time indicated. Δn is negative.

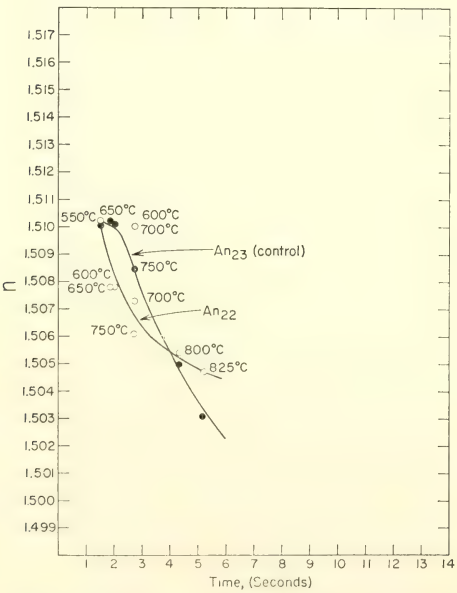

Fig. 59. Annealing data for An_{22} and control sample An_{23}.

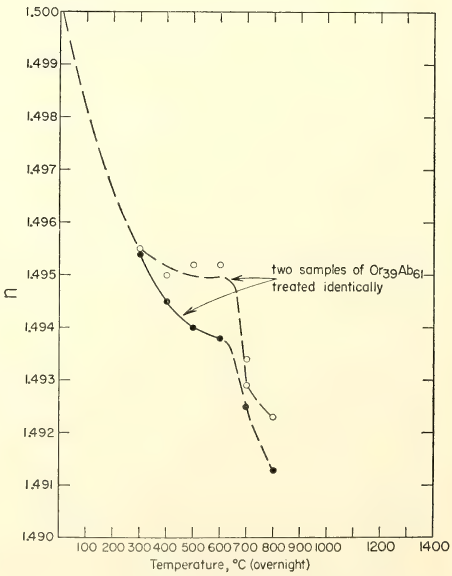

Fig. 60. Overnight heat treatment of two grains of $Or_{39}Ab_{61}$.

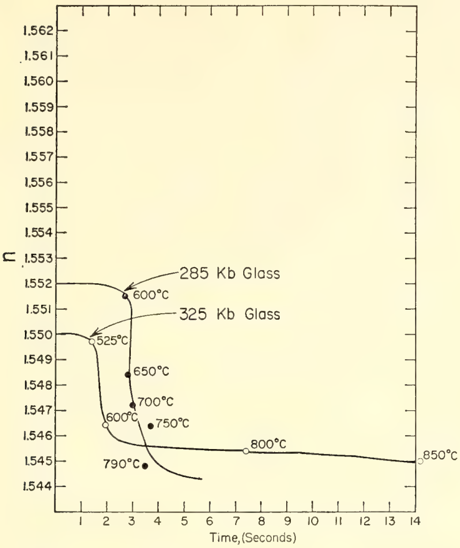

Fig. 61. Annealing data for two synthetically shocked glasses, DA-21 and DA-24.

shock waves at 285 kb (sample DA-21) and 325 kb (sample DA-24), were treated by the standard annealing procedure. Figure 58 shows change of index with annealing for these and other glasses studied. The final indices, measured after the quench, are shown in Fig. 61.

Interpretation of the Results

It is well known that the maximum density of a feldspar glass at peak shock pressure is not preserved on culmination of the shock event. Ahrens and Rosenberg (1968) gave a Rankine-Hugoniot plot of feldspar at two shock pressures, showing that the final density is more dependent on the release adiabat than on the peak pressure. In fact, with higher shock pressures, the effects of the release adiabat can be more severe. Comparison of the changes in the indices of refraction measured in the present study of shocked glasses from the Ries Crater with those of the dense glasses produced at static pressure (*Year Book 67*) suggests that a shock density corresponding to only about 10 kb is preserved in the Ries glasses.

Great changes in the index of refraction occurred during these short annealings, suggesting that the temperatures during the shock events were not high. For example, the two synthetically shocked glasses, DA-21 and DA-24, exhibited rapid changes above 550°–600°C. The natural glasses exhibited similar behavior but the times were even shorter (1–3 seconds). The present set of experiments has involved rapid annealment, with times in seconds, like those to be expected in natural impacts. The results could be helpful in interpreting observations on extraterrestrial samples.

Andalusite and "β-Quartz$_{ss}$" in Macusani Glass, Peru

Bevan M. French and H. O. A. Meyer*

Andalusite and a "β-quartz solid solution" along the join $LiAlSi_2O_6$-SiO_2 have been identified in glass collected by Barnes (see Barnes *et al.*, 1970) from near the town of Macusani, southern Peru. This is believed to be the first report of the natural occurrence of a "β-quartz solid solution" and also the first chemically substantiated account of andalusite occurring in possible equilibrium with a presumably volcanic glass.

Macusani glass, which occurs as pebbles and cobbles in glacial and alluvial deposits, is unique because it is not comparable in composition with tektites nor with any naturally occurring volcanic glass (Linck, 1926; Martin and de Sitter-Koomans, 1955; Elliott and Moss, 1965). It is characterized (Table 49) by a high content of alumina and mineralizers. Barnes *et al.* (1970) have shown that the glass composition is similar to that of a sillar (altered ash flow) that outcrops near the glacial deposits that contain the Macusani glass; furthermore, the K/Ar ages of glass and sillar

* Planetology Branch, National Aeronautics and Space Administration, Goddard Space Flight Center, Maryland.

TABLE 49. Analyses of Minerals from Macusani Glass

	Macusani Glass *	Andalusite	"β-Quartz$_{ss}$"	Chromite	Spinel †
SiO_2	71.6	36.3	77.4	0.02	0.09
TiO_2	0.04	...	0.00	0.16	0.02
Al_2O_3	16.7	63.2	17.0	9.41	56.0
Cr_2O_3	...	...	...	51.6	<0.01
FeO	0.6	0.39	0.00	31.4	17.0
MgO	tr	0.00	0.00	5.98	0.5
CaO	0.4	0.00	0.00	0.00	0.0
MnO	0.05	...	...	0.45	0.3
ZnO	...	...	...	...	27.0
Li_2O	0.8	...	~ 5 ‡	...	...
Na_2O	4.7	...	< 0.1	...	...
K_2O	3.6	...	< 0.1	...	...
B_2O_3	0.4	...	...	...	...
P_2O_5	0.4	...	...	...	...
F	1.4	...	...	...	...
H_2O	0.2	...	...	...	...
Totals	100.4 (less O = F = 0.6)	99.9	(99.4)	99.0	(100.9)

* Elliott and Moss, 1965.
† Matrix effects for Zn approximated.
‡ Determined qualitatively by laser microprobe.

are comparable at 3–4 million years. In an attempt to discover the origin and chemical history of this glass, we have analyzed several discrete mineral phases that occur with the glass, namely, andalusite, "β-quartz$_{ss}$," quartz, chromite, and gahnite.

Andalusite

Andalusite occurs as clear, almost euhedral, prismatic crystals elongated parallel to a well-defined flow banding. Many of the crystals are boudinaged, suggesting that they were present during flowage and consolidation of the glass. From optical properties, Linck (1926) identified similar crystals in comparable glass from Paucartambo (approximately 100 miles northwest of Macusani) as andalusite. The ideal composition Al_2SiO_5 has been proved by us for the crystals in the Macusani glass (Table 49). Also the preliminary X-ray diffraction powder data agree with that obtained for a standard andalusite.

The only other occurrence known to the authors of andalusite in a volcanic glass is in the pyrometamorphosed sediments of the Asama volcano, Japan (Aramaki, 1961). In this occurrence, however, it appears that the andalusite is a relict from the sediments, for when it occurs in the glassy part of the rock it shows evidence of resorption. The stable aluminum-silicate mineral in the Asama glass is a silica-deficient sillimanite, whose composition is reported to be about halfway between ideal sillimanite and ideal mullite. Sillimanite was also identified in the Macusani glass (Linck, 1926; Martin and de Sitter-Koomans, 1955), occurring as very small elongated crystals. This phase is much less abundant than andalusite and has not yet been verified by us.

In the systems Al_2O_3-SiO_2 (Bowen and Greig, 1924; Aramaki and Roy, 1962), Al_2O_3-SiO_2-$(Na,K)_2O$ (Schairer and Bowen, 1955, 1956) a composition equivalent to that of Macusani glass (excluding volatites) would produce mullite in equilibrium with the melt at a minimum temperature of about 1100°C. Unfortunately the reactions andalusite or sillimanite $\rightarrow$ mullite and quartz are not clearly understood. G. C. Kennedy (in preparation) has demonstrated the existence of a solid solution relationship between mullite and sillimanite. This rela-

tionship complicates the andalusite-sillimanite boundary, but below 3 kb and above 700°C the amount of sillimanite in mullite is restricted to less than 10%. The recent work of Richardson, Gilbert, and Bell (1969), however, demonstrates that it is possible to obtain andalusite on the liquidus if one considers the intersection of the minimum melting curve for granitic systems containing excess H_2O (Luth, Jahns, and Tuttle, 1964) with the andalusite-sillimanite equilibrium curve.

The occurrence of andalusite (and sillimanite?) in the Macusani glass may result from the presence of sufficient volatiles in the melt (as evidenced by the presence of B, F, H_2O in the glass) to lower the liquidus below the andalusite $\rightarrow$ sillimanite $\rightarrow$ mullite reaction temperature. The possible presence of small, minor sillimanite crystals in the Macusani glass suggests that the temperature lay close to the andalusite $\rightarrow$ sillimanite boundary.

"β-Quartz$_{ss}$"

The mineral interpreted as a member of the β-quartz and spodumene solid solution series occurs as numerous small rosettes, which together form bands parallel to the flow banding in the glass. These rosettes have the appearance of quench crystals, whose present distribution may reflect slight compositional differences in adjacent layers of glass. Electron-probe analysis (Table 49) of this material, together with the high Li_2O content of the glass (0.8%; Elliott and Moss, 1965), suggested that this mineral might contain appreciable lithium. This belief was confirmed by laser microprobe analysis,* which indicated a greater concentration of lithium in the mineral phase (~5 wt % Li_2O) than in the glass.

From the analysis (Table 49) this phase would have a composition approximating to $(LiAlSi_2O_6)_{62}(3SiO_2)_{38}$ mole %. Preliminary cell data based on a β-quartz type structure are $a = 5.14$ Å, $c = 5.46$ Å. These values give a chemical composition (Munoz, *Year Book 67,* p. 138) of $(LiAlSi_2O_6)_{63}(3SiO_2)_{37}$, in excellent agreement with the analytical value.

The mineral in the Macusani glass is believed to be the first reported occurrence in nature of a mineral having such a composition and structure.

Phases having the same structure as hexagonal β-quartz (cf. $LiAlSi_2O_6$-III, Li, 1968) have been synthesized along the join SiO_2-$LiAlSi_2O_6$ at pressures above 10 kb (Munoz, *Year Book 67*). Unfortunately there is much confusion in the literature with regard to the identification of "β-eucryptite$_{ss}$" and "β-quartz$_{ss}$" in the phase studies that have been done at 1 atm. This confusion has arisen from the similarity of X-ray powder data for the two series. Single-crystal work is essential for positive identification. Until such work is completed the status of true β-quartz structures along the join spodumene-quartz at 1 atm must remain in doubt.

It seems likely that the formation of andalusite, which was aided by the presence of volatiles, was inhibited when the temperature suddenly dropped as quenching (loss of volatiles?) took place. At this point, rapid but limited growth of the "β-quartz$_{ss}$" occurred. Perhaps, in view of the work of Richardson, Gilbert, and Bell (1969) on the andalusite-sillimanite equilibrium, we may suggest a possible maximum temperature of formation for the glass and andalusite in the region of 850°C.

Quartz, Chromite, and Gahnite

Other minerals that occur within the glass from Macusani and have been identified by electron-probe analysis include quartz, spinel, and chromite. The quartz is present as a single crystal whose edges show some resorption. The chromite is of the magnesiochromite variety

* This analysis was performed qualitatively by J. J. Bussey, of Jarrell-Ash Division, Fisher Scientific Company, Waltham, Massachusetts.

($a = 8.36$ Å), whereas the spinel is an iron gahnite (Table 49). Both these spinellids were obtained from HF residue, and their petrographic relations to the glass and other minerals are uncertain. The occurrence of two spinellids of such diverse composition in a homogeneous glass is puzzling; one (or both) could be relicts from sediments assimilated by a superheated granitic magma.

STAFF ACTIVITIES

Washington Crystal Colloquium

Beginning in September 1968 the Washington Crystal Colloquium, an informal monthly assembly of crystallographers from the Baltimore-Washington-Virginia area, moved its meeting place from the George Washington University campus to the Geophysical Laboratory. Attendance varied between twenty and fifty persons. The following eight lectures were presented:

"The crystal structure, at 5.5 Å resolution, of the hemoglobin from *Glycera dibranchiata,* a marine annelid worm," by Eduardo A. Padlan (The University of the Philippines), presented by Warner E. Love (The Johns Hopkins University), September 26, 1968.

"Recent investigations on the salamander toxin" and "The crystal structure of the π complex of picric acid with 1 bromo-2 amino naphthalene," by Gerhard G. Habermehl (Institute for Organic Chemistry, Darmstadt, Germany), October 25, 1968.

"The crystal structure of low chalcocite," by Howard T. Evans, Jr. (U. S. Geological Survey), November 22, 1968.

"Crystal structures of anti-radiation drugs and of products of photo rearrangements," by Louise I. Karle (*pro tem.,* Universität Marburg) and Isabella L. Karle (U. S. Naval Research Laboratory), December 19, 1968.

"Crystal structures and crystal chemistry of two borate minerals, veatchite and howlite," by Joan R. Clark (U. S. Geological Survey), January 31, 1969.

"High-pressure X-ray diffraction studies of single crystals; the crystal structure of benzene at 25 kb," by Stanley Block (U. S. National Bureau of Standards), March 6, 1969.

"The crystal structure of a 1,3-diglyceride and its relevance to the study of biological membranes," by Albert Hybl (University of Maryland), April 18, 1969.

"Cyclotetradepsipeptide," by J. Konnert (U. S. Naval Research Laboratory), and "The crystal structure of 8,14-anhydrodigitoxigenin, a variant of the cardiac-active steroid, digitoxigenin," by R. D. Gilardi (U. S. Naval Research Laboratory), May 16, 1969.

Journal of Petrology

Two of the founding members of the Editorial Board of the *Journal of Petrology* have retired from their posts this year after ten years of service. Dr. H. S. Yoder, Jr., is succeeded as Coeditor by Dr. E. D. Jackson, U. S. Geological Survey (Menlo Park, California). The post of Senior Managing Editor held by Prof. G. Malcolm Brown will not be filled; however, Dr. J. D. Bell of Oxford University has been added to the staff of Managing Editors. Both men will continue to serve the Journal as members of the Honorary Advisory Board.

Volume 9 for 1968 consisted of 488 pages and contained a contribution by a Fellow of the Laboratory. Members of the staff of the Laboratory act as reviewers along with their international colleagues. The *Journal of Petrology* continues to provide a format of outstanding quality for data papers of long lasting value.

Lectures

During the report year Staff Members and Fellows were invited to present lectures as follows:

P. H. Abelson made a total of 16 invited public appearances. He made speeches in the following capacities: As Distinguished Lecturer ("Science and Society") at the University of Arkansas, Fayetteville; as organizer and participant in a Symposium on Science and Engineering Policies in Transition at the Carnegie Institution of Washington; as a participant in a Symposium on "The New View of the Origin of Life" ("Chemical Reactions on the Primitive Earth") at the annual meeting of the American Association for the Advancement of Science at Dallas, Texas; as speaker ("Science, Technology, and Ethics—An Agenda for the Future") at the dedication of a new Science Center and lecturer ("Chemical Events on the Primitive Earth") at a seminar at St. Olaf College, Northfield, Minnesota; as speaker ("Challenges for Tomorrow") at Centennial Year Symposium at Oregon State University, Corvallis; as speaker ("Science and Engineering Policies") at dinner of International Symposium on "A Critical Review of the Foundations of Relativistic and Classical Thermodynamics" at the Department of Chemical and Petroleum Engineering, University of Pittsburgh; and as a participant in a special meeting sponsored by the British and American Associations for the Advancement of Science at Boulder, Colorado.

P. M. Bell gave a series of three talks at the Geology Department, University of Cincinnati. He also addressed the Department of Geology at Northwestern University and the Department of Geochemistry and Mineralogy at Pennsylvania State University.

Gabrielle Donnay served as guest lecturer at the Sulfide Institute at Lehigh University.

P. E. Hare gave invited lectures at a Symposium on Organic Geochemistry of the Precambrian at the Annual Meeting of the Geological Society of America at Mexico City, a Symposium on Penetration of $CaCO_3$ Substrates by Lower Plants and Invertebrates at the Annual Meeting of the American Association for the Advancement of Science at Dallas, and a Symposium on Calcification and Skeletal Mineralogy at a Meeting of the Southeastern Section of the Geological Society of America at Columbia, S. C. He also addressed the Paleontological Society of Washington, the Institute of Molecular Evolution at the University of Miami, the Geology Department at Indiana University, and the Lamont Geological Observatory of Columbia University.

T. C. Hoering lectured on "Organic Geochemistry and the Record of Ancient Life" at a Symposium on the Origin of Life at California State College at Los Angeles.

T. E. Krogh addressed the Miller Geology Club at the Geology Department of Queen's University at Kingston, Ontario.

G. Kullerud continued as Adjunct Professor in Geochemistry at Lehigh University where he supervised the sulfide research program and lectured on sulfide phase equilibria. He served as a Visiting Professor at Heidelberg University and as Consulting Professor to the Department of Geosciences, Texas Technological College, Lubbock, Texas, where he also presented lectures on ore deposits. He served as director of a six-week Summer Institute in Sulfide Phase Equilibria and their Applications to Ores for College Teachers of Economic Geology sponsored by the National Science Foundation. In addition, he lectured at the Max Planck Institut für Kernphysik in Heidelberg, at the University in Tübingen, and at the University in Clausthal, Germany. He addressed the Geology Club at the Franklin and Marshall College, Lancaster, Pennsylvania, and lectured in the Department of Geology, University of Toronto, and the Mineral Sciences Di-

vision, Department of Energy, Mines, and Resources, at Ottawa, Canada. He was elected to the Council of the Mineralogical Society of America.

D. H. Lindsley addressed the Department of Geology at Queen's University, Kingston, Ontario. He spent the first six months of 1969 as Visiting Associate Professor at the Division of Geological Sciences, California Institute of Technology, where he led a seminar on experimental petrology.

H. O. A. Meyer participated in a meeting at Cologne to celebrate the 60th anniversary of the Deutsche Mineralogische Gesellschaft. He addressed the Geological Society of Washington and gave an invited lecture at the Department of Geological Sciences of Virginia Polytechnic Institute. In addition, he presented lectures at the Planetology Branch, National Aeronautics and Space Administration, Goddard Space Flight Center, and at the Department of Geochemistry and Mineralogy of the Pennsylvania State University.

H. S. Yoder, Jr., presented a talk on the "Experimental Data Bearing on the Calcalkaline Andesites" at the Andesite Conference in Eugene and Bend, Oregon, sponsored by the University of Oregon Center for Volcanology and the International Upper Mantle Committee. He participated in the discussions at the International Volcanological Association meeting at the University of Laguna, Tenerife, Canary Islands, and jointly presented a paper with Dr. Schairer. Invited lectures were also given by Yoder at Amherst College, University of Massachusetts, and Pennsylvania State University. He gave the principal address entitled "Major Problems of the Alkali Magma Series" at the Alkaline Rock Symposium held in conjunction with the joint annual meeting of the Geological Association of Canada and the Mineralogical Association of Canada in Montreal, Quebec.

Petrologists' Club

Five meetings were held during the 58th year of the Petrologists' Club. The following lectures were presented:

"Experimental studies of metamorphic reactions of haplopelites within the system K_2O-MgO-Al_2O_3-SiO_2-H_2O," by Freidrich Seifert (The Ruhr University, Bochum, Germany), October 15, 1968.

"Mineralogy and petrology of an olivine diabase sill and associated unusually potassic granophyres in central Arizona," by Douglas Smith (Geophysical Laboratory), January 14, 1969.

"State of water in the upper mantle and role of water in the formation of crustal materials," by I. Kushiro (Geophysical Laboratory), February 18, 1969.

"Meteorites, analytical error, kimberlite nodules, secondary alteration, and the composition of the upper mantle," by A. J. Erlank (Department of Terrestrial Magnetism), April 1, 1969.

"A petrogenetic grid in the system Al_2O_3-K_2O-FeO-SiO_2-H_2O and its application to the basement rocks of the Venezuelan Andes," by L. Kovisars (University of Pennsylvania), May 27, 1969.

BIBLIOGRAPHY

Allmann, R., *see* Donnay, G.

Bell, P. M., and F. R. Boyd, Phase equilibrium data bearing on the pressure and temperature of shock metamorphism, in *Shock Metamorphism of Natural Materials,* B. M. French and N. M. Short, eds., Mono Book Corp., Baltimore, Md., 43–50, 1968 (Geophysical Laboratory Paper 1533).

Bell, P. M., and B. T. C. Davis, Melting relations in the system jadeite-diopside at 30 and 40 kb, *Am. J. Sci., Schairer Vol., 267A,* 17–32, 1969 (G. L. Paper 1521).

Bell, P. M., *see also* Richardson, S. W.

Boyd, F. R., Electron-probe study of diopside inclusions from kimberlite, *Am. J. Sci., Schai-*

rer Vol., 267A, 50–69, 1969 (G. L. Paper 1522).

Boyd, F. R., *see also* Bell, P. M.

Bryan, W. B., L. W. Finger, and F. Chayes, Estimating proportions in petrographic mixing equations by least-squares approximation, *Science, 163,* 926–927, 1969 (G. L. Paper 1532).

Burnham, C. W., *see* Finger, L. W.

Carmichael, I. S. E., *see* Lindsley, D. H.

Chayes, F., A least squares approximation for estimating the amounts of petrographic partition products, *Mineral. Petrogr. Acta, 14,* 111–114, 1968 (G. L. Paper 1519).

Chayes, F., *see also* Bryan, W. B.

Davis, B. T. C., *see* Bell, P. M.

Davis, G. L., S. R. Hart, and G. R. Tilton, Some effects of contact metamorphism on zircon ages, *Earth Planet. Sci. Letters, 5,* 27–34, 1968 (G. L. Paper 1515).

Donnay, G., and R. Allmann, Si_3O_{10} groups in the crystal structure of ardennite, *Acta Cryst., B24,* 845–855, 1968 (G. L. Paper 1506).

Donnay, G., *see also* El Goresy, A.; Gaines, R. V.; Kullerud, G.

Donnay, J. D. H., *see* Kullerud, G.

El Goresy, A., and G. Donnay, A new allotropic form of carbon from the Ries crater, *Science, 161,* 363–364, 1968 (G. L. Paper 1513).

El Goresy, A., and G. Kullerud, Phase relations in the system Cr-Fe-S, in *Meteorite Research,* P. M. Millman, ed., D. Reidel Publishing Co., Dordrecht, Holland, 638–656, 1969 (G. L. Paper 1536).

Finger, L. W., and C. W. Burnham, Peak-width calculations for equi-inclination diffraction geometry, *Z. Krist., 127,* 101–109, 1968 (G. L. Paper 1507).

Finger, L. W., *see also* Bryan, W. B.

Gaines, R. V., G. Donnay, and M. H. Hey, Sonoraite, *Am. Mineralogist, 53,* 1828–1832, 1968 (G. L. Paper 1517).

Gilbert, M. C., High-pressure stability of acmite, *Am. J. Sci., Schairer Vol., 267A,* 145–159, 1969 (G. L. Paper 1523).

Gilbert, M. C., *see also* Richardson, S. W.; Wones, D. R.

Hadidiacos, C. G., Solid-state temperature controller, *J. Geol., 77,* 365–367, 1969 (G. L. Paper 1537).

Hart, S. R., *see* Davis, G. L.

Hey, M. H., *see* Gaines, R. V.

Huckenholz, H. G., Synthesis and stability of Ti-andradite, *Am. J. Sci., Schairer Vol., 267A,* 209–323, 1969 (G. L. Paper 1524).

Kullerud, G., The lead-sulfur system, *Am. J. Sci., Schairer Vol., 267A,* 233–256, 1969 (G. L. Paper 1525).

Kullerud, G., G. Donnay, and J. D. H. Donnay, Omission solid solution in magnetite: kenotetrahedral magnetite, *Z. Krist., 128,* 1–17, 1969 (G. L. Paper 1514).

Kullerud, G., *see also* El Goresy, A.; Naldrett, A. J.

Kushiro, I., The system forsterite-diopside-silica with and without water at high pressures, *Am. J. Sci., Schairer Vol., 267A,* 269–294, 1969 (G. L. Paper 1526).

Kushiro, I., H. S. Yoder, Jr., and M. Nishikawa, Effect of water on the melting of enstatite, *Geol. Soc. Am. Bull., 79,* 1685–1692, 1968 (G. L. Paper 1516).

Kushiro, I., *see also* Yoder, H. S., Jr.

Lindsley, D. H., I. S. E. Carmichael, and J. Nicholls, Iron-titanium oxides and oxygen fugacities in volcanic rocks: a correction, *J. Geophys. Res., 73,* 3351–3352, 1968 (G. L. Paper 1504).

Lindsley, D. H., and J. L. Munoz, Subsolidus relations along the join hedenbergite-ferrosilite, *Am. J. Sci., Schairer Vol., 267A,* 295–324, 1969 (G. L. Paper 1527).

Munoz, J. L., *see* Lindsley, D. H.

Naldrett, A. J., and G. Kullerud, Emplacement of ore at the Strathcona Mine, Sudbury, Canada, as a sulfide-oxide magma in suspension in young noritic intrusions, *Intern. Geol. Congr., 23rd, 7,* 197–213, 1968 (G. L. Paper 1503).

Nicholls, J., *see* Lindsley, D. H.

Nishikawa, M., *see* Kushiro, I.

Richardson, S. W., Staurolite stability in a part of the system Fe-Al-Si-O-H, *J. Petrol., 9,* 467–488, 1968 (G. L. Paper 1509).

Richardson, S. W., P. M. Bell, and M. C. Gilbert, Kyanite-sillimanite equilibrium between 700° and 1500°C, *Am. J. Sci., 266,* 513–541, 1968 (G. L. Paper 1508).

Richardson, S. W., M. C. Gilbert, and P. M. Bell, Experimental determination of kyanite-andalusite and andalusite-sillimanite equilibria; the aluminum silicate triple point, *Am. J. Sci., 267,* 259–272, 1969 (G. L. Paper 1518).

Schreyer, W., and F. Seifert, High-pressure phases in the system MgO-Al_2O_3-SiO_2-H_2O, *Am. J. Sci., Schairer Vol., 267A,* 407–443, 1969 (G. L. Paper 1534).

Seifert, F., *see* Schreyer, W.

Steiger, R. H., *see* Tilton, G. R.

Tilton, G. R., and R. H. Steiger, Mineral ages and isotopic composition of primary lead at Manitouwadge, Ontario, *J. Geophys. Res., 74,* 2118–2132, 1969 (G. L. Paper 1535).

Tilton, G. R., *see also* Davis, G. L.

Wones, D. R., and M. C. Gilbert, The fayalite-magnetite-quartz assemblage between 600° and 800°C, *Am. J. Sci., Schairer Vol., 267A,* 480–488, 1969 (G. L. Paper 1528).

Yoder, H. S., Jr., and I. Kushiro, Melting of a hydrous phase: phlogopite, *Am. J. Sci., Schairer Vol., 267A,* 558–582, 1969 (G. L. Paper 1529).

Yoder, H. S., Jr., *see also* Kushiro, I.

REFERENCES CITED

Ahrens, T. J., and J. T. Rosenberg, Shock metamorphism: experiments on quartz and plagioclase, in *Shock Metamorphism of Natural Materials,* B. M. French and N. M. Short, eds., Mono Book Corp., Baltimore, Md., 59–85, 1968.

Akimoto, S., H. Fujisawa, and T. Katsura, Synthesis of $FeSiO_3$ pyroxene (ferrosilite) at high pressures, *Proc. Japan Acad., 40,* 272–275, 1964.

Akimoto, S., and I. Kushiro, Natural occurrence of titanomaghemite and its relevance to the unstable magnetization of rocks, *J. Geomag. Geoelec., 11,* 94–110, 1960.

Akimoto, S., T. Nagata, and T. Katsura, The $TiFe_2O_5$-Ti_2FeO_5 solid solution series, *Nature, 179,* 37–38, 1957.

Alexander, L. E., and G. S. Smith, Single-crystal diffractometry: The improvement of accuracy in intensity measurements, *Acta Cryst., 17,* 1195–1201, 1964.

Aoki, K., Petrology of alkali rocks of the Iki Island and Higashi-Matsuura district, Japan, *Sci. Rept. Tohoku Univ., Third Ser., 6,* 261–310, 1959.

Aramaki, S., Sillimanite and cordierite from volcanic xenoliths, *Am. Mineralogist, 46,* 1156–1165, 1961.

Aramaki, S., and R. Roy, Revised phase diagram for the system Al_2O_3-SiO_2, *J. Am. Ceram. Soc., 45,* 229–242, 1962.

Arnold, R. G., Mixtures of hexagonal and monoclinic pyrrhotite and the measurement of the metal content of pyrrhotite by X-ray diffraction, *Am. Mineralogist, 51,* 1221–1227, 1966.

Arnold, R. G., Range in composition and structure of 82 natural terrestrial pyrrhotites, *Can. Mineralogist, 9,* 31–50, 1967.

Arnold, R. G., Pyrrhotite phase relations below $304° \pm 6°C$ at <1 atm total pressure, *Econ. Geol., 64,* 405–419, 1969.

Bailey, D. K., and R. MacDonald, Alkali-feldspar fractionation trends and the derivation of peralkaline liquids, *Am. J. Sci., 267,* 242–248, 1969.

Bailey, D. K., and J. F. Schairer, Feldspar-liquid equilibria in peralkaline liquids—the orthoclase effect, *Am. J. Sci., 262,* 1198–1206, 1964.

Bailey, D. K., and J. F. Schairer, The system Na_2O-Al_2O_3-Fe_2O_3-SiO_2 at 1 atmosphere, and the petrogenesis of alkaline rocks, *J. Petrol., 7,* 114–170, 1966.

Baker, I., and S. E. Haggerty, The alteration of olivine in basaltic and associated lavas, Part II, Intermediate and low-temperature alteration, *Contrib. Mineral. Petrol., 16,* 258–273, 1967.

Baker, P. E., I. G. Gass, P. G. Harris, and R. W. LeMaitre, The volcanological report of the Royal Society expedition to Tristan de Cunha, 1962, *Phil. Trans. Roy. Soc. London, Ser. A, 256,* 439–578, 1964.

Balchan, A. S., and H. G. Drickamer, High pressure electrical resistance cell, and calibration points above 100 kb, *Rev. Sci. Instr., 32,* 308–313, 1961.

Baltitude, R. J., and D. H. Green, Experimental study at high pressures on the origin of olivine nephelinite and olivine melilitite nepheline magmas, *Earth Planet. Sci. Letters, 3,* 325–337, 1967.

Banno, S., Garnet-pyroxene equilibrium in granulite facies rocks and inclusions in kimberlite and alkali basalt, *Japan. J. Geol. Geography, 36,* 23–36, 1965.

Banno, S., I. Kushiro, and Y. Matsuii, Notes on rock-forming minerals (20): Enstatite from a garnet-peridotite inclusion in kimberlite, *J. Geol. Soc. Japan, 69,* 157–159, 1963.

Barnes, V. E., G. Edwards, W. A. McLaughlin, I. Friedman, and D. Joensuu, Macusanite occurrence, age, and composition, Macusani, Peru, *Geol. Soc. Am. Bull.,* in press, 1970.

Bassett, W. A., T. Takahashi, and P. W. Stook, X-ray diffraction and optical observations on crystalline solids up to 300 kb, *Rev. Sci. Instr., 38,* 37–42, 1967.

Bergman, W., Evolutionary aspects of the sterols, in *Cholesterol,* R. P. Cook, ed., Academic Press, New York, 435–444, 1958.

Berner, R. A., Stability fields of iron minerals in anaerobic marine sediments, *J. Geol., 72,* 826–834, 1964.

Biggar, G. M., and M. J. O'Hara, Temperature control and calibration in quench furnaces and some new temperature measurements in the system CaO-MgO-Al_2O_3-SiO_2, *Mineral. Mag., 37,* 1–15, 1969.

Birle, J. D., G. V. Gibbs, P. B. Moore, and J. V. Smith, Crystal structures of natural olivines, *Am. Mineralogist, 53,* 807–824, 1968.

Bonatti, E., and Y. R. Nayudu, Origin of manganese nodules on the ocean floor, *Am. J. Sci., 263,* 17–39, 1965.

Bowen, N. L., The crystallization of haplobasaltic, haplodioritic and related magmas, *Am. J. Sci., 40,* 161–185, 1915.

Bowen, N. L., *Evolution of Igneous Rocks,* Princeton University Press, 1928.

Bowen, N. L., and J. W. Greig, The system Al_2O_3-SiO_2, *J. Am. Ceram. Soc., 7,* 238–256, 1924.

Bowen, N. L., and J. F. Schairer, The system MgO-FeO-SiO_2, *Am. J. Sci., 29,* 151–217, 1935.

Bown, M. G., and P. Gay, An X-ray study of exsolution phenomena in the Skaergaard pyroxenes, *Mineral. Mag., 32,* 379–388, 1960.

Boyd, F. R., Hydrothermal investigations of amphiboles, in *Researches in Geochemistry,* Vol. 1, P. H. Abelson, ed., John Wiley and Sons, Inc., New York, 377–396, 1959.

Boyd, F. R., Petrological problems in high pressure research, in *Researches in Geochemistry,* Vol. 2, P. H. Abelson, ed., John Wiley and Sons, Inc., New York, 593–618, 1967.

Boyd, F. R., Electron-probe study of diopside inclusions from kimberlite, *Am. J. Sci., Schairer Vol., 267A,* 50–69, 1969.

Boyd, F. R., and G. M. Brown, Electron-probe study of pyroxene exsolution, *Mineral. Soc. Am. Spec. Paper, 2,* 211–216, 1969.

Boyd, F. R., and J. L. England, Apparatus for phase-equilibrium measurements at pressures up to 50 kb and temperatures up to 1750°C, *J. Geophys. Res., 65,* 741–748, 1960.

Boyd, F. R., and J. F. Schairer, The system $MgSiO_3$-$CaMgSi_2O_6$, *J. Petrol., 5,* 275–309, 1964.

Bridgman, P. W., Polymorphic transitions of 35 substances to 50,000 kg/cm^2, *Proc. Am. Acad. Arts Sci., 72,* 45–136, 1937.

Bridgman, P. W., The compression of twenty-one halogen compounds and eleven other simple substances to 100,000 kg/cm^2, *Proc. Am. Acad. Arts Sci., 76,* 1–7, 1945.

Brookins, D. G., Re-examination of pyrope from the Stockdale kimberlite, Riley Co., Kansas, *Mineral. Mag., 36,* 450–452, 1967.

Brooks, E. R., Multiple metamorphism along the Grenville Front, north of Georgian Bay, Ontario, *Geol. Soc. Am. Bull., 78,* 1267–1280, 1967.

Bryan, W. B., Relative abundance of intermediate members of the oceanic basalt-trachyte association: evidence from Clarion and Socorro Islands, Revillagigedo Islands, Mexico, *J. Geophys. Res., 69,* 3047–3049, 1964.

Bryan, W. B., History and mechanism of eruption of soda-rhyolite and alkali basalt, Socorro Island, Mexico, *Bull. Volcanol., 29,* 453–480, 1966.

Bryan, W. B., Geology and petrology of Clarion Island, Mexico, *Geol. Soc. Am. Bull., 78,* 1461–1476, 1967.

Bryan, W. B., Low-potash dacite drift pumice from the Coral Sea, *Geol. Mag., 105,* 431–439, 1968.

Bryan, W. B., L. W. Finger, and F. Chayes, Estimating proportions in petrographic mixing equations by least-squares approximation, *Science, 163,* 926–927, 1969.

Bunch, T. E., and K. Keil, Chromite and ilmenite from non-chondritic meteorites, submitted to *Am. Mineralogist,* 1969.

Bunch, T. E., K. Keil, and E. Olsen, Mineral compositions and petrology of silicate inclusions in iron meteorites, *Contrib. Mineral. Petrol.,* in press, 1969.

Bundy, F. P., Fe-Co and Fe-V alloys for pressure calibration in the 130- to 300-kb region, *J. Appl. Phys., 38,* 2446–2449, 1967.

Burnham, C. W., J. R. Clark, J. J. Papike, and C. T. Prewitt, A proposed crystallographic nomenclature for clinopyroxene structures, *Z. Krist., 125,* 109–119, 1967.

Burns, R. G., Apparatus for measuring polarized absorption spectra of small crystals, *J. Sci. Instr., 43,* 58–60, 1966.

Burns, R. G., Optical absorption in silicates, in *The Application of Modern Physics to the Earth and Planetary Interiors,* S. K. Runcorn, ed., John Wiley and Sons, Inc., New York, in press, 1969.

Burns, R. G., and W. Fyfe, Crystal-field theory and the geochemistry of transition elements, in *Researches in Geochemistry,* Vol. 2, P. H. Abelson, ed., John Wiley and Sons, Inc., 259–285, 1967.

Carmichael, I. S. E., Natural liquids and the phonolitic minimum, *Geol. J., 4,* 55–60, 1964.

Carmichael, I. S. E., and W. S. MacKenzie, Feldspar-liquid equilibria in pantellerites: an experimental study, *Am. J. Sci., 261,* 382–396, 1963.

Chayes, F., Relative abundance of intermediate members of the oceanic basalt-trachyte association, *J. Geophys. Res., 68,* 1519–1534, 1963*a*.

Chayes, F., Author's reply to the preceding discussion, *J. Geophys. Res., 68,* 5108–5109, 1963*b*.

Chayes, F., Variance-covariance relations in some published Harker diagrams of volcanic suites, *J. Petrol., 5,* 219–237, 1964.

Chayes, F., The chemical composition of Cenozoic andesites, in "Proceedings of the Andesite Conference," A. R. McBirney, ed., *Oregon Dept. Geol. Mineral. Ind. Bull., 65,* 1–11, 1969.

Chayes, F., On estimating the magnitude of the hidden zone and the compositions of the residual liquids of the Skaergaard layered series, *J. Petrol.,* in press, 1970.

Chikashige, M., and T. Aoki, Metallographic investigation of the system aluminum-selenium, *Mem. Coll. Sci. Kyoto Imperial Univ., 2,* 249–254, 1917.

Chikashige, M., and J. Nosé, Metallographic investigation of the system aluminum-tellurium, *Mem. Coll. Sci. Kyoto Imperial Univ., 2,* 227–232, 1917.

Chinner, G. A., and J. F. Schairer, The join $Ca_3Al_2Si_3O_{12}$-$Mg_3Al_2Si_3O_{12}$ and its bearing on the system CaO-MgO-Al_2O_3-SiO_2 at atmospheric pressure, *Am. J. Sci., 260,* 611–634, 1962.

Clark, A. H., Stability field of monoclinic pyrrhotite, *Trans. Inst. Mining Met., Sect. B, 75,* 232–235, 1966.

Clark, J. R., and J. J. Papike, Crystal-chemical characterization of omphacites, *Am. Mineralogist, 53,* 840–868, 1968.

Clark, L. A., and G. Kullerud, The sulfur-rich portion of the Fe-Ni-S system, *Econ. Geol., 58,* 853–885, 1963.

Clark, S. P., Jr., Infrared spectra of minerals, *Am. Mineralogist, 42,* 732–740, 1957.

Clark, S. P., and A. E. Ringwood, Density distribution and constitution of the mantle, *Rev. Geophys., 2,* 35–88, 1964.

Corlett, M., Low-iron polymorphs in the pyrrhotite group, *Z. Krist., 126,* 124–134, 1968.

Cromer, D. T., Anomalous dispersion corrections computed from self-consistent field relativistic Dirac-Slater wave functions, *Acta Cryst., 18,* 17–23, 1965.

Cromer, D. T., and J. B. Mann, X-ray scattering factors computed from numerical Hartree-Fock wave functions, *Acta Cryst., A24,* 321–324, 1968.

Cronan, D. S., and J. S. Tooms, The geochemistry of manganese nodules and associated pelagic deposits from the Pacific and Indian Oceans, *Deep-Sea Res., 16,* 1–25, 1969.

Curtis, C. D., Applications of the crystal-field theory to the inclusion of trace transition elements in minerals during magmatic differentiation, *Geochim. Cosmochim. Acta, 28,* 389–403, 1964.

Davis, B. T. C., and F. R. Boyd, The join $Mg_2Si_2O_6$-$CaMgSi_2O_6$ at 30 kb pressure and its application to pyroxenes from kimberlites, *J. Geophys. Res., 71,* 3567–3576, 1966.

Deer, W. A., R. A. Howie, and J. Zussman, *Rock-Forming Minerals,* Vol. 4, John Wiley and Sons, Inc., New York, 1963.

Degens, E. T., *Geochemistry of Sediments,* Prentice-Hall, Inc., Englewood Cliffs, N. J., 1965.

Deland, A. N., The boundary between the Timiskaming and Grenville subprovince in the Surprise Lake area, Quebec, *Proc. Geol. Assoc. Can., 8,* 127–141, 1956.

Desborough, G. A., and R. H. Carpenter, Phase relations of pyrrhotite, *Econ. Geol., 60,* 1431–1450, 1965.

Destenay, D., Structure cristalline de la triphyline, *Mém. Soc. Roy. Sci. Liège, 10,* no. 3, 5–28, 1950.

DeVries, R. C., and E. F. Osborn, Phase equilibria in high-alumina part of the system CaO-MgO-Al_2O_3-SiO_2, *J. Am. Ceram. Soc., 40,* 6–15, 1957.

Donnay, G., J. M. Stewart, and H. Preston, The crystal structure of sonoraite, $Fe^{3+}Te^{4+}O_3(OH)\cdot H_2O$, *Tschermaks Mineral. Petrog. Mitt.,* in press, 1969.

Doyle, R. W., Identification and solubility of iron sulfide in anaerobic lake sediment, *Am. J. Sci., 266,* 980–994, 1968.

Drickamer, H. G., The effect of high pressure on the electronic structure of solids, *Solid State Phys., 17,* 1–133, 1965.

Drickamer, H. G., G. K. Lewis, Jr., and S. C. Fung, The oxidation state of iron at high pressure, *Science, 163,* 885–890, 1969.

Elliott, C. J., and A. A. Moss, Natural glass from Macusani, Peru, *Mineral. Mag., 35,* 423–424, 1964.

Elliott, R. P., *Constitution of Binary Alloys,* 1st Suppl., McGraw-Hill Book Co., Inc., New York, 1965.

Erd, R. C., H. T. Evans, and H. D. Richter, Smythite, a new iron sulfide and associated pyrrhotite from Indiana, *Am. Mineralogist, 42,* 309–333, 1957.

Eremenko, V. N., and G. I. Kruchinina, On the composition diagram of the system nickel-antimony, *Tr. Inst. Chernoi Met. Kiev, 5,* 110–122, 1951.

Ernst, W. G., *Amphiboles; Crystal Chemistry, Phase Relations, and Occurrence,* Springer-Verlag, New York, 1968.

Fiala, J., Pyrope of some garnet peridotites of the Czech massif, *Krystalinikum, 3,* 55–74, 1965.

Finger, L. W., The crystal structure and cation distribution of a grunerite, *Mineral. Soc. Am. Spec. Paper, 2,* 95–100, 1969.

Fischer, K., A further refinement of the crystal structure of cummingtonite, $(Mg,Fe)_7Si_8O_{22}(OH)_2$, *Am. Mineralogist, 51,* 814–818, 1966.

Fiske, R. S., Recognition and significance of pumice in marine pyroclastic rocks, *Geol. Soc. Am. Bull., 80,* 1–8, 1969.

Fleet, M. E., On the lattice parameters and superstructures of pyrrhotites, *Am. Mineralogist, 53,* 1846–1855, 1968.

Foerstner, H., Das Gestein der Insel Ferdinandea (1831) und seine Beziehungen zu den jüngsten Laven Pantellerias und des Aetnas, *Tschermaks Mineral. Petrog. Mitt., 5,* 388–396, 1883.

Foshag, W. F., Mineralogical studies on Guatemalan jade, *Smithsonian Inst. Misc. Collections, 135,* no. 5, Publ. 4307, 60 pp., 1957.

Fox, P. J., and B. C. Heezen, Sands of the Mid-Atlantic Ridge, *Science, 149,* 1367–1370, 1965.

Fukao, Y., H. Mizutani, and S. Uyeda, Optical absorption spectra at high temperatures and radiative thermal conductivity of olivines, *Phys. Earth Planet. Interiors, 1,* 57–62, 1968.

Fürst, U., and F. Halla, Röntgenographische Untersuchungen in den Systemen Mn-Bi, Co-Sb, Ni-Sb, *Z. Physik. Chem., Abt. B, 40,* 285–307, 1938.

Fyfe, W., The possibility of *d*-electron coupling in olivine at high pressures, *Geochim. Cosmochim. Acta, 19,* 141–143, 1960.

Gaines, R. V., G. Donnay, and M. H. Hey, Sonoraite, *Am. Mineralogist, 53,* 1828–1832, 1968.

Gaskell, T. F., Comparisons of Pacific and Atlantic Ocean floors in relation to ideas of continental displacement, in *Continental Drift,* S. K. Runcorn, ed. Academic Press, New York, 299–307, 1962.

Gass, I. G., P. G. Harris, and M. W. Holdgate, Pumice eruption in the area of the South Sandwich Islands, *Geol. Mag., 100,* 321–330, 1963.

Gast, P. W., Trace element fractionation and the origin of tholeiitic and alkaline magma types, *Geochim. Cosmochim. Acta, 32,* 1057–1086, 1968.

Geller, S., and J. L. Durand, Refinement of the structure of $LiMnPO_4$, *Acta Cryst., 13,* 325–331, 1960.

Gheith, M. A., Differential thermal analysis of certain iron oxides and oxide hydrates, *Am. J. Sci., 250,* 677–695, 1952.

Gheith, M. A., Lipscombite, a new synthetic "iron lazulite," *Am. Mineralogist, 38,* 612–628, 1953.

Ghose, S., The crystal structure of a cummingtonite, *Acta Cryst., 14,* 622–627, 1961.

Ghose, S., A scheme of cation distribution in the amphiboles, *Mineral. Mag., 35,* 46–54, 1965.

Ghose, S., and E. Hellner, The crystal structure of a grunerite and observations on the Mg-Fe distribution, *J. Geol., 67,* 691–701, 1959.

Gilluly, J., Geological contrasts between continents and ocean basins, *Geol. Soc. Am. Spec. Paper, 62,* 7–18, 1955.

Gossner, B., and H. Strunz, Über strukturelle Beziehungen zwischen Phosphaten (Triphylin) und Silicaten (Olivin) und über die chemische Zusammensetzung von Ardennit, *Z. Krist., 83,* 415–421, 1932.

Green, D. H., Origin of basalt magmas, in *Basalts: The Poldervaart Treatise on Rocks of Basaltic Composition,* Vol. 2, H. H. Hess and A. Poldervaart, ed., Interscience Publishers, New York, 835–862, 1968.

Greenwood, H. J., The synthesis and stability of anthophyllite, *J. Petrol., 4,* 317–351, 1963.

Greig, J. W., and T. F. W. Barth, The system $Na_2O \cdot Al_2O_3 \cdot 2SiO_2$ (nepheline, carnegieite)-$Na_2O \cdot Al_2O_3 \cdot 6SiO_2$ (albite), *Am. J. Sci., 35A,* 113–125, 1938.

Grønvold, F., and H. Haraldsen, On the phase relations of synthetic and natural pyrrhotites ($Fe_{1-x}S$), *Acta Chem. Scand., 6,* 1452–1469, 1952.

Haggerty, S. E., The Fe-Ti oxides in Icelandic basic rocks and their significance in rock magnetism, unpublished Ph.D. thesis, University of London, 1968.

Hall, H. T., and R. A. Yund, Pyrrhotite phase relations below 325°C (abstract), *Geol. Soc. Am. Spec. Paper, 101,* 82–83, 1966.

Hamilton, W. C., On the treatment of unobserved reflexions in the least-squares adjustment of structures, *Acta Cryst., 8,* 185–186, 1955.

Hamilton, W. C., On the isotropic temperature factor equivalent to a given anisotropic temperature factor, *Acta Cryst., 12,* 609–610, 1959.

Hamilton, W. C., Significance tests on the crystallographic R factor, *Acta Cryst., 18,* 502–510, 1965.

Hansen, M., and K. Anderko, *Constitution of Binary Alloys,* McGraw-Hill Book Co., Inc., New York, 2nd ed., 1958.

Haraldsen, H., Über die Hocktemperaturumwandlungen der Eisen (II)-Sulfidmischkristalle, *Z. Anorg. Allgem. Chem., 246,* 195–226, 1941.

Harrison, C. G. A., and M. N. A. Peterson, A magnetic mineral from the Indian Ocean, *Am. Mineralogist, 50,* 704–712, 1965.

Hart, S. R., and L. T. Aldrich, Fractionation of potassium/rubidium by amphiboles: Implications regarding mantle composition, *Science, 155,* 325–327, 1967.

Haug, P. A., Applications of mass spectrometry to organic geochemistry, Ph.D. thesis, University of California, Berkeley, 1963.

Henderson, J. R., Structural and petrographic relations across the Grenville province–Southern province boundary, Sudbury district, Ontario, unpublished Ph.D. thesis, McMaster University, October 1967.

Henry, N. F. M., Some data on the iron-rich hypersthenes, *Mineral. Mag., 24,* 221–226, 1935.

Hess, H. H., Pyroxenes of common mafic magmas, Part 2, *Am. Mineralogist, 26,* 573–594, 1941.

Hijikata, K., and K. Yagi, Phase relations of Ca-Tschermak's molecule at high pressures and temperatures, *J. Fac. Sci. Hokkaido Univ., Ser. IV, 13,* 407–417, 1967.

International Tables of X-Ray Crystallography, Vol. 3, Kynoch Press, England, 1962.

Irvine, T. N., Chromian spinel, a petrogenetic indicator, Part 2, Petrologic applications, *Can. J. Earth Sci., 4,* 71–103, 1967.

Ito, T., and N. Morimoto, Anthophyllite, in *X-Ray Studies on Polymorphism,* Maruzen Co., Ltd., Tokyo, 42–49, 1950.

James, O. B., in Geological Survey Research 1969, *U. S. Geol. Surv. Prof. Paper,* in press, 1969.

Jamieson, J. C., and B. Olinger, Pressure inhomogeneity—a possible source of error in using internal standards for pressure gages, in *Symposium on the Accurate Characterization of the High-Pressure Environment,* October 1968, U. S. Department of Commerce, National Bureau of Standards, 1968.

Johansson, K., Vergleichende Untersuchungen an Anthophyllits, Grammatit und Cummingtonit, *Z. Krist., 73,* 31–51, 1930.

Johnston, W. G. Q., Geology of the Temiskaming-Grenville contact southeast of Lake Temagami, northern Ontario, Canada, *Bull. Geol. Soc. Am., 65,* 1047–1074, 1954.

Katz, L., and W. N. Lipscomb, The crystal structure of iron lazulite, a synthetic mineral related to lazulite, *Acta Cryst., 4,* 345–348, 1951.

Keen, M. J., Magnetization of sediment cores from the eastern Atlantic Ocean, *Nature, 187,* 220–222, 1960.

Kendall, M. G., *Rank Correlation Methods,* Griffin & Co., London, 1948.

Kennedy, G. C., and B. E. Nordlie, The genesis of diamond deposits, *Econ. Geol., 63,* 495–503, 1968.

Kingston, G. A., The occurrence of platinoids and bismuthotellurides in the Merensky reef at Rustenburg platinum mine in the western Bushveld, *Mineral. Mag., 35,* 815–834, 1966.

Klein, C., Jr., and D. R. Waldbaum, X-ray crystallographic properties of the cummingtonite-grunerite series, *J. Geol., 75,* 379–392, 1967.

Kracek, F. C., Phase relations in the system sulfur-silver and the transitions in silver sulfide, *Trans. Am. Geophys. Union, 27,* 364–374, 1946.

Krogh, T. E., and P. M. Hurley, Strontium isotope variation and whole-rock isochron studies, Grenville province of Ontario, *J. Geophys. Res., 73,* 7107–7125, 1968.

Kullerud, G., Sulfide studies, in *Researches in Geochemistry,* Vol. 2, P. H. Abelson, ed., John Wiley and Sons, Inc., New York, 286–321, 1967.

Kullerud, G., and R. A. Yund, The Ni-S system and related minerals, *J. Petrol., 3,* 126–175, 1962.

Kuno, H., Study of orthopyroxenes from volcanic rocks, *Am. Mineralogist, 39,* 30–46, 1954.

Kuno, H., Mafic and ultramafic nodules from Itinome-gata, Japan, in *Ultramafic and Related Rocks,* P. J. Wyllie, ed., John Wiley and Sons, Inc., New York, 337–342, 1967.

Kuno, H., Mafic and ultramafic nodules in basaltic rocks of Hawaii, *Geol. Soc. Am. Mem., Poldervaart Vol.,* in press, 1969.

Kushiro, I., Si-Al relation in clinopyroxenes from igneous rocks, *Am. J. Sci., 258,* 548–554, 1960.

Kushiro, I., Compositions of magmas formed by partial zone melting in the earth's upper mantle, *J. Geophys. Res., 73,* 619–634, 1968.

Kushiro, I., Clinopyroxene solid solutions formed by reactions between diopside and plagioclase at high pressures, *Mineral. Soc. Am. Spec. Paper, 2,* 179–191, 1969.

Kushiro, I., and K. Aoki, Origin of some eclogite inclusions in kimberlite, *Am. Mineralogist, 53,* 1347–1367, 1968.

Kushiro, I., Y. Syono, and S. Akimoto, Effect of pressure on garnet-pyroxene equilibrium in the system $MgSiO_3$-$CaSiO_3$-Al_2O_3, *Earth Planet. Sci. Letters, 2,* 460–464, 1967*a*.

Kushiro, I., Y. Syono, and S. Akimoto, Stability of phlogopite at high pressures and possible presence of phlogopite in the earth's upper mantle, *Earth Planet. Sci. Letters, 3,* 197–203, 1967*b*.

Kushiro, I., Y. Syono, and S. Akimoto, Melting of a peridotite nodule at high pressures and high water pressures, *J. Geophys. Res., 73,* 6023–6029, 1968.

Kushiro, I., H. S. Yoder, Jr., and M. Nishikawa, Effect of water on the melting of enstatite, *Geol. Soc. Am. Bull., 79,* 1685–1692, 1968.

LaBerge, G. L., Microfossils and Precambrian iron formations, *Geol. Soc. Am. Bull., 78,* 331–342, 1967.

LaCroix, A., Les ponces dacitiques flottant sur l'ocean, entre des Fiji, les Nouvelles-Hebrides, et la Nouvelle-Calédonie, *Compt. Rend., 208,* 853–857, 1939.

Lambert, I. B., and P. J. Wyllie, Stability of hornblende and a model for the low velocity zone, *Nature, 219,* 1240–1241, 1968.

Lausen, C., The occurrence of olivine bombs near Globe, Arizona, *Am. J. Sci., 14,* 293–306, 1927.

Lepp, H., Stages in the oxidation of maghemite, *Am. Mineralogist, 42,* 679–681, 1957.

Li, C. T., The crystal structure of $LiAlSi_2O_6$ III (high-quartz solid solution), *Z. Krist., 127,* 327–348, 1968.

Linck, G., Ein neuer kristallführender Tektit von Paucartambo in Peru, *Chem. Erde, 2,* 157–174, 1926.

Lindberg, M. L., Manganoan lipscombite from the Sapucaia pegmatite mine, Minas Gerais, Brazil; first occurrence of lipscombite in nature, *Am. Mineralogist, 47,* 353–359, 1962.

Lindemann, W., Beitragzur Struktur des Anthophyllits (abstract), *Fortschr. Mineral., 42,* 205, 1965.

Lindsley, D. H., and J. L. Munoz, Subsolidus relations along the join hedenbergite-ferrosilite, *Am. J. Sci., Schairer Vol., 267A,* 295–324, 1969.

Lippincott, E. R., L. S. Whatley, and H. C. Duecker, Microtechniques using miniaturized diamond optics, in *Applied Infrared Spectroscopy,* D. Kendall, ed., Reinhold Book Corp., New York, 435–461, 1966.

Love, L. G., and G. C. Amstutz, Review of microscopic pyrite from the Devonian Chattanooga Shale and Rammelsberg Banderz, *Fortschr. Mineral., 43,* 273–309, 1966.

Luth, W. C., R. H. Jahns, and O. F. Tuttle, The granite system at pressures of 4 to 10 kb, *J. Geophys. Res., 69,* 759–773, 1964.

Lynn, D. C., and E. Bonatti, Mobility of manganese in diagenesis of deep-sea sediments, *Marine Geol., 3,* 457–474, 1965.

Macdonald, G. A., Dissimilarity of continental and oceanic rock types, *J. Petrol., 1,* 172–177, 1960.

MacGregor, I. D., The system MgO-SiO_2-TiO_2 and its bearing on the distribution of TiO_2 in basalts, *Am. J. Sci., Schairer Vol., 267A,* 342–363, 1969.

Mansuri, Q. A., Intermetallic actions; the system thallium-arsenic, *J. Inst. Metals, 28,* 453–468, 1922.

Mao, H. K., The pressure dependence of the lattice parameters and volume of ferromagnesian spinels and its implications to the earth's mantle, Ph.D. thesis, University of Rochester, Rochester, New York, 1967.

Mao, H. K., W. A. Bassett, and T. Takahashi, Effect of pressure on crystal structure and lattice parameters of iron up to 300 kb, *J. Appl. Phys., 38,* 272–276, 1967.

Mao, H. K., T. Takahashi, W. A. Bassett, J. S. Weaver, and S. Akimoto, Effect of pressure and temperature on the molar volumes of

wüstite and of three $(Fe,Mg)_2SiO_4$ spinel solid solutions, *J. Geophys. Res., 74,* 1061–1069, 1969.

Martin, R., and C. de Sitter-Koomans, Pseudotectites from Colombia and Peru, *Leidse Geol. Mededel., 20,* 151–164, 1955.

Mason, B., Kaersutite from San Carlos, Arizona, with comments on the paragenesis of this mineral, *Mineral. Mag., 36,* 997–1002, 1968.

Medaris, L. G., Jr., Partitioning of Fe^{++} and Mg^{++} between coexisting synthetic olivine and orthopyroxene, *Am. J. Sci., 267,* 945–968, 1969.

Melson, W. G., 1967–1968 eruption of Metis Shoal, Tonga: description and petrology, *Smithsonian Contrib. Earth Sci.,* in press, 1969.

Melson, W. G., E. Jarosewich, V. T. Bowen, and G. Thompson, St. Peter and St. Paul Rocks: A high temperature, mantle-derived intrusion, *Science, 155,* 1532–1535, 1967.

Menard, H. W., *Marine Geology of the Pacific,* McGraw-Hill Book Co., New York, 1964.

Mero, J. L., Ocean floor manganese nodules, *Econ. Geol., 57,* 747–767, 1962.

Meyer, H. O. A., Chrome pyrope: an inclusion in natural diamond, *Nature, 160,* 1446–1447, 1968.

Milton, C., B. Ingram, J. R. Clark, and E. J. Dwornik, Mckelveyite, a new hydrous sodium barium rare-earth uranium carbonate mineral from the Green River formation, Wyoming, *Am. Mineralogist, 50,* 593–612, 1965.

Mrose, M. E., Vernadskite discredited: pseudomorphs of antlerite after dolerophanite, *Am. Mineralogist, 46,* 146–154, 1961.

Muir, I. D., and C. E. Tilley, Mugearites and their place in alkali igneous rock series, *J. Geol., 69,* 186–203, 1961.

Nicholls, G. D., Geochemical studies in the ocean as evidence for the composition of the mantle, in *Mantle of the Earth and Terrestrial Planets,* S. K. Runcorn, ed., Interscience Publishers, New York, 285–304, 1967.

Nixon, P. H., and G. Hornung, A new chromium garnet end member, knorringite, from kimberlite, *Am. Mineralogist, 53,* 1833–1840, 1968.

Nixon, P. H., O. von Knorring, and J. M. Rooke, Kimberlites and associated inclusions of Basutoland: A mineralogical and geochemical study, *Am. Mineralogist, 48,* 1090–1132, 1963.

O'Hara, M. J., Primary magmas and the origin of basalts, *Scot. J. Geol., 1,* 19–40, 1965.

O'Hara, M. J., Mineral parageneses in ultrabasic rocks, in *Ultramafic and Related Rocks,* P. J. Wyllie, ed., John Wiley and Sons, Inc., New York, 393–403, 1967.

O'Hara, M. J., The bearing of phase equilibria studies in synthetic and natural systems on the origin and evolution of basic and ultrabasic rocks, *Earth Sci. Rev., 4,* 69–133, 1968.

O'Hara, M. J., and G. M. Biggar, Diopside + spinel equilibria, anorthite and forsterite reaction relationships in silica-poor liquids in the system $CaO\text{-}MgO\text{-}Al_2O_3\text{-}SiO_2$ at atmospheric pressure and their bearing on the genesis of melilites and nephelinites, *Am. J. Sci., Schairer Vol., 267A,* 364–390, 1969.

O'Hara, M. J., and E. L. P. Mercy, Petrology and petrogenesis of some garnetiferous peridotites, *Trans. Roy. Soc. Edinburgh, 65,* 251–314, 1963.

O'Hara, M. J., and E. L. P. Mercy, Exceptionally calcic pyralspite from South African kyanite eclogite, *Nature, 212,* 68–69, 1966.

O'Hara, M. J., and H. S. Yoder, Jr., Formation and fractionation of basic magmas at high pressures, *Scot. J. Geol., 3,* 67–117, 1967.

Opdyke, N., B. Glass, J. D. Hays, and J. Foster, Paleomagnetic study of Antarctic deep-sea cores, *Science, 154,* 349–357, 1966.

Osawa, A., and N. Sibata, An X-ray investigation of nickel-antimony alloys, *Nippon Kinzoku Gakkaishi, 4,* 362–368, 1940.

Osborn, E. F., The system $CaSiO_3$-diopside-anorthite, *Am. J. Sci., 240,* 751–788, 1942.

Oxburgh, E. R., Petrological evidence for the presence of amphibole in the upper mantle and its petrogenetic and geophysical implications, *Geol. Mag., 101,* 1–19, 1964.

Pankey, T., and F. Senftle, Magnetic susceptibility of natural rutile, anatase, and brookite, *Am. Mineralogist, 44,* 1307–1309, 1959.

Parks, C. F., A magnetite "flow" in northern Chile, *Econ. Geol., 56,* 431–436, 1961.

Pauling, L., The principles determining the structure of complex ionic crystals, *J. Am. Chem. Soc., 51,* 1010–1026, 1929.

Phemister, T. C., The boundary between the Timiskaming and Grenville subprovinces in the townships of Neelon, Dryden, Dill, and Broder, District of Sudbury, *Ontario Dept. Mines Prelim. Rept., 1961–5,* 1961.

Phillipi, G. T., On the depth, time and mechanism of petroleum generation, *Geochim. Cosmochim. Acta, 29,* 1021–1049, 1965.

Philpotts, A. R., Origin of certain iron-titanium oxide and apatite rocks, *Econ. Geol., 62,* 303–315, 1967.

Powell, H. E., and L. N. Ballard, Magnetic susceptibility of 34 manganese-bearing minerals, *U. S. Bur. Mines Inform. Circ., 8359,* 1–10, 1968.

Quirke, T. T., and W. H. Collins, The disappearance of the Huronian, *Geol. Surv. Can. Mem., 160,* 1930.

Rabbitt, J. C., A new study of the anthophyllite series, *Am. Mineralogist, 33,* 263–323, 1948.

Ramdohr, P., *Die Erzmineralien und ihre Verwachsungen,* Akademie-Verlag, Berlin, 1950.

Raup, D. M., Crystal orientations in the echinoid apical system, *J. Paleont., 39,* 934–951, 1965.

Raup, D. M., The endoskeleton, in *Physiology of Echinodermata,* R. A. Boolootian, ed., Interscience Publishers, New York, 379–395, 1966.

Reinders, W., and F. Goudriaan, Die Röstreaktionsarbeit bei Kupfer; Gleichgewichte in System Cu-S-O, *Z. Anorg. Chem., 126,* 85–103, 1923.

Richards, A. F., Transpacific distribution of floating pumice from Isla San Benedicto, Mexico, *Deep-Sea Res., 5,* 29–35, 1958.

Richards, A. F., Geology of the Islas Revillagigedo, Mexico, 1, Birth and development of Volcan Barcena, Isla San Benedicto, *Bull. Volcanol., 22,* 73–123, 1959.

Richardson, F. D., and J. H. E. Jeffes, The thermodynamics of substances of interest in iron and steel making; III, Sulfides, *J. Iron Steel Inst. (London), 171,* 1034–1038, 1952.

Richardson, S. W., P. M. Bell, and M. C. Gilbert, Kyanite-sillimanite equilibrium between 700° and 1500°C, *Am. J. Sci., 266,* 513–541, 1968.

Richardson, S. W., M. C. Gilbert, and P. M. Bell, Experimental determination of kyanite-andalusite and andalusite-sillimanite equilibria; the aluminum silicate triple point, *Am. J. Sci., 267,* 259–272, 1969.

Ringwood, A. E., Mineralogy of the mantle, in *Advances in Earth Science,* P. M. Hurley, ed., M.I.T. Press, Cambridge, Mass., 357–399, 1966.

Ringwood, A. E., The pyroxene-garnet transformation in the earth's mantle, *Earth Planet. Sci. Letters, 2,* 255–263, 1967.

Roberts, H. S., Polymorphism in the FeS-S solid solution, I, Thermal study, *J. Am. Chem. Soc., 57,* 1034–1038, 1935.

Robie, R. A., and D. R. Waldbaum, Thermodynamic properties of minerals and related substances at 298.15°K (25.0°C) and 1 atmosphere (1.013 bars) pressure and at higher temperatures, *U. S. Geol. Surv. Bull., 1259,* 1968.

Roedder, E., Liquid CO_2 inclusions in olivine-bearing nodules and phenocrysts from basalts, *Am. Mineralogist, 50,* 1746–1782, 1965.

Roedder, E., and D. S. Coombs, Immiscibility in granitic melts, indicated by fluid inclusions in ejected granitic blocks from Ascension Island, *J. Petrol., 8,* 417–451, 1967.

Rogers, D. P., The extrusive iron oxide deposits, "El Laco," Chile (abstract), Geological Society of America, Program with Abstracts of the 1968 Annual Meetings, Mexico City, Mexico, 252–253, 1968.

Romano, R., New petrochemical data of volcanites from the island of Pantelleria (Channel of Sicily), *Geol. Rundschau, 57,* 773–783, 1968.

Rooymans, C., and W. Albers, High-pressure polymorphism of Cr_2FeS_4 and related compounds, preprint, pp. 63–66, 1967.

Rosenqvist, T., A thermodynamic investigation of the system silver-silver sulfide, *Trans. Am. Inst. Mining Met. Engrs., 185,* 451–460, 1949.

Rosenqvist, T., Magnetic and crystallographic studies on the higher antimonides of iron, cobalt, and nickel, *Acta Met., 1,* 761–763, 1953.

Ross, C. S., M. D. Foster, and A. T. Myers, Origin of dunites and of olivine-rich inclusions in basaltic rocks, *Am. Mineralogist, 39,* 693–737, 1954.

Roy, R., A. J. Majumdar, and C. W. Hulbe, The Ag_2S and Ag_2Se transitions as geologic thermometers, *Econ. Geol., 54,* 1278–1280, 1959.

Roy, S., Mineralogy of the different genetic types of manganese deposits, *Econ. Geol., 63,* 760–786, 1968.

Sato, M., and T. L. Wright, Oxygen fugacities directly measured in magmatic gases, *Science, 153,* 1103–1105, 1966.

Schairer, J. F., Melting relations of the common rock-forming oxides, *J. Am. Ceram. Soc., 40,* 215–235, 1957.

Schairer, J. F., and N. L. Bowen, The system K_2O-Al_2O_3-SiO_2, *Am. J. Sci., 253,* 681–746, 1955.

Schairer, J. F., and N. L. Bowen, The system Na_2O-Al_2O_3-SiO_2, *Am. J. Sci., 254,* 129–195, 1956.

Schairer, J. F., and H. S. Yoder, Jr., The nature of residual liquids from crystallization, with data on the system nepheline-diopside-silica, *Am. J. Sci., 258A,* 273–283, 1960.

Segnit, E. R., The section $CaSiO_3$-$MgSiO_3$-Al_2O_3, *Mineral. Mag., 31,* 255–264, 1956.

Shand, S. J., *Eruptive Rocks,* John Wiley and Sons, Inc., New York, 1943.

Shankland, T. J., The pressure shift of infrared absorption bands in minerals and its effect on radiative heat transport (abstract), *Trans. Am. Geophys. Union, 50,* 357, 1969.

Shannon, R. D., and C. T. Prewitt, Effective ionic radii in oxides and fluorides, *Acta Cryst.,* in press, 1969.

Shoemaker, E. M., and E. C. T. Chao, New evidence for the impact origin of the Ries Basin, Bavaria, Germany, *J. Geophys. Res., 66,* 3371–3378, 1961.

Sibata, N., Equilibrium diagram of the nickel-antimony system, *Sci. Rept. Tôhoku Univ., First Ser., 29,* 697–727, 1941.

Skinner, B. J., F. R. Boyd, and J. L. England, A high-pressure polymorph of chalcocite, Cu_2S (abstract), *Trans. Am. Geophys. Union, 45,* 121–122, 1964.

Skinner, B. J., R. C. Erd, and F. S. Grimaldi, Greigite, the thio-spinel of iron; a new mineral, *Am. Mineralogist, 49,* 543–555, 1964.

Sobolev, N. V., Jr., The xenoliths of eclogites from the kimberlite pipes of Yakutia as fragments of the upper mantle substance, *Intern. Geol. Congr., 23rd,* vol. 1, 155–163, 1968.

Sobolev, N. V., Jr., I. K. Kuznetsova, and N. I. Zyuzin, The petrology of grospydite xenoliths from the Zagadochnaya kimberlite pipe in Yakutia, *J. Petrol., 9,* 253–280, 1968.

Sorem, R. K., and D. W. Gunn, Mineralogy of manganese deposits, Olympic Peninsula, Washington, *Econ. Geol., 62,* 22–56, 1967.

Strangway, D. W., R. M. Honea, B. E. McMahon, and E. E. Larson, The magnetic properties of naturally occurring goethite, *Geophys. J., 15,* 345–359, 1968.

Sugaki, A., and H. Shima, Synthetic sulfide minerals (1), *Mem. Fac. Eng., Yamaguchi Univ., 15,* 15–31, 1965.

Swift, I. H., and E. T. P. Tyndall, Elasticity creep of lead single crystals, *Phys. Rev., 61,* 359–364, 1942.

Takahashi, T., W. A. Bassett, and H. K. Mao, Isothermal compression of the alloys of iron up to 300 kb at room temperature: iron-nickel alloys, *J. Geophys. Res., 73,* 4717–4725, 1968.

Takeuchi, Y., The absolute structure of ullmannite, NiSbS, *Mineral. J. (Sapporo), 2,* 90–102, 1957.

Taylor, L. A., The system Ag-Fe-S: phase equilibria and geologic applications, Ph.D. thesis, Lehigh University, 1968.

Thompson, R. N., and W. S. MacKenzie, Feldspar-liquid equilibria in peralkaline acid liquids: an experimental study, *Am. J. Sci., 265,* 714–734, 1967.

Tilley, C. E., The dunite-mylonites of St. Paul's Rocks (Atlantic), *Am. J. Sci., 245,* 483–491, 1947.

Tilley, C. E., and H. F. Harwood, The dolerite-chalk contact of Scawt Hill, Co. Antrim, *Mineral. Mag., 22,* 439–468, 1931.

Tilley, C. E., and I. D. Muir, Intermediate members of the oceanic basalt trachyte association, *Geol. Forën. Stockholm Förh., 85,* 434–443, 1964.

Tokes, L. G., Mass spectrometric fragmentation mechanisms in the steroid series, Ph.D. thesis, Stanford University, Palo Alto, 1965.

Towe, K. N., Echinoderm calcite: single crystal or polycrystalline aggregate, *Science, 157,* 1048–1050, 1967.

Tunell, G., and E. Posnjak, The stability relationships of goethite and hematite, *Econ. Geol., 26,* 337–343, 1931.

Van Schmus, W. R., G. W. Wetherill, and M. E. Bickford, Rb-Sr age determinations of the Nipissing diabase, north shore of Lake Huron, Ontario, Canada, *J. Geophys. Res., 68,* 5589–5593, 1963.

Verhoogen, J., Distribution of titanium between silicates and oxides in igneous rocks, *Am. J. Sci., 260,* 211–220, 1962.

Wade, A., and R. T. Prider, The leucite-bearing rocks of the west Kimberley area, Western Australia, *Quart. J. Geol. Soc. London, 96,* 39–98, 1940.

Wager, L. R., The major element variation of the layered series of the Skaergaard intrusion and a re-estimation of the average composition of the hidden layered series and of the successive residual magmas, *J. Petrol., 1,* 364–398, 1960.

Warren, B. E., and D. I. Modell, The structure of anthophyllite $H_2Mg_7(SiO_3)_8$, *Z. Krist., 75,* 161–178, 1930.

Washington, H. S., The volcanoes and rocks of Pantelleria, Part II, *J. Geol., 21,* 683–713, 1913.

Watkins, N. D., and H. D. Goodell, Geomagnetic polarity change and faunal extinction in the Southern Ocean, *Science, 156,* 1083–1087, 1967.

Watkins, N. D., and S. E. Haggerty, Primary oxidation variation and petrogenesis in a single lava, *Contrib. Mineral. Petrol., 15,* 251–271, 1967.

Weir, C. E., A. Van Valkenburg, and E. R. Lippincott, Optical studies at high pressures using diamond anvils, in *Modern Very High Pressure Techniques,* R. H. Wentorf, Jr., ed., Butterworths, Washington, 51–69, 1962.

Wheeler, E. P., II, Fayalitic olivine in northern Newfoundland-Labrador, *Can. Mineralogist, 8,* 339–346, 1965.

White, R. W., Ultramafic inclusions in basaltic rocks from Hawaii, *Contrib. Mineral. Petrol., 12,* 245–314, 1966.

Whittaker, E. J. W., The crystal chemistry of the amphiboles, *Acta Cryst., 13,* 291–298, 1960.

Whittaker, E. J. W., The structure of the orthorhombic amphibole, holmquistite, *Acta Cryst., B25,* 394–397, 1969.

Williams, A. F., *The Genesis of the Diamond,* 2 vol., E. Benn Ltd., London, 1932.

Wilson, J. T., Orogenesis as the fundamental geological process, *Trans. Am. Geophys. Union, 33,* 444–449, 1952.

Wilson, R. L., and S. E. Haggerty, Reversals of the earth's magnetic field, *Endeavour, 25,* 104–109, 1966.

deWys, E. C., and W. R. Foster, The system diopside-anorthite-akermanite, *Mineral. Mag., 31,* 736–743, 1958.

Yagi, K., and K. Onuma, An experimental study on the role of titanium in alkalic basalts in light of the system diopside-akermanite-nepheline-$CaTiAl_2O_6$, *Am. J. Sci., Schairer Vol., 267A,* 509–549, 1969.

Yoder, H. S., Jr., The jadeite problem, *Am. J. Sci., 248,* 312–334, 1950.

Yoder, H. S., Jr., Calcalkalic andesites: Experimental data bearing on the origin of their assumed characteristics, in "Proceedings of the Andesite Conference," A. R. McBirney, ed., *Oregon Dept. Geol. Mineral. Ind. Bull. 65,* 77–89, 1969.

Yoder, H. S., Jr., and I. Kushiro, Melting of a hydrous phase: phlogopite, *Am. J. Sci., Schairer Vol., 267A,* 558–582, 1969.

Yoder, H. S., Jr., and C. E. Tilley, Origin of basalt magmas: An experimental study of natural and synthetic rock systems, *J Petrol., 3,* 342–532, 1962.

Yund, R. A., and H. T. Hall, The miscibility gap between FeS and $Fe_{1-x}S$, *Mater. Res. Bull., 3,* 779–784, 1968.

Yund, R. A., and H. T. Hall, Hexagonal and monoclinic pyrrhotites, *Econ. Geol., 64,* 420–423, 1969.

Zachariasen, W. H., The crystal structure of metaboric acid, *Acta Cryst., 16,* 385–389, 1963.

Zahner, J. C., and H. G. Drickamer, Effect of pressure on crystal-field energy and covalency in octahedral complexes of Ni^{2+}, Co^{2+}, and Mn^{2+}, *J. Chem. Phys., 35,* 1483–1490, 1961.

Zemann, J., The crystal chemistry of the tellurium oxide and tellurium oxosalt minerals, *Z. Krist., 127,* 319–326, 1968.

Zies, E. G., Chemical analyses of two pantellerites, *J. Petrol., 1,* 304–308, 1960.

Zies, E. G., A titaniferous basalt from the island of Pantelleria, *J. Petrol., 3,* 177–180, 1962.

Zies, E. G., A new analysis of cossyrite from the island of Pantelleria, *Am. Mineralogist, 51,* 200–205, 1966.

PERSONNEL

Scientific Staff

Director: P. H. Abelson

Emeritus Research Associate: E. G. Zies, *Chemist*

Physical Chemists: F. R. Boyd, T. C. Hoering,[1] J. F. Schairer

Petrologists: F. Chayes, D. H. Lindsley,[2] H. S. Yoder, Jr.

Geochemists: G. L. Davis, T. E. Krogh, G. Kullerud

Organic Geochemist: P. E. Hare

Geophysicist: P. M. Bell

Physicist: J. L. England

Crystallographer: Gabrielle Donnay

Fellows: W. B. Bryan, University of Queensland, Brisbane, Australia; A. El Goresy, Max Planck Institut für Kernphysik, Heidelberg, Germany;[3] L. W. Finger,

[1] On leave of absence at Space Sciences Laboratory, University of California, Berkeley, from September 1, 1968.

[2] On leave of absence at Division of Geological Sciences, California Institute of Technology, from January through June 1969.

[3] Appointment terminated November 30, 1968, to return to position at Heidelberg.

University of Minnesota; [4] M. C. Gilbert, University of California at Los Angeles; [5] S. E. Haggerty, Imperial College of Science and Technology, University of London, England; E. Hansen, Yale University; [6] J. E. Kalb, American University; [7] I. Kushiro, University of Tokyo; [8] H. K. Mao, University of Rochester; [9] H. O. A. Meyer, University College, London; S. A. Morse, Franklin and Marshall College; [10] H. R. Puchelt, University of Tübingen, Germany; [11] W. H. Scott, Yale University; [12] D. Smith, California Institute of Technology; [13] L. A. Taylor, Lehigh University.[9]

Guest Investigators: M. Bird, U. S. Geological Survey; E. Chao, U. S. Geological Survey; J. D. H. Donnay, Johns Hopkins University; K. Fink, University of Maine; M. C. Gilbert, Virginia Polytechnic Institute; S. Hafner, University of Chicago; Odette James, U. S. Geological Survey; K. King, Lamont Geological Observatory; J. Kutina, Lehigh University (visiting from Charles University, Prague, Czechoslovakia); W. R. Lees, Texas Technological College; V. R. Meenakshi, Duke University; G. Moh, University of Heidelberg, Germany; R. G. Platt, University of Western Ontario; G. R. Rapp, Jr., University of Minnesota; Dr. Friedrich Seifert, Bochum University, Germany; A. Shinyayev, Soviet Academy of Sciences, Baikov Institute of Metallurgy, Moscow; A. C. Turnock, University of Manitoba; D. Veblen, Harvard University; J. F. Wehmiller, Lamont Geological Observatory.

Operating and Maintenance Staff

Executive Officer: A. D. Singer
Accountant: C. B. Petry
Editor and Librarian: Dolores M. Thomas
Stenographers: Patricia S. Garrett, Marjorie E. Imlay
Clerk: H. J. Lutz
Electronic Technician: C. G. Hadidiacos
Research Assistant: J. F. Kocmaneck, W. D. Stanbro [14]
Chief Mechanician: F. A. Rowe
Instrument Makers: C. A. Batten, L. C. Garver, W. H. Lyons, G. E. Speicher
Mechanic and Carpenter: E. J. Shipley
Machinists: W. R. Reed, J. R. Thomas
Building Engineer: R. L. Butler,[15] H. L. Moore [16]
Mechanic's Helper: M. Ferguson
Janitor: D. B. Patrick, [17] L. B. Patrick [18]

[4] Appointment terminated June 30, 1969, to accept position as Crystallographer on Geophysical Laboratory staff from July 1, 1969.

[5] Appointment terminated August 31, 1968, to accept position as Assistant Professor of Petrology, Virginia Polytechnic Institute, Blacksburg, Virginia.

[6] Appointment terminated December 31, 1968, to accept position with Shell Development Company, Houston, Texas.

[7] Appointment terminated December 31, 1968.

[8] Appointment terminated June 30, 1969, to return to position at University of Tokyo.

[9] Appointment from September 1, 1968.

[10] Appointment terminated August 31, 1968, to return to position at Franklin and Marshall College.

[11] Appointment terminated September 30, 1968, to return to position at University of Tübingen.

[12] Appointment terminated June 30, 1969.

[13] Appointment from October 1, 1968.

[14] Appointment on a part-time basis from June 2, 1969.

[15] Retired December 31, 1968.

[16] Appointment from November 1, 1968.

[17] Appointment from July 1 through 3, 1968.

[18] Appointment from July 15, 1968.

PLATES

Plate 1. All products from runs at 1225°C and 10 kb. (A) Large forsterite crystal containing inclusion consisting of glass holding a liquid in which moves a bubble of gas. Free balls of glass and quench mica also exhibited in photograph. Initial total water content $= 23.1$ wt %; no CO_2 was present. From products of run interpreted to be from $Fo + L + G$ region. (B) Several elongated forsterite crystals containing inclusions consisting of glass holding a liquid bubble. Note large number of free glass balls. Initial H_2O content $= 65.8$ wt % and $CO_2 =$ 3.4 wt %. From products of run interpreted to be from $Fo + L + G$ region. (C) Left center: Inclusion in forsterite showing glass holding a crystal (bright spot) and a liquid with a large gas bubble. Initial H_2O content $= 15.4$ wt % and $CO_2 = 8.4$ wt %. From products of run interpreted to be from $Ph + Fo + G$ region. (D) Two forsterite crystals among books of phlogopite having, respectively, several and no inclusions. Initial H_2O content $= 5.6$ wt % and $CO_2 = 9.4$ wt %. From products of run interpreted to be from $Ph + Fo + G$ region. (E) Forsterite crystal holding glass inclusion in which are a large faceted phlogopite crystal and at least two forsterite (?) crystals (bright dots to the immediate right of the phlogopite crystal). Liquid and vapor bubbles were not discernible. Initial H_2O content $= 15.4$ wt % and $CO_2 =$ 8.4 wt %. From products of run interpreted to be from $Ph + Fo + G$ region. (F) Large crystal of forsterite containing several complex inclusions. Initial H_2O content $= 10.0$ wt % and $CO_2 = 8.9$ wt %. From products of run interpreted to be from $Ph + Fo + G$ region.

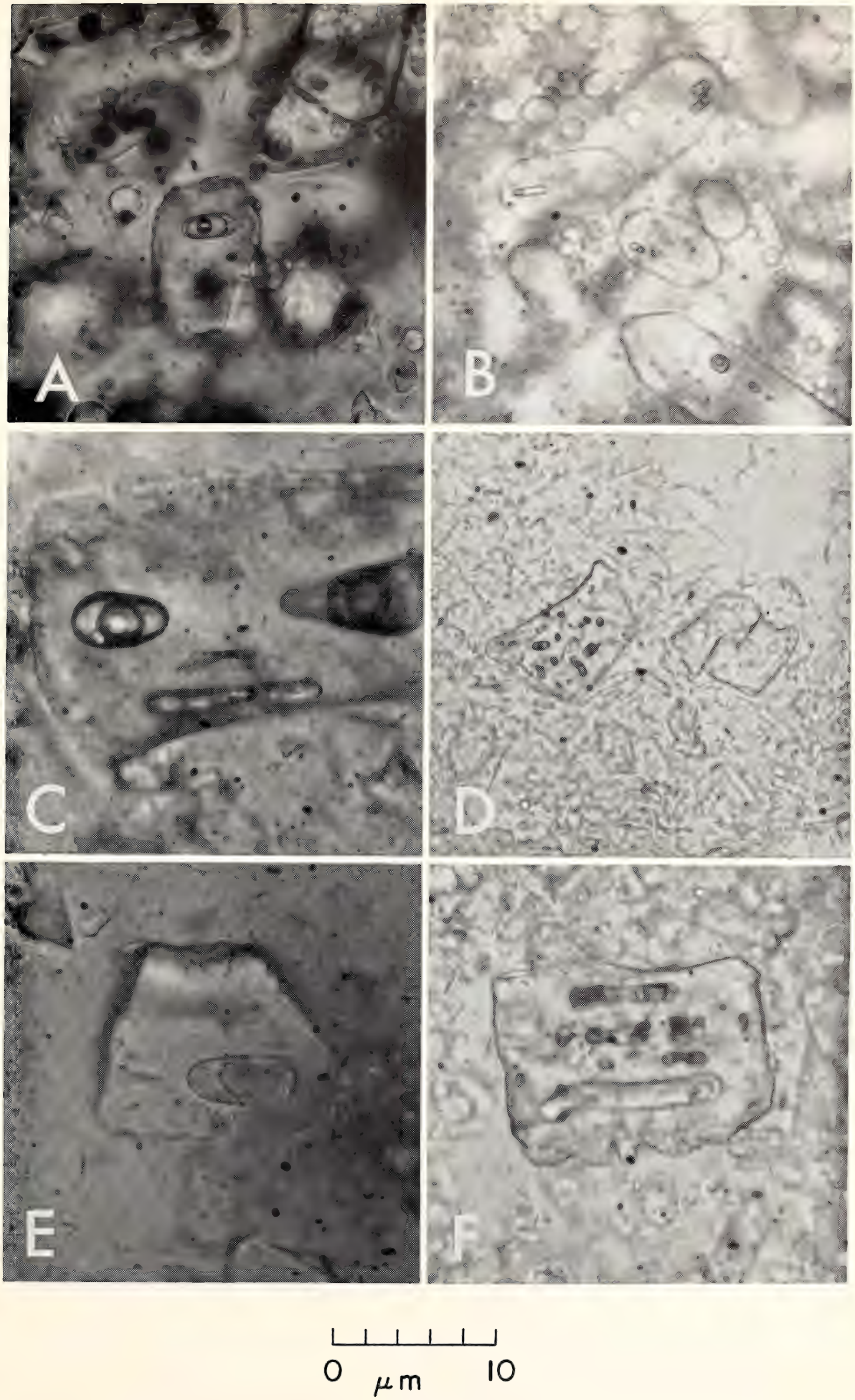
A
B
C
D
E
F
0 μm 10

Plate 2. (A) An aggregate of euhedral crystals of zoned magnetite that show various stages of oxidation to hematite. Note that certain concentric zones are selectively oxidized, but that oxidation also takes place along (111) planes. (B) Sharply terminating crystal faces of hematite, pseudomorphous after magnetite, showing complex radiating, fibrous, and colloform overgrowths of goethite and hematite. (C) A new iron-phosphate mineral, $Fe_4(PO_4)_3$, showing good polysynthetic twinning. The phase is interstitial to magnetite. Incipient oxidation of magnetite, to maghemite and hematite, is present along grain boundaries and cracks. (Crossed nicol 10°.) (D) Iron phosphate containing dark, irregular veinlets of oxidized material. This phase shows no difference in Fe or P content and is considered to be due to the oxidation of Fe^{2+} to Fe^{3+}. The surrounding magnetite is in an advanced stage of oxidation to hematite.

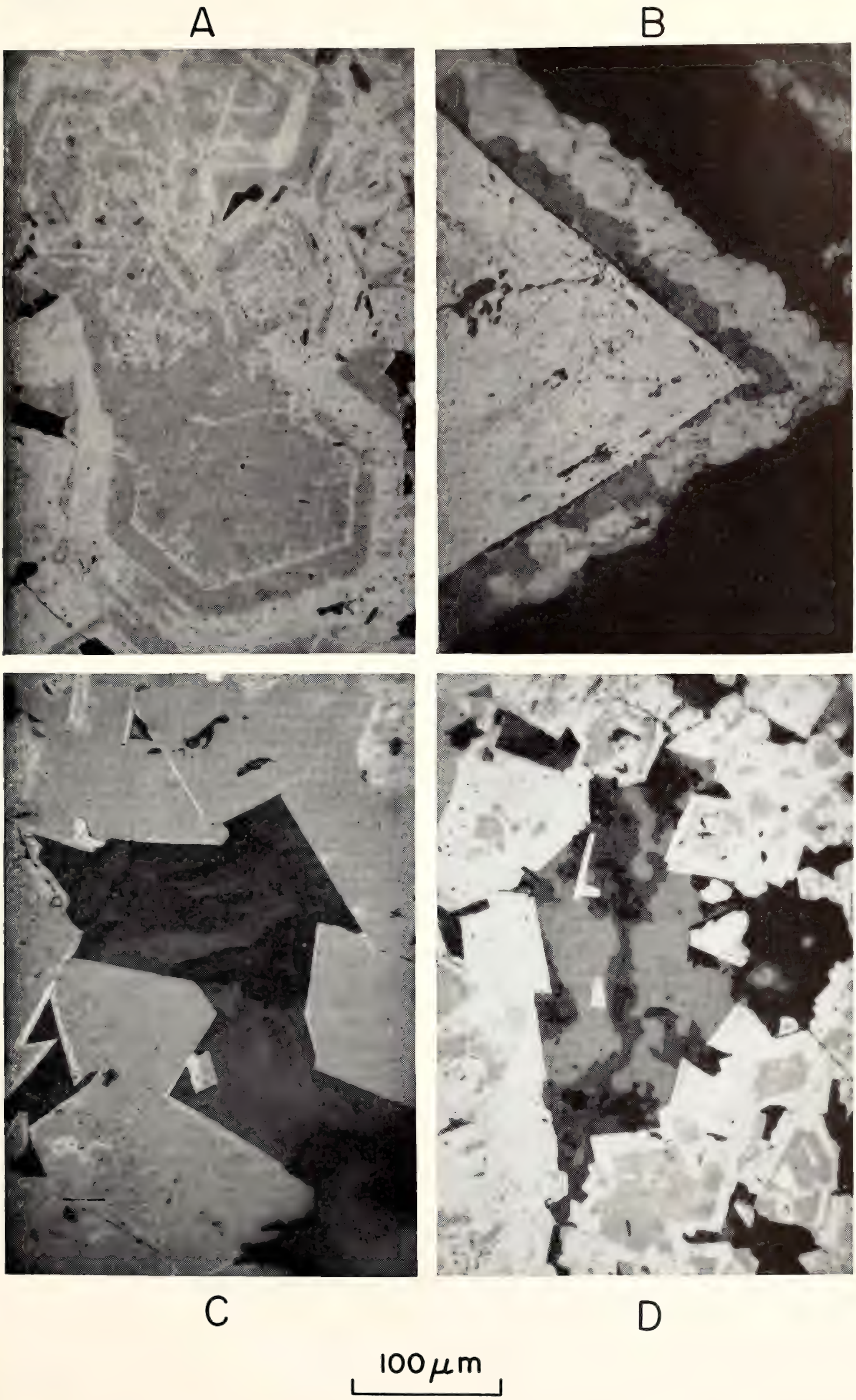
A
B
C
D
100 μm

Department of Terrestrial Magnetism

Washington, District of Columbia

Ellis T. Bolton
Director

L. Thomas Aldrich
Associate Director

Contents

INTRODUCTION

One of the truly profound sources of energy in the earth is held within the strain fields of rock formations at depths ranging from the surface to several hundred kilometers. As the strain is released, physical dislocation within the rock occurs, often resulting in readily detectable events at the surface—dramatically signified by earthquakes. When these occur "pent-up aching rivers" pour forth in a few seconds their energies and shake the solid ground as though it were jelly. Occurring in or near the sea, great waves, tsunamis, may be generated to smash against shores thousands of miles from the source. Lakes inland are tilted and their waters oscillate like those in a tipped saucer, sloshing from one end to the other until gravitational influence quiets them.

Anyone who has ever felt an appreciable earthquake has experienced deeply the fearful and mysterious maturation of his Mother Earth which, for all her nurturing, lasting solidity, shudders with uncertainty as she struggles to form herself into a space ball of maximum conformity to the physical laws of the Universe. For him this once imperturbable foundation has been shaken and is no longer the ultimate immutability.

Man has long known of, but until recently little appreciated, the lessons potential in an earthquake. Even the great earthquake of April 18, 1906, along the San Andreas fault, which effected large scale change in the visible earth, not to mention the equally significant change in human endeavor in California, went relatively unnoticed after the initial human shock wore off, except for the continuing interest of a small band of intrepid men, until the Carnegie Institution of Washington stepped in and bailed out a laggard local legislature by publishing the first coherent report of damage, disruption, and desecration brought upon the land. This work was completed in the years 1908 and 1910 as CIW Publication No. 87.

In this first truly comprehensive attempt to understand earthquake mechanics scientifically, which comprises volume II, 1910, of CIW Publication 87, *The California Earthquake of April 18, 1906*, one finds on page 31 these words of Harry Fielding Reid of Johns Hopkins University: "As strains always precede the rupture and as the strains are sufficiently great to be easily detected before the rupture occurs, in order to foresee tectonic earthquakes it is merely necessary to devise a method of determining the existence of the strains . . ."

Wise and prophetic words, these, but easier said than done in 1910. Now, sixty years later, Reid's dream may be on the verge of becoming reality as a result of the invention of an inexpensive and extraordinarily sensitive volume strain rate meter by Dr. I. Selwyn Sacks, Staff Member of the Department and Mr. Dale Evertson of the Applied Research Laboratories of the University of Texas at Austin. This omnidirectional strain rate meter is concreted into solid rock in a 150-foot-deep hole on the DTM grounds and has worked continuously since its installation in August 1968. The cost of the installation, including drilling the hole and the cost of subsidiary recording devices, was a little over $2000. Its frequency response covers a wide range of geophysical interests—from strain changes induced by microseisms through those caused by microbarometric pressure influences on the solid rock to those resulting from the gravitational deformation of the earth by the moon. Distortions as minute as 10^{-7} microns (.001Å, or a thousandth the distance between atoms in an ordinary chemical bond) are readily detected and strain

changes of somewhat over 1 part in 10^{14} can, in principle, be detected. As a practical matter, for a single instrument, earth noise of the order of 10^{-10} dominates the records in the 6–20 second period range while the earth tide induces changes of about 4×10^{-8} at Washington's latitude. The system is many times more sensitive than the most sensitive strain meters heretofore available. This new device bids fair to add much to our knowledge of the structure of the earth and the causes of earthquakes. It is described in the pages which follow and some illustrative results are presented.

Of course, many other areas of endeavor are described. One will find a number of fascinating and important new discoveries in fields as different as astrophysics and biophysics as well as in the various aspects of geophysics. Almost every topic discussed has been undertaken by the Staff in cooperation with Fellows in the Department and with scientists and institutions elsewhere. This spirit of symbiotic personal working relationships is traditional at DTM, lending immeasurable support and giving great strength to the diversity which we enjoy in our activities.

ASTROPHYSICS

G. E. Assousa, L. Brown, S. D'Odorico, J. W. Erkes, W. K. Ford, Jr., C. Petitjean, K. C. Turner, M. A. Tuve, and C. M. Varsavsky

The astrophysics program this year has included observations of the neutral hydrogen around the Magellanic Clouds, new observations of the velocities of emission regions in the Andromeda nebula, considerable analysis of scattering data from polarized protons, and foil excitation spectrograms from the Van de Graaff accelerator. Unfortunately, an intense fire in the pressure tank of the Van de Graaff accelerator did sufficient damage to make the accelerator inoperative for almost one year. However, the damage has now been repaired and there is a backlog of experiments waiting to be performed.

Optical Astronomy

W. K. Ford, Jr., Vera C. Rubin, and S. D'Odorico

Andromeda nebula. Spectra of 67 emission regions from 3 to 24 kpc from the nucleus of M31 have been obtained with the DTM image tube spectrograph attached to the 72-inch telescope of the Ohio State and Ohio Wesleyan Observatories at Lowell Observatory, and the 82-inch telescope of Kitt Peak National Observatory. At a dispersion of 135 Å/mm radial velocities, principally from Hα emission, have been determined with an accuracy of ± 10 km/sec. No emission regions have been identified from the nucleus out to 3 kpc. However, spectrograms of the nucleus and the major and minor axes out to 4 kpc show the [NII] λ 6583 line in emission against the stellar continuum, and velocities have been obtained by measuring this line.

From the rotation curve for $r \leq 24$ kpc, the following parameters for a disk model of M31 are obtained. There is a dense rapidly rotating nucleus of total mass $M = 5 \times 10^9$ $\mathfrak{M}_\odot$ Near $r = 2$ kpc the density is very low and the rotational velocities are very small. In the region 500 pc–1400 pc, ionized gas is observed moving out from the nucleus. Beyond $r = 4$ kpc, the total mass of the galaxy increases approximately linearly to about 14 kpc, and more slowly thereafter. The circular velocities are nearly constant in this region. The total mass in the disk of radius of 24 kpc is 1.85 ± 10^{11} $\mathfrak{M}_\odot$; one-half of this mass is located in the disk interior to $r = 9$ kpc. In contrast, the neutral hydrogen mass calculated from 21 cm

observations is $6.7 \times 10^9\ \mathfrak{M}_\odot$; one-half of it is contained in the disk interior to $r=$ 13.4 kpc. There is no significant difference between the optical and 21-cm circular velocities for M31. This is seen in Fig. 1 where the optical observations and the 21-cm rotation curve from Burke, Turner, and Tuve (*Year Book 63*) are superimposed.

There is a remarkable similarity between the M31 rotation curve and that adopted by Schmidt (1965)[1] for our galaxy. However, the rotation curve for M31 has a slightly higher maximum velocity, and decreases more slowly with large distance from the nucleus, which results in a 20% larger mass for M31 than for our galaxy (Burke, Turner, and Tuve, *Year Book 63*, p. 341).

Infrared observations: An experimental refrigerated RCA cascaded image tube with an S1 photocathode has been used in the DTM image tube spectrograph to obtain spectra of stars and galaxies in the region 6800Å–11000Å. Much of this observing has been done with the 36-inch NASA telescope at Greenbelt, Maryland. Exposures as long as 7 hours have been necessary. Nevertheless, highly useful infrared spectrograms of galaxies NGC 1068, 4151, and M82 have been obtained; all show strong lines of [SIII] λ 9069, λ 9532 and He I λ 10830. The NASA telescope has also been used to obtain photographs of M82 and several other galaxies through narrow-band interference filters.

Image tubes. Much of the work of the Carnegie Image Tube Committee has in the past years been carried out at the Department of Terrestrial Magnetism. This activity has included evaluating and testing experimental image intensifiers,

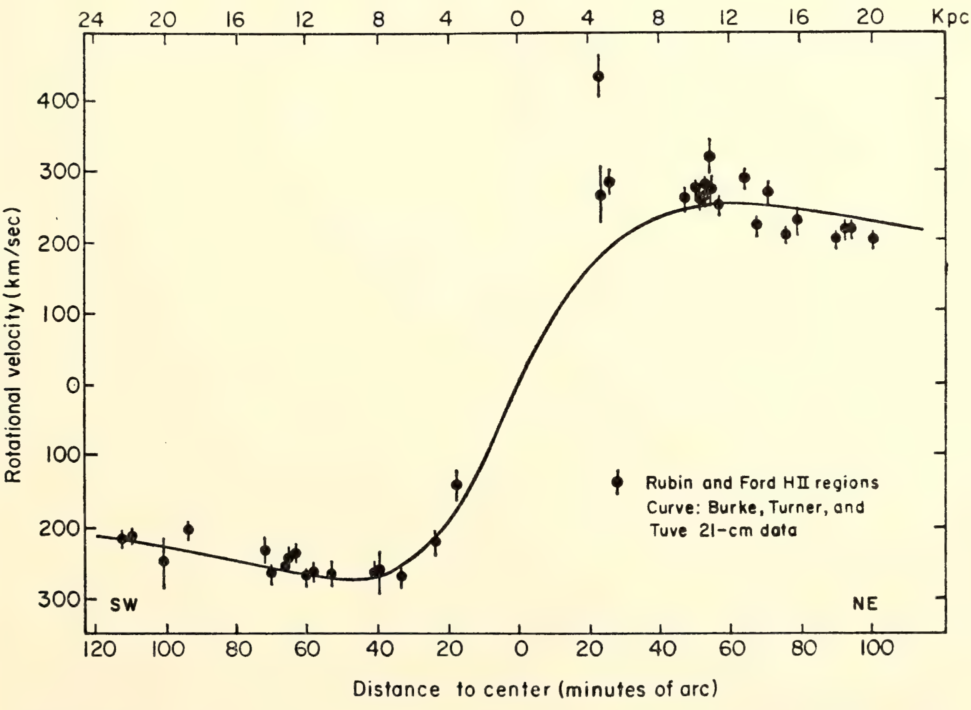

Fig. 1. Rotational velocities in the plane of M31, as a function of distance from the center. Black circles are velocities determined from optical spectra of H II regions; the solid line is rotation curve determined by Burke, Turner, and Tuve from 21-cm radio observations.

and more recently procuring, assembling, and testing a number of image-tube systems that have been allocated to observatories. The image tube program has been supported by the National Science Foundation and the Carnegie Institution of Washington, and we wish to express our thanks for this continuing support.

Radio Astronomy

J. W. Erkes, K. C. Turner, M. A. Tuve, and C. M. Varsavsky

It has been a very active year in both hemispheres for the radio astronomy group. As in the past two years, the major emphasis in the northern hemisphere has been on equipment development, and in the southern hemisphere on observations. Dr. Tuve has obtained many additional records of H-line emission with the 60-foot radio telescope at Derwood, Maryland.

We wish to express our thanks to the Office of Naval Research for the continuing loan, provided under contract No. Nonr-3021(00), of 38 tons of pig lead that serves as counterweights for this instrument.

Equipment

J. W. Erkes and K. C. Turner

The major accomplishment this year is certainly the completion of the electronics for the Derwood–Avery Road interferometer in nearby Maryland. The entire apparatus has successfully seen "imitation fringes" from an artificial radio source. A block diagram of the system is shown in Fig. 2. Provision has been made in the front-end switches of the two telescopes, so that the Avery Road instrument may be operated either as an interferometer, or as a continuum receiver for pointing and calibration measurements, and the Derwood telescope may be used either as an interferometer element or in our standard hydrogen-line spectrometer mode. As of this writing, the system is awaiting the installation of the interferometer front-end package on the Derwood telescope.

Modernization of our H-line spectrometer continues. The latest improvement is a digital timing system, which will give increased flexibility in choosing integration times, and will eliminate a variation of a few percent in the old timing system.

Data Analysis

K. C. Turner

All data from the one degree spacing survey of the region between the two Magellanic Clouds have been reduced. Figures 3 and 4 present some results. Figure 3 is a map of the total neutral hydro-

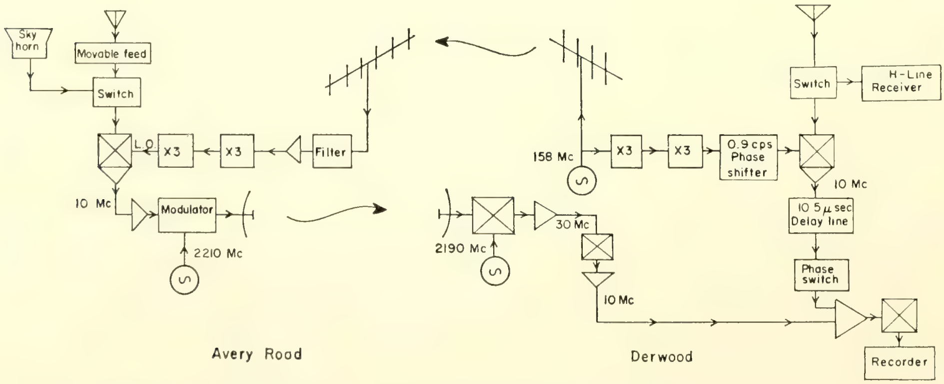

Fig. 2. Block diagram of Derwood–Avery Road interferometer system.

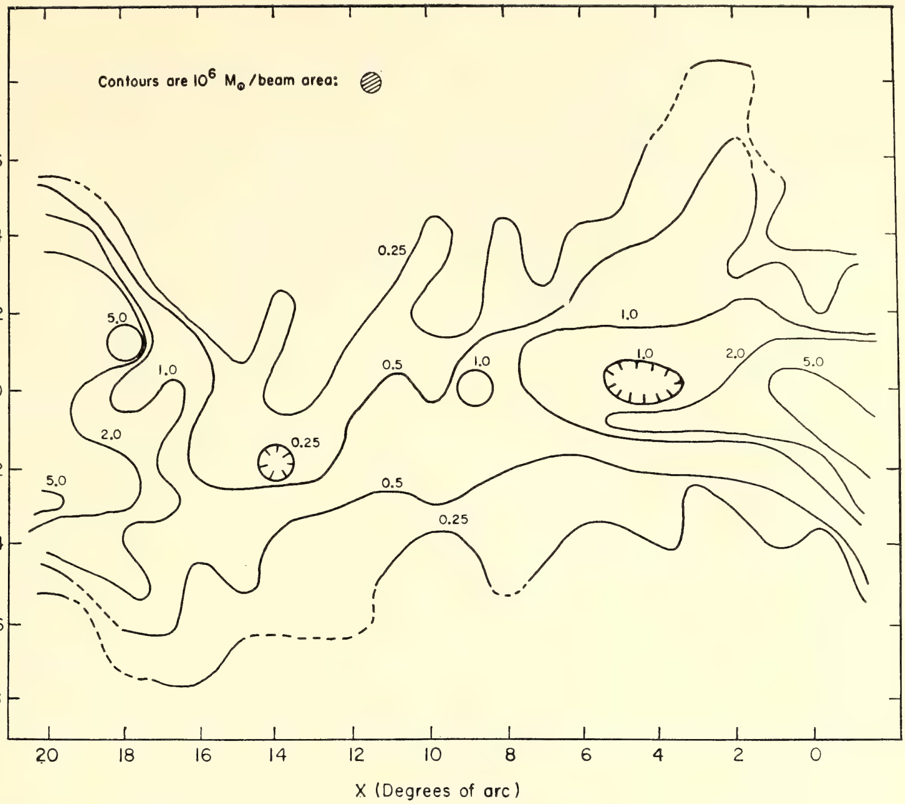

Fig. 3. Total neutral hydrogen between the Magellanic Clouds.

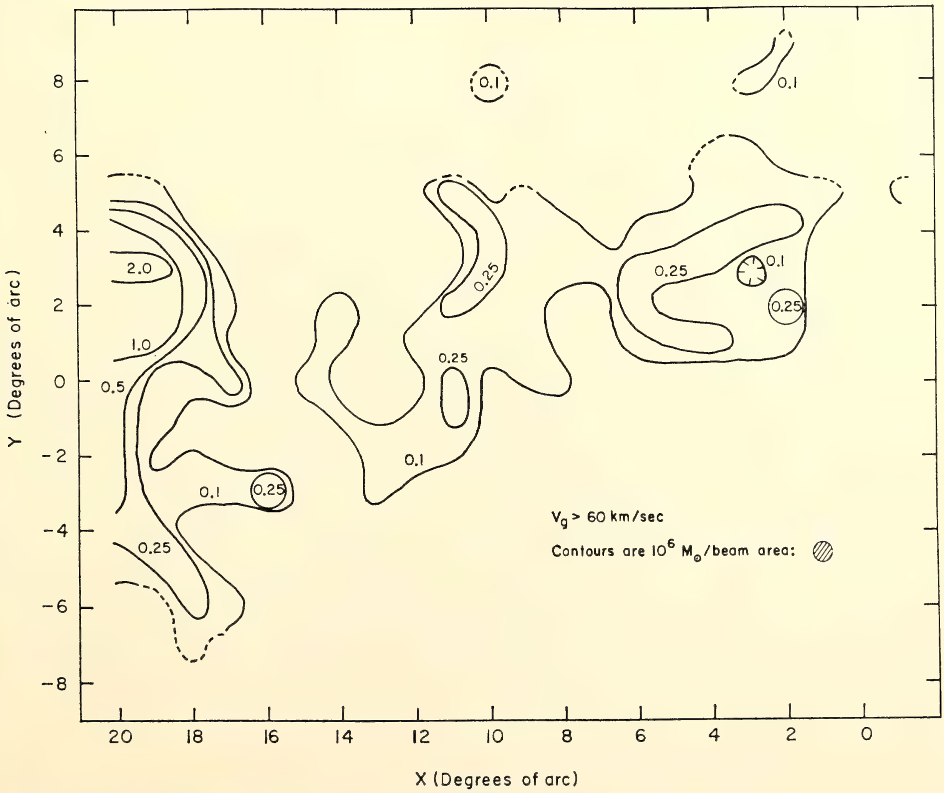

Fig. 4. High-velocity gas in the Magellanic Cloud system.

gen observed, and Fig. 4 shows the distribution of gas moving at high velocities with respect to the Magellanic Cloud system. Analysis of the very complex structures observed here is continuing, in an effort to understand something of the history and dynamics of the Magellanic Cloud system.

A Study of HB 21

J. W. Erkes

Observations of the distribution of neutral hydrogen around the supernova remnant HB 21 were begun, using the 60-foot Derwood dish and the 60-channel H-line spectrometer. This supernova remnant was chosen for analysis for two reasons: its large angular size (nearly two degrees) permitted the neutral hydrogen distribution near it to be mapped in some detail; moreover, continuum observations show that HB 21 has been seriously deformed, as if by a strong interaction with the surrounding interstellar material.

A preliminary contour map showing the distribution of neutral hydrogen in the velocity range from 0 to 10 km/sec can be seen in Fig. 5. The broken line shows the outermost extent of the supernova remnant as seen on high-resolution continuum radio maps. The neutral hydrogen is arranged in a ringlike structure whose diameter is roughly equal to that of HB 21. A detailed analysis of these observations is in progress.

Southern Hemisphere Observations

J. W. Erkes and K. C. Turner

Between October 14 and November 20, 1968, a survey of the Small Magellanic Cloud was initiated. Observations were made on a half-degree grid (at one beamwidth intervals). Observations at closer spacing over the brighter regions were then undertaken. Figure 6, a map of the total amount of neutral hydrogen observed, represents a preliminary result.

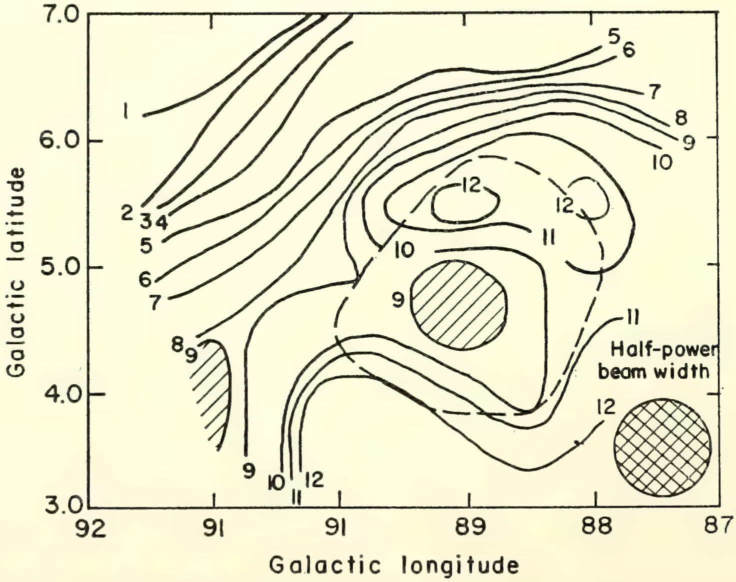

Fig. 5. The neutral hydrogen near HB 21, in the velocity range 0–10 km/sec. The contour interval is 4.56×10^{19} H atoms/cm^2. The hatched areas are depressions.

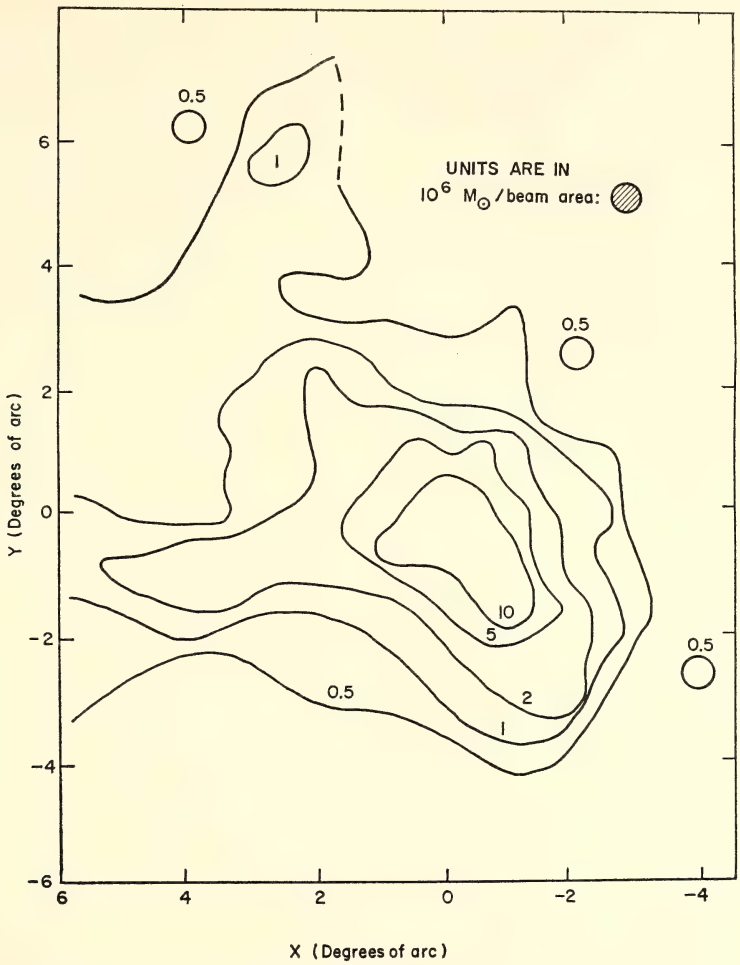

Fig. 6. Total neutral hydrogen near the Small Magellanic Cloud.

Previously published observations of Hindman and Balnaves [2] at higher spatial resolution lie approximately within the 5×10^6 $\mathfrak{M}_\odot$ contour. We estimate that about 40% more points will be necessary to complete the survey. The Small Magellanic Cloud is of great interest not only because it is one of our nearest neighbor galaxies, but also because of its extremely complicated structure. Double-peaked hydrogen profiles are the rule in the small cloud, and Hindman has suggested that several very violent explosions took place there in the past. Whether or not this is the case, it seems clear that large-scale events have occurred in the small cloud for which we have no evidence in our own galaxy.

Activities of the Instituto Argentino de Radioastronomía

C. M. Varsavsky

During the period that extends between July 1, 1968, and June 30, 1969,

the Instituto Argentino de Radioastronomía–Carnegie Institution of Washington Radio Astronomy Station began to materialize one of its basic aims, namely, the training of young Latin American astronomers. Three students completed their Ph.D. thesis at the station: Dr. Edemundo da Rocha Vieira, from the University of Rio Grande do Sul, in Brazil, and Drs. Silvia Garzoli and Esteban Bajaja, from the University of La Plata, in Argentina. In addition, three more students are currently writing their Ph.D. theses at the station: Mr. Wolfgang Pöppel, of the University of Buenos Aires, and Miss Dora Goniadzki and Mr. Raúl F. Colomb, of the University of La Plata. Two more, younger graduate students, Mr. Fernandez, from the University of Buenos Aires, and Mr. Quiroga from the University of La Plata, are beginning to get their first research experience at the station while completing the course requirements for their doctoral degrees. It is hoped that the flow of graduate students to the station will continue at a rate of two to three new students per year.

The progress of research activities at the station showed itself at the last meeting of the Argentine Astronomical Society, held at San Juan on October 10, 11, and 12, 1968. Members of the staff of IAR presented ten papers, or one-fourth of the total number of papers presented at the meeting. This shows that the IAR–CIW joint project has become a very significant fraction of the total astronomical effort in Argentina.

Most of the work is concerned with the correlation of the gaseous and dust components of interstellar matter and with the general distribution of hydrogen, particularly outside the galactic plane. It is expected that a brief summary of three years' work on these problems will be presented at a symposium organized by the International Astronomical Union on the "Spiral Structure of the Galaxy," to be held August 1969.

Construction of the second 100-foot steerable dish, which will be able to move on rails up to a distance of 750 meters from the first dish, has progressed considerably and it is expected that it will be completed in early 1970. The foundations, the drive, and the dish proper are practically finished; still to be done are the rail system, pedestal, and the final assembly.

Nuclear Physics

L. Brown and C. Petitjean

The force law for strong nuclear interactions, still elusive after half a century of study, has long been known to be dependent on the relative orientation of the intrinsic angular momenta (spins) and orbital angular momentum with one another and with the radius vectors connecting the particles. It is the strong spin-dependence of nuclear forces that has motivated the work that has combined the Van de Graaff machine of the Carnegie Institution with the polarized ion source of the University of Basel. The nucleon-nucleon force is fairly well understood phenomenologically at nonrelativistic velocities, but it has proved difficult to apply this force to describe even slightly more complicated structures. Our collaborator, the theorist Dr. R. G. Seyler, is now attempting to do just that with our earlier measurements of proton-deuteron scattering[3] (*Year Book 66,* pp. 64–66). At low energies, the nuclear force is given for convenience in terms of a potential function that now has four terms for which there is experimental evidence: a central, a spin-spin, a tensor, and a spin-orbit term. The central potential depends on the magnitude of the separation of the particles, which here are the target nucleus and the incident nucleon; the spin-spin po-

tential depends on the relative orientation of the spins of the particles; the tensor potential depends on the relative orientation of the spins and the radius vector connecting them; the spin-orbit potential depends on the relative orientation of the spins and orbital angular momentum.

If one of the two particles has spin zero, then only the central and spin-orbit terms apply. This simplification lay behind our earlier choice of $^4He(p,p)^4He$, $^{12}C(p,p)^{12}C$ and $^{16}O(p,p)^{16}O$ as reactions for the study of scattering by polarized protons. Scattering nucleons from medium and heavy nuclei show strong effects of the central and spin-orbit terms but little of the spin-spin or tensor forces. This has made our analysis of $^6Li(p,p)^6Li$ especially appealing, since the phase shifts derived from the measurements show strong spin-spin effects that can be examined independently of the other force terms. Lithium-6 has spin-one and protons spin-half.

The phase shift analysis of spin-half particles on spin-one is discussed in *Year Book 66,* pp. 64–66, and *Year Book 67,* pp. 297–298, and Seyler recently published a complete theoretical description.[4] For low energies there are thirteen states with orbital angular momentum 0, 1, and 2. Elastic scattering has a real phase shift for each state, if inelastic processes are excluded, and complex phase shifts, if inelastic processes take place, e.g., nuclear reactions. Mixing between states of the same angular momentum and parity, whereby particles leave the interaction from a different state than that by which they entered, can also occur. Figure 7 shows the thirteen S, P, and D states that account for 26 parameters in $^6Li(p,p)^6Li$; one must add 7 mixing parameters, denoted by arrows linking states that mix. This large number of parameters caused us to fear that the analysis might prove to be "too easy" or, in other words, that we might find many sets of parameters from which good fits to the experimental data could

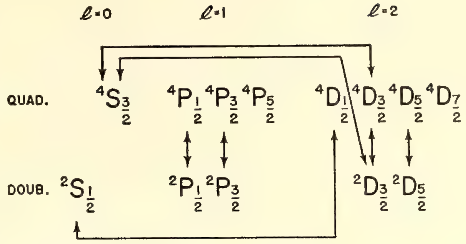

Fig. 7. Parameters describing the states for the elastic scattering of protons by ^6Li. For orbital angular momentum $\ell_{max} = 2$, there are 13 phase shifts associated with the 13 states. Since inelastic channels are open, the phase shifts are complex. The 7 arrows represent mixing parameters coupling states of the same J^{π}. If mixing parameters are real, a total of 33 parameters is needed to describe $^6Li(p,p)^6Li$ for S-, P-, and D-waves.

be calculated. Nature has proved far simpler than we expected, for only two sets of phase shifts were found, and one of these could be eliminated by straightforward reference to another experiment.

Figure 8 shows the phase shifts needed to describe $^6Li(p,p)^6Li$. Reference to Fig. 7 discloses that phases for neither the D states nor the ^2P states are required; with these states absent, at least insofar as the accuracy of our data allows, no mixing can occur between them and any other, hence all mixing parameters must be zero. This is not the place for a review of our extended efforts to find other sets of parameters, which are described elsewhere in detail.[5] Our phases predict the results for scattering polarized ^6Li on hydrogen and may be subjected to further experimental test in the future, as two sources of polarized lithium have been recently constructed.[6,7]

The splitting of the ^2S and ^4S phases is noteworthy. This results from a spin-spin interaction; the quadruplet state, i.e., the ^4S, has parallel spins and the doublet state has spins which are antiparallel. The two phases are not identical, indicating that the potential for the two orientations is different. What is particularly striking and a bit puzzling is that the doublet phase is larger in

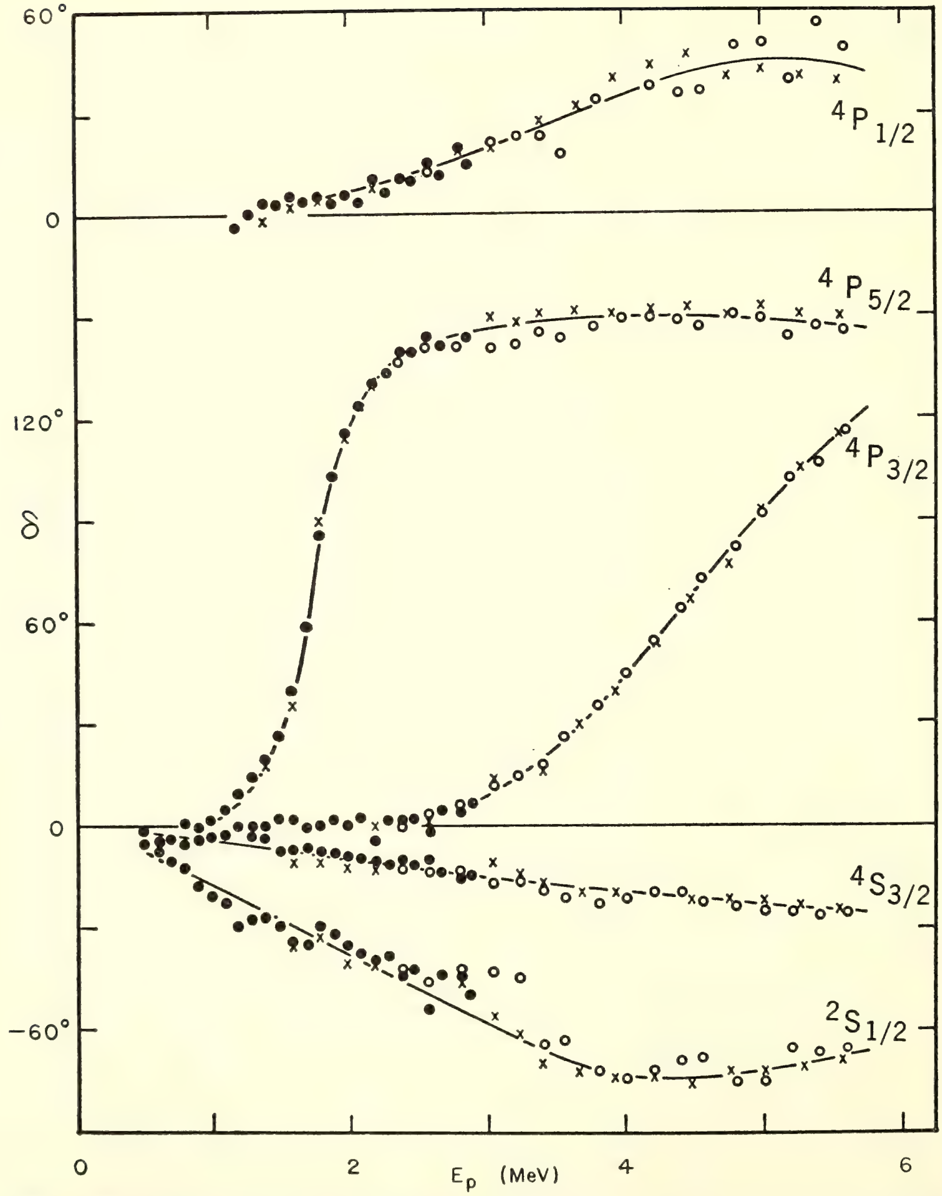

Fig. 8. Phase shifts as functions of energy. The points show the phase shifts that were obtained as the best fit to the experimental data. A second, equally good set of phase shifts results if one interchanges the $^4P_{3/2}$ and the $^4P_{1/2}$ phases. The second set is eliminated by a previous identification of the state near 5 MeV as $3/2^-$.

absolute value than the quadruplet; this finding is the opposite of the effect that we found in D(p,p)D and seems hard to reconcile with the negligible values for the ^{2}P phases. Imaginary components of the phases are not plotted in Fig. 8. They are not particularly sensitive to the inelastic scattering data, which here is the total cross section for ^{6}Li$(p,^3$He$)^4$He. The imaginary components were, therefore, inaccurately determined in this analysis, but that inaccuracy is not strongly reflected in the real components.

The ^{4}P phases have strong splitting effects attributable to the spin-orbit force and showing two resonances: a $^4P_{5/2}$ at 1.8 MeV and a $^4P_{3/2}$ at 5 MeV. Incidentally, our data and analyses are unable to distinguish between a $^4P_{3/2}$ and a $^4P_{1/2}$ resonance at 5 MeV, and we obtained a second set of phases that is identical to the one shown in Fig. 8 except that these two phases are interchanged. An independent experiment had previously determined the spin and parity of the 5-MeV state, thereby eliminating the second set of phases.

Figure 9 presents the polarization in ^{6}Li$(p,p)^6$Li in the form of a contour map. The proton laboratory energy is plotted along the abscissa, the laboratory scattering angle is plotted along the ordinate, and polarization efficiency is given by the contours in units of 0.01. Our data are distributed from 1.2 to 3.2 MeV over scattering angles from 40° to 135°.

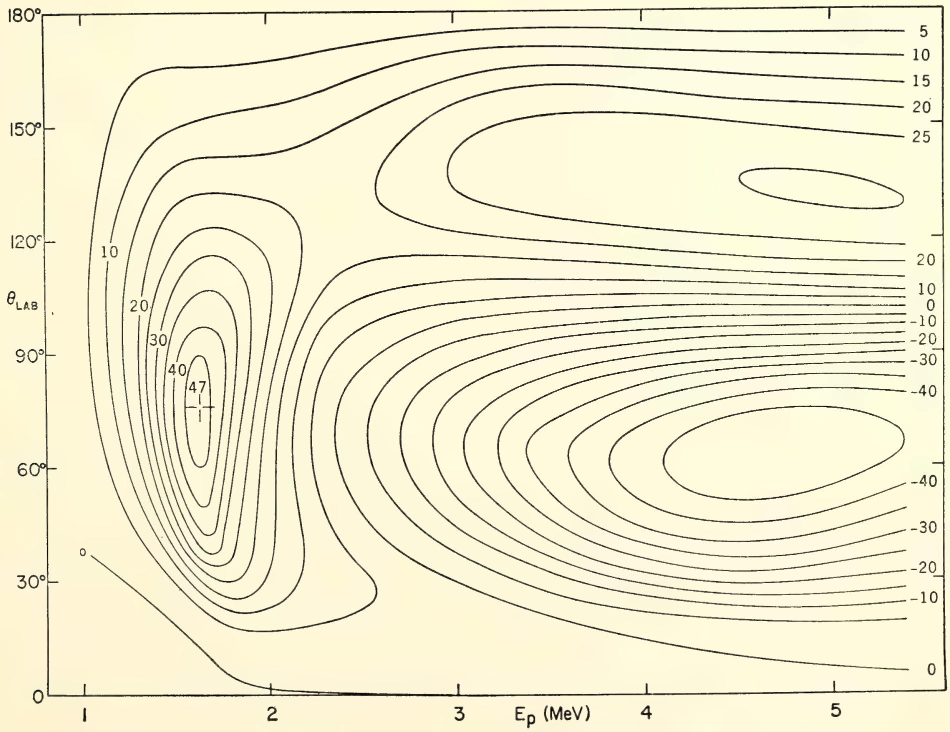

Fig. 9. Polarization contour map of ^{6}Li$(p,p)^6$Li. Analyzing efficiency contours of 0.05 spacing, which are calculated from the smooth curves of the phase shifts in Fig. 8, are shown plotted on a coordinate system of lab scattering angle against lab proton energy. Polarization data were used in the phase shift analysis only up to 3.2 MeV, so this map may be unreliable above that energy.

Atomic Physics

G. E. Assousa, L. Brown, and W. K. Ford, Jr.

We had hoped to present the results of extensive observations using foil excitation spectroscopy in this report. A new deflection magnet allowed us to use beams of much heavier ions than had been possible with the old magnet. Unfortunately, shortly after changing our experimental program from nuclear physics to atomic physics a terrible fire burned the charging belt of the Van de Graaff and did much damage to equipment located within the pressure tank. Fortunately, the machine was not seriously damaged structurally and could be repaired. The repairs cost us dearly in time and removed the possibility of doing experimental work until just recently.

The characteristic of our first work with a beam of sodium ions (*Year Book 67*, 299–300) was a bewildering number of lines that could not be matched in wavelength to classified lines. We went to lower beam energies with neon, 0.4 MeV for Ne^+, and found that a much more normal spectrum results. Numerous unidentified lines appeared as the energy was raised, but only a few lines remained at 2.5 MeV. From plates exposed to a 0.4 MeV beam excited by a self-supporting carbon foil 10 $\mu g/cm^2$ thick, we have identified several transitions originating in the 3p levels of Ne I and the 4f levels of Ne II. There are several measurements of the lifetimes of the Ne I levels from other techniques which do not agree well with one another, but none whatsoever of Ne II. Our measurements agree sufficiently well with the results of pulsed electron beam excitation [8] to give us confidence in the technique. An apparent discrepancy, which troubled us for some time, was removed when we learned that a misalignment of the spectrograph slit caused an attenuation of the observed intensity of the beam along its length; data for ascertaining the size of this effect were present on plates exposed to the gas-excited beam. We have remeasured these lifetimes but have not yet analyzed the plates.

BIOPHYSICS

E. T. Bolton, R. J. Britten, J. A. Chiscon, D. B. Cowie, L. J. Grady, B. H. Hoyer, D. E. Kohne, N. J. Reed, and R. B. Roberts

Our interests, as in the past, have centered on the nucleic acids of a variety of organisms. Of particular interest have been the large amounts of repeated DNA sequences present in the genomes of higher organisms, as well as the nonrepetitious (unique) DNA contained in all living cells. A portion of this year's report summarizes the major properties of the repetitious DNA and serves as a brief review of five years of intensive research and as reference material for our continuing interests in the DNAs of many types of organisms. In addition to this summary, the detailed reports of our year's work with the DNAs of a variety of organisms are presented.

Studies of the DNA of the calf demonstrated that while the quantity of repetitious DNA is large, it is found in only a few classes and that these classes contained a high frequency of family members which empirically are a collection of polynucleotide chains found to be similar in nucleotide sequences. On the other hand, there is a scarcity of low-frequency sequences. These results imply saltatory replication rather than long-term, gradual processes of growth of families. Another series of interesting experiments revealed that there is marked interspersion of the repeated nucleotide sequences among the nonrepetitive sequences within the bovine genome.

Preliminary investigations of the repetitious DNA of the rat (and mouse) indicate that the range of sequence di-

vergence in a family appears to be extremely broad. Furthermore, the DNA from families having the largest number of members has the highest thermal stability, implying lack of evolutionary divergence.

Among the bacteria and the blue-green algae the amount of repetitious DNA appears to be small and the frequency of family members low. In the bacteria a portion of the repeated nucleotide sequences has been identified with ribosomal DNA (*Year Book 67,* p. 310). This year another fraction of the DNA having multiple copies was observed in *E. coli.* The number of copies present is dependent upon the growth state of the cell. Such a correlation with the phase of growth suggests that these multiple copies are extrachromosomal and not under the same control of replication as the bacterial genome.

The DNA of the blue-green algae, and of their viruses, has also been studied. Taxonomic relationships among the blue-green algae have been investigated by measuring the amount of genetic material held in common among the species and by the thermal stability of their DNA-DNA reaction products. Certain blue-green algae, sensitive to the same virus, were shown to be closely related; others of the same family showed evolutionary divergence from these virus-sensitive algae, and in one case a family member showed no indication of evolutionary relationship. Furthermore, other blue-green algae, taxonomically classified in other orders among the Cyanophyta, were shown to contain nucleotide sequences common to the virus-sensitive strains. It is evident that we have just begun to decipher in an objective way a portion of the taxonomic interrelationship among the blue-green algae.

One important aspect of these investigations was the discovery of a new blue-green algae virus which appears to be lysogenic to one strain, *Oscillatoria prolifera,* and is virulent to several other strains. This is the first example of lysogeny to be reported outside of the bacterial systems.

No genetic similarities, as measured by DNA-DNA interactions, could be detected between blue-green algae and *E. coli* or some of the lysogenic viruses of these bacteria. These studies will be continued to search for an evolutionary pathway coupling the blue-green algae to other living organisms.

Most of the lysogenic bacteriophages investigated thus far have been shown to contain nucleotide sequences in common (*Year Book 67,* p. 301). A defective phage, obtained by inducing strains of *E. coli* 15, appears to be an exception. Studies investigating the nature of the DNA of this virus, and of the relationship of this viral DNA to that of its bacterial host (and to nonlysogenic *E. coli* strains) have been carried out. Preliminary evidence suggests that the high degree of reaction observed between the viral DNA and the DNA of these *E. coli* strains occurs because most of the DNA of these viruses appears to reside in a limited portion of the *E. coli* chromosomes and this viral DNA is preferentially replicated a large number of times, and packaged in a viral protein coat.

Finally, a new and very rapid method for DNA extraction has been developed, which makes use of hydroxyapatite to bind native, sheared DNA. While the method is very convenient, a greater importance may lie in the potentially more complete extraction of DNA with the concomitant reduction in the risk of missing minor components. DNA prepared by the new method from the fungus *Neurospora* shows a component (25% of the total) which is almost absent from DNA extracted by standard methods. This component appears to reassociate at the same rate as the principal DNA. It is therefore not primarily repeated DNA. The reassociation of *Neurospora* DNA measured spectrophotometrically exhibits the normal time course expected for single-copy DNA

with a small, rapid initial component. Due to the presence of relatively large quantities of mitochondrial DNA it is not yet certain whether or not *Neurospora* contains repeated sequences.

Observed Properties of Repeated DNA Sequences (April 1969)

R. J. Britten

In the four years since the recognition of repeated sequences in DNA a large number of observations of their properties have been made. The generality of their occurrence, their transcription to form RNA, and the striking differences in transcription between different cell types indicate that repeated sequences at present have a major role and probably have had during much of evolution. Nevertheless their mode of origin and function remains unknown. Table 1 lists the major observations that have been made up to the present about repeated sequences. The following comments on the items in the table are intended to be a status report of current knowledge.

1. Measurements of several kinds (hydroxyapatite, optical hypochromicity, DNA agar) have shown that for the more than 60 plant and animal species examined so far a large fraction of the DNA reassociates much more rapidly than can be expected from the DNA content per cell. In bacteria, repetition of ribosomal cistrons has been observed, and a number of copies of episomal DNA are present under certain conditions.

2. The DNA of a number of species has been separated into repetitive and nonrepetitive fractions on hydroxyapatite after samples have been incubated appropriately. These measurements give the best available estimates of the quantity of repeated sequences and the results vary from 20% for sea urchin DNA to at least 80% for salmon and wheat DNA under a standard criterion of precision (see 4, below). The boundary between repeated and nonrepeated sequences is somewhat arbitrary. The amount of repeated DNA measured depends on the length of the fragments as well as the criterion of precision. Future observations are likely to increase the total quantity of repetitive DNA that can be recognized.

3. The rates of reassociation of various observed families of repeated sequences range from 50 times that expected for single copy DNA in *Drosophila* to 2,000,000 times the single copy rate in guinea pig (see 7, below).

4. With several of the assay methods it is possible to measure the thermal stability of the reassociated DNA. A wide range of thermal stability is observed for reassociated repeated sequences including melting temperatures

TABLE 1. Observed Properties of Repeated DNA Sequences

1. Occurrence	Observed in all tested species above the fungi.
2. Quantity	From 20% to 80% of the total nuclear DNA.
3. Frequency	From 50 to 2,000,000 related sequences per family.
4. Precision	All degrees of thermal stability seen in reassociated repeated DNA.
5. Arrangement	Scattered throughout the length of the genome.
6. Age	Several hundred million years up to very recent.
7. Variety	Patterns of frequency and precision vary widely even among vertebrates.
8. Expression	RNA complementary to some repeated DNA sequences has been observed in every cell type examined.
9. Control of expression	Different sets of repeated sequences are transcribed in different tissues and stages of development.

as low as 40° below that of perfectly matching reassociated DNA. A large part of the reduction can be attributed to imperfect matching of the strand pairs and thus to divergence of some of the sequences in a family from others in the same family. A part may also be due to the short length over which the homology occurs in certain cases. A correlation seems to exist between rate of reassociation and thermal stability (see p. 386 in this report) indicating that the families with the highest frequency (largest number of members) also have the highest thermal stability and presumably have originated most recently.

5. Long single strands of higher organism DNA ($\sim 10^7$ daltons) form large "network" particles when incubated so that only repeated sequences reassociate. All but 1–5% of calf DNA is included in such particles and their formation is specific; for example, calf and pea DNA form separate particles when incubated together. This observation indicates that almost all fragments of moderately large size contain somewhere in their length a segment of repeated sequence. Many fragments, of course, must contain more than one. Recent experiments (described on p. 378 of this report) have shown that such interspersion occurs on an even finer scale. Most fragments, about 1.5 million daltons, appear to contain both repeated sequences and nonrepeated sequences.

6. Two lines of evidence suggest the great age of some families of repeated sequences. One is the great difference in nucleotide sequence among the members of some families. The other is the existence of repeated sequences held in common between organisms such as fish and mammals whose common ancestors existed hundreds of millions of years ago. There are also families of repeated sequences which are not shared between closely related species such as the mouse and rat. These must have originated relatively recently.

7. Each species appears to have a distinct pattern of precision and frequency of repeated sequences, and the differences among them are not small. Calf DNA, for example, has a frequency spectrum dominated by a 66,000-copy component making up one-third of the DNA (described on p. 379 of this report). In the human, a component with about this frequency does occur but it contains much less DNA, while a moderate amount of repeated DNA occurs with about 1000 copies. In the calf no families have been observed in the range of about a thousand members. However, a 1000-member family appears to dominate the frequency spectrum of *Xenopus laevis*. More observations are required for correlations and systematic patterns to be discerned. Nevertheless, from the patterns of the few species that have been examined it appears that only a relatively small number of "families" of repeated sequences are present in individual species. It is not known whether a "family" arises in an event in which a segment of DNA is multiplied or a series of events in which shorter segments are multiplied to an approximately equal extent.

8 and 9. Except for a few specifically designed experiments (e.g., *Year Book 67*, p. 320), all of the large number of measurements of RNA hybridization to DNA of higher cells measure only sequence homologies of RNA to repeated sequences of DNA. The results do not indicate what part of a family of repeated sequences has been transcribed. Measurements of the saturation of DNA with RNA thus indicate the size of the families of repeated sequences rather than the "information content" or sequence length of the transcribed RNA. After this realization, the observations apparently must be described in new terms. A role is suggested for repeated sequences in gene expression, or its control. For example, more different repeated DNA sequences are represented in RNA that never leaves the nucleus than in that which reaches the cytoplasm (mouse "L" cells, rabbit kidney cells and

mouse liver cells). During embryonic development of the African clawed toad, *Xenopus,* the changes which occur in the populations of RNA molecules are so great that all of the families of repeated DNA sequences which are observed to be transcribed at some stages are apparently distinct from all of those observed at other stages of development. It is not known that any of the transcribed repeated sequences are translated to yield protein.

A Bovine Genome

R. J. Britten and Jean Smith

The general properties of the repeated sequences of calf DNA have been previously reported (e.g., *Year Book 66,* Fig. 43). The intensive study of the DNA of this one species continues to be rewarding. In the following sections experimental results are described which give insight into three aspects of the organization of this genome. The first aspect is the scattering of interspersion of the repeated sequences throughout the DNA. The second is a more detailed description of the major classes of repeated DNA, including the identification of one class making up about one-third of the total DNA and present in 66,000 "copies." The third is the apparent absence of low frequency repetition such as might be expected if much of the DNA resulted from "gene amplification" by means of copying DNA segments.

Interspersion of repeated and nonrepeated sequences in the bovine genome. Previous experiments (*Year Book 64,* 324–327) have indicated that for mammalian DNA almost all long fragments (5–10 million daltons) contain segments of repeated sequences. Since more than half of the DNA is made up of nonrepeated sequences a majority of these long fragments must also contain nonrepeated sequences as well as repeated sequences. The results shown in Fig. 10 indicate that this interspersion occurs on an even finer scale.

In this series of measurements a rela-

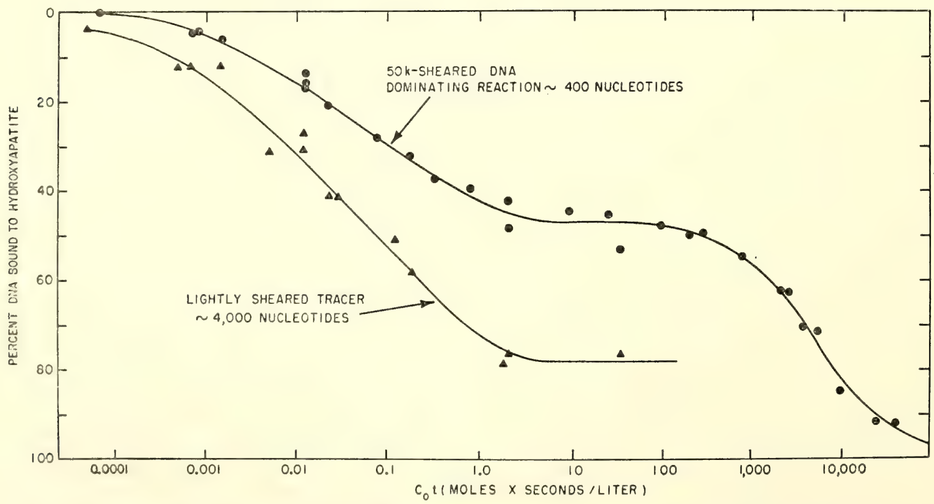

Fig. 10. The demonstration of fine-scale intermixing of repeated and nonrepeated sequences in the calf genome. The upper curve shows the reassociation of calf DNA fragments sheared to about 400 nucleotides. Incubation at 60°C in 0.12 *M* PB and hydroxyapatite assay under the same conditions. The lower curve shows the reassociation of a small quantity of labeled 4000-nucleotide-long fragments with the majority of 400-nucleotide-long fragments. For the upper curve, data have been included from a number of other measurements (all 50-k sheared) in order to give a more complete picture of calf DNA reassociation kinetics.

tively high concentration of DNA sheared to short fragments (400 nucleotides long) was mixed with a small quantity of C^{14}-labeled calf DNA which had been sheared (blender at 7000 rpm) to yield fragments 4000 nucleotides long. This mixture was denatured and samples were incubated for various times in 0.12 *M* PB at 60°C* and passed over hydroxyapatite. The reassociation of the small fragments was assayed by the optical density of the bound DNA, and that of the longer fragments by the bound radioactivity.

Since the longer fragments were present at a very low concentration, no measurable amount of pairs was formed between long fragments. Therefore, in order for a labeled long fragment to bind, a complementary strand pair had to be formed with one of the short unlabeled fragments. Nevertheless, at all times a much greater proportion of the long DNA fragments are bound than of the short ones.

This result indicates that most of the 4000-nucleotide-long pieces contain nonrepeated as well as repeated DNA. It appears that at least two-thirds of the nonrepeated DNA occurs adjacent to repeated sequences. In other words, most stretches of nonrepeating DNA are interrupted at least every 4000 nucleotides by segments of repeated DNA.

Clearly, a great deal of interspersion of the different sequences is present in calf DNA. This test does not go so far as to demonstrate that all repeated sequences are interspersed with the nonrepeated DNA. A minimum of 10–20% of the repeated DNA scattered rather evenly throughout the genome would suffice. This evidence relates mostly to the intermediate rate fraction (66,000 copies) since the more rapidly reassociating DNA was partly removed from the long tracer by a preparative hydroxyapatite fractionation.

There are two major alternative explanations for the interspersion, and future measurements might make it possible to decide between them. First, there could be a functional requirement for distribution of repeated sequences throughout the genome. For example, the repeated sequences might be involved in the regulation of transcription and expression of the adjacent regions of the genome. Second, their interspersion might simply be a measure of the extent to which events of translocation have occurred during evolution.

Resolution of the highly repetitive fractions of bovine DNA. It is difficult to identify the quantities and rates of reassociation of individual components of the spectrum of repeated sequences from a curve such as the upper one in Fig. 10. However, the DNA can be fractionated on hydroxyapatite after various degrees of incubation. Study of the kinetics of reassociation of individual fractions then gives a more detailed view of the spectrum and may allow identification of individual components.

Figure 11 shows diagrammatically the steps of fractionation used in this analysis. Three of the resulting fractions (underlined on Fig. 11) were used for detailed kinetic analysis with hydroxyapatite. The results are shown in Figs. 12, 13, and 14.

Figure 12 shows the results for the largest of the components, identified as intermediate on Fig. 11. The curve drawn on this figure is the time course of an ideal second-order reassociation reaction fitted to the data by a least-squares method. The fit is obviously within error and there is no sign of heterogeneity in this component. Seventeen percent of the DNA does not appear to reassociate and this is due either to partial degradation

* PB represents neutral phosphate buffer made up of equal parts of Na_2HPO_4 and Na H_2PO_4, pH = 6.8. C_0t is an acronym for the product of concentration and time (Mols nucleotides × seconds per liter). It is the parameter that controls the reassociation of DNA when the temperature, salt concentration, and fragment size are defined.

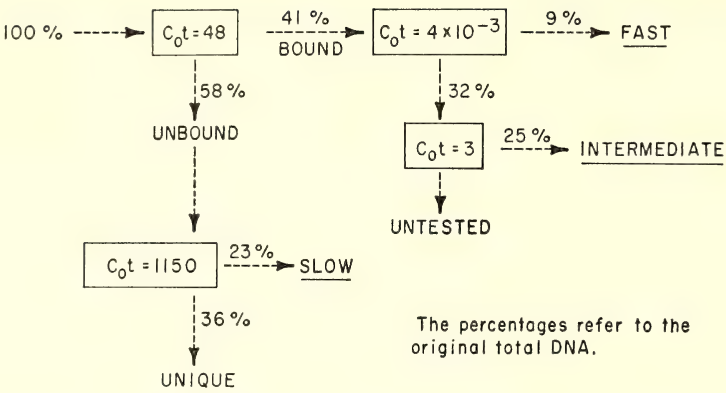

Fig. 11. Diagram of the steps of fractionation used in the study of the repeated sequences of calf DNA. The boxes represent incubations and hydroxyapatite fractionations, done at 60°C in 0.12 *M* PB. The number in each box is the C_0t used in the incubation. DNA which is unbound and thus not reassociated moves to the right, while that which is reassociated moves downward. Data on the reassociation of the three underlined fractions: "intermediate," "fast" and "slow" are presented on the succeeding three figures. C^{14}-thymidine labeled, primary culture, calf kidney DNA prepared by the Marmur method was mixed with DNA extracted from calf brain tissue by the new MUP method described on p. 400 of this report. In each fractionation step the quantity of the two DNAs bound was equal within error ($= \pm 3\%$).

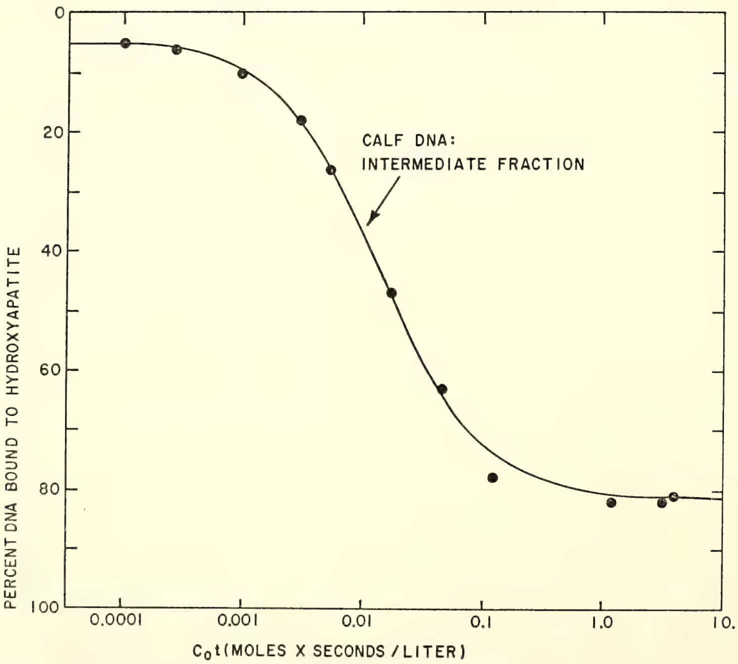

Fig. 12. Reassociation of the "intermediate" fraction of calf DNA, measured with hydroxyapatite. C^{14} labeled calf DNA was fractionated by partial reassociation and passage over hydroxyapatite, as shown in Fig. 11. The fraction marked "intermediate" was then denatured and samples incubated for various times, and passed over hydroxyapatite in 0.12 *M* PB at 60°C. The percentage bound to hydroxyapatite is shown on the ordinate and the incubation C_0t on a logarithmic scale on the abscissa. The curve is the time course of an ideal second-order reaction fitted to the data by a least-squares method using an IBM 1130 computer. RMS error is 1.5%.

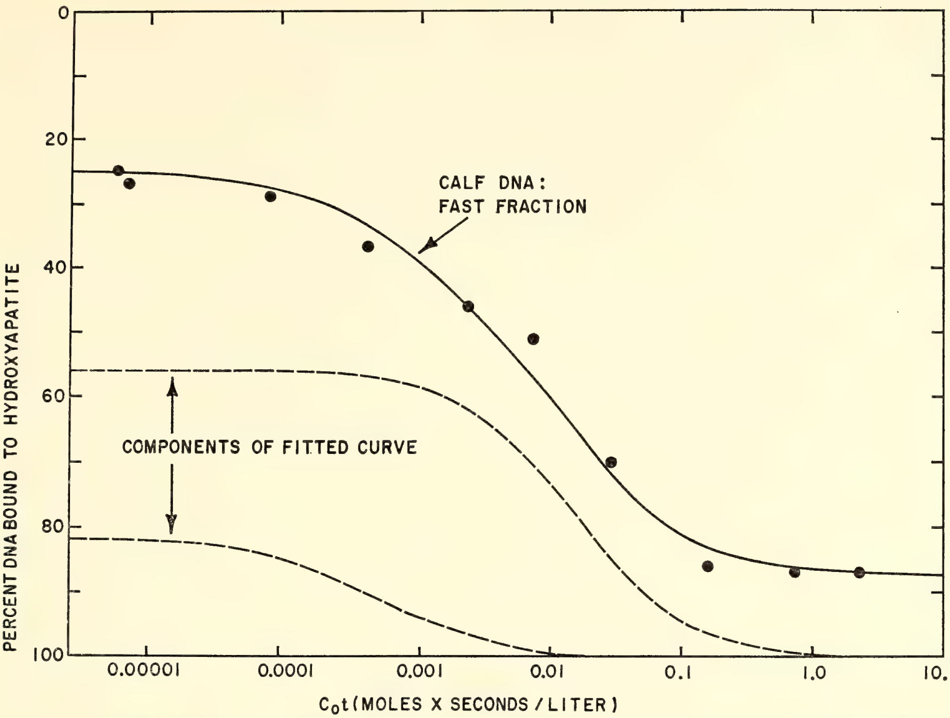

Fig. 13. Reassociation of the "fast" fraction of calf DNA measured with hydroxyapatite. Conditions were as described in caption of Fig. 12, except that two second-order reaction components were used to derive the upper solid curve. RMS error is 2.2%. The individual components are shown on the two lower curves. The slower component has the same rate constant within 15% as the intermediate fraction of Fig. 12. The very fast component which appears to be half reacted at $C_0t = 3 \times 10^{-4}$ is probably a sequence 60 nucleotides long which is repeated 1 million times in the calf genome. Little is yet known of the fraction which is bound at $C_0t = 10^{-5}$. It may represent fragments that can form complementary regions by folding back on themselves.

of the DNA during extensive processing or to imperfect fractionation.

The actual yield of this component is about 30% of the DNA and it may be estimated that it amounts to 37% of the original total DNA. The rate constant for this component is 60.6 $M \times$ sec/liter, while that for *E. coli* under identical conditions is 0.25. The complexity or total length of the DNA that is repeated (*Year Book 65,* p. 89) is therefore about 17,000 nucleotide pairs. Since it makes up 37% of the DNA there are about 66,000 copies present in the calf genome.

It is puzzling, even shocking, that more than one-third of the calf genome should be given over to a population of nucleotide sequences with an apparently single large frequency of repetition. This fraction after reassociation exhibits the very broad range of thermal stability often observed for families of repeated DNA. It should be noted that while the data of Fig. 12 do not imply any heterogeneity in this class of DNA some may nevertheless be present. A limited resolution of different frequency components is set simply by the time course of second-order reactions. Thus, several families of repeated sequences could be in this fraction, differing from the mean by a factor of 2 to 4 or even more for potential small components.

What sort of mechanism could lead to

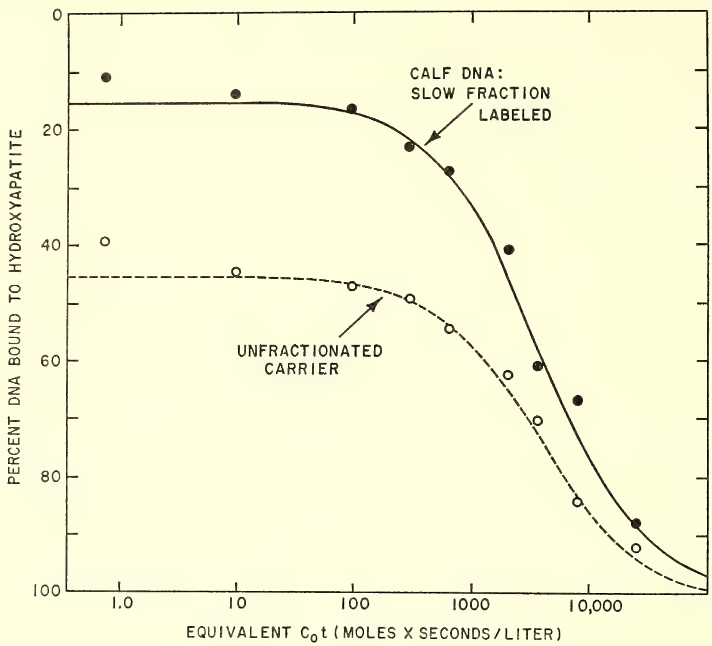

Fig. 14. Reassociation of the "slow" fraction of calf DNA measured with hydroxyapatite. Conditions were as described in the caption of Fig. 12, except for incubation in 0.6 *M* PB at 65°C. A high concentration of unfractionated, unlabeled calf thymus DNA was added to accelerate the reaction and serve as a reference. The two curves are ideal second-order reactions fitted by a least-squares method, except the first point in each instance. They are half completed at $C_0t = 4050$ for the upper curve (tracer; RMS = 3.3%) and $C_0t = 4130$ for the lower curve (carrier; RMS = 1.3%). The abscissa is equivalent C_0t as defined in the text.

the incorporation into the genome of 66,000 copies of a segment or segments of DNA? Perhaps a single event was responsible, in which a length of DNA the size of the genome of a small virus was multiplied many times. Later the individual copies might have diverged from each other and fragments have been scattered throughout the genome by translocation. Another, but less likely, possibility is that at various times small fragments of DNA have been copied. For reasons of structure or function in each case about 66,000 copies would have been incorporated into the genome.

The most rapidly reassociating DNA of the calf. Measurements have been made of the reassociation of the 9% fraction identified on Fig. 11 as "fast." The results are shown in Fig. 13. There appear to be three major components in this fraction. The slowest has a reassociation rate constant about equal to that of the intermediate component (Fig. 12). Some of the intermediate component is expected as a "contaminant" in the "fast" fraction since it partially reacts at the C_0t (4×10^{-3}) used in the fractionation.

The faster component shown on Fig. 13 appears to be half reassociated at a C_0t of 3×10^{-4}. Due to the relatively small amount of it there is a large potential error in the estimate of its rate of reaction and its quantity. However, there is little doubt that it exists. This component may be an analog of the mouse "satellite," which consists of a million copies of a sequence several hundred nucleotides long. The sequence

that has been repeated in the calf is shorter, perhaps only 60 nucleotides long, but there are apparently about a million copies present. This component (or family of repeated sequences) makes up only 2 or 3% of a calf DNA but it could be purified relatively easily. We have not yet done so and thus do not have measurements of its thermal stability or composition. It is not known whether it corresponds to the "dense satellite" that is observed in CsCl density gradient analysis of calf DNA.

About 25% of the DNA of the "fast" fraction is bound at the earliest measurement ($C_0t=10^{-5}$). It appears that no collisions are required between DNA strands, i.e., no reassociation in the usual sense, is required for the binding of this fraction to hydroxyapatite. The binding of this fraction of calf DNA may be attributed to some specific characteristic which makes it mimic the behavior of double-stranded DNA, as far as its binding to hydroxyapatite. It seems likely that an unusually high degree of local complementary pairing can occur among the bases of individual "single-stranded" fragments.

The thermal stability and hyperchromicity observed when this fraction is "melted" in the spectrophotometer give further clues to its nature. The melting occurs continuously over a broad range of temperatures from 60 to 90°C. Therefore, this fraction probably is not cross-linked in such a way that native-type double-stranded secondary structure can form. On melting, the hyperchromicity is only about 10% of the optical density in the denatured state. Thus, perhaps only half, or less, of the bases are paired. A large reduction in optical density (8–10%) is observed when this fraction is subsequently cooled even at very low salt concentration ($10^{-3}M$ EDT). This observation also indicates that collisions between separate fragments are not necessary for double-stranded type secondary structure to be formed in this fraction.

Possibly these fragments are the result of nucleotide sequence inversions and thus contain complementary stretches of bases which can "fold back" on themselves, as suggested by Peter Walker originally for the mouse satellite as a whole and later for a small fraction of it.

"Internal" base-pairing within a single strand could consist of extended regions of homology which, for example, permit a "hairpin" to form. Many other patterns can also be imagined, particularly since there are only a few facts to go on. The base sequence could contain a kind of "intimate self-complementarity" such as is present in the alternating "dAT" which makes up 30% of the DNA of some crabs. The sequences in this fraction of the calf DNA cannot be quite as simple as dAT since, in the reassociated state, this DNA melts over a very broad range of temperatures. Another possibility is that there could be local clusters of bases complementary to clusters elsewhere on the fragment. The double-stranded regions of sRNA might contain the requisite secondary structure for binding to hydroxyapatite under our conditions. Thus, the genes for sRNA might appear in the "foldback" DNA fraction.

DNA with similar characteristics has been observed in several creatures. The first demonstration of such a "fold-back" in mouse DNA was made jointly with Peter Walker during his visit to this laboratory in 1966. Only 1% of mouse DNA is in this form compared to about 3% for calf. The African clawed toad *Xenopus laevis* contains about 11% while human DNA contains about 3%. In some preparations a certain degree of instability has been observed. That is, the yield of this "foldback" fraction falls during sequential steps of binding to hydroxyapatite.

All of these estimates have been made with DNA that had been sheared at 50,000 psi and has an average fragment size of 400 or 500 nucleotides, single stranded. One measurement, made with calf DNA of a larger fragment size, sug-

gests that a greater fraction of the DNA can be bound to hydroxyapatite because of "foldback." In preparation for the experiment of Fig. 10, the labeled DNA that had been sheared at 7000 rpm (fragments about 4000 nucleotide pairs long) was denatured, rapidly cooled to 60°C and quickly passed over HAP in 0.12 *M* PB. The effective C_0t was about 10^{-4} and 31% of the DNA was bound. A part of this binding was due to the rapidly reassociating families of repeated sequences, but it is likely that the principal binding was due to the "foldback." The implication is, of course, that the "foldback" regions are also scattered throughout the genome and are individually fairly short, at least in comparison with the long fragments used in this test. No significant comment can yet be made on the mechanism of origin or possible function of these "foldback" sequences. However, there is one bit of evidence suggesting that they may be related to the repetitive DNA. Apparently they occur with relatively high frequency in mouse satellite DNA[9]. About 20% of one of the complementary strands prepared by density gradient centrifugation binds to hydroxyapatite at extremely low C_0t.

Limit on low-frequency sequences. The fraction labeled "slow" on Fig. 11 contains sequences which had not reacted at $C_0t=48$ but in a second incubation did reassociate at $C_0t=2000$. A large part of this fraction is made up of nonrepeated sequences, but in addition there would be present in this fraction sequences repeated at a low frequency in the original calf DNA if they existed. Their relative concentration would be increased depending on their frequency of repetition. By calculation at least, those present in about 10 copies would be increased fourfold, while those with greater or less numbers of copies would be less amplified.

In order to test sensitively for such low repetition DNA, an excess of unlabeled, unfractioned calf DNA was added to the labeled "slow" fraction. This added "carrier" DNA had been sheared in the same way as the labeled DNA (50,000 psi) so that it would have the same rate of reassociation. The "carrier" DNA was present at a high concentration (3 mg/ml) and the salt concentration was also raised to 0.6 *M* PB so that nonrepeated DNA would reassociate in a reasonable time (the last point was taken at 8 days). This mixture was denatured and samples were incubated for various times at 65°C, diluted to 0.12 *M* PB and passed over hydroxyapatite at 60°C. Figure 14 shows the results of the assay for the binding of both the labeled "slow" fraction and the carrier DNA.

The abscissa scale on Fig. 14 introduces a new term, equivalent C_0t, which has become necessary as a result of the use of high salt concentrations to accelerate reactions of slowly reassociating DNA. The effect of salt concentration on the rate of the reaction is now rather accurately known from the measurements made by Wetmur and Davidson.[10] In order to calculate equivalent C_0t we use the empirical formula given in *Year Book 67,* which includes the following term for the variation of rate with monovalent cation concentration (κ):

$$\kappa^{(.24/\kappa)^{.42}}$$

Unfortunately, in formula 16, pp. 333 and 334, *Year Book 67,* the upper exponent was omitted in printing. As this equation is somewhat inconvenient, Table 2 was prepared. Using the above constants, it gives the rate of reassociation relative to that expected in 0.12 *M* PB. Wetmur and Davidson's data, on which this table is based, was obtained in each case at the optimum temperature, about 25°C below the melting temperature at the particular salt concentration. Observed rates will be less at other temperatures.

There is no evidence from the curves in Fig. 14 for any low repetition frequency sequences. Clearly no large popu-

TABLE 2. Rate of DNA Reassociation * versus Salt Concentration

Monovalent cation concentration	Relative reassociation rate	PB † molarity	Monovalent cation concentration	Relative reassociation rate	PB molarity
0.015	0.0000	0.01	0.465	3.8841	0.31
0.030	0.0016	0.02	0.480	4.0085	0.32
0.045	0.0133	0.03	0.495	4.1300	0.33
0.060	0.0453	0.04	0.510	4.2487	0.34
0.075	0.1021	0.05	0.525	4.3646	0.35
0.090	0.1831	0.06	0.540	4.4778	0.36
0.105	0.2858	0.07	0.555	4.5884	0.37
0.120	0.4063	0.08	0.570	4.6964	0.38
0.135	0.5410	0.09	0.585	4.8019	0.39
0.150	0.6867	0.10	0.600	4.9049	0.40
0.165	0.8404	0.11	0.615	5.0056	0.41
0.180	1.0000	0.12	0.630	5.1040	0.42
0.195	1.1633	0.13	0.645	5.2001	0.43
0.210	1.3288	0.14	0.660	5.2941	0.44
0.225	1.4954	0.15	0.675	5.3860	0.45
0.240	1.6619	0.16	0.690	5.4758	0.46
0.255	1.8277	0.17	0.705	5.5636	0.47
0.270	1.9920	0.18	0.720	5.6495	0.48
0.285	2.1544	0.19	0.735	5.7335	0.49
0.300	2.3146	0.20	0.750	5.8157	0.50
0.315	2.4722	0.21	0.825	6.2009	0.55
0.330	2.6271	0.22	0.900	6.5478	0.60
0.345	2.7791	0.23	0.975	6.8613	0.65
0.360	2.9280	0.24	0.050	7.1457	0.70
0.375	3.0739	0.25	1.125	7.4047	0.75
0.390	3.2167	0.26	1.200	7.6413	0.80
0.405	3.3563	0.27	1.275	7.8582	0.85
0.420	3.4929	0.28	1.350	8.0575	0.90
0.435	3.6263	0.29	1.425	8.2412	0.95
0.450	3.7567	0.30	1.500	8.4110	1.00

* Calculation based on an empirical formula (see text) fitted to the data of Wetmur and Davidson.[10] At optimum temperature, 25°C below melting temperature.

† Neutral phosphate buffer.

lation of such sequences is present in calf DNA. What limits can be set from this experiment? A component present in 10 copies and making up 2% of the original DNA would make up 8% of a "slow" fraction. It would very likely be recognizable, but a smaller one might not be. Suppose, for example, that half of the slowly reassociating DNA was present in two copies, the remainder being present as single copies. In such a case the calculated average rate of reaction of the labeled "slow" DNA would be greater than that of the carrier by only 7%, which would be difficult to distinguish. The two curves in Fig. 14 show the time course of ideal second-order reactions fitted to the data by a least-squares method. (The earliest point at $C_0t=0.8$ was not included since some of the very fast component remains.) There is no sign of any systematic deviation of the data points from these curves, and the RMS errors are 3% for the tracer and 1% for the carrier. Half reaction for these fitted curves occurs at $C_0t=4050$ for the tracer and at $C_0t=4130$ for the unfractionated carrier. Therefore, there is no evidence at a moderate level of sensitivity for sequences present in a small number of copies.

This result is of general interest since there are several lines of theoretical argument which might suggest the existence of recognizable quantities of low frequency repetition. First, it appears

that gene duplication has often occurred during evolution. Even though the resulting gene sequences undergo changes of various sorts, the evidence of sequence homology remains among the proteins themselves, as, for example, in the well-known case of vertebrate hemoglobins. Second, there may have occurred events of duplication at other levels of organization during the evolution of the ungulates. Specific chromosome duplications would, under the proper conditions, leave traces recognizable in this way. Third, it has recently been proposed that during the development of an individual many or most genes are copied a number of times to form "slave" genes [11, 12]. It was thought that the "slaves" would be the DNA actually transcribed while "master" copies were preserved for hereditary service in the germinal line of cells with less risk of damage. Finally, there is direct evidence that certain genes are "amplified"; that is, a number of copies are made at given times or in specific cell types. The best example is the set of ribosomal genes which not only exist in many copies in the DNA of every cell, but are present in even larger quantities in amphibian eggs and certain other tissues. The negative evidence presented above of course does not rule out such models, since only a few genes might be amplified in particular tissues.

The failure to observe small numbers of copies of DNA sequences implies that repeated sequences originate in events of large-scale multiplication (saltatory replications) rather than from many single duplications spread over a long period of time. In the latter case one would expect to observe a continuous distribution of frequencies, rather than what is actually observed in calf DNA: relatively discrete large families with many members and a paucity or absence of low-frequency repetition.

Fractionation of Rat Repeated Sequences According to Thermal Stability

Nancy Reed

Families of repeated sequences, commonly characterized according to their reassociation rates, may also be described in terms of the thermal stability of the reassociated products. Such an approach can provide a roughly quantitative measure of the degree of sequence divergence within a given family. Cross-reaction of an isolated family with heterologous DNA, furthermore, might furnish additional insights into the family's evolutionary history. Results reported here are preliminary explorations of such questions, and deal with (1) the properties of isolated reassociated DNA fractions of varying thermal stability and (2) relationships among the fractions.

Studies have been performed with mouse or rat DNA which had been sheared at 50,000 psi, incubated to $C_0t \cong 100$ at 50° or 60°C in 0.14 *M* phosphate buffer, and applied to hydroxyapatite at the incubation temperature. Following elution of the adsorbed DNA at 5°C intervals (Fig. 15), each fraction was reincubated at $C_0t \cong 10$, again at 50° or 60°C. Reassociated material was then recovered from hydroxyapatite by elution at 0.4 *M* PB, 50°C. Thermal behavior of the fractions was similar to that described by Britten and Kohne for salmon DNA (*Year Book 66*). As with salmon DNA, each fraction exhibits an optical T_m within a few degrees of its original HA elution temperature. The hyperchromicity of a fraction was found to vary directly with its thermal stability: values ranged from about one-third to more than three-fourths the hyperchromicity of native DNA for DNA fractions eluting at 65°C and at 90°C, respectively. However, while the fractions exhibited specificity with respect to T_m and hyperchromicity, their melting profiles, particularly among the low stabil-

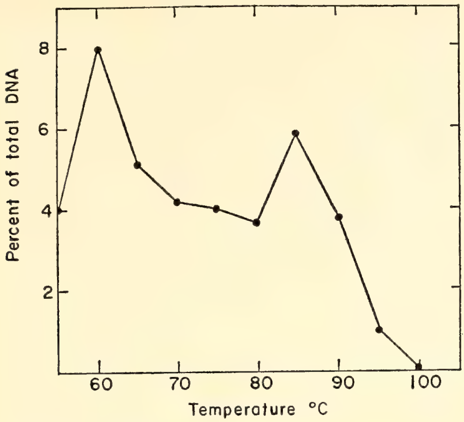

Fig. 15. Thermal elution of the reassociated repeated sequences of rat DNA. Rat DNA at 400 μg/ml in 0.14 *M* PB was heated to 100°C for 5 minutes, then incubated at 50°C for 20 hours. About 40% of the DNA subsequently bound to a hydroxyapatite column at 50°C in 0.14 *M* PB. The bound material was eluted at 5°C intervals.

ity fractions, exhibited considerable overlap.

Since heterogeneity of a DNA sample can be revealed in its reassociation profile (see *Year Book 65*), reassociation rates of the rat thermal fractions were determined both optically and by HA chromatography. Without exception it was found that the higher the T_m of a fraction of rat DNA, the higher was its average reassociation rate. The rat 90°C fraction, for example, exhibited 50% reassociation at $C_0t \cong 7 \times 10^{-3}$ (HA assay 0.14 *M* PB) the 65°C fraction reached 50% reassociation at $C_0t \cong 2 \times 10^{-1}$. Fractions of intermediate stability revealed intermediate reassociation rates (see Fig. 16). Further, it was found that while each fraction could be characterized by a unique reassociation profile, the profiles in most cases were broader than expected for a homogeneous sample. Thus, each fraction appeared to contain more than one component.

The possibility that there are sequences common to several (or many) of the fractions was investigated through the use of radioactive rat DNA. A rat $C^{14}-90$°C fraction, for example, has been incubated with fiftyfold excesses of various nonradioactive fractions. Considerable cross-reaction among the fractions was observed. A majority of the radioactive 90° or 80°C fractions, in fact, was found to be capable of re-

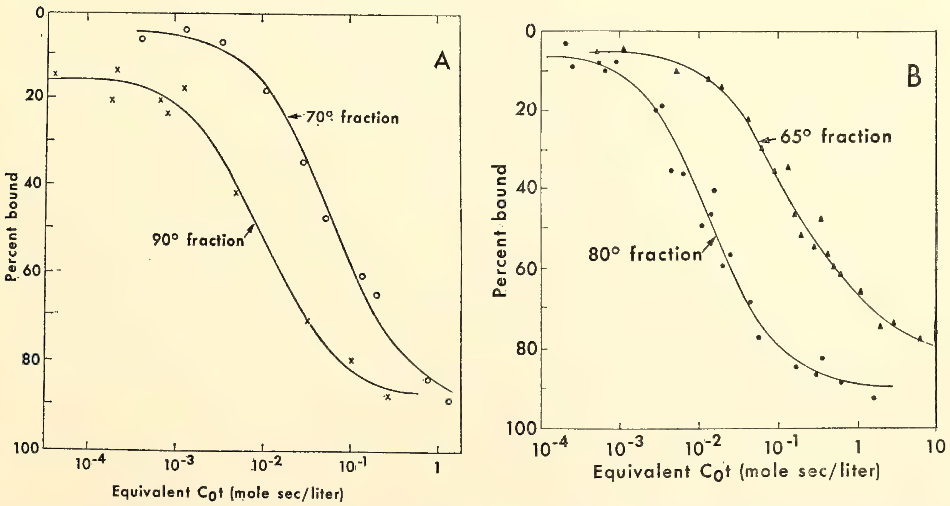

Fig. 16. Reassociation of thermal fractions of rat DNA. C^{14}-DNA fractions (prepared as described in text) were incubated in 0.14 *M* PB at 50°C at varying C_0t values. Subsequent binding of radioactivity to hydroxyapatite (0.14 *M* PB, 50°C) was measured.

association with unlabeled 90°, 80°, 70°, or 65°C fractions. From the observed rates of reaction, it has been possible to estimate that about two-thirds of the unlabeled 80°C fraction and slightly less than one-third of the unlabeled 65°C fraction may be homologous to material in the $C^{14}-90$°C fraction.

The presence of more than one component in the 65°C fraction was directly demonstrated in a slightly different experiment. A $C^{14}-65$°C fraction was incubated with excess unlabeled 90°C fraction under conditions sufficient to allow the reassociation of most of their common sequences. The remaining unreassociated radioactive material was then observed to be greatly reduced in its ability to reassociate with a second 90°C fraction, but still capable of extensive reaction with a 70°C fraction. Therefore, at least two classes of sequences are indicated in the $C^{14}-65$°C fraction. The precise number of families in the rat genome is not yet known, but these and other preliminary data are consistent with a low value (less than 10). Several of the families may comprise a substantial fraction of the genome.

To summarize: the repeated sequences in rat or mouse DNA can be fractionated according to their thermal stability; the fractions exhibit specificity in thermal behavior and reassociation rate. Cross-reaction of the fractions, however, reveals the presence of sequences common to many of them and indicates that the range of sequence divergence within families may be extremely broad.

DNA Sequences Present as Multiple Copies in *E. coli*

J. A. Chiscon and D. E. Kohne

Reports of previous experiments (*Year Book 67,* p. 310) describe methods for the isolation and characterization of bacterial rR-cistrons, those nucleotide sequences coding for ribosomal RNA. These experiments also demonstrate that such cistrons represent small amounts of repeated nucleotide sequences in the bacterial genome. A recent attempt has been made to explore further the possibility that additional repetitious DNA does in fact exist in such prokaryotes as the bacteria. Experimentation utilizing *E. coli* has resulted in the isolation and purification of a small DNA fraction which exists as multiple copies within the bacterial cell. The copy number is dependent upon the growth stage of the bacterial population.

E. coli BB $P^{32}-$DNA from stationary phase cells was isolated, sheared, denatured, and allowed to reassociate partially during incubation (*Year Book 67,* p. 311). This fraction was recovered from hydroxyapatite, denatured, allowed to reassociate partially, and the reacted fraction again recovered. Conditions for five such consecutive cycles were chosen so that, from cycle to cycle, the amount of nonrepetitive *E. coli* DNA able to reassociate would decrease greatly. Repeated DNA sequences, however, would react more rapidly and be conserved in the reassociated fraction of each cycle. Table 3 gives both expectations and observed data which, at the conclusion of the five cycles of purification, show the percentage of reassociation expected of nonrepeated *E. coli* BB P^{32}-DNA to be 0.006%, and the actual percentage of re-

TABLE 3. Reassociation Rate Fractionation of *E. coli DNA*

Cycle	P^{32}-DNA C_0t	Original input P^{32}-DNA adsorbed, %	Calculated P^{32}-DNA expected to be adsorbed, %
1	0.44	14.2	14.5
2	0.44	2.5	2.1
3	0.44	1.3	0.3
4	0.44	0.57	0.044
5	0.44	0.48	0.006

Note: Data showing the fraction of original input P^{32}-DNA from *E. coli* BB adsorbing to hydroxyapatite when reacted with itself, and the calculated fraction of nonrepetitive DNA expected to adsorb to hydroxyapatite at the given C_0t values.

association obtained, prior to removal of rR-cistrons and their complementary strands, to be 0.48%.

Following cycle 5, rR-cistrons were removed from the recovered DNA by incubating the solution with a large aliquot of R-RNA, Rnasing, passing the solution through hydroxyapatite to trap DNA-RNA hybrids, and passing the nonreassociated DNA over Dowex-50 to remove basic protein. DNA complementary to the rR-cistrons was then removed by incubating the remaining DNA for a time sufficient for almost complete reassociation ($C_0t=0.3$) of DNA for which complementary strands were available. The reassociated DNA, now amounting to 0.3% of the bulk *E. coli* DNA, was recovered from hydroxyapatite.

Figure 17 illustrates the time course of reassociation of this final isolated fraction of P^{32}-DNA. The rapidly reassociating fraction has a C_0t for half reaction of about 1.8×10^{-2}, and the reaction follows an ideal second-order reaction curve with reasonable precision. The $C_0t_{1/2}$ suggests a DNA information content of about 1.8×10^7 daltons. Figure 18 shows the reassociation kinetics of the isolated fraction of P^{32}-DNA and bulk *E. coli* DNA isolated separately from both mid-log and stationary stages of culture growth. The experimental points for the bulk DNA from both stages follow the ideal curve. The isolated P^{32} fractions, incubated separately with bulk DNA from each stage of growth, differ both from the bulk DNA and each other in time course of reassociation. The fraction incubated with mid-log bulk DNA reassociated about two times faster than the bulk DNA; the fraction incubated with stationary bulk DNA reassociated about seven times faster. The multiple copies, then, may represent as much as 4–5% of the total

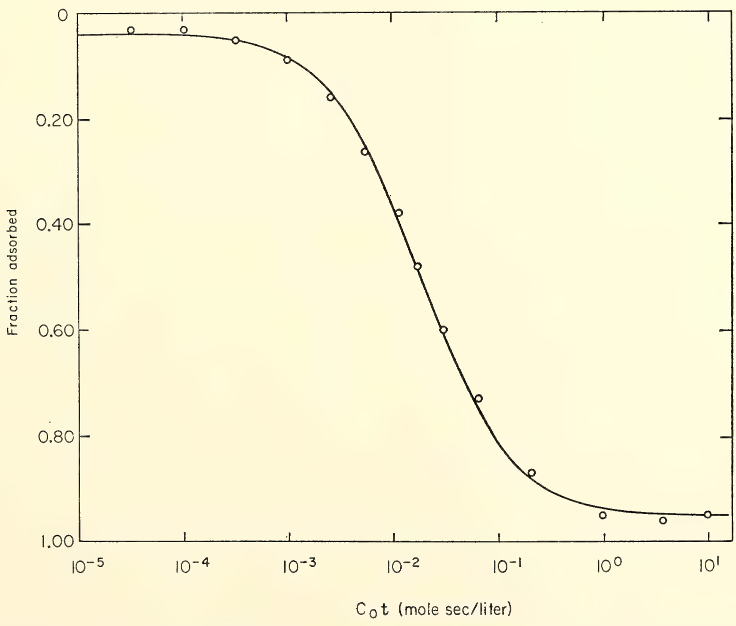

Fig. 17. The kinetics of reassociation of an isolated fraction of *E. coli* BB P^{32}-DNA. Each point represents an aliquot taken from one of two incubation mixtures containing different DNA concentrations. Following denaturation, the mixtures were incubated for the indicated C_0t before the aliquots were withdrawn, passed through hydroxyapatite, and the front and back peaks monitored for radioactivity.

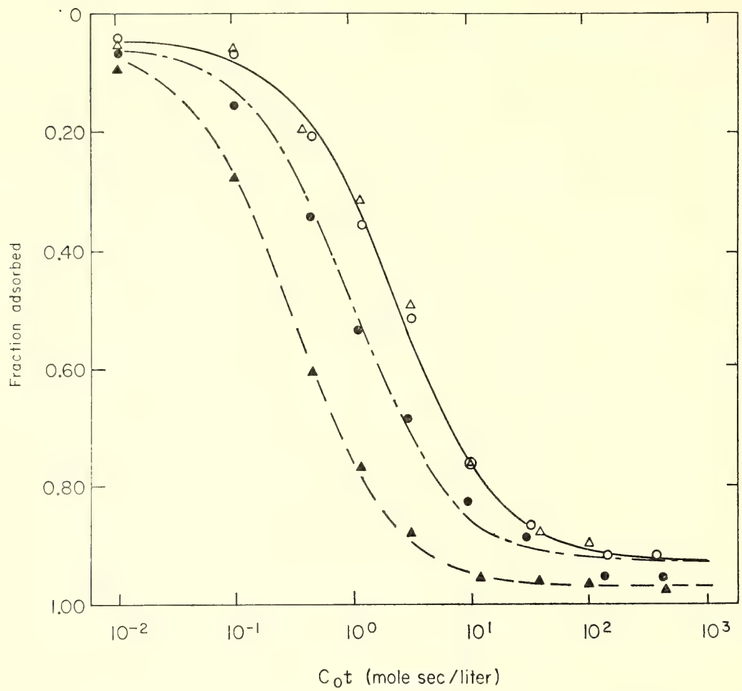

Fig. 18. The reassociation kinetics of an isolated fraction of *E. coli* BB P^{32}-DNA incubated separately with *E. coli* unlabeled bulk DNA isolated from mid-log and stationary stages of culture growth. Open circles represent the reassociation of mid-log bulk DNA; open triangles, stationary bulk DNA. Solid circles represent the reassociation of the small quantities of P^{32}-DNA incubated with the mid-log bulk DNA (1/1,800). Solid triangles refer to the P^{32}-DNA incubated with stationary phase bulk DNA. Each point represents an aliquot taken from one of four incubation mixtures containing different DNA concentrations. Following denaturation, the mixtures were incubated for the indicated C_0t before the aliquots were withdrawn, passed through hydroxyapatite, and the front and back peaks measured for optical density and monitored for radioactivity.

DNA of the stationary stage bacterial cell. Further analysis of the data points to possible heterogeneity of the isolated fraction. At mid-log, two components appear to be represented unequally as a large fast fraction and a smaller slow fraction, while in the stationary phase the two appear to approach equality in copy number.

The ability of the P^{32}-DNA to hybridize with a mixture of 16S and 23S R-RNA subunits was found to be low (2.7%). In addition, although half of the cold bulk DNA reassociated in each of the experiments, the ability of the P^{32}-DNA to form duplexes with DNA from salmon (0%), *Salmonella typhimurium* (2.0%), *Proteus mirabilis* (3.5%) and *Enterobacter aerogenes* (5.0%) was also low.

It appears that, in addition to rR-cistrons, other DNA nucleotide sequences present as multiple copies within bacterial cells can be isolated from those cells, utilizing the purification methods outlined above. Differing degrees of multiplicity during different stages of culture growth suggest that this DNA is not a part of the actual bacterial genome, but is extrachromosomal in nature. The possibility does exist that selective and varying amplification of a small fraction of the genome itself has been detected. It is known, however, that certain extra-

chromosomal elements escape normal regulation and apparently form multiple copies each time a bacterial chromosome is replicated once. In addition, there must be metabolic restriction of excessive multiplication of these elements during growth of the bacterial population. The probability, then, is great that in this case it is DNA from extrachromosomal elements that has been studied. If this is so, a relatively quick, simple, useful method is available for isolation and characterization of episomal and plasmid DNA.

Cyanophyta and their Viruses

D. B. Cowie and Lillian K. Prager

Blue-green algae and bacteria are classified in a super-kingdom, the prokaryotes, characterized as organisms lacking well-defined nuclei. This distinction represents a basic difference from higher cell types, the eukaryotes, in which true nuclei exist bounded by nuclear envelopes. Our studies in this laboratory of the nucleic acid composition of both types of cells have shown another significant distinction: the DNA of prokaryotes is nonrepetitive except for small amounts of ribosomal or episomal DNAs, while that of the eukaryotes consists of large quantities of repeated DNA sequences as well as the nonrepetitive DNA.

The investigation of genetic material held in common among bacteria and temperate bacteriophages has provided some information concerning taxonomic relationships as well as indicating probable evolutionary patterns among these organisms. These studies have been enlarged to include the blue-green algae in the hope that these organisms may serve as an experimental system bridging the apparent evolutionary discontinuity between the prokaryotic and eukaryotic types of cells. Unlike the bacteria, the blue-green algae share the property of an oxygen-evolving photosynthesis with eukaryotic algae and higher plants.

Our first discovery was that the taxonomic classification of the blue-green algae is often confusing and many references are obscure or unattainable. As a guide for experimentation and for discussion, we have selected a classification of Smith [13] shown in Table 4.*

The discovery and isolation by Safferman and Morris [15] of a virus (LPP-1) capable of lysing certain species of the three blue-green genera *Lyngbya, Plectonema* and *Phormidium* suggested that these organisms, all having a common viral host-range specificity, might be evolutionally related. It is of interest to note that *Lyngbya* and *Phormidium* have been classified in Suborder 1 as Oscillatorineae (Table 4) while *Plectonema* is listed in Suborder 2, Family 2 under Scytonemataceae.

Figure 19 demonstrates that nucleotide sequence homologies exist among the three blue-green algae sensitive to the LPP-1 virus. Radioactive *Plectonema boryanum* (597) DNA fragments were reacted with *Lyngbya* (488) and Phormidium (485) DNA embedded in agar. The degree of reassociation and the thermal stability of the reaction products were examined by means of the DNA–DNA-agar thermal chromatography method.[16] Since the blue-green alga *Fremyella diplosiphon* (481) had been included by Smith in the same family as *Plectonema boryanum* (597) it was included in these reaction tests with *Plectonema* DNA. No reaction between these two DNAs was observed, however, indicating that *Fremyella* (481) probably belongs in another family of blue-green algae.

Figure 19 also shows that the thermal stability of the reaction products formed between *Plectonema* (597) DNA fragments and the DNAs of *Phormidium* (485) and *Lyngbya* (488) is almost as high as that observed when the *Plectonema* (597) DNA fragments are reacted

* All blue-green algae used are from the Culture Collection of Algae at Indiana University [14] unless otherwise identified.

TABLE 4. Cyanophyta *

Order 1. CHROOCOCCALES	Order 2. CHAMAEDIPHONALES	Order 3. OSCILLATORIALES
Family 1. Chroococcaceae	Family 1. Pleurocapsaceae	Suborder 1. Oscillatorineae
Chroococcus	Family 2. Dermocarpaceae	Family 1. Oscillatoriaceae
Gloeocapsa	Family 3. Chamaesiphonaceae	*Oscillatoria prolifera* (1270)
Synechocystis		*Arthrospira*
Aphanocapsa		*Borzia*
Microcystis		*Romeria*
Chondrocystis		Phormidium sp. (485)
Eucapsis		*Trichodesmium*
Synechococcus		*Spirulina*
Gloeothece		Lyngbya sp. (488)
Chroothece		Lyngbya sp. (621)
Rhabdoderma		*Porphyrosiphon*
Bacillosiphon		*Symploca*
Dactylococcopsis		*Microcoleus*
Aphanothece		*Hydrocoleum*
Anacystis nidulans (625)		*Schizothrix*
Merismopedia		Suborder 2. Nostochineae
Holopedium		Family 1. Nostocaceae
Coelosphaerium		*Anabaena*
Marssoniella		*Aulosira*
Gomphosphaeria		*Anabaenopsis*
Glaucocystis nostochinearum (64)		Nostoc sp. (588)
Gloeochaete		*Wollea*
Family 2. Entophysalidaceae		*Aphanizomenon*
		Cylindrospermum
		Nodularia
		Family 2. Scytonemataceae
		Scytonema
		Tolypothrix
		Plectonema boryanum
		Plectonema boryanum (597)
		Diplocolon
		Desmonema
		Fremyella diplosiphon (481)
		Family 3. Stigonemataceae
		Family 4. Rivulariaceae

* Condensed from Gilbert M. Smith, *The Fresh-Water Algae of the United States,* McGraw-Hill Book Company, Inc., New York, 1950.

TABLE 5. Reaction between *Lyngbya* (621) DNA Fragments and the DNA of Other Blue-Green Algae

DNA in agar	Radioactivity bound (c/m)	Percentage radioactivity bound relative to control
Lyngbya (621)	6686	100
Phormidium (485)	1510	23
Plectonema (597)	981	15
Oscillatoria (1270)	4163	62
Anacystis (625)	2108	32

Note: Less than 0.01 μg of *Lyngbya* (621) DNA fragments were reacted with DNA-agar each containing approximately 10 μg embedded algal DNA. Fifty-five percent of the *Lyngbya* (621) DNA fragments reacted with the *Lyngbya* (621) DNA in agar.

with *Plectonema* (597) DNA-agar. This result indicates a high degree of precision of base pairing among the reacting nucleotide sequences. Table 5 shows that compared to the reaction of the *Plectonema* (597) DNA fragments with the identical DNA in agar, 62% of the *Plectonema* (597) fragments reacted with the *Lyngbya* (488) and 51% with the *Phormidium* (485) DNAs under the experimental conditions employed (see legend, Fig. 19).

The LPP-1 virus. The LPP-1 virus, which is capable of infecting all of the above blue-green algae except *Fremyella* (481) has been isolated and some of the characteristics of its DNA examined.

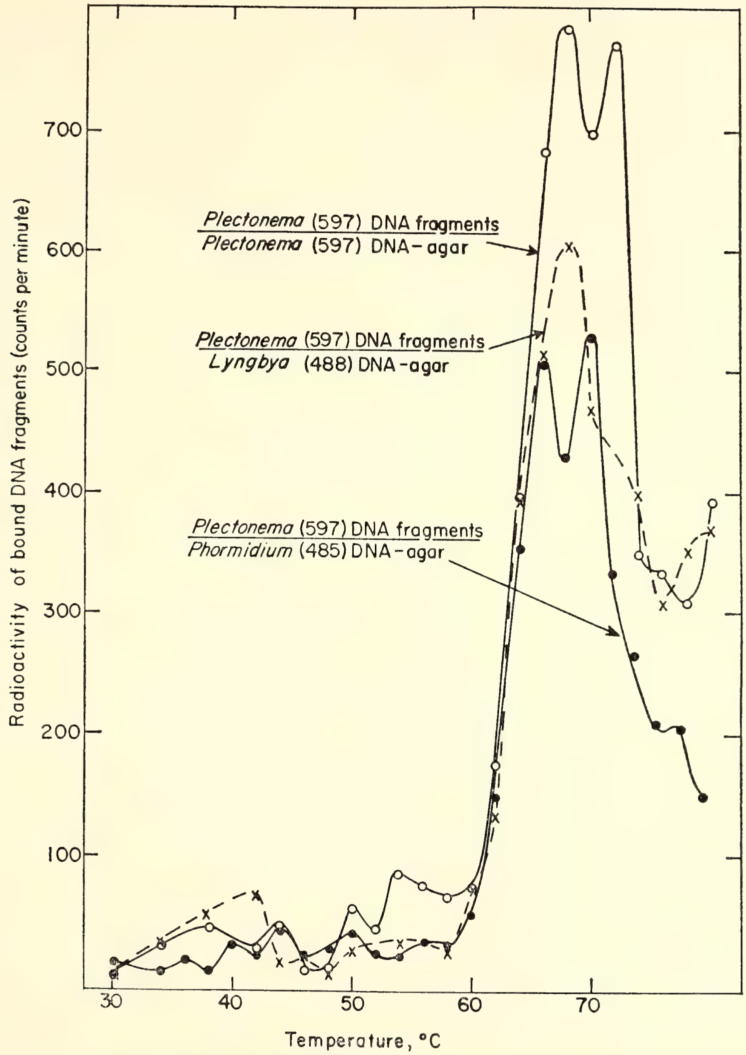

Fig. 19. Thermal elution profiles characteristic of the reaction of radioactive *Plectonema* (597) DNA fragments with *Plectonema* (597) DNA-agar (circles and solid lines); with *Lyngbya* (488) DNA-agar (crosses and broken lines); and with *Phormidium* (485) DNA-agar (solid circles and solid lines). Two μg of the radioactive fragments were incubated overnight at 60°C with approximately 10 μg of the algae DNAs embedded in agar. The thermal elutions were carried out in SSC/30 (SSC is 0.15 *M* NaCl to 0.015 *M* Na citrate).

Figure 20 shows the thermal elution profile obtained from studies of the reaction of LPP-1 DNA fragments with LPP-1 DNA-agar.

When LPP-1 DNA fragments obtained from the infection of *Plectonema* (597) are reacted with DNA-agar preparations of *Plectonema* (597), *Phormidium* (485), *Lyngbya* (488), or *Fremyella* (481), no DNA-DNA reactions are observed. The lower curve shown in Fig. 20 (solid circles) was obtained from a study of LPP-1 DNA fragments after incubation with *Lyngbya* (488) DNA-

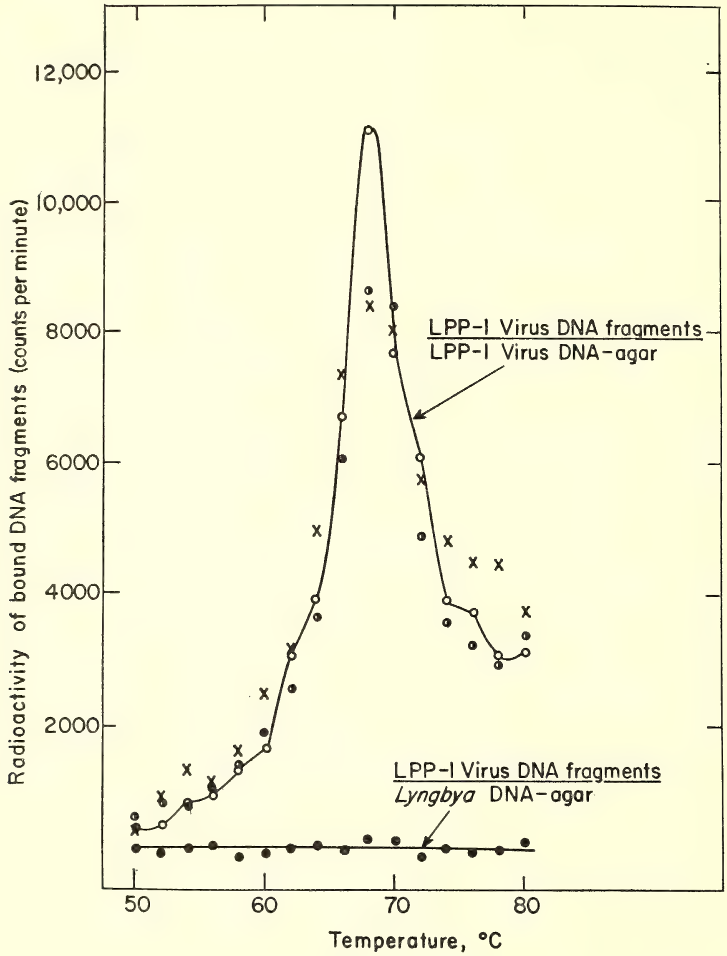

Fig. 20. Thermal elution profiles obtained from studies of the reaction of three different radioactive preparations of LPP-1 DNA fragment preparations (circles with solid line; crosses; circles) with 18 μg of LPP-1 DNA-agar, and with 7 μg *Lyngbya* (488) DNA in agar (solid circles). More than 35% of the LPP-1 DNA fragments reacted with the LPP-1 DNA agar, while less than 1% reacted with the *Lyngbya* DNA after overnight incubation at 60°C. Less than 1 μg of the labeled LPP-1 DNA fragments were used for each test and the elution was carried out in SSC/30.

agar. Similar results were obtained when the other blue-green algae DNAs were tested. These results are in agreement with those obtained by Luftig and Haselkorn [17] who measured the degree of hybridization of RNA synthesized in vitro on an LPP-1 DNA template with *Plectonema* (597) and LPP-1 DNAs; no hybridization was observed with the *Plectonema* (597) DNA and 18% hybridization was obtained with the LPP-1 DNA. Thus this blue-green virus-host system is similar to that obtained with virulent, nonlysogenic bacteriophages and their bacterial hosts (*Year Book 67*, p. 309).

Similarly no reaction was observed when the DNAs of several bacteriophages—λ, 434 hy, φ 80 and P_{22}—were incubated with LPP-1 DNA. Thus, it ap-

pears that genetic similarities do not exist between these two types of the prokaryotes tested, the blue-green algae and the Enterobacteria, and some of their viruses.

Lysogeny and the blue-green algae. Several other blue-green algae viruses have been recently described. SM-1, a phycovirus isolated by Safferman and his co-workers,[18] which infects unicellular blue-green algae, appears to be virulent against *Synechococcus elongatus* and *Microcystis aeruginosa*. Another virulent virus $G_{111'}$ isolated by Padan *et al.*[19] and having numerous similar features to LPP-1 including the same host-range sensitivity, appears to be quite similar or identical to LPP-1.

While culturing various blue-green algae by aeration in synthetic media, it was noticed that a culture of *Oscillatoria prolifera* (1270) appeared more foamy than other strains of algae, suggesting spontaneous lysis of a small portion of the cells. A liter culture of this blue-green algae was clarified by low-speed centrifugation for 10 minutes and the clear supernatant recentrifuged (20,000 rpm for 100 minutes) in a Spinco Model L ultracentrifuge.

After ultracentrifugation, a small, crystal-clear pellet was observed. Dr. Russell L. Steere of the Plant Virology Laboratory, U. S. Department of Agriculture, agreed to make an electron microscopic examination of an aliquot of the purified pellet. Particles were seen strikingly different from the LPP-1 or the SM-1 blue-green algal virus previously reported.*

The enthusiasm spontaneously generated at that time resulted in an agreement to collaborate and to enlarge this collaboration by the participation of Dr. Robert Safferman.† A sample of the *Oscillatoria* (1270) virus was given to Dr. Safferman to test for viral infectivity among many of the numerous strains of blue-green algae maintained at his laboratory. Within a few weeks, Safferman reported that our virus was capable of infecting three blue-green algae, *Lyngbya* (488), *Plectonema* (597) and *Phormidium* (485). All others tested, including several species of *Oscillatoria*, were immune. In spite of our excitement, there was the sobering apprehension that a contamination of LPP-1 might have crept into the virus sample given to Dr. Safferman. This fear was allayed when Safferman further reported that his strain of *Oscillatoria* (1270), independently obtained from Indiana University Algae Culture Collection two years earlier, also contained virus capable of infecting *Plectonema boryanum* (597).

Lysogeny has been known to occur only among bacteria. Hopefully suspecting that the *Oscillatoria* virus seen in the electron microscope might represent the first known example of lysogeny other than that among bacteria, an attempt was made to induce the *Oscillatoria* algae with mitomycin C (1 g/ml). The culture lysed and the supernatant (after removal of algal cells and cellular debris by low-speed centrifugation) yielded a clear, glassy pellet when ultracentrifuged.

At this time we can report that a virus has been obtained which appears spontaneously in cultures of *Oscillatoria prolifera* (1270) and has morphological characteristics markedly different from LPP-1; it is unable to lyse the *Oscillatoria* blue-green algae, and yet is capable of infecting and lysing *Lyngbya* (488), *Plectonema* (597) and *Phormidium* (485). We are currently attempting to ascertain whether the *Oscillatoria* (1270) virus independently isolated by Dr. Safferman (1) has the same morphological

* It was at this time, in his laboratory, that we were first informed by Dr. Steere of the discovery and characterization of a second blue-green algal virus, SM-1. (Safferman, Schneider, Steere, Morris, and Diener.[18])

† Federal Water Pollution Control Administration, U. S. Dept. of Interior, Cincinnati, Ohio.

features characteristic of the virus isolated in this laboratory and (2) whether the virus's DNA shows any homology with the DNA of the *Oscillatoria* (1270) host.

The lysogenic virus obtained from cultures of *Oscillatoria* (1270) apparently has the same host range as the virulent blue-green virus, LPP-1. Studies were carried out to ascertain whether the DNA of *Oscillatoria* (1270) contained nucleotide sequences similar to the DNA of the three blue-green algae sensitive to the lysogenic virus.

Table 6 shows the results obtained where radioactive *Lyngbya* (621) DNA fragments were reacted with DNA-agars of *Lyngbya* (621), *Phormidium* (485), *Plectonema* (597) and *Oscillatoria* (1270). Control DNA-agar containing the DNA of *Anacystis nidulans* (625) was used, as this blue-green alga is classified by Smith (Table 4) and by others into an order different from that of the other four algae used in this experiment. The results were somewhat unexpected. The *Lyngbya* (621) DNA did react with the DNA of *Phormidium* (485) and *Plectonema* (597); however, the reaction was extremely low considering the reaction observed when *Plectonema* (597) fragments were tested against another strain of *Lyngbya* (488) DNA-agar (Fig. 19 and Table 5). In addition to giving a lower reaction, *Lyngbya* (621) differs from *Lyngbya* (488) in being insensitive to infection by the LPP-1 virus (3). The suggestion is made that *Lyngbya* (621) is markedly different genetically from the more closely related group comprising *Lyngbya* (488), *Phormidium* (485) and *Plectonema* (597).

TABLE 6. Reaction between *Plectonema boryanum* (597) DNA and the DNA of Other Blue-green Algae

DNA in agar	Radioactivity bound (c/m)	Percentage radioactivity bound relative to control
Plectonema (597) control	15200	100
Lyngbya (488)	9460	62
Phormidium (485)	7762	51
Fremyella (481)	52	0.6

Note: 2.1 μg *Plectonema* (597) DNA fragments were reacted with various DNA-agar preparations each containing approximately 10 μg of embedded algal DNA. Thirty-four % of the *Plectonema* (597) DNA fragments reacted with the *Plectonema* (597) DNA in agar.

The data shown in Fig. 21 support this conclusion. Thermal chromatograms obtained from studies of the reaction of *Lyngbya* (621) DNA fragments with the DNA of other blue-green algae show that the reaction products are less thermally stable than those observed in the previous experiment (Fig. 19). A large portion of the bound radioactive *Lyngbya* (621) fragments was eluted at temperatures much lower than that observed for the reaction of *Lyngbya* (621) fragments with the identical DNA in agar. This result implies imperfect base pair matching among the reacting nucleotide sequences of the heterologous DNAs, and evolutionary divergence. In part, however, some of the homologous segments which elute at lower temperatures also may reflect portions having a lower GC content (with almost perfect base pairing) than the overall GC content of either of the reacting heterologous DNAs.

Lyngbya (621) showed a high degree of reaction, however, with *Oscillatoria* (1270) and consequently could appropriately be classified in Order 3, the Oscillatoriales (Table 4).

Surprisingly, the *Lyngbya* (621) DNA fragments reacted with the *Anacystis* (625) DNA to a greater extent than that of either the *Phormidium* (485) or *Plectonema* (597) DNAs. Two references subsequently located indicated that *Anacystis nidulans* has probably been improperly classified as a member of the Chroococcales. Silva [20] states: "The formation of short but multicellular filaments by the algae extensively cultured and investigated under the name '*Anacystis nidulans*' indicates that this strain should not be assigned to the Chroococ-

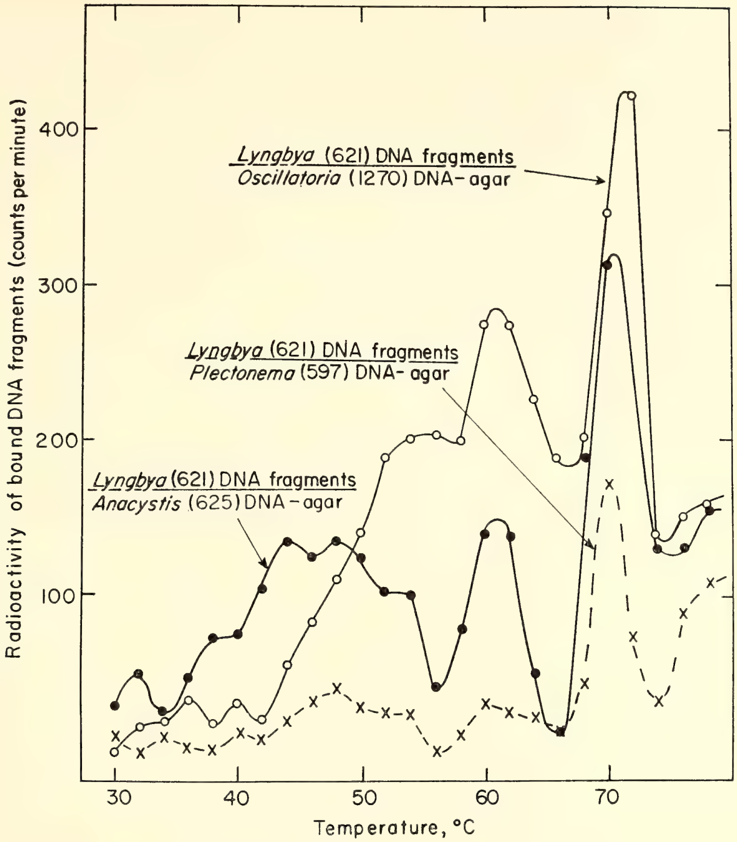

Fig. 21. Elution profiles obtained from studies of the reaction of 0.01 μg *Lyngbya* (621) DNA fragments with DNA-agars containing approximately 10 μg blue-green algae DNAs. Circles with solid lines, *Oscillatoria* (1270) DNA; crosses with broken lines, *Plectonema* (597) DNA; solid circles with solid lines, *Anacystis* (625) DNA. Incubation and elution procedures as in Figs. 19 and 20.

cales. Drouet (personal communication) has tentatively identified it as *Phormidium mucicola* (Nostocales)."

Polyphyletic origins for members of this group are suggested by the results of Edelman, *et al.*[21] who found that six members of the Order Chroococcales examined had base compositions varying from 35 to 71% GC. These authors observed that "the genera placed in this order are characterized by negative rather than positive characteristics, and form the residuum left after exclusion of the strictly filamentous and regularly endospore-forming Cyanophyta." Thus, it appears that the reaction observed between the *Lyngbya* (621) DNA and the *Anacystis* (625) DNA supports Drouet's suggestion[22] that this *Anacystis* might be identified as *Phormidium mucicola* and should therefore not be classified as a member of Order 1, the Chroococcales, but probably among the Oscillatoriales.

DNA of the Defective Bacteriophage of *E. coli* Strain 15

Leo J. Grady

The existence of common nucleotide sequences has been observed among the

DNAs of genetically related bacteria and some of these bacteria and their lysogenic bacteriophages and finally among the lysogenic viruses themselves. In the latter case even bacteriophages which attack different bacterial species, such as a λ and P_{22}, have been shown to contain homologous DNA sequences (for review see *Year Book 67,* p. 301). An exception among the temperate phages previously studied is the defective phage carried as prophage by strain 15 of *E. coli* which, while sharing common nucleotide sequences with its host, does not react with any of the other phage DNAs studied. Four other features distinguishing the 15 phage are: (1) While unable to undergo a complete cycle of phage replication on any strain of *E. coli* yet tested,[23, 24] the 15 phage can exert a bacteriostatic effect somewhat reminiscent of that produced by colicins and T_2 or T_4 phage "ghosts". However, unlike colicins which have no influence on the strain producing them, the 15 phage only exhibits a bacteriostatic effect against *E. coli* 15, the same strain from which it arises [25, 26]. (2) The 15 phage appears to be unrelated serologically to other *E. coli* bacteriophage (A. Weisbach, personal communication). (3) There is too much homology between the DNA of *E. coli* and that of the 15 phage to be accounted for, as was done by Cowie and McCarthy [27] in the case of λ, on the basis of the existence of one phage genome per host chromosome. (4) The presence of the 15 phage as prophage appears to increase resistance of *E. coli* 15 to ionizing radiation.[28] This is contrary to the results obtained by Marcovich using *E. coli* K12 (λ).[29]

Several of the characteristics of the *E. coli* 15 system are also manifested in a case of defective lysogeny involving *B. subtilis,* namely: (1) *B. subtilis* is not normally sensitive to the phage, but uncured mutants can be isolated in which a bacteriostatic effect is produced.[30] (2) An unusually high degree of homology exists between phage and host DNA.[30, 31] (3) The presence of the phage seems to affect at least one response of *B. subtilis* to ionizing radiation.[32] In this instance, part of the explanation appears to be that no phage DNA is synthesized after induction and, instead, *B. subtilis* DNA is cut into fragments of appropriate size and incorporated into phage protein.[30, 31, 32] The host DNA contained in the phages consists of some material synthesized before induction and some made afterwards.[33] There is also evidence suggesting that a limited portion of the *B. subtilis* chromosome is preferentially replicated a great many times.[33]

The possibility of a similar situation existing in the *E. coli* 15 system was initially investigated by resolving whether any significant portion of the DNA incorporated into phages had been synthesized prior to induction. The thymine-auxotroph *E. coli* 15 T^- was adapted to growth in a minimal medium containing D_2O and $N^{15}H_4Cl$. Once successfully adapted, the bacteria were grown in the presence of thymine-1-^{14}C to an approximate titer of 3×10^8 cells/ml and then transferred to a medium containing H_2O, $N^{14}H_4Cl$, thymine-2-^{14}C and mitomycin C at a concentration of 2 γ/ml. Upon completion of lysis, the phage were isolated and the DNA extracted. The composition of this DNA was determined by comparing it with appropriate heavy or light H^3-labeled DNA markers in a CsCl gradient. The results are shown in Fig. 22. All of the DNA isolated from the phage banded with the light marker, indicating that it had been synthesized in the light medium after induction. No evidence was found for either heavy DNA, or for hybrid DNA of intermediate density. This result is not in agreement with the situation existing in *B. subtilis* and suggests that there is a difference between the two systems. It does not, however, rule out the possibility that some newly synthesized bacterial DNA is incorporated into phage particles.

A second set of experiments was undertaken to establish the extent of ho-

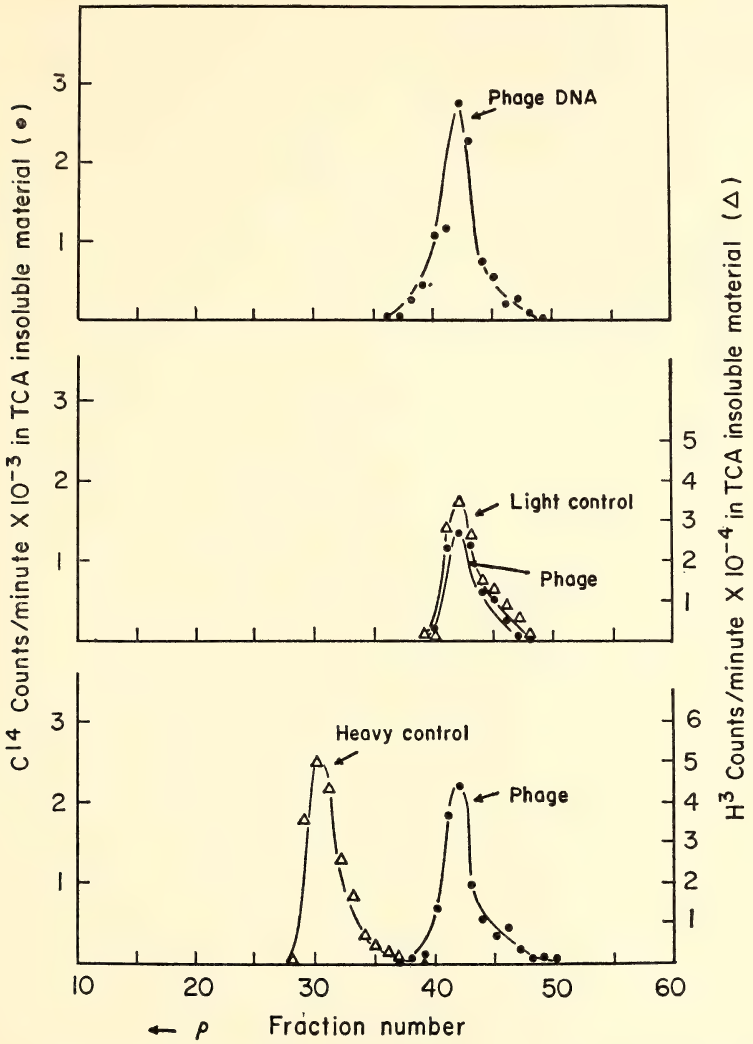

Fig. 22. Density in a CsCl gradient of DNA isolated from the defective 15 phage. Phages were obtained from *E. coli* 15 T$^-$ which had been grown in a minimal medium containing N_{15} and D_2O, and then shifted to a similar medium containing N_{14} and H_2O and the time of induction with Mitomycin C. Starting from the top, banding patterns are shown for: (1) phage DNA; (2) phage DNA compared to a light, or normal density control; (3) a comparison of phage DNA with a heavy marker. Centrifugation was for 72 hours at 30,000 rpm in a SW39L rotor and a Spinco model L ultracentrifuge.

mology between 15 phage DNA and that of *E. coli* strains 15 T$^-$, BB, and JG 151. These strains are, respectively, lysogenic, nonlysogenic (*Year Book 64*, p. 340), and cured.[34]

The proportion of the phage DNA homologous to the DNA of each strain of *E. coli* was measured by incubating a small amount of radioactive phage DNA with a sample of the appropriate DNA agar. In all three cases, at least 40% of the phage genome was capable

of hybridizing with *E. coli* DNA. No difference could be detected between lysogenic and nonlysogenic strains.

Saturation experiments to measure the amount of *E. coli* DNA homologous to the DNA of the phage are currently in progress. Preliminary results show that a considerable portion of the bacterial DNA is capable of hybridizing with the DNA of the phage and also suggest that a difference may exist between the nonlysogenic strain on the one hand and the lysogenic and cured strains on the other. Certain anomalies in the data, however, demand further work before these results can be viewed with confidence.

A New Method for DNA Purification

R. J. Britten, M. Pavich, and Jean Smith

Passage of a crude cell lysate through hydroxyapatite at room temperature in the presence of 8 *M* urea and 0.14 *M* phosphate buffer (PB) permits the DNA to be absorbed while most other cell constituents pass through. The DNA may be recovered in a high degree of purity simply by eluting from the hydroxyapatite with 0.4 *M* PB. Table 7 gives a detailed protocol for the method.

Milan Pavich, a summer student, had made a series of exploratory measurements of the effect of urea and of various concentrations of PB on the binding of DNA and RNA to hydroxyapatite. This work led to a method for the separation of RNA from DNA. The urea was originally added as a denaturating agent to establish a reasonable criterion of precision for recognization of nucleic acid strand pairs at room temperature. To our surprise, experiments showed that RNA was not bound under these conditions. Therefore, tests were made to see if DNA could be prepared directly from tissues by this method. A sample of calf kidney was ground in a blender in the presence of sodium lauryl sulfate (SLS) as a lytic agent and ethylene diamine tetraacetate (EDT) to inhibit nuclease action. When the mixture was passed over HAP the RNA did indeed pass through and a certain fraction of the protein and other macromolecules were bound. Very little of these other cellular constituents are eluted under the conditions which eluted the DNA (0.4 *M* PB, 25°C). Tests with C^{14}-valine labeled mouse "L" cells indicated that

TABLE 7. DNA Extraction Procedure

Lysis [a]	Suspend tissue in 8 *M* urea, 0.24 *M* PB, 1% SLS, .01 *M* EDT.[b]
Shear [c]	Blender 10–20,000 rpm; sealed, filled container.
Absorption [d]	Pass over hydroxyapatite; stir to prevent channeling.
Washing	Several volumes of MUP: 8 *M* urea, 0.24 *M* PB.
Washing	Several volumes of .014 *M* PB to remove urea.
Elution [e]	With 0.4 *M* PB, after a final stir.

[a] For certain tissues a preliminary grinding in the presence of dry ice or freeze-drying, increases yield by breaking down cell structure. All subsequent operations at room temperature.

[b] PB is neutral phosphate buffer; SLS is sodium lauryl sulfate; EDT is ethylene diamine tetraacetate. See footnote in text for an improved buffer.

[c] Frozen tissue lumps may be processed. Run twice for 1 min. Avoid heating. Other methods such as a fine hypodermic syringe or a pressure cell could be used.

[d] Heavy loads of tissue may plug a column. It is possible to use a batch method in a centrifuge, readjust the elutriant to MUP, absorb on a column and elute in a relatively small volume, for a two-step purification.

[e] In the batch method the total HAP pellet volume may be taken as diluent in adjusting the PB to .4 *M* for elution. A refractometer is convenient for adjusting salt concentrations and checking urea removal.

less than 1/1000 of the cellular protein was present in the DNA fraction. The purity of the DNA has been checked in a number of cases by "melting" in the spectrophotometer. Typically, hyperchromicities of 25–28% of the optical density at 98°C are observed. In comparison, DNA of comparable purity (by hyperchromicity test) prepared by standard methods requires a lengthy procedure including successive stages of enzyme treatment deproteinization and precipitation. Urea very likely acts to denature many proteins, reducing the danger of enzymatic activity. It may also disrupt the cell and chromatin structure. There is preliminary evidence that the urea reduces the affinity of RNA for the hydroxyapatite and unexpectedly increases the affinity of native DNA for the HAP.

The choice of this method * or the standard method depends on the quantity of tissue available, the quantity of DNA required, and the fragment size desired. This method is very convenient for the preparation of DNA if the quantity of tissue is small or even microscopic, for example, with labeled tissue culture cells. The avoidance of the alcohol precipitation steps can increase the recovery markedly. The MUP method is limited by the capacity of the hydroxyapatite to absorb DNA. The capacity in turn depends on the surface condition and thus the method of preparation or source of the hydroxyapatite crystals. We customarily use a commercial dry form (Bio-Rad HTP) for convenience. It is likely that an increase in capacity could be achieved with finely ground crystals. Under our conditions, very large fragment size DNA cannot be efficiently eluted. Since others have chromatographed 60 million-dalton DNA on HAP at room temperature, this is probably not an insoluble problem. Nevertheless it is our practice to shear the tissue lysate in a blender at 10,000 or 20,000 rpm. This, of course, reduces the DNA fragment size and improves recovery. It also is a convenient way to disperse the tissue. Due to the presence of the SLS and the released proteins, foaming is severe if air is present during blending. Therefore, a medium or small sealable blender vessel is used and it is filled with lysing solution.

Having a method which did not depend on precipitation, it naturally occurred to us that new minor fractions of DNA might be recovered which differed in molecular weight or state from the principal part of the DNA. We were nevertheless astonished to find that a major component of *Neurospora* DNA had been effectively discriminated against in the standard Marmur procedure. Figure 23 shows a melting curve for DNA extracted by S. Dutta of Howard University by this method. The low melting temperature fraction amounts to about 25% of this DNA. A component in this melting temperature range is barely present or absent in DNA prepared by the Marmur method or the various modifications that have been used to extract DNA from *Neurospora*. It does not show up at all as a low

* Further development of this method is likely to occur. At the time this section was being written Neltje Van de Velde and Bill Hoyer tested it on plant materials as described in Table 7 and failed to recover DNA. However, two modifications led to a good yield. Molar sodium perchlorate was added to the lysing mixture and the lysate was extracted with an equal volume of chloroform (5% octanol) centrifuged and the supernatant passed over hydroxyapatite. Surprisingly, molar $NaClO_4$ does not reduce the binding of DNA under these conditions. At this moment it appears advisable to add these two features to the protocol listed in Table 7, particularly in difficult cases. In one test, 19 mg of DNA were recovered on 20 ml of hydroxyapatite from 20 g of human liver. In this case the DNA was contaminated with about 5% RNA and the hydroxyapatite capacity was greater than expected. In another trial Nancy Reed recovered 30 mg of DNA from 20 g of rat liver, using a 30 ml HAP column. No measurable quantity of RNA was present with the DNA. Batch variation of the hydroxyapatite is indicated, and it appears that for critical use tests must be made on each batch of hydroxyapatite.

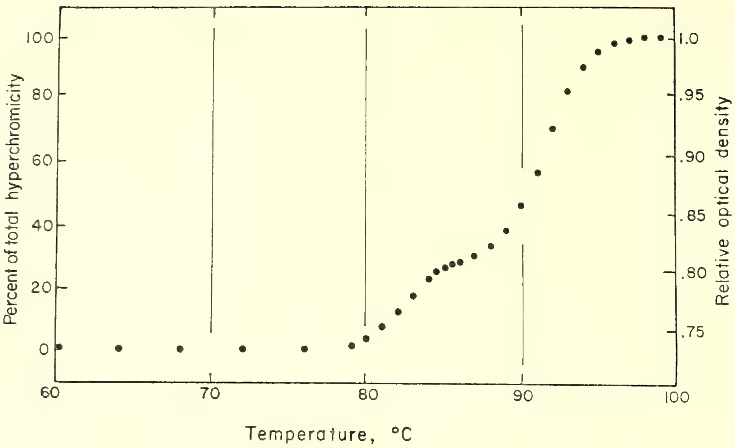

Fig. 23. *Neurospora* DNA prepared by the MUP method–optical melting curve. Hyphae of *Neurospora crassa* strain were freeze dried and suspended in the MUP lysing solution. The DNA was extracted and purified on hydroxyapatite by the method described in Table 7. The low melting component is barely observable in samples of DNA prepared by standard methods. Melting curve done on the Gilford spectrophotometer in 0.12 *M* PB.

density component in any of the published CsCl equilibrium measurements for *Neurospora* DNA.

Up to this time DNA has been successfully extracted from the following species: calf, brachiopod, mouse, *Neurospora,* iguana, human, *E. coli,* several kinds of blue-green algae, chicken, *Lactobacillus,* wheat, king crab, *Amphioxus.* In the case of *Fremyella* it proved necessary to grind the frozen tissue with dry ice in a blender in order to make the extraction reasonably efficient. The *Neurospora* DNA was extracted from tissue that had been freeze-dried. The extraction failed with *Amoeba hystolytica,* but succeeded using a modification much like the one described in the footnote.

Sensitive tests have been made for calf and human DNA to assay any difference in the quantity and pattern of repeated sequences between DNAs extracted by this method and the standard (modified Marmur) procedure. C^{14}-adenine HELA cell DNA prepared by the standard method was mixed with human liver DNA prepared with this method. Both DNAs were sheared to small fragments and the mixture was denatured and incubated for various periods in 0.12 *M* PB at 60°C. The single strands and reassociated double strands were separated by hydroxyapatite fractionation and always had equal specific radioactivity within error. Similar tests were done with C^{14}-thymidine calf kidney DNA (standard extraction) and calf brain DNA extracted with the new method.

Brain

R. B. Roberts

The Biophysics Section continues to maintain its interest in the mechanisms of the brain and particularly in the biochemical basis of long-term memory. This is achieved for the most part by continuing our collaboration with Drs. Louis B. Flexner and Josefa B. Flexner of the University of Pennsylvania. During the past year they have demonstrated the long persistence of peptidyl puromycin in the brain after injections of puromycin sufficient to block memory. Experimental work here has been sharply curtailed after the departure of Dr.

Adrian Rake. We maintain close contact with his experimental program now carried on at Pennsylvania State University. Our present activity is focused on exploring the possibility that puromycin acts by blocking receptor sites for norepinephrine or epinephrine in the central nervous system.

GEOPHYSICS

S. E. Forbush, S. R. Hart, I. S. Sacks, J. S. Steinhart, L. T. Aldrich, M. A. Tuve, C. Brooks, D. E. James, A. J. Erlank, A. T. Linde, G. Saa, S. Suyehiro, M. Casaverde, R. Salgueiro, P. Aparicio, A. Rodriguez, D. Simoni, L. Tamayo, A. A. Giesecke, Jr., E. Deza, J. Frez, E. Kausel, E. Gajardo, F. Volponi, J. Mendiguren, R. Cabre, L. Fernandez, S. del Pozo, and J. Santa Cruz

In seismology this year the Andean plateau has received special attention. Both in obtaining new measurements of its seismic properties and in interpreting the old measurements, we have sought to describe with increasing depth and precision the physical properties of this unusual part of the earth's crust. These properties must be satisfied by any model describing the process of continent formation. Attempts to examine the process itself were made in the Canadian shield where isotope studies of ancient volcanic rocks have placed bounds on any model which describes the chemical association of rubidium and strontium in the earth. Another tool for studying the process, the bore-hole strainmeter, has been tested and perfected. The simplicity and sensitivity of this device give promise of increased availability both of strain measurements in earthquake regions and measurements of long-period (1 hour or more) variations in the strain field due to distant seismic events. These are among the reports which follow.

GEOCHEMISTRY AND GEOCHRONOLOGY

S. R. Hart, T. E. Krogh, G. L. Davis, L. T. Aldrich, C. Brooks, and A. J. Erlank

Sea Floor Basalts

S. R. Hart

The hypothesis of sea-floor spreading calls for the formation of an igneous crust on the oceanic ridges and rises, followed by lateral spreading and reassimilation of the crust into the mantle along the oceanic trenches. Dredging in the deep oceans has provided many samples of the upper oceanic crust; this material with few exceptions appears to be a tholeiitic or high-alumina basalt characterized by unusually low ($<0.5\%$) potassium content. Unlike continental or oceanic island basalts of similar composition, however, the dredge basalts are generally depleted in the large oxyphile trace elements such as U, Th, Rb, Cs, and Ba, and show high ratios of K/Rb, K/Cs and Sr/Ba.

Considering the uniqueness in the trace element composition of these submarine basalts and the hostile nature of the environment in which the rocks must be preserved, we have investigated the possible role of sea water alteration in producing the anomalous trace element characteristics. It has been noted that the basalts tend to become increasingly altered with distance from the median valley (zone of origin) and that truly fresh material is unusual beyond some tens of kilometers from the median valley. In part this effect is due to aging in the sea water environment; in part it may be due to variable degrees of burial metamorphism, since the basalts which occur on the flanks of the ridges may only be exposed by fault uplift. Material ranging from fresh glassy basalts from the East Pacific Rise to relatively altered basalts dredged at 7-km depth in

the Puerto Rico Trench were obtained through the cooperation of A. E. J. Engel, Scripps Institution of Oceanography; A. J. Nalwalk, University of Connecticut; M. N. Bass, University of California; and W. G. Melson, Smithsonian Institution.

Since alteration of these basalts commonly proceeds inward from the surfaces of pillows, joint blocks and flows, the first test was to analyze the fresh interior and compare it with the more altered exterior or margin. We have done this for the elements K, Rb, Cs, and Sr. We found that for Sr the differences between interior and margins are relatively slight (maximum of 20%), whereas for the alkalies the differences are very large. In most samples the alteration causes an enrichment of the alkalies; for several altered basalt glasses the K and Rb were depleted. For the six samples which showed enrichments during alteration, the average increase was a factor of two for potassium, a factor of five for rubidium, and a factor of twenty for cesium. The results are shown in Fig. 24 in terms of K/Cs and K/Rb ratios as a function of potassium content. In all cases, the alteration drastically lowers the K/Rb and K/Cs ratios; the trends of the "alteration" lines joining the interior-exterior pairs are generally similar, and of negative slope.

To explain these results in terms of the simplest possible model, we propose that the first effect of sea water alteration will be to produce secondary minerals such as chlorites, zeolites, and clay minerals. Then these minerals, in particular the clay minerals, will undergo base-exchange reactions with sea water and will absorb the alkalies preferentially as a function of ionic radius. The altered basalts might then be viewed as mixtures of "fresh" basalt and a fully exchanged clay mineral. If we assume a typical clay mineral of 1.5% K, K/Rb = 250, K/Cs = 4700, then the mixing line for fresh basalt plus clay mineral is as shown in Fig. 24 (dashed line). Such a mixing line provides an adequate representation of the alteration data.

The alkalies in sea water are strongly depleted in the heavier elements, as evidenced for example from calculated residence times: Na—120 m.y.; K—10 m.y.; Rb—4 m.y.; Cs—0.6 m.y. This observed depletion is in fact rather complementary to the order of enrichment in these altered basalts, with cesium being selectively enriched during alteration. The relative depletion of Cs and Rb in the oceans is usually related to adsorption on detrital clay minerals eroded from the continents. Recently, however, it has been suggested (Kharkar, Turekian, and Bertine, 1968)[35] that these clays may be saturated prior to reaching the ocean and may act as a source of cations, not as a sink. If this concept is true, sea-floor basalt would provide a very convenient sink for many elements, as it is being continuously generated on the ridges and is immediately accessible to sea water for alteration. Control of sea-water chemistry by interaction with silicates has received much attention recently. There is the possibility that the sea-floor basalts may play a very active role in this process.

The difficulties for K-Ar dating of dredge basalts which these alteration studies imply are rather serious. Obviously the demonstration of a consistent aging pattern for sea-floor basalts is an important aspect of the hypothesis of sea-floor spreading. However, as the basalts move away from the ridges and age, they also become increasingly altered and more difficult to date. From our results we would predict generally that alteration will lead to increased potassium contents which, coupled with possible loss of argon during the alteration process, will lead to K-Ar ages that are erroneously young. Separation of unaltered minerals from these rocks for dating is possible in many cases—for example, plagioclase is quite common as phenocrysts or xenocrysts. However, the potassium levels in these minerals are

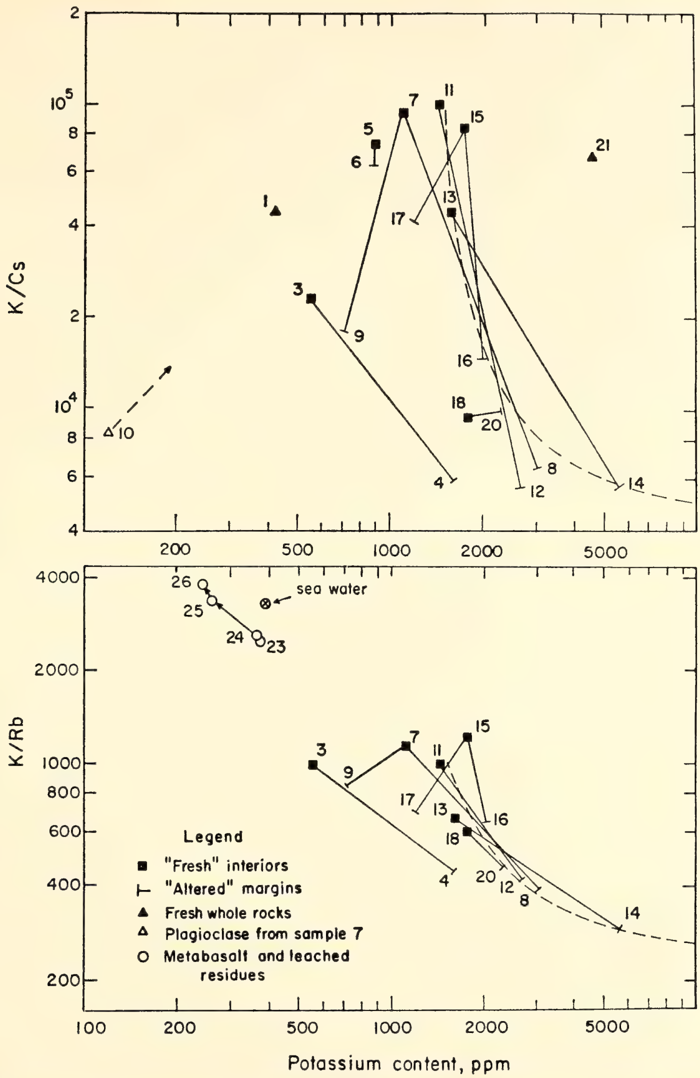

Fig. 24. K/Rb and K/Cs versus K content of midoceanic ridge submarine basalts. The lines connect analyses of interior and marginal portions of corresponding samples. Dashed curve represents a mixing line for an average fresh basalt and a typical clay mineral. Open circles show trend of a submarine metabasalt as a result of various leaching treatments.

very low (<0.01%) creating a difficult analytical problem. In addition, the presence of excess argon in xenocrystic minerals may also be serious. We feel that the prospects for accurate K-Ar dating of sea-floor basalts are rather poor and that other methods such as fission-track dating may prove more promising.

In studying the oldest areas of oceanic crust one naturally considers the oceanic trenches, where the oceanic crust is presumably consumed some hundreds of millions of years after formation. In collaboration with A. Nalwalk, we have undertaken the study of selected trace elements in a suite of basalts dredged

from 7-km depth on the north wall of the Puerto Rico Trench. Most of the samples show some indication of secondary alteration, such as chloritization of the olivines and pyroxenes, high ratios of ferric to ferrous iron and high water contents. The problem is to determine whether this is an initial high-temperature deuteric type of alteration, a low-temperature metamorphic alteration, a sea-water alteration, or some combination of these.

Results of K, Rb, and Cs analyses on these trench basalts are shown in Fig. 25.

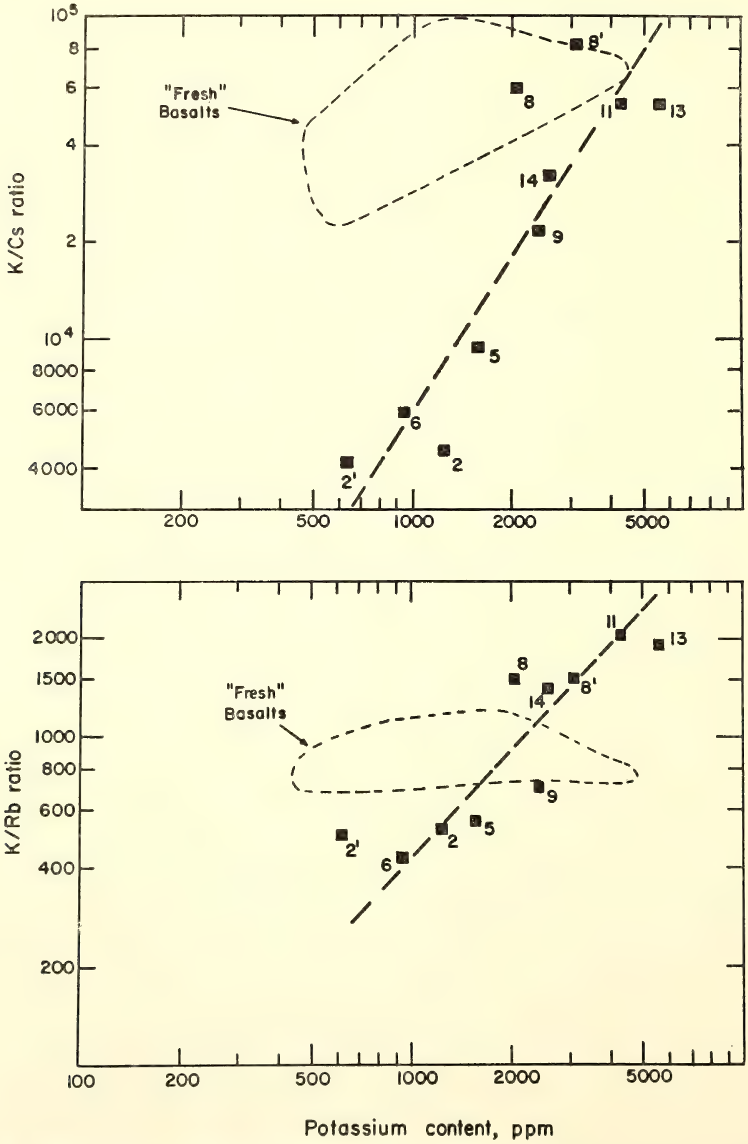

Fig. 25. K/Rb and K/Cs versus K content of submarine basalts from Puerto Rico trench. The dashed area is drawn to include the freshest midocean ridge basalts of Fig. 24.

The alkali data define rather distinct trends in terms both of K/Rb and K/Cs ratios. However, these trends are distinctly different from those shown by the fresher basalts of Fig. 24, shown here as an outline area. There is in fact almost no overlap of the data for the trench basalts and that for fresh ridge basalts. There are other chemical parameters of these trench basalts which show significant interrelationships, and several of these are shown in Fig. 26. Of particular interest is the CaO trend between 48% and 51% SiO_2—essentially a pure "calcium-loss" trend which would be difficult to produce by any combination of mineralogical effects during differentiation. Leaching of calcium from glass occurs very rapidly during aqueous alteration, and as many of the trench basalts are rich in glass, we feel that this CaO versus SiO_2 trend is a strong indication of alteration in an aqueous environment.

Because the strontium contents of these basalts show rather large and consistent variations relative to the other elements (Fig. 26), we have analyzed selected samples for Sr^{87}/Sr^{86}. For sample No. 6 (least altered by petrographic

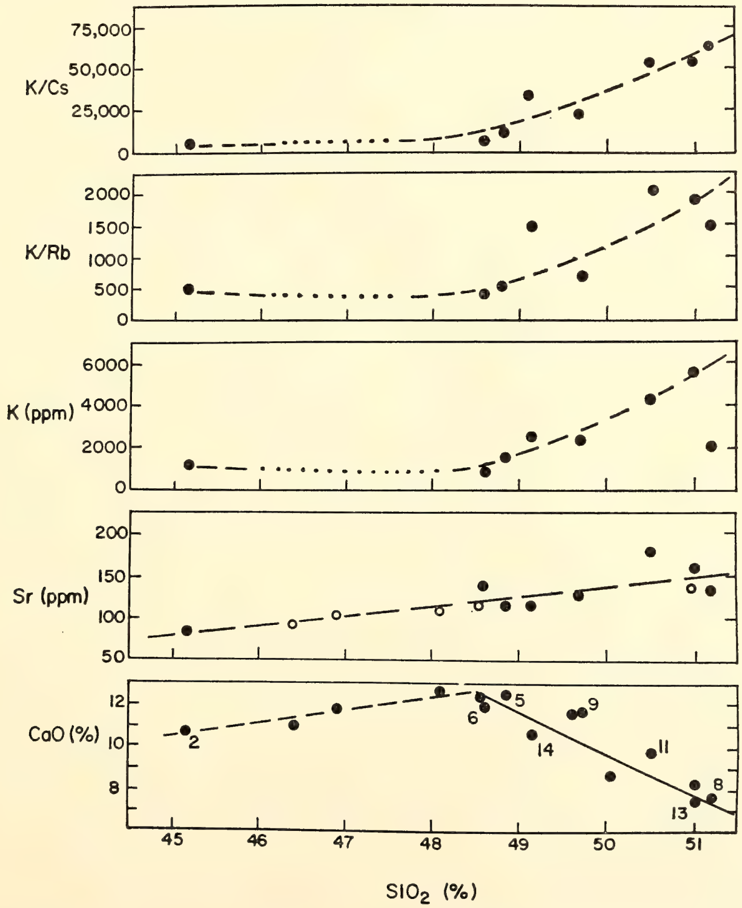

Fig. 26. Trends of K/Cs, K/Rb, K, Sr, and CaO versus SiO_2 for Puerto Rico trench basalts. Solid line on CaO plot is calculated for pure Ca loss.

criteria) the Sr^{87}/Sr^{86} ratio is 0.7033; for sample No. 2, 0.7047 and for sample No. 11, 0.7061. A Sr^{87}/Sr^{86} ratio of 0.7033 is very similar to that in average fresh oceanic basalts; on the other hand, ratios as high as 0.706 are very unusual in oceanic basalts. Because sea-water strontium has a ratio of about 0.709, we feel that the high ratios in sample Nos. 2 and 11 probably represent partial exchange with sea water. Furthermore, as we have previously shown that the alkali elements are affected by alteration to a greater degree than strontium, we infer that the K, K/Rb and K/Cs trends of Figs. 25 and 26 are also related to alteration by sea water. While the present study leaves unanswered the question of what the primary trace element characteristics of the trench basalts were, it does show that alteration processes can produce high as well as low values of K/Rb and K/Cs and that trace element values for the alkali metals and alkaline earths in sea-floor basalts must be viewed with considerable caution.

Finally, having pointed out many of the difficulties involved in dealing with these basalts, we should also consider what we have learned regarding their primary trace element characteristics. The unusually high K/Rb and K/Cs ratios observed by Gast (1965)[36] are substantiated. However, the general trend of decreasing K/Rb with increasing K content is probably the result of chemical alteration. When we group our freshest basalts geographically and consider the variation of K/Rb ratio, we find that this variation is largely independent of potassium content. For example, three of our freshest samples are from the East Pacific Rise (sample Nos. 1, 5, and 21) and they have K/Rb ratios of 700, 800, and 740, though the potassium contents vary by more than a factor of ten (from 430 ppm to 4600 ppm). Samples from the mid-Atlantic ridge show a larger variation in K/Rb (980 to 1200) but there again is no correlation with potassium content.

The Grenville Front in the Chibougamau–Surprise Lake Area

T. E. Krogh, C. Brooks, S. R. Hart, and G. L. Davis

A metamorphic transition in the Surprise Lake area near Chibougamau, Quebec, was studied and described as a transitional Grenville front by Deland (1956).[37] A brief report of preliminary results was included in *Year Book 67*.

The Rb-Sr ages of muscovites and biotites from this metamorphic transition are shown in Fig. 27. Figure 28 presents the isotopic data for several whole-rock samples.

It is clear from the muscovite ages that the metamorphic transition had occurred and the region had cooled more than 2500 m.y. ago. Biotite Rb-Sr ages on the other hand range from a minimum value of about 900 m.y. in the southeast part of the map area to 2100 m.y. in the northwest. In cases where two biotites were analysed, the coarser fraction always yielded an older age, and biotites from the granites give older age values than those from the metasediments. Biotites have lost variable amounts of radiogenic strontium by diffusion, probably about 900 m.y. ago, whereas muscovites have retained almost all of their radiogenic strontium under the same conditions.

The occurrence of this Archaean metamorphic transition near the thermal effect of the $\sim$1 b.y. Grenville metamorphism may be simply a coincidence, but an alternate explanation is possible. A metamorphic gradient, developed vertically 2500 m.y. ago, may have been exposed in a lateral direction as a result of later uplift, perhaps at 900 m.y. Mineral isograds exposed along the Grenville front by this mechanism would pre-date the front itself.

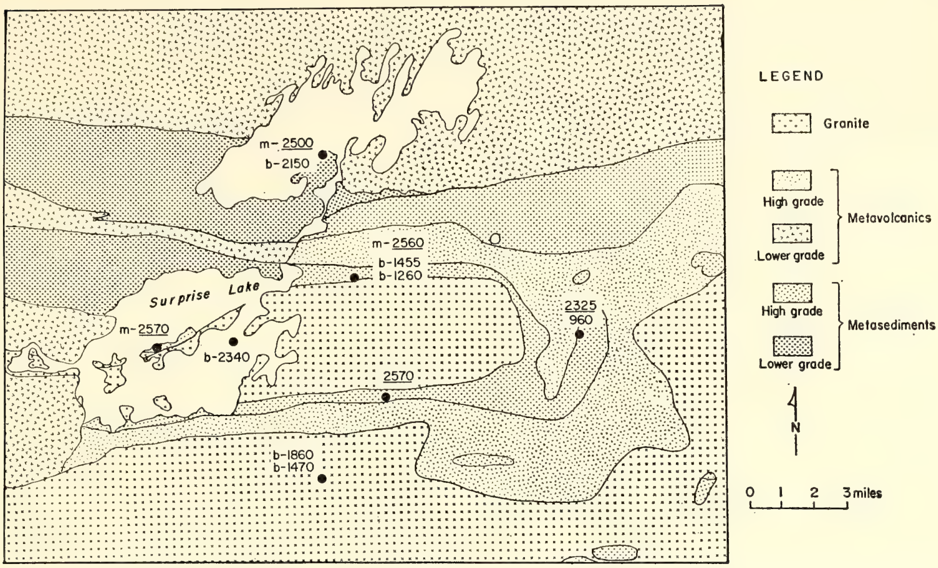

Fig. 27. Generalized geologic map of Surprise Lake area, Quebec. Muscovite Rb-Sr ages (*m*) are shown underlined; other ages are biotite Rb-Sr ages. In two cases both coarse- and fine-grain-size fractions of biotite were analyzed, the coarse fraction giving the greater age in each case. As the muscovites from the metasediments are metamorphic minerals, they establish minimum ages for the metamorphic transition in this area.

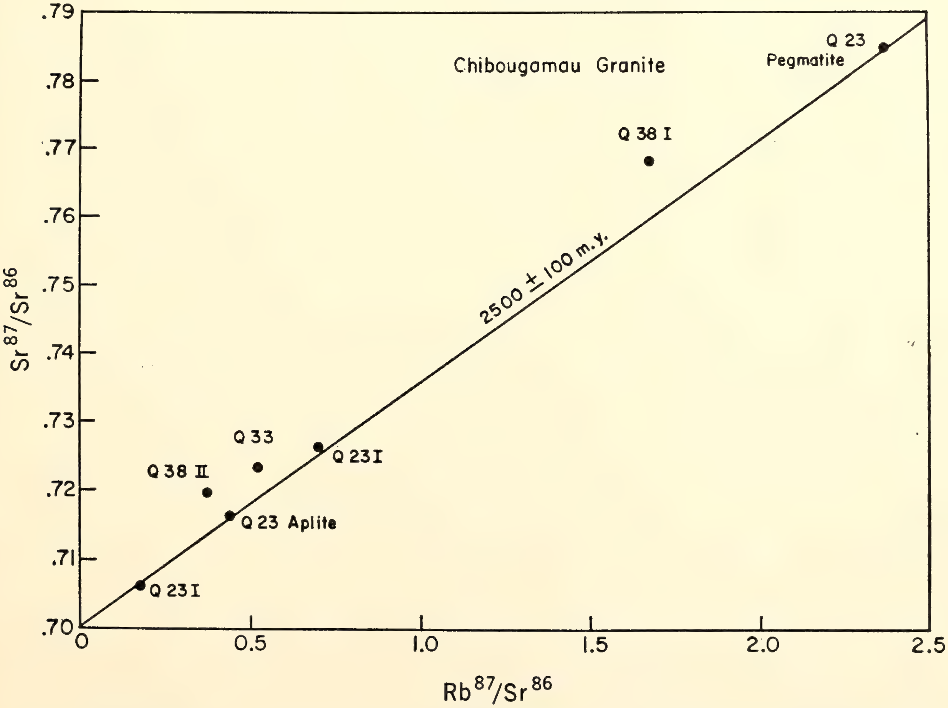

Fig. 28. Rb-Sr isochron diagram for whole rock samples from Surprise Lake area, Quebec. Q23 samples are from an island in the eastern part of Surprise Lake. Q33 and Q38 are samples of granitic gneiss located south of Surprise Lake.

Isotopic analysis of whole-rock granite samples from several locations does not show any marked effect resulting from the younger metamorphism. A poorly defined isochron with an age of 2500 ± 100 m.y. was obtained from several samples from a single outcrop area. Samples from other locations suggest a similar age but with an anomalously high initial ratio.

Rb-Sr Relationships for Igneous Rocks of the Corryong Province, Victoria, Australia

C. Brooks

The Siluro-Devonian igneous rocks of the Corryong District, Victoria, Australia, have been the subject of an intensive geochemical investigation.[38] The rocks consist of granites, dykes of variable composition, volcanics and leucogranites. The geochemical investigation has revealed that the province is relatively enriched in Rb, and consequently the Sr^{87}/Sr^{86} of any aging magma will change considerably over short intervals of time. In order to attempt a documentation of this possibly changing isotopic composition, and also to decipher the complex chronology, a Rb-Sr investigation has been initiated in collaboration with M. Leggo.

Isochrons have been determined for the dominant "basement" granite (the Corryong-Koetong batholith, Fig. 29), muscovite dykes cutting the Corryong granite (Fig. 30), the Mt. Mittamitite leucogranite (Fig. 31), the Pine Mountain leucogranite (Fig. 32) and for the spatially associated Jemba rhyolites (Fig. 33). Caution must be exercised in

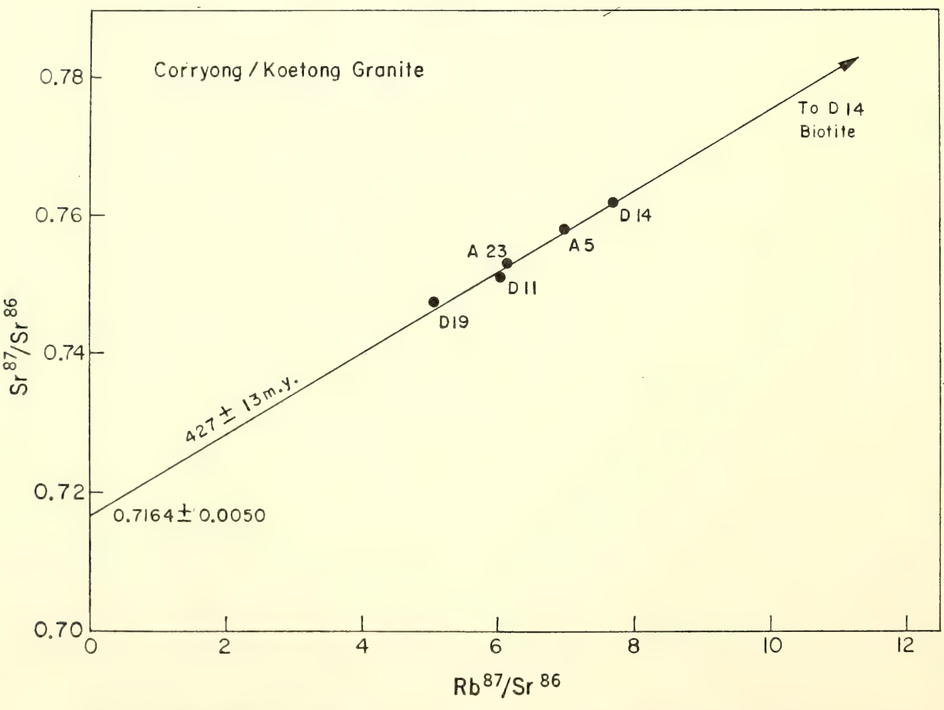

Fig. 29. Rb-Sr isochron diagram for total rock samples of the Corryong/Koetong granite batholith (Victoria). Deleting the biotite (excluded by scale requirements) does not change the age estimate but raises the isochron error to ± 97 m.y. at the 95% level of confidence.

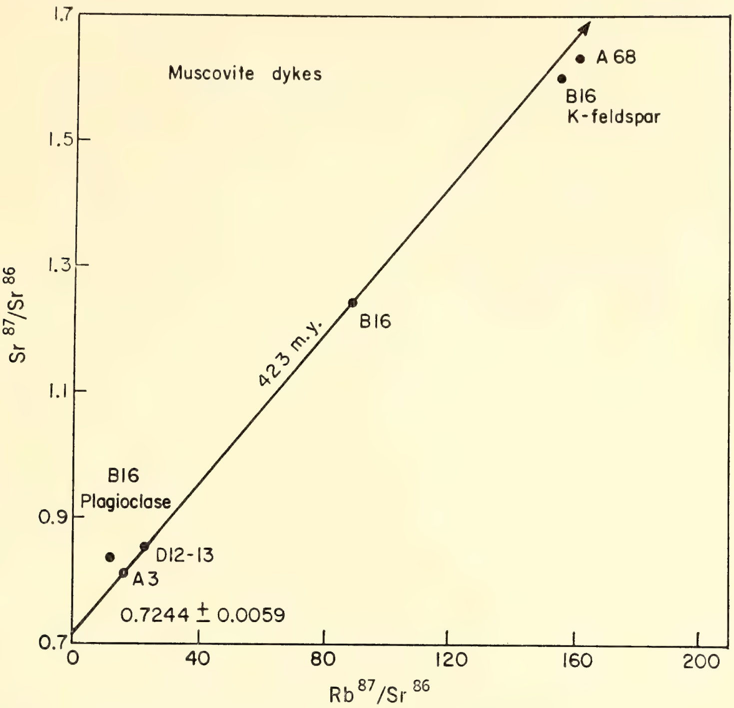

Fig. 30. Rb-Sr isochron diagram for total rock and mineral samples from muscovite dykes which cut the Corryong/Koetong batholith. Both D12–13 muscovite and B16 muscovite plot on the 423-m.y. isochron but are excluded by scale requirements.

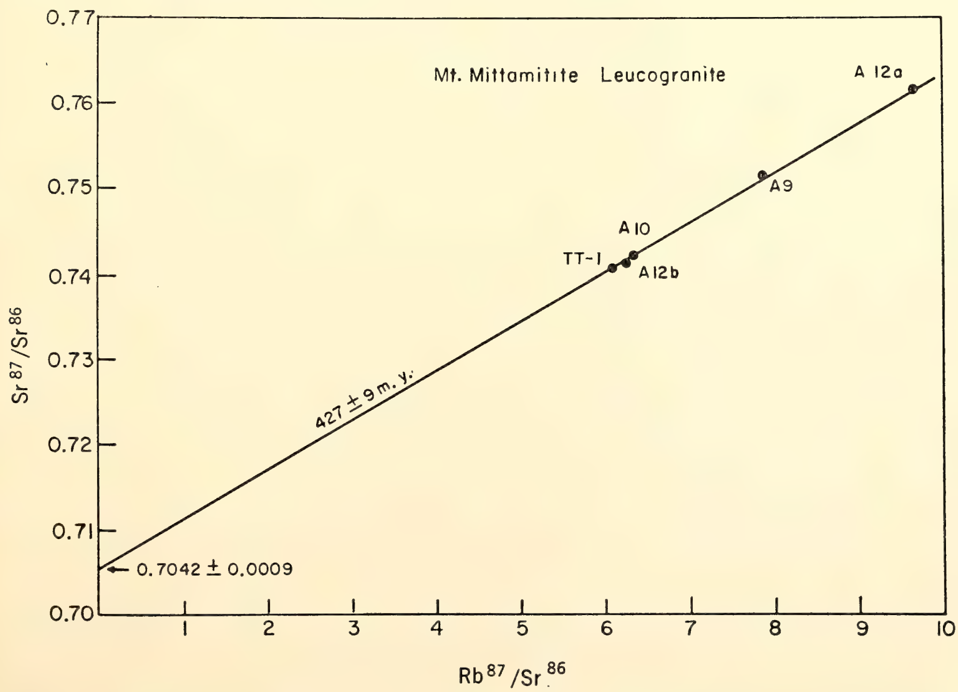

Fig. 31. Rb-Sr isochron diagram for total rocks of the Mt. Mittamitite leucogranite, Victoria. The age and initial Sr^{87}/Sr^{86} error estimates are given at the 95% level of confidence.

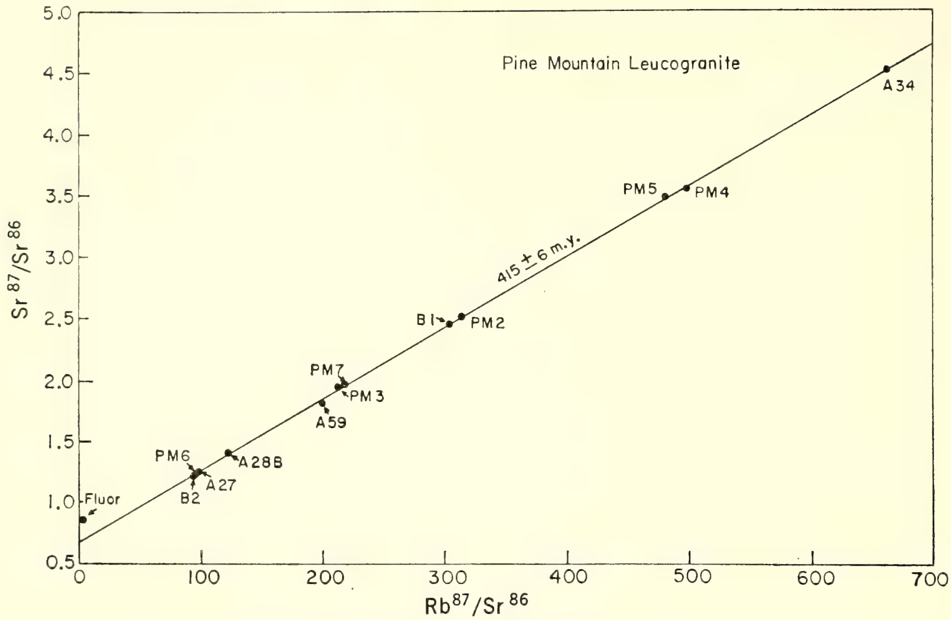

Fig. 32. Rb-Sr isochron diagram for total rocks of the Pine Mountain leucogranite, Victoria, and associated dykes (B2, A27, PM 6, A28B). Age error is at the 95% level of confidence.

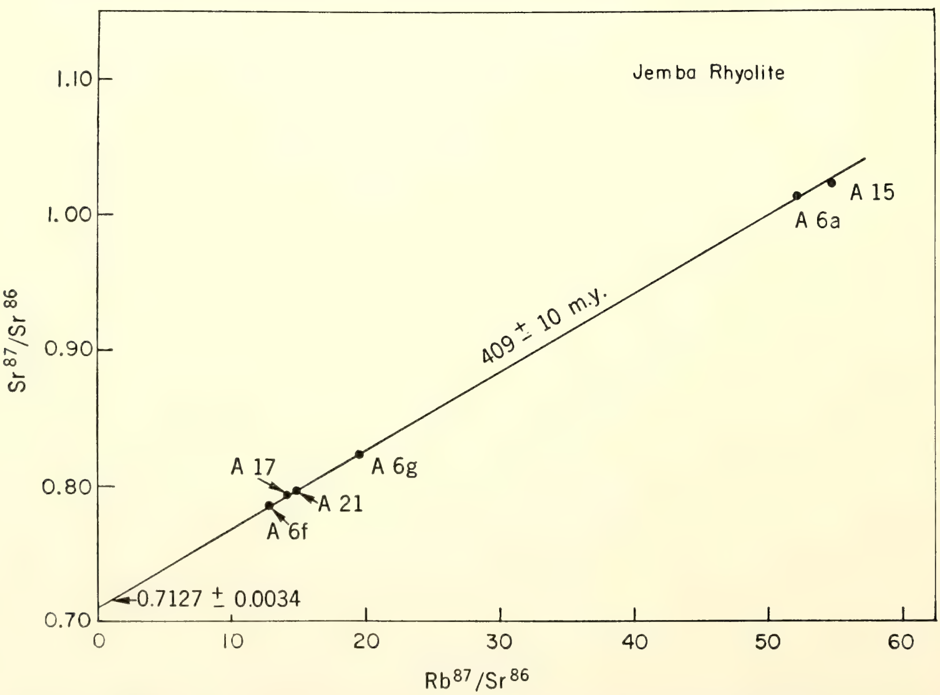

Fig. 33. Rb-Sr isochron diagram for total rocks of the Jemba rhyolite subsidence caldera, Victoria. Error estimates are given at the 95% level of confidence.

interpreting the isochron estimates given in the figures because different linear least-squares statistical models give different errors for the fits. Although work is progressing to improve this situation, it is not yet completed. However, the data suggest that the period of igneous activity lasted approximately 20 m.y., from the formation of the Corryong granite at 427 m.y. to the extrusion of the Jemba rhyolites at 409 m.y. The Jemba rhyolite, which has an uncertain stratigraphic relationship with the leucogranites, is apparently similar in age to the leucogranites. The initial ratio data is less informative due to the large errors resulting from the lack of range in Rb/Sr ratio. The preliminary data indicate no significant difference between the initial Sr^{87}/Sr^{86} of the Corryong granite, Jemba rhyolite or the muscovite dykes. The initial ratio of the Mt. Mittamitite leucogranite, however, is significantly lower, which is somewhat contradictory to the proposal that this leucogranite is a later-stage product of the Corryong batholith. Unfortunately, the Pine Mountain leucogranite is too enriched in Rb to provide an initial Sr^{87}/Sr^{86} estimate. Work is continuing in an effort to determine more accurately the initial Sr^{87}/Sr^{86} ratios.

Discussion of the Use of Rb-Sr Isochron Regression Treatments

C. Brooks and S. R. Hart

The publication of the new initial Sr^{87}/Sr^{86} value [39] for achondrites defines a new level of precision of Sr isotope measurement. Although it is highly unlikely that any suite of terrestrial samples will have been as perfectly chemically closed throughout their history as the reported achondrite suite, this improved level of precision requires a detailed appraisal of isochron regression treatments. These treatments, which are used to estimate the Rb-Sr isochron parameters, are not in a satisfactory state, since all proposed regression models incorporate certain shortcomings. An investigation of these models is being completed. Some aspects of the investigation, however, have been finished.

Normality of error distribution. A basic assumption in any application of least-squares analysis is that all errors affecting the fit of the regression line are normally distributed. Qualitatively, the more nonnormally distributed the errors are, the less "certainty" one can place on the errors calculated for the fit. The degree of normality of the error distribution function can be graphically examined by calculating a cumulative distribution analysis for replicate data and testing for linearity on probability paper. The only laboratory which has published sufficient duplicate data for such a treatment is the Department of Geophysics and Geochemistry of the Australian National University. The results for 100 total rocks, 52 feldspars, and 50 micas are displayed in Fig. 34. Inspection of this figure reveals that most of the measurement errors for whole rocks, feldspars, and biotites show somewhat sigmoidal trends. On plotting theoretical replicate error-data taken from a known normal distribution, similar trends were observed. This effect is apparently a direct result of small-sample statistics, and we conclude that the A. N. U. error data are for the most part normally distributed. It is clear that for laboratories such as A. N. U., where most of the data ($>90\%$) is demonstrably normal in error distribution, the general least-squares analysis is applicable with little reservation.

Correlation of errors. A recent least-squares isochron regression development has been published [40] in which the experimental errors in X and Y are correlated. For Rb/Sr isochrons, where the Sr isotope ratios and concentration are measured together, correlation between the Sr^{87}/Sr^{86} and Rb^{87}/Sr^{86} is obviously possible. This correlation is expressed as a coefficient which varies from -1 to 0 to $+1$. Minus 1 indicates perfect negative correlation, i.e., a $(+1\%)$ error in X produces a (-1%) error in Y, zero indicates

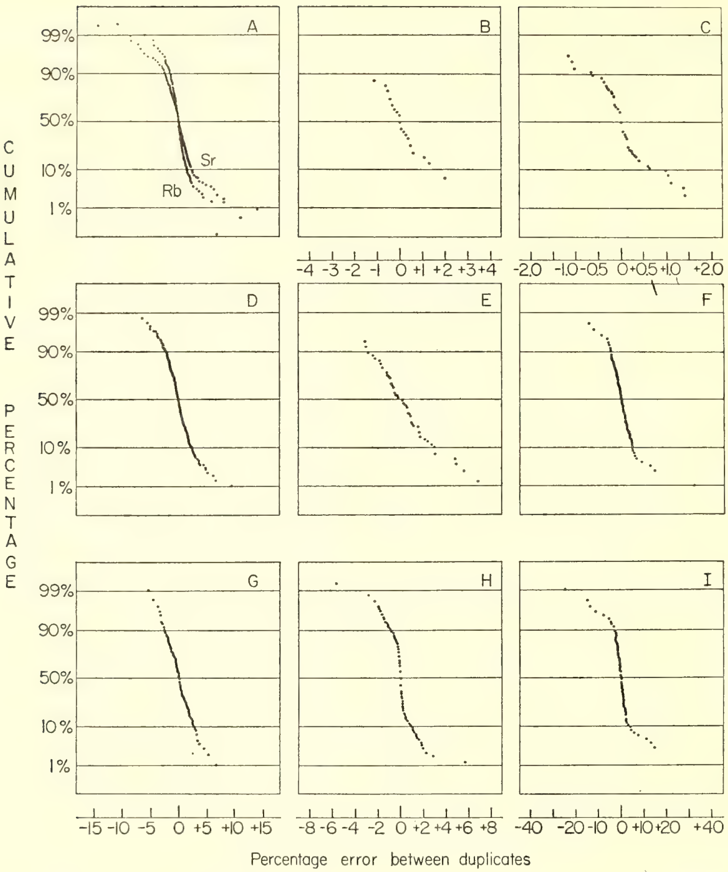

Fig. 34. Probability plot displaying cumulative distribution analyses of the difference between duplicates expressed as a percentage of their mean. The identification is as follows: A. Rb and Sr for 100 total rocks. B. Unspiked Sr^{87}/Sr^{86} for 15 feldspars. C. Calculated Sr^{87}/Sr^{86} for 38 feldspars. D. Rb^{87}/Sr^{86} for 100 total rocks. E. Unspiked Sr^{87}/Sr^{86} for 34 total rocks. F. Rb^{87}/Sr^{86} for 50 micas (biotites, muscovites). G. Rb^{87}/Sr^{86} for 52 feldspars. H. Calculated Sr^{87}/Sr^{86} for 100 total rocks. I. Calculated Sr^{87}/Sr^{86} for 50 micas (biotites, muscovites).

no correlation at all, and +1 indicates a (+1%) error in Y. To calculate a value for the correlation coefficient (r), the A. N. U. replicate data used in the error distribution analysis has been treated with a statistical package developed at the National Bureau of Standards, Washington, D. C. In this treatment the paired X and Y errors are plotted on conventional axes, and the resulting trend or lack of trend fitted by simple least-squares analysis. The parameters of the fitted line allow calculation of the correlation coefficient and the error in the coefficient for that data. Figures 35 and 36 display the trends for total rocks, feldspars and micas. Consideration of the sample correlation coefficients shown in Figs. 35 and 36 indicate that (1) for total-rock data ($Sr^{87}/Sr^{86}<1.0$), the correlation coefficient is not significant at the 95% level of confidence; (2) for the remaining data the correlation coefficients are significant at the 95% level and in the case of the micas at the 99% level. Since most total-

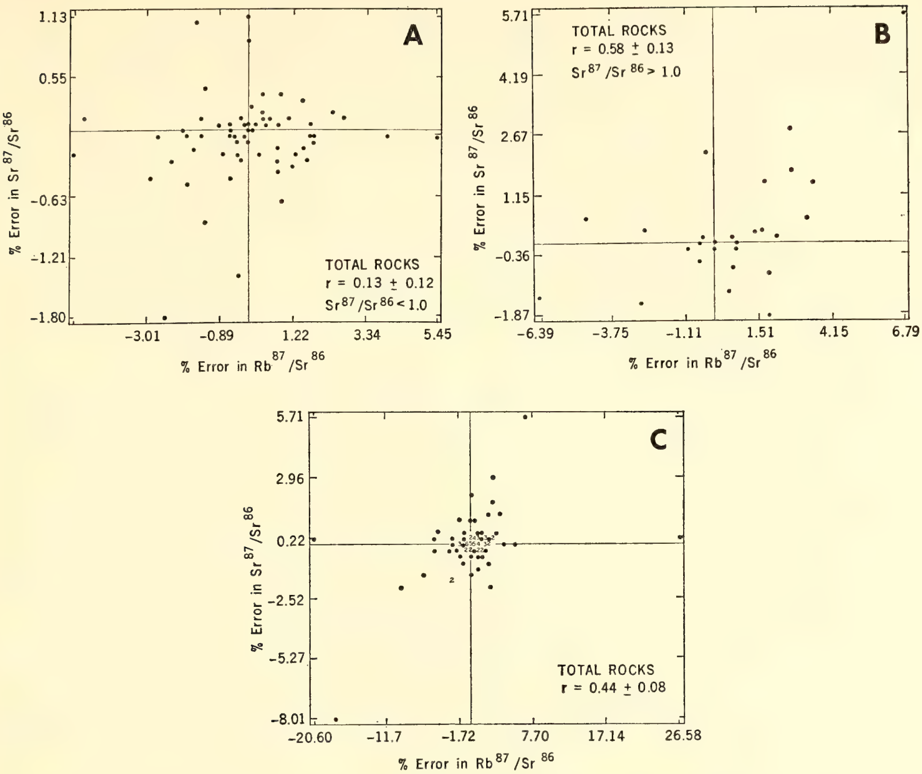

Fig. 35. Plots of the errors between duplicate total rock data expressed as a percentage of the mean value. The correlation coefficients (r) are given for each set of data, which are distinguished by the mean $Sr^{87}/Sr^{86} < 1.0$ (A), mean $Sr^{87}/Sr^{86} > 1.0$ (B) and all data (C). A plotted number indicates the number of points coincident at that point.

rock regressions involve data whose Sr^{87}/Sr^{86} is less than 1.0, it is apparent that the assumption of zero correlation between Sr^{87}/Sr^{86} and Rb^{87}/Sr^{86} is a valid one. If regressions are to be made involving micas or high Sr^{87}/Sr^{86} total rocks, a positive value of r should be used. A reasonable estimate may be adopted from the data of this investigation.

Some "nonstatistical" realities. Although analysis of the degree of normality and correlation of data is part of a detailed investigation of regression treatments, we feel that there still remains the need for human evaluation in the decimal-point game of statistical argument; the very nature of geological analysis necessitates a degree of human evaluation.

For example, minimization of Student's t-multiplier by the analysis of additional samples will produce smaller values for the calculated isochron errors. However, if these samples do not represent increased geological coverage of the parent body, then this minimization of the errors is artificial with respect to predictions about the parent body.

A second example involves the testing of differences between ages and initial Sr^{87}/Sr^{86} ratios of isochrons. The increase of the error estimates of the isochron fit due to the raising of the levels of confidence introduces the possibility that statistics can be forced to support a pre-

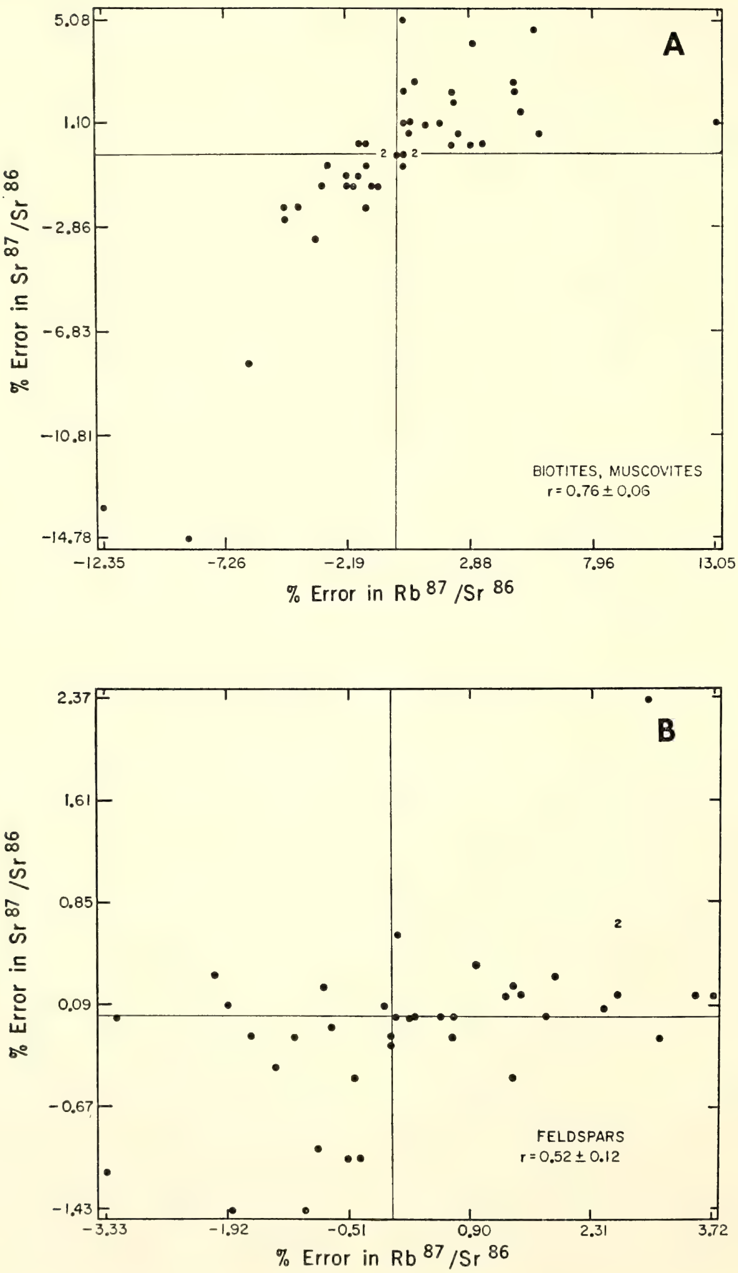

Fig. 36. Plots of the errors between duplicate biotite/muscovite data (A) and feldspar data (B). The correlation coefficients (r) are given.

conceived idea. For example, consider the following age estimates at the 1σ level of confidence for two six-data point isochrons.

Isochron I 100 ± 10 m.y.
Isochron II 200 ± 10 m.y.

At all levels of confidence up to about 99.7%, the isochrons show distinctly different ages. At the 99.99% level, however, there is *no* significant age difference. In other words, statistical differences can always be eliminated by unrealistic raising of confidence levels. This example should properly be described as showing a significant difference in age at all levels of confidence less than 99.7%.

Some comment must also be made regarding the relative errors obtained from a total-rock isochron as opposed to a single very enriched sample from the same body. An age error can be assigned to this enriched sample (on the basis of analytical precision and possible uncertainty in the initial ratio) which may be considerably smaller than the calculated errors of the isochron. This age error for the single sample, however, can in no way be used to determine our confidence level regarding the body as whole and as a result cannot be used for testing for differences between this body and any other. In the same way, the single-sample precision in Sr^{87}/Sr^{86} cannot be applied to a single low isochron point to predict the initial ratio of the parent body. To determine useful confidence limits for the age and initial ratio estimates of a geologic body, a sufficient number of samples is required to overcome small-sample limitations.

Perhaps nowhere in the application of statistics to the field of geology is there such inordinate extrapolation based on so few observations. A recent published example extrapolated an age and initial Sr^{87}/Sr^{86} from four hand specimens to at least 1000 cubic miles of rock. The only constructive suggestions that can be made in this type of analysis are the desirability of increasing the number of samples analyzed, the need for adequate, small-sample theory consideration, and the realization that even carefully determined, precise isochron-parameters may still misinterpret a geological state which is not necessarily subject to statistical laws of normal distribution.

Intelligent use of the available regression models even on closely controlled statistical grounds will not completely eliminate nonrealistic use, unless full account is taken of small-sample theory. To make this clearly unambiguous, we strongly suggest that isochron parameters be given with a stated level of confidence, with stated assigned experimental errors, and with a statement defining the method and the number of samples used in calculating these errors. This will, we hope, minimize the isochron "errors of ignorance," and lead to more emphasis in the literature on the statistical concept of *prediction* about the parent geological unit or body from isochron regression results.

Potassium/Rubidium Ratio of Red Sea Brines

S. R. Hart

Remarkable occurrences of hot brines are found in at least three depressions or closed basins on the floor of the Red Sea. These brines, with temperatures up to 56°C and with salinities about eight times higher than sea water, occur at depths of about 2000 m along the median rift zone of the Red Sea. A number of theories have been proposed for their origin: (1) extreme evaporation of the entire Red Sea at some earlier stage, (2) local solution of exposed salt deposits on the sea floor, (3) evaporation in coastal areas with later density flow to the deep pockets, (4) leaching of evaporites in underlying strata. A variation of the last process has been proposed by Craig (1966)[41] in which normal Red Sea water enters the evaporite sequence comprising the shallow sill separating the Red Sea from the Gulf of Aden, undergoes geo-

thermal heating as it is driven downward by density flow, travels in fracture systems along the axis of the Red Sea finally to emerge from beneath the sea floor into the closed depressions, more than 400 km north of where it started. Samples of the 56°C Atlantis brine, the 44°C Discovery brine, and several of the intermediate mixed layers separating the brines from normal Red Sea water were analyzed for K and Rb to see if the K/Rb ratio could be used as an effective tracer for investigating the origin of the brines.

Samples were made available by R. Weiss and H. Craig of the Scripps Institution of Oceanography. Results of the K/Rb analyses are shown in Fig. 37. The two brines are quite similar in K and Rb content (they have similar salinities as well), with the small differences probably representing the analytical uncertainties. Furthermore, the two intermediate or mixed waters are on a perfect mixing line between the brines and present-day normal Red Sea water. This strongly suggests that the mixing which formed the intermediate waters has taken place under present-day conditions, since the salinity of the Red Sea has probably varied widely in the past because of climatic effects. The Red Sea is at present open to the ocean at its south end through a channel only 100 meters deep. Lowering of sea level during glacial periods would have isolated the Red Sea from the open ocean, and its salinity would then be entirely controlled by the local evaporation-precipitation budget. The fit of points to the mixing line suggests that at the time of mixing the potassium content (and salinity) of the Red Sea did not differ from the present value by more than ±3–4%.

The K/Rb ratio of the brines is about 970, compared with 3200 for sea water and about 200–400 for most igneous rocks. Clearly the brines have not been formed by simple evaporation of sea water (this conclusion had also been noted previously, based on consideration

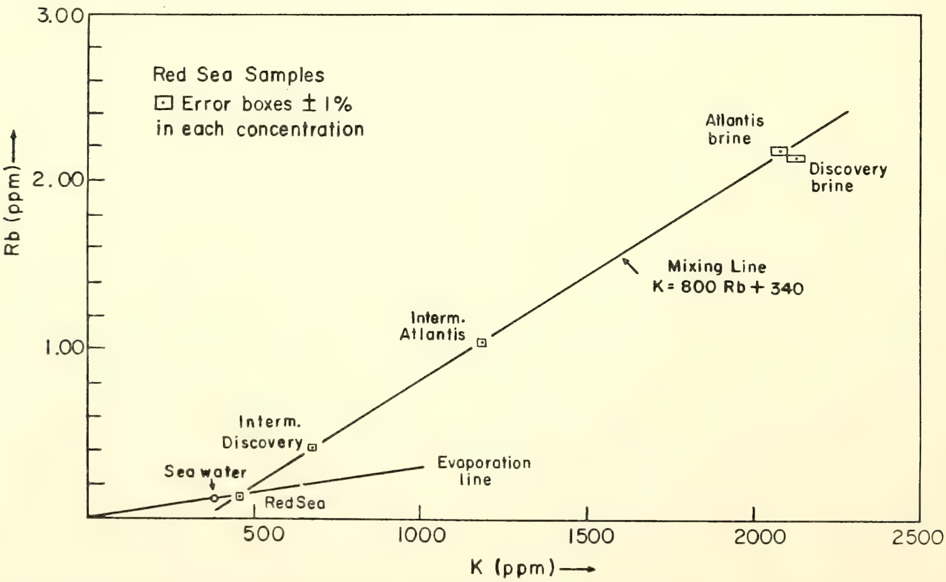

Fig. 37. K and Rb contents of brines, intermediate mixed layers, and normal sea water from the Red Sea. Mixing line for Red Sea samples is an approximate best-fit line to the data points. Evaporation line is a line of constant K/Rb ratio equal to that in open ocean water (3160).

of the major-element chemistry of the brines). Furthermore, the K/Rb ratio is unlike that in most crustal rocks, ruling out possible origins related to bulk weathering or leaching of common rock types. From the equation of the mixing line it is clear that, even if the brines are not at original strength, the K/Rb of the original source must have been greater than 800 (since the K/Rb of the mixing equation approaches 800 asymptotically for large K concentrations). Ocean-floor basalts have K/Rb ratios which are typically 800 and higher, and since the Red Sea rift is a zone of generation of new oceanic basaltic crust, these rocks would be a potential source for alkalies with high K/Rb as well as a source of heat. However, the oxygen and hydrogen isotope data of Craig [41] clearly shows that the water of the brines is related to normal southern Red Sea water, and that most of the dissolved salts are compatible with extraction from evaporite sequences—rather than having any relationship to magmatic water and basaltic chemistry. Data on the K/Rb ratios of typical evaporite deposits are rather poor, but it does seem that certain evaporite minerals such as sylvite will have very high K/Rb ratios (2000–10,000), whereas other minerals such as carnallite will have low K/Rb ratios (100–200). Thus, depending on the particular mineralogy of a given evaporite sequence it would be possible to obtain brine solutions with K/Rb ratios as high as those observed in the Red Sea brines. The overall K/Rb of an evaporite sequence must ultimately trace back to the drainage system which fed the original salt lake. (Here it is interesting to note that most fresh-water streams from a variety of drainage basins contain dissolved alkalies with K/Rb ratios ~800–1000.) The K/Rb data thus add some positive support to the "evaporite-leaching" theory of Craig [41] for the source of the Red Sea brines.

Sr-Isotopic Evidence Bearing on the Early Heterogeneity and Continuous Differentiation of Earth's Mantle

The abundance of Sr^{87} has been increasing since the time of nucleosynthesis because of the natural radioactive decay of Rb^{87}. If we express this abundance as a ratio with a nonradiogenic isotope such as Sr^{86}, then in every geological environment (such as Earth's mantle), the rate of change of Sr^{87}/Sr^{86} will be proportional to the Rb/Sr ratio that existed in that environment. This has important implications concerning the evolution of Earth, since the change of the Sr^{87}/Sr^{86} ratio with time can be used as a "tracer" in testing possible models for the chemical evolution in Rb and Sr in the mantle.

The use of the Sr^{87}/Sr^{86} "tracer" in this way depends entirely on the availability of rocks that have been directly derived from Earth's mantle. To date, most investigators concerned with rocks derived from the mantle have confined their efforts almost exclusively to the modern volcanics for which no age correction is necessary. Almost no work has been done on older volcanics or other rocks of presumed mantle origin, consequently our knowledge concerning the development of Sr^{87} in the mantle with time is severely limited.

Because of the lack of data, previous workers have considered strontium development in the mantle in terms of "end-member" models, with one end-member being the primordial strontium ratio as defined by Rb-poor meteorites. The other end-member is taken as modern volcanic strontium, and a linear growth during mantle evolution is usually assumed. We have attempted to close this gap in our knowledge of mantle evolution by investigating volcanics from the oldest accessible Precambrian terrane in North America, the 2.7-b.y. Superior Province in the Canadian Shield. The metavolcanic belts sampled are shown in Fig. 38.

The Archaean volcanic suites sampled

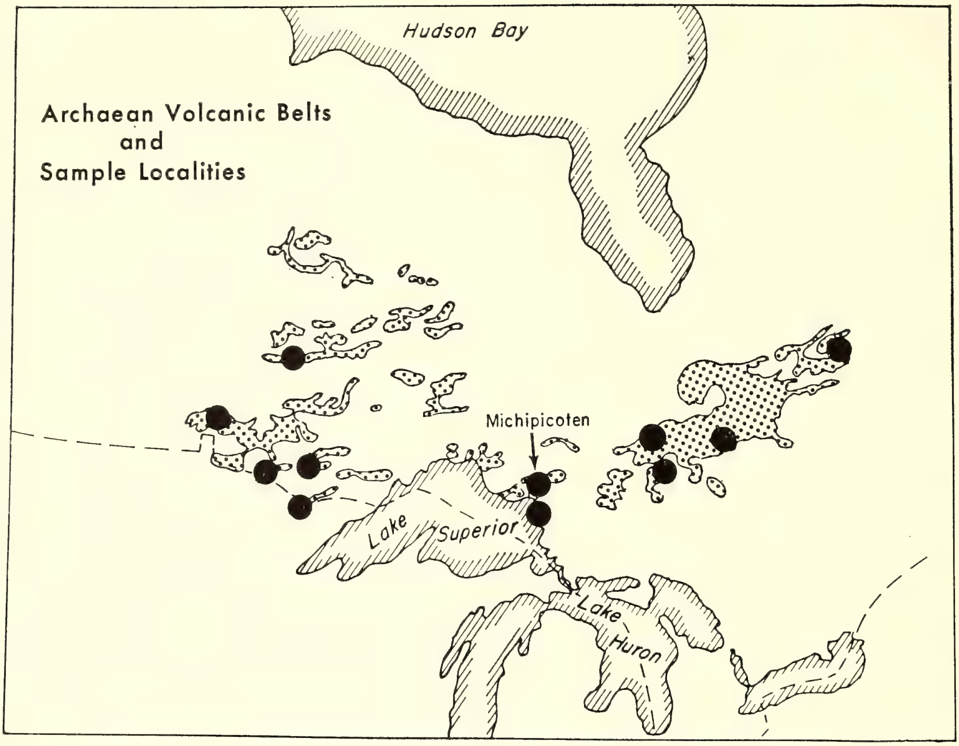

Fig. 38. Generalized map showing location of principal metavolcanic belts in the Superior Province, Canadian Shield. Solid circles show localities from which metavolcanic samples have been obtained and analyzed for Rb, Sr, and Sr^{87}/Sr^{86}.

range typically from basalt to rhyolite with the basalts being similar in composition to modern subalkaline basalts such as those dredged from the oceans. Unlike their modern counterparts, however, the older rocks have been metamorphically upgraded to either zeolite, greenschist or amphibolite facies. This metamorphism provides a mechanism whereby it may be argued that any Sr^{87}/Sr^{86} value measured in a Precambrian volcanic has been modified due to movement of Sr and/or Rb during the metamorphism. This possibility, together with such problems as the one implied by the calcite content of the metavolcanics, has been investigated in detail. Our data provide strong evidence that a considerably higher Sr^{87}/Sr^{86} value existed in Earth's mantle 2.7 b.y. ago than that predicted by a linear growth from the "meteoritic" primordial value. In addition, the Sr^{87}/Sr^{86} data suggests that the heterogeneity recorded for the present-day mantle appears to have existed also in the mantle 2.7 b.y. ago. Various limiting cases for the evolution of mantle Sr are considered. Several models are found to be compatible with our observations; one of these is a simple differentiation model with continuous transport of Rb and Sr from the mantle.

Carbonate Contents and Sr^{87}/Sr^{86} Ratios of Calcites from Archaean Metavolcanics

C. Brooks, T. E. Krogh, S. R. Hart, and G. L. Davis

Volcanic magmas crystallize into mineral assemblages that are highly sus-

ceptible to alteration by weathering and metamorphic events. Any proposed investigation of the initial Sr^{87}/Sr^{86} in total-rock samples of metavolcanics must include consideration of the type and degree of alteration. In the case of Archaean greenstones, the most obvious indication of alteration is ubiquitous carbonate and silica.

We do not here attempt to relate the formation of carbonate to any particular time in the history of the metavolcanics. If this alteration is associated with either the parent vulcanism or the subsequent metamorphism that led to formation of the "greenstones," the problem of the effect of alteration on the Rb/Sr isotope parameters of the total rock is considerably simplified. Any later open-system behavior of the total rock or its alteration products would prevent sensible Rb/Sr chronology.

The carbonate component of the greenstones was determined by means of gas chromatography to a precision of ±2–3%. A distinction was made between *vein* and *disseminated* calcites; the former were separated from discrete veins, while the latter were separated from crushed rock that had been previously hand-picked to exclude calcite veins. Residues after preliminary 2N HCl treatment indicated that the separates were between 40% and 99% pure (the contaminants were predominantly quartz, with variable amounts of altered plagioclase and composite calcite-clinozoisite grains).

The histogram of calcite contents (Fig. 39) reveals that 52% of the Archaean greenstones examined (Fig. 38) contained less than 1% calcite, and 79% contained less than 3% calcite. These data are supported by a composite prepared from 40 other greenstone samples that gave a calcite content of 1.1%.

The histogram for the present-day Sr^{87}/Sr^{86} ratios of the calcites analyzed (Fig. 40) shows that whereas the vein calcites range from 0.701 to 0.718 in this ratio, with one exception the disseminated calcite ratios form a mode at 0.702. (The exception is a disseminated calcite taken from a rock collected in close proximity to the Grenville front.) The surprisingly high Sr^{87}/Sr^{86} ratios of some of the calcites are worthy of consideration especially since some of the values observed are significantly higher than the present-day Sr^{87}/Sr^{86} of the host greenstone. The isotopic distinction between these "radiogenic" calcites, which generally have lower Rb/Sr ratios than the host greenstones, implies that either (a) the calcite strontium was introduced under nonreactive conditions (groundwater?) and did not reach isotopic equilibrium with the host rock, or (b)

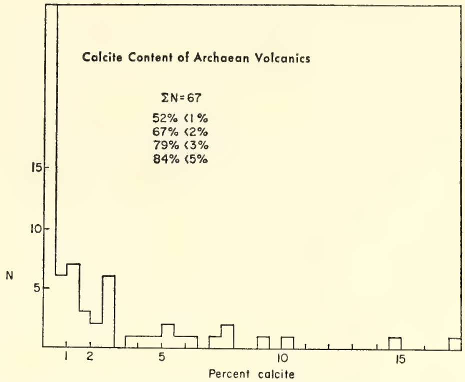

Fig. 39. Histogram showing calcite contents of 67 Archaean metavolcanics. Fifty-two percent of the samples contain less than 1% calcite; 79% contain less than 3% calcite.

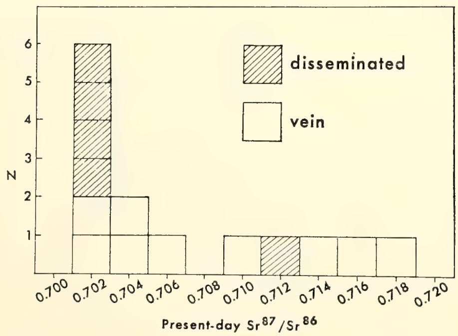

Fig. 40. Histogram showing measured Sr^{87}/Sr^{86} ratios of vein and disseminated calcites separated from Archaean metavolcanics.

the calcite strontium was derived locally by limited and selective leaching of only the rubidium-enriched mineral phases.

Providing that the four disseminated calcites measured are typical, then it is apparent that the initial Sr^{87}/Sr^{86} ratios of greenstones will not be affected by even as much as 10–20% of this calcite. Vein calcites can have a measurable effect on the Sr ratios of greenstones, however. We conclude that careful field sampling of Archaean greenstones, with the exclusion of visible vein calcite, will allow Rb-Sr isotope investigation in which the measured isotopic parameters have not been significantly affected by alteration attributable to the calcite.

The Initial Sr^{87}/Sr^{86} Ratios of the Upper Metavolcanics, Ontario, Canada and Lower Series, Michipicoten

C. Brooks, T. E. Krogh, S. R. Hart, and G. L. Davis

The Michipicoten area has been the subject of extensive geological investigation and our ground control is based upon the excellent account given by Goodwin.[42] He distinguishes lower, middle, and upper series of metavolcanics in the Michipicoten basin. Our sampling has followed this internal division. Figure 41 displays Goodwin's geological relationships and gives the location of our sampling sites.

The Rb/Sr results for 22 metavolcanics are displayed in the isochron diagram, Fig. 42. Inspection of this figure reveals that two separate lines must be fitted to the data, one corresponding to the upper series volcanics, one to the lower series. Statistical analysis of the lower series data indicates that there are sources of "geological" scatter about the isochron. Rejection of data (especially the higher Rb^{87}/Sr^{86} data points) to reduce this scatter could not be supported on geological grounds, and hence the most realistic isochron parameters are believed to be those given in Fig. 42. The initial Sr^{87}/Sr^{86} ratio for the lower series meta-

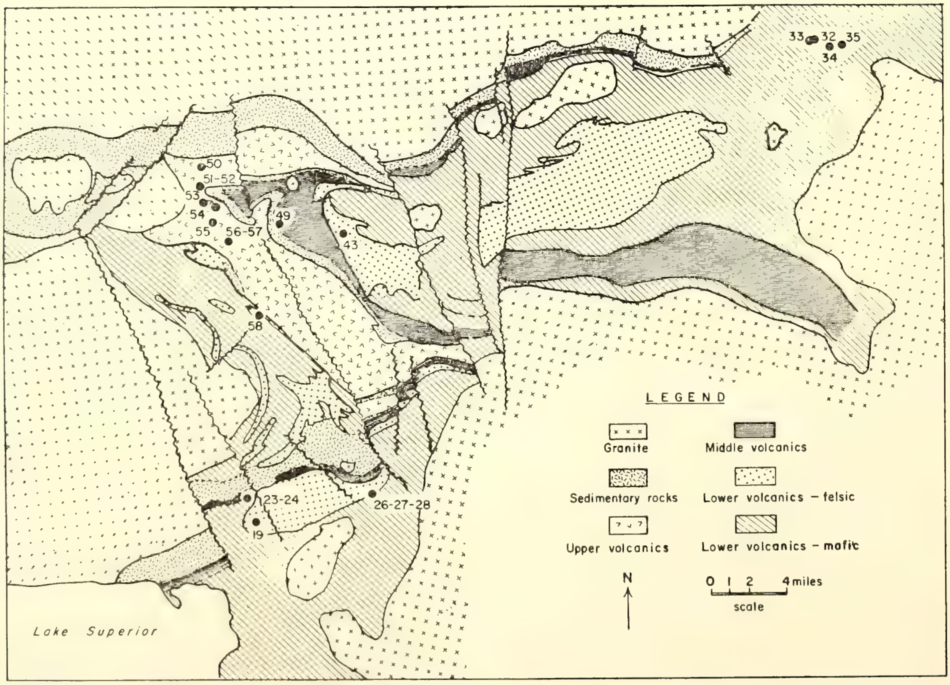

Fig. 41. Geologic map of the Michipicoten metavolcanic basin, adapted from Goodwin.[42] Sample localities shown as solid circles; numbers are sample reference numbers.

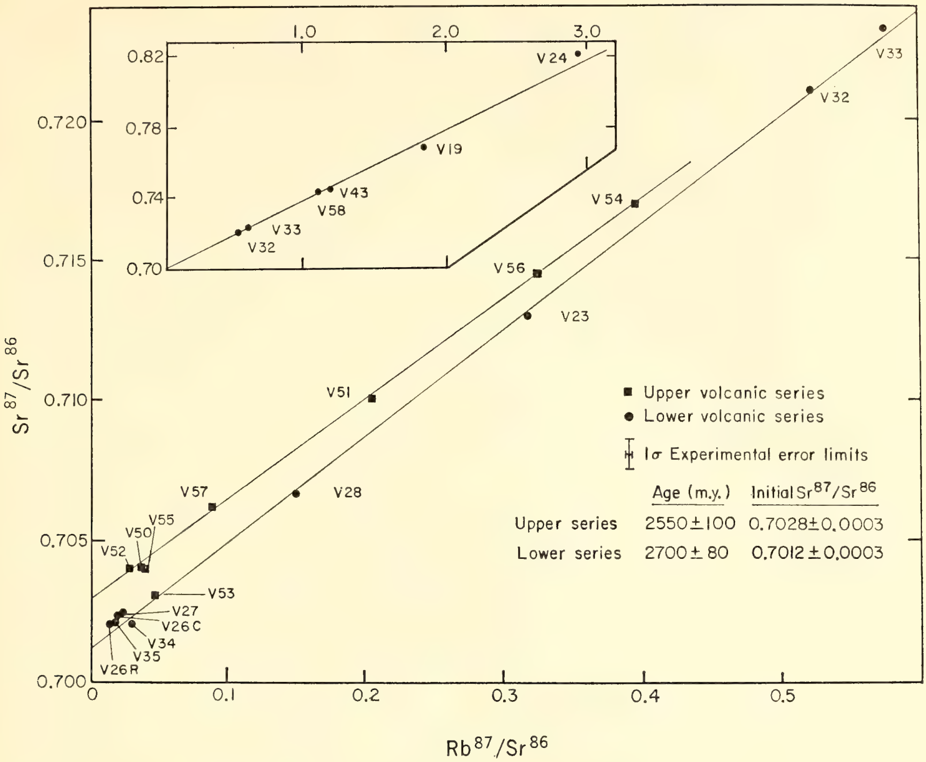

Fig. 42. Rb-Sr isochron diagram for Michipicoten metavolcanics. Inset shows samples from the lower series which have high Rb/Sr ratios. Samples from the lower series and upper series define distinctly different isochrons. Error limits are at 95% level of confidence.

volcanics remains constant despite the deletion of high Rb/Sr data points.

Whereas some of the lower series data reflect geological scatter, the upper series of metavolcanics (with one exception) fit an isochron exceedingly well. The exception (sample V53) is statistically distinct, and the isochron for the remaining upper series data gives an age estimate of 2550 ± 100 m.y. and an initial Sr^{87}/Sr^{86} ratio of 0.7028 ± 0.0003.

Testing between the recommended isochrons for the upper and lower series data according to the McIntyre *et al.* procedure [43] indicates that the series are distinctly different in initial Sr^{87}/Sr^{86} estimates at very high levels of confidence (+99.9%), and significantly different in age estimates at any level of confidence less than 98.5%. However, metavolcanics are frequently found to record ages that conform with times of regional metamorphism or plutonism. The 150-m.y. age difference between the upper and lower metavolcanic series, and the agreement between the age of the upper series and the average K/Ar mineral age recorded throughout the Superior Province of the Canadian Shield, demands that the possibility of metamorphic isochron rotation during whole-rock redistribution of strontium be considered for the upper series volcanics.

There are variations in the metamorphic grade within the Michipicoten basin. In the northeast it is low amphibolite facies (samples V32–V35) while in the southwest it is low-to-middle greenschist facies (samples V19–V27). The upper volcanics (V50–V57) fall inter-

mediate in metamorphic grade between the lower volcanics from different parts of the basin. To produce a metamorphic isochron requires that a metamorphic event distinguish the upper from the lower series in a single volcanic pile. This pulse would then be required to upgrade both volcanic series while initiating isotopic redistribution in the upper series only. The persistence of an excellent isochron on which fall lower volcanics of quite different metamorphic grades, e.g., V32 and V23, argues against metamorphic rotation of the isochron. In the light of these considerations, we feel that the initial Sr^{87}/Sr^{86} ratios of the Michipicoten metavolcanics are not metamorphic or apparent values.

One method of attempting to eliminate local mixing effects in the isotopic composition produced by metamorphism of volcanics is to analyze composites consisting of numerous samples representative of large exposures. Two composites were collected (samples V27 and V28) which together represent a sampling volume of about 4×10^7 kilograms of lower volcanics. These were found to possess quite different Rb/Sr ratios, yet each fell within experimental error on the lower-series isochron, thereby adding further weight to the primary nature of that isochron.

Although metamorphic effects seem inadequate to explain the difference in the observed initial ratios, effects due to crustal contamination, crustal or subcrustal magma aging, and remelting must also be considered. The average value of Rb for the lower-series section is calculated to be 19 ppm, of Sr 217 ppm, and of Rb/Sr 0.09. The average upper-series section, which contains few felsic members, is quite similar to the average lower series section in these parameters (Rb = 14 ppm, Sr = 194 ppm, Rb/Sr = 0.07).

It could be proposed that part of the parent magma giving rise to the lower-series volcanics aged in a molten or semimolten state for 150 m.y. and was then extruded to form the upper volcanics. To generate the observed Sr^{87}/Sr^{86} difference in 150 m.y., the aging magma would need a Rb/Sr of 0.27, a value considerably higher than that observed in either the average upper- or lower-series members. Clearly this process is not consistent with the observations. For the same reason, remelting of the lower-series volcanics after 150 m.y. will not produce a magma with the observed initial Sr^{87}/Sr^{86}. Preferential melting of V24-type acidic lavas could fulfill the Sr isotopic requirements, but is contraindicated by the lack of felsic volcanics in the upper series (and the low Rb/Sr ratio).

Crustal contamination has led to variations in the initial Sr^{87}/Sr^{86} of modern continental volcanics, and it could be suggested that the upper- and lower-series volcanics differ in Sr^{87}/Sr^{86} due to the incorporation (prior to extrusion) of different amounts of contaminant. If we take as the contaminant a sialic crust 500 m.y. older than the volcanics and with a Rb/Sr ratio of 0.25, about 40% of this would be required to produce the observed difference in Sr^{87}/Sr^{86}. This degree of contamination is inconsistent with the Rb/Sr data and with the generally mafic character of the upper volcanics. In addition, it is doubtful that any significant amount of crustal contaminant was available at that time (Hart and Davis, 1969).[44]

The effect of sea-water contamination on modern oceanic volcanics is considerably greater than had been thought before (see pp. 403–408 of this report). Consequently interaction with an Archaean sea could have caused modification of the Sr isotopic composition. Analysis of both an epidotized rim (sample V26R) and a core (sample V26C) from a pillow indicates no difference in the isotopic composition. While strontium contamination has been observed in modern oceanic volcanics, possible effects during the Archaean will be greatly minimized because of the similarity of the sea-water strontium and volcanic strontium at that time.

Evaluation of the possible metamorphic processes, crustal contamination, magma aging, and magma regeneration leads to the conclusion that the initial ratios obtained for the Michipicoten metavolcanics are most probably primary features of the volcanic magmas. The initial ratio difference of 0.0016 (significant at the 99.9% level of confidence) is taken to reflect a heterogeneity in the isotopic composition of the Sr of the magma source regions prior to 2.6–2.7 b.y. ago.

Initial Sr^{87}/Sr^{86} Ratios of Regionally Sampled Metavolcanics from the Canadian Shield

C. Brooks, S. R. Hart, T. E. Krogh, and G. L. Davis

A histogram for the initial Sr^{87}/Sr^{86} ratios of 32 metavolcanics sampled on a regional scale, the Michipicoten metavolcanics discussed above, and modern oceanic volcanics is given in Fig. 43. Whereas the ratios from the modern oceanic volcanics are direct isotopic measurements, the metavolcanic values have been calculated from present-day Sr^{87}/Sr^{86} ratios assuming a 2.7-b.y. growth period for radiogenic Sr. The major error in any single projected ratio is a combination of the estimated experimental error in the measured Sr^{87}/Sr^{86} ratio and the uncertainty in the age correction. For a $\pm$100-m.y. value for the latter, the combined limit of error for over two-thirds of the projected initial Sr^{87}/Sr^{86} ratios is less than $\pm$0.0005 at the 95% level of confidence. For the few samples with high Rb/Sr ratios (up to 0.14), the uncertainty in the corrected initial ratio is a maximum of $\pm$0.001.

The spread in the calculated initial

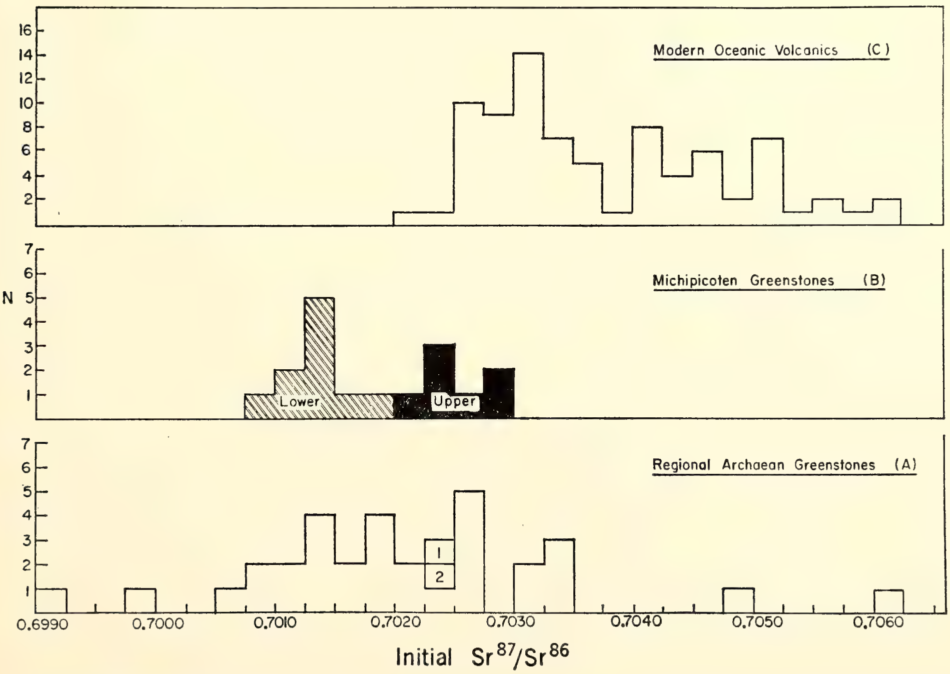

Fig. 43. Histogram of initial Sr^{87}/Sr^{86} ratios for (A) Archaean metavolcanics from the various localities shown in Fig. 38; (B) metavolcanics from Michipicoten area, individually corrected for age from Fig. 42; (C) modern oceanic volcanics, compiled from the literature. Also shown are two Archaean metavolcanic composites: (1) 20 samples from Abajevis Hills, Quebec; (2) 70 samples from the various localities of Fig. 38.

ratios of the regionally distributed Archaean metavolcanics is considerably larger than the maximum uncertainty in any single ratio. This spread was not found to correlate with either the geographical location of the samples, their Rb content or Rb/Sr ratio. Individual analyses of this type are prone to the incorporation of some spurious data; for instance, the highest projected Sr^{87}/Sr^{86} for the regional data was for a sample taken from the Grenville front zone. If the other three extreme values are similarly spurious, the remaining spread (from 0.7005 to 0.7035) is essentially the same as that observed for the Michipicoten data. In considering the Michipicoten data we evaluated possible effects due to metamorphic processes, crustal contamination, magma aging, and magma regeneration. We concluded that the initial ratios and their range of values are probably primary features of the volcanic magmas. The similarity between the regional values and the Michipicoten data suggests, furthermore, that these differences of initial ratio are regional in scale and reflect heterogeneity in the Archaean mantle on a broad scale.

In comparing the modern values and the Archaean data (Fig. 43), the present-day isotopic heterogeneities in the oceanic mantle appear to be only somewhat larger than the inferred Archaean mantle values. Implications of this result are discussed in a later section.

The mean value of the regionally selected metavolcanics is 0.7020 ± 0.0003, and is compared with the calculated ratios for the two composites shown in Fig. 43. Composite 1 is composed of 20 samples from the Abajevis hills, Quebec, and composite 2 is composed of 70 volcanics collected from the different areas shown in Fig. 38. The projected Sr^{87}/Sr^{86} values for the two composites are not significantly different from the mean of the 32 individual samples, thereby establishing the validity of the mean regional value. This Archaean mean ratio is clearly lower than the average value for modern oceanic volcanics, and may be used in evaluating models for the chemical evolution of Rb and Sr in the mantle.

Rb-Sr Mantle Evolution Models

S. R. Hart and C. Brooks

The Sr data which we wish to apply toward interpretation of mantle evolution models are presented in Table 8. For the present-day mantle we have chosen average oceanic volcanic strontium, since these volcanics appear to be least affected by problems of magma aging and contamination with sialic crust. For the primordial strontium of Earth we have chosen the strontium from the Rb-poor achondrites. There is, of course, no direct evidence that Earth started with such strontium, and we must bear in mind the evolutionary consequences of a different primordial strontium value. We use the average initial

TABLE 8. Initial Sr^{87}/Sr^{86} Data Relating to Mantle Evolution

Rock type	Average initial Sr^{87}/Sr^{86}	Age (m.y.)	Source of data
Oceanic volcanics	0.7038 ± 0.0002	modern	63 basalts from Gast (1967)[45] and 40 basalts from Bence (1966)[46]
Archaean metavolcanics	0.7018 ± 0.0002	2600–2700	30 regional basic volcanics, 22 Michipicoten volcanics and two composites of 70 and 20 samples each
Achondritic meteorites	0.6990 ± 0.0003	4500	analyses of Gast (1960)[47] and isochron of Papanastassiou *et al.*, (1969)[39]

Note: Errors are estimated standard errors of each population in relation to a common value for the E and A standard of 0.7082.

strontium from the Archaean volcanics discussed above as an intermediate time point. This ancient volcanic association is most similar to the orogenic basalt-andesite-rhyolite association of the modern island arcs and should, strictly speaking, not be compared to modern oceanic volcanics, which may sample a different type of mantle. However, Sr analyses of modern calcalkaline island arc volcanics are not abundant, and so we are forced for now to use Archaean and modern strontium data which are derived from somewhat different types of occurrences. Also, while the Sr evidence from both the Archaean and modern volcanic data indicates a heterogeneous mantle, our initial considerations will be of an "averaged" mantle.

Figure 44 is an evolution diagram showing the data of Table 8. As discussed earlier, the Archaean point falls distinctly above a line (marked $k=0$ in the figure) joining "primordial" strontium and modern mantle strontium. The *linear evolution model*, $k=0$, might be termed an infinite reservoir model, as it requires the Rb/Sr ratio of the regions which we sample throughout time to be a constant. While this model has been commonly used in the past to describe mantle evolution (Hedge, 1966),[48] it is not in accord with our Archaean data. Furthermore, both Gast (1968)[49] and Hurley (1968)[50] have advanced strong arguments showing that the mantle is not an infinite reservoir with respect to supplying crustal quantities of Rb and Sr. Their data show that the mantle as a whole cannot follow a simpler linear evolution trend. However, it is possible that the mantle is not well mixed on a large scale and that the same mantle region is never sampled twice. Thus each new generation of magma could take place in a mantle region which was a closed system until that time, and the "apparent" evolution curve would be linear. In view of the Archaean data, however, it seems more reasonable to consider various nonlinear evolution models.

One approach to a nonlinear model would be to consider a multistage evolution in which periodic extractions of ma-

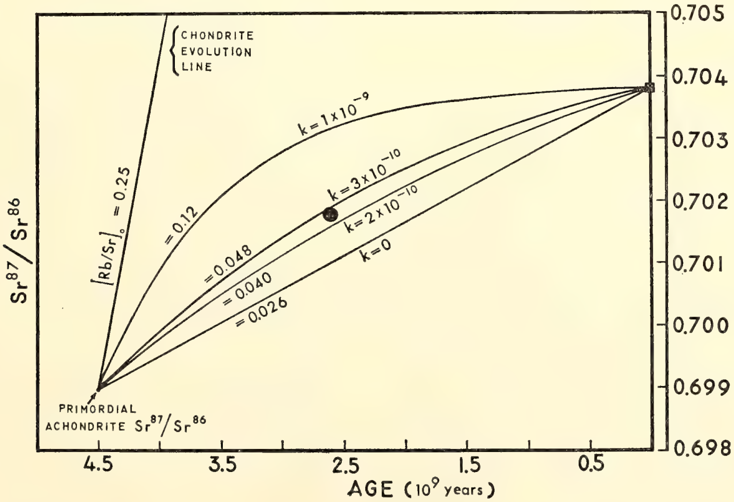

Fig. 44. Rb-Sr evolution diagram. Curves connecting primordial strontium ($Sr^{87}/Sr^{86} = 0.6990$) and modern oceanic strontium (0.7038) are calculated for a continuous transport model. Values of k are the transport parameters; other values are the initial Rb/Sr ratios required by the model. Also shown is the evolution line of a typical chondritic meteorite with initial Rb/Sr ratio of 0.25. Black circle at 2.6-b.y. age is our best average value for Archaean metavolcanics.

terial from the mantle leave it successively depleted in Rb relative to Sr (Hurley, 1968). The three points of Fig. 44 can be fitted with an infinite number of two-stage models, and there do not exist enough data to adequately assess a *multistage evolution model.* However, the number of unconstrained parameters can be reduced simply by approximating a multistage process with a *continuous transport model.* For example, assume that both Rb and Sr are transported from mantle to crust continuously, and at a rate proportional to their instantaneous concentration in the mantle. Thus,

$$\frac{d(\mathrm{Rb}^{87})}{dt} = -\lambda\,\mathrm{Rb}^{87} - \gamma\,\mathrm{Rb}^{87}$$

$$\frac{d(\mathrm{Sr}^{86})}{dt} = -\alpha\,\mathrm{Sr}^{86}$$

$$\frac{d(\mathrm{Sr}^{87})}{dt} = \lambda\,\mathrm{Rb}^{87} - \alpha\,\mathrm{Sr}^{87}$$

where λ is the radioactive decay constant for Rb^{87}, γ is the transport coefficient for Rb^{87}, and α is the transport coefficient for Sr^{86} and Sr^{87}.

The solution may be written in the form

$$\left(\frac{\mathrm{Sr}^{87}}{\mathrm{Sr}^{86}}\right)_t = \left(\frac{\mathrm{Sr}^{87}}{\mathrm{Sr}^{86}}\right)_0 + \frac{\lambda\,(\mathrm{Rb}^{87}/\mathrm{Sr}^{86})_0\,[1-e^{-(\lambda+k)t}]}{\lambda+k},$$

where k is a combined transport coefficient $= (\gamma-\alpha)$. We will assume Rb is transported at a higher rate than Sr $(\gamma>\alpha)$.

We can also derive the fraction of Rb and Sr left in the mantle as a function of time,

$$(\mathrm{Rb}^{87})_t/(\mathrm{Rb}^{87})_0 = e^{-(\lambda+\gamma)t}$$

$$(\mathrm{Sr}^{86})_t/(\mathrm{Sr}^{86})_0 = e^{-\alpha t}$$

and the time variation of the Rb/Sr ratio,

$$(\mathrm{Rb}^{87}/\mathrm{Sr}^{86})_t/(\mathrm{Rb}^{87}/\mathrm{Sr}^{86})_0 = e^{-(\lambda+k)t}.$$

Similar models for uranium and lead evolution have been discussed by Patterson (1964),[51] Wasserburg (1966),[52] and Gast (1967).[45]

The obvious feature of this model is that for every value of initial Rb/Sr ratio, there is only one value of the combined transport coefficient which will satisfy the two $\mathrm{Sr}^{87}/\mathrm{Sr}^{86}$ end-points. Figure 44 shows curves for this continuous model for $k=0$, 2×10^{-10}, 3×10^{-10}, and 1×10^{-9} yr^{-1}, corresponding to initial Rb/Sr ratios of 0.026, 0.040, 0.048 and 0.12. The Archaean data point is consistent with a k value of 2–3×10^{-10} and an initial Rb/Sr ratio of 0.04–0.05. This k value then also sets limits on the extent of transport of Rb and Sr from the mantle. For the limiting case of no Sr transport $(\alpha=0)$, we find that 65–80% of the Rb has been removed from the mantle. For a ratio of Rb and Sr transport of $\gamma/\alpha \approx 3$, 75–90% of the mantle's Rb and 40–55% of its Sr has been moved into the crust. Hurley (1968) has estimated the Rb/Sr ratio of the total crust to be about 0.15. This value, coupled with the initial value of about 0.05 for Earth suggested by Fig. 44, leads to a value of γ/α of about three.

It is interesting to note that, for $k\sim2$–3×10^{-10}, Rb and Sr are transported to the crust almost linearly as a function of time and if we equate this Rb and Sr movement to the formation of continental crust, then the model requires a relatively constant rate of continental growth.

One of the main difficulties with this model, at least as fitted to the Archaean data, is its requirement of very extensive removal of Rb from the mantle. Gast (1968) has pointed out that it is unlikely that Rb will be more extensively removed from the mantle than radiogenic argon, and that for an extreme case where Earth starts with only 120 ppm K, about 70% of its radiogenic argon (and 55% of its K) is now present in the crust and atmosphere. This value is to be compared with the estimate of 75–90% removal of rubidium according to the con-

tinuous transport model. To some extent these comparisons are misleading, because the argon calculation refers to Earth as a whole whereas the Rb-Sr evolution model may in fact only relate to the upper mantle regions from which magmas have actually been derived throughout geologic time. Hence, while total Earth may be only 20–30% outgassed with respect to radiogenic argon (assuming a more reasonable initial K content of 300 ppm), the upper mantle regions could be 100% outgassed. Furthermore, the estimated uncertainties in the data of Table 8 allow the fractional removal of Rb to be as low as 40–50%.

The present-day Rb-Sr ratio of the mantle, as determined by the k value of $2\text{–}3 \times 10^{-10}$, would be 0.012–0.015, or about one-third of its initial value. A number of authors have commented on the fact that submarine basalts have Rb/Sr ratios which are too low to generate the observed Sr^{87}/Sr^{86} ratios of the basalts in 4.5 billion years, and they suggest this finding may indicate a derivation of basalt from a mantle region which was recently depleted in Rb. Our model for continuous Rb depletion in the mantle is consistent with the submarine basalt data, as the average Rb/Sr ratio of these basalts ($\sim$0.01) is very similar to that predicted by the continuous model for the present-day mantle. The high K/Rb ratio of these submarine basalts may also be related to a continuous depletion model in which the transport of Rb would take place at a faster rate than the transport of K, throughout geologic time, leaving a residual mantle with a relatively high K/Rb ratio.

Finally, we may consider what constraints the continuous evolution model implies with regard to development of the observed isotopic heterogeneities in the mantle. There are two limiting ways in which heterogeneities can be developed in the mantle. (1) There can be a uniform initial Rb/Sr ratio throughout the mantle, but with subsystems of different values for the transport coefficients. Or (2) there can be uniform transport coefficients throughout geologic time, but with subsystems of different initial Rb/Sr ratio.

Either way heterogeneities will develop at a different rate, which may be specified as the ratio of the range in Sr^{87}/Sr^{86} during Archaean times to that at present. For (1), the Archaean range will be 30% of the present range; for (2), it will be about 55%. The actual observed ranges, as derived from Fig. 43, are almost the same for the Archaean data and the modern data, and are thus in contrast to the model prediction of a range for the Archaean of one-third to one-half of the present range. We suspect that some of the Archaean variation may be geological, related to the difficulty of preserving primary initial ratios in volcanic rocks for long periods of time. Moreover, the inherent precision of the Archaean points is less than that of modern data because of the necessary time correction. Clearly, a definitive test of evolution models such as these requires more analyses of better ultimate precision, not only for Archaean volcanics but for volcanics of other ages.

The K, Rb, Cs, and Sr Geochemistry of Archaean Metavolcanics

S. R. Hart, G. L. Davis, C. Brooks, and T. E. Krogh

By comparing the trace element content of Archaean and modern volcanic rocks, we may gain insight into the changing nature of the mantle and of the derivation processes which supply volcanic material to the surface. This approach is complementary to the studies of strontium isotope abundances reported in preceding sections.

The geologic setting and major element chemistry of Archaean volcanics clearly shows that they are similar to the modern continental and island-arc calcalkali volcanic series (Wilson *et al.*, 1965).[53] We are unable, for lack of chemical data, to assign rock names to the Archaean vol-

canics which we have analyzed for trace elements. However, Wilson *et al.* (1965) suggest that typical Archaean volcanic belts contain more basalts than andesites. Baragar (1968),[54] through systematic sampling of two volcanic belts, showed that basalts and andesites were more nearly equal in abundance, with both being more abundant than the more siliceous rocks (dacites and rhyolites). Basing our classification on Baragar's work, we have simply divided our volcanics into two classes: $K<0.6\%$, basic; $K>0.6\%$, siliceous. In this way we are able to calculate trace element averages for comparison with modern volcanic types; Table 9 presents the averaged data for the basic Archaean volcanics, along with data for a basic composite formed from 70 samples. The individual values are also presented in Figs. 45 and 46. Many previous investigators have noted the depletion of potassium in Archaean volcanics relative to younger volcanics; our data show that this depletion extends to the trace elements, Rb and Sr, as well. In the Archaean volcanics, K, Rb, and Sr are depleted by approximately equal amounts relative to the young tholeiites, so that the K/Rb and K/Sr ratios in the old and young basic volcanics are essentially identical. Looked at in terms of trace element trends (Figs. 45 and 46) the data, though scattered, appear to lie in areas somewhat separated from the trends of young calcalkaline volcanic series such as those in New Zealand. This divergence is especially pronounced in the more basic Archaean rocks, since the New Zealand trend does not extend very far into the low potassium region. The data for the siliceous Archaean volcanics is not greatly different from the New Zealand trend.

Is the depletion of K, Rb, and Sr in Archaean volcanics a primary or secondary feature? Since all of these volcanics have undergone metamorphism to some degree, it is natural to consider this metamorphism as a possible cause for depletion of K, Rb, and Sr. The data of Fig. 45 are separated according to area, and therefore may be considered in respect to the overall metamorphic grade of each area. The Abajevis-Clericy area, generally zeolite-greenschist facies, has a rather restricted range of K/Rb, with 15 out of 17 samples falling within the range 230–400. The Surprise Lake area shows a transition in metamorphic grade (related to the Grenville front) from greenschist to amphibolite facies and the K/Rb ratios show a much larger scatter than at Abajevis-Clericy. However, the average K/Rb ratio is the same in both the low grade and high grade areas. Similarly, in the Michipicoten area, the volcanic series range in metamorphic grade from low greenschist to low amphibolite facies. Again there is no obvious correlation of K/Rb with grade of metamorphism, though the scatter may be somewhat larger in the higher grade areas. There is some suggestion that changes in K/Rb may occur in either direction; volcanics which are siliceous enough to form muscovite during metamorphism tend to have low K/Rb ratios, whereas basic volcanics which form amphibole during metamorphism tend to have high ratios.

At extreme grades of metamorphism it is likely that major changes in trace

TABLE 9. Comparison of K, Rb, and Sr Contents of Archaean and Modern Basic Volcanics

Group	K, %	Rb, ppm	Sr, ppm	K/Rb	K/Sr
46 individual Archaean volcanics	0.19	6.1	123	310	15.5
Archaean composite, 70 samples	0.21	5.9	173	360	12.0
Orogenic andesites	1.1	4.5	260	250	42.0
Tholeiitic basalts	0.6	1.7	450	340	12.9

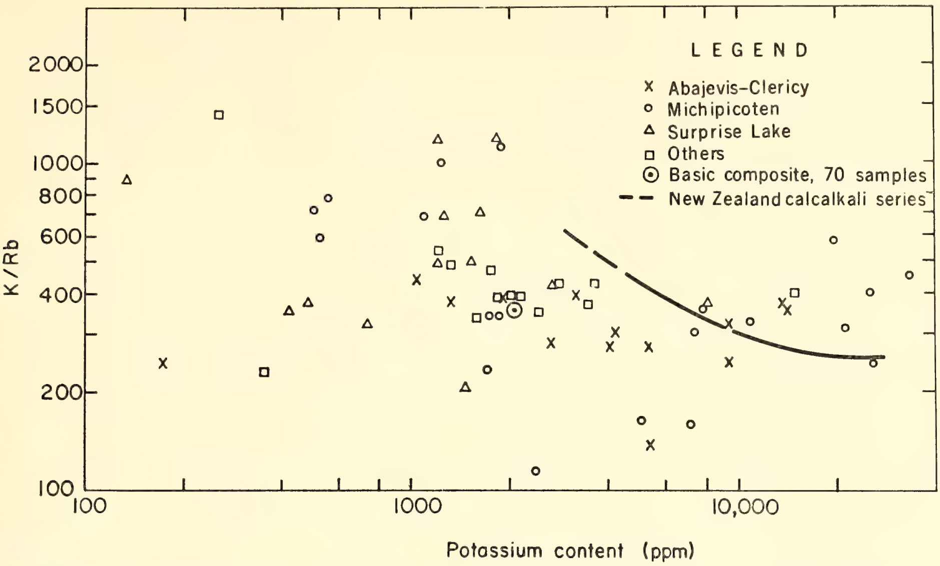

Fig. 45. K/Rb versus K content of Archaean metavolcanics from the various localities of Fig. 38. Solid line is the average trend line for samples from the modern island arc calcalkaline series of New Zealand.

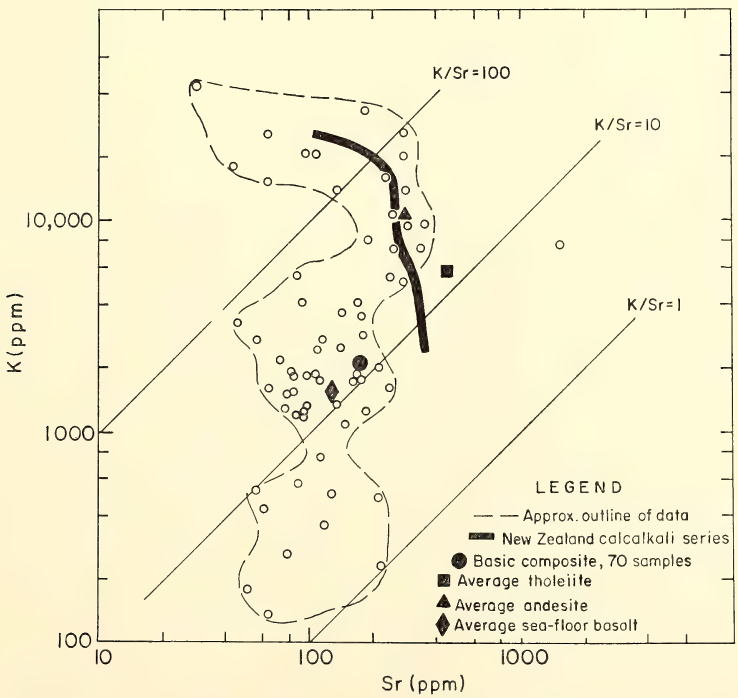

Fig. 46. Logarithmic plot of K and Sr contents of Archaean metavolcanics. Strontium contents show little variation compared with large variations in potassium content. Modern island-arc volcanics from New Zealand shown for comparison.

TABLE 10. Effect of Metamorphism on K, Rb, and Sr

Area	Facies	K, %	Rb, ppm	Sr, ppm	K/Rb	K/Sr
Emeryville	amphibolite	0.87	21.5	230	404	38
Colton	granulite	0.48	5.8	150	830	32

element chemistry can take place, as illustrated by the data in Table 10. These data were obtained on composites of a major amphibolite unit which crosses regional metamorphic gradients in the classic Adirondack area of Engel and Engel; samples were generously provided by A. E. J. Engel. The K, Rb, and Sr contents of these amphibolite units have been drastically reduced in the high-grade granulite facies area. The K/Sr ratio has remained relatively unchanged, while the increased loss of Rb relative to K has caused a doubling of the K/Rb ratio. However, even these extreme grades of metamorphism have not depleted the potassium to the 0.2% level observed in the Archaean volcanics, strongly suggesting that this abnormally low potassium content is a primary feature of Archaean basic lavas. In general, while there may be a tendency toward local redistribution of trace elements during low grade metamorphism, we consider gross changes throughout a thick volcanic pile to be very unlikely. There is certainly no obvious field or petrographic evidence for large-scale migration of alkalies in metavolcanic sequences. A case of local redistribution of major elements during burial metamorphism has been described (Smith, 1968)[55] and it is possible that the trace elements will respond, on a local scale, to this development of mineralogical "patchiness." More extensive studies of trace element behavior during metamorphism are clearly needed; however, use of large representative samples and sample composites may help to minimize metamorphic effect.

If the K, Rb, and Sr depletions noted for Archaean volcanics in Table 11 are primary features, then what possible interpretations can be formed regarding the nature of the Archaean mantle? While there are no young calcalkaline orogenic volcanics with similar depletions of K, Rb, and Sr, the submarine basalts of the ocean floors have certain characteristics which are similar to Archaean volcanics. Average contents of K, Rb, Cs, and Sr for these two volcanic types are compared in Table 11. The submarine basalts have low K and Sr contents, similar to the Archaean volcanics; however, Rb and Cs are further depleted in the submarine basalts, leading to considerably higher K/Rb and K/Cs ratios.

A preliminary model relating Archaean and modern volcanism might be formulated as follows. Submarine basalts are formed in a region of high thermal gradient (on the upwelling plume of mobile mantle under the mid-ocean ridges), and probably represent products of partial melting at shallow depths. We suggest a similar low pressure mode of

TABLE 11. K, Rb, Cs, and Sr in Archaean and Submarine Basalts

Rock type	K, %	Rb, ppm	Cs, ppm	Sr, ppm	K/Rb	K/Cs	K/Sr
Archaean volcanics	0.20	6.0	0.36	150	330	5500	13
Submarine basalts	0.16	1.8	0.02	125	900	80,000	13

formation for Archaean volcanics, as it is probable that geothermal gradients were considerably higher during the earlier periods of Earth history. Perhaps partial melting at shallow depths is more extensive than partial melting at high pressure, leading to a magma with low contents of K, Rb, Cs, and Sr. The similarity of K and Sr contents in Archaean and submarine basalts not only suggests a similar mode of origin but suggests that removal of K and Sr from the mantle since Archaean times has not exceeded 20–30%. On the other hand, the marked depletions of Rb and Cs in submarine basalts may be explained by relatively large removals of Rb and Cs from the mantle since Archaean times. Thus a transport model similar to that proposed for the Sr isotopic evolution of the mantle could be applied to these other elements as well, with relative transport coefficients in the order

$$Cs > Rb > K \approx Sr$$

Distribution of Potassium in Mafic and Ultramafic Nodules

A. J. Erlank

Many workers have considered that the mafic and ultramafic nodules and inclusions found in volcanic rocks, and specifically those occurring in kimberlite, may represent fragments of the upper mantle. Recent studies on these materials have paid particular attention to the distribution of K and related elements Rb, Cs, Ba, Sr, Th, U, and Pb, as well as the Sr^{87}/Sr^{86} ratio, in these nodules and their component minerals, and these abundances have been used to postulate models for the composition and differentiation history of the upper mantle. Two questions are crucial to the interpretation of such data; both ultimately deal with the possibility of modification of the original composition of these rocks and their minerals. In the first place, where analysis of whole-rock samples is concerned, secondary alteration and contamination by crustal material is likely, particularly for kimberlite nodules. In this case it is difficult, if not impossible, to evaluate the primary abundance patterns. Several workers have analyzed individual mineral separates of the primary phases to overcome this difficulty. Apart from the question of whether it is possible to obtain pure separates, this raises the second question as to whether the elemental composition now observed is reflective of the composition of the mineral at depth, i.e., whether or not the composition of the minerals has changed upon release of the high temperatures and pressures under which they formed.

These questions can only be answered by a thorough knowledge of the location of the elements mentioned, i.e., the precise internal distribution as revealed by a technique such as electron-probe analysis. This study is concerned with the distribution of K in a variety of possible upper mantle materials. Of the elements mentioned above, only potassium occurs in high enough concentrations to be amenable to electron-probe analysis. By implication, however, the K abundances to be discussed provide reliable information concerning the distribution of these associated elements.

During this work it has consistently been possible to obtain a detection limit on the order of 20 ppm K. Many of the minerals analyzed have K contents at or near the detection limit, and these results will consequently be imprecise. For this reason particular care has been taken in making corrections for background; full details of the technique used together with an assessment of accuracy will be given elsewhere. In general, it may be noted that the pure minerals are considered to yield more reliable data than the alteration products. For this reason the values quoted for the alteration products are best considered in a relative manner by comparison with the pure minerals. Analysis locations on the

pure minerals were chosen by use of both the reflected and transmitted light facilities in those regions where the grains were considered to be clear and fresh, but it is considered likely that the electron-probe detects alteration, in the form of high K abundances, that is not optically visible.

Material examined comprises both rock sections and mineral fractions and is derived mostly from African kimberlite pipes. These include eclogites, garnet peridotites, garnet pyroxenites and a phlogopite nodule. For comparison a garnet pyroxenite from Salt Lake Crater, Hawaii, and an eclogite from Kakanui, New Zealand, have also been studied.

Secondary alteration. The possibility of secondary contamination of nodules and inclusions has been commented on by several workers. Particularly relevant to this work are the observations by Gurney, Berg, and Ahrens (1966)[56] concerning anomalously high Cs concentrations in eclogites from the well-known Roberts Victor Mine, and the subsequent detailed account by Berg (1968)[57] concerning the nature of the alteration processes affecting these nodules.

All the kimberlite nodules studied show, in varying degrees, evidence of secondary alteration and contamination processes, and it is clear that the distribution of potassium is affected by these processes. It has not yet been possible to delineate the type and number of alteration effects experienced by the nodules, because (1) the alteration products are extremely variable in nature even within small areas of the same primary mineral in single nodules, (2) the type of secondary minerals found varies from nodule to nodule, even for similar rock types from the same pipe, and (3) there is some dependence on geographical distribution because garnet peridotites from Lesotho (where the kimberlites are found higher in the stratigraphic sequence intruding Karroo lavas) do not appear to have such high K concentrations associated with their alteration products as do those from South Africa. Likewise the type of secondary veining observed in two eclogites from Tanzania is different from that observed in eclogites from the Roberts Victor Mine. However, much of the K contained in these rocks, apart from that present in phlogopite, is located in cracks, along grain boundaries, secondary minerals, and alteration products. This is the essential feature of significance if it be considered that the alteration took place either during transit and emplacement of the kimberlite or during subsequent weathering of the kimberlite, as both processes would carry the imprint of the crustal environment.

Berg (1968)[57] considers that the Roberts Victor eclogites, which have been especially severely affected, have been subjected to two stages of alteration, as suggested above, and this work for the most part supports his contention. The type of alteration which has affected the garnets is dissimilar in composition to that affecting the omphacites. The latter type is important because of interest in the K content of clinopyroxenes, as discussed elsewhere in this report. Plate 1 shows the fine-grained, turbid alteration typical of Roberts Victor omphacites. The electron beam scanning photographs reveal a phase with a high K concentration, which is also depleted in Ca and Mg relative to unaltered omphacite. Plate 1 (A) indicates the location of two traverses, X and Y, which are shown in Figs. 47 and 48. Berg (1968) identified an analcime-type zeolite as an alteration product of the omphacite, but a study of Figs. 47 and 48 suggests that at least three phases are chemically distinguishable, although optically they are not. The relevant point of interest concerns the presence of up to 10% K in one of the phases, in comparison with $\sim$0.12% K in the pure omphacite. This, together with the fine-grained nature of the alteration (note, for example, that the K-rich phases are often less than 10 μm wide) causes con-

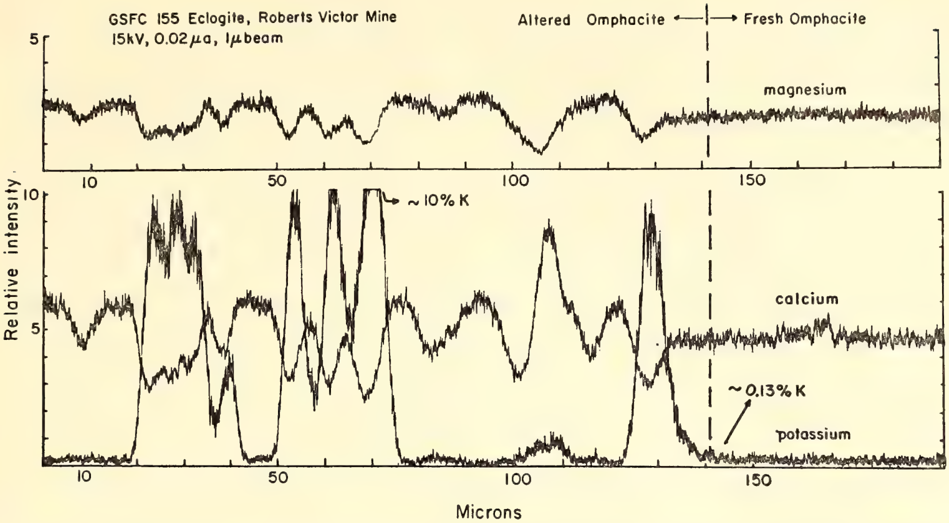

Fig. 47. Electron-probe traverses for Mg, Ca, and K along line *X* in Plate 1A showing variation in composition between fresh and altered omphacite from Roberts Victor eclogite.

cern with respect to obtaining pure separates of the fresh omphacite. Several separates have been examined by electron-probe analysis and all, to varying degrees, show the presence of K-rich alteration. One, which had been leached with dilute HCl, still revealed the presence of up to 5% K in altered areas. Hence, it would be desirable, when analyzing omphacite separates, to monitor

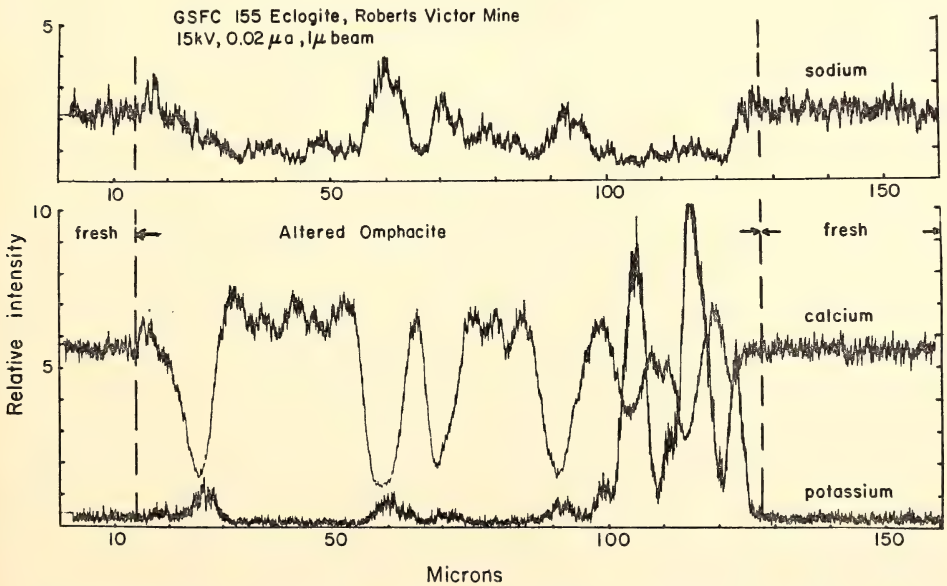

Fig. 48. Electron-probe traverse for Na, Ca, and K along line *Y* in Plate 1A showing variation in composition between fresh and altered omphacite from Roberts Victor eclogite.

the purity of the separates by comparing the K content of these mineral fractions, as determined, for example, by isotope dilution analysis, with that obtained by electron-probe analysis on pure material.

The type of alteration found in cracks and surrounding the garnets from Roberts Victor eclogites is presumably related to the emplacement of the kimberlites. The term kelyphite has been used to describe this alteration, but this term is not considered appropriate for these samples, as it seems clear that extraneous material has been introduced. Some of the material is phlogopite, and some is related to phlogopite in having high Mg and K contents (the latter often up to 5%), but at the same time the concentrations of other elements such as Na and Ca are too high (locally up to 9% Na and 7% Ca) to be pure phlogopite. In several of the reaction rims surrounding garnets, potash feldspar is also present. It may be noted that these semi-opaque alteration products (kelyphite) are more readily identified by the use of the reflected light than the transmitted light facility. However, in many cases these phases are too variable in composition and too fine grained to be identified. For all Roberts Victor eclogites, the amount of K located within the reaction rims is far in excess of that present in the fresh garnets, which in all rocks analyzed have less than 20 ppm K.

As mentioned previously, the type of alteration found in other eclogites differs from that observed in the Roberts Victor samples. Two eclogites from Tanzania have virtually all their K located along cracks and grain boundaries, and the omphacite does not show the fine-grained, turbid alteration characteristic of the Roberts Victor omphacites. Plate 2 indicates the location of K in one of the Tanzanian eclogites. This sample is considered to be the freshest kimberlite eclogite available to the author. The K-rich phase could not be identified, but is not phlogopite. Elsewhere, along cracks in the garnets, small 10-μ grains of potash feldspar ($\sim$13.5% K) were observed. The garnets and omphacites in both samples have less than 30 ppm K. A petrographic description and photomicrograph of the nodule shown in Plate 2, sample 501, is given by Williams (1932, plate 82).[58]

The discussion above deals largely with the Roberts Victor eclogites, as recent workers have shown particular interest in these nodules. However, many of the comments regarding Roberts Victor eclogites apply in a general way to the other nodules found in kimberlite. Plate 3 indicates the type of alteration found in garnets from a garnet peridotite nodule. The alteration is not phlogopite, but again has phlogopite affinities in having high K ($\sim$3.5–4.0%) and Mg contents. This type of "kelyphitic" alteration is common to all garnet pyroxenites and peridotites examined, although those from Lesotho apparently have suffered less K metasomatism than those from South Africa. The diopside in these nodules is invariably veined with a fine alteration product, although this does not contain as much K as that observed for the omphacite alteration product, the highest concentration found being about 1.5% K. An unexpected feature is the presence of local and erratic areas of high K concentration in serpentine filling olivine cracks, where K contents of approximately 4–6% K are encountered. No separate mineral phase could be identified. Sometimes, however, the serpentine veining could be traced to a phlogopite grain, and it could be shown that the two minerals have reacted with evident leaching of the phlogopite; this may partly explain the redistribution of K during the serpentinization process. These features again demonstrate the difficulty of obtaining pure mineral separates. It should also be noted that the examples shown in Plates 1, 2, and 3 have been chosen to provide obvious and clear demonstrations of the distribution of K in the rocks examined. In many cases, however, the K-rich alteration is not so

clearly defined and not amenable to analysis by the electron beam scanning technique.

Preliminary work carried out on nodules from other environments indicates distributions similar to that revealed above. A garnet pyroxenite from Salt Lake Crater, Hawaii, contains less than 35 ppm K in both pyroxenes and in the garnet, while a K-rich phase contained within a zeolite-carbonate vein carries up to 3% K. An eclogite from the Kakanui volcanic breccia, New Zealand, has less than 30 ppm K in both clinopyroxene and garnet. Primary hornblende contains 1.2% K, but the highest concentration of K in this rock up to 2.8% K, is in veinlike alteration along cracks between the garnet and pyroxene. Hence, even in these nodules it is likely that whole-rock trace element work will be of limited significance.

Potassium content of primary minerals. The features described above demonstrate that high concentrations of K are to be found in alteration products, secondary minerals, veins, and cracks, but no comment has yet been made regarding the contribution from such phases towards the overall K content of these rocks, nor of the role played by phlogopite in this respect. Phlogopite is a frequent constituent of the kimberlite nodules, and there has been some controversy over its mode of origin. While there is every indication that phlogopite may be present in small amounts in upper mantle material, it appears that some of the nodules, notably the Roberts Victor eclogites, contain such large amounts that at least some of the phlogopite is probably of secondary origin. Detailed modal analyses and whole-rock analyses for K are required to resolve the question raised above, but the available data indicates that, irrespective of the mode of origin of phlogopite and of its contribution towards the K content of the rock, much of the K in these rocks is of secondary origin (Berg, 1968; [57] Griffin, and Rama Murthy, 1968; [59] Allsopp, Nicolaysen, and Hahn-Weinheimer, 1969).[60] At this stage it is pertinent to discuss the K content of the primary minerals of these nodules.

For reasons given above the role of phlogopite will not be further considered, and discussion will be limited to the olivine, garnet and pyroxene phases in these rocks. Only three olivines have been analyzed in detail and, as expected, only small amounts of K are present; all three contain less than 20 ppm. Of 7 orthopyroxenes studied, one has 35 ppm K, and the remainder have on the order of 20 ppm or less. One orthopyroxene separate analyzed by Griffin and Murthy (1968) contained 170 ppm K. All the above minerals are in peridotites and pyroxenites.

Particular attention has been paid to the K content of garnets from all types of garnet bearing nodules, a total of 18 being examined. In most of these, three separate measurements were made on different grains. While occasional values slightly above the detection limit were recorded in single measurements, as would be statistically expected, the individual average for all rocks is below the detection limit, i.e., less than 20 ppm K. This contrasts sharply with measurements made on mineral separates from similar nodules. Griffin and Rama Murthy (1968) report K contents ranging from 30 to 490 ppm K in 6 garnets from volcanic nodules, while Allsopp, Nicolaysen, and Hahn-Weinheimer (1969) found from 200 to 1340 ppm K in garnets from 5 kimberlite nodules. Taken together with the alteration features previously described, this indicates that it may not be possible to separate garnet concentrates which are pure, at least with respect to K.

The above observations show that olivines, garnets, and orthopyroxenes are not important in controlling the distribution of K in the upper mantle. There may be some speculation regarding the presence of larger amounts of K in these minerals at high temperatures and pres-

sures but this is considered unlikely, as work reported elsewhere in this report on synthetic garnets in potassium-rich systems reveals that even at 70 kb and 1500°C only trace amounts of K (<100 ppm) are able to enter the garnet structure.

The K content of clinopyroxenes is larger and more variable, and hence important when considering the location of K in upper mantle material. All data obtained in this study are summarized in Fig. 49. Measurements made on volcanic nodules other than those from kimberlite, together with a few samples from the Bushveld Igneous Complex, are given in Fig. 49 (A) and show a maximum K content of 40 ppm. Figure 49 (B) indicates the K content of 6 normal diopsides from nodules in kimberlite, with a maximum value of 120 ppm being found in a phlogopite nodule. Also shown are two subcalcic diopsides, previously analyzed by Boyd (1961)[61] and which have the highest concentrations so far observed for diopsides, namely, 280 and 340 ppm K.

Figure 49 (C) reveals that the distribution of K in omphacite from eclogite nodules in kimberlite is apparently bimodal. Seven samples (4 from the Roberts Victor pipe) carry from less than 20 to 150 ppm K, while 8 others, all from Roberts Victor, contain 800–1350 ppm K. The first group obviously have concentrations similar to that observed for the normal diopsides, but the second group contain concentrations higher than expected from crystal-chemical observations. Similar variations have been observed by other workers. Berg (1968), Griffin and Murthy (1968) and Allsopp, Nicolaysen, and Hahn-Weinheimer (1969) report concentrations ranging from 200 to 2100 ppm K in a variety of omphacites from eclogite nodules in kimberlite. It is not clear at this stage how pure the mineral separates analyzed by these workers are, but the electron-probe measurements demonstrate the existence of omphacites with 1000 ppm or more K, and which are apparently fresh and homogeneous at the 1-μ level. The presence of a clinopyroxene with K concentrations of this order as a major upper mantle phase has important implications when considering the production of basaltic magmas, and raises difficulties for any differentiation scheme such as proposed by O'Hara (1968).[62] However, work described elsewhere in this report on synthetic clinopyroxenes in potassium-rich systems indicates that, at least up to 32 kb and 1450°C, the maximum amount of K likely to enter the clinopyroxene structure is on the order of 150 ppm, in agreement with the concentrations found in natural diopsides and the low K omphacites. It is noteworthy that a diopside inclusion from a diamond analyzed by Boyd (1969), yields a K content of less than 40 ppm.

Papike (1968),[63] using single-crystal X-ray techniques, has shown the presence of submicroscopic intergrowths of amphibole in high-K Roberts Victor omphacite, and this appears to be the most likely explanation for these high K concentrations. Possibly this may reflect the presence of limited solid solution between clinopyroxene and amphibole at

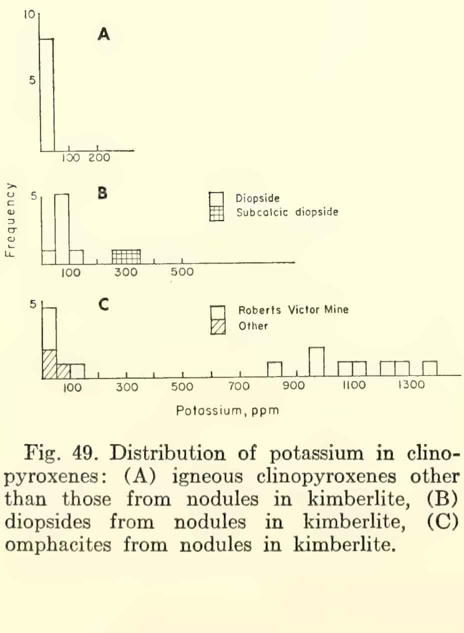

Fig. 49. Distribution of potassium in clinopyroxenes: (A) igneous clinopyroxenes other than those from nodules in kimberlite, (B) diopsides from nodules in kimberlite, (C) omphacites from nodules in kimberlite.

great depth. It is not considered that these amphibole intergrowths are due to the type of alteration process described in the first section of this report, as one of the samples examined (belonging to the low-K group), which was chosen because of the extreme alteration it had undergone, still showed homogeneous K concentrations (45 ppm) in small relict areas of clear omphacite. It is possible of course that the intergrowths reflect an earlier, higher temperature alteration.

Recent research on kimberlite eclogites has suggested the presence of at least two types of eclogite nodule. Both Rickwood, Mathias, and Siebert (1968)[64] and Macgregor and Carter (1969)[65] suggest a classification in terms of Group I and Group II eclogites (the former authors also treat kyanite and corundum eclogites as separate groups), and it appears that both classifications may refer to the same types of eclogites. Seven of the samples analyzed by Rickwood, Mathias, and Siebert have been analyzed in this study, and for these all high-K omphacites belong to Group I and all low-K omphacites to Group II of their classification. Hence this may reflect a different mode or location of formation for the two eclogite groups. It is considered unlikely that the low-K types are differentiates of the high-K eclogites, as this is contrary to the known geochemical behavior of K.

It is clear that the high-K omphacites, coupled with their high K/Rb and low Sr^{87}/Sr^{86} ratios (Allsopp, Nicolaysen, and Hahn-Weinheimer, 1969) are of prime importance in understanding upper mantle differentiation processes. Other compositional differences are also likely to be important. Preliminary electron-probe data show that the low-K omphacites have distinctly higher Ca contents than the high-K omphacites, and it seems likely that other fundamental differences also exist.

Potassium Contents of Synthetic Pyroxenes at High Temperatures and Pressures

A. J. Erlank and I. Kushiro

Electron-probe analyses of presumed upper mantle materials, in particular kimberlite nodules, have revealed that olivines, garnets, and orthopyroxenes in general contain less than 30 ppm potassium and hence do not play an important role in the distribution of potassium in the upper mantle. The K content of clinopyroxenes is considerably larger and is crucial when considering the production of basaltic liquids with K contents varying from 0.05 to 1.5%.

Garnet peridotites, such as those found in kimberlites, are often assumed to be the dominant rock type present in the upper mantle. Chrome diopsides from these nodules generally contain on the order of 100 ppm K or less. The highest concentrations measured to date by electron-probe analysis have been observed in two subcalcic diopsides (Boyd, *Year Book 66,* pp. 331–334); concentrations of 280 ppm and 340 ppm K in these two pyroxenes have been measured in this study. Even allowing for 15% modal abundance for diopsides in garnet peridotite, the K content of the resultant assemblage does not satisfactorily account for the high K contents of alkali basalts, provided at least 1% direct partial melting is involved in the production of the basalt.

Potassium contents of eclogitic omphacites from African kimberlites are more difficult to interpret. Electron-probe analyses given elsewhere in this report demonstrate that the K distribution of omphacites is apparently bimodal, with some containing from 20 to 150 ppm K, while others carry from 800 to 1400 ppm K. The comments expressed above with respect to the diopsides obviously apply to the low-K omphacites. However, the K content of the second group is larger than expected and difficult to explain on crystal-chemical grounds. It is

clear that the presence of clinopyroxene with K contents of this order as an upper mantle phase would be important for controlling the distribution of K in basaltic liquids. Hence, it appeared desirable to seek confirmation of this feature.

We have attempted to determine experimentally the amount of K which could enter the clinopyroxene lattice under upper mantle conditions by reacting together, at high temperatures and pressures, various clinopyroxenes and potassium-rich phases and measuring the potassium content of the resultant pyroxenes by electron-probe analysis.

The experiments were made in the pressure range 15–32 kb with a piston-cylinder apparatus similar to that designed by Boyd and England (1960).[66] Sealed Pt tubes were used for the hydrous runs. The starting materials are mechanical mixtures of the following materials: synthetic pure diopside made by Hytonen and Schairer; a mixture of phlogopite composition consisting of forsterite, quench forsterite, and glass; a mixture crystallized at 1 atm from a glass of composition anorthite 50 forsterite 50 (by mole); a natural omphacite from Kaminaljuyu, Guatemala (originally described by Foshag, 1957)[67] which has a composition close to diopside 45 jadeite 55 (by mole) (Clarke and Papike, 1968);[68] and a natural potassic richterite from Wolgidee, Australia, which is similar in composition to that analyzed by Wade and Prider (1940)[69] and is described in this report, pp. 442–443.

In all of the hydrous runs, diopside and omphacite were recrystallized to euhedral∼subhedral crystals even at subsolidus temperatures. During the electron-probe analysis for K the other two spectrometers were set for Ca and Mg, and comparison of the starting materials and reactants indicated the recrystallization of the clinopyroxenes. Additional measurements for Na also revealed the nature of the pyroxenes formed. Phlogopite occurs as hexagonal plates forming thick books; however, when glass is present, it often appears as feathery crystals, which are believed to be quench crystals. Richterite which had been ground finely was also recrystallized to relatively large, euhedral∼subhedral crystals. Because of recrystallization in the presence of excess vapor, equilibrium is believed to have been attained in the hydrous runs. In the anhydrous run made for the 1:1 mixture of diopside and phlogopite composition, the temperature was raised to above the solidus to secure equilibrium.

A great deal of difficulty has been experienced in making the electron-probe measurements. Partly this is due to the small size of the reaction products, necessitating the use of a 1–2-μm electron beam and low sample current (0.025 μa) with resultant low intensity. The main problem has, however, been caused by the presence of minute inclusions and intergrowths of these crystals with K-rich phases (phlogopite and glass), frequently resulting in anomalously high K contents for apparently clear clinopyroxene grains. Consequently, several runs have been discarded and we report here only those measurements for which a fair amount of consistency has been established. Particular care has been taken in making background measurements, often by using the pure starting materials which were always mounted together with the reaction products. It is to be noted that the results have only been corrected for background and drift, but it is believed that they are accurate to within 10–20% of their true values; this level of accuracy is adequate for present purposes. A detailed account of the technique used will be given on p. 443 of this report.

The assembled data are listed in Table 12. It is immediately apparent that regardless of variation in mineral assemblage, temperature, pressure, and water content, the amount of K which has entered the clinopyroxene reaction products is small, less than 150 ppm. Even where clinopyroxene has crystallized di-

TABLE 12. Potassium Contents of Synthetic Clinopyroxenes and Garnets

Reactants	P, kb	T, °C	Duration, hours	H_2O, %	Products	Ppm K in clinopyroxene
Di + Anhy Phl (1:1)	15	1100	4	11.4	Di, Fo, Phl, Gl, gl	140
	30.5	1150	3⅔	13.1	Di, Fo, Phl, Gl, gl	90
	32	1000	4	4.6	Di, Phl, gl	70
	21	1450	2¼	...	Di, Fo, Gl	140
Omph + Anhy Phl (1:1)	25	1000	5⅙	5.0	Omph, Phl	110
(2:1)	25	1000	6	40.0	Cpx, Phl, Fo, gl	50
(1:1)	26.5	1050	4	7.4	Cpx, Phl, Gl	<50
	30	1100	3	22.2	Cpx, Fo, Phl, gl	50
Rich + An_1Fo_1 (2:1)	20	1000	3	4.7	Rich, Phl, Cpx	120
Rich + Di (1:1)	24	1000	2	10.4	Rich, Cpx	<50
						ppm K in garnet
Anhy Phl + An_1Fo_1 (1:4)	30	1100	3	12.6	Gt, Cpx, Phl	<50
Phl *	70	1500	⅔	...	Gt, Phl, q-Phl, X	<100

* Run prepared by Kushiro, Syono, Akimoto (1967).[70]

Abbreviations: Di = diopside; Anhy Phl = anhydrous phlogopite composition; Phl = phlogopite; Fo = forsterite; Gl = glass; gl = glass balls considered to be quenched vapor; Omph = omphacite; Cpx = clinopyroxene solid solution; Rich = potassic richterite; Gt = garnet; An_1Fo_1 + crystalline mixture of anorthite and forsterite (1:1 by mole) ≡ pyrope-grossular (2:1 by mole); q-Phl = quench phlogopite; X = unknown phase.

rectly from liquid under anhydrous conditions and in the absence of phlogopite, nearly all the K has remained in the liquid, as measured by the K content of ~13% in the glass. At this stage it is not clear to what extent variations in temperature, pressure, and sodium content affect the substitution of potassium. These results seem in accord with the natural diopsides and low-K omphacites previously discussed, and we have found no experimental evidence to explain the presence of 1000–1500 ppm K in omphacite. The most likely explanation appears to be that these high-K contents are due to the presence of submicroscopic intergrowths of amphibole in the omphacite structure, as suggested by Papike (1968)[63] on the basis of X-ray studies. This possibility has important implications regarding the genesis of eclogites and basaltic lavas, and requires further confirmation. In our runs with amphibole and pyroxene, no reaction has occurred between these minerals.

Also given in Table 12 are measurements made on garnets produced in two runs. Potassium was not detected in either one. One of the runs had previously been analyzed with an electron probe, and up to 5.8% K reported in the garnets (Kushiro, Syono, and Akimoto, 1967).[70] The original electron-probe section was available, and further study showed that the earlier analysis was in error. The discrepancy is most likely due to the beam's overlapping high-K mica in the original analysis. During the analysis of this section, one of the breakdown products of phlogopite was found to have a very high potassium content (phase X in Table 12). Semiquantitative analysis indicates that this phase has of the order of 29% K_2O and 32% MgO, but with an anomalously low SiO_2 content of 1% or less. Unfortunately, the fine-grained nature of this phase and poor surface of the section prevented proper analysis, and we are not able at this stage to identify this phase. It seems clear that clinopyroxenes and garnets will not accept sufficient potassium in their structures, even at high temperature and pressures, to provide that required to form basalt by simple partial melting. In this case, the rocks which are parental

to basalt must contain potassium-rich phases such as phlogopite and/or K-rich amphibole.

The Occurrence of Potassic Richterite in a Mica Nodule from the Wesselton Kimberlite, South Africa

A. J. Erlank and L. W. Finger

The presence of amphibole as a constituent of the upper mantle has been suggested by several workers, and cogent geochemical and geophysical arguments have been presented in support of this contention (Oxburgh, 1964; [71] Ringwood, 1964; [72] Hart and Aldrich, 1967).[73] Amphibole, usually in the form of hornblende or pargasite, has frequently been observed in rocks of possible upper mantle origin, such as the amphibole peridotites from St. Paul's rocks on the mid-Atlantic Ridge, and as xenocrysts and in xenoliths from basic volcanic rocks and tuffs (Mason, 1968),[74] but to our knowledge has not been recorded as a definite primary constituent of the mafic and ultramafic nodules found in Southern African kimberlite pipes.

During the course of electron-probe analysis of a mica pyroxenite nodule from the Wesselton kimberlite pipe, South Africa, a mineral with an unusual potassium content was encountered and subsequently identified as the rare amphibole, potassic richterite (magnophorite). These nodules, also referred to as phlogopite nodules, are distinctive in that they consist almost entirely of phlogopite (>90%) with minor amounts of diopside. Garnet, olivine, and ortho-

TABLE 13. Electron Microprobe Analyses of Kimberlitic Potassic Richterites and Diopside

	Richterite 1	Richterite 2	Richterite 3	Diopside
SiO_2	54.3	54.4	54.1	54.2
TiO_2	0.59	0.60	0.59	0.10
Al_2O_3	1.22	1.25	1.24	0.71
FeO *	4.36	4.34	4.22	5.07
MnO	0.07	0.07	0.07	0.17
MgO	20.9	21.4	21.2	16.0
CaO	7.06	7.14	7.15	20.7
Na_2O	3.19	3.20	3.34	1.50
K_2O	4.70	4.77	4.69	0.01
Cr_2O_3	0.07	0.06	0.04	0.42
Total	96.5	97.2	96.6	98.8

Numbers of ions on the basis of 23 oxygens	1		2		3		Number of ions on the basis of 6 oxygens		
Si	7.80	8.00	7.75		7.76		Si	2.010	
Al	0.20		0.21	8.00	0.21	8.00	Ti	0.003	
Ti	...		0.04		0.03		Al	0.031	
Al	0.01		...		...		Ca	0.820	
Ti	0.06		0.02		0.03		Cr	0.012	
Mg	4.46	5.00	4.55	5.00	4.52	5.00	Fe	0.157	2.018
Cr	0.01		0.01		0.01		Mn	0.005	
Fe	0.46		0.42		0.44		Ca	0.820	
Fe	0.05		0.10		0.07		Mg	0.881	
Mn	0.01		0.01		0.01		Na	0.108	
...	...	2.00	...	2.00	...	2.00	K	0.001	
Ca	1.09		1.09		1.10				
Na	0.84		0.80		0.82				
Na	0.05	0.91	0.08	0.95	0.11	0.97			
K	0.86		0.87		0.86				

* Total Fe expressed as FeO.

pyroxene are absent. A petrographic description and chemical analysis of the nodule in question, WESS 156, are given by Williams (1932),[58] pp. 347, 350.

The potassic richterite found in this nodule is present in the form of small subhedral grains, usually about 100 μm in length, contained within the diopside, and appears to be of primary origin. Optical characteristics are consistent with those available for other richterites. Three of these grains together with the associated diopside, have been analyzed by electron-probe analysis, while a fourth identified by probe analysis in a grain mount of separated diopside grains has been partially isolated and analyzed by single-crystal X-ray diffraction.

Relevant chemical data are presented in Table 13. Multiple measurements show each grain to be homogeneous with very little, if any, variation between grains. Compared with the type analysis for potassic richterite (Wade and Prider, 1940),[69] the Wesselton richterite has slightly differing FeO and K_2O contents, but the most striking difference is the lower TiO_2 content of the Wesselton potassic richterite (0.6% TiO_2) compared with the value of 3.5% TiO_2 given by Wade and Prider. The significance of this feature and its possible dependence on pressure is discussed on p. 000 of this report. The average of the three analyses expressed in the amphibole formula, is $(K_{.86}Na_{.08})(Na_{.82}Ca_{1.09}\ Mn_{.01}\ Fe_{.07})(Fe_{.45}Mg_{4.51}Ti_{.04}Cr_{.01})(Si_{7.77}Al_{.21}\ Ti_{.02})\ O_{22}\ (OH)_2$.

The composition of the enclosing diopside is given for comparison purposes. It has a lower chrome content than diopsides that occur in the peridotite nodules, and is similar to a diopside inclusion from a diamond studied by Boyd (*Year Book 67,* pp. 133–135).

The Wesselton potassic richterite grain examined by single crystal techniques was only partially separated from the enclosing diopside because of difficulties in handling small grains. The interfering diffraction pattern handicapped the orientation of the grain but the following cell data were obtained from precession photographs: *a,* 10.00 Å; *b,* 18.00 Å; *c,* 5.26Å; *β,* 104.8°; *V,* 917 Å^3. The cell data of the diopside at 23°C were measured from back-reflection Weissenburg photographs and yielded the following results: *a,* 9.734 ± 0.002 Å; *b,* 8.9135 ± 0.0005 Å; *c,* 5.261 ± 0.006 Å; *β,* 106.06 ± 0.03°; *V,* 438.6 ± 0.6 Å^3.

It is difficult at this stage to assess the importance of the occurrence of potassic richterite in the mica nodule. Certainly it appears to be of primary origin, and work described by Kushiro and Erlank in "Stability of Potassic Richterite," p. 231 of this report, shows that in the absence of phases other than diopside it is stable to higher temperatures and pressures than any other amphibole so far examined. Hence, although it occurs only as a trace constituent in the nodule examined, it may indicate the type of amphibole likely to occur in the upper mantle. However, preliminary work described elsewhere in this report indicates that it may not be stable in the presence of nonpotassic aluminous phases such as garnet. Nevertheless, if one percent of potassic richterite of the type analyzed occurs in upper mantle material, the resulting K content of 400 ppm is sufficient, when such material is subjected to partial melting and fractionation along the lines suggested by O'Hara (1968), to account for the K content of most basaltic lavas. This would also apply to other elements related to K, specifically Rb and Ba, and hence it would be of some interest to determine the trace element content of potassic richterites.

Stability of Potassic Richterite

I. Kushiro and A. J. Erlank

This report may be found in the annual report of the Geophysical Laboratory (*Year Book 68,* pp. 231–233).

Strontium Isotope Abundances in Layered Ultramafic Rocks

A. J. Erlank

The continental crust has been intruded by a number of ultramafic layered complexes during its geologic history, and these are generally believed to originate in the upper mantle. Hence they can provide information on the isotopic characteristics of the liquids from which they crystallized, and, by implication, on the source areas of these bodies at the time of intrusion. The South African continent has been intruded by several pre-Cambrian layered complexes, and preliminary Sr isotopic work on two of these is here described.

The well-known Bushveld Igneous Complex has been adequately described in the literature and hardly requires further description. The related but smaller Losberg Complex, also located in Transvaal, South Africa, has recently been comprehensively described by Abbott and Ferguson (1965)[75] and Danchin and Ferguson (1969).[76] Of special interest to this study are the different K/Rb ratios reported for equivalent rock types from these two complexes (Erlank, Danchin, and Fullard, 1968;[77] Danchin, 1968[78]). Sr isotope analyses have been made on some of the mafic and ultramafic rock types analyzed by these authors and the results are shown in the Rb-Sr isochron plot of Fig. 50. (Analysis of the standard Eimer and Amend $SrCO_3$ during this period yielded a value of 0.7085 ± 0.0003.)

For convenience, the Losberg data are considered first. Least-squares analysis of the data indicates an age of 1918 ± 350 m.y. and an initial Sr^{87}/Sr^{86} ratio of 0.7061 ± 0.0027 (95% confidence limits). The uncertainties in these values are

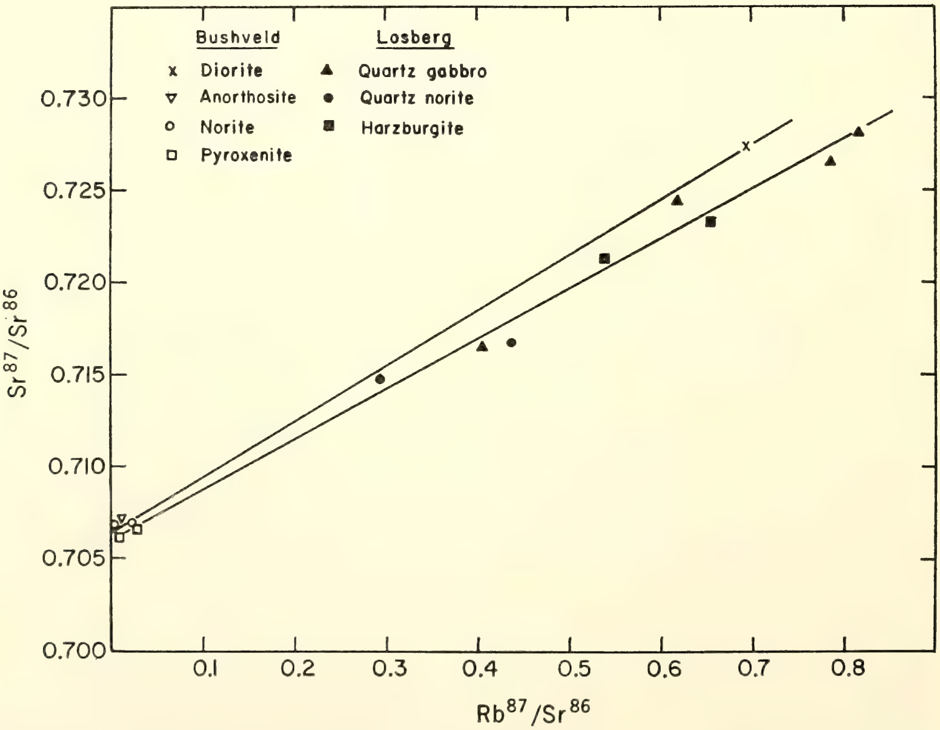

Fig. 50. Rb-Sr relationships in rocks from the Bushveld and Losberg igneous complexes.

certainly partly because of the narrow spread of the Rb/Sr ratios, consistent with the overall range of magmatic differentiation observed, and partly because of the fact that the Rb and Sr concentrations have only been determined by X-ray fluorescence. However, it is believed that the spread shown on the isochron is also influenced by geological processes. Electron-probe analysis of a few of the rocks indicates that some redistribution of alkalies has occurred. For example, the Harzburgites in the Losberg are characterized by the presence of traces of biotite ($\sim$1–2%), a feature not characteristic of the Bushveld rocks. The electron-probe studies show clearly that the mica has been "leached" by subsequent serpentinization processes and the question naturally arises as to the extent of the redistribution. More detailed work is required to resolve this question; nevertheless it is clear that the Losberg rocks define an isochron which is not significantly different in age from that previously established for the acid rocks from the Bushveld Igneous Complex, i.e., 1970 ± 70 m.y. (Nicolaysen, de Villiers, Burger, and Strelow, 1958 [79]), but which is younger than that found for rocks from the related Great Dyke in Rhodesia, i.e., 2530 ± 30 m.y. (Allsopp, 1965).[80]

The Bushveld mafic and ultramafic rocks have an insufficient spread in Rb/Sr ratio to establish a reliable age and, in fact, have such low ratios that the measured Sr^{87}/Sr^{86} ratios effectively yield the initial isotope ratios. The single diorite analysis is difficult to interpret, as the genesis of these rocks is not clearly established. If it is considered that this rock is an iron-rich differentiate of the basic suite, and if the initial ratio of the basic rocks is taken as $Sr^{87}/Sr^{86} = 0.7065$, the age of this rock is 2125 m.y. This is not significantly different in age from the Losberg rocks, but the possibility exists that the mafic rocks from the Bushveld are slightly older than those from the Losberg. However, the simplest interpretation of the available data suggests that both complexes were emplaced during the same period of magmatic activity and may in fact be cogenetic in origin, the Losberg rocks being more differentiated than those from the Bushveld.

The initial Sr isotope ratios of the two complexes are not in agreement with those inferred from other studies for the upper mantle at that time. The initial Sr^{87}/Sr^{86} ratios for these complexes are clearly within the range 0.7060–0.7065 and are significantly higher than the ratio of 0.7025 for rocks of the Great Dyke (Allsopp, 1965) and the ratios given elsewhere in this report for 2700-m.y. metavolcanics from the Canadian Shield.

If the Bushveld and Losberg rocks reflect the initial Sr isotope compositions of their source areas, this could imply an origin either in the upper mantle or lower crust. The latter possibility is generally considered unlikely on petrological grounds, but is quite feasible from the point of view of Rb-Sr abundance relationships. Derivation from the upper mantle necessitates that the latter be inhomogeneous in nature, with regions of high radiogenic Sr^{87} content. The low Rb/Sr and high K/Rb ratios of the Bushveld rocks would further restrict the composition of the source areas, if these ratios are in any way reflective of these regions.

It is perhaps more likely that the rocks studied do not reflect the Sr isotope compositions of their source areas, i.e., the upper mantle, and have been modified or contaminated during or after emplacement. If so, such processes must account for the similarity of the Sr^{87}/Sr^{86} ratios in both complexes, and yet also be consistent with the different Rb/Sr and K/Rb ratios observed. Bulk assimilation of crustal material could explain these relationships in the Losberg rocks, but the high K/Rb and low Rb/Sr ratios of the Bushveld rocks are not easily accounted for by this process unless extensive differentiation occurred subse-

quent to contamination. Previous work (Erlank, Danchin, and Fullard, 1968) has already suggested that the Bushveld mafic rocks are depleted in Rb because of mineralogical effects.

It is also possible that selective diffusion of radiogenic Sr^{87} into the magmas of these rocks has occurred, without the K/Rb and Rb/Sr ratios being significantly changed. It is difficult to see how such a process would affect both complexes equally, unless a common magma chamber is assumed. The same type of comment would apply to a subsequent Sr homogenization process.

The data presented in this study are in agreement with data reported for other ultramafic layered complexes and continental tholeiites in that high initial Sr^{87}/Sr^{86} ratios are observed, and it is clear that such ratios are more common than previously supposed.

COSMIC-RAY RESEARCH

S. E. Forbush

The variation in the cosmic-ray diurnal anisotropy with a period of two sunspot cycles. Two preceding annual reports described the statistical analyses which led to the discovery of a well-determined variation with a period of two solar cycles in the cosmic-ray diurnal anisotropy recorded by Carnegie Institution of Washington cosmic-ray ionization chambers. Figure 3 in *Year Book 66* (p. 12) showed that the yearly means of the diurnal anisotropy in the asymptotic direction 128° E of the sun, after removing the effects associated with magnetic activity, were well fitted by a 20-year wave. This 20-year wave, twice the sunspot period of 10 years for the interval 1937–1965, passed through a zero near the end of 1958 close to the time when, as shown by Babcock from measurements at the Mt. Wilson Observatory, the sun's poloidal magnetic field reversed.

It is well known that the period of the sunspot cycle varies from about 10 to 13 years with an average near 11 years. Consequently, the interval between successive reversals of the sun's poloidal magnetic field is expected to vary from about 10 to 13 years (period 20 to 26 years). If when such variation in reversals occur they correspond with those in the reversal of sign in the asymptotic component 128° E of the sun in the cosmic-ray diurnal anisotropy this would provide additional strong evidence that reversal of the sun's general magnetic field is responsible.

In addition to results shown for the years 1937–1965 in Fig. 1, *Year Book 66,* p. 10, Fig. 51 of this report includes results, shown by triangles, for the four years 1936, 1966, 1967 and 1968. The 20-year wave in Fig. 51 (this report) passes through a zero near the end of 1968. The yearly mean diurnal anisotropy component for 1968 lies significantly above the dashed curve (with a period of 20 years). Analysis of solar magnetograms made at Mt. Wilson Observatory gives no indication of any tendency for reversal in the sun's poloidal field as late as March 1969 which would accord with the cosmic-ray result for 1968 in Fig. 51. Valuable additional evidence concerning a causal relation between the two phenomena should be available in the next few years.

In collaboration with Pomerantz and Duggal of the Bartol Research Foundation, a study based on Simpson's neutron-monitor data from Huancayo was made of the magnitude of the variation, with a period of 20 years, in the asymptotic component of the diurnal anisotropy 128° E of the sun and of that in the component 90° E of the sun (20-year variation removed). Both of these variations were found in agreement with those from the ionization chambers during the interval 1953 to 1966 for which the neutron-monitor data were available.

Cosmic-ray ionization chamber for Christchurch, New Zealand. The Carnegie Institution of Washington cosmic-ray ionization chamber No. C-4 was

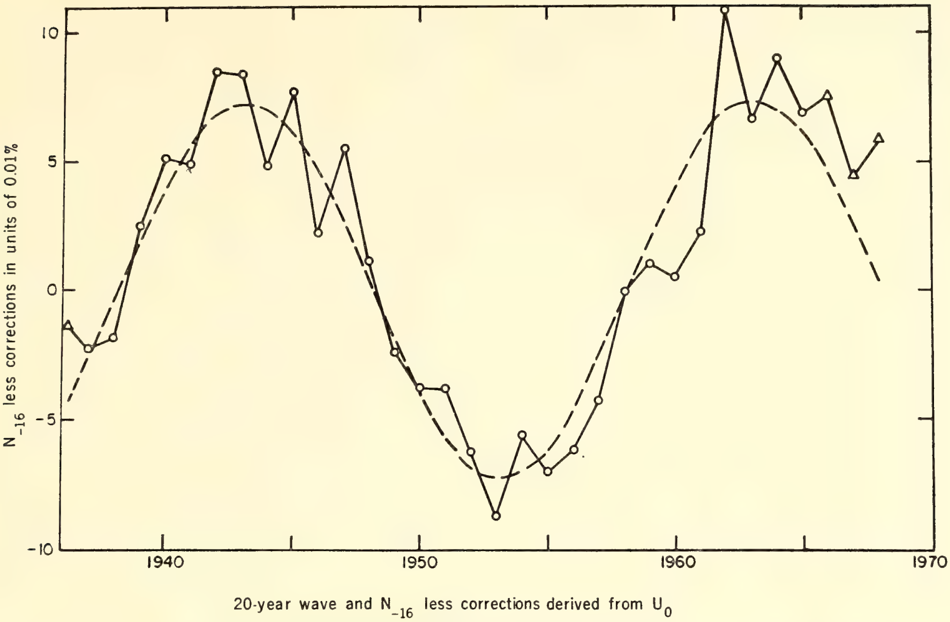

Fig. 51. Twenty-year wave in the amplitude of the component of the diurnal anisotropy in the asymptotic direction 128° east of the sun corrected for variations due to magnetic activity U_0.

installed in Christchurch in March 1969. The Geophysical Observatory in Christchurch constructed housing within a large building used for storing equipment and supplies for research projects in Antarctica. The Geophysical Observatory has kindly arranged for one of its technicians to carry out operation of the meter and its routine maintenance.

Most of the measurements from the ionization chamber records will be made promptly by the Geophysical Observatory at Christchurch in order to provide data to correct radiation measurements for the variable cosmic-ray background. These radiation measurements by the National Radiation Laboratory are made by special detectors mounted within the Carnegie Institution of Washington ionization chamber which was operated in Christchurch from 1937 to 1961.

Publication of cosmic-ray results. The manuscript and tables for Carnegie Institution of Washington Publication No. 175, vol. XXII, have been turned over to the Institution's editorial office which anticipates that this volume will be available late in 1969. This publication will contain results for January 1960 through December 1968 from Huancayo and Fredericksburg, for the period 1959 to 1961 from Christchurch, and for 1951 to 1953 from Godhavn.

Observations and reduction of data. Cosmic-ray ionization chambers were operated throughout the report year at Huancayo, Peru, and at Fredericksburg, Virginia. Scalings and reduction of records have been maintained on a current basis for both stations. The reductions have been greatly facilitated by the use of the IBM 1130 computer. Registration from the cosmic-ray meter at Christchurch commenced near the end of March 1969.

Cooperation in operation of cosmic-ray meters. Grateful appreciation is expressed to the U. S. Coast and Geodetic Survey and the staff of its magnetic observatory at Fredericksburg for efficient operation of the meters during the past report year, and to the Government of

Peru and to the Director and staff of the Instituto Geofísico del Peru for making cosmic-ray records from Huancayo available.

Grateful appreciation is expressed to the Director and staff of the Geophysical Observatory at Christchurch, New Zealand, for providing housing for the ionization chamber and for greatly assisting in the installation of the equipment as well as its reception through customs. We are also grateful to the National Science Foundation for having shipped the equipment and for providing air transportation for Dr. Forbush from Washington to New Zealand on an Air Force Deep Freeze plane.

SEISMOLOGY

A Sensitive Borehole Strain-rate Meter

I. S. Sacks and D. W. Evertson

The measurement of strain changes in the earth is fundamentally important to the understanding of earthquakes. The amplitude of the change in the strain field in the vicinity of an earthquake decreases as the square of the distance from the hypocenter, and therefore instruments of high sensitivity are required to detect and measure these changes for smaller earthquakes, and for those at longer distances.

A borehole strain-meter has been developed jointly by the Department of

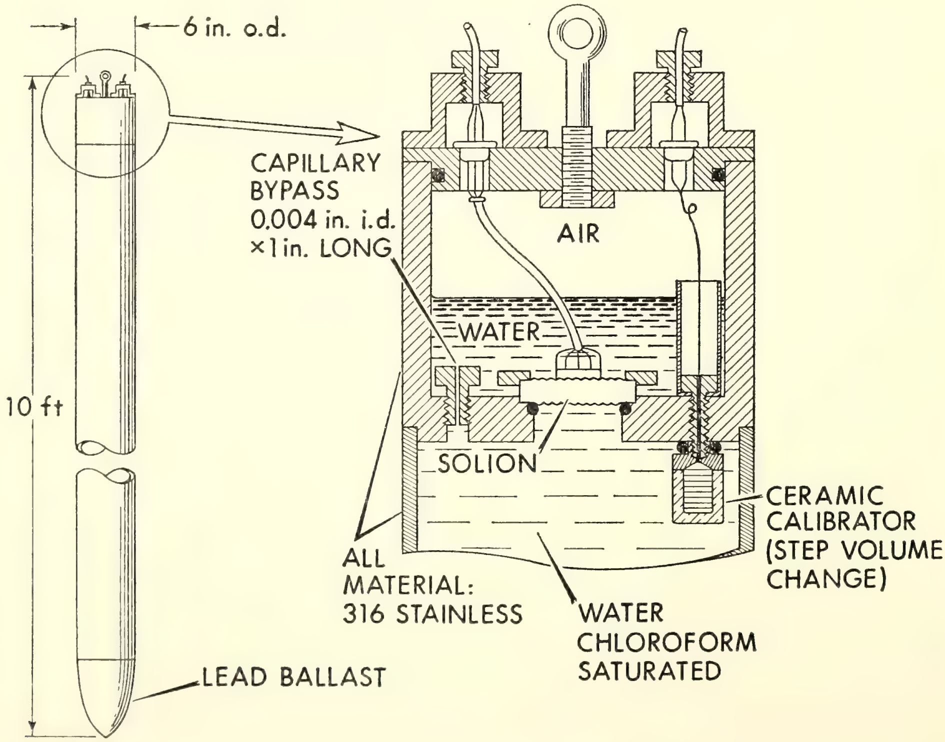

Fig. 52. Prototype of the borehole strain-rate meter. The first instrument was installed in a borehole 150 feet deep on the DTM campus. Solid rock was intersected at a depth of 70 feet. The water in the instrument is saturated with chloroform to inhibit microbial growth.

Terrestrial Magnetism and the Applied Research Laboratory of the University of Texas at Austin. In essence, it consists of a water-filled resilient tube in intimate contact with the walls of a borehole. As the strain in the surrounding rock changes, the tube is deformed, forcing liquid through a flow sensor into an air space. A drawing of the instrument is shown in Fig. 52. All metallic parts are fabricated from 316 stainless steel, because of its corrosion resistance. It is, of course, imperative that the tube faithfully follow the minute distortions (down to 10^{-7} microns) of the hole. This is ensured by prestressing the ⅛-inch-thick steel tube with an expanding cement which bonds the strain-meter to the rock. After curing for about one month, the cement expansion is such as to cause a prestress on the tube of about 7 psi.

The flow sensor used is a linear solion (Larkam, 1965)[81] developed by ARL. This is a device in which the current flowing between an anode and a cathode is modulated by the pumping of the electrolyte (in this case due to the deformation of the steel tube) through a porous cathode. Two such cathodes are arranged in a push-pull system (Fig. 53). Flow in the direction of the arrow would cause the current in cathode 1 to increase and the current in cathode 2 to decrease.

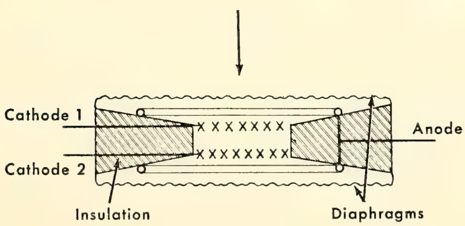

Fig. 53. Schematic drawing of the solion flow velocity sensor. The cathodes are made from very fine platinum basket weave. The electrolyte is potassium iodide and free iodine, and the solion body is made of Kel-F. The two half cells have a bias voltage of about 0.5 volts applied; the current in each cathode is a measure of the flow velocity of the electrolyte through the cathodes.

Solion noise measurements (by D. W. Evertson), gave a noise current of 10^{-8} amperes, dominantly in the period range 20–100 seconds. The noise of the two cathodes was coherent, however, suggesting fluid pumping, and the actual noise is probably substantially less than 10^{-8} amperes. Typical flow sensitivity of this type of solion is 40 amps/cc/sec; therefore, the threshold sensitivity is 0.4×10^{-10} cc/sec. The velocity sensitivity is flat down to 20-sec period; then the sensitivity gradually decreases towards shorter periods. The volume of water in the steel tube is 30 liters, giving a volume strain-rate threshold sensitivity of 1.2×10^{-14}/sec. The frequency response of the strain-meter as installed in the DTM campus is shown in Fig. 54. The departure from a velocity law at periods longer than one day is due to the capillary bypass (Fig. 52). The purpose of this bypass is to avoid permanent deformation of the solion diaphragms caused by tube deformation due to concrete prestress, temperature changes during installation, and any long-term volume changes of the immediate environment of the strain-meter.

Results after the concrete had cured (less than 3 months) showed that the site noise was well above the internal noise of the instrument. In the period range covered by this instrument, the earth noise is dominated by microseisms in the 6–20 sec range with strain rarely less than 10^{-10} and occasionally an order of magnitude higher. The earth tide (due to the attraction of the moon) is about 4×10^{-8} at this latitude. The noise in the period range between the microseisms ($\sim$8 seconds) and about one hour has been found to be locally generated by small atmospheric pressure fluctuations which typically seem to be about 30 microbars. If one considers the effect of very long wavelength disturbances, where wavelength $\lambda/4$ is significantly greater than the depth of the strain-meter, there is no attenuation, and the strain ϵ, is given by $\epsilon = P/E$ where P is the pressure and E

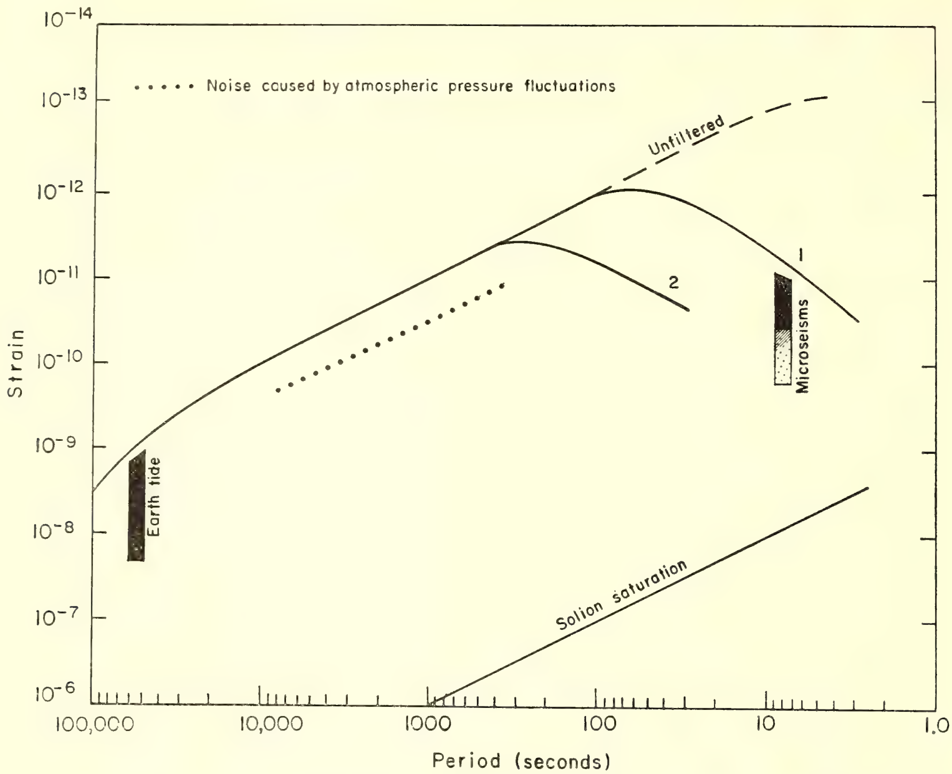

Fig. 54. Frequency response of the prototype strain-meter. The response below 100,000-second period falls off at 12 db/octave due to the capillary bypass (Fig. 52). The response at short periods is modified by electronic double integration to reduce the sensitivity in the microseism range, 6–20 second period.

is Young's modulus for the rock. Assuming pressure fluctuations of 30 microbars and E for rock of 10^7 psi, the resulting strain (vertical component) would be 4.5×10^{-11}. Because this was the level of strain noise actually found (see Fig. 55), a microbarograph with matched frequency response was installed. Figure 56 shows the correlation between the microbarograph and the strain-meter. The low pass filter which has been applied to both instruments cuts the sensitivity at a rate of 6 db/octave at periods shorter than 200 seconds. The correlation is extremely high at all times (except of course during large earthquakes). It would appear from this very high correlation that the earth noise in the period range one hour to three minutes must be at least one order of magnitude less than the atmosphere-induced noise, i.e., less than 10^{-12}. The wavelengths of the atmospheric disturbances are relatively short, since this noise seems to be associated mainly with weather fronts which travel at velocities as low as 15/km/hour. Therefore, the wavelength of a one-minute period disturbance is only 250 meters. It is found that the close waveform correlation that exists at periods longer than about 3 minutes deteriorates towards the shorter periods, i.e., down to 30 sec. Figures 55 and 57 show typical records. Figure 55 is the recording of a New Guinea earthquake.

Setting up a network of similar instru-

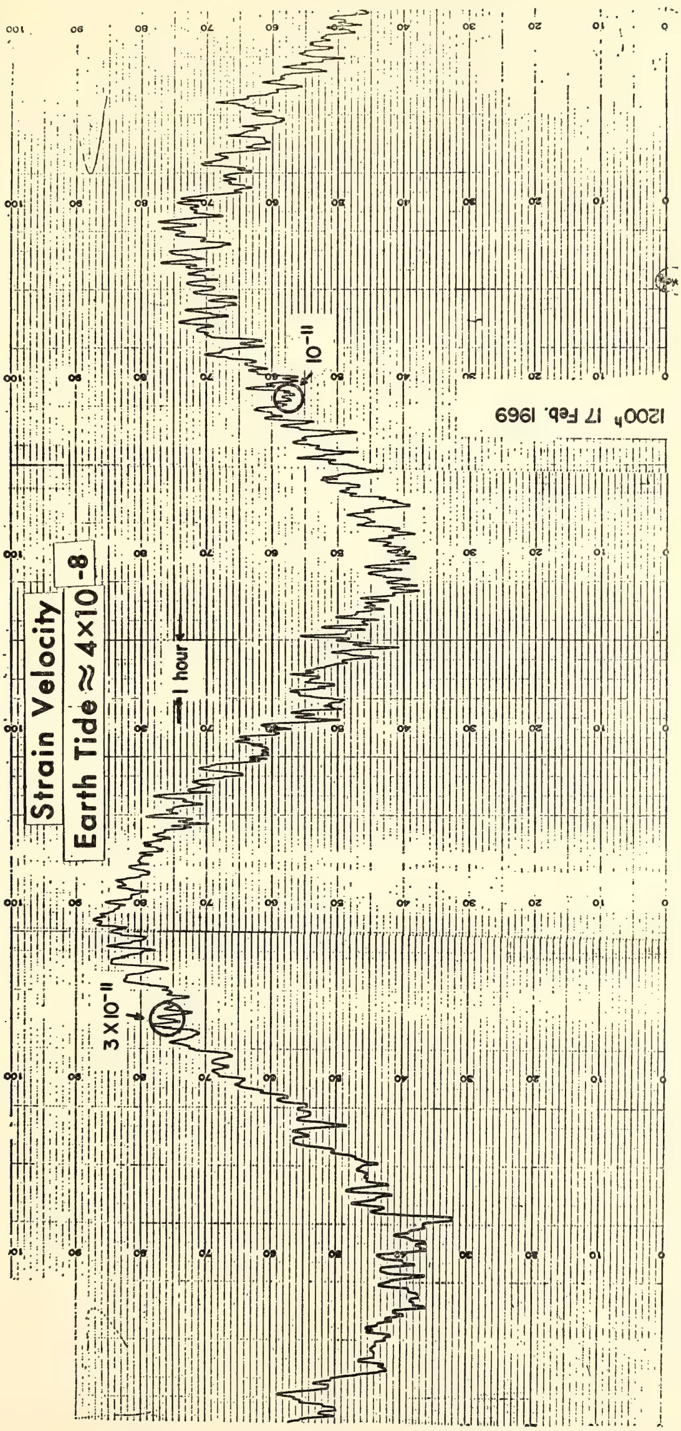

Fig. 55. Strain velocity recording of earth tide and superimposed noise caused by atmospheric pressure fluctuations. The strain sensitivity as a function of period is given in curve 2, Fig. 54.

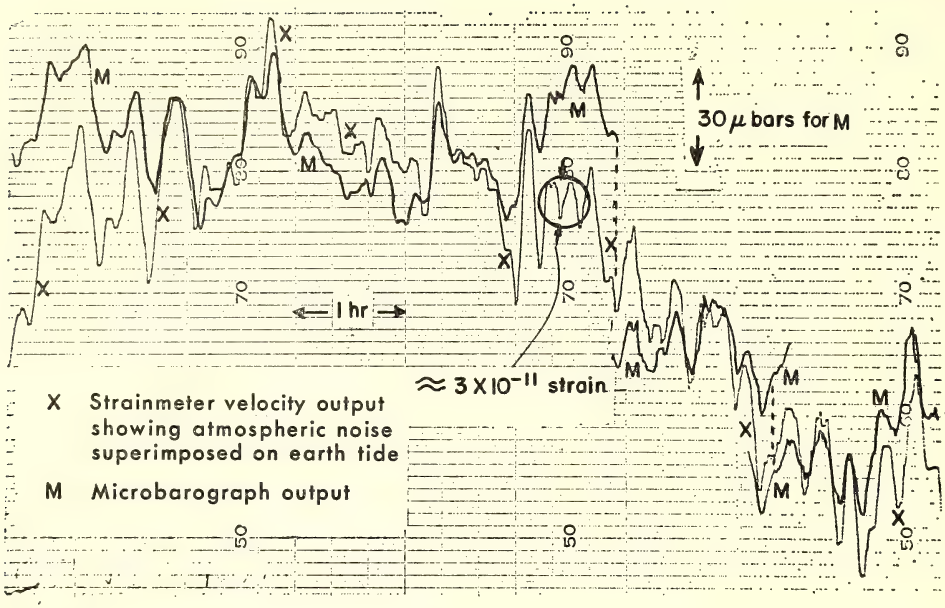

Fig. 56. Comparison of microbarograph and strain-meter records. The microbarograph trace has been broken into three sections and displaced vertically to compensate for the large low-frequency excursion on the strain-meter record due to the earth tide. The close correlation of the two traces at periods of less than 1 hour suggests that most of the noise on the strain-meter is caused by atmospheric pressure fluctuations.

ments of high sensitivity and relatively low cost might be a practical way to learn the behavior of the stresses and strains in earthquake regions of the earth.

Time Anomalies and Structure Beneath the Andes

I. S. Sacks, G. Saa, and P. Aparicio

The Carnegie Analysis Center was set up in Lima, Peru, in 1965. One of the subsidiary goals of the Center was the collection of data to see what, if any, correlation existed between surface expression and what lies beneath—for example, the Andes Mountains, and anomalous velocities in the upper mantle. Otsuka made a few preliminary determinations using near-vertically incident *PKP* waves (*Year Book 65*); and Prof. Volponi in San Juan, Argentina, has been engaged in a similar project in west central Argentina for a number of years. The study reported here covered the region between 12° S and 24° S. The earthquake waves used in this investigation are shown in Fig. 58.

P waves. The compressional waves in the distance range 30°–90° travel wholly in the mantle and have angles of incidence ranging from 40° to 20°. The earthquake regions within this distance range were divided into twelve 30° sectors as shown in Fig. 59. Each sector was treated independently. The group of stations available (see Plate 4) were treated as a wide-spaced array. A discussion of the statistical approach follows.

Arrival time at reference stations:

$$t_e + t_t\ (\Delta) + \Delta t_r = t \qquad (1)$$

where t_e is the origin time, or location, error, expressed as time; $t_t(\Delta)$ is the theoretical travel time (Jeffreys-Bullen) if there were no location errors or station

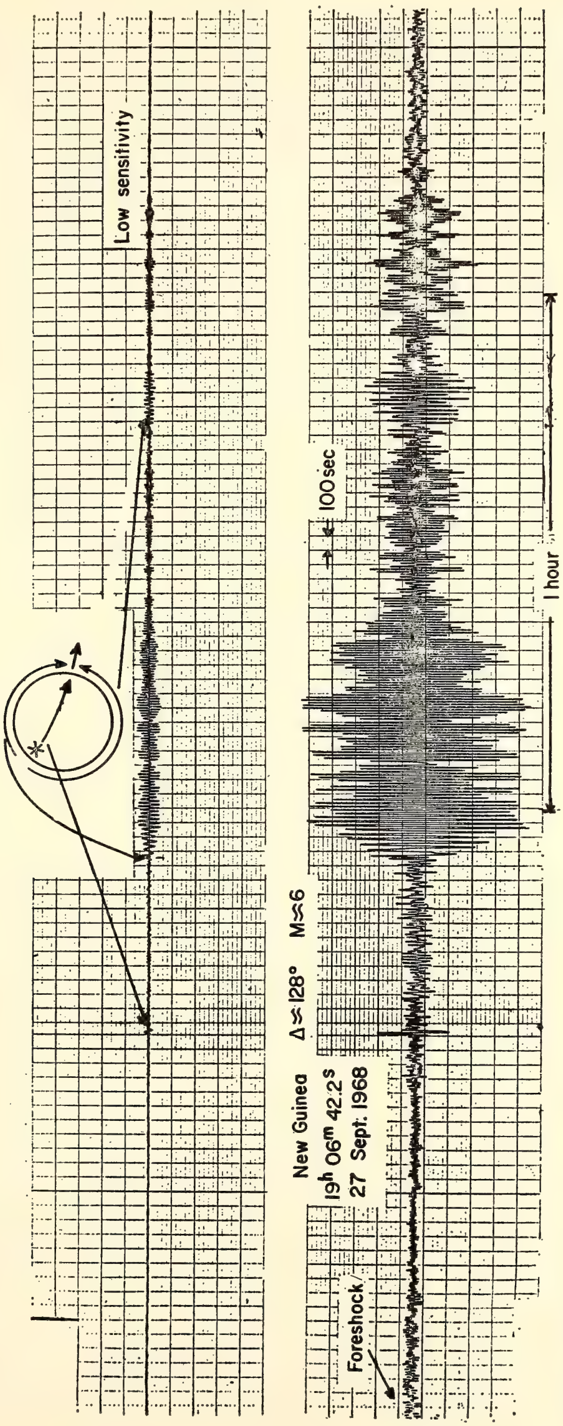

Fig. 57. Strain-meter recording of an earthquake in New Guinea. The strain sensitivity as a function of period is given in curve 1 in Fig. 54.

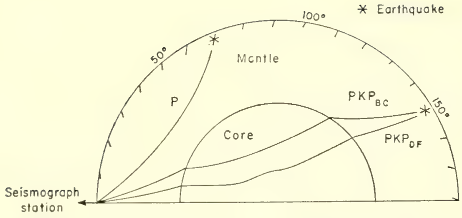

Fig. 58. Seismic wave paths used for determination of seismograph station time residuals. The time residual is defined as the difference between the actual phase arrival time and the theoretical arrival time calculated from the Jeffreys-Bullen 1958 travel-time tables. The asterisks indicate earthquakes.

residuals; t_r is an arrival time reading error at the seismograph station; $r(\theta)$ is the station residual (as a function of azimuth θ) to be determined (θ has been divided into 30° independent sectors in this study).

If a sufficient number of earthquakes are studied in each sector, the reading error t_r will be much reduced, as well as the nonsystematic part of t_e. In some sectors the earthquakes occupy a small region, e. g., in sector F dominated by the South Sandwich Island events, whereas

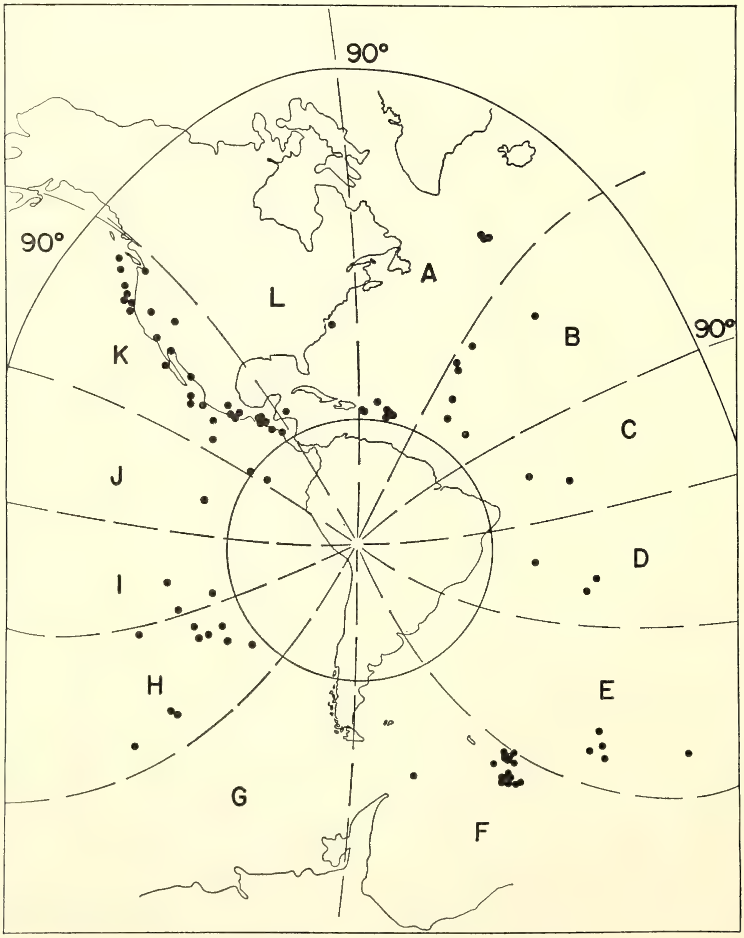

Earthquakes for P-wave residuals

Fig. 59. Earthquakes used for the *P*-wave study. The earthquake epicentral region was divided into 12 sectors which were analyzed independently.

in others, e. g., in sector K, they are well dispersed. In sector F, the systematic part of t_e may be substantial and must remain unknown. There may also be deviations from the travel-time tables used in this particular region of the earth. Distances greater than 30° were used to minimize this error—at distances less than 20°, these deviations are known to be large (James and Sacks, *Year Book 67*). Residuals were calculated as above for some "reference" stations which, as a part of the worldwide network of standardized stations, were also used by other investigators. Table 14 shows the mean residuals (each sector being given equal weight) of some stations compared with those determined by Herrin and Taggart (1968).[82] The agreement is good.

If one treats the network of stations in South America as an array, and determines residuals relative to reference stations, the major uncertainties in equation 1 disappear, as follows:

$t_e + t_t\ (\Delta) + r(\theta)_1 = t_1$ reference station minus
$t_e + t_t\ (\Delta_2)^1 + r(\theta)_2 = t_2$ of another station
is $r(\theta)_1 - r(\theta)_2 = t_1 - t_2$.

Because time comparisons with a reference station are generally made over small distances ($<3°$), the error $t_t\ (\Delta_2)$ will be small. To the extent that $r(\theta)_1$ is known from equation 1, and bearing in mind the limitations $[t_e,\ \theta,\ t_t\ (\Delta_1)]$, the absolute residual $r(\theta)_2 = t_2 - t_1 + r(\theta)_1$ may be calculated for all stations and all sectors. Some sectors (C, D, G, J, L) had too few earthquakes to allow reliability tests, and residuals determined for these sectors are given lowest weight in the results shown in Fig. 60.

TABLE 14. Mean Residuals for Reference Stations *

Station	Herrin and Taggart	Sacks, Saa, and Aparicio
ANT, Antofagasta, Chile	—0.52	—0.7
ARE, Arequipa, Peru	+0.54	0.0
LPB, LaPaz, Bolivia	+0.38	+0.4
PNS, Penas, Bolivia		+0.7
HUA, Huancayo, Peru	+1.58	+1.2
NNA, Nana, Peru	—0.09	—0.55

* Comparison of residuals determined in this study with those determined by Herrin and Taggart (1968).[82]

A similar study was undertaken using *PKP* waves at distances greater than 145°. At shorter distances, the GH branch is the first arrival and the emergent nature and low amplitudes of this phase make the arrival time hard to determine with good precision. Between 145 and 155 there is dominant, impulsive arrival between the DF and AB branches. Travel times for this phase were determined (Fig. 61) and were used as well as DF for the residual study. Earthquake epicenters were divided into 12 regions in the same manner as for the *P*-wave residuals. The residuals in certain sectors could be determined with greater accuracy than those in others for the same reasons given in the *P*-wave case. Region H, which is dominated by Banda Sea earthquakes, is particularly well determined. These earthquakes have very sharp onsets, are numerous, and their arrival times can be read with great accuracy. Figure 63 shows the residuals for the H direction, together with the standard deviations of the residual determinations. The residuals are plotted as a function of the elevation of the station. The mean (*M*) residual, which was determined by giving each sector equal weight, is also plotted on Fig. 63. It will be seen that the difference between mean residuals in direction H is always less than the standard deviation. This is not too surprising because these *PKP* waves have angles of incidence of about 7° for DF, and 11° for the BC branch so that the cone covered by the various sectors is only 14° for DF or 22° for BC, and the waves are effectively normally incident. In contrast, the *P*-waves from the various sectors cover a cone of about 80°.

Some system of comparison has to be

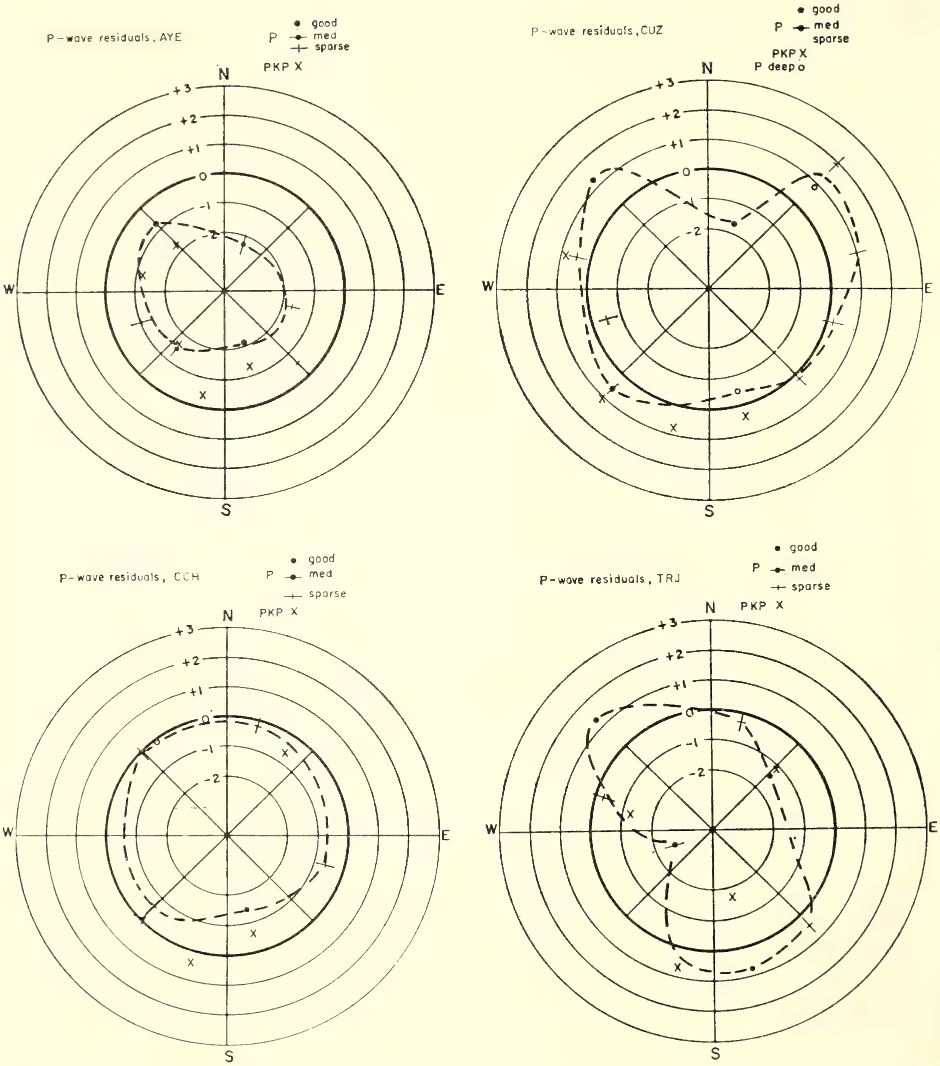

Fig. 60. *P*-wave residuals as a function of azimuth for some South American seismographs. The results of the following four stations are displayed: AYE, (Ayanquera, coastal station, southern Peru); CUZ, (Cuzco, Andean station, southern Peru); CCH, (Cochabamba, eastern flank of the eastern cordillera, Bolivia); TRJ, (Tarija, eastern flank of the Cordillera de Mochara, southern Bolivia). The geographical location of these stations and the relationship of the time residuals to the position of the mountain chains is shown in Fig. 64.

adopted to assess the normalcy of these results. If one makes the usual assumption that the various topographic features are in isostatic equilibrium, a comparison criterion can be developed. This assumption implies that the weight of any column, with excess mass above sea level (which may represent the mountain region) is supported by a lower density root, i. e., that the crust is thicker under the mountain so that the excess mass of the mountain is supported. Unfortunately, to date, neither the seismic velocities nor the gravity in this area have been

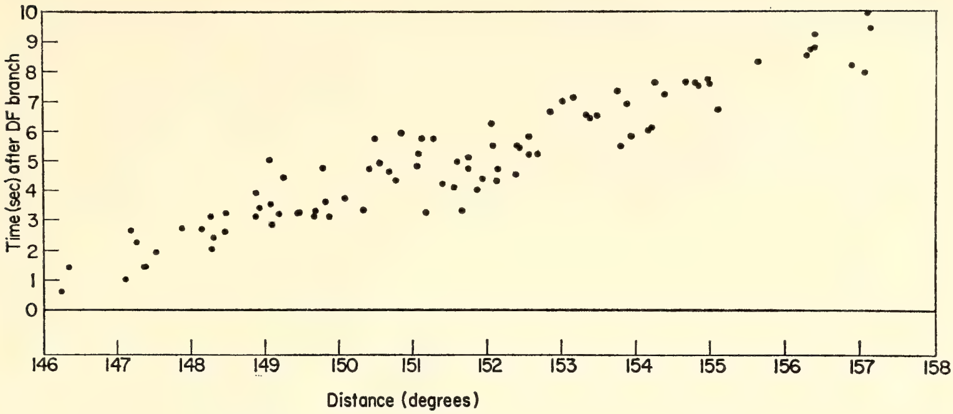

Fig. 61. Travel-time difference between the BC and DF branches of *PKP*. The BC branch is dominant in the distance range 145–155 degrees.

determined very fully. The figures adopted for seismic velocities and density above and below the Moho are suggested to some extent by the work that has been done. (See the following article in this report, *Explosion Studies in the Altiplano.*) However, these figures are to be used only for comparison of the residuals and are not to be taken as determined models. The expected residuals, plotted as a function of elevation and based on an isostatic model, are shown in Fig. 62. Some features are suggested from the comparison of the "isostatic line" (Fig. 62) and the actual observations. The results from the bulk of the stations from sea level up to about 4-km elevation fall fairly close to the isostatic line. There is, however, a cluster of stations at elevation between 3 and 4 km which have arrival-time residuals well in excess of the "isostatic" line, and also some stations up to an elevation of more than 5 km at which the arrivals are slightly early. Figure 63 is a schematic section through the topography, showing the position of stations having *PKP* arrival-time residuals which are late, early, or as expected. A certain pattern is seen to obtain: stations on the west, i.e., on the Pacific Ocean side of the divide of the mountain ranges, are somewhat early, whereas those to the east of center are substantially late. Stations on the coast, or on the flanks, and surprisingly enough on the altiplane, show no anomaly.

It became apparent as the study progressed that various groups of stations track together, i.e., that the variation of the residuals of one station, for azimuth and angle of incidence, was similar to the variation for other stations of the same group. The coastal group (AYE, ATI, SGP, etc.), the mountain group (HUA, CUZ, PUN) and the altiplano group, (LPB, PNS, SCS, DSG) all had residuals which behaved coherently. Plate 5 shows the azimuthal results from the *P*-wave studies plotted on a topographical map. It can be seen on the coastal station, AYE, that the *P*-wave residuals are greater for paths along and below the Andes, i.e., when the waves approach from the northwest. This is also true for the mountain station Cuzco. Cuzco also has large residuals when the waves approach from the northeast, i.e., up the eastern flank of the mountain. The TRJ station has large residuals when waves approach from either the northwest or the south. This once again follows the line of the Andes. The station on the west of the Andes, CCH, has rather small azimuthal effects; the waves are slightly delayed from the northwest.

One qualitative model which explains

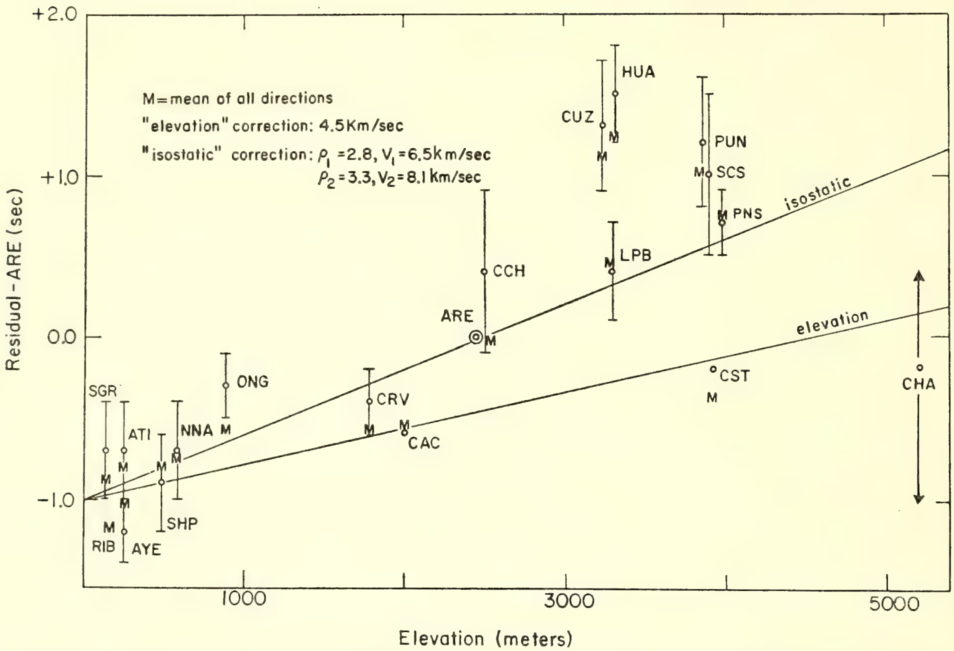

Fig. 62. Time residuals for *PKP* waves. The standard deviation, determined for the H direction, is shown by the length of the bars. *M* indicates the mean residual which has been calculated from the results of all sectors, giving each sector equal weight. Since the residuals of other sectors are not as well determined as those of the H direction, the uncertainty of the *M* residuals may be greater than those of the H direction. Note that the residuals of CUZ, HUA, and PUN are significantly greater than predicted by the isostatic model.

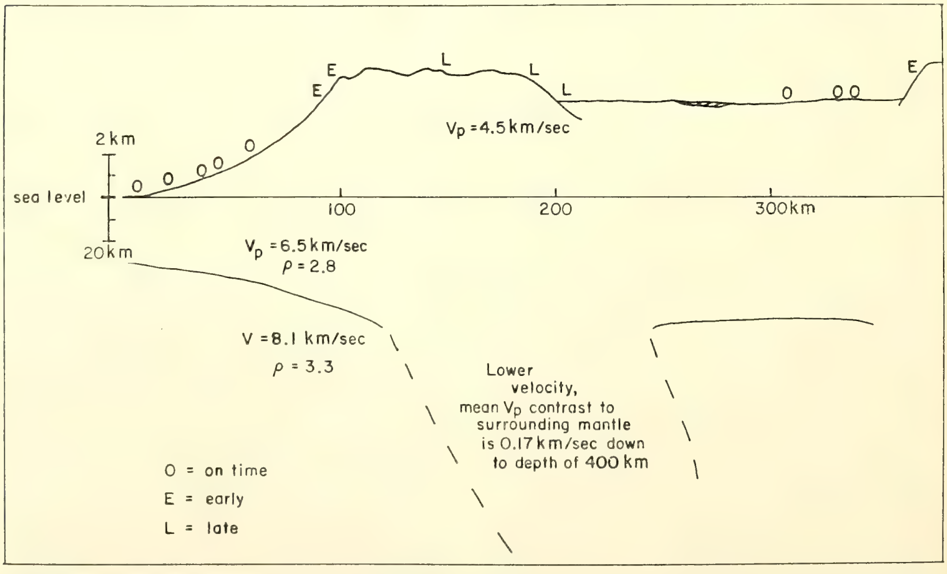

Fig. 63. Crust and upper mantle model that explains the residuals in Figs. 63 and 65. *O, E,* and *L* indicate relative positions of the groups of seismograph stations whose arrivals are on time, early, or late, respectively. The earthquake activity is generally east of the low velocity tongue and also dips away from the west coast.

the data is shown in Fig. 63. It will be seen that it departs from an isostatic model in that there is a low-velocity tongue dipping down below the mountain away from the ocean. The mean velocity discontinuity across the tongue must be about 0.2 km per sec if the tongue persists to a depth of 400 km. It should be noted that the earthquake activity is generally to the west of the tongue, i.e., towards the Pacific Ocean side.

It was, of course, of considerable interest to know that the residuals would be on the eastern side of the Andes, i.e., on the western edge of the Brazilian shield. A station was installed at Riberalta in the northern Bolivian jungle, to determine this residual. This proved to be a rather difficult area in which to operate a seismograph, and only a few results were obtained during one year of operation. They did indicate, however, that the residual on the edge of the Brazilian shield is about the same as those of the coastal stations on the west coast. The Riberalta (RIB) mean residual is plotted in Fig. 62.

The following conclusions may be drawn from this study about the uppermost mantle under western South America. (1) The Andes mountain chain has a root of lower-velocity material which dips away from the west coast. The width of the root is about 100 km, and the velocity difference between the root and the surrounding mantle is about 0.2 km/sec if the length (down dip) of the root is 400 km. If the root is shallower, the velocity contrast will prove to be greater. (2) The earthquake activity, which also dips away from the west coast, reaching a depth of 600 km, lies on the west side of the low-velocity tongue. (3) Apart from the low-velocity tongue, there does not seem to be a substantial change in the mean velocity of the uppermost mantle between the west coast and the low-elevation pampas of western Brazil. (4) The high plateau (the altiplano) between two mountain ranges, which probably has some tens of thousands of feet of sediments, seems to have a relatively normal delay for near-vertical arrivals.

The data obtained from this study resulted from the observations of a number of short-period vertical seismometers. The NSF supported the construction and operation of many of these stations.

Explosion Studies in the Altiplano

DTM Staff: collaborators from the University of Wisconsin, the Southwest Center for Advanced Studies, the Instituto Geofísico Boliviano, the Instituto Geofísico del Peru, and the Instituto Geofísico, Universidad Nacional de San Agustín

As part of the Department's contributions to the activities of the International Geophysical Year, studies of the crustal properties in southern Peru and eastern Bolivia were made using explosions in copper mines. In *Year Book 57* the results of these efforts were reported in detail. In summary, a normal refraction profile was found along the western flank of the Andes with seismic arrivals refracted from both crustal and mantle layers in the earth. Attempts to find similar arrivals for paths into the altiplano were frustrating. No waves refracted from the mantle were observed. The crustal structure determined from the 1957 observations is given in Table 15.

It was decided more than two years ago that another attempt to determine these elusive seismic parameters of the crust should be made. This decision was based on several factors, among which

TABLE 15. Andean Crustal Models

Velocity km/sec	Layer thickness, km: Peru, 1957	Layer thickness, km: Bolivia, 1968
5.0	1.5	10
6.0	8.0	15
6.6	30.0	35
8.0	...	...
Crustal thickness, km	39.5	60

were (1) the technological improvements in our seismic equipment, which gave more sensitivity at lower frequencies; (2) the existence of many very sensitive, semipermanent seismic stations in Peru and Bolivia in the region to be studied; (3) the growing competence of collaborators in Peru and Bolivia; and (4) the opportunity to participate in studies directly related to the upper mantle program agreed to by the geophysics community in South America. The extensive official arrangements in the two countries were ably accomplished by the Instituto Geofísico del Peru, Ing. A. A. Giesecke, Jr., executive director; and by the Instituto Geofísico Boliviano, R. Cabré, S. J., coordinator. We are indebted to these institutions, as well as to the members of the staff of the Geophysical Institute, University of San Agustín, Arequipa, Peru, A. Rodriguez B., director; and of the Observatorio San Calixto, La Paz, Bolivia, R. Cabré, director. These are representative of a large group of interested scientists and officials of both countries whose efforts made these observations possible. The participation of our colleagues at the University of Wisconsin and the Southwest Center for Advanced Studies was supported in part by grants from the Harry Oscar Wood fund.

The experiment was designed to provide 5 one-ton chemical explosions in each of two lakes, one in southern Peru and the other in southern Bolivia, separated by about 850 km as shown in Fig. 64. It was anticipated that seismic energy from each lake might be detected up to a distance of 600 km, and that possibly a complete reverse profile between the two lakes would be obtained. For the first events we therefore concentrated our observations in the middle 250 km of the line. No seismic arrivals from explosions in either lake were observed in this region. Subsequent explosions provided arrivals shown in Fig. 65.

It is seen that the data are not suffi-

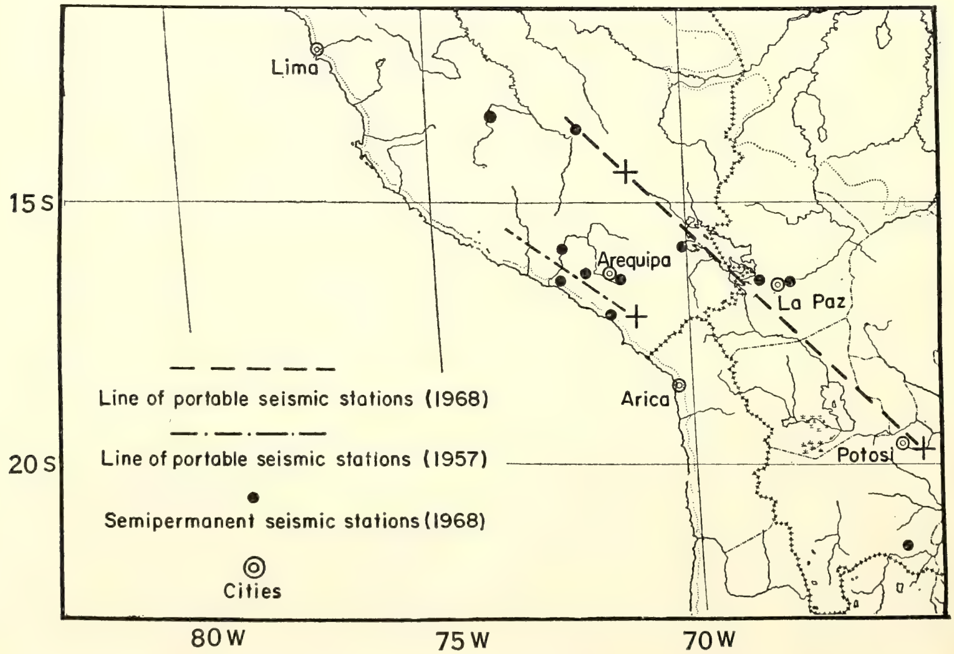

Fig. 64. Locations of explosion studies in the altiplano region.

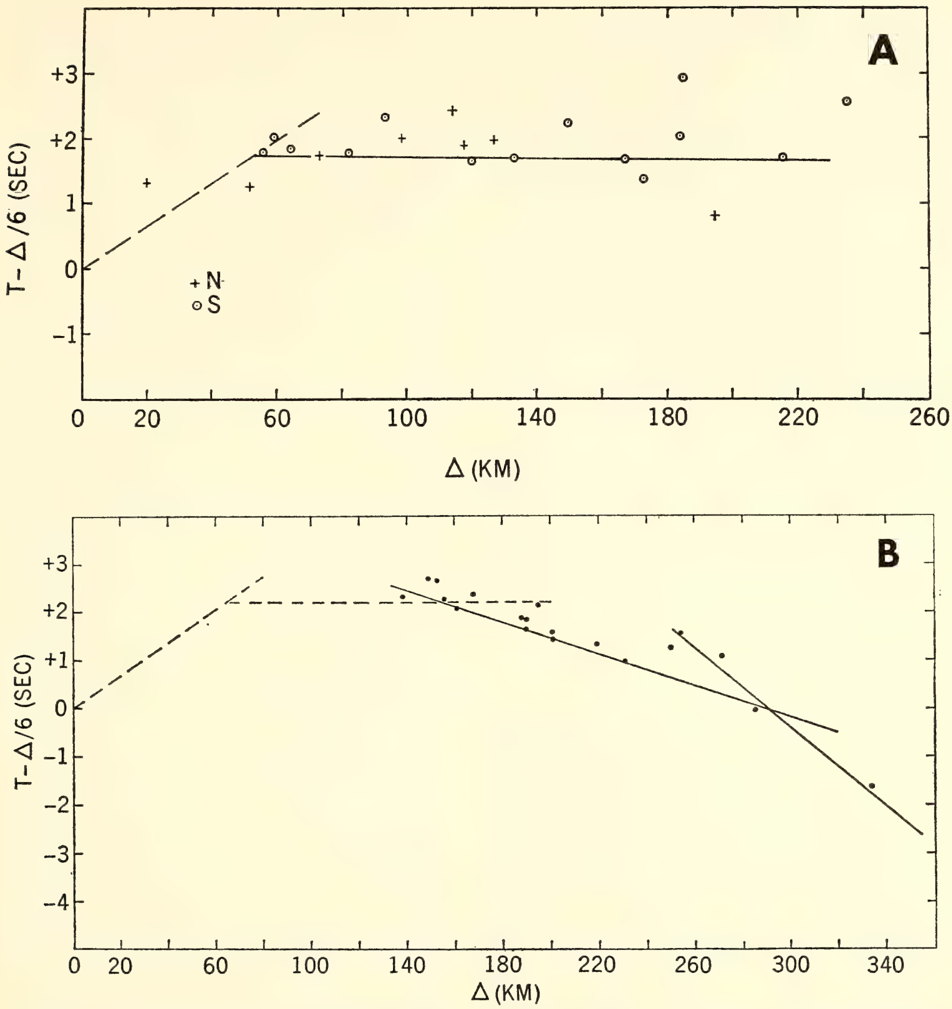

Fig. 65. (A) Travel-time curve, 1968 Peruvian explosions; (B) travel-time curve, 1968 Bolivian explosions.

cient in either country to provide a complete crustal model. It is also apparent that no seismic energy from the mantle could be identified as such in Peru. To estimate the crustal thickness in Bolivia, the dashed lines of Fig. 65b were drawn to approximate the near-shot data in Peru. For the travel-time curve indicated, we may calculate the results of Table 15. In Bolivia, the data for the first layer are nonexistent. The crossover between arrivals attributed to a layer of velocity of 6 km/sec and arrivals due to a layer of velocity of 6.6 km/sec is sketchily observed, as is the crossover between arrivals from the 6.6-km layer and the 8.0-km mantle. The crustal model obtained agrees reasonably well with that estimated by other techniques. It may be pointed out that 10–12 tons of explosives are needed to complete a reverse profile which would define the crustal velocities and structure of the Bolivian altiplano. It is not probable

that any reasonable amount of explosive material would provide needed data in Peru.

A comparison of the two results of Table 15 is of some interest. If one assumes that the mantle velocity of 8 km/sec persists to 60 km, the time difference of the two models, for waves having vertical incidence to the crust at this depth, is 1.2 seconds and is not sufficient to explain even half the variation found between coastline and altiplano stations discussed in the report of Sacks and Saa.

These newest efforts to define a crustal model of the altiplano have again shown a region of anomalously high absorption of seismic energy in southern Peru and have given preliminary results which demonstrate the possibility of measuring completely the seismic parameters of the crust in the central Bolivian region of this unusual tectonic province.

Model Seismology

D. E. James

To facilitate analysis of seismic waves, seismologists have traditionally partitioned the earth into radially homogeneous spherical shells. In the early studies of the earth this simplification was not especially restrictive within the limits of the available data and, until recently, was not regarded as a serious obstacle to interpretation of structure within the earth.

The past several years, however, have been almost revolutionary in seismology. More abundant and sophisticated seismic data which demonstrate widespread lateral inhomogeneities have led to the recognition that spherically homogeneous layers can no longer be considered viable approximations to the earth. Given these conditions, it is clearly time to admit that the earth is inhomogeneous, nonlinear, and anisotropic, and to proceed toward a quantitative evaluation of the heterogeneity.

Before it is possible to attempt such an evaluation, however, it is necessary to understand something of wave propagation through inhomogeneous media of the kind likely to exist in the earth. At least two approaches to the problem are possible—theoretical studies and model studies. Several groups are engaged in theoretical treatment of some of the problems; however, it seems to us that the necessary assumptions are too restrictive for direct application to the earth. We have therefore undertaken two-dimensional model seismology as a means of studying wave propagation under conditions analogous to those we believe exist in the earth. Our progress in this past year suggests that it will be possible to fabricate two-dimensional models incorporating velocity gradients. Before reporting our preliminary results it is appropriate to review briefly the justifications and limitations of thin sheets as cross-sectional models of the earth.

Two-dimensional models. A rather extensive discussion of the advantages of two-dimensional models over three-dimensional models can be found in a classic paper by Oliver, *et al.* (1954),[83] in which they introduce the concepts of two-dimensional modeling. There are, however, a few assumptions and limitations that we shall examine further before proceeding. The most important of these is the relationship between plate dilatational velocity, wavelength, and sheet thickness. Specifically, a fundamental assumption made in two-dimensional modeling is that the wavelength is long relative to plate thickness, so that the plate dilatational velocity goes to a limiting value for infinitely thin sheets.

We examine this problem in more detail by considering dispersion in plates. The details of the mathematical development leading to the period equation for plates has been presented elsewhere (see Tolstoy and Usdin, 1953,[84] for derivation and earlier references) and will not be repeated here.

The dispersion curves for the first two-symmetric modes and the first anti-

symmetric mode in $\frac{1}{16}$-inch plexiglas, and the first symmetric mode in $\frac{1}{32}$-inch aluminum are shown in Fig. 66.

Three records were obtained for $\frac{1}{16}$-inch plexiglas and bandpassed, one between 20 khz and 160 khz, one between 80 khz and 320 khz, and the third between 160 khz and 640 khz. These records were digitized and analyzed using a multiple filtering technique described by Dziewonski, *et al.* (1969).[85] The authors kindly provided us with their computer program which we have modified slightly.

The analysis of the 80–320 khz record is shown in Fig. 67. The numbers are linear amplitudes normalized to a maximum value of 99 and printed as a function of group velocity and period. The minus signs denote local maxima along a column. ALPHA and BAND are filter parameters defined by Dziewonski, *et al.,* and were chosen to maximize resolution. The solid line is a fit by eye to the maxima indicated for each period and represents the dispersion curve for $\frac{1}{16}$-inch plexiglas. The light dashed lines indicate the approximate limits of uncertainty. The values of the group velocity indicated by the minus signs at the display periods for the three analyzed records are shown in Fig. 66A for comparison with the theoretical dispersion curve for plexiglas. It can be seen that the shape of the two curves matches extremely well; it is not surprising that the observed dispersion curve indicates lower velocities in view of the fact that velocities are normally calculated for the first break and the main energy packet arrives slightly later.

It is important to observe that the plate dilatational velocity, which we shall take to be our compressional velocity in the model studies, is significantly dispersive even in $\frac{1}{16}$-inch plexiglas. Ideally, we should prefer that the plate dilatational waves be non-dispersive and that they behave as much like genuine body waves as possible. We consider a dispersion of $<10\%$ in velocity over the entire range of observed frequencies to be acceptable. In general, this requires sheet thicknesses of ~ 1 mm or less.

The plate wave dispersion affects the apparent value of the specific attenuation factor, Q. The value of Q in nonmetallic modeling materials is significantly lower than in the earth and is the one important parameter that does not scale in model experiments. In addition to the value of Q being intrinsically lower in the plastics commonly used in modeling, the dispersion of the dilatational waves results in a further decrease in effective Q. This effect is quite significant and studies are now in progress to determine quantitatively the decrease in apparent Q due to dispersion.

Modeling techniques. The apparatus employed in our experiments is quite similar to that used elsewhere and is shown in Fig. 68. The pulses are produced by thyratron pulsers and have rise times of <0.2 μsec and tails of a few microseconds.

Our efforts have been aimed principally at producing thin sheets of various velocities with the use of polyester resins and various kinds of filler. Depending upon the composition and amount of the filler used, the velocities of the cast sheets can be increased over the velocity of pure cast polyester by at least 25%. Thus far, the most successful results for increasing velocity (and Q) have been obtained using powdered limestone and powdered aluminum as filler. Polyester mixtures with a volume ratio of one part resin to one part aluminum or limestone are comparatively nonviscous and can be easily cast into large sheets 1 mm thick. A list of a few velocity measurements in cast sheets is given in Table 16.

Radiation patterns and free surface amplitudes. In the model studies that are anticipated, we shall in general wish to measure amplitudes of waves arriving at the free surface from a source located either on the free surface or in the interior of the model. As a preliminary to any study involving amplitudes, it is necessary to establish radiation patterns

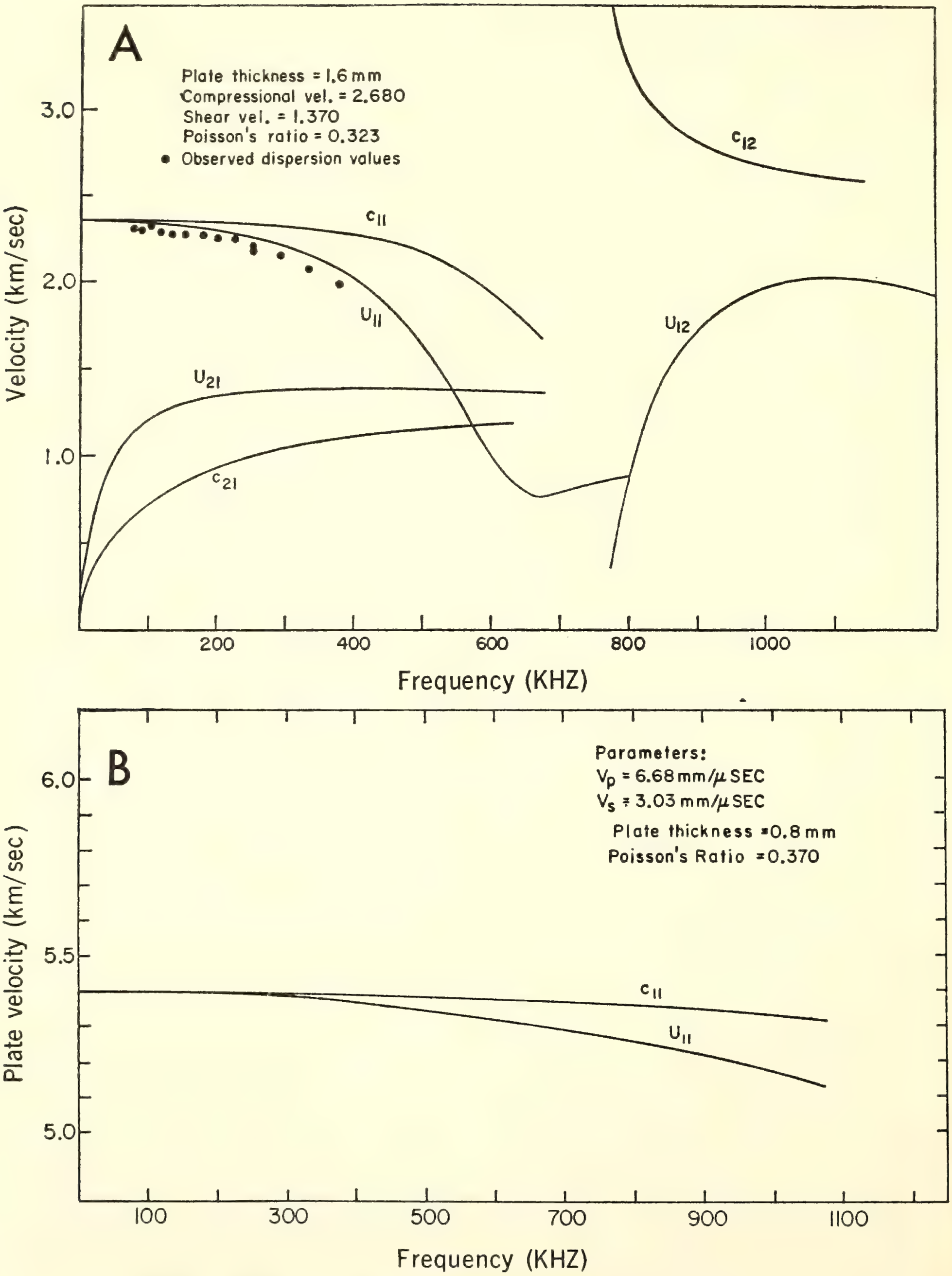

Fig. 66. Dispersion curves for plexiglas and aluminum. Observed dispersion as measured using multiple filtering is shown for the first symmetric mode in plexiglas. Notation: U denotes group velocity, c phase velocity, and the subscripting follows Tolstoy and Usdin (1953)[84].

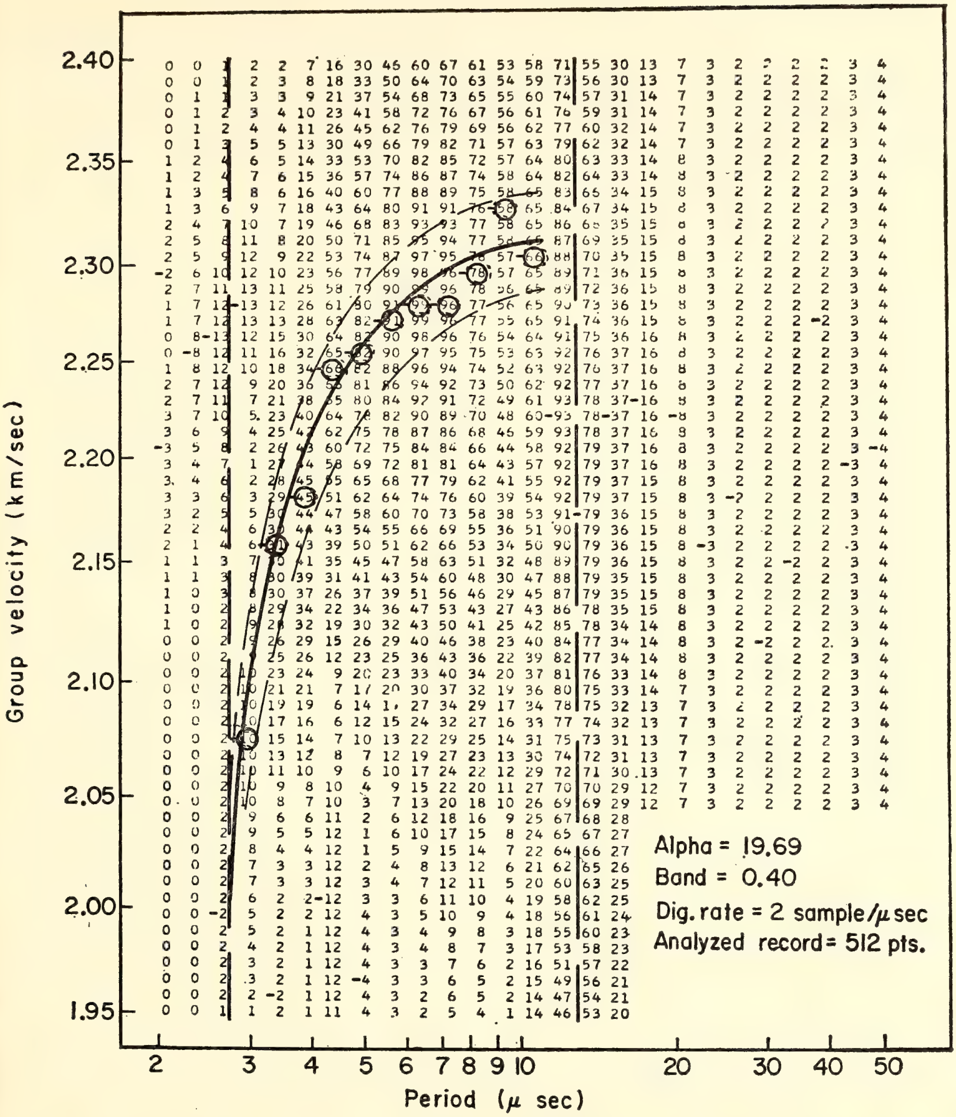

Fig. 67. Group velocities for 1/16-inch plexiglas sheet determined by multiple filtering technique. Minus signs denote local maxima along the various columns. The numbers in each column give spectral amplitudes on a linear scale. The dispersion curve is traced by following the maximum from column to column. The maxima circled are plotted as observed dispersion values in plexiglas in Fig. 66. The solid line gives the preferred dispersion curve, and the light dashed lines indicate estimated limits of reliability. The heavy dashed vertical lines denote filter cuts.

for *P*- and *S*-waves from the transducers and to measure free surface displacements as a function of incident angle and wave type. By reciprocity (Gupta, 1965),[86] it is comparatively straightforward to demonstrate that for plane waves the vertical displacement due to incident *P*- or *S*-waves yields an angle-dependent pattern of displacements identical in shape and relative magnitude

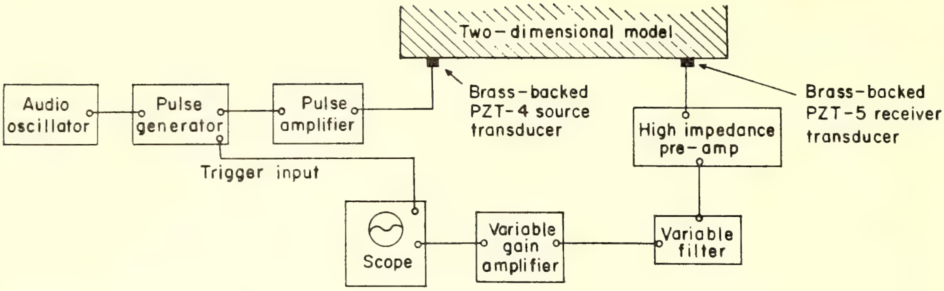

Fig. 68. Experimental apparatus.

TABLE 16. Properties of Polyester Sheets with Various Fillers

Resin (type and volume)	Filler (composition and dry volume)	Plate thick-ness, mm	V_p, mm/μsec	V_s, mm/μsec	Pseudo-Poisson's ratio	Temp., °C
MR-480; 1.5 liters	none	1.5	2.01	1.16	0.251	23.5
MR-480; 1.4 liters	Al powder; 0.4 liters (1 lb.)	1.55	2.21	1.28	0.242	23.6
MR-480; 1.3 liters	Al powder; 1.2 liters (3 lbs.)	1.6	2.46	1.42	0.250	22.5
MR-480; 1.3 liters	Pulverized limestone; 1.1 liters	1.6	2.56	1.48	0.248	23.2

to the radiation patterns for *P*- and *S*-waves resulting from a vertical displacement at the free surface. Fig. 69 shows the angles and our notation for incident and reflected waves at the free surface. *A* and *B* are directly proportional to the amplitudes of the incident *P* and *SV* waves, respectively.

Although the problem of determining free surface displacements has been treated numerous times in the literature (Jeffreys, 1926;[87] Knott, 1899;[88] Gutenberg, 1944;[89] Nuttli, 1961;[90] Gupta, 1965[86]), the results are not in a particularly useful form for our purposes. The following, therefore, is a brief development, following Jeffreys' notation, of vertical displacements and energy partitioning at a free boundary.

Case I: Incident P-*wave.* If A, A_1, and

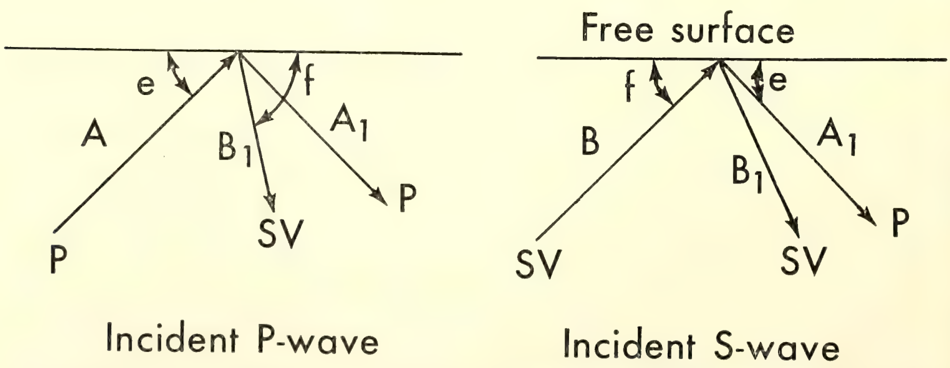

Fig. 69. Illustration giving notation and angular relations for incident and reflected waves at a free surface.

B_1 are as shown in Fig. 69, then for any choice of velocities we have

$$B_1 = A \cdot \frac{4 \tan e \,[(1+F)\tan^2 e + 1]}{2F \tan e \tan f + [(1+F)\tan^2 e+1]\,(\tan^2 f - 1)}$$

$$A_1 = A \cdot \frac{4F \tan e \tan f - [(1+F)\tan^2 e+1]\,(\tan^2 f-1)}{2F\tan e \tan f + [(1+F)\tan^2 e + 1]\,(\tan^2 f - 1)}$$

where $F = \dfrac{2V_s^2}{(V_p^2 - 2V_s^2)}$, V_s = shear velocity, and V_p = plate dilatational velocity. To use A_1 and B_1 as initial amplitudes of waves now traveling to the opposite free surface (as in the single-layer case described below), it is necessary to conserve energy, so that

$A^2 = B_1^2 \dfrac{\tan f}{\tan e} + A_1^2$ (Ewing, *et al.*, 1957, p. 29)[91] and the amplitude of reflected $SV = B_1\left(\dfrac{\tan f}{\tan e}\right)^{\frac{1}{2}}$ and that of $P = A_1$.

The vertical displacement at the free surface is given by

$$w = i\kappa[\tan e\,(A - A_1) + B_1]$$

where the exponent term has been dropped.

$$\kappa = \text{wave number} = {}^{\omega}/c$$

where ω = angular frequency, c = apparent velocity of wave in the x direction along the surface, and $i = \sqrt{-1}$. Replacing κ by $^{\omega}/c$, and tan e by $[c^2/V_p^2) - 1]^{\frac{1}{2}}$ (Ewing, *et al.*, 1957, p. 26), we have

$$w = i\frac{\omega}{V_p}\left[\left(1 - \frac{V_p^2}{c^2}\right)^{\frac{1}{2}} (A - A_1) + \frac{V_p}{c} B_1\right]$$

where V_p = plate dilatational velocity and $V_p/c = [1(\tan^2 e + 1)]^{\frac{1}{2}}$.

This equation gives the vertical free surface displacement due to an incident P-wave with amplitude coefficient, A. The angular displacement pattern also gives the radiation pattern of P for a vertical displacement at the free surface. This pattern, together with that for incident SV, is shown in Fig. 70.

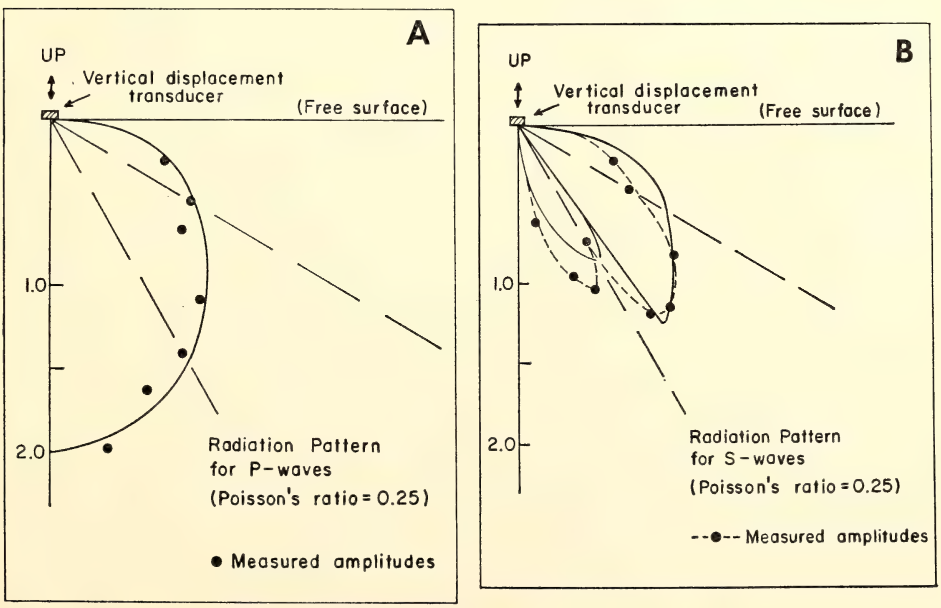

Fig. 70. Radiation patterns for P and S due to a vertical displacement at the surface.

Case II: Incident SV *wave.* Again, following the notation given in Fig. 69, we have

$$B_1=B\cdot\frac{2\,F\tan e\tan f+((1+F)\tan^2 e+1)\,(1-\tan^2 f)}{2\,F\tan e\tan f-((1+F)\tan^2 e+1)\,(1-\tan^2 f)}$$

$$A_1=B\cdot\frac{2\,F\tan f\,(1-\tan^2 f)}{2\,F\tan e\tan f-((1+F)\tan^2 e+1)\,(1-\tan^2 f)}$$

where F is given above and B is directly proportional to the amplitude of the incident SV wave.

By partitioning of energy at the boundary, we have

$$B^2=A_1^2\frac{\tan e}{\tan f}+B_1^2$$

so that the reflected P-wave amplitude is equal to A_1 $(\tan e/\tan f)^{\frac{1}{2}}$.

The vertical amplitude due to an incident SV wave with amplitude coefficient$=B$ is given by:

$$w=i\,\kappa\,[(B+B_1)-\tan e\,A_1].$$

Replacing κ by ω/c and $\tan e$ by $(c^2/V_p^2-1)^{\frac{1}{2}}$, we have

$$w=i\frac{\omega}{V_p}\left[\frac{V_p}{c}\,(B+B_1)-\left(1-\frac{V_p^2}{c^2}\right)^{\frac{1}{2}}A_1\right]\,[(90^\circ-f)>\theta_c]$$

where the variables are as given above. θ_c=critical angle of SV greater than which no P-wave is reflected and SV is totally reflected and phase shifted.

The free surface displacement pattern for incident SV is given in Fig. 70B. It should be noted that for both P and SV an incident wave of *unit* amplitude has been assumed so that the relative amplitudes of P and SV are correct for a displacement at the surface.

The discrepancy for S-waves between measured and theoretical results in Fig. 70b may be due largely to interference effects that have made precise measurements of S amplitudes difficult. We do not believe the differences to be significant. Use of a bender bimorph as described by Chowdhury and Dehlinger (1963)[92] should provide more reliable measurements. The amplitude measurements described below for PP and PS phases give a more precise indication of the general applicability of plane-wave theory to the radiation patterns of vertical motion transducers over typical model dimensions.

Propagation and amplitudes in a single layer. As a test of the applicability of plane-wave free surface reflection theory, a single-layer model was investigated. A series of record tracings (Fig. 71) are shown for the various phases diagrammed in Fig. 72. These results are virtually identical to those reported by Press, *et al.* (1954).[93] The only phase of particular interest is the refracted SPS phase. It is not especially prominent on

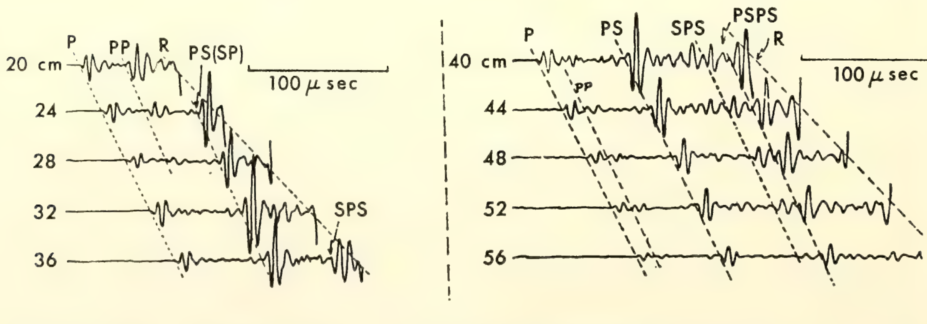

Fig. 71. Record tracings showing the various phases diagrammed in Fig. 72.

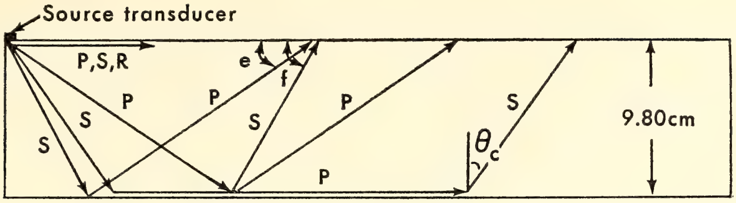

Fig. 72. Ray paths for the various phases shown in Fig. 77. θ_c is the critical angle for S-waves. Note the large amplitude of PS (SP) and $PSPS$ ($SPSP$).

the records shown in Fig. 71 because of the relatively high frequency pass band. The SPS pulse has very large amplitude at low frequencies, a fact which may indicate that it is produced by curvature of incident S at the free surface.

Amplitudes for a fixed frequency have been computed for the PP and PS (SP) phases using the radiation patterns and vertical displacement expressions given above. To obtain amplitudes which can be compared to amplitudes measured experimentally, geometric spreading and attenuation must be taken into consideration so that over any path length between the free surfaces we have

$$A_d = A_o \exp\left(\frac{-\pi fT}{Q}\right)$$

where A_o = initial amplitude of wave
A_d = amplitude of wave at distance d from source
f = frequency
T = travel time over path length $= d/V_p$.

It should be noted that this expression must be calculated for each path separately between the free surfaces.

Geometric spreading can be calculated on the basis of total path length, and in sheets is:

$$A = \left(\frac{r_o}{r_1}\right)^{\frac{1}{2}} A_o$$

where r_o is an arbitrary normalizing path length, A_o is initial amplitude, A is final amplitude, and r_1 is the path length traveled by the ray in question.

The amplitudes for the plexiglas layer have been computed and are shown together with experimental values in Fig. 73. For the purpose of amplitude calculations, plexiglas was a poor choice because of the low and highly temperature-sensitive Q value. Thus the theoretical amplitude curves shown depend not so much on the reflection and conversion coefficients at the free surfaces as they do on Q. In this case, and those following, the relative positions of the theoretical amplitude curves of PP and PS are as predicted by the radiation or vertical displacement patterns shown in Fig. 70. These curves have not been shifted relative to one another to provide a better fit to the individual curves. We have assumed in all cases that the amplitude of PS is equal to that of SP. This assumption is correct if the relative radiation patterns of P and S for the source and pickup transducer are the same.

Because of the dominating effect of Q on amplitudes in plexiglas, amplitudes were measured in a single-layer sheet of $\frac{1}{32}$-inch soft aluminum. Aluminum has an extremely high Q, variously measured between about 1000 and 200,000 (Knopoff, 1964),[94] and therefore attenuation plays little role in the amplitude result (provided the sheet is thin enough that no significant dispersion takes place). Measured amplitudes should depend only on free surface reflection and conversion coefficients. Results for two different frequency pass bands are shown in Fig. 74. The slope of PS appears to agree very well with theory as does the relative position of the PS and PP curves. It is clear, however, that the slope of PP does not provide an ideal fit to the experi-

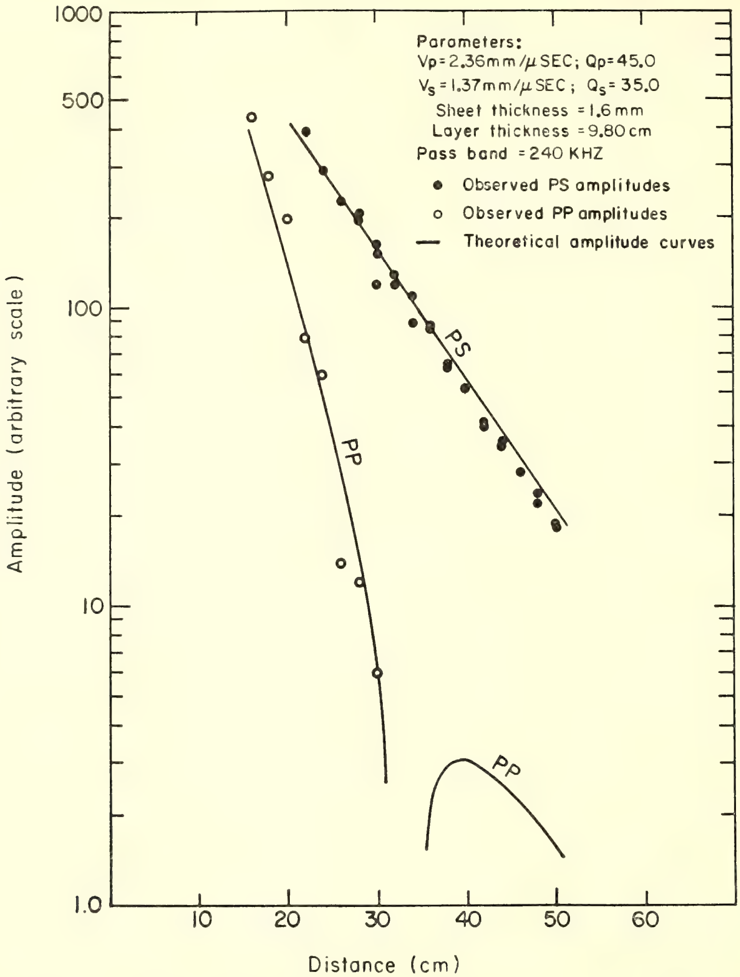

Fig. 73. Amplitudes for *PP* and *PS* (*SP*) in plexiglas. It has been assumed that the amplitude of *PS* is equal to that of *SP* by reciprocity. Solid lines are theoretical curves assuming the parameters given in the figure. Effects due to *Q* and geometric spreading have been taken into account.

mental data, particularly at 320 khz, although the discrepancy is not especially large. The fit for both *PS* and *PP* appears to be everywhere better than about 25% and over most of the curves less than 15%. The different values of *Q* used in the two sets of calculations do not change significantly either the slopes or the relative positions of the two curves.

The interference effect suggested by the sigmoidal shape of the *PS* measured amplitudes may be due in part to the effect of *PPPP*. Within the range 38–55 cm, *PPPP* has approximately the same arrival time as *PS*. Within this range, however, its amplitude is more than an order of magnitude less than that of *PS* and does not appear to be sufficient to account for all the effects observed in the *PS* amplitudes.

It is clear from the results described above that plane-wave theory provides a

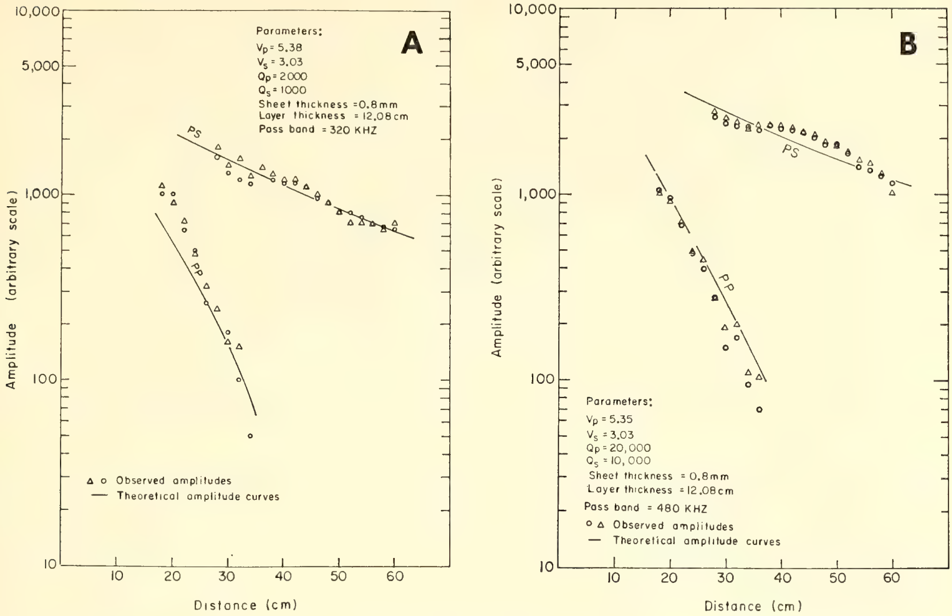

Fig. 74. Amplitudes in 1/32-inch aluminum layer for different pass bands.

good approximation to the measured vertical displacements at a free surface over dimensions and wavelengths appropriate for model studies. For future experiments, the problem in general will be one of calculating the amplitude of the incoming wave from the measured displacement at the surface.

Change in Earthquake Spectrum Before and After the Matsushiro Swarm

Shigeji Suyehiro

The Matsushiro Earthquake Swarm started on August 3, 1965. Its region was limited to a small area of about 10×10 km. The Worldwide Standard Seismograph of short period (Vmax: 100,000) at the Matsushiro Seismological Observatory in the swarm region recorded 663,142 earthquakes from the swarm through August 1967, and 61,005 of these were perceptible at the Observatory. This swarm was accompanied by tremendous land deformations. In October 1966 a horizontal extension of 116 cm was observed in the swarm region over a distance of about 3 km, corresponding to a linear strain of 3.8×10^{-4} (see Fig. 75). This enormous amount of strain cannot be explained merely by pure elastic deformation, but nonelastic deformations such as fractures or creep must have taken place.

As many fractures have developed in the swarm region since the start, the transmission of high-frequency energy through this fractured region must be affected by scattering. Many fractures were seen at the surface and many others must exist under the ground.

Prior to the start of the swarm, observations of local earthquakes had been made at the Observatory, and information was obtained pertaining to the transmission of high-frequency energy before the swarm. To study changes in the predominance of high-frequency energy, observations were repeated in January 1967 at the same spot and with the same instrumentation, which has a recording response of up to 250 cps. These observa-

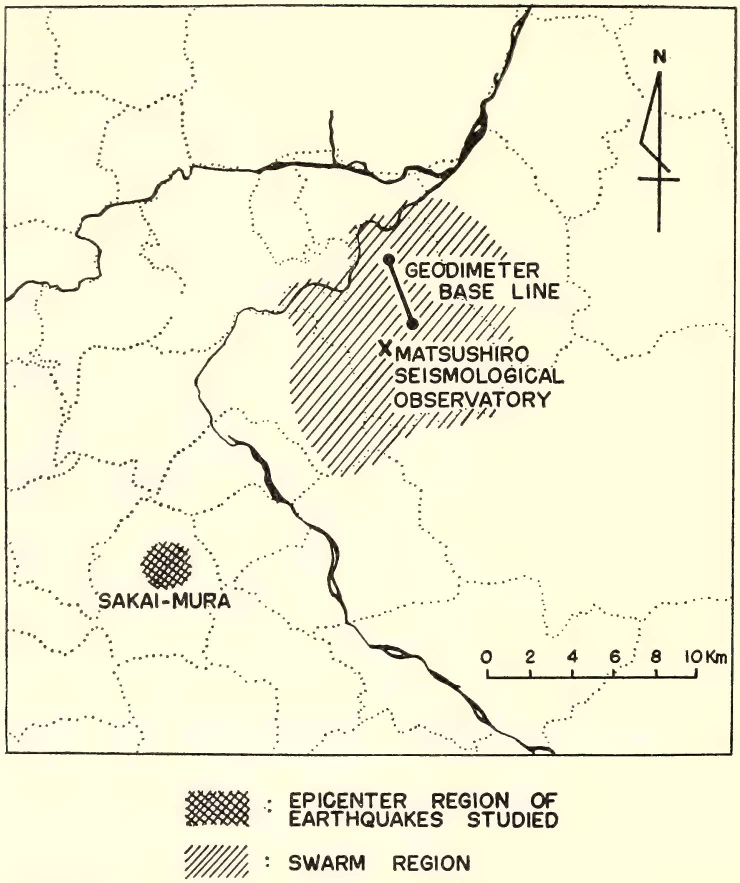

Fig. 75. Matsushiro swarm region, epicenter region of earthquakes studied, and geodimeter base line which showed a linear strain of 3.8×10^{-4}.

tions were compared with the pre-swarm observations of December 1963 and January 1964 for earthquakes occurring in the same area outside the swarm region with a similar depth of 3–10 km (see Fig. 75).

Data. Toward the end of 1966, the swarm had been restricted to within 5 km of the Observatory. From January 1967 the swarm activity started diffusing into the surrounding area, and a series of earthquakes occurred about 15 km southwest of the Observatory with depth ranging from 3 to 10 km. During the pre-swarm observation, earthquakes occurred also in this region with the same depth range. Fortunately, in that period, observations were made at the Matsushiro Observatory with a tripartite net and hypocenters were estimated solely from these observations. To eliminate as many uncontrollable elements as possible, the same source region, order of magnitude, instrumentation, and receiving point were used to compare the transmission of high-frequency energy through the swarm region before and toward the end of the swarm.

The selected earthquakes which satisfied the conditions were replayed from magnetic tape through a varying band-pass filter of one-third octave from 2.0–2.5 cps to 200–250 cps, and the maximum amplitude was measured within 0.6 sec from the onset at each different band-pass. Examples of filtered seismograms

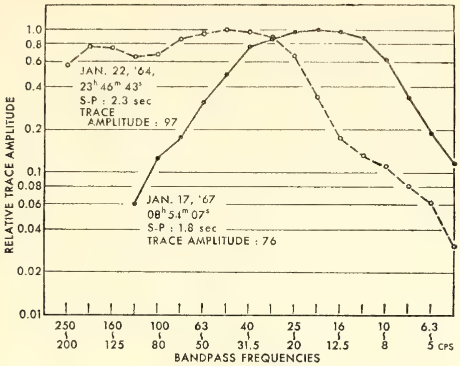

Fig. 76. Relation between relative trace amplitude and band-pass frequency.

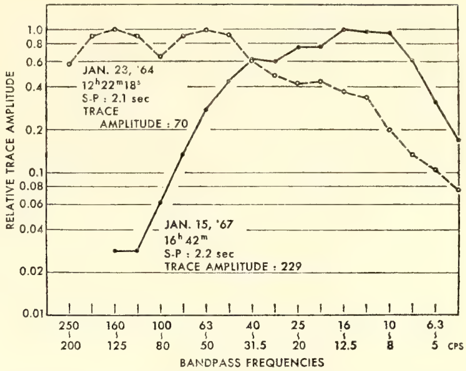

Fig. 78. Relation between relative trace amplitude and band-pass frequency.

are shown in Plate 6. Figures 76, 77, and 78 show three examples of the relation between relative trace amplitude and band-pass frequency. Spectra of seismograms of earthquakes which differ only in the time of occurrence, namely before and toward the end of the swarm, are compared in Plate 6 and Figs. 76, 77, and 78.

Figures 75–78 show the high-frequency energy, which was more abundantly recorded for the 1964 earthquakes than for the 1967 earthquakes. Many earthquakes in the present category have been examined, and in no case is there conflict with the statement made above. What caused this variation? No change has taken place in the instrumentation or in the receiving station. The magnitude of earthquakes analyzed and their path of propagation remain the same. Therefore, only changes in the source spectrum or in the nature of the crust along the path of propagation, or in both, could cause such a difference. For the following reasons, the nature of the path is inferred to have changed rather than the source of the spectrum.

1. The source used in this study was outside the swarm region and had shown no extraordinary activity until January 1967 when the seismicity in that area increased. Even in the swarm region, no volcanic activity was found and no increase of underground temperature could be deduced from geomagnetic observations. It is difficult to assume any substantial change in the elastic constants of material in the source region which could have affected the source spectrum of earthquakes of the same order of magnitude.

2. Earthquakes that took place closer to the Observatory in the swarm region in 1967 were analyzed to determine whether the source still produced high-frequency energy. In Fig. 79 the trace amplitude 125–100 cps/trace amplitude of 63–50 cps, most of which are for 1967 earthquakes, is plotted against $S-P$ time, that is, the epicentral distance; if earthquakes are close enough to the receiving station, high-frequency waves are observable. This proves that the source still produces high-frequency waves, but

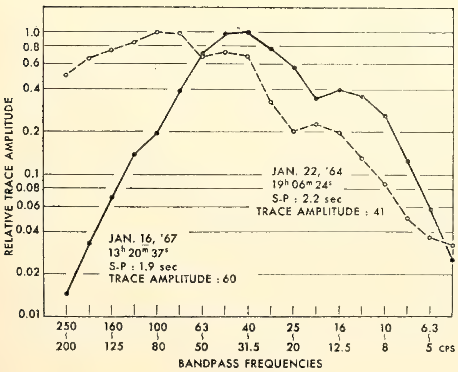

Fig. 77. Relation between relative trace amplitude and band-pass frequency.

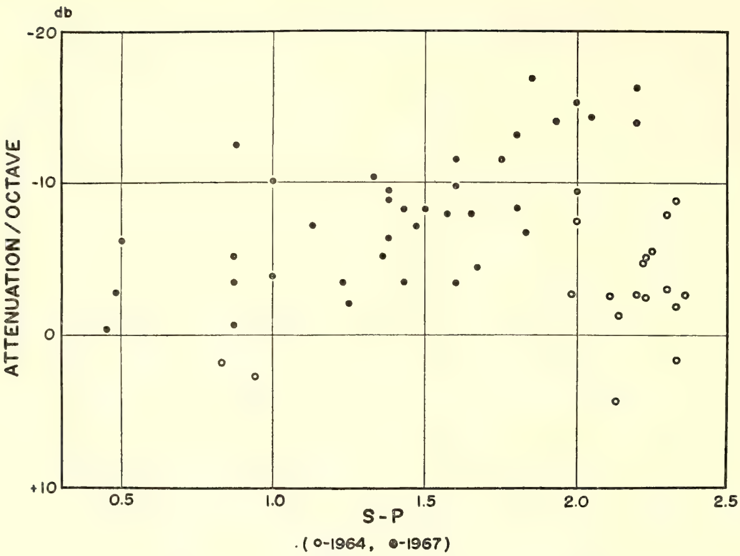

Fig. 79. Relation between $S-P$ time and attenuation of trace amplitude over one octave.

the medium along the path was not so conductive for the high frequencies in January 1967 as it had been before the swarm.

3. Very large ground deformations have been observed in the swarm region, especially in the north-south direction. A strain of 3.8×10^{-4} was observed from October 1965 to September 1966. This deformation could not have been caused by elastic strain alone, but is probably the result of considerable fissuring, some of which was observed on the surface. It is very likely that the crust under the swarm region has been highly fractured as a result of an extremely large number of earthquakes. The reduction of high-frequency waves in January 1967, as compared with those which existed before the swarm, must be attributed to the medium along the path.

4. If the high-frequency energy is at-

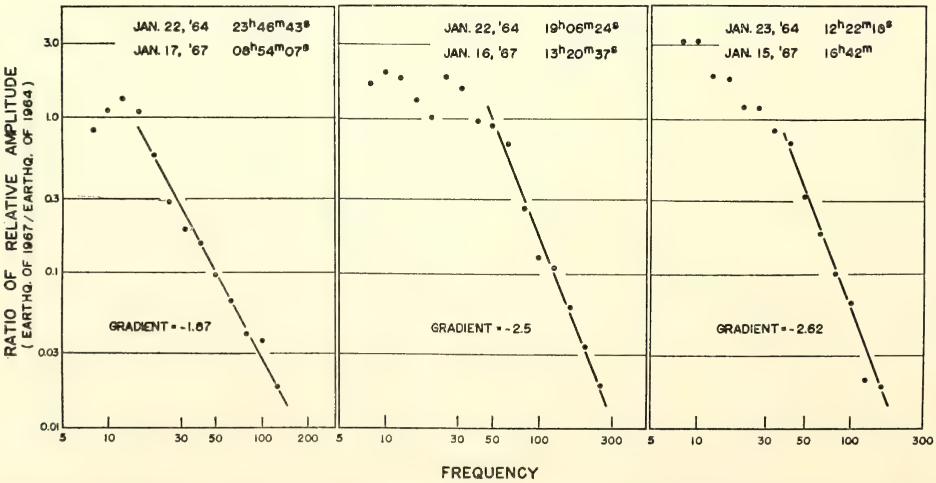

Fig. 80. Relative amplitude ratio of earthquake of 1967 to earthquake of 1964, amplitude 67(f)/amplitude 64(f).

tenuated in the medium during propagation, what type of attenuation is conceivable? Is it due to absorption or scattering? As stated previously, it is difficult to assume any substantial change in the physical or chemical nature of the medium which might change the Q-value to that extent. To study the dependency of attenuation on frequency, the amplitude ratio of 1967 and 1964 earthquakes was plotted against frequency. Three examples are shown in Fig. 80. As seen from the figure, the amplitude ratio is proportional to the nearly inverse cube of the frequency for high frequencies. Such a high dependency on frequency strongly suggests that the attenuation is due to scattering.

5. From Fig. 80, it is seen that the frequency dependency becomes appreciable from about 20 cps. Assuming the velocity of a P wave in the region is 5 km/sec, the wavelength at 20 cps is 250 m. Again assuming that $\log E = 11.4 + 1.5\,M$ and the maximum strain energy stored in a unit volume is 3×10^3 erg/cm^3 (strain energy: $0.5\ eX^2$; e: elastic const.$=5\times10^{11}\sim10^{12}$ c.g.s.; $X=1\sim2\times10^{-4}$), the magnitude of an earthquake released by breaking rock volume of $250\times250\times250$ m will be 3.5. Such earthquakes are perceptible in a small region. The present swarm consists of many small earthquakes without any outstanding one. The magnitude of the larger, perceptible, earthquakes which occur frequently, is 3.5–3.0.

The size of fissures, which may be produced by those larger earthquakes in the swarm, agrees with the wavelength with which the scattering effect becomes appreciable.

6. In Plate 6, the amplitude decays after P arrival in the frequency range of 50 cps more rapidly in the pre-swarm earthquakes than in the earthquakes of 1967. This difference in the seismogram can also be explained by the increased scattering effect after the swarm.

From the present study, it is concluded that the swarm region has been highly fractured. The magnitude of the largest swarming earthquakes agrees well with the frequency of seismic waves with which the scattering becomes effective.

It seems likely that the highly heterogeneous region was under strain, started breaking by many fractures, and was eventually released from the strain, as experiments suggested.

Difference in the Relationship of Magnitude to Frequency of Occurrence between Aftershocks and Foreshocks for an Earthquake of Magnitude 5.1 in Central Japan

S. Suyehiro

An earthquake of magnitude 5.1 occurred in central Japan in September 1967 in almost the same place where the event of 1964 took place with different "b" values for foreshocks and aftershocks. The 1967 sequence was completely recorded by a set of comprehensive magnetic tape seismographs of broad frequency band and large dynamic range; b values of 0.59 and 0.89 were found for foreshocks and aftershocks as compared with 0.35 and 0.76 found for the 1964 sequence.

The main points of difference between the events of 1964 and 1967, which shared the same epicenter region and the same pattern in sequence, are the magnitude of main shocks and the background seismic activity. The magnitude of the main shock was 3.3 in 1964 and 5.1 in 1967. The background activity was very quiet in 1964, while in 1967 the Matsushiro swarm had grown outward to include the present region where the activity was already high. If similarities are assumed in larger and smaller earthquakes, the difference in the combination of b values for foreshocks and aftershocks must be attributed to the difference in the background activities rather than the magnitudes of main shocks. Accordingly, the larger b value of 0.59 for foreshocks in 1967, as compared with the 1964 event, was interpreted as resulting from the superposition of high background activity of $b=1$ and pure foreshock activity with the same b value of

0.35 as in 1964. A slight difference of b value in the two aftershock sequences can also be explained in the same way. Without the high background activity in 1967, b values of foreshocks and aftershocks in the same region should have been as they were in 1964.

Introduction

On January 22, 1964, a perceptible earthquake of magnitude 3.3 occurred about 16 km to the southwest of the Matsushiro Seismological Observatory. Twenty-five foreshocks and 173 aftershocks associated with this earthquake were recorded at the Observatory. From the analysis of these records, a considerable difference in the relationship of magnitude to frequency of occurrence was found between the foreshocks and aftershocks, i. e., the coefficient b in the Gutenberg-Richter formula was only 0.35 for the foreshocks as compared with 0.76 in the aftershocks (S. Suyehiro, T. Asada, and M. Ohtake, 1964).[95] The same difference was also observed in the foreshocks and aftershocks of the Great Chilean Earthquake of 1960 (S. Suyehiro, 1966).[96]

In August 1965 a large swarm of earthquakes started near the Matsushiro Seismological Observatory (Earthquake Research Institute, 1966 and 1967).[97] For about one and a half years this swarm was limited to a region of 10 km × 10 km, but later the swarm region grew outward to include the region where the sequence of January 1964 took place (Fig. 81). The activity in this region continued with the form of swarm until September 1967 when a strong earthquake of magnitude 5.1 occurred with many foreshocks and aftershocks. The earthquake was much larger than preceding and following earthquakes, which indicated that the present sequence is of the fore-, main-, and aftershock type rather than being one of the rises in a swarm activity. Furthermore, the origin of the main shock was only 2 km from that of the main shock of January 1964.

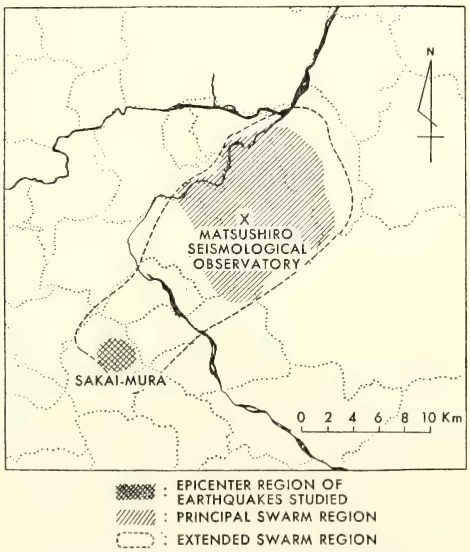

Fig. 81. Area of earthquake swarm near Matsushiro Seismological Observatory.

Naturally, a question was raised as to whether the present sequence manifested the same character as was found in December 1964, in which different b values were assigned to foreshocks and aftershocks.

Fortunately, two months before this event, a set of seismographs of large dynamic range and of broad frequency band, developed by I. S. Sacks, was installed in the Matsushiro Seismological Observatory (I. S. Sacks, 1966),[98] and the whole sequence was recorded from the level of background noise up to the main shock adequately without saturation. The results of the analysis and related discussions are reported in this section.

Instrumentation

The present multichannel recording system has velocity and displacement responses in a frequency range of $\frac{1}{30}$–30 cps, and its dynamic range covers background noise from an assumed quietest site to earthquake motions of intensity IV or more (JMA scale). The specially designed pendulum of low distortion is housed in vacuum, and its operational period is 15 sec for the horizontal component and 5 sec for the

vertical component. Accordingly, the present pendulum of comparatively long period is free from distortion in the short-period vibration field, which is not true of most types of seismographs now in operation. The output of the transducers is fed into a system of chopper amplifiers and filters and recorded in three levels for displacement response and in two levels for velocity response on slow-speed magnetic tape of 0.17 mm/sec by the direct recording method.

With this system, all shocks from foreshocks or aftershocks of small magnitude barely above the background noise up to the main shock of magnitude 5.1, which gave the intensity IV at the site of observation, were properly recorded by the same frequency response without saturation. Such an instrumental set-up is very valuable for studies of magnitude and frequency of occurrence, and for comparison of spectra of large and small earthquakes.

Material

Seismogram. The magnetic tape of about 40 hours in real time before and after the main shock, namely, from 08 hours on September 13, 1967, to 11 hours on September 16, 1967, was replayed and recorded on ink-writing paper by a specially designed read-out system at the Department. Examples are shown in Fig. 82 in which earthquakes with large differences in magnitude are well covered by a large dynamic range.

Earthquakes of $S-P$ time from 1.4 sec to 2.2 sec were all considered as foreshocks or aftershocks for the following reasons. (1) The activity in the principal swarm region had already calmed down,

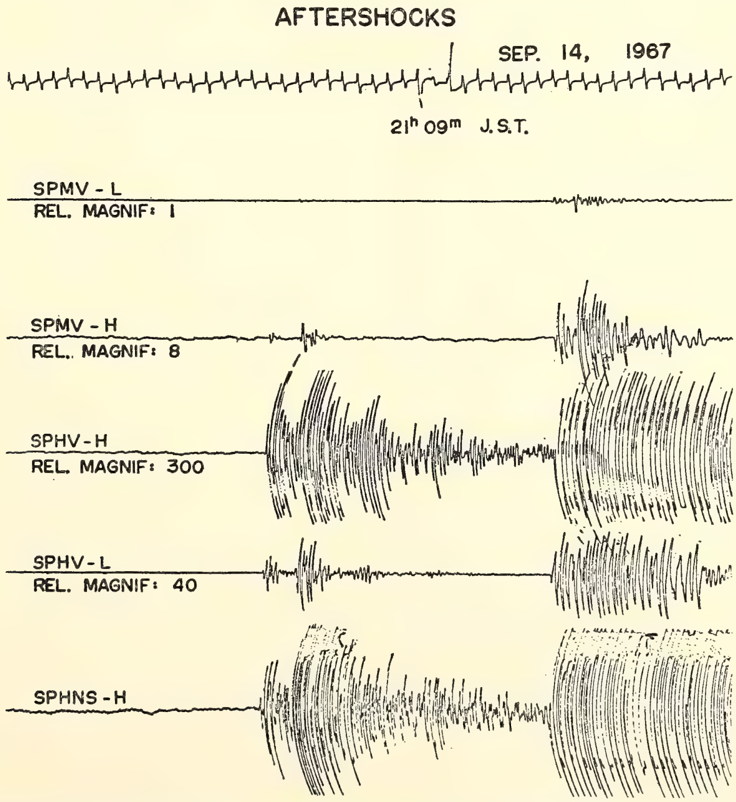

Fig. 82. Seismograms showing that earthquakes with large differences in magnitude are well recorded by a large dynamic range.

and earthquakes of the same $S-P$ range in different azimuth were very small in number. (2) The frequency of occurrence of earthquakes of the said $S-P$ time rose abruptly about 40 hours before the main shock. (3) Nearly all earthquakes of magnitude larger than 1.8 gave a clear initial motion, and the azimuth was checked from the direction of the initial motion. (4) Even if some foreign shocks from different azimuths had leaked in, they would have increased the frequency of occurrence slightly in the magnitude range of the first or second shock, which could not have distorted the statistics. Such a distortion, furthermore, could not favor the present conclusion of a smaller b value for foreshocks, but would work toward the opposite conclusion. For aftershocks of much higher frequency of occurrence, such a distortion is inconceivable.

Magnitude Determination. Earthquakes corresponding to the above criteria occurring within 40 hours before and after the main shock were read from the ink-writing records. Amplitudes measured from the middle- or low-sensitivity channel were all reduced to what should have been recorded by the high-sensitivity channel. Since the trace amplitude of the background noise is about 1 mm, earthquakes of maximum trace amplitude of less than 3 mm were all eliminated from the statistics. Magnitudes were assigned on the following assumptions.

1. The epicentral distance from the Observatory is nearly the same, and the difference of magnitudes of two earthquakes is equal to the difference of logarithms of maximum trace amplitudes of two earthquakes ($\Delta M_{12} = \log A_1 - \log A_2$).

2. The magnitude of the main shock, 5.1, and that of one foreshock, 4.1, determined by JMA, were used to reduce the relative magnitude scale by 1 to the scale in common use.

3. Frequency of occurrence and magni-

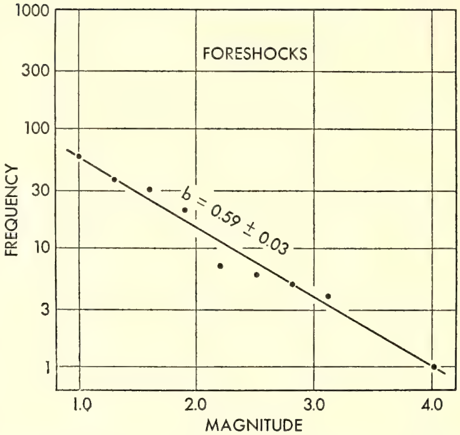

Fig. 83. Relation between frequency of occurrence and magnitude for foreshocks.

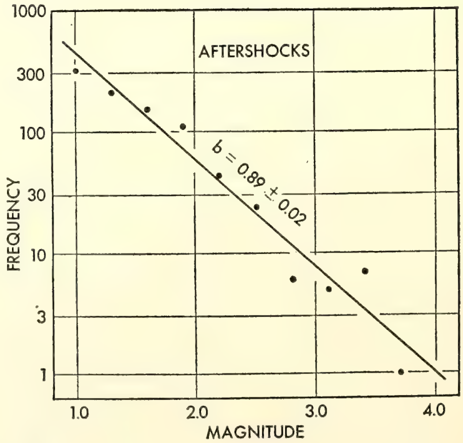

Fig. 84. Relation between frequency of occurrence and magnitude for aftershocks.

TABLE 17. Magnitude and Frequency of Occurrence of Foreshocks and Aftershocks

Trace amplitude, mm	Magnitude	Frequency of occurrence: Foreshocks	Frequency of occurrence: Aftershocks
3.0–5.9	1.0	59	316
6.0–11.9	1.3	37	212
12.0–23.9	1.6	31	151
24.0–47.9	1.9	21	110
48.0–95.9	2.2	7	44
96.0–191.9	2.5	6	24
192.0–383.9	2.8	5	6
384.0–767.9	3.1	4	5
768.0–1535.9	3.4	0	7
1536.0–3071.9	3.7	0	1
3072.0–6143.9	4.0	1	0

tude were considered. Class interval in trace amplitude and frequency of occurrence and corresponding magnitude for foreshocks and aftershocks are listed in Table 17. Figure 83 shows the relation between frequency of occurrence and magnitude for foreshocks, and Fig. 84 shows that relation for the aftershocks.

4. Frequency distribution of $S-P$ times. Frequency distribution of $S-P$ times for foreshocks and aftershocks is shown in Fig. 85.

5. Background activity in the region of the event. The swarm region started growing, and the NE–SW diameter reached 20 km as of August 1966, but the present region was not yet included. On January 16 and February 3, 1967, earthquakes of intensity V took place in the present region, called Sakai-mura Village, and this region became active. Table 18 shows the frequency of occurrence of perceptible earthquakes and intensity observed at the village office of Sakai-mura from January 1967 to August 1967, just before the present event. All earthquakes originating in other regions but perceptible at Sakai-mura village were eliminated. Magnitudes were assigned on the basis of instrumental determinations, and also according to the relation of magnitude to intensity, ($M = \frac{1}{2}I + \text{const.}$, for local shocks of nearly constant epicentral distance).

TABLE 18. Perceptible Earthquakes in the Sakai-mura Region from January to August 1967

	Intensity				
	I (Mag. 2.5)	II (Mag. 3.0)	III (Mag. 3.5)	IV (Mag. 4.0)	V (Mag. 4.5)
January	60	18	3	3	3
February	155	62	11	2	1
March	55	16	1	0	0
April	44	6	5	2	0
May	90	29	2	2	0
June	29	8	4	1	0
July	17	3	1	0	0
August	13	9	3	0	0
Total	463	151	30	10	4

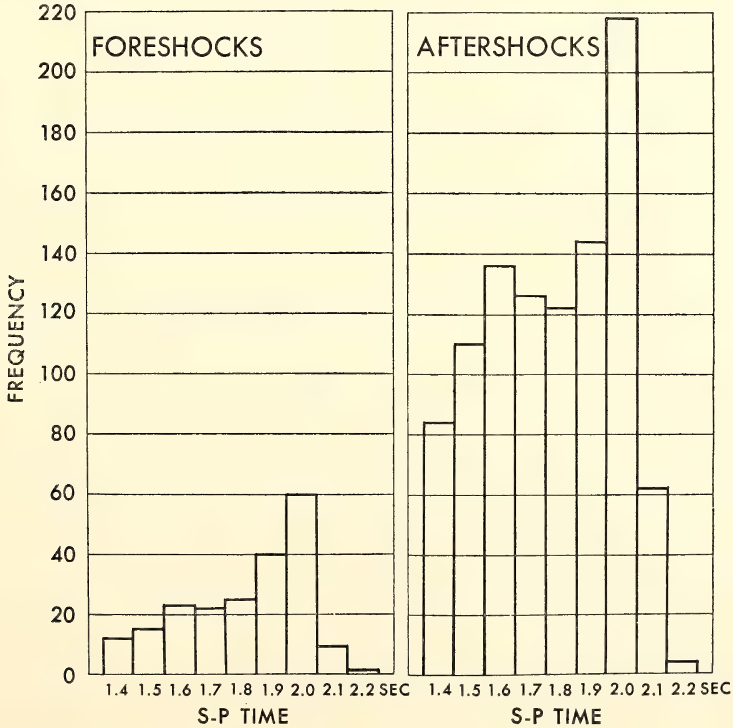

Fig. 85. Distribution of $S-P$ times.

This activity is considered as the background activity in the region when the present event took place, and the relation between frequency of occurrence and magnitude is shown in Fig. 86.

Discussion

1. b values. In the event of 1964, $b=0.76\pm0.02$ for aftershocks and $b=0.35\pm0.01$ for foreshocks while in the present event, $b=0.89\pm0.02$ for aftershocks and $b=0.59\pm0.03$ for foreshocks. In both cases, a smaller b value was found for foreshocks and a larger value for aftershocks. The difference between b values for foreshocks and aftershocks, however, is not so large for the present event as it was for the event of 1964. The two events took place in almost the same region, so why were b values not similar for each?

Two points of difference can be raised between the events of 1964 and 1967. One is that the magnitude of the main shock was 5.1 in 1967 as against 3.3 in 1964, and the other is that the 1964 event took place when the regional background activity was very quiet, while the 1967 event occurred when the regional activity was already high and of swarm type (see Table 18 and Fig. 86). Since many similarities have been found between large and small earthquakes, especially in the relation of frequency of occurrence to magnitude, the first point alone scarcely counts. The second point can most likely be attributed to the fact that some relative difference in b values existed, particularly for foreshocks, in the events of 1967 and 1964, although a smaller b for foreshocks was retained.

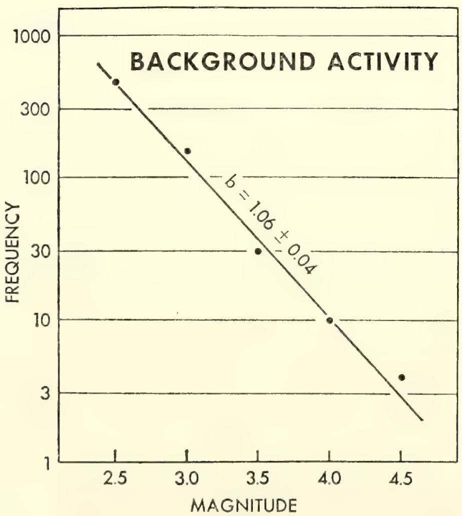

Fig. 86. Relation between frequency of occurrence and magnitude for background activity.

2. Superposition of two activities of different b value. Let us first consider the two foreshock sequences, which gave a comparatively large difference in b value. It is assumed that the foreshock activity for the main shock of September 1967 had the same b value of 0.35 as the foreshock activity of 1964. With this value superposed on the already existing swarming background activity the superposition of two activities was observed.

The well-known formula, which represents the relationship of frequency of occurrence to magnitude, $\log N=a-bM$, does not follow the law of superposition. In Fig. 87, two straight lines,

$$\log N_1=-0.35\,M \text{ and } \log N_2=-1.00\,M,$$

are drawn, having the same frequency of occurrence at a relative magnitude of 0; and $\log\,(N_1+N_2)$ is also given as a function of M. Evidently, $\log\,(N_1+N_2)=f(M)$ can no longer be expressed by a straight line, but is a convex curve downward. However, the observable magnitude range is usually not large enough to see the curvature, and the fraction which is observed would be considered a straight line. In a region where one activity overwhelms the other, the existence of minor activity has practically no effect on the major activity. Only in a region where two activities have comparable frequency of occurrence does the resultant "apparent b" have an intermediate value of two b's.

It is assumed that the frequency distribution for the present foreshock ac-

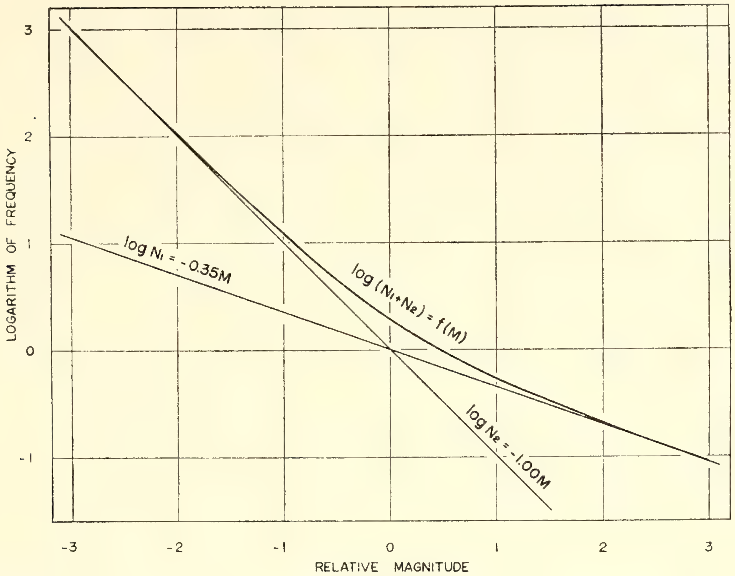

Fig. 87. Superposition of two activities of different b's.

tivity shown in Fig. 85 is actually a part of the resultant curve. The mean frequency of occurrence of $M=3$ earthquakes in pure background activity is calculated to be 0.022/hour (Fig. 86), while that of $M=3$ earthquakes in superposed activity is 0.097/hour (Fig. 83). Accordingly, the same value for pure foreshock activity must be $0.097-0.022=0.075$, which is 3.4 times larger than the value of pure background activity. The magnitude range 1–4 in Fig. 83 corresponds to the magnitude range -1.2 to 1.8 in Fig. 87 if a difference of 3.4 times between $b=0.35$ pure foreshock activity, and $b=1.00$ pure background activity, at magnitude 3, is applied. If the curve, $\log (N_1+N_2)$, between $M=-1.2$ and $M=1.8$ in Fig. 87 is approximated by a straight line, its b value is

$$\log (N_1+N_2)_{-1.2}-\log (N_1+N_2)_{1.8}/M_{-1.2}-M_{1.8},$$

which is calculated to be 0.62.

The observed value, 0.59, and the calculated value, 0.62, on the above assumption show good agreement. Thus, the difference in b values for the foreshocks of 1964 and 1967 can be interpreted as being caused by the superposition of pure foreshock activity and pure background activity. The aftershock activity of a higher frequency of occurrence is much less influenced by the background activity than the foreshock activity. However, if the same consideration is applied to the aftershock activity, assuming that the pure aftershocks have a b value of 0.76 as in 1964, the resultant b should be 0.80. Again, this value has a fair agreement with the observed value of 0.89.

3. Foreshocks and aftershock region. Figure 85 shows the frequency distribution of $S-P$ time of foreshocks and aftershocks. Considering that the difference between the upper and lower limits of $S-P$ time is 0.8 sec and that the wave velocity of an imaginary $S-P$ wave is 7.0 km/sec, the linear dimension of the region becomes 5.6 km. From the Utsu-Seki formula of $\log A=1.02\ M_0-4.0$ (M_0: magnitude of the main shock, A: area of aftershock region in km^2), using $M_0=5.1$, a linear dimension of 4.0 km is obtained, which is in good agreement

with the observed value. Similar agreement was found in 1964.

Conclusion

The difference in *b* values for foreshock and aftershock activities in 1964 and 1967 can be interpreted as being caused by the superposition of high background seismic activity and pure foreshock activity. The same order of difference in *b* values for foreshocks and aftershocks seems to be characteristic of earthquakes of fore-, main-, and aftershock type which take place in the present region near the Matsushiro Seismological Observatory.

REFERENCES CITED

1. Schmidt, M., *Galactic Structure,* A. Blaauw and M. Schmidt, eds., Chicago: Univ. of Chicago Press, p. 513, 1965.
2. Hindman, J. V., and K. M. Balnaves, *Australian J. Phys.,* Astrophysical Supplement, No. 4, 1967.
3. Trächslin, W., L. Brown, T. B. Clegg, and R. G. Seyler, *Phys. Letters, 25B,* 585, 1967.
4. Seyler, R. G., *Nucl. Phys., A124,* 253, 1969.
5. Petitjean, C., L. Brown, and R. G. Seyler, *Nucl. Phys., 129,* 209, 1969.
6. Ebbinghaus, H., U. Holm, H. U. Klapdor, and H. Neuert, *Z. Phys., 199,* 68, 1967.
7. Miers, R. E., and L. W. Anderson, *Rev. Sci. Instr., 39,* 336, 1968.
8. Klose, J. Z., *Beam-Foil Spectroscopy,* S. Bashkin, ed., Gordon and Breach Publishers, New York, 1968.
9. Flamm, W. G., P. M. Walker, and M. McCallum, *J. Mol. Biol., 40,* 423, 1969.
10. Wetmur, J. G., and N. Davidson, *J. Mol. Biol., 31,* 349, 1968.
11. Callan, H. G., *J. Cell. Sci., 2,* 1, 1967.
12. Whitehouse, H. L. K., *J. Cell. Sci., 2,* 9, 1967.
13. Smith, M., in *The Fresh-Water Algae of the United States,* McGraw-Hill Book Co., New York, 1950.
14. Starr, R. C., *Am. J. Botany, 51,* 1013, 1964.
15. Safferman, R. S., and M. E. Morris, *Science, 140,* 679, 1963.
16. Cowie, D. B., and P. Szafranski, *Biophys. J., 7,* 567, 1967.
17. Luftig, R., and R. Haselkorn, *Virology, 1,* 344, 1966.
18. Safferman, R. S., I. R. Schneider, R. L. Steere, M. E. Morris, and T. O. Diener, *Virology, 37,* 386, 1969.
19. Padan, E., and M. Shilo, *Virology, 32,* 234, 1967.
20. Silva, P. C., in *Physiology and Biochemistry of Algae,* p. 827. Academic Press, New York and London, 1962.
21. Edelman, M., D. Swinton, J. A. Schiff, H. T. Epstein, and B. Zeldin, *Bacteriol. Rev., 31,* 315, 1967.
22. Drouet, F., *Proc. Acad. Nat. Sci. Phila., 115,* 261, 1963.
23. Frampton, E. W., and B. R. Brinkley, *J. Bacteriol., 90,* 446, 1965.
24. Sandoval, H. K., H. C. Reilly, and B. Tandler, *Nature, 205,* 522, 1965.
25. Ryan, F. J., P. Fried, and F. Mukai, *Biochim., Biophys. Acta, 18,* 131, 1955.
26. Endo, H., K. Ayabe, K. Amako, K. Takeya, *Virology, 25,* 469, 1965.
27. Cowie, D. B., and B. J. McCarthy, *Proc. Natl. Acad. Sci. U. S., 50,* 537, 1963.
28. Grady, L. J., and E. C. Pollard, *Radiation Res., 36,* 68, 1968.
29. Marcovich, H., *Ann. Inst. Pasteur, 90,* 303, 1956.
30. Seaman, E., E. Tarmy, and J. Marmur, *Biochemistry, 3,* 607, 1964.
31. Okamoto, K., J. A. Mudd, J. Mangan, W. M. Huang, T. V. Subbaiah, and J. Marmur, *J. Mol. Biol., 34,* 413, 1968.
32. Grady, L. J., and E. C. Pollard, *Biochim. Biophys. Acta, 145,* 836, 1967.
33. Haas, M., and H. Yoshikawa, *Virology, 3,* 248, 1969.
34. Ishibashi, M., and Y. Hirota, *J. Bacteriol., 90,* 1496, 1965.
35. Kharkar, D. P., K. K. Turekian, and K. K. Bertine, Stream supply of dissolved silver, molybdenum, antimony, selenium, chromium, cobalt, rubidium and cesium to the oceans. *Geochim. Cosmochim. Acta, 32,* 285, 1968.

36. Gast, P. W., Terrestrial ratio of potassium to rubidium and the composition of earth's mantle. *Science, 147,* 858, 1965.

37. Deland, A. N., The boundary between the Timiskaming and the Grenville Subprovince in the Surprise Lake area, Quebec. *Proc. Geol. Assoc. Can., 8,* 127–141, 1956.

38. Leggo, M., Unpublished Ph.D. thesis, Australian National University, Canberra, Australia, 1968.

39. Papanastassiou, D. A., and G. J. Wasserburg, Initial Sr isotopic abundances and the resolution of small time differences in the formation of planetary objects. *Earth Planet. Sci. Letters, 5,* 361–376, 1969.

40. York, D., Least-squares fitting of a straight line with correlated error. *Earth Planet. Sci. Letters, 5,* 320–324, 1969.

41. Craig, H., Isotopic composition and origin of the Red Sea and Salton Sea geothermal brines, *Science, 154,* 1544–1548, 1966.

42. Goodwin, A. M., Structure, stratigraphy, and origin of iron formations, Michipicoten area, Algoma District, Ontario, Canada. *Geol. Soc. Am. Bull., 73,* 561–586, 1962.

43. McIntyre, G. A., C. Brooks, W. Compston, and A. Turek, The statistical assessment of Rb-Sr isochrons. *J. Geophys. Res., 71,* 5459–5468, 1966.

44. Hart, S. R., and G. L. Davis, Zircon U-Pb and whole-rock Rb-Sr ages and early crustal development near Rainy Lake, Ontario. *Geol. Soc. Am. Bull., 80,* 595–616, 1969.

45. Gast, P. W., Isotope geochemistry of volcanic rocks, in *Basalts,* 325–358, Interscience Publishers, New York, 1967.

46. Bence, A. E., The differentiation history of the earth by rubidium-strontium isotopic relationships. Ph.D. thesis, M. I. T., 1966.

47. Gast, P. W., Limitations on the composition of the upper mantle. *J. Geophys. Res., 65,* 1287–1297, 1960.

48. Hedge, C. E., Variations in radiogenic strontium found in volcanic rocks. *J. Geophys. Res., 71,* 6119–6128, 1966.

49. Gast, P. W., Upper mantle chemistry and evolution of the earth's crust, in *The History of the Earth's Crust,* R. A. Phinney, ed., Princeton Univ. Press, 1968.

50. Hurley, P. M., Correction to: Absolute abundance and distribution of Rb, K and Sr in the earth. *Geochim. Cosmochim. Acta, 32,* 1025–1030, 1968.

51. Patterson, C. C., Characteristics of lead isotope evolution on a continental scale in the earth, in *Isotopic and Cosmic Chemistry,* 244–268, North Holland Publ., Amsterdam, 1964.

52. Wasserburg, G. J., Geochronology and isotopic data bearing on development of the continental crust, in *Advances in Earth Science,* 431–459, M. I. T. Press, Boston, 1966.

53. Wilson, H. D. B., P. Andrews, R. L. Moxham, and K. Ramlal, *Can. J. Earth Sci., 2,* 161–175, 1965.

54. Baragar, W. R. A., *Can. J. Earth Sci., 5,* 773–790, 1968.

55. Smith, R. E., *J. Petrol., 9,* 191–219, 1968.

56. Gurney, J. J., G. W. Berg, and L. H. Ahrens, Observations on caesium enrichment and the potassium/rubidium/caesium relationship in eclogites from the Roberts Victor Mine, South Africa. *Nature, 210,* 1025–1027, 1966.

57. Berg, G. W., Secondary alteration in eclogites from kimberlite pipes. *Am. Mineralogist, 53,* 1336–1346, 1968.

58. Williams, A. F., *The Genesis of the Diamond,* 2 vols., E. Benn, Ltd., London, 1932.

59. Griffin, W. L., and V. Rama Murthy, Abundances of K, Rb, Sr and Ba in some ultramafic rocks and minerals. *Earth Planet. Sci. Letters, 4,* 497–501, 1968.

60. Allsopp, H. L., L. O. Nicolaysen, and P. Hahn-Weinheimer, Rb/K ratios and Sr-isotopic compositions of minerals in eclogitic and peridotitic rocks. *Earth Planet. Sci. Letters, 5,* 231–244, 1969.

61. Boyd, F. R., Electron-probe study of diopside inclusions from kimberlite. *Am. J. Sci., 267-A,* 50–69, 1969.

62. O'Hara, M. J., The bearing of phase equilibria studies in synthetic and natural systems on the origin and evolution of basic and ultrabasic rocks. *Earth Sci. Revs., 4,* 69–133, 1968.

63. Papike, J. J., personal communication, 1968.

64. Rickwood, P. C., M. Mathias, and J. C. Siebert, A study of garnets from eclogite and peridotite xenoliths found in kimberlite. *Contrib. Mineral Petrol., 19,* 271–301, 1968.

65. Macgregor, I. D., and J. L. Carter, The genesis of eclogite xenoliths from the Roberts Victor kimberlite pipe, South Africa. *Trans. Am. Geophys. Union, 50,* 342, 1969.

66. Boyd, F. R., and J. L. England, Apparatus for phase-equilibrium measurements at pressures up to 50 kb and temperatures up to 1750°C. *J. Geophys. Res., 65,* 741–748, 1960.

67. Foshag, W. F., Mineralogical studies on Guatemalan jade. *Smithsonian Misc. Collections, 135,* No. 5, Publ. 4307, 60 pp., 1957.

68. Clarke, J. R., and J. J. Papike, Crystal-chemical characterization of omphacites. *Am. Mineralogist, 53,* 840–868, 1968.

69. Wade, A., and R. T. Prider, The leucite-bearing rocks of the West Kimberley Area, Western Australia. *Quart. J. Geol. Soc., London, 96,* 39–98, 1940.

70. Kushiro, I., Y. Syono, and S. Akimoto, Stability of phlogopite at high pressures and possible presence of phlogopite in the earth's upper mantle. *Earth Planet. Sci. Letters, 3,* 197–203, 1967.

71. Oxburgh, E. R., Petrological evidence for the presence of amphibole in the upper mantle and its petrogenetic and geophysical implications. *Geol. Mag., 101,* 1–19, 1964.

72. Ringwood, A. E., Mineralogy of the Mantle, in *Advances in Earth Science,* P. M. Hurley, ed., M. I. T. Press, 357–399, 1964.

73. Hart, S. R., and L. T. Aldrich, Fractionation of potassium/rubidium by amphiboles: Implications regarding mantle composition. *Science, 155,* 325–327, 1967.

74. Mason, B., Kaersutite from San Carlos, Arizona, with comments on the paragenesis of this mineral. *Mineral. Mag., 36,* 997–1002, 1968.

75. Abbott, D., and J. Ferguson, The Losberg intrusion, Fochville, Transvaal. *Geol. Soc. S. Africa Trans., 68,* 31, 1965.

76. Danchin, R. V., and J. Ferguson, Differentiation trends in the Bushveld and Losberg intrusions. *Geol. Soc. S. Africa Trans.* (Willemse Volume), in press, 1969.

77. Erlank, A. J., R. V. Danchin, and C. C. Fullard, High K/Rb ratios in rocks from the Bushveld Igneous Complex, South Africa. *Earth Planet. Sci. Letters, 4,* 22–29, 1968.

78. Danchin, R. V., K and Rb in the Losberg intrusion, Transvaal, South Africa. *Earth Planet. Sci. Letters, 5,* 41–44, 1968.

79. Nicolaysen, L. O., J. W. L. de Villiers, A. J. Burger, and F. W. E. Strelow, New measurements relating to the absolute age of the Transvaal system and the Bushveld Igneous Complex. *Geol. Soc. S. Africa Trans., 61,* 137–173, 1958.

80. Allsopp, H. L., Rb-Sr and K-Ar measurements on the Great Dyke of Southern Rhodesia. *J. Geophys. Res., 70,* 977–984, 1965.

81. Larkam, C. W., Theoretical analysis of the solion polarized cathode acoustic linear transducer. *J. Acoust. Soc. Am., 37,* 664–678, 1965.

82. Herrin, E., and J. Taggart, Regional variations in P travel times. *Bull. Seis. Soc. Am., 58,* 1325–1337, 1968.

83. Oliver, J., F. Press, and M. Ewing, Two-dimensional model seismology. *Geophysics, 19,* 202–219, 1954.

84. Tolstoy, I., and E. Usdin, Dispersive properties of stratified elastic and liquid media: A ray theory, *Geophysics, 18,* 844–870, 1953.

85. Dziewonski, A., S. Block, and M. Landisman, A technique for the analysis of transient seismic signals. *Bull. Seis. Soc. Am., 59,* 427–444, 1969.

86. Gupta, I., Note on the use of reciprocity theorem for obtaining radiation patterns. *Bull. Seis. Soc. Am., 55,* 277–281, 1965.

87. Jeffreys, H., The reflection and refraction of elastic waves. *Monthly Notices Roy. Astron. Soc., Geophys. Suppl., 1,* 321–334, 1926.

88. Knott, C. G., Reflexion and refraction of elastic waves with seismological applications. *Phil. Mag., 48,* 64–97, 1899.

89. Gutenberg, B., Energy ratio of reflected and refracted seismic waves. *Bull. Seis. Soc. Am., 34,* 85–102, 1944.

90. Nuttli, O., The effect of the earth's surface on the S-wave particle motion. *Bull. Seis. Soc. Am., 51,* 237–246, 1961.

91. Ewing, M., W. Jardetzky, and F. Press, *Elastic Waves in Layered Media,* McGraw-Hill, New York, 1957.

92. Chowdhury, D. K., and P. Dehlinger, Elastic wave propagation along layers in two-dimensional models. *Bull. Seis. Soc. Am., 53,* 593–618, 1963.

93. Press, F., J. Oliver, and M. Ewing, Seismic model study of refraction from a layer of finite thickness. *Geophysics, 19,* 388–401, 1954.

94. Knopoff, L., *Q. Revs. Geophys., 2,* 625–660, 1964.

95. Suyehiro, S., T. Asada, and M. Ohtake, Foreshocks and aftershocks accompanying a perceptible earthquake in central Japan. *Papers Meteorol. Geophys. (Tokyo), 15,* 71–87, 1964.

96. Suyehiro, S., Difference between aftershocks and foreshocks in the relationship of magnitude to frequency of occurrence for the great Chilean earthquake of 1960. *Bull. Seis. Soc. Am., 56,* 185–200, 1966.

97. The Party for Seismographic Observation of Matsushiro Earthquakes and the Seismometrical Section, 1966 and 1967: Matsushiro Earthquakes Observed with a Temporary Seismographic Network. Parts 1–4, *Bull. Earthquake Res. Inst., Tokyo Univ., 45,* 67–90; *45,* 197–223; *45,* 887–917.

98. Sacks, I. S., A broad-band large dynamic range seismograph. *Geophys. Mono. 10, Am. Geophys. Union,* 543–553, 1966.

BIBLIOGRAPHY

Assousa, G. E., L. Brown, and W. K. Ford, Jr., Lifetimes of excited states in Ne I and Ne II (abstract). *Bull. Am. Phys. Soc., 14,* 485, 1969.

Baum, W. A., J. S. Hall, L. L. Marton, and M. A. Tuve, Annual Report of the Committee on Image Tubes for Telescopes. *Carnegie Inst. Wash. Year Book 67,* 389–391, 1967–1968.

Bolton, E. T., The evolution of polynucleotide sequences in DNA, in *Mendel Centenary: Genetics, Development and Evolution,* pp. 76–85, R. M. Nardone, ed., Wash., D. C., Catholic Univ. of America Press, 1968.

Brandt, W., see Brown, L.

Britten, R. J., and D. E. Kohne, Repeated sequences in DNA. *Science, 161,* 529–540, 1968.

Brooks, C., and S. R. Hart, On the realistic use of Rb-Sr isochron regression treatments (abstract). Joint Annual Meeting Geol. and Mineral. Associations of Canada, with summer meeting of the Mineral. Soc. Am., Montreal, Canada, Univ. of Montreal, June 5, 6, 7, 1969, *General Programme and Abstracts of Papers,* pp. 5–6.

Brooks, C., S. R. Hart, and T. Krogh, Implications about the mantle from K, Rb, Sr concentrations and Sr^{87}/Sr^{86} ratios of Archean volcanic rocks (abstract). *Geol. Soc. Am. Program,* 81st Ann. Meeting, Mexico City, Mexico, p. 39, Nov. 11–13, 1968.

Brooks, C., S. R. Hart, T. E. Krogh, and G. L. Davis, Carbonate contents and $^{87}Sr/^{86}Sr$ ratios of calcites from Archaean metavolcanics. *Earth and Planetary Sci. Letters, 6,* 35–38, 1969.

Brooks, C., S. R. Hart, T. E. Krogh, and G. L. Davis, The initial Sr^{87}/Sr^{86} of Michipicoten greenstones and its bearing on the development of the mantle (abstract). Joint Annual Meeting Geol. and Mineral. Associations of Canada, with summer meeting of the Mineral. Soc. Am., Montreal, Canada, Univ. of Montreal, June 5, 6, 7, 1969, *General Programme and Abstracts of Papers,* p. 6.

Brown, L., W. K. Ford, Jr., Vera Rubin, W. Trächslin, and W. Brandt, Foil- and gas-excitation of sodium spectra, in *Beam-Foil Spectroscopy, I,* pp. 45–77, S. Bashkin, ed., N.Y., Gordon and Breach, 1968.

Brown, L., and C. Petitjean, $^6Li(p, {}^3He)^4He$ reaction with polarized protons from 0.4 to 3.2 MeV. *Nucl. Phys., A117,* 343–352, 1968.

Brown, L., see also Assousa, G. E., and Petitjean, C.

Cowie, D. B., see Falkow, S.

Davis, G. L., S. R. Hart, and G. R. Tilton, Some effects of contact metamorphism on zircon ages. *Earth and Planetary Sci. Letters, 5,* 27–34, 1968.

Davis, G. L., see also Brooks, C., and Hart, S. R.

De La Haba, G., see Flexner, L. B.

Duggal, S. P., see Forbush, S. E.

Erlank, A. J., Microprobe investigation of potassium distribution in mafic and ultramafic nodules (abstract). *Trans. Am. Geophys. Union, 50,* 343, 1969.

Falkow, S., and D. B. Cowie, Intramolecular heterogeneity of the deoxyribonucleic acid of temperate bacteriophages. *J. Bacteriol., 96,* 777–784, 1968.

Fischer, G. von, W. Schreyer, G. Troll, G. Voll, and S. R. Hart, Hornblendealter aus dem ostbayerischen Grundgebirge. *Neues Jahrb. Mineral. Monatsh., 11,* 385–404, 1968.

Flexner, J. B., see Flexner, L. B.

Flexner, L. B., J. B. Flexner, G. De La Haba, and R. B. Roberts, Loss of memory as related to inhibition of cerebral protein synthesis. *J. Neurochem., 12,* 535–541, 1965.

Forbush, S. E., Variation with a period of two solar cycles in the cosmic-ray diurnal anisotropy and the superposed variations correlated with magnetic activity. *J. Geophys. Res., 74,* 3451–3468, 1969.

Forbush, S. E., S. P. Duggal, and M. A. Pomerantz, Monte Carlo experiment to determine

the statistical uncertainty for the average 24-hour wave derived from filtered and unfiltered data. *Can. J. Phys., 46,* S985–S989, 1968.

Ford, W. K., Jr., Electronic image intensification. *Ann. Rev. Astron. Astrophys., 6,* 1–12, L. Goldberg, ed., Palo Alto, Calif., Annual Reviews, Inc., 1968.

Ford, W. K., Jr., A. T. Purgathofer, and Vera C. Rubin, Optical spectra near 1 micron: the Seyfert galaxy NGC 4151 and the planetary nebula NGC 6543. *Astrophys. J., 153,* L39–L40, 1968.

Ford, W. K., Jr., and Vera C. Rubin, Spectra of emission regions in M31 (abstract). *Bull. Am. Astron. Soc., 1,* 188, 1969.

Ford, W. K., Jr., and Vera C. Rubin, The spectrum of the 1968 supernova in NGC 2713. *Publ. Astron. Soc. Pacific, 80,* 466–469, 1968.

Ford, W. K., Jr., see also Assousa, G. E., Brown, L., and Rubin, Vera C.

Hall, J. S., see Baum, W. A.

Hart, S. R., Discussion of 'K/Rb in amphiboles and amphibolites from northeastern Minnesota'. *Earth Planet. Sci. Letters, 4,* 30–31, 1968.

Hart, S. R., K, Rb, and Cs concentrations in fresh and altered abyssal tholeiites (abstract). *Geol. Soc. Am. Program,* 81st Ann. Meeting, Mexico City, Mexico, p. 128, Nov. 11–13, 1968.

Hart, S. R., and G. L. Davis, Zircon U-Pb and whole-rock Rb-Sr ages and early crustal development near Rainy Lake, Ontario. *Geol. Soc. Am. Bull., 80,* 595–616, 1969.

Hart, S. R., G. L. Davis, R. H. Steiger, and G. R. Tilton, A comparison of the isotopic mineral age variations and petrologic changes induced by contact metamorphism, in *Radiometric Dating for Geologists,* pp. 73–110. E. I. Hamilton and R. M. Farquhar, eds., N. Y. Interscience Publs., 1968.

Hart, S. R., see also Brooks, C., Davis, G. L., Fischer, G. von, and Steinhart, J. S.

James, D. E., and I. S. Sacks, Instabilities in locating hypocenters using a small number of stations—a discussion and a solution (abstract). *Earthquake Notes, Eastern Section Seis. Soc. Am., 39,* 9, 1968.

James, D. E., I. S. Sacks, E. Lazo L., and P. Aparicio G., On locating local earthquakes using small networks. *Bull. Seis. Soc. Am., 59,* 1201–1212, 1969.

Kohne, D. E., Isolation and characterization of bacterial ribosomal RNA cistrons. *Biophys. J., 8,* 1104–1118, 1968.

Kohne, D. E., Taxonomic applications of DNA hybridization techniques, in *Chemotaxonomy and Serotaxonomy, 2,* 117–130, J. G. Hawkes, ed., N. Y. Academic Press, Inc., 1968.

Kohne, D. E., see also Britten, R. J.

Krogh, T., see Brooks, C.

Marton, L. L., see Baum, W. A.

Petitjean, C., L. Brown, and R. Seyler, Polarization and phase shifts in $^6Li(p,p)^6Li$ from 0.5 to 5.6 MeV (abstract). *Bull. Am. Phys. Soc., 13,* 1448, 1968.

Petitjean, C., L. Brown, and R. Seyler, Polarization and phase shifts in $^6Li\ (p,p)^6Li$ from 0.5 to 5.6 MeV. *Nucl. Phys., A 129,* 209–219, 1969.

Petitjean, C., see also Brown, L.

Pomerantz, M. A., see Forbush, S. E.

Purgathofer, A. T., see Ford, W. K., Jr.

Roberts, R. B., *et al., A Report on National Uses and Needs for Separated Stable Isotopes,* Wash., D. C., National Academy of Sciences–National Research Council, 37 pp., July 29, 1968.

Roberts, R. B., see also Flexner, L. B.

Rubin, Vera C., and W. K. Ford, Jr., Spectrographic study of the Seyfert galaxy NGC 3227. *Astrophys. J., 154,* 431–445, 1968.

Rubin, Vera C., see also Brown, L. and Ford, W. K., Jr.

Saa, G., and I. S. Sacks, The effect of elevation and region on the P and S waves of some South American seismograph stations (abstract). *Trans. Am. Geophys. Union, 50,* 237, 1969.

Sacks, I. S., see James, D. E. and Saa, G.

Schreyer, W., see Fischer, G. von.

Seyler, R., see Petitjean, C.

Steiger, R. H., see Hart, S. R.

Steinhart, J. S., and S. R. Hart, Calibration curves for thermistors. *Deep-Sea Res., 15,* 497–503, 1968.

Stueber, A. M., Abundances of K, Rb, Sr and Sr isotopes in ultramafic rocks and minerals from western North Carolina. *Geochim. Cosmochim. Acta, 33,* 543–553, 1969.

Tilton, G. R., see Davis, G. L., and Hart, S. R.

Trächslin, W., see Brown, L.

Troll, G., see Fischer, G. von.

Turner, K. C., Dynamics of the galaxy–Magellanic Cloud system (abstract). *Astron. J., 73,* S121, 1968.

Tuve, M. A., Letters: An Open Forum, Re: Solid-earth geophysics after the termination of the Upper Mantle Project. *Trans. Am. Geophys. Union, 49,* 448–449, 1968.

Tuve, M. A., Odd Dahl at the Carnegie Institution, 1926–1936, in *Festskrift til Odd Dahl,* Fra Venner Og Kolleger, pp. 40–46, Bergen, A. S. John Griegs Boktrykkeri, 1968.

Tuve, M. A., see also Baum, W. A.

Varsavsky, C. M., Dust and atomic hydrogen in interstellar space. *Astrophys. J., 153,* 627–632, 1968.

Voll, G., see Fischer, G. von.

PERSONNEL

Director
Ellis T. Bolton

Associate Director
L. Thomas Aldrich

Staff Members

Roy J. Britten
Louis Brown
Dean B. Cowie
Scott E. Forbush [1]
W. Kent Ford, Jr.
Stanley R. Hart
Bill H. Hoyer [2]
Richard B. Roberts
I. Selwyn Sacks
John S. Steinhart [3]
Kenneth C. Turner

Staff Associates

David E. James [4]
David E. Kohne
Vera C. Rubin

Distinguished Service Member of Carnegie Institution
M. A. Tuve

Section Chairmen

Astrophysics: W. Kent Ford, Jr.
Biophysics: Dean B. Cowie
Geophysics: L. Thomas Aldrich

Fellows

George E. Assousa, Florida State University, Tallahassee, Florida
Willy Z. Barreda R., Universidad Nacional de San Agustín, Arequipa, Peru [5]
Christopher Brooks, Australian National University, Canberra, Australia [6]
J. Alfred Chiscon, Purdue University, Lafayette, Indiana [7]
Sandro D'Odorico, Osservatorio Astrofisico, Asiago, Italy [8]
Joseph W. Erkes, University of Illinois, Urbana, Illinois [9]

[1] Retired June 30, 1969.
[2] From November 1, 1968.
[3] On leave of absence from October 7, 1968, resigned June 30, 1969.
[4] From September 1, 1968.
[5] From June 1, 1969.
[6] Through November 30, 1968.
[7] Through May 31, 1969.
[8] From January 1, 1969.
[9] From September 1, 1968.

Anthony J. Erlank, University of Cape Town, Rondebosch, South Africa [10]

Leo J. Grady, Pennsylvania State University, University Park, Pennsylvania [11]

Jaime Guzman, Observatorio San Calixto, La Paz, Bolivia [12]

Kyoichi Ishizaka, Kyoto University, Kyoto, Japan [13]

David E. James, Stanford University, Stanford, California [14]

Alan T. Linde, University of Queensland, Brisbane, Australia [15]

Claude Petitjean, University of Basel, Basel, Switzerland [16]

Adrian V. Rake, University of British Columbia, Vancouver, British Columbia [17]

Nancy J. Reed, Fellow of the National Institute of General Medical Sciences, Bethesda, Maryland [18]

German Saa, S. J., Universidad del Norte, Antofagasta, Chile

Erich Steiner, University of Basel, Basel, Switzerland [19]

Research Associates

Mateo Casaverde, Instituto Geofísico del Peru, Lima, Peru

Reynaldo Salgueiro, Instituto Geofísico Boliviano, La Paz, Bolivia

Shigeji Suyehiro, Meteorological Research Institute, Tokyo, Japan

Collaborators and Visiting Investigators

Pablo Aparicio, Y.P.F.B., La Paz, Bolivia.

John Bannister, Universidad de Chile, Santiago, Chile

Francesco Bertola, Osservatorio Astrofisico, Asiago, Italy

Don J. Brenner, Walter Reed Army Institute of Research, Washington, D. C.

Ramon Cabre, S. J., Observatorio San Calixto, La Paz, Bolivia

Dorothy Canter, George Washington University, Washington, D. C.

Eric H. Davidson, Rockefeller University, New York, New York

Salvador del Pozo, Instituto Geofísico Boliviano, La Paz, Bolivia

David Denham, Geophysical Laboratory, Port Moresby, Papua and New Guinea

Ernesto Deza, Instituto Geofísico del Peru, Lima, Peru

S. Dutta, Howard University, Washington, D. C.

Dale Evertson, Applied Research Laboratory, University of Texas, Austin, Texas

Stanley Falkow, Georgetown University, Washington, D. C.

Luis Fernandez, S. J., Observatorio San Calixto, La Paz, Bolivia

Louis B. Flexner, University of Pennsylvania, Philadelphia, Pennsylvania

Josefa B. Flexner, University of Pennsylvania, Philadelphia, Pennsylvania

Jose Frez, Universidad de Chile–Zona Norte, Antofagasta, Chile

Enrique Gajardo, Centro Regional de Sismologia Para America del Sur, Lima, Peru

Albert Gelderman, National Institutes of Health, Bethesda, Maryland

Alberto A. Giesecke, Instituto Geofísico del Peru, Lima, Peru

Daniel Haapala, Georgetown University, Washington, D. C.

Anton L. Hales, Southwest Center for Advanced Studies, Dallas, Texas

Pembroke J. Hart, National Academy of Sciences, Washington, D. C.

Edgar Kausel, Universidad de Chile, Santiago, Chile

Roman Laubert, New York University, New York, New York

Eduardo Lazo, Universidad Nacional de San Agustín, Arequipa, Peru

Alfred Marshak, Tulane University, New Orleans, Louisiana

[10] From July 1, 1968.

[11] From September 1, 1968.

[12] From September 1, 1968 through October 31, 1968.

[13] Through August 31, 1968.

[14] Through August 31, 1968.

[15] From January 1, 1969.

[16] Through September 30, 1968.

[17] Through August 31, 1968.

[18] From November 11, 1968.

[19] From June 1, 1969.

Martin F. McCarthy, S. J., Observatorio Astronomico, Specola Vaticana, Italy
Jorge Mendiguren, Universidad Nacional de Cuyo, San Juan, Argentina
Robert P. Meyer, University of Wisconsin, Madison, Wisconsin
Anthony Morse, Franklin and Marshall, Philadelphia, Pennsylvania
A. J. Nalwalk, University of Connecticut, Groton, Connecticut
Jose Oblitas, Observatorio San Calixto, La Paz, Bolivia
Daniel Ochoa, Universidad Nacional de San Agustín, Arequipa, Peru
Ricardo Olea, Universidad de Chile, Santiago, Chile
Alois Th. Purgathofer, Universität Sternwarte, Vienna, Austria
Anibal Rodriguez, Universidad Nacional de San Agustín, Arequipa, Peru
Robert Safferman, U. S. Dept. of Interior, Cincinnati, Ohio
Jaime Santa Cruz, Observatorio San Calixto, La Paz, Bolivia
Richard G. Seyler, Ohio State University, Columbus, Ohio
Robert Shleser, Purdue University, Lafayette, Indiana
Diglio V. Simoni, Universidad Nacional de San Agustín, Arequipa, Peru
Russell L. Steere, U. S. Dept. of Agriculture, Beltsville, Maryland
Neil A. Straus, University of Toronto, Toronto, Canada
Lupe Tamayo, Universidad Nacional de San Agustín, Arequipa, Peru
Carlos Varsavsky, Instituto Argentino de Radioastronomía, Villa Elisa, Argentina
Fernando Volponi, Universidad Nacional de Cuyo, San Juan, Argentina
Robert F. Wing, Ohio State University, Columbus, Ohio

Design Engineer

Everett T. Ecklund

Electronic Research Specialists

Kenneth D. Burrhus
John B. Doak
Charles A. Little
Glenn R. Poe

Laboratory Assistants

Liselotte Beach
Margaret E. Chamberlin [20]
Lillian K. Prager [21]
Jean F. Smith [22]
Neltje W. van de Velde

Office

Chief, Fiscal Section: Helen E. Russell
Office Manager: William N. Dove
Assistant Fiscal Officer: Niels M. Pedersen
Librarian: Lelah J. Prothro (part time)
Secretary: Claudine C. Ator
Stenographers: Dorothy B. Dillin, E. Kathleen Hill
Typist: Mary T. Sheahan [23]

Shop

Shop Manager and Electronics Research Specialist: Paul A. Johnson
Instrumentation Research Specialist: Michael Seemann
Instrument Makers: Robert Hoffmaster, Carl M. Rinehart
Machinist: Francis J. Caherty

[20] Through August 31, 1968.
[21] From October 1, 1968.
[22] From November 4, 1968.
[23] Through March 15, 1969.

Buildings and Grounds

Carpenter and Maintenance Foreman: Leo J. Haber
Assistant Maintenance Foreman: Elliott M. Quade
Maintenance Assistant: Stanley Gawrys
Caretakers: Bennie Harris, Willis Kilgore, Jr.

Part-Time and Temporary Employees

George F. Brigham, Jr.
Joseph A. Darr
Allen Forsbacka
Kimberly A. Matthews
Stephen Nezezon
Milan Pavich
Jerome Roddy
John Roddy
Victor A. Scuderi
Carl L. Shears
Robert Tapscott

PLATES

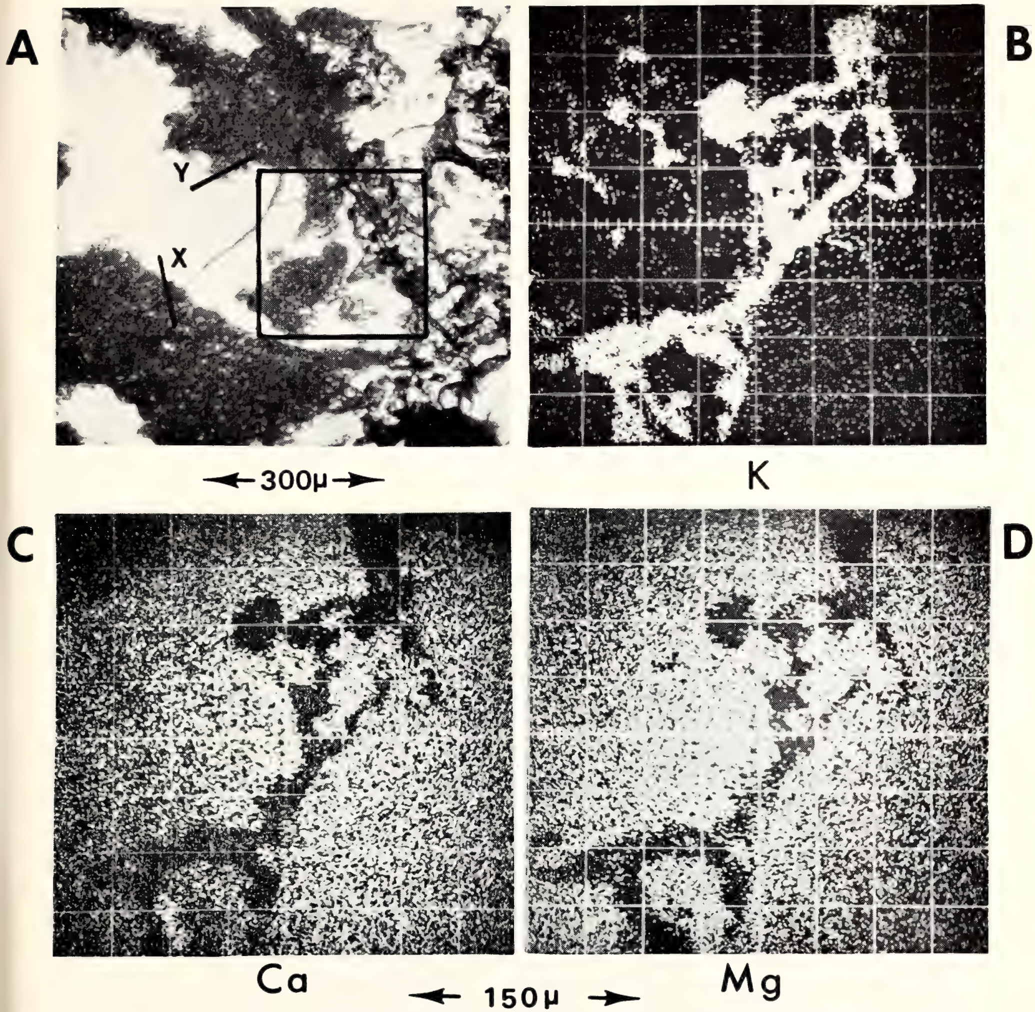

Plate 1. Secondary alteration in Roberts Victor omphacite. (A) Photomicrograph showing fresh (clear) and altered (turbid) omphacite. Boxed area indicates area covered in (B), (C), and (D) which are electron beam scanning photographs for K, Ca, and Mg radiation respectively.

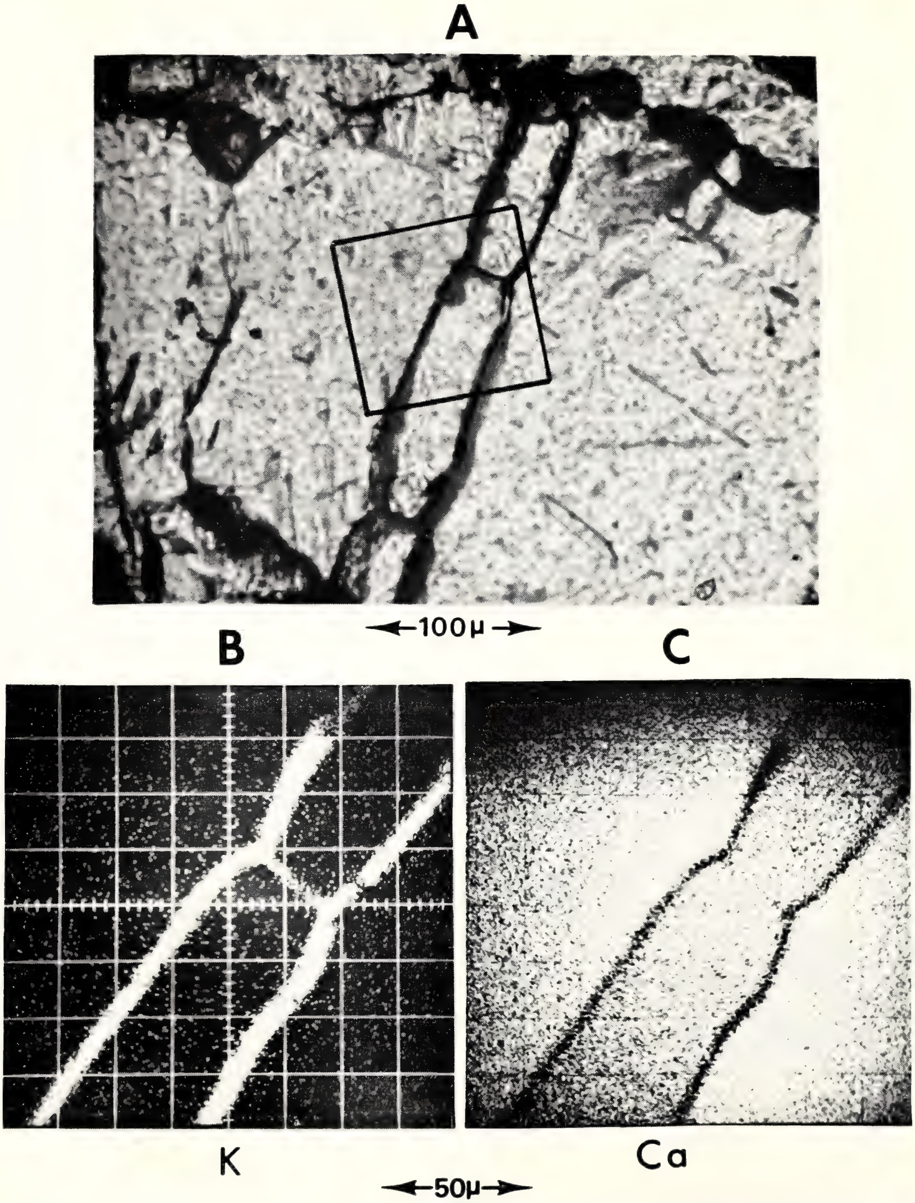

Plate 2. Location of potassium along grain boundaries in an eclogite from Tanzania. (A) Photomicrograph showing stubby garnet grains enclosed by omphacite. Boxed area indicates area covered in (B) and (C) which are electron beam scanning photographs for K and Ca radiation. Note concentration of K along cracks separating garnet and omphacite.

Plate 3. (A) Photomicrograph showing kelyphite type of alteration in garnet from a garnet peridotite. Boxed area indicates area covered in (B) which shows K X-ray radiation from an electron beam scanning photograph.

A

← 300μ →

B

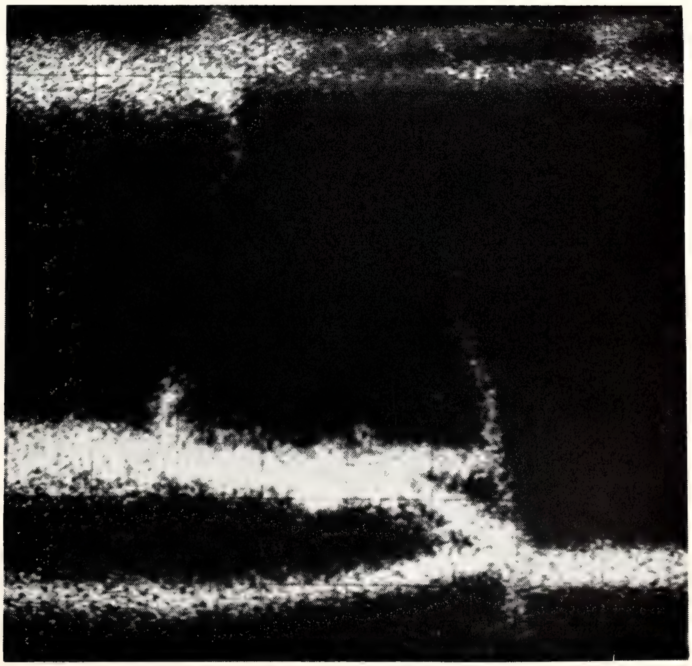

K

← 75μ →

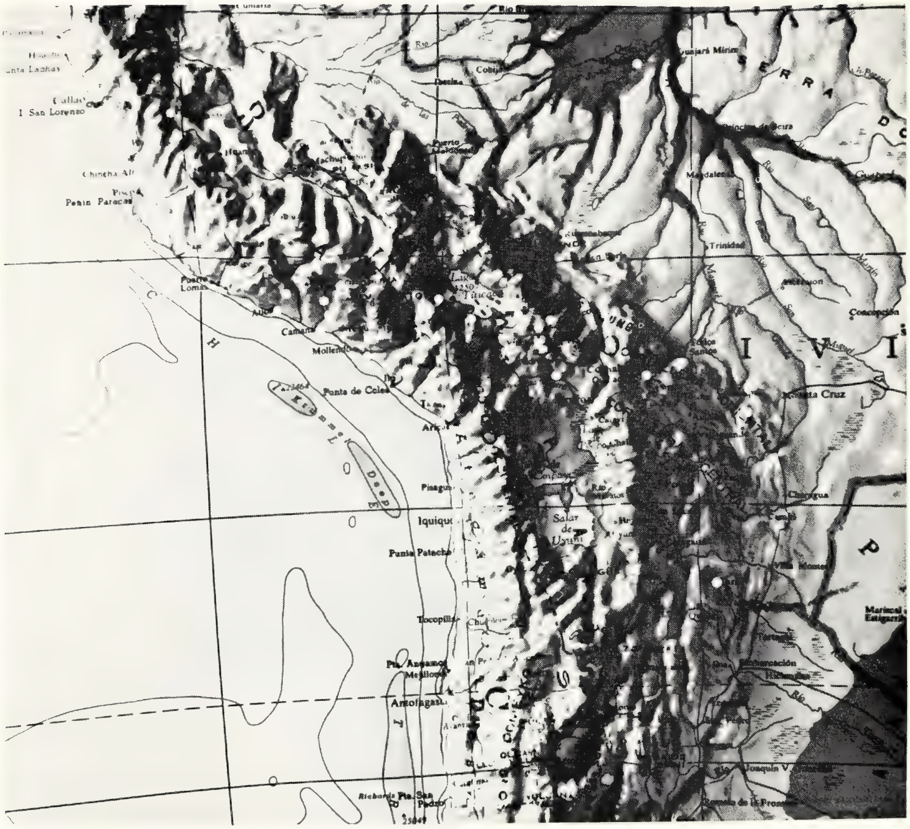

Plate 4. Seismograph stations used in this study. Most of the stations have DTM-type drum recording seismographs with a broadly peaked response having maximum sensitivity at 1.5 cps. The worldwide standard stations were used as reference stations.

Plate 5. The relationship between azimuthal variation of *P*-wave residuals and mountain chains. It was generally found that the *P*-wave arrivals were most delayed when the seismic ray path lay along and beneath the Andes cordillera.

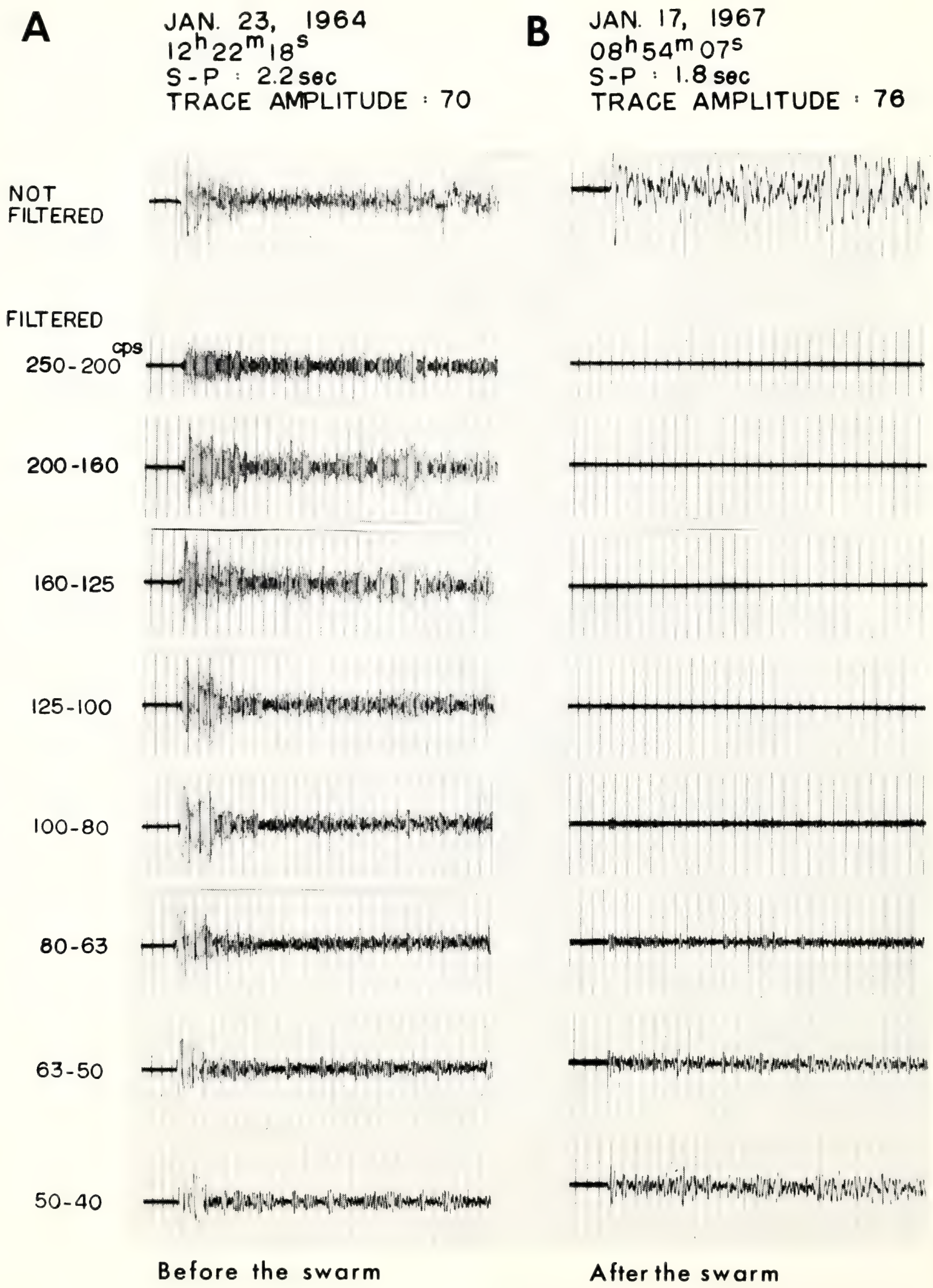
A
JAN. 23, 1964
$12^h 22^m 18^s$
S-P : 2.2 sec
TRACE AMPLITUDE : 70
B
JAN. 17, 1967
$08^h 54^m 07^s$
S-P : 1.8 sec
TRACE AMPLITUDE : 76
NOT FILTERED
FILTERED
cps
250-200
200-160
160-125
125-100
100-80
80-63
63-50
50-40
Before the swarm
After the swarm

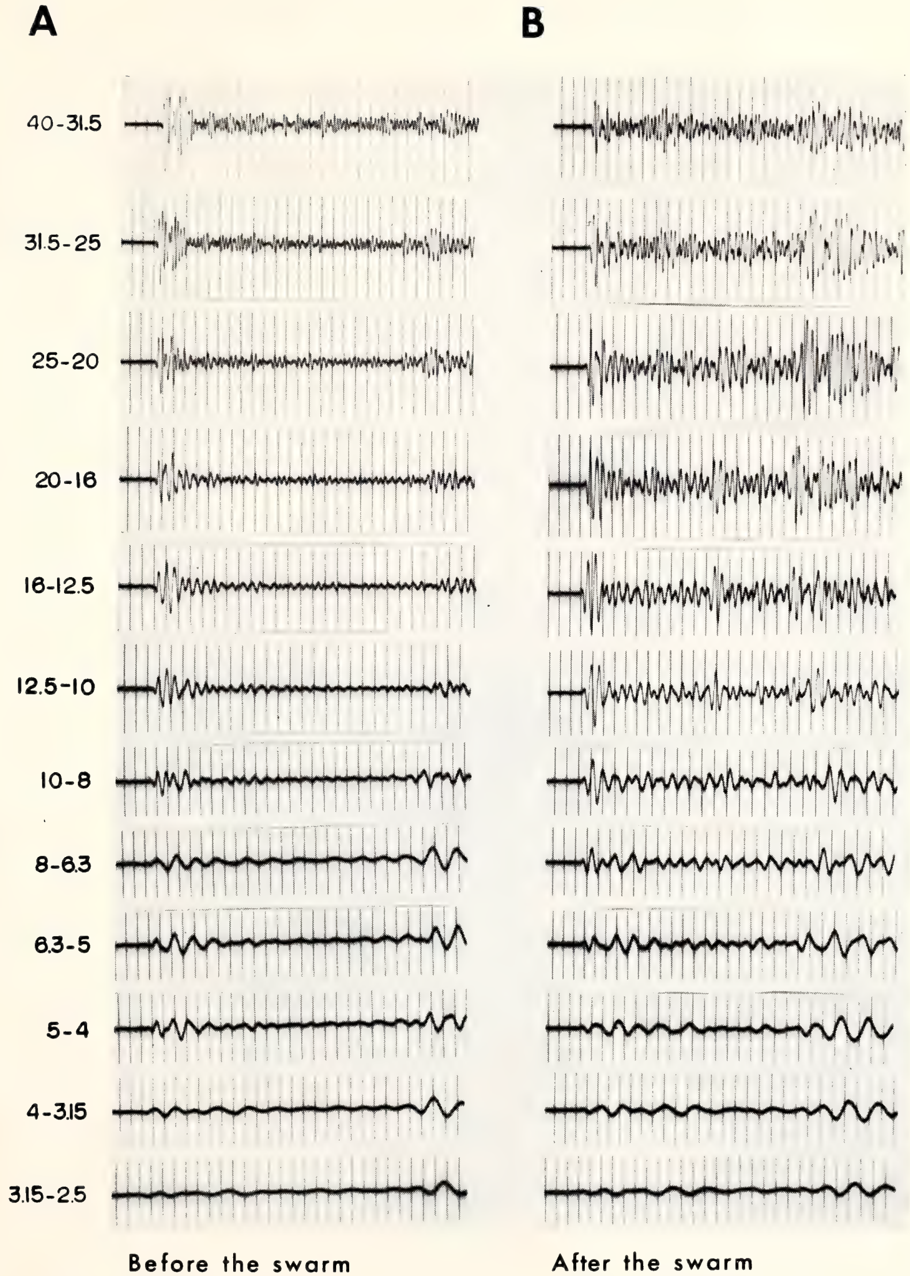

Plate 6. Records of two earthquakes of the same region which represent the year of 1964 before the swarm (A) and the year of 1967 toward the end of the swarm (B).

Committee on Image Tubes for Telescopes

Cooperative Project of Mount Wilson and Palomar Observatories, Department of Terrestrial Magnetism, Lowell Observatory, National Bureau of Standards, and United States Naval Observatory

W. A. Baum
Lowell Observatory

John S. Hall (*Chairman*)
Director, Lowell Observatory
Flagstaff, Arizona

L. L. Marton
National Bureau of Standards

M. A. Tuve
Department of Terrestrial Magnetism

REPORT OF THE COMMITTEE

The Carnegie Image Tube Committee was originally set up primarily to evaluate various methods of electronic image intensification. Many different approaches to the problem were investigated. Several years ago various tests indicated that the cascaded type of intensifier could provide an appreciable gain over unaided photography for many sorts of astronomical observations. This permanently scaled tube, which is similar in some respects to an end-on photomultiplier, multiplies primary photoelectrons internally, and displays on a phosphor screen an intensified image that is recorded photographically. Cascaded tubes developed by RCA for the Committee were found in 1963 (*Carnegie Institution of Washington Year Book 64*) to provide gains in exposure time of 10 or more over conventional photographic techniques.

Until 1963 the task of the Carnegie Committee had been to evaluate experimental tubes and to provide the manufacturers of tubes with a vigorous feedback of information and criticism of the performance of their devices. The Committee's emphasis then shifted from this evaluation and testing program to a program of procuring, assembling, and testing a number of image tube systems that could be fairly readily adapted to observational problems. These complete systems were made available to observatories requesting them through a joint NSF-Carnegie Allocations Committee. Since the inception of this activity in 1965, three dozen systems have been provided to astronomical investigators at various observatories. Nearly a third of these are outside of the United States.

The allocations program has thus been successful in introducing a powerful, new technique in astronomical research. Results obtained with these Carnegie-RCA devices appear regularly in the astronomical literature. The rate of failure of these allocated tubes due to breakage, the slumping of cathodes, or the loss of vacuum has been gratifyingly low. Fortunately, tubes of high quality continue to be available from RCA (Type C33011).

During the past year or two, the emphasis of the Carnegie Committee has changed once again. With the completion of the allocation program, more effort has been put into improving the techniques for using these tubes. In particular, Dr. I. S. Bowen * has designed several spectrograph cameras that are especially suited to image intensifier work. A contract for engineering services and a purchase order for improved tubes with high performance specifications are leading to the development at RCA of a high-gain, low-distortion version of the cascaded tube. Progress on this improved tube has thus far been most encouraging, leading us to hope that it will be completed during the coming year.

During this report year Dr. Bowen has succeeded in designing two transfer optical devices of high quality. The transfer lens has long been the weakest link in the cascaded-tube system, and we look forward to exploiting the better image quality that Dr. Bowen's new optics provide.

The development, procurement, and distribution of image tubes have been supported by the National Science Foundation and the Carnegie Institution of Washington, and the Committee wishes to express its thanks for this continuing support. We wish to acknowledge and thank Dr. W. Kent Ford, Jr., for carrying out so effectively the work on the image tube systems at the Department of Terrestrial Magnetism. We are most fortunate to have Dr. I. S. Bowen's continuing interest and assistance in solving the optical problems associated with image intensifiers.

* Distinguished Service Member, Carnegie Institution of Washington.

Department of Embryology

Baltimore, Maryland

James D. Ebert
Director

Contents

INTRODUCTION

It was an eventful year in the Department of Embryology. Although there were no serious distractions, and the work of the Department continued on an even course, a decision was reached that will affect the Department's program in the years to come. Over the next two years, the Department will undergo its most extensive reorganization since the realignment of its program after the Second World War, and possibly the most extensive in its history.

Almost since its beginning the Department has fostered three separate lines of research: human embryology, reproductive physiology (the mammalian embryo and its environment), and experimental embryology. Faithful readers of these reports hardly need be told that over the past decade more and more emphasis has been placed on exploring mechanisms of development at cellular and molecular levels. Descriptive human embryology and studies of maternal-fetal interactions have diminished perceptibly in quantity, although, happily, there has not been a corresponding drop in the quality of published work.

However, what were once three relatively small fields of research, in which the subject matter and techniques could be mastered by one or two devoted, energetic investigators, have become three vast areas for exploration, requiring a new depth and range of knowledge and technical sophistication. The "critical mass" of investigators in each of these areas is no longer one or two. Thus the decision was made to focus the Department's efforts almost entirely on studies at cellular and molecular levels. The programs in human embryology, in the conventional descriptive sense, and anatomic and physiologic studies of maternal-fetal interactions will gradually be terminated.

Fields of research evolve. The Department of Embryology was for over forty years the leader in the field of human embryology. Its Collection is by a considerable margin the finest in the world. Yet in the past decade its use has diminished. The intellectual climate of the Department has shifted. The Collection is no longer the focal point it once was—and might still be, in a different setting.

The Department also played a key role in the initiation and nurturing of the field of reproductive physiology in the primates. Now the field is expanding rapidly, largely under the impetus and leadership provided by the National Institute of Child Health and Human Development.

These considerations enabled—in fact required—that the Department's resources be marshalled so as to permit the exploration of the basic mechanisms of determination and differentiation in increasing depth.

What are the practical consequences of this far-reaching decision? Some of them will more properly be included in future reports. However two steps of the long-range program are firm enough to permit their announcement at this time.

Dr. Douglas M. Fambrough, Carnegie Fellow, and Dr. Ronald H. Reeder, Helen Hay Whitney Fellow, joined the research staff on July 1, 1969, thereby further strengthening the Department's competence in molecular biology.

In July 1971 or shortly thereafter, the Carnegie Embryological Collection (including the Bluntschli Collection) will be transferred to Wayne State University, where it will be housed in space specifically designed for it in the new Kresge Eye Institute. It is understood that qualified visiting scholars will continue to have access to it. Professor Ronan O'Rahilly, who has used the Collection extensively in recent years (and who is in residence at the Department of

Embryology in 1969–1970), will be the Director of Embryology in the Kresge Institute, and Dr. Bent G. Böving will move to Wayne State University in 1970 as Professor of Anatomy and Gynecology-Obstetrics. It is expected that under their leadership in its new location, the Collection will be used more extensively than it has been in recent years.

The history of embryology shows that the problems of development exist on many levels of complexity from the molecular to the evolutionary. They must be approached on many levels; in addition, a variety of tools and viewpoints are required, which can only be provided by the interplay of various specialized disciplines.

The most fruitful new generalizations of the immediate future are likely to emerge from the frame of perception provided by molecular genetics: the concept of levels of control, and their interactions; the concept of regulation. This is more than an expression of faith. The approaches that are increasingly characteristic of the field should permit new ideas to be perceived and new syntheses to be effected more readily than ever before. A glimpse of the possibilities that lie ahead is provided by the progress reported by Brown, Dawid, Reeder, and Wensink in their continuing study of the genes coding for ribosomal RNA. These genes are the first to be isolated from an animal genome, the ribosomal DNA and its products having been analyzed in detail in *Xenopus laevis* and other amphibians. In *Xenopus* the ribosomal RNA sequences are initially transcribed as a large 40S precursor molecule, which is then cleaved to give one 18S and one 28S rRNA molecule. The 40S precursor contains few (if any) sequences other than those for 18S and 28S rRNA. Sequences for 40S rRNA account for about half of the total length of the isolated homogeneous DNA component which has been designated as ribosomal DNA (rDNA). The 40S sequences have an average deoxyguanylic–deoxycytidylic acid (GC) content of 62%. The other half of the rDNA, called "spacer," is interspersed with the 40S sequences and has a GC content of about 77%. The spacer sequences are probably not transcribed in vivo. The 40S and spacer sequences alternate along the length of the DNA, and the unit repeats about 450 times at each nucleolar organizer in somatic cells of *X. laevis*. The active and inactive lengths of DNA are illustrated strikingly in electron micrographs by Miller and Beatty of the Oak Ridge National Laboratory. In primary oocytes of *X. laevis* the rDNA is amplified so that an individual oocyte contains about 4000 nuclear equivalents of rDNA or 1000-fold more rDNA than would be predicted from its tetraploid complement of chromosomes.

In *Year Book 67* (pp. 403–404) it was reported that the somatic rDNA (present at the nucleolar organizer of somatic cells) and the extra replicas of this DNA in oocytes differ from each other in buoyant density, the buoyant density of somatic RNA being lower by 6 mg/cm^3 than that of the extra copies. Having obtained both the somatic rDNA and extra copies in oocytes in pure form, Brown and his colleagues have been able to show that the two DNAs differ in the degree to which they are methylated, the somatic rDNA containing about 4–5% 5-methyl deoxycytidylic acid (MeC), while the extra copies contain less than 0.2% MeC. The presence of methyl groups is known to lower the density of DNA in cesium chloride and the content of MeC in somatic rDNA is probably sufficient to account for its lower buoyant density.

However it is not sufficient to isolate and describe these genes. That is only a beginning. What we need to know is how their activities are regulated. What is the basis of differential gene expression? Little is known about the way in which cytoplasmic factors may impinge upon the genome. It is known that in *Xenopus*, rDNA functions during oogenesis and

again after gastrulation, but not during cleavage. K. Shiokawa and K. Yamana of Kyushu University have described a cytoplasmic factor obtained from cleaving embryos which inhibits the formation of rRNA when it is added to embryonic cells at stages when the rDNA is known to be otherwise active. However the evidence presented does not permit one to decide whether it is an inhibition of transcription, i.e., synthesis of 40S rRNA, or "processing" of 40S rRNA to the 28S and 18S components. The potential importance of the observation is clear; we have few leads to the isolation of possible repressors in embryonic cells. However, it will be necessary to establish the *level* of the inhibition.

To do so requires first that rDNA and rRNA be isolated and characterized; that has been accomplished. A further step would be the development of a system for the synthesis of the products of rDNA in vitro. Brown, Reeder, and their colleagues have searched for conditions under which rDNA is transcribed with high fidelity in vitro. Substantial progress is now reported (pp. 506–509), using a system in which *Xenopus* rDNA is transcribed by *E. coli* RNA polymerase. The assay developed measures how much of each strand of the double-stranded rDNA is transcribed, as well as the amount and kind of RNA transcribed from the spacer region. The technique actually separates the heavy (H) strand, which is transcribed in vivo, from the light (L) strand. Studies of the complementary RNA synthesized using rDNA as template shows that it contains both rRNA and some RNA corresponding to the spacer DNA. Chain initiation appears to be very accurate, but chain termination less so, some polymerase molecules apparently continuing to transcribe beyond the 40S sequences into the spacer region.

An analogous approach is being taken by Dawid and his colleague, R. F. Swanson, a Fellow of the U. S. Public Health Service. Dawid has continued to center his attention on mitochondrial DNA and its immediate RNA products in *Xenopus*. He has now offered additional evidence that the 21S and 13S RNAs of mitochondria clearly differ from the 28S and 18S ribosomal RNAs. Moreover, preliminary hybridization experiments suggest that the 21S and 13S RNAs do not share sequence homologies. It seems likely, therefore, that different parts of the mitochondrial DNA act as templates in their formation.

At the same time Swanson has made substantial headway in studying protein synthesis in mitochondria isolated from ovaries of *Xenopus laevis*. It is known that mitochondria have the ability to synthesize proteins in vitro. However little is known of the source of informational RNA, the products themselves, or the details of the process. Swanson has developed a system in which the polynucleotides polyuridylic, polyadenylic and polycytidylic acids are taken up by isolated mitochondria. The transport of polyuridylic acid (poly U) across the mitochondrial membrane results in an increase in the incorporation of phenylaline. The system appears to offer promise of identifying the site of protein synthesis within the mitochondrion.

Another striking example of the effectiveness of interdisciplinary studies is seen in the relationship between developmental biology and virology. It was over fifty years ago that Peyton Rous discovered the tumorigenic virus that bears his name. It is less appreciated, however, that in those studies he used two techniques later to be developed further and exploited by students of development. One was the technique of transplantation of tissue fragments to the embryonic membranes of the chick embryo later used by several generations of embryologists to study the ability of embryonic tissues to differentiate when isolated in a favorable environment well removed from their normal relations with other tissues, and by students of developmental immunology in elucidating the graft-

versus-host reaction. The second was the use of the enzyme trypsin to liberate cells from clotted plasma on which they were growing, the forerunner of today's techniques of dissociating tissues into their component cells, now widely employed in studies of the manner in which embryonic cells interact in forming their characteristic patterns of tissue architecture.

But if virology contributed those techniques to the study of development, it was an embryologist, Ross Harrison, who provided the method that is widely recognized as one of the principal technical cornerstones of virology, that of tissue culture. Viruses may be now propagated in clonal lines of cells from a variety of sources, normal and abnormal; and clonally derived cells provide the most convenient and reproducible material for studies of the mechanisms of action of viruses in destroying or transforming cells.

Even now, several new developments offer promise for the future. One arises out of an idea discussed in previous *Year Books,* namely that in order to transform a cell, a tumor virus must first stimulate the synthesis of the cell's DNA. During the year, Yoshikawa-Fukada, a Carnegie Fellow, and Ebert have continued to probe into the mechanism whereby oncogenic viral infection activates part of the cellular genome. Their earlier studies (*Year Book 67,* p. 431) showed that Rous sarcoma virus RNA (RSV-RNA) contains base sequences complementary to those of DNA from a variety of sources. They now report further progress in characterizing these sequences and are attempting to determine their significance in oncogenesis. As noted a year ago (*Year Book 67,* p. 436), the portion of RSV-RNA which hybridizes with DNA from chicken cells has a high content of adenylic acid. Further studies now reveal this to be a general pattern, i.e., the segment of RSV-RNA that is enriched in adenylate is also observed in hybrids with piscine and mammalian DNAs. Is this specific segment of RSV-RNA directly involved in the transformation process? It is noteworthy that DNAs of other oncogenic viruses, e.g., adenoviruses and SV40 virus, also have a high content of deoxyadenylate. Moreover there is evidence that DNA from oncogenic viruses is integrated into the genome of the host cell.

These and other findings suggest that there may be, so to speak, a "viral oncogenic sequence," with, possibly, a corresponding sequence in the cellular genome. If such a "viral oncogenic sequence" exists, it should be revealed in viral homologies. As a first test of this scheme, Yoshikawa-Fukada and Ebert have studied the relations between RSV-RNA and the DNAs of three adenoviruses, types 2, 4, and 12. This family of adenoviruses is interesting in that types 2 and 4 are not oncogenic, while type 12 is highly oncogenic. The results are striking. RSV-RNA hybridizes far more extensively with DNA from type 12 (oncogenic) than with DNAs from types 2 and 4; moreover, preliminary analyses indicate that the RSV-RNA combining with adenovirus 12-DNA again has a high adenylate content. Experiments are also in progress to further characterize the part of the cellular DNA involved and to determine its role. The initial findings are recorded on pages 521–531. It is at this point that Yoshikawa-Fukada's and Robert J. Hay's programs interact. Hay, also working in consultation with Ebert, has continued to search for the mechanism whereby DNA synthesis is stimulated in myotubes by Rous sarcoma virus.

Mention has already been made of five Fellows and Assistant Investigators, Fambrough, Hay, Reeder, Swanson, and Yoshikawa-Fukada, whose programs are discussed more fully in the body of the Report. They are representative of a larger group of visiting scientists who have contributed impressively to the Department's vitality and well-being.

In the final year of his stay as a Fellow of Carnegie Institution, Dr. Hayden G.

Coon's work ranged widely in exploring possible applications of the technique of virus-assisted cell hybridization he developed last year in cooperation with Dr. Mary Weiss (*Year Book 67*, pp. 424–427). One of the systems being analyzed is a cross between cells producing large amounts of collagen and cells producing little or none, e.g., myeloma cells. In this work Coon was joined during part of the year by Dr. Lewis N. Lukens, on leave from Wesleyan University. On September 1, 1969, Coon took up a new position as Associate Professor of Zoology at Indiana University.

Another Carnegie Fellow, Yoshiaki Suzuki, formerly of the National Institute of Health, Tokyo, joined Brown in an attempt to isolate the genes coding for the messenger RNA that directs the synthesis of the silk protein, fibroin, in the silkworm, *Bombyx mori.* Their initial observations are described briefly later in the Report.

Dr. Francis J. Manasek, on leave from the Children's Hospital Medical Center, Boston, spent the year with R. L. DeHaan, continuing his earlier electron microscopic studies of the formation of the epicardium. In addition, he and Coon initiated an investigation of the fine structure of cells differentiating in vitro.

In July 1969, Dr. Harold E. Kasinsky, a Fellow of the U. S. Public Health Service for the past two years, took up an appointment as Assistant Professor of Zoology in the University of British Columbia.

Finally, special mention should be made of Dr. Harold R. Misenhimer who in his second year as a Carnegie Fellow brought to his collaboration with Dr. Elizabeth M. Ramsey not only intense interest and uncommon technical abilities, but a deep understanding of the difficult problems that lie ahead in the field of maternal-fetal interactions. Dr. Ramsey's program has long enjoyed close ties with the Johns Hopkins School of Medicine by virtue of her continuing association with M. W. Donner and S. I. Margulies. Now through Dr. Misenhimer there are new links to Baltimore City Hospitals, thus further strengthening the research base in the community.

During the year two students completed the requirements for the doctorate at Johns Hopkins: Iris Polinger, who had been working with DeHaan, has taken up a post in New York University College of Dentistry, and Merry C. Schwartz, one of Brown's students, has become Assistant Professor of Biology at Morgan State College. Other students whose contributions are mentioned specifically in the Report include Lynn Billingsley (with Böving), John Chase (with Dawid), Criss Hartzell (in Fambrough's laboratory) and Pieter Wensink (associated with Brown).

RIBOSOMAL RNA AND ITS GENES DURING OOGENESIS AND DEVELOPMENT OF *XENOPUS LAEVIS*

D. Brown, I. B. Dawid, R. H. Reeder, and P. Wensink

(with the technical assistance of E. Jordan and M. Rebbert)

The DNA coding for ribosomal RNA is the first group of genes to be isolated in pure form from an animal genome (see *Year Book 67*, pp. 401–404). This ribosomal DNA and its products have been analyzed in detail in the amphibian *Xenopus laevis.* In this species the ribosomal RNA (rRNA) sequences are initially transcribed as a large 40S precursor molecule, which is then cleaved to give one 18S and one 28S rRNA molecule. Several lines of evidence suggest that the 40S precursor contains few, if any, sequences other than those for 18S and 28S rRNA. Sequences for 40S rRNA account for about half of the total length

of the isolated DNA component which we have designated as ribosomal DNA (rDNA). The 40S sequences have an average deoxyguanylic-deoxycytidylic acid (GC) content of 62%. The other half of the rDNA, called "spacer," is interspersed with the 40S sequences and has a GC content of about 77%. The spacer sequences are probably not transcribed in vivo. The 40S and spacer sequences alternate along the length of the DNA, and the unit repeats about 450 times at each nucleolar organizer in somatic cells of *X. laevis.* In primary oocytes of *X. laevis* the rDNA is amplified so that an individual oocyte contains about 4000 nucleolar equivalents of rDNA or 1000-fold more rDNA than would be predicted from its tetraploid complement of chromosomes.

Two problems have concerned us during the past year. *First,* we have analyzed some physical and chemical characteristics of the rDNA which is present at the nucleolar organizer of somatic cells (somatic rDNA) as well as the extra replicas of this DNA in oocyte nuclei. Both the somatic rDNA and extra copies in oocytes have been obtained in pure form. *Second,* we have synthesized RNA in vitro using the purified rDNA as primer. The aim of these experiments is to reestablish in vitro the conditions which control both the kinds and amounts of rDNA transcribed in vivo.

The Structure of rDNA

The somatic rDNA and the extra copies in the oocyte differ from each other in buoyant density (*Year Book 67,* pp. 403–404). The buoyant density in CsCl of somatic rDNA is lower by 6 mg/cm^3 than that of the extra copies. Two possible reasons for this difference would be a difference in nucleotide sequence, or a secondary modification of one of the DNAs, such as methylation. To test these hypotheses, (^{32}P)-rDNA was prepared from cultured kidney cells (somatic rDNA) and from the ovaries of newly metamorphosed froglets (extra copies). The DNAs were enzymatically hydrolyzed to mononucleotides, the labeled nucleotides were separated by thin layer chromatography and located by radioautography (Plate 1). A single qualitative difference was detected between the two hydrolysates. The hydrolysate of somatic rDNA contains a spot identified as 5-methyl deoxycytidylic acid (MeC) which is missing in the hydrolysate of oocyte rDNA. Bulk *X. laevis* DNA contains about 1.5% of its total residues as MeC. Somatic rDNA has about 4–5% of its residues as MeC, while the extra copies do not contain any detectable MeC (less than 0.2%). The presence of methyl groups is known to lower the density of DNA in CsCl, and the content of MeC in somatic rDNA is probably sufficient to account for its lower buoyant density.

The two rDNAs have been compared by other techniques. Both rDNAs exhibit a two-part melting curve. The 40S sequences melt at a lower temperature than the spacer sequences because of the difference in their GC content. Judging from the relative hyperchromicity, the ratio of spacer to 40S sequences is similar for both rDNAs.

Another comparison of the DNAs was made by analyzing the RNA products made with RNA polymerase in vitro. Hereafter we shall refer to these RNAs made in vitro as "complementary RNA" (cRNA). The base compositions of the cRNAs synthesized on the two rDNAs are indistinguishable. At present, the only detectable difference between the somatic rDNA and extra rDNA of oocytes is that the somatic rDNA contains about 4–5% MeC, while the extra copies contain less than 0.2% MeC.

Transcription of rDNA in vitro

In the living cell rDNA is transcribed in a highly specific manner. Only one of the two DNA strands is transcribed (which we will hereafter call the heavy

strand, H), and only the 40S sequences are copied from this strand. As far as is known at present the spacer sequences and the other strand (light, L) are not transcribed. We have searched for conditions in vitro under which rDNA would be transcribed with high fidelity, i.e., in the same way as in the intact cell.

As a beginning we have used RNA polymerase from *E. coli* and have developed an assay to measure fidelity of transcription in vitro. This assay measures how much of each rDNA strand is transcribed as well as the amount of RNA transcribed from the spacer region. For the strand selection assay approximately 1 μg of rDNA is denatured, hybridized in solution with a 200-fold excess of unlabeled 18S and 28S rRNA, and then centrifuged to equilibrium in a CsCl density gradient. The rRNA hybridizes only with the strand which is transcribed in vivo (H) and since the resulting RNA-DNA hybrid is denser than the unhybridized strand (L), the two DNA strands separate in the CsCl gradient. The gradient is divided into 15 fractions, each fraction is treated with alkali to release bound RNA, and the DNA from each fraction is trapped on a separate nitrocellulose filter. One such set of filters can be hydridized with radioactive RNA synthesized in vitro to test the RNA for its homology to the strands.

The fact that this technique actually separates the H and L strands of rDNA is illustrated in Fig. 1. ^{3}H-labeled rDNA separated into two equal-sized peaks, and ^{32}P-labeled rRNA hybridized almost exclusively with the denser of the two peaks, i.e., the H strand.

The *E. coli* RNA polymerase used in these experiments was purified by the method of Burgess. Recently Burgess and his colleagues have shown that *E. coli* polymerase is composed of four different subunits. One subunit is called the S protein; it affects the specificity of chain initiation but not chain elongation. They have also shown that the S protein is

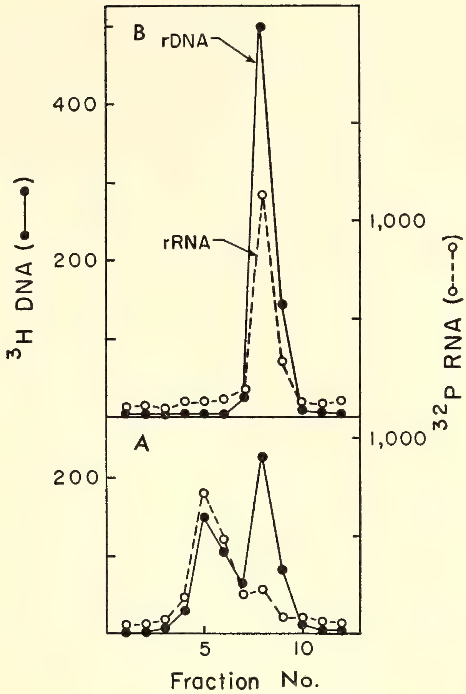

Fig. 1. Strand separation of rDNA. (A) ^{3}H-labeled rDNA was prehybridized in solution at 60°C with excess unlabeled rRNA, spun in a CsCl gradient, and collected in fractions. Each fraction was alkali treated to remove rRNA, trapped on a nitrocellulose filter, and rehybridized with ^{32}P rRNA. (B) Same as (A) except that the mixture of rDNA and unlabeled rRNA was added directly to CsCl without prehybridizing at 60°C.

largely removed from the enzyme by chromatography on phosphocellulose (PC enzyme). Other methods of enzyme purification, such as centrifugation in glycerol gradient (GG enzyme), leave the S protein attached to the enzyme.

We have tested the complementary RNA (cRNA) synthesized using rDNA as template with both RNA polymerases, i.e., with and without S protein. The cRNA was made under identical conditions with (^{3}H)-CTP and (^{32}P)-CTP included in the reaction mixtures with the GG enzyme and PC enzyme, respectively. The purified cRNAs were mixed and hybridized with a series of strand-

separated filters (Fig. 2A). *E. coli* RNA polymerase purified on a glycerol gradient (GG enzyme), and presumably containing S protein, has better than 95% specificity for reading the H strand of native rDNA. Phosphocellulose purified enzyme (PC enzyme) is less specific but still prefers the H strand. Whether this partial specificity of PC enzyme is due to some residual S protein is not yet known. Another sample of the same mixture of cRNA was assayed for sequences complementary to the spacer region by hybridization in the presence of an excess of unlabeled 28S and 18S RNA (Fig. 2b). The radioactivity remaining after competition represents spacer transcription. In other experiments it has been shown that this uncompeted RNA has a GC content of about 77%, corresponding to that of the spacer DNA. About 12% of the cRNA which hybridized to the H strand is a copy of the spacer region, suggesting that while chain initiation with the GG enzyme is very accurate, chain termination is less accurate. The PC enzyme product resembles that of the GG enzyme in this respect. Some polymerase molecules apparently continue to transcribe beyond the 40S sequence into the spacer region. These experiments suggest that the nucleotide sequence of initiation sites has been conserved during evolution, since a bacterial enzyme can identify them in an animal DNA with considerable fidelity.

Electron microscope techniques are being developed to map the gene sequences of rDNA molecules. Several methods are being investigated whose common purpose is to distinguish single-stranded from double-stranded regions of the molecule. Because of the different base compositions of the rDNA sequences, it is hoped that a "denaturation" map may be constructed as has been done by Inman with lambda phage DNA. In this method the DNA is partially melted and the denatured regions

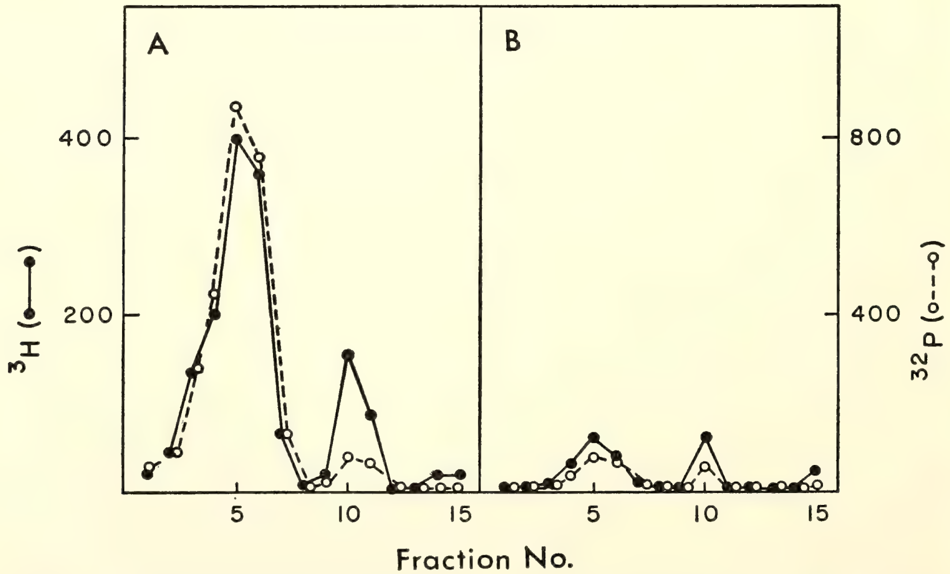

Fig. 2. Comparison of cRNAs transcribed from native rDNA by the phosphocellulose enzyme (^{3}H, solid circles, solid lines) and by the glycerol gradient enzyme (^{32}P, open circles, broken lines). The two cRNAs were mixed and hybridized on filters containing strand-separated rDNA. (A) Hybridization without competition. (B) Hybridization with excess unlabeled 18S and 28S rRNA present.

prevented from reassociating by reaction with formaldehyde. A denatured region is visualized as two thinner strands bifurcating from a thicker strand and then rejoining it. We are attempting to melt out the 40S sequences while leaving the spacer DNA double-stranded. In a second method single-stranded rDNA will be hybridized with rRNA and examined with the electron microscope. Hybrid regions should be thicker than single-stranded DNA. If this distinction can be made, then a "hybridization" map of DNA will be constructed.

GENES AND GENE PRODUCTS IN OTHER ANIMALS

I. B. Dawid, D. D. Brown and Y. Suzuki

The DNA of *Urechis caupo* Oocytes

I. B. Dawid and D. D. Brown

Urechis oocytes can be obtained in large numbers free of contaminating somatic cells. Their DNA has been isolated and characterized. The haploid DNA complement of the *Urechis* genome is 1 $\mu\mu$g. The oocyte, which is "tetraploid," contains about 10 $\mu\mu$g of DNA, more than twice the complement predicted from its chromosome content (see Schwartz, this Report, p. 511). About 60% of this DNA has been characterized as mitochondrial DNA by its presence in a mitochondrial pellet, its rapid renaturation, and the presence of circular DNA in the preparation. Furthermore, this DNA forms common networks during joint renaturation with chick mitochondrial DNA. Circular molecules of *Urechis* mitochondrial DNA have contour lengths of 5.85μ; mitochondrial DNA of *X. laevis* which was spread under identical conditions had a closely similar contour length (5.86μ).

The DNA of *Urechis* oocytes contains excess copies of rDNA. This is of particular interest since the oocyte has only a single nucleolus, a common feature of oocytes from marine invertebrates. The nuclear DNA of *Urechis* oocytes contains about 6 times as much rDNA as does sperm DNA; this corresponds to about 24 nucleolar equivalents per oocyte instead of the four predicted for a tetraploid cell. This observation extends the generality of rDNA gene amplification in oocytes to include not only amphibians, fish, several orders of insects—but now an echiuroid worm.

Differentiation of the Silk Gland in *Bombyx mori*

Y. Suzuki and D. D. Brown

An analysis of genes and gene products has been undertaken for the posterior portion of the silk gland in the silkworm, *Bombyx mori*. It is our hope to isolate in pure form the genes which code for the messenger RNA which in turn directs the synthesis of the silk protein, fibroin. Although ribosomal RNA genes have been isolated from animal DNA, no purification of a gene which codes for a specific cellular protein has been successful. It is the regulation of these latter genes which best characterizes a differentiated cell. During the fifth instar the posterior part of the silk gland synthesizes most of its protein as silk fibroin. This unusual protein contains alternating glycine residues in the crystalline region and about 73% of its total amino acids as glycine and alanine. Of particular interest is the predicted nucleotide composition of its gene which can be estimated from the codons for glycine and alanine (GGX and GCY, respectively). The messenger RNA (and gene) for fibroin should have a base composition of between 62 and 82% GC depending upon the identity of the terminal nucleotide (X and Y above). Bulk *Bombyx* DNA is 38% GC. This difference in base composition should help in

the separation of the fibroin gene from bulk DNA.

Work to date has involved learning how to grow the animals and the isolation and labeling methods for their DNA. Of particular importance is the availability of an established cell line from ovarian tissue of *Bombyx* which is now growing in the laboratory. We have benefited greatly in these initial experiments by the advice and generosity of Dr. J. L. Vaughn of the U. S. Agricultural Research Service at Beltsville, Maryland, and Dr. M. Himeno of Kyoto University, Japan, both of whom are experts in raising *Bombyx*.

NUCLEIC ACID METABOLISM IN OOCYTES AND EMBRYOS OF *URECHIS CAUPO*

Merry C. Schwartz

The advantages of the echiuroid worm *Urechis caupo* for the analysis of nucleic acid metabolism during both gametogenesis and embryogenesis were discussed in *Year Book 67,* pp. 413–417.

A survey of the nucleic acid content of *Urechis* embryos throughout embryogenesis is summarized in Fig. 3. In the mature fertilizable oocyte, 10% of the total RNA is 4S RNA, with rRNA (i.e., 18S and 28S ribosomal RNAs) accounting for about 90% of the total. Thus there are 10 molecules of 4S RNA in the oocyte for each ribosome present. The 5S RNA, the third structural RNA of the ribosome, represents approximately 1% of the total RNA, or about one molecule per ribosome present. These relative amounts of 4S RNA, 5S RNA, and rRNA are similar to those found in most adult somatic tissues.

The embryo's content of both total RNA (reflecting primarily rRNA) and 4S RNA remain virtually unchanged throughout embryogenesis. However, net increases in minor RNA species, e.g., messenger RNAs or specific transfer RNAs, would not be detected by these methods. Such synthesis, although quantitatively relatively insignificant, could be qualitatively very important for embryogenesis.

The haploid DNA complement for *Urechis,* as determined in sperm, is 1 pg. A mature oocyte is tetraploid and contains 10 pg of DNA, 4 pg of nuclear DNA, and approximately 6 pg of mitochondrial DNA (see Dawid and Brown, this Report, p. 509). By the trochophore stage the larva's DNA content has increased to 1.8 mμg, corresponding to 900 diploid cells. Thus, with regard to net nucleic acid synthesis, DNA is the primary product of embryogenesis in *Urechis caupo.*

Since the embryo's RNA content is approximately constant, one would like to know whether the maternal RNAs stored in the oocyte are conserved or replaced during embryogenesis. Therefore, the relative synthesis of RNA and DNA was monitored at several embryonic stages. Embryos were incubated with ^{32}P-phosphate and the relative incorporation of radioactivity into various nucleic acids reflects their relative rates of synthesis. As shown in Fig. 4, DNA synthesis predominates during embryogenesis up to and including the post-gastrula stage. Since the amount of DNA synthesized during embryogenesis (1.8 mμg per embryo) is much less than the total RNA content of the embryo (14 mμg), and since the synthesis of DNA greatly exceeds that of RNA throughout this period, then only a small fraction of the embryo's RNA could be synthesized after fertilization. Other experiments measured the total amount of RNA synthesized and accumulated up to the post-gastrula stage and demonstrated that less than 9% of the 4S RNA and 3% of the rRNA present in the post-

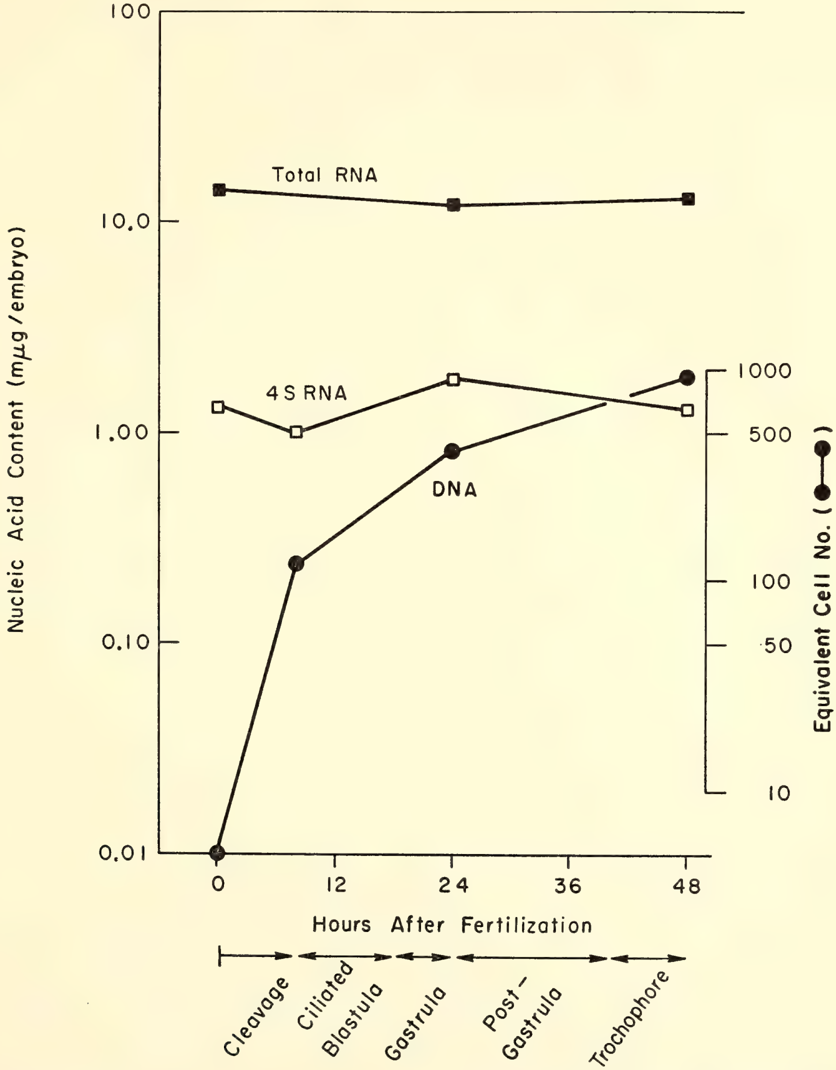

Fig. 3. Nucleic acid content (μmg/embryo) of *Urechis* embryos. The 4S RNA, total RNA, and DNA content per embryo are plotted as a function of time after fertilization. The equivalent cell numbers (solid circles) were calculated from the DNA content per embryo using 2 pg as the DNA content of each diploid cell.

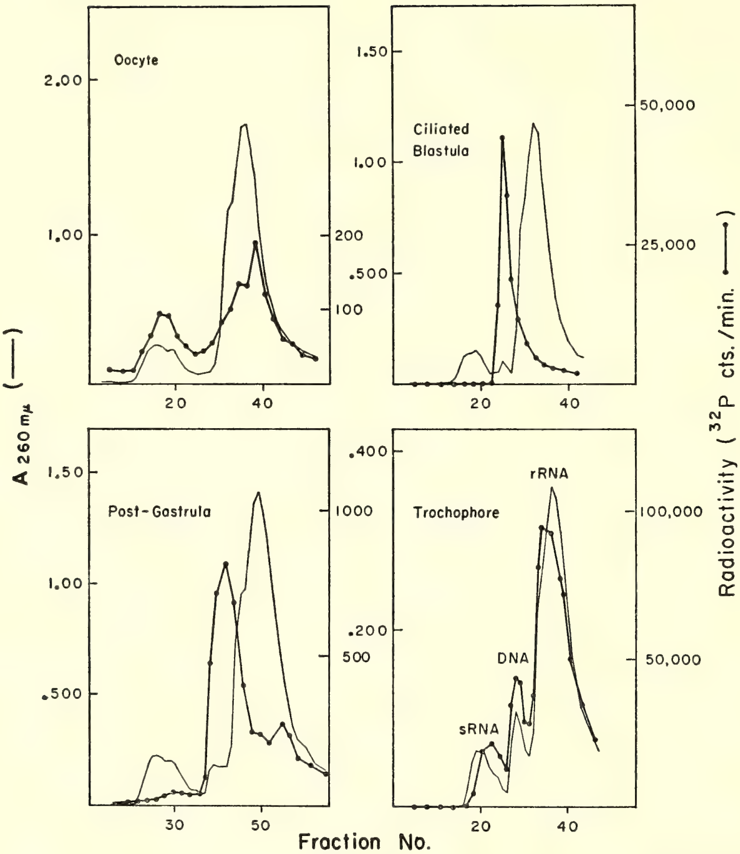

Fig. 4. Nucleic acid synthesis in the mature oocyte, ciliated blastula, post-gastrula, and trochophore larva of *Urechis*. Eggs and embryos were incubated in ^{32}P-phosphate and the nucleic acids were extracted and fractionated on a MAK column. No comparisons of the radioactivity incorporated at different stages can be made because of variations in the number of embryos and differences in the incubation conditions.

gastrula embryo could have been synthesized after fertilization.

RNA synthesis is not totally absent during embryogenesis: the synthesis of rRNA, 4S RNA, 5S RNA, and heterogeneous RNA was observed. The measurement of the relative rates of synthesis of specific classes of RNA can provide insights into the mechanisms which regulate RNA transcription during embryogenesis. During cleavage both 4S RNA and heterogeneous, nonmethylated high molecular weight RNAs are synthesized. The rate of synthesis of 4S RNA per cell remains virtually constant through cleavage, gastrula, and post-gastrula stages. During this same period the synthesis of rRNA, which is not detectable during cleavage, increases at least 13-fold. The dramatic increase in the synthesis of rRNA relative to 4S RNA synthesis between ciliated blastula and post-gastrula stages is shown in Fig. 5. Thus, during embryogenesis, the synthesis of 4S RNA is regulated independently of the synthesis of rRNA.

Similarly, the relative synthesis of 4S RNA and 5S RNA has been compared at various developmental stages. The synthesis of 5S RNA relative to 4S RNA is much greater in the trochophore larva than in the earlier stages of embryogene-

sis or in the mature oocyte. By combining data of this type with the preceding comparison of 4S RNA and rRNA synthesis, it is seen that whereas the synthesis of 4S RNA is independent of rRNA synthesis, the regulation of 5S RNA is coordinate with the synthesis of the other two ribosomal RNAs.

These results obtained in a spirally cleaving embryo can be compared with the synthetic patterns observed in the radially cleaving embryo of *Xenopus laevis.* Two basic features are common to both embryos: maternal RNAs are conserved throughout embryogenesis and must function significantly in protein synthesis in the embryo; and, the synthesis of the three RNAs of the ribosome appears to be coordinate and regulated independently of the synthesis of 4S RNA. Thus, basic differences in nucleic acid metabolism between mosaic and regulative embryos, if indeed such differences do exist, must be more subtle than are the general patterns observed in this investigation.

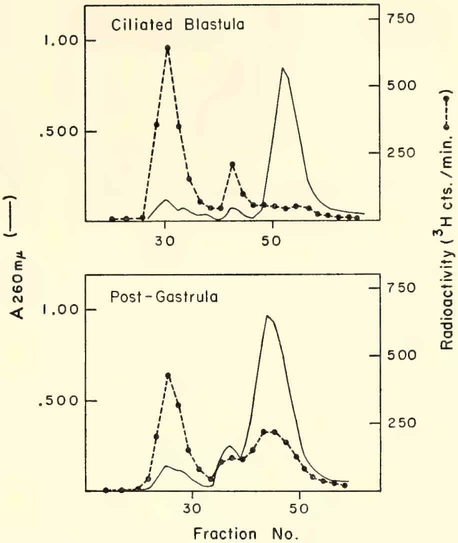

Fig. 5. The methylation of nucleic acids in ciliated blastulae and post-gastrulae of *Urechis.* Two suspensions of sibling embryos were incubated with ^{3}H-methyl L-methionine at ciliated blastula and post-gastrula stages. At the end of the pulse the nucleic acids were extracted and fractionated on MAK.

HISTONE SYNTHESIS IN CLEAVING EMBRYOS OF *XENOPUS LAEVIS*

H. E. Kasinsky

In our studies of the role of protein synthesis in early development (*Year Book 67,* p. 417), we have concentrated on following up an observation made by Hallberg (*Year Book 67,* pp. 409–413) in the course of his study of ribosomal protein synthesis in *Xenopus laevis* embryos. Hallberg noted that about 8% of the total protein synthesized by cleaving embryos pulsed with $^{14}CO_2$ eluted as a single peak from a carboxymethyl cellulose column (see Fraction C, *ibid.,* Fig. 9). Electrophoresis of this radioactive protein on acrylamide gels showed the presence of two radioactive bands which were distinct from known ribosomal proteins (*Ibid.,* Plate 2). Furthermore, these two proteins were accumulated by the swimming tadpole to the extent that they were visible as both stainable and radioactive bands in both normal and anucleolate embryos (*Ibid.,* Plate 3). Our experiments now suggest that both proteins are histones.

Nuclei were prepared from erythrocytes of adult *Xenopus* by lysing the cells in distilled water. Chromatin was prepared from these nuclei by the method of Bonner *et al.* in *Methods in Enzymology,* XII:B (1968). Nuclear sap and ribosomal proteins were extracted with saline-EDTA and 0.05 *M* Tris buffer, *p*H 8, respectively. The chromatin was purified by centrifugation through a sucrose gradient, the sucrose dialyzed away and the histone extracted from the

chromatin with 0.4 N H_2SO_4. The histones were pretreated with 50 mM dithiothreitol and then electrophosed on 15% gels of polyacrylamide at *p*H 4.5 in urea. Gels were stained with amido black, photographed, and the band pattern traced in the Joyce-Loebl microdensitometer. In order to determine the position of radioactive bands, the gels were dried on filter paper and autoradiographed according to the method of Fairbanks *et al.* (*Biochem. Biophys. Res. Commun., 20,* 393, 1965). Microdensitometer tracings of the radioactive bands exposed on X-ray film were recorded.

Figure 6 shows that two proteins in Fraction C from embryos coelectrophorese with two of the three main bands of *Xenopus* erythrocyte histones. Furthermore, as seen in Plate 2, the position of the fast-moving band in Fraction C coincides with arginine-rich histone IV (Fambrough and Bonner, *Biochemistry 5,* 2563, 1966), which is known to have almost the same amino acid sequence in both pea and calf. (Pea histone IV was generously donated to us by Douglas Fambrough.) In Plate 2, the bands at the top, close to the origin, are those of bovine serum albumin used as a marker in these experiments. In Fig. 6 we have reproduced only the tracings of the center portion of each gel and have omitted the albumin bands. We conclude that the fast-moving band in Fraction C from both cleaving embryos and swimming tadpoles is probably histone IV, the ubiquitous histone whose structure has been conserved almost completely during evolution.

The data from Hallberg's experiments suggest that these two proteins are synthesized *de novo* during early *Xenopus* development and represent a large fraction of the protein made during cleavage. If there are 5 major types of histone in *Xenopus,* as has been described for other eukaryotes, then as much as 20% of the proteins synthesized before gastrulation may be of this class of proteins.

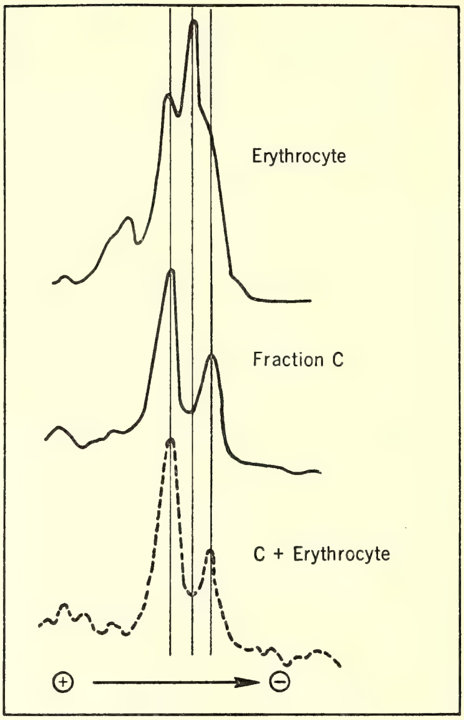

Fig. 6. Microdensitometer tracings of acrylamide gels after electrophoretic fractionation of *Xenopus* erythrocyte histones and Fraction C proteins from swimming tadpoles: solid lines, amidoblack stain; broken lines, radioautogram.

STUDIES ON MITOCHONDRIA FROM *XENOPUS LAEVIS*: THEIR COMPOSITION, FUNCTIONS, AND BIOGENESIS

I. B. Dawid, R. F. Swanson, J. W. Chase, and M. Rebbert

Mitochondrial RNA

I. B. Dawid, with the assistance of Martha Rebbert

Last year it was reported (*Year Book 67,* p. 418) that mitochondria from *Xenopus laevis* oocytes contain two unique RNA species which behave in electrophoresis on polyacrylamide gels as is expected of 21S and 13S RNA. In addition, these preparations contain 4S RNA and

some 28S and 18S RNA (rRNA). The 28S and 18S RNAs are considered contaminants since they can be largely eliminated by RNase treatment of intact mitochondria, or by removing the outer mitochondrial membrane with digitonin.

How and where do the two mitochondrial RNAs (M-RNAs) originate, i.e., on which DNA templates are they transcribed: nuclear or mitochondrial? Hybridization experiments were carried out in an attempt to answer this question. ^{32}P-labeled RNA was prepared from mitochondria obtained from cultured *X. laevis* kidney cells that had been labeled for several generations. Such preparations contained large amounts of rRNA in addition to the 21S and 13S RNA species. These contaminants did not interfere in the hybridization experiments, for the purified mitochondrial DNA (M-DNA) employed had been extensively characterized as being free of contamination with nuclear DNA. DNA and 4S RNA were removed from the labeled RNA which was then tested for its ability to hybridize with mitochondrial and with nuclear DNA (Table 1). M-DNA hybridized well with this RNA and the level of hybridization was not reduced by the addition of excess nonradioactive rRNA. Nuclear DNA hybridized at a much lower level and unlabeled rRNA competed in this hybridization. It appears likely that the mitochondrial components in the mixture (21S and 13S RNAs) hybridized with M-DNA, whereas the ribosomal components (28S and 18S) hybridized with the nuclear DNA. This conclusion is supported by determinations of the base composition of the RNA hybridized with nuclear or mitochondrial DNAs. It has been shown earlier that M-RNA has a base composition low in GC content (45%), whereas the GC content of rRNA is much higher (62%). The results in Table 2 show that RNA which hybridized with M-DNA has a much lower GC content than that which hybridized with nuclear DNA. Preliminary hybridization experiments suggest that 21S and 13S RNAs do not share sequence homologies; therefore it is likely that different portions of the M-DNA act as templates in the formation of these RNA species.

TABLE 1. Hybridization of Partially Purified Mitochondrial RNA

	Unlabeled rRNA	RNA in Hybrid, cpm
M-DNA, 5 μg	0	3960
M-DNA, 5 μg	50 μg	4270
N-DNA, 40 μg	0	710
N-DNA, 40 μg	50 μg	106

Note: The ^{32}P-RNA was used at a concentration of 5 μg in 2 ml of 4 × SSC; the preparation contained about 65% rRNA (18S and 28S) and 35% mitochondrial RNA (13S and 21S). N-DNA is nuclear DNA.

TABLE 2. Base Composition of Hybridized ^{32}P-RNA

Acid	In Hybrid with N-DNA	In Hybrid with M-DNA
Cytidylic	32	25
Guanylic	26	16
Adenylic	25	36
Uridylic	17	23

The nature and function of the 21S and 13S mitochondrial RNA is as yet unknown. The 21S component is present in about twice the concentration of the 13S component and, although their molecular weights are not known accurately, it appears likely that the two components are present in a stoichiometric ratio of one.

Protein Synthesis in Mitochondria from Ovaries of *Xenopus laevis*.

R. F. Swanson

In recent years it has been shown that mitochondria have the ability to synthesize proteins in vitro. While the fact itself is well established, the nature of the products, the source of the informational RNA, and the mechanism of synthesis are not well understood. Ribosomelike particles have been isolated from *Neurospora* and yeast mitochondria, but a submitochondrial system of protein synthesis has not been established.

Several aspects of protein synthesis in mitochondria isolated from *X. laevis* ovaries have now been investigated. Bacterial counts, energy requirements, stability to ribonuclease, inhibition by chloramphenicol, and lack of inhibition by cycloheximide suggest that the observed protein synthesis is not due to contamination of the mitochondrial system by either bacteria or cytoplasmic ribosomes.

Several characteristics of mitochondrial protein synthesis could be studied by following up the observation that polyuridylic acid (poly U) is able to enter isolated mitochondria and subsequently direct polypeptide synthesis. This observation also provides a possible basis for a model system for the study of the coding properties of nonmitochondrial RNA, both natural and synthetic, in mitochondrial protein synthesis. In addition to poly U, polyadenylic and polycytidylic acids are taken up by isolated mitochondria. Incorporation of ^{3}H-polynucleotides was measured as incorporation of radioactivity into a form which is no longer digested by pancreatic ribonuclease. The reaction has an absolute requirement for magnesium ions and is greatly stimulated by mercaptoethanol. Incorporation does not occur at 0°C. Neither *Xenopus* RNA nor DNA, native or denatured, was incorporated under these conditions, nor was RNA from bacteriophage MS 2. Mitochondrial incorporation of poly U was also followed by measuring the stimulation of ribonuclease-insensitive phenylalanine incorporation (Table 3). In the absence of poly U, or when ribonuclease and poly U are added simultaneously, the rate of phenylalanine incorporation is very low. Ribonuclease had no effect when added after mitochondria were incubated with poly U for a short period of time. These results indicate that a mechanism exists for the transport of "messenger RNA" across the mitochondrial membrane.

In an attempt to identify the intramitochondrial site of protein synthesis, mitochondria were incubated with a mixture of ^{14}C-amino acids or with poly U and ^{3}H-phenylalanine. The mitochondria were disrupted with the nonionic detergent NP40 and the distribution of acid insoluble radioactivity was analyzed after sedimentation through sucrose gradients (Fig. 7). In the absence of any further treatment radioactivity was spread throughout the gradient. However, when a small amount of ribonuclease was added before centrifugation there was an increase in the amount of labeled material having a sedimentation coefficient of 55S and a decrease in more rapidly sedimenting radioactive material. The UV-absorbing material sedimenting at 80S probably represents cytoplasmic ribosomes which contaminate the mitochondrial preparation, since this material is removed by incubation of intact mitochondria with ribonuclease and by other means (see above) which do not affect mitochondrial protein synthesis.

A possible interpretation of these results is that the 55S material represents single mitochondrial "ribosomes," the amount of which is increased as a result of digestion of "polyribosomes" by ribonuclease. If this suggestion were corroborated, the mitochondrial ribosome would be the smallest known.

TABLE 3. Polyuridylic Acid Stimulation of Phenylalanine Incorporation by *Xenopus Mitochondria*

	Radioactivity (cpm) incorporated
	60 min
Complete system	2700
Ribonuclease added after poly U	2880
Ribonuclease added before poly U	90
Minus poly U	80

Note: Mitochondria were incubated with poly U (500 μg/ml) for 10 minutes at 22°C. Ribonuclease (100 μg/ml) was added either before or after incubation of mitochondria with poly U as indicated. Aliquots of mitochondria were assayed in a second incubation period for ability to incorporate ^{3}H-phenylalanine into hot TCA precipitable material.

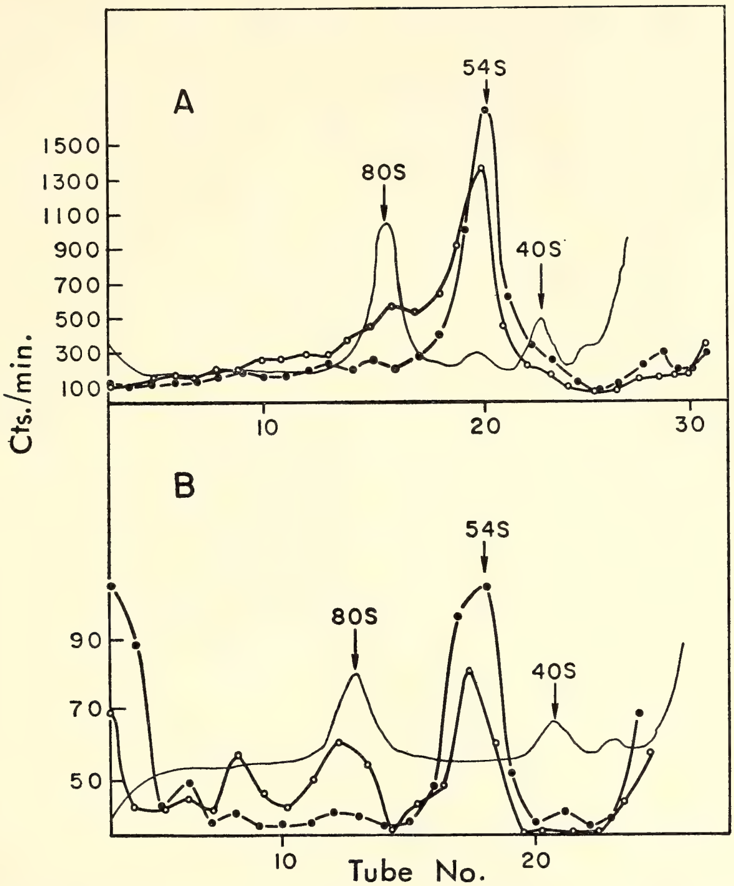

Fig. 7. Sedimentation of mitochondrial extracts. (A) Mitochondria were incubated with poly U and then with ^{3}H-phenylalanine. After disruption of the mitochondria with the detergent NP40, debris were removed by centrifugation at 20,000 $\times$ *g* and the supernatant was layered on buffered 15–30% sucrose gradients containing magnesium and potassium ions. After centrifugation the distribution of hot TCA precipitable radioactive material was determined. No additions (open circles). Ribonuclease (1 μg/ml) added before centrifugation (solid circles). Solid line represents O.D. 260. (B) Mitochondria were incubated with a mixture of ^{14}C–amino acids. Detergent treatment and sedimentation and sedimentation analysis were then carried out as described under (A).

Formation of Mitochondria During Embryogenesis of *Xenopus laevis*

J. W. Chase

During the past year we have begun a study of mitochondrial biogenesis in the embryonic development of *Xenopus laevis*. The study is intended to determine the time course of the formation of mitochondria and some mitochondrial components during embryogenesis. Initially, we have determined the content of total mitochondrial protein and the amount of cytochrome oxidase activity per embryo throughout development. The content of mitochondrial protein in the unfertilized egg is about 10 μg and does not change until just after hatching (stages 37–39). It then increases, and has doubled by stage 45 (feeding). Cytochrome oxidase activity is about 0.03 μatom oxygen/min/egg in the unfertil-

ized egg, remains constant until stages 37–39, and doubles by feeding. Thus, we find no change in the specific activity of cytochrome oxidase during early development of *Xenopus,* contrary to the earlier report of Weber and Boell. This difference may be due to a different method of preparation of the mitochondria. Earlier work had been done with particles washed by differential centrifugation; used on frog eggs and embryos, however, this technique yields preparations containing varying amounts of pigment which contributes to the apparent mitochondrial protein. In the present work continuous sucrose and discontinuous ficoll gradients were used to obtain mitochondria. The sucrose technique introduced a difficulty: since the particles obtained were similar to osmotically lysed mitochondria when examined with the electron microscope, it appeared possible that we had lost most of the soluble proteins during the purification, which loss would result in inaccurate values for total mitochondrial protein. However, we have discounted this explanation of our results on the basis of experiments which show that the same proportion of soluble protein can be extracted from the mitochondria from eggs and embryos prepared by either differential centrifugation or by sucrose gradients, and that glutamic dehydrogenase (a soluble mitochondrial enzyme) is localized only in the mitochondrial band in sucrose gradients.

We are now concentrating on mitochondrial nucleic acid synthesis during development. The experiments on mitochondrial protein content were conducted to determine the stage at which mitochandrial protein, and presumably the mitochondrial population, increases. Studies on the synthesis of mitochondrial nucleic acids will be related to this time course of the rise in mitochondrial protein.

CELL DIFFERENTIATION AND VIRAL SUSCEPTIBILITY

R. J. Hay, M. Yoshikawa-Fukada, and J. D. Ebert
(assisted by D. Somerville and B. Smith)

Do Isolated Myotubes Synthesize DNA After Exposure to Rous Sarcoma Virus?

The observation that DNA synthesis occurs in myotubes of muscle colonies in culture after infection with Rous Sarcoma Virus (RSV) raises several questions (*Year Book 67,* pp. 429–431). One phase of our program this year involved attempts to determine whether or not *isolated* myotubes could be induced to synthesize DNA after exposure to RSV. Three methods for separating myotubes and myoblasts were employed. The first required exposure of clonal cultures to vincoleucoblastine (VLB) as described previously (*Year Book 67,* p. 431). Our main objection to this method is the possibility that VLB induces irreversible changes in myotube metabolism not apparent by morphological examination.

The second method of separation involved subcultivation, at high dilution, on collagen-coated culture dishes. Clonal cultures were washed three times in succession with Hanks' BSS minus divalent cations. Trypsin (Difco 1:250) at 0.01%, which had been brought to 37°C, was added. The solution was allowed to cover the culture surface and was then removed immediately. After incubation at 37°C for 5 minutes, a suspension of fibroblasts, myoblasts, and myotubes was prepared in medium F12 215 by gentle mixing using a wide-bore pipette. Aliquots of this suspension were then added to culture vessels containing F12 215. Typical muscle syncytia (Plate 3A)

could be located 15–24 hours after addition to the culture vessel. Individual syncytia could be isolated physically from myoblasts and fibroblasts by using conventional porcelain penicylinders if a suitable dilution factor had been used initially.

We exposed myotubes, isolated by either of these methods, to dilutions of RSV ranging from 5×10^5 to 10^7 focus-forming units per ml. The cultures were then pulsed for 3 hours with tritiated thymidine at 12, 24, 48, or 72 hours after exposure to the virus. Despite repeated attempts, varying the time between isolation and infection as well as virus dose, we could obtain no unequivocal evidence for thymidine incorporation in syncytia exposed to RSV. These negative findings add support to the hypothesis that RSV gains entry and exerts its effect on the myotube by infecting the myoblast at some time prior to fusion. Additional support for this assumption derives from work done with the third system for separating myoblasts and myotubes, using somewhat different culture conditions, described below.

Effects of RSV in a Relatively Synchronous Mass Muscle Culture System

The formation of myotubes in clonal culture is an asynchronous process in which myoblast fusion takes place over an interval of 7–9 days (*Year Book 62*, p. 441). Myoblast fusion in mass muscle culture is very synchronous in comparison. It seemed probable that in gaining insight into the mode of action of RSV on DNA synthesis in myotubes, a higher degree of synchrony than that offered by clonal cultures would be required, especially because of the role of the myoblast suggested above. For this reason we developed a novel mass culture system for muscle which we have used extensively in more recent studies. The procedure finally adopted consisted of the following general steps.

Cell suspensions were prepared from 11-day embryonic chick leg muscle and were seeded in F12 215 at high density (4×10^7 cells/9 cm plate). After 18–26 hours of incubation the monolayer was washed three times with Hanks' BSS minus divalent cations and was treated briefly with 0.05% trypsin. The trypsin was removed and the cells were suspended in F12 215 warmed to 37°C. The cell number was adjusted to 10^6/ml and the suspension was added to 9 cm plates (10 ml/plate). After incubation for 90 minutes to allow fibroblasts to adhere preferentially, the cells still in suspension (predominantly myoblasts) were removed. The adhering cells were washed gently three times with medium and the washes were added to the cell suspension obtained. This differential adhesion (DA) method for increasing the ratio of myoblasts to fibroblasts gives a higher cell yield, more reproducible results and at least as high a ratio of myoblasts (80% or more by clonal analysis) as does the differential trypsinization method used earlier (*Year Book 64*, p. 484).

Cell suspensions prepared by the DA method were used to seed collagen-coated, 35 mm Falcon plates ($2.5–5 \times 10^5$ cells/plate). By microscopic examination at 16- and 8-hour alternating intervals, it was found that myoblast fusion is most extensive during the interval from 40 to 72 hours after DA cell seeding. Although this period of active fusion varies slightly among experiments, the system is much more predictable than that used previously.

Muscle cultures at the end of the active fusion period were exposed to various doses of RSV and were pulsed for 3 hours at 12, 24, 48, and 72 hours after infection. No examples of thymidine incorporation attributable to exposure to RSV were ever noted. In addition, brief pretreatment of the cultures with trypsin or with the polyanion DEAE-dextran, known to enhance infectivity of some RSV types, did not

lead to DNA synthesis in myotubes after exposure to the virus.

Time of infection and the effect of RSV on DNA synthesis in myotubes. Our attention now focused on the effects of RSV following exposure at earlier times, prior to myotube formation. The cultures were pulse labeled after myotubes had formed. Two very striking findings emerged as a result of a long series of experiments of this kind. *First,* early infection of myoblasts prepared by the DNA method yielded cultures with relatively small and often abnormal-looking myotubes by 60–72 hours after seeding. *Second,* a high proportion of myotubes in such cultures synthesized DNA. In some experiments we have estimated that 20–30% of the myotubes were affected. Typical examples are shown in Plate 3B and C. The time of infection was critical. The best results, in terms of proportion of myotubes labeled, were obtained when the myoblasts were infected within the first 24 hours after preparation by the DA method. The cultures were usually pulse labeled for 3 hours 65–96 hours after DA seeding. Myotubes in control cultures showed virtually no DNA synthesis.

It is interesting to speculate that the requirement for early infection may be associated with a wave of DNA synthesis in the myoblast population. O'Neill and Strohman, using somewhat different culture conditions, observed that there is an early phase of DNA synthesis and cell division prior to the onset of active myoblast fusion. This is probably a prerequisite for fixation of the transformed state in myoblasts as is the case for transformation of chick fibroblasts.

Infection of preformed myotubes by infected myoblasts. Having developed a reproducible method for induction of DNA synthesis in myotubes using RSV, we wanted to demonstrate unequivocally that myotube nuclei can be derepressed. Myoblasts prepared by the DA method were exposed to high doses of RSV and were incubated for 12–40 hours in medium containing tritiated thymidine (2–5 μc/ml). Such infected and heavily labeled myoblasts, after trypsinization and removal of diffusible label, were added to muscle cultures set up earlier. We found, as has also been observed by Bischoff and Holtzer, that the more mature myoblasts have a greatly reduced capacity to accept new myoblasts. Accordingly, we added the infected and labeled myoblasts to muscle cultures at late stages of the fusion process (72 hours or more after DA seeding). By this time addition of RSV alone will not induce DNA synthesis in the myotubes present. We then pulsed such cultures for 3 hours at about 6, 16, 24, 48, or 72 hours after addition of the infected cells, using either tritiated thymidine (0.5–1 μc/ml) or ^{14}C-thymidine (0.25 μc/ml).

At this writing no extensive secondary labeling has been noted under any conditions. The usual finding is that heavily labeled nuclei are incorporated into myotubes but DNA synthesis is not detected in adjacent nuclei. It has been possible, however, to obtain secondary labeling in a few nuclei adjacent to heavily labeled nuclei under certain specific conditions. Two variables which seem to be most important are the time interval between infecting the myoblasts and adding them to recipient cultures, and the time between addition of the infected myoblasts and pulsing of the recipient cultures. The secondary labeling was observed, at low frequency, after pulsing with either label but recent results after ^{14}C- and ^{3}H-thymidine labeling are shown in Plate 3D and E.

Detection of the secondary labeling in myotube nuclei is consistent with the hypothesis that infected myoblasts release derepressor molecules into the muscle sarcoplasm, but other interpretations are still possible. The occurrence of DNA synthesis in mature myotubes in clonal culture (*Year Book 66,* p. 600), although rare, also argues for this concept.

Our present working hypothesis is that derepressor molecules are synthesized in the myoblasts prior to fusion. The ability of myoblasts to fuse is impaired once active release of virus begins. This could explain the apparent critical timing between infection and use of myoblasts to challenge preformed myotubes. The low incidence of DNA synthesis occurring in large, mature myotubes can be explained partly on this basis, but also by the observation that myotubes become less able to accept new myoblasts as they mature. We further suppose that the hypothetical derepressor molecules are unstable in the myotube and can act on myotube nuclei for only a short period after their release into the sarcoplasm. Thus, in a synchronous system such as we are using, DNA synthesis could only be detected in recipient myotubes by pulse labeling over a critical time interval. This interval may indeed be shorter than the usual S phase of a given cell population, since only part of the genome may be involved in DNA synthesis in nuclei of affected myotubes (*Year Book 66,* p. 600 and Plate 3B). This could explain the difficulty of obtaining extensive secondary labeling using the system outlined above. An alternative explanation might be that treatment of the infected myoblast population with trypsin causes premature leakage of derepressor molecules.

Experiments designed to test aspects of this hypothesis and improve the proportion of secondary labeling are planned or in progress. Very gentle techniques for subcultivation of infected myoblasts are being adopted to minimize damage to the cell surface. Suspensions of myoblasts obtained by these new techniques will be used to infect myotubes as usual.

We have been able to reduce the proportion of mononucleated cells in mass muscle cultures by adding excess thymidine (2.5 millimolar) at 24 hours after the DA seeding (Plate 3F and G). Myoblasts so treated fuse and form muscle normal by morphological criteria, but secondary proliferation of myoblasts or contaminating fibroblasts is eliminated or at least markedly reduced. This culture system offers the advantage that background labeling due to mononucleated cells is minimal. It may even be possible to quantitate DNA synthesis induced in these myotube populations after addition of infected myoblasts. Attempts to increase the incidence of fusion of infected myoblasts with cultures of mature myotubes through the use of Sendai virus are also being made.

Comparative Studies on the Hybridization of RSV-RNA with DNA from Various Sources

Our earlier studies have shown that RSV-RNA contains some base sequences complementary to those of DNA from a variety of avian and mammalian species (*Year Book 67,* p. 431). Particular attention has been directed this year towards characterizing these sequences, and attempts have been made to determine their significance in oncogenesis.

Before presenting the results, a discussion of reports from other laboratories may be useful. Temin attempted to demonstrate the existence of DNA complementary to RSV-RNA in RSV-infected chick cells using DNA-RNA hybridization techniques. Although his findings have been cited as evidence in favor of the existence of a DNA "provirus," the low levels of specific radioactivity reported render this conclusion doubtful. Nevertheless, the requirement of DNA synthesis for cell transformation and productive infection by RSV, as well as by other oncogenic viruses, is also consistent with this hypothesis.

However, contradictory findings were reported by Harel *et al.* and by Wilson and Bauer, who found that RSV and the related avian myeloblastosis virus (AMV) RNAs hybridized to the same extent with DNA from infected and from

uninfected cells. Harel observed about 20% competition with cellular RNA, while Wilson and Bauer obtained over 80% competition. The relatively high saturation values (almost equivalent to those of ribosomal RNA genes in animal cells) and very different levels of competition could be due to contamination of the RSV-RNA preparations with cellular RNAs.

Because of the low specific activity of labeled RSV-RNA, such negative findings do not exclude the possibility that one or more DNA molecules, homologous to RSV-RNA, are present in infected cells. However, the existence of viral particles and of actively replicating RSV-RNA in nonvirus producing (NP) cell cultures makes it unnecessary to postulate proviral DNA. Moreover, within the framework of current molecular biology, the proviral DNA hypothesis requires the production of a new kind of enzyme—an RNA-dependent DNA polymerase—to synthesize proviral DNA copies from RSV-RNA as template. Furthermore, a proviral DNA or RSV-RNA–dependent RNA polymerase would be required to make progeny RSV-RNA in infected cells. We assume that the content of DNA in a chick fibroblast is about 2.4×10^{12} daltons and that one proviral DNA molecule (1.2×10^{7} daltons per single strand) exists in a nucleus. A maximum of 0.0005 μg of RSV-RNA hybridizes with 100 μg of DNA under the best conditions. This figure corresponds to about 5% of the avian genome which hybridizes with RSV-RNA. If 50 μg of cellular DNA and 10^{5} cpm/μg of RSV-RNA are used for hybridization, then we are speaking of having to detect a difference of less than 25 cpm in 500 cpm; in other words, 0.00025 μg of DNA in 0.005 μg. A difference of this low magnitude, even if deemed statistically significant, is not sufficient in itself to justify the novel concepts we have just outlined.

Homology Between RSV-RNA, RAV-RNA, and DNA from Various Species

The ability of RSV-RNA to hybridize with DNA from various sources was determined using the hybridization technique described in *Year Book 67*, p. 432. It should be emphasized that the hybridization experiments were done in the presence of chick ribosomal RNA at concentrations 100 to 300 times those of RSV-RNA to avoid possible competition with cellular RNA.

The DNAs extracted from pea, *Euglena,* salmon sperm, and *Rana pipiens,* organisms which are not susceptible to infection with RSV, hybridize with RSV-RNA to about the same extent (Fig. 8A–D). The small radioactive peak associated with yeast DNA (Fig. 8E) is thought to be nonspecific because of the low ratio of radioactivity to optical density. A similar peak was observed with DNA from *E. coli* (*Year Book 67,* p. 435). The DNAs from pea, *Euglena, Rana pipiens,* and yeast were generously provided by Dr. John Sinclair.

The Bryan high titer strain of RSV used in these studies contains 4–10 times more of the helper, Rous Associated Virus (RAV), than of RSV itself. Preliminary experiments comparing RAV with RSV in terms of hybridization with DNA from various sources have been performed using the same techniques. The highest specific activity obtained thus far after ^{32}P-labeling is 6×10^{4} cpm/μg of RAV-RNA. As shown in Fig. 9A and B, RAV-RNA, like RSV-RNA, hybridizes with mammalian DNA but not with bacterial DNA. Similar saturation levels are also obtained with various DNAs when RSV-RNA and RAV-RNA are compared (see Table 4).

Base Ratio Analyses of the Segment of RSV-RNA Which Hybridizes with DNA from Several Sources

As noted earlier (*Year Book 67,* p. 436), that portion of RSV-RNA which hybridizes with chick DNA has a higher

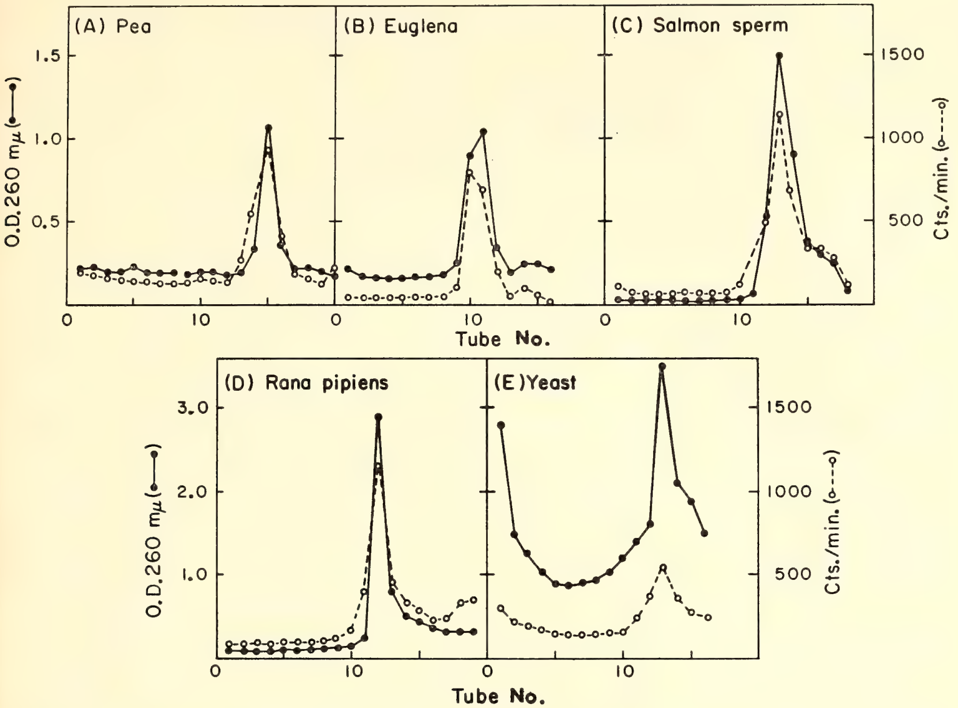

Fig. 8. Hybridization of ^{32}P–RSV-RNA with DNA from various organisms.

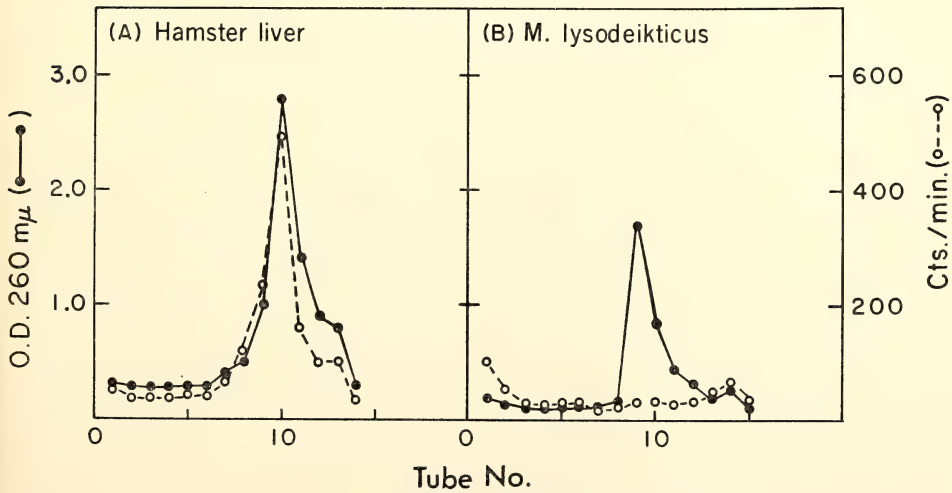

Fig. 9. Hybridization of ^{32}P–RAV-RNA with mammalian and bacterial DNAs.

TABLE 4. Saturation Values of Hybridized RSV-RNA and RAV-RNA with Various DNAs

Source of DNA	Amount of RNA Saturating 100 μg of DNA	
	RSV-RNA μg	RAV-RNA μg
Spafas chick fibroblast	0.009–0.010	0.010
RSV-infected chick fibroblast (72 hr. p.i.)	0.009–0.010	0.011
Calf thymus	0.004	0.005–0.006
Salmon sperm	0.008	0.007
Hamster liver	0.003 *	...
Clone 2	0.003 *	...
Adeno 2 virus	0.003 *	0.003 *
Adeno 12 virus	0.04 *	...

Note: Figures marked with asterisk represent the results of one experiment. Others are the average of 3–4 experiments using several different preparations of labeled RNA and DNA. Filters contained various amounts of DNA, and saturation values were standardized to per 100 μg of DNA.

adenylate content than the average for whole RSV-RNA. Similar analyses were performed after hybridization of RSV-RNA with DNA from several species.

About 200 μg of DNA were hybridized with ^{32}P-labeled RSV-RNA in the presence of 300 μg of chick ribosomal RNA. The preparation was treated with RNase and fractionated by CsCl centrifugation. Material in tubes, corresponding to the radioactive peak shown in Fig. 8, was pooled, and the hybridized RNA was precipitated by TCA with carrier yeast RNA. It was hydrolyzed in KOH, and the resulting nucleotides were separated by two-dimensional paper chromatography. Base ratio analyses are shown in Table 5. Although small differences are observed in the actual figures, the base ratio of hybridized RSV-RNA is generally characterized by high A and G, and low U. This is true for both mammalian and avian DNAs.

TABLE 5. Base Ratio of Hybridized RSV-RNA with Various DNAs in the Presence of Chick Ribosomal RNA

Source of DNA	A	U	G	C
Spafas chick fibroblast	30.7	11.9	38.6	18.8
Calf thymus	30.1	10.2	41.0	18.7
Salmon sperm	29.6	11.0	40.6	18.8

Note: Figures are the average of 3 analyses.

These observations suggested the possibility that the specific segment of RSV-RNA which hybridizes with cellular DNA might be involved in the transformation process. Findings consistent with such a general hypothesis are available from work with oncogenic viruses containing DNA, reported by others, and can be outlined as follows. (1) The DNAs of the oncogenic adenoviruses and SV40 have more deoxyadenylate than do those of nononcogenic adenoviruses. (2) Considerable evidence suggests that DNA from oncogenic viruses is integrated into the host cell genome. (3) RNA synthesized in vitro with DNA of SV40 or Polyoma viruses as template hybridizes with cellular DNA. With this background information in mind, we are attempting to answer the following questions. Does RSV-RNA hybridize with DNA from oncogenic viruses? What is the base composition of the segment of RSV-RNA which hybridizes with this DNA? How is this RSV-RNA fragment distributed in the host cell, particularly in the nucleus. And finally, what is the biological significance of this hybridizing portion of RSV-RNA?

Homology between RSV-RNA and Adenovirus-DNA

Adenovirus (Adeno) types 2, 4, and 12 were chosen for study. On the one hand, they are related viruses of the same "family"; on the other, they show clear differences in oncogenicity. The first two are not oncogenic while the last is highly oncogenic. Viral DNA was extracted after purification of the virus particles by treatment with genetron 113 followed by two centrifugation steps using CsCl of density 1.34. The initial results have been striking. RSV-RNA hybridizes much more extensively with DNA from Adeno 12 (oncogenic) than with that of Adeno 2 or 4 (Fig. 10A–C).

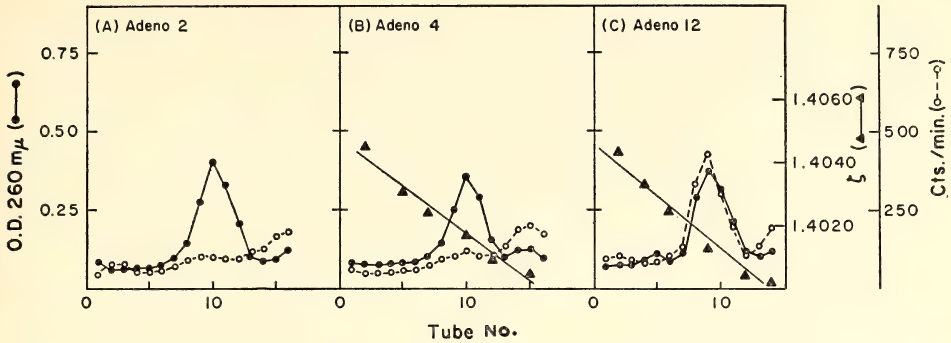

Fig. 10. Hybridization of 32P–RSV-RNA with Adenovirus DNAs.

The density of DNA from Adeno 2, 4, 12, and KB cells is 1.716, 1.717, 1.708, and 1.699, respectively. Since there is no detectable optical density peak at refractive index 1.4000 in 2×SSC, the viral DNA preparations were not contained with host cell DNA.

Preliminary analyses of the base ratios of the segment of RSV-RNA which hybridizes with Adeno 12–DNA indicate a high A and low U content. The technique employed was similar to that described for Table 5, but no ribosomal RNA was added during hybridization. Additional experiments to characterize this segment of RSV-RNA are in progress.

For saturation experiments, a Millipore filter holding 50–100 μg of cellular DNA or 10–30 μg of viral DNA was incubated in 1 ml of 4×SSC containing 100 μg of chick ribosomal RNA (both 18S and 28S) and different amounts of ^{32}P-labeled RSV-RNA (specific activity varies between 4×10^4 cpm and 4×10^5 cpm per μg RNA from preparation to preparation) at 62°C for 12 hours with constant shaking. The filters were washed once with 4×SSC and were incubated in 2×SSC with 50 μg/ml RNase (pretreated at 80°C for 10 minutes) at 37°C for 30 minutes. Each filter was then washed thoroughly with 50 ml of 4×SSC. Release of DNA from filters during hybridization was significant, as was observed from the increase in counts and optical density of blank filters when they were incubated with DNA-filters. Therefore, only one kind of DNA-filter was incubated in each vial, and blank filters for background determinations were incubated in separate vials. The background for RSV-RNA was about 0.1% of input RNA. This is about 10 times higher than ribosomal RNAs incubated and treated as described above. The addition of 0.1% SDS (purified by ethanol crystallization twice), which had been reported to be effective in decreasing background counts of RNA synthesized in vitro, did not decrease background counts under the conditions described above.

A typical saturation curve is shown in Fig. 11. About 1–2 μg of RSV-RNA per ml is necessary to saturate 50 μg of DNA from either mammalian or avian source material. The amounts of RSV-RNA required to saturate DNA from various sources are indicated in Table 4. Although the saturation value obtained for Adeno 2–DNA is close to that obtained for mammalian DNAs, it can be shown that this must be due to nonspecific background labeling rather than to specific hybridization. The molecular weight of Adeno 2–DNA is reported to be 2.4×10.7. Therefore, the saturation figure 0.003% can correspond only to a DNA fragment of molecular weight 720 (2 nucleotide pairs) in one Adeno-DNA molecule. Niyogi and Thomas reported

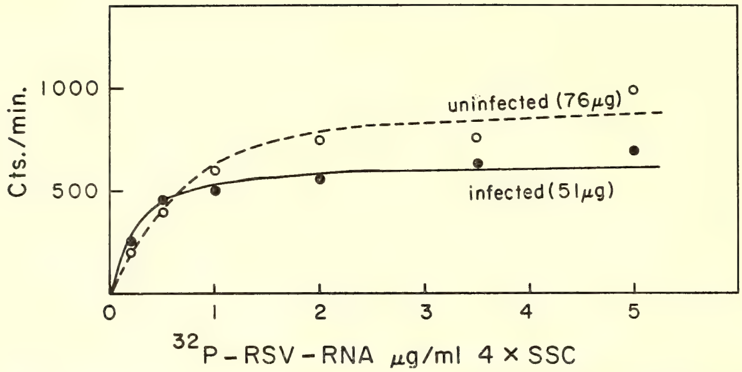

Fig. 11. Saturation curve of ^{32}P-RSV-RNA hybridized with chick embryo DNA. A filter holding DNA from uninfected cells contains an average of 76 μg DNA; filters prepared using material from RSV-infected cells contain an average of 51 μg DNA (72 hours postinfection). Each point represents an average from 4 filters (2 filters/ml incubation mixture).

that eleven nucleotide pairs are the minimum number detectable by current hybridization techniques.

Attempts to Demonstrate Natural Hybrid Formation Between RSV-RNA and Cellular DNA

The cytoplasmic and nuclear RNAs of chicken fibroblasts infected with purified ^{3}H-uridine and ^{32}P-labeled RSV were fractionated by sucrose density gradient centrifugation. Between 3 and 6 hours postinfection, about 80% of intracellular radioactive RNA was found in the nucleus and 20% in the cytoplasm. Both RNAs have a molecular size similar to that of the smaller component of RSV-RNA (Fig. 12). The DNA of ^{32}P-RSV-infected chick fibroblasts 6 hours postinfection was extracted gently in 2 × SSC to keep hydrogen bonds intact. This DNA was then treated with SDS, preincubated with pronase, and fractionated

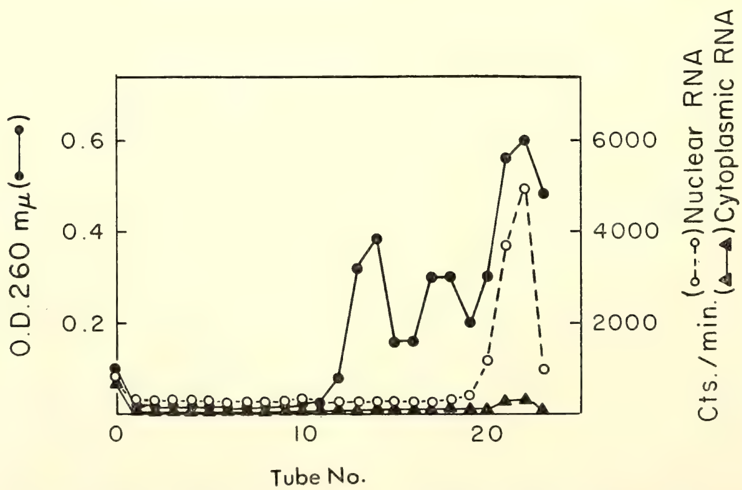

Fig. 12. Sucrose density gradient centrifugation of ^{32}P-RSV-infected chick embryo RNA. Cytoplasmic and nuclear RNAs were extracted 72 hours postinfection and centrifuged on a sucrose gradient of 5-20% at 24,000 rpm for 20 hours in SW 25.3 rotor.

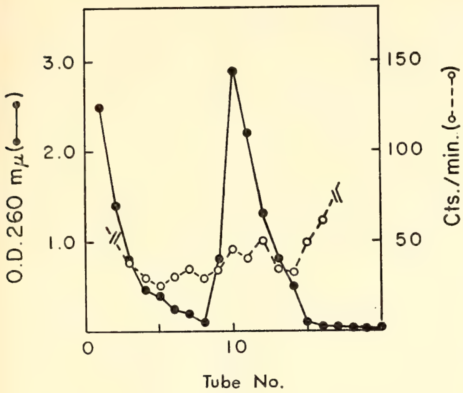

Fig. 13. CsCl centrifugation of DNA from chick embryo cells infected with ^{32}P-RSV. ^{32}P-RSV was adsorbed for 2 hours and then removed. The DNA was extracted after an additional 6 hours of incubation in growth medium.

by CsCl centrifugation (Fig. 13). In spite of repeated attempts, it was not possible to obtain reproducible evidence for a radioactive peak associated with cellular DNA. Only at much later stages after infection was a radioactive peak detected with ribosomal RNA and with DNA from cells infected with ^{32}P- or ^{3}H-uridine–labeled RSV. Thus, in vivo hybridization of RSV-RNA with a cellular DNA has not yet been proved.

These results suggest, however, that most of the RSV-RNA moves into the nucleus soon after infection. In addition, the possibility that degradation products from labeled RSV-RNA may be incorporated into DNA and thus obscure the presence of a natural hybrid cannot yet be excluded.

Hybridization of RSV-RNA with DNA from Chinese Hamster Chromosomes

A Chinese hamster cell line, provided initially by Dr. M. M. Elkind, was partially synchronized by thymidine block and the chromosomes were isolated from the cells at metaphase. The chromosomes were separated into 3 size-groups, comparable to those described by Mendelsohn *et al.*, by slight modifications of established methods. RSV-RNA was hybridized as usual with DNA prepared from the three chromosome fractions (Table 6). Although the actual amount hybridized varied from preparation to preparation, there was so significant difference between the three fractions of different size. Furthermore, the sum of amounts of RSV-RNA which hybridize at saturation with DNA from the three fractions is very close to the value determined for mammalian DNA. This suggests that DNA homologous to RSV-RNA is not located on any one chromosome or in any one size-group, but that these genes are dispersed among the chromosomes in all three size-groups.

Hybridization of RSV-RNA with Membrane-Associated DNA

The preparation and some characteristics of a DNA fraction associated with nuclear membranelike lipid has recently been reported for calf thymus chromatin source materials. Experiments using the same general technique were designed to compare the hybridization of RSV-RNA with membrane-associated DNA

TABLE 6. Comparison of 3 Classes of Chinese Hamster Chromosomes

Experiment Number (different preparations of chromosomes)	RSV-RNA (cpm/μg DNA) Hybridized with Chromosomes of 3 Size-Groups		
	Large	Medium	Small
I	338/65	231/52	332/70
II-1	1710/27	2458/71	1789/30
II-2	1390/24	2495/75	1319/29
III-1	640/60	450/66	692/66
III-2	649/65	433/50	501/50
IV (saturation)	0.004 μg/100 μg	0.006 μg/100 μg	0.004 μg/100 μg

versus nonassociated DNA. The possibility that RSV-RNA might hybridize more extensively with membrane-associated DNA was suggested from the following observations: (1) RSV can induce DNA synthesis in myotubes and in contact-inhibited cells; (2) the initiation of DNA replication in bacterial and in mammalian cells is generally supposed to involve an interaction between membranes and DNA; and (3) the DNA homologous to RSV-RNA is apparently dispersed among the chromosomes of the Chinese hamster cell (Table 6).

DNA extracted from the precipitate fraction of calf thymus chromatin sheared under conditions of low ionic strength, showed a higher level of hybridization with RSV-RNA than did DNA from the supernatant fraction. Interestingly, a much more striking difference was observed between similar fractions prepared from Chinese hamster cells collected in S-phase (Table 7).

Chinese hamster cells were partially synchronized by thymidine block (2.5 m*M*. It is estimated that above 30% of the cells were in synchrony after release of the thymidine block. They were harvested in S-phase and fractionated into cytoplasm and nuclei by homogenizing in "lysis buffer" (10 m*M* KCl, 10 m*M* Tris *p*H 7.5, 1.5 m*M* $MgCl_2$). Nuclei were suspended in 20-fold diluted lysis buffer and sonicated in a Branson Sonifier at power 4 for 90 seconds. The supernatant obtained after centrifugation at $10{,}000 \times g$ for 20 minutes was referred to as the soluble fraction. The precipitate, collected after one wash under the same conditions, was called the membrane-associated fraction. DNA extracted from both fractions was used for hybridization (Table 7).

TABLE 7. Comparison of Soluble Chromatin and Membrane-Associated DNAs

Source of DNA	Hybridized RNA of Different Experiments (cpm/100 μg DNA)	
Calf thymus		
soluble chromatin	3316	4217
membrane-associated	3877	4663
Chinese hamster		
soluble fraction	676	820
membrane-associated	1810	1630

Note: Each figure is the average of four filters.

Initial Attempts to Determine the Biological Role of Cellular DNA Homologous to RSV-RNA

Studies to define more fully the properties of the above-mentioned DNA fractions were undertaken using HeLa cells as source material. These were preferred to Chinese hamster cells since they were much more susceptible to synchronization by excess thymidine.

The cytoplasmic fraction of HeLa cells in S phase (90% synchronized) was prepared as described above and after centrifugation at $10{,}000 \times g$ for 20 minutes, the supernatant was dialyzed against DNA polymerase-buffer (2.5 m*M* EDTA, m*M* 2-mercaptoethanol, 50 m*M* phosphate-buffer *p*H 7.5) and used as cytoplasmic extract. It contains less than 0.2% cellular DNA. Isolated nuclei were suspended in 20-fold diluted lysis-buffer and sonicated in the Branson Sonifier at power 4 for 30, 90, 180, and 300 seconds followed by centrifugation at $10{,}000 \times g$ for 20 minutes. The washed sediment was dialyzed against DNA polymerase buffer and referred to as the membrane-associated fraction. The same precipitate fraction of the nuclear sonicate that was used for DNA extraction (Table 7) has the ability to incorporate ^{3}H-TTP into the acid-soluble fraction in the absence of added primer DNA. In the case of the 90-second sonicate, 90% of its incorporation is dXTP-dependent (Table 8).

Cytoplasmic extracts, of course, need template DNA to incorporate ^{3}H-TTP into the acid-insoluble fraction and about 80% is dXTP-dependent. There is a lag of 10 minutes in the initial time course of ^{3}H-TTP incorporation. This lag disappeared, however, when the cytoplasmic extract and DNA were preincubated at

TABLE 8. DNA Synthesis in vitro

Source of Enzyme	TCA-Insoluble Radioactivity (cpm)		
	Complete	— DNA	— dXTP
(1) Cytoplasmic extract	31335	1284	...
(2) Cytoplasmic extract	4423	...	1125
(3) Membrane-associated fraction sonicated for			
30 seconds	3509	...	188
90 seconds	4871	...	552
180 seconds	1702	...	617
300 seconds	1222	...	142

Note: Complete system (0.25 ml) for (1) and (2) consists of 20 μmoles Tris pH 7.8, 2 μmoles $MgCl_2$, 1 μmole 2-mercaptoethanol, dXTP each 50 mμmoles, ^{3}H-TTP (2 μc/mμmoles) 1 μc, heat-denatured calf thymus DNA 30 μg and 100 μg of protein. Extract (1) is a fresh preparation and extract (2) was stored at 4°C for 2 weeks. Complete system for (3) is the same as for (1) and (2), except calf thymus DNA.

4°C or 37°C for 10 minutes (Fig. 14). This suggests that free DNA polymerase first forms an active complex with template DNA to start DNA synthesis.

As shown in Fig. 15, in the case of the membrane-associated fraction, no time lag was detected in the initial incorporation, and in 10–15 minutes the incorporation reached a plateau. Addition of cytoplasmic extract did not induce any marked increase of DNA synthesis, but the addition of heat-denatured DNA

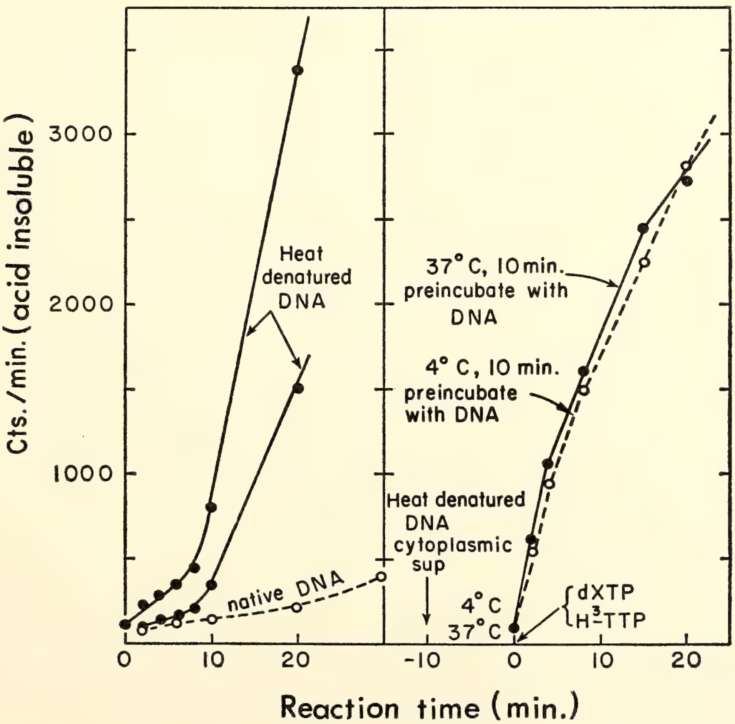

Fig. 14. Time course of ^{3}H-TTP incorporation by cytoplasmic extracts.

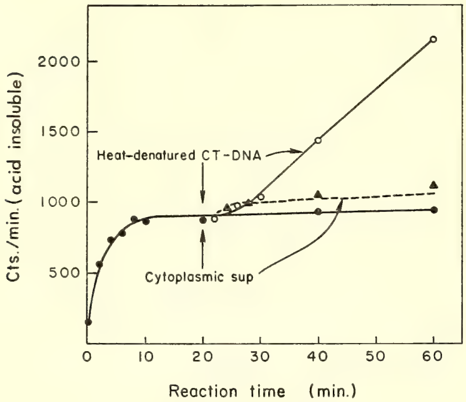

Fig. 15. Time course of ^{3}H-TTP incorporation by membrane-associated fractions.

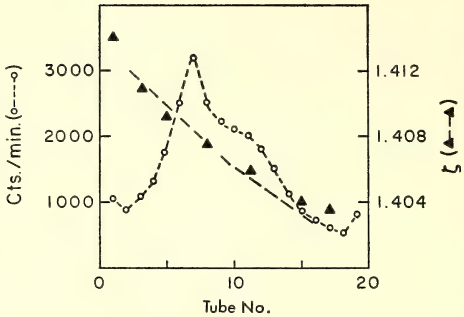

Fig. 16. Alkaline sucrose density gradient centrifugation of DNA synthesized in vitro with membrane-associated fractions. The membrane-associated fraction sonicated for 90 seconds was used for DNA synthesis. DNA synthesis was stopped after 45 minutes by adding NaOH and EDTA with final concentrations of 0.1 *N* and 0.01 *N*, respectively. The supernatant, after low-speed centrifugation, was layered on a 5–20% gradient and centrifuged at 50,000 rpm for 15 hours at 5°C in SW 65 rotor.

caused incorporation at a rate similar to that observed with the cytoplasmic extract and heat-denatured DNA. These results indicate that in the membrane-associated fraction DNA-polymerase and DNA exist forming an active complex. Hence DNA synthesis starts immediately if substrates are supplied. However, once DNA polymerase finishes reading the membrane-associated template DNA, which is probably double-stranded, it is released from DNA as free enzyme. As such, it could not form an active complex, and would be unable, therefore, to read native DNA efficiently. After the initial incorporation reaches a maximum upon the addition of single-stranded DNA to the membrane-associated fraction, released free DNA polymerase will react with the added DNA and start synthesis in the same way as in the cytoplasmic extracts.

The nature of DNA synthesized in vitro with the membrane-associated fraction was studied by alkaline sucrose gradient (Fig. 16) and alkaline CsCl centrifugation (Fig. 17). Dispersed radioactive peaks from 10S to 2S, comparable to the values obtained by sedimentation equilibrium with original DNA from the membrane-associated fraction, were observed. A sharp peak of about 2S would represent the minimum unit. The centrifugation pattern in alkaline CsCl suggests (although peaks are not clear) that the two strands will be separable because of their heterogeneous base sequences. Thus the possibility for isolation and further characterization of this DNA appears promising.

Westphal and Dulbecco found an homology between RNA (synthesized in vitro) complementary to DNA of polyoma or SV40 viruses and cellular DNA from 3T3 or BHK cells. In their experiments DNA-filters trapping 160 μg cellular DNA were incubated with various amounts of RNA complementary to viral DNA (0.04–0.1 μg). From 0.0001 μg to 0.0003 μg of RNA hybridized with 100 μg of normal cellular DNA, with a linear increase of hybridization according to input RNA. There was no difference observed between the complementary RNAs to polyoma and SV40 DNAs. The saturation values were not reported, but a low ratio of input RNA to DNA was used, RNA being added at about one-tenth of an estimated saturation value. (One μg of RNA was necessary to saturate 10^{-4} μg of polyoma DNA. We assume that the DNA of one nucleus con-

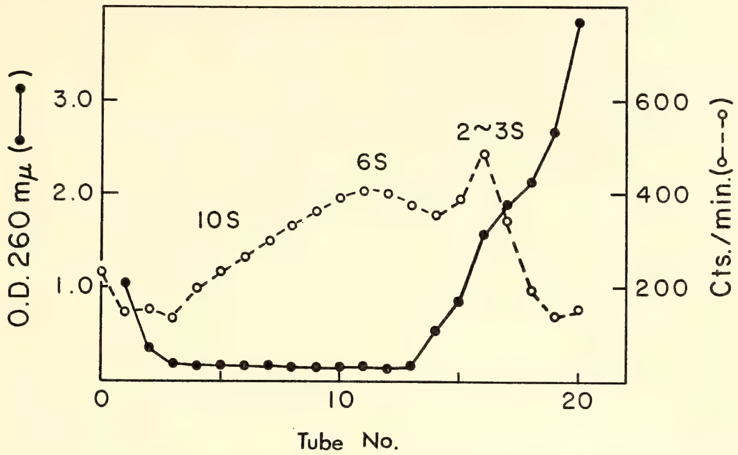

Fig. 17. Alkaline CsCl centrifugation of DNA synthesized in vitro with the membrane-associated fraction. The sample was prepared as described for Fig. 16. After centrifugation each fraction was neutralized, adjusted to 4 × SSC and trapped on a Millipore filter.

tains at least one region homologous to a molecule of viral DNA. The ratio of the weight of DNA in a virus particle to the weight of DNA per cell is 5×10^{-7}. We can calculate, therefore, that 200 μg of cellular DNA will be saturated by 1 μg RNA in the system described.) The region on mammalian DNA which is homologous to RNA complementary to polyoma and SV40 viruses may be the same gene that is homologous to RSV-RNA. Adeno 12–DNA could also contain this gene.

About 0.04% of Adeno 12–DNA (m.w. 2.3×10^7) is homologous to RSV-RNA. Therefore, a segment of 9000 daltons corresponding to 27 nucleotides in one Adeno-DNA molecule hybridizes with RSV-RNA. Since an eleven-nucleotide base sequence is the minimum detectable by hybridization, 9000 daltons will represent one unit of the homologous region. With a given saturation value of 0.004% (Table 4) and knowing that a mammalian nucleus contains about 5×10^{12} daltons of DNA, we can calculate that 2×10^8 daltons (which correspond to 2×10^4 units) exist in the nucleus. If we assume that this homologous unit is a recognizing site of DNA polymerase or an initiating site of replication, there are 2×10^4 initiating points for DNA replication in a mammalian nucleus and the average replicating unit is 2.5×10^8 daltons. It is interesting to note that direct measurements with the electron microscope by Taylor, Huberman, and Riggs indicate that the average replicating unit in Chinese hamster cells ranges from 1.2 to 7.6×10^8 daltons.

TROPHIC EFFECTS OF NERVE ON MUSCLE

Douglas Fambrough, Criss Hartzell, and Arlyne Musselman

Motor neurons and the muscle fibers they innervate interact in several ways. Most obviously, the action potentials conducted by the motor nerves trigger the release of a chemical transmitter, acetylcholine, from the nerve terminals. The acetylcholine interacts with the muscle fiber membranes to initiate a change in

permeability which leads indirectly to contraction of the muscle. This functional interaction is comparatively well understood. More subtle interactions between nerve and muscle are inferred from observations concerning both the formation of neuromuscular connections in the embryo and the behavior of adult nerve and muscle when they are disconnected. These subtle interactions are collectively termed "trophic interactions."

Besides being interesting in their own right, trophic interactions between nerve and muscle are relevant to the broader questions concerning the molecular basis of interactions between different cell types and the mechanisms controlling the surface properties of cells. In particular, the nerve-muscle system may serve as a model for interactions between functionally connected neurons in the brain.

Our research during the past year has focused upon the morphological, biochemical, and physiological changes in rat skeletal muscle following denervation. Most experiments have been done on the left hemidiaphragm. It has long been known that, following denervation, this muscle undergoes a marked transient hypertrophy involving greatly increased DNA and protein synthesis. It is also well known that denervated diaphragm is typical of denervated muscle in becoming supersensitive to acetylcholine. Understanding the molecular details of these changes is prerequisite to understanding the mechanisms by which these changes are prevented by the presence of functioning motor nerves.

DNA and Protein Metabolism in Denervated Rat Diaphragm

The rate of DNA synthesis in adult rat diaphragm is very low. Following denervation the rate of DNA synthesis increases dramatically. We have determined the time course of this increase by excising and culturing diaphragms denervated for varying lengths of time in vitro for 1 hour in a balanced salt solution with glucose and ^{3}H-thymidine and then either processing them for autoradiography or precipitating the DNA and counting it in a liquid scintillation counter. The results are shown in Table 9. A significant increase in the rate of DNA synthesis is apparent 12 hours after denervation and the rate is maximal at two to three days. By the sixth day the rate has returned to the control level. These data are in excellent agreement with the data of Zak *et al.* obtained by measuring the in vivo incorporation of ^{3}H-thymidine into DNA in denervated rat diaphragm. Our autoradiographic studies correlate well with the incorporation data.

The mechanism responsible for the increased rate of DNA synthesis in denervated muscle is unknown. While muscle fibers constitute the overwhelming bulk of muscle tissue, there are other

TABLE 9. Incorporation of ^{3}H-Thymidine into DNA* of Rat Diaphragms Denervated for Varying Lengths of Time

Days Denervated	Number of Animals	Cpm/mg Protein	S.E.	% Control
0 (control)	4	915	531	100
0.5	4	3,407	800	370
1	4	7,870	1205	860
1.5	4	11,937	645	1300
2	4	13,920	334	1520
3	4	5,232	202	570
4	5	4,198	109	460
5	5	1,238	199	135
6	3	924	76	101
7	5	919	175	100

* 10% TCA precipitable, 0.3 *N* NaOH (37°C, 18 hr) stable counts.

cell types present. Before the mechanism can be understood, we must identify the cell types involved. Unfortunately, the resolution of light microscope autoradiographic techniques is not adequate to determine whether the labeled nuclei are subsarcolemmal or extramuscular. The majority of the labeled nuclei are closely apposed to the muscle fibers but not visibly beneath the basement of the individual fibers. Due to reports that satellite cells are more abundant in denervated gastrocnemius (Lee) and are the only cells in regenerating (Resnik) or neonatal (Moss) rat muscle to incorporate ^{3}H-thymidine, it is tempting to speculate that the labeled nuclei of denervated muscle belong to satellite cells. The possibility that denervated muscle tissue is invaded by dividing, exogenous cells is disfavored because cells labeled with ^{3}H-thymidine by a series of injections prior to denervation do not appear later in denervated muscle.

To determine whether the frequency of nuclear division as well as the rate of DNA synthesis is increased by denervation, denervated diaphragms were cultured 5 hours in vitro in the presence of a mitotic inhibitor, vincristine sulfate. In control muscle there were no mitoses in a typical longitudinal section (except in some connective tissue cells), whereas in comparable sections of three-day denervated muscle there were three to eight mitotic figures. Experiments are now underway in which rats are being injected with ^{3}H-thymidine followed by injections of vincristine sulfate to determine whether labeled cells undergo a subsequent mitosis. This in vivo technique should eliminate any possible enhancement of the frequency of mitosis caused by in vitro conditions. If labeled mitoses are found, electron microscopic study should provide a rapid identification of the cell types responsible for DNA synthesis in denervated muscle.

We have investigated the increase in rate of protein synthesis and of incorporation of glucosamine into glycoproteins in denervated muscle. The time courses of these rate changes are similar to that for DNA synthesis (see Table 9). The increased rate of protein synthesis in denervated rat diaphragm represents an increased synthesis of all the major types of muscle tissue proteins. This was determined by labeling control and denervated muscle proteins with ^{3}H-leucine and ^{14}C-leucine and then fractionating the combined proteins by differential centrifugation and by disc electrophoresis. Similarly the threefold increase in the rate of glucosamine incorporation into glycoproteins was found to represent increased incorporation into the major glycoprotein fractions.

We have no evidence for the synthesis of a new species of protein in denervated muscles or for an exceptionally large increase in the rate of synthesis of any individual protein. However, our studies of the changes in muscle membrane properties following denervation suggest that such changes in protein metabolism may indeed occur.

Control of Acetylcholine Receptors in Muscle Fiber Membranes

Each muscle fiber is functionally connected to its controlling motor neuron through a single neuromuscular junction. Acetylcholine (ACh) released from a nerve terminal interacts with receptors in the muscle fiber membrane to trigger excitation of the muscle fiber. The ACh receptors are concentrated in an area of about 1000 μ^2 at each nerve-muscle junction, while the surface of an entire muscle fiber may exceed $5 \times 10^5 \mu^2$. There is no effect upon the resting potential of a muscle fiber when ACh is applied to the fiber surface at a distance from the neuromuscular junction. When the nerve-muscle connection is interrupted, however, the entire muscle fiber membrane becomes very sensitive to applied ACh.

Standard electrophysiological methods developed by Nastuk, del Castillo and Katz, and Miledi are used to measure

ACh sensitivity. A recording microelectrode is positioned for intracellular recording, a second electrode containing 3 *M* ACh is positioned just outside the muscle fiber, and minute, metered pulses of ACh are liberated from this second pipette by iontophoresis. The change in the transmembrane potential, caused by the ACh, is amplified and displayed on an oscilloscope. Photographic records of the oscilloscope traces are analyzed and the ACh sensitivity of the muscle membrane is calculated as millivolts depolarization per nanocoulomb of current passed through the ACh pipette. The lower limit of detectable ACh sensitivity is about 0.001 mV/nC. Ten-day denervated rat diaphragm fibers have a uniform ACh sensitivity of about 100–200 mV/nC.

In order to study the development of ACh sensitivity in denervated rat diaphragm, we have developed a method for maintaining pieces of adult rat diaphragm in organ culture. Such pieces will still contract when electrically stimulated after two to three weeks in culture. ACh supersensitivity develops in these cultured muscles at about the same rate as that of muscles denervated in vivo. Two days after denervation, the ACh sensitivity outside the endplate region is still less than 0.001 mV/nC. After three days postdenervation, fibers show a uniform ACh sensitivity of 2–20 mV/nC, and after 5 days in culture the sensitivity always exceeds 10 mV/nC. Actinomycin D (1 μg/ml), an inhibitor of RNA synthesis, or puromycin (10 μg/ml), an inhibitor of protein synthesis, added to cultures of denervated diaphragm will totally inhibit the development of ACh supersensitivity at any point in time. However, neither actinomycin D nor puromycin nor cycloheximide, at concentrations which inhibit virtually all RNA or protein synthesis, will abolish ACh supersensitivity which has already developed. Cultured diaphragm will not tolerate these agents indefinitely but can survive 48-hour incubations with no diminution in ACh sensitivity. These results support the hypothesis that ACh receptors are at least part protein and that their construction requires normal RNA and protein synthesis. The RNA must have a short half-life since actinomycin D can halt the development of supersensitivity. The positioned receptors appear to be very stable.

Some factor secreted from the motor nerve terminals may act as a regulator of ACh receptor production. This hypothesis is strengthened by the results of an experiment in which fragments of diaphragm devoid of nerve terminals were maintained in organ culture. These became ACh supersensitive more rapidly than whole denervated fibers (in which the nerve endings remain active for a limited time) and had an ACh supersensitivity of up to 3 mV/nC after two days. We have added homogenates and extracts of sciatic nerve to diaphragm cultures as single doses or by replacement of the medium every day, but have achieved no striking repression of the development of ACh supersensitivity. Likewise, various doses of ACh or of ACh and eserine sulfate (a cholinesterase inhibitor) have had no marked effect.

CHARACTERIZATION OF HEART CELLS OF THE CHICK EMBRYO

R. L. DeHaan, F. J. Manasek, I. S. Polinger and E. W. Schaefer, with the assistance of K. A. Magness

During the past year we have focused most of our attention on defining a set of properties which characterize the cell types of embryonic heart in vivo, and

on comparing these with characteristics of cells isolated from the heart in tissue culture.

Epicardial Investment, Glycogen Content, and Secretory Activity of the Early Myocardium

Although most of the gross anatomic changes occurring during cardiac organogenesis have been described, developmental events at the cell and tissue level remain relatively poorly understood. F. J. Manasek's major efforts over the past few years have been devoted to elucidating events at this level, largely with the use of the electron microscope. It is anticipated that these descriptive studies will provide the groundwork for further experimental approaches.

The epicardium, the tissue layer investing the myocardium, was previously thought to arise *in situ* from the developing myocardial wall. Consequently this structure was called the "epimyocardium." An earlier study by Manasek showed that the wall of the tubular heart contains only myocytes; it is not covered by an epicardium and does not contain undifferentiated cells that could give rise to the epicardium. During the past year he completed a light and electron microscopic study of epicardium formation showing that the epicardium arises from an extramyocardial source. The epicardium is initially a single sheet of flattened cells, first seen in the chick embryo at stage 17+, partially covering the myocardium. The epicardium eventually spreads over the entire myocardial surface. Later, a subepicardial connective tissue layer is formed. Since the epicardium is not formed from the outer myocardial cell layer, it is suggested that the term "epimyocardium" be abandoned in favor of the more accurate and simple "developing myocardium." This work is currently being extended in collaboration with DeHaan. Serial sections of pertinent stages are being reconstructed and the pattern of epicardial migration over the myocardium will be described.

An electron microscopic and histochemical analysis of glycogen distribution in the intact early embryonic heart showed that large pools of this polysaccharide are only present in cardiac myocytes. Glycogen therefore provides a convenient marker for the identification of muscle cells at the light microscopic level (Plates 4, 5). Polinger demonstrated that this relationship also holds true in vitro (described below) and that glycogen is a stable marker. Preliminary experiments with organ-cultured hearts suggest that the stored intracellular glycogen may not be available to the cells as an energy source until late in embryonic life.

Embryonic myocardial glycogen also appears to be resistant to breakdown by phagocytes. In an electron microscopic study of normal myocardial cell death, Manasek showed that even after phagocytes have ingested dead muscle cells and digested most of their organelles, glycogen particles are still recognizable. Experiments are now being planned to determine whether embryonic myocardial glycogen is truly present in a metabolically unavailable form.

Unlike other striated muscle, embryonic cardiac muscle contains a large fenestrated Golgi system throughout most of embryonic life. Beginning at about the 4th day of development in the chick, dense granules can be seen within Golgi lamellae, suggesting a specific myocardial secretory function. In the chick, unlike mammals, these dense granules are present in ventricular (Plates 4, 5) as well as atrial myocytes. The composition of these granules remains unknown, but experiments performed earlier this year suggest they are not lipid soluble. Manasek and D. M. Fambrough, working in collaboration, are attempting to isolate, purify, and characterize these granules.

Characterization of 7-Day Heart Cells In Vivo and In Vitro

This year Iris Polinger completed her analysis of the ultrastructure and behavioral properties of 7-day heart cells. Her problem was twofold: To develop criteria for identifying cell types in order to determine if myocardiallike (M) and fibroblastlike (F) cells in culture represent two distinct populations, or are merely different manifestations of a single cell type; and to compare M- and F-cells in vitro with the cell types present in the heart in vivo, using criteria other than gross morphology.

In her recently submitted doctoral dissertation, she employed seven criteria for characterizing heart cells: (1) spontaneous activity, (2) nucleolar number, (3) glycogen content, (4) myofibrillar content, (5) adhesiveness to the plastic culture substratum, (6) growth rate, and (7) DNA synthesis.

Extending the observations of Manasek, Polinger has confirmed that glycogen is present in the 7-day chick heart only in cardiac muscle cells, not in epicardium, endocardium, or fibrous cell types. Since, as noted above, particulate glycogen is retained for extended periods in culture, this substance could act as a marker for heart muscle cells at this stage. She has, in fact, found that after the heart is dissociated, those cells which contain glycogen "always and without exception contain myofibrils with Z-bands." (Polinger, Doctoral Dissertation, p. 39, Johns Hopkins University, 1969). Clearly the correlation between myofibrils and glycogen in heart muscle cells is retained after dissociation with trypsin. From counts on over 150 glycogen-containing cells, removed from such culture plates and examined with the electron microscope, she has also demonstrated that the same correlation still exists after 24 hours in vitro.

With these facts in mind, it was possible to correlate cells categorized live in culture as M or F on the basis of their morphology, with the presence or absence of glycogen. For this study cultures were grown by standard techniques in medium 629. Thirty-seven microscopic fields including 538 cells were photographed live with phase optics on Polaroid film. Each cell was scored as a beating or quiescent M- or F-cell. The plates were fixed and stained for glycogen and RNA, the photographed fields were relocated and the same cells were examined for glycogen. The results were striking. Every cell categorized as an M-cell, beating or not, contained glycogen, as did that small group of cells (3.7%) scored as beating F-cells. Among the quiescent F-cells, 85% were completely devoid of glycogen.

Since glycogen is always correlated in these cells with myofibrils, it may be concluded that all cells categorized in culture as M or "beating F," and a fraction (as high as 15%) of quiescent F-cells, are in fact myocardial muscle cells. The glycogen-free cells are presumably derived from epicardium, endocardium, and fibrous tissues. Moreover, inasmuch as the beating F category normally represents no more than 0.5% of the total cells in a culture, and F-cells usually constitute 25–30%, the error in assaying M- and F-cells in a culture may be calculated as only about 5% ($0.5\% + 15\% \times 30\%$). This is a satisfactory level of accuracy for an assay based upon morphological criteria.

The observation that F-cells are well spread, while M-cells remain rounded on the culture plate for at least the first day or two, prompted experiments to determine if this difference in spreading reflected a difference in adhesiveness of the two cell types, and if such a difference could be exploited to separate M- and F-cells. As mentioned in *Year Book 67* (and described in detail in her dissertation) Polinger has devised a separation technique which depends upon the differential rate of attachment of M- and F-cells to Falcon plastic dishes. With this method she has obtained cultures containing over 85% of either cell type.

The separation technique may be described briefly. Each of a series of plastic culture dishes is inoculated with a suspension of cells. After swirling the medium the supernatant is removed from one dish immediately, and at varying intervals after inoculation from the replicate plates. Each supernatant is transferred to another culture dish. These latter dishes, referred to as supernatant (S) dishes, contain those cells which have not yet attached to the original dishes. The original or residual (R) plates then contain those cells which have been able to attach to the substratum in the time between inoculation and removal of the supernatant.

Whereas control cultures (23-hour R plates) contain 63% M-cells, these are enriched to a maximum of 88% in 2-hour S plates. In contrast in 1-hour R plates, M-cells constitute only about 20% of the population. Figure 18 shows the rate of attachment of total cells and M- and F-cells in the residual plates. By 1 hour after seeding, 34% of the cells that will ever attach in the R plates have already done so. By 6 hours, 100% of the cells that will attach have done so.

The initial rate of attachment of F-cells is rapid (Fig. 18). By ½ hour 42% of the total F-cell population, but only 7.7% of the total M-cell population, have attached. Thus, the high rate of attachment of cells during the first half hour is due almost entirely to the attachment of F-cells. After 1 hour in culture, the rate of attachment of M-cells (Fig. 18) increases while the rate of attachment of F-cells levels off. By 4 hours after seeding, when 92% of attachable cells have attached, 100% of the F-cells and 82% of the M-cells have attached. By 6 hours, all the cells that will ever attach have done so. This value represents 32% of the inoculum in these experiments.

When the percentage of M-cells in residual culture plates was determined using phase optics, and the plates were stained with periodic acid-Schiff and azure B (for glycogen and RNA), the percentage of M-cells was again found to be directly correlated with the percentage of cells containing glycogen.

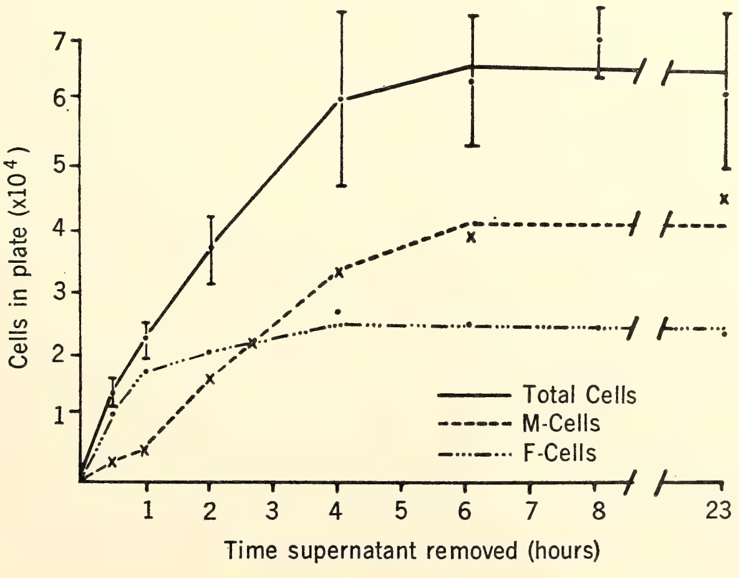

Fig. 18. Rate of attachment of M- and F-cells in residual plates.

A further difference between M- and F-(glycogen and nonglycogen) cells investigated by Polinger is their strikingly different rates of mitotic activity. During the first two days in growth medium the majority of cells which incorporate ^{3}H-thymidine into DNA are rapidly dividing glycogen-free cells. Even at day 1, the percentage of these cells which become labeled is significantly greater than that of cells containing glycogen. On the other hand, this difference in labeling index is not reflected in the intact chick heart. When 7-day embryonic hearts are labeled in vivo by injecting ^{3}H-thymidine through the amnion, the labeling index of glycogen-rich muscle cells in the ventricular myocardial wall is found to be similar to that of epicardial and endocardial cells, which are devoid of glycogen.

Potassium-Inhibition of Pacemaker Capacity

In previous reports (*Year Book 66, 67*) and other publications DeHaan and Gottlieb defined a pacemaker heart cell in culture as any single isolated cell seen to beat rhythmically. A potent regulator of pacemaker function was shown to be potassium. Employing dissociation procedures and media tested to yield maximal numbers of active cells, DeHaan found that the number of pacemaker M-cells which manifest their capacity for spontaneous contraction at any given moment was a function of the concentration of potassium in the medium $(K^+)_o$. At low levels of potassium (1 m*M*), 70–80% of the M-cells derived from a 7-day heart beat spontaneously. As K_o is raised progressively by small incremental injections of KCl into the culture medium, a fraction of the cells become quiescent ("switch off") at each steplike rise in K_o. At normal serum potassium concentration (4–5 m*M*) only about 40% of latent pacemakers beat. In high-potassium media, no more than 10–20% continue spontaneous activity. This result is reversible, at least over a short period, in that if the high-K medium is removed from these cells and replaced by one containing 1 m*M* K_o, 70–80% of the M-cells begin beating again. Some cells switch off at a given K_o while others remain active, which suggests the possibility that each pacemaker cell may have an individual threshold of K-inhibition.

To test this possibility, DeHaan and E. W. Schaefer, an undergraduate student at Johns Hopkins, designed an experiment to answer the following questions:

1. Do the cells which are beating at a given K_o remain on for extended periods (hours), or does the %BC counted at a particular time represent the statistical average of a larger number of pacemaker cells which are intermittently on and off?
2. Does each heart cell in a culture exhibit its own threshold of K-inhibition?
3. To what extent does this threshold remain constant with time?

Cultures of isolated 7-day heart cells, prepared by techniques described previously by DeHaan and Gottlieb, were incubated in medium containing 1.3 m*M* K for 22–27 hours. Care was taken to maintain *p*H, CO_2-level, and osmolarity constant during all phases of the experiment. Microscopic fields in a culture, including about 30 actively beating pacemaker cells, were photographed on Polaroid film at the beginning of an experiment, and each beating cell was then numbered on the photographs. A small aliquot of 0.25 *M* KCl saline was injected into the culture dish. After a 5-minute equilibration period the numbered cells were reexamined and those which had stopped were identified on the photographs. A second aliquot of KCl was added; the cells were again examined. A third injection brought the K_o-level to 9.6 m*M*. After recording which of the 30 original cells had switched off and which ones were still beating, the plate was flushed twice with prewarmed, pregassed 1.3 m*M* K medium,

TABLE 10. Spontaneous Pacemaker Activity of Identified Isolated Single Heart Cells Observed Through Two Cycles of K_o-Increase

	Experimental					Control				Experimental
	(1) K_o (mM)	(2) Total pm counted	(3) Pm on	(4) % on	(5) % S.E.	(6) K_o (mM)	(7) Total pm counted	(8) Pm on	(9) % on	(10) % on norm.*
Cycle I	1.3	267	267	100	—	1.3	59	59	100	100
	3.8	266	198	75.2	2.6	1.3	59	58	98.4	76.8
	7.0	266	116	43.8	5.1	1.3	59	57	96.5	47.3
	9.6	265	71	26.6	5.0	1.3	59	54	91.4	35.4
Cycle II	1.3	246	190	77.2	2.9	1.3	56	47	84.2	93.2
	3.8	243	147	61.0	2.7	1.3	55	46	84.0	7.0
	7.0	234	100	42.7	5.9	1.3	50	42	84.2	58.7
	9.6	189	60	31.0	4.6	1.3	50	42	84.2	47.7

* % on norm. = The percentage of active pacemaker cells normalized to discount control decrement with time; = % $\text{on}_{\text{exp.}}$ + (100 − % $\text{on}_{\text{contr.}}$).

restoring the culture to its original condition. The culture was allowed to equilibrate for 1.5–2.0 hours, and the cycle of three injections was repeated, with observations on the same population of 30 cells after each increment of K_o. This experiment was repeated nine times, yielding a total of 267 cells observed (903 observations). Two control experiments were performed (total 58 cells) in which plates were treated in an identical way except that the injected aliquots of solution were free of potassium and therefore produced no increase in K_o-level.

Cells were counted as either beating or quiescent at each K_o-level. Each cell either beating (++) or not beating (−−) at a particular level of K_o in both was then scored as "same" (S) if it was cycles of K-injections.

The data from preliminary studies completed in recent months are presented in Table 10 in terms of the percentage of the original pacemaker population which remained active ("on") at each potassium concentration through the two cycles. The dramatic potassium-inhibition effect, previously reported, is illustrated in column 4. In column 9 the decrement in pacemaker activity with time is shown among control cells. The experimental data, normalized to discount this time decrement, are provided in column 10. In Table 11 the behavior of individual cells is compared during the two cycles. The symbols shown in columns 3 to 6 indicate that cells were spontaneously active at a given K_o during both cycles (++), quiescent during both cycles (−−), active during cycle I but not during cycle II (+−), or "off"

TABLE 11. Constancy of Pacemaker Activity of Identified Isolated Single Heart Cells Observed Through Two Cycles of K_o-Increase

Experimental							Control		
(1) K_o (mM)	(2) Total pm counted	(3) ++	(4) −−	(5) +−	(6) −+	(7) % same ++ −−	(8) K_o (mM)	(9) Total pm	(10) % same
1.3	267	248	0	19	0	92.9	1.3	56	84.2
3.8	266	191	48	13	14	89.8	1.3	55	85.6
7.0	266	125	109	1	31	88.0	1.3	50	85.5
9.6	265	85	129	9	42	80.8	1.3	50	90.6
Mean						87.9			86.5

during cycle I but "on" during cycle II (−+).

Tentative answers to the three questions raised above are provided by these results. Control cells examined once, and again two to three hours later (Table 11, column 10), appear in these experiments to be remarkably constant. Although there was some effect of the manipulation of the culture (transfer of the culture plate from incubator to microscope warm stage, injection of control medium, mechanical agitation, etc.) and especially of the time intervening between observations, more than 85% of the cells exhibited the same behavior over a period of 2–3 hours. Moreover, when pacemakers were shifted from one level of K_o to another, and the results were corrected for the predictable decrement with time, 87.9% of the cells exhibited an individual threshold for potassium-inhibition, which remained constant over the same 2- to 3-hour period.

This estimate of constancy can be shown to be a conservative one, as a result of an arbitrary convention employed in scoring cell behavior. At the beginning of an experiment, all the cells counted were isolated singlets, beating independently. During the course of an experiment lasting up to four hours, occasional cells became conjoint with beating neighbors. Since, in these cases, it became impossible to determine whether each cell was acting as its own pacemaker or responding to a stimulus from its conjoint partner, such cells were eliminated from consideration after contact was observed. This is the reason for the decline in total number of pacemakers counted (columns 2 and 7, Table 10) throughout an experiment.

It can be concluded, therefore, that at least 88% of pacemaker cells derived from a 7-day embryonic heart exhibit individual thresholds for K-inhibition which remain constant for several hours in culture under the conditions described.

Other experiments now being conducted by DeHaan appear to indicate that the potassium-inhibition threshold relationship of cells from hearts earlier than 7 days are quite different than from older hearts, suggesting that after the heart forms and begins to beat, dramatic changes occur in the transmembrane Na-K ratios and, presumably, in ionic fluxes. Techniques of culture and electrophysiology previously reported are now being modified for application to cells from 2-day hearts, at the time the organ begins beating, to study the differentiative changes presumed to take place in the pacemaker membranes during this critical time.

Electron Microscopy of Cultured Cells

Hayden G. Coon and Francis J. Manasek

Active cilia have been found on some of the cells of the established line of *Xenopus laevis* kidney originated by Dr. Keen Rafferty of the Department of Anatomy of the Johns Hopkins University School of Medicine. During the three years this line has been carried it has retained its predominantly epithelial nature as well as a tendency toward formation in crowded cultures of vesicles reminiscent of kidney tubules. In the course of producing a somatic hybrid cell strain between this amphibian cell line and the established mouse fibroblast LM (TK^-) Cl 1 D (propagating mononucleate hybrids apparently *are* possible and will be the subject of a future communication), we observed that patches of cells possessed active cilia in cultures grown for 3 weeks or more in our standard culture medium (F12 with doubled concentrations of amino acids and pyruvate, supplemented with 15 μg/ml ascorbic acid and 5% fetal calf serum, the whole diluted with water by 10% for amphibian culture). To the best of our knowledge, this is the first time that cilia have been reported in continuously propagated cell cultures. These organelles

have been studied previously in explants of tissue maintained for short times in vitro as "organ cultures." The occurrence of the ciliated cells in small patches suggested a clonal origin, and we are attempting to clone cell lines with high and low probabilities of expressing the ciliated phenotype. This observation also prompts us to reexamine cell cultures from the more familiar ciliated tissues such as lung and oviduct of mammalian embryos. The relationships among the centriolar apparatus and the basal bodies during cell division and the action of cilia under varied conditions of cell fusion will be investigated.

The ultrastructure of the cilium is characteristic and also serves as a definitive demonstration. Consequently, Coon joined forces with Manasek in studying these and other cultured cells with the electron microscope. Plate 6 shows the typical cilia found in regions where visible ciliary activity was identified before preparation for the electron microscope.

The logical way to cut sections of cells showing cilia is in the plane normal to the substrate—in this case, normal to the plastic petri dish. Manasek has discovered that it is possible to section the epon embedding medium containing the cells and the polystyrene petri dish at the same time. The result has produced the series of unusual micrographs shown in Plates 6–9. Previously it was standard practice to separate the embedding plastic from the culture dish, and usually sections were taken in the plane parallel to the freed surface. We believe that this new method of examining the interface between cells and their substrate will yield valuable information on the adhesion of cells to neighboring substances and the modifications of the basal surfaces of cells induced by a variety of substrates. The whole dimension of ultrastructural comparisons between cells in vivo and their counterparts in cell culture is still virtually unexplored.

Because of the novelty of this method we include some details here. The cultures were first rinsed in cold Hanks' balanced salt solution and then fixed for 10 minutes at room temperature in cold 2G fixative: 2.5% glutaric dialdehyde and sodium cacodylate buffer (0.025 *M*) in Hanks' solution. They were rinsed with fresh Hanks' solution and then postfixed with 1% OsO_4 in 0.1 *M* cacodylate buffer, *p*H 7.6. Cultures were then dehydrated with a graded ethanol series. Some cultures were given a final rinse with a weak solution of uranyl acetate in absolute alcohol. Following absolute alcohol, the cultures were embedded directly in epon. After polymerization, small pieces were sawed out and sectioned normal to the culture dish on glass or diamond knives. The plastic dish was not removed from the epon and no difficulty was experienced in sectioning the block, half of which was polystyrene culture dish and the other half epon. Sections were mounted on uncoated copper grids, stained with lead citrate and examined in an Hitachi HU-11E microscope operated at 50 kV.

Plates 7 and 8 illustrate an alteration which we have found in each of the three different epithelial cells in culture which we have examined. The *Xenopus* kidney line, kidney cells of the Chinese hamster, and rat liver cells have shown a specialization of the basal cell surface similar in appearance to the terminal web which is commonly seen at the apical surface of many epithelia in vivo. A detailed view of this "basal web" of filamentous material is shown in Plate 8. It is present on both the basal and apical surfaces of many of these cultured epithelial cells. It seems unlikely that this basal web is merely a specialized portion of a cell cortex, since the latter feature is generally absent in these cultured cells. The confusion of cellular polarity which results when this kind of specialization is present may significantly change the function and behavior of cells in culture. The discovery of structural alterations of these cultured cells suggests experiments to be done in order

to determine the change, if any, of this region of contact as the substrate is changed. We are beginning by asking whether the same basal cytoplasmic specializations are produced when these cells are cultured on coatings of collagen, fibrin clot, agar, cellophane, or other types of plastic.

Plate 9 shows some new features of cultures of rat liver cells (see *Year Book 67*) revealed by electron microscopy. In regions where the cells of the typical "monolayer" or epithelial sheet are packed closely together, we were surprised to find that they overlap one another much more than could be detected with phase optics. No typical junctional complexes were found despite the epithelial growth pattern of these liver cells. In these old cultures (the rat liver cell population had been maintained in the same petri dish for ten weeks after the sheet had reached confluence) a large amount of material had accumulated between the cells and the plastic culture dish. The presence of a fibrous-appearing material similar to the "reticular fibers" of normal liver had been seen with phase microscopy (*Year Book 67*). We had believed that this material was mostly collagen because of its digestion in purified collagenese (Worthington CLSPA) and because of the incorporation into protein of large amounts of hydroxyproline from ^{3}H-proline precursor. However, we have found by electron microscopy an amorphous material more like elastin or basement membrane collagen in appearance, and we have found no evidence of the typical banded pattern of mature connective tissue collagen. Parallel alignments of electron-dense material were also present (Plate 9C). Possibly it is this material which contains the collagenlike hydroxyproline synthesized by these cells. We plan further studies of these secretion products by the technique of combining electron microscopy and autoradiography of cultures which have been pulsed with ^{3}H-proline and "chased" with cold proline. Further characterization of this product will be attempted by chromatographic analysis of protocollagen and its constituent polypeptide chains. It seems possible that this epithelial cell produces either a portion of the collagen molecule or an imperfectly aligned polymer. It is tempting to speculate that because of the clonal isolation of a purified line of epithelial cells, an intermediate or a deficient product has accumulated. The addition of mesenchymal cells or fibroblasts might result in the final elaboration of a product more like that formed in the normal tissues.

COLLAGEN SYNTHESIS IN SOMATIC CELL HYBRIDS BETWEEN LYMPHOCYTES AND FIBROBLASTS

Hayden G. Coon and Lewis N. Lukens in collaboration with Phillip Periman, National Institutes of Health

(*with the technical assistance of Mrs. Isabelle Williams and Mrs. Virginia Hicks*)

Hybrid cells between a pigmented hamster melanoma and a nonpigmented mouse fibroblast have been found by Davidson, Ephrussi, and Yamamoto not to express pigmentation. These hybrid cells have also been shown not to possess the activity of DOPA-oxidase, a key enzyme in the pathway for melanin biosynthesis. Earlier work by Green, Ephrussi, Yoshida, and Hamerman had established that hybrid cells between two collagen producing fibroblast strains did produce collagen and that the level of collagen production by these hybrids was approximately intermediate between that of the two parental strains. These two results have been cited by Davidson, Ephrussi, and Yamamoto as suggesting

that "differentiated" or specialized synthesis by vertebrate cells is under "negative control," i.e., in the hybrids the negative control function of the non-pigmented fibroblast was dominant to the pigment synthesizing control mechanism of the melanoma. It was hypothesized that the control mechanism which prevents or represses pigment synthesis in the fibroblast is also able to prevent pigment production by the melanoma. While it is not yet clear which characteristics will be found to exhibit negative control in hybrid cells and which ones will not, the working hypothesis proposed by Richard Davidson is that parental cells showing the same differentiated function will continue to exhibit that function as a cellular hybrid, whereas parental strains with dissimilar differentiated functions will produce hybrids which exhibit negative control or failure of expression of either specialized function. We find evidence from the hybrids between rat liver (which cell strains synthesize serum antigens) and the mouse fibroblast "L" cells (which do not) that the hybrids do not form any serum antigens, neither those of the rat nor those of the mouse (see *Year Book 67,* and the Wistar Symposium No. 9, 1969). This result is consistent with the notion of negative control of differentiated syntheses in hybrid cells.

Because collagen synthesis represents the best example of persistent production of a specialized molecule in hybrid cells, and because of Dr. Lukens' experience in the field of collagen biosynthesis, we decided to continue the inquiry into the control of collagen biosynthesis by hybrid cells. Specifically, we wanted to know whether hybrid cells were also capable of exhibiting negative control for collagen synthesis. While comparative studies are not complete, most cells of the adult body do synthesize some collagen, and certainly the cells from most adult organs do so in cell culture. Certain cells of the blood and lymphoid system, however, are known not to synthesize collagen. Collagens are well adapted for this kind of study because they are very sensitively detected by their large amount (about 9%) of a virtually unique amino acid, hydroxyproline. We have decided to study hybrid cells between lymphocytes which have been shown by Green, Goldberg, and Todaro not to produce collagen, and the established mouse fibroblast "L" cell, Cl 1 D, which does synthesize collagen. This fibroblast cell line characteristically produces only small amounts of collagen, but it has the advantage that it can be selectively killed in tissue culture, which greatly simplifies isolation of hybrid cell strains. If the hybrids were to be capable of exhibiting negative control of collagen synthesis, then we would expect no collagen to be synthesized by the lymphocyte $\times$ fibroblast hybrid cells. If collagen were made by these hybrids, then we would possibly have found evidence of a counter example to the current generalization.

We have isolated 10 independently derived rat lymphocyte (RLy) $\times$ mouse fibroblast (Cl 1 D) hybrid cell strains. These hybrids were produced by a modification of the inactivated Sendai virus procedure previously described (see *Year Book 67*). We have found, as did Henry Harris and his collaborators, that the thoracic duct lymphocyte is especially difficult to fuse with other cells. We believe that our method will be of sufficient interest that some details should be presented here.

Cl 1 D cells were first plated in petri dishes at 4×10^6/100 mm dish. Four hours later, after the cells had attached, the dishes were rinsed with Hanks' saline and drained nearly dry. The dishes were kept cool by placing them on a metal plate resting in a tray of crushed ice. A few drops of β-propiolactone–inactivated Sendai virus (300 HAU/ml) were placed in the center of each dish and were allowed to spread uniformly to the edges of the dish. Meanwhile, washed suspensions of rat lymphocytes (prepared by

thoracic duct cannulation and purified by overnight incubation at 37°C in cell culture medium generously supplied by Dr. S. Strober of the NIH) were suspended in the same concentration of cold βPL-inactivated Sendai virus so as to yield 10^8 viable lymphocytes/ml. A few drops (0.2 ml) of the lymphocyte-virus suspensions were added to the center of each of the cold dishes. As these drops spread to the edges of the dishes, lymphocytes became stuck to the Cl 1 D cells already attached to the dish. After ten minutes in the cold, the dishes were gently transferred to a moist 37°C incubator for about 90 minutes before standard culture medium was added. After 48 hours, the medium was changed to selective medium HAT and renewed twice weekly thereafter. An average of 34 macroscopic hybrid colonies per dish appeared after three weeks of incubation. Only colonies from separate dishes were considered certainly of independent origin. Since the selective medium HAT killed all Cl 1 D cells, and this culture regime did not yield any rat cell colonies (lymphocytes died and were effectively washed away by medium changes) the system is a fully selected method for the production of hybrid colonies. Only hybrids which possessed the fibroblast parent's characteristic attachment to the plastic culture surface were preserved by this method. However, in one series the floating cells harvested with the exhausted medium were collected and cultured separately. None of these cultures yielded a viable hybrid. It may be concluded that a nonadhering lymphocytelike hybrid is relatively rare.

Our first results from this study are presented in Table 12. As is conventionally done, we have taken incorporation of radioactivity into hydroxyproline found in the protein from the cells and medium after incubation in ^{3}H-proline as evidence of collagen production. The ratio of the radioactivity of hydroxyproline in protein to the radioactivity of proline in protein is a measure of the quantity of collagen synthesized relative to other cellular proteins. All five of the independently isolated hybrid cell strains between rat lymphocytes and Cl 1 D (RLy $\times$ Cl 1 D) which we have tested were found to be synthesizing collagen. Furthermore, the hybrids are synthesizing collagen at a rate equal to, or in 4 cases greater than, that of the Cl 1 D parent! Negative control of collagen syn-

TABLE 12. Collagen Synthesizing Ability of Parental and Hybrid Cell Strains
[Disintegrations per minute (DPM) ^{3}H-proline and ^{3}H-hydroxyproline (after purification to constant specific activity) 15- to 24-hour incubations]

Cell Strain	No. of Replicate Plates Pooled	DPM Hydroxy-proline	Total DPM in Acid Hydrolysate	DPM Hydroxy-proline / Total DPM × 100	Cells/ Plate × 10^6	DPM Hydroxy-proline / 10^6
Cl 1 D	1	67,200	8,040,000	0.84	13	5,160*
Cl 1 D	2	71,900	10,160,000	0.71	13	2,760†
RLy × Cl 1 D #3	2	41,200	5,450,000	0.76	3.5	5,900*
RLy × Cl 1 D #6	6	387,500	29,200,000	1.33	9	7,180†
RLy × Cl 1 D #7	2	33,850	2,635,000	1.29	1	16,900*
RLy × Cl 1 D #9	2	21,300	1,950,000	1.09	0.86	12,500*
RLy × Cl 1 D #10	3	194,000	14,550,000	1.33	15	4,300†
BRL 3C4	1	82,600	825,500	10.0	2.55	32,300†
BRL 3C4	1	81,800	711,900	11.5	3.02	27,300†
BRL 62	2	105,000	4,145,000	2.54	3	17,500*

Note: These measurements of rat liver strains were cited in the section with Dr. Manasek; they are included here as examples of high collagen producing cell strains. Note that the clonal strain BRL 62 produces relatively less collagen than the separate clonal strain BRL 3C4. This may be accounted for in part by the fact that 62 cells were in log phase of growth, whereas the 3C4 cells were in older stationary cultures. * = 150 μC/plate/10 ml; † = 100 μC/plate/10 ml.

thesis does not appear to operate in these hybrids.

This result does not, however, mean that we have completely ruled out negative control for collagen biosynthesis. There are two considerations which make that strong a conclusion premature. In Sendai virus to increase the probability of hybrid strain formation, the absolute rate of hybridization or the mating rate was low (the calculated hybridization frequency was about $1/10^5$ in these experiments). The first objection to such a conclusion, then, is that the hybrids could have arisen from a minor contaminant of the lymphocyte population. If the supposed contaminants came from the vascular system, then they might be expected to be capable of synthesizing collagen and our result would still be substantially in agreement with that of Green, Ephrussi, Yoshida, and Hamerman. We believe that this possibility is remote and that our examination of 5 separately derived hybrids effectively increases the probability that at least one of these 5 came from the great majority of lymphocytes in the parental cell population. A second and even more difficult problem is posed by the fact that most of the cells in these strains had "segregated" or lost as many as one half of the distinguishable rat marker chromosomes by the time that the hybrids were sufficiently numerous to be tested (about 25 cell generations). If the postulated negative control of collagen synthesis depends on the presence of a specific rat chromosome, it is possible that each of these hybrid strains had lost that chromosome. Again, the more hybrid cell strains we examine, the less likely that a specific chromosome is missing in each of them. If, however, several chromosomes from the rat lymphocyte must be present at the same time in order to achieve negative control of collagen synthesis in the hybrid, then it may prove very difficult ever to obtain the desired evidence. Our overall conclusion at this point must be that we cannot be sure, but that it is very possible that collagen synthesis is not subject to the same kind of negative control as melanin synthesis or serum antigen synthesis. We shall have to study many more independently derived lymphocyte × fibroblast hybrids to have an answer to our original question. Fortunately, improved technology has made the production of these hybrids highly efficient.

The possibility of hybrids having been formed by a "contaminant" cell type is removed if a cloned culture line is used as the original parent. We have chosen as one of these parents the mouse myeloma cell line MOPC-315B originated by Dr. Michael Potter at the NIH and adapted to cell culture and cloned by his associate, Dr. Phillip Periman. Dr. Periman has collaborated with us in producing hybrid cell lines between two of his culture adapted, functional myeloma cell lines and the selectable "L" cells, Cl 1 D and A9. These fascinating hybrid cells will be studied in great detail because of the parent myeloma cells' plasma cell-like ability to synthesize specific immunoglobulins. Our results indicate that these myeloma cells, like normal plasma cells, do not synthesize collagen. In addition to these mouse myeloma cells, we have produced hybrid cell strains from human lymphocytes (supplied courtesy of Dr. Periman) which have been extensively purified by passage through glass columns and an interval in cell culture. These fresh human lymphocytes and still another culture cell line (HL-G) derived from human lymphocytes have been used as parents in further hybridizations with Cl 1 D. Neither the lymphocytoid cell line, HL-G, nor the fresh human lymphocyte population produces collagen. We have not yet assayed the hybrids for collagen production.

If we assume that these hybrids will show the same collagen synthesizing ability that we have found in all five rat lymphocyte × Cl 1 D hybrids tested, then another very interesting variation of the basic "control of synthesis" experiment

can be done. Because of species differences recently discovered between the polypeptide $\alpha 2$ chains of rats, mice, and men, these peptides can be separated and individually quantitated. Now the question can be posed: are the polypeptides characteristic of both species produced, or is the collagen produced by the hybrid only an augmented synthesis of the Cl 1 D parent? Is a hybrid molecule of a specialized structural protein like collagen produced in these cells as was found for the ubiquitous metabolic enzyme LDH by Weiss and Ephrussi in 1966? Can a "tribrid" be made in which the chromosomes of three separate species, combined in a single multiply hybrid cell, conspire to produce a trebly hybridized collagen triple helix? The separation and analysis of the different collagen polypeptides is being done in collaboration with Dr. George Martin at the NIH. It would be especially exciting if we were able to find evidence for the "turn on" of a previously repressed specific cell function by observing the synthesis of human collagen in the human lymphocyte $\times$ Cl 1 D hybrids.

THE MAMMALIAN EMBRYO IN RELATION TO ITS ENVIRONMENT

The Spacing of Blastocysts

B. G. Böving and L. M. Billingsley

Rabbit blastocysts become approximately equidistantly spaced along the uterine horn containing them. Their spacing is a consequence of their being pushed apart by waves of contraction that arise from each end of the uterus and from wherever the uterus is distended by a blastocyst within.

The first and older conclusion (*Year Book 55*) derived from measurements of distances between conceptuses, summarized by dividing the standard deviation by the mean. The mean of such coefficients of variation (one for each horn) is not significantly different from the mean of randomized models at 3, 4, and 5 days after mating, but it becomes increasingly and significantly more nearly even at 6 and 7 days after mating—indicating the time to look for the spacing mechanism at work. An indication of where to look and what to look for is provided by the fact that spacing occurs with blastocysts well separated from each other. This suggests that the uterus conducts whatever activity it is that separates blastocysts from each other and from the ends of the horn after waves of contraction have arisen and spread from those points where it is distended by a blastocyst. Accordingly, at 6 to 7 days after mating, rabbits were opened under anesthesia. The uterus was exposed but kept warm and moist by a specially devised fanned steam generator and, for fine control, a thermistor controlled heat lamp. With the benefit of the previously described ring light (*Year Book 66*), uterine motion was photographed at 4 frames per second for subsequent study at 6 times normal speed.

The second and newer conclusion derives from the following observations. (1) Waves of uterine contraction arise from each end of the horn and from wherever it is distended by a blastocyst within. (2) They are propagated along the uterine horn. (3) Such propagated uterine contraction waves, usually called "peristalsis," differ from peristalsis by moving equally in both directions from the point of distention and by not propelling the distending object. (4) Similar contraction waves are stimulated by beads of blastocyst size inserted into the uterus. (5) Similar contraction waves are able to move beads the size of unattached blastocysts, but (6) they are unable to move attached blastocysts or beads the size of attached blastocysts. Formally, preimplantation conceptus spacing by

the rabbit may be explained in terms of stimulus (distention + spontaneous movement), effector (uterine muscle), action (propagated contraction) and result (equidistant spacing), giving some assurance that no major aspect of the mechanism has been overlooked.

With conceptus spacing worked out for one species, the rabbit, comparative study was next. The rat was chosen, because it has repeatedly been claimed to have even spacing, yet its blastocysts do not exhibit the remarkable expansion (*Year Book 67*) characteristic of the rabbit's. Thus, it might have the potential to reveal a different spacing mechanism. On the other hand, the "even spacing" claimed for rat conceptuses has not been supported by distance measurements but by counts showing tubal and cervical halves of uterine horns to contain approximately equal numbers. Such equal filling might have occurred with conceptuses spaced randomly and presumably passively, whereas equidistant spacing is statistically discriminated from random spacing and may imply that the uterus was stimulated by each conceptus individually and exerted a spacing reaction appropriate to the number of conceptuses in the particular horn. That implication of interaction applies if the conceptuses do not touch each other, but it does not apply in a string-of-beads situation where equidistant spacing may have resulted from nothing more than the equality in size of the abutting conceptuses. The first situation was usually found at 5.5 days after estimated time of mating, which is near the time of implantation (Plate 10B), but the second situation might develop as early as 6.5 days after mating if there were many conceptuses (Plate 10C). With fewer conceptuses, it tended to occur later (Plate 10D). If some information on locations of placental scars observed postnatally may be borrowed from the literature and added to the present prenatal data, it may be inferred that, as conceptuses grow, spacing by abutting continues to equalize the distances between their centers slightly and gradually until term (Fig. 19). By that time, rat spacing is as equidistant as rabbit spacing at the time of implantation. At implantation time, however, while significantly more even than random, rat spacing is significantly less regular than rabbit spacing (Fig. 19).

Exploring the rat's less accurate and distention-free preimplantation spacing mechanism requires a determination of when it operates. Accordingly, earlier data are now being sought. External examination for swellings and inspection after clearing are unreliable below the 5.5 day stage (Plate 10B). But if rat uterine horns are dissected open, some of the conceptuses are likely to be missed because they are so small. At 4.5 days after mating, it has been found possible to take advantage of increased capillary permeability at presumptive implantation sites, which lets them be marked by intravenous injection with 5% Evans blue in 0.8% NaCl solution (Plate 10A). More such preparations are needed before the spacing typical of 4.5 days can be measured and expressed quantitatively. To estimate the spacing typical of 3.5 days, it will probably be necessary to employ histological methods, which are more troublesome but also less subject to the occasional doubt in diagnosing an implantation site by the dye marking method.

The comparative study, in addition to pointing to the need for earlier rat data, has suggested the desirability of later data for rabbits to see if their nearly equidistant spacing achieved by implantation time is made even more regular by conceptuses abutting when numerous enough and big enough. More philosophically, the rat-rabbit comparison provides another example of more or less closely related mammals accomplishing a superficially similar result by at least partly different mechanisms.

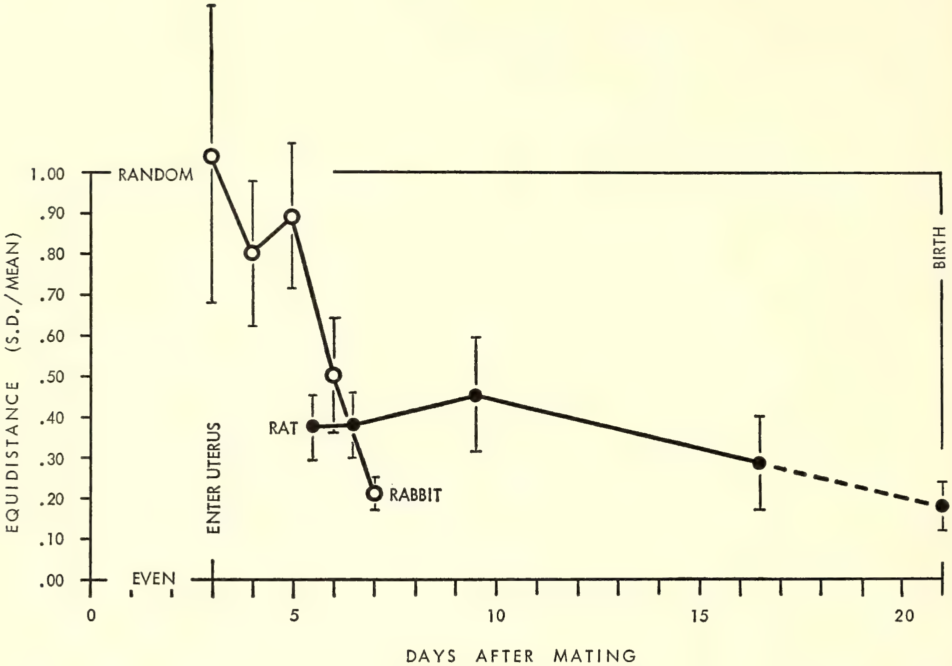

Fig. 19. The spacing of rabbit and rat conceptuses in the uterine horn at various times after mating is compared by coefficients of variation (standard deviation divided by mean distance between centers). Perfectly equidistant spacing is reflected by zero; large samples with random spacing tend to an average of unity. Vertical bars extend ± 2 S.E. Rabbit spacing is significantly more regular than rat spacing when implantation begins (rat 5.5 days; rabbit 7.0 days).

Anatomy and Physiology of the Placenta

E. M. Ramsey, H. R. Misenhimer, M. W. Donner, S. I. Margulies, and C. B. Martin, Jr.

Baseline Studies

Because of the rapidity with which the rhesus monkey has gained popularity as an experimental model for reproductive physiology, plans for investigative procedures have far outdistanced the body of information on such fundamental matters as normal blood pressure, blood constituents, etc., in both the mother and the fetus. The sparse data which are available have usually been assembled as control values from the point of view of some specific research plan and hence have only limited general usefulness. Data on the subhuman primates are almost entirely lacking.

This situation has presented an increasingly serious obstacle in our own work as our studies have come to deal more and more with physiology rather than anatomy. It is obvious that results obtained under experimental conditions which modify basal body functions can only be evaluated in comparison with the normal values for the given functions. Perhaps less apparent but of fundamental importance is the fact that many of the surgical and pharmacological procedures which form necessary preliminaries to experimental manipulations are in themselves factors which modify normal conditions. For example, most of the experiments which deal with uteroplacental circulation require the administration of an anesthetic prior to experimental manipulation. Bonica has shown in humans that anesthesia may

produce profound changes in blood pressure, blood gases, etc. and that these changes are variable and dependent upon several factors including the agent being employed.

It may be recalled (*Year Book 67*, p. 460) that previously, in collaboration with Bonica, we commenced an investigation of the effect of anesthesia on the uteroplacental circulation in the rhesus monkey. We compared the effects of intravenous pentobarbital sodium and nitrous oxide–oxygen anesthesia and found the effects to be essentially the same. We did not, however, analyze the effect of the anesthetic agent *per se* on the various parameters which might influence uteroplacental circulation, largely because baseline data for these critical parameters were not available.

For some years we have realized that "someday" we would have to take time from the forward progress of our program to establish certain of these requisite baseline values. Such an experimental parenthesis duplicates the experience of an earlier period in the work when Ramsey and Corner devoted several years to the establishment of normal myometrial activity patterns in pregnant rhesus monkeys, as a baseline for subsequent radiologic studies (see *Year Books 56–60*). The results of that exercise in self-discipline have been extremely useful not only in our own work but in that of other reproductive physiologists who employ rhesus monkeys.

In attempting to collect data upon those vital functions which form the focal points of our current interest a first hurdle lies in the fact that the monkey must be anesthetized for most procedures, including those which are easily and quite comfortably carried out in conscious, cooperative human patients. The second obstacle is presented by the monkey's ability to remove chronically implanted catheters, probes and the like, an ability which most other laboratory animals do not have. These difficulties have been largely overcome by utilizing a primate restraining chair into which the animal is placed after the initial anesthetic and surgery and where she is allowed to recover to a normal, awake state. Most animals tolerate such a restraining chair for protracted periods of time, during which continuous monitoring can be carried out without interference from the animal.

Employing these devices we have made continuous recordings of both maternal and fetal systemic blood pressure and pulse rate and have been able to obtain arterial blood samples from both the mother and fetus for simultaneous blood gas studies. These measurements have been made via plastic catheters inserted into the femoral artery of both the mother and the fetus. Values for maternal blood pressure obtained by simultaneous ausculation, employing a premature infant blood pressure cuff, were found to be unreliable and actually misleading because of the high values registered. Technically no satisfactory cuff could be obtained or devised and psychologically the animal reacted to inflation of the cuff, and indeed to the mere presence of the investigator, with an agitation which greatly increased the peripheral blood pressure while minimal effect was noted on the central pressure. The direct recordings, made hour after hour in a quiet, isolated room, were dependable and reproducible.

Our results thus far indicate a broad range of maternal mean blood pressure (diastolic pressure $+\frac{1}{3}$ pulse pressure) from 81.5 to 126.5 mm Hg with an average value of 104.6 (S.D. = 15.6) and a similarly wide variation in maternal pulse rate from 129 to 214 beats per minute with an average of 178 (S.D. = 21.6). Maternal pH and blood gases have also been studied and show a more consistent pattern, except for pO_2 which is quite variable and does not always follow the trends of the other gases or of pH. The mean values for these parameters are as follows:

Maternal arterial pH	7.40 (S.D. = 0.06)
Maternal arterial pO_2	103.7 (S.D. = 13.8) mm Hg
Maternal arterial pCO_2	26.5 (S.D. = 2.1) mm Hg
Maternal arterial HCO_3^-	18.5 (S.D. = 1.7)

The data on blood pressure, pulse rate, and blood gases have been collected from pregnant animals in which the gestational age ranged from 101 to 156 days. An insufficient number of observations has yet been made to determine whether or not the individual variations are related to gestational age; they do not appear to be influenced by the weight of the animal. Additional data are being collected to expand this body of information so that these factors and other pertinent variables can be evaluated with greater statistical validity.

An inadequate number of observations of these parameters has been made on fetuses to permit the calculation of means and standard deviations.

The effect of anesthesia on maternal and fetal blood pressure, pulse rate, and arterial pH is illustrated in Figure 20, which is a graphic analysis of a typical study. The prompt and transient decrease in both maternal and fetal mean blood pressure is a consistent observation. In approximately half of the animals studied the maternal hypotension has been followed by a period of hypertension which usually exceeds the limit of two standard deviations above the mean and persists for 2–4 hours. This observation warrants further study.

The arterial pH of both the mother and the fetus decreases after intravenous pentobarbital anesthesia. The magnitude of this decrease appears to be dependent upon the dose of pentobarbital and its duration upon the route of administration, being most persistent when part of the agent is given intramuscularly. Even though a decrease in arterial pH is a consistent finding following this anesthetic technique, it is seldom more than 2 S.D. below the mean. This trend toward acidosis probably reflects the depressing effect of pentobarbital on the respiratory center of the brain, as has been reported by other investigators. In general the blood gas values tend to support this observation by a concomitant drop in pO_2 and HCO_3^- and a rise in pCO_2. However, the latter parameters are subject to erratic variations that are sometimes unassociated with the clinical condition and are considered less reliable than arterial pH in reflecting the well-being of the mother or the fetus.

Another of the vital functions which forms a focal point of our current interest is the normal uterine artery blood flow. Study of this, using an electromagnetic flow meter, is in progress.

An additional experimental modality which may affect the vital parameters is the contrast medium employed for the radioangiographic studies. It is considered nontoxic in the usual clinical doses, but its effect upon mother and fetus in our studies is being investigated.

Although we do not feel that our study of baselines is by any means complete, we believe that enough basic data are now in hand to permit us to evaluate experimental findings with some degree of assurance.

Experimental Production of Hypertension

All of the monkeys upon whose uterine arteries Drs. Hodari and Hodgkinson placed constricting bands in 1967 (*Year Book 67,* p. 461) have now been pregnant, some of them twice, since the banding. Clinical and laboratory data are being carefully collected and collated. Each pregnant animal is subjected to radioangiography close to term and fetuses and placentas are weighed and examined. The study is being continued in the expectation that some tentative conclusions may be formulated following one or two more breeding seasons.

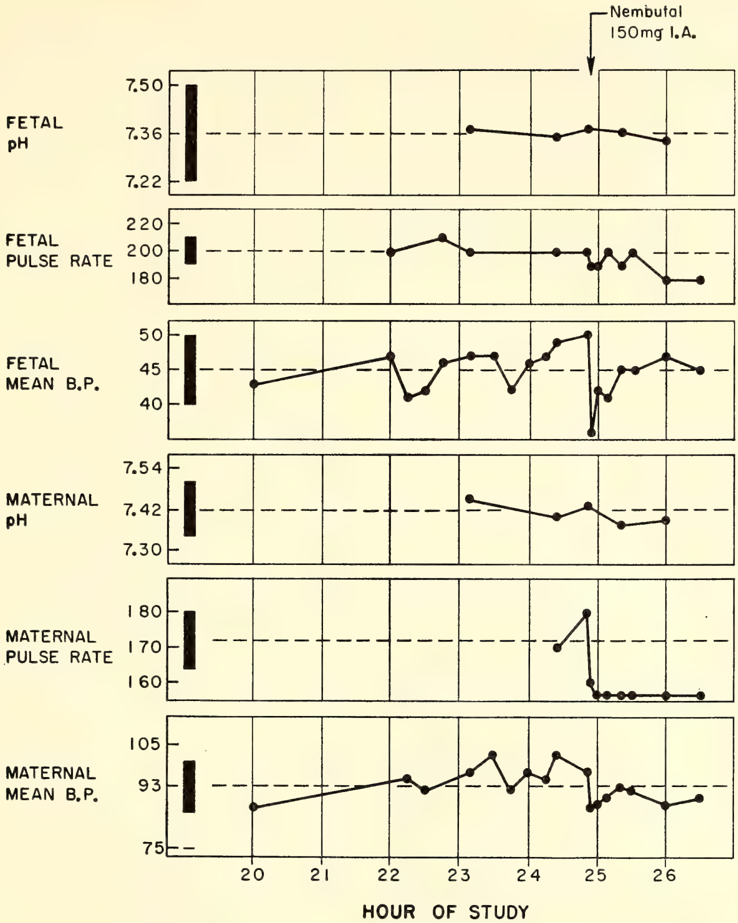

Fig. 20. Graphic analysis of a typical study showing the effect of anesthesia upon maternal and fetal blood pressure, pulse rate, and arterial *p*H. The broken line in each instance represents the mean, and the solid black bar at the left, two standard deviations. Monkey 67–97, 135 days pregnant. Study CP14.

Placenta Extrachorialis in Monkeys

G. M. Harbert, C. B. Martin, Jr., and E. M. Ramsey

Circumvallate or extrachorial placenta is an infrequent anomaly of human pregnancy, though not altogether rare. It has not previously been recorded in the rhesus monkey and this fact has been noted as bearing possible relevance to the pathogenesis of the condition, since monkey implantation is of the superficial type and human implantation is interstitial.

Occurrence of three single disc circumvallate placentas in rhesus monkeys within a single year, all associated with normal term gestations, was of striking interest. Two of the cases occurred among members of the Carnegie colony and one in the colony of the University of Virginia School of Medicine. Dr. Harbert of the Department of Obstetrics and Gynecology at the University of Virginia made an intensive study of the specimens which conformed both grossly and microscopically to the pattern char-

acteristic of human cases. The usual occurrence of a single disc placenta (80% bidiscoid in the Carnegie monkey colony) added a further element which Dr. Harbert considered in his study. Since all three specimens came from term pregnancies, no inferences could be drawn about the original depth of implantation though some weight was given to the fact that the trophoblast, always less invasive in the monkey than in the human, displayed no augmented invasiveness.

The cases are being recorded in the literature as contributory evidence which must be considered by all students of human placenta circumvallata in attempting to evolve a concept of the condition's pathogenesis.

THE COLLECTION OF HUMAN EMBRYOS

B. G. Böving and E. M. Ramsey

With the assistance of Lynn Billingsley, Böving is rearranging the serial sections of human embryos so that they will be in one continuous developmental sequence running through Streeter's Horizons and then by millimeters of crown-rump length.

Those interested in the early human embryo will be glad to hear of an excellent embryo in Horizon IX in the possession of Dr. J. E. Jirasek, Chief of the Embryological Laboratory of the Institute for the Care of Mother and Child, in Prague. This embryo, which Böving was privileged to examine, is important, because Horizon IX is represented by only 2 specimens in the Carnegie collection plus drawings and photographs of a third. More specifically, this specimen was obtained at surgery and is well preserved. Thus, its freedom of the sharp dorsal flexion present in some degree in the other specimens suggests that the flexion is not characteristic of the stage, as had been suspected.

The Development of the Human Heart at Seven Postovulatory Weeks

M. H. Cooper and R. O'Rahilly

Serial sections at stages 19, 20, and 21 (approximately 17–23 mm, C.–R.) were studied in detail. At stage 19, most of the features characteristic of the heart were present, with the exception of the septum secundum, which was seen during stage 20. Moreover, the interventricular foramen, which was patent at stage 19, was closed at stage 20. A significant growth in thickness of the myocardium of both the atria and the ventricles occurred from stage 19 to stage 21. This was particularly noticeable in the portion of the atria that would develop into the musculi pectinati. The embryonic connective tissue at the atrioventricular sulcus was evident at stage 19 and, at stage 21, it was seen descending along the external surface of the ventricles.

STAFF ACTIVITIES

Among the symposia and conferences in which various members of the staff participated during the past year were the following:

Sixth International Congress of Embryology (Paris); Symposium on Cellular Senescence in vitro (Zinkovy, Czechoslovakia); Second Congress of the National Academy of Medicine of Mexico (Mexico City); Twenty-fourth International Congress of Physiological Sciences (Washington, D. C.); Park City International Symposium on RNA in Development (Park City, Utah); Symposium on Fetal Growth and Development (San Diego); Symposium in Ob-

stetrics and Gynecology (San Francisco); Conference on Reproductive Physiology (Seattle); Fifteenth Cancer Retreat (University of Michigan); Symposium on Heterospecific Genome Interactions (Philadelphia); Symposium on Comparative Physiology of the Heart (Hanover, New Hampshire); Conference on Conduction Development (Bethesda, Maryland); Second Conference on Studies of Cellular Aging (Belmont, Maryland).

Lectures were presented at a number of campuses, including Emory University, Goucher College, Illinois Institute of Technology, Indiana University, Morgan State College, Reed College, State University of New York (Binghamton), the Universities of British Columbia, California (San Francisco), Chicago, Connecticut, Florida, Illinois, Massachusetts, Miami (Florida), Oregon, Toledo, Washington, and Wisconsin, and Wayne State University. Members of the staff also spoke at a number of hospitals and research centers, including Baltimore City Hospitals, Beth Israel Medical Center (New York), and Worcester Foundation for Experimental Biology.

Special presentations included the Janet Baldwin Memorial Lecture at Cornell University Medical School; the First Victor E. Hall Annual Lecture at the University of California (Los Angeles); a lecture before La Sociedad Venezolana de Puericultura y Pediatría and El Departamento de Clinica Pediatría y Puericultura of the Central University of Venezuela in Caracas; one at the Centennial Program of Dalhousie University Faculty of Medicine; the Keynote Address at the Junior Sciences and Humanities Symposium (Baltimore); and a lecture at the dedication of new facilities for the health sciences at the University of Vermont.

Members of the group took part in meetings of a number of learned societies, including, in addition to those already mentioned, the American Association of Anatomists, American Chemical Society, American College of Obsetricians and Gynecologists, American Philosophical Society, American Society of Biological Chemists, American Society for Cell Biology, Federation of American Societies for Experimental Biology, National Academy of Sciences, National Society for Medical Research, Society for Experimental Biology and Medicine, and Society for Gynecologic Investigation.

Advisory and consultative services included membership on the editorial boards of *Anales del Desarrollo, Developmental Biology, International Journal of Cancer, Journal of Cell Biology, Journal of Embryology and Experimental Morphology, Excerpta Medica* (section on Human Developmental Biology), *Current Topics in Developmental Biology,* and *Quarterly Review of Biology.*

Members of the staff continued to serve on the University Science Development Advisory Panel, National Science Foundation; and the Visiting Committees of the Departments of Biology of Harvard University, Massachusetts Institute of Technology, State University of New York (Buffalo), University of Oregon, and University of Toledo. In addition, service was rendered on Advisory Committees of the Center for Oral Health Research (University of Pennsylvania) and the International Institute for the Study of Human Reproduction (Columbia University).

Members of the staff also acted in these capacities: Member of the Board of Scientific Overseers, Jackson Laboratory; Trustee, Marine Biological Laboratory; Member of the Board of Scientific Counselors, National Cancer Institute; and Member of the Board of Directors, Oak Ridge Associated Universities.

Other posts occupied by members of the Department include the following: in the American Association for the Advancement of Science, Committee on Science in the Promotion of Human Welfare and Newcomb Cleveland Prize Com-

mittee; in the American Association of Anatomists, Representative to Division of Medical Sciences of the National Research Council and Representative to the National Society for Medical Research; in the American Institute of Biological Sciences, Chairman of the Committee on Laboratory Animal Care, Member, Public Responsibilities Committee and Council of Past Presidents; in the American Society of Zoologists, President-elect; and in the Society for Developmental Biology, Member of Executive Committee.

Formal teaching has been largely confined to the Johns Hopkins Department of Biology, but during the year lectures were offered in other departments of the University as well, among them Anatomy, Obstetrics and Gynecology, Pathobiology and Pediatrics.

Other activities directed largely toward teaching included the participation of members of the Department in lectures offered at high schools and junior high schools, e.g. Dunbar High School (Baltimore) and the Baltimore City–County Science Seminars; and in the Embryology Course at the Bermuda Biological Station.

The Carnegie motion picture *Uteroplacental Circulation in the Rhesus Monkey* was shown to 22 audiences during the period from November 1, 1967, through June 30, 1969.

Seminars. The roster of speakers at the seminars organized by the Department to serve all those working in developmental biology in the region included David Epel (Stanford University); Chandler Fulton (Brandeis University); Joel Huberman (Stanford University); Tom Humphreys (University of California, San Diego); Thomas Lentz (Yale University); K. Marushige (University of British Columbia); Bruce Nicklas (Duke University); Y. Nishizuka (Kyoto University); A. Paes de Carvalho (University of Rio de Janeiro); Gordon Sato (Brandeis University); Lauri Saxen (University of Helsinki); Richard Sidman (Harvard Medical School); J. E. Till (Ontario Cancer Institute); and David Wolstenholme (Kansas State University).

BIBLIOGRAPHY

Billingsley, L. M., *see* Böving, B. G.

Böving, B. G., *Review of* Ultrastructure of Fertilization, by C. R. Austin. *Science, 163,* 1187–1188, 1969.

Böving, B. G., and Billingsley, L. M., Rat conceptus spacing. *Anat. Record, 163,* 158, 1969.

Brown, D. D., *see* Green, H., Reeder, R. H.

Coon, H. G., and M. C. Weiss, A quantitative comparison of spontaneous and virus-produced viable hybrids. *Proc. Natl. Acad. Sci., 62,* 852–859, 1969.

Cooper, M. H., and R. O'Rahilly, The development of the human heart at seven postovulatory weeks. *Anat. Record, 163,* 172, 1969.

Dawid, I. B., Cytoplasmic DNA in differentiation and development. *J. Animal Sci., 27,* Suppl. I, 61–69, 1968.

Dawid, I. B., and D. R. Wolstenholme, The structure of frog oocyte mitochondrial DNA. In *Biochemical Aspects of the Biogenesis of Mitochondria,* E. C. Slater, J. M. Tager, S. Papa, and E. Quagliariello, eds., Adriatica Editrice, Bari, pp. 83–90, 1968.

Dawid, I. B., and D. R. Wolstenholme, Renaturation and hybridization studies with mitochondrial DNA. *Ibid.,* pp. 283–297.

Dawid, I. B., *see also* Wolstenholme, D. R.

DeHaan, R. L., Emergence of form and function in the embryonic heart. *Develop. Biol.,* Suppl., *2,* 208–250, 1968.

DeHaan, R. L., Guest Editorial—Congenital heart disease: A plea for an experimental approach. *New Engl. J. Med., 279,* 44–45, 1968.

DeHaan, R. L., *Review of* Epithelial-Mesenchymal Interactions. *Science, 162,* 784, 1969.

DeHaan, R. L., and S. H. Gottlieb, The electrical activity of embryonic chick heart cells isolated in tissue culture singly or in interconnected cell sheets. *J. Gen. Physiol., 52,* 643–665, 1968.

DeHaan, R. L., *see also* Stalsberg, H.

Ebert, J. D., Preface I. In *Dynamics of Development: Experiments and Inferences,* by Paul A. Weiss, Academic Press, New York, pp. v–vi, 1968.

Ebert, J. D., Discussion. In *Symposium on Molecular Aspects of Differentiation, J. Cell Physiol., 72* (Suppl. 1), pp. 222–223; 227, 1968.

Ebert, J. D., Levels of control: A useful frame of perception? In *Current Topics in Developmental Biology,* vol. 3, A. A. Moscona and A. Monroy, eds., Academic Press, New York, xv–xxv, 1968.

Ebert, J. D., The Public Information Committee of the Jackson Laboratory: *An Editorial. JAX, 16,* (4), 14–15, 1969.

Ebert, J. D., *Review of* Immunologic Deficiency Diseases in Man, R. Good, ed., *Medical Tribune,* February 24, 1969.

Ebert, J. D., *Review of* Lymphocyte Stimulation, by N. R. Ling. *BioScience, 19,* 376–377, 1969.

Ebert, J. D., *Review of* Cellular Aspects of Developmental Pathology, by R. P. Bolande. *Quart. Rev. Biol., 44,* 110, 1969.

Goldberg, B., *see* Green, H.

Gottlieb, S. H., *see* DeHaan, R. L.

Green, H., B. Goldberg, M. Schwartz, and D. D. Brown, The synthesis of collagen during the development of *Xenopus laevis. Develop. Biol., 18,* 391–400, 1968.

Harbert, G. M., C. B. Martin, Jr., and E. M. Ramsey, Placenta extrachorialis in rhesus monkeys. *Anat. Record, 163,* 195, 1969.

Kaltreider, D. F., *see* Misenhimer, H. R.

Manasek, F. J., Myocardial cell death in the embryonic chick ventricle. *J. Embryol. Exp. Morphol., 21,* 271–284, 1969.

Martin, C. B., Jr., *see* Harbert, G. M.

Misenhimer, H. R., and D. F. Kaltreider, Preterm delivery of patients with decreased glucose tolerance. *Obstet. Gynecol., 33,* 642–646, 1969.

O'Rahilly, R., *see* Cooper, M. H.

Ramsey, E. M., Radioangiography of the placenta. In *Fetal Homeostasis,* vol. III. Ralph M. Wynn, ed., Appleton-Century-Crofts, New York, N. Y., pp. 151–170, 1968.

Ramsey, E. M., *Review of* Reproduction in the Female Mammal, G. E. Lamming and E. C. Amoroso, eds., Plenum, New York; Butterworths, London, 1967 and Biology of Gestation, vol. I, The Maternal Organism. N. S. Assali, ed., Academic Press, New York, 1968. *Science, 162,* 447–448, 1968.

Ramsey, E. M., *see also* Harbert, G. M.

Reeder, R. H., and D. D. Brown, An assay for the control of ribosomal RNA gene transcription *in vitro. Federation Proc., 28,* 349, 1969.

Ristow, H., *see* Wolstenholme, D. R.

Schwartz, M. C., *see* Green, H.

Stalsberg, H., The origin of heart asymmetry: right and left contributions to the early chick embryo heart. *Develop. Biol., 19,* 109–127, 1969.

Stalsberg, H., and R. L. DeHaan, Endodermal movements during foregut formation in the chick embryo. *Develop. Biol., 18,* 198–215, 1968.

Stalsberg, H., and R. L. DeHaan, The precardiac areas and formation of the tubular heart in the chick embryo. *Develop. Biol., 19,* 128–159, 1969.

Wolstenholme, D. R., and I. B. Dawid, A size difference between the mitochondrial DNA molecules of urodele and anuran Amphibia. *J. Cell Biol., 39,* 222–228, 1968.

Wolstenholme, D. R., I. B. Dawid, and H. Ristow, An electron microscope study of DNA molecules from *Chironomus tentans* and *Chironomus thummi. Genetics, 60,* 759–770, 1968.

Wolstenholme, D. R., *see also* Dawid, I. B.

PERSONNEL

Year Ended June 30, 1969

(including those whose services began or ended during the year)

Research Staff

Bent G. Böving, Physiology
Donald D. Brown, Biochemistry
Igor B. Dawid, Biochemistry
Robert L. DeHaan, Experimental Embryology
James D. Ebert, Director
Elizabeth M. Ramsey, Placentology and Pathology

Assistant Investigator

Robert J. Hay

Research Associates (extramural)

Louis B. Flexner, Philadelphia, Pa.
Arthur T. Hertig, Boston, Mass.
Irwin R. Konigsberg, Charlottesville, Va.
Samuel R. M. Reynolds, Chicago, Ill.

Fellows

Hayden G. Coon, Fellow of Carnegie Institution
Douglas M. Fambrough,[1] Fellow of Carnegie Institution

[1] Appointed Staff Member beginning July 1, 1969.

Masako Fukada, Fellow of Carnegie Institution
Harold Kasinsky, Fellow of U. S. Public Health Service
Harold R. Misenhimer, Fellow of Carnegie Institution
Ronan O'Rahilly, Fellow of Carnegie Institution
Kenjiro Ozato,[2] Fellow of Carnegie Institution
Ronald H. Reeder,[1] Fellow of the Helen Hay Whitney Foundation
Yoshiaki Suzuki, Fellow of Carnegie Institution
Ronald F. Swanson, Fellow of U. S. Public Health Service

Students

John Chase, Graduate, Biology, Johns Hopkins University
John O. Dunning, Graduate, Biology, Johns Hopkins University
L. D. Frye, Graduate, Johns Hopkins University
H. Criss Hartzell, Jr., Graduate, Johns Hopkins University
G. B. Pogoriler, Graduate, Johns Hopkins University
Iris S. Polinger, Graduate, Biology, Johns Hopkins University
M. C. Rechsteiner, Graduate, Johns Hopkins University
E. W. Schaefer, Undergraduate, Biology, Johns Hopkins University
Merry C. Schwartz, Predoctoral Fellow, National Science Foundation, Johns Hopkins University
R. Stern, Graduate, Johns Hopkins University
Thomas G. Storch, Johns Hopkins Medical School
Pieter C. Wensink, Graduate, Johns Hopkins University

Visiting Investigators

John Bonica, Seattle, Wash.
Louis E. DeLanney, Ithaca, N. Y.
Martin W. Donner, Baltimore, Md.
Marlene Eng, Seattle, Wash.
Raymond F. Gasser, New Orleans, La.
Daniel Goor, New York, N. Y.
Peter Gruenwald, Philadelphia, Pa.
G. M. Harbert, Charlottesville, Va.
Alberto Hodari, Detroit, Mich.
Paul Hodgkinson, Detroit, Mich.
J. E. Jirasek, Prague, Czechoslovakia
Maurice Lambiotte, Bellevue, France
Lewis N. Lukens, Middletown, Conn.
F. J. Manasek, Boston, Mass.
S. I. Margulies, Baltimore, Md.
C. B. Martin, Jr., Augusta, Ga.
Dorcas H. Padget, Baltimore, Md.
Fernando Porturas, Lima, Peru
Glenn C. Rosenquist, Baltimore, Md.

Clerical and Technical Staff

James E. Abbott, Recorder
Grace M. Andrews, Secretary-Receptionist
Mary N. Barton, Librarian (part time)
James Blackwell, Custodian
William J. Cleary, Recorder
Diane M. Dombrowski, Technician
William H. Duncan, Senior Technician
Ernestine V. Flemmings, Laboratory Helper
Richard D. Grill, Photographer
Ernest Harper, Chief Custodian
Virginia Hicks, Laboratory Helper
Eddie Jordan, Technician
Elizabeth Legum, Technician
Edna G. Lichtenstein, Secretary
Alice H. Mabin, Laboratory Helper
Kathleen Magness, Technician
Thomas F. Malooly, Business Manager
Juanita Mandy, Laboratory Helper
Arlyne Musselman, Senior Technician
John Pazdernik, Building Engineer
Betty Lou Phebus, Bookkeeper-Clerk
Conrad Pott, Custodian
Margaret J. Proctor, Secretary
Martha Rebbert, Technician
Arthur G. Rever,[3] Fiscal Officer
Bessie Smith, Laboratory Helper
Delores Somerville, Technician
SuatLu Toh, Technician
Isabelle P. Williams, Technician
Leroy Williams, Custodian
David Wilmoth, Assistant Recorder
John L. Wiser, Machinist

Student Assistants

Lynn Billingsley, University of Maryland
Jeff Sollins, Drew University
Roberta M. Truitt, Morgan State College

[1] Appointed Staff Member beginning July 1, 1969.

[2] Resigned after only four months because of family illness.

[3] Retired, June 30, 1969.

PLATES

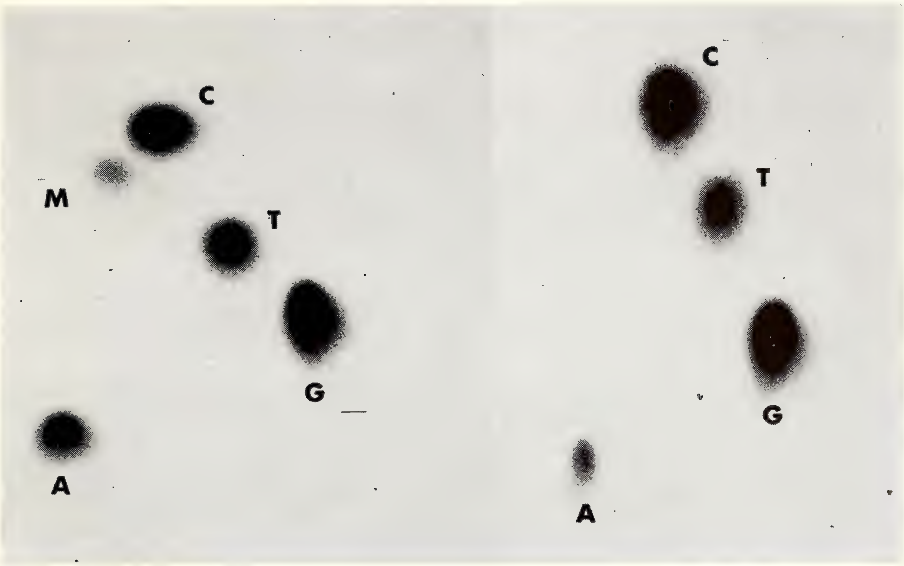

Plate 1. Autoradiogram of a two-dimensional chromatogram of the 5′-(^{32}P)-deoxyribonucleotides isolated from hydrolysates of the somatic rDNA (left) and the extra copies of rDNA in oocytes (right). The lack of complementarity seen in the nucleotides from extra rDNA is due to unequal pool sizes during labeling and does not give an exact base composition of the DNA. *A,* deoxyadenylic acid; *G,* deoxyguanylic acid; *T,* deoxythymidylic acid; *C,* deoxycytidylic acid; *M,* 5-methyl deoxycytidylic acid.

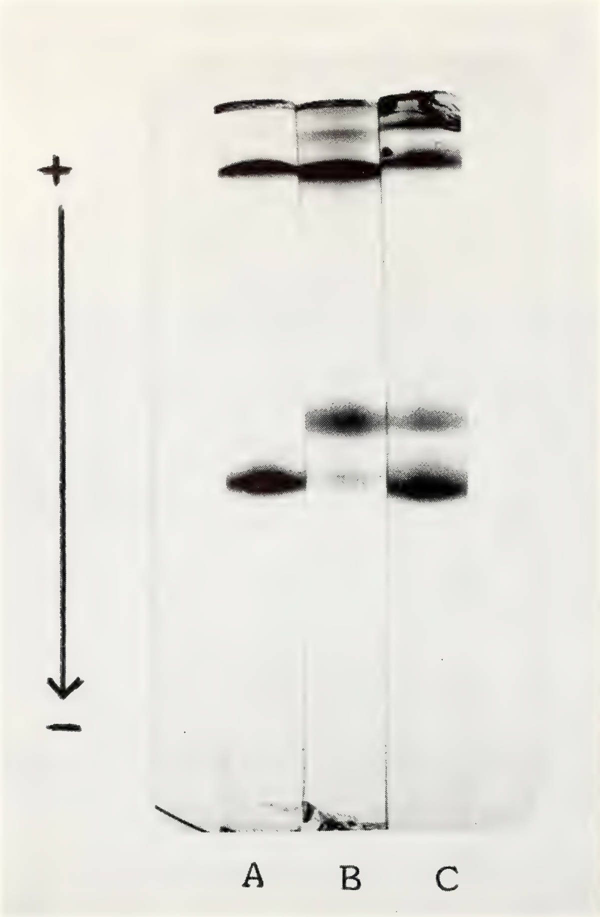

Plate 2. Coelectrophoresis of *Xenopus* Fraction C proteins with arginine-rich histone IV from pea. (*A*) Pea histone IV (*B*) Fraction C (*C*) Pea IV + Fraction C. Bands near the top of gel are bovine serum albumin protein which was added as a marker.

Plate 3. (A) Myotube isolated as described in text. Fixed with glutaraldehyde 16 hours after isolation. Phase contrast, $\times 250$. (B) Myotube of a culture infected with 5×10^5 FFU of RSV immediately after DA seeding. Pulsed beginning 67 hours after infection. Note apparently more dense labeling in the mononucleated cells. Phase contrast, $\times 250$. (C) Sister culture to B. Phase contrast, $\times 250$. (D) Myoblasts, which had been infected with RSV 45 hours earlier, were added to DA muscle cultures 96 hours after seeding. They were pulsed with ^{14}C-thymidine beginning at 22 hours after addition of infected myoblasts. Note that the grains due to ^{14}C are not localized as is the case with ^{3}H labeling. Phase contrast, $\times 250$. (E) Sister culture to D. In this case the infected myoblasts were labeled, as described in the text, with ^{3}H-thymidine before being added to the muscle culture. Note secondary labeling in nuclei adjacent to heavily labeled nuclei from infected myoblast cultures (arrow). Phase contrast, $\times 250$. (F) Muscle culture to which excess thymidine was added 24 hours after DA seeding. The culture was fixed with glutaraldehyde 56 hours later. Phase contrast, $\times 100$. (G) Sister culture to F, fixed after an additional 72 hours (a total of 152 hours after DA seeding). Phase contrast, $\times 100$.

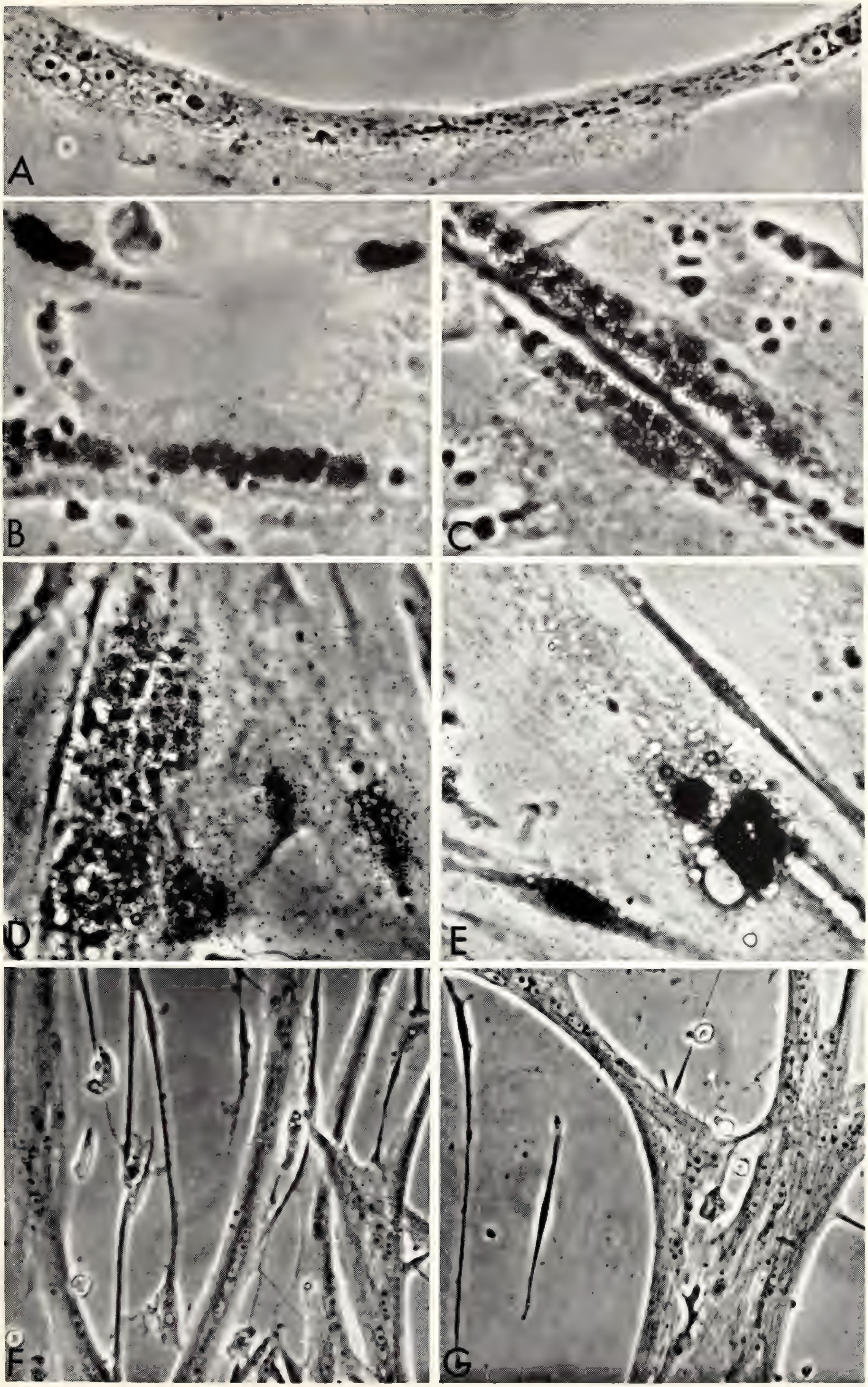
A
B
C
D
E
F
G

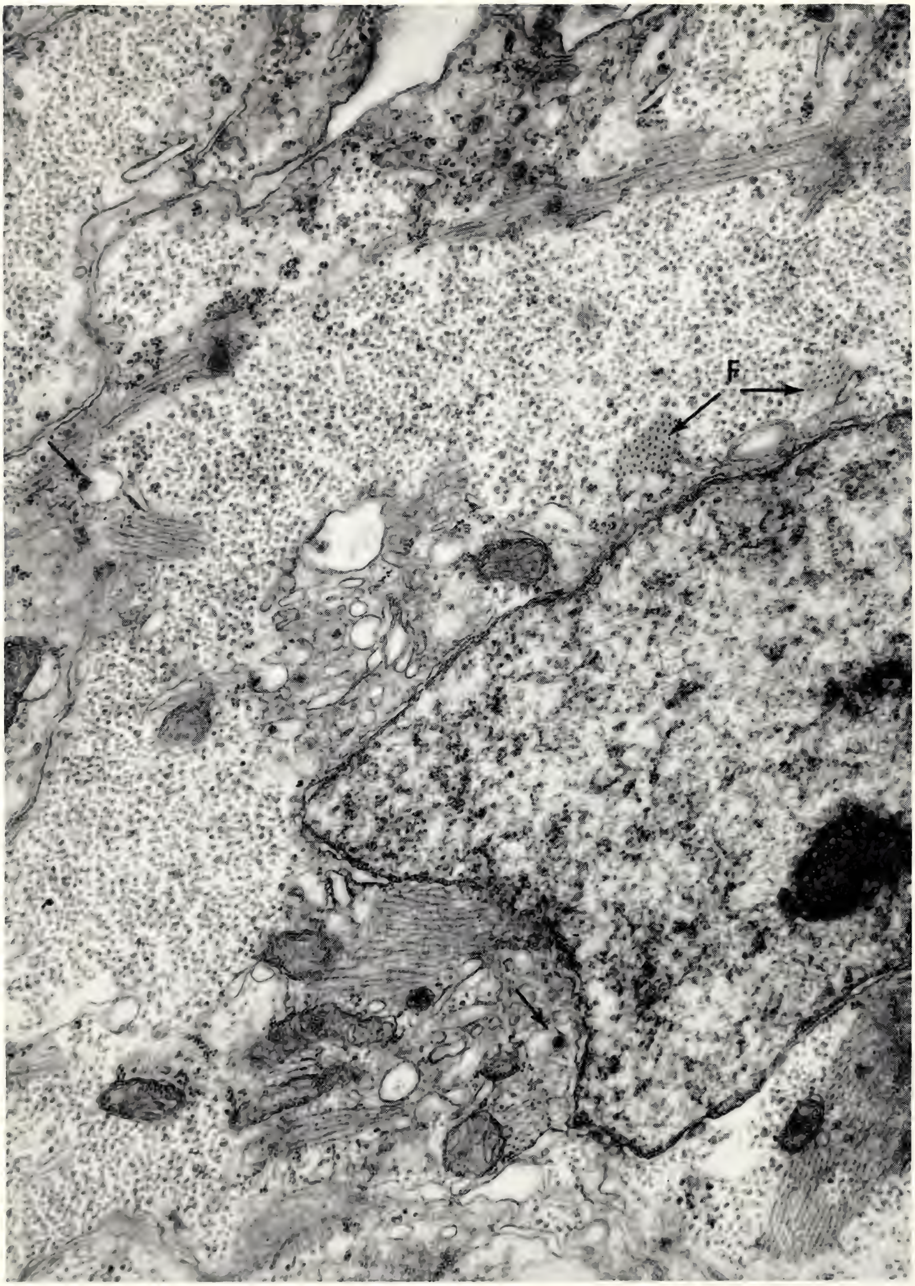

Plate 4. A portion of a ventricular myocyte from the heart of an 8-day-old chick embryo is shown in this electron micrograph. A large part of the cytoplasm is filled with glycogen granules and cardiac muscle cells of this age embryo characteristically contain large pools of this polysaccharide. In this cell, myofibrils do not appear to be packed in an orderly fashion. Several fibrils are tangentially sectioned, whereas two small bundles (*F*) are cut in cross section. The Golgi region is prominent and the arrows mark two of the many putative secretory granules seen in this cell. $\times$ 28,600.

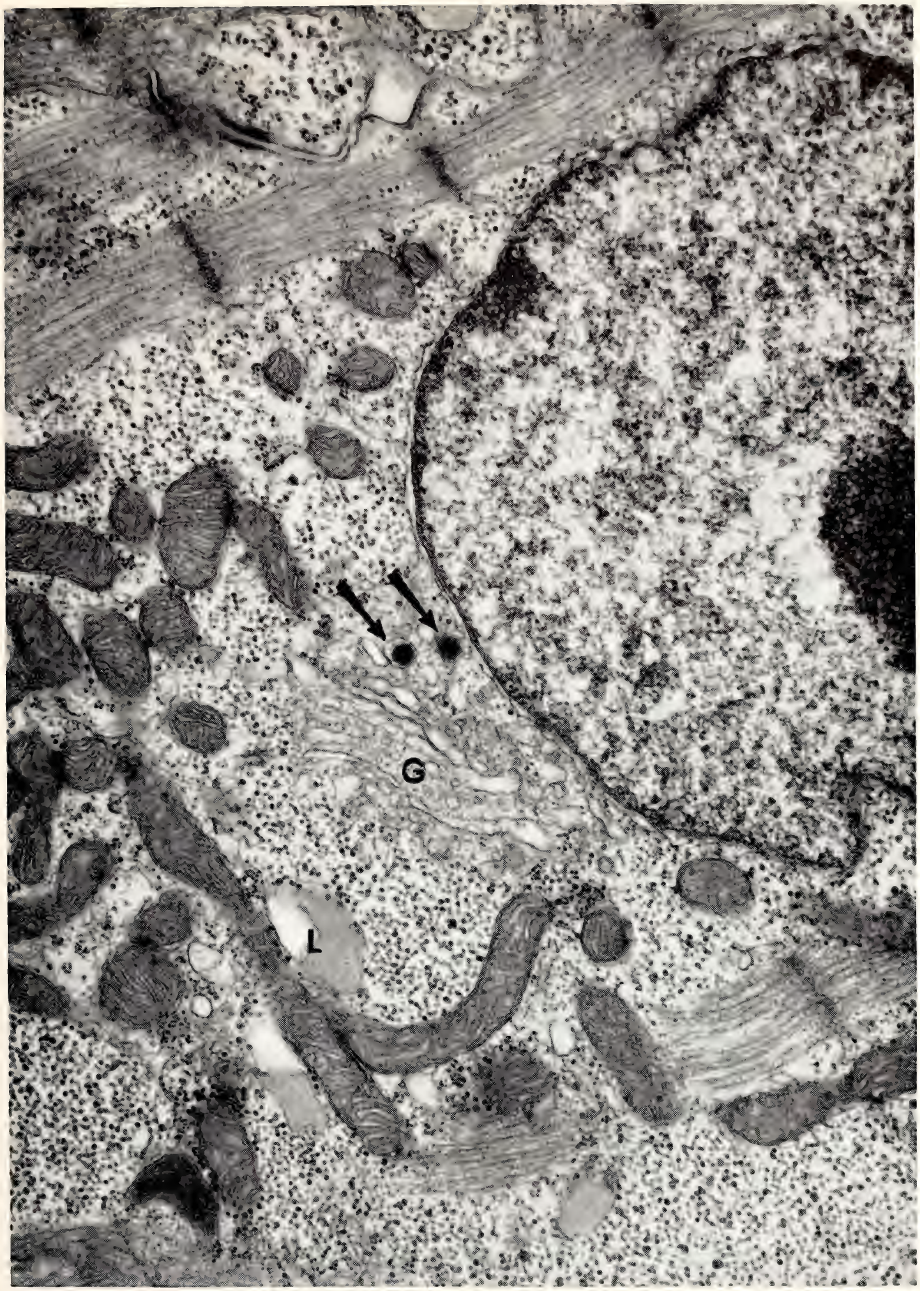

Plate 5. Ventricular myocytes of newly hatched chicks still demonstrate large amounts of glycogen, especially within the sarcoplasmic core, a portion of which is shown in this electron micrograph. Mitochondria and lipid (*L*) droplets abound in this region. Two electron-dense, membrane-bound granules are seen (arrows) within the Golgi system (*G*). A developing intercalated disc is seen in the upper left. × **29,700**.

Plate 6. Typical cilia are seen projecting from the apical surface of a small percentage of cultured *Xenopus* kidney cells. A prominent ciliary rootlet is present (arrow) and both members of a diplosome are visible near the bottom of the plate. In this electron micrograph portions of two cells are visible and a prominent space separates their lateral surfaces. $\times$ 46,000.

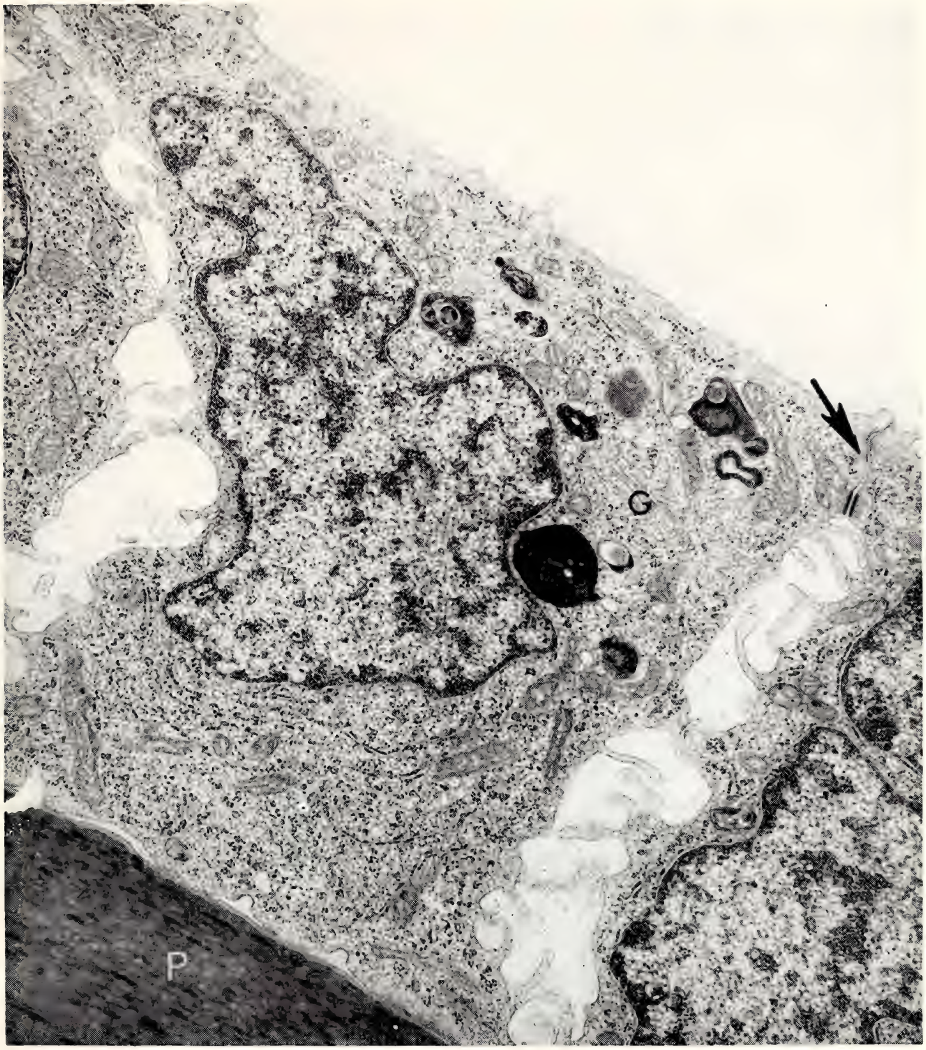

Plate 7. Portions of several cultured *Xenopus* kidney cells are seen in this low magnification ($\times$ 27,000) electron micrograph. The monolayer of low columnar epithelial cells are joined near their apical surfaces by typical apical junctional complexes (arrow). Numerous microvilli project into the large intercellular spaces between the lateral cell boundaries. The basal surface is in close contact with the plastic culture dish (*P*). These cells contain electron-dense inclusions and their cytoplasmic matrix consists largely of ribosomes, both free and membrane bound. Scattered mitochondria are present and a large Golgi system (*G*) is seen to the right of the nucleus. The electron microscope does not reveal the presence of an extracellular matrix.

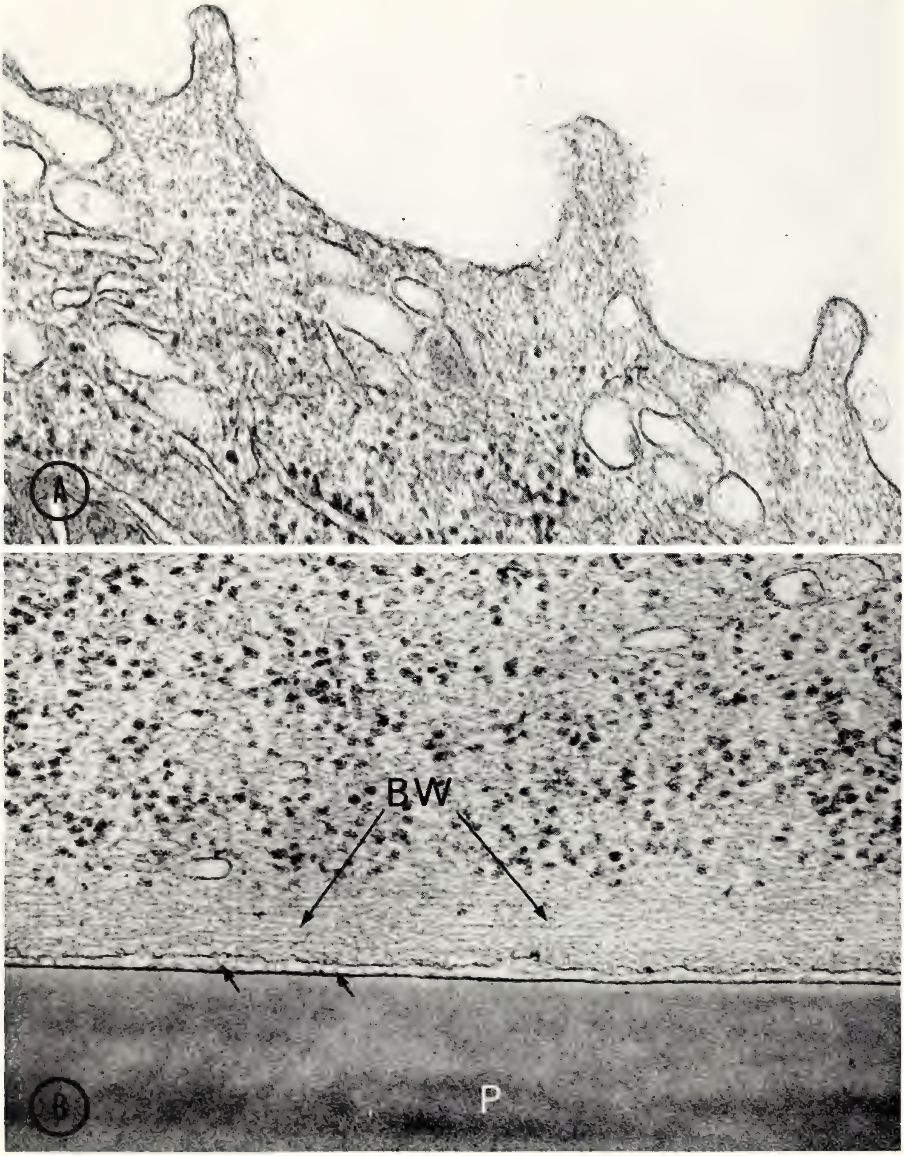

Plate 8. (A) At higher magnification the apical microvilli demonstrate a filamentous material similar in appearance to *antennulae microvillares*. Similar projections are seen along the entire apical surface. The microvilli along the lateral surface (see Plate 7) are devoid of this substance, suggesting a functional difference. $\times$ 71,000. (B) The basal surfaces of cultured *Xenopus* kidney cells are separated from the plastic culture substrate (*P*) by a narrow space. Occasionally small amounts of material can be demonstrated in this space (arrows). Wherever the cells demonstrate this close relationship to the plastic substrate they appear to develop a cytoplasmic specialization characterized by parallel filaments. In many respects this basal web (*BW*) appears similar to the terminal web of many epithelia. These cultured cells do not generally contain a well-defined cortex, and the basal web may be a specific response to the culture substratum. No specialized attachments to the substrate have ever been seen in these cells. $\times$ 90,000.

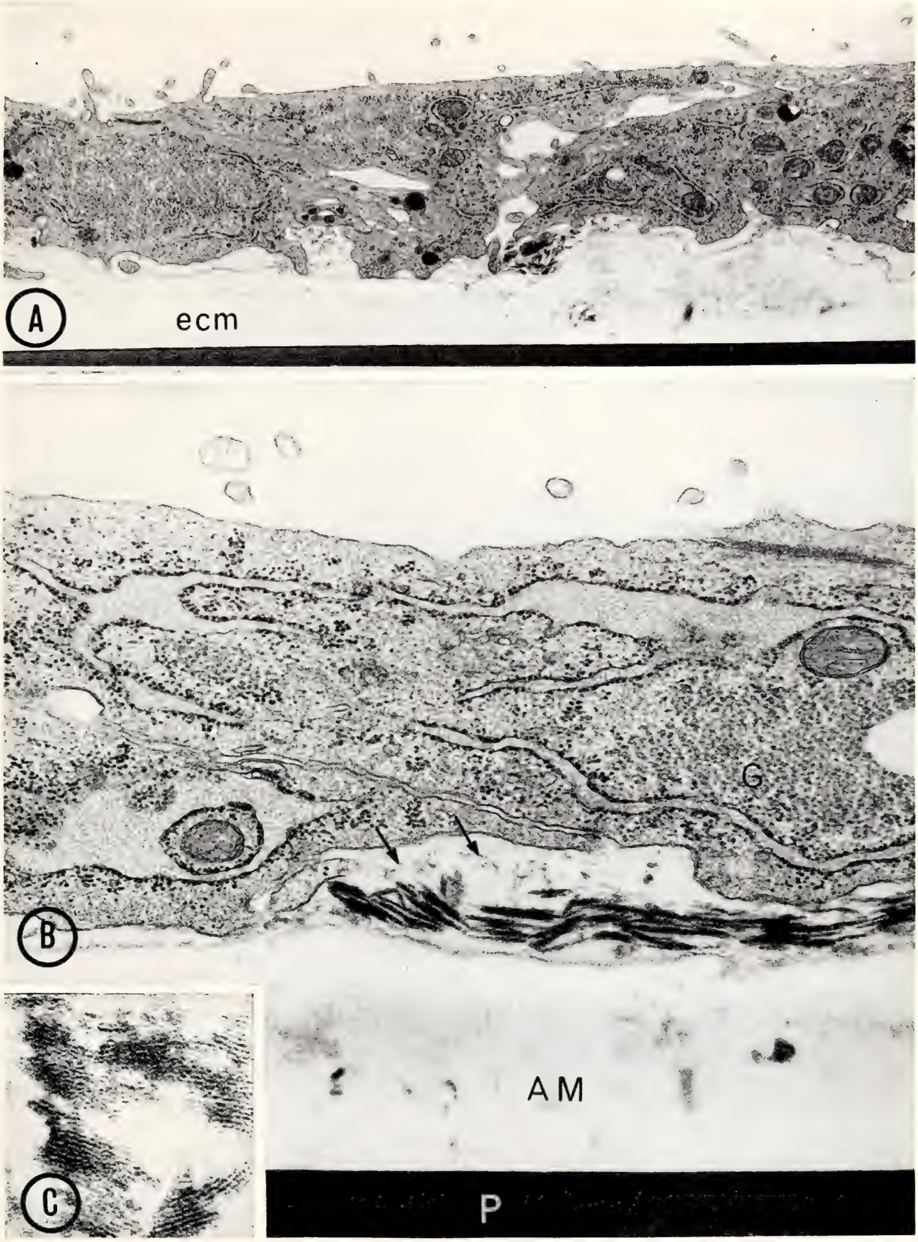

Plate 9. (A) Cultured Buffalo rat liver cells form an epithelial sheet that is often several cells thick. The apical surface has numerous microvilli, and the basal surface is widely separated from the plastic substrate of the culture dish by a layer of extracellular material (*ecm*). $\times$ 9,250. (B) Under higher magnification ($\times$ 31,000) most of the extracellular material between the culture dish (*P*) and the cell layer appears amorphous (*AM*). Occasional clumps of electron-dense material are also present. In addition, a flocculent material, similar in appearance to the material comprising basal laminae can also be demonstrated (arrows). Note the prominent granular endoplasmic reticulum and the large glycogen accumulations (*G*) within the cells. (C) Under higher magnification ($\times$ 150,000) the extremely dense extracellular material is resolved into parallel repeating subunits with a separation of approximately 45 Å.

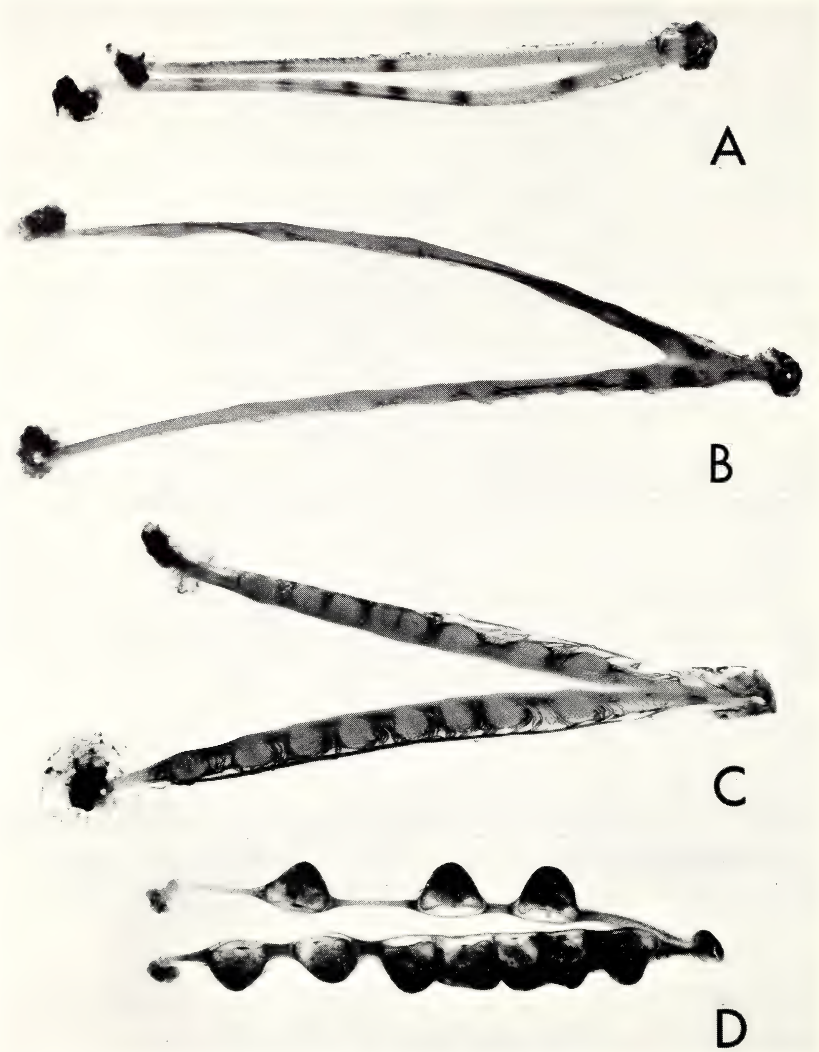

Plate 10. (A) Rat uterus with presumptive implantation sites marked by intravenously injected Evans blue; 4.5 days after mating. (B) Rat uterus with positions of conceptuses marked by slight swellings. Spacing is more even than random; 5.5 days after mating. (C) Rat uterus with conceptuses very obvious as swellings and translucent regions. With numerous conceptuses, there may be little or no spacing between them after they reach this size. Spacing approaches equidistance; 7.5 days after mating. (D) Rat uterus with pronounced swellings from conceptuses. With few (upper horn) there may still be space between them and no spacing by crowding. With more conceptuses (lower horn) the spacing by crowding begins where the crowding is most severe; 13.5 days after mating.

Department of Plant Biology

Stanford, California

C. Stacy French
Director

Contents

INTRODUCTION

In recent years photosynthesis investigations have centered on the kinetic relations between the substances that make possible the flow of electrons from water to those carbon compounds whose reduction is the significant function of the whole process. These oxido-reduction reactions are coupled to phosphorylation systems that also store chemical energy as adenosine triphosphate. Thus by a linked series of complex reactions carbon dioxide is turned into the required organic components of living matter, and power for their further interconversion is provided in usable form.

The main tide of scientific effort in the study of photosynthesis flows increasingly toward the more precise refinement of a theoretical picture describing the interrelations between the pigments, enzymes, and intermediate compounds that make up the photosynthetic system. The drawing power of this tide had for some years left an ebb in the field of knowledge from which the main tide originated. This was the descriptive and comparative type of plant physiology through which the general significance and biological function of photosynthesis became apparent over a century ago. Such types of investigation have now been revived by many vigorous groups.

Experimental taxonomy. One aspect of the work of the Experimental Taxonomy Group of the Department might now be described as an effort to bring the advances in the detailed understanding of the mechanisms of photosynthesis to bear on explanations for the diverse physiology of contrasting kinds of plants. To apply effectively the relevant parts of the vast body of intricate concepts about photosynthesis to broader biological problems—such as a determination of the physiological basis of adaptation and of natural selection and evolution in plants—almost requires that investigators themselves be active contributors to the main body of theoretical progress as well as users of that new information for the clarification of fundamental ecological questions. A strong collaborative effort on these lines has been developed by Drs. Björkman, Hiesey, and Nobs with several members of the Stanford faculty and their graduate students.

In the Experimental Taxonomy Section, this year's activities include continuing studies at the altitudinal transplant stations at Stanford, Mather, and Timberline as well as intensive laboratory investigations directed toward further penetration into unknown mechanisms underlying natural selection and plant evolution.

In 1947 the Experimental Taxonomy Group met with university colleagues having similar interests at the Department Laboratory and at the mountain stations. The purpose of this conference was to select the type of plant material best suited for long-term studies of the adaptation mechanisms of plants to contrasting environments. The resulting choice, the Erythranthe group of *Mimulus* (monkey flower), has amply proved its anticipated value as an experimental group of species for such investigations. Cross-fertilization experiments have been combined with studies of growth characteristics both at the Department's three field stations and in controlled environments. Field work has been correlated to laboratory measurements of the photosynthetic characteristics of first-, second-, and third-generation progeny. Each generation was studied for several years.

A strong correlation was found between the inheritance of certain morphological characters and the ability to survive in specific environments. The action of combinations of genes caused nearly all of the significant characters to

be inherited in groups, that is, a purely random assortment of characters did not take place. Hybrid vigor was found to depend as much upon the environment in which it was tested as upon the genetic inheritance of the plants. The genetic recombinations of some of the various steps of the photosynthetic process suggest the mechanisms underlying the ability of hybrids to flourish in contrasting environments.

This long series of studies on the basic question of biological quality, as determined by the interplay of genetic and of environmental influences, is being prepared for publication as an Institution monograph. This fifth volume in the series *Experimental Studies on the Nature of Species* appropriately marks Dr. William M. Hiesey's retirement after forty-four years devoted to basic research on this problem of the comparative influences of environment and of heredity on the performance of an individual.

Many of the questions arising from the work of the Experimental Taxonomy Group under Dr. Clausen's and Dr. Hiesey's leadership can now be investigated in a more definitive manner than was possible at the time their significance was first perceived. As Dr. Björkman now has assumed responsibility for experimental taxonomy work at the Department, the biochemical basis for physiological characteristics of plant adaptation to contrasting environments is receiving greater emphasis. Thus there is an increasing amount of collaboration, and of similarity in the experimental techniques, of the two groups in the Department, although their objectives remain distinct.

Recently Dr. Björkman and Mr. Eckard Gauhl, an Institution Research Fellow from Professor Egle's laboratory at Frankfurt, have been able to measure simultaneously with high precision not only the rates of carbon dioxide uptake and water vapor release, but also the rate of oxygen evolution during photosynthesis in higher plants. Such measurements are made possible by the development of new equipment and are of special value in the current comparative studies of contrasting ecological races and species.

In the growing field of comparative studies of photosynthesis in plants from ecologically diverse environments, recent developments have revealed that photosynthetic differentiation in higher plants is not limited only to differences in the *capacities* of component steps of photosynthesis, but that differences in the biochemical *pathways* of the process also exist. During the past few years it has been established that certain grass species, whose main distribution is in tropical regions, possess a different pathway for photosynthetic carbon dioxide fixation than do plants from temperate regions. Members of at least three dicotyledonous families have also been found to possess this newly discovered pathway. In the saltbush genus *Atriplex* some members have this pathway, whereas others do not.

The discovery of different CO_2-fixation pathways in photosynthesis has opened up an exciting field of investigation for those concerned with the biochemical and physiological basis of adaptation. Dr. Björkman and Mr. Gauhl have undertaken a comparative study of two *Atriplex* species of differing CO_2-fixation pathways. Their work is an integral part of a broad study of mechanisms of photosynthetic adaptation to environmental factors, particularly with regard to temperature. One of these *Atriplex* species, *A. patula,* which occurs mainly in cool coastal areas, fixes CO_2 by the normal reductive pentose phosphate pathway, whereas the other species, *A. rosea,* which grows primarily in hot, semiarid habitats, fixes CO_2 by the more recently discovered C_4-dicarboxylic acid pathway. The two species differ with regard to certain key photosynthetic enzymes, and they have profoundly different photosynthetic characteristics. For

example, the strong inhibitory effect of oxygen on photosynthetic CO_2 fixation in normal air, which appears to be a widespread phenomenon among higher plants from temperate climates, is present in *A. patula* but absent in *A. rosea*. The two species also differ markedly in their internal leaf structure. Other investigators have linked these combinations of differences to contrasts in plants of tropical and temperate climates, and these characteristics are thought to represent fundamental differences in evolutionary steps.

That these differences occur within a single genus makes possible comparative studies of functional adaptability that are more pertinent than would be the case if they occurred only in widely separated taxa. Still more important, however, the inheritance of the function, and biochemistry of the various components by which the two species differ, may now be studied. Recently, Dr. Nobs has been able to hybridize these two species of *Atriplex*. First-generation hybrids are now being analyzed by Dr. Björkman with regard to their photosynthetic and biochemical characteristics. Dr. John Boynton, an Institution Research Fellow from Duke University, is making a study of cell and chloroplast fine structure of the F_1-hybrid compared with that of the parental species. It is hoped that second-generation progeny can also be obtained, a development that would open up new opportunities for genetic studies of the molecular and physiological basis of natural selection and speciation.

Mr. Gauhl has also completed a two-year study on contrasting ecological races of the European bittersweet, *Solanum dulcamara,* in which distinct inherited differences in photosynthetic characteristics were demonstrated.

The relationships between certain North American and European species of goldenrod (*Solidago*) have long been a subject of speculation among botanists. The physiological studies on sun and shade races of European forms of *Solidago virgaurea* by Drs. Björkman and Holmgren have created new interest in ascertaining these relationships. Results from hybridizations, most of which were made by Dr. Nobs, now clearly demonstrate that the European members and the North American counterparts (referable to *S. multiradiata*) are forms which have evolved moderate genetic barriers to intercrossing. Within either group, highly diverse ecological races are completely interfertile.

Biochemical investigations. The Biochemical Investigations Group continues to center most of its interest on the functional relationships between photosynthetic pigments and their associated enzymes in the two photosystems. Each of these systems contains a mixture of pigments and enzymes in the form of particles. Many laboratories are trying to improve techniques for the separation of the two photosystems of chloroplasts. Thorough resolution of the two requires both adequate disintegration methods and sharp separation procedures. The primary test for successful fractionation of chloroplasts into the two groups of particles involved in system 1 and system 2 is the ratio of the rates of two chemical reactions, which are specific for one or the other system. The pigment composition of the systems is also different. In general there is more chlorophyll *b* and more of a "C*a* 670" form of chlorophyll *a* in system 2 than in system 1. In system 1 a "C*a* 680" form of chlorophyll *a* predominates, and system 1 also contains some of the forms of chlorophyll that have still longer wavelength absorption maxima.

We are trying to analyze the absorption spectra of chloroplast fractions in order to identify the specific chlorophyll *a* complexes associated with each system. Different species of algae have greatly varying relative proportions of the different forms of chlorophyll. Furthermore, the system-1 and system-2 fractions of many chloroplasts show striking con-

trasts in their absorption spectra. Dr. Brown has separated fractions of chlorophyll-containing particles from a variety of plants and has measured both their absorption and fluorescence spectra at low temperature. The collection and interpretation of these data, and of data resulting from older lines of investigation, are still in progress. It is expected that comparisons of a comprehensive series of spectra resolved by digital computer methods will show whether the spectra for the different individual forms of chlorophyll are alike or different in the corresponding fractions of all species.

In determining whether all the chlorophyll in one fraction is actually a functional part of that system, it is essential to compare the absorption spectra of both fractions with the action spectra for the two chemical reactions of each fraction. Action spectra, the relative effectiveness of different wavelengths in causing a specific chemical effect, match the absorption spectra of only the *photochemically active* pigments in the mixture. Absorption spectra, however, show *all* the pigments present, even though some of them may not be functional for the systems tested. It is therefore very important to learn how to measure action spectra with high precision for system-1 and system-2 activity of fractions of disintegrated chloroplasts.

Action spectra for oxygen exchange in whole cells have been measured for some time with adequate accuracy, and the results can be plotted automatically, like absorption spectra, with moderately satisfactory results. However, for the partial reactions associated with the separate steps of photosynthesis in chloroplast fractions, the precision so far attainable is lamentable, and the band widths of the monochromatic light for action spectroscopy are about ten times the routine width for absorption spectroscopy.

In an effort to improve this situation Dr. Eckhard Loos, an Institution Research Fellow from Munich, has made a study of ways to improve measurements of action spectra for chloroplast fractions. So far his work has been on photosystem 1 as determined by the photochemical reduction of the dye methyl viologen. Initially attempts were made to introduce a controlled oxygen leak into the system in such a way as to balance the reduction of the dye by the photochemical reaction. The intensities needed at different wavelengths to maintain a constant concentration of reduced dye would reflect the relative photochemical action of each wavelength. Such an arrangement would have made automatic plotting possible. There were, however, difficulties with the oxygen leak sufficient to make this approach impractical at the present time.

The same dye reduction system was therefore used in a sealed vessel for point-by-point measurements. The optimum concentrations of the critical components of the reaction mixture were determined. The system as worked out gives easily measurable rates at low light intensities. With a high pressure mercury lamp, monochromator slits giving a half-band width of 1.5 nm can be used. The reproducibility of rate determinations, however, is still inadequate. The preliminary results of Dr. Loos' work have shown close agreement between the action and absorption spectra of system-1 particles from spinach chloroplasts.

Dr. Zdenak Šesták, a Visiting Investigator from Prague, followed the changes in the relative amounts of system-1 and system-2 pigments in developing leaves. In young radish leaves he found about 25 percent of the chlorophyll to be in system-1 particles while in older leaves only 15 percent was in system 1. Young leaves are therefore preferable for preparation of system-1 fractions.

Several mild treatments, such as gentle heating, ultraviolet exposure, and incubation with enzymes, disrupt the "C*a* 680" form of chlorophyll responsible for system-1 photochemistry and change it to a form with a shorter wavelength peak.

Similar treatments that reduce the photochemical activity of system 2 in spinach chloroplasts have been investigated by Dr. Kenneth Mantai, a Carnegie Corporation Fellow who came to us from Professor Bishop's laboratory at Oregon State University. The common basis for the effects of ultraviolet radiation and the effects of treatments by destructive enzymes is believed to be the disruption of the structural unit comprising the pigment-enzyme complex that is specific for the functioning of system 2 in the chloroplasts.

The energy of a light quantum absorbed by a chlorophyll molecule is not immediately used for making chemical changes but instead is passed on through many chlorophyll molecules until it arrives at a particular reaction center. All the chlorophyll molecules, acting together as an antenna to catch light quanta for one reaction center, constitute a photosynthetic unit. Emerson and Arnold originally determined the size of this unit by dividing the number of chlorophyll molecules in a sample of algae by the number of oxygen molecules the algae could produce from a single flash of bright light.

The same concept can be applied to groups of photosynthetic units whose products may depend on a single enzyme for further processing. Thus each pigment system can be thought of as a small group of chlorophyll molecules feeding energy to a particular reaction center, while the products from several such centers are serviced by a single enzyme molecule, which action defines a larger composite unit. The size of this larger unit can be determined by testing whether the action of a single molecule of an enzyme poison can render the enzyme molecule ineffective.

A somewhat similar experiment was done this year by Dr. Lars Olof Björn, a Visiting Investigator from Lund, who calculated a photosynthetic unit of about 10^5 chlorophyll molecules. This result was obtained from the stimulating effect of phenazine methosulfate on the slow emission of delayed light from cells following the activation of photosystem 1 by far-red light. The size of the functional unit so measured is approximately that of the morphological unit called a thylacoid that is recognizable in electron-microscope photographs of chloroplasts.

The connections to two large computers at Stanford, described last year by Dr. David Fork, have been used extensively, and a Dataphone line to the IBM 360/67 Computer has been added. The effective use of these facilities has been made possible by a grant from the National Science Foundation (No. GB 8630) for "Pigment-Enzyme Interactions in the Electron-Transport Mechanism of Photosynthesis." This grant gives our work on the subject far greater scope than could be managed on the Department budget alone. In fact, the application of computer analysis to a wide variety of comparable chlorophyll spectra is the essential difference between one aspect of the present project and the somewhat similar, but very limited, approach to the problem that we have made in the past. Our experience in applying for this grant has, however, made clear the extreme importance of flexible funds that can be appropriated without delay. Without the interim support of the Institution to pay for computer use during the grant processing period, a severe loss of momentum and of investigators' time would have occurred. In addition to serving their computational purposes, the computers have been a means of reducing the secretarial work of manuscript revision and of handling our reprint distribution list.

The rate of publication on photosynthesis, like the rate of publication in all fields of science, has increased so much that each scientist must continually narrow and redefine the limits of his specialty. Because of the quantity of published work, the value of good review articles is now far greater than that of all but a very few original "contribu-

tions" to the subject. The important public service of the Kettering Laboratory and of a Japanese group in preparing and circulating lists of titles of papers on photosynthesis and related matters has made it possible at least to be aware of work relevant to one's current enterprises. Reading even a reasonable fraction of the important papers is already impossible. There are no longer any experts on the whole subject of photosynthesis.

In 1965 we started a cooperative card-file system to list papers of particular interest under 75 subject headings. Each card is punched for needle selection by several subject headings, by author, and by laboratory. The designation of papers for card listing requires only a few cryptic symbols on the journal or on the reprint itself made by the interested scientist. The whole operation is handled by the Department secretary. This apparently adequate and simple system has in four years produced so many cards that the selection of those in a desired category is approaching the limit of practicality.

We see no satisfactory solution to the problem of literature listing and searching that can be carried out efficiently by a small group of research workers, even with complete secretarial support. Cost and programming problems seem to make computer use for literature searching an unrealistic approach for a single laboratory. Some sort of a centralized computer selection and listing system serving the entire community of photosynthesis workers seems to be an eventual necessity. However, the practical problems of interlaboratory agreement on organization of the system and on methods for its efficient use are serious even for the literature of photosynthesis. A greater difficulty than incomplete listing will be the danger of swamping the interrogator with information only partially relevant to his immediate concerns.

The purpose of a useful literature search system is to go beyond the title or abstract in order to retrieve buried information about specific findings and experimental techniques. A central computer could perhaps answer an inquiry by searching its internally stored library and reporting only a reference and page listing of the desired information that would already be in the worker's own library. Presumably we will have to wait until such systems have been developed for other types of scientific work before it would be reasonable to attempt their use for our subject. It would, of course, be useful if some group of enterprising computerized-library specialists could be induced to use the publications on photosynthesis for developing a system to search scientific literature.

BIOCHEMICAL INVESTIGATIONS

Studies on Fractions of Chlorophyll Complexes from a Variety of Plants

J. S. Brown

In order to study the various forms of chlorophyll, the forms should first be separated. Detergents have been used for this purpose for several years, but in using them there is the disadvantage that the detergent may adhere to the chlorophyll-lipoprotein complexes, modify the spectra of the material, and complicate further analysis. Therefore the nondetergent, physical method of fractionation devised last year by J.-M. and M.-R. Michel is especially valuable (*Year Book 67*, p. 508). Briefly, the procedure consists of disintegrating the chloroplasts or algae suspended in a KCl-Tricine buffer with the French press, layering the broken material on a sucrose density-gradient, and centrifuging the layered material for 30–60 minutes to separate the two kinds of chlorophyll-containing particles.

The light fraction-1 particles are similar to the system-1 particles separated by detergent fractionation procedures. They show relatively more long wavelength absorption and fluorescence and have a lower fluorescence yield per chlorophyll than the denser particles in fraction 2. These two kinds of particles were obtained from several higher plants and algae (*Year Book 67,* p. 516).

This year further experiments have been performed to study some parameters of the procedure itself: to fractionate non-green algae, including the red alga *Porphyridium,* the diatom *Phaeodactylum,* and three blue-green algae, *Anacystis, Anabaena* and *Plectonema;* and to compare the absorption and fluorescence of the various pigmented particles. The effect of mild heating and of trypsin or porcine pancreatic lipase digestion on the absorption of spinach particles was also investigated.

The way in which the algae were grown and harvested, and the way the chloroplasts were prepared, apparently had little or no effect upon the subsequent fractionation. A buffer of 0.05 *M* $K_2HPO_4-KH_2PO_4$ at *p*H 8 has proved to be as suitable as the Tris or Tricine used previously.

For the experiments reported here the algae were suspended in 0.3 *M* KCl, 0.05 *M* Tricine, *p*H 8, and forced through the needle valve three or more times. Since the amount of breakage by the needle valve was low with certain algae, we tried the Braun "MSK" mechanical cell homogenizer. Rapid shaking of a dense algal suspension in the same buffer as above with glass beads 0.25–0.30 mm in diameter for 2 minutes was sufficient to break practically all of the cells. We have not yet standardized this breaking method completely, but if conditions such as the ratio of cells to beads and the temperature during shaking are optimal, this homogenate, after spinning in the sucrose gradient, will yield the same fractions as the material broken by the needle valve. Cells of *Scenedesmus, Porphyridium,* and *Anacystis* have been successfully fractionated after disintegration by the MSK homogenizer.

Whether the bands in the sucrose gradient contain different kinds of chlorophyll particles has been determined by at least one of the following spectroscopic criteria: low-temperature absorption or fluorescence-emission spectra, and relative fluorescence yields of the chlorophyll.

Table 1 shows the relative fluorescence yields of chlorophyll *a* in fractions of chloroplasts and algae studied since those listed in Table 9, *Year Book 67,* p. 518. These yields were determined by the same method as before, except that the concentration of chlorophyll *a* alone has been used in the current calculations in order to compare algae that lack chlorophyll *b*.

TABLE 1. Relative Fluorescence Yield of Chlorophyll *a* in Fractions 1 and 2 at 20°C and the Long-Wavelength Emission Maximum of Fraction 1 at —196°C

Plant Material	Fluorescence Yield		Fluorescence Peak
	Fraction 1	Fraction 2	Position, nm
Spinach	2.2	7.1	734
Atriplex semibaccata	0.72	2.2	735
Chlamydomonas rheinhardii	2.9	5.9	711
Scenedesmus obliquus	5.0	9.2	720
Botrydiopsis alpina	1.4	2.5	715
Phaeodactylum tricornutum	1.9	9.6	No peak
Anacystis nidulans	0.54		715
Anabaena cylindrica	0.91		726
Plectonema boryanum	0.24		728

Low-temperature absorption and fluorescence spectra in Fig. 1 of *Chlamydomonas* and *Scenedesmus* illustrate typical separations in which fraction 2 has proportionately more chlorophyll *b*, absorbing at 650 nm, and less long wavelength absorption than fraction 1. Fraction 1 has greater emission at longer wavelengths than fraction 2 relative to the peak near 680 nm. The small absorption band near 700 nm was first observed in *Scenedesmus* by Butler, 1960, and called C-705. Butler, 1966, suggested that C-705 may be the same form of chlorophyll as C*a* 695 in *Euglena,* and that it is also the fluorescence-excitation band seen in all the green plants that were examined. However, we have not detected this band in spectra of other algae closely related to *Scenedesmus.*

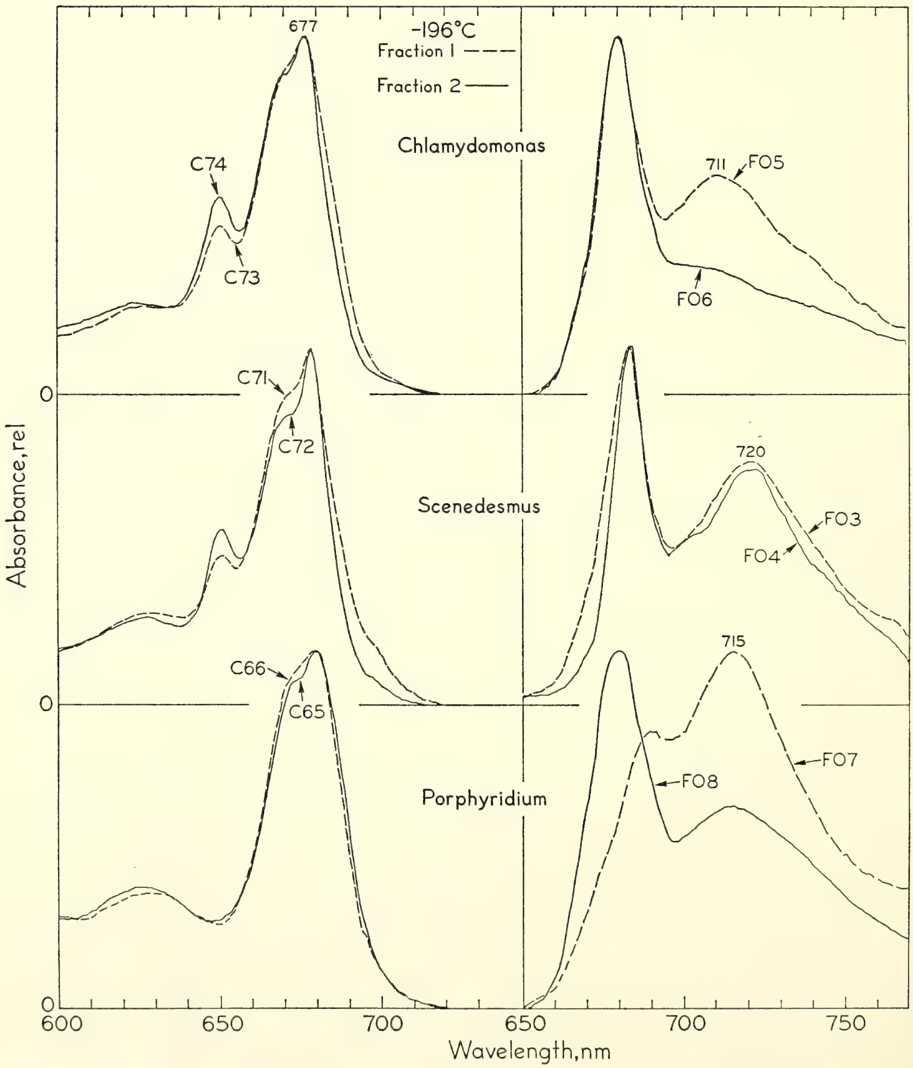

Fig. 1. Absorption and fluorescence spectra of fractions 1 and 2 from *Chlamydomonas, Scenedesmus* and *Porphyridium* recorded at —196°C. Excitation at 435 nm.

The fluorescence yields of fractions from *Porphyridium* were not measured, but differences in the absorption and emission spectra can be seen in Fig. 1 and do indicate that two kinds of chlorophyll fractions were obtained. Most of the phycoerythrin remained at the top of the sucrose after centrifugation.

Attempts to fractionate the three species of blue-green algae were originally made by initially breaking the cells in the needle valve. Since disruption was incomplete, only a relatively small amount of chlorophyll-containing particles were dispersed through the sucrose gradient. Spectroscopic tests of samples from various levels in the centrifuge tube revealed no differences. More recently, *Anacystis* was thoroughly broken by shaking with glass beads in the MSK homogenizer. Centrifugation of this homogenate in sucrose produced a layering of phycocyanin at the top of the tube and two well-separated green bands below. However, these bands had very similar absorption and emission spectra.

Since we have so far failed to find two chlorophyll fractions from the blue-green algae, we must consider the possibility that the separation of phycocyanin from the denser fraction 2 type of chlorophyll, with which it is thought to function, may have altered the whole particle. The particles of blue-green algae all had the relatively low fluorescence yields characteristic of fraction 1.

Fig. 2 shows low-temperature absorption and emission spectra of particles from three species of blue-green algae. The differences in the relative proportions of the biological forms of chlorophyll are striking. All the spectra were measured with submicroscopic particles of about the same density and chlorophyll concentration. A positive correlation is evident between the amount of absorption at 710 nm and the height of the long-wavelength (relative to the short-wavelength) fluorescence band.

The question of which chlorophyll absorption band is the source of the long-wavelength fluorescence band, enhanced in fraction 1 at low temperature, has often been asked. Different experimenters have reported widely different peak positions for the long-wavelength emission band in different kinds of plants. Since a part of this variation might have been due to errors inherent in different spectrofluorimeters and to the measurement

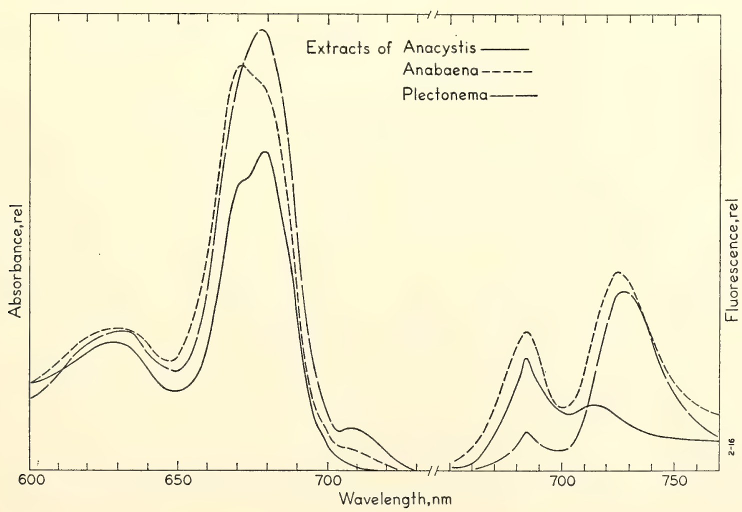

Fig. 2. Absorption and fluorescence spectra of particles of *Anacystis, Anabaena* and *Plectonema* recorded at —196°C. Excitation at 435 nm.

of samples with too much chlorophyll, we compared the fluorescence emission spectra, measured in the same way, of very dilute fraction-1 particles from a number of species. The peak positions, listed in Table 1, varied from 711 to 735 nm and showed no apparent correlation with a particular absorption band except for the case of the blue-green algae mentioned above. The source of this emission band still remains largely unexplained.

An investigation of the stability of the chlorophyll-lipoprotein binding that may determine the characteristic absorption spectra of the biological forms of chlorophyll was attempted. With spinach, heating the homogenate to 40°C for 10 minutes, or storing it at 4°C for 2 days, had no effect upon its subsequent ability to fractionate in the sucrose gradient or upon the absorption spectra of the fractions. This is in contrast to broken cells of some algae such as *Tribonema* and *Botrydiopsis,* in which a considerable transformation of the "C*a* 680" chlorophyll peak to about 670 nm occurs within a day of storage at 4°C.

Both fractions 1 and 2 from spinach were incubated at 25°C with trypsin and in separate experiments with porcine lipase for several hours. No change appeared in the low-temperature chlorophyll absorption spectra of the treated particles even though the fraction-2 particles clumped after 15 minutes.

In contrast to this lack of an enzyme effect, Michel-Wolwertz (*Year Book 67,* p. 505) observed that a protease (from *Streptomyces griseus*) caused shifts in the proportions of chlorophyll forms in particles of *Euglena* and *Chlorella.* Wheat lipase also changed the absorption of *Chlorella* particles. Either these enzymes from different sources act differently, or the chlorophyll complexes in spinach are more resistant to their action. However, treatment with trypsin and porcine lipase, more than sufficient to inhibit DCIP reduction completely (see Mantai, this *Year Book,* p. 601), need not be reflected in any detectable change in chlorophyll absorption.

References

Butler, W. L., *Biochem. Biophys. Res. Commun., 3,* 685, 1960.

Butler, W. L. in *The Chlorophylls,* Leo P. Vernon and Gilbert R. Seely, eds., Academic Press, N. Y., p. 343, 1966.

Absorption and Fluorescence of Chlorophyllide *a* in vivo

J. S. Brown

The accumulation of chlorophyllide *a* (chlorophyll *a* without phytol) in a *Chlorella* mutant "SCA" makes it possible to measure the absorption and fluorescence spectra of that pigment in vivo. Ellsworth and Aronoff, 1968, determined that chlorophyllide *a* is the major porphyrin in this mutant, but that it is easily converted in part to pheophorbide *a* (chlorophyllide minus Mg) by exposure of the cells to strong light or during extraction by organic solvents. Dr. Ellsworth kindly supplied us with a culture of the "SCA" mutant induced by ultraviolet irradiation.

The absorption peaks of ethyl chlorophyllide and of chlorophyll *a* in ether are both near 660 nm. The two major biological forms of chlorophyll *a* absorb between 670 and 683 nm. The absorption maximum of chlorophyllide *a* in *Chlorella* is here reported at 690 nm. This long wavelength peak position of chlorophyllide in vivo shows that the wavelength shift caused by the arrangement of chlorophyll molecules on a carrier is not dependent on the presence of the phytol tail.

The cells were grown on a glucose-agar medium in darkness for 6 days. Absorption and fluorescence spectra of both the intact cells and their homogenates were measured near the temperature of liquid N_2 (Fig. 3). The homogenates were prepared by passing the cells, suspended in a 0.15 *M* KCl, 0.05 *M* Tricine buffer at

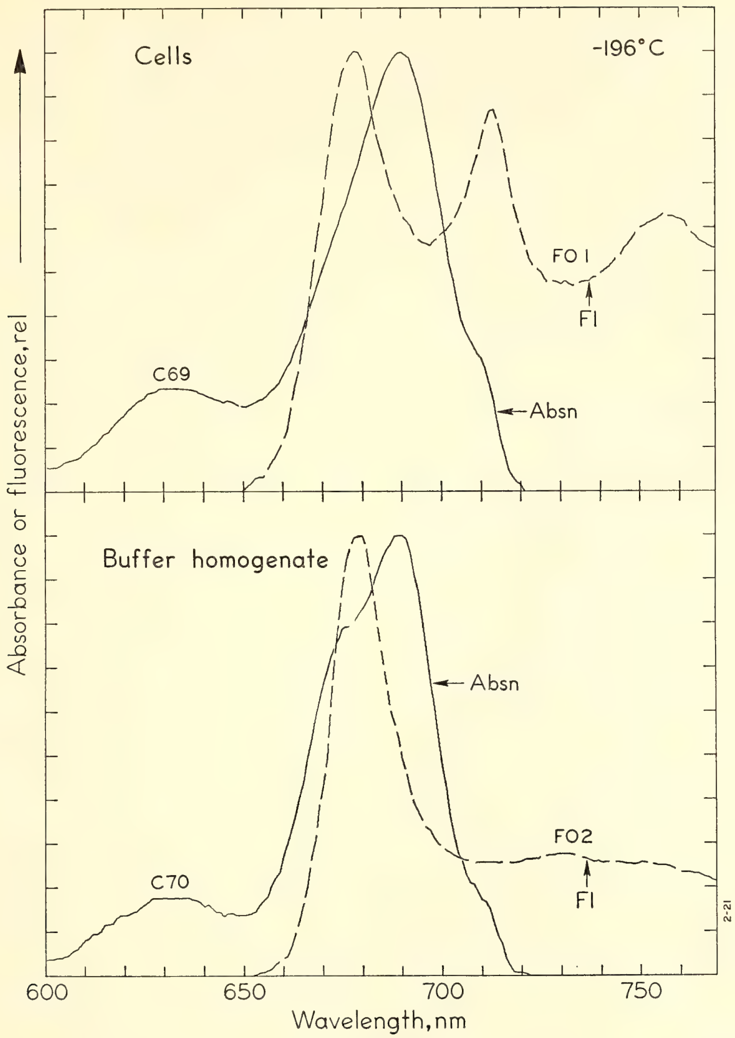

Fig. 3. Absorption and emission spectra measured at —196°C of *Chlorella* mutant "SCA" cells and their homogenate. Excitation at 435 nm.

*p*H 8, through the needle valve several times and centrifuging at 3000 *g* for 10 minutes to remove the larger particles.

An approximate check on the pigment content of the homogenate was made by extracting these pigments with 80% acetone in water and measuring the absorption spectrum. Characteristic absorption maxima of pheophorbide *a* at 410 and 535 nm indicated that some of this porphyrin was indeed present in the homogenates.

The absorption spectrum shows the in vivo absorption maximum of chlorophyllide *a* at 690 nm. The shoulder between 670 and 680 nm that is more prominent in the homogenate than in the cells is probably due to pheophorbide *a* because this pigment is known to be formed from chlorophyllide by extrac-

tion. The pigment causing the small band near 710 nm is unknown. A form of pheophorbide *a* absorbing at 710 nm has been observed in aged *Euglena* (*Year Book 61,* p. 352) and in *Ginkgo* leaves by Kunieda and Takamiya, 1965. However, the main peak in damaged *Ochromonas* (Brown, 1968) and in acid-treated chloroplasts was found at 671 nm. Whether *Ochromonas* contained pheophorbide or pheophytin was not determined, but the two porphyrins have very similar spectral characteristics.

The peak positions in the emission spectra are difficult to explain unless we assume that chlorophyllide *a* in vivo does not fluoresce, and that the emission band near 680 nm is from the pheophorbide. This is reasonable since the pheophorbide in *Ochromonas* fluoresced at 683 nm. The emission peak at 713 nm is from a second, unknown pigment form that is destroyed by breaking the cells. The diatom *Phaeodactylum* also has a similarly labile emission band at 714 nm (*Year Book 65,* p. 486).

References

Brown, J. S., *Biochim. Biophys. Acta, 153,* 901–902, 1968.

Ellsworth, R. K., and S. Aronoff, *Arch. Biochem. Biophys., 125,* 35–39, 1968.

Kunieda, R., and A. Takamiya, *Plant and Cell Physiol., 6,* 431–439, 1965.

Photosystem 1 and 2 Particles from Leaves of Diverse Ages

Z. Šesták

During the development of a leaf from unfolding to abscission its photosynthetic rate displays characteristic changes. The rate increases to the phase of photosynthetic maturity followed by a steady decline that may go below the compensation point. Although changes of chlorophyll content have a similar character, the slower decline of chlorophyll is reflected in a gradual lowering of assimilation numbers with the aging of leaves. This was already observed in 1918 by Willstätter and Stoll (for review see Šesták and Catsky, 1967). One of the reasons for these ontogenetic changes in assimilation numbers may be an interconversion of the forms of chlorophyll in vivo and/or a changed ratio of photosystems 1 and 2.

To test this possibility the fractionation method of Michel and Michel-Wolwertz (*Year Book 67,* pp. 508–514) was employed to separate chloroplast fractions enriched in photosystem 1 or 2. In experiments with young, middle-aged, and old spinach and radish leaves purchased at the local market, the method was used with only one minor modification: besides linear gradients, step gradients (5 ml, 12.5% sucrose solution; 20 ml, 30%; 5 ml, 50%) were used. Centrifugation times of 30 or 35 minutes were chosen for radish and 40 or 45 minutes for spinach. The standard procedure was found unsuitable for glass-house plants of *Mimulus cardinalis* whose chloroplasts and photosystems were probably too heavily damaged by the procedure.

With linear gradients the method affords a reasonable separation of three bands. In step gradients band 2 often appears only as an elongated tail of band 1 or in front of band 3, while band 3 is usually located at the boundary of the last two sucrose concentrations. This results in irregularities in the flow-cuvette evaluation of the results (see bands of photosystem 2 in Fig. 4).

The disadvantage of the method is that in various steps of the chloroplast isolation procedure a great deal of chlorophyll-containing material is rejected. Consequently the chloroplasts thus fractionated may represent only a specific fraction of the total plant tissue initially used, i.e., the mature chloroplasts, chloroplasts with resistant membranes, small chloroplasts, etc.

Absorption spectra of particles in bands 1 and 3 (containing particles enriched in photosystems 1 and 2, respectively) measured both at room tempera-

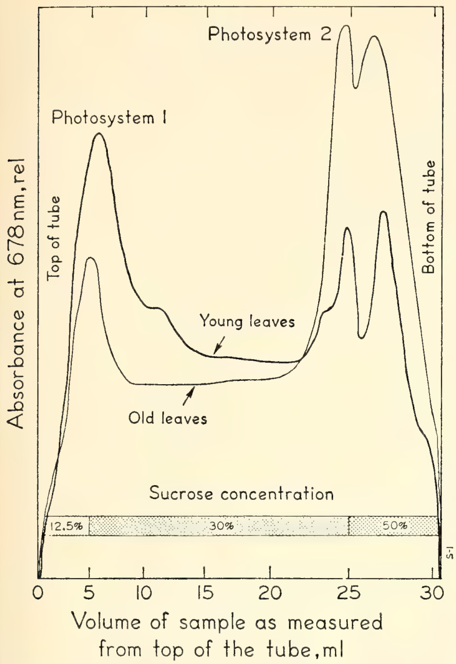

Fig. 4. The distribution of chloroplast particles from young and old radish leaves fractionated by step-gradient centrifugation in sucrose. The absorbance at 678 nm is plotted against the quantity of sample withdrawn, as measured from the top of the tube.

ture and at liquid nitrogen temperature agreed with those given by Michel and Michel-Wolwertz. No obvious difference in the spectral characteristic other than that corresponding to a different chlorophyll *a/b* ratio was found between particles from young and from old leaves.

On the other hand, visual inspection of centrifuged sucrose gradients indicated a different distribution of particles from young and old leaf chloroplasts into the individual bands. To test this the spectrophotometric system for light-scattering samples described by French and Lawrence (*Year Book 66*, pp. 175–177) was adapted for flowing the contents of the centrifuge tube through the cuvette. (The cuvette was modified by Mr. R. W. Hart.) Starting with the bottom layer, the gradient flowed through the cuvette by gravity only. The resulting nonlinear flow speed (see abscissa in Fig. 4) induces difficulties in the quantitative evaluation of the records and needs to be improved by slow pumping of the gradient through the cuvette. The accuracy was, however, found suitable (values always within the limits of ±10%) by comparing centrifuge tubes with different amounts of broken chloroplasts put on its top (Table 2).

The records (e.g., Fig. 4) confirmed that chloroplasts from young leaves contained more photosystem-1 and less photosystem-2 particles than chloroplasts from old leaves. Thus, for example, band 1 from young radish leaf chloroplasts included approximately 25% of the total chlorophyll in the original homogenate, whereas the same band from old leaves had only about 15% of the total chlorophyll.

Particles of both photosystems from young leaf chloroplasts had a significantly lower ratio of chlorophylls *a/b* and a 20–30% higher fluorescence at 683 nm per chlorophyll $(a+b)$ than those from old leaves. This difference was more clearly pronounced by calculation per chlorophyll *a* only in photosystem 2 which has a lower chlorophyll *a/b* ratio. With the aging of the dialyzed separated particles, these differences in fluorescence yield between preparations from young and old leaves diminished. This may be due to a more rapid decay of the photo-

TABLE 2. An Accuracy Test for the Estimation of Relative Chlorophyll Contents of Different Fractions of the Homogenate of an Old Radish Leaf *

Amount of Sample Applied, ml	Band Area: Entire Sample	Band 1	Bands 2 and 3
100	100	100	100
150	150	141	159
200	207	211	210

* The absorbance of a sucrose step-gradient was measured in a flow-through cuvette at 678 nm. The area under the curves were computed giving that for the lowest concentration a value of 100.

systems after isolation from young leaves.

Although the results have to be confirmed on a large number of plant species by analyses either of individual leaves on a plant or of one leaf during its whole life cycle, they suggest that with the maturation and aging of leaves the amount of photosystem-1 particles in isolated chloroplasts declines in relation to photosystem-2 particles. At the same time their photoactivity relative to amount of chlorophyll falls. Because particles of the (middle) band 2 were found by Michel and Michel-Wolwertz to display photosystem-2 activity (their absorption spectra are also similar to those of photosystem-2 particles), it seems that there is a surplus of photosystem-2 particles in chloroplasts, and, therefore, the amount of photosystem-1 particles and the amount of chlorophyll in them may limit the photosynthetic rate.

Reference

Šesták, Z., and J. Catsky, in *Le chloroplaste, croissance et vieillissement,* C. Sironval, ed., Masson et Cie., Paris, pp. 213–262, 1967.

An Action Spectrum for Methyl Viologen Reduction by Fractionated Spinach Chloroplasts

Eckhard Loos

In the last few years chloroplast fragments have become available which are enriched in one or the other of the two photosystems (systems 1 and 2) operating in photosynthesis of algae and higher plants. To obtain better insight into these two systems, especially with regard to their pigment composition, one should have them separated as cleanly as possible. An important criterion for the completeness of a fractionation is the degree of coincidence of the absorption spectrum of a fraction with the action spectrum for a reaction specific for system 1 or 2.

Several absorption spectra of subchloroplast particles containing predominantly photosystem-1 or photosystem-2 pigments have been published (Boardman and Anderson, 1964; Anderson and Boardman, 1966; Ogawa *et al.,* 1966; Vernon *et al.,* 1966; Briantais, 1967; Michel and Michel-Wolwertz, 1969; Bril *et al.,* 1969). There are also a number of action spectra for system-1 and system-2 activity (Müller *et al.,* 1963; Kelly and Sauer, 1965; Vidaver, 1966; Joliot *et al.,* 1968; Ludlow and Park, 1969). However, they were measured with whole chloroplasts or algal cells, which are known to have flattened absorption and action spectra. In the present study an attempt was made to obtain an action spectrum with fractionated chloroplasts. It was hoped to gain in this way more exact knowledge of the pigments sensitizing a partial reaction of photosynthesis and to be able to estimate the degree of separation of the two photosystems. Because system-2 enriched particles are quite labile and tricky to experiment with, the attempt was made first with system-1 particles. Methyl viologen reduction was chosen as a system-1 reaction (Arnon, 1963; Kok *et al.,* 1965) using an artificial electron donor and DCMU to block any activity from system 2.

Material and Methods

About 180 g spinach leaves were homogenized for 10 seconds in the Waring blendor with 65 ml of buffer "A" (Jensen and Bassham, 1966) from which $NaNO_3$ and Na-isoascorbate were omitted. The resulting brei was filtered through 8 layers of cheesecloth and the filtrate centrifuged for 2.5 minutes at $3000 \times g$. The pellet was resuspended in 5–10 ml 0.05 *M* Tricine (*p*H 7.9), 0.15 *M* KCl and forced twice through a needle valve. Unbroken chloroplasts were then removed by centrifuging for 5 minutes at $3000 \times g$. From the homogenate so obtained, 2 ml (equivalent to 500–1500 μg chlorophyll) were layered on 30 ml of a linear sucrose gradient (10–50%) con-

taining 0.15 *M* KCl and 0.05 *M* Tricine *p*H 7.9. After 45 minutes' centrifugation at 65,000 × *g*, system-1 enriched particles were withdrawn from the green top band in the centrifuge tube and, henceforth in this report, are called fraction 1.

Unless otherwise indicated, the reaction mixture used contained in moles/liter: Tricine, 0.05 (*p*H 7.8–8.0); KCl, 0.15; NH_4Cl, 10^{-3}; cysteine, 0.04; DCPIP, 2×10^{-5}; DCMU, 10^{-5}; methyl viologen 2×10^{-4}. The chlorophyll concentration was 2.5 μg ml^{-1}. To make this mixture anaerobic, 1-ml plexiglas cuvettes were filled, bubbled for 1 minute with N_2, and closed with a screw cover.

Methyl viologen reduction was followed spectrophotometrically by recording the increase of absorption at 386 nm, a secondary peak of the reduced form of methyl viologen. The measuring light was isolated with an interference filter (10-nm half bandwidth) and after passage through the sample detected by an RCA photomultiplier (type IP 22), which was protected from stray actinic light by two Corning filters, No. 9782 and No. 5543. The measuring beam and the actinic light were at right angles to each other, the path-lengths being 7.9 and 4.8 mm respectively. In action spectra measurements the cuvette was backed with an aluminum foil for a more even illumination of the sample. Actinic light was obtained from a 2000-w high pressure mercury lamp used in conjunction with a monochromator, and was filtered through 4 cm water, a Balzers Calflex heat-reflecting filter and for the wavelengths 600–660 nm, through Corning filter No. 2404, for 645–680 nm, through Corning filter No. 2408 and, for 680 nm and longer, through Schott filter RG5. In experiments not dealing with action spectra, actinic light was provided by a ribbon filament lamp and a 680-nm interference filter (10-nm half bandwidth) plus a Calflex filter. Light intensity was monitored continuously by deflecting part of the beam onto a calibrated silicon cell whose output was amplified and integrated over the time interval of the exposure. Absorption spectra were measured with a spectrophotometer specially suited for light scattering samples (French and Lawrence, 1968).

Results

A. Methyl viologen reduction using cysteine-DCPIP as electron donor

The cysteine-DCPIP couple was used as electron donor because with ascorbate-DCPIP no activity was detected, confirming the results of Arnon (1963).

Kinetics. Two types of kinetics were encountered. The first one, illustrated in Fig. 5A, is characterized by a rapid increase of absorption upon the onset of illumination, after which the rate tapers off to a constant value in the course of several seconds; shutting off the light causes a sudden decrease of absorption followed by a more or less sloping back rate.

The second kind lacks the transients (Fig. 5B). The reason for the two kinetic

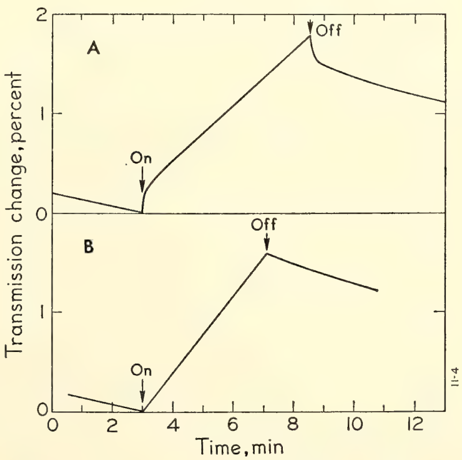

Fig. 5. Kinetics of methyl viologen reduction. In the experiment for Fig. 5A the DCPIP concentration was 1.4×10^{-4} *M* and the cysteine concentration was 5×10^{-3} *M*. Upward trace corresponds to a decrease of absorption. Wavelength of light was 696 nm for part A of the figure and 680 nm for part B, nonsaturating light intensities.

types is not yet clear. It may be a seasonal variability in the spinach leaves, for the kinetics with the transients were observed from December through March and could not be reproduced in the summer time.

The rate of the back reaction increased during the course of an experiment after many alternating light and dark periods, apparently concurrently with the accumulation of reduced dye (Fig. 6). The steady-state rate of methyl viologen reduction in the following experiments was corrected for the back reaction, using the average of the steady rates before and after a light exposure.

Optimizing the reaction conditions. The concentration of some components of the reaction mixture was varied to find optimum conditions, to be able to use the relatively weak light intensities available with a narrow spectral bandwidth of the actinic light.

A schedule of 5.5 minutes dark alternating with 5.7 minutes light was employed. The light intensity was about 3000 ergs cm^{-2} sec^{-1}, and the wavelength, 680 nm. Each point represents the average of at least two measurements.

The influence of DCPIP concentration. Table 3 shows the dependence of the rate of methyl viologen reduction on the DCPIP-concentration. The optimum is around 3×10^{-5} *M* DCPIP, the decline

TABLE 3. Rate of Methyl Viologen Reduction at Different DCPIP-Concentrations *

Concentration of DCPIP, *M*	Rate of Methyl Viologen Reduction, Rel.
3×10^{-4}	10.5
1×10^{-4}	48
3×10^{-5}	125
1×10^{-5}	100
3×10^{-6}	58.5
1×10^{-6}	25

* The cysteine concentration was 5×10^{-3} *M*.

in activity being sharper towards the higher concentrations than towards the lower ones. For all further experiments a DCPIP concentration of 2×10^{-5} *M* was chosen.

The influence of cysteine concentration. The concentration of cysteine, which keeps the DCPIP reduced, may affect considerably the rate of methyl viologen reduction, as is illustrated in Table 4. The optimum rates were observed only in the relatively small concentration range between 0.04 and 0.08

TABLE 4. Rate of Methyl Viologen Reduction at Different Cysteine Concentrations

Concentration of Cysteine, *M*	Rate of Methyl Viologen Reduction, Rel.
4×10^{-3}	3.7
8×10^{-3}	12.7
1.6×10^{-2}	17.2
4×10^{-2}	25.6
8×10^{-2}	25.0

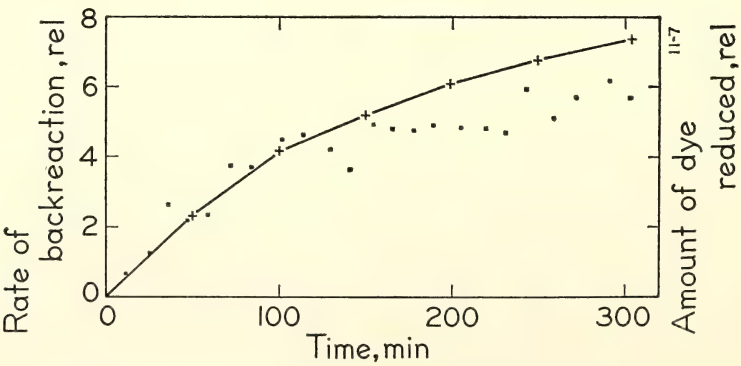

Fig. 6. Accumulation of reduced methyl viologen (line through crosses) and rates of reoxidation during the dark periods (points). Periods of 7–8 minutes light alternated with 4–5 minutes dark. Nonsaturating light intensities; chlorophyll concentration 1.3 g ml^{-1}. Data are taken from an action spectrum experiment.

TABLE 5. Rate of Methyl Viologen Reduction at Different Methyl Viologen Concentrations

Concentration of Methyl Viologen, *M*	Rate of Methyl Viologen Reduction, Rel.
10^{-5}	11.6
5×10^{-5}	11.9
2×10^{-4}	13.4
5×10^{-4}	11.1
1×10^{-3}	12.9

M. With the highest concentration tested (0.08 *M*) in some cases the rate declined with time. The reason for the relatively low rates at weaker cysteine concentrations may be a too slow re-reduction of DCPIP, which becomes oxidized in the light by the chloroplast fragments.

The influence of methyl viologen concentration. One experiment was carried out varying the concentration of methyl viologen; it did not seem to be critical under the chosen conditions (Table 5).

Dependence of the rate of methyl viologen reduction on light intensity. A four minutes light to four minutes dark schedule was used for these experiments. In general the light intensity curves were S-shaped (Fig. 7) and only in a few

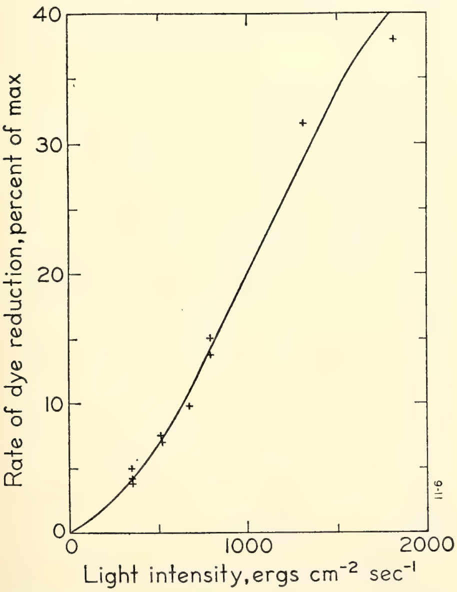

Fig. 7. The dependence of rate of methyl viologen reduction on light intensity, wavelength 680 nm.

cases was a linear relationship found. The slopes of the curves attained their greatest steepness at rates which amounted to 10% or less of the light-saturated value. The reason for the nonlinearity in the lower intensity range is not yet known. One explanation is a limited cyclic electron transport, preferentially driven at low light intensities.

B. Action spectrum for methyl viologen reduction

To minimize errors due to the nonlinear intensity-versus-rate curves, two measurements were taken:

1. The light intensities at a certain wavelength and at a reference wavelength were so adjusted as to yield approximately equal rates.

2. The measurements were made in the linear portion of the light intensity curve. In order to compare also somewhat differing rates obtained with different wavelengths, all rates were corrected by adding the value of the intercept, which is produced on the rate coordinate at zero intensity by an extension of the linear part of the light curve. This correction usually amounted to 30–80% of the measured rates. Points for light intensity curves were measured at the beginning and in the middle or at the end of an experiment.

Each wavelength was given for 3–4 minutes and immediately followed or preceded by an exposure to a reference wavelength, which was 680 nm in the range 645–700 nm and 625 nm for the region between 600 and 660 nm. The dark periods lasted for 3–5 minutes.

Fig. 8 shows the points of an action spectrum obtained in six experiments involving five preparations of fraction 1. For measurements between 645 and 700 nm (points in Fig. 8) a half bandwidth of 1.5 nm was used; the chlorophyll concentration was about 1.3 μg ml^{-1} corresponding to an optical density of about 0.05 at 680 nm. Two experiments for points between 600 and 660 nm (crosses in Fig. 8), however, were car-

ried out with 2.5 and 1.5 nm half-bandwidth and chlorophyll concentrations of approximately 6 and 2.5 μg ml^{-1}. These points were obtained using 625 nm as a reference wavelength. They were joined to the other points with 680 nm as reference by two wavelengths (645 and 650 nm) in the overlapping region, and the average values were calculated from sets of points. The factor was determined by which the average of the 645-nm points from the one set (625 nm as reference) differed from the corresponding 645-nm average of the other set (680 nm as reference). Similarly such a factor was obtained for the 650-nm values. The average of those two factors was finally used to multiply all points of the one set (625 nm as reference) and so connect to the other set.

As can be seen in Fig. 8 the absorption spectrum (solid line) fits closely the measurements for the relative action. The divergence in the part between 670 and 680 nm is considered to be insignificant, for it was not evident in two other experiments which showed more scatter.

Discussion

The data in Fig. 8 suggest that the absorption spectrum of fraction 1 represents also the spectrum of the pigments active in light reaction 1. However, the action spectrum measurements are not accurate enough to establish firmly slight disagreements with the absorption spectrum; for instance no evaluation can be made of the degree of activity of chlorophyll *b*. For a more precise action spectrum, therefore, another way to measure system 1 activity must be sought.

The action spectrum from fractionated chloroplasts is less flattened than the action spectrum for methyl viologen reduction in whole spinach chloroplasts obtained by Joliot *et al.* (1968) (the broken line and circles in Fig. 8). This underlines the necessity to use as finely dispersed chloroplast material as possible for further action spectra.

References

Anderson, J. M., and N. K. Boardman, *Biochim. Biophys. Acta, 112,* 403–421, 1966.

Arnon, D. I., *Photosynthetic Mechanisms of Green Plants,* Publ. 1145 N.A.S.–N.R.C. Washington, D. C., pp. 195–212, 1963.

Boardman, N. K., and J. M. Anderson, *Nature, 203,* 166–167, 1964.

Briantais, J. M., *Photochem. Photobiol., 6,* 155–162, 1967.

Bril, C., D. J. Van der Horst, S. R. Poort, and J. B. Thomas, *Biochim. Biophys. Acta, 172,* 345–348, 1969.

Butler, W. L., *Arch. Biochem. Biophys., 93,* 413–422, 1961.

French, C. S., and M. Lawrence, *Carnegie Institution Year Book 66,* pp. 175–177, 1968.

Jensen, R. G., and J. A. Bassham, *Proc. Natl. Acad. Sci., 56,* 1095–1101, 1966.

Joliot, P., A. Joliot, and B. Kok, *Biochim. Biophys. Acta, 153,* 635–652, 1968.

Kelly, J., and K. Sauer, *Biochemistry, 4,* 2798–2802, 1965.

Kok, B., H. J. Rurainski, and O. von H. Owens, *Biochim. Biophys. Acta, 109,* 347–356, 1965.

Ludlow, C. J., and R. B. Park, *Plant Physiol., 44,* 540–543, 1969.

Michel, J., and M. Michel-Wolwertz, *Carnegie Institution Year Book 67,* pp. 508–514, 1969.

Müller, A., D. C. Fork, and H. T. Witt, *Z. Naturfschg., 18b,* 142–145, 1963.

Ogawa, T., F. Obata, and K. Shibata, *Biochim. Biophys. Acta, 112,* 223–234, 1966.

Vernon, L. P., E. R. Shaw, and B. Ke, *J. Biol. Chem., 17,* 4101–4107, 1966.

Vidaver, W., *Plant Physiol., 41,* 87–89, 1966.

The Forms of Chlorophyll *a* in Fractions of Chloroplasts from Different Sources

C. S. French

The previously reported attempts to resolve the complicated absorption spectra of chlorophyll complexes into spe-

cific components representing the different natural forms of chlorophyll have been continued. This year's work represents a level of approximation that has served more to clarify the limits of usefulness of the curve analysis procedure than to define the spectra of specific chlorophyll components. Rather than reporting in detail on the extensive but still unsatisfactory curve analyses carried out this year, we will present, on identical scales, some of the spectra of different investigators that illustrate the complex nature and the range of variation within the red region of the spectrum which is caused by the presence of different forms of chlorophyll *a*.

The spectra of normally green cells or of whole chloroplasts cannot truly represent the sums of the spectra of the component forms because of the well-known flattening effect due to the high optical density of the particles themselves. Therefore, our recent curve analyses have been mainly restricted to spectra of small particles of broken or fractionated chloroplasts.

Methods for separating chloroplasts into two fractions corresponding roughly to the pigments of photosystem 1 and photosystem 2 are being intensively investigated in many laboratories. Previously we found the longer-wavelength form of the two major chlorophyll *a* components, C*a* 680, to have a much narrower bandwidth in the system-2 fractions than in the system-1 fractions. Dr. Brown's recent measurements with fractions from numerous species of plants have amply confirmed the generality of this situation. Since the absorption bands near 680 nm in the spectra of the two fractions differ in half-width, it is obvious that spectra of whole chloroplasts, or of their unfractionated homogenates, are more complex than was expected from the old assumption that they were both made up of a small number of forms of chlorophyll *a* similar in shape and differed only in their proportions in the two fractions.

The spectra of separated chloroplast fractions, therefore, appear to offer the greatest promise for resolution into the spectra of the individual components, and most of the recent work has been on such material. Because the spectra are sharper at liquid nitrogen temperature, most of the curve analyses have been done with low-temperature data.

The extreme sharpness of the C*a* 680 peak in fraction 2 is consistent with the previously discussed idea that its shape may be greatly influenced by refractive index changes of the pigment near its absorption band. Devising methods for the routine measurement of such wavelength dependent scattering in a way that can lead to a calculation of the true absorbance is of great importance. Various possible methods have been considered although we have not yet attempted to make experimental tests of possible procedures. The main difficulty is to devise a measurement system that would be usable at liquid N_2 temperature as well as for suspensions at room temperature.

Theories. A basic question is whether the spectra for different chloroplast preparations are made up of identical chlorophyll components in different proportions or whether the wavelength maxima and the widths of the components themselves are different in the various preparations of corresponding chloroplast fractions. We hope to answer this question by curve analysis.

To account for the variations in observed spectra and yet to maintain the simplest realistic concept of the minimum number of chlorophyll forms that must exist, we wish to distinguish between the three alternative hypotheses illustrated in Table 6. According to the constant components concept, the basic major bands are assumed to correspond to actual forms of chlorophyll that always have the same peak position and width. Since variation in the proportions of these components can give peaks or shoulders at many different wavelength positions, the observed variation in

TABLE 6. Three Alternative Concepts to Account for the Observed Band Positions of Chlorophyll *a* Types

Constant Components Concept		Extra Components Concept		Variable Components Concept
The components have peaks of constant wavelength and width while the observed variety of spectra is due to differences in the proportions of these forms.		The major components have peaks of constant position and width, extra bands may or may not be present.		The major components have peak positions and/or widths that vary from one sample to another within a specific range for each type.
Name of component	Range of possible peak position due to mixtures of these components[1]	Universal forms	Extra forms	Range of variation for each type of component
		Approximate wavelength, nm		
C*a* 665			665	662–667
	665–670			
		670[2]		668–673[2]
C*a* 670[2]			675	
	670–680			
		680[3]		
				678–683[3]
C*a* 680[3]			685	684–689
	680–695		688	
C*a* 695			695	690–696
	695–700			
C*a* 700			700	697–702
	700–705			
C*a* 705			705	703–708
	705–710			
C*a* 710			710	709–713
	710–715			
C*a* 715			715	714–718

[1] The presence of other components can modify the peak position for the sum of any pair of components.

[2] Predominant in system 2.

[3] Predominant in system 1.

wavelength position need not signify the existence of a large number of different chlorophyll forms.

Curve analyses of spectra for a single sample or for a small number of samples no matter how precise, cannot distinguish between basic components and the broader bands with intermediate peak positions that are the sums of several basic components. If the constant component idea is correct, we should be able to find the minimum number of invariant components that when added with appropriate height factors, will fit all spectra.

The concept of extra components, by contrast with that of constant components, posits that there are two major and universal forms in each system with constant peaks at about 670 and 680 nm. In addition, however, there may also be any of a number of other invariant forms also present in any particular sample. The probable peak positions of some of these less common extra forms are given in Table 6. The two ideas should be distinguishable by comparison of the results of many curve analyses. For the one, identical components should fit all spectra, while the other requires extra com-

ponents which also would always be at specific wavelengths.

A third hypothesis, that of variable components, unlike the other two, presumes that the chlorophyll *a* forms of any one type are not constant but may vary in their peak positions over a range of about ± 3 nm and possibly also in their widths. If this is actually true, then an almost unlimited number of components would result from an extensive series of curve analyses.

Curve analysis with Gaussian components. During the past year we have attempted to resolve various absorption spectra of chloroplast fractions most of which were prepared by Dr. Brown from a variety of algae and leaves. We have also analyzed spectra of some purified chlorophyll-protein complexes prepared by Dr. J. Philip Thornber of the Brookhaven National Laboratory. One procedure used in analyzing these spectra has been to match the experimental curves by adding together simpler curves, usually Gaussian probability functions. The reason for doing so is that the Gaussian curves thus obtained may represent the individual bands of the different chlorophyll forms and, therefore, serve as a means for specifying their wavelength peaks and their widths at half-height. Neither of these parameters of a single band is directly identifiable in a composite absorption spectrum. There is no reason to expect Gaussian curves necessarily to fit even a single isolated band over its entire extent. Nevertheless, that shape has been found to be adequate for use with chlorophyll spectra except at the long wavelength tails. Lorentzian (Cauchy) curves are far less useful.

Each of the major forms of chlorophyll *a* that we wish to identify has a main peak in the 660–700 nm region, a wider and lower band near 620–640 nm, and a still wider and lower band with a maximum somewhere near 580 nm. So far we have not been able to distinguish between the bands of the different forms of chlorophyll *a* in the 570–640 nm region. The long wavelength tails of 620–640 nm bands do overlap the main peaks and hence have some small effect on the apparent shape of the main peak. This overlap of unidentifiable low and broad bands has been a source of some uncertainty in determining the height and, to a smaller extent, the half-width of the major bands.

These curve analyses made with the RESOL program have resulted in a number of adequate matches of Gaussian curves to the experimental spectra. The interpretation of the results by attributing particular Gaussian curves to the absorption bands of specific chlorophyll complexes has not yet been very successful. There are two difficulties in the use of this method. One difficulty can probably be greatly reduced by program modifications that are being explored. That trouble is the sometimes extreme modification by the program of the wavelength peaks and half-widths of the estimated input bands with which the computation starts. When this happens the resulting fit may be excellent even though the bands so determined cannot possibly be considered as representing the absorption bands of chlorophyll complexes.

Dr. Tunnicliff has recently shown us how to restrict the amount of wavelength adjustment allowed for each iteration. Mr. Lawrence is working on a modification of the program using this principle. The plan is to make a restriction for both the peak wavelength change and the width change per iteration independently specifiable for each input band. If these modifications can be made to operate successfully, the program will be much more useful for complex spectra. For instance, the whole curve for a known or suspected chlorophyll component describable as the sum of several Gaussian or Lorentzian functions can be entered and either rigidly held or allowed minor adjustments while the program determines the remaining components of the system. In this way

the difficulties that have caused so much trouble in curve analysis this year may be avoided. With these modifications it should be possible to use enough input bands to allow for the main peaks of the minor components as well as for the side bands of the major chlorophyll forms. This has not yet been possible with the present program lacking the restraints on band adjustments.

Another and more serious difficulty is that many of the spectra do not have sharp enough characteristics to require only a single combination of Gaussian curves for a precise fit. With such spectra we have to use some other method for determining the band shapes. Characterless curves are, however, valuable for testing the reality of component spectra that have been determined from other data.

One partially successful attempt to derive the separate chlorophyll spectra in a two-component mixture is illustrated in Fig. 9. This is the room-temperature spectrum of Dr. Thornber's purified system-2 pigments from spinach. This spectrum is of particular interest because it contains the highest proportion of chlorophyll *b* of any fraction we have seen. In this case the RESOL program gave a very rough resolution of the 570–640 nm region but reasonable bands for the main 652 chlorophyll *b* and 671 chlorophyll *a* peaks. The larger of the minor component bands at 632 nm, however, is probably too wide, too high, and at too long a wavelength. Combining the 652-nm and 604-nm components with a portion of the 575 band to represent the spectrum of chlorophyll *b* in vivo gives a completely objective, although inadequate, solution to this curve resolution problem. The derived curves are given in the upper part of Fig. 9. The analogous addition of the 671-nm and 632-nm bands with part of that at 575 nm to represent the spectrum of C*a* 670 of system 2 is also not satisfactory. However, this figure illustrates a method

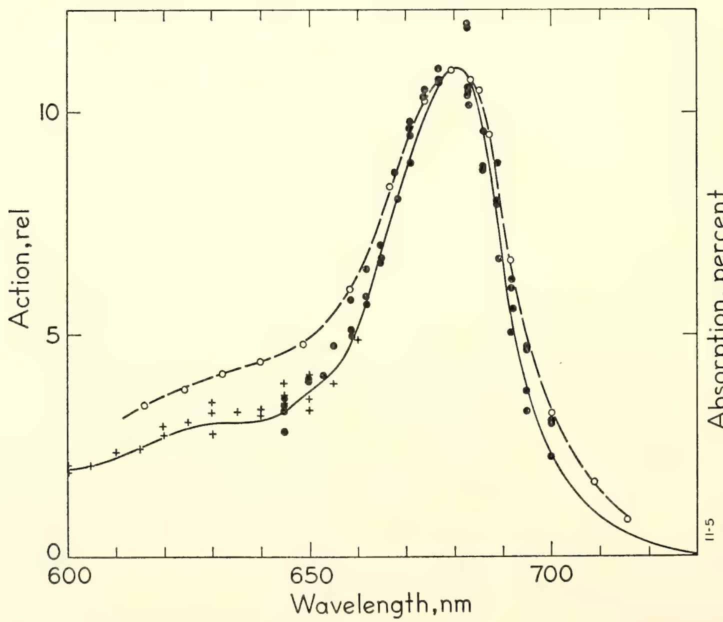

Fig. 8. Wavelength dependence of relative action for methyl viologen reduction by fraction 1 (points and crosses). Solid line: absorption spectrum of fraction 1. Broken line and circles: action spectrum for methyl viologen reduction in whole chloroplasts; adapted from Joliot *et al.* (1968).

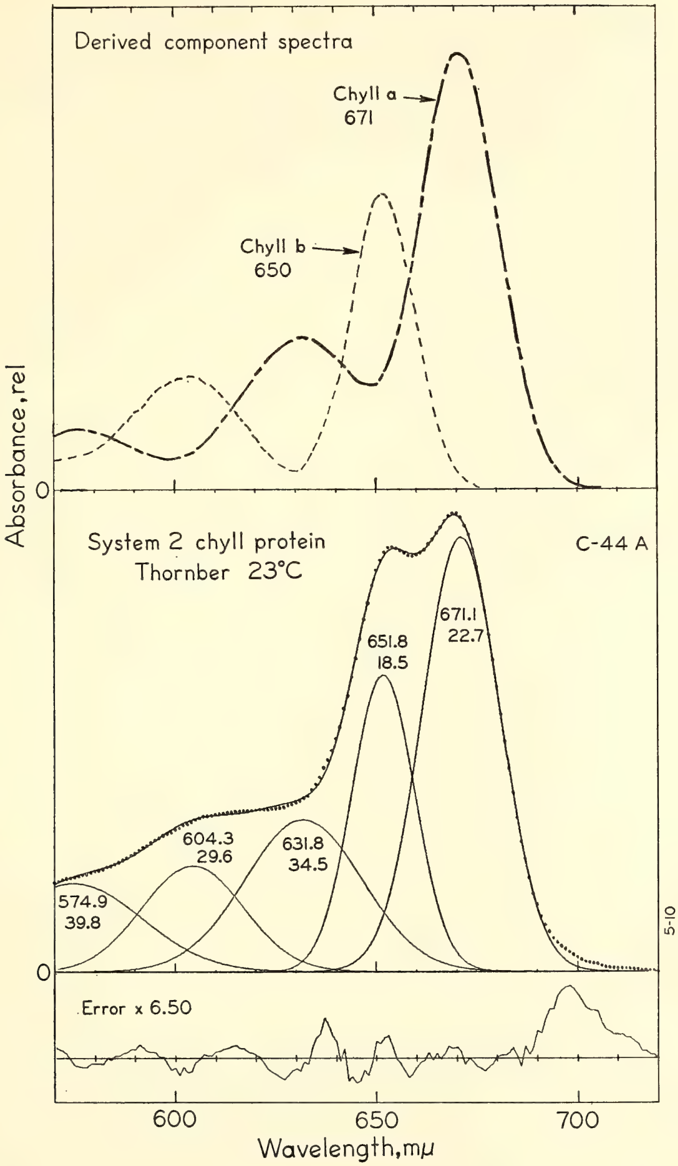

Fig. 9. The absorption at room temperature of Dr. Thornber's purified system-2 chlorophyll protein matched with Gaussian curves. In the upper part the components have been added to approximate very roughly the spectra of the chlorophyll *b* and chlorophyll *a* components.

that may be valuable in the future after the curve analysis program is improved.

Comparison of spectra by subtraction. One procedure occasionally useful for related pairs of characterless spectra is nearly the same except for the relative amounts of a common component. If that requirement is more or less true, then the difference spectra give a reasonable approximation to the band shape of

one component. This procedure, described last year, has been applied to a number of curve pairs and has frequently shown that the spectra selected differ by several unexpected bands. One of the more significant of these calculations by the DSPEC program came from two spectra of a fraction from homogenized *Botrydiopsis* that were prepared on successive days. That from the fresh homogenate had a large C*a* 680 band while that from the same homogenate stored overnight at 4°C had very little of that component. Even this pair of spectra showed an unexpected difference near 665 nm as well as the major difference peak at 680 nm (French *et al.,* 1968).

This comparative procedure for deriving the spectra of component bands eventually should have more utility if enough appropriate pairs of spectra can be found. The method has the advantage over the approximation by Gaussian components in that it gives the entire spectrum of a component rather than only the width and position of its main band. So far, however, these difference spectra have been more useful in emphasizing the presence of unsuspected components than in finding the precise shape of the components that are obviously present.

To compare curves with each other we have found it well worth the extra expense to have all spectra plotted on the same scale with a peak height of 7.5 inches and a wavelength scale of 1 nm = $\frac{1}{15}$ inch. Such a graph made by the SPLOT program also serves to make any errors of curve digitizing strikingly apparent. An even greater convenience is the file of 4×5 positive film photographs of the standard-scale plots that are accurately aligned with each other. Many of these can be superimposed to compare all spectra of a particular type. For visual study they are held in a plastic frame with slots. When arranged in order of the increasing height of a particular band such a set of spectra gives a three-dimensional view of the interrelations of several bands.

To search for the less obvious components the spectra measured at −196°C are being compared within the following groups of preparations:

(a) Particles prepared by sucrose-gradient centrifugation of algae lacking chlorophyll *b,* and purified chlorophyll-protein preparations free of chlorophyll *b* (13 spectra).

(b) Fraction-1 particles from various sources (6 spectra).

(c) Comparable fraction-2 particles (6 spectra).

(d) Miscellaneous: unfractionated homogenates, (following centrifugation at 3000 *g* for 10 minutes to remove large particles), and spectra of whole cells that are pale enough to give comparatively undistorted spectra (9 spectra).

Some very revealing information about the complexity of spectra appears when two apparently similar spectra are superimposed, as shown in Fig. 10. In that figure are absorption spectra kindly supplied by Dr. Thornber for two of his purified samples of chlorophyll protein from the blue-green algae *Tolypothrix* and *Phormidium* (Thornber, 1969). Small bulges, caused by minor components, are more clearly seen by comparison with a curve that is similar but lacks these smaller bands. Figure 10 clearly shows that the *Phormidium* preparation absorbs relatively more at 633, 665, 688, and 708 while the *Tolypothrix* material has proportionately more absorption near 678 and 695 nm. Both have a major component at about 672 nm with a secondary band at about 620–635 nm. It also seems that the *Phormidium* may have the peak of its second largest component at 680 rather than at 678 nm, its apparent position in the *Tolypothrix* preparation. It is possible, however, that the apparent difference may be only in the relative proportions of identical components. If, in fact, each of the two spectra does consist of a mixture of 665, 672, 678–680, 688, 695, and

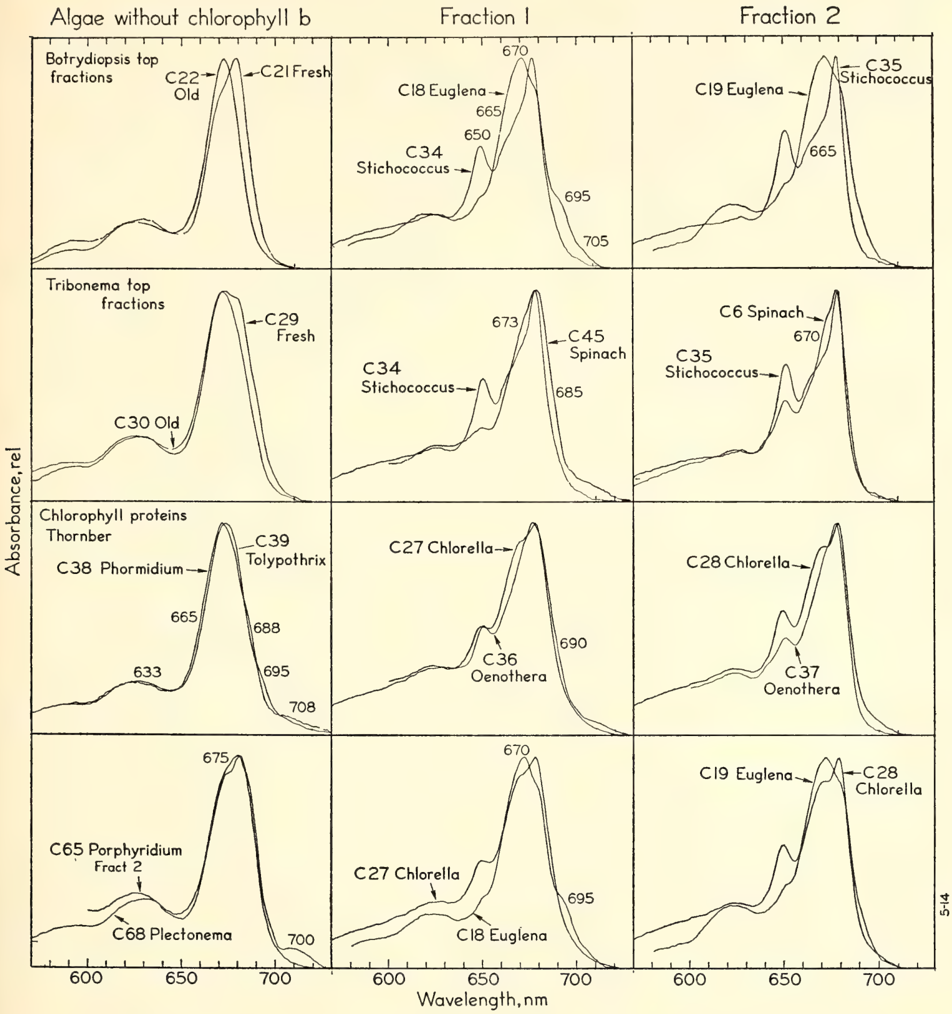

Fig. 10. Some selected spectra at —196°C showing various forms of chlorophyll. Comparisons of similar spectra suggest the presence of small amounts of extra chlorophyll forms in addition to those common forms giving the major peaks. The data was kindly provided by the following workers: M.-R. Michel-Wolwertz, C6, C18, C19, C27, C28; J. S. Brown, C34, C35, C65, C68; P. Thornber, C38, C39; L. Prager, C21, C22, C29, C30; D. C. Fork, U. Heber and M.-R. Michel-Wolwertz, C36, C37.

708 components, each with a side band in the 620–640 region, it is not surprising that the RESOL resolution of the *Tolypothrix* spectrum into 6 Gaussian components gave the oversimplified picture shown in Fig. 11 with the indicated errors of this match.

For the *Phormidium* spectrum, C38, three widely different curve analyses were obtained, all with about the same error of fit. None of them gave interpretable components. A visual comparison of selected spectra, as in Fig. 10, gives a preference to the interpretation that differences between comparable fractions result from different propor-

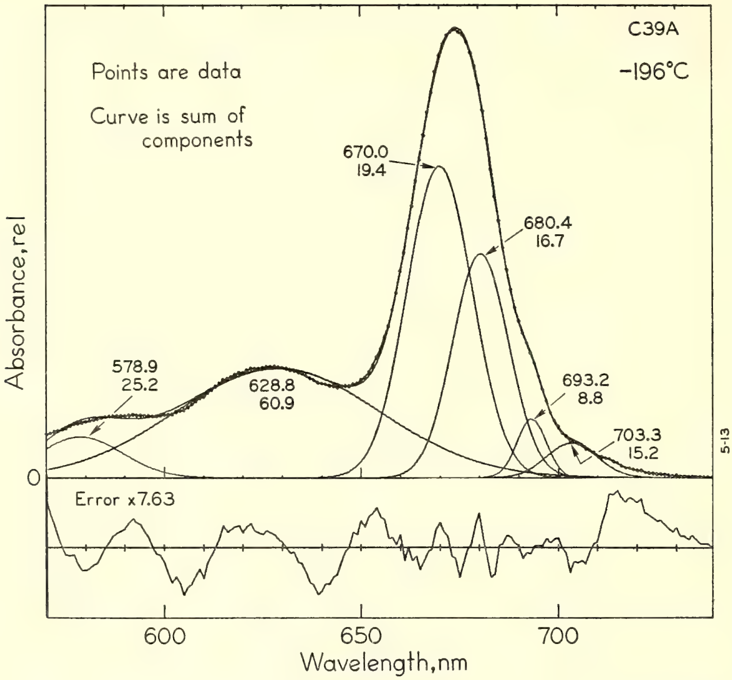

Fig. 11. A partial resolution of Dr. Thornber's spectrum at —196°C for purified chlorophyll protein from *Tolypothrix.* It is not yet possible to resolve the 600–640 nm region into its components.

tions of similar components, provided enough separate components are considered for each curve. Smaller amounts of extra forms, however, may also exist in some of these algae.

Considered from the point of view of the constant component theory the spectra for the sharpest and for the smoothest spectra of fractionated chloroplasts of Fig. 10 show that if the *Euglena* fractions 1 and 2 each contain a C*a* 680 component as sharp as those in *Stichococcus,* then there must be at least two components in the 665–675 region of *Euglena* that are low or absent in *Stichococcus.* The 695-nm and 705-nm components of *Euglena* show clearly in this comparison.

Euglena must have a higher proportion of components at about 665, 670, and 675 nm than does *Stichococcus.* Furthermore, *Stichococcus* has the highest chlorophyll *b* peak and the sharpest C*a* 680 component of any alga so far investigated. These two pairs of spectra for fractions 1 and 2 of *Stichococcus* and *Euglena* are the most difficult ones to explain by the theory of constant components. A better comparison is of the same *Stichococcus* data with that for spinach fractions. Here, apparently, an increase in the amount of a 673-nm component added to the *Stichococcus* curve for either fraction could bring them up to the spinach curves in that region. For fraction 2 in addition to the other obvious differences, a component near 685 nm appears to be larger in spinach than in *Stichococcus.*

In brief, the results of the past year's work have emphasized the presence in most preparations of more forms of chlorophyll than are evident unless some sort of curve analysis is carried out.

Continuing improvements in the methods of curve analysis applied to a

large collection of precisely measured spectra from a wide variety of preparations from many diverse plant species may eventually decide between the three concepts here described.

The costs of computer use for this work since March 15, 1969, have been covered by NSF Grant No. GB 8630, which has made it possible to increase greatly the number of spectra investigated. It is a pleasure to thank Mr. Mark Lawrence for programming help, Mrs. Helen Kennedy for digitizing the curves, and various colleagues for their contributions of selected spectra.

References

Brown, J. S., submitted to *Biophys. J.*, 1969.

French, C. S., and Lillian Prager in *Progress in Photosynthesis Research,* H. Metzner, ed., II, 11 pp., (in press), 1969.

French, C. S., M. R. Michel-Wolwertz, J. M. Michel, J. S. Brown, and Lillian Prager in *Biochemical Society Symposia Number 28, Porphyrins and Related Compounds,* T. W. Goodwin, ed., Academic Press, London and New York, pp. 147–162, 1968.

Thornber, J. P., *Biochim. Biophys. Acta, 172,* 130–144, 1969.

A Comparative Study of the Light-Induced Carotenoid Change and Fluorescence in the Chlorophyll-*b*-less Alga *Botrydiopsis alpina* (Xanthophyceae)

David C. Fork and Yaroslav de Kouchkovsky

Introduction

A number of absorbance changes having similar kinetics were seen upon illumination of the yellow-green alga *Botrydiopsis alpina* that were apparently produced by a transient shift to longer wavelengths of the absorption bands of a carotenoid pigment (*Year Book 66,* p. 160; *Year Book 67,* p. 496). Action spectra measurements reported last year (*Year Book 67,* p. 496) demonstrated that both photochemical systems caused the shift in this particular, as yet unidentified, carotenoid. Inhibition of system 2 by DCMU permitted the observation that system 1 mediated a rapid shift of the carotenoid absorption to longer wavelengths which reversed again during illumination. The subsequent addition of the electron donor couple DAD and ascorbate produced a sustained carotenoid shift in the light, again sensitized by system 1. System 2 was also shown to be responsible for a sustained carotenoid shift that was relatively slow at the light intensities used.

We studied here the dependence of the carotenoid shift and of chlorophyll fluorescence upon treatments that would influence the primary photoreactions. A number of treatments were investigated in an attempt to obtain separately the carotenoid shift produced by each of the two photosystems. We have found both the initial rise and decay of the carotenoid shift follow first-order kinetics and an indication for another, slower first-order component.

It may be that the carotenoid pigment showing these shifts, like chlorophyll *b*, undergoes slight absorption changes when its supporting membrane is disturbed by electron transport. The carotenoid shift is discussed in relation to the chlorophyll-*b* change, electron transport and a high-energy "intermediate" produced during photophosphorylation.

Materials and Methods

Botrydiopsis alpina was cultured as previously described (Fork, 1969). Light-induced differences of absorbance at 515 nm were used to follow the carotenoid changes. These measurements were done as described earlier (de Kouchkovsky and Fork, 1964). The half-bandwidth of the measuring beam was 2 nm. The algae were diluted with culture medium so that the final transmission of the cell suspension was around 10% at 515 nm. The temperature was 20°C and the gas phase was air. Sometimes the results were also compared, using

wavelengths other than 515 nm (such as 482 and 497 nm) where absorbance changes typical of the carotenoid can be seen.

Fluorescence was measured simultaneously with absorbance changes. Actinic light to excite fluorescence and the carotenoid shift was incident on the top surface of the cell suspension, which was contained in an open cuvette. The photomultiplier, for monitoring fluorescence, was located above and to one side of this cuvette. The actinic light used in all these experiments had a wavelength of 652 nm and a half-band of about 9 nm. The light produced by using Schott RG 1, 3 mm in combination with a Balzers heat-reflecting filter Calflex C, a water filter (27 mm), and a Baird-Atomic interference filter type B-1. The intensity of this beam was about 2.9 nanoeinstein cm^{-2} sec^{-1} (5.3×10^3 ergs cm^{-2} sec^{-1}). A combination of Schott RG 10 (3 nm) and Baird-Atomic interference filters (742 nm, type B-1, half-band, about 9 nm) transmitted fluorescent light of this wavelength but absorbed 652 nm actinic light. Fluorescence at 742 nm is very likely a "satellite" of the main emission band at 685 nm, and is, therefore, a reflection of the functioning of system 2 (compare the composite fluorescence band in vitro which is nearly an image of the absorption band and the experiments made in vivo that were reported by Lavorel, 1962).

A schedule of 6 seconds light and 48 seconds dark was used.

Results

The top trace of Fig. 12 shows kinetics typical for the absorbance change produced at 515 nm upon illumination of *Botrydiopsis alpina* (*Year Book 67*, p. 496). The initial increase of absorbance

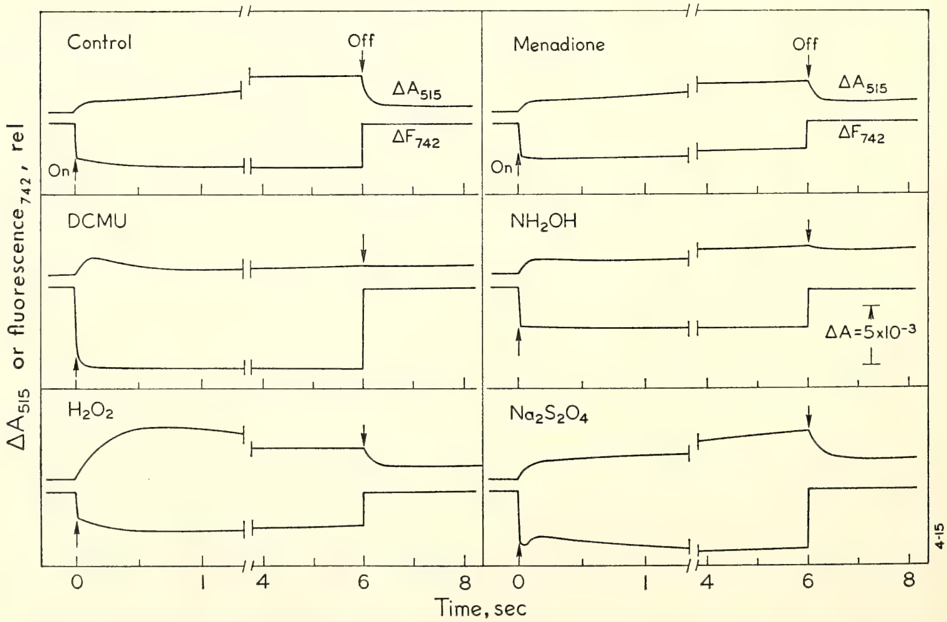

Fig. 12. Kinetics of light-induced absorbance changes at 515 nm produced upon illumination of *Botrydiopsis alpina* with red actinic light (described in the text) and the effect of DCMU, H_2O_2, NH_2OH, $Na_2S_2O_4$ and menadione. The concentrations (M) used were: DCMU, 5×10^{-6} M; H_2O_2, 5×10^{-3} M; NH_2OH, 1×10^{-2} M; $Na_2S_2O_4$, 5×10^{-3} M; and menadione, 1.6×10^{-6} M. Note that a faster recording was made for the "on" than for the "off" portions of the traces.

produced upon illumination is followed by a much slower rise which was completed within about 6 seconds in the light (the length of the exposures used for Fig. 12). Darkening produced a rapid decrease of absorbance to the former dark baseline.

Fig. 13 reveals that both the initial rise and the decay of the carotenoid shift are caused by first-order reactions. The decay curve was obtained by plotting the absorbance change that still remained at intervals after darkening the cell suspension. The rise curve was obtained by plotting the carotenoid that remained unreacted at intervals after the actinic light was given. The half times ($t_{1/2}$) and the rate constants (k) for the rise and decay are similar in both cases. The values for the rise are $t_{1/2}=0.07$ sec and $k=9.5$ sec^{-1}, and for the decay, $t_{1/2}=0.09$ sec and $k=7.9$ sec^{-1}. In some cases it was possible to analyze the decay as the sum of two first-order reactions.

The absorbance change produced by carotenoids, like those caused by chlorophyll *b*, are strongly dependent upon the dark interval given between exposures. This effect was described in *Year Book 63*, p. 441 for the chlorophyll *b* change. In essence, the carotenoid change also increases up to a certain maximum with increasing dark intervals between exposures. This increase is not proportional to the dark interval but varies in a complex way. Therefore, in all experiments reported here, a uniform dark interval (48 sec) was given between successive exposures until a reproducible response was obtained.

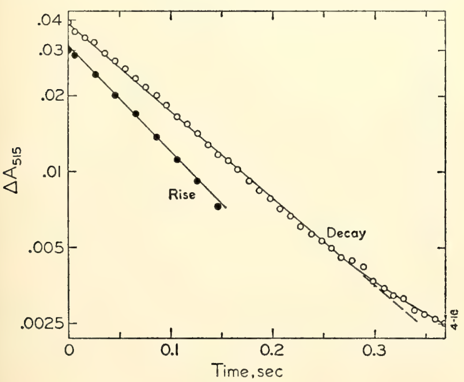

Fig. 13. Semilogarithmic plot of the rise and decay of the 515-nm absorbance change in *B. alpina* measured as described in the text.

Having determined conditions needed to obtain reproducible results it was then possible to investigate the effects on the carotenoid change and on fluorescence of substances which are known (or could be expected) to exert strong effects on the early reactions of photosynthesis. Fig. 12 shows examples of the results produced on the carotenoid change and on fluorescence after addition of the inhibitors DCMU and NH_2OH, of a reductant, $Na_2S_2O_4$, an oxidant, H_2O_2, and of vitamin K_3 (menadione). As noted previously (*Year Book 67*, p. 498), DCMU had only a partial inhibiting effect on the carotenoid change. The on-rate in DCMU (V_i, measured as shown in the insert of Fig. 14) was unaffected but the initial deflection, X_i, (see insert) was increased. DCMU almost completely inhibited the steady-state part of the change, X_s, and greatly depressed the off-rate, V_s. Illumination in the presence of the oxidant, H_2O_2, produced a large increase in the initial deflection (X_i) but a decrease in the on-rate, V_i, resulting in maximum deflection being reached at longer times than in the control. The steady-state deflection, X_s, and the off-rate, V_s, were decreased in the presence of H_2O_2. Hydroxylamine at the concentration used for Fig. 12 (10^{-2} M) had no effect on the on-rate, increased the initial deflection slightly but lowered the steady state and off-rate. Hydrosulfite (10^{-2} M) slowed down the decay of the 515-nm change and at the same time produced increased fluorescence. A transient decrease of fluorescence appeared after about 0.5 sec of illumination.

Measurements of the parameters of the 515-nm absorbance change and those

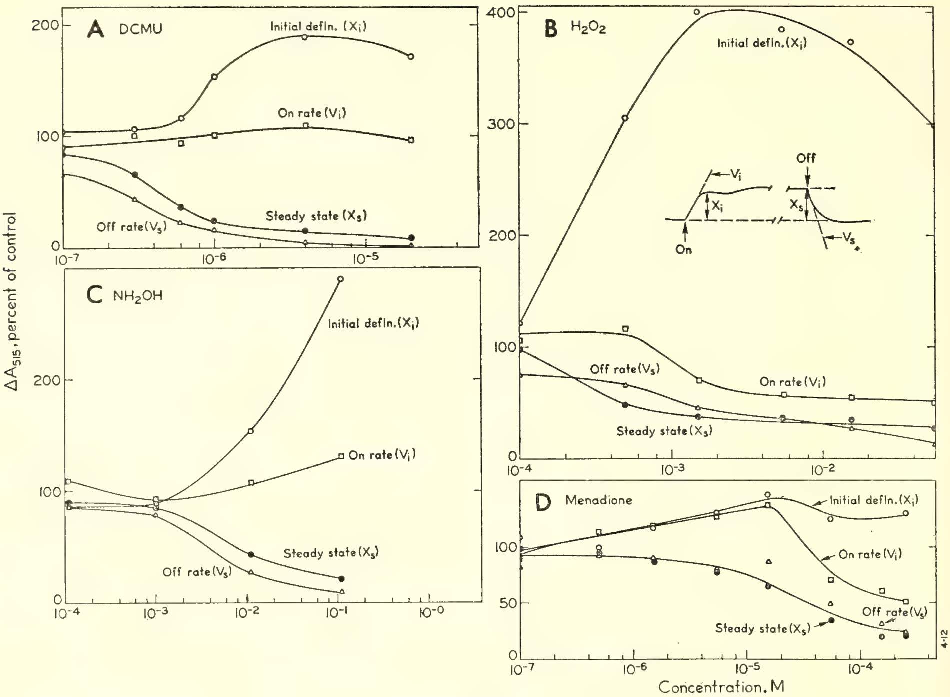

Fig. 14. The effect of concentration of DCMU, H_2O_2, NH_2OH, and menadione on various parameters of the absorbance change at 515 nm in *B. alpina* measured as shown in the insert.

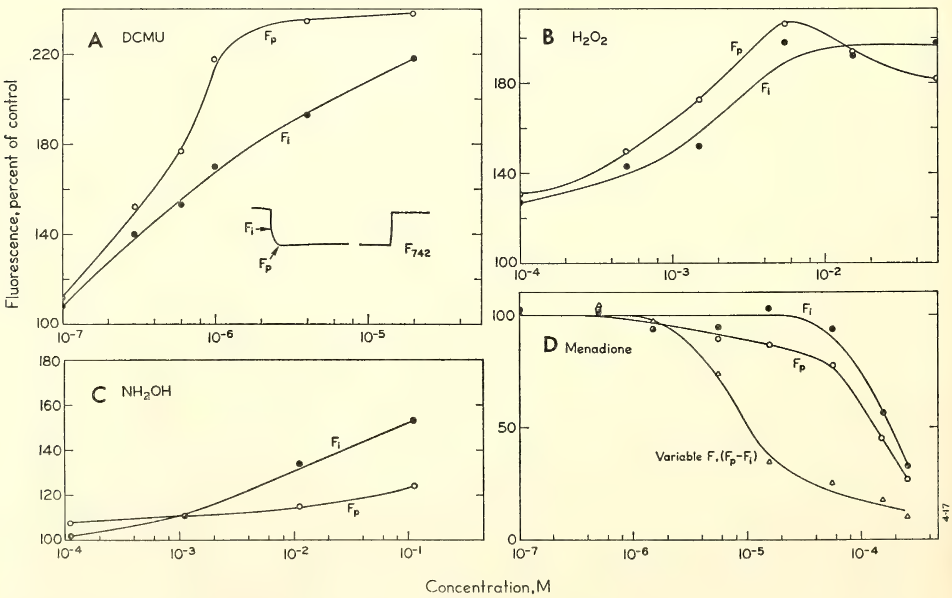

Fig. 15. The initial, F_i, and peak, F_p, fluorescence (measured as shown in the insert) as a function of the concentrations of DCMU, H_2O_2, NH_2OH, and menadione. The measurements were made simultaneously with those for absorbance changes given in Fig. 14.

of fluorescence (determined as shown in the inserts) are given in Figs. 14 and 15 as a function of the concentration of H_2O_2, DCMU, NH_2OH, and menadione (vitamin K).

An increase in the DCMU concentration from 10^{-7} to 2×10^{-5} M had little effect on the on-rate of the 515-nm change, but it gave rise to strong inhibition of the steady-state change as well as to the off-rate (Fig. 14A). By 4×10^{-6} M the initial deflection was doubled. As customarily observed, the initial fluorescence, F_i, increased with increasing DCMU concentrations (Fig. 15A). The maximum peak fluorescence, F_p, was doubled already at a concentration somewhat below 10^{-6} M. (At about this concentration and above, the initial deflection of the 515-nm change was increasing strongly.) It should be noted that measurements of F_i are somewhat difficult to make with certainty because the response time of the recorder makes possible an overestimation by including in this measurement part of the fast rise of variable fluorescence.

Hydrogen peroxide, at concentrations higher than 5×10^{-4} M inhibited the on- and off-rates as well as the steady state 515-nm deflection, but it dramatically increased the initial deflection (Fig. 14, part B). Both the initial and the maximum peak fluorescence were increased by addition of up to about 5×10^{-3} M H_2O_2 (Fig. 15, part B). Further addition of H_2O_2 did not change F_i but it decreased F_p.

A thousandfold variation in the concentration of hydroxylamine (from 10^{-4} to 10^{-1} M) produced relatively little effect on the on-rate of the 515 change (Fig. 14, part C). At concentrations above 10^{-3} M, NH_2OH produced a progressive inhibition of the steady state and the off-rate of this change concomitantly with a large increase in the initial deflection. Figure 15, part C, shows NH_2OH had only a slight effect on the maximum of peak fluorescence. Initial fluorescence was increased more than F_p at concentrations above 10^{-3} M. Since the curves are plotted as percent of the control and not as actual values of F_i or F_p, the crossing over of the two curves does not mean that F_i becomes larger than F_p. Below 10^{-3} M, however, there was little effect of NH_2OH on either F_p or F_i.

Menadione (Fig. 14, part D) below 10^{-5} M had a slightly stimulatory effect on both the initial deflection and the on-rate of the 515-nm change, but it inhibited slightly the steady-state change and the off-rate. Above 10^{-5} M, all parameters measured for the 515-nm change declined, the on-rate declining most rapidly. The initial fluorescence was not effected by menadione at concentrations up to about 2×10^{-5} M (Fig. 15, part D). Above this it produced a strong inhibition of the initial fluorescence. By contrast, the peak fluorescence began to be inhibited at concentrations above about 10^{-6} M. The effect of menadione on variable fluorescence (the difference between the peak and initial fluorescence) is also shown in part D of Fig. 15. The maximum effect of menadione on variable fluorescence occurred between concentrations of 10^{-6} and 10^{-5} M. At 10^{-5} M variable fluorescence was reduced by 50 percent.

Figure 16 shows the effect on fluorescence and on the carotenoid change of combined additions of DCMU+H_2O_2, NH_2OH+H_2O_2, and DCMU+NH_2OH.

As was seen earlier in Fig. 14, H_2O_2 alone gave a large stimulation of the initial deflection of the 515 change. Fig. 16 shows, as described above for Fig. 12, that the time needed to attain the maximum deflection t was increased by addition of 14 peroxide. Variable results were sometimes obtained for fluorescence (but not for the carotenoid change) when using hydrogen peroxide. In the experiments shown in Fig. 16, H_2O_2 (5×10^{-3} M) decreased somewhat both F_i and F_p while in the experiment shown in Fig. 14 the same concentration produced increased fluorescence. However, H_2O_2 al-

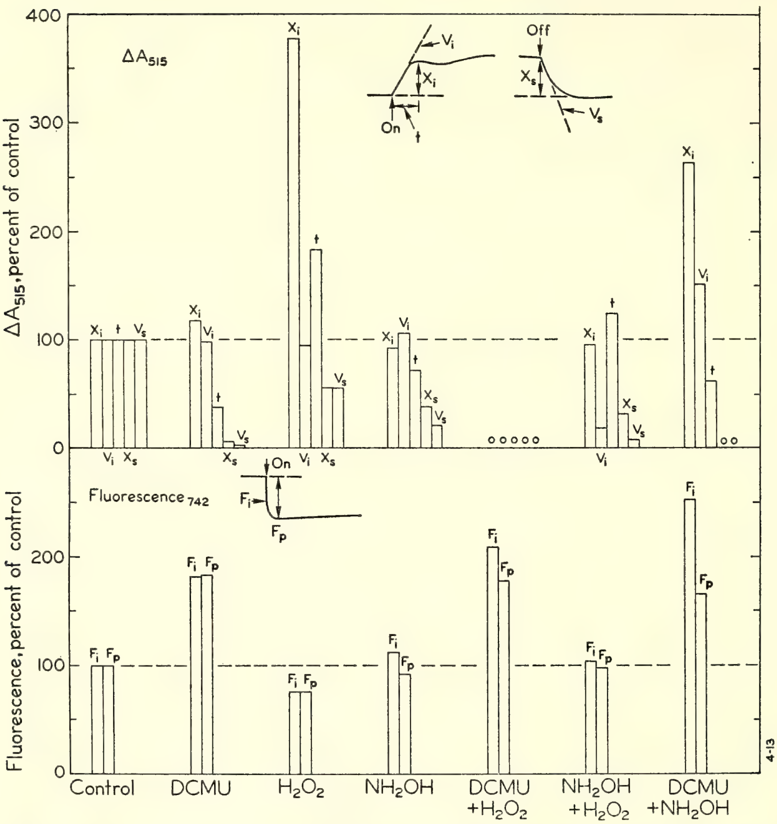

Fig. 16. The effect of DCMU, H_2O_2, NH_2OH, and DCMU plus H_2O_2, NH_2OH plus H_2O_2, and DCMU plus NH_2OH measured simultaneously on the 515-nm absorbance change and fluorescence (as shown in the inserts). The concentrations used are given in the legend for Fig. 12.

ways had an effect on the kinetics of the F_i to F_p rise (Fig. 12).

Interestingly, the combination of both DCMU and H_2O_2 completely inhibited the carotenoid change while at the same time it produced the usual approximate doubling of fluorescence.

The combination of hydroxylamine plus hydrogen peroxide did not produce the dramatic inhibiting effect shown by the combination of DCMU and H_2O_2. Although the values could not be determined precisely, the initial deflection of the 515 change was decreased slightly and the time, *t*, needed to attain the maximum deflection was increased thus producing a decrease of the initial on-rate. Fluorescence was almost unaffected by this combination.

Hydroxylamine plus DCMU gave a 2.5-fold stimulation of the initial deflection of the 515 change in addition to increasing the on-rate and, as a consequence, the time needed to attain the maximum initial deflection was shortened to about 50% of the control. The steady-state 515 absorbance change was completely inhibited. This combination also produced a 2.5-fold increase of the initial fluorescence and about half as much increase in the peak height of fluorescence.

Discussion

Since DCMU apparently acts by preventing reoxidation of reduced *Q* (Duysens and Sweers, 1963), it leads to the inactivation of the traps of system 2.

The carotenoid change produced by system 2 is also inhibited with DCMU because the action spectrum for the change persisting after treatment showed system 1 sensitization (*Year Book 67,* p. 496). DCMU had almost no effect on the on-rate of this carotenoid change over the range of concentrations tested (10^{-7} to 2×10^{-5} *M*) suggesting that the change produced by system 2 is slower than that produced by system 1. Action spectra for the slow change appearing after a few seconds of illumination showed system-2 activity. In these experiments the addition of H_2O_2 gave rise to a large, but slow, change (Fig. 12). Since peroxide is a strong oxidant, it may act by oxidizing a component near system 1 such as P700 (see Fig. 17). If the effect of H_2O_2 is to allow only a system-2 carotenoid change to persist, then DCMU would be expected to abolish the change. This was what actually occurred when H_2O_2 and DCMU were combined as shown in Fig. 16. Inactivation by H_2O_2 of some component near system 1 would then allow accumulation of intermediates reduced by system 2 and produce increased fluorescence. Such a result was described in Fig. 15 for fluorescence. It is not known what conditions are required with H_2O_2 to produce both a slow carotenoid change and increased fluorescence since H_2O_2 sometimes did not stimulate fluorescence. In most cases, however, this is what was seen.

Hydroxylamine apparently acts on system 2 by blocking reactions near water splitting (de Kouchkovsky, 1961; Joliot, 1968). This compound at 10^{-3} *M* produced nearly complete inhibition of oxygen evolution but had almost no effect on the dark-decay of the 515-nm change and on the fluorescence of *Chlorella* (de Kouchkovsky, 1969). Apparently, hydroxylamine (NH_2OH) at this concentration replaces water (H-OH) as the electron donor giving rise to strong inhibition of oxygen evolution and little effect on fluorescence. Similarly, in *Botrydiopsis* low concentrations of hydroxylamine (10^{-4}–10^{-3} *M*) had almost no effect on fluorescence nor much effect on the carotenoid change. At concentrations above 10^{-3} *M*, however, this substance acted like DCMU by increasing the initial deflection and the on-rate but inhibiting the steady state and the off-rate of the carotenoid change and at the same time increasing fluorescence. Thus hydroxylamine at concentrations higher than a certain level may interact additionally at another site by preventing the return of Y^+ to the Y state (Fig. 17).

Menadione has been shown (*Year*

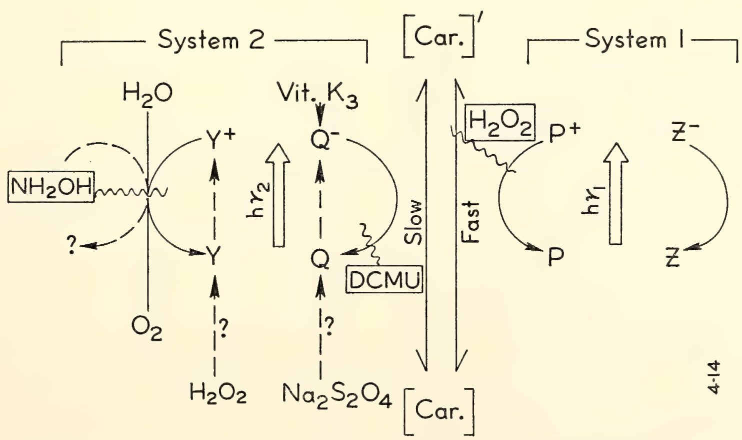

Fig. 17. Generalized scheme showing the effect of various substances on the carotenoid change in *B. alpina.* For details see the text.

Book 66, p. 165; Amesz and Fork, 1967) to be an effective quencher of the variable fluorescence originating in system 2. This quenching process is apparently caused by a direct interaction of chlorophyll and quinone molecules and not by a stimulation of electron transport. More evidence that menadione acts close to system 2 was provided by the observation that this substance inhibited the reduction of the *f*-type cytochrome in light absorbed mainly by system 2. In these experiments menadione inhibited the slow phase of the change (steady state) mediated by system 2. Concomitantly with this, menadione was extremely effective in quenching variable fluorescence in *Botrydiopsis.* The concentration for 50% quenching was 10 μM. By comparison, *Ulva* required a concentration of 50 μM (Fork and Amesz, 1967).

In contrast to this inhibiting effect on the steady-state 515-nm change, menadione produced a stimulation of the initial deflection over more than a hundredfold variation in concentration. Menadione produced a decline in the on-rate at concentrations greater than about 1.5×10^{-5} M and a decline of the steady state. Interestingly, DCMU, also acting close to system 2, did not have an effect on the on-rate of the 515-nm change. Quanta absorbed by system-2 traps inactivated by DCMU may become available to system 1 by a "spill-over" type of mechanism (Myers and Graham, 1963). Amesz *et al.* (1969) found in the blue-green alga *Anacystis nidulans* that light absorbed by system 2 could, in the presence of DCMU, be used for such system-1 reactions as the oxidation of cytochrome or P700. Subsequent addition of 1,4-naphthoquinone, a close relative of menadione (2-methyl-1,4-naphthoquinone) and an effective quencher, prevented this spill-over. Menadione is apparently effective in quenching fluorescence since it provides "artificial" traps for quanta absorbed by system 2 (Amesz and Fork, 1967). Thus it would prevent spill-over of quanta to system 1 and would decrease the on-rate of the 515-nm change mediated by system 1. Under these conditions the initial deflection would not be much affected (Fig. 14) but would take longer to appear.

There is no evidence to date to indicate that the carotenoid showing these light-induced shifts participates as a redox catalyst in the electron-transport chain. Rather, it appears that the change may reflect, as does the chlorophyll-*b* change, a disturbance of the supporting membrane as a result of electron transport. Junge and Witt (1968) recently postulated that the chlorophyll-*b* change (seen at 475, 515, and 650 nm in plants containing this chlorophyll) is produced by the formation of an electrical field across the thylakoid membrane, which in some unknown way, gives rise to a change in the absorption of chlorophyll *b* and then a translocation of H^+. The chlorophyll-*b* change was found (Junge and Witt, 1968) to have a biphasic decay after a short light flash that could be decomposed into two first-order reactions. Analysis made here of the rise and decay of the carotenoid change showed that both followed first-order kinetics, and there is some indication for another, slower, component also exhibiting first-order kinetics. Junge and Witt observed a linear relationship between the rate of phosphorylation and the amplitude of the slow phase of the chlorophyll-*b* change in spinach chloroplasts. Conditions producing phosphorylation accelerated the decay of this change by the same amount as electron transport.

In bacteria Amesz and Vredenberg (1966) found a quantum yield of 3 for the carotenoid shift, suggesting that these changes are not produced by a chemical reaction. More likely, electron transport in the membrane causes a change in the environment of the carotenoids resulting in a small change in their absorption spectrum. Baltscheffsky (1969) has suggested that an energy-rich intermediate of phosphorylation coupled to electron transport produced a membrane con-

formation resulting in the carotenoid shift in bacteria. Fleischman and Clayton (1968) suggested, on the basis of studies with inhibitors and uncouplers, that the carotenoid shift in *Rhodopseudomonas spheroides* depends upon the formation of an energy-rich intermediate of phosphorylation. It will be of interest to determine whether the carotenoid shift that can be seen in algae and higher plants can be related in a similar manner to a membrane change and photophosphorylation.

References

Amesz, J., and D. C. Fork, *Biochim. Biophys. Acta, 143,* 97–107, 1967.

Amesz, J., and W. J. Vredenberg, in *Currents of Photosynthesis,* J. B. Thomas and J. C. Goedheer, eds., Donker, Rotterdam, pp. 75–83, 1966.

Amesz, J., W. Noteboom, and D. H. Spaargaren, in *Progress in Photosynthesis Research,* H. Metzner, ed., Proc. Intern. Congr. Photosynthesis Research, Freudenstadt, Germany, in press, 1969.

Baltscheffsky, M., *Arch. Biochem. Biophys., 130,* 646–652, 1969.

Duysens, L. N. M., and H. E. Sweers, in *Studies on Microalgae and Photosynthetic Bacteria, Special Issue of Plant and Cell Physiol.,* Jap. Soc. of Plant Physiologists, The Univ. of Tokyo Press, pp. 353–372, 1963.

Fleischman, D. E., and R. K. Clayton, *Photochem. Photobiol., 8,* 287–298, 1968.

Fork, D. C., in *Progress in Photosynthesis Research,* H. Metzner, ed., Proc. Intern. Congr. Photosynthesis Research, Freudenstadt, Germany, in press, 1969.

Joliot, A., Thesis, Univ. of Paris (1968).

Junge, W., and H. T. Witt, *Z. Naturforsch, 23b,* 244–254, 1968.

de Kouchkovsky, Y., *Comp. Rend. Acad. Sci., Fr., 252,* 2026–2028.

de Kouchkovsky, Y., in *Progress in Photosynthesis Research,* H. Metzner, ed., Proc. Intern. Congr. Photosynthesis Research, Freudenstadt, Germany, in press, 1969.

de Kouchkovsky, Y., and D. C. Fork, *Proc. Natl. Acad. Sci. U. S., 52,* 232–239, 1964.

Lavorel, J., *Biochim. Biophys. Acta, 60,* 510–523, 1962.

Myers, J., and J. R. Graham, *Plant Physiol., 38,* 105–116, 1963.

The Effect of Ultraviolet Irradiation on the Carotenoid Change, Electron Transport, and Photosynthesis of *Botrydiopsis alpina*

David C. Fork and Kenneth E. Mantai

Many similarities exist between the absorbance changes produced by chlorophyll *b* in green algae and higher plants and those attributed to a long-wavelength shift of a carotenoid in the yellow-green alga *Botrydiopsis alpina* (cf. Fork, 1969, and elsewhere in this report). The light-induced difference spectrum for the carotenoid change in this alga has maxima at 450, 482, and about 515 nm (and minima at 466 and 497 nm). The carotenoid change may be conveniently followed at any of these peak wavelengths; for this study we have chosen 482 nm. The difference spectrum in an alga with chlorophyll *b* such as *Ulva,* by contrast, has a positive maximum around 515 nm and negative minima near 475 and 650 nm (Fork *et al.,* 1966).

The kinetics of the chlorophyll *b* change and the carotenoid change have many features in common. Both show upon illumination a rapid initial deflection followed by a slower and larger change in the light. Darkening produces a rapid decay to the former base line. An example of the kinetics seen at 482 nm is given in the trace on the left side of Fig. 18. As explained in another section of this report, these absorption changes are dependent upon the dark interval given between exposures. Therefore, for the experiments reported here, an appropriate scheduling was used until reproducible changes were attained.

Action spectra for the initial deflection have shown sensitization by system 1 for both the chlorophyll-*b* change

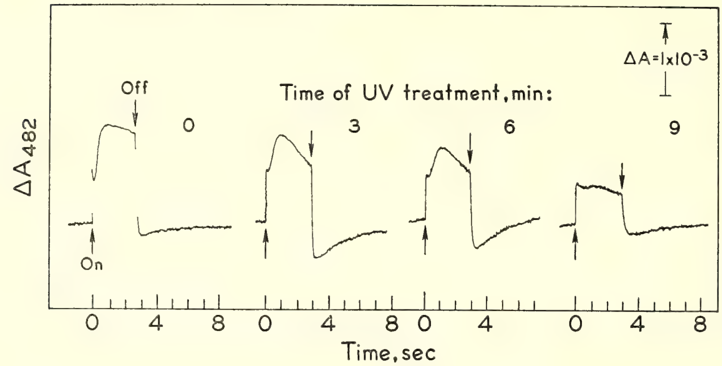

Fig. 18. The effect of ultraviolet irradiation (253.8-nm mercury line) on the kinetics of light-induced absorbance changes at 482 nm in *Botrydiopsis alpina*. A schedule of 3 seconds light and 6 seconds dark was used. Half-band width of the measuring beam was 2 nm. The red actinic light was a broad band from 620 to about 800 nm and had an intensity of 1.2×10^5 ergs cm^{-2} sec^{-1}.

(Fork *et al.,* 1966) and the carotenoid change (*Year Book 67,* p. 496; Fork, 1969). The slow phase appearing after several seconds of illumination is activated by system 2 in both cases. Earlier studies with *Scenedesmus* have shown (Mantai and Bishop, 1967) that the slow phase of the chlorophyll-*b* change is more sensitive to ultraviolet irradiation than is the rapid, initial deflection. Because of the similarities between the changes described above, it was expected that the slow phase of the carotenoid change mediated by system 2 would be more sensitive to ultraviolet irradiation than would the initial deflection. Figure 18 shows that this actually was the case. After 6 minutes of UV treatment the slow phase was strongly affected. The slow phase of the change was measured as the maximum excursion of the trace above the initial, rapid on-deflection. By contrast, the height of the initial deflection of the 482-nm change was hardly affected until longer times of irradiation had passed. After this ultraviolet treatment the cells produced a time course having a large, transient negative change upon darkening. Fig. 19A shows a semilogarithmic plot of the slow phase remaining after increasing times of irradiation with UV. Since the absorbance change observed consists of several components, a strict measurement of the fast and slow phases is difficult (see Fig. 18). As shown in Fig. 19A, there is an initial lag period of about 5 minutes during the ultraviolet treatment before inhibition of the slow phase begins. This suggests that some reaction other than the one being inhibited by the UV irradiation is rate limiting for the absorbance change, and it is not until the process affected by the irradiation itself becomes rate limiting that a decrease in the absorbance change occurs. After the initial lag period, the decay of activity with time follows first-order kinetics; and back extrapolation of the linearly decreasing part of the curve yields a half time ($t_{1/2}$) for decay of about 5 minutes. This lag period was not always seen, however. The absorbance changes shown in Fig. 18 (obtained from a different sample than that used for Fig. 19) did not show this lag in the UV effect. Nevertheless, the slow phase, when measured as described above, also decayed by first-order kinetics and had a $t_{1/2}$ of about 6 minutes. The decay of the chlorophyll-*b* change in spinach chloroplasts after irradiation was also found to be first order (Mantai, unpublished).

A study was made of the effect of UV irradiation on the reaction centers of system 2. For this we measured the

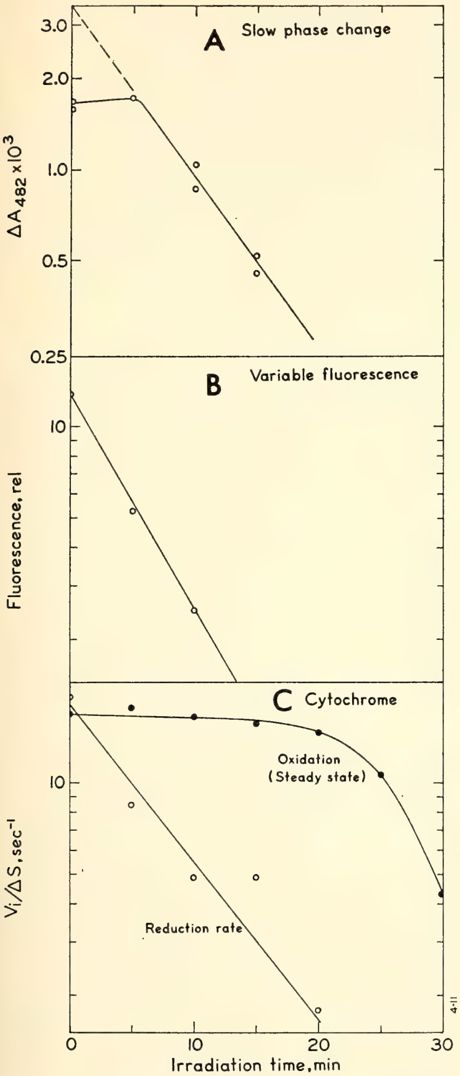

Fig. 19. (A) The slow phase of the 482-nm change in *B. alpina* as a function of increasing times of UV irradiation. The slow part of the change was measured as described in the text. The actinic light was the same as described in Fig. 18. The same culture of cells was used for all the measurements shown in Fig. 19. (B) Variable fluorescence in *B. alpina* treated with DCMU (1×10^{-4} *M*) as a function of the time of exposure to UV. Variable fluorescence was measured as the difference in level between the fluorescence produced immediately upon illumination and the maximum level produced. Dark interval between exposures, 30 seconds. Measurements were made at 685 nm (half-band 15 nm) by using interference and colored glass filters that transmitted fluorescent light but absorbed the blue actinic light. The latter had a peak near 420 nm, a half-band of 40 nm, and an intensity of about 10^2 ergs cm^{-2} sec^{-1}. (C) Light-induced reactions of the *f*-type cytochrome in *B. alpina* as a function of exposure time to ultraviolet. Measurements were made at 420 nm, half-band width 2 nm. The difference spectrum matched that of cytochrome *f* and had a maximum at 403 nm, with a Soret band near 419 nm. For each measurement the rate of reduction upon darkening was measured and was corrected for the endogenous cytochrome reduction remaining after the cells were poisoned with DCMU as described in (B). The initial rate of absorbance increase (reduction) divided by the steady-state level of oxidation attained in the light (in DCMU) was plotted as shown. Oxidation was taken as the light-induced steady-state absorbance decrease produced in the presence of DCMU. Red actinic light was as described for Fig. 18.

amount of variable-yield fluorescence remaining after increasing periods of UV treatment. Duysens and Sweers (1963) have shown that fluorescence having a variable yield during illumination is controlled by the reduction state of the system-2 reaction centers. When these traps are reduced, fluorescence is high; and when they are oxidized, the traps serve as quenchers (*Q*) and decrease fluorescence. Fig. 19B shows that the variable-yield fluorescence also decayed by first-order kinetics, with a half-time for inactivation similar to that of the carotenoid change (4–5 minutes). Similar results have been reported earlier for the effect of UV on variable fluorescence in spinach chloroplasts (Mantai, 1968; Malkin and Jones, 1968).

Light-induced reactions of the *f*-type cytochrome in *Botrydiopsis* were followed by measuring absorbance changes at 420 nm. This cytochrome has been shown by many workers in many different types of plants to be oxidized by system 1 and reduced by system 2. This effect was confirmed also for *Botrydiopsis*. Fig. 19C shows that the reduction of the cytochrome was sensitive to UV and decayed by first-order kinetics with a $t_{1/2}$ of about 6 minutes. In contrast to re-

duction, the oxidation of the cytochrome (mediated by system 1) was unaffected by irradiation times up to about 20 minutes. After this, oxidation was also affected. It should be noted that all these comparative measurements on the carotenoid change, variable fluorescence, cytochrome reduction, and oxidation were made with the same sample.

The data given above supports also the hypothesis that the slow phase of the carotenoid change is produced by system 2. Since the kinetics and the effects of UV on both the carotenoid and chlorophyll-*b* changes are very similar, it would appear that both of these absorbance changes result from similar reactions, although the compound responsible for the change in each case may be quite different. If these changes reflect some type of disturbance produced in their supporting membrane by a process such as electron transport (for example, by generation of an electric field across a membrane as proposed by Junge and Witt, 1968), then UV may act by disrupting membranes in some way. Other evidence (Mantai, 1968) has also suggested that ultraviolet light produces a disruption of lamellar membranes.

References

Duysens, L. N. M., and H. E. Sweers, in *Studies on Microalgae and Photosynthetic Bacteria, Special Issue of Plant and Cell Physiol.,* Jap. Soc. of Plant Physiologists, The Univ. of Tokyo Press, pp. 353–372, 1963.

Fork, D. C., J. Amesz, and J. M. Anderson, in *Energy Conversion by the Photosynthetic Apparatus, Brookhaven Symp. in Biol., 19,* Brookhaven National Laboratory, Upton, N. Y., pp. 81–94, 1967.

Fork, D. C., in *Progress in Photosynthesis Research,* H. Metzner, ed., Proc. Intern. Congr. Photosynthesis Research, Freudenstadt, Germany, in press, 1969.

Junge, W., and H. T. Witt, *Z. Naturforsch., 23b,* 244–254, 1968.

Malkin, S., and L. W. Jones, *Biochim. Biophys. Acta, 162,* 297–299, 1968.

Mantai, K. E., Thesis, Oregon State Univ., Corvallis, Oregon, 1968.

Mantai, K. E., and N. I. Bishop, *Biochim. Biophys. Acta, 131,* 350–356, 1967.

Electron Transport and Degradation of Chloroplasts by Hydrolytic Enzymes and Ultraviolet Irradiation

Kenneth E. Mantai

Recent development of the chemiosmotic hypothesis for the mechanism of both oxidative and photosynthetic phosphorylation has led to increased interest in membrane structure and integrity as a vital factor in efficient operation of the energy trapping reactions. Measurement of various chloroplast reactions after treatments which disrupt the membrane structure could help to elucidate the role that the structural integrity of membranes plays in these reactions. Because chloroplast membranes consist of about 50% lipid and 50% protein, digestion of these substances with appropriate enzymes could provide information on their importance in the membrane structure. There is evidence that the inhibition of photosynthesis by ultraviolet irradiation is due to a structural disruption of the chloroplast membranes. The following report compares the effects of UV irradiation, pancreatic lipase digestion, and trypsin digestion on electron transport as measured by DCIP (2,6 dichlorophenolindophenol) reduction in spinach chloroplasts.

Both UV irradiation and lipase digestion decrease the level of fluorescence in chloroplasts (Kok, *et al.,* 1967; Okayama, 1964), suggesting that the photochemistry itself is being affected by the treatments. Fig. 20 shows the effects of UV irradiation, pancreatic lipase, and trypsin digestion on the relative quantum yield of DCIP reduction. As seen in the figure, all three treatments decreased the quantum yield, confirming that the

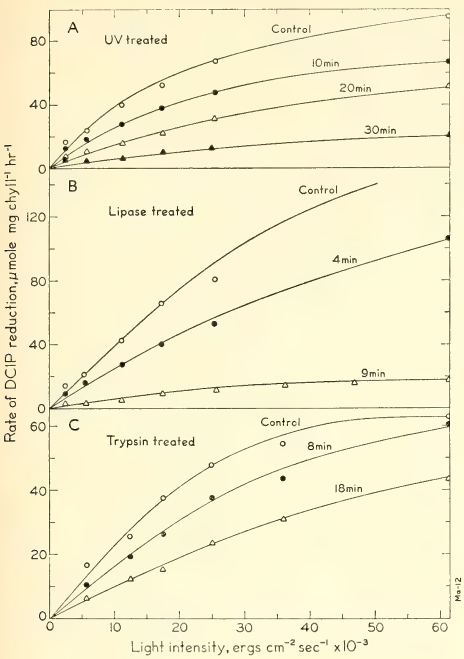

Fig. 20. Effects on relative quantum yield of DCIP reduction after UV irradiation, pancreatic lipase digestion, or trypsin digestion. Reaction mixtures consisted of: sucrose, 0.4 M; KCl, 15 mM; Tricine, 50 mM (pH 7.6); DCIP, 33 μM and chloroplasts containing about 40 μg chlorophyll, the exact amount varying slightly from experiment to experiment. The total volume was 3.0 ml. Enzyme digestions were carried out at 25°C in 0.4 M sucrose, 15 mM KCl, and 50 mM Tricine (pH 7.6). UV irradiation was performed as previously described (Mantai and Bishop, 1967).

photochemistry was indeed being inhibited.

There is considerable evidence for two pathways of electron transport in chloroplasts, only one of which is coupled to photophosphorylation. Therefore, the possibility that there might be a difference in the sensitivity of these pathways to the action of trypsin, lipase, or UV irradiation was tested by treating the chloroplasts and then measuring the rate of DCIP reduction in the presence or absence of a chemical uncoupler (CCCP, methylamine, NH_4Cl, atebrin, or gramicidin D).

Electron transport measurements made after UV irradiation, Fig. 21, shows that there was no difference in the rates at which coupled or uncoupled electron transport was inhibited (compare irradiated and methylamine uncoupled curves). CCCP uncoupled less effectively, and finally inhibited slightly, as the period of irradiation increased (see also below). In this experiment, a high concentration of CCCP (33 μM) was used. Reducing the CCCP concentration to 3.3 μM did not qualitatively change the results. The rates shown in the figure are under light saturating conditions. It should be mentioned that in this type of experiment if the two pathways have initial steps in common (e.g., trapping centers), and one of these steps is rate limiting, any differences in sensitivity between the rest of the two pathways would not be detected.

A similar experiment measuring DCIP reduction after digestion with pancreatic lipase is shown in Fig. 22. In this case

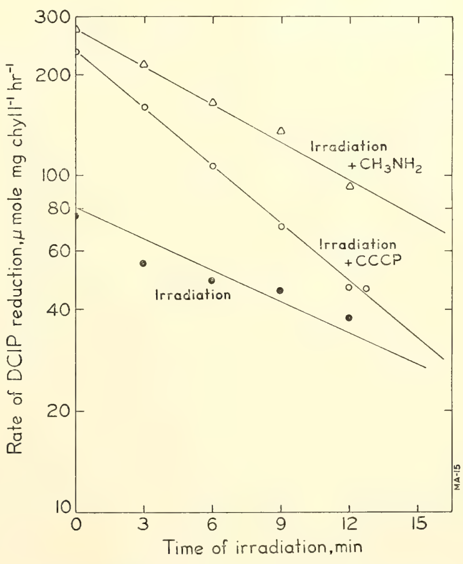

Fig. 21. Effect of uncoupling agents on DCIP reduction after UV irradiation. Conditions as in Fig. 20 with uncouplers added to give the following concentrations: CCCP, 33 μM and methylamine, 20 mM.

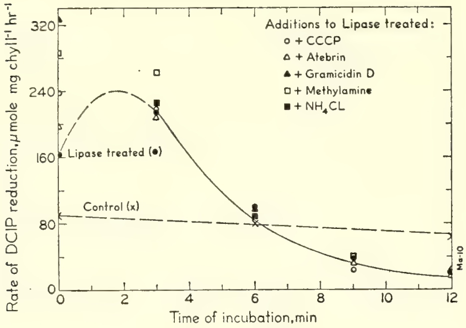

Fig. 22. Effect of uncoupling agents on DCIP reduction after digestion with pancreatic lipase. Reaction conditions as in Fig. 20 with uncouplers added to give the following concentrations: CCCP, 3.3 μM; atebrin, 10 μM; NH_4Cl, 1 mM; methylamine, 20 mM and Gramicidin D, 0.5 g ml^{-1}. Solid line shows lipase treated sample in absence of added uncouplers. Dashed line shows control sample without added uncouplers.

the lipase itself acts initially as an efficient uncoupler as shown by the increased electron flow. The zero-time sample shows considerable uncoupling because about 30 seconds elapsed between the time the enzyme was added and a sample removed. The uncoupling is complete after a short time, and addition of chemical uncouplers causes no further stimulation of electron flow. After continued digestion the total rate of light-saturated DCIP reduction decreases.

Trypsin digestion also uncouples chloroplasts (Fig. 23A), although not as effectively as lipase as seen by further stimulation of electron transport after addition of methylamine. Again, continued digestion led to a decrease in photoreductive capacity. In the experiment shown in Fig. 23B the uncoupler CCCP was added to trypsin-treated chloroplasts. Under these conditions CCCP acted as a potent inhibitor of electron transport. This inhibition appears to affect only the "extra" or coupled electron transport pathway. The same concentration of CCCP (3.3 μM) caused a doubling (Fig. 23B) of electron transport in untreated chloroplasts and did not inhibit either UV- or lipase-treated samples. However, there did appear to be a slight inhibitory effect in UV treated chloroplasts as irradiation time increased (Fig. 21). CCCP has been reported to inhibit electron transport at relatively high concentrations in untreated chloroplasts, but, as shown in Table 7, the inhibition was not concentration-dependent in trypsin-treated chloroplasts. CCCP did

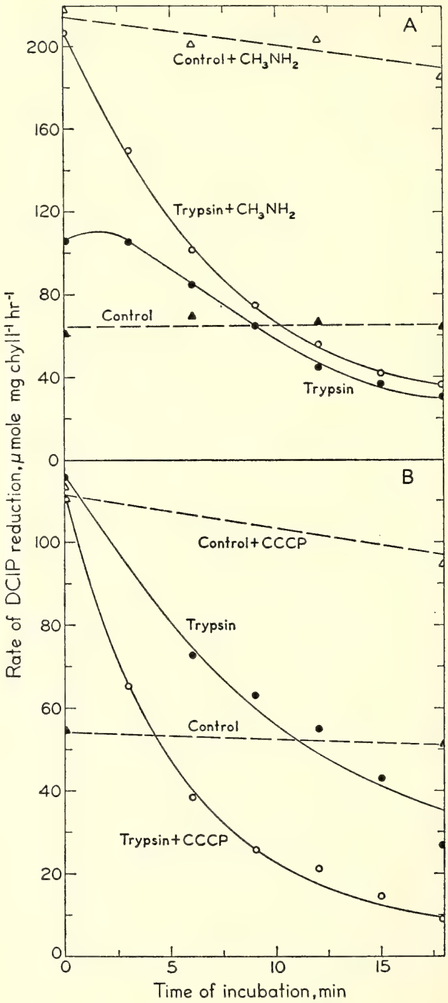

Fig. 23. Effect of methylamine or CCCP on DCIP reduction after trypsin digestion. Conditions as in Figs. 20 and 21.

TABLE 7. The Effect of Various Concentrations of CCCP on the Rate of DCIP Reduction* in Control and Trypsin Treated Spinach Chloroplasts

	CCCP Concentration, μM					
	0.0	0.33	0.66	1.70	3.33	9.99
Control	79.1	81.6	...	88.9	107.0	161.2
Trypsin treated	45.8	46.6	39.4	...	32.0	...

* Expressed as μ moles red. mg. chl^{-1} hr^{-1}. Conditions as in Fig. 20.

not stimulate DCIP reduction at concentrations as low as 0.33 μM in trypsin digested chloroplasts nor did it inhibit untreated chloroplasts at concentrations as high as 10 μM. Treatment of chloroplasts with papain, another proteolytic enzyme, gave similar results.

Reports from Park's laboratory have shown that glutaraldehyde-fixation of chloroplasts stabilized system-2 activity (Park, *et al.*, 1966). Although the initial activity of these chloroplasts is low, the rate of DCIP reduction is stimulated by the uncoupler methylamine and inhibited by DCMU, suggesting that the activity is the result of true photosynthetic reactions and not of artifacts in the fixation procedure. It has also been shown that glutaraldehyde cross-links proteins, both inter- and intramolecularly, without greatly affecting their conformation. In view of this, experiments were performed to determine whether fixation would provide protection against the action of trypsin, lipase, or UV irradiation. In Fig. 24 the effects of UV irradiation on DCIP reduction in fixed and normal chloroplasts are shown. The fixation procedure had no effect on the inhibition by UV irradiation. Figure 25 shows the results of similar experiments measuring the effects of fixation on the inhibition by (A) pancreatic lipase and (B) trypsin. Glutaraldehyde-fixation afforded striking protection against the inhibitory effects of these two enzymes. Measurement of the fatty acids liberated after lipase digestion did not reveal any great difference between fixed and unfixed samples, indicating that the lipase was still able to attack the fixed chloroplasts. No attempt was made to assay the activity of the trypsin in fixed and unfixed samples. The possibility thus remains that the fixation procedure made the lamellar proteins unavailable to the trypsin, perhaps simply by steric hindrance. However, fixed chloroplasts exhibited partial uncoupling by trypsin, suggesting that the enzyme attacks the membrane.

Since glutaraldehyde-fixation protects against the effects of lipase, it would appear that those lipids readily hydrolyzed

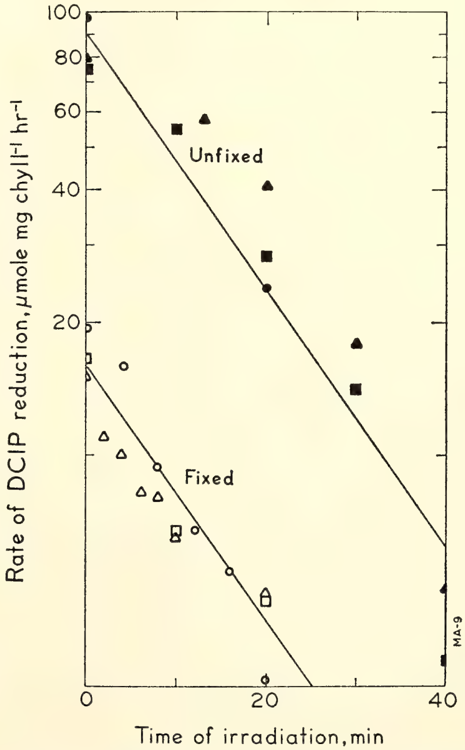

Fig. 24. Effect of UV irradiation on normal and glutaraldehyde-fixed chloroplasts. Reaction mixture consisted of phosphate buffer, 0.01 M (pH 7.3); DCIP, 33 μM and chloroplasts containing about 40 μg chlorophyll.

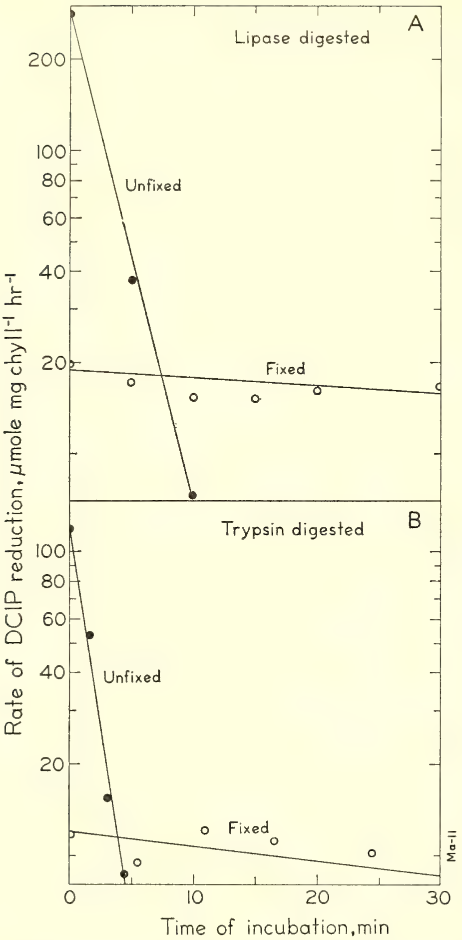

Fig. 25. Effect of pancreatic lipase or trypsin digestion on DCIP reduction in normal and glutaraldehyde-fixed chloroplasts. Conditions as in Fig. 24.

by pancreatic lipase are required only as a "glue" and not as obligate components for electron transport. The protection afforded by fixation against trypsin is somewhat less easily explained. Trypsin preferentially attacks peptide bonds in which the carboxyl group is donated by a basic amino acid residue, usually arginine or lysine. Chloroplast lamellar and structural protein is rather low in both of these amino acids and relatively few breaks in the protein molecules would be expected. Glutaraldehyde, by cross-linking both inter- and intramolecularly, may hold the protein conformation in its original state in spite of the breaks in the protein molecules themselves.

UV irradiation inhibits in a manner similar to trypsin and lipase, with some striking exceptions. The most evident is the lack of uncoupling by UV irradiation (see Fig. 21). PMS-mediated cyclic photophosphorylation is inhibited by UV irradiation at about the same rate as the loss of Hill reaction activity, at least with relatively low (although still saturating for the Hill reaction) actinic light intensities. However, lack of uncoupling implies that the site of inhibition may be in the electron transport chain rather than in the phosphorylation mechanism. As shown in Fig. 20, the relative quantum yield of DCIP reduction decreases after UV irradiation (as does the variable fluorescence) indicating that system 2 is being affected. Moreover, since cyclic photophosphorylation is at least one component removed from system 2 (DCMU blocks after the primary electron acceptor for system 2, but does not inhibit cyclic photophosphorylation), UV irradiation must either produce a general effect on the membrane system or inhibit at two separate sites. There is no strong evidence that UV irradiation destroys a specific component or components of the electron transport chain. Although plastoquinone and other quinones are in fact destroyed by UV irradiation, it does not appear that this is the major cause of the inhibition (Mantai and Bishop, 1967).

It seems reasonable to conclude that the inhibition of electron transport by pancreatic lipase, trypsin, and probably UV irradiation as well, is caused by a structural disruption of the lamellar membranes rather than inactivation of a specific component. The inhibition by UV irradiation, however, appears to be more specific and does not uncouple although phosphorylation is inhibited.

References

Kok, B., *et al., Energy Conversion by the Photosynthetic Apparatus, Brookhaven Symp. in Biol. No. 19,* Brookhaven National Laboratory, Upton, New York, pp. 446–458, 1967.

Mantai, K. E., and N. I. Bishop, *Biochim. Biophys. Acta, 131,* 350–356, 1967.

Okayama, S., *Plant and Cell Physiol., 5,* 145–156, 1964.

Park, R., *et al., Proc. Natl. Acad. Sci., 55,* 1056–1062, 1966.

Effects of *N*-Methylphenazonium Methosulfate and Pyocyanine on Delayed Light Emission in *Chlorella* Cells and Spinach Chloroplasts

L. O. Björn

In trying to understand the process of photosynthesis it is useful to study the reverse process, i.e., the delayed light emission (afterglow) that comes from plants even several minutes after they have been transferred from light to darkness.

That the light emission is closely related to photosynthesis is indicated by the fact that many chemical agents which influence the latter also change the former. Thus the substances reported below to change the pattern of light emission are known to be efficient, although artificial, catalysts of photosynthetic phosphorylation.

One aim of biological research is to determine the minimum unit that can perform a certain function and to identify this unit structurally. It has long been known that the chlorophyll molecules do not function separately in photosynthesis, but rather cooperate in groups. The number of cooperating molecules found in a group or "photosynthetic unit" depends on the kind of experiment by which it is measured. The unit for the primary conversion of light into chemical energy contains a few hundred chlorophyll molecules, while several such units might form a larger unit capable of more complex functions. The experiments described below indicate that a specific kind of afterglow originates in units containing about the same number of chlorophyll molecules as the structural unit called a thylacoid.

In these experiments the plant sample was first illuminated for 30 seconds. The exciting light was then shut off and the afterglow measured for a few minutes. The exciting wavelength, isolated with interference filters, was either 648 or 730 nm. The sample was either *Chlorella pyrenoidosa* (Indiana Culture No. 252) or spinach chloroplasts ("whole chloroplasts" in 0.34 *M* NaCl buffered to *p*H 7.7–7.8 with 0.05 *M* Tricine). The light emission was recorded from about one second to a few minutes after the end of excitation. Air had free access to the samples, and the *Chlorella* were kept suspended by a continuous stream of air bubbles during irradiation and measurement.

With intact cells the decay kinetics vary with the wavelength used for excitation. With 648 nm a monotonic decay is obtained; but after excitation with 730-nm irradiation of sufficient intensity and duration the light emission drops to a minimum, rises again to a maximum and finally slowly declines. This maximum at about 1 minute in the decay curve was first described by Bertsch and Azzi (1965). This so-called component *V* (nomenclature of Shuvalov and Litvin, 1969) that is induced only by long-wavelength light, differs from other kinds of afterglow not only by its action spectrum and time dependence, but also by the emission spectrum (Litvin and Shuvalov, 1966). It also has a different temperature dependence (Bertsch and Azzi, 1965; Shuvalov and Litvin, 1969), and is strongly influenced by oxygen.

Among the more interesting results of the current experiments are the effects of *N*-methylphenazonium methosulfate (PMS) and its photooxidation product, pyocyanine, on the afterglow. Both seem to enter *Chlorella* rapidly. PMS accele-

rates the emission of component *V*. The effect can be detected with a PMS-concentration of only 10^{-9} *M* (Figures 26 and 27). The 648-nm–induced emission is affected only by much higher concentrations. Pyocyanine gives the same effects as PMS, but a ten times higher concentration is required. The same effect of pyocyanine has been described by Rubin and Venediktov (1967) for *Vallisneria,* but the concentration used in their investigation was very high (10^{-2} g 1^{-1} = 4.8×10^{-5} *M*).

The results in Figures 26 and 27 were obtained with dilute suspensions of algal cells, and in this case the effect of PMS depends on its concentration but is independent of the algal concentration. If very dense suspensions are employed, PMS is somewhat less effective on a concentration basis. However, when the amount of PMS is expressed in relation to the amount of *Chlorella,* the efficiency is higher in dense suspensions. In one series of experiments a suspension with the following characteristics was used: cell concentration, 1.0×10^{11} 1^{-1}; chlorophyll concentration, 1.77 m*M* (chl *a* 1.34 m*M,* chl *b* 0.43 m*M*); packed cell

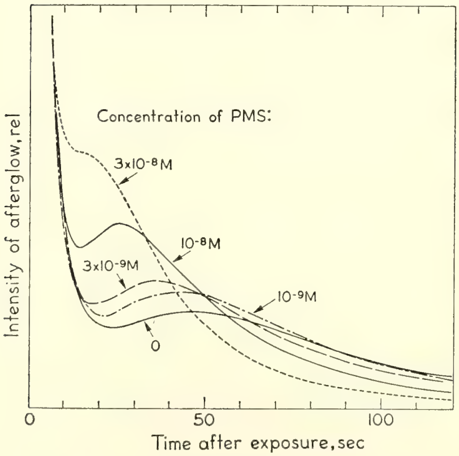

Fig. 26. PMS accelerates the slow light emission, component *V,* in a suspension of *Chlorella.* Concentration of chlorophylls $a + b = 4.3 \times 10^{-5}$ *M,* excitation by 30 seconds far red, 730 nm, at about 4×10^4 erg cm^{-2} sec^{-1}.

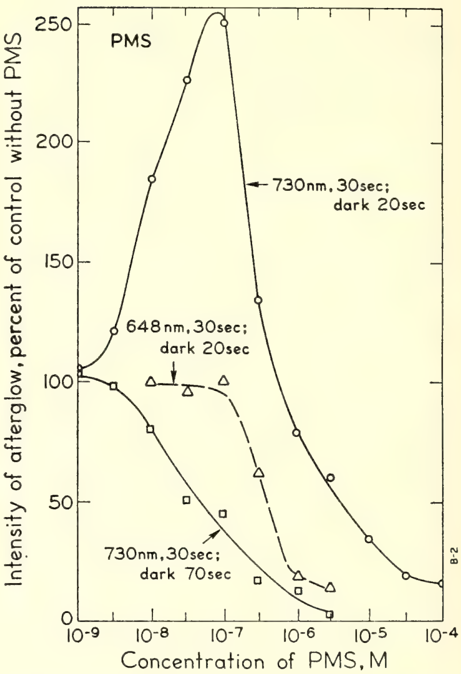

Fig. 27. Effect of PMS on the afterglow from *Chlorella* suspensions (concentration of chlorophylls $a + b$ ranging from 6.6×10^{-6} to 6.8×10^{-4} *M*) excited by 30 seconds of either red (648-nm) or far red (730-nm) light. The abscissa indicates the concentration of PMS, the ordinate the afterglow intensity 20 seconds or 70 seconds after end of exposure, as indicated on the curves.

volume, 29% of suspension volume. Table 8 shows the effect of 1×10^{-8} *M* and 3×10^{-8} *M* PMS at this high cell concentration. It was found that, when a sufficiently long time had elapsed after the end of excitation, the luminescence intensity with PMS declined to a certain fraction of the intensity without PMS, and that this fraction eventually reached a fixed value. For 1×10^{-8} *M* PMS, this limiting value was 0.62.

If we assume that there are "afterglow units" of approximately uniform size (perhaps related to the "photosynthetic units"), the result of the above experiment can be used to determine a maximum concentration of these units (corresponding to a minimum size). If

at any time the intensity of luminescence with PMS is only the fraction x of that without PMS, then at least the fraction $(1-x)$ of the luminescent units are in some way affected. A unit which is affected must be associated with at least one molecule of PMS. Thus the molar concentration of afterglow units cannot exceed (molarity of PMS)/$(1-x)$.

In the present case with [PMS] = 1×10^{-8} M and $x=0.62$, the maximum molarity of afterglow units is $(1\times10^{-8})/0.38$ $M=2.63\times10^{-8}$ M. Since the concentration of chlorophyll is 1.77×10^{-3} M, there are *at least* 6.7×10^{4} molecules of chlorophyll per unit.

The unit estimated in this way is considerably larger than the "classical" photosynthetic unit. It may be identical with the unit estimated by Junge and Witt (1968) for the light-induced chlorophyll-*b* change. They estimate a size of about 10^5 chlorophyll molecules, and believe the unit to be one thylacoid.

This estimate of unit size applies of course only to component *V* afterglow. The other afterglow components may emanate from units of different sizes.

Low concentrations of PMS only increase the rate of emission but do not change the amount of light emitted. In the experiment shown in Table 8, the long-term emission was decreased to 62 and 39% by the two concentrations of PMS, but the light integrated from 5 to 370 seconds after the end of excitation was 105 and 102% of the value of the control without PMS. However, with a high concentration of PMS the total amount of light is decreased.

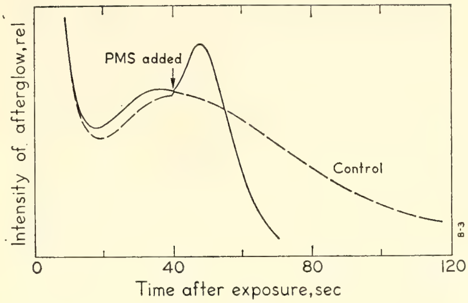

Fig. 28. Afterglow from 2.5 ml *Chlorella* suspension (concentration of chlorophylls $a+b=1.6\times10^{-4}$ M) excited by 30 seconds far red (730-nm) light at about 4×10^{4} erg cm^{-2} sec^{-1}. Forty seconds after the end of the exposure, approximately 0.5 ml of either water (dashed line) or 10^{-5} M PMS (solid line) were injected.

The acceleration of emission by PMS can also be demonstrated by injecting it into the sample in the dark period after excitation. In the experiment shown in Figure 28 a large amount of PMS was used, and it is readily seen that the total amount of light emitted was decreased by PMS.

Although leaves of many plants (including spinach) were found to give decay curves of essentially the same type as *Chlorella,* isolated chloroplasts seem to lack most of component *V* of the delayed light. With spinach chloroplasts the decay curves appear very similar (monotonic decline) whether the emis-

TABLE 8. Effect of PMS on the Afterglow from a Dense *Chlorella* Suspension Excited for 30 sec at 730 nm, Average of Four Experiments

Dark Time, sec	Time Course: Relative Intensity without PMS	Ratio of Luminescence with PMS to Luminescence without PMS: 1×10^{-8} M PMS	3×10^{-8} M PMS
20	860	1.21	1.87
70	1009	1.08	1.05
120	611	0.75	0.58
170	319	0.74	0.51
220	176	0.72	0.46
270	106	0.63	0.37
320	59	0.62	0.40
370	35	0.62	0.39

sion is induced by 648 or 730 nm light. A few differences between the effects of the two wavelengths were observed:

1. Pyocyanine at a concentration of 3×10^{-6} M slightly increases the 20-second delayed light excited by 730 nm, but decreases that excited by 648 nm (Fig. 29). The effects are not as pronounced as those found by Mayne (1967) for delayed light in the millisecond range.

2. Ascorbate (0.01 M) increases the long-lived afterglow excited by 730 nm (remnants of component V?), but has no effect on that excited by 648 nm (when no other additions are made, see below and Fig. 30).

3. The afterglow excited by weak 648-nm light is diminished by a previous exposure to 730-nm light, but enhanced by a previous exposure to strong 648-nm light. This holds even when the dark time after the first exposure is so long that the afterglow induced by it has become negligible. A similar effect was reported by Litvin and Shuvalov (1966).

Although ascorbate alone has no effect on the 648-nm–induced emission, it

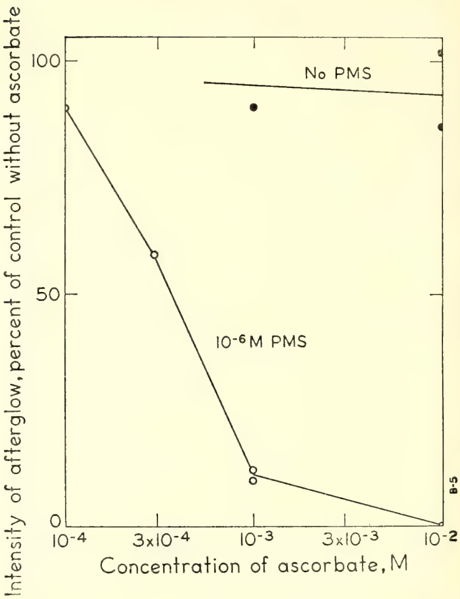

Fig. 30. Afterglow from spinach chloroplasts (concentration of chlorophylls $a + b = 4.1 \times 10^{-5}$ M) 20 seconds after the end of 30-second excitation by red (648-nm) light at about 1.5×10^{3} erg cm^{-2} sec^{-1}. Afterglow intensity is decreased by ascorbate only in the presence of PMS.

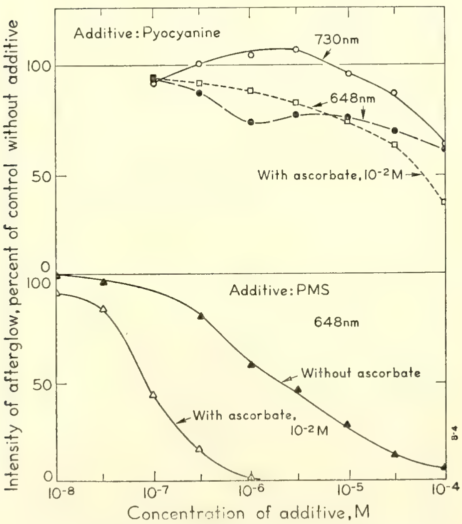

Fig. 29. Effect of PMS and pyocyanine on the afterglow from spinach chloroplasts 20 seconds after the end of 30-second excitation by either red (648-nm) or far red (730-nm) light.

greatly enhances the effect of PMS, probably because PMS is reduced by ascorbate (Fig. 30). Ascorbate can be replaced by isoascorbate. Bertsch *et al.* (1969) found no effect of PMS alone on the fast delayed light (1–20 msec) from chloroplasts, while PMS (3×10^{-5} M) plus ascorbate (5×10^{-3} M) produced almost complete inhibition. In the present experiments PMS alone inhibits at a high concentration, but in the presence of ascorbate the same effect is produced by less than one tenth as much PMS.

In my experiments pyocyanine alone had less effect than PMS alone. In this respect the late delayed light differs from that in the millisecond range investigated by Bertsch *et al.* (1969). As expected, ascorbate did not radically change the effect of pyocyanine (which is not reduced by ascorbate). Ascorbate does have an effect at very high concentra-

tions of pyocyanine, possibly due to traces of PMS in the pyocyanine preparation.

References

Bertsch, W. F., and J. R. Azzi, *Biochim. Biophys. Acta, 94,* 15–26, 1965.

Bertsch, W., J. West, and R. Hill, *Biochim. Biophys. Acta, 172,* 525–538, 1969.

Junge, W., and H. T. Witt, *Z. Naturforsch., 23b,* 244–254, 1968.

Litvin, F. F., and V. A. Shuvalov, *Biokhimiya, 31,* 1264–1275, 1966.

Mayne, B. C., *Photochem. Photobiol., 6,* 189–197, 1967.

Rubin, A. B., and P. S. Venediktov, *Fiziol. rastenii 15,* 34–40, 1967.

Shuvalov, V. A., and F. F. Litvin, *Molekulyarnaya Biologiya, 3,* 59–73, 1969.

A Test of Fiber Optics for Fluorescence Spectroscopy

C. S. French, R. W. Hart, N. Murata, and C. Wraight

The ideal geometry of a system for exciting fluorescence and for collecting the emitted light to give the minimum distortion of the emission spectrum by reabsorption of the fluorescent light within the sample is to have both optical axes perpendicular to the surface of the sample. Collection of the emitted light over a large solid angle with simultaneous perpendicular illumination is difficult with lenses or mirrors.

However, the availability of glass fiber optics in sheet form makes possible a convenient fluorescence excitation and light collection system for use in fluorescence spectrophotometers with the axes for both beams perpendicular to the sample surface. With alternate sheets of fibers for the incident and for the emitted light nearly half the sample surface may be exposed to the collector fibers.

The efficiency of light collection depends on the acceptance angle of the individual fibers and on the overlapping of the cones of illuminated spaces with the cones of the space seen by the collection fibers. The numerical aperture of the fibers, 0.5 in air, corresponds to a light cone of 60° for the ends in air and to about 83° for the ends in water. For a sample in immediate contact with the ends of the fibers the overlapping is zero at the surface but becomes high a short distance below the surface of the sample.

The original recording fluorescence spectrophotometer with automatic correction for variation in sensitivity of the detector and of the monochromator's transmission with wavelength (French, 1956) was modified to test the fiber optics system as shown in Fig. 31. Although the principle seems useful, the system we developed was not satisfactory.

The soft plastic backing of the 0.003-inch diameter fibers was removed by softening with chloroform and scraping to avoid waste space in the bundle ends. However, sheets of glass fibers parallel to each other can be bought with the backing material omitted from the ends (Fiber Photics Inc., 2557 Soquel Drive, Santa Cruz, California, 95060).

The width of each fiber optic sheet was chosen to match the length of an image of the exit slit of the monochromator

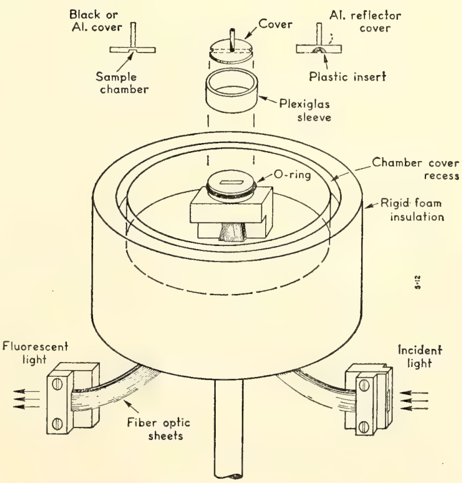

Fig. 31. An arrangement for measuring fluorescence spectra with fiber optics.

used for the excitation light. The width of this image required the use of 12 sheets in the bundles for the incident light. At the sample position the sheets carrying the excitation light alternate with the collecting sheets, and one extra collecting sheet was added outside the last excitation sheet. The ends of each bundle of sheets were coated with epoxy cement and pressed into cavities of rectangular cross section in plastic blocks for the bundles going to the two monochromators. For the sample position an aluminum block was used. The ends of the three bundles were ground and polished.

The aluminum block has a horizontal surface so a solid sample may be laid on it. A removable plastic sleeve fitted over the round top of the block and sealed with an O-ring, holds liquid samples. A box with a light-tight cover and plastic foam insulation supports the aluminum sample block and can be filled with liquid N_2 or other liquid to hold the desired temperature long enough for a spectral measurement.

An aluminum cover can be used to define the thickness of a liquid sample and to act as a reflector for increasing the light collection efficiency with weakly absorbing solutions. Other aluminum inserts giving various sample depths are used to check for distortion of the emission spectrum by internal reabsorption. Spectra of identical shape for sample depths differing by a factor of two provide adequate evidence for lack of such distortion.

At the suggestion of Dr. Charles Weiss we have also made curved focusing reflectors, as shown in the upper part of Fig. 31, to increase the light collecting efficiency for dilute liquid samples. In these reflectors the space between the reflector and the sample chamber is filled with clear plastic. For highly scattering samples, such as those with ice crystals, black covers that do not reflect were made.

The system we built, although providing a convenient method for handling samples, gave 71% of the overall efficiency of our previous lens system instead of an anticipated gain. This test was made on a fragment of fluorescent Corning glass No. 3387 in a flat reflecting aluminum holder. Some of the loss may be attributed to the microscopically visible chipping of some of the ends of the glass fibers in the grinding process.

A more serious loss, however, occurs from the fact that the angle of divergence of the beam entering the monochromator exceeds the f 2.5 cone of the collector lens. An improvement of 20% was achieved by adding a small field lens inside the slit.

In testing the system, chlorophyll adsorbed on the epoxy cement in which the fibers were embedded. To remove the contaminant the fibers and plastic were cut back 0.02 inch and the space filled with epoxy cement. A $\frac{1}{16}$-inch lucite plate was added to keep the sample from sticking to the epoxy. These modifications led to disastrous light losses.

The fiber optics system with these modifications was compared to the old lens and mirror system. The lens and mirror system was then about 30 times more efficient than the modified fiber optics system which has been, at least temporarily, abandoned. The fiber optics arrangement could probably be made to give reasonably good performance if the sample end of the fibers were covered with a very thin layer of material to which the sample did not adhere.

Reference

French, C. Stacy, in *The Luminescence of Biological Systems*, Frank H. Johnson, ed., A.A.A.S., Wash. D. C., pp. 51–74, 1955.

Use of the ACME Computer for Analysis of Real-Time Data

David C. Fork

We have developed several programs, largely as the result of the competent help of Linda Crouse of the ACME com-

putation center, that enable us to use the computer to handle real-time data. (A description of the ACME facility is given in last year's report, *Year Book 67,* p. 534).

As presently written, the programs allow us to vary the rate at which the analog signals will be sampled (up to about 1000 points per second using an IBM 1800 or up to about 20,000 points per second with the IBM 270X interface). Depending upon the needs of the experiment, a variable number of time-course curves can be analyzed. For each of these curves, measurements of up to ten differences of amplitude can be made. The data can be returned as obtained by the IBM 1800 or, to avoid a flood of unwanted numbers, averaged over a particular region of interest.

In addition, a second channel of analog input is reserved for data received from a photocell that monitors the actinic light. The program determines when the light has been turned on and off and measures its intensity. A value at any point in time, along a curve, can be obtained by entering in the program the time the measurement is to be made in relation to the time the light went on or off.

The programs are also designed to measure slopes over designated time intervals. Thus, by entering appropriate factors the quantum yields can readily be determined.

EXPERIMENTAL TAXONOMY INVESTIGATIONS

The *Mimulus* Investigations

William M. Hiesey, Malcolm A. Nobs, and Olle Björkman

A considerable part of the current effort of the Experimental Taxonomy Group has been directed towards bringing to conclusion the long-term investigations on the Erythranthe section of *Mimulus.* This group of species was selected for combined cytotaxonomic, transplant, and physiological investigation in a multiple-approach study aimed at improving our understanding of the many-sided biological question of how differentiation between species and ecological races within species is related to mechanisms of inheritance, to major external factors of contrasting natural environments, and to internal physiological functions. Plants are better suited than animals for such studies primarily because plants can be cloned and manipulated experimentally with much greater freedom in cytogenetic, transplant, and physiological investigations needed in such an integrated program.

Earlier *Year Books* (*50,* 1951; and *53,* 1954, to *67,* 1969) have reported progress on various aspects of the *Mimulus* investigations. The results from these and more recent researches are incorporated in a Carnegie Institution monograph to appear as Volume V of the series, *Experimental Studies on the Nature of Species.* It seems appropriate to review the major features of this monograph.

Mimulus as an experimental object. In searching for basic principles regarding mechanisms of evolution in higher plants, the choice of experimental materials is of utmost importance. Earlier studies by the Experimental Taxonomy Group on various species-complexes such as *Potentilla glandulosa, Achillea millefolium,* and the grass genus *Poa* pointed to characteristics lacking in these groups that would have been helpful for extending the earlier studies to include quantitative physiological investigations. The latter are needed to fill an important gap in our knowledge relating to the genetic structure of species and races, the environments in which they evolved, and their internal functioning. The Erythranthe section of *Mimulus* was chosen primarily as a vehicle to bridge this gap.

The features of the Erythranthe section that make this group particularly suitable for experimental investigations include a unique combination of essential characteristics. The most important are (1) all members are diploid with the same chromosome number ($n=8$); (2) all of the five species that have been brought into culture can be intercrossed in any combination to produce vigorous first-generation hybrids; (3) these F_1 hybrids range from completely fertile to highly sterile, and reflect different degrees of genetic compatibility within the section that clearly evolved from a common ancestral stock; (4) the species, and often races within species, have distinct marker characters that can be followed through successive generations in genetic experiments; (5) the flower structure of all the members of the group favors easily controlled pollinations, and in interfertile combinations many seedling progeny may be obtained from a single flower; (6) species and ecological races within the Erythranthe section differ widely in their capacity to survive in contrasting climates such as are found at the Stanford, Mather, and Timberline transplant stations; (7) all members of the section can be readily propagated vegetatively as clones to obtain genetically identical plants that can be used in diverse kinds of transplant and physiological experiments and (8) all members have leaves and stems suitable for use in quantitative physiological measurements involving gas exchange on intact living plants. Few plant groups meet all of these requirements as well as this group of *Mimulus* species.

Biosystematic relationships within the Erythranthe section. As reported in *Year Book 64*, pp. 427–429, there are two major interfertile groups within the Erythranthe section, one composed of the two most widely distributed species, *M. lewisii* and *M. cardinalis,* and the other of the three southernmost species, *M. verbenaceus, M. eastwoodiae,* and *M. nelsonii.* The species of either group when intercrossed produce F_1 hybrids that are partially sterile to varying degrees. One of the most sterile combinations, *M. lewisii*×*M. nelsonii,* gave rise to a fertile, vigorous, distinctive amphiploid (see *Year Book 65,* pp. 468–471), thus establishing the close ancestral relationship between the genetically most diverse members of the section. The varying degrees of interfertility among inter- and intra-specific combinations reveal in finer detail different stages of genetic isolation that have evolved within the section.

Recombinations of morphological characters in hybrid populations. From an experimental point of view it is a most fortunate circumstance that *M. lewisii* and *M. cardinalis,* the two species of widest geographic distribution, are interfertile and occur in distinct but complementary climates. *Mimulus lewisii* occurs in more northernly areas and at higher altitudes in contrast with *M. cardinalis* of more southern distribution, mostly at lower altitudes. First-generation hybrids between ecologically extreme forms of the two species are interfertile, and their progeny provide a means for studying the mode of inheritance of the distinctive morphological characters differentiating the two species in relation to their responses in the contrasting climates at the Stanford, Mather, and Timberline transplant stations.

The numerous morphological characters that distinguish the two species include flower color, flower structure, patterns of pigment distribution in localized areas in the corollas, and such vegetative characteristics as leaf shape and number of dentations along leaf margins. The segregation of 20 characters distinguishing *M. lewisii* and *M. cardinalis* has been studied extensively in F_1, F_2, and F_3 populations when cloned and grown at Stanford and at the Mather and Timberline transplant stations.

Inheritance of morphological markers in relation to capacity for survival at the transplant stations. Of the many

morphological characters studied, only one distinguishing *M. lewisii* from *M. cardinalis* has been found to be inherited in a simple Mendelian manner. The presence or absence of yellow carotenoid pigment in the upper epidermis of the corollas is determined by a single gene. Its presence in *M. cardinalis* in conjunction with other pigments causes the flowers of this species to have the bright orange-red appearance. In *M. lewisii* this pigment is absent, and the corollas are pale pink or purple, depending on the particular race. In the F_1 hybrid the expression of the yellow carotenoid pigment carried by *M. cardinalis* is suppressed by a dominant gene carried by *M. lewisii.* In F_2 and F_3 progeny this character is inherited in the ratio of 3 without carotenoid pigment to one with carotenoid pigment, its expression or lack of it being superimposed upon a wide array of independently inherited pigment characters governed in inheritance by complex gene systems. The resultant number of phenotypic expressions of flower color in F_2 and F_3 progeny is, therefore, very large.

All other characters distinguishing *M. lewisii* and *M. cardinalis* that we have studied have a complex hereditary basis that cannot be resolved in simple Mendelian terms. An example is the inheritance of leaf characteristics. *Mimulus lewisii* has relatively narrow oblanceolate leaves with nearly entire edges, as illustrated in the top row in Fig. 32 at the left. The array shown is typical of that found in seedlings obtained by self-pollinating the *M. lewisii* parent. Corresponding leaves of the *M. cardinalis* parent used in crossing experiments are shown in the same figure (top row at the right). As compared with *M. lewisii,* the leaves of *M. cardinalis* are broader, more obtuse at the tips, and have toothed margins.

The leaves of F_1 hybrids between *M. lewisii* and *M. cardinalis* are clearly intermediate, but with variations overlapping both parental populations, as shown in Fig. 32 (row next to the top). In the second generation the assortment of recombinations in leaf characters covers the entire range from one parental extreme to the other, with maximum frequencies in intermediate classes that fall within the range of the F_1 progeny.

Third-generation progenies derived by self-pollinating selected F_2 individuals possess leaf characters that may differ appreciably from one another, depending on the characteristics of the particular F_2 parent. The leaves from the series of F_3 population shown in Fig. 32 are examples. The first of this series, No. 7541, was derived from a *lewisii*-like F_2 individual. The leaf types segregated in this F_3 population include the range of variation of the original *M. lewisii* parent plus that found in F_1 progeny. The flowers produced by this same F_3 population ranged over various *lewisii*-like shades of pink, all having short styles and stamens, characters of *M. lewisii.* The correlation in the inheritance of predominantly *lewisii*-like characters in this population in both leaf and floral characters is clearly evident on analysis.

In contrast, the F_3 progeny derived from a *cardinalis*-like F_2 individual had broad, obtuse leaves with toothed margins, as shown in Fig. 32 (culture No. 7565, bottom row). In this population the range of variation in leaf characters included that of the original *M. cardinalis* parental population and the F_1 progeny. The flowers of this same F_3 population segregated into an array having predominantly *cardinalis*-like characters. The bias in segregation towards *M. cardinalis* in this population is as striking as in the previous F_3 progeny whose characters segregated strongly towards *M. lewisii.*

Third-generation progenies derived from F_2 individuals in classes intermediate between those of the parental types segregate over a considerably wider range than in the two examples just mentioned. Examples are shown by the arrays of leaves in Fig. 32 including the F_3

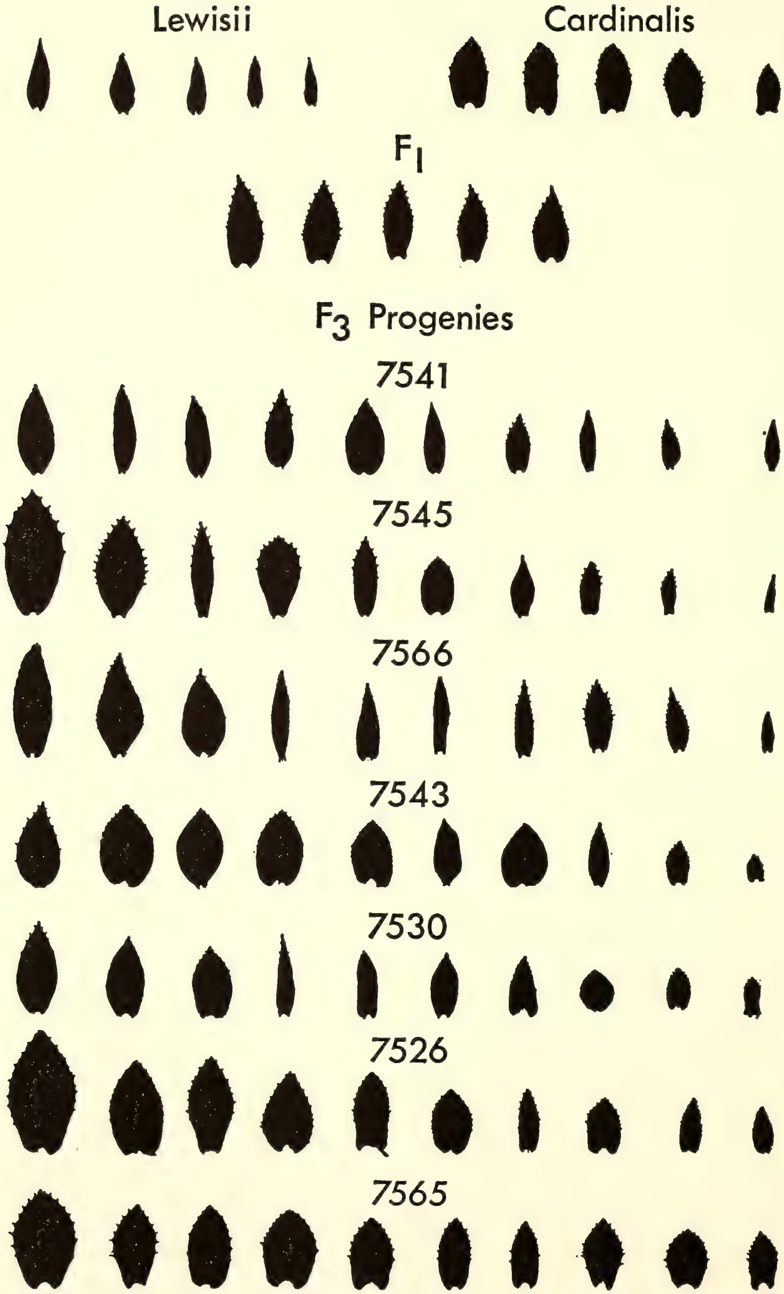

Fig. 32. Differences in leaf characters between subalpine *M. lewisii* and coastal *M. cardinalis*, their F_1 hybrid, and ranges of segregation within F_3 progenies derived from F_2 individuals of different genetic composition. See text.

populations 7545, 7566, 7543, 7530, and 7526. Some of these populations, notably 7545 and 7530, approach the diversity found in F_2 populations.

The responses of cloned transplants at the altitudinal field stations at Stanford, Mather, and Timberline of parental, F_1, F_2, and F_3 progenies which have been studied over a long period of years show definite correlations between the morphological characters they inherit and their capacity to survive in contrasting climates. The plants shown in Plate 1A, photographed in the Timberline garden in 1967, summarize the responses of *M. lewisii, M. cardinalis,* and their F_1 hybrid at the subalpine station. The photograph was taken in early September after the onset of early autumn frosts and the season's first light snowfall and shows the already matured and dormant *M. lewisii* (left) with the withered remains of its flowering stems. The spot marked by the tape measure at the right is where coastal *M. cardinalis* was repeatedly planted and died from winterkill. In the center is their F_1 hybrid showing marked vigor and the ability to withstand the freezing weather to a considerably higher degree than even the *M. lewisii* parent native to the Timberline area.

Plate 1B shows a small portion of the Timberline garden in 1967 in which the responses of three F_3 progenies were being tested. The row marked (1) is a planting of the offspring of the *lewisii*-like F_2 plant 7111-16, row (2) the offspring of the F_1-like plant 7111-17, and row (3) the offspring of the *cardinalis*-like F_2 plant 7135-35. Plate 1B was taken in 1967 two years after the cloned propagules were planted in the garden. At this time the F_3 progeny of the *lewisii*-like F_2 plant shown in row 1 were nearly all well established and vigorous, and most of the plants flowered. The F_3 progeny of the F_1-like F_2 plant 7111-17 were highly variable, ranging from weak to vigorous, with a high frequency of nonsurvivors. The F_3 progeny of the *cardinalis*-like plant 7135-35 were uniform and at that time had mostly survived, but all were later in seasonal development. Plate 1C was taken in the same garden a year later (1968). Here the plants in row 1, the offspring of the *lewisii*-like F_2 individual, are quite uniformly vigorous and starting to flower, those in row 2 from the F_1-like F_2 plant show extreme variability due to segregation, with only a small proportion of survivors, and those in row 3, the offspring of the *cardinalis*-like F_2, have all succumbed to winter-killing.

Genetic coherence. Earlier *Year Books* (*62,* pp. 387–391 and *63,* pp. 433–435) have reported evidence for partial genetic linkages between groups of marker characters that distinguish such species as *M. lewisii* and *M. cardinalis.* Such combinations of characters are inherited in second- and third-generation progenies in recombination frequencies that indicate that purely random assortment of such characters does not occur; parental combinations of characters tend to segregate together with greater frequency than would be predicted on the basis of free random recombination. That such characters also tend to be correlated with the responses and survival of individual plants at the transplant stations is now also fully evident. Extensive data from repeated crossings of both F_2 and F_3 progeny in *Mimulus* have been analyzed statistically with the help of an IBM 360/67 computer and clearly reveal the existence of such partial linkages. Although the observed recombinations of characters in the F_2 are always striking and spectacular, they are fewer than would be predicted on the basis of free random recombination. The expression of hybrid vigor, or heterosis, in first- and second-generation progeny in both inter- and intra-specific combinations in relation to the parental races is about as dependent on the environment in which it is observed (i.e., at the transplant stations) as upon the genetic constitution of the parents.

Physiological studies. The comparative study of species, races, and hybrids at the physiological and biochemical level as a means of probing further into mechanisms underlying natural selection requires the development of quite different techniques from those employed in the cytogenetic and transplant studies. It is, however, of enormous advantage to use the same cloned plant materials in comparative quantitative physiological studies from which a wealth of background information is available in order that the data from the various approaches can be effectively integrated. This does not, however, preclude the use of other species that may be valuable as reference points in comparative studies.

The physiological studies on *Mimulus* have centered on the study of the photosynthetic performance under a variety of controlled variables. These studies have led to ramifications that involve basic questions concerning the mechanism of some of the various steps in the photosynthetic process itself and how alterations in particular steps appear to affect the resultant performance of genetically distinct ecological races and species. Earlier *Year Books* have reviewed these developments, and current new findings are reported in the following pages. In the *Mimulus* monograph the physiological work will be reviewed to date, together with a report of preliminary studies on the culture of excised tissues under aseptic conditions as an aid in the comparative study of physiological and biochemical characteristics of ecological races and species.

Growth, Photosynthetic, and Biochemical Responses of Contrasting *Mimulus* Clones to Light Intensity and Temperature

Olle Björkman, Malcolm A. Nobs, and William M. Hiesey

In recent months we have concentrated on a study of two contrasting clones of *Mimulus* and their F_1 progeny. The parental clones, as shown by the transplant and genetic investigations, are among the most contrasting members of the Erythranthe section with respect to their growth and survival at the Stanford, Mather, and Timberline transplant stations, yet are genetically compatible and differ in a large number of conspicuous morphological characters. One clone, 7635-2, is a form of *M. lewisii* from Logan Pass, Glacier National Park, at an elevation of 2100 m, and the other is a clone of *M. cardinalis,* 7211-4, originally from the hot foothills of the Sierra Nevada of California at Jacksonville at an altitude of 250 m. The environments of the two races represent temperature extremes at which members of the Erythranthe section naturally occur.

Responses when grown under different light intensities. Figure 33 shows the mean dry weight increases in growth of the two clones over a 17-day experimental period when subjected to incident light intensities of 18,000, 53,000, and 106,000 ergs cm^{-2} sec^{-1}. In the experiment the daylength was 16 hours, and temperature was held constant at 21°C. The CO_2 and O_2 concentrations were those of normal air. The plants were grown in Perlite in plastic pots and were watered with Hoag-

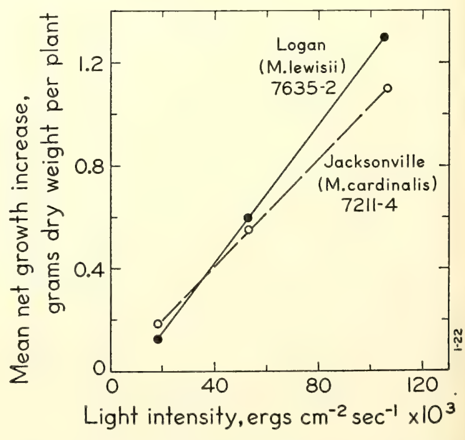

Fig. 33. Effect of light intensity on dry matter increase in the Logan and Jacksonville clones of *Mimulus.* Temperature was held constant at 20°C, and CO_2 concentration at 0.03%.

land's nutrient solution. The 17-day experimental period was considered long enough to provide a good measure of growth response to different light intensities, and short enough for growth to be exponential. As shown in Fig. 33 the growth rates of the two clones under these experimental conditions were directly proportional to the incident light intensity. The growth rate increase for *M. lewisii* with increasing light intensity was somewhat greater than for *M. cardinalis.*

The light-saturated photosynthetic rates of both clones when measured at 20°C both at concentrations of 21.0% and 1.5% of O_2 are generally higher as the light intensity during growth is increased, as shown in the upper part of Table 9. A significant difference between the two clones is evident, however, in their relative rates when grown under the intermediate intensity of 53,000 ergs cm^{-2} sec^{-1} as compared with the highest at 106,000 ergs cm^{-2} sec^{-1}. In Logan the increase in photosynthetic rate at the higher light intensity when measured in 21% O_2 is much smaller than in Jacksonville. The differences are even greater when the light-saturated photosynthetic rates are measured in 1.5% O_2. The rates measured on this Logan clone are higher than those observed on *M. lewisii* from Timberline, clone 7405-4 (*Year Book 65,* pp. 464–468). This suggests that considerable diversity exists within *M. lewisii* in light-saturated photosynthetic rates when measured under 21% O_2 present in normal air.

Anatomical sections of leaves of the two clones reveal parallel modifications in leaf thickness and in number of cell layers when grown under the three light intensities. Leaf thickness of both clones was approximately doubled when grown under the highest light intensity as compared with the lowest (i.e., at 106,000 versus 18,000 ergs cm^{-2} sec^{-1}). At the intermediate light intensity the leaves were of intermediate thickness. The leaves of the *M. lewisii* clone were about 25% thicker than those of *M. cardinalis* under any given intensity. The increase in leaf thickness as a result of increased light intensity is attributable to a greater number of cell layers in both the palisade and spongy parenchyma as well as to greater cell size.

It might be anticipated that the rate of light-saturated photosynthesis on the basis of leaf area should increase with increasing leaf thickness if the composition of biochemical components inside the leaves that determines the capacity

TABLE 9. Effect of Light Intensity During Growth on Subsequent Light-Saturated Rate of Photosynthesis, Carboxydismutase Activity, and Contents of Chlorophyll and Soluble Protein in the Leaves of Two *Mimulus* Clones

	Logan 7635-2			Jacksonville 7211-4		
Light Intensity for Growth, erg cm^{-2} sec^{-1} $\times 10^3$	18	53	106	18	53	106
Photosynthesis at 20°C and 0.03% CO_2, μmole CO_2 dm^{-2} min^{-1}						
In 21% O_2	6.6	11.0	12.4	4.1	8.8	12.9
In 1.5% O_2	8.8	17.9	17.2	5.6	13.0	18.7
Carboxydismutase Activity,[1] μmole CO_2 (g fresh wt.)$^{-1}$ min^{-1}	4.7	10.0	11.3	4.4	7.9	13.5
Chlorophyll $a + b$, mg (g fresh wt.)$^{-1}$	1.33	1.53	1.70	1.44	1.25	1.87
Soluble protein,[2] mg (g fresh wt.)$^{-1}$	9.3	20.6	20.7	8.2	15.9	25.1

[1] Assay conditions: 0.05 *M* $NaHCO_3$; 4×10^{-4} *M* ribulose-1,5-diphosphate; *p*H 8.0, 30°C.
[2] Protein was determined by the Folin-Lowry method.

for light-saturated photosynthesis remains constant. On the other hand, in normal air where photosynthesis is partially limited by CO_2 concentration, one might predict that light-saturated photosynthesis would not increase proportionally to leaf thickness because of the greater diffusion resistance to CO_2 in the thicker leaves. The actual experimental data reveal that photosynthesis increases faster as the leaves become thicker than would even be predicted on the basis of the first hypothesis. This result points to a third possibility, namely, that biochemical components inside the leaves that limit light-saturated photosynthesis have increased with increasing light intensity when computed on a fresh-weight or unit-volume basis.

The data presented in Table 9 support this conclusion. In both clones carboxydismutase activity is highly modified by the light intensity during growth; the higher activities occur in plants grown under the higher light intensities. The pattern of modification in the two contrasting clones differs in that Logan shows little increase in the activity of the enzyme when grown under the intermediate as compared with the highest light intensity, whereas the activity in Jacksonville in this step is approximately doubled. There is, thus, a good correlation between rate of photosynthesis at light saturation and the carboxydismutase activity. This is in agreement with the results obtained in this laboratory with other species (Björkman, 1968, a, b; Gauhl, this *Year Book*).

The chlorophyll content, expressed on a fresh weight basis in the leaves of both clones, generally increases with increasing light intensity during growth, but the increase is much smaller than that for carboxydismutase activity. This result is not surprising since the content of light-harvesting pigment would not be expected to have much influence on the rate of photosynthesis in the light-saturated state. The content of soluble protein, on the other hand, closely parallels the carboxydismutase activity and the photosynthetic rate in both clones. This suggests that the levels of enzymes other than carboxydismutase may also be modified in a similar manner by different light intensities during growth.

Responses to differences in temperature. The differential effects of the two temperatures, 10°C as compared with 30°C, on the growth of the *M. lewisii* clone 7635-2 (Logan) and the *M. cardinalis* clone 7211-4 (Jacksonville) are illustrated in Plate 2. The photographs shown were taken one month after comparable cuttings of each clone were placed in controlled cabinets and subjected to a light intensity of 53,000 ergs cm^{-2} sec^{-1} for 16-hour days, the temperatures being held constant at 10, 20, and 30°C day and night. The nonsurvival of the Logan clone at 30°C under these conditions, as compared with good growth and flowering of the Jacksonville clone, and, conversely, the more active growth of Logan at 10°C as compared with Jacksonville during the 30-day experimental period, is consistent with the very divergent responses of these two clones when grown at the Stanford, Mather, and Timberline transplant stations.

Propagules of the same two clones were subjected to the same experimental treatment and then harvested after a 15-day period before the Logan clone had succumbed at 30°C. This clone had then developed abortive precocious flowering stems having small green leaves. The average net increases in dry weights of the clones during this period are shown in Table 10. It can be seen that the increase in growth of the Jacksonville clone was 2.4 times greater at 30 than at 10°C, whereas in Logan the difference in increment of growth at these contrasting temperatures was approximately the same with a ratio of 0.9.

In view of the marked hybrid vigor observed at the altitudinal transplant stations in F_1 progeny between *M. lewisii* and *M. cardinalis* described in the pre-

TABLE 10. Effect of Temperature on Growth

Clone	Net Mean Dry Weight Increase in 15 Days, mg: Grown at 10°C	Grown at 30°C	Ratio, Growth at 30°C to Growth at 10°C
Logan 7635-2	139 ± 8.9*	126 ± 24.4	0.9
Jacksonville 7211-4	140 ± 7.0	337 ± 32.2	2.4
F_1 Logan 7635-2 × Jacksonville 7211-4	232 ± 14.7	277 ± 25.0	1.2

* Standard error of the mean.

ceding section, an experiment was conducted in which the growth of F_1 seedling progeny of the *M. lewisii* clone Logan 7635-2 and the *M. cardinalis* clone Jacksonville 7211-4 was compared with the growth of rooted cuttings of the parents at 10 and 30°C. The conditions of illumination and CO_2 and O_2 concentration were the same as in the preceding temperature experiments. Although the 14 seedling F_1 replicates grown at each temperature were fairly variable, their growth response at 30°C was intermediate between the parents, as shown by the mean net dry weight increases listed in Table 10. Evidence of hybrid vigor under the high temperatures is therefore lacking, but at 10°C the apparently greater growth of the hybrid over that of the parents may be significant.

Determinations of carboxydismutase activity, of the content of soluble protein, and of chlorophyll in the leaves were made on the Logan and Jacksonville clones grown at 10, 20, and 30°C. All determinations were made during the period when both clones were in active growth at all three temperatures. The results of these determinations are listed in Table 11.

In both clones the soluble protein content of the leaves was higher at 10 than at 20 or 30°C. This marked accumulation of soluble protein at low temperature is a point of interest for which no satisfactory explanation is at hand. In the Jacksonville clone where this accumulation is particularly great, there is no corresponding increase in carboxydismutase level. The activity of this enzyme is about the same regardless of whether the clone was grown at 10, 20, or 30°C.

In the Logan clone the carboxydismutase activity is about the same in leaves that have been grown at 10 and 20°C.

TABLE 11. Effect of Temperature During Growth on Subsequent Levels of Carboxydismutase, Chlorophyll and Soluble Protein in the Leaves of Two *Mimulus* Clones

	Logan 7635-2			Jacksonville 7211-4		
	Temperature During Growth					
	10°C	20°C	30°C	10°C	20°C	30°C
Carboxydismutase activity,[1] μmole CO_2 (g fresh wt.)$^{-1}$ min^{-1}	10.6	10.0	3.62	5.2	7.9	6.5
Chlorophyll $a + b$, mg (g fresh wt.)$^{-1}$	1.62	1.53	0.78	1.21	1.25	1.00
Soluble protein,[2] mg (g fresh wt.)$^{-1}$	26.2	20.0	13.9	39.9	15.9	16.3

[1] Assay conditions: 0.05 *M* $NaHCO_3$; 10^{-4} *M* ribulose-1,5-diphosphate; *p*H 8.0, 30°C.

[2] Protein was determined by the Folin-Lowry method.

The activity is considerably higher than in the Jacksonville clone. However, in the Logan clone growth at 30°C results in a very much reduced carboxydismutase activity. Similarly, the chlorophyll content of the leaves was much reduced at 30° as compared with 20° and 10°C in Logan whereas in Jacksonville the corresponding values were essentially the same at the three different temperatures. These results point to a breakdown of the photosynthetic apparatus in the Logan clone at 30°C, whereas there is no evidence of any detrimental effects of high temperature in the Jacksonville clone. We do not know whether the detrimental effects of high temperature in the Logan clone are primarily due to an intrinsically low degree of temperature stability of its photosynthetic apparatus, or whether processes responsible for the continuous synthesis of its components, such as photosynthetic pigments and enzymes, are adversely affected by high temperature so that the rate of their synthesis does not keep up with the rate of their breakdown.

Light-saturated photosynthesis in *Mimulus* and in many other higher plants as measured in air containing normal CO_2 and O_2 concentrations is often characterized by a comparatively small dependence on temperature in the range 15–30°C. This relatively weak effect of temperature on light-saturated photosynthesis has been generally interpreted to mean that photosynthesis is limited mainly by physical barriers to CO_2 diffusion since any process that is limited by enzyme activity would be expected to exhibit marked temperature dependence.

Newer evidence now indicates that the small effect of temperature on the photosynthetic rate as observed in normal air is largely due to the inhibiting effect of O_2 on photosynthetic CO_2 uptake. As shown in Fig. 34, the temperature dependence in both the Jacksonville and Logan clones is much greater in 1.5% than in 21.0%. These results are in close agreement with those obtained by Joliffe and Tregunna (1968) for wheat leaves, and by us with *Marchantia* (*Year Book 67*, pp. 479–482), but are at variance with those previously reported by us for *Mimulus* (*Year Book 66*, pp. 222–225).

In 1.5% O_2 and 0.03% CO_2 the Arrhenius equation is approximately valid for both the Logan and Jacksonville clones of *Mimulus* in the range 5–15°C. At the higher CO_2 concentration of

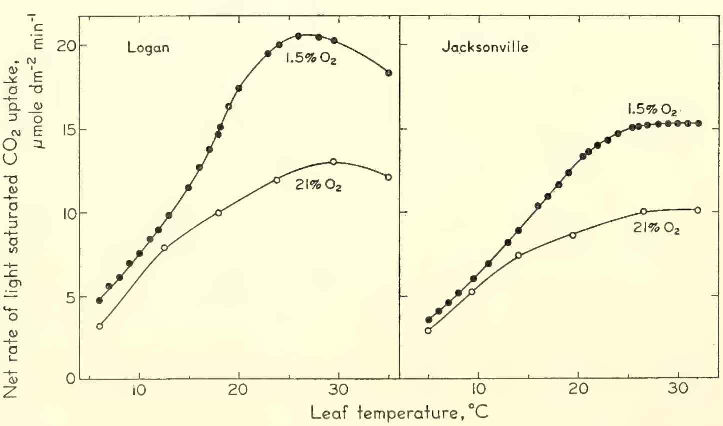

Fig. 34. Temperature dependence of light-saturated photosynthetic rate in the Logan and Jacksonville clones of *Mimulus* under 1.5% and 21.0% O_2. Measurements were made under saturating white light of 3.4×10^5 erg cm^{-2} sec^{-1} intensity (400–700 nm) from a 2.5 KW Xenon lamp and a CO_2 concentration of 0.030%.

0.07% a linear relationship between the logarithm of the photosynthetic rate and the inverse of absolute temperature is obtained up to at least 27°C (cf. this *Year Book,* Fig. 51). Energies of activation calculated from Arrhenius plots for the *Mimulus* clones yielded values of approximately 16 to 19 Kcal mol^{-1} equivalent to Q_{10} values of 2.7 to 3.3. These are comparatively high values for biological reactions.

It is of great interest that we have obtained very similar values for CO_2 fixation in vitro with partially purified preparations of carboxydismutase from both *Mimulus* and *Marchantia.* The close agreement between the activation energies for photosynthesis and the carboxylation reaction in vitro might, of course, be coincidental. On the other hand, it could reflect a causal relationship. A close agreement between measurements of the two processes would be expected if the activation energies for the carboxydismutase-catalyzed reaction in vitro is approximately the same as in vivo, and if the carboxylation reaction is a major limiting step of light-saturated photosynthetic rates at temperatures below 15°C.

No marked differences in activation energy for light-saturated photosynthesis were found between the Logan and the Jacksonville clones when both were previously grown at 20°C at a light intensity of 53,000 erg cm^{-2} sec^{-1} (400–700 nm). The main difference between the two is that Logan exhibits a higher rate of photosynthesis than Jacksonville at all temperatures in the range 5–30°C. Another difference is that in Logan the rate declines at temperatures above approximately 25°C, whereas in Jacksonville such a decline is not apparent until the temperature considerably exceeds 30°C.

A question of great importance is to what extent the temperature dependence of photosynthesis may be affected by the temperature under which the plants are previously grown. This problem was investigated on *Marchantia* last year (*Year Book 67,* pp. 479–482). The results of similar experiments using the Jacksonville clone 7211-4 of *Mimulus* are shown in Fig. 35. The dependence of the light-saturated rate of CO_2 uptake on temperature was determined on intact attached leaves of plants previously grown at 10, 20, and 30°C.

As is evident in Fig. 35, the rate of photosynthesis at 15°C and 1.5% O_2 was

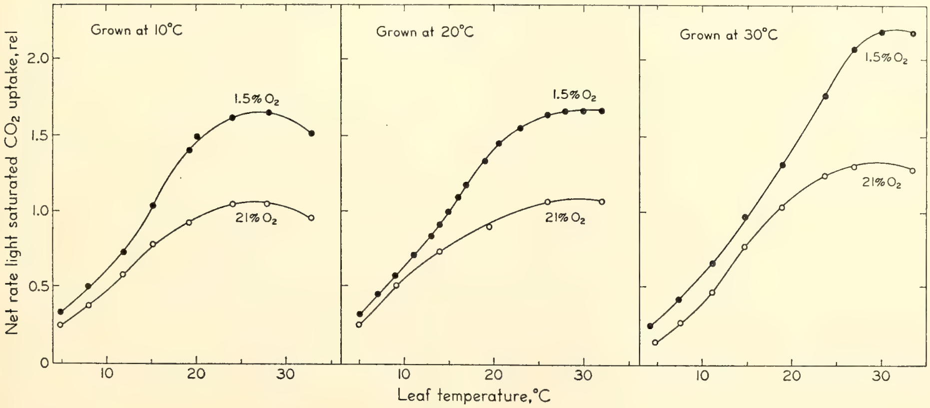

Fig. 35. Effect of temperature during growth on subsequent temperature dependence of light-saturated photosynthetic rates under 1.5% and 21.0% O_2 in the Jacksonville clone of *M. cardinalis.* Conditions for measurements were the same as in Fig. 34. The rate at 15°C in 1.5% O_2 was set to unity for each leaf.

little affected by the temperature under which the plants were grown. To facilitate direct comparisons of the temperature curves shown, the light-saturated photosynthetic rate as measured at 15°C and under 1.5% O_2 is plotted as equal to unity for each of the three clone-members previously grown at the three temperatures.

The temperature dependence of photosynthesis when measured under both 1.5% and 21.0% O_2 concentrations is very similar for leaves previously grown at 10 and 20°C. There is, however, a slight shift of the optimum toward lower temperatures in the clone-member grown at 10°C as compared with the one at 20°C. When grown at 30°C, a more pronounced change in the shape of the temperature curve takes place, with considerably higher light-saturated photosynthetic rates at the higher temperatures than in the clone-members grown at 10 or 20°C. This effect is evident in measurements made both in 21.0% and 1.5% O_2, but it is more pronounced at the lower O_2 concentration. This suggests that the modification in temperature dependence is not caused by changes in the rate of the processes underlying the inhibiting effect of O_2 (photorespiration). The activation energy from photosynthesis in the range 5–10°C is, nevertheless, not significantly affected by any of the three temperatures under which the Jacksonville clone of *M. cardinalis* was grown.

Conclusions. At this stage of our still incomplete understanding of the physiological and biochemical mechanisms that operate in higher plants, each increment of new experimental information changes our concepts of them. An example is our current interpretation of temperature dependence for light-saturated photosynthesis as a result of measurements made under low as compared with high O_2 concentration, discussed above.

It is evident that the two contrasting clones of *M. lewisii* and *M. cardinalis* differ markedly in both physiological and biochemical characteristics when studied under certain sets of controlled conditions. At the same time they possess many characteristics in common that are also shared by such unrelated plants as the liverwort *Marchantia.* The experimental techniques for exploring the physiological and biochemical basis of natural selection have now been developed to a point where new basic information is coming to light that needs further exploration and analysis before a satisfying understanding can be achieved.

References

Björkman, O., *Physiol. Plantarum, 21,* 1–10, 1968a.

Björkman, O., *Physiol. Plantarum, 21,* 84–99, 1968b.

Joliffe, P. A. and E. B. Tregunna, *Plant Physiology, 43,* 902–906, 1968.

Comparative Studies of *Atriplex* Species with and without β-Carboxylation Photosynthesis and their First-Generation Hybrid

Olle Björkman, Eckard Gauhl, and Malcolm A. Nobs

The recent discovery of a new CO_2 fixation pathway in photosynthetic organisms, first found to be operative in sugar-cane (Kortschak *et al.,* 1965; Hatch and Slack, 1966), has stimulated new interest in comparative studies of photosynthesis among higher plants. Several groups of investigators, particularly in Australia, Canada, and the United States, are currently studying the biochemistry of the new carboxylation pathway and its relation to photosynthetic characteristics and leaf structure. This pathway is commonly referred to as the C_4-dicarboxylic acid pathway since oxaloacetate, malate and aspartate are the first products of CO_2 fixation, or as β-carboxylation photosynthesis since it involves β-carboxylation of phospho(enol)pyruvate. Members of at least five different families of higher plants

belonging to both the monocotyledoneae and the dicotyledoneae (Hatch *et al.,* 1967; Johnson and Hatch, 1968) have been shown to possess this pathway. Within each of four different genera, including *Atriplex,* some species possess the pathway while others do not.

Of particularly great interest to those of us concerned with mechanisms of adaptation and natural selection in plants are the observations that (1) the β-carboxylation pathway seems to be mainly limited to taxonomic groups distributed mostly in tropical and subtropical regions, and (2) that plants which possess this pathway apparently have profoundly different photosynthetic characteristics than do plants in which it is absent. In the plants possessing β-carboxylation the compensation point for CO_2 exchange in air approaches zero, and illuminated leaves do not release CO_2 into CO_2-free air. Moreover, the strong inhibiting effect of oxygen on the rate of photosynthetic CO_2 uptake in normal air, which is a very widespread phenomenon among plants without the β-carboxylation pathway, is absent in plants having this pathway.

The finding that differentiation in carboxylation pathways exists among species within the same genus provides a unique opportunity for studying biochemical and physiological mechanisms of adaptation. Not only are such species a more favorable material for comparative work than plants of unrelated taxonomic groups, but also they may permit studies of the inheritance of the different photosynthetic pathways if the species have sufficient genetic compatibility to allow hybridization between them. In those cases where different carboxylation pathways have been found among species within a single genus heretofore, the species belonged to different subgenera and may not be sufficiently closely related to permit intercrossing.

In our own search for suitable experimental plants, we chose two species of the family *Chenopodiaceae, Atriplex patula* ssp. *hastata* and *A. rosea* L., both of which are very common in California. In their biosystematic work on North American species of *Atriplex,* Hall and Clements (1923) wrote: "The most closely related species (to *A. patula*) seem to be the *rosea* group. . . . There is no direct connection with any other group." Both species are annuals and are diploid with nine pairs of chromosomes.

A. patula L. is a common species in coastal marshes throughout North America with the possible exception of Mexico, and is widely distributed also in Europe and Asia. There is great morphological variation in this species, and many subspecies have been recognized; frequently these subspecies have morphological variation in this species, The *A. patula* material used in the present work was collected in a coastal salt marsh close to San Mateo Beach State Park, Pescadero, California, and was identified as ssp. *hastata* Hall and Clem. (=var. *hastata* Gray). It is a common plant in salt marshes along the Pacific coast of California, Oregon, and Washington.

A. rosea L. is a native of Eurasia with its main distribution from central Asia through southeastern Europe and the Orient. It is also common in major Mediterranean Islands as well as in Morocco and Egypt. The species is naturalized in western United States and is very abundant in semiarid places in the hot interior of the region, where it often occurs together with *A. semibaccata,* a naturalized introduction from Australia. In California *A. rosea* is a common plant in the interior valleys, but it occurs also in the southern part of the San Francisco Bay area where the present material was collected. Interestingly, both *A. patula* ssp. *hastata* and *A. rosea* are abundant in this area although also here the latter species occupies much drier locations than does the former.

Up to the present time species that have been found to possess β-carboxyla-

tion photosynthesis also possess a specialized leaf anatomy characterized by a layer of large chloroplast-containing cells which surround the vascular bundles. Whether or not this specialized leaf anatomy is essential for the functioning of β-carboxylation photosynthesis has not yet been established, but it is nevertheless a valuable characteristic in preliminary screening of species. Moser (1934) described almost 100 *Atriplex* species, many of which, including *A. rosea,* possess this specialized leaf structure, whereas others such as *A. patula* do not. This characterization of *A. rosea* and *A. patula* has recently been confirmed by Downton *et al.* (1969) and in this laboratory for our own material.

During the past year comparative studies of the two species' growth, as well as their biochemical and photosynthetic characteristics, have been made and are reported below. Concurrently we attempted to hybridize the two *Atriplex* species. This led to success only recently when F_1 hybrids between *A. rosea* and *A. patula* were obtained; some early results with these hybrids are included at the end of this report.

The plant material used in the comparative studies on biochemical and photosynthetic characteristics was grown in controlled growth cabinets under a light intensity of 1.1×10^5 erg cm^{-2} sec^{-1} (400–700 nm), a temperature of 25°C, and a photoperiod of 16h/day, except in the experiments summarized in Table 5 where the light intensity during growth was half of that given above. Young, mature leaves were used throughout the investigation. All photosynthesis measurements were made on single leaves attached to intact plants.

Activities of carboxylation enzymes. In plants with β-carboxylation photosynthesis, oxaloacetate, malate, and aspartate are the first products to be labeled when $^{14}CO_2$ is fed to photosynthesizing leaves. There is strong evidence that phospho(enol)pyruvate (PEP) serves as substrate in the carboxylation reaction. This is further supported by the finding that plants with β-carboxylation photosynthesis have very high activities of PEP carboxylase whereas plants lacking this pathway have low activity of this enzyme (Hatch *et al.*, 1967; Johnson and Hatch, 1968). As shown in Table 12, *A. rosea* has about 50 times higher PEP carboxylase activity than *A. patula.* The values are in excellent agreement with those reported by Hatch and co-workers for other species with and without β-carboxylation photosynthesis.

Although the activity of carboxydismutase is considerably higher in *A. patula* than in *A. rosea,* the values for the latter species are very much higher than those reported by Hatch and co-workers for other species with β-carboxylation. A comparison of carboxydismutase activity in species with β-carboxylation and species that lack this pathway revealed that the activity found in *A. rosea* is not unusually high in comparison with other β-carboxylation species; neither was there consistently lower

TABLE 12. Activity of PEP Carboxylase and Carboxydismutase in Extracts of *A. patula* and *A. rosea* *

Species	PEP Carboxylase Activity, μmol CO_2 per min per			Carboxydismutase Activity, μmol CO_2 per min per		
	Fresh Weight, g	Soluble Protein, mg	Chlorophyll, mg	Fresh Weight, g	Soluble Protein, mg	Chlorophyll, mg
A. patula	0.6	0.03	0.44	11.52	0.590	8.41
A. rosea	26.8	1.54	14.41	4.60	0.265	2.47

* Enzyme activities were measured at 30°C as described by Björkman and Gauhl (1969).

carboxydismutase activity in the species that have β-carboxylation photosynthesis as compared to those that lack it. *A. patula* is outstanding in that it has the highest activity of all species investigated. These results are summarized in Table 13 and a full account of the study is given elsewhere (Björkman and Gauhl, 1969).

Fractionation of total soluble leaf protein on Sephadex G-200 (see pp. 636–637, this *Year Book*) in two species with similar carboxydismutase activities and protein contents, one with β-carboxylation and one without, indicated that approximately half of the total soluble protein was located in the "fraction 1" protein peak in both species. Therefore, the presence of comparatively high carboxydismutase *activities* for species with β-carboxylation is apparently indicative of similarily high *concentrations* of this enzyme. Other experiments showed that it is unlikely that the great differences between the carboxydismutase levels obtained here and those reported by Hatch and co-workers are caused by differences in the light, or in the temperature regimes under which the plants were grown.

Experiments in which different grinding procedures were compared revealed that, while nearly complete cell breakage could readily be achieved with leaves of *A. patula* and other species without β-carboxylation, breakage of the thick-walled sheath cells surrounding the vascular bundles in *A. rosea* and other species with β-carboxylation proved quite difficult. Special measures were required to break these cells. The mesophyll cells of *A. rosea* leaves were, on the other hand, very easy to break. High carboxydismutase activity in leaf extracts of species with β-carboxylation was obtained only when a high degree of breakage of the bundle sheath cells had been achieved. Further experiments in which *A. rosea* leaves were subjected to progressively more vigorous grindings showed that carboxydismutase activity increased as an increasing fraction of the protein was released from the bundle sheath cells, indicating that the chloroplasts in these cells contain carboxydismutase levels similar to those present in the mesophyll cells of species without β-carboxylation photosynthesis. These results strongly suggest that, in *A. rosea* and other species with β-carboxylation, at least the bundle sheath cells are capable of CO_2 fixation via the reductive pentose-phosphate pathway.

PEP carboxylase activity in leaf extracts of *A. rosea* was, on the other hand, high even when only a minor fraction of the bundle sheath cells had been broken, and the activity did not increase with increased breakage of these cells. These results provide evidence that high PEP carboxylase levels are present in the mesophyll cells of *A. rosea*. Apparently, the bundle sheath cells contain little or no PEP carboxylase. This finding would indicate that the chloroplast-containing bundle sheath cells in plants with β-carboxylation photosyn-

TABLE 13. Carboxydismutase Activity in Species With and Without β-Carboxylation *

Species with β-carboxylation	Carboxy-dismutase Activity	Species without β-carboxylation	Carboxy-dismutase Activity
Distichlis spicata	3.6	*Elymus mollis*	4.1
Paspalum distichum	2.2	*Mimulus cardinalis*	5.2
Zea mays	2.3	*Solanum dulcamara*	3.7
Amaranthus edulis	2.0	*Plantago lanceolata*	3.0
Atriplex semibaccata	4.9	*Solidago spathulata*	4.5
Atriplex rosea	2.5	*Atriplex patula*	8.4

* Assay conditions were as described by Björkman and Gauhl (1969). Activity at 30°C is expressed in μmole CO_2 (mg chlorophyll)$^{-1}$ (min)$^{-1}$.

thesis are not responsible for the β-carboxylation of PEP. However, since PEP carboxylase seems to be rather unstable in crude enzyme preparations of *A. rosea* leaves, the results cannot be taken as conclusive evidence for the absence of PEP-carboxylase in bundle sheath cells.

These results appear to be consistent with the hypothesis that there are two consecutive carboxylation reactions in plants with β-carboxylation photosynthesis. In the first carboxylation, CO_2 reacts with PEP to form C_4-dicarboxylic acids, the reaction being catalyzed by PEP carboxylase. This newly formed carboxyl group might then be transferred to ribulose-1,5-diphosphate to form phosphoglyceric acid either by a "transcarboxylation," or the carboxyl group may be first decarboxylated to CO_2, which is then fixed in a conventional Calvin cycle carboxylation, mediated by carboxydismutase. If PEP carboxylase is indeed absent in the bundle sheath cells, then it seems likely that the first carboxylation occurs in the mesophyll cells, and the second occurs primarily in the bundle sheath cells.

Glycolate oxidase activity. There is considerable evidence to support the hypothesis that the inhibitory effect of O_2 on photosynthetic CO_2 uptake in higher plants without β-carboxylation photosynthesis is caused primarily by a reoxidation of photosynthetic products (that is, photorespiration), and that glycolate is a major component of the evolution of CO_2 by illuminated leaves in CO_2-free air. Previous studies in which it was found that the activity of glycolate oxidase was very much lower in species with β-carboxylation than in species lacking this pathway suggest that this enzyme is responsible for the evolution of CO_2 in the light (Tregunna, 1966; Oeser *et al.*, 1968). In later work where species of the dicotyledonous genera *Amaranthus* (Tolbert *et al.*, 1969) and *Atriplex* (Osmond, 1969) were included, the differences in glycolate oxidase activity between species with and those without β-carboxylation were much less pronounced although still considerable.

Table 14 shows the rates of O_2 uptake in leaf homogenates of *A. patula* and *A. rosea* in the presence and in the absence of glycolate. Evidently, the activity of glycolate oxidase in *A. rosea* is about two-thirds as high as that found in *A. patula.* The true values for *A. rosea* may possibly be even higher than shown here since the breakage of the vascular bundle sheath cells was not quite complete. As with carboxydismutase, high activities of glycolate oxidase in *A. rosea* extracts were obtained only when good breakage of bundle sheath cells had been achieved.

In view of the high glycolate oxidase activity in *A. rosea* extracts, it appears unlikely that the absence of an effect of O_2 concentration on photosynthetic CO_2 uptake, and of other characteristics commonly attributed to photorespiration, can be explained by differences in the activity of glycolate oxidase.

CO_2 compensation point for photosynthesis. The CO_2 compensation point (the CO_2 concentration at which the rates of CO_2 fixation and production are equal) is known to be close to zero at O_2 concentrations of less than one or two percent, and to increase linearly with increased O_2 concentration in species without β-carboxylation photosynthesis. In species with β-carboxylation, however, the CO_2 compensation point remains very low regardless of the O_2 concentration. As shown in Fig. 36, the response in *A. patula* is typical of species without

TABLE 14. Glycolate Oxidase Activity at 21°C and *p*H 8.0 in Leaf Homogenates of *A. patula* and *A. rosea* *

Species	Addition	Oxygen Uptake nmol min^{-1} (mg chlorophyll)$^{-1}$
Atriplex patula	None	30
Atriplex patula	Glycolate	200
Atriplex rosea	None	40
Atriplex rosea	Glycolate	150

* Glycolate concentration was 0.01 *M*.

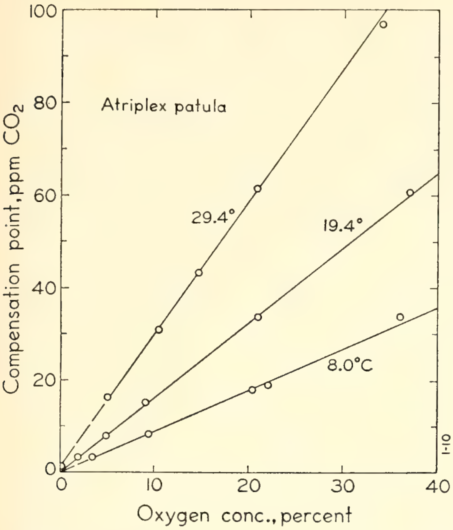

Fig. 36. Effect of O_2 concentration on CO_2 compensation point for photosynthesis in 21% O_2 in *A. patula* at three different leaf temperatures. Light intensity was 1.0×10^5 erg cm^{-2} sec^{-1} (400–700 nm).

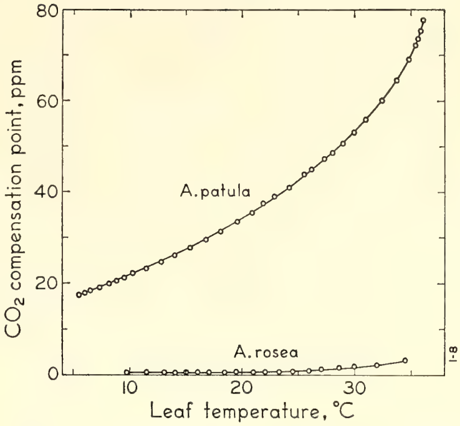

Fig. 37. Temperature dependence of CO_2 compensation point for photosynthesis in 21% O_2 in *A. patula* and *A. rosea*. Light intensity was 1.0×10^5 erg cm^{-2} sec^{-1} (400–700 nm).

β-carboxylation. The compensation point is strongly dependent on temperature, but at any given temperature the compensation point is directly and linearly related to O_2 concentration. In *A. rosea* the compensation point is less than a few ppm CO_2 at all O_2 concentrations in the range 0–40%, a response characteristic of species with β-carboxylation photosynthesis.

The differential response between the two *Atriplex* species with regard to the CO_2 compensation point is further illustrated in Fig. 37 where the compensation point in 21% O_2 is plotted as a function of leaf temperature. In *A. patula* the compensation point increases exponentially with increasing leaf temperature, whereas in *A. rosea* it remains very low throughout the entire temperature range from 5 to 36°C. Incidentally, even though the compensation point is not in itself a rate, the data given in Fig. 37 for *A. patula* yield a nearly straight line in an Arrhenius plot. The "activation energy" derived from such a plot is equal to approximately 7600 calories ($Q_{10} = 1.56$).

Transient changes in photosynthetic rate following changes in light intensity. Fig. 38 illustrates the time-course of photosynthetic CO_2 uptake by *A. patula* and *A. rosea* leaves in response to a sudden decrease in light intensity under 1% and 21% O_2. In *A. patula* the steady-state rates at both the higher and the lower light intensities are about 50% greater in 1% than in 21% O_2, whereas in *A. rosea* the rates are unaffected by O_2 concentration. Under 21% O_2 *A. patula* leaves show a pronounced "undershoot" in the rate of CO_2 uptake when light intensity is suddenly decreased, a phenomenon which is presumably closely related to the "post-illuminative burst" of CO_2 evolution that takes place in higher plants without β-carboxylation photosynthesis. Under 1% O_2 these effects are absent. In corn, a species with β-carboxylation, the transient effects are absent under both 1% and 21% O_2 (*Year Book 66*, pp. 224–227).

These results are consistent with the hypothesis that the effects reflect the temporary continuation of a process leading to CO_2 production which occurs in the previous steady-state, in plants

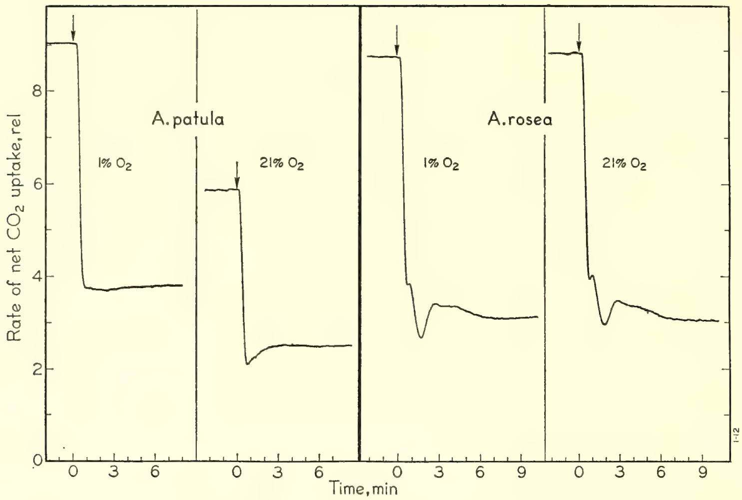

Fig. 38. Time-course of photosynthetic CO_2 uptake in 1% and 21% O_2 by *A. patula* and *A. rosea* leaves following a sudden decrease in light intensity. Arrows indicate the time at which light intensity was reduced from 2×10^5 to 5×10^4 erg cm^{-2} sec^{-1} (400–700 nm). Leaf temperature was 25°C, and CO_2 concentration 0.030–0.033%.

without β-carboxylation photosynthesis. However, as shown in Fig. 38, a complex transient change in the rate of CO_2 uptake occurs in *A. rosea* leaves after the light intensity is suddenly reduced. This effect is absent in corn, but a similar effect was found to be present in another species with β-carboxylation, namely, *Amaranthus edulis* (*loc. cit.*). The transient effect in *A. rosea* and *Amaranthus* is an interesting phenomenon for which no explanation is at hand. Its presence in both 1% O_2 and 21% O_2 suggests that it may be related to a different process than the effect observed in species without β-carboxylation in 21% O_2.

Effect of O_2 concentration on the light-saturated photosynthetic rate and on the resistance to gas diffusion. At constant temperature, CO_2 concentration and CO_2 uptake decrease continuously in *A. patula* with increasing O_2 concentrations in the range of 1–21%, whereas the rate is little affected in *A. rosea* (Fig. 39). It is of considerable importance to know whether or not this higher rate of light-saturated photosynthesis in *A. patula* in low O_2 concentration is accompanied by a lower resistance to CO_2 diffusion from the ambient atmosphere into the leaf. If, as is often assumed, the light-saturated rate of photosynthesis in air of normal CO_2 and O_2 concentration

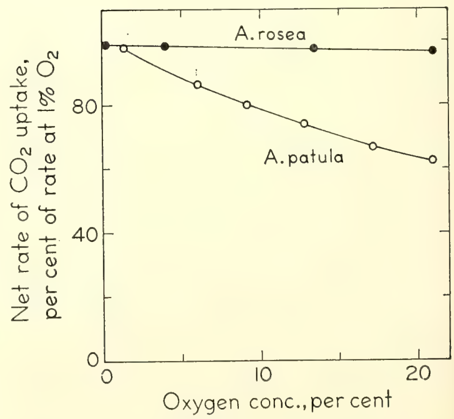

Fig. 39. Effect of O_2 concentration on light-saturated rate of photosynthetic CO_2 uptake in *A. patula* and *A. rosea*. Light intensity was 4×10^5 and 6×10^5 erg cm^{-2} sec^{-1} (400-700 nm) with *A. patula* and *A. rosea*, respectively. Leaf temperature was 25°C, and CO_2 concentration 0.030–0.032%.

is limited mainly by physical resistance to gas diffusion, then a marked increase in the photosynthetic rate due to a decreased O_2 concentration could not occur without a concomitant decrease in diffusion resistance.

Of the various component physical resistances to gas diffusion, only the one imposed by the stomata can be expected to be influenced by changes in the gaseous composition of the atmosphere. Since any changes in stomatal resistance that would affect the diffusion of CO_2 would also affect the rate of the diffusion of water vapor from the leaf, the influence of O_2 concentration on resistance to CO_2 diffusion can be followed by measuring the rate of transpiration. Simultaneous measurements of CO_2 uptake and transpiration were therefore made at different O_2 concentrations on *A. patula* and *A. rosea* leaves. Some of the results of these measurements are presented in Table 15. A full account of this work is given elsewhere (Gauhl and Björkman, 1969).

The results clearly show that resistance to CO_2 diffusion in the gas phase is not significantly influenced by O_2 concentration in leaves of either *A. patula* or *A. rosea* in spite of the fact that the rate of light-saturated CO_2 uptake in the former species is enhanced by approximately 50% when the O_2 concentration is reduced from the normal 21% to 1.5%. It can be concluded, therefore, that at least in *A. patula* the rate of light-saturated photosynthesis in normal air is not limited primarily by physical resistance to gas diffusion even at the

TABLE 15. Effect of O_2 Concentration on the Rates of CO_2 Uptake and Water Vapor Release by *A. patula* and *A. rosea* Leaves *

Species	CO_2 Uptake, μmole cm^{-2} min^{-1}		Water Vapor Release, mg dm^{-2} min^{-1}	
	21% O_2	1.5% O_2	21% O_2	1.5% O_2
A. patula	12.3	18.7	51.6	51.6
A. rosea	21.2	21.9	48.0	48.0

* Measurements were made under saturating white light, and 0.031–0.032% CO_2 at 26°C.

comparatively high temperature of 25°C (see p. 634, this *Year Book*).

Other experiments in which the rate of transpiration in the two *Atriplex* species was measured at 6 different O_2 concentrations gave no evidence of any effect of O_2 concentration on stomatal diffusion resistance. The resistance of the stomata to water vapor transfer varied from 1.0 to 1.4 sec cm^{-1} with *A. patula* and from 1.1 to 1.3 sec cm^{-1} for *A. rosea*. Thus, there is no significant difference in resistance to water loss between the two species when they are grown and kept under conditions of ample water supply. This does not, of course, preclude the possibility that the two species may differ in their transpiration rates under water stress. Since under low O_2 concentration the light-saturated rate of photosynthesis is similar in the two *Atriplex* species, there is no intrinsic difference in the ratio of photosynthesis to transpiration. However, because of the strong inhibiting effect of 21% O_2 on photosynthesis in *A. patula*, but not in *A. rosea*, the efficiency of photosynthesis in normal air in terms of water loss is greater in the latter species.

Temperature dependence of light-saturated photosynthesis. There are several reports that species which possess β-carboxylation photosynthesis have higher optimum temperatures for photosynthesis in normal air than plants that lack this pathway. Figs. 40 and 41 show the temperature dependence for photosynthetic CO_2 uptake at a high light intensity of 3.5×10^5 erg cm^{-2} sec^{-1} (400–700 nm) for *A. patula* and *A. rosea*, respectively. This light is not fully saturating for *A. rosea* at high temperatures (Fig. 43). The curve for *A. rosea* was determined in 21% O_2, but since the rate of photosynthesis in this species is unaffected by O_2 concentration in the range from 6 to 38°C, the curve is also valid for low O_2 concentrations.

The temperature dependence of light-saturated photosynthesis in *A. patula* is markedly affected by O_2. As was also

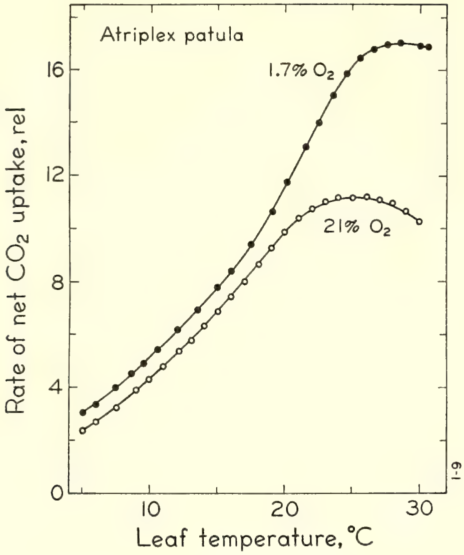

Fig. 40. Temperature dependence of the rate of photosynthetic CO_2 uptake in 1.7% and 21% O_2 by an *A. patula* leaf. Light intensity was 3.5×10^5 erg cm^{-2} sec^{-1} (400–700 nm) and CO_2 concentration 0.032–0.035%.

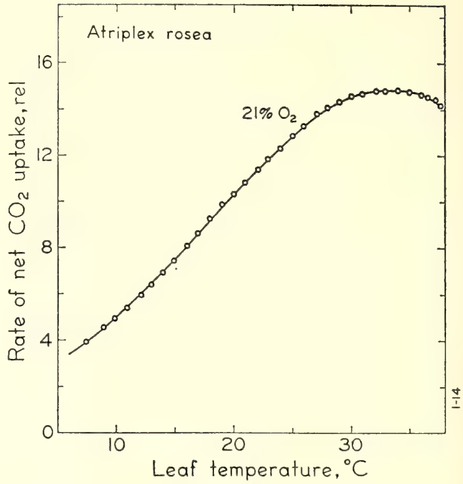

Fig. 41. Temperature dependence of the rate of photosynthetic CO_2 uptake in 21% O_2 by an *A. rosea* leaf. Light intensity was 4.3×10^5 erg cm^{-2} sec^{-1} (400–700 nm) and CO_2 concentration 0.031–0.034%.

found with *M. cardinalis* (see p. 618, this *Year Book*), the inhibitory effect of O_2 increases with increasing temperature. (It should be noted, however, that the *light-limited* rate of CO_2 uptake in both *A. patula* and *Mimulus* is markedly inhibited by 21% O_2 at both high and low temperatures; see *Year Book 67*, p. 482). A comparison of the rates of CO_2 uptake by the two *Atriplex* species in strong light and normal air shows that in *A. rosea* the rate is more temperature dependent in the upper range. This is consistent with previously reported differences between unrelated species with and without β-carboxylation photosynthesis. However, the temperature dependence is remarkably similar in the two *Atriplex* species when the O_2 concentration is kept at a low level, particularly in the low temperature range where the Arrhenius equation is approximately valid. In this range the activation energy is high, and no significant differences in activation energy are apparent between the two species.

These results fail to support the hypothesis that the differences in photosynthetic response to temperature between species with and without β-carboxylation are indicative of different temperature characteristics of the carboxylation enzymes. They rather suggest that the rate-limiting step is either the same in the two species, or, if different steps are limiting, these have approximately the same energies of activation. It is tempting to speculate that carboxydismutase may be a rate-limiting enzyme in both species at low temperatures (*cf.* p. 619, this *Year Book*).

CO_2 dependence of light-saturated photosynthesis. The response of light-saturated photosynthesis to CO_2 concentrations in the two *Atriplex* species is of special interest in view of the presence of high PEP carboxylase activities in *A. rosea* but not in *A. patula.* PEP carboxylase has been reported to have a much higher affinity for CO_2 ($K_m \sim 10^{-4}$ *M*) than carboxydismutase ($K_m \sim 10^{-2}$ *M*). If these different affinities in vitro result in differences in CO_2 depend-

ence of photosynthesis between the two species, then such differences should be apparent under low O_2. Comparisons of the CO_2 dependence of photosynthesis in the two species when in 21% O_2 are complicated by the inhibiting effect of O_2, particularly since the degree of the inhibition by O_2 increased with decreasing CO_2 concentration.

Figure 42 depicts the CO_2 dependence of photosynthetic O_2 evolution under 0.15% O_2 in the two species. The measurements were made as described on pages 637–638. The response to CO_2 concentration is very similar in *A. patula* and *A. rosea,* with half of the maximum rate being reached at approximately 0.02% CO_2 in both species. The somewhat earlier saturation in *A. rosea* in comparison with *A. patula* may possibly be significant. However, at the light intensity used (4×10^5 erg cm^{-2} sec^{-1}; 400–700 nm) photosynthesis in *A. patula* is light saturated under all CO_2 concentrations, but it is not fully saturated at the highest CO_2 concentrations in *A. rosea.* This may have resulted in a somewhat lower CO_2 saturation in the latter species. The results thus indicate that the two *Atriplex* species do not differ markedly in their photosynthetic response to CO_2 concentration when reoxidation of photosynthetic products in the light is suppressed by keeping the leaves at a low O_2 concentration.

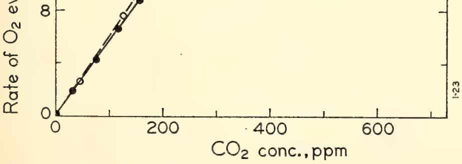

Fig. 42. Dependence of CO_2 concentration on the rate of photosynthetic O_2 evolution by *A. patula* and *A. rosea* leaves in 0.15% O_2. CO_2 concentration is given as the mean of the concentrations of the gas entering and that leaving the leaf chamber. Light intensity was 3.7×10^5 erg cm^{-2} sec^{-1} (400–700 nm) and leaf temperature 26°C. Photosynthesis measurements were made with the device described on pp. 636–640.

The saturation of photosynthesis at low CO_2 concentrations in *A. patula* appears to be inconsistent with the high K_m-values that have been reported for carboxydismutase. However, recent work (Cooper *et al.,* 1969) provides evidence that carboxydismutase cannot utilize bicarbonate, and that only CO_2 itself can serve as substrate for the enzyme. At the *p*H used for the determination of the K_m, the concentration of CO_2 is only on the order of one percent of the total "CO_2" added to the reaction mixture. If the K_m is recalculated for CO_2, it becomes 100 times lower than the value based on total "CO_2". The differences in the K_m-values between PEP carboxylase and carboxydismutase based on total "CO_2" may, therefore, not be relevant to photosynthetic CO_2 fixation.

Dependence of photosynthesis on light intensity. It is well known that unusually high light intensities are required to saturate photosynthesis in corn and certain other species recently found to possess β-carboxylation photosynthesis. As shown in Fig. 43 this is also true for *A. rosea.* Complete light saturation is not reached even at light intensities equal to full sunlight (approximately 5×10^5 erg cm^{-2} sec^{-1}, 400–700 nm) in this species whereas in *A. patula* light saturation is essentially reached at about half this intensity. In normal air (21% O_2, 0.032% CO_2) the rate at high light intensities is considerably higher in *A. rosea* than in *A. patula,* but at low light intensities the rates are approximately equal.

Since the degree of enhancement of photosynthesis that takes place in *A. patula* when O_2 concentration is lowered is approximately the same at all light intensities, and since no enhancement

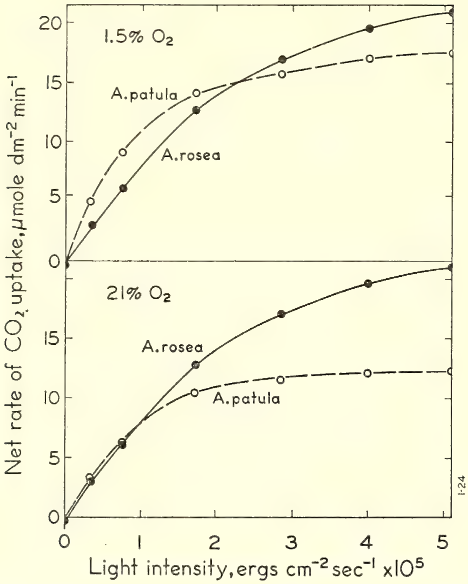

Fig. 43. Effect of light intensity on the rate of photosynthetic CO_2 uptake in 1.5% and 21% O_2 by *A. patula* and *A. rosea* leaves. Leaf temperature was 25°C and CO_2 concentration 0.030–0.034%.

at all occurs in *A. rosea,* the former species becomes more efficient in utilizing light of low intensities than *A. rosea* under 1.5% O_2. These results suggest that the quantum yield for CO_2 uptake under low O_2 is higher in *A. patula* than in *A. rosea.*

Experiments in which light-limited rates of CO_2 uptake of the two species were measured in monochromatic light (at 665 nm) provided further evidence that this is indeed the case. As shown in Fig. 44 the quantum requirement for CO_2 uptake under low O_2 concentration is 35–40% higher in *A. rosea* than in *A. patula.* This indicates that β-carboxylation photosynthesis may be intrinsically less efficient than conventional photosynthesis in terms of the amount of CO_2 reduced to carbohydrate per amount of energy expended. This would be the case if β-carboxylation photosynthesis requires more ATP or $NADPH_2$ for each CO_2 fixed.

If this is true the main advantage of

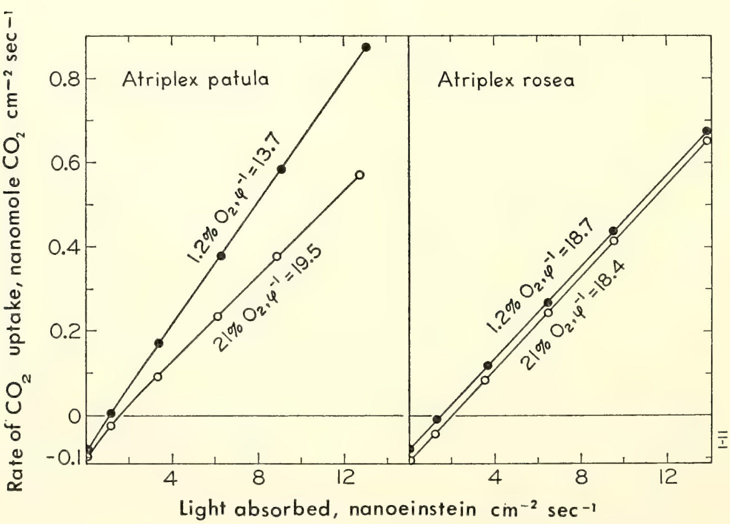

Fig. 44. Light-limited rate of photosynthesis of *A. patula* and *A. rosea* leaves in 1.2% and 21% O_2 as a function of light intensity in nanoeinstein sec^{-1} absorbed by each cm^2 leaf area. Quantum requirement (ϕ^{-1}) is expressed in einstein per mole CO_2. CO_2 uptake was measured at 665 nm (half-band width, 12 nm), 25°C, and 0.031–0.032% CO_2. Leaf absorptance (measured in an Ulbricht integrating sphere) was 86% and 89% at 665 nm for *A. patula* and *A. rosea,* respectively.

β-carboxylation photosynthesis appears to be the conservation of carbon under high levels of irradiance and high temperatures. Under saturating light intensities the supply of chemical energy would not be expected to be limiting and, therefore, a higher ATP or $NADPH_2$ requirement than in conventional photosynthesis would have no effect on the light-saturated rate of CO_2 uptake. It should be remembered, however, that photosynthesis in species with β-carboxylation is not completely light-saturated even in full sunlight, and consequently the rate of CO_2 uptake in such plants in natural habitats will always be partially dependent on the supply of chemical energy. Under low light intensities the benefits gained by eliminating the inhibitory effect of O_2 in plants with β-carboxylation photosynthesis would be counteracted by the greater requirement for chemical energy. This is consistent with the finding that the quantum requirement for CO_2 uptake is approximately the same for the two *Atriplex* species in normal air (Fig. 44). Comparative measurements of light-limited rates of photosynthesis in other species should reveal whether or not the higher quantum requirement of *A. rosea* in comparison with *A. patula* under low O_2 concentration is indeed attributable to β-carboxylation photosynthesis *per se.*

Growth responses. Our comparative studies on the photosynthetic characteristics of the two *Atriplex* species demonstrate that in normal air under conditions of high light intensity and high temperature *A. rosea* is capable of considerably higher rates of photosynthetic CO_2 uptake than *A. patula*. The differences between the two species decreased with decreasing light intensity and decreasing temperature, and disappeared at rate-limiting light intensities. A question of considerable interest is whether or not these differences in photosynthetic performance are reflected in growth.

Preliminary experiments in which the two *Atriplex* species were grown at different light intensities indicate that *A. rosea* requires higher light intensities for maximum growth than *A. patula.* Nevertheless, both species grow slowly at low light intensity (1.5×10^4 erg cm^{-2} sec^{-1}, 400–700 nm) and must be considered to be sun species.

When the two *Atriplex* species were grown under a light intensity of 1.1×10^5 erg cm^{-2} sec^{-1}, the optimum temperature for growth was in the range 20–25°C for *A. patula* and 25–30°C for *A. rosea.* The growth rate of *A. rosea* was much greater at 30 than at 15°C, whereas there was no marked difference in growth at these two temperatures with *A. patula.* At 38°C *A. patula* grew poorly, whereas *A. rosea* grew considerably better at this temperature than at 15°C.

The differences that exist between the two *Atriplex* species in response of growth to different light intensities and temperatures thus seem consistent with differences in photosynthetic characteristics. Comparative growth experiments at high temperatures and different oxygen concentrations might provide further information on the causal relationship that appears to exist between growth response and photosynthetic characteristics that distinguish plants with and without β-carboxylation photosynthesis. Such growth experiments are planned.

Characteristics of F_1 hybrids: A. rosea $\times$ A patula. As mentioned earlier, attempts to hybridize the two *Atriplex* species were successful only very recently, and only by using *A. rosea* as the female parent. The hybrid material is currently being subjected to intensive investigation with regard to biochemistry, leaf anatomy, and cytogenetics. Some early results are reported here.

Like both of the parents, the F_1 hybrids are diploid, and are highly uniform in appearance, having intermediate morphology and growth habit. As shown in Fig. 45, leaf shape and size are clearly intermediate. This is also true of the

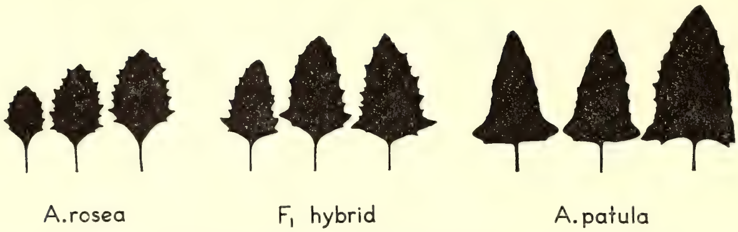

Fig. 45. Comparison of the leaf shape of the F_1 hybrid, *A. rosea* × *A. patula,* with the leaf shape of the parents.

betacyanin content in the lower leaf epidermis; in *A. rosea* the betacyanin is very prominent, whereas it is absent in *A. patula.*

Examination of leaf sections with the light microscope revealed that the general leaf anatomy of the F_1 hybrid is also roughly intermediate between the parents. The mesophyll of the hybrid leaves resembles that of *A. patula,* but the palisade cells are less densely packed. There is also a greater density of chloroplasts in cells around vascular bundles in the hybrid than in *A. patula,* but the large thick-walled bundle sheath cells, characteristic of *A. rosea* and many other species with β-carboxylation photosynthesis, are absent. Cell and chloroplast ultrastructure of the hybrid in comparison with the parental species is now being studied in this laboratory by Dr. John Boynton.

The data presented in Table 16 show clearly that the F_1 hybrid is definitely *not* intermediate between the parental species with regard to photosynthetic characteristics. Photosynthesis is strongly affected by O_2 concentration in the F_1 hybrid, apparently even more so than in *A. patula,* the male parent. The rate of photosynthesis in the F_1 hybrid is lower than in either parent under 21% O_2.

The activity of carboxydismutase in the F_1 hybrid is only about half of that in *A. patula,* but higher than in *A. rosea.* PEP carboxylase activity in the F_1 hybrid is only about one-tenth of the activity present in *A. rosea,* the female parent, even though it may be slightly higher than in *A. patula.* The chlorophyll content of the leaves, which is about the same in both parental species, is about one-third lower in the hybrid.

These results demonstrate that, in

TABLE 16. Some Photosynthetic and Biochemical Characteristics of the F_1-Hybrid Between *A. rosea* and *A. patula* in Comparison with the Parental Species *

Species	Photosynthesis Rate		Enhancement in 1.5% O_2, %	PEP Carboxylase Activity	Carboxydismutase Activity
	1.5% O_2	21% O_2			
A. rosea	3.8	3.8	0	14.7	3.4
A. rosea × *A. patula* F_1	4.1	2.4	69	1.4	5.1
A. patula	6.0	4.1	48	0.8	9.6

* Photosynthetic rates as well as enzyme activities are expressed in μmole CO_2 min^{-1} (g fresh wt.)$^{-1}$. Photosynthesis was measured in white light of an intensity of 1×10^5 erg cm^{-2} sec^{-1} (400–700 nm), at a leaf temperature of 25°C, and a CO_2 concentration of 0.032–0.034%. Enzyme assays were made at 30°C; other conditions were as described by Björkman and Gauhl (1969). The plants were grown at a light intensity of 5.5×10^4 erg cm^{-2} sec^{-1} (400–700 nm).

Atriplex, photosynthetic and biochemical characteristics associated with β-carboxylation photosynthesis are not transmitted simply by the plastids from the female parent to the progeny. Instead, inheritance of these characteristics appears to be predominantly under nuclear control. The results further suggest that the number of genes that govern the processes underlying β-carboxylation photosynthesis, and the absence of an inhibitory effect of oxygen on CO_2 uptake, may be small.

Attempts are currently being made to obtain second-generation progeny from the F_1 hybrids. If these attempts are successful, it may be possible to find out which of the several correlated characteristics, physiological, biochemical, and anatomical, are essential to photosynthetic function in plants with β-carboxylation photosynthesis, as well as to analyze genetically the inheritance of these characteristics. This could greatly enlighten our understanding of the physiological and molecular mechanisms of adaptive differentiation and natural selection in plants.

References

Björkman, O., and E. Gauhl, *Planta, 88,* 197–203, 1969.

Cooper, T. G., D. Filmer, Marcia Wishnick, and M. D. Lane, *J. Biol. Chem., 244,* 1081–1083, 1969.

Downton, J., T. Bisalputra, and E. G. Tregunna, *Can. J. Botany,* in press, 1969.

Gauhl, E., and O. Björkman, *Planta, 88,* 187–191, 1969.

Hall, H. M., and F. E. Clements, *The Phylogenetic Method in Taxonomy; The North American Species of Artemisia, Chrysothamnus, and Atriplex,* Carnegie Inst. of Wash. Publ. 326, Washington, D. C., 1923.

Hatch, M. D., and C. R. Slack, *Biochem. J., 101,* 103–111, 1966.

Hatch, M. D., C. R. Slack, and H. S. Johnson, *Biochem. J., 102,* 417–422, 1967.

Johnson, H. S., and M. D. Hatch, *Phytochem., 7,* 375–380, 1968.

Kortschak, H. P., C. E. Hartt, and G. O. Burr, *Plant Physiol., 40,* 209–213, 1965.

Moser, H., *Beih. Bot. Zentr., 52,* 378–388, 1934.

Oeser, A., N. E. Tolbert, R. H. Hageman, R. K. Yamazaki, and T. Kisaki, *Plant Physiol. Abstr.,* 5–12, 1968.

Osmond, C. B., *Biochim. Biophys. Acta, 172,* 144–149, 1969.

Tolbert, N. E., A. Oeser, R. K. Yamasaki, R. H. Hageman, and T. Kisaki, *Plant Physiol., 44,* 135–147, 1969.

Tregunna, E. B., *Science, 151,* 1239–1241, 1966.

Leaf Factors Affecting the Rate of Light-Saturated Photosynthesis in Ecotypes of *Solanum dulcamara*

Eckard Gauhl

As reported last year (*Year Book 67,* pp. 482–488), clones of *Solanum dulcamara* L. from sunny and shaded habitats show marked differences in their response to light intensity during growth. When propagules of clone Mb 1, originally from a densely shaded habitat in a reed-grass marsh near Mönchbruch, Germany, were grown under a low light intensity of 24×10^3 erg cm^{-2} sec^{-1} (400–700 nm) and subsequently exposed to a high intensity of 11×10^4 erg cm^{-2} sec^{-1}, the leaves showed evidence of photoinhibition. After a few days under the higher light intensity the quantum efficiency of photosynthesis was markedly reduced. No such detrimental effect was detected in leaves of clone Fe 2, which originated from a sunny habitat on an open sand dune on Fehmarn Island in the Baltic Sea. Fully mature leaves of this clone show a considerable increase in light-saturated photosynthetic rate after transfer to a high light intensity. More recent work revealed that when leaves of the clone from the shaded habitat are subjected to prolonged exposure to high light intensities, not only light-limited rates but also the light-saturated rate of photosynthesis is reduced, as shown in Fig. 46.

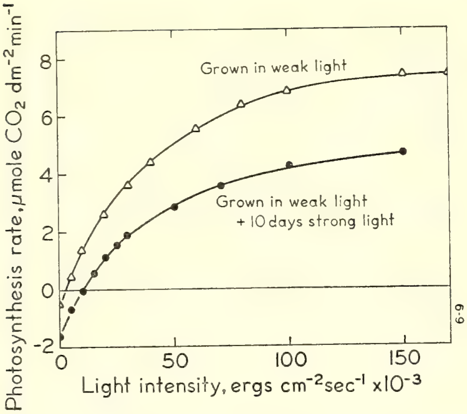

Fig. 46. Rate of CO_2 uptake as a function of light intensity for a leaf of *Solanum dulcamara,* clone Mb 1, grown in weak light and after exposure to strong light for 10 days.

The light-saturated rate of apparent photosynthesis in normal air may be limited by physical resistances to gas diffusion as well as by the capacities of enzymatic reactions. It is also affected by the rate of reoxidation of photosynthetic products with O_2 (photorespiration). An attempt was made to determine which of these factors are of greatest importance in determining (1) the decline in photosynthesis when leaves of the shaded habitat clone are transferred from a low to a high light intensity and, conversely, (2) the increase in photosynthesis that takes place when leaves of the sunny habitat clone are transferred from a low to a high light intensity.

Diffusion resistance and O_2 effect. To determine whether the changes in the rates of photosynthesis of the *Solanum* ecotypes are caused simply by changes in physical diffusion resistances, simultaneous measurements of CO_2 uptake and transpiration were made with the method described by Gauhl and Björkman (1969). When the transpiration rate is known, the resistance against the transfer of water vapor from the surface of the mesophyll cells to the ambient atmosphere (R_w) can be calculated. This resistance includes the resistance to gas diffusion through the stomatal openings and that of the external boundary layer. Photosynthetic CO_2 uptake involves these same resistances and an additional resistance due to the diffusion of CO_2 in the liquid phase from the mesophyll cell walls to the carboxylation sites in the chloroplasts.

Of these three resistances, only the stomatal diffusion resistance can be expected to be influenced by changes in the gaseous composition of the ambient atmosphere. Since it is well established that the rate of CO_2 uptake of many plants, including *S. dulcamara,* is enhanced when the oxygen concentration surrounding the leaf is reduced from 21% to a lower level, photosynthesis and transpiration were measured simultaneously under alternate O_2 concentrations of 21% and 1.5%, and a constant CO_2 concentration of 300 ppm. If physical barriers to the diffusion of CO_2 into the leaf are mainly limiting the rate of light-saturated CO_2 uptake, enhancement of photosynthesis due to the lower O_2 concentration could not take place without a decrease in the resistance R_w. The results summarized in Table 17 show that the enhancement of the photosynthetic rate in low O_2 found in the leaves investigated is not accompanied by a decrease in R_w. The degree of enhancement was about 50% in all leaves.

Carboxydismutase activity and protein content. There is strong evidence that the activity of certain photosynthetic enzymes, particularly carboxydismutase, may be a major limiting factor determining the light-saturated rate of photosynthesis in leaves (Björkman, 1968; Wareing *et al.,* 1968). Parallel increases in protein content and light-saturated photosynthesis found in the leaves of clone Fe 2 originally from a sunny habitat after exposure to strong light for 1 to 6 days suggested that synthesis of one or several photosynthetic enzymes could, at least in part, account for the increased rate of CO_2 uptake. The activity of carboxydismutase was,

TABLE 17. Resistance to Water Vapor Transfer, R_w and Rate of CO_2 Uptake in 21% and 1.5% Oxygen

	21% O_2		1.5% O_2	
	R_w, sec cm^{-1}	CO_2 Uptake, μmole dm^{-2} min^{-1}	R_w, sec cm^{-1}	CO_2 Uptake, μmole dm^{-2} min^{-1}
Clone Mb 1 grown in weak light	1.74	7.07	1.78	10.35
After 12 days in strong light	2.22	3.90	2.25	5.77
Clone Fe 2 grown in weak light	1.95	5.07	1.95	7.35
After 6 days in strong light	1.75	12.55	1.73	18.32

Note: The measurements were made under saturating light and a CO_2 concentration of 300 ppm.

therefore, determined in leaves of this clone grown in weak light and again after the leaves had been exposed to strong light for 2, 4, and 6 days. Procedures used for the preparation of the leaf extracts and for the enzyme assays were as described by Björkman (1968). The results of these determinations are summarized in Table 18. The activity of carboxydismutase increased when computed on the basis of fresh weight and chlorophyll, but the specific activity remained constant. These data strongly indicate that the increased protein synthesis that takes place upon exposure to strong light includes *de novo* synthesis of carboxydismutase.

There is much evidence that carboxydismutase and fraction-1 protein of leaves are the same protein entity. Fraction-1 protein, which comprises a major portion of the total soluble protein in leaves, can readily be separated by gel-filtration on Sephadex G-200. This technique was used in the present work to follow changes in the amount of fraction-1 protein in leaves of the clone Fe 2 grown in weak light and then transferred to strong light for 2, 4, and 6 days. Leaves with the major veins excluded were homogenized in a buffer containing 0.1 *M* Tris-HCl, 0.01 *M* $MgCl_2$, 2.5×10^{-4} *M* EDTA, 1 gl^{-1} isoascorbate and 5 m*M* DTT (dithiothreitol). The final *p*H was 7.95. The homogenate was spun at 25,000 rpm for 20 minutes, the supernatant treated on a Sephadex G-50 column (0.9×15 cm), and the protein-containing portion of the eluate subsequently applied to a Sephadex G-200 column (2.5×40 cm). Both columns were equilibrated with the same buffer used for homogenization except that isoascorbate and DTT were omitted. All operations were carried out at 2°C. The eluate from the Sephadex G-200 column was collected in 2.5-ml fractions, and the protein in each fraction precipitated with CCl_3COOH and determined with the Folin-Lowry method. Fig. 47 shows the elution pattern of the protein from leaves grown in weak light and after being placed for 4 days in strong light. The prominent peak in these curves represents fraction-1 protein. Table 19 lists the content of total soluble protein and fraction-1 protein in leaves grown

TABLE 18. Carboxydismutase Activity in Leaf Extracts from *Solanum dulcamara,* Clone Fe 2, Grown in Weak Light and Transferred to Strong Light for 2, 4, and 6 Days

Days in Strong Light	Enzyme Activity, μmole CO_2 per min		
	Per dm^2 Leaf Area	Per mg Chlorophyll	Per mg Soluble Protein
0	6.21	0.96	0.17
2	8.41	1.36	0.17
4	11.44	1.65	0.17
6	13.92	2.45	0.17

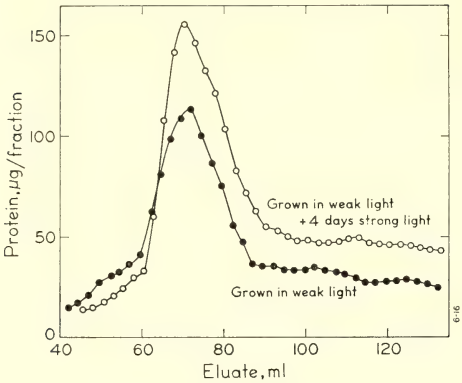

Fig. 47. Elution curves of protein separations on Sephadex G-200 of leaf extracts of *Solanum dulcamara,* clone Fe 2, grown in weak light and after exposure to strong light for four days. The same amount of leaf material (fresh weight) was used for both separations.

in weak light and after exposure to strong light for 2, 4, and 6 days. Both total protein and fraction-1 protein increase in a roughly parallel way during the exposure to strong light.

Conclusions. A change in the O_2 concentration surrounding the leaf from 21% to 1.5% did not have any effect on the degree of stomatal opening. Photosynthesis was enhanced almost 50% in all leaves tested regardless of origin or preconditioning. This indicates that the change in light-saturated photosynthesis that takes place in the different ecotypes as a result of short-term exposure to high light intensities cannot be due to changes in physical barriers to diffusions of CO_2, or in the rate of reoxidation of photosynthesis in the light (photorespiration). The causes of the reduction in the light-saturated rate of CO_2 uptake in the shaded habitat clone upon exposure to strong light are still unknown. The parallel increase in photosynthesis, protein content and carboxydismutase activity in leaves of the sunny habitat clone as a result of exposure to strong light suggests strongly that synthesis of key photosynthetic enzymes may be the major factor increasing the rate of photosynthesis after transfer to a higher light intensity.

TABLE 19. Soluble Protein and Fraction-1 Protein Content of Leaves of *Solanum dulcamara,* Clone Fe 2, Grown in Weak Light and Transferred to Strong Light for 2, 4, and 6 Days

Days in Strong Light	Total Soluble Protein, mg per g Fresh Weight	Fraction-1 Protein, mg per g Fresh Weight
0	16.65	7.63
2	21.76	8.28
4	29.10	10.13
6	32.00	12.26

References

Björkman, O., *Physiol. Plantarum, 21,* 1, 1968.

Gauhl, E., and O. Björkman, *Planta, 88,* 187–191, 1969.

Wareing, P. F., M. M. Khalifa, and K. J. Treharne, *Nature, 220,* 453, 1968.

Application of a New O_2 Sensing Device to Measurements of Higher Plant Photosynthesis

Olle Björkman and Eckard Gauhl

Until recently no technique for measurements of photosynthetic O_2 exchange by leaves that combines the accuracy, simplicity, and convenience in operation of the infrared analyzer for measurements of CO_2 was available. Almost all information on photosynthetic O_2 exchange by higher plants has been obtained from mass spectrometric measurements.

Polarographic measurements of O_2 exchange have been widely used in studies of algal photosynthesis for many years. Last year we successfully adapted this technique for measurements of photosynthesis by thalli of the liverwort *Marchantia polymorpha.* Unfortunately, however, the technique is unsuited for use with higher plant leaves.

Very recently, a greatly improved version of the paramagnetic O_2 analyzer

was tested for use with higher plants in Professor Egle's laboratory in Frankfurt, Germany, with promising results (Schaub *et al.*, 1968). In addition to this improved paramagnetic analyzer, an entirely new O_2 sensing device, exploiting the high ionic conductivity to oxygen of a newly developed ceramic, has become commercially available. Because of its very high sensitivity, it appeared to be potentially useful for measurement of photosynthetic O_2 evolution and the testing of the device for this purpose was therefore undertaken in this laboratory. The sensor is manufactured by the Westinghouse Electric Corporation, New Products Division, Pittsburgh, Pa., and is incorporated in Model 209 O_2 Monitor of this company. Scientific Products, Menlo Park, California, kindly made one such instrument available for testing.

The sensor consists of a nonporous tube of a calcium stabilized zirconium oxide ceramic to which porous electrodes are attached. It is also equipped with a furnace operating at 850°C. This temperature is kept constant with a solid-state proportional controller.

The gas to be analyzed is admitted to one side of the ceramic tube and the reference gas to the other side. Oxygen molecules on the side with the higher O_2 pressure gain electrons to become ions, while simultaneously on the other side, oxygen molecules are formed by reverse action. The potential of the cell is then given by

$$V = (RT/nF)\ ln\ (P_s/P_r) \qquad (1)$$

where R is gas constant; T, absolute temperature; F, Faraday; P_s, partial pressure of O_2 in the sample gas; and P_r, partial pressure reference gas (Burke, 1969). With the cell used in the present study the open circuit potential (mV) is given by

$$V = 55 \log\ (P_s/P_r) \qquad (2)$$

The cell voltage is unaffected by the presence of noncombustible gases such as water vapor and carbon dioxide, but care has to be taken not to introduce combustible gases into the cell since at the high operating temperature these will react with oxygen and reduce its concentration.

In measurements of photosynthesis with an open flow system under rate-limiting CO_2 concentrations it is usually desirable that the uptake of CO_2 by the leaf does not result in an excessive reduction of the CO_2 concentration in the leaf chamber. In most cases a reduction exceeding 25% would be undesirable. Under a CO_2 concentration of normal air this would amount to about 80 ppm. Since the uptake of one mole of CO_2 can be expected to correspond to a roughly equal amount of O_2 being evolved, the change in O_2 concentration also should not exceed this value. It is therefore desirable that a concentration change of about 1 ppm be resolved by the device.

Figure 48 shows the calculated rela-

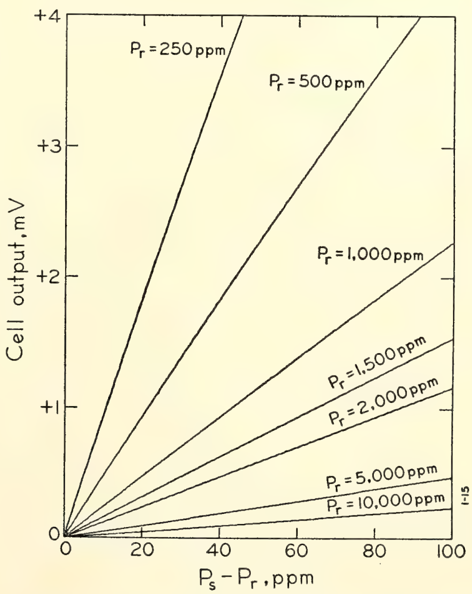

Fig. 48. The open circuit voltage produced by the zirconium-oxide ceramic cell as a function of the difference in O_2 concentration between the sample and the reference gas, at different O_2 concentrations in the reference gas.

tionship between the cell voltage and the difference in O_2 concentration between the sample and the reference gas at various O_2 concentrations. From these data it may be predicted that sufficient sensitivity can be obtained at O_2 concentrations of less than 2000–10,000 ppm O_2. In the photosynthesis measurements reported here the O_2 concentration of the gas entering the leaf chamber was kept at 1500 ppm. At this concentration the sensitivity of the device was sufficiently high and there was no evidence of adverse metabolic effects that might be caused by anaerobic conditions. The O_2 concentration in the leaf chamber was kept in the range of 1500–1560 ppm. As shown in Fig. 48, the relationship between the O_2 concentration and the cell voltage is very close to linear in this narrow range.

The output voltage of the O_2 cell was measured with a Keithley Model 150 B Microvoltmeter and the amplified signal displayed with a dual channel Hewlett-Packard 7100 BM potentiometric recorder. The indicating circuitry and other accessory components that are integral parts of the Westinghouse Model 209 Monitor were either inadequate or unnecessary for the present application. With the exception of the O_2 cell assembly and the temperature controller, all circuits in the Model 209 O_2 Monitor were disconnected. An open system similar to that described by Björkman (1966) was employed. All measurements were made on single leaves, attached to the plants.

With the O_2 concentrations used in our photosynthesis measurements the noise level of the output voltage from the O_2 cell was very low. The estimated signal-to-noise ratio of the amplified and recorded signal was about 500 to 1. A change in concentration of 0.2 ppm could easily be detected when the O_2 concentration was kept at about 1500 ppm. Under these same conditions the base line drift was estimated to be 1% of full scale deflection over a 10-hour period. These data suggest that a considerably higher amplification factor could be used while a tolerable noise level could still be maintained. As far as we are aware, there is no other O_2 sensing device presently available with as high a sensitivity in this concentration range.

The instrument was completely unaffected by vibrations from pumps and other equipment that were mounted on the same bench. It was also unaffected by considerable changes (some $\pm 5°C$) in the ambient temperature. Another attractive feature is that no elaborate calibrations are needed. The response of the cell to changes in O_2 concentration can readily be predicted from equation 2. Experimental values obtained by diluting pure O_2 with N_2 agreed with these predicted values within the experimental error of the calibration procedure. This error was approximately $\pm 3\%$ and that of the analyzer is presumably smaller.

Figures 49–51 show typical results of experiments in which the dependence of photosynthesis on light intensity and temperature was determined. Tracings from the recorded charts presented in Fig. 49 illustrate the time course of photosynthesis when the leaves were subjected to changes in light intensity. The rate of O_2 evolution, calculated from the predicted response of the O_2 cell, was in very close agreement with the rate of CO_2 uptake in all cases where both rates were measured. Results of determinations of the dependence of photosynthetic O_2 evolution on CO_2 concentration in leaves of *Atriplex patula* and *A. rosea,* using this new O_2 sensing device, are shown in another section of this *Year Book* (p. 629, Fig. 42).

The response time of the O_2 measuring system is determined by the volume of the leaf chamber and the gas connections between it and the O_2 cell, and by the flow rate. The response time of the O_2 cell itself is, according to the manufacturer, only one millisecond.

Because of its insufficient sensitivity

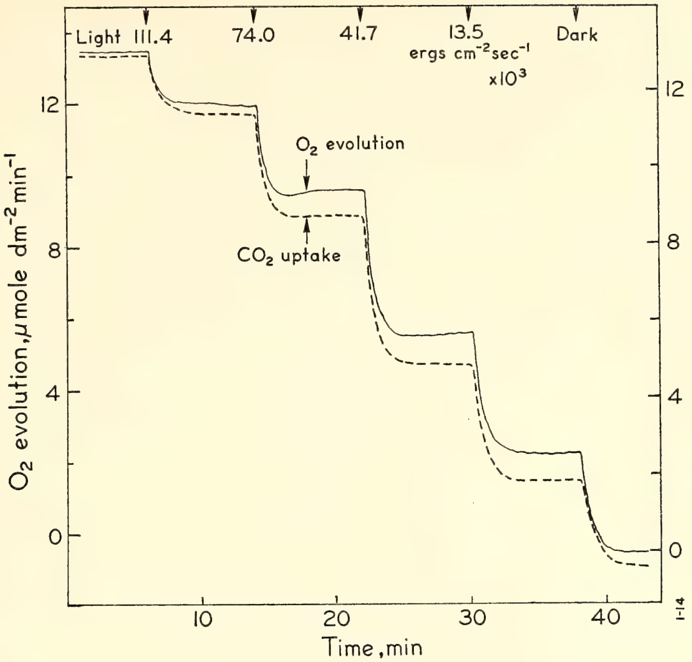

Fig. 49. Recorder traces of the time courses of O_2 evolution and CO_2 uptake in a *Mimulus verbenaceus* leaf subjected to decreases in light intensity. The leaf temperature was 25°C and the CO_2 concentration in the leaf chamber was approx. 0.08%. White light was provided by a 2.5 kW high pressure Xenon lamp.

at high O_2 concentrations, the device is of limited usefulness in photosynthesis measurements under field conditions and

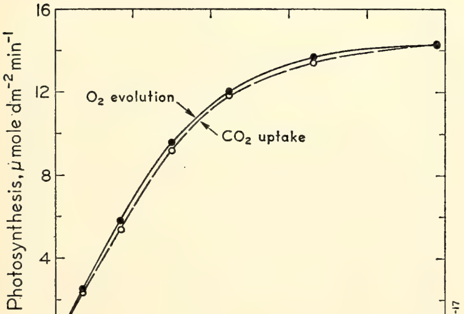

Fig. 50. Effect of light intensity on the rates of O_2 evolution and CO_2 uptake in an *M. verbenaceus* leaf. Conditions were as given under Fig. 49.

in studies on the inhibitory effect of O_2 on net photosynthesis (photorespiration). It is, however, probably the best instrument currently available for kinetic studies of higher plant photosynthesis under low O_2 concentrations where reoxidation of photosynthetic products in the light is inhibited.

A particularly valuable feature of the O_2 cell is its complete insensitivity to CO_2. This greatly simplifies measurements of the dependence of photosynthesis on CO_2 concentration, and of photosynthetic responses under saturating CO_2 concentrations where the infrared CO_2 analyzer has a relatively poor resolution. The O_2 analyzer, described here, provides an excellent supplement to the infrared CO_2 analyzer in comparative studies of photosynthetic characteristics in higher plants, and it has

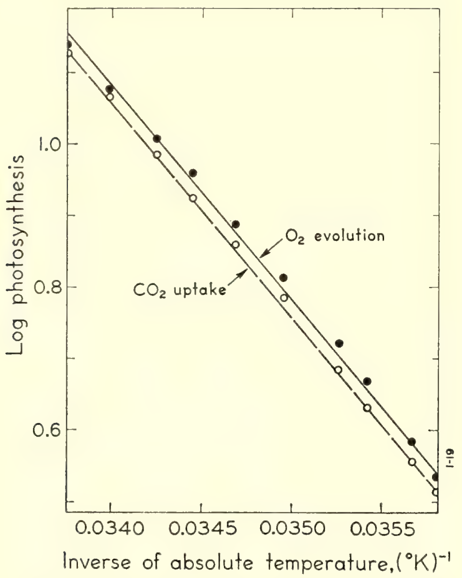

Fig. 51. Arrhenius plots of the effect of leaf temperature in the range 6–24°C on the rates of O_2 evolution and CO_2 uptake in an *M. verbenaceus* leaf. Saturating white light of an intensity of 2.5×10^5 erg cm^{-2} sec^{-1} (400–700 nm) was from a 2.5 kW high-pressure Xenon lamp.

now been incorporated into our photosynthesis measuring system.

References

Björkman, O. E., *Physiol. Plantarum, 19,* 618–633, 1966.

Burke, J. E., *Science, 161,* 1205–1212, 1968.

Schaub, H., W. Hilgenberg, and H. Fock, *Z. Pflanzenphysiol., 60,* 64–71, 1968.

Intercontinental Crosses in *Solidago*

Malcolm A. Nobs

The goldenrods of the sunflower family (the genus *Solidago*) comprise about 100 species that are distributed mostly in the Northern Hemisphere with only a few representatives in South America. The greatest diversity occurs in Eastern North America with about 75 species. On the Pacific Slope only about 12 species are found, while in the vast continent of Eurasia only a single widespread species, *Solidago virgaurea* L., is considered to be native.

Dr. Jean Beaudry and his co-workers at the University of Montreal (Beaudry, 1963; Kapoor and Beaudry, 1966) are making a comprehensive biosystematic study of the North American members of the genus. Results from comparative physiological studies on contrasting ecotypes of *Solidago virgaurea* from northern Europe by Björkman and Holmgren interested us in the long-standing question regarding the degree of relationship between the Old World *S. virgaurea* and Pacific Slope forms of the genus that appeared to be ecological counterparts. Crossings begun by us in 1965 (*Year Book 65,* p. 471) and continued during the last two years have yielded hybrids that now provide information relating to our original question.

Table 20 lists the species used in the crossings, their origins, the pollen fertilities and chromosomal pairing of both parents, and of their F_1 hybrids. The crossings included, as far as possible, combinations of pairs of races from similar ecological habitats in western Europe and western North America. One pair consists of arctic forms, a member of *S. virgaurea* from northern Norway, and a form of *S. multiradiata* from Umiat, Alaska. Both are continental interior forms from approximately 70° N. latitude. Another pair consists of an alpine form of *S. virgaurea* from the Sierra Nevada of Spain at 3000 m elevation and 38° N. latitude and a form of *S. multiradiata* from the Sierra Nevada of California at the same altitude and latitude. A third pair of lowland counterparts were crossed. These were a tall, branched form of *S. virgaurea* from near Barcelona, Spain, and a coastal form of *S. spathulata* D.C. from central California, both from approximately 38° N. latitude. Another North American representative, *S. spectabilis* (D.C. Eat.) Gray from Mono Lake, California, at

TABLE 20. Pollen Fertilities and Chromosome Pairing in Parental and Hybrid Combinations of *Solidago*

Species or Hybrid Combination	Culture No.	Origins (Elevations and Latitudes)	Percent Normal Pollen *	Meiotic Pairing (Metaphase I)
Parental Species:				
S. multiradiata Ait.	7654	Timberline, Sierra Nevada of California, 3100 m, 38° N.	90	Regular, 9 pairs
S. multiradiata Ait.	7338	Umiat, Alaska, 100 m, 70° N.	78	Regular, 9 pairs
S. spectabilis (D.C. Eat.) Gray	7657	Mono Lake, California, 2000 m, 38° N.	92	Regular, 9 pairs
S. spathulata D.C.	7659	Coastal Central California, San Mateo Co., 50 m, 38° N.	87	Regular, 9 pairs
S. spathulata D.C.	7335	Coastal Central California Ft. Ross, 20 m, 38° N.	90	Regular, 9 pairs
S. virgaurea L.	B 039	Beskades, Norway, 600 m, 70° N.	80	Regular, 9 pairs
S. virgaurea L.	HV 124	Hallands Vadero, S. Sweden, 50 m, 56° N.	90	Regular, 9 pairs
S. virgaurea L.	7612	Barcelona, Spain, 600 m, 41° N.	89	Regular, 9 pairs
S. virgaurea L.	7613	Sierra Nevada, Spain, 3000 m, 38° N.	80	Regular, 9 pairs
Hybrid Combinations:				
multiradiata × *multiradiata*	7592	Umiat × Timberline	82	Regular, 9 pairs
multiradiata × *spectabilis*	7668	Timberline × Mono Lake	54	Moderately regular, 15% with univalents
multiradiata × *spathulata*	7672	Timberline × Coastal San Mateo	51	Moderately regular, 12% with univalents
multiradiata × *spathulata*	7590	Timberline × Coastal Ft. Ross	60	Nearly regular, 6% with univalents
virgaurea × *virgaurea*	7568	South Sweden × N. Norway	80	Nearly regular, 5% with univalents
virgaurea × *virgaurea*	7692, 7693	South Sweden × Barcelona and Reciprocal	78	Nearly regular, 6% with univalents
virgaurea × *multiradiata*	7573	South Sweden × Timberline	15	Irregular, 7 pairs + 2 tetravalents
virgaurea × *multiradiata*	7678	Sierra Nevada (Spain) × Timberline (California)	19	Irregular, 7 pairs + 2 tetravalents or univalents
virgaurea × *spectabilis*	7679, 7680	Barcelona (Spain) × Mono Lake (California)	23	Irregular, 7 pairs + 2 tetravalents
virgaurea × *spathulata* (2n)	7682-102	Sierra Nevada (Spain) × Coastal California (San Mateo)	13	Irregular, univalents plus chains
virgaurea × *spathulata* (4n)†	7682-111	Ditto	50	Multivalents plus univalents
virgaurea × *spathulata*	7684	Barcelona (Spain) × Coastal California (San Mateo)	18	Irregular, 7 pairs + 2 tetravalents and univalents
virgaurea × *spathulata*	7690	Beskades (Norway) × Coastal Central California (San Mateo)	20	Irregular, 7 pairs + 2 tetravalents
virgaurea × *spectabilis*	7691	Beskades (Norway) × Mono Lake (California)	12	Irregular, 6 pairs + 2 tetravalents and univalents

* Pollen stainable with lacto-phenol and cotton blue.
† Spontaneous tetraploid F_1 hybrid.

2000 m elevation has also been included.

As indicated in Table 20, the F_1 hybrids of all the combinations indicate that there is a high degree of homology between their chromosomes and those of the parental species. Even the most highly irregular combinations as, for example, F_1 hybrids between different forms of *S. virgaurea* and *S. multiradiata,* or between *S. virgaurea* and *S. spathulata,* have about 80% chromosomal pairing. That some structural repatterning of the chromosomes has taken place is, however, very evident. These appear to be primarily due to segmental interchange. The strong sterility barriers, as indicated by the high percentage of aborted pollen, also suggests that accumulated gene differences as well as other small undetectable structural rearrangements may have taken place in the differentiation of the North American and European counterparts. The combination 7683 (Table 20) between *Solidago virgaurea* from the Sierra Nevada in Spain and *S. spathulata* from coastal Central California yielded a spontaneous tetraploid with $n=18$ chromosomes. The pollen of the tetraploid is 50% normal as compared with only 13% for the diploid hybrid plants, suggesting that the tetraploid may have considerably higher fertility than the diploids. The extreme vigor of the tetraploid in the Stanford garden as contrasted with the diploids further indicates that it is an amphiploid, and implies that a fairly high degree of genetic divergence has taken place between the parental species.

The very close homology between the chromosomes of even the most contrast-

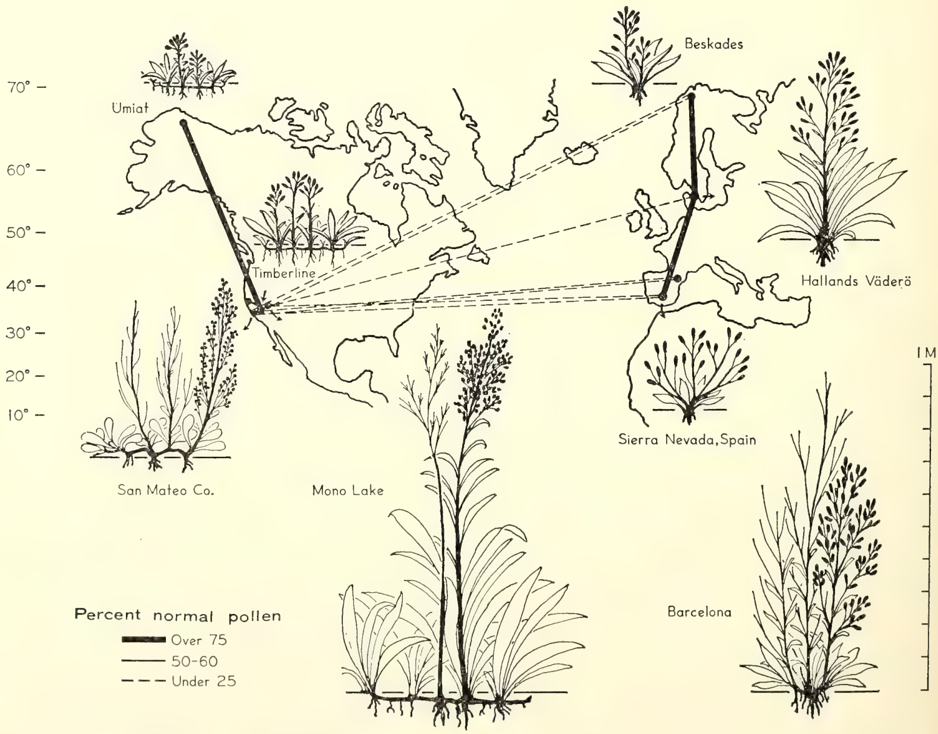

Fig. 52. Fertilities of first-generation hybrids between European and North American forms of *Solidago*. The habit sketches of the parental forms are drawn to scale from plants grown in the Stanford garden. See text.

ing ecological races of the European *S. virgaurea,* and also between corresponding North American forms of *S. multiradiata,* is evident from Table 20. That parallel differentiation in the two species has taken place in the two continents is now clear. It is equally clear that the two species have been derived from the same ancestral stock and are closely enough related to have preserved most of their chromosomal homology.

Figure 52 summarizes the relationships between the North American and European forms of *Solidago* in graphic form and illustrates the major morphological differences between the parental forms used in the crossings. The drawings of the parental plants are made to scale as the plants are observed in the Stanford garden. It should be remembered that such vegetative characters as stem height may be strongly modified in contrasting environments.

References

Beaudry, Jean R., *Can. J. Genet. Cytol., 5,* 150–174, 1963.

Kapoor, B. M. and J. R. Beaudry, *Can. J. Genet. Cytol., 8,* 422–443, 1966.

Vegetation of the Harvey Monroe Hall Natural Area

Jens Clausen

Occasioned by the XIth International Botanical Congress meeting at the University of Washington, Seattle, August 24 to September 3, 1969, two major field excursions are planned that include the Institution's Department of Plant Biology field stations and central laboratory. The Mather and Timberline transplant stations will be featured, the latter situated in the Harvey Monroe Hall Natural Area. A list of plant species native to this unique area that has been compiled over a period of years is being printed by the Institution in booklet form and will be available to the visiting botanists.

In view of the wide biological interest in the Harvey Monroe Hall Natural Area a brief review of its history appears to be appropriate. In his annual report (*Year Book 32,* pp. 20–21) President John C. Merriam discussed the establishment of this Natural Reserve Area in connection with future research on fundamental problems in biology, such as environment and heredity. Dr. Herman A. Spoehr, then Chairman of the Division of Plant Biology, in his report the same year (p. 180) discussed the significance of the Area "combining an unusual complex of environmental conditions and biological materials."

Dr. Harvey M. Hall proposed the establishment of such a "natural area." He emphasized that "natural conditions will be preserved virtually free from disturbance excepting those necessary for the conduct of scientific research." Hall's proposal was unique in that it would permit scientific research consistent with the conservation of the native vegetation, animal life and other natural features in essentially undisturbed form. Hall's very extensive first-hand field knowledge of the entire flora of California enabled him to perceive the special value of having available for basic experimental work such a strategically located preserve. After Hall's death, in 1932, a mutual contract between the U. S. Forest Service and the Carnegie Institution was drawn setting up the area as Hall had proposed, to be named in his honor.

The approximately 20-square-kilometer area (about 7 square miles) includes diverse topographic features that are truly representative of the high Sierra Nevada of California. Included are three valleys lying in an east-west direction that touch the east rim of the Sierra Nevada at 38° N. latitude. The valleys lie at altitudes between 3000 and 4000 m (about 10,000–13,000 ft.), and each has steep north- and south-facing slopes that provide unusual ranges of temperature, with cold night air collect-

ing at the bottom of the valleys (*Year Book 64,* pp. 431–435).

The present-day vegetation includes a total of 347 species-complexes and 4 interspecific hybrids, an unusually high number of species for an area above 3000 m altitude. Within the Hall Area are local edaphic niches that range from bogs and moist meadows to dry screes, rough, rocky talus and glacial moraines that extend up to the still active Conness Glacier. It appears the Sierra Nevada was uplifted more than 1000 m during the 1–2 million years since the midglacial period. During the shifts in altitude and climate the species, possessing genetic flexibility, evolved new ecological races as they were raised in altitude with the mountains.

Within the Hall Area the present-day vegetation consists of what appear to be 72 species that are members of circumpolar to circumboreal complexes that must have immigrated from the north through the Cascade-Sierran mountain ranges. About 68 species belong to complexes that have related races and species along the Pacific slope, some spilling over to the east of the Sierras; related to this group are 32 high-alpine, endemic Sierra Nevada species that could have occupied ice-free refuges during the period of heaviest glaciation. The remaining 175 species appear to have their relatives in the Great Basin–Rocky Mountain region, and must have entered the Hall Area over the dry mountain ridges from the east, although many spill over to the higher altitudes on to the Sierran west slope. Of these, 14 reach the Atlantic, and 31 occur in Alaska.

As the Sierras gradually rose, the aridity of the Great Basin increased, providing habitats for the multiple forms of sagebrushes and rabbitbrushes. The Hall Area itself is geologically recent, probably having been free of ice only within the last 2000–6000 years, although forms of hardier species may have occupied refuges for longer periods.

STAFF ACTIVITIES

Dr. William M. Hiesey retired on June 30, 1969. He joined the Institution in 1926 and has led the Experimental Taxonomy Group since 1956. Dr. Hiesey plans to remain active for the completion of an Institution monograph, *Experimental Studies on the Nature of Species,* Vol. V., Biosystematics, genetics, and ecological physiology of the Erythranthe section of *Mimulus,* by William M. Hiesey, Malcolm A. Nobs, and Olle Björkman.

Because of overlapping interests of the Experimental Taxonomy Group and of several Stanford professors, the ties between the Institution and the Department of Biological Sciences of Stanford University have become closer. In addition to direct experimental collaboration with Professors Harold Mooney, Peter Ray, and Peter Raven, and their graduate students, a Stanford Seminar on Plant Physiology and Ecology has met weekly at our Department under Professor Ray's direction. Plans are in preparation for expansion of the collaborative work of Drs. Björkman and Nobs with the Stanford group at the mountain stations and at the laboratory.

Dr. Jens Clausen was invited to attend the Vth Congress of EUCARPIA, the European Association for Research in Plant Breeding, meeting at Milan, an international symposium in Denmark of the Scandinavian Association of Geneticists in honor of Professor C. Syrach Larsen's retirement, and a meeting of the Danish Botanical Society. His talk on "Genecology and Breeding" will be published in English and in Russian. Dr. Clausen has prepared a description of the Harvey Monroe Hall Natural Area, with a check list of its plants showing also their relatives in other

regions. This Institution publication which developed from his talk at the Danish Botanical Society is available to two groups of botanists visiting the mountain stations in connection with the XI International Botanical Congress held in Seattle in August, 1969.

Dr. Fork and Dr. Jan Amesz of Leiden, a former Carnegie Corporation Fellow, have collaborated on an article, "Action spectra and energy transfer in photosynthesis," for *Annual Reviews of Plant Physiology* and have also contributed a chapter, "Spectrophotometric studies on photosynthesis," for a comprehensive text on photophysiology, edited by Professor Giese of Stanford.

Dr. Norio Murata, an Institution Research Fellow has been awarded the prize for promotion of research by the Japanese Biochemical Society for his accomplishments in the study of fluorescent pigments of photosynthesis.

Mr. Jan Kowalik was awarded the Jurzykowski Award by the Alfred Jurzykowski Foundation on January 24, 1969, in recognition of his outstanding achievements in the field of bibliography.

Drs. Brown and Murata attended the Gordon Conference on Photosynthesis at Holderness, New Hampshire, June 29 to July 4, 1969.

During the year the Institution's Bush Cabin at Inverness, California was built in a heavily wooded area close to the Tomales Bay State Park and the Point Reyes National Seashore. This was made possible by Dr. Bush's gift to the Institution for staff recreation. The cabin shell was built by a contractor while completion of the roof, deck, interior finish, wiring, and finish plumbing is providing an abundance of recreational challenge for the Department's Staff and Fellows.

BIBLIOGRAPHY

449* Amesz, Jan, *see* Fork, David C.

453 Björkman, Olle, and Eckard Gauhl, Carboxydismutase activity in plants with and without β-carboxylation photosynthesis. *Planta, 88,* 197–203, 1969.

458 Björkman, Olle, and Eckard Gauhl, Use of the zirconium oxide cell for measurements of photosynthetic oxygen evolution by intact leaves. *Photosynthetica,* in press, 1969.

454 Björkman, Olle, *see* Gauhl, Eckard.

Björkman, Olle, Characteristics of the photosynthetic apparatus as revealed by laboratory measurements. *IBP/PP Technical Meeting, Trebon, Czechoslovakia, Productivity of Photosynthetic Systems, Models and Methods,* Czechoslovakia Academy of Science, ed., Preliminary texts of invited papers, pp. 136–148, April 10, 1969.

Brown, Jeanette S., Selective and reversible absorption changes of chloroplast particles. *Fifth Intern. Congr. Photobiol., Hanover, New Hampshire, Abstracts of Congress, 5,* p. 101, 1968.

* Department of Plant Biology publication numbers.

Brown, Jeanette S., Fluorescence of fractionated chloroplast particles (abstract). *Biophysical Journal, 9,* A-124, 1969.

442 Brown, Jeanette S., *see* French, C. S.

449 Fork, David C., and Jan Amesz, Action spectra and energy transfer in photosynthesis. *Ann. Rev. Plant Physiol., 20,* Leonard Machlis, ed., Annual Reviews, Palo Alto, Calif., pp. 305–328, 1969.

445 French, C. S., Biophysics of plastid pigments. Closing Session Summary, Internatl. Congr. of Photosynthesis Research, Freudenstadt, June 4–8, 1969, *Photosynthetica, 3*(1), 94–96, 1969.

French, C. S., Absorption and fluorescence spectra of forms of chlorophyll. *Fifth Intern. Congr. Photobiol., Hanover, New Hampshire, Abstract of Congress, 5,* 73, 1968.

French, C. S., Analysis of spectra of chloroplast fractions (abstract). *Biophys. J., 9,* A-124, 1969.

French, C. S., The forms of chlorophyll *a* in plants (abstract). *Plant Physiol., 43,* Suppl., S 20, 1968.

442 French, C. S., M. R. Michel-Wolwertz, J. Michel, J. S. Brown, and L. Prager, Naturally occurring chlorophyll types

and their functions in photosynthesis. *Biochemical Society Symposia, 28, Porphyrins and Related Compounds,* T. W. Goodwin, ed., London, pp. 147–162, 1969.

454 Gauhl, Eckard, and Olle Björkman, Simultaneous measurements on the effect of oxygen concentration on water vapor and carbon dioxide exchange of leaves. *Planta, 88,* 187–191, 1969.

Gauhl, Eckard, *see* Björkman, Olle.

446 Heber, Ulrich, Conformational changes of chloroplasts induced by illumination of leaves in vitro, *Biochim. Biophys. Acta, 180,* 302–319, 1969.

442 Michel, J. M., *see* French, C. S.

442 Michel-Wolwertz, M. R., *see* French, C. S.

442 Prager, L., *see* French, C. S.

SPEECHES

Björkman, Olle, Adaptive differentiation of photosynthetic characteristics among species and races of higher plants from ecologically diverse habitats. Advanced Plant Physiology and Biochemistry Seminar, MSU/AEC Plant Research Laboratory, Michigan State University, East Lansing, Michigan, March 4, 1969.

Björkman, Olle, Comparative studies of photosynthesis and growth in species with different pathways of carboxylation. Advanced Plant Physiology and Biochemistry Seminar, MSU/AEC Plant Research Laboratory, Michigan State University, East Lansing, Michigan, March 5, 1969.

Björkman, Olle, Ecological aspects of photosynthesis. Department of Botany Seminar, University of California at Davis, Davis, California, November 5, 1968.

Björkman, Olle, Oxygen inhibition of photosynthesis and growth, photorespiration, β-carboxylation photosynthesis, and related matters. Stanford Plant Physiology Graduate Seminar, Carnegie Institution, Stanford, California, May 7, 1969.

Björn, Lars O., Delayed light emission. Stanford University Plant Physiology Graduate Seminar, Carnegie Institution, Stanford, California, April 23, 1969.

Brown, Jeanette S., Selective and reversible absorption changes of chloroplast particles. Fifth International Congress on Photobiology, Hanover, New Hampshire, August 29, 1968.

Brown, Jeanette S., Fluorescence of fractionated chloroplast particles. Biophysical Society, Los Angeles, California, February 27, 1969.

Brown, Jeanette S., Biological forms of chlorophyll *a*. Stanford University Plant Physiology Graduate Seminar, Carnegie Institution, Stanford, California, October, 1968.

Brown, Jeanette S., Spectroscopic analysis of different chlorophyll containing particles. Gordon Research Conference, Holderness School, Plymouth, New Hampshire, June 30, 1969.

Clausen, Jens, Genecology and breeding. Vth Congress of Eucarpia, European Association for Research in Plant Breeding, Milan, Italy, October 2, 1968.

Clausen, Jens, Genecology and breeding. Scandinavian Association of Geneticists Symposium on Seed Orchards, in honor of Dr. C. Syrach Larsen, Scandinavian Seminar College, Holte, Denmark, October 7, 1968.

Clausen, Jens, Genecology and breeding. Mendelian Society, Botanical Society, Lund, Sweden, October 17, 1968.

Clausen, Jens, Populationsstudier over traeer i en alpin-subalpin dal i Sierra Nevada, California (Population studies on trees in an alpine-subalpine valley in Sierra Nevada, California). Danish Botanical Society, Botanical Laboratory, University of Copenhagen, Copenhagen, Denmark, October 23, 1968.

Fork, David C., Recent studies on intermediates of electron transport in photosynthesis. Biology Department Seminar, University of Chicago, Chicago, Illinois, May 23, 1969.

Fork, David C., Intermediates of photosynthetic electron transport. Biology Department Seminar, California Institute of Technology, Pasadena, California, June 2, 1969.

Fork, David C., Photosynthetic electron transport. Stanford University Plant Physiology Graduate Seminar, Stanford, California, January 15, 1969.

French, C. S., Absorption and fluorescence spectra of forms of chlorophyll. Fifth International Congress on Photobiology, Hanover, New Hampshire, August 28, 1968.

French, C. S., The forms of chlorophyll *a* in plants. American Society of Plant Physiologists, Amherst, Massachusetts, August 31, 1968.

French, C. S., Analysis of spectra of chloroplast fractions. Biophysical Society, Los Angeles, California, February 27, 1969.

Gauhl, Eckard, Photosynthetic differentiation among *Solanum dulcamara* ecotypes from exposed and shaded habitats. Stanford University Plant Physiology Graduate Seminar, Carnegie Institution, Stanford, California, December 4, 1968.

Hiesey, William M., Biosystematic and comparative physiological studies in *Mimulus*. Stanford University Plant Physiology Graduate Seminar, Carnegie Institution, Stanford, California, February 19, 1969.

Hiesey, William M., Experimental studies on comparative plant physiology at the Carnegie Institution Laboratory. Biology Department Seminar, San Jose State College, San Jose, California, May 7, 1969.

Mantai, Kenneth E., Effect of hydrolytic enzymes on photosystem 2. Stanford University Plant Physiology Graduate Seminar, Carnegie Institution, Stanford, California, February 12, 1969.

Mantai, Kenneth E., Effects of hydrolytic enzymes and UV irradiation on electron transport in chloroplasts. Biology Department Seminar, Oberlin College, Oberlin, Ohio, April 28, 1969.

Nobs, Malcolm, Genetic diversity in *Mimulus* species and races and their responses to contrasting climates. Biology Department Seminar, University of Iowa, Iowa City, Iowa, January 9, 1969.

PERSONNEL

Biochemical Investigations

Staff: C. Stacy French, *Director;* Jeanette S. Brown, David C. Fork; James H. C. Smith, *Emeritus*

Carnegie Corporation Fellow: Kenneth E. Mantai [1]

Institution Research Fellows: Eckhard E. Loos,[2] Lars Olof Björn,[3] Norio Murata,[4] Colin Wraight [5]

Visiting Investigators: Zdenek Šesták,[6] Marcel Andre,[7] Yaroslav de Kouchkovsky [8]

Guest Investigator: Teruyo Murata [9]

Technical Assistants: Lillian Prager,[10] Mary Holzer,[11] Helen Kennedy,[12] Gregory S. Martinelli [13]

Experimental Taxonomy

Staff: Olle Björkman, William M. Hiesey, Malcolm A. Nobs; Jens C. Clausen, *Emeritus*

Institution Research Fellows: Eckard Gauhl,[14] John E. Boynton [15]

Technical Assistant: Frank Nicholson

Gardener: Archibald H. Lawrence

Summer Research Assistants: Stephen G. Wood,[16] Peter G. Mika [17]

Part Time Garden Helpers: Andrew Libertone,[18] Charles Wright II [19]

Clerical Assistant: Marylee Eldredge [20]

Administrative Secretary-Accountant: Clara K. Baker

General Department Secretary: Wilta M. Stewart,[21] Karen D. Roberts [22]

Mechanical Engineer: Richard W. Hart

Electrical Engineer: Mark C. Lawrence

Custodian: Jan Kowalik

Custodian Helper: Dietrich G. Seaman [23]

[1] From September 5, 1968. From Oregon State University, Corvallis, Oregon.

[2] From January 6, 1968. From Institut für Angewandte Botanik, Technische Hochschule, Munich, Germany.

[3] From January 3, 1969. From University of Lund, Lund, Sweden.

[4] From June 3, 1969. From University of Tokyo, Tokyo, Japan.

[5] From June 23, 1969. From University of Bristol, Bristol, England.

[6] From September 11, 1968, through October 20, 1968. From Czechoslovak Academy of Sciences, Prague, Czechoslovakia.

[7] From October 14, 1968, through November 21, 1968. From Commisariat a l'Énergie Atomique, Centre d'Études Nucléaires de Cadarache., France.

[8] From November 27, 1968, through December 22, 1968, from CNSR, Gif-sur-Yvette, France.

[9] From June 3, 1969. From University of Tokyo, Tokyo, Japan.

[10] From July 1, 1967, through August 2, 1968.

[11] From July 1, 1968, through February 7, 1969.

[12] From February 3, 1969.

[13] From June 19, 1969.

[14] From April 11, 1967, through June 30, 1969. From Botanisches Institut der Johann Wolfgang Goethe-Universität, Frankfurt, Germany.

[15] From June 9, 1969. From Duke University, Durham, North Carolina.

[16] From June 18, 1968, through September 3, 1968.

[17] From June 16, 1969.

[18] From October 3, 1967, through February 7, 1969.

[19] From May 13, 1969.

[20] From October 15, 1956, through February 15, 1969.

[21] From November 3, 1967, through March 31, 1969.

[22] From March 24, 1969.

[23] From January 22, 1969, through February 15, 1969.

PLATES

Plate 1(A). Subalpine *M. lewisii* (left), the F_1 hybrid between *M. lewisii* × *M. cardinalis* (center), and the vacant position of the nonsurviving coastal *M. cardinalis* parent (right, marked by tape) in the Timberline garden, September 1967, after an early autumn snowfall.

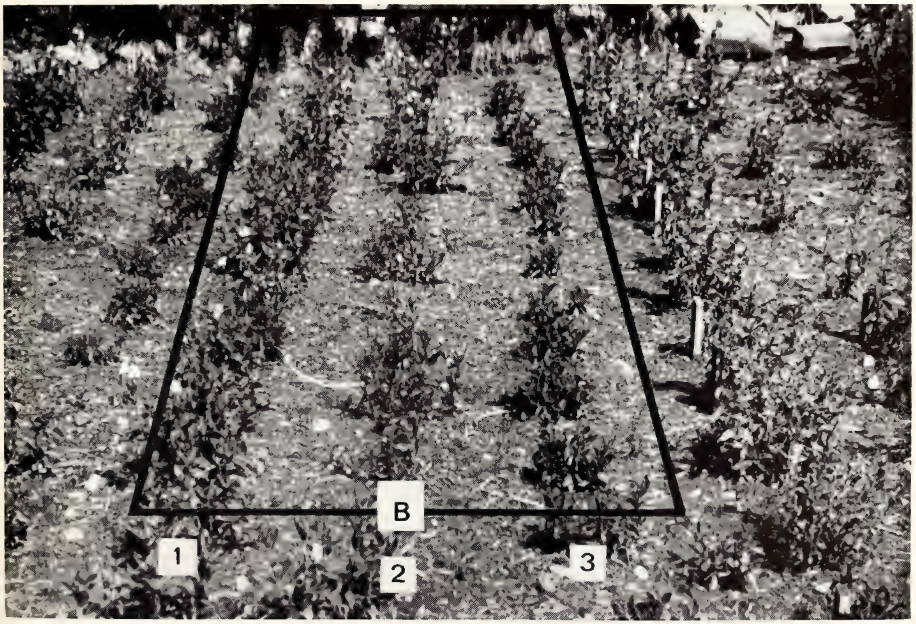

Plate 1(B). Three third-generation progenies from the above cross in the Timberline garden, summer of 1967; row 1, F_3 plants from the *M. lewisii*-like F_2 plant, 7111-16; row 2, F_3 plants from the F_1-like F_2 plant 7111-17; and row 3, plants from the *M. cardinalis*-like F_2 plant 7135-35.

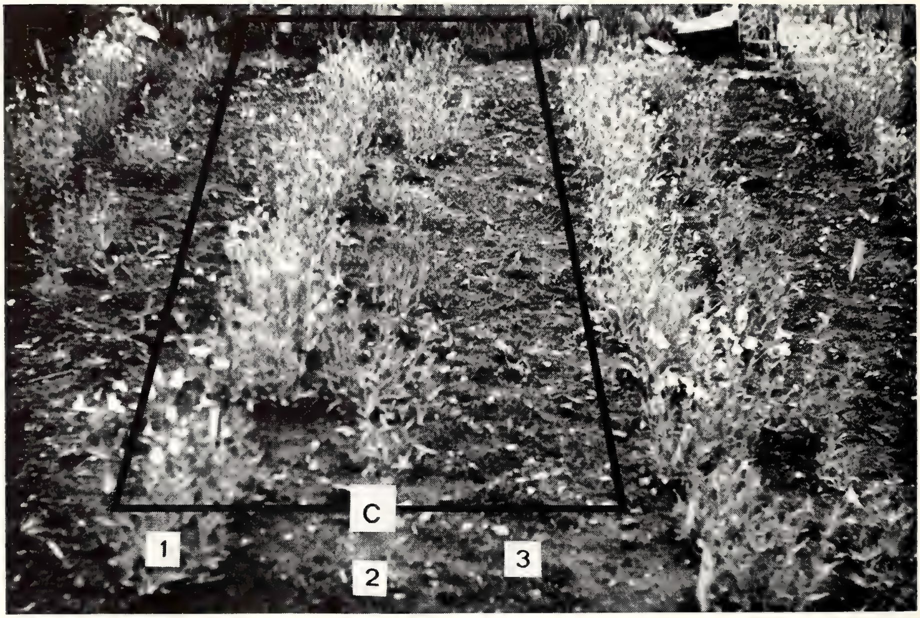

Plate 1(C). The same scene in the summer of 1968, all plants in row 3 having been eliminated by winter-kill.

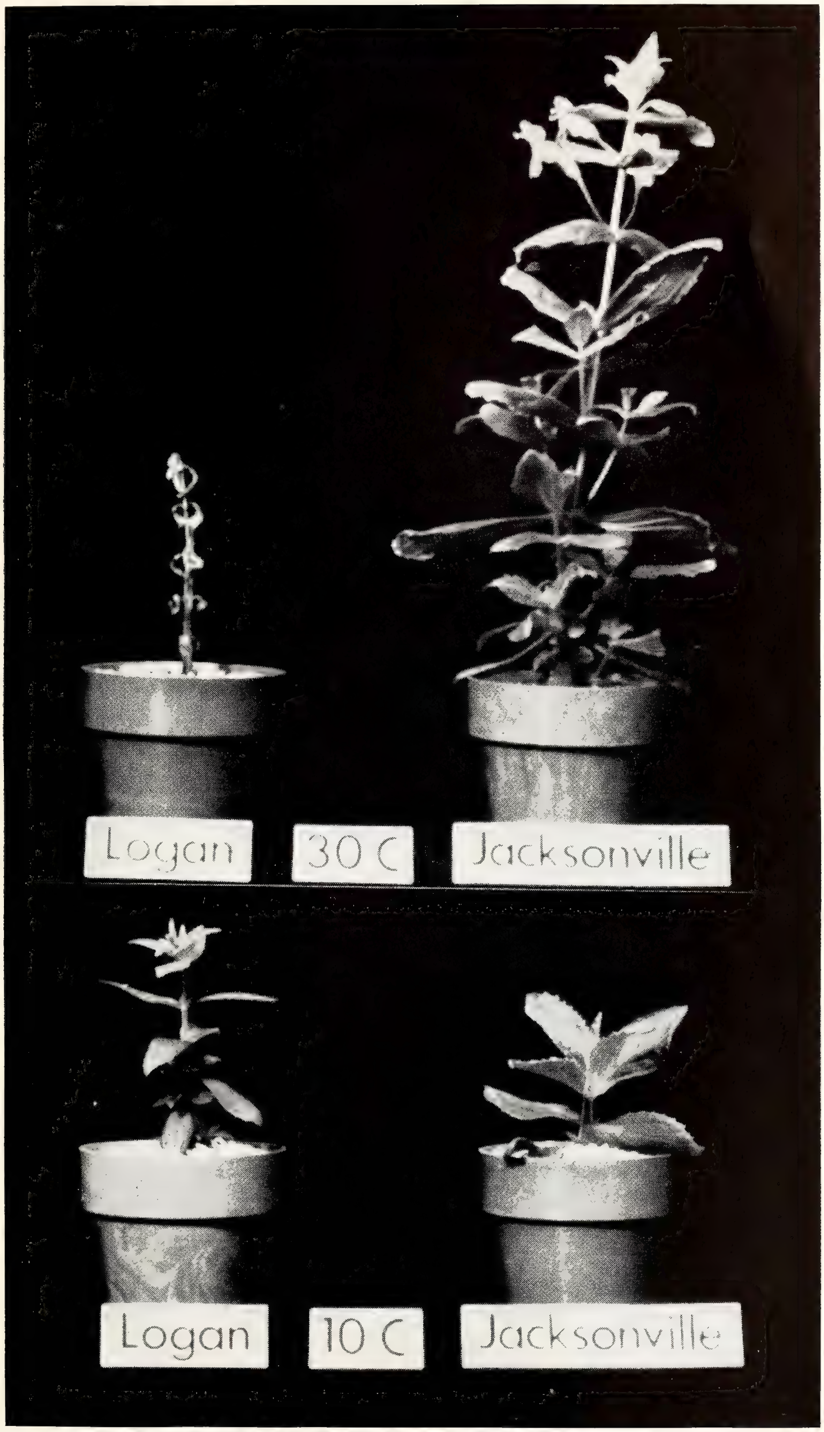

Plate 2. The Logan and Jacksonville clones of *Mimulus* after a 30-day period at 10 and 30°C. The light intensity was maintained at 5.3×10^4 erg cm^{-2} sec^{-1} (400–700 nm) during a 16-hour photoperiod, and the CO_2 concentration at 0.03%.

Genetics Research Unit

Cold Spring Harbor, New York

Alfred D. Hershey
Director

Carnegie Institution Year Book 68, 1968–1969

Contents

GENES AND HEREDITARY CHARACTERISTICS

Determination of Phenotype

Historically influential ideas have to be simple. Since natural phenomena need not be simple, we master them, if at all, by formulating simple ideas and exploring their limitations. The notion that genes determine the characteristics of biological individuals and species is exceptional among simple ideas: its limitations have consistently diminished with the passage of time. In these notes I consider both the simplicity and the limitations of our ideas about genetic determination.

The early students of heredity were forced to distinguish between the genetic constitution of an animal or plant (its *genotype*) and the expression of its genes in visible characters (its *phenotype*). The distinction is particularly clear in a heterozygous individual that received dissimilar genes from its two parents: the dual genotype clearly gives rise to a single phenotype. But even an individual with a single set of genes exhibits a phenotype that depends on stage of development, environmental influences, and accidental factors.

The notion that genotype controls phenotype is pure tautology in the typical breeding experiment in which genotype means differences between genotypes, and phenotype means differences between phenotypes. Mendel brought the tautology to light by showing that inheritance depends on unit factors. The generality of his discovery may be summarized by saying that we know of no biological characters, including developmental patterns, that are immune to gene mutations. The importance of his discovery lay in showing that inheritance could be analyzed: he initiated the collaboration between nature and scientists that has characterized the study of inheritance to this day. Nevertheless, the more general relation between genotype and phenotype for many years seemed infinitely complicated, as indeed it was in the prechemical era of genetics.

In 1940 Beadle and Tatum redirected attention to Mendel's unit factors when they described their first experiments with the bread mold *Neurospora*. This organism was unique at the time in permitting both genetic and nutritional experiments. Thus Srb and Horowitz (1944) could analyze fifteen *Neurospora* mutants unable to synthesize the amino acid arginine and show that each biochemical step in the synthesis is, in general, the province of a single gene functioning in the synthesis of a single enzyme. This result, epitomized in the phrase "one gene–one enzyme," obviously conflicted with what everybody knew: that the relation between genotype and phenotype was infinitely complicated. Chiefly because of this conflict, and partly too because the meaning of the phrase was not precisely defined, the new hypothesis met with strenuous opposition.

Actually, the hypothesis consisted of two parts: only one gene functions specifically in the synthesis of a single enzyme, and one gene functions specifically in the synthesis of only one enzyme (if any). Both parts were necessarily a little vague, because the significance of the word "specifically" was not clarified for another decade or more. (We now say that one gene determines the amino acid sequence of one enzyme.)

I don't suppose it is possible to assign a date to the eventual acceptance of the one gene–one enzyme hypothesis, but I remember clearly the Cold Spring Harbor Symposium of 1951 at which the controversy reached its climax. At that meeting Horowitz and Leupold presented their paper entitled "Some recent studies bearing on the one gene–one enzyme hypothesis," a paper that would be better

known today if it had been called "Confirmation of the one gene–one enzyme hypothesis by the use of conditional lethal mutations." In the stormy discussion that followed I was unable to grasp the issues, but it was clear to me that nearly everyone was quarreling with Beadle and Tatum, who were absent, and ignoring the results just presented.

Horowitz and Leupold offered rather subtle arguments in support of the hypothesis that only one gene functions "in a direct manner" in the synthesis of a single enzyme. They also showed that there are relatively few genes concerned with functions common to synthesis of proteins in general, and proposed that the immediate precursors of proteins are single amino acids or their derivatives, not polypeptides. Their paper is historic both for cogency of argument and because it describes the first systematic use of temperature-sensitive mutants.

In the context of the one gene–one enzyme hypothesis, subsequent developments are mainly the discovery of two smaller classes of genes: regulator genes (Jacob and Monod), whose products in the well-known examples are proteins interacting directly with DNA to interfere with the expression of other genes or groups of genes (Gilbert, Ptashne); and genes in which the structures of ribosomal and transfer RNA's are encoded (Spiegelman). At the present time there are no clear indications that additional classes remain to be discovered, though of course not all gene-determined proteins are properly called enzymes.

It is well to keep in mind that classical genetics was a perfected discipline some time before chemical genetics was invented: no real conflict between them was possible. (Read, for example, Sewall Wright's paper published in the *Physiological Reviews* in 1941, then G. W. Beadle's published in the *Chemical Reviews* in 1945.) The initial aim of chemical genetics called for elucidation of the structural and functional basis of the determination of phenotype by genotype. This aim, as nearly everyone agrees, has been achieved in large measure, and largely through elucidation of the structure of DNA (1953). The chief element of surprise, I think, was the simplicity of the denouement, anticipated in part by Beadle and Tatum.

If the overall plan is simple, one ought to be able to put it into a few words, which I attempt as follows.

First, the genotype resides in DNA—more importantly, in the one-dimensional sequence of the four nucleotides in single DNA strands.

Second, nucleotide sequences in single DNA strands represent a code transcribable into complementary sequences according to simple one-to-one rules: the four bases form only two interstrand pairs, guanine-cytosine and adenine-thymine. This code is used for DNA replication, gene transcription, and synthesis of ribosomal and transfer RNA's. It also regulates the structure of typical double-strand DNA molecules.

Third, sequences in one of the two complementary strands, transcribed into messenger RNA, represent a second code translatable into amino acid sequences in proteins. This is a nonoverlapping triplet code (three bases per amino acid) usually called *the* genetic code.

Fourth, the phenotype, insofar as it is understood at all, resides exclusively in amino acid sequences. This can be seen in several ways. For one thing, enzyme activities, which depend on specific protein structures, constitute a large part of the analyzable phenotype. For another thing, the three-dimensional structures of proteins are directly determined by the one-dimensional sequences of their constituent amino acids, as first suggested by the reversible thermal inactivation of enzymes, and currently being proved by the artificial synthesis of enzymes.

Finally, gross structure can be directly determined by subunit structure, as seen in the reconstitution of certain virus particles from their molecular con-

stituents, and in the joining of phage tails and heads to make viable phage particles. These demonstrations that specific three-dimensional structures can arise spontaneously out of appropriate one-dimensional structures did much to resolve old biological puzzles quite independently of the many detailed mechanisms now being brought to light.

My summary is necessarily abstract. Perhaps I should mention one concrete fact. Rüst and Sinsheimer have shown that either complementary strand of DNA from the phage called ϕX can infect bacterial cells to give rise to identical viral progeny. Therefore the two strands contain the same genetic information: they encode the same genotype. If we could examine these two strands in detail, we should find that they differ from each other in a systematic way: each adenine residue in one is matched by a thymine residue at the corresponding position in the other, and similarly for the pair guanine and cytosine. We are sure of this in spite of the fact that we cannot read nucleotide sequence directly. How we know is fairly simple too, but the evidence cannot be put into a few words.

So far I have made what I consider to be factual statements. Perhaps the best way to assess my judgment in this matter is to look at the criticisms raised by the few people who have made serious efforts to challenge it.

Carl Lindegren, a perceptive man with a brave disregard for the rules of debate, once pointed out in *Nature* (1955) that the city of Chicago existed for some time before it became dependent on electricity. He inferred that if DNA happened to be a late-comer on the biological scene, contemporary research would be hard put to discover that fact. Lindegren's analogy is not very apt, since towns do not acquire public utilities by inheritance. Nevertheless, it is fair to ask why biologists should believe in something not visible in the historical record. The answer, to which molecular genetics has contributed significantly, can be given as follows.

If we assume kinship of living things, we at once imagine an evolutionary family tree stemming from an aboriginal branch point that represents an event of singular importance. That event, the invention of hereditary differences, I take to be conceptually equivalent to the origin of life. If we find DNA in both aboriginal branches, we conclude either that DNA function antedates the origin of life or that DNA was independently created two or more times. In fact, biochemists find a common genetic code exploited in all members of a reasonable sample of biological species. To most people, the hypothesis of unique origin provides the only economical explanation.

The same issues are raised in extreme form by those experimental evolutionists who suggest that life is being continually recreated. There are really two issues. On the one hand, the unity of biology suggests kinship of living things. On the other hand, the complexity of the simplest forms of life suggests an inordinately low frequency of spontaneous generation: at least once on earth to be sure, but perhaps not at all in an unexplored universe. I am aware that these arguments are logically ambiguous. I am also aware that they were advanced before the phrase molecular genetics was coined. But I wish to make two less obvious points. First, in spite of the simplicity of the overall plan of inheritance, recent advances in molecular genetics serve only to augment, not diminish, our appreciation of biological complexity. For example, Peter Lengyel recently added up 130 known macromolecular components necessary just for the synthesis of protein. Second, without evidence for the unity of biochemistry, a unity now clearly evident in the universality of the genetic code, the doctrine of the unity of biology would be insecure indeed, particularly with respect to the simpler forms of life. In short, life exists

and we infer that it had a beginning. To find anything credible in either the fact or the inference is to miss the point.

Barry Commoner has devoted more thought to the search for weaknesses in molecular biology than anyone else (excepting, of course, molecular biologists). His paper in *Nature,* October 26, 1968, presumably reflects his maturest judgment. In it he cites the discovery by Speyer that mutations affecting Kornberg's DNA polymerase (an enzyme concerned with DNA synthesis) can influence the rate of further mutation. This fact shows, according to Commoner, that heritable characteristics are determined in part by nucleotide sequences in DNA, in part by the properties of enzymes. He has also remarked somewhere, presumably to defend his inference against obvious forms of attack, that it has not been shown that information theory is applicable to biological problems. Both these statements strike me as irresponsible: they are not untrue, just obtuse and misleading. Because Commoner has written eloquently and at length, using such phrases as "theoretical crisis," "illusory successes of molecular biology," and "collision course" to manufacture conflict between "two kinds of biology," it seems worth while to try to straighten out the technical basis of his argument. (Quotations from *Science and Survival,* Viking Press, 1967.)

Long before 1953 it was evident that general mutation rates are themselves gene determined. The early geneticists described this situation as follows. The heritable characteristics of organisms are determined by genes received from their parents and transmitted to their progeny, genes that must, therefore, be duplicated in each generation. But genes are not perfectly stable, or are not duplicated with perfect fidelity, whence arise the variations (mutations) that serve evolutionary purposes. Thus it is necessary to distinguish between a mechanism of duplication, on which inheritance depends, and the occasional failures of that mechanism, which may give rise to new lines of inheritance. The frequency of failure depends on all sorts of things—external radiation, exposure to various chemicals, temperature, ionic milieu, as well as genetic constitution itself—including, we now know, the gene-determined structure of at least one enzyme. Thus information theory, insofar as it is needed in this context, is just the common sense of geneticists, who saw fit to distinguish between speech and noise. I am forced to conclude that Commoner is quarreling with the principles of genetics, and that he hasn't told us anything about molecular biology.

To separate my counter-criticism from the arbitrary meanings of words, I repeat it in a form that avoids loaded phrases entirely. I noted above that factors external to the cell, such as ambient temperature, affect mutation rates. According to Commoner's reasoning we ought, on that account, to abandon our notion that living cells can reproduce themselves.

There are, I think, more interesting limitations to current biological principles than anything pointed out by the carpers. The discovery by early geneticists that a unique set of genes determines the characteristics of the individual at once raised the question whether or not heritable characteristics are determined exclusively by those genes. This question remains unanswered and is, in fact, difficult to phrase intelligibly. The demonstration by molecular biologists that a linear genetic code can be translated into three-dimensional structure, as in the assembly of virus particles, showed that in principle the known mechanisms of inheritance could be the only mechanisms. (The example of the viruses is important because there one can observe the regeneration of quite different viral species in the same cellular milieu, depending only on the kind of DNA molecule introduced at the start.) The inference that all three-dimensional structure is encoded in

nucleotide sequences does not necessarily follow, however. I shall call that inference the unwritten dogma, since it must be shared at least by those biologists who consider molecular biology all but finished.

The problem is defined by beautiful experiments with protozoa (see T. M. Sonneborn, "Does preformed cell structure play an essential role in cell heredity?" in *The Nature of Biological Diversity,* McGraw-Hill, 1963; and Vance Tartar, *The Biology of Stentor,* Pergamon Press, 1961). Experiments of similar import with fertilized eggs of the African toad have been reported by A. S. G. Curtis (*Endeavour,* 1963).

In the work cited, diverse sorts of experiment bring to light a primordium in the cell cortex that is indispensable to development and, at least in *Paramecium,* persists through both sexual and asexual reproduction. I propose to discuss this and related problems in a superficial way, mainly to place my wager that the status of the unwritten dogma is likely to remain ambiguous for some time.

First of all, what sort of problem is it that the cell seems to have solved by inventing its cortical primordium? The important thing, it seems to me, is to preserve by growth and division an element that persists in the cell in only one copy. This requirement is clear because experimental duplication of the cortical primordium produces a dual monster. The same problem is presented by genes and chromosomes themselves, and we have no real idea how it is solved. In bacteria, there is some evidence that DNA replication too is controlled by a cortical primordium.

How can this problem be solved in principle? Perhaps by making use of another obscure fact, that cellular differentiation often appears to be irreversible. If irreversible differentiation can occur during the life of the individual, it could have occurred in the remote history of all living cells.

Given the fact that a cortical structure forms part of the cellular inheritance, how can we account for its persistence? Suppose, as a minimum hypothesis, that the cortical primordium is a molecular structure composed of two typical gene products that interact spontaneously with each other in a characteristic fashion. Suppose too that the functioning of the pertinent genes is controlled in such a way that the two reactants are produced alternately, never appearing free in the cytoplasm at the same time. This is a necessary condition to avoid production of supernumerary cortical primordia, and a sufficient condition to permit an inherited primordium to grow. Then inheritance is assured by centering the structure on the cleavage line at each cell division. Of course this scheme, even if it should prove correct, says nothing about the reason for being of the cell primordium. The scheme serves, therefore, merely to bring us to the conceptual stage at which molecular principles cease to help.

Throughout these notes, I have tried to show that the contemporary phase of molecular biology, while giving decisive answers to genetic questions, did not alter the framework of those questions, and indeed could not have succeeded so well if important alterations had proved necessary. I wish now to comment briefly on those aspects of cell biology to which genetics, molecular or not, has contributed very little. In short, what are the limitations of molecular biology?

The cell theory, dating from 1839 or earlier, engenders lengthy discussions in textbooks of biology, discussions that are interesting but do not, I think, succeed very well in stating a theory. The central notions are: that living things come in cellular form, that cells arise only from pre-existing cells, and that all cells are homologous. Without the last proviso, it is not clear what the word "cell" means, for the "typical" cell pictured in schoolbooks is an abstract thing. Thus the cell theory stands or falls in company

with the assertion that all cells share a common ancestry, which is basically an article of faith. Discussion of the theory commonly ends with the statement that the cell is "the structural unit of life," or even "life's minimum unit" (*Life,* Simpson and Beck, 1969). Such statements serve chiefly as a reminder that scientific theories cannot be profitably discussed outside their proper experimental context.

According to Tartar (*The Biology of Stentor,* 1961), the pertinent experiments are nearly as venerable as the cell theory. For instance, Gruber (1885), pursuing earlier work, showed that a single cell of the protozoan genus *Stentor* could be cut into three parts, from each of which a complete animal would regenerate. In subsequent experiments with other ciliates, pieces as small as $\frac{1}{80}$ of the cell volume were found capable of regeneration. Such experiments reveal, of course, that cells of certain protozoan species are multinucleate. More important to my purpose, they show that the cell is a homeostatic unit of life, not a minimum unit, and raise the question, what is the minimum unit? By suppressing this question, the cell theory in effect keeps living things out of the laboratory.

The experiments with *Stentor* penetrate beyond the cortical primordium to reveal what is usually called cell polarity. Polarity might be defined for present purposes as a vital principle not accounted for by any useful hypothesis. In *Stentor,* this principle seems to reside in all parts of the cell cortex.

Stentor coeruleus is an aquatic one-celled animal bearing feeding organs at its head end and a hold-fast at its tail end. The entire surface is marked by longitudinal stripes of two kinds: clear stripes carrying cilia, alternating with granular stripes without cilia. During the life of the animal, its cortical stripes grow both in width and in number. The splitting of old (wide) stripes into young (narrow) ones occurs on the ventral surface and proceeds asymmetrically, producing a circumferential (left–right) gradient of stripe widths meeting as a visible boundary on the median ventral surface.

At the start of normal cell division, or during regeneration of decapitated animals, new mouth parts start to form in the region of stripe multiplication on the ventral surface. (The parts afterwards migrate to their normal position.) These observations define an oral primordium site lying near the junction between wide and narrow stripes. However, this site is not itself a hereditary structure, because the dorsal half of a longitudinally bisected animal regenerates a new one, which appears in a newly created junction between wide and narrow stripes. Thus the oral primordium develops when required at the poles of a left–right gradient, and near the equator of a longitudinal gradient.

Likewise the tail structure (hold-fast) comes not from a specific hereditary primordium but from the posterior pole of a longitudinal gradient. Thus if the hold-fast is tucked forward by surgical means, a second one develops at the newly created posterior pole. Animals with two mouths and one tail, or with two tails and one mouth, once created by surgical interference, survive as hereditary biotypes with varying degrees of stability.

A piece of cortex grafted in reverse orientation into a normal animal may rotate to restore normal polarities, may degenerate and disappear, or may develop its own mosaic stripe pattern. Similarly, an animal bisected transversely and reconstructed with the head portion rotated 180° with respect to the tail, may regain its normal stripe pattern either by rotatory slippage of the two halves with respect to each other or by replacement of stripes in one of the halves through outgrowth from the other. These and other experiments show that polarity resides in every part of the cortex.

According to Tartar, Prowazek (1904,

1913) understood the situation about as well as anybody. The cell nucleus can only provide substances for growth and differentiation. Neither the nucleus with its arbitrary orientation nor the fluid endoplasm can account for the evolution of specific cell structures: that calls for patterns hidden in a rigid ectoplasm.

In *Stentor* and certain other cells, all reasonably large pieces of the cell cortex are equipotent with respect to regeneration of cortical patterns—patterns that are, moreover, subject to metastable variations. In bacteriophages, supramolecular patterns do not persist as such but recur, apparently residing exclusively in the gene-determined structures of individual molecules. Taken together, these facts encourage us to see in cortical polarity a historical invention that ought to be analyzable in terms of structure and process. They do not encourage us to think that the task of molecular biology is finished, even at the cellular level. In Tartar's words, "our greatest lack and most fruitful opportunity in biology lies in conceiving and testing the nature and capabilities of persistent supramolecular patterns." To the ambitious young molecular biologist seeking prospects, I recommend a careful reading of Tartar's book.

DNA Phenotypes

Many years ago methylcytosine was found as a minor constituent in wheat germ DNA. However, no clue to the significance of unusual bases in DNA appeared until the discovery of glucosylated hydroxymethylcytosine in phages T2, T4, and T6. In these phages, the replacement of cytosine by its hydroxymethyl derivative was found to be complete (Wyatt and Cohen, 1953). The glucosylation also proved to be massive, but showed a distinctive pattern in each of the three species (Volkin, 1954; Sinsheimer, 1956; Lehman and Pratt, 1960; Kornberg, Zimmerman, and Kornberg, 1961). Since the three phage species were known to be very similar in function, the pattern of glucosylation could be recognized at once as part of the phenotype. A more general argument was clear too: since diverse phage species can multiply in cells of a single bacterial species, many phages must use a common genetic language. Therefore hydroxymethylcytosine is equivalent to cytosine, and uracil (found in some phage DNA's as well as in RNA) is equivalent to thymine, in the genetic dictionary. In fact, experiments with Kornberg's DNA polymerase later showed that a dozen or more bases, including artificial ones, are equivalent to one or another of the four kinds of which DNA is typically composed. Thus the genetic message is a specified sequence of four nonequivalent units. Equivalent units are those expected and found to be interchangeable in the base pairing rules of Watson and Crick. The choice among equivalent units generates optional phenotypes, optional sometimes at the discretion of the experimenter.

The notion that DNA, the bearer of the genetic message, itself exhibits diverse phenotypes occasioned some surprise, though the biological rationale was clear enough. Speciation may be regarded as the acquisition of devices by which living things compete (and sometimes cooperate) to preserve and disseminate their genes. One might have anticipated modification of DNA structure as a particularly direct means to this end. Indeed, Seymour Cohen suggested that hydroxymethylcytosine in T2 DNA might serve to protect against the action of degradative enzymes. His suggestion has proved correct for the glucosylated DNA.

The role of glucosylation as a species marker in the DNA of phage T2 is particularly dramatic. When its DNA contains glucose, this phage multiplies in bacterial cells and destroys the nonglucosylated DNA of the host. When the DNA of the phage does not contain glucose, it is rejected by the host, though it

can function normally without glucosylation under special conditions (Arber, *Annual Reviews of Microbiology,* 1965).

The example of phages T2, T4, and T6 is rather special since few DNA's contain glucose. However, similar purposes are accomplished by more subtle chemical means in other species. In *Escherichia coli* and many of its phages, methylation serves as a strain-specific marker. Here the common features of several systems are "modification" of DNA at a few specific sites by a bacterial methylating enzyme, and "restriction" by a nuclease that can cleave the DNA at the same sites provided they have not been methylated previously. A number of such genetic systems are known, each characteristic of a different bacterial strain. Thus in *E. coli* strain A, the DNA of phage λ is methylated (or cleaved) at just one critical site lying between genes c_{II} and O. In *E. coli* strain B, λ DNA is methylated or cleaved at two or more sites not including the A-specific site. The terms "modification" and "restriction" refer to the biological consequences of methylation and cleavage: in general, phage particles cannot infect a given strain of *E. coli* with high frequency unless they contain DNA previously marked by the methylating system of that strain. The bacterial DNA is subject to the same modifications and restrictions, which therefore give to DNA itself a number of alternative mating types (Arber and Linn, *Annual Reviews of Biochemistry,* 1969).

It should be added that the DNA of *E. coli* contains numerous methylated adenine and cytosine residues that do not play any known role as compatibility factors, although their distribution in the DNA is strain specific. Their significance is unknown.

Diverse phenotypes are seen also in gross structure of DNA. Thus the DNA of phage ϕX comes in single-strand rings, T2 DNA as circularly permuted rods, T5 DNA with characteristic single-strand cuts, several phage DNA's with terminal repetitions, others with terminal cohesive sites. The significance of these variations is obscure but they probably reflect modalities of DNA replication on the one hand and, on the other, alternative means of getting the proper length of DNA into phage particles. The variations repeat a common theme: exploitation of the structural principle of complementary base sequences to permit cleavage and rejoining of DNA molecules without loss of message content. As expected according to this principle, one cut in the single-strand ring of ϕX DNA appears to be biologically irreparable. Idiosyncrasies of DNA structure have been discussed in annual reports from this laboratory for several years. Important examples are reviewed by C. A. Thomas, Jr. (*Journal of Cellular Physiology,* Supplement 1, 1967).

The amount of DNA per cell is another complex variable with phenotypic aspects. The primary component of the variation is the species-specific number of genes per set, which varies from three or four to a few hundred just among the viruses. Since evolutionary specialization often calls for new genes without making old ones obsolete ("ontogeny recapitulates phylogeny"), the maximum number must be very large. The question of nongenic DNA remains open and may prove unanswerable since some genes probably function only under special conditions, during embryonic life for instance. Several genes in T4 are dispensable or not, depending on functions provided by the host. Perhaps the proper way to phrase the question about nongenic DNA is to ask what functions of DNA remain to be discovered.

Repetitious DNA is fairly common (Britten and Kohne, *Science,* August 9, 1968). It is of course an obligatory feature of DNA replication, especially during phage growth where it probably plays a physiological role in terms of gene dosage. A more interesting example has been analyzed by Brown and Dawid

(*Science,* April 19, 1968). Oocytes of the African toad contain large amounts of DNA that consists mainly of sequences matching those present in ribosomal RNA. Apparently the repetitious DNA is used for rapid synthesis of ribosomal RNA during oogenesis.

The extreme case of variation in amount of DNA is of quite another sort. RNA viruses dispense with the DNA phase of genetic determination entirely, having invented one or two genes permitting direct replication of RNA. What once seemed a major historical puzzle turns out to be a typical biological quirk.

Britten and Kohne give evidence for the existence of repeating sequences within single gene sets. They detect such sequences only in vertebrate species, but their methods may not be applicable to species with fewer genes. The striking feature of the data is multiple repetition of a few sequences, which cannot represent simply production of supernumerary gene copies because the repeated sequences are not perfectly identical. Britten and Kohne interpret their data in historical rather than functional terms, but the possibility of special function should be considered too. Current ideas about the genetic origin of antibodies are a case in point.

Adams, Jeppesen, Barrell, and Sanger (Cold Spring Harbor Symposium, 1969) have detected a complementary sequence in the RNA of phage R17 (in DNA, the equivalent structure would be called an inverted repetition). These authors directly determined the sequence of 57 ribonucleotides found in a particular fragment of the viral nucleic acid. The sequence can be written in the form of a hairpin cross linked by 19 out of 25 possible base pairs. Evidently such a structure could be accounted for by a series of historical accidents. More interesting is the likelihood that specified sequences affect secondary structure in RNA to permit control of replication or translation or both. The general implication seems to be that nucleotide sequences are subject to evolutionary constraints that have nothing to do with the genetic message proper—an inevitable correlate, perhaps, of the redundancy of genetic language.

The arrangement of genes within DNA molecules has subtle phenotypic consequences (Stahl, *Journal of Cellular Physiology,* Supplement 1, 1967). These are well illustrated by a single example. In λ prophage, nearly all phage functions have to be repressed, and the function of a single gene called c_{I} serves this purpose. Ptashne and Hopkins showed that the c_{I} product is a protein that attaches specifically at two binding sites in the DNA bracketing the genes c_{I} and *rex.* Szybalski and Taylor showed that in the absence of the c_{I} product, transcription starting in the vicinity of c_{I} proceeds outward in both directions. Evidently the repressor interferes with transcription at two starting points to meet the needs of the prophage in a remarkably direct way. This scheme of control depends on the arrangement of two genes and two repressor binding sites and, owing to the polarity of the genetic message, on the orientation and control mechanisms of outlying genes as well. Thus a highly specified chromosomal arrangement that serves functional needs also links together several genetic elements whose shuffling by genetic recombination has to be discouraged. The example conforms nicely to the operon model of Jacob and Monod, with special features attributable to the fact that lysogeny compresses the entire phage genome into just two mutually exclusive functions.

The λ repressor system also illustrates an evolutionary principle that is too often ignored: biological adaptation always means coadaptation, ultimately involving entire genomes, organisms, and populations. This principle accounts in part for the paradox that evolution utilizes mutations that are individually deleterious. The same principle suggests

that attempts to distinguish between adaptive variation and "non-Darwinian evolution" through neutral mutation (King and Jukes, *Science,* May 16, 1969) are doomed to failure. Lest my remarks be construed as a defense of Darwinism, I offer the following propositions. Only strong theories generate alternatives. Darwinian theory is characteristically weak.

Perhaps the most puzzling aspect of DNA phenotypes has to do with the distribution of nucleotides within the molecules. Since recent discussions of this subject (Skalka, Burgi, and Hershey, *Journal of Molecular Biology,* 1968; *Year Book 67,* pp. 558–560) are already out of date, I recapitulate here the main historical facts before presenting some recent results obtained by Yamagishi and Skalka.

Perhaps the best way to state the problem is to describe the methods of study. Owing to the base-paired structure of DNA, the average composition of a molecule or fragment can be expressed by a single number, the molar fraction of guanine plus cytosine (G+C), which is equivalent to the fraction of guanine-cytosine pairs. The remaining fraction, if we neglect exceptional bases, represents adenine-thymine pairs.

The distribution of nucleotides within molecules can be determined by breaking them into fragments of known size, separating the fragments into classes of diverse composition, and measuring the G+C content in each class. Since the distribution is necessarily dependent on size of fragments, the analysis has to be repeated with fragments of various sizes. This sort of analysis has now been carried out for a few phage and bacterial species.

The nature of the problem could be seen only dimly in 1953, when interest was first focused on base sequence as the clue to the genetic message. The DNA species known at that time contained about 44% G+C, which seemed reasonable in a way, since an efficient language would use all letters with similar frequency. This thought was short lived because Lee, Wahl, and Barbu (1956) and Belozersky and Spirin (1958) reported a number of bacterial DNA species whose G+C contents ranged from 26% to 74%. Thus it appeared that DNA language, like human language, was not designed primarily for efficient communication.

The discovery that the buoyant density of DNA is strongly dependent on composition (Rolfe and Meselson, 1959; Sueoka, Marmur, and Doty, 1959) yielded the first results concerning nucleotide distribution in DNA. For instance, Rolfe and Meselson found that the standard deviation of G+C content among fragments of *E. coli* DNA (fragment length probably about 10^4 nucleotide pairs) was less than $\pm 3\%$, to be compared with the 48% range covered by variations among species. Thus diverse bacterial species, surely possessing many functions in common, do not contain many DNA segments of similar composition. Rolfe and Meselson concluded that the compositions of protein and DNA could not be directly related to each other by a universal code.

Sueoka (1961) studied directly the relation between composition of DNA and composition of protein by analyzing the whole cellular protein of a number of microbial species. He found that the frequencies of the amino acids leucine, valine, and threonine showed no correlation with the G+C content of DNA. However, glycine, alanine, and arginine showed a weak positive correlation, and lysine, glutamic acid, and isoleucine showed a weak negative correlation. Sueoka's results can now be interpreted in terms of the degeneracy of the genetic code, in which 61 codons specify one or another of just 20 amino acids (Crick, *Cold Spring Harbor Symposia on Quantitative Biology,* 1966). Thus there are four valine triplets each containing either one or two guanine or cytosine residues, and the abundance of valine

could not be favored by either extreme DNA composition. Alanine triplets contain two or three guanine or cytosine residues, and lysine triplets zero or one, in agreement with Sueoka's results. Sueoka's main conclusion, that compositions of DNA and protein are not strongly correlated, is also consistent with the coding dictionary, which allows a stretch of DNA specifying one each of 15 frequently occurring amino acids to vary in G+C content between 29% and 67%. Furthermore, both mutational study of individual proteins and comparative analysis of homologous proteins from different species show that functional requirements do not impose severe restrictions on the composition of protein. Therefore the observed variations in composition of DNA cannot signify diverse requirements with respect to the composition or function of proteins.

Having reached the conclusion just stated, Sueoka (1962) and Freese (1962) proposed that the composition of DNA was determined mainly by the genetically determined rates of mutational interconversion between guanine-cytosine pairs and adenine-thymine pairs. These authors also assumed that DNA composition as such had no functional significance and therefore could not respond to selective pressures. The latter assumption was perhaps superfluous to their main proposal because, however divergence in composition of DNA among different species may arise, one might expect it to be accompanied by coadaptive variation in mutational habit.

If DNA composition in a given species were determined primarily by mutational habit, guanine-cytosine pairs should be distributed at random among DNA fragments of gene size or larger. Recent analyses of several phage and bacterial DNA's by Yamagishi and Skalka show that the distributions are never random (see below). One must conclude either that DNA composition does reflect specialized functional adaptations or that interspecific genetic recombination is frequent with respect to the evolutionary time scale. Perhaps both possibilities should be considered likely. In any case, the hypothesis of domination by mutational equilibria loses its force.

Last year Yamagishi and Skalka proposed that an asymmetric distribution of G+C in bacterial DNA in the vicinity of λ prophage might be designed to favor the types of genetic recombination that give rise to transducing phage (*Year Book 67*, pp. 558–560). They are no longer enthusiastic about this hypothesis for two reasons. First, it now appears that the *bio*-transducing phage analyzed last year is atypical, having picked up bacterial DNA not proper to the *bio* region of *E. coli*. Its structure may not be relevant to the hypothesis under test. Second, the recognition that unselected fragments of *E. coli* DNA are rather dissimilar in composition neutralizes the significance of departures from the average composition in the vicinity of prophage insertion sites.

Miyazawa and Thomas (1965) first demonstrated that the DNA of *E. coli* contains segments of dissimilar composition. Yamagishi has carried the analysis further, and some of his results are presented in Fig. 1. The upper part of the figure confirms previous work in showing that large fragments of the DNA are uniform in composition. The lower part of the figure shows that fragments of the order of size of individual genes range in G+C content from 39% to 56%. The distribution is asymmetrical, with an average at 51%. The distribution is nevertheless rather compact: its standard deviation is ± 3.8 percentage units in G+C content, as compared with ± 6.7 units for λ DNA (Skalka, Burgi, and Hershey, 1968).

Yamagishi also examined *E. coli* DNA fragments of other lengths. His results show that stretches of the extreme composition 39% G+C range in length up to about 35,000 nucleotide pairs and comprise 3% of the total DNA. The asym-

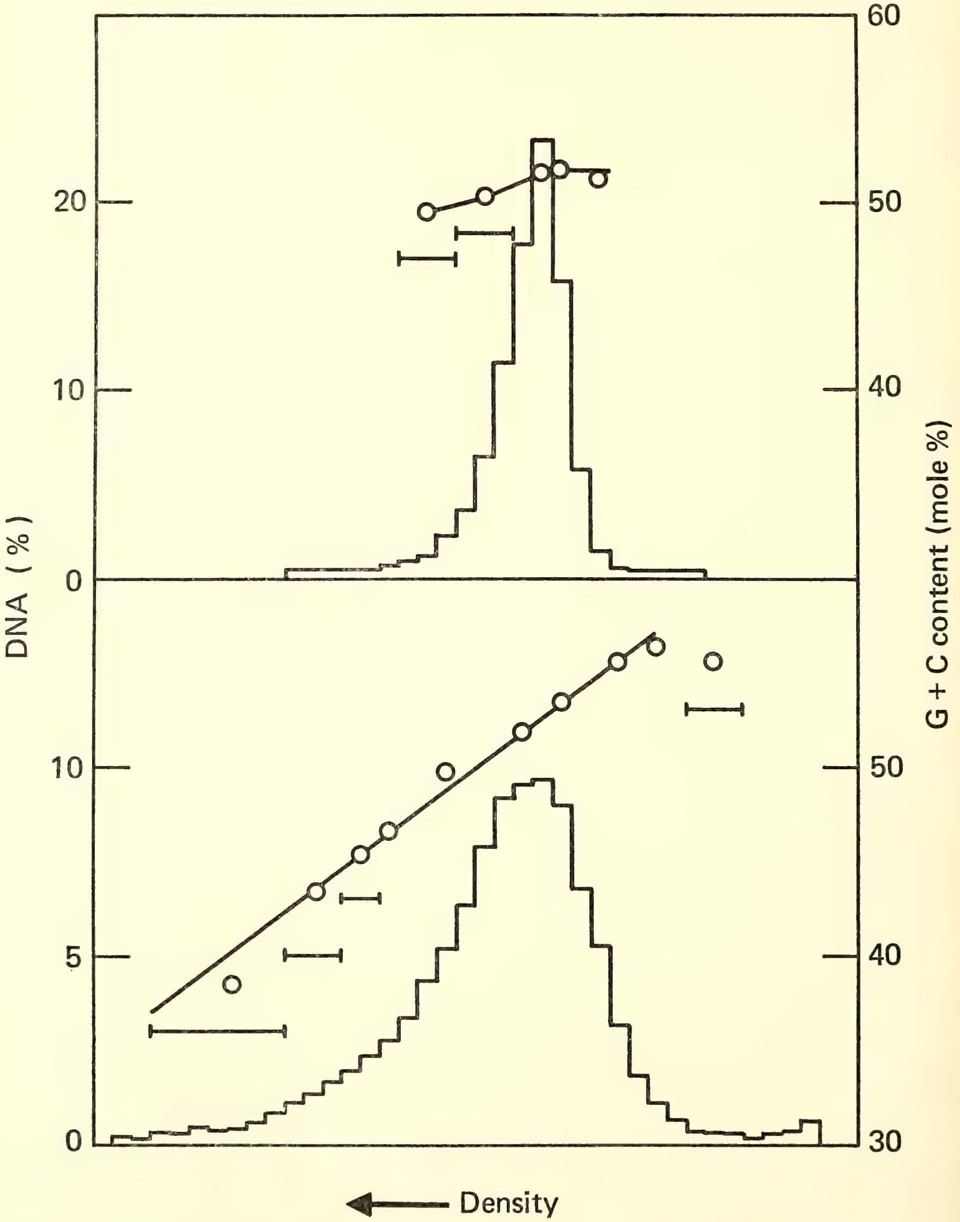

Fig. 1. Distribution of fragments of *E. coli* DNA with respect to guanine + cytosine content. Upper part: fragments of molecular weight 70 million (about 10^5 nucleotide pairs). Lower part: fragments of molecular weight 1.3 million (2000 nucleotide pairs). In both parts, distributions of DNA with respect to buoyant density in Hg-Cs_2SO_4 are shown by histograms, and the G + C content of fractions by the curves. Single fractions, or pooled fractions indicated by horizontal bars, were analyzed directly to get the points on the curves. For methods, see Skalka *et al.*, *Journal of Molecular Biology, 34,* 1–16, 1968.

metry of the distribution shown in Fig. 1 is characteristic, and signifies that long stretches of low G+C content are more numerous than long stretches of high G+C content.

The DNA of *Bacillus subtilis* is generally similar to that of *E. coli* except that its fragments range from 35% to 50% in G+C content, with an average of 44%. In collaboration with I. Takahashi of McMaster University, Yamagishi could show by genetic tests that regions of exceptional G+C content in *B. subtilis* include typical bacterial genes. Therefore local variations in composition do not reflect merely temporary residents in the bacterial chromosome such as prophages.

Yamagishi also analyzed several specific segments of *E. coli* DNA recovered from various ϕ80 transducing phage lines. Here the content of bacterial genes can be identified by genetic tests, and the corresponding DNA can be recognized by fractionation with respect to density combined with hybridization tests to distinguish between components of phage and bacterial origin. A segment containing the tryptophan operon consists of DNA ranging in G+C content from 45% to 57%. A segment containing lactose genes is more homogeneous, with an average G+C content of 54%. Among the various segments examined, only the *gal* region contains DNA corresponding to the average for the entire chromosome, 51% G+C (Yamagishi and Skalka, *Year Book 67*, p. 559).

Skalka has examined a number of phage DNA species by density analysis of molecular halves and smaller fragments (about 2000 nucleotide pairs). By this method λ DNA molecules are readily shown to consist of dissimilar halves and to be made up of four or more distinct segments containing 37%, 43%, 48.5%, and 57% G+C (Skalka, Burgi, and Hershey, 1968). The closely related phages 434, 82, and 21 are very similar to λ except that the 37% G+C section is absent in phage 21. Phage ϕ80, related to λ, and the unrelated phage 186 resemble each other in containing only two distinct segments, the molecular halves, measuring approximately 50% and 55% G+C, respectively. The DNA of phage P2 also contains dissimilar halves, and resolves into three widely dissimilar segments. The DNA of phage P22 contains at least two dissimilar segments. Molecular halves of this DNA have the same composition, presumably because the molecules come with circularly permuted nucleotide sequences. Unlike the others, phages T5, T7, and P1 contain DNA's that are strikingly uniform in composition, though not absolutely so because small fragments exhibit asymmetrical density distributions. Phage P1 contains 5% of DNA of only 37% G+C.

Two conclusions emerge. First, all DNA's so far examined contain relatively long segments that differ in composition. Second, the phage DNA's so far examined fall into two classes. DNA molecules from phages λ, 186, P2, and probably P22 are composed of a few long segments of dissimilar composition. Since the effect is to produce dissimilar halves, these may be called asymmetric DNA's. By contrast, phages T5, T7, and P1 contain DNA's of relatively uniform composition. The grouping suggests that phage λ may be taken as representative of a class. If so, asymmetry of DNA structure, clustering of genes of related function in the genetic map, and propensity toward interspecific genetic recombination form a seemingly harmonious set of class characteristics.

BIBLIOGRAPHY

Bear, P. D., and A. Skalka, The molecular origin of lambda prophage mRNA. *Proc. Natl. Acad. Sci. U.S., 62,* 385–388, 1969.

Makover, S., A preferred origin for the replication of lambda DNA. *Cold Spring Harbor Symp. Quant. Biol., 33,* 621–622, 1968.

Skalka, A., Nucleotide distribution and functional orientation in the deoxyribonucleic acid of phage ϕ80. *J. Virology, 3,* 150–156, 1969.

Skalka, A., *see also* Bear, P. D.

Yamagishi, H., Single strand interruptions in PBS 1 bacteriophage DNA molecule. *J. Mol. Biol., 35,* 623–633, 1968.

PERSONNEL

Year ended June 30, 1969

Elizabeth M. Bocskay, Chief Clerk
Elizabeth Burgi, Associate in Microbiology
Agnes C. Fisher, Secretary to Director; Editor
Alfred D. Hershey, Director
Laura J. Ingraham, Research Assistant
Shraga Makover, Carnegie Institution Fellow
Barbara McClintock, Distinguished Service Member
David H. Parma, National Science Foundation Postdoctoral Fellow
Jennie S. Pope, Curator of Drosophila Stocks
Anna Marie Skalka, Carnegie Corporation Fellow
Carole E. Thomason, Technical Assistant
Hideo Yamagishi, Carnegie Institution Fellow

Temporary

Robert A. Weisberg, Guest Investigator

Bibliography

July 1, 1968–June 30, 1969

PUBLICATIONS OF THE INSTITUTION

Carnegie Institution of Washington Year Book 67. Octavo, xii + *76* + 609 pages, 22 plates, 262 figures, Washington, D. C., January 1969.

PUBLICATIONS BY THE PRESIDENT

Caryl P. Haskins

Report of the President. Reprinted from *Carnegie Institution of Washington Year Book 67,* 86 pages, 2 plates, 6 figures, January 1969.

The way of the future (An address presented at Queens College of the City University of New York, March 28, 1968), Queens College Press, Flushing, New York, 1968.

The humanities and the natural sciences: partnership and paradigm. *ACLS Newsletter,* Vol. 20, No. 1, January–February 1969, pp. 20–37.

The inspiration of the amateur. *Graduate School Chronicle* (University of Maryland), Spring 1969, pp. 1, 3–6.

The testament of the years between (The *Encyclopaedia Britannica* Lecture, presented at the University of Edinburgh, 1968), Edinburgh University Press, 1969.

PUBLICATION BY THE EXECUTIVE OFFICER

Edward A. Ackerman

Recursos Naturales y Desarrollo Industrial, Provincia de Magallanes. With David F. Bramhall and Orris C. Herfindahl. Published for the Ford Foundation Urban and Regional Development Advisory Program in Chile, Santiago, Chile, 1968.

Administrative Reports

Report of the Executive Committee

To the Trustees of the Carnegie Institution of Washington

Gentlemen:

In accordance with the Provisions of the By-Laws, the Executive Committee submits this report to the Annual Meeting of the Board of Trustees.

During the fiscal year ending June 30, 1969, the Executive Committee held four meetings. Printed accounts of these meetings have been or will be mailed to each Trustee.

The estimate of expenditures for the fiscal year beginning July 1, 1969, has been reviewed by the Executive Committee.

The terms of office of the Chairmen of all Committees of the Board expire on May 2, 1969. The terms of the following members of Committees also expire on May 2, 1969:

Executive Committee
Carl J. Gilbert
Crawford H. Greenewalt
Richard S. Perkins

Finance Committee
Richard S. Perkins

Nominating Committee
Carl J. Gilbert

Henry S. Morgan, *Chairman*

May 2, 1969

Report of Auditors

LYBRAND, ROSS BROS. & MONTGOMERY

REPORT OF INDEPENDENT CERTIFIED PUBLIC ACCOUNTANTS

To the Auditing Committee of
Carnegie Institution of Washington:

We have examined the statement of assets and funds balances of Carnegie Institution of Washington as of June 30, 1969, and the related summary statement of changes in funds for the year then ended and the supporting exhibits and schedules. Our examination was made in accordance with generally accepted auditing standards, and accordingly included confirmation from the custodian of investments held at June 30, 1969, and such tests of the accounting records and such other auditing procedures as we considered necessary in the circumstances. We previously examined and reported upon the financial statements of the Institution for the year ended June 30, 1968.

These statements have been prepared on the general basis of cash receipts and disbursements and, as a result, omit accrued income, liabilities and provision for depreciation. Accordingly, they do not purport to present financial position or results of operations as they would appear had generally accepted accrual basis accounting principles been applied in their preparation.

In our opinion, the accompanying financial statements and supporting exhibits and schedules (Pages 4-17) present fairly the assets and funds balances of Carnegie Institution of Washington at June 30, 1969 and 1968, and the changes in funds for the year ended June 30, 1969, on the basis indicated above consistently applied.

Lybrand, Ross Bros. & Montgomery

Washington, D. C.
October 2, 1969

STATEMENT A ASSETS AND FUNDS

JUNE 30, 1969 and 1968

ASSETS

	1969	1968
Cash	$ 688,866.39	$ 273,715.58
Advances	38,410.02	44,265.83
Investments (cost)*, Schedule 2:		
Governmental obligations	1,892,625.00	2,907,695.31
Nongovernmental bonds	39,123,254.31	41,176,949.69
Corporate stocks	37,711,702.61	34,539,849.64
Mortgage	13,983.06	16,397.31
Land (cost)	389,306.96	368,760.86
Buildings and equipment (cost)	6,748,789.29	6,497,273.68
Total assets	$86,606,937.64	$85,824,907.90

FUNDS

Operating Fund, Exhibit 1	$ 2,318,156.83	$ 918,043.52
Restricted Grants, Exhibit 2	105,817.51	(5,893.90)
Endowment and Special Funds, Exhibit 3	77,044,867.05	78,046,723.74
Land, Buildings, and Equipment Fund, Exhibit 4	7,138,096.25	6,866,034.54
Total funds	$86,606,937.64	$85,824,907.90

* Approximate market value on June 30, 1969: $109,262,034.

STATEMENT B

SUMMARY STATEMENT OF CHANGES IN FUNDS

FOR THE YEAR ENDED JUNE 30, 1969

	Operating Fund (Exhibit 1)	Restricted Grants (Exhibit 2)	Endowment and Special Funds (Exhibit 3)	Land, Buildings and Equipment (Exhibit 4)	Total
Balance, July 1, 1968	$ 918,043.52	($ 5,893.90)	$78,046,723.74	$6,866,034.54	$85,824,907.90
Additions:					
Realized capital gain, net	....	....	360,107.91	....	360,107.91
Investment income					
Interest	....	....	2,077,434.79	....	2,077,434.79
Dividends	....	....	2,135,892.53	....	2,135,892.53
Restricted grants	....	677,943.00	....	....	677,943.00
Gifts	....	....	66,494.44	....	66,494.44
Other income	....	....	59,125.64	....	59,125.64
Expenditures capitalized					
Current year	....	....	....	303,981.32	303,981.32
Prior year	....	....	....	120,656.01	120,656.01
Appropriations					
Budget	4,697,212.00	....	(4,697,212.00)	....	....
Carnegie Southern Observatory	1,000,000.00	....	(1,000,000.00)	....	....
Employee benefits, Bush Gift	3,700.00	....	(3,700.00)	....	....
	5,700,912.00	677,943.00	(1,001,856.69)	424,637.33	5,801,635.64
Deductions:					
Expenditures	4,300,798.69	566,231.59	....	....	4,867,030.28
Disposition of equipment	....	....	....	152,575.62	152,575.62
	4,300,798.69	566,231.59	....	152,575.62	5,019,605.90
Net change during year	1,400,113.31	111,711.41	(1,001,856.69)	272,061.71	782,029.74
Balance, June 30, 1969	$2,318,156.83	$105,817.51	$77,044,867.05	$7,138,096.25	$86,606,937.64

EXHIBIT 1 CHANGES IN OPERATING FUND

FOR THE YEAR ENDED JUNE 30, 1969

Balance, July 1, 1968		$ 918,043.52
Appropriations, Statement B:		
Budget, July 1, 1968, to June 30, 1969—Exhibit 3	$4,697,212.00	
Carnegie Southern Observatory	1,000,000.00	
Employee benefits, special, Bush Gift	3,700.00	5,700,912.00
Total available for expenditures		6,618,955.52
Expenditures:		
Salaries	2,205,623.72	
Laboratory	365,788.18	
Employee benefits, retirement contributions	276,077.39	
Employee benefits, other	133,806.87	
Equipment	297,557.98	
Fellowships	155,794.89	
Building	181,157.51	
Operating	138,456.43	
Travel	94,243.81	
Publications	84,097.99	
Awards	76,930.16	
Financial advisory services	74,016.26	
Taxes	78,367.75	
Consulting fees and insurance	77,620.94	
Rent	24,606.09	
Shop	18,309.70	
Entertainment	9,708,59	
Dormitory	8,634.43	
Total expenditures		4,300,798.69
Balance, June 30, 1969		$2,318,156.83

EXHIBIT 2 CHANGES IN RESTRICTED GRANTS

FOR THE YEAR ENDED JUNE 30, 1969

	Balance July 1, 1968	Grants	Expenditures Salaries	Expenditures Other	Balance June 30, 1969
Carnegie Corporation of New York	$49,886.14	$ 80,000.00	......	$104,799.13	$ 25,087.01
Helen Hay Whitney Foundation	583.37	8,500.00	......	8,458.37	625.00
Jet Propulsion Laboratory....	351.18	....	......	48.20	302.98
National Aeronautics & Space Administration	(32,876.58)	182,272.00	$ 6,171.28	158,071.88	(14,847.74)
National Science Foundation	(12,445.02)	332,500.00	15,454.39	208,151.79	96,448.80
Office of Naval Research.....	(9,119.39)	27,133.00	2,594.76	16,248.85	(830.00)
Public Health Service........	(3,662.18)	47,538.00	19,556.64	25,287.72	(968.54)
University of Minnesota......	1,388.58	....	......	1,388.58	......
Total	($5,893.90)	$677,943.00	$43,777.07	$522,454.52	$105,817.51*

* Does not include grants to be received as follows:

National Aeronautics & Space Administration.....	$105,211.00
National Science Foundation.....................	254,023.05
Office of Naval Research.........................	6,164.00
Public Health Service	4,650.00
	$370,048.05

EXHIBIT 3

CHANGES IN ENDOWMENT AND SPECIAL FUNDS

FOR THE YEAR ENDED JUNE 30, 1969

	Balance July 1, 1968	Realized Capital Gain, net	Investment Income	Gifts and Other Income	Appropriations	Transfers	Balance June 30, 1969
Endowment Fund:							
Gifts							
Andrew Carnegie	$22,000,000.00	....	....	....	....	....	$22,000,000.00
Carnegie Corporation of New York	10,000,000.00	....	....	....	....	....	10,000,000.00
Realized capital gain, net	31,380,349.98	$298,592.65	....	....	....	....	31,678,942.63
Unrestricted Capital Fund							
Gifts	105,268.99	....	....	$ 1,875.00	....	....	107,143.99
Realized capital gain, net	5,292,382.15	58,309.16	....	....	....	....	5,350,691.31
Income							
Andrew Carnegie, reserve	2,500,000.00	....	....	....	....	....	2,500,000.00
Other	538,829.29	....	....	....	....	....	538,829.29
Working Capital Fund							
Income	4,725,093.92	....	$4,175,009.13	....	$4,978,273.71	$ 59,125.64	3,980,954.98
Sales							
Assets	....	....	....	14,177.35	....	(14,177.35)	....
Publications	....	....	....	18,394.61	....	(18,394.61)	....
Services	....	....	....	4,126.77	....	(4,126.77)	....
Refunds	....	....	....	17,647.16	....	(17,647.16)	....
Publication royalties	....	....	....	4,779.75	....	(4,779.75)	....
Special Funds:							
Astronomy	683,683.29	....	....	....	683,683.29	....	....
Bush Gift	19,709.43	141.52	1,654.15	....	5,200.00	....	16,305.10
Colburn	190,172.51	892.33	10,429.76	....	10,110.00	....	191,384.60
Hale Relief	6,996.38	31.54	368.56	....	350.00	....	7,046.48
Harkavy	9,475.26	38.98	455.57	....	450.00	....	9,519.81
Morgenroth	32,806.25	105.45	1,226.77	218.55	290.00	....	34.067.02
Special Instrumentation	....	4.76	905.74	64,400.89	....	....	65,311.39
Teeple	19,351.50	87.09	1,018.06	....	985.00	....	19,471.65
Wood	542,604.79	1,904.43	22,259.58	....	21,570.00	....	545,198.80
Total	$78,046,723.74	$360,107.91	$4,213,327.32	$125,620.08	$5,700,912.00	—0—	$77,044,867.05

EXHIBIT 4

CHANGES IN LAND, BUILDINGS, AND EQUIPMENT FUND

FOR THE YEAR ENDED JUNE 30, 1969

	Balance July 1, 1968	Expenditures *	Deductions	Balance June 30, 1969	Classification of June 30, 1969, Balance: Land	Buildings	Equipment
Department of Plant Biology	$ 212,831.07	$ 6,340.36	$ 1,695.06	$ 217,476.37	....	$ 75,371.81	$ 142,104.56
Geophysical Laboratory	910,307.93	66,300.42	29,142.00	947,466.35	22,907.27	147,476.52	777,082.56
Mount Wilson Observatory	1,809,679.94	73,035.12	15,872.55	1,866,842.51	47,824.97	313,087.27	1,505,930.27
Department of Terrestrial Magnetism	1,155,576.85	172,320.65	72,397.06	1,255,500.44	74,449.98	323,864.47	857,185.99
Department of Embryology	452,130.70	96,258.05	16,846.71	531,542.04	....	....	531,542.04
Genetics Research Units	1,271,428.13	5,464.43	6,945.54	1,269,947.02	29,880.54	964,465.47	275,601.01
Office of Administration	1,054,079.92	4,918.30	9,676.70	1,049,321.52	214,244.20	718,943.49	116,133.83
Total	$6,866,034.54	$424,637.33	$152,575.62	$7,138,096.25	$389,306.96	$2,543,209.03	$4,205,580.26

* Expenditures for Equipment:	
Operating Fund	$297,557.98
Restricted Grants	5,614.16
Expenditures Capitalized:	
Current Year	809.18
Prior Year	120,656.01
Total	$424,637.33

SCHEDULE 1

BUDGET SUMMARY OF OPERATING FUND

FOR THE YEAR ENDED JUNE 30, 1969

	Unexpended Appropriations July 1, 1968	Appropriations	Transfers and Allotments	Total Expenditures	Unexpended Appropriations June 30, 1969
Plant Biology	$ 5,183.88	$ 268,654.94	($ 16,292.79)	$ 252,762.04	$ 4,783.99
Geophysical Laboratory	38,045.53	796,708.70	(29,005.51)	761,190.00	44,558.72
Mount Wilson Observatory	13,139.79	1,886,508.86	(72,894.49)	887,599.64	939,154.52
Terrestrial Magnetism	65,772.43	865,548.70	(41,791.36)	844,217.36	45,312.41
Embryology	33,351.75	657,156.90	(25,167.18)	617,574.99	47,766.48
Genetics Research Units	2,954.11	175,148.90	(28,758.76)	142,330.54	7,013.71
Research Projects, etc.	83,229.20	78,725.00	(25,205.40)	85,978.24	50,770.56
Office of Administration	8,486.22	469,460.00	(41,827.70)	433,357.62	2,760.90
Consulting fees, insurance, taxes	6,171.00	45,000.00	30,044.77	79,799.11	1,416.66
Contingent operating fund	80,421.06	200,000.00	(253,921.06)	....	26,500.00
Financial advisory services	16,739.22	76,000.00	(2,722.96)	74,016.26	16,000.00
General publications	6,500.00	67,600.00	(21,591.94)	45,078.06	7,430.00
Employee benefits, retirees	326,357.48	96,100.00	(10,366.67)	64,949.53	347,141.28
Employee benefits, special	7,991.85	7,700.00	(2,789.47)	11,945.30	957.08
Unallocated Appropriations	223,700.00	10,600.00	542,290.52	....	776,590.52
Total	$918,043.52	$5,700,912.00	—0—	$4,300,798.69	$2,318,156.83

Principal Amount	Description	Maturity	Book Value	Approximate Market Value
	Federal Agency Bonds			
$ 400,000	Federal National Mortgage Association, 4⅝s	1970	$ 394,500.00	$ 390,248
500,000	Federal National Mortgage Association, 5⅛s	1972	498,125.00	465,000
1,000,000	Federal National Mortgage Association, Part. Certificates, 5½s	1973	1,000,000.00	932,500
$ 1,900,000	Total		$ 1,892,625.00	$ 1,787,748
	Foreign and International Bank Bonds			
$ 700,000	Alberta Government Telephone, Commission Deb., 4¾s	1989	$ 700,000.00	$ 469,000
750,000	Alcan Aluminum Corporation, Prom. Note, 4¾s	1984	750,000.00	575,625
489,000	Aluminium Co. of Canada, Ltd., S. F. Deb., 4½s	1980	494,013.40	386,310
146,000	Australia (Commonwealth of), 4½s	1971	143,810.00	136,145
114,000	Australia (Commonwealth of), 5s	1972	114,000.00	104,310
466,000	Australia (Commonwealth of), 5½s	1982	467,843.20	391,440
750,000	Bell Telephone Co. of Canada, 1st Mtg. Series X, 4⅞s	1988	747,300.00	523,125
250,000	British Columbia Power Commission, S. F. Deb. Series L, 4⅜s	1987	245,000.00	170,000
750,000	Industrial Acceptance Corp. Ltd., Sec. Note Series Z, 5¼s	1982	750,000.00	534,375
125,000	Intl. Bank for Reconstruction & Development, 3s	1976	125,000.00	100,000
125,000	Intl. Bank for Reconstruction & Development, 3⅜s	1975	123,125.00	100,000
250,000	Intl. Bank for Reconstruction & Development, 4½s	1977	250,000.00	205,000

Principal Amount	Description	Maturity	Book Value	Approximate Market Value
	Foreign and Industrial Bank Bonds—Continued			
751,000	Quebec Hydro-Electric Commission, S. F. Deb., 5s........................	1988	737,857.50	510,680
200,000	Shawinigan Water & Power Co., 1st Mtg. & Collat. Tr. S. F. Series M, 3s.......	1971	200,720.00	182,500
1,000,000	Shell Funding Corp., Collat. Tr. Series B, 4¾s........................	1985	1,000,000.00	800,000
500,000	Toronto (Municipality of Metropolitan), S. F. Deb., 5s........................	1979	498,637.50	400,000
$ 7,366,000	Total		$ 7,347,306.60	$ 5,588,510
	Public Utility Bonds			
$ 750,000	Colonial Pipeline Co., Sec. Note Series A, 4.829s......................	1990	$ 750,000.00	$ 558,750
250,000	Columbia Gas System, Inc., Series F, 3⅞s........................	1981	245,937.50	177,500
237,000	Columbus & Southern Ohio Electric Co., 1st Mtg., 3¼s......................	1970	237,938.01	223,076
300,000	Consolidated Edison Co. of N.Y., 1st & Ref. Mtg. Series N, 5s..........	1987	301,406.52	229,500
4,000	Consumers Power Co., 1st Mtg., 4¾s......................	1987	4,015.48	3,055
200,000	Minnesota Power & Light Co., 1st Mtg., 3⅛s......................	1975	200,935.77	158,750
250,000	Niagara Mohawk Power Corp., Gen. Mtg., 3⅝s......................	1986	251,843.98	165,938
400,000	Niagara Mohawk Power Corp., Gen. Mtg., 4⅞s......................	1987	402,098.79	310,500
200,000	Pacific Gas & Electric Co., 1st & Ref. Mtg. Series X, 3⅛s........	1984	200,874.90	127,750
250,000	Pacific Gas & Electric Co., 1st & Ref. Mtg. Series BB, 5s.........	1989	251,209.26	192,500
250,000	Pacific Power & Light Co., 1st Mtg., 4⅜s........................	1986	251,818.07	165,313
236,000	Potomac Electric Power Co., Deb., 4⅝s	1982	239,125.84	171,985
200,000	Public Service Co. of Indiana, 1st Mtg. Series F, 3⅛s...............	1975	201,068.99	159,000
400,000	Public Service Co. of Indiana, 1st Mtg. Series L, 4⅞s..............	1987	400,000.00	277,000

Principal Amount	Description	Maturity	Book Value	Approximate Market Value
	Public Utility Bonds—Continued			
500,000	Public Service Electric & Gas Co., 1st & Ref. Mtg., 4⅞s	1987	502,888.77	388,125
250,000	Southern California Edison Co., 1st & Ref. Mtg. Series H, 4¼s	1982	250,937.56	180,000
200,000	Southern California Edison Co., 1st & Ref. Mtg. Series J, 4⅞s	1982	201,130.17	150,500
300,000	Washington Water Power Co., 1st Mtg., 4⅞s	1987	300,000.00	209,250
$ 5,177,000	Total		$ 5,193,229.61	$ 3,848,492
	Communication Bonds			
$ 400,000	Illinois Bell Telephone Co., 1st Mtg. Series E, 4¼s	1988	$ 402,981.08	$ 283,500
200,000	Mountain States Telephone & Telegraph Co., Deb. 3⅛s	1978	200,280.00	148,750
100,000	New York Telephone Co., Ref. Mtg. Series E, 3⅛s	1978	100,394.47	73,500
200,000	Pacific Telephone & Telegraph Co., Deb., 3¼s	1978	200,882.86	148,750
250,000	Southern Bell Telephone & Telegraph Co., Deb. 4s	1983	250,601.26	181,563
300,000	Southwestern Bell Telephone Co., Deb., 3⅛s	1983	302,250.00	196,500
$ 1,450,000	Total		$ 1,457,389.67	$ 1,032,563
	Railroad Bonds			
$ 100,000	Chesapeake & Ohio Railway Co., Gen. Mtg., 4½s	1992	$ 99,500.00	$ 68,500
267,000	Fort Worth & Denver Railway Co., 1st Mtg., 4⅜s Guar.	1982	268,108.23	181,560
$ 367,000	Total		$ 367,608.23	$ 250,060
	Industrial and Miscellaneous Bonds			
$ 1,000,000.00	Boeing Co., Notes, 6⅜s	1986	$ 1,000,000.00	$ 855,000
550,000.00	C.I.T. Financial Corp., Deb., 4¾s	1970	536,937.50	522,500
960,000.00	Columbia Broadcasting System, Inc., Prom. Note, 5½s	1991	960,000.00	794,400
400,000.00	Commercial Credit Co., Note, 3⅝s	1976	402,761.12	302,000
700,000.00	Commercial Credit Co., Note, 4¾s	1982	700,000.00	500,500

Principal Amount	Description	Maturity	Book Value	Approximate Value Market
	Industrial and Miscellaneous Bonds—Continued			
325,000.00	Crown Zellerbach Corp., Prom. Note, 4⅜s	1981	325,000.00	268,125
483,000.00	Erie Mining Company, 1st Mtg. Series B, 4½s	1983	468,935.04	326,025
1,000,000.00	First National City Bank, Capital Conv. Notes, 4s	1990	1,075,715.00	975,000
500,000.00	FMC Corp., S. F. Deb., 3.8s	1981	500,000.00	355,000
187,000.00	Four Corners Pipe Line Co., Sec. Note, 5s	1982	187,000.00	159,418
500,000.00	General Electric Credit Corp. (N.Y.), Sub. Note, 4¾s	1987	500,000.00	318,750
500,000.00	General Electric Credit Corp. (N.Y.), Prom. Note, 5s	1975	500,000.00	422,500
200,000.00	General Motors Acceptance Corp., Deb., 3½s	1972	200,000.00	177,500
480,000.00	General Motors Acceptance Corp., Deb., 4s	1979	435,037.50	355,200
1,000,000.00	General Motors Acceptance Corp., Deb., 4⅞s	1987	990,000.00	743,750
200,000.00	General Motors Acceptance Corp., Deb., 5s	1977	195,000.00	168,500
200,000.00	General Motors Acceptance Corp., Deb., 5s	1981	199,000.00	162,500
150,000,00	General Portland Cement Co., Conv. Sub. Deb., 5s	1977	154,500.00	117,000
190,000.00	Grant W. T. Financial Corporation, Promissory Note	1969	190,000.00	190,000
750,000.00	Household Finance Corp., Deb., 4⅞s	1993	746,250.00	517,500
1,000,000.00	Hystron Fibers, Inc., Notes, 5¾s	1986	1,000,000.00	842,500
357,913.55	Instlcorp, Inc., Collat. Tr. Notes, A-16	1991	345,957.98	290,804
297,069.72	Instlcorp, Inc., Collat. Tr. Note Series A-19	1991	287,240.18	240,626
161,820.38	Instlcorp, Inc., Collat. Tr. Note, A-21	1991	156,156.69	130,670
208,335.32	Instlcorp, Inc., Collat. Tr. Note, A-23	1991	204,960.39	168,751
640,659.68	Instlcorp, Inc., Collat. Tr. Note, A-36	1992	614,494.87	501,316
400,000.00	Intl. Harvester Credit Corp., Deb., 4⅝s	1979	398,000.00	300,000
232,000.00	Kaiser Aluminum & Chemical Corp., 1st Mtg., 5½s	1987	232,000.00	182,120
676,666.67	Kresge (S. S.) Company, Prom. Note, 4⅞s	1983	676,666.67	512,574
200,000.00	Montgomery Ward Credit Corp., Deb., 4⅞s	1980	199,000.00	138,000

Principal Amount	Description	Maturity	Book Value	Approximate Market Value
	Industrial and Miscellaneous Bonds—Continued			
95,000.00	National Dairy Products Corp., Deb., 2¾s	1970	94,654.50	88,825
700,000.00	Owens-Illinois, Inc., Notes, 5s	1991	700,000.00	514,500
1,871,000.00	Penney (J. C.) Company, Inc., Conv. Sub. Deb., 4¼s	1993	2,092,961.25	2,072,133
525,000.00	Sears Roebuck Acceptance Corp., Sub. Deb., 4⅝s	1977	511,505.00	425,250
1,000.000.00	Shell Oil Company, Deb., 5s	1991	1,000,000.00	777,500
250,000.00	Spiegel, Inc., Deb., 5s	1987	250,000.00	175,625
456,000.00	Statewide Stations Inc., Sec. Note, 4⅝s	1994	456,000.00	318,060
215,000.00	Talcott (James) Inc., Senior Note, 5½s	1980	212,850.00	179,525
700,000.00	Texas Gulf Sulphur Co., Prom. Note, 4.7s	1989	700,000.00	540,750
452,963.01	Trailer Train Co., 4⅞s	1976	452,963.01	391,813
296,000.00	Tremarco Corporation, 1st Mtg. Series E, 5s	1983	296,000.00	244,200
700,000.00	United Air Lines, Inc., Notes, 5s	1984	700,000.00	521,500
680,000.00	United Shoe Machinery Corporation, S. F. Deb., 5¾s	1992	678,300.00	567,800
542,500.00	U.S. Steel, S. F. Sub. Deb., 4⅝s	1996	443,873.50	381,106
1,048,000.00	Westinghouse Electric Corp., Demand Note		1,048,000.00	1,048,000
250,000.00	Whirlpool Corporation, S. F. Deb., 3½s	1980	250,000.00	171,875
490,000.00	Woolworth (F. W.) Company, Prom. Note, 5s	1982	490,000.00	344,225
$24,720,928.33	Total		$24,757,720.20	$20,301,216
$40,980,928.33	Bonds, funds invested		$41,015,879.31	$32,808,589
	Mortgage			
$ 13,983.06	Alfred D. Hershey and Harriet D. Hershey, 5½s	1974	$ 13,983.06	$ 13,983

Number of Shares	Description	Book Value	Approximate Market Value
	Common Stocks		
23,110	American Electric Power Co., Inc.	$ 162,703.74	$ 768,408
65,868	American Smelting & Refining Co.	1,360,609.98	2,083,076
42,352	American Telephone & Telegraph Company	1,161,275.59	2,297,596
32,000	Armstrong Cork Company	131,908.39	1,168,000
11,000	Avon Products, Inc.	956,691.61	1,702,250
2,000	Burlington Industries, Inc.	86,634.16	70,000
34,800	Caterpillar Tractor Co.	601,472.84	1,757,400
24,000	Chesebrough-Pond's Inc.	746,765.43	1,047,000
16,500	Chicago Pneumatic Tool Co.	601,964.31	561,000
39,200	Coca-Cola Company (The)	628,984.09	2,724,400
36,000	Continental Oil Company (Del.)	146,960.65	1,255,500
2,500	Corning Glass Works	59,631.83	677,500
43,972	Eastman Kodak Company	443,434.12	3,297,900
24,000	Federated Department Stores, Inc.	582,805.81	900,000
15,104	First National City Bank	348,278.77	979,872
19,400	Ford Motor Company	577,047.36	916,650
30,627	General Electric Company	767,899.37	2,756,430
13,800	General Foods Corp.	1,210,911.44	1,124,700
35,419	General Motors Corporation	1,143,847.99	2,758,255
36,200	Gillette Company	1,239,112.08	1,905,025
83,424	Goodyear Tire & Rubber Company	1,702,971.74	2,450,580
40,012	Gulf Oil Corporation	154,333.51	1,530,459
31,668	International Business Machines Corp.	851,095.87	10,695,867
61,175	International Nickel Co. of Canada Ltd.	1,296,074.87	2,240,534
57,000	International Paper Company	2,112,936.24	2,194,500
12,900	Johnson & Johnson	750,762.93	1,460,925
47,630	Kennecott Copper Corporation	1,308,403.57	1,952,830
15,000	Merck & Co., Inc.	107,286.55	1,389,375
17,000	Minnesota Mining & Manufacturing Co.	1,691,650.93	1,717,000
30,700	Mobil Oil Corporation	1,099,916.18	1,799,788
5,000	National Cash Register Company	720,712.50	639,375
33,600	Panhandle Eastern Pipe Line Co.	1,067,554.69	1,033,200
9,000	Penn. Central Co.	614,232.68	444,375
61,400	Philip Morris Incorporated	1,551,034.72	1,765,250
4,600	Sears, Roebuck and Co.	207,078.03	318,550
32,800	Southern Co.	878,283.72	885,600
23,561	Standard Oil Co. (New Jersey)	671,594.17	1,828,923
24,190	Texaco Inc.	249,172.89	1,826,345
43,500	Texas Gulf Sulphur Co.	1,257,455.80	1,103,813
44,000	TRW Inc.	2,214,408.91	1,540,000
7,600	Texas Utilities Co.	104,621.78	400,900
56,800	U. S. Plywood-Champion Papers Inc.	697,928.16	1,874,400
35,999	Virginia Electric & Power Co.	636,133.86	967,473
20,000	Whirlpool Corporation	943,953.26	1,100,000
26,100	Xerox Corp.	1,863,165.49	2,528,438
1,372,511	Common stocks, funds invested	$37,711,702.61	$ 76,439.462
	Aggregate investments	$78,741,564.98	$109,262,034

SUMMARY OF INVESTMENT TRANSACTIONS
FOR THE YEAR ENDED JUNE 30, 1969

Cash, July 1, 1968				($ 184,712.31)
	Sales and Redemptions			
	Capital Gain	Capital Loss	Book Value	
Bonds	$ 127,466.65	$ 744,943.36	$ 9,262,253.15	
Mortgage	....	....	2,414.25	
Common Stocks	1,081,000.03	103,415.41	4,950,804.21	
	1,208,466.68	848,358.77	14,215,471.61	
Realized capital gain, net—Statement B	....	360,107.91	360,107.91	
	$1,208,466.68	$1,208,466.68		
Total sales and redemptions				14,575,579.52
Income applied to amortization of bond premium				5,154.61
Gifts				49,768.54
Total				14,445,790.36
	Acquisitions			
Bonds			6,198,642.07	
Common Stock			8,122,657.18	
Total acquisitions				14,321,299.25
Cash, June 30, 1969				$ 124,491.11

Abstract of Minutes

of the Seventy-First Meeting of the Board of Trustees

The annual meeting of the Board of Trustees was held in the Board Room of the Administration Building on Friday, May 2, 1969. Chairman James N. White called the meeting to order.

The following Trustees were present: Michael Ference, Jr., Crawford H. Greenewalt, Caryl P. Haskins, Robert A. Lovett, Keith S. McHugh, Henry S. Morgan, William I. Myers, Garrison Norton, Robert M. Pennoyer, Richard S. Perkins, William M. Roth, William W. Rubey, Frank Stanton, Charles P. Taft, Charles H. Townes, Juan T. Trippe, and James N. White.

The minutes of the Seventieth Meeting were approved.

William T. Golden was elected a member of the Board of Trustees.

The following were elected for one-year terms: Henry S. Morgan as Chairman of the Executive Committee, Richard S. Perkins as Chairman of the Finance Committee, Garrison Norton as Chairman of the Nominating Committee, Keith S. McHugh as Chairman of the Auditing Committee, and Frank Stanton as Chairman of the Retirement Committee.

Vacancies in standing committees, with terms ending in 1972, were filled as follows: Garrison Norton was elected a member of the Nominating Committee; Carl J. Gilbert, Crawford H. Greenewalt, and Richard S. Perkins were elected members of the Executive Committee; and Robert M. Pennoyer and Richard S. Perkins were elected members of the Finance Committee.

The reports of the Executive Committee, the Finance Committee, the Retirement Committee and the Auditing Committee were accepted. On the recommendation of the latter it was resolved that Lybrand, Ross Bros. and Montgomery be appointed as public accountants for the fiscal year beginning July 1, 1969.

The annual report of the President was accepted.

To provide for the operation of the Institution for the fiscal year beginning July 1, 1969, and upon recommendation of the Executive Committee, the sum of $4,651,730 was appropriated, the appropriation to be made specifically in the amount of $4,484,130 from the Working Capital Fund, $10,110 from the Colburn Fund, $370 from the Hale Fund, $450 from the Harkavy Fund, $290 from the Morgenroth Fund, $985 from the Teeple Fund, $21,995 from the Wood Fund, and $133,400 from Restricted Grants.

Articles of Incorporation

Fifty-eighth Congress of the United States of America;

At the Second Session,

Begun and held at the City of Washington on Monday, the seventh day of December, one thousand nine hundred and three.

AN ACT

To incorporate the Carnegie Institution of Washington.

Be it enacted by the Senate and House of Representatives of the United States of America in Congress assembled, That the persons following, being persons who are now trustees of the Carnegie Institution, namely, Alexander Agassiz, John S. Billings, John L. Cadwalader, Cleveland H. Dodge, William N. Frew, Lyman J. Gage, Daniel C. Gilman, John Hay, Henry L. Higginson, William Wirt Howe, Charles L. Hutchinson, Samuel P. Langley, William Lindsay, Seth Low, Wayne MacVeagh, Darius O. Mills, S. Weir Mitchell, William W. Morrow, Ethan A. Hitchcock, Elihu Root, John C. Spooner, Andrew D. White, Charles D. Walcott, Carroll D. Wright, their associates and successors, duly chosen, are hereby incorporated and declared to be a body corporate by the name of the Carnegie Institution of Washington and by that name shall be known and have perpetual succession, with the powers, limitations, and restrictions herein contained.

SEC. 2. That the objects of the corporation shall be to encourage, in the broadest and most liberal manner, investigation, research, and discovery, and the application of knowledge to the improvement of mankind; and in particular—

(a) To conduct, endow, and assist investigation in any department of science, literature, or art, and to this end to cooperate with governments, universities, colleges, technical schools, learned societies, and individuals.

(b) To appoint committees of experts to direct special lines of research.

(c) To publish and distribute documents.

(d) To conduct lectures, hold meetings, and acquire and maintain a library.

(e) To purchase such property, real or personal, and construct such building or buildings as may be necessary to carry on the work of the corporation.

(f) In general, to do and perform all things necessary to promote the objects of the institution, with full power, however, to the trustees hereinafter appointed and their successors from time to time to modify the conditions and regulations under which the work shall be carried on, so as to secure the application of the funds in the manner best adapted to the conditions of the time, provided that the objects of the corporation shall at all times be among the foregoing or kindred thereto.

SEC. 3. That the direction and management of the affairs of the corporation and the control and disposal of its property and funds shall be vested in a board of trustees, twenty-two in number, to be composed of the following individuals: Alexander Agassiz, John S. Billings, John L. Cadwalader, Cleveland H. Dodge, William N. Frew, Lyman J. Gage, Daniel C. Gilman, John Hay, Henry L. Higginson, William Wirt Howe, Charles L. Hutchinson, Samuel P. Langley, William Lindsay, Seth Low, Wayne MacVeagh, Darius O. Mills, S. Weir Mitchell, William W. Morrow, Ethan A. Hitchcock, Elihu Root, John C. Spooner, Andrew D. White, Charles D. Walcott, Carroll D. Wright, who shall constitute the first board of trustees. The board of trustees shall have power from time to time to increase its membership to not more than twenty-seven members. Vacancies occasioned by death, resignation, or otherwise shall be filled by the remaining trustees in such manner as the by-laws shall prescribe; and the persons so elected shall thereupon become trustees and also members of the said corporation. The principal place of business of the said corporation shall be the city of Washington, in the District of Columbia.

SEC. 4. That such board of trustees shall be entitled to take, hold and administer the securities, funds, and property so transferred by said Andrew Carnegie to the trustees of the Carnegie Institution and such other funds or property as may at any time be given, devised, or bequeathed to them, or to such corporation, for the purposes of the trust; and with full power from time to time to adopt a common seal, to appoint such officers, members of the board of trustees or otherwise, and such employees as may be deemed necessary in carrying on the business of the corporation, at such salaries or with such remuneration as they may deem proper; and with full power to adopt by-laws from time to time and such rules or regulations as may be necessary to secure the safe and convenient transaction of the business of the corporation; and with full power and discretion to deal with and expend the income of the corporation in such manner as in their judgment will best promote the objects herein set forth and in general to have and use all powers and authority necessary to promote such objects and carry out the purposes of the donor. The said trustees shall have further power from time

to time to hold as investments the securities hereinabove referred to so transferred by Andrew Carnegie, and any property which has been or may be transferred to them or such corporation by Andrew Carnegie or by any other person, persons, or corporation, and to invest any sums or amounts from time to time in such securities and in such form and manner as are permitted to trustees or to charitable or literary corporations for investment, according to the laws of the States of New York, Pennsylvania, or Massachusetts, or in such securities as are authorized for investment by the said deed of trust so executed by Andrew Carnegie, or by any deed of gift or last will and testament to be hereafter made or executed.

SEC. 5. That the said corporation may take and hold any additional donations, grants, devises, or bequests which may be made in further support of the purposes of the said corporation, and may include in the expenses thereof the personal expenses which the trustees may incur in attending meetings or otherwise in carrying out the business of the trust, but the services of the trustees as such shall be gratuitous.

SEC. 6. That as soon as may be possible after the passage of this Act a meeting of the trustees hereinbefore named shall be called by Daniel C. Gilman, John S. Billings, Charles D. Walcott, S. Weir Mitchell, John Hay, Elihu Root, and Carroll D. Wright, or any four of them, at the city of Washington, in the District of Columbia, by notice served in person or by mail addressed to each trustee at his place of residence; and the said trustees, or a majority thereof, being assembled, shall organize and proceed to adopt by-laws, to elect officers and appoint committees, and generally to organize the said corporation; and said trustees herein named, on behalf of the corporation hereby incorporated, shall thereupon receive, take over, and enter into possession, custody, and management of all property, real or personal, of the corporation heretofore known as the Carnegie Institution, incorporated, as hereinbefore set forth under "An Act to establish a Code of Law for the District of Columbia, January fourth, nineteen hundred and two," and to all its rights, contracts, claims, and property of any kind or nature; and the several officers of such corporation, or any other person having charge of any of the securities, funds, real or personal, books or property thereof, shall, on demand, deliver the same to the said trustees appointed by this Act or to the persons appointed by them to receive the same; and the trustees of the existing corporation and the trustees herein named shall and may take such other steps as shall be necessary to carry out the purposes of this Act.

SEC. 7. That the rights of the creditors of the said existing corporation known as the Carnegie Institution shall not in any manner be impaired by the

passage of this Act, or the transfer of the property hereinbefore mentioned, nor shall any liability or obligation for the payment of any sums due or to become due, or any claim or demand, in any manner or for any cause existing against the said existing corporation, be released or impaired; but such corporation hereby incorporated is declared to succeed to the obligations and liabilities and to be held liable to pay and discharge all of the debts, liabilities, and contracts of the said corporation so existing to the same effect as if such new corporation had itself incurred the obligation or liability to pay such debt or damages, and no such action or proceeding before any court or tribunal shall be deemed to have abated or been discontinued by reason of the passage of this Act.

SEC. 8. That Congress may from time to time alter, repeal, or modify this Act of incorporation, but no contract or individual right made or acquired shall thereby be divested or impaired.

SEC. 9. That this Act shall take effect immediately.

J G Cannon

Speaker of the House of Representatives.

Wm P Frye

President of the Senate pro tempore.

Approved.
April 28. 1904.
Theodore Roosevelt

By-Laws of the Institution

Adopted December 13, 1904. Amended December 13, 1910, December 13, 1912, December 10 1937, December 15, 1939, December 13, 1940, December 18, 1942, December 12, 1947, December 10, 1954, October 24, 1957, May 8, 1959, May 13, 1960, May 10, 1963, May 15, 1964, March 6, 1967, and May 3, 1968.

ARTICLE I

The Trustees

1. The Board of Trustees shall consist of twenty-four members with power to increase its membership to not more than twenty-seven members. The Trustees shall hold office continuously and not for a stated term.

2. In case any Trustee shall fail to attend three successive annual meetings of the Board he shall thereupon cease to be a Trustee.

3. No Trustee shall receive any compensation for his services as such.

4. All vacancies in the Board of Trustees shall be filled by the Trustees by ballot at an annual meeting, but no person shall be declared elected unless he receives the votes of two-thirds of the Trustees present.

5. If, at any time during an emergency period, there be no surviving Trustee capable of acting, the President, the Director of each existing Department, and the Executive Officer, or such of them as shall then be surviving and capable of acting, shall constitute a Board of Trustees *pro tem,* with full powers under the provisions of the Articles of Incorporation and these By-Laws. Should neither the President, nor any such Director, nor the Executive Officer be capable of acting, the senior surviving Staff Member of each existing Department shall be a Trustee *pro tem* with full powers of a Trustee under the Articles of Incorporation and these By-Laws. It shall be incumbent on the Trustees *pro tem* to reconstitute the Board with permanent members within a reasonable time after the emergency has passed, at which time the Trustees *pro tem* shall cease to hold office. A list of Staff Member seniority, as designated annually by the President, shall be kept in the Institution's records.

ARTICLE II

Officers of the Board

1. The officers of the Board shall be a Chairman of the Board, a Vice-Chairman, and a Secretary, who shall be elected by the Trustees, from the members of the Board, by ballot to serve for a term of three years. All vacancies shall be filled by the Board for the unexpired term; provided, however, that the Executive Committee shall have power to fill a vacancy in the office of Secretary to serve until the next meeting of the Board of Trustees.

2. The Chairman shall preside at all meetings and shall have the usual powers of a presiding officer.

3. The Vice-Chairman, in the absence or disability of the Chairman, shall perform the duties of the Chairman.

4. The Secretary shall issue notices of meetings of the Board, record its transactions, and conduct that part of the correspondence relating to the Board and to his duties.

ARTICLE III

Executive Administration

The President

1. There shall be a President who shall be elected by ballot by, and hold office during the pleasure of, the Board, who shall be the chief executive officer of the Institution. The President, subject to the control of the Board and the Executive Committee, shall have general charge of all matters of administration and supervision of all arrangements for research and other work undertaken by the Institution or with its funds. He shall prepare and submit to the Board of Trustees and to the Executive Committee plans and suggestions for the work of the Institution, shall conduct its general correspondence and the correspondence with applicants for grants and with the special advisers of the Committee, and shall present his recommendations in each case to the Executive Committee for decision. All proposals and requests for grants shall be referred to the President for consideration and report. He shall have power to remove, appoint, and, within the scope of funds made available by the Trustees, provide for compensation of subordinate employees and to fix the compensation of such employees within the limits of a maximum rate of compensation to be established from time to time by the Executive Committee. He shall be *ex officio* a member of the Executive Committee.

2. He shall be the legal custodian of the seal and of all property of the Institution whose custody is not otherwise provided for. He shall sign and execute on behalf of the corporation all contracts and instruments necessary in authorized administrative and research matters and affix the corporate seal thereto when necessary, and may delegate the performance of such acts and other administrative duties in his absence to the Executive Officer. He may execute all other contracts, deeds, and instruments on behalf of the corporation and affix the seal thereto when expressly authorized by the Board of Trustees or Executive Committee. He may, within the limits of his own authorization, delegate to the Executive Officer authority to act as custodian of and affix the corporate seal. He shall be responsible for the expenditure and disbursement of all funds of the Institution in accordance with the directions of the Board and of the Executive Committee, and shall keep accurate accounts of all receipts and disbursements. Following approval by the Executive Committee he shall transmit to the Board of Trustees before its annual meeting a written report of the operations and business of the Institution for the preceding fiscal year with his recommendations for work and appropriations for the succeeding fiscal year.

3. He shall attend all meetings of the Board of Trustees.

4. There shall be an officer designated Executive Officer who shall be appointed by and hold office at the pleasure of the President, subject to the approval of the Executive Committee. His duties shall be to assist and act for the President as the latter may duly authorize and direct.

5. The President shall retire from office at the end of the fiscal year in which he becomes sixty-five years of age.

ARTICLE IV

Meetings and Voting

1. The annual meeting of the Board of Trustees shall be held in the City of Washington, in the District of Columbia, in May of each year on a date fixed by the Executive

Committee, or at such other time or such other place as may be designated by the Executive Committee, or if not so designated prior to May 1 of such year, by the Chairman of the Board of Trustees, or if he is absent or is unable or refuses to act, by any Trustee with the written consent of the majority of the Trustees then holding office.

2. Special meetings of the Board of Trustees may be called, and the time and place of meeting designated, by the Chairman, or by the Executive Committee, or by any Trustee with the written consent of the majority of the Trustees then holding office. Upon the written request of seven members of the Board, the Chairman shall call a special meeting.

3. Notices of meetings shall be given ten days prior to the date thereof. Notice may be given to any Trustee personally, or by mail or by telegram sent to the usual address of such Trustee. Notices of adjourned meetings need not be given except when the adjournment is for ten days or more.

4. The presence of a majority of the Trustees holding office shall constitute a quorum for the transaction of business at any meeting. An act of the majority of the Trustees present at a meeting at which a quorum is present shall be the act of the Board except as otherwise provided in these By-Laws. If, at a duly called meeting, less than a quorum is present, a majority of those present may adjourn the meeting from time to time until a quorum is present. Trustees present at a duly called or held meeting at which a quorum is present may continue to do business until adjournment notwithstanding the withdrawal of enough Trustees to leave less than a quorum.

5. The transactions of any meeting, however called and noticed, shall be as valid as though carried out at a meeting duly held after regular call and notice, if a quorum is present and if, either before or after the meeting, each of the Trustees not present in person signs a written waiver of notice, or consent to the holding of such meeting, or approval of the minutes thereof. All such waivers, consents, or approvals shall be filed with the corporate records or made a part of the minutes of the meeting.

6. Any action which, under law or these By-Laws, is authorized to be taken at a meeting of the Board of Trustees may be taken without a meeting if authorized in a document or documents in writing signed by all the Trustees then holding office and filed with the Secretary.

7. During an emergency period the term "Trustees holding office" shall, for purposes of this Article, mean the surviving members of the Board who have not been rendered incapable of acting for any reason including difficulty of transportation to a place of meeting or of communication with other surviving members of the Board.

ARTICLE V

Committees

1. There shall be the following Standing Committees, *viz.* an Executive Committee, a Finance Committee, an Auditing Committee, a Nominating Committee, and a Retirement Committee.

2. All vacancies in the Standing Committees shall be filled by the Board of Trustees at the next annual meeting of the Board and may be filled at a special meeting of the Board. A vacancy in the Executive Committee and, upon request of the remaining members of any other Standing Committee, a vacancy in such other Committee may be filled by the Executive Committee by temporary appointment to serve until the next meeting of the Board.

3. The terms of all officers and of all members of Committees, as provided for herein, shall continue until their successors are elected or appointed.

Executive Committee

4. The Executive Committee shall consist of the Chairman, Vice-Chairman, and Secretary of the Board of Trustees, the President of the Institution *ex officio,* and, in

addition, not less than five or more than eight Trustees to be elected by the Board by ballot for a term of three years, who shall be eligible for re-election. Any member elected to fill a vacancy shall serve for the remainder of his predecessor's term.

5. The Executive Committee shall, when the Board is not in session and has not given specific directions, have general control of the administration of the affairs of the corporation and general supervision of all arrangements for administration, research, and other matters undertaken or promoted by the Institution. It shall also submit to the Board of Trustees a printed or typewritten report of each of its meetings, and at the annual meeting shall submit to the Board a report for publication.

6. The Executive Committee shall have power to authorize the purchase, sale, exchange, or transfer of real estate.

Finance Committee

7. The Finance Committee shall consist of not less than five and not more than six members to be elected by the Board of Trustees by ballot for a term of three years, who shall be eligible for re-election.

8. The Finance Committee shall have custody of the securities of the corporation and general charge of its investments and invested funds, including its investments and invested funds as trustee of any retirement plan for the Institution's staff members and employees, and shall care for and dispose of the same subject to the directions of the Board of Trustees. It shall have power to authorize the purchase, sale, exchange, or transfer of securities and to delegate this power. It shall consider and recommend to the Board from time to time such measures as in its opinion will promote the financial interests of the Institution and of the trust fund under any retirement plan for the Institution's staff members and employees, and shall make a report at each meeting of the Board.

Auditing Committee

9. The Auditing Committee shall consist of three members to be elected by the Board of Trustees by ballot for a term of three years.

10. Before each annual meeting of the Board of Trustees, the Auditing Committee shall cause the accounts of the Institution for the preceding fiscal year to be audited by public accountants. The accountants shall report to the Committee, and the Committee shall present said report at the ensuing annual meeting of the Board with such recommendations as the Committee may deem appropriate.

Nominating Committee

11. The Nominating Committee shall consist of the Chairman of the Board of Trustees *ex officio* and, in addition, three Trustees to be elected by the Board by ballot for a term of three years, who shall not be eligible for re-election until after the lapse of one year. Any member elected to fill a vacancy shall serve for the remainder of his predecessor's term, provided that of the Nominating Committee first elected after adoption of this By-Law one member shall serve for one year, one member shall serve for two years, and one member shall serve for three years, the Committee to determine the respective terms by lot.

12. Sixty days prior to an annual meeting of the Board the Nominating Committee shall notify the Trustees by mail of the vacancies to be filled in membership of the Board. Each Trustee may submit nominations for such vacancies. Nominations so submitted shall be considered by the Nominating Committee, and ten days prior to the annual meeting the Nominating Committee shall submit to members of the Board by mail a list of the persons so nominated, with its recommendations for filling existing vacancies on the Board and its Standing Committees. No other nominations shall be received by the Board at the annual meeting except with the unanimous consent of the Trustees present.

Retirement Committee

13. The Retirement Committee shall consist of three members to be elected by the Board of Trustees by ballot for a term of three years, who shall be eligible for re-election and the Chairman of the Finance Committee *ex officio*. Any member elected to fill a vacancy shall serve for the remainder of his predecessor's term.

14. The Retirement Committee shall, subject to the directions of the Board of Trustees, be responsible for the maintenance of a retirement plan for staff members and employees of the Institution and act for the Institution in its capacity as trustee under any such plan, except that any matter relating to investments under any such plan shall be the responsibility of the Finance Committee subject to the directions of the Board of Trustees. The Committee shall submit a report to the Board at the annual meeting of the Board.

ARTICLE VI

Financial Administration

1. No expenditure shall be authorized or made except in pursuance of a previous appropriation by the Board of Trustees, or as provided in Article V, paragraph 8, hereof.

2. The fiscal year of the Institution shall commence on the first day of July in each year.

3. The Executive Committee shall submit to the annual meeting of the Board a full statement of the finances and work of the Institution for the preceding fiscal year and a detailed estimate of the expenditures of the succeeding fiscal year.

4. The Board of Trustees, at the annual meeting in each year, shall make general appropriations for the ensuing fiscal year; but nothing contained herein shall prevent the Board of Trustees from making special appropriations at any meeting.

5. The Executive Committee shall have general charge and control of all appropriations made by the Board. Following the annual meeting, the Executive Committee may allocate these appropriations for the succeeding fiscal year. The Committee shall have full authority to reallocate available funds, as needed, and to transfer balances.

6. The securities of the Institution and evidences of property, and funds invested and to be invested, shall be deposited in such safe depository or in the custody of such trust company and under such safeguards as the Finance Committee shall designate, subject to directions of the Board of Trustees. Income of the Institution available for expenditure shall be deposited in such banks or depositories as may from time to time be designated by the Executive Committee.

7. Any trust company entrusted with the custody of securities by the Finance Committee may, by resolution of the Board of Trustees, be made Fiscal Agent of the Institution, upon an agreed compensation, for the transaction of the business coming within the authority of the Finance Committee.

8. The property of the Institution is irrevocably dedicated to charitable purposes, and in the event of dissolution its property shall be used for and distributed to those charitable purposes as are specified by the Congress of the United States in the Articles of Incorporation, Public Law No. 260, approved April 28, 1904, as the same may be amended from time to time.

ARTICLE VII

Amendment of By-Laws

1. These By-Laws may be amended at any annual or special meeting of the Board of Trustees by a two-thirds vote of the members present, provided written notice of the proposed amendment shall have been served personally upon, or mailed to the usual address of, each member of the Board twenty days prior to the meeting.

Index